PB88-145297

Kinetics of Ingested (222)Rn in Humans Determined from Measurements with (133)Xe

Massachusetts General Hospital, Boston

Prepared for

Health Effects Research Lab.
Research Triangle Park, NC

Dec 87

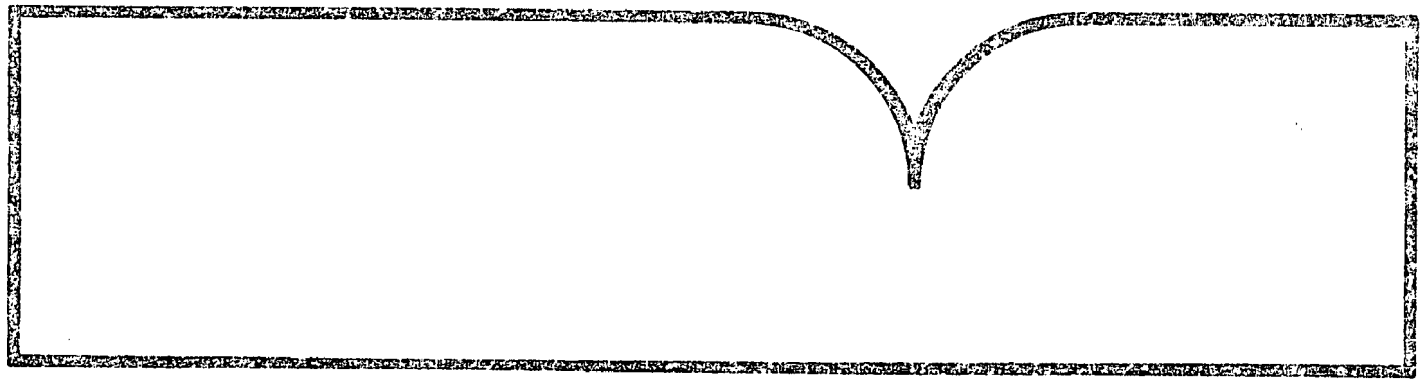

EPA/600/1-87/013
December 1987

The Kinetics of Ingested ^{222}Rn In Humans Determined from Measurements with ^{133}Xe

by

John A.Correia, Ph.D., Steven B. Weise, Ronald J. Callahan, Ph.D. and H. William Strauss, M.D.

Department of Radiology
Division of Radiological Sciences and Division of Nuclear Medicine

Massachusetts General Hospital
Boston, MA 02114

CR810942

Project Officer

Norman E. Kowal
Toxicology and Microbiology Division
Health Effects Research Laboratory
U.S. Environmental Protection Agency
Cincinnati, Ohio 45268

HEALTH EFFECTS RESEARCH LABORATORY
OFFICE OF RESEARCH AND DEVELOPMENT
U.S. ENVIRONMENTAL PROTECTION AGENCY
RESEARCH TRIANGLE PARK, NORTH CAROLINA 27711

TECHNICAL REPORT DATA
(Please read Instructions on the reverse before completing)

1. REPORT NO.	2.	3. RECIPIENT'S ACCESSION NO.
EPA/600/1-87/013		PB88 145297/AS

4. TITLE AND SUBTITLE	5. REPORT DATE
THE KINETICS OF INGESTED ^{222}Rn IN HUMANS DETERMINED FROM MEASUREMENTS WITH ^{133}Xe	December 1987
	6. PERFORMING ORGANIZATION CODE
7. AUTHOR(S)	8. PERFORMING ORGANIZATION REPORT NO.
John A. Correia, Steven B. Weise, Ronald J. Callahan, and H. William Strauss	
9. PERFORMING ORGANIZATION NAME AND ADDRESS	10. PROGRAM ELEMENT NO.
Department of Radiology, Division of Radiological Sciences and Division of Nuclear Medicine, Massachusetts General Hospital, Boston, MA 02114	CBMC1A
	11. CONTRACT/GRANT NO.
	CR810942
12. SPONSORING AGENCY NAME AND ADDRESS	13. TYPE OF REPORT AND PERIOD COVERED
Health Effects Research Laboratory (HERL) Office of Research and Development (ORD) U.S. Environmental Protection Agency (USEPA) Research Triangle Park, North Carolina 27711	Project Report/Summary
	14. SPONSORING AGENCY CODE
	EPA-600/11

15. SUPPLEMENTARY NOTES
P.O. Norman E. Kowal, BMTB/TMD/HERL/USEPA (CI)

16. ABSTRACT

The problem of naturally occurring ^{222}-radon contamination has received a great deal of public and scientific attention over the past several years, and has become a major public health issue worldwide. The purpose of the work reported in this document was to provide information about the behavior of ingested ^{222}-radon in the digestive system and other organs of the human body. ^{133}-Xenon, an element which behaves in the same manner as ^{222}-radon in tissue and differs only in tissue solubility, was used in studies on human subjects. The tissue solubility differences were accounted for by using the tissue/blood partition coefficients of the two gases. This report was submitted in fulfillment of cooperative agreement CR810942 by Massachusetts General Hospital, Boston, MA, under the sponsorship of the U.S. Environmental Protection Agency. This report covers a period from 24 October 1983 to 23 April 1886, and work was completed as of 26 August 1987.

17. KEY WORDS AND DOCUMENT ANALYSIS

a. DESCRIPTORS	b. IDENTIFIERS/OPEN ENDED TERMS	c. COSATI Field/Group

18. DISTRIBUTION STATEMENT	19. SECURITY CLASS (This Report)	21. NO. OF PAGES
RELEASE TO PUBLIC	UNCLASSIFIED	900
	20. SECURITY CLASS (This page)	22. PRICE
	UNCLASSIFIED	

EPA Form 2220-1 (Rev. 4-77) PREVIOUS EDITION IS OBSOLETE

NOTICE

This document has been reviewed in accordance with U.S. Environmental Protection Agency policy through cooperative agreement CR810942 to Massachusetts General Hospital, Boston, MA and approved for publication. Mention of trade names or commercial products does not constitute endorsement or recommendation for use.

FOREWORD

The many benefits of our modern, developing, industrial society are accompanied by certain hazards. Careful assessment of the relative risk of existing and new man-made environmental hazards is necessary for the establishment of sound regulatory policy. These regulations serve to enhance the quality of our environment in order to promote the public health and welfare and the productive capacity of our Nation's population.

The complexities of environmental problems originate in the deep interdependent relationships between the various physical and biological segments of man's natural and social world. Solutions to these environmental problems require an integrated program of research and development using input from a number of disciplines. The Health Effects Research Laboratory, Research Triangle Park, NC and Cincinnati, OH, conducts a coordinated environmental health research program in toxicology, epidemiology, and clinical studies using human volunteer subjects. Wide ranges of pollutants known or suspected to cause health problems are studied. The research focuses on air pollutants, water pollutants, toxic substances, hazardous wastes, pesticides, and nonionizing radiation. The laboratory participates in the development and revision of air and water quality criteria and health assessment documents on pollutants for which regulatory actions are being considered. Direct support to the regulatory function of the Agency is provided in the form of expert testimony and preparation of affidavits as well as expert advice to the Administrator to assure the adequacy of environmental regulatory decisions involving the protection of the health and welfare of all U.S. inhabitants.

This document reports the results of research on the behavior of ingested radon in the human digestive system and other organs of the body, which was performed because of the recently recognized public health problem of human exposure to naturally occurring radon in the environment.

F. Gordon Hueter, Ph.D.
Director
Health Effects Research Laboratory

ABSTRACT

The problem of naturally occurring ^{222}-radon contamination has received a great deal of public and scientific attention over the past several years, and has become a major public health issue worldwide. The purpose of the work reported in this document was to provide information about the behavior of ingested ^{222}-radon in the digestive system and other organs of the human body. ^{133}-Xenon, an element which behaves in the same manner as ^{222}-radon in tissue and differs only in tissue solubility, was used in studies on human subjects. The tissue solubility differences were accounted for by using the tissue/blood partition coefficients of the two gases. This report was submitted in fulfillment of cooperative agreement CR810942 by Massachusetts General Hospital, Boston, MA, under the sponsorship of the U.S. Environmental Protection Agency. This report covers a period from 24 October 1983 to 23 April 1886, and work was completed as of 26 August 1987.

CONTENTS

Chapter 1

INTRODUCTION

The purpose of the work reported in this document was to provide information about the behavoir of ingested ^{222}Rn in the digestive system and other organs of the body. The problem of naturally occuring ^{222}Rn contamination has received a great deal of public and scientific attention over the past several years and has become a major public health issue worldwide [36][8] [45].

One potentially serious source of radiation dose to the population at large from ^{222}Rn comes from the ingestion of drinking water laden with this substance [13][1][5] [44]. To date this problem has been studied only in a preliminary way. Very little data has been collected in human subjects. There have been several studies in which a small number of subjects ingested radon laden water and were followed over time either by whole body counting of the penetrating emissions from the ^{222}Rn daughter or by measuring equilibrated ^{222}Rn daughters in expired air ^{214}Bi [3][48] [1][17][13] [5] [19]. All of these studies suffer from the limitation that direct regional measurements of organ concentrations could not be carried out with the experimental preparation used, and the fact that they depend on inferring ^{222}Rn and daughter concentrations from an equilibrated mixture of the parent and daughters. Also, because of the difficulties in carrying out the measurements, only a few subjects were evaluated in each experiment.

In the present work we have attempted to use an alternative preparation which would overcome these limitations. Rather than using ^{222}Rn itself we have used a substance, ^{133}Xe, which behaves in the same manner as ^{222}Rn in tissue, differing only in tissue solubility. The tissue solubility

differences may be accounted for in situations where organ concentrations are equilibrated at all times (a usual assumption for compartmental models) using the tissue/blood partition coefficients of the two gases[51][16][28].

^{133}Xe is used routinely as in gaseous form for clinical nuclear medicine lung ventilation and brain organ flow studies[40] [50][29][11][18][37] [32][12][25][10] It has not however been used routinely in dissolved form. ^{133}Xe emits penetrating photons at 81 and 35 keV, the former being within the range of energy for which clinical scintillation cameras are designed [2][42][15][35]. [26]. A significant effort was expended at the early stages of the project to develop a method for producing and administering sterile doses of ^{133}Xe in solution and to the development of human imaging protocols. A series of animal studies, not reported in this work, were carried out as part of this development phase.

Thirty-five subjects were imaged after the administration of a drink of water laden with millicurie levels of ^{133}Xe. They were followed for periods of up to ten hours with a scintillation camera. Organ radioactivity concentration *vs* time curves were generated for the digestive system, quantitated in absolute concentration units and converted to ^{222}Rn kinetic curves using partition coefficient data gleaned from the literature. Various parameters were then computed from these ^{222}Rn concentrations, including cumulative radioactivity concentrations for ^{222}Rn and its five daughters, organ mean transit time for ^{222}Rn and a set of average analytical organ rate constants for ^{222}Rn kinetics determined from least squarares fits. Fifteen of the subjects were also studied with high frequency imaging (1hz) during the initial post-ingestion period to test for rapid escape of radioactivity from the body.

An additional twelve subjects were studied after inhalation of ^{133}Xe to assess the contribution of ^{222}Rn recirculated from the lungs to the organs of the body. These studies were conducted because recirculation was felt to be the major source of muscle and fat radioactivity following ingestion of ^{222}Rn and might also be a significant source of radioactivity in other organs.

This project was carried out in a university hospital environment (Massachusetts General Hospital) because such an institution is the only place where the imaging technology, experience in handling large (mCi) quantities of radioisotopes for use in human subjects, and expertise in mathematical modeling and data handling could all be found in the same institution.

The following chapters of this report present the details of experimental

methods (Chapter 2), Results (chapter 3) and conclusions (chapter 4).

Chapter 2

EXPERIMENTAL METHODS

2.1 Introduction

The purpose of this chapter is to describe the experimental and computational approaches used in producing the results reported in other sections. The overall goal of the work was to determine regional quantitative radioactivity concentrations and cumulative radioactivity concentrations which result from the ingestion of ^{222}Rn. The experimental preparation was based on the administration of a drink of ^{133}Xe, a chemical analog of radon, to a series of volunteer subjects and following the regional radioactivity distribution in the body over time with a nuclear medical imaging device. ^{133}Xe was chosen because it emits penetrating photons (81keV and 30keV) which are easily imaged and because it is routinely used in gaseous form for nuclear medical studies.

The remainder of this chapter describes the details of the measurements and data analysis that were carried out to achieve the stated goal. It is organized as a series of sections, each describing a separate aspect of methodology. The order of presentation is chosen to approximate as closely as possible the chronological steps in arriving at the results. The topics discussed include:

- Subject recruitment and population characteristics
- Xenon and Radon Partition Coefficients
- Radioactivity Dose Preparation and Calibration

- Experimental Imaging Methodology
- Data Analysis

2.2 Experimental Study Population

Paid normal volunteer subjects were recruited by advertising on bulletin boards at local academic institutions and within the local community. The advertisments were reviewed and approved by the Massachusetts General Hospital (MGH) human studies committee. Approximately seventy responses to the advertisements occured during a two year period. An initial interview by telephone was conducted with each respondent. In this interview the nature of the study and its goals as well as the specific measurements to be done were explained to the respondent by an experienced interviewer. A set of questions concerning the subject's reasons for volunteering were also asked for the purpose of psychological screening. During the phone interviews twenty percent of the responding subjects were eliminated by the interviewer or themselves decided against participation based on a disproportionate perception of radiation risk. Approximately ten percent were eliminated based on their psychological status or state of health.

Potential subjects from the above group were re-contacted by telephone and a time for either an ingestion or an inhalation a study was scheduled. Subjects scheduled for ingestion studies were instructed at this time either to fast for eight to twelve hours, to eat a low fat meal four to six hours before the study, or to eat a low fat meal one hour before the study. When a subject arrived on the day of the study, one of the investigators again explained the overall goals of the study and the specifics of the measurements. In the course of this discussion the subject was shown the equipment to be used. A medical history was taken and the subject's digestive status was confirmed. Finally, the subject was asked to read and sign an approved consent form and was asked to express any concerns or questions that he/she might have concerning the study. No subjects dropped out at this stage. œB Five studies were judged to be technical failures based on equipment problems or inability of the subject to cooperate. A total of thirty sucessful ingestion studies and twelve successful inhalation studies were performed. The characteristics of the ingestion study population, including the time of each participant's last meal prior to the study, is shown in Table 2.1. This

Table 2.1: Subject Population for Ingestion Studies

Subject ID	*Age (yrs)*	*Sex*	*weight (lbs)*	*height (in)*	*time Since Last Meal (hrs)*
ahern	48	m	180	72	12
arrol	48	f	108	60	1.5
ayer	49	f	115	63	1
brock	32	f	103	62	5
byrne	44	m	165	69	6
cline	27	f	115	67	6
elmden	25	f	150	65	5
epling	39	m	150	69	5
freedman	33	m	225	70	1
gallop	42	m	180	69	6
gmckinley	20	f	150	67	0.5
hand	54	f	120	63	1
hawkins	40	m	140	68	1
hill	41	f	130	66	12
hutchins	25	f	66	135	1
jmckinley	45	m	175	70	6
kelleher	28	m	155	70	11
littell	45	m	228	72	1.5
maio	21	m	150	67	12
malcom	29	m	165	73	11
macmillan	21	m	150	70	10
miller	25	f	120	66	4
morgan	38	m	140	70	2
monroe	28	m	174	68	1.5
muchrche	27	m	190	71	1.5
park	21	m	150	73	1.5
taates	27	m	155	71	1.5
taylor	25	f	175	62	5
wesolek	25	m	180	74	1
wiltse	32	f	130	60	4
AVERAGE	33.1	—	168.7(m), 120.9(f)	70.3(m), 64.3(f)	—
S.D.	10.	—	30(m), 39(f)	1.9(m), 2.6(f)	—

population consisted of twelve females and eighteen males. Their mean age was 33.1 ± 10.0 years. All but five of the subjects (2 males and 3 females) had normal body weight for their height and those five were mildly obese. Six subjects had fasted for more than eight hours, fifteen had had a light meal within one and one half hours before the study and nine had had a similar meal four to six hours before the study.

2.3 Xenon and Radon Partition Coefficients

This study exploits the fact that Radon and Xenon, both chemically inert , behave in a very similar way in tissue and blood. The main differences in their behavior result from differences in solubility in tissues, a physical effect. Both elements diffuse freely into tissue and blood and their typical root of egress is by diffusion into to venous blood and subsequent transfer to air in the lungs. If one assumes that two tissues, blood and intestinal wall for example, are equilibrated with respect to a given inert gas, then the concentrations of in the two tissue types i and j are related by a constant called the partition coefficient, λ_{ij} citeWeathersby80[49][28]. The rate of clearance of inert gas depends on the partition coefficient and the local tissue blood flow in the following way[9][20][29] [39][49]:

$$f = \lambda k \tag{2.1}$$

where λ is the tissue blood partition coefficient, f is the local tissue blood flow and k is the compartmental rate constant for tracer clearance. The rates of clearance of two different inert gas tracers in the same tissue are then related in the following way:

$$k_i/k_j = \lambda_j/\lambda_i \tag{2.2}$$

The equilibrium concentrations of the the gasses in the tissue are also related in a similar way. Thus, if the tissue clearance rate constants or tissue concentrations for one inert gas are known, and partition coefficients for it and another inert gas are also known, the former quantities for the second inert gas may be inferred from those of the first.

In order to relate tissue clearance of ^{133}Xe to that of ^{222}Rn, partition coefficient data from the literature was collected and reviewed (refs). There is a large amount of data available in animals for both of these gases

[38][7][9][14][41] [52][53] as well as a resonable amount of human data[38][20] [23][24][33][39][46] [51][28][6][13][17].

For the purposes of the work reported here the human data was used where possible. In several instances (the digestive organs in particular) no human Xe data was available. In these cases however data was available for animals and for another inert gas, Kr[4][22] [21][31][33][41][51] [27]. Digestive organ partition coefficients for Xe were inferred from human Kr and Rn partition coefficents. This was felt to be justifiable since, for other organs where partition coefficients were known for all three gases, the ratios among the three were constant. Also, comparisons of partition coefficients in all three gases in several animal species yielded approximately the same ratios. The partition coefficients used in the computations undertaken as part of this work are given in table 2.2.

In the case of fat there is wide range of Rn partition coefficients reported (from 10 to 20). For the computations in this work the value 11.93 was assumed to be correct but this decision is arbitrary.

For most of the other organs of interest in this work, the Radon and Xenon partition coefficients were very similar. This allowed us to make the assumption of a single phase for these gasses in the digestive system rather than being concerned about whether the two substances would behave differently in the gas phase before entering tissue. One problem with this assumption is that differing amounts of fat in the food present in the digestive system would dissolve Xe and Rn differently. Therefore experimental subjects ate only low fat foods in the period before the studies.

Table 2.2: Human Tissue-Blood Partition Coefficients for Rn and Xe

Organ	Radon λ	Xenon λ
liver	0.75	0.75
stomach	0.76	0.72
intestines	0.76	0.72
kidney	0.70	0.68
muscle	0.54	0.69
fat	11.93 (20.0)	9.5
brain	0.76	0.92

2.4 Radioactivity Administration and Calibration

In order to provide a sterile preparation of ^{133}Xe for ingestion, it was necessary for us to develop a method of producing individual (unit) doses of this gas dissolved in liquid (dissolved Xenon doses are not currently available commercially) and to develop a safe and effective method of administering the dose to a human subject. The unit dose and subject delivery systems must be both sterile and resistant to corrosion from saline. To provide unit doses from a high-radioactivity source a chrome-plated stainless steel vessel was constructed. The vessel contains a screw-driven press which can be operated from the outside when the vessel is closed and two fittings which are compatible with standard sterile hospital fittings. A commercially purchased glass ampule containing approximately one Curie of ^{133}Xe is placed in the chamber, the chamber is then sealed and filled with saline from a reservoir which remains connected. The screw press is then operated from the outside to crush the ampule and the Xe gas is dissolved. Unit doses may be drawn form the device by adding saline to the inlet port and collecting displaced saline, already equillibrated with the gas, in a sterile syringe at the outlet port. The gas/saline solution in the vessel then equilibrates at slightly lower ^{133}Xe concentration. A schematic of this device is shown in figure 2.1. It is sterilized before each new ampule is loaded.

The unit dose, about 5cc in volume, is then injected into a sterile plastic bag containing 100cc of saline with no air bubbles. The transfer is made through a sterile injection membrane which was fitted to it along with a three way valve and a plastic straw. The straw serves as the administration route to the subject. A sketch of this device is also shown in figure 2.1.

Typically, a unit dose was made up between four and eight hours before the study to allow for ^{133}Xe equilibration within the bag. Such a dose consisted of 3-6 mCi of ^{133}Xe with the assumption that 1-3 mCi would be delivered to the subject and the remainder would adhere to the plastic bag and valves. The radioactivity level in each dose was measured just prior to administration and immediately after administration using a standard nuclear pharmacy dose calibrator (ionization chamber based well counter calibrated to $\pm 10\%$ for ^{133}Xe).

At the start of an ingestion study, the subject was told to seal his/her

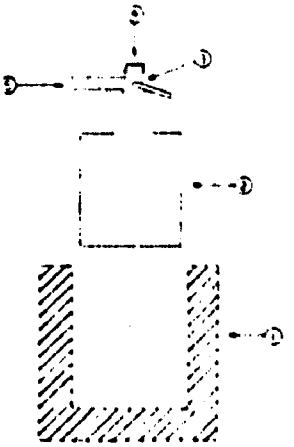

1 - Lead Shield
2 - Vinyl Bag
3 - Valve
4 - Filling Port
5 - Drinking Stem

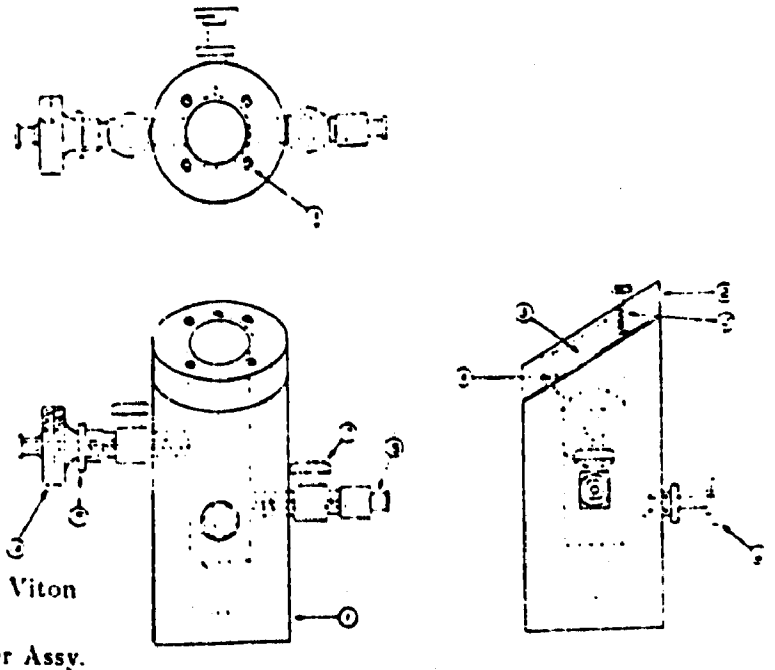

1 - Base
2 - Cover
3 - Window
4 - O-Ring #2-124 Viton
5 - Bleeder Valve
6 - Ampule Crusher Assy.
7 - Valve (2) Circle Seal
8 - Luer Lock Adapter
9 - Pipe Fitting 1/8 to 1/4 NPT (#316SS)
10 - Millipore Filter Assy. (Cat.#XX35-52500)
11 - (4) #6-32(SS) x 1/2in. Cap Screws

Figure 2.1: Upper: Diagram of Sterile Administration Aparatus for ^{133}Xe Ingestion. Lower: Machine Drawing of ^{133}Xe Unit Dose Dispenser

lips around the plastic straw and at a signal from the investigator to begin drinking normally. The bag was then opened to the subject. During drinking the bag was squeezed slightly by the investigator to prevent the formation of gas bubbles. Typically, it took a subject about twenty seconds to swallow the 100cc dose. This simple system worked very well in practice. In approximately 35 administrations there were no subject complications or radioactivity spills.

Radioactivity was administered to inhalation subjects from a commercial ^{133}Xe gas delivery system which is routinely used for clinical lung scans. It consists of a rebreathing reservior containing 3-6 mCi per liter of radioactive gas mixed with air, and an activated charcoal trap. The subject is connected to the reservoir via a tight fitting mask. During the first 2.5 minutes of the study, the subject breathed from the reservior and for the subsequent ten minutes he/she breathed in room air and exhaled into the activated charcoal trap. The mask was removed after 12.5 minutes and the subject continued breathing normally for the remainder of the study.

2.5 Experimental Imaging Methodology

2.5.1 instrumentation and data collection for ingestion studies

All imaging studies were carried out at the Massachusetts General Hospital Nuclear Medicine Division in clinical scanning rooms. The radioactivity distribution in each subject's torso was imaged from the anterior projection during and after the administration of ^{133}Xe using a nuclear medical scintillation camera. All but four of the subjects were studied using a Technicare Ω500 rectangular field camera. This camera was chosen because its large imaging field (56 x 38 cm) and its rectangular geometry allow for the viewing of all of the digestive system and the pelvic area in most adults. A smaller circular field camera was used to image the remaining four subjects at times when the Ω500 camera was unavailable due to an emergency clinical study. Both of these devices give a projection image with a spatial resolution of approximately 1 cm (Full Width at Half Maximum response of a point source of radioactivity). The dead time characteristics of these devices are such that no significant deadtime effects occur below 20,000

detected events per second. This fact was experimentally verified for both of the imaging cameras used in this study. Since no patient data set was collected at countrates in excess of the 20,000 event per second limit, no deadtime corrections were made to the data. The sensitivity and limiting detectibility of the Ω500 imaging camera were measured using point and plane sources of ^{133}Xe in a torso equivalent scatterer. The sensitivity was determined to be 11.3 detected events per second perμCi for a uniform distribution of ^{133}Xe in a torso-like phantom. The main source of limitation to detectibility was found to be the presence of a 1,980 event per minute background due to cosmic rays and other sources of environmental radiation. It was determined that the detection, at 90% confidence, of 0.75μCi distributed in the torso requires a approximately fifteen minute imaging time. This was assumed to be the practical lower limit of detectibility for our studies.

Image data were acquired using a Technicare 560 nuclear medical computing system which is interfaced to the imaging cameras. This computer has a specially designed operating system which allows for acquisition and display of image data, simple image arithmetic and the selection of a region to be identified on all images in a given data set (Regions of Interest or ROI's). It was used to produce events *vs* time curves. Since the Technicare computer does not have the capacity to carry out sophisticated computations on large numerical data sets, all processing beyond the extraction of ROI data was done on a Digital Equipment Corporation VAX 11/780 computer. Software for the transfer of data from the Technicare 560 to the VAX 11/780 was developed as part of this project.

A simple device to monitor expired air during inhalation and ingestion studies was constructed. It consists of a constant speed pump which withdraws a continous sample of expired air from a mask or nasal canula, through a fixed geometry coil in a sodium iodode well detector. The events measured in one second epochs are recorded on a multichannel analyzer operated in multiscalar mode. This device gives relative air concentration.

2.5.2 subject study protocol

ingestion studies

The overall approach to collecting ^{133}Xe kinetic radioactivity concentration data was to place the subject's torso in contact with the scintallation camera in anterior (front) view and to then administer a 100 c.c drink containing between 1 and 5 mCi ^{133}Xe in saline via a straw connected to the sterile administration device. At the start of ingestion the image collection computer was started and images collected for some time period in order to follow the tranisit of radioactivity through the digestive system. In practice, about half the subjects were given the drink while standing because they were concerned about gagging while drinking in the supine position. These subjects were followed for ten minutes in the standing position and then placed in the supine position on the imaging table, realigned, and imaging continued. The remainder of the subjects received the drink while lying on the imaging table. Images of short duration were collected during the initial 25 minutes. These consisted, in half the subjects, of sixty-four 5 second images, then thirty-two 15 second images, and then thirty-two 30 second images. In the remaining half of the subjects, high frequency sampling of 1 or 2 seconds per image was used for the first 4 minutes and then the 5, 15 and 30 second sampling protocol just described was followed. After the inital thirty minutes, images summing events over one minute intervals were collected for the remainder of the study. Most subjects were not able to lie still in the supine position for more than four hours. Therefore, they were allowed to get up at between three and four hours to take a one hour break. Before a subject was allowed to get up, three marker sources were taped to his/her skin at known anatomical points and the sources imaged. The reference points used were the zyphoid bone at the bottom of the sternum and the left and right iliac protrusions of the pelvis. The positions of the sources were marked on the skin before removal as a secondary reference. The subject then returned after one hour, the marker sources were again placed on the body, and he/she was repositioned. A second imaging session of sixty second images was then carried out for two to four hours and, if necessary, the subject took another break, being repositioned again after one hour and imaged. The cycle of imaging sessions and breaks was repeated ,as long as the subject could tolerate it, for up to ten hours. In ten of the subjects, only the first imaging session was undertaken due either to

equipment scheduling difficulties or subject fatigue.

The image data sets resulting from the above described measurements, consist of three to ten hours of data having time gaps of approximately one and one half to two hours including repositioning time in those which extend beyond four hours. Five subjects were also brought back for imaging at twenty-four to thirty hours post ingestion to determine if residual ^{133}Xe radioactivity above the 0.75 μCi detectability threshold was present. These subjects were imaged for twenty minutes and a twenty minute background was collected immediately before or after the imaging study. In all cases, at least one twenty minute background measurement was made during the day of the study.

In ten subjects who were imaged at high frequency (typically 1 image per second), the expired air was sampled through a nasal canula to determine if a large amount of radioactivity escaped through the lung at early times after ingestion. Figure 2.2 shows a example of selected images from an ingestion study.

2.5.3 inhalation studies

The purpose of the inhalation studies which were done as part of this work was to characterize the response of tissues, particularly muscle and fat but other organs as well, to ^{222}Rn recirculated form the lung in arterial blood. Each subject was positioned in the same manner as for the ingestion studies and then connected to the breathing reservoir containing between three and six mCi of^{133}Xe mixed with air. The subject breathed from the reservoir system for two and one half minutes and then breathed room air for the remainder of the study. The subject's exhalations during the first twelve minutes of the study were trapped in an activated charcoal trap to minimize room background. The imaging protocol used in these studies is the same as that for the ingestion studies. A continous sampling of the subject's expired air during the breathup period and subsequent ten minutes was measured using the counting system described above. These data were used to infer the blood arterial radioactivity concentration as a function of time in order to provide input functions for the various organs (see subsection on data analysis). Figure 2.3 shows a selection of images from an inhalation study.

Figure 2.2: Anterior Scintillation Camera Images at Selected Times During a Ten Hour Imaging Protocol After Ingestion of ^{133}Xe. The time (min) at which each image was taken is shown.

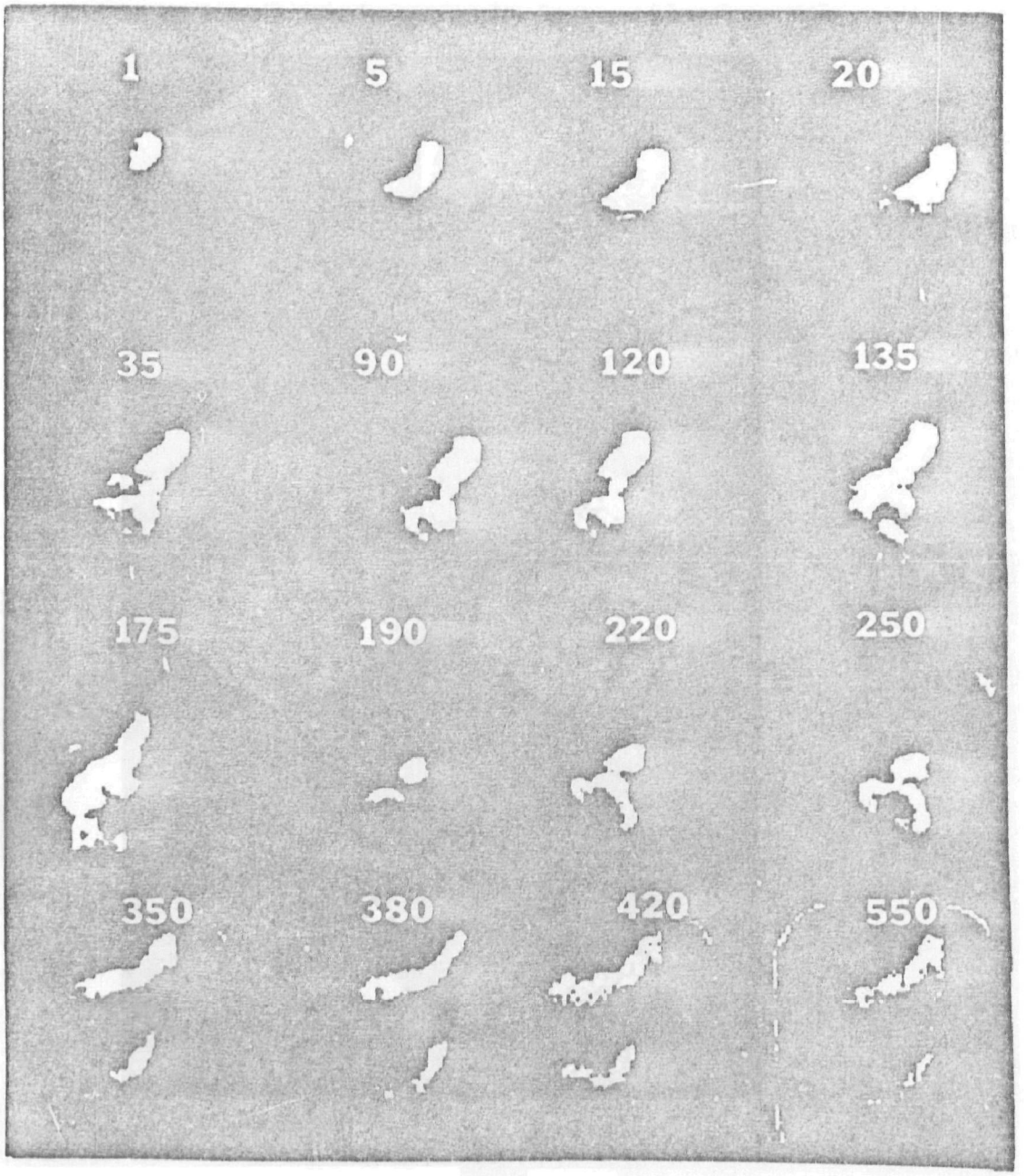

Figure 2.3: Selected Scintillation Camera Images from Inhalation Study. The times at which the images were taken are shown at the right. Lung is seen in the early phaze while radioactivity is being breathed. Liver, kidney and fat are seen in later images in this female subject

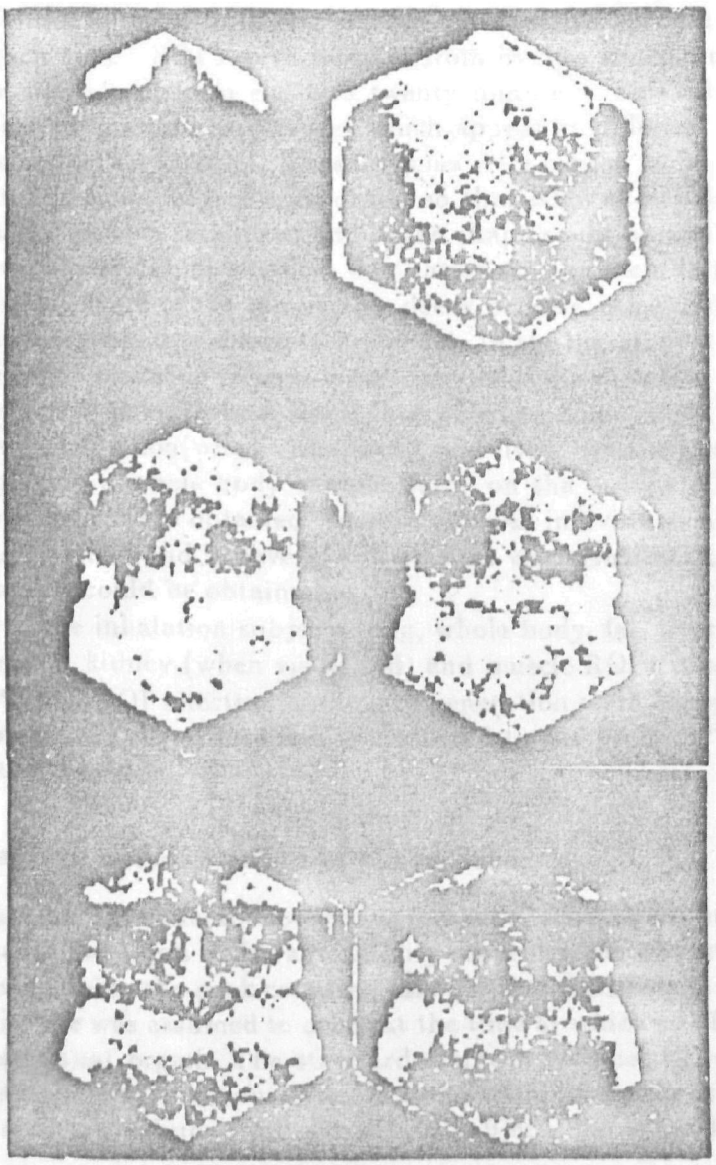

.5 , 2.0 min.

1.0 , 1.5 hr.

6.0 , 7.0 hr.

2.5.4 data analysis

preliminary data manipulation

Initial analysis of image data was carried out on the Technicare 560 imaging computer. This anlysis consisted of selecting regions of interest and the production of data sets consisting of events recorded in each region at each time. ROI's were selected from images which were summed over time periods of from eight to twenty minutes. This allowed the visualization of anatomic structures which appear at different times during the data collection interval. These regions were chosen to be smaller than the anatomic boundary of each organ so that edge effects due to finite scintillation camera resolution and organ shape could be minimized, but large enough to minimize stastical fluctuations in the measurements due to the Possion nature of the radioactive decay process. An example of the region selection process is shown in figure 2.4. In the ingestion studies an attempt was made to define regions for all organs of the digestive system including stomach, small intestine, whole intestine, ascending colon, transverse colon, descending colon(when visualized), and liver. Also a muscle sample from thigh and a whole body sample based on the outline of the torso in the image field, were obtained. In several small individuals a lung sample was also obtained and in several subjects fat was visualized to a degree where a sample could be obtained.

In the inhalation subjects lung, whole body, fat, liver, whole intestine, stomach, kidney (when visualized) and muscle ROI's were selected.

When ROI selection and curve generation were completed for a given subject, the curve data was transmitted to the VAX 11/780 computer for further analysis.

absolute normalization of curve data

A normalization factor converting measured events per minute per unit ROI area (N) to organ ^{133}Xe radioactivity concentration was determined for each subject using the peak counting rate per unit ROI area in the stomach (C). This rate was assumed to occur at the time at which all of the radioactivity was in that organ. The standard stomach volume, V_s = 402.0cc[45][47] , was used in this computation. In order to minimize the effects of variations in stomach volume from subject to subject, the subjects who ate before

Figure 2.4: Example of Region of Interest Selection for an Ingestion Study. At left is shown a fifteen Minute Summation Image Used to Define Regions. At Right is Shown the Selected Regions for stomach, liver, small intestine, descending colon and ascending colon

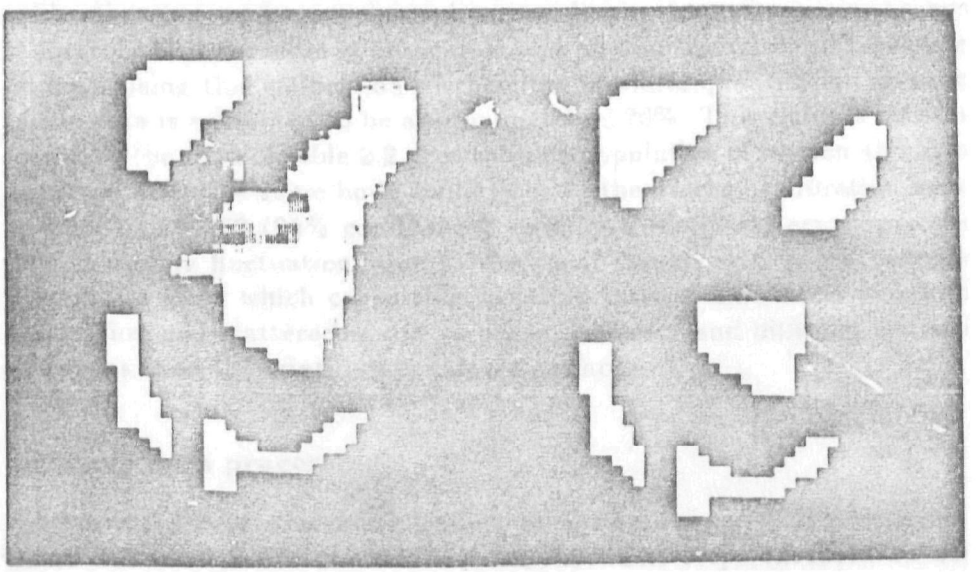

the study were asked to eat only a small (100-200 cc chewed) volume of food. The calibration factor (F) is given by $F = D/(V_s C)$ where D is the administered dose determined by measuring the dose container immediately before and immediately after administration. The calibration factors along with administered doses of ^{133}Xe are shown in Table 2.2.

Four of the studies listed in table 2.2 were not performed on the Ω500 Gamma Camera. Their calibration factors are not included in the average which is displayed in the table for that camera.

This method of calibration was compared to the use of a generic camera calibration derived from a chest phantom. It was deemed superior because it controls for differences in absorption and photon scatter in different sized bodies. Using this calibration method the absolute quantitative accuracy of the data is estimated to be approximately ±20%. This claim is substantiated by the data of table 2.2. For the sub-population of women all having approximately the same body build ($n = 7$) the average calibration factor is 0.0067±0.00082 (95% confidence) yielding a fractional error spread of 24% including fluctuations due to the small sample size. The sources of systematic error which cause this variation include differences in photon absorption and scatterering due to organ geometry and differing distances of organs from the scintillation camera surface.

primary data processing

The primary data processing leading to absolute organ ^{222}Rn concentrations was carried out on the VAX 11/780. The steps executed on each organ curve for each subject are as follows:

- Normalize data for different collection times yielding data in events/minute and account for collection gaps.
- Inspect curve data for transfer errors, verify errors and correct.
- Integrate data to uniform one minute time samples. This was done to reduce the size of the data sets and to make variance weighting and other aspects of non-linear least squares fitting more tractable. The early data, sampled at high frequency was also treated separately (see below).

- Subtract background. An individual background correction for each region in each subject was generated from background images collected at the time of each study.

- Convert Curves to absolute concentrations using measured calibration factors, correct for partition coefficient differences where appropriate and correct for difference between ^{133}Xe and ^{222}Rn half lives. The latter correction results in a ^{222}Rn data set which is not decay corrected (i.e., as measured).

- Interpolate data between collection gap endpoints. Single exponential interpolation was chosen over linear, spline and colocation polinomial interpolations because it gave the best visual impression of the transitions, most of which occur at late times in the data sets. This interpolation is only a convenience to simplify plotting and data integration computations.

- Smooth data once with unweighted three point smoothing to reduce stastical fluctuations and variations in the data due to minor subject motion and contractions of digestive organs.

These steps lead to absolute organ curve data sets which are sampled uniformly at one minute intervals. The entire data base is presented in graphical form in Appendix A and in numerical form in appendix B. An example of a data set in one subject is presented in Figure 2.5. A separate data base, which preserves the rapid time sampling of the early phase of the studies was also prepared for separate analysis. This database includes data from fifteen subjects and covers the first ten to fifteen minutes of data collection (to the time when one minute collection intervals were begun) in each subject. This data has also been included in the larger data base but has been integrated to one minute epochs there. A sample of an early data set is shown in figure 2.6. Air sampling data (by nasal canula) collected in eleven subjects was also transferred to the VAX 11/780. An example of this data in the is also presented in figure 2.6.

The inhalation data sets were treated in the same manner as the ingestion data sets to produce organ curves uniformly sampled at one minute intervals. The resulting data sets, however are in relative and not absolute concentration units. Expired air data in all of these subjects was also

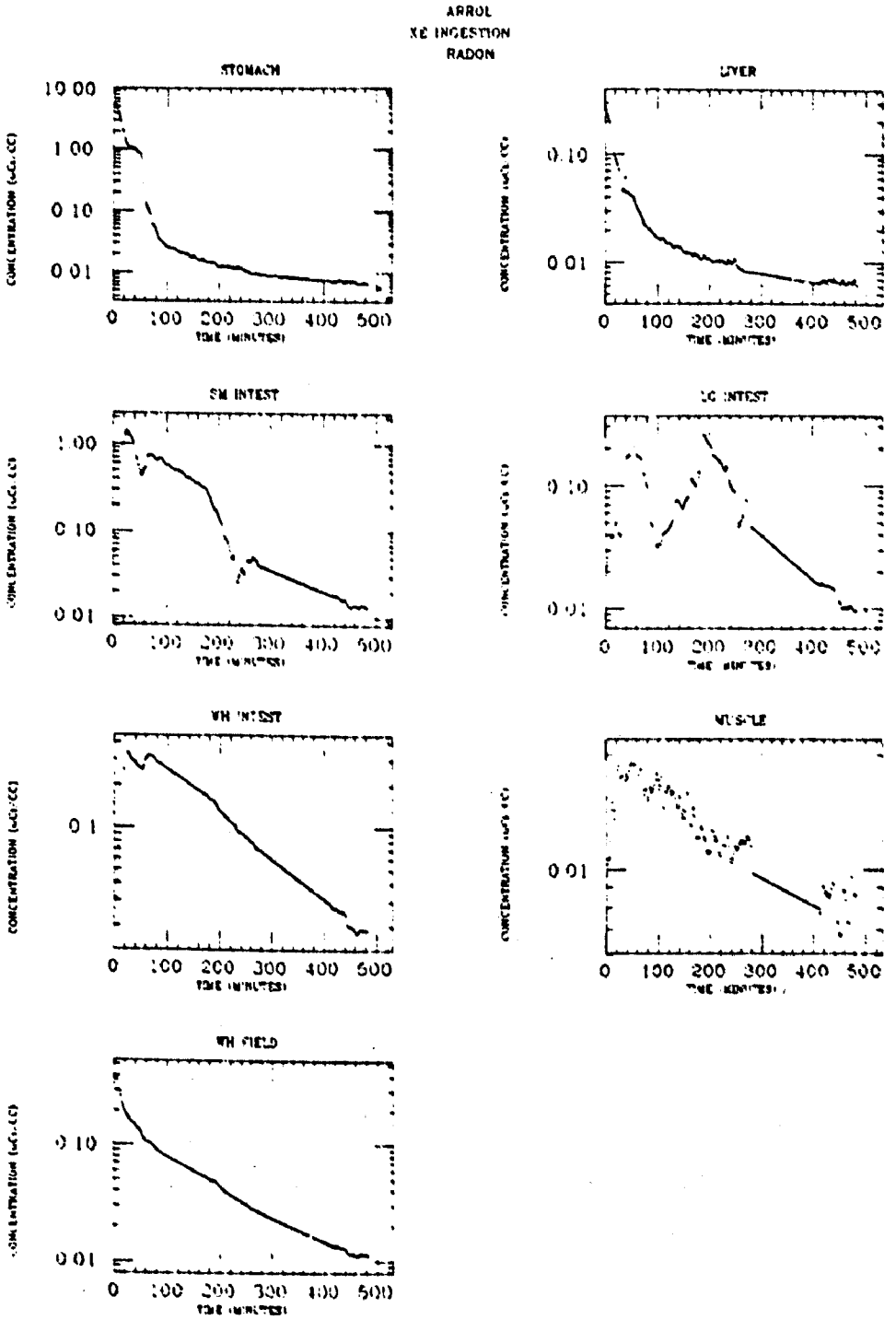

Figure 2.5: Example of Quantitative Radioactivity *vs* Time Curves for an Ingestion Study

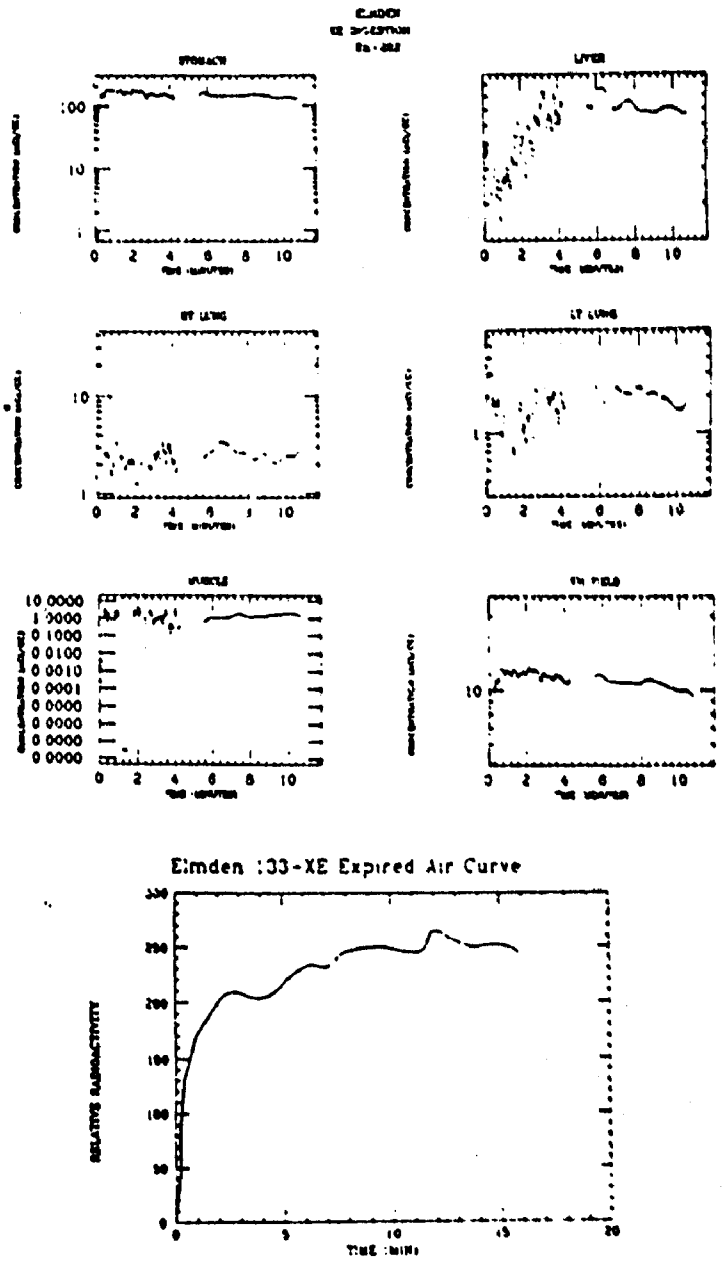

Figure 2.6: Example of Radioactivity vs Time Curves at High Sampling Frequency for the First Ten Minutes of an Ingestion Study. Also shown is the early expired air curve for this subject

transferred to the VAX 11/780. A complete inhalation data curve data set is shown in figure 2.7.

Analysis of Ingestion Studies

direct cumulative radioactivity computations Cumulative radioactivity concentrations of ^{222}Rn and its sucessive daughters ^{218}Po ($T_{1/2}$ = 0.051hr), ^{214}Pb ($T_{1/2}$ = 0.447hr), ^{214}Bi ($T_{1/2}$ = 0.328hr), ^{214}Po ($T_{1/2}$ = $4.44 \times 10^{-6} hr$) and ^{21} Po ($T_{1/2}$ = 22.yrs) were determined form the data sets uniformly sampled at one minute. The ^{222}Rn cumulative radioactivity concentration($\dot{C}_{Rn}$)was computed from the following expression:

$$\dot{C}_{Rn} = \int_0^{t_{max}} C_{Rn}(t')\, dt' + C_{Rn}(t_{max})/\lambda_{tail} \qquad (2.3)$$

where t_{max} is the time at the end of data collection λ_{tail} ia a rate constant determined from a single exponential fit of the last part of the curve (last 25 points typically), and A_{tail} is the radioactivity concentration at the end of the study as determined from the average of the last 5 points.

Based on inspection of the curves and least squares fit results (described below), the time cutoff (t_{max}) was established for each integral. The criterion used was that integration was stopped for major organs if and when extraneous signal from overlying muscle and other tissues became the dominant signal. In all but a few instances, there were no significant differences between the cut-off integrals and integrals carried out to the end of the imaging period. The second term of the above expression is a correction to 20 hour time based on the (monoexponential) tail of the organ signal. In most instances this was a negligible correction but for a few of the studies which were terminated before three hours it was five to twenty percent in organs such as the descending colon. The above equation was programmed as a numerical integration routine including the tail correction and applied directly to the absolute curve data sets. Tabulated data from these integrations is presented in the results section.

Daughter cumulative radioactivities were computed sucessively from the radon curves by the following expression which assumes that the radioactivity concentration in a one minute epoch is the instantaneous concentration at the beginning of the epoch. This is a very good approximation except in the case of the short lived daughter, where it leads to an overestimate of

the cumulative activities.

$$D_{i+1}(t) = D_i(t)(1 - e^{-\lambda_i \delta t}) + D_{i+1}(t - \delta t)e^{-\lambda_{i+1}\delta t} \qquad (2.4)$$

where $D_i(t)$ is the concentration of daughter i at time t, λ_i is the decay constant of the i'th daughter, and δt is the collection time interval (1 minute). This expression takes into account the production of daughter nuclide in the current epoch plus the production of daughter at that time from residual parent assuming that the daughters, once produced do not migrate from the organ within times on the order of five to ten halflives. The resulting daughter concentrations were integrated, including a tail correction, using the numerical integration routine mentioned above to produce daughter cumulative radioactivity concentrations In the case of the daughters, the tail correction is fairly large in some instances due to buildup of daughter.

Tables of daughter cumulative radioactivities averaged over the subject population are given in the Results section.

Mean transit times of ^{222}Rn radioactivity through the organs of the body were computed from the absolute radioactivity curves by numerically evaluating the following expression:

$$\bar{T} = \int_0^{t_{max}} tC_{organ}(t)\, dt / \int_0^{t_{max}} C_{organ}(t)\, dt \qquad (2.5)$$

where $C_{organ}(t)$ is the ^{222}Rn organ concentration.

These mean transit times represent the average time for a molecule of ^{222}Rn to transit a given organ after a δ-function of radioactivity is introduced into the stomach. The traditional organ transit time is the average time for a molecule to transit an organ after the introduction of a δ-function into the organ, can easily be computed from the transit times defined above but are not useful for dosimetry calculations in practical situations and therefore have not been considered. Transit time data averaged over the subject population and several sub-populations are presented in the results section of this report.

non-linear least squares fits to uniformly sampled data sets It can be seen from the examples shown in figure 2.5 and in Appendix A, that there is considerable structure in the digestive system curves, especially those of the stomach, small intestine, ascending colon and descending colon.

This is due to the fact that the digestive system is pulsitile in the sense that food and digestive biproducts are moved through it by non-periodic muscular contractions. A number of approaches to the modeling of this data were investigated[43] including the possibility of fitting the data to pulsitile models. The pulsitile model approach was abandoned when the results of our simulation studies demonstrated that it was very difficult to achieve convergence of the fit in the presence of noise. Further simulation studies demonstrated that simple compartmental models did fit the noisy pulsitile data well on the average and hence this approach was persued.

All nonlinear least squares fitting was done using the Marquardt- Levenberg Method[30][34] on the VAX 11/780. An interactive fitting package including a curve display was written to handle the data sets as part of this project. Using this package, each fit, its residuals and the raw data were displayed and evaluated on-line and the fits were repeated as necessary to achieve acceptable convergence and fit quality. In most cases the errors in the parameter sets determined from the fits (diagonal elements of the variance-covariance matrix from the fitting routine) were less than ten percent. Typically the residuals of the fits showed structure which was associated with pulsitile changes in organ data.

The stomach and whole field were fit to a sum of exponentials under the assumption that they behave like compartmental systems into which a δ-function input has been injected. The function fitted was of the form:

$$\sum_{i=1}^{n} A_i e^{-k_i t} \tag{2.6}$$

where A_i and k_i are the unknown parameters.

The small intestine and whole intestine were treated as compartmental systems whose input functions were given by the rate of change of radioactivity in the stomach. The model for the concentration in the target organ in this case is:

$$C_{organ}(t) = \sum_{i=1}^{n} \int_0^t A_i e^{-k_i(t-t')} \, I(t') \, dt' \tag{2.7}$$

where $I(t)$ is the input function to the organ.

Two approaches to fitting these data were tried. In the first the concentration curve from the organ feeding the organ of interest was used to directly compute an input function and in the second the organ of interest

data were fit to a function which is the analytic convolution of the feeding organ output function, determined from least squares, with the exponential response function of the organ of interest. For a single exponential input (denoted by subscript f) and response this function has the form:

$$C_i(t) = \{A_f A_i k_f/(k_i - k_f)\}(e^{-k_f t} - e^{-k_i t}) \qquad (2.8)$$

There were a number of convergence difficulties with the fits using the direct numerical the input function from the organ data. As a result of this, the information reported here is based on fits to the convolved analytic model. However, in cases where good fits were achieved with the direct approach (approximately two thirds of the subjects) the results of both approaches were in good agreement.

Convergence difficulties were enountered in attempting to fit the ascending colon and descending colon data either to an analytic model or to the model based on a numerical input from the previous organ. Since this difficulty is still unresolved, no analytic results for these organs are presented.

An attempt was made to fit the liver data to the convolved model using analytic input functions derived from the whole intestine data. The estimated liver rate constants were consistently very large, indicating that radioactivity was cleared by the liver as fast as it was input. The liver was therefore treated in the same manner as the whole body and fit to a sum of exponentials. Lung data were derived from the liver data assuming that all radioactivity reaching the liver from the portal circulation was rapidly transferred to the lung. The lung concentrations under this assumption are related to the liver concentrations by a scale factor which is the ratio of the organ volumes.

Muscle data (and the few direct fat samples obtained) were modeled as a compartment which was driven by the fraction of the lung radioactivity that is re-dissolved in the arterial blood and recirculated. Thus the muscle input function was taken to be the lung curve times the radon blood/air partition coefficient. Muscle and fat samples were indirectly obtained in fitting stomach and liver curves. The ROI's placed over these organs tended to view muscle in young males and fat in obese males and most females at late times . The parameters estimated from exponential components corresponing to muscle and fat were grouped with muscle and fat parameters from direct samples.

Cumulative radioactivities of ^{222}Rn were computed from the compartmental parameter sets obtained by least squares fitting. The cumulative radioactivity for each organ in each subject was computed and then these results combined to form a population average. Average values of the parameter sets for each organ over the subject population were also computed. These data are presented in the results section of this report. The fit parameters and concentration data computed from them are presented in the results section of this report where they are compared to computations by the direct approach described above. Examples of several least squares fits to the data are shown in figures 2.8.

separate evaluation of early data In order to determine whether or not significant amounts of radioactivity leave the body at early times after ingestion by direct transfer through the stomach wall, the early data in 15 subjects was analysed separately. The stomach and whole body curves in these subjects for the first 5-10 minutes were fit to a sum of exponentials and were also qualitatively inspected in an effort to observe any peaks or very fast decays. The time of appearance of radioactivity in the organs of the intestinal system was also noted. Expired air curves measured in ten of these subjects were also qualitatively graded.

2.5.5 analysis of inhalation data

The inhalation data sets were also analysed by nonlinear least squares. In this case the the arterial input function which drives a given organ is determined by computing the curve of end tidal expired air concentration. This method is used routinely for inert gas cerebral blood flow measurements[10] . The organ curves were fit to a model which is a convolution of the arterial input function determined in this way with a sum of exponentials representing the organ response(equation 2.6).

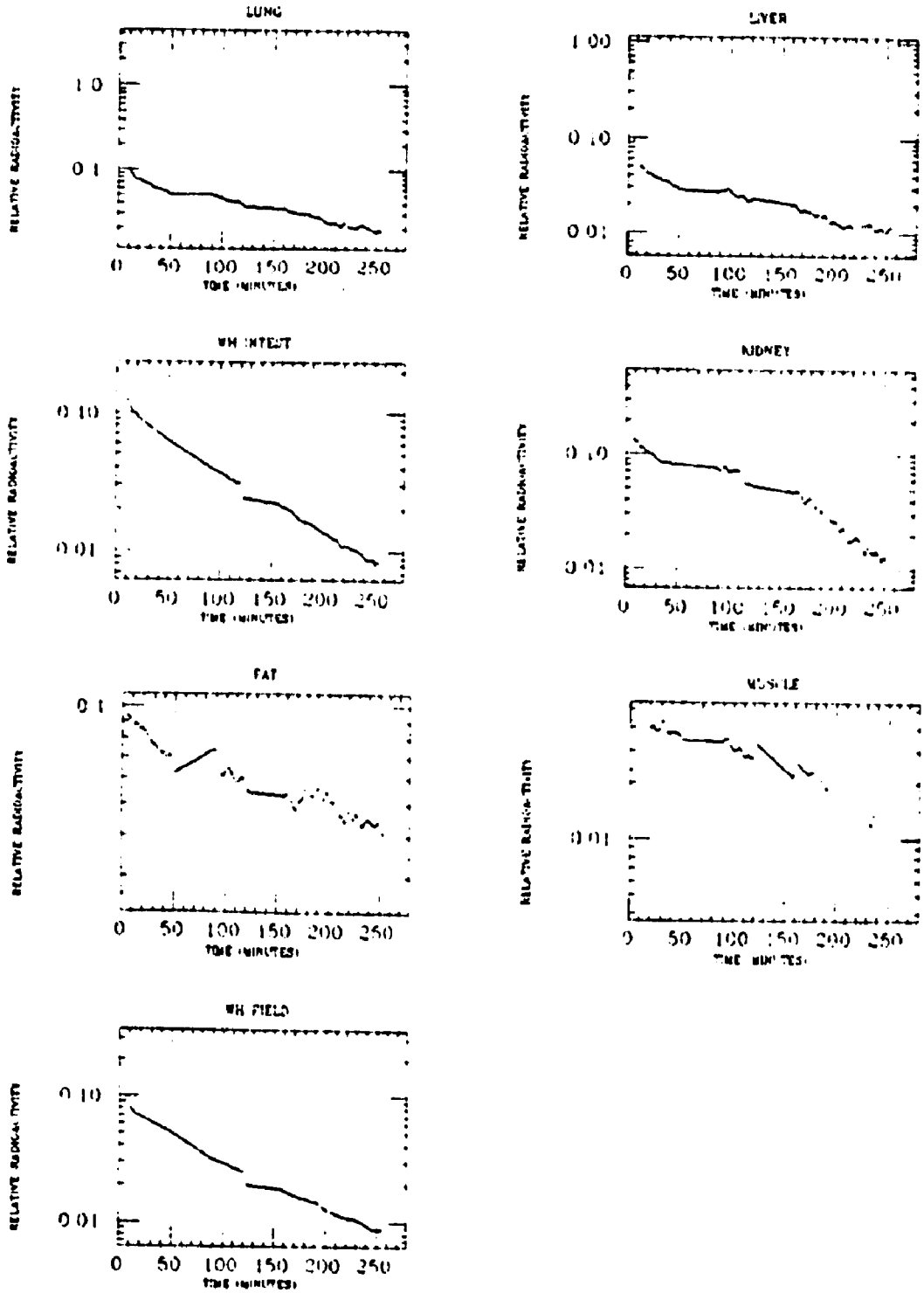

Figure 2.7: Relative Radioactivity *vs* Time Curves for an Inhalation Study in a Female Subject

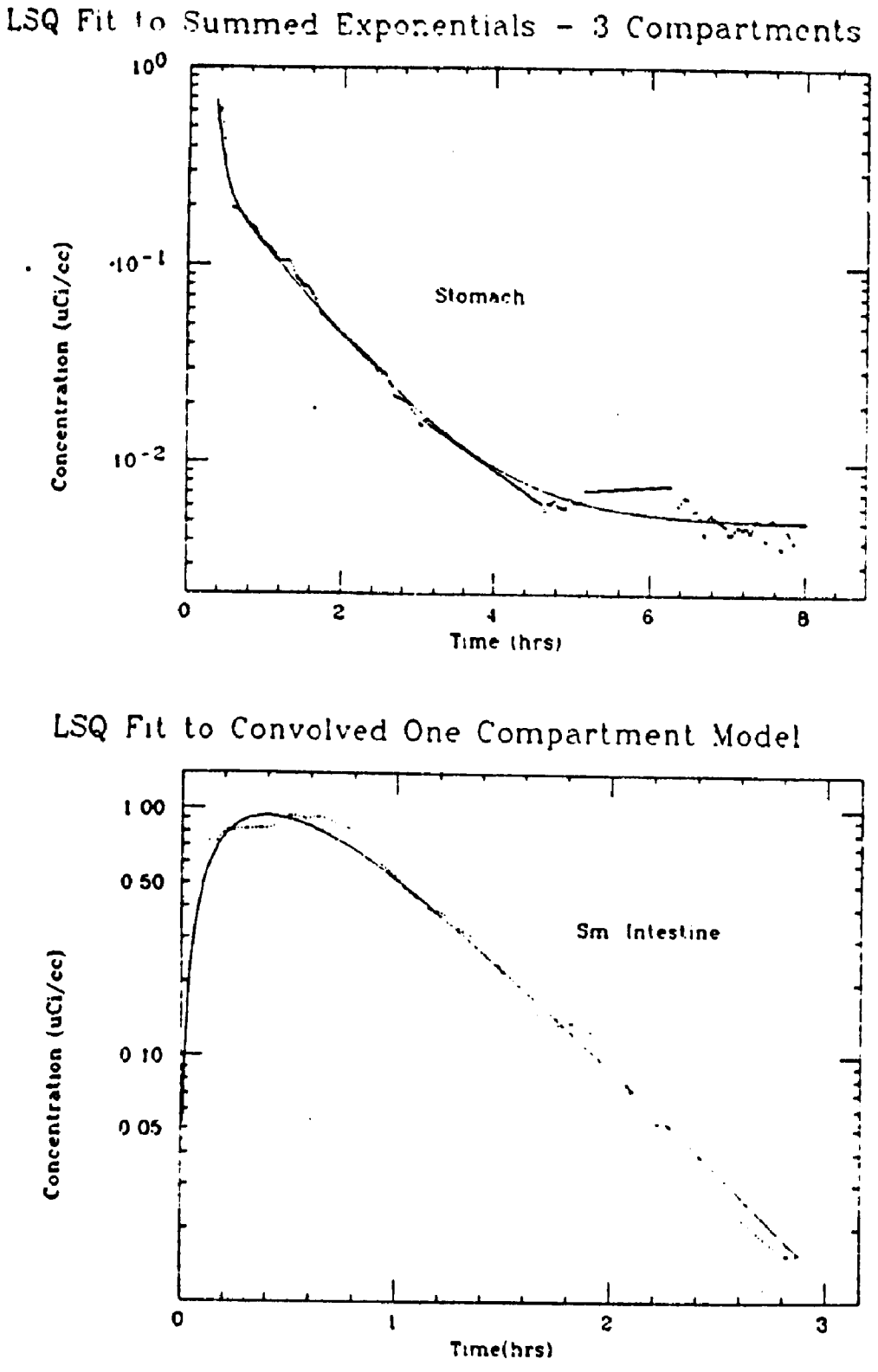

Figure 2.8: Examples of Nonlinear Least squares Fits to a Stomach Curve (Summed Exponentials) and a Small Intestine Curve (Convolved Model)

Table 2.3: Scintillation Camera Calibration Factors Measured for Each Subject

Subject ID	Radioactivity Administered (mCi)	Calibration Factor
ahern	0.86	0.0104
arrol	2.13	0.0077
ayer	1.46	0.0061
brock	1.40	0.0066
byrne	1.36	0.0081
cline	1.25	0.0082
elmden	1.13	0.012
epling	0.64	0.0145*
freedman	2.93	0.0447*
gallop	0.90	0.0109
gmckinley	1.89	0.0187
hand	0.95	0.0074
hawkins	0.60	0.0081
hill	2.22	0.0062
hutchins	1.94	0.0053
jmckinley	0.35	0.0315*
kelleher	2.80	0.012
littell	0.50	0.022
maio	1.62	0.0106
malcom	1.79	0.0076
macmillan	2.00	0.0100
miller	2.50	0.007
morgan	0.50	0.0054
monroe	2.87	0.0168
muchrche	1.47	0.0106
park	2.47	0.0131
taates	2.42	0.019
wesolek	1.62	0.0131*
wiltse	0.42	0.0075
AVERAGE	1.54	0.0103
S.D.	0.77	0.0040

Chapter 3

RESULTS

3.1 Introduction

This chapter presents the results of the measurements and computations described in the chapter on methods. As evidenced by appendices A and B, a very large volume of data has been produced from the original image measurements. In order to provide an understandable and useful presentation of these results, the information presented here is mostly in the form of tables of averages over the subject population and several sub-populations. The results presented here were selected because of their pertinence to dosimetry calculations. Since it may be of interest to some users of this report to compute other information, the quantitative radioactivity concentration data base for ^{222}Rn and it five daughters is included in the Appendices in both graphical and numerical forms. This data, as well as the original image data are available on industry-standard magnetic tape. Also available, though not included in the appendices, are the separate database of ingestion curves sampled at high frequencies and early times, and the inhalation study data base. The latter two data bases are not included in the appendices since both provide secondary information in some sense.

In the case of the ingestion studies the results fall into two catagories, those generated directly from the quantitative data base (direct results) and those generated from parameters derived from least-squares fits to the curves in the database (analytic results). As discussed in the chapter on methods, the direct results are more complete than the analytic results (do to difficulties in fitting some of the data to simple models) and are

therefore treated as the primary results. The analytic results are, however, fairly complete and are presented as supplimentary support for the direct results.

The main purpose of the inhalation studies was to determine the effect of radioactivity reaching the various organs, particularly muscle and fat, via recirculation from the lungs after ingestion. The results reported here are therefore aimed toward that purpose at the expense of a detailed reporting of cumulative radioactivity concentrations and other parameters associated with the inhalation of ^{222}Rn.

3.2 Results from Direct Analysis of Quantitative Data

Table 3.1 summarizes the results of direct computation of cumulative radioactivy concentrations of ^{222}Rn and its daughters per ingested millicurie of ^{222}Rn. These data represent averages over the entire population of ingestion subjects and have been computed as described in the Methods chapter. In the case of stomach, small intestine, whole intestine, whole body , liver and muscle the averages presented are over thirty subjects, while that for ascending colon is over twenty two subjects and that for descending colon is over ten subjects. The smaller samples in the latter organs are due to difficulties in selecting unambiguous regions in some cases and to lack of visualizitation of those organs in others, the latter being true particularly for the descending colon in studies having relatively short imaging times and in some fasted subjects where no radioactivity was observed.

The lung cumulative radioactivity concentrations reported in table 3.1 are derived from the liver data assuming that all of the radioactivity appearing in the portal circulation was delivered to the lung over very short times.

In most organs the ^{222}Rn concentration was close to zero at the end of the measuring interval. There are some exceptions to this in the short studies of the tail correction used to extrapolate the data to long times adequately corrects for this,as demonstrated by computer simulation, in most instances. The possible exceptions to this are the fat and muscle samples for which the data of Table 3.1 show significant underesitimates of ^{222}Rn cumulative radioactivity concentrations compared to the analytic

estimates presented in the following sections.

The standard deviations given in table 3.1 are sample deviations and in most instances they are fairly large. This reflects normal physiological variability and differences in digestive status among the subjects.

The daughter cumulative radioactivity concentrations per millicurie of ^{222}Rn ingested are given in (nCi/cc)-hrs and are computed under the assumption that deposited daughter atoms remain where they are deposited and do not migrate during the intervals over which the measurements and computations are carried out. Measurements in five subjects at times greater than twenty four hours post-ingestion indicate that the level of ^{222}Rn radioactivity in the body per ingested millicurie is less than 0.75μCi. This supports the arguement that all of the deposited energy due to the daughters is local with the possible exception of long lived ^{210}Pb. Refinements of these estimates could be made by accounting for the kinetics of the heavy metal daughters.

For the long lived product ^{210}Pb, the entries of table 3.1 are expressed as total radioactivity concentration under the assumption that virtually all atoms produced are still present in an organ at the end of the computation interval.

Table 3.2 gives the mean transit time of ^{222}Rn through each organ averaged over the subject population for a δ-function input to the stomach. It should be noted that the sample standard deviations in this parameter are somewhat smaller (percentagewise) than for the cumulative activities. This is probably due to the fact that the mean transit time is independent of the absolute calibration factor for each subject and the uncertainty in the calibration factor is approximately $\pm$20% (Methods chapter). These numbers represent a convienient, model independent characterization of each organ and could be used, in combination with estimates of initial organ radioactivity concentrations, for simple dosimetry calculations.

3.3 Results from Analytic Treatments of Quantitative Data

Non-linear least squares fits were carried out on the quanitiative ^{222}Rn curves as described in the Methods chapter. The parameter estimates from these fits, averaged over the subject population are presented in table 3.3.

Table 3.1: Average ^{222}Rn and daughter Cumulative Activities Computed Directly from Time-Activity Curves

Organ	^{222}Rn (μCi/cc)-hr	^{218}Po (nCi/cc)-hr	^{214}Pb (nCi/cc)-hr	^{214}Bi (nCi/cc)-hr	^{214}Po (nCi/cc)-hr	^{210}Pb (nCi/cc)
stomach	2.66±2.31	1.64±1.43	12.63±11.33	9.64±8.62	0.31±0.29	99.15±12.22
small intestine	0.44±0.41	0.29±0.25	21.55±19.54	0.15±0.14	0.051±0.049	15.5±17.28
whole intestine	0.37±0.45	0.23±0.28	1.62±1.91	1.17±1.27	0.39±0.44	8.44±8.07
ascending colon	0.21±0.20	0.14±0.13	0.93±0.87	0.68±0.59	0.027±0.023	5.46±5.70
descending colon	0.33±0.31	0.20±0.19	1.66±1.27	0.89±0.77	0.023±0.023	3.36±3.21
liver	0.096±0.078	0.059±0.048	0.45±0.38	0.35±0.30	0.011±0.009	3.17±3.66
lung	0.18±0.14	0.204±0.166	1.52±1.28	0.037±0.033	0.020±0.017	5.82±6.71
muscle	0.038±0.033	0.023±0.020	0.17±0.15	0.12±0.11	0.004±0.003	0.89±1.06
whole body	0.29±0.26	010±0.16	1.42±1.30	1.07±0.98	0.035±0.033	10.49±13.8
fat	.026±.015	0.017±0.009	0.12±0.08	0.081±0.060	0.003±0.0021	0.79±0.76

Table 3.2: Organ Mean Transit Times of ^{222}Rn after Ingestion

Organ	Mean Transit Time (min)
stomach	43.8±20.2
small intestine	94.1±51.5
whole intestine	102.6±38.5
liver	83.0±33.1
lung	87.0±33.0
whole body	80.7±27.8

In all cases a compartmental model was assumed. As explained in detail in the Methods chapter, the stomach, whole body and liver curves were fit to sums of exponentials while the other organs were fit to a model which is an analytic convolution of an input function derived from a fit to the output function of the previous organ and a sum of exponentials. Difficulties with convergence of the fits were encountered in attempting to fit the ascending and descending colon data. Therefore no results are reported in the table for those organs. The number of parameters used to describe each organ was chosen retrospectively after fitting the data to different numbers of exponentials. In some instances the signal from a given organ was contaminated by a contribution from overlying muscle or fat. These contaminants were accounted for by the fits and the parameters of the muscle and fat components stripped out of the organ curves were grouped with the pure muscle and fat parameters. Most of the fat samples reported here were obtained as contaminant signals.

As in the case of the directly computed cumulative radioactivity concentration data, the large sample standard deviations in table 3.3 reflect physiological and digestive-status variations in the subject population The errors in the individual parameter estimates as determined from the variance-covariance matrix of the fits are less than 10% in all cases and thus represent only a small contribution to the overall variances. Since the amplitude parameters of the fits are in quantitative units, these average parameters can be used to compute cumulative radioactivity concentrations. A possible problem with this is that in some organs there is a wide variation (an order of magnitude in the case of the stomach) in the rate constants and the average rate constant might not yield the correct cumulative activity as compared to the average of the individual cumulative activities due to the non-linear effects introduced by exponentiation.

Table 3.4 presents cumulative ^{222}Rn radioactivity concentrations computed from individual analytic cumulative concentrations averaged over the subject population. A comparison with table 3.1 shows that these argee well with comulative activities computed from the averaged rate constants in most instances. Also shown in table 3.4 are the organ cumulative concentrations for ^{222}Rn computed by the direct approach. Again the agreement is quite good except in muscle and fat. In these cases the analytic values are deemed to be the more reliable for the reasons discussed in the last section.

Table 3.3: Average Analytic Rate Constants and Ampltudes from Fits to ^{222}Rn Ingestion Quantitative Concentration Curves

organ	n	A_1	k_1	A_2	k_2	A_3	k_3
stomach	27	4.25±2.43	2.67±2.80	-	-	-	-
small intestine	23	0.60±0.56	1.25±0.69	-	-	-	-
liver	27	0.20±0.25	3.29±2.76	0.06±0.07	0.88±0.50	-	-
whole body	28	0.25±0.19	3.37±1.97	0.21±0.28	0.84±0.33	0.042±0.041	0.15±0.13
lung	28	0.50±0.35	3.37±1.97	0.34±0.51	0.838±0.33	0.077±0.075	0.53±0.127
muscle	25	0.042±.049	0.44±0.18	-	-	-	-
fat	10	0.021±0.019	0.698±0.026	-	-	-	-
whole intestine	28	0.25±0.38	0.815±0.47	-	-	-	-

Table 3.4: Analytic vs Direct Average ^{222}Rn Cumulative Radioactivity Concentratiom in (μCi/cc)-hr

Organ	*analytic*	*Direct*
stomach	1.67±2.42	2.66±2.31
small intestine	0.46±0.41	0.44±0.41
whole intestine	0.47±0.45	0.37±0.45
ascending colon	—	0.21 ±0.20
descending colon	—	0.33±0.31
liver	0.099±0.08	0.096±0.078
lung	0.18±0.15	0.17±0.14
muscle	0.099±0.10	0.038±0.033
whole body	0 35±0.29	0.29±0.26
fat	0.019±0.014	0.026±0.015

Table 3.5 gives an example of the rate constants and cumulative ^{222}Rn radioactivity concentrations (both direct and analytic) in the individual subjects for the small intestine. This data, averaged over subjects yields one entry in table 3.1 or table 3.3.

Table 3.5: Example of Organ Rate Constants and Cumulative Concentrations in Individual Subjects - Small Intestine

Subject	*A (μCi/cc)*	*k (hr^{-1})*	*Analytic (μCi/cc)-hr*	*Direct (μCi/cc)-hr*
Ahern	0.243	0.772	0.33	0 31
Arrol	0.76	0.74	1.69	1.93
Ayer	0.032	0.?5	0.255	0.108
Brock	0.217	1.74	0.219	0.260
Cline	1.62	2.11	1.01	1.023
Elmdon	0.122	0.15	1.01	0.76
Epling	0.23	1.24	0.15	0.18
Gallop	0.25	0.43	0.42	0.60
Hand	0.036	0.84	0.22	0.076
Hawk	3.88	0.90	0.09	0.07
Hill	1.20	1.06	1.036	0.80
Hutch	0.17	1.19	0.43	0.53
Jmcknley	0.152	1.02	0.078	0.075
Kelleher	0.117	1.81	0.55	0.20
Littell	0.018	0.29	0.096	0 02
Maio	0.23	0.36	1.042	0.99
Malcom	0.022	0.53	0.34	0.57
MacMillan	2.13	2.53	0.38	0.48
Morgan	0.215	1.13	0.17	0.19
Muchre	0.049	0.69	0.09	0.11
Park	0.572	2.72	0.57	0.68
Teates	0.160	2.06	0.20	0.25
Wiltse	0.35	1.39	0.16	0.15

3.4 Comparisons of Sub-populations

^{222}Rn cumulative radioactivity concentrations and mean transit times computed by the direct approach were compared among several sub-groups of subjects. These include males, females, fasted subjects and the two catagories of fed subjects. The cumulative radioactivity concentration values for the groups are presented in table 3.6 and the transit time values in

table 3.7. As before, the standard deviations are sample standard deviations.

One tailed T-tests[34] comparing these two parameters among the groups were carried out to test for differences. The results of these tests are summarized in tables 3.8 and 3.9. These tables give the precentage differences between pairs of subject groups for a given parameter and the probability that this difference is due to noise alone from the T-tests. Differences with P 0.10 are not assumed to be significant but may demonstrate trends which would emerge if a larger population were studied. More differences reached significance for the mean transit times than for the concentrations. This is again a reflection of the superior statistical quality of the transit time estimates.

Several features of these differences should be mentioned. First, females show higher cumulative radioactivity concentrations and corrispondingly longer transit times in most organs than males. This is probably due to the fact that overall body retention of inert gases is expected to be higher in females than in males due to the presence of more fatty tissue. The stomach in females shows a faster mean transit time while the stomach cumulative concentration difference does not reach significance. This is consistent with the fact that stomach emptying times in females are faster than those in males. Both of the fed groups (4hr and 1hr pre-study) show lower cumulative concentrations and transit times in most organs than the fasted group, the exceptions being stomach where the differences are equivocal and descending colon which shows the opposite behavior. These differences might be explained by the fact that the digestive system is more active in fed subjects and that there is still food waste ,which retains radioactivity, in the descending colon . However, one might expect that, in fasted subjects, cumulative radioactivity concentrations should be smaller than those in fed subjects because of the fast component of transit through the stomach and small intestine. This point requires further elucidation before a conclusive explanation can be offered.

The subjects who have eaten one hour before the study show higher cumulative concentrations and longer transit times than those who ate at four to six hours again indicating higer retention of ^{222}Rn except in ascending colon and descending colon, neither of the latter differences reaching significance.

Organ	fasted	fed (1hr)	fed (4-6hr)	males	females
stomach	2.24±2.60	3.14±2.34	1.65±0.71	2.49±2.00	2.87±2.63
small intestine	0.48±0.32	0.44±0.46	0.49±0.34	0.31±0.18	0.53±0.52
whole intestine	0.37±0.16	0.40±0.54	0.29±0.18	0.28±0.18	0.49±0.63
ascending colon	0.25±0.24	0.17±0.15	0.31±0.31	0.20±0.15	0.11±0.25
descending colon	0.20±0.09	0.43±0.36	0.20±0.07	0.18±0.08	0.13±0.36
liver	0.17±0.04	0.10±0.09	0.06±0.03	0.09±0.07	0.10±0.08
lung	0.30±0.07	0.19±0.16	0.12±0.06	0.17±0..15	0..18±0 .14
muscle	0.06±0.04	0.04±0.03	0.02±0.01	0.04±0 04	0.04±0.03
whole body	0.29±0.15	0.34±0.31	0.17±0.06	0.31±0.31	0.29±0.21

Table 3.6: Average Radon Cumulative Activity Concentrations in (μCi/cc)-hrs for Different Subject Sub-Groups

Table 3.7: Mean Transit Times (min) of Ingested ^{222}Rn for Different Subject Sub-Groups

Organ	fasted	fed (1hr)	fed (4-6hr)	males	females
stomach	37.9±18.6	48.1±21.32	37.8±10.4	39.6±15 0	49.0±24.0
small intestine	114.7±66.7	94.8±45.0	69.6±24.0	81.2±31.2	111.3±65.7
whole intestine	138.3±47.5	107.9±33.8	74.7±19.6	101.0±39.7	105.5±36.8
ascending colon	141.6±70.6	126.4±61.5	101.0±21.0	116.0±39.4	147.1±75.2
descending colon	167.8±62.2	144.0±88.5	81.6±4.8	103.2±21.9	171.0±92.2
liver	93.3±30.0	89.5±31.3	51.0±13.5	77.4±29.0	89.6±36 3
lung	93.3±30.0	89.5±31.3	51.0±13.5	77.4±29.0	89 6±36.3
muscle	180.6±42.7	137.0±53.5	85.4±11.3	138.3±59 7	133.3±50 3
whole body	105.8±24.6	78.9±24.1	55.6±35.4	73.6±21.8	87 4±31.5

Table 3.8: Percent differences and levels of significance by T test 0f cumulative radioactivity concentrations in sub groups

Organ	Fasted/Fed	Fasted/(5hr)	Fed/(5hr)	male/female
stomach	-25 (P .20)	[illegible] (P .25)	47 (P .03)	-13 (-)
small intestine	8 (-)	-2 (-)	-1 (-)	-42 (P .03)
whole intestine	7 (-)	22 (P .25)	28 (-)	-43 (P .10)
ascending colon	32 (P .25)	19 (-)	45 (P .25)	45 (P .25)
descending colon	-53 (P .10)	0.01 (-)	53 (P .10)	-58 (P .10)
liver	41 (P .05)	64 (P .01)	40 (P .10)	-10 (-)
lung	37 (P .02)	60 (P .01)	40 (P .12)	-10 (-)
muscle	50 (P .10)	67 (P .01)	50 (P .05)	0 (-)
whole body	15 (-)	41 (P .05)	50 (P .10)	6 (-)

Table 3.9: Mean transit time differences and levels of significance by T-Test among sub-groups

Organ	Fasted/Fed	Fasted/(5hr)	Fed/(5hr)	male/female
stomach	21 (P .10)	10 (-)	21 (P .10)	19 (P .10)
small intestine	17 (P .20)	39 (P .10)	26 (P .10)	-30 (P .05)
whole intestine	22 (P 0.10)	46 (P .01)	31 (P .03)	-4 (-)
ascending colon	14 (-)	11 (P .10)	20 (P .20)	-21 (P .12)
descending colon	14 (-)	51 (P .05)	43 (P 0.12)	-40 (P.10)
liver	4 (-)	45 (P .01)	43 (P .01)	-24 (P .10)
lung	4 (-)	45 (P .01)	43 (P .011)	-24 (P .10)
muscle	24 (P .05)	52 (P .01)	38 (P .01)	4 (-)
whole body	25(P .03)	20 (P .01)	29 (P .05)	-16 (P .08)

3.5 Results of Separate Analysis of Early Ingestion Data

A group of fifteen ingestion subjects were imaged at high frequency (typically 1 sec images for 2min and 5sec images thereafter) during the initial ten minutes after the beginning of ingestion. In nine of these subjects the expired air from the respiratory system was sampled during the same period. The purpose of these measurements was to determine if there were large transfers of radioactivity out of the body via routes such as direct transfer across the stomach wall.

The results presented in table 3.10 suggest that such loss does not occur. As can be seen in the table, when single exponental rate constants fit to the early stomach data are compared to the stomach rate constants from fits to the full data sets, in many cases the early rate constants are smaller than those from the complete data set reflecting the pulsitile nature of the stomach and in all other cases they are approximately the same as the rate constants from the full data sets. In the fasted subjects there was a rapid disapearance of radioactivity from the body ($k \sim 10hr^{-1}$) but the radioactivity can be traced through the small intestine to the lung. In all instances where the expired air was monitored, the appearance of radioactivity in the lung correlated with arrival of radioactivity at the liver via the small intestine. The whole body rate constants show the same type of behavior as the stomach rate constants again yielding no evidence of an early escape from the body of large amounts of radioactivity.

3.6 Results from Inhalation Studies

The purpose of the inhalation studies was to assess the effect of ^{222}Rn radioactivity reaching the various organs via recirculation from the lung. Recirculation occurs because a fraction of the radioactivity reaching the lung from the portal circulation of the liver is dissolved in arterial blood and carried throughout the body by blood flow. This phenominon is the primary source of radioactivity in the muscle and fat following ingestion of an inert gas[49][51].

Table 3.11 shows the rate constants for the clearance ^{222}Rn from various organs after inhalation of ^{222}Rn. These rate constants were obtained

by non-linear least squares fits to the inhalation organ curves. The model assumed was a sum of exponentals convolved with the experimentally measured arterial input function from the lung.

All of the major organs showed a very fast turnover of ^{222}Rn which was consistent with clearance by blood flow. In Table 3.11 organs have been grouped for simplicity. The data of table 3.11 for all organs other than muscle and fat may be interpreted as meaning that recirculation effects in high flow organs are negligible compared to direct effects of ingestion because of the rapid clearance of radioactivity due to blood flow. In fat and resting muscle however the accumulated radioactivity is significant because of slow clearance by blood flow. Multiple fat and muscle samples were taken in each individual. Many of these samples were slower components of fits to the organ curves. The mildly obese subjects in the inhalation group usually had a fat component in each abdominal curve and most females showed distinct fat deposits in the hips and breasts in the image data. Muscle samples were reliably obtained from the abdominal curves of lean males as well as from hip and thigh muscle when possible. The rate constants for muscle and fat determined from the inhalation studies agree well with those obtained from the ingestion studies.

Muscle and fat cumulative radioactivity concentrations for ingestion were computed from the inhalation single exponential rate constants and amplitudes. The amplitudes were put on an absolute scale by using the average scintillation camera calibration factor from table 2.3 (methods section). The input function used for this computation is made up of the two fast components from the ingestion lung curves multiplied by the air-blood partition coefficient for ^{222}Rn ($\lambda = 0.187$). The result of this calculation is compared to the direct and analytic esitmates of muscle and fat cumulative ^{222}Rn concentrations computed from the ingestion data in Table 3.12. The inhalation fat estimate agrees fairly well with the direct ingestion computation but is low compared to the ingestion analytic estimate by a factor of three. The inhalation muscle estimate is about a factor of two lower than either of the ingestion results. A possible explanation for these discrepancies is that, since the rate constants are very similar, many of the muscle and fat samples used in the ingestion computations may have been contaminated with signal from digestive organs producing artifically high curve amplitudes. Another possible explanation is that the radioactivity is more uniformly distributed in the body as a result of inhalation than

Table 3.10: Early Ingestion Rate Constants for Stomach and Whole Body

subject	sample time (sec)	early stomach rate (hr^{-1})	stomach rate from 1 min data (hr^{-1})	early whole body rate (hr^{-1})	fastest whole body rate from 1 min data (hr^{-1})	air sampling
ayer	1	0.12	0.85	0.013	0.57	-
arrol	1	1.83	3.48	1.40	3.89	-
cline	1	0.13	2.97	.009	2.07	-
elinden	1	1.20	1.24	0.88	0.92	-
gallop	2	0.004	1.82	0.008	.71	-
gmckinley	1	1.17	0.89	1.99	0.66	-
hand	1	3.5	2.07	1.55	6.35	-
hill	1	11.4	9.77	2.93	6.63	-
hutchins	1	2.0	1.70	0 45	3.68	-
kelleher	1	7.2	6.99	1.57	3.25	-
maio	1	4.1	4.33	.64	5.77	8 5.77-
malcom	2	0.82	9.28	1.17	1.96	-
monroe	2	2.0	5.78	1.21	3.68	-
park	2	1.45	2.72	1.42	2.25	-
tantes	1	0.20	2.84	0.02	2.29	-

Table 3.11: Average Organ Rate Constants from Inhalation Studies

organ	N	Average Rate Constant (hr^{-1})
liver, spleen, kidney	9	31.9±13.8
stomach, small intestine	9	36.8±22.0
ascending colon, descending colon	5	9.88±3.55
muscle	27	0.41±0.12
fat	14	0.115±0.037

it is for ingestion, causing the calibration factors to undercompensate for absorption and scatter in the inhalation case. A separate calibration for the inhalation studies could possibly remedy this.

Table 3.12: Comparison of Muscle and Fat results from Inhalation and Injestion Studies

parameter	ingestion muscle	inhalation muscle	ingestion fat	inhalation fat
amplitude (μCi/cc)	0.042	0.052	0.021	0.027
rate constant (hr^{-1})	0.442	0.437	0.092	0.087
Analytic cumulative concentration (μCi/cc)-hr	0019	0.0107	0 099	0.0343
Direct cumulative concentration (μCi/cc)-hr	0.026	-	0.038	-

Chapter 4

CONCLUSIONS

A database consisting of Quantitative radioactivity concentrations per ingested mCi of ^{222}Rn has been produced from measured data in thirty subjects. ^{133}Xe ingestion kinetic curves were measured in each subject for the organs of the digestive system, muscle, fat, lung and whole body. From these data, kinetic curves of radioactivity concentration per mCi of ^{222}Rn ingested for the five radon daughters have also been produced. These data are presented in graphical and tabular forms in the appendices of this report. They may be used as a basis for dosimetry calculations and kinetic studies by other investigators. In addition, a database of ^{222}Rn kinetic curves at high sampling frequency (1 sec) and a data base of ^{222}Rn relative concentrations after inhalation of that gas have also been produced. These latter databases are not included in the appendices but are available along with the primary data base on industry standard magnetic tape.

Quantitative cumulative radioactivity concentrations for ^{222}Rn and its daughters have been computed by direct manipulation of the kinetic curves. For ^{222}Rn, these concentrations vary from a high of 2.66 μCi/cc per mCi ingested for the stomach through values in the range of 0.30 μCi/cc per mCi ingested for the intestinal system and whole body to a low of 0.038 and 0.026 μCi/cc per mCi ingested for muscle and fat respectively (table 3.1). The cumulative concentrations of radon daughters, presented in table 3.1 , are in the one to ten nanocurie range for all daughters except the long lived ^{210}Pb for which the stomach concentration is 99.15 nCi/cc. These cumulative concentration data constitute a body of information for radon dosimetry computations.

Fits of compartmental models to the ^{222}Rn kinetic curves confirm the results of the direct computations and also form a useful data set for dosimetry studies and additional, more detailed, modeling studies. The average kinetic rate constants over the subject population are given in table 3.3.

Organ Mean transit times for ^{222}Rn after ingestion have also been computed. These data indicate that the majority of the radioactivity is cleared from most organs within ten hours. Exceptions to this are fat and to some degree muscle. Measurements in five subjects at times greater than twenty four hours post ingestion indicate that no ^{133}Xe radioactivity was present in any individual at the 0.75μCi level (table 3.2).

The results of high frequency measurements at early times post-ingestion indicate that there is no rapid escape of radioactivity from the body by routes other than through the intestines. Although a fast component was observed in fasted subjects, it was consistent with a fast component seen in the analysis of the one minute data extending over the entire imaging period and it correlated with radioactivity transiting the small intestine at early times.

Inhalation measurements confirm that the turnover of ^{222}Rn radioactivity recirculated from the lungs is rapid in the major organs and does not, therefore, contribute significantly to cumulative radioactivities. Estimates of rate constants for muscle and fat from the inhalation studies agree well with those from the ingestion studies. However, estimates of muscle and fat tissue concentration using the inhalation data vary by up to a factor of two with respect to those computed directly from the ingestion data. These differences are most likely due to technical factors such as the inappropriate use of ingestion calibration factors for the inhalation studies.

Differences between the male and female sub-populations were observed as were differences between subpopulations having different digestive status. Females appear to have higher cumulative radioactivity concentrations and longer mean transit times than males. Fasted subjects have higher concentrations and longer transits than fed subjects in general and those fed one hour before the study have higher values of these parameters than those fed five hours before the study. Differences among the digestive status groups reached significance in fewer instances than those in the male/female groups possibly because of small sample sizes. The digestive group differences mentioned here are not conclusive for this reason.

The work completed in this project can be extended and improved in

several ways. Organ radiation doses can be generated for ^{222}Rn and its daughters directly from the cumulative concentration data. The kinetic curves can be used as a basis for attempting to model the digestive system in more detail, to model the migration of the daughters within the body and to take into account ^{222}Rn bound to food in the digestive system. . The inhalation data could be used to generate a separate dosimetry data base for ^{222}Rn inhalation, although more subject measurements might be needed first. Further work could be done to improve the fits of convolved models to the organs of the lower digestive system since this presented a source of difficulty in the present investigation.

Also, the experimental preparation developed in the course of this work could be used for more extensive studies of the effects of digestive status and different types of dietary intake on ^{222}Rn kinetics.

Bibliography

[1] I O Andersson, I Nilsson, and A B Atomenergi. Exposure following ingestion of water containing radon-222. IAEA, Sweden, 1964.

[2] H O Anger. *Instrumentation in Nuclear Medicine*, chapter Radioisiotope cameras, page 486. Volume , Academic Press, New York, 1967.

[3] K Aurand and A Schraub. Uber das verhalten des radons und seiner folgeprodukte im organismus bei peroraler verabreichung. *Strahlentherapie*, 94:272–286, 1954.

[4] G Bell and M Harper. Measurement of local blood flow in the renal cortex from the clearance of ^{85}Kr. *J Surgical Res*, 5(9):382–386, 1965.

[5] Snyder W S, editor. *Ingested radon as a source of human radiation exposure*, Proceedings of the first international congress of radiation protection, Pergamon Press, Oxford and New York, 1968.

[6] P Celsis, T Goldman, L Henriksen, and N A Lassen. A method for calculating regional cerebral blood flow from emission computed tomography of inert gas concentrations. *Journal of Computer Assisted Tomography*, 5(5):641–645, 1981.

[7] R Y Chen, F C Fan, S Kim, and et al. Tissue blood partition coefficient for xenon: temperature and hematosit dependence. *J Appl Physiol Resp Enviorn Exerc Phys*, 49:178–183, 1980.

[8] W Cohn. Toxicity of inhaled or ingested radioactive products. *Health Physics*, 38:1015–1020, 1980.

[9] H Conn. Equilibrium distribution of radioxenon in tissue: xenon hemoglobin association curve. *J Applied Physiol*, 16(6):1065–1070, 1961.

[10] J A Correia, R H Ackerman, and N A Alpert. *Textbook of Nuclear Medicine*, chapter Cerebral Blood Flow Studies Using Xenon-133. Volume I, Lea and Febiger, Philadelphia, 1984.

[11] J A Correia, R H Ackerman, F Buonanno, and et al . A portable device for the measurement of rCBF in the icu and or using CdTe detectors and a fourier transform based data analysis. *IEEE Trans Nucl Sci*, 2:1979 , 1981.

[12] S Davis, R H Ackerman, J A Correia, and et al . Cerebral blood flow and reactivity in stroke age normal controls. *J Cereb Blood-flow Metab (Suppl)*, 1:547 , 1981.

[13] W Dobeln and B Lindel. Some aspects of radon contamination following ingestion. *Arkiv for Fys*, 27:32:531–572, 1964.

[14] M Ercan. Solubility coefficient of ^{133}Xe in water, saline, dog blood and organs. *Intern J of Applied Radiation and Isotopes*, 30:757–759, 1979.

[15] S Genna, S Pang, and A Smith. Digital scintigraphy:principles, design and performance. *J Nucl Med*, 22:365, 1981.

[16] M Guter. Gas versus liquid:the question of solubility. *Prog nucl Med*, 5:1–34, 1978.

[17] J H Harley, E Jetter, and N Nelson. *Elimination of radon from the body*. Volume , Health and Safety Laboratory, United States Atomic Energy Commission, New York, 1958.

[18] W D Heiss, I Podreka, and A Roszuczky. Regional cerebral blood flow measurement with a scintilation camera after intracarotid and iv injection of xenon. *Cerebral Vascular Disease*, 2:25, 1979.

[19] J B Hursh, D A Morken, P D Thomas, and A Lovaas. The fate of radon ingested by man. *Health Physics*, 11:465–476, 1965.

[20] W H Ibister, P F Schofield, and H B Torrance. Measurement of the solubility of Xe^{133}in blood and human brain. *Phys Med Biol*, 10(2):243-250, 1965.

[21] W Kirk and D Morken. In-vivo kinetic behaviour and whole body partitian coefficients for ^{85}kr in guinea pigs. *Health Physics*, 28:263-273, 1975.

[22] W Kirk and P Parish. In-vivo solubility of ^{85}kr in guinea pig tissues. *Health Physics*, 28:249-261, 1975.

[23] J T Kuikka, M T Keinanen, E M R Suolinna, and E O H Solin. Effect of instantaneous partition coefficient of xenon on the organ, the blood flow measurements. *Phys Med Biol*, 25(4):735-739, 1980.

[24] T Lahtinen, P Karjalainen, A Uuananen, R Lahtinen, and E Alhava. The partition coefficients of ^{133}Xe between human blood bone. *Phys Med Biol*, 6(1):125-132, 1981.

[25] M O Leach and C M J Bell. Blood flow measurements and the partition coefficient of ^{133}Xe in bone. *Phys Med Biol*, 27:1401-1403, 1982.

[26] C M Lederer, J M Hollander, and I Perlman. *Table of Isotopes*. Volume , John Wiley and Sons, New York, London and Sydney, 1967.

[27] D P Leiberman, R T Mathie, A M Harper, and L H Blumgart. The hepatic arterial and portal venous circulations of the liver studied with a krypton-85 clearance technique. *Journal of Surgical Research*, 25:154-162, 1978.

[28] A Leo, C Hansch, and D Elkins. Partition coefficients and their uses. *Chemical Reviews*, 71:525-616, 1971.

[29] B L Mallet and N Veall. Measurement of regional cerebral clearance rates in man using Xenon-133. *Clin Sci*, 29:179 , 1965.

[30] D W Marquardt. An algorithm for least squares estimation of nonlinear parameters. *J Soc Indust Appl Math*, 11:431, 1963.

[31] R T Mathie, D P Leiberman, A M Harper, and L H Blumgart. The solubility of ^{85}krypton in the regenerated, liver of the rat. *Br J Exp Path*, 58:231, 1977.

[32] J Merory, Thomas D J, P R Humphrey, and et al . Cerebral blood flow after surgery for recent subarachnoid hemorrhage. *J Neurol Neurosurg Psychiatry*, 43:214 , 1980.

[33] M Meyer. Technique for measurement of inert gases in liquids by gas chromatography. *Pflugers, Arch*, 375:161–165, 1978.

[34] S L Meyer. *Data analysis for scientists and engineers*. Volume , John Wiley and Sons, Inc, 1975.

[35] N G Moody, W Paul, and M K G Joy. A survey of medical gamma-ray cameras. IEEE, 1970.

[36] A V Nero, M B Schwehr, W W Nazaroff, and K L Revzan. Distribution of airborne radon-222 concentrations in u.s. homes. *Science*, 234:992–997, 1986.

[37] B Norrving, B Nilsson, and Risberg J . RCBF in patients with carotid occlusion: resting and hypocapnic flow related to collateral pattern. *Stroke*, 15:155 , 1983.

[38] E Nussbaum. Radon solubility in body tissues and fatty acids. In , editor, *AEC Research and Development Report UR-503*, University of Rocheser, 1957.

[39] M D O'Brien and N Veal. Partition coefficients between various brain tumors and blood for ^{133}Xe. *Phys Med Biol*, 19:472–475, 1974.

[40] W D Obrist, H K Thompson, H S Wang, and et al. Regional cerebral blood flow estimated by ^{133}Xe inhalation. *Stroke*, 6:245, 1975.

[41] Y Ohta, A Amos, and L E Farhi. Solubility and partition coefficients for gases in rabbit brain and blood. *J Appl Physiol Resp Environ Exercise Physiol*, 46(6):1169–1170, 1979.

[42] J A Patton, F D Rollo, Brill, and A B. Recent advances in nuclear medicine instrumentation. *IEEE Trans Nucl Sci*, 27:1066, 1980.

[43] A E Posewitz. *Simulation and modeling analysis of ingested xenon data in human volunteers, Masters Thesis*. Master's thesis, University of Lowell, 1986.

[44] H Prichard and T Gesell. An estimate of population exposures due to radon in public water supplies in the area of houston, texas. *Health Physics*, 41(4):599-606, 1981.

[45] Task Group 4 (Radon and Daughters). *Evaluation of occupational and environmental exposures to radon and radon daughters in the United States*. Volume , National Council on Radiation Protection and Measurements, Bethesda, Maryland, 1984.

[46] T F Richard, Foun-Chung Fan Chen, Syngcuk Kim, Kung-Ming J, Shunichi Usami, and Shu Chien. Tissue blood partition coefficient for xenon: temperature and hematocrit dependence. *J Applied Physiol Resp Environ Exerc Physiol*, 49:178-183, 1980.

[47] W S Snyder, M J Cook, L R Karhausen, E S Nasset, G P Howells, and I H Tipton. *Report of the task group on reference man*. Volume Publication 23, Pergamon Press, Oxford, New York, Toronto, Sydney, Paris and Frankfurt, 1975.

[48] M Suomela and H Kahlos. Studies on the elimination rate and the radiation exposure following ingestion of ^{222}Rn rich water. *Health Physics*, 23:641-652, 1972.

[49] C A Tobias, H B Jones, J H Lawrence, and J G Hamilton. The uptake and elimination of krypton and other inert gases by the human body. *J Clin Invest*, 28:1375-1385, 1949.

[50] A G Waltz, A R Wanek, and R E Anderson. Comparison of analytic methods for calculation of cbf. *J Nucl Med*, 13:66 , 1972.

[51] P K Weathersby and L D Homer. Solubility of inert gases in biological fluids and tissues: a review. *Undersea Biomed Research*, 7(4):277-296, 1980.

[52] S Yeh and R Peterson. Solubility of kryton and xenon in blood, protein solutions, and tissue homogenates. *J Appl Physiol*, 20(5):1041-1047, 1965.

[53] I H Young and P D Wagner. Solubility of inert gases in homogenates of canine lung tissue. *J Applied Physiol:Respiratory Environ. Exercise, Physiol*, 46:1207-1210, 1979.

APPENDIX A

Quantitative ^{222}Rn and Daughter Concentrations vs Time in Graphical Form

The following graphs present the quantitative radioactivity *vs* time curves for ^{222}Rn and its daughters for the ingestion subjects studied in this project. The ^{222}Rn and the daughter curves both have units of μCi/cc. The order of presentaiton is such that the ^{222}Rn curves for all subjects are given first then all subject curves for each daughter are sucessively presented.

This data is available in tabular form (Appendix B) and on industry standard magnetic tape along with subroutines to read and manipulate it in FORTRAN 77.

AHERN
XE INGESTION
RADON

SM INTEST

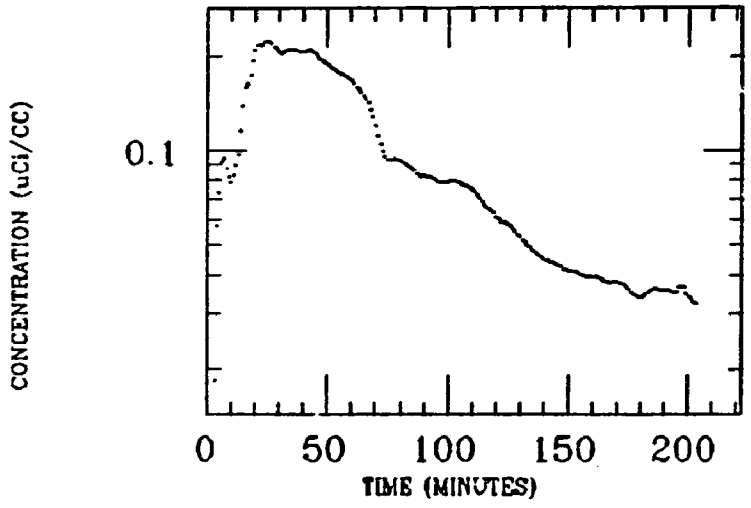

STOMACH

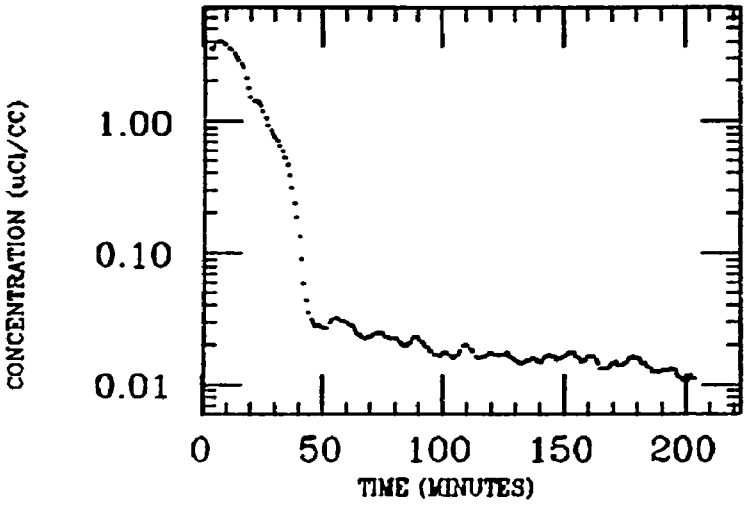

WH FIELD

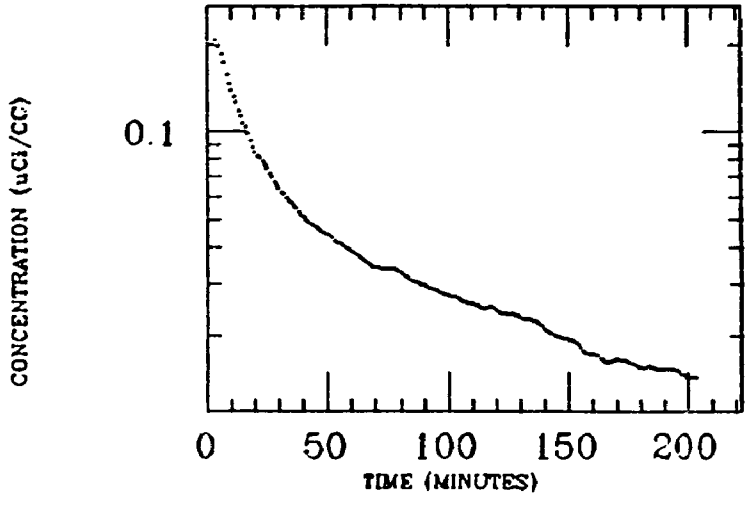

WH INTEST

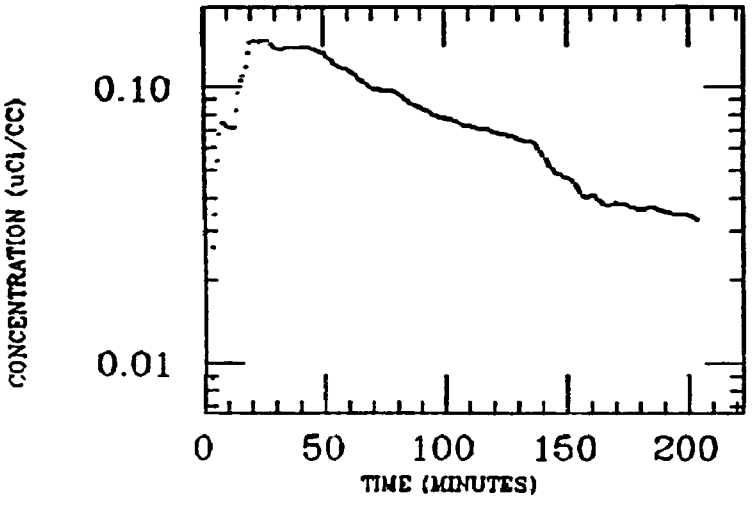

AHERN
XE INGESTION
RADON

ASC COLON

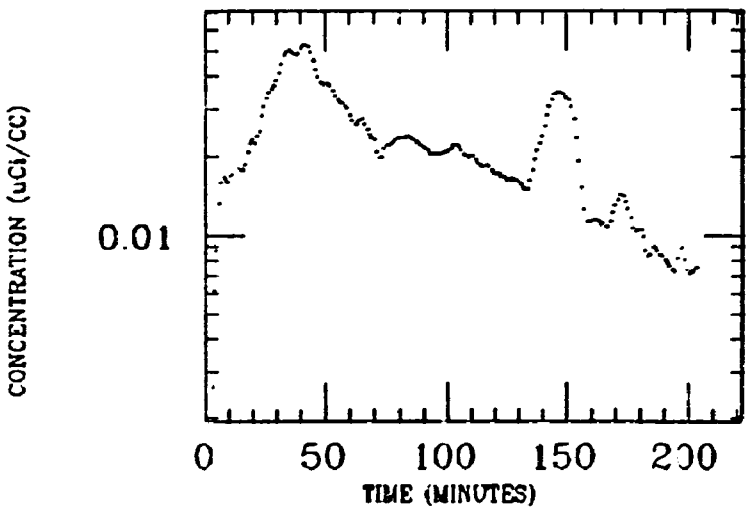

HIP

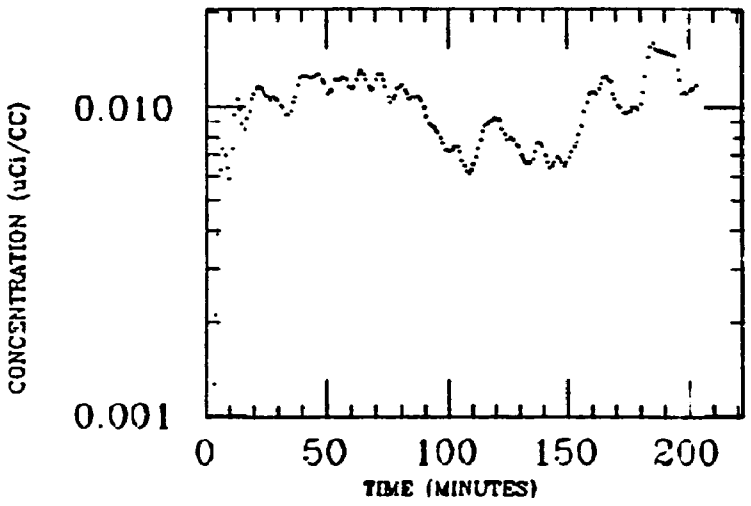

LIVER

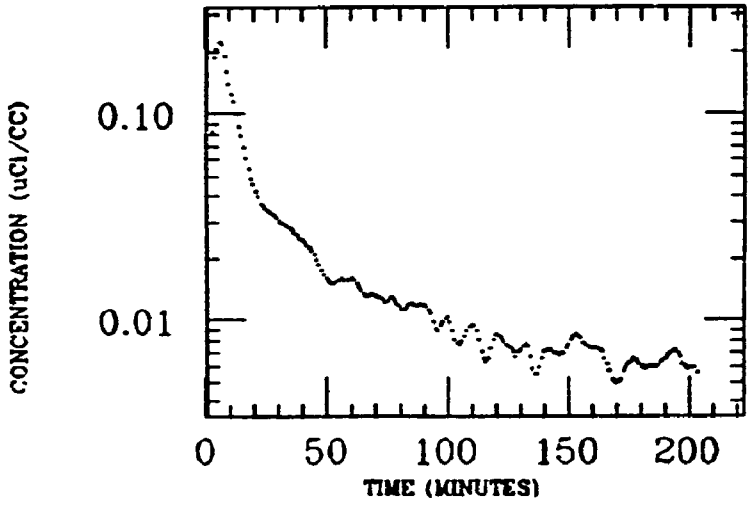

ARROL
XE INGESTION
RADON

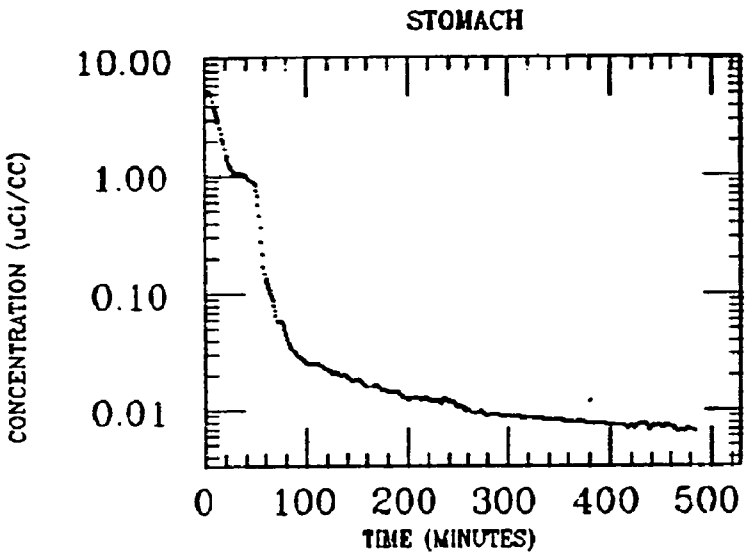

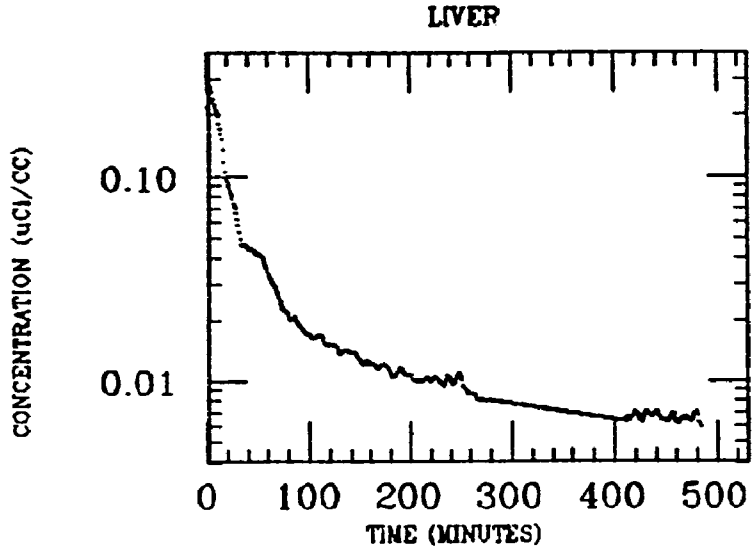

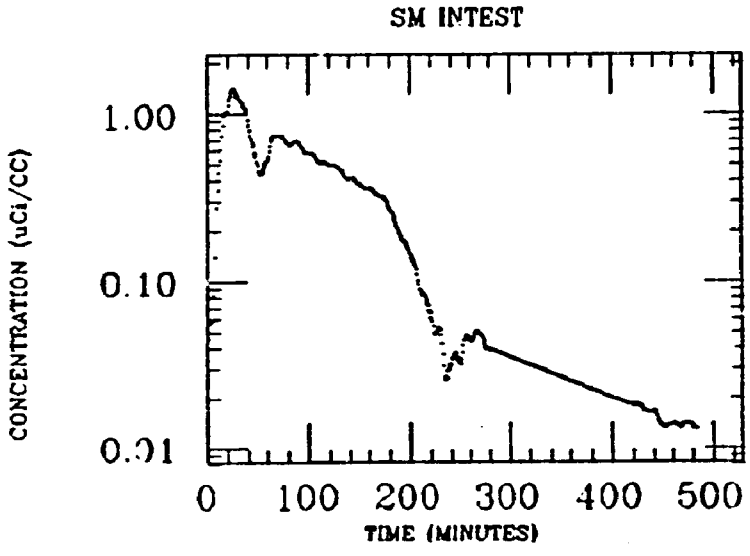

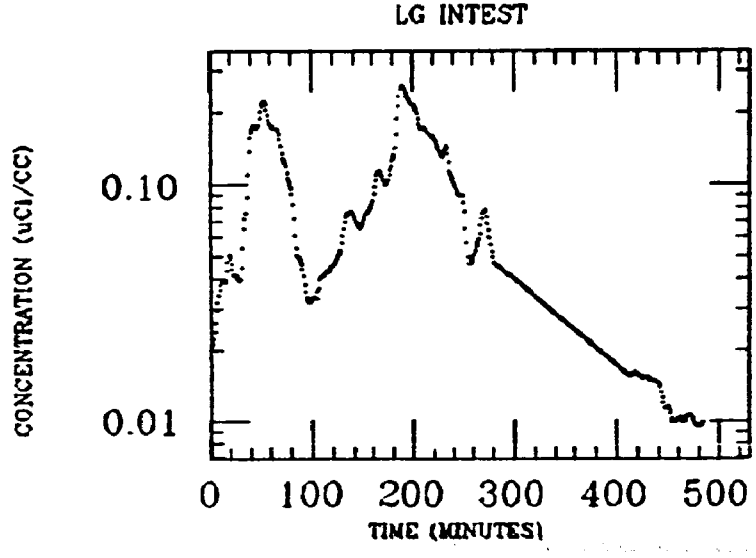

ARROL
XE INGESTION
RADON

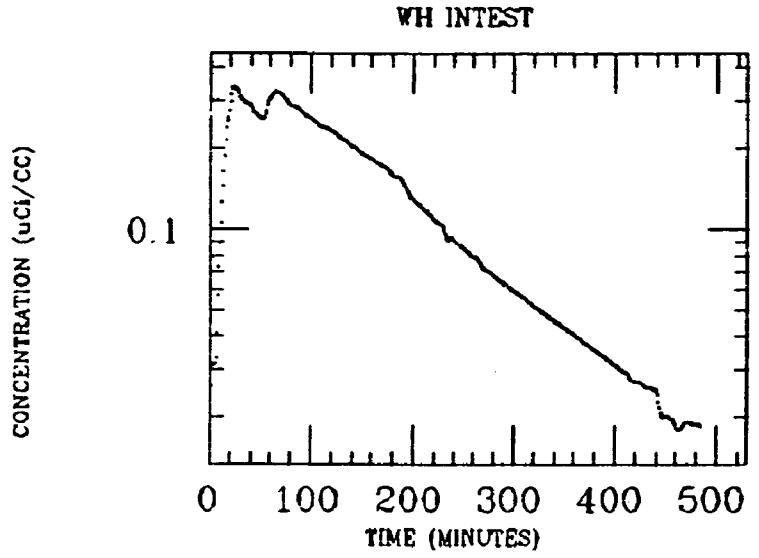

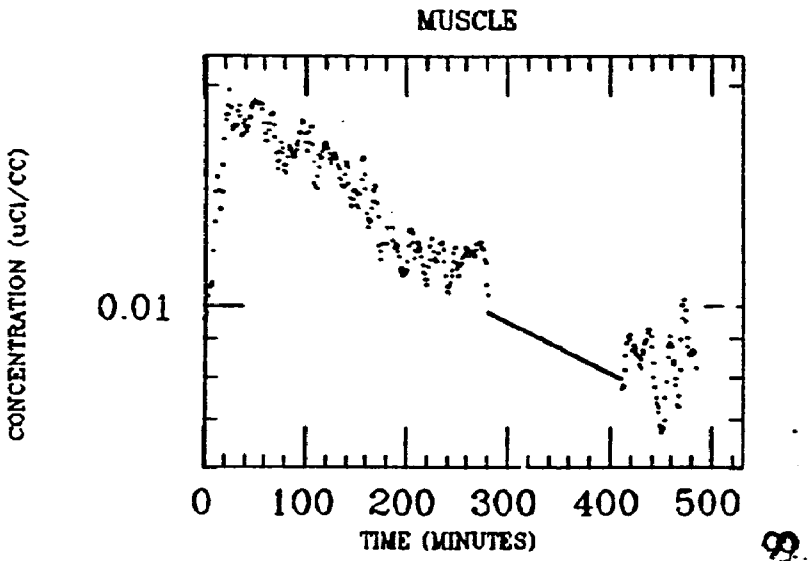

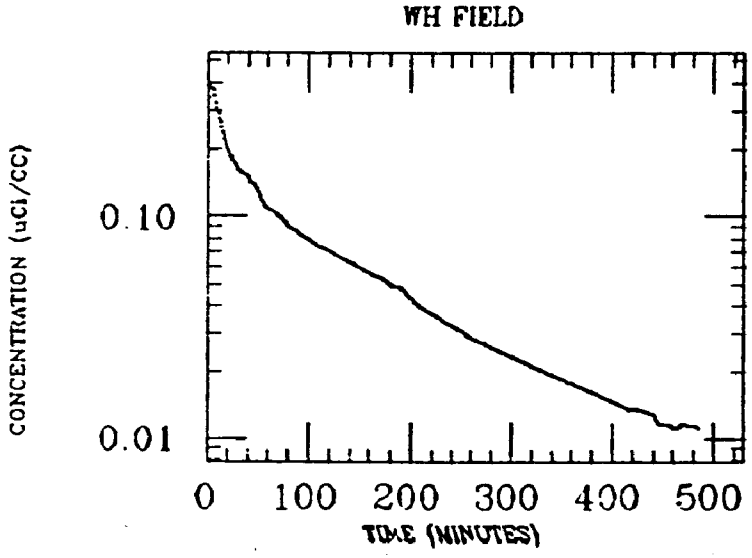

AYER
XE INGESTION
RADON

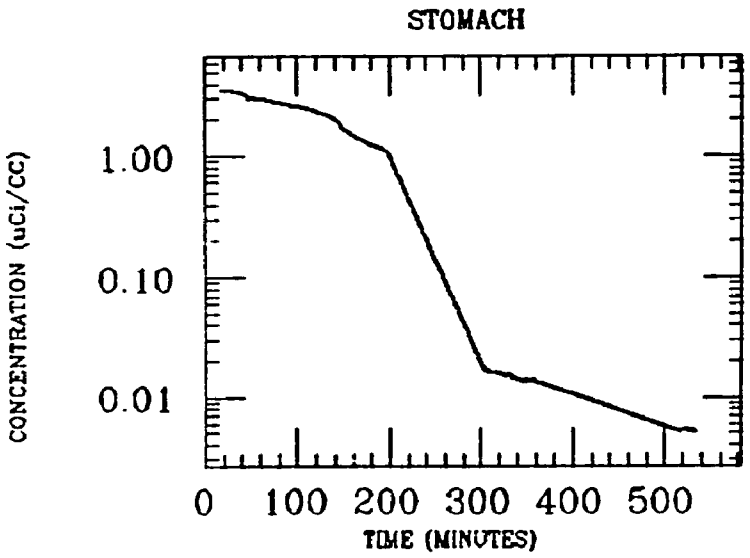

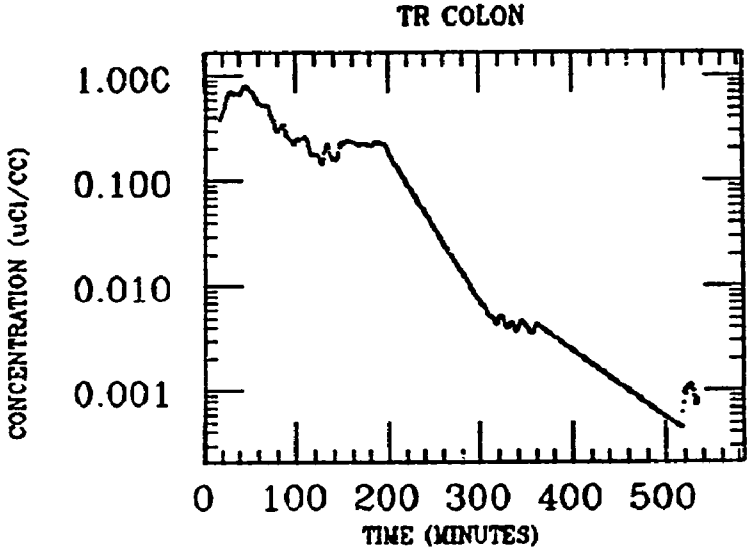

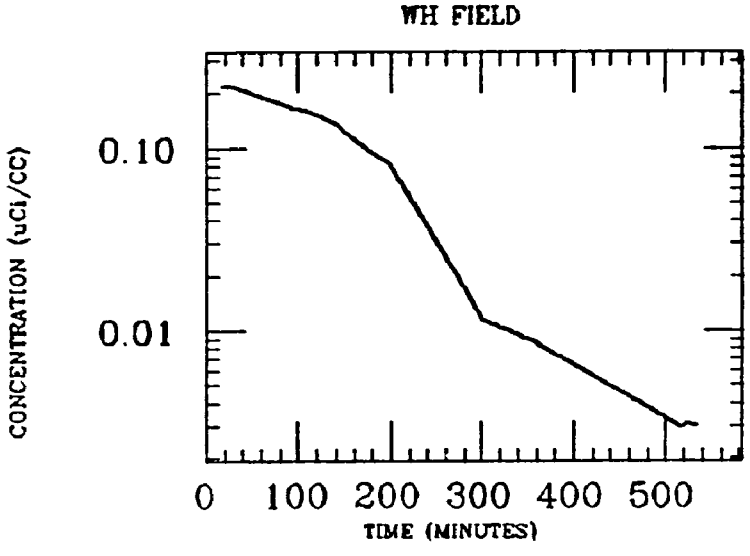

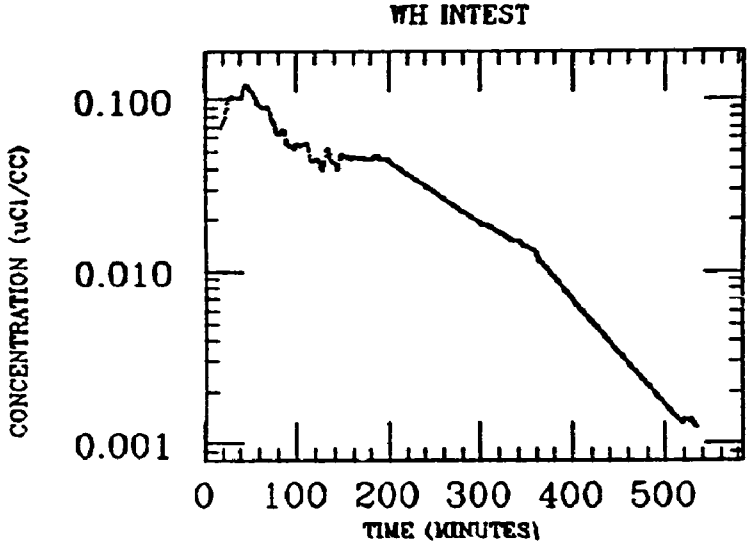

AYER
XE INGESTION
RADON

ASC COLON

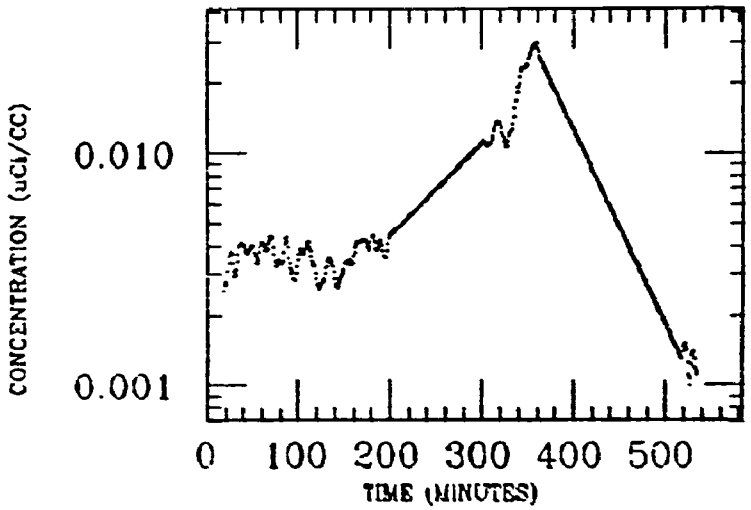

DES COLON

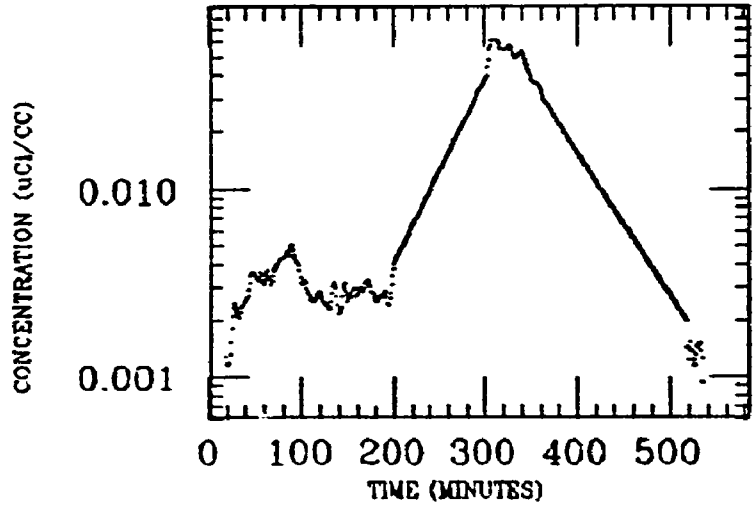

LIVER

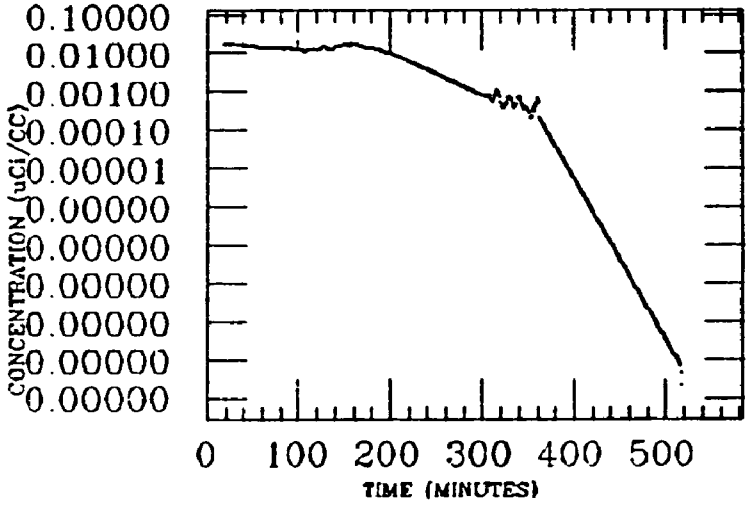

SM INTEST

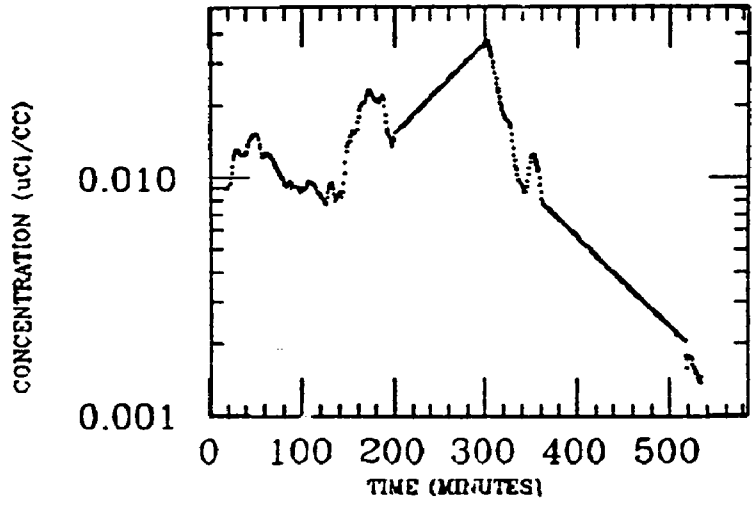

60

AYER

XE INGESTION

RADON

STOMACH

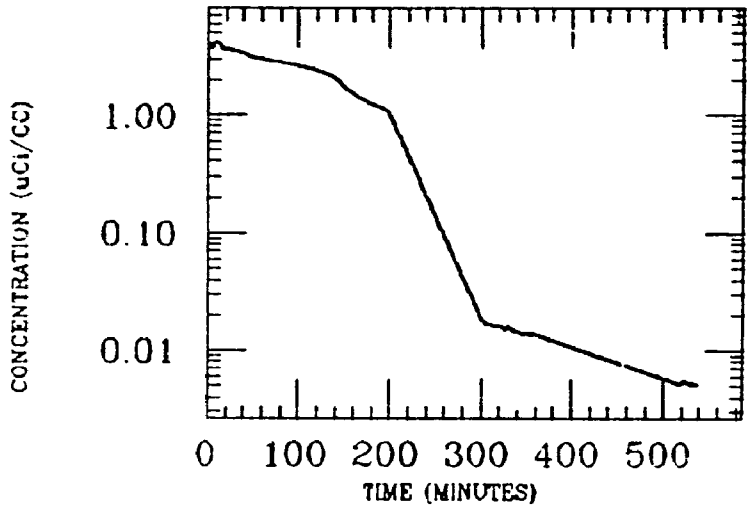

LIVER

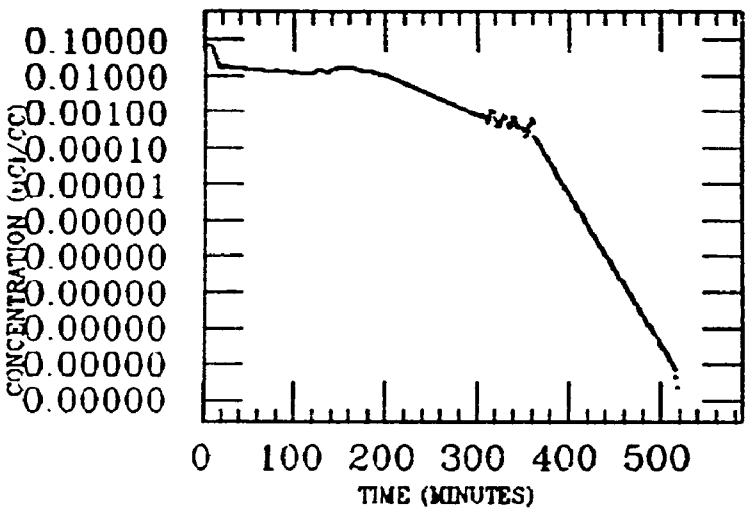

WH FIELD

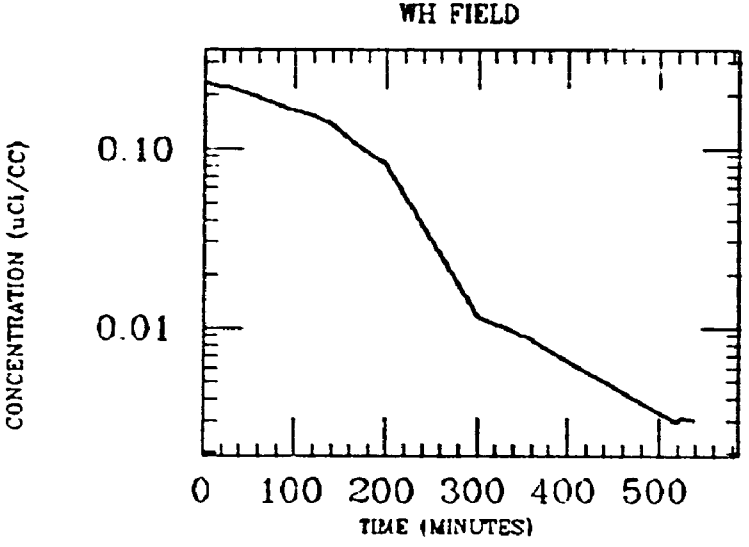

BROCK
XE INGESTION
RADON

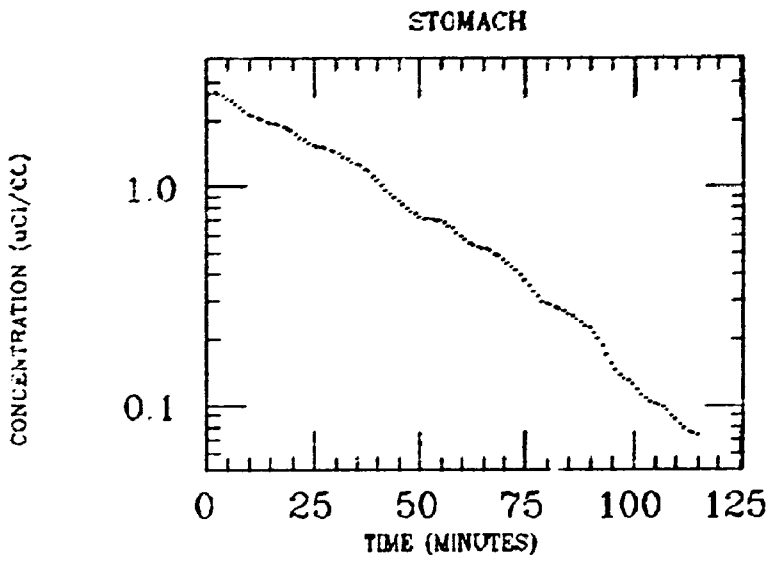

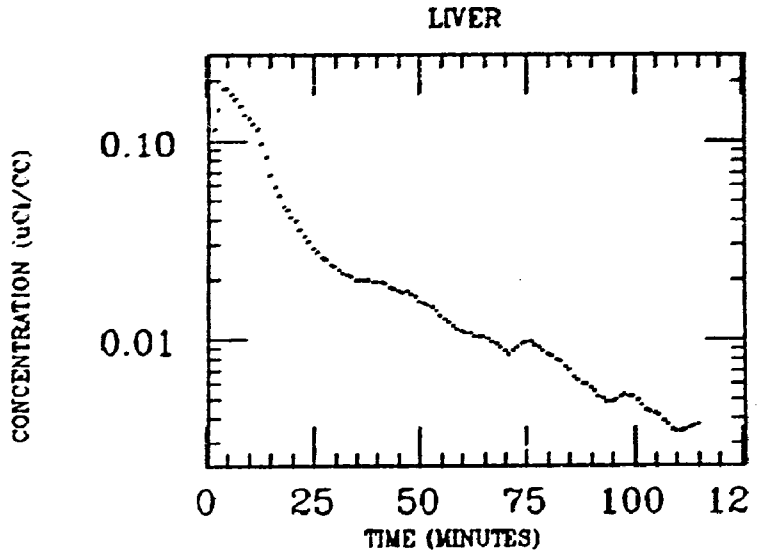

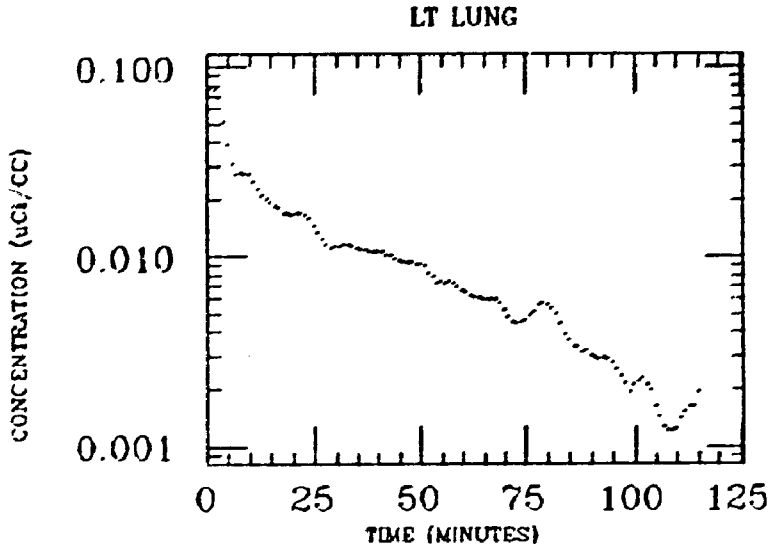

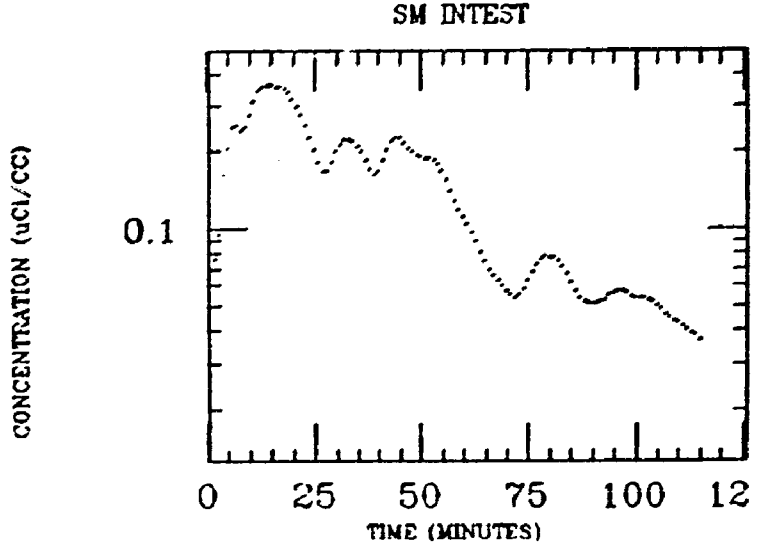

BROCK
XE INGESTION
RADON

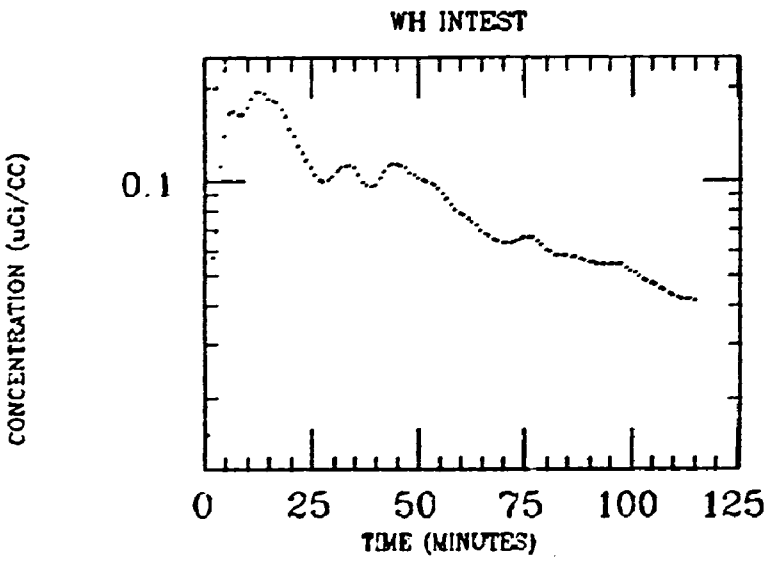

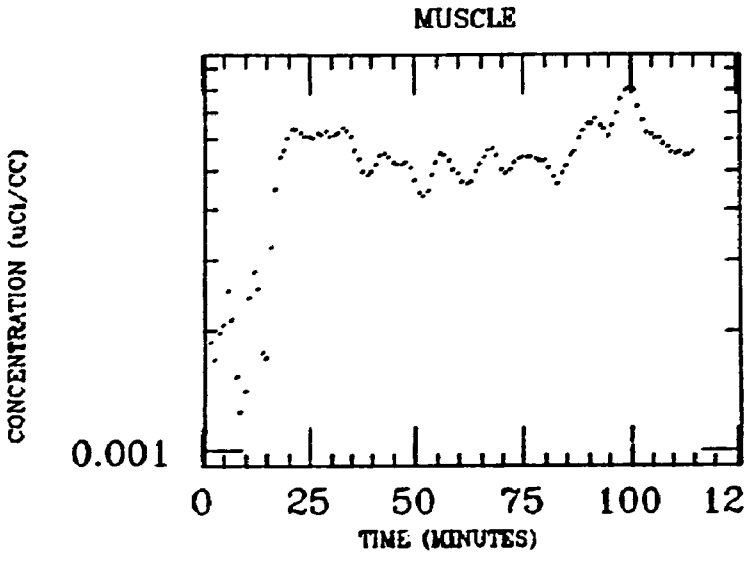

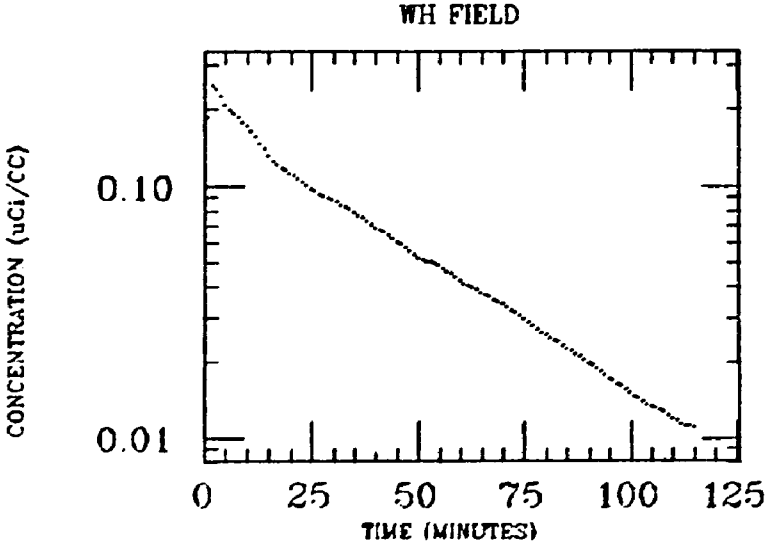

BYRNE
XE INGESTION
RADON

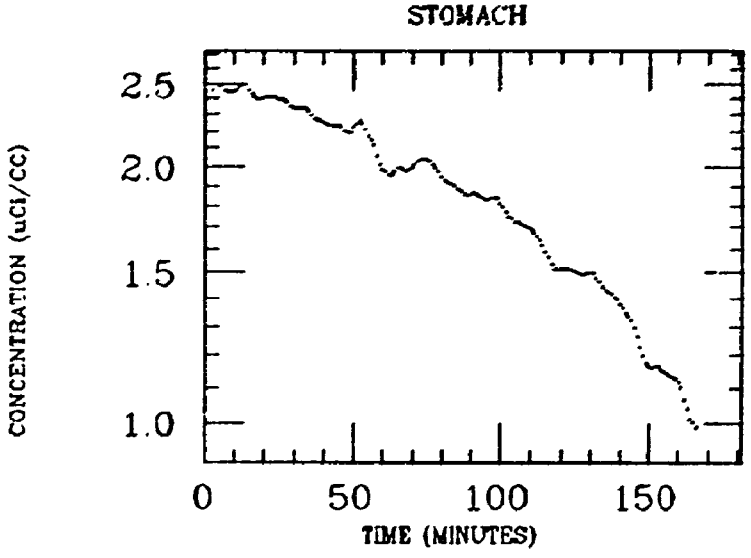

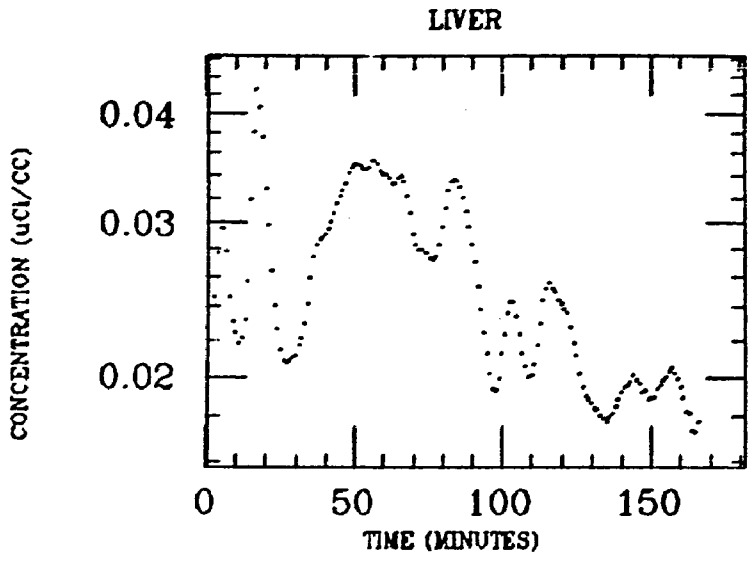

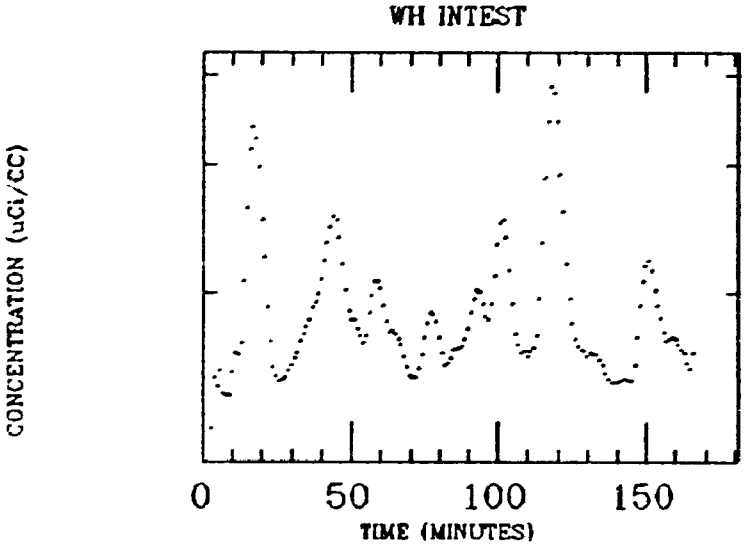

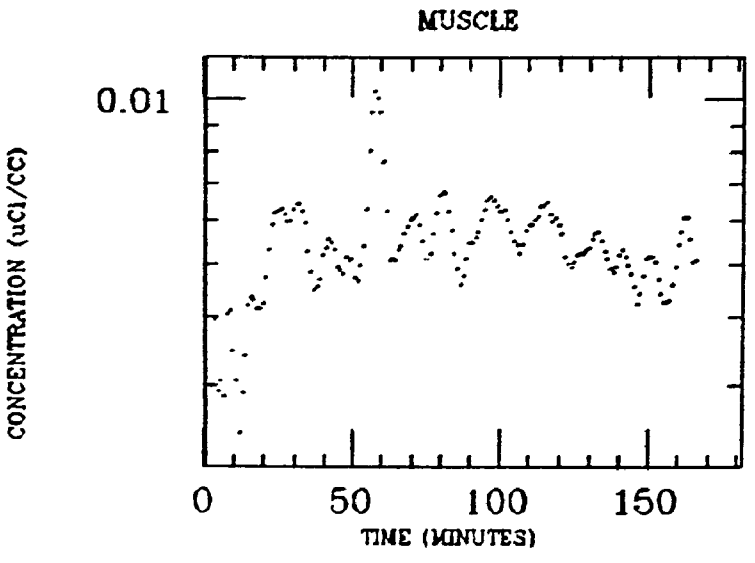

BYRNE
XE INGESTION
RADON

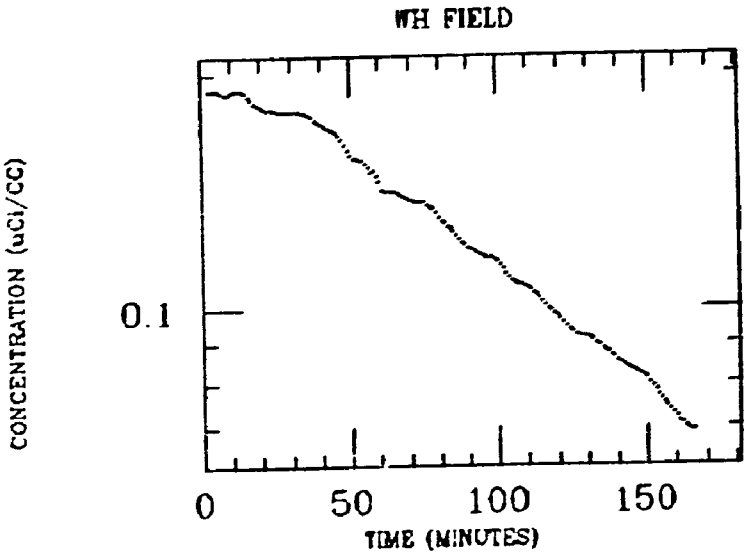

CLINE
XE INGESTION
RADON

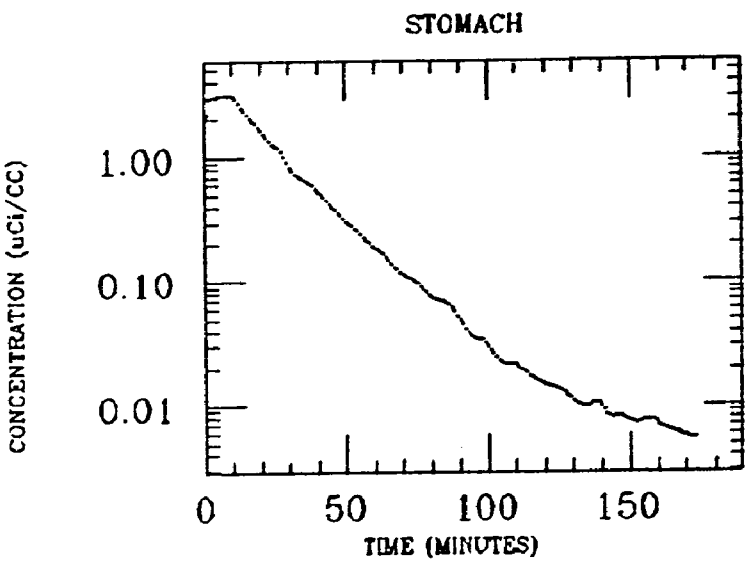

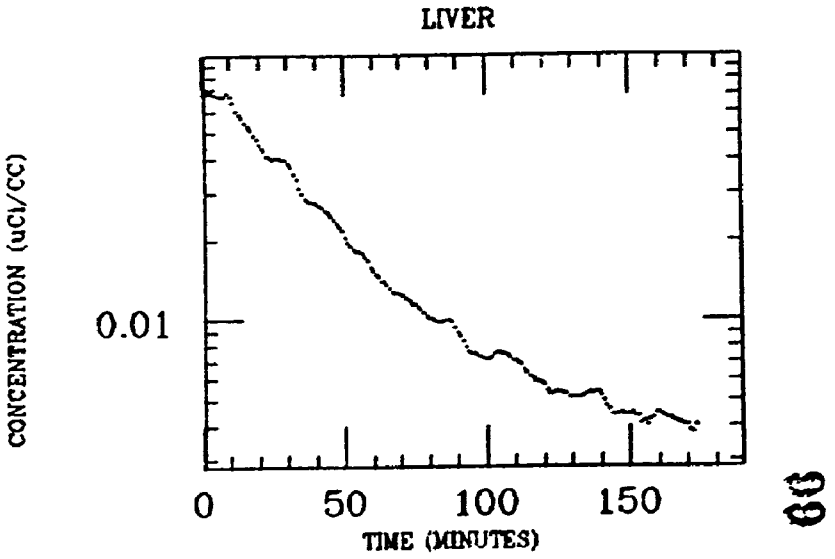

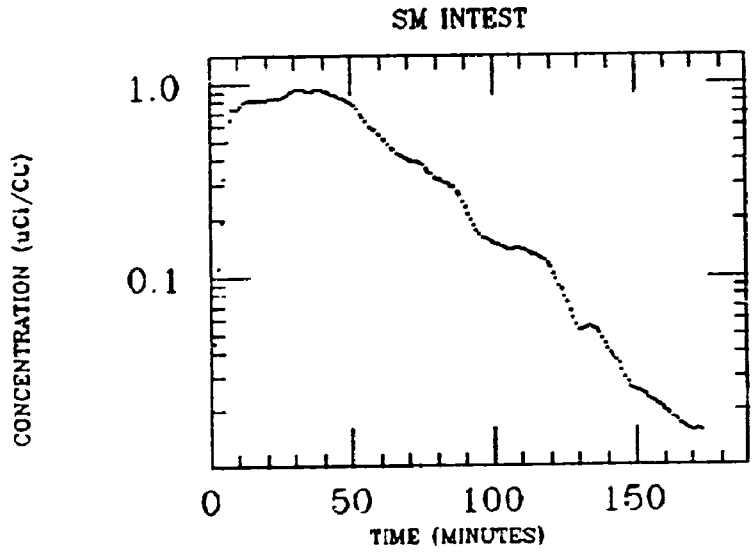

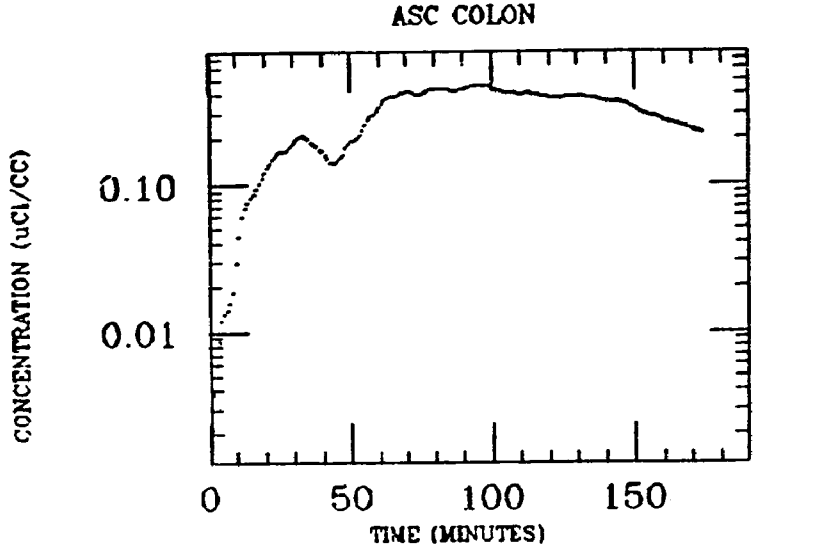

CLINE
XE INGESTION
RADON

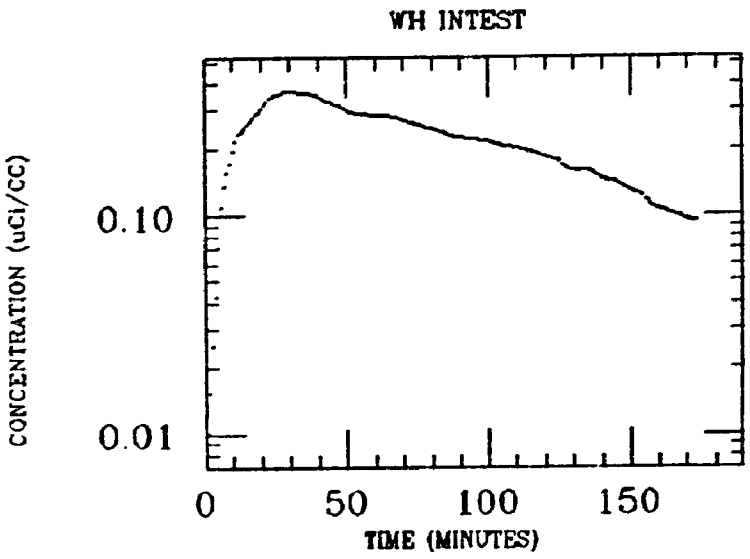

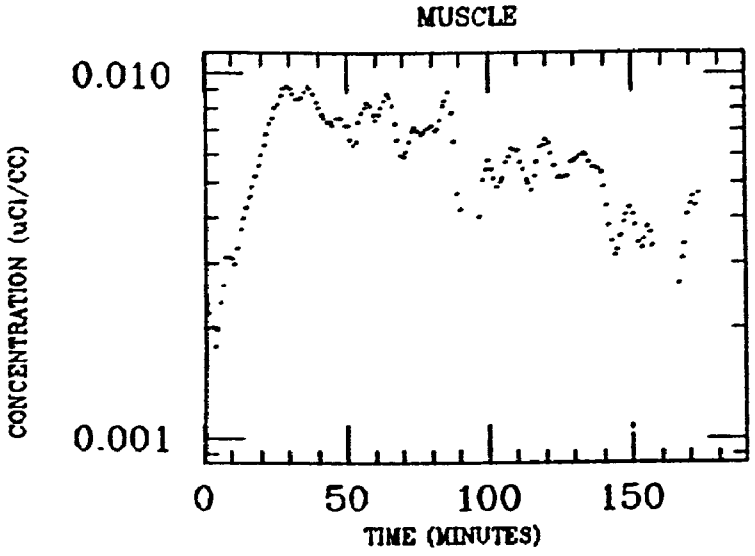

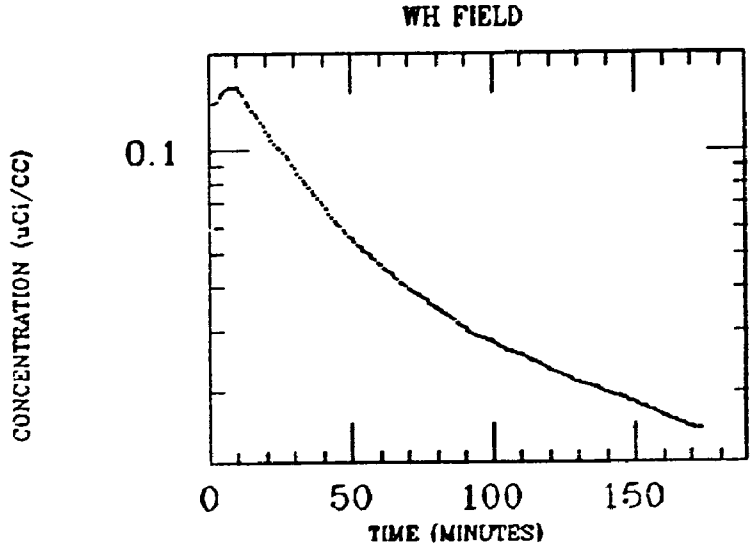

ELMDEN
XE INGESTION
RADON

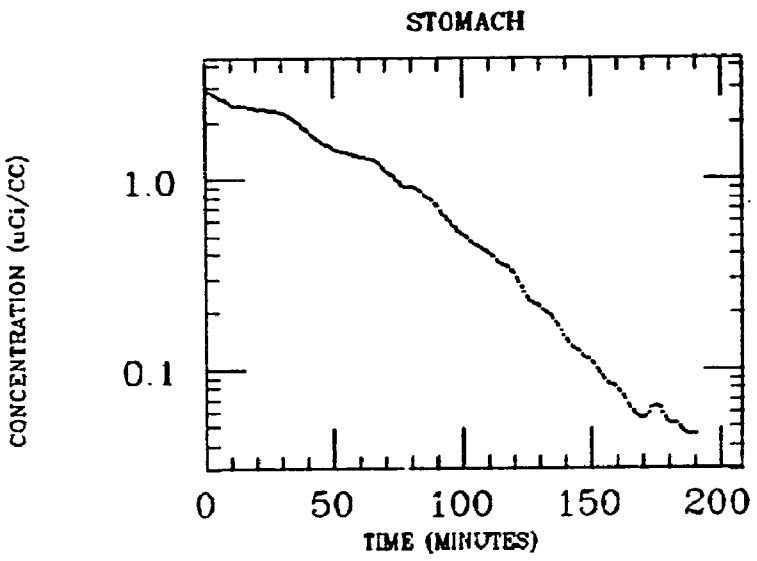

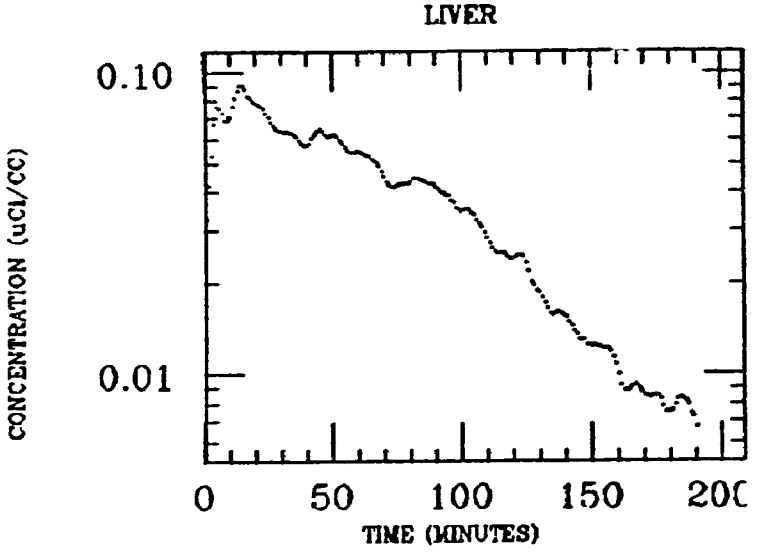

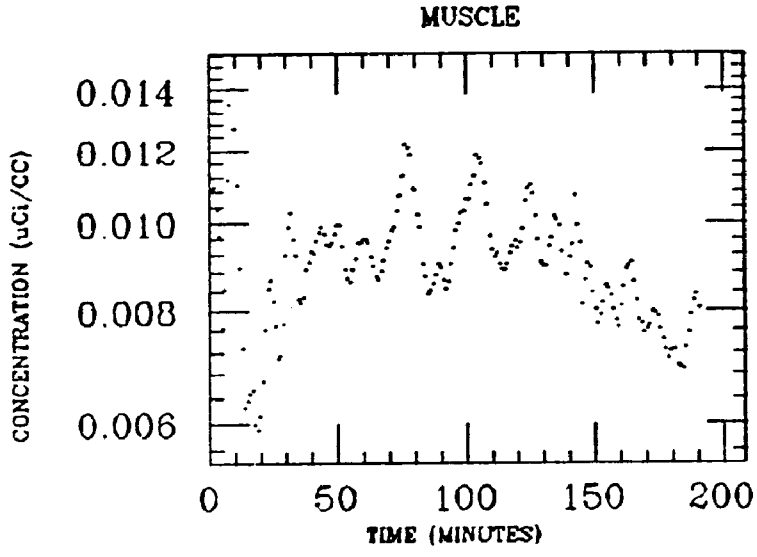

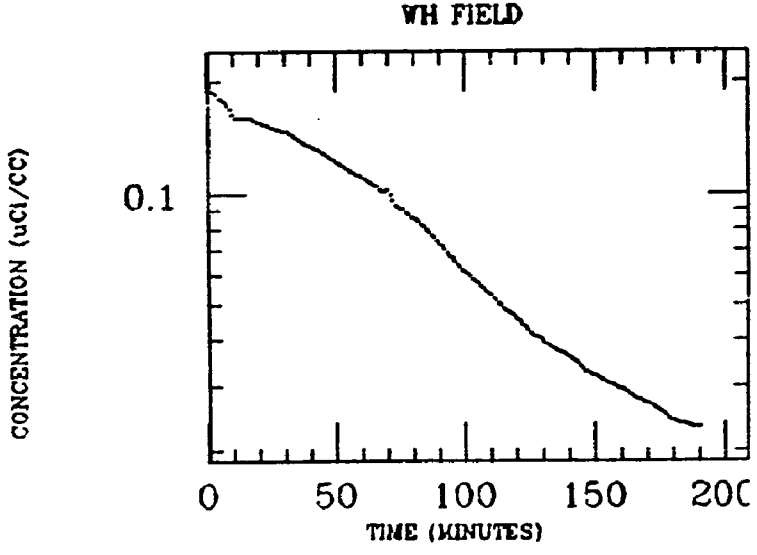

ELMDEN
XE INGESTION
RADON

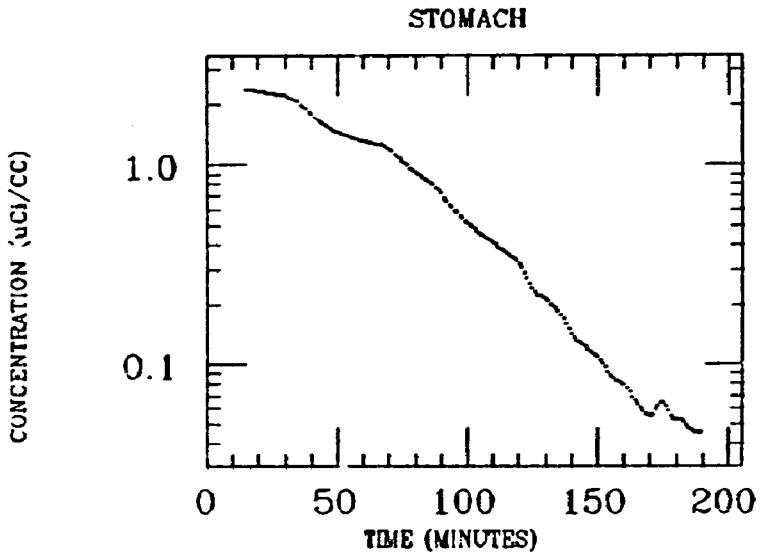

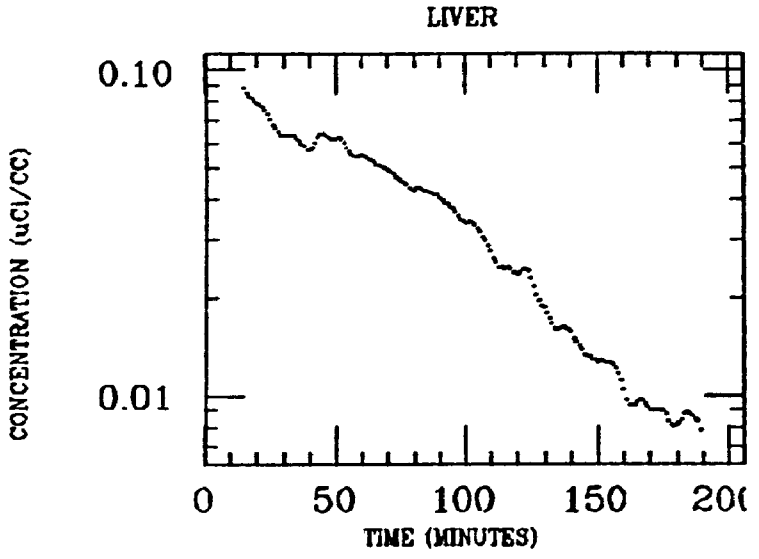

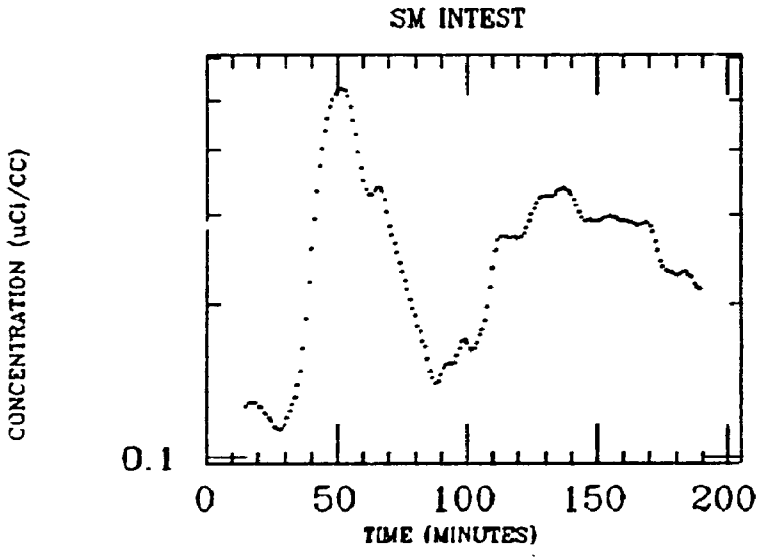

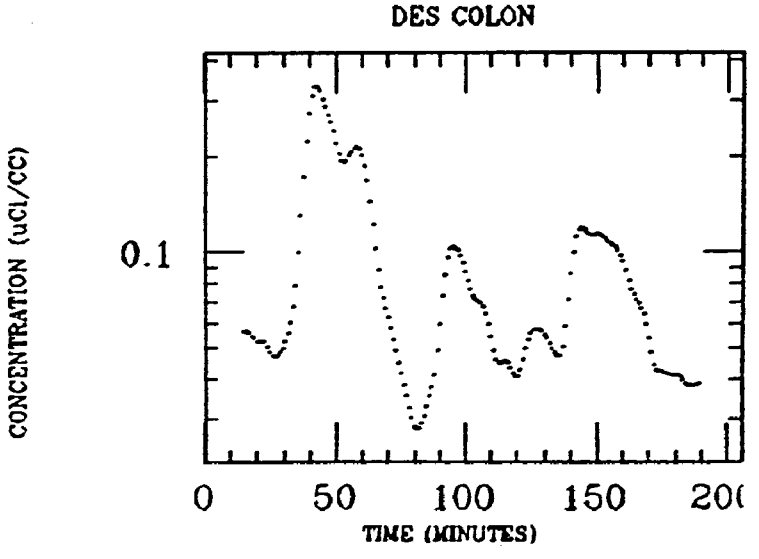

ELMDEN
XE INGESTION
RADON

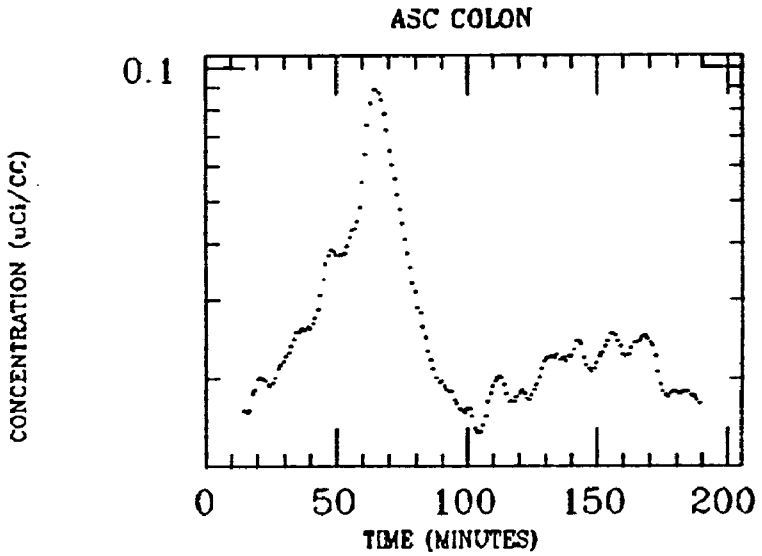

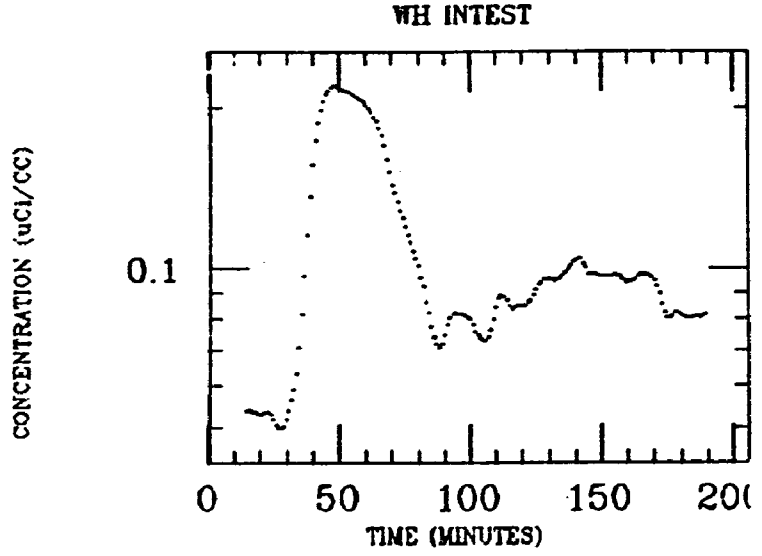

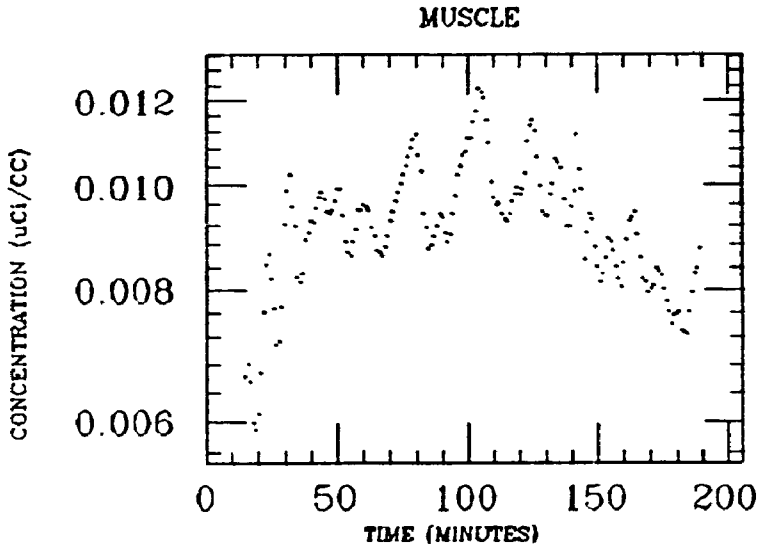

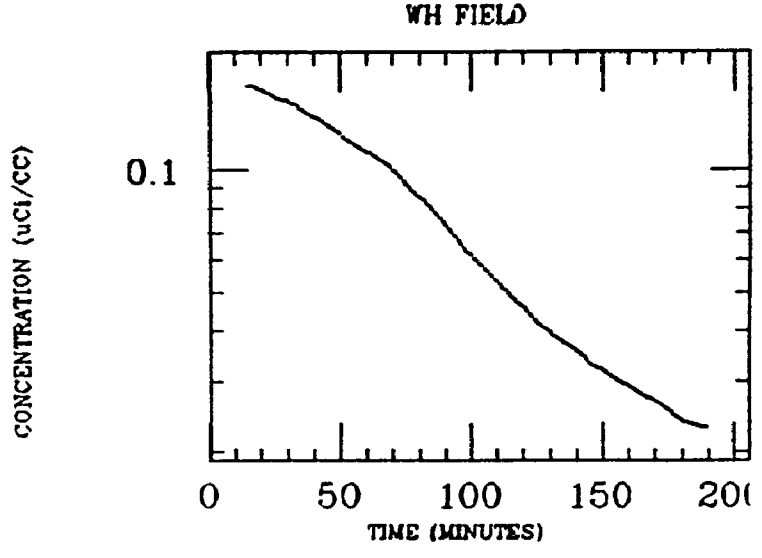

EPLING
XE INGESTION
RADON

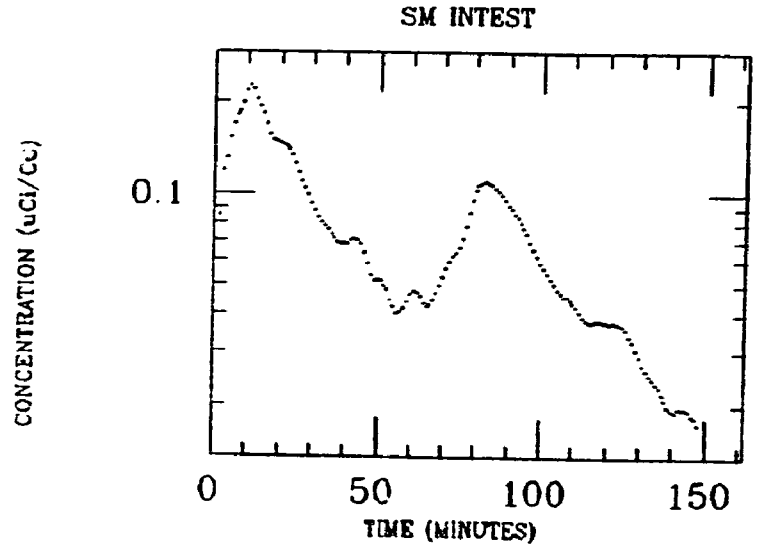

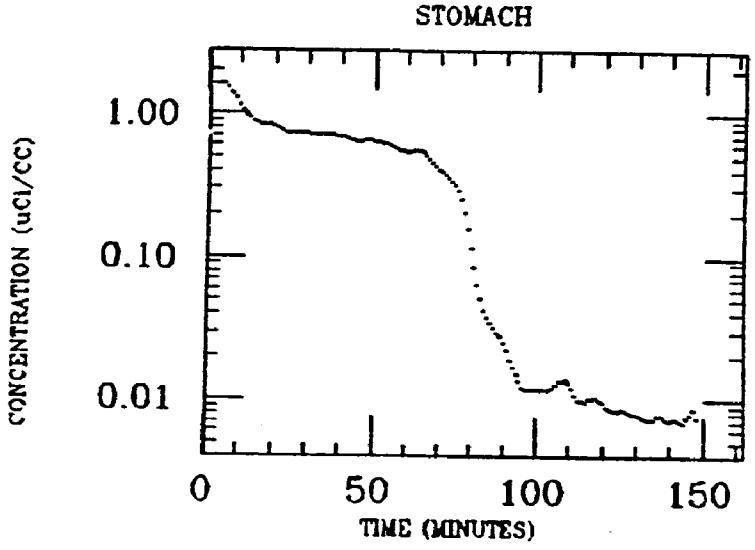

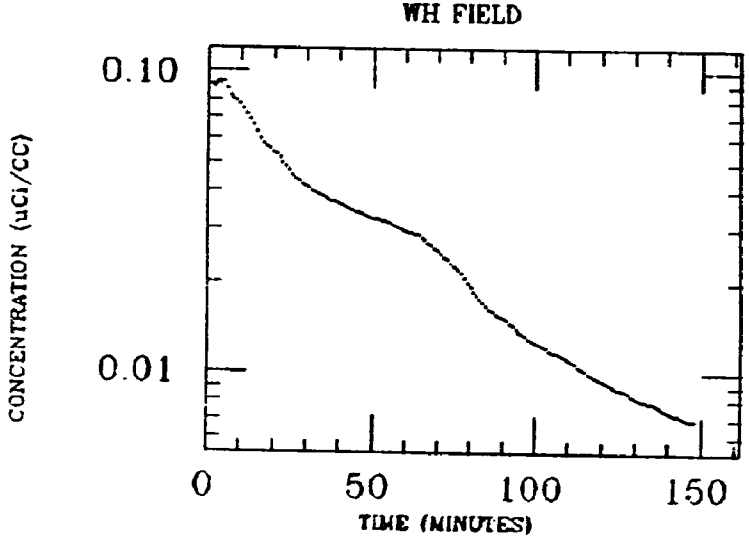

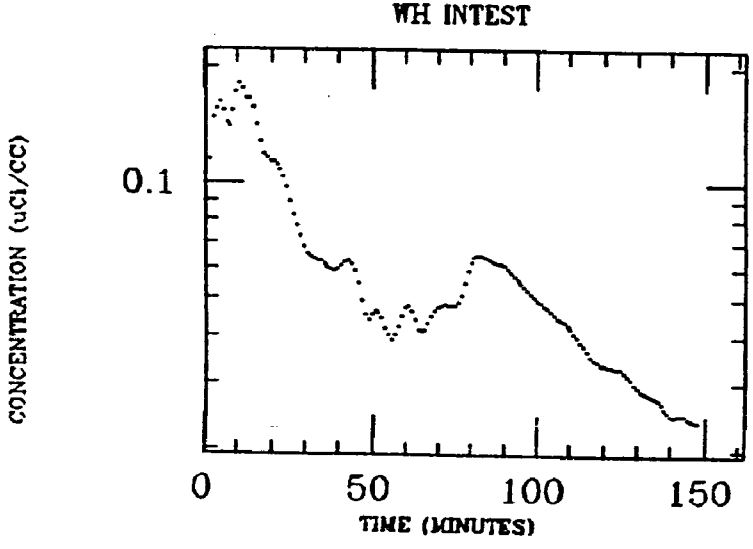

EPLING
XE INGESTION
RADON

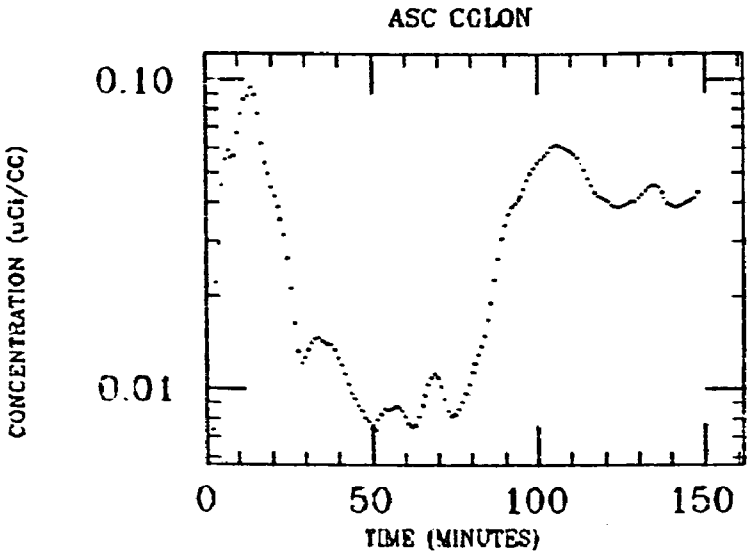

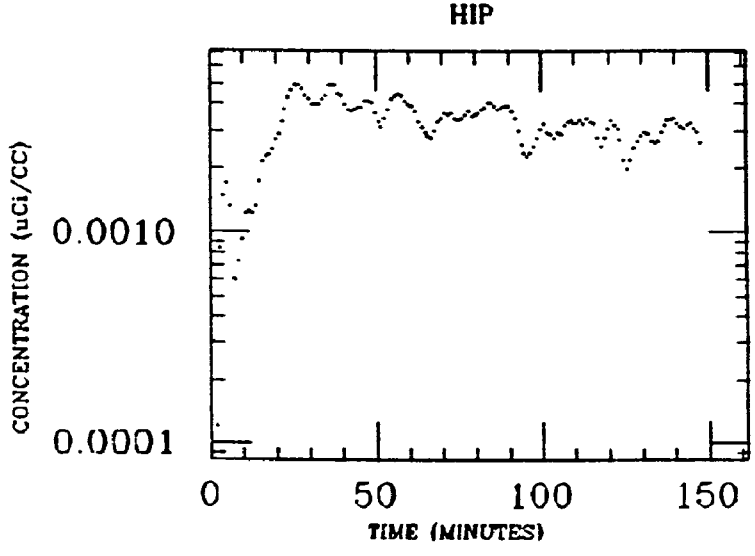

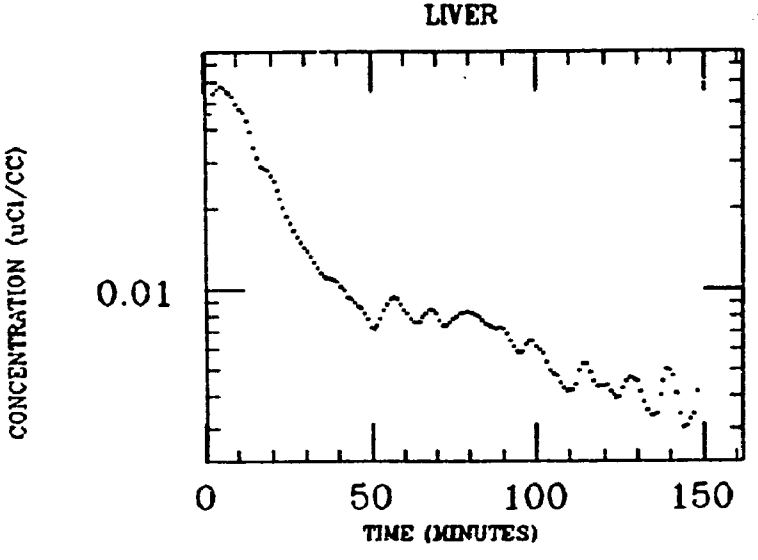

GALLOP
XE INGESTION
RADON

STOMACH

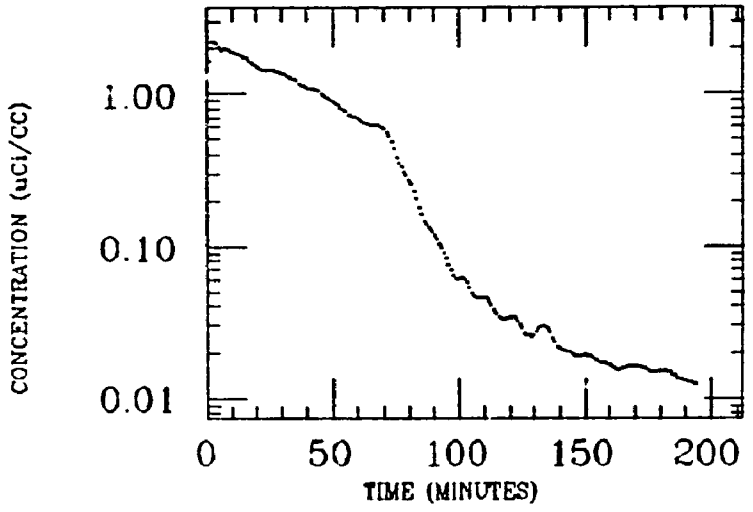

MUSCLE

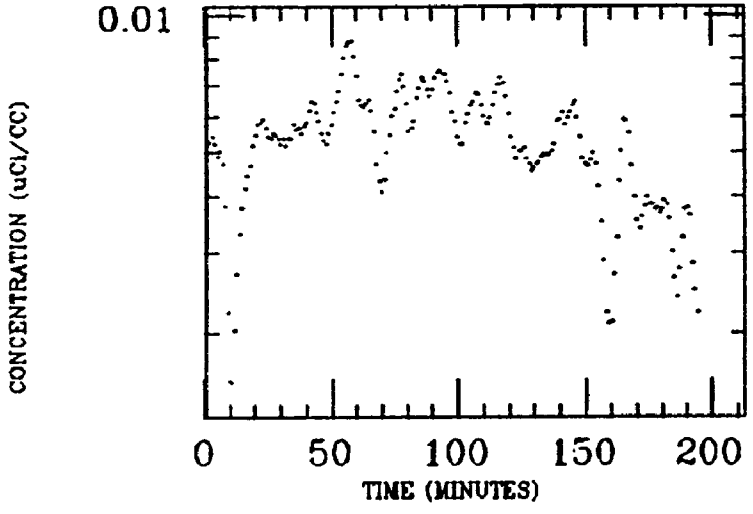

LIVER

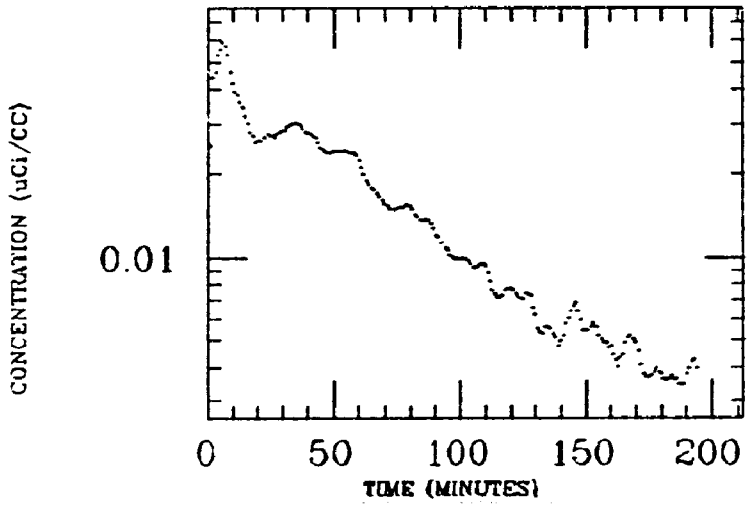

WH FIELD

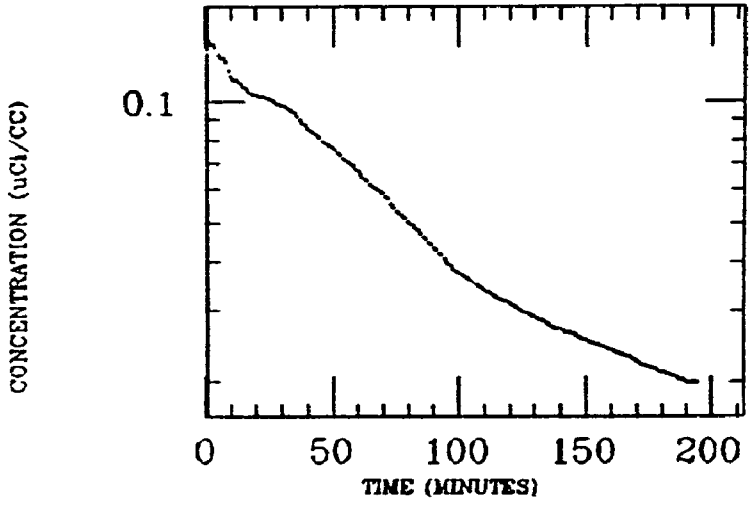

GALLOP
XE INGESTION
RADON

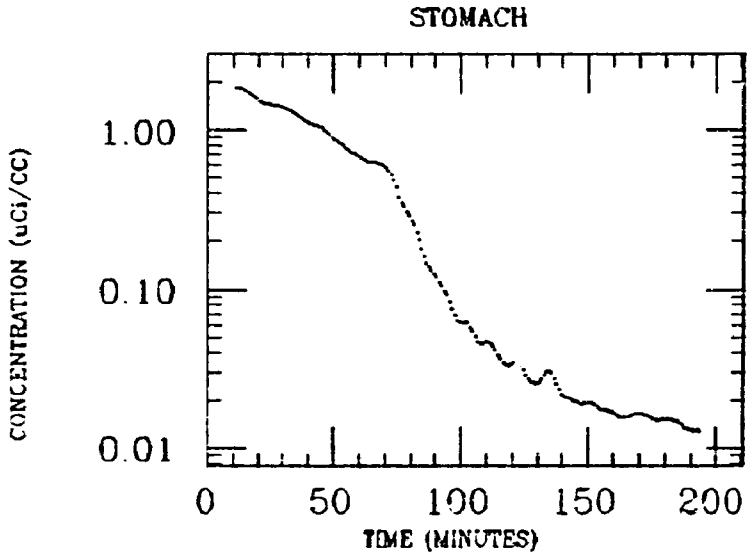

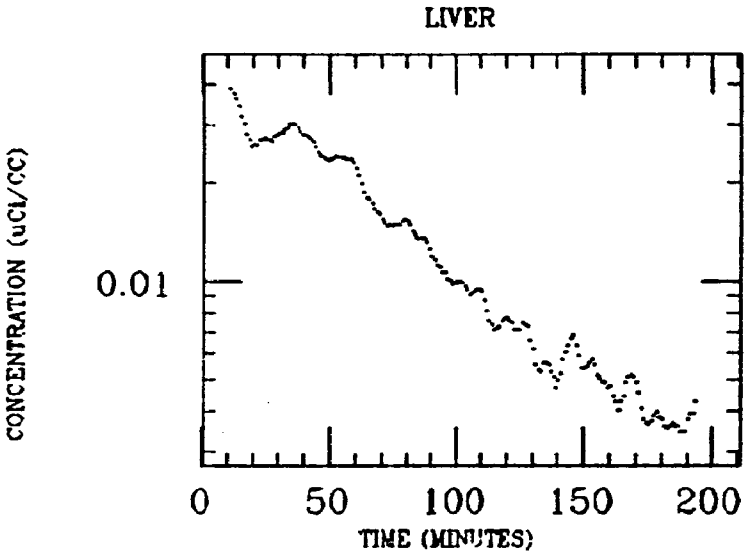

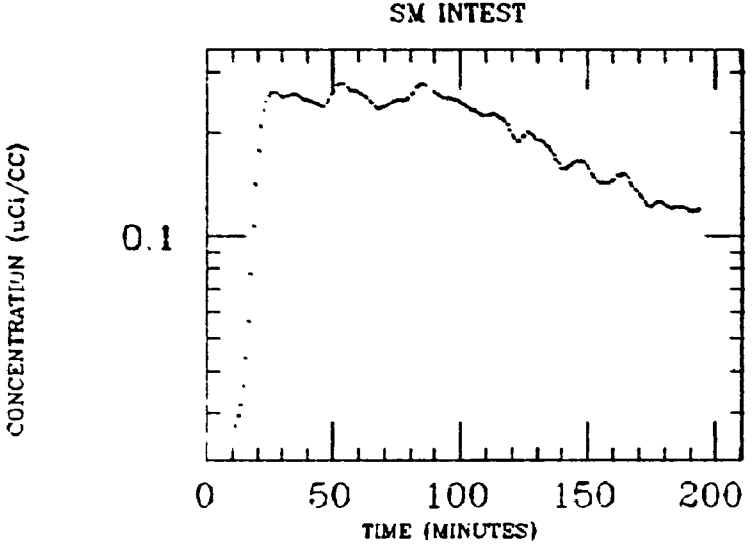

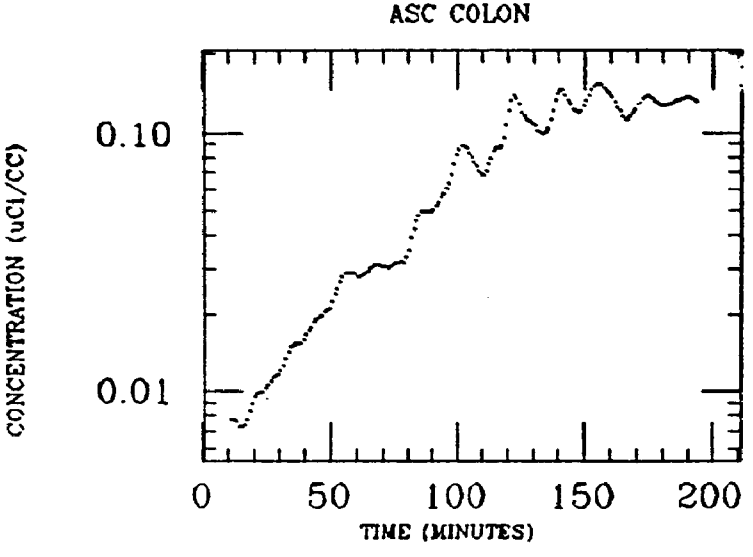

GALLOP
XE INGESTION
RADON

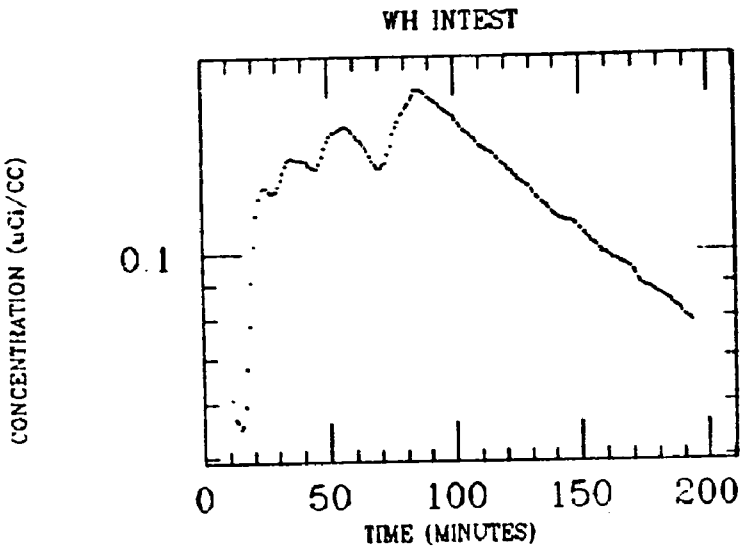

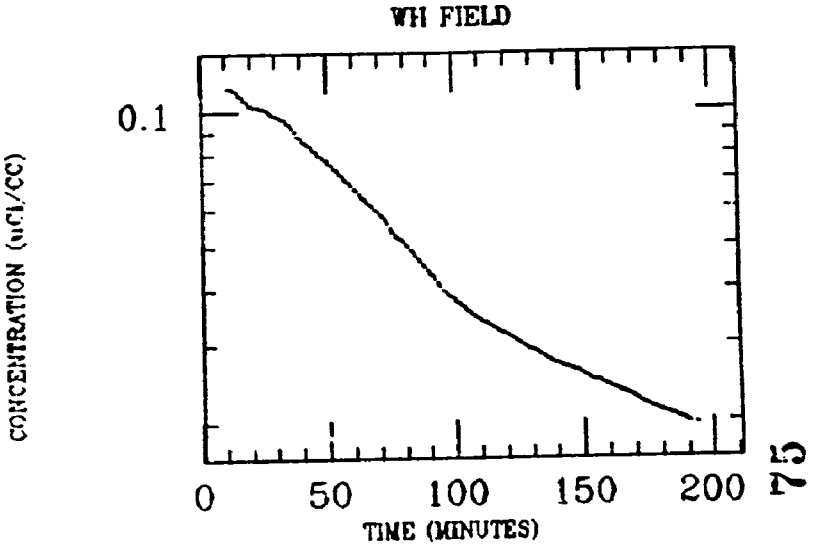

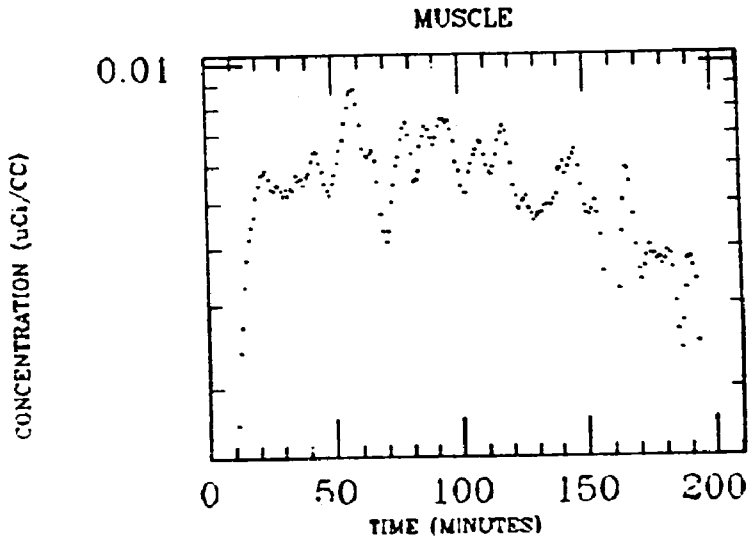

G.MCKINLEY
XE INGESTION
RADON

STOMACH

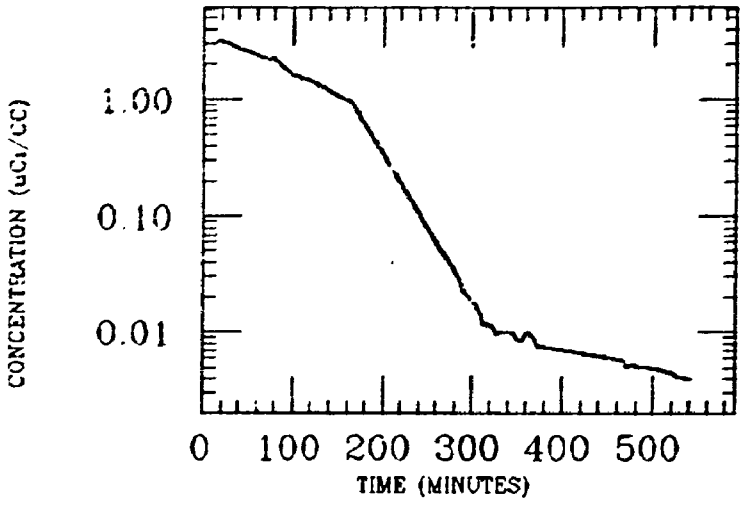

LIVER

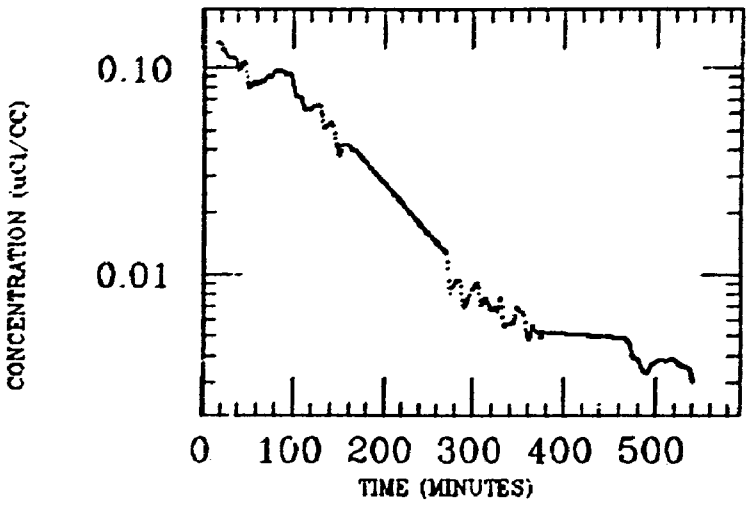

SM INTEST

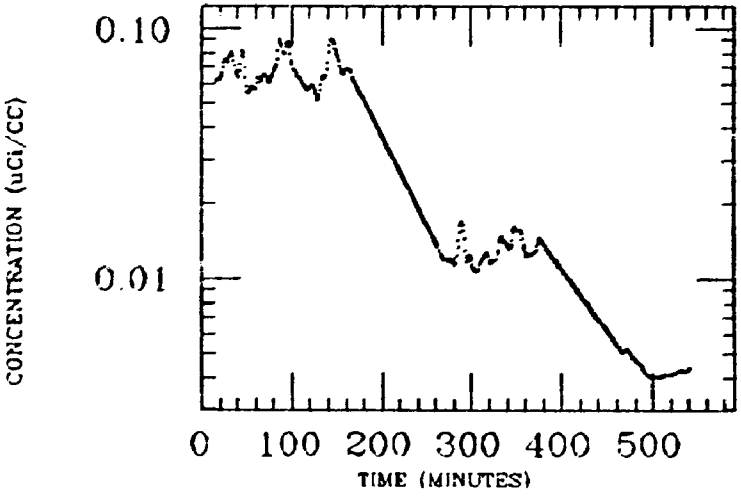

WH INTEST

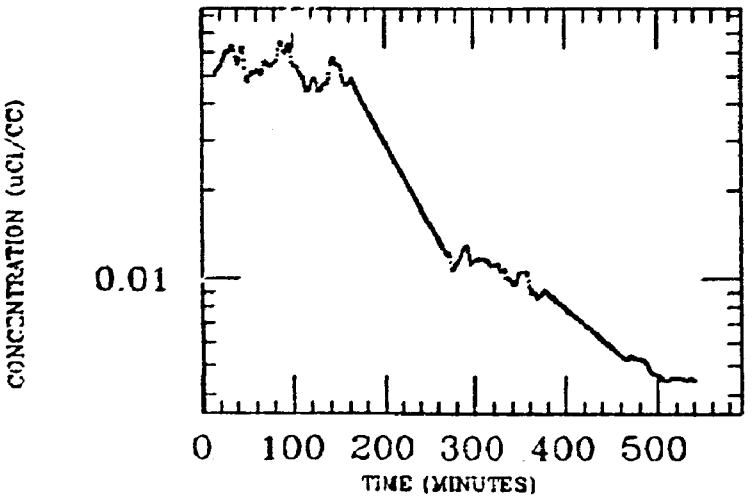

C.MCKINLEY
XE INGESTION
RADON

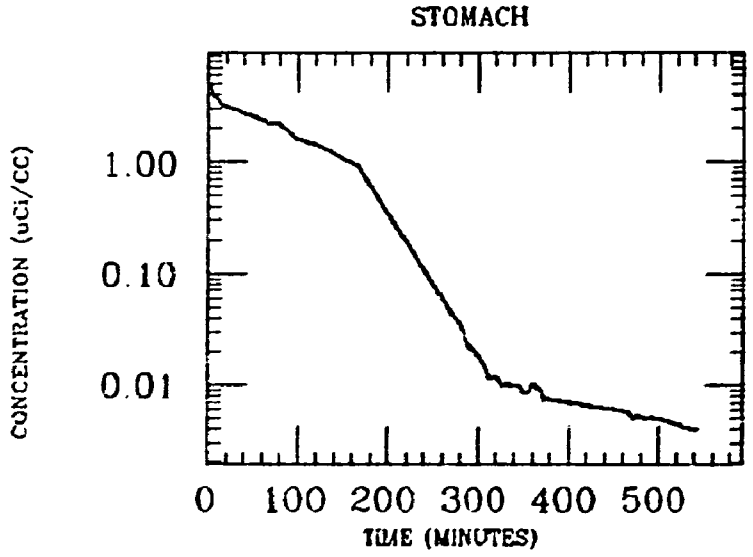

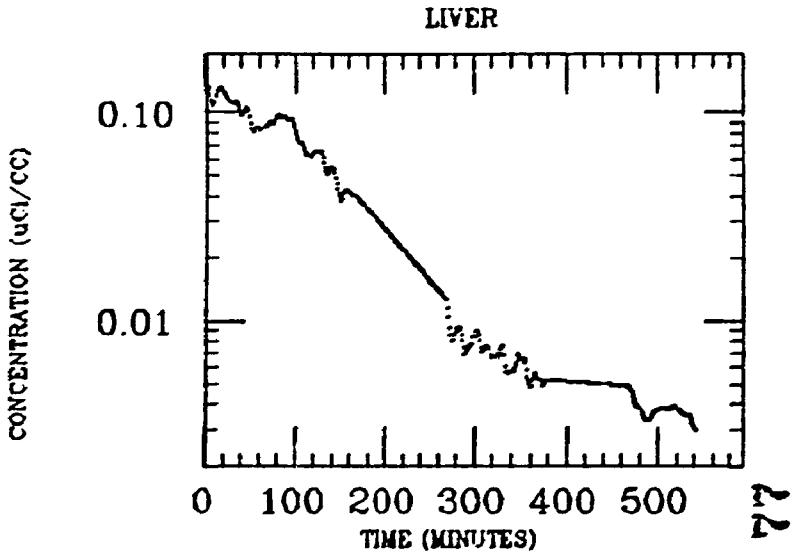

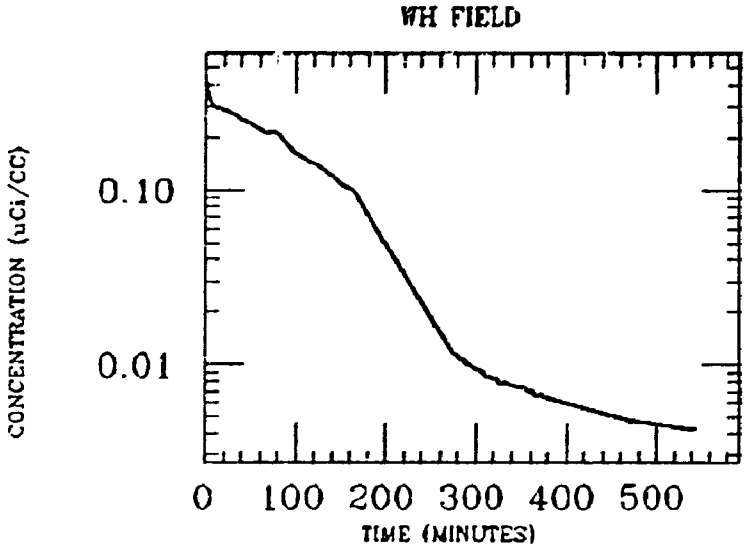

C.MCKINLEY
XE INGESTION
RADON

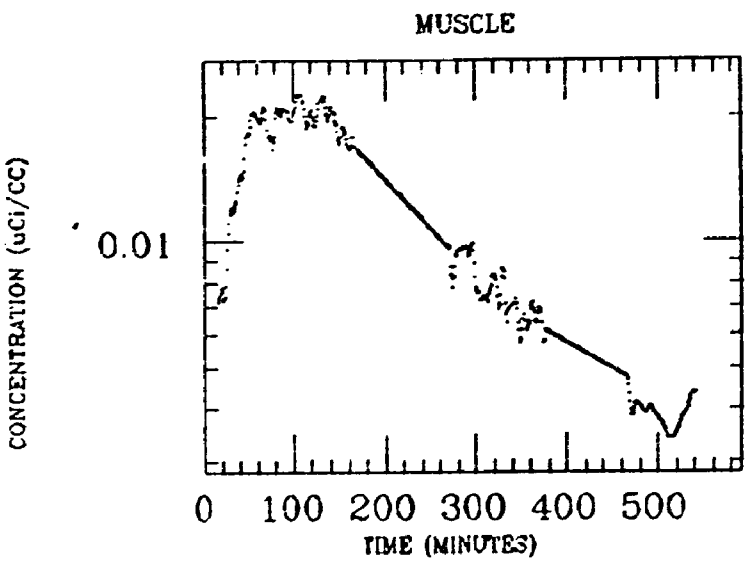

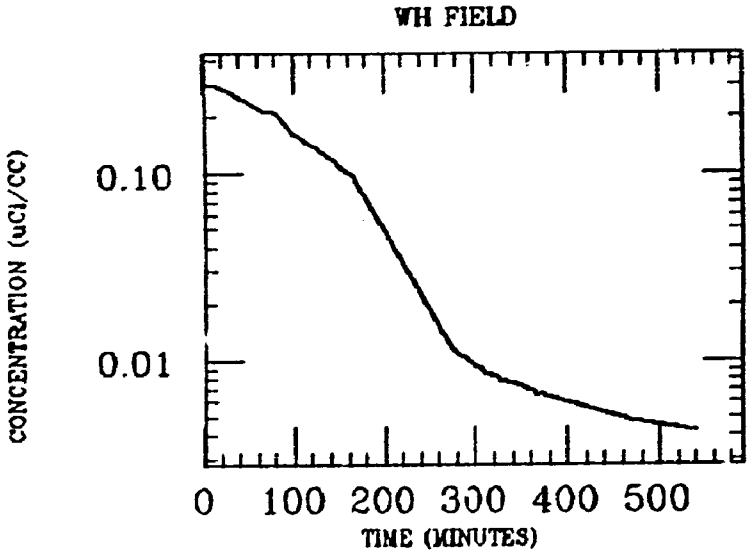

HAND
XE INGESTION
RADON

STOMACH

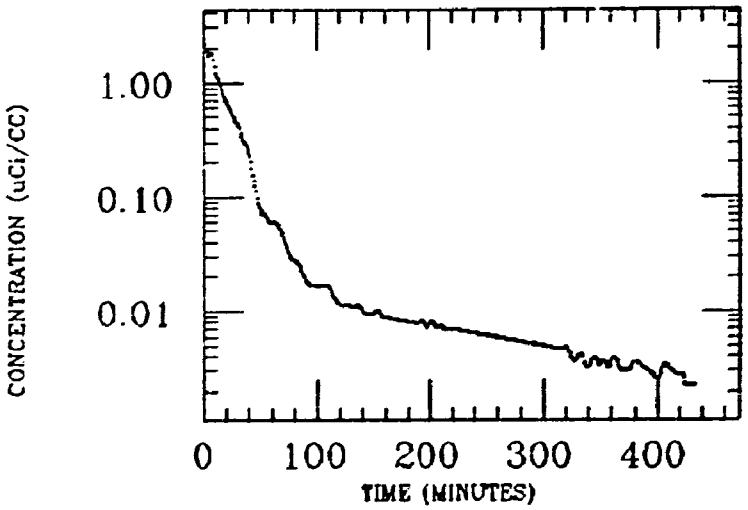

LIVER

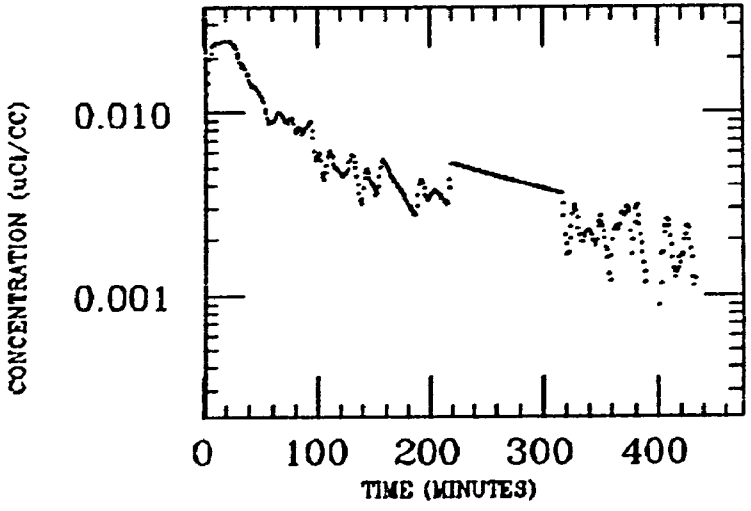

LT LUNG

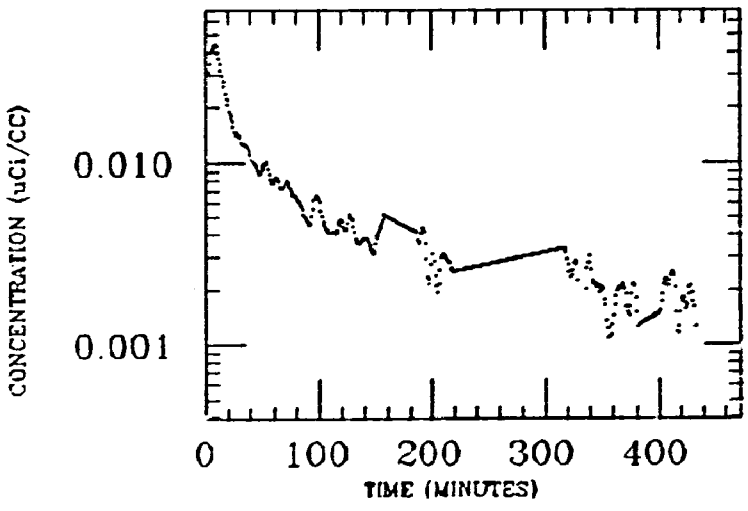

WH INTEST

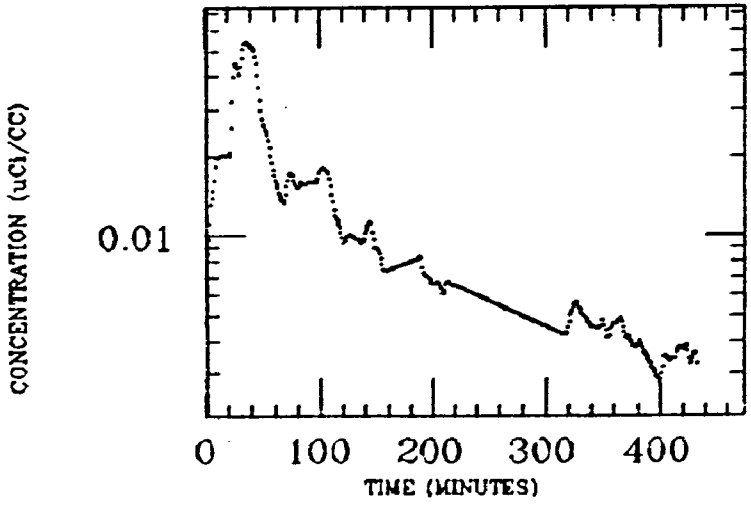

HAND
XE INGESTION
RADON

STOMACH

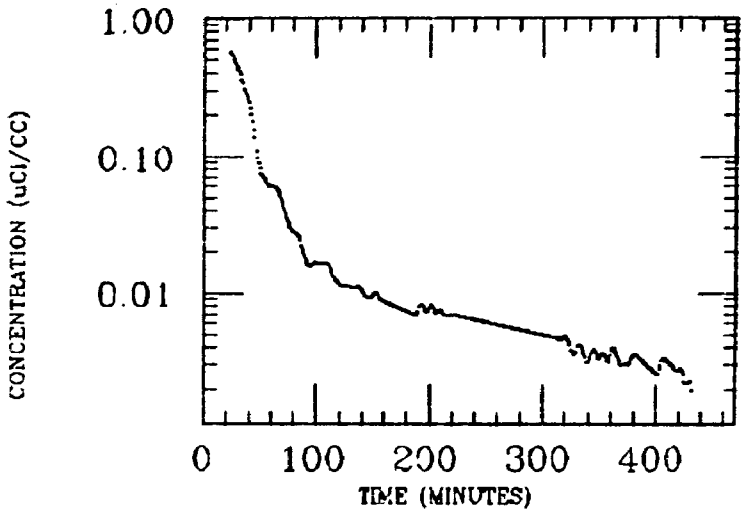

LIVER

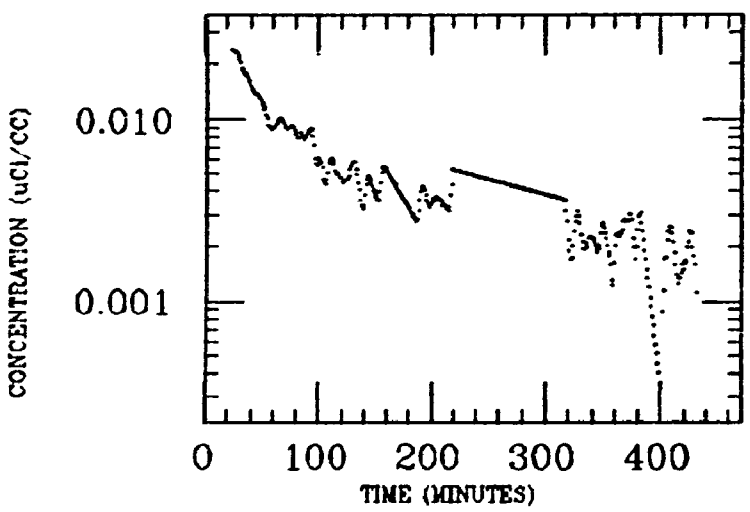

LT LUNG

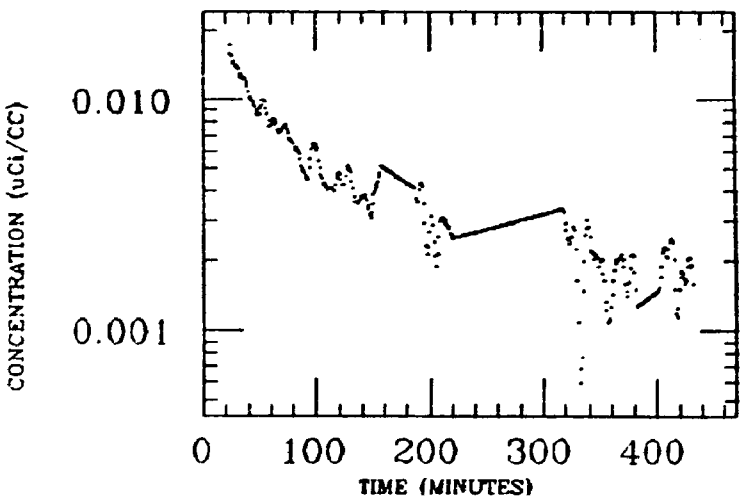

SM INTEST

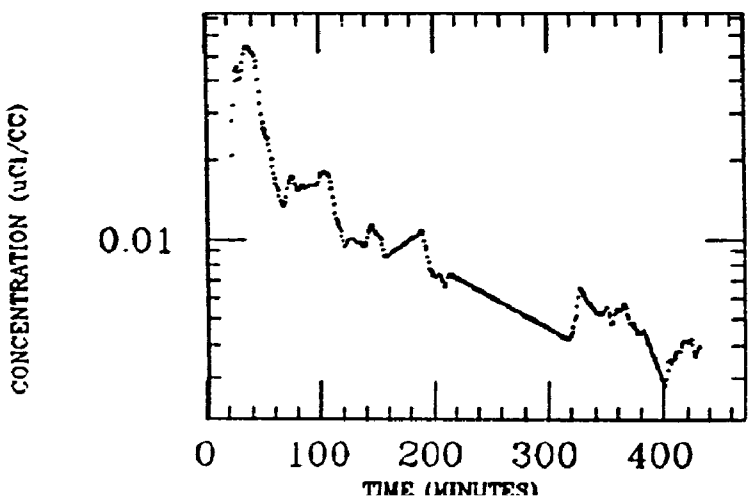

HAND
XE INGESTION
RADON

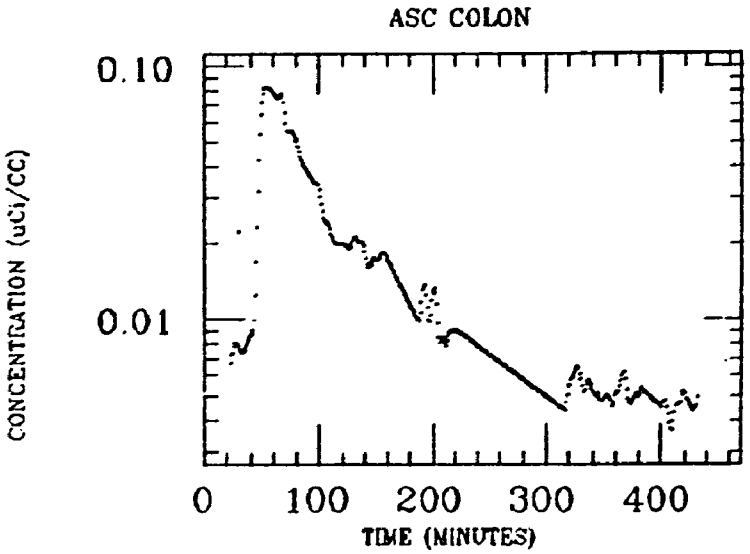

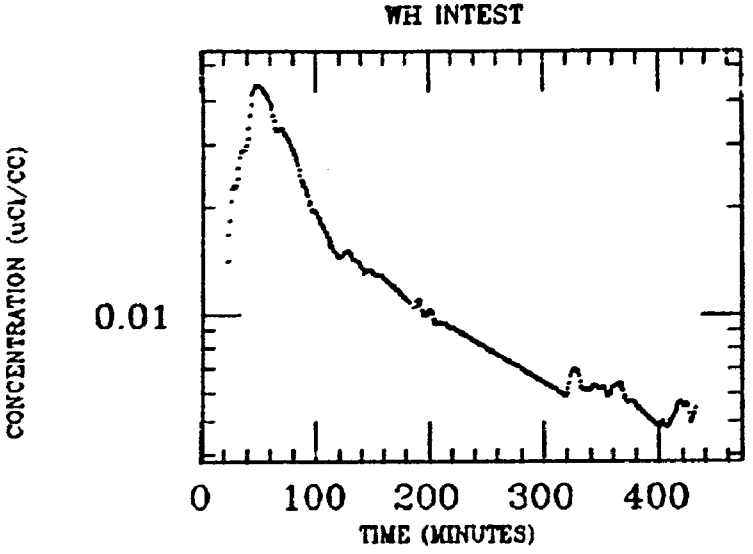

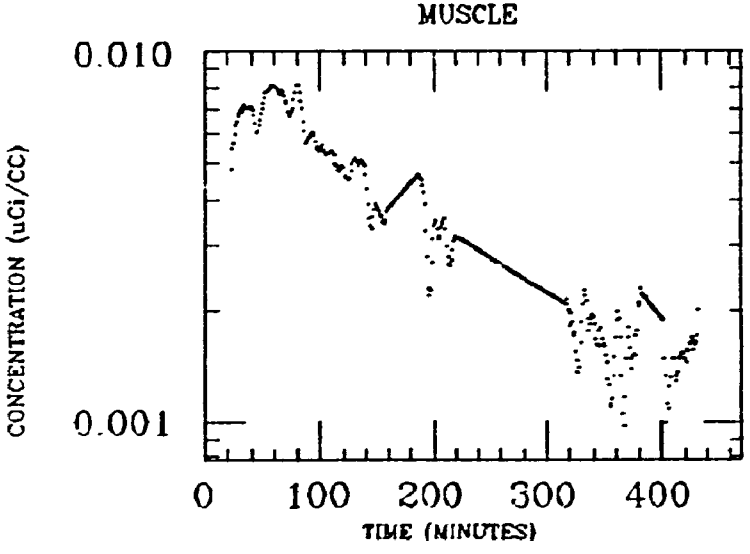

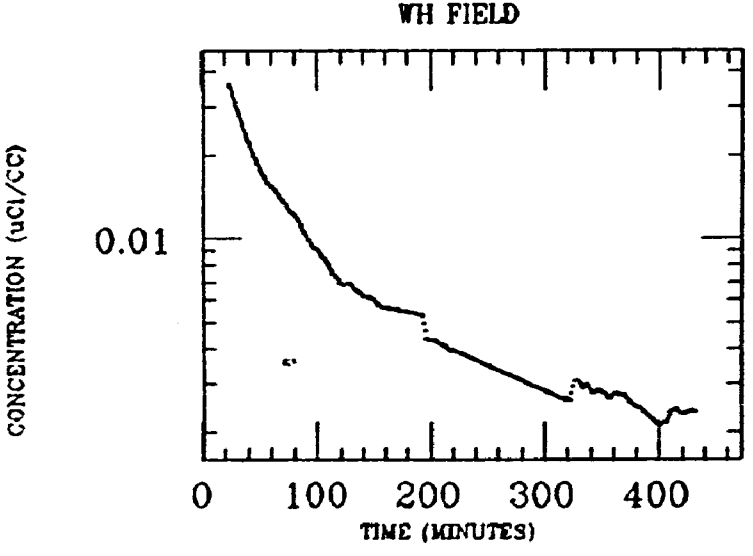

HAWKINS
XE INGESTION
RADON

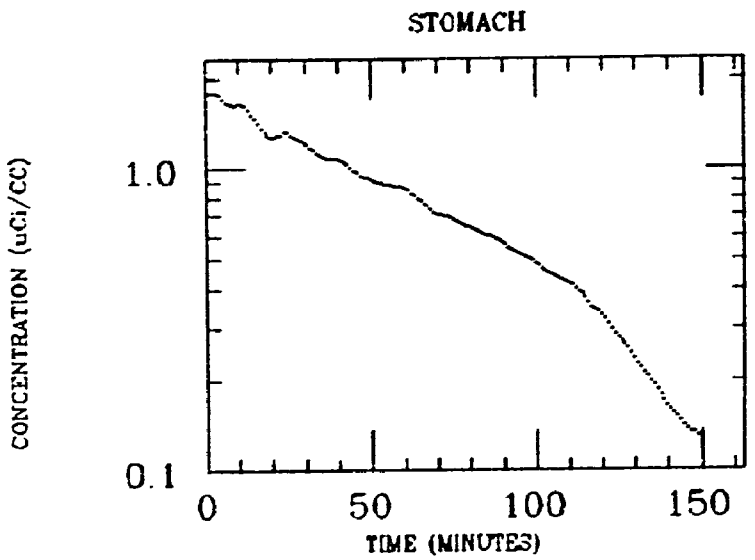

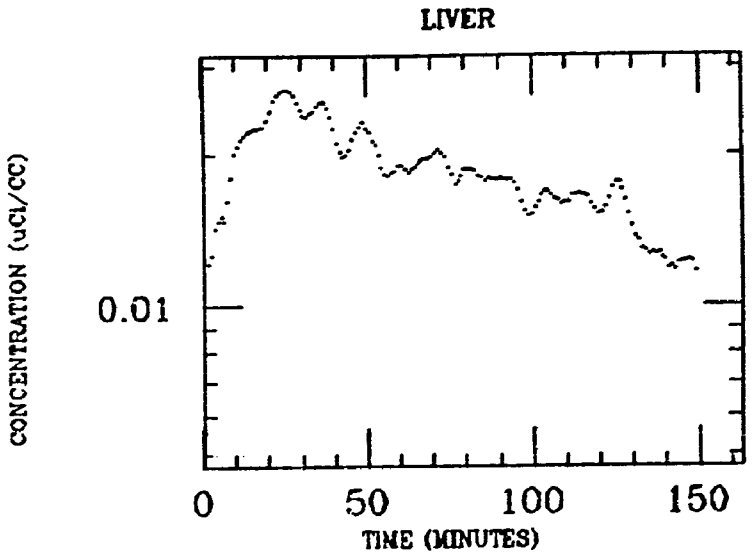

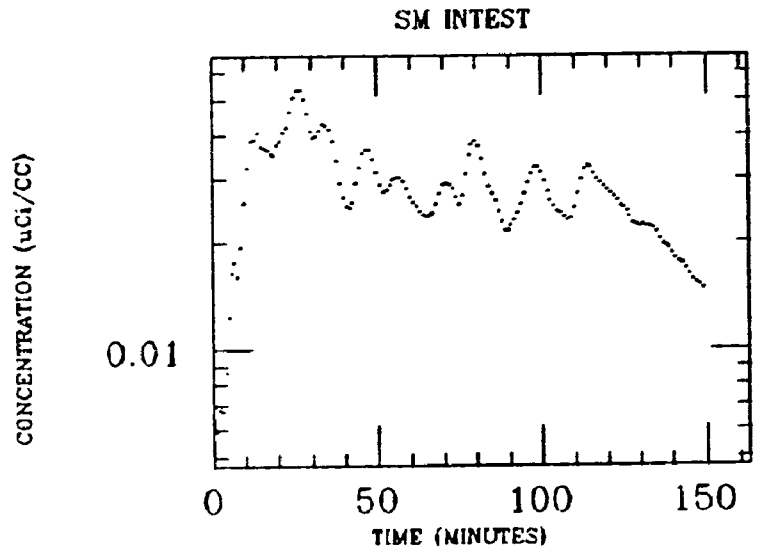

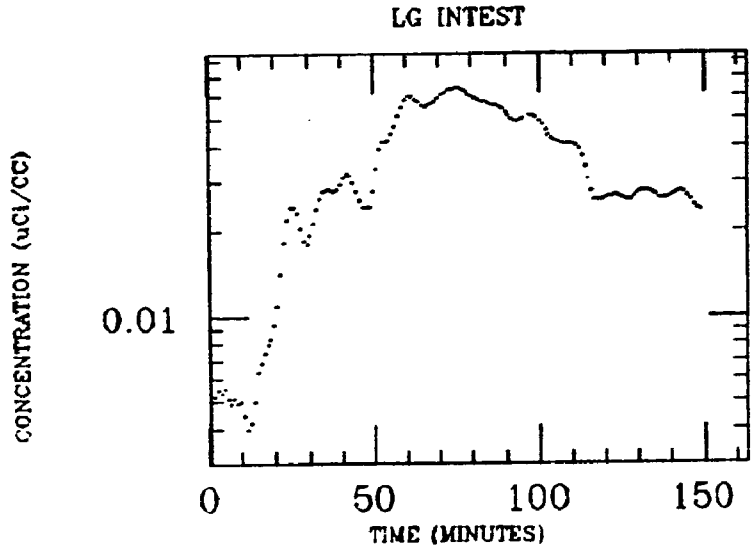

HAWKINS
XE INGESTION
RADON

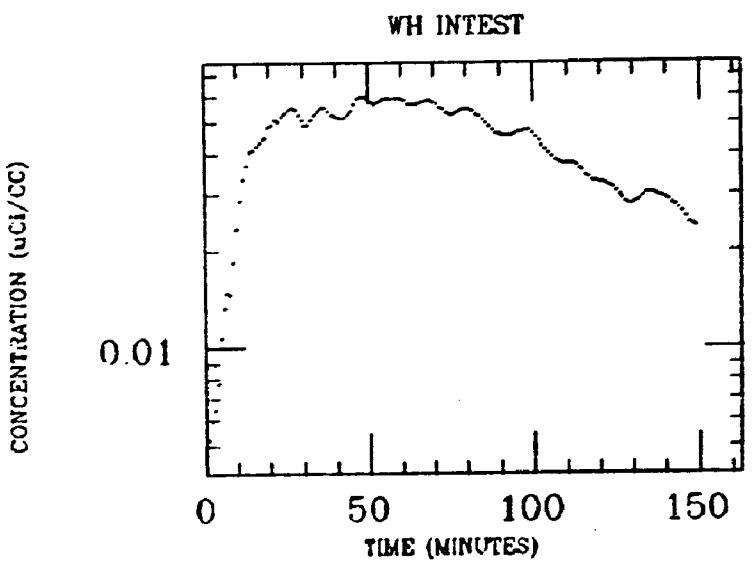

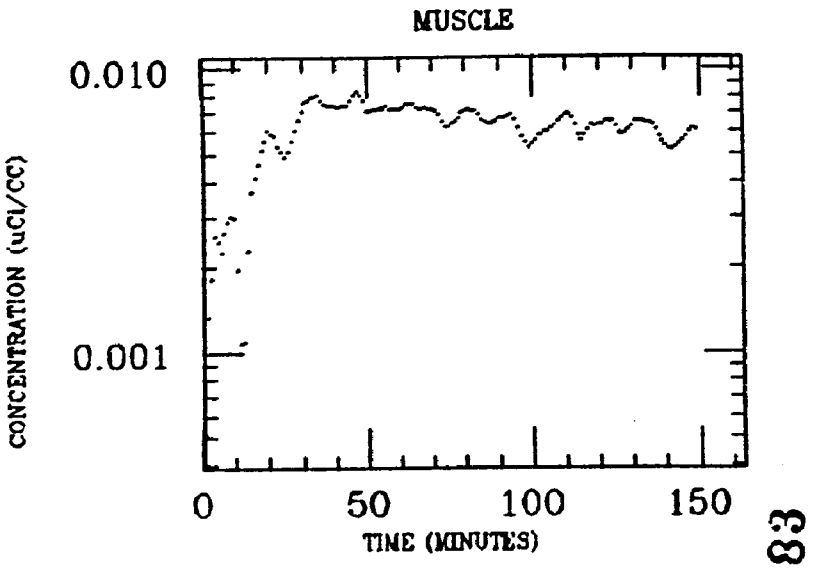

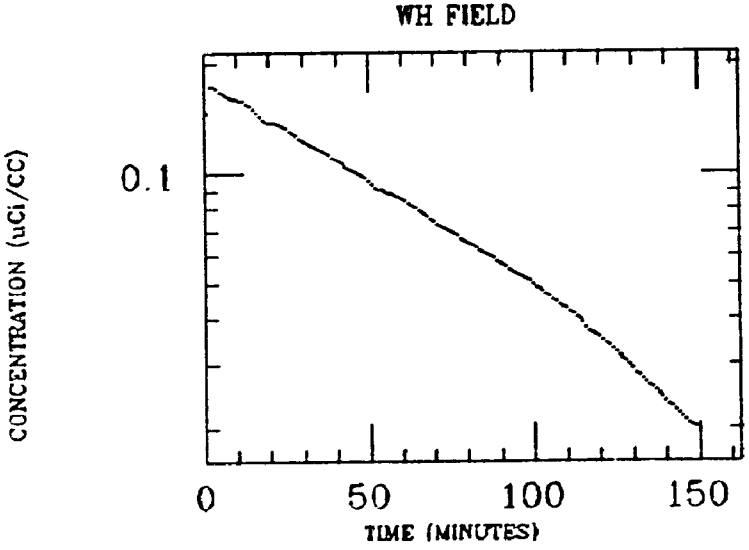

HILL
XE INGESTION
RADON

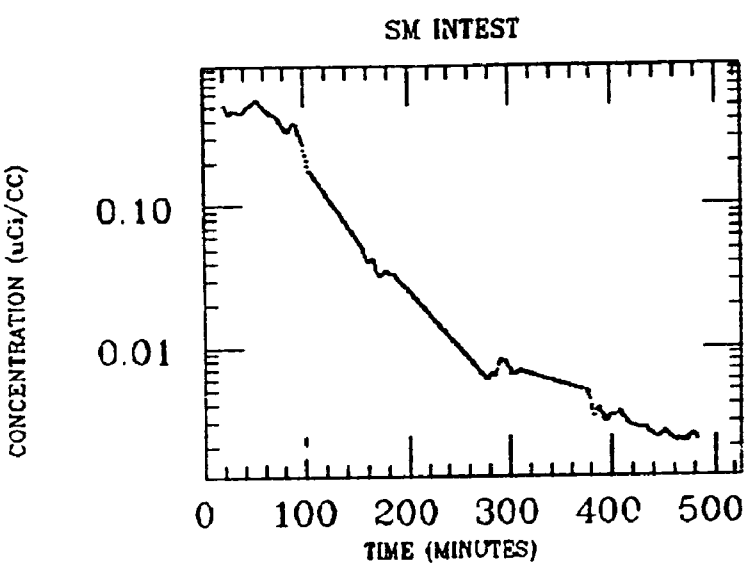

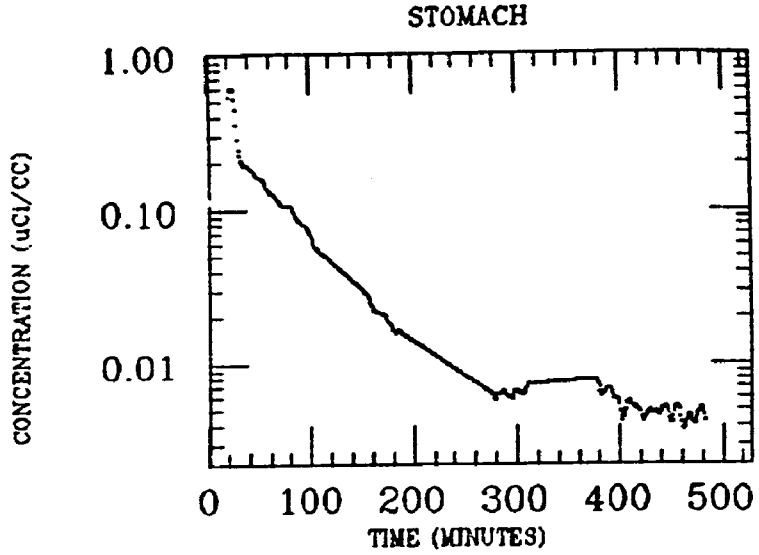

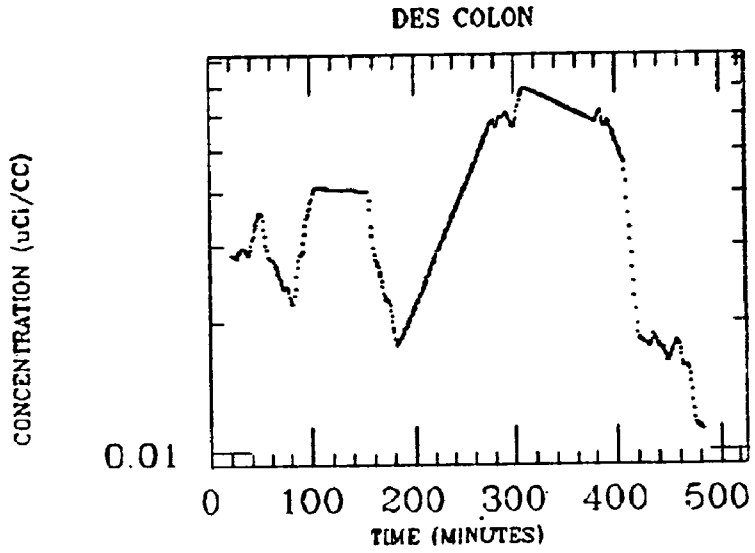

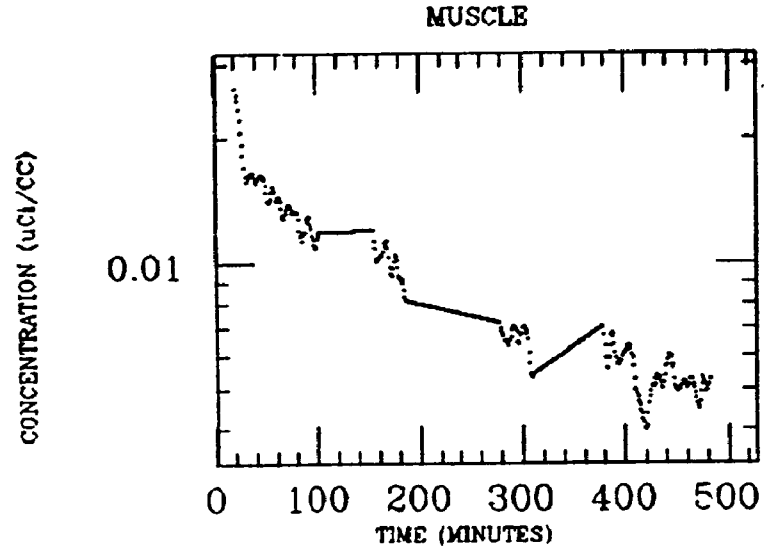

HILL
XE INGESTION
RADON

LIVER

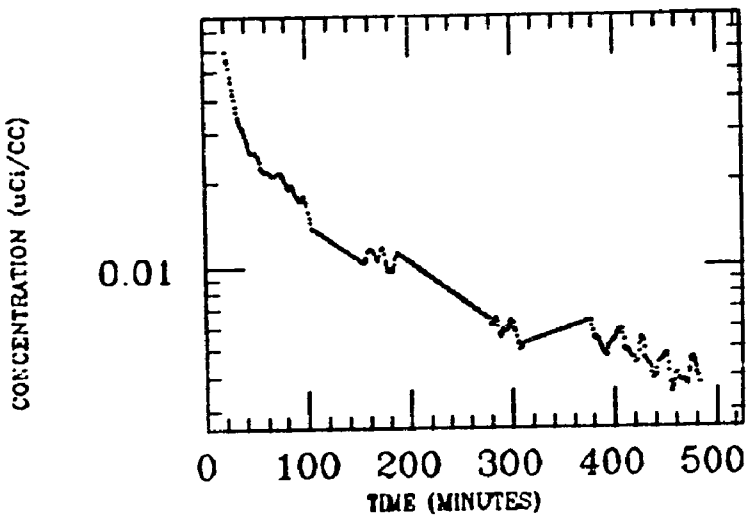

WH FIELD

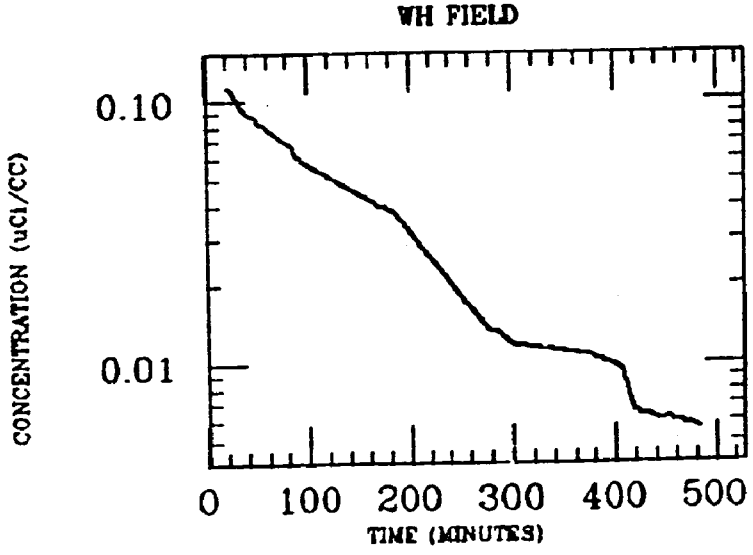

HILL
XE INGESTION
RADON

STOMACH

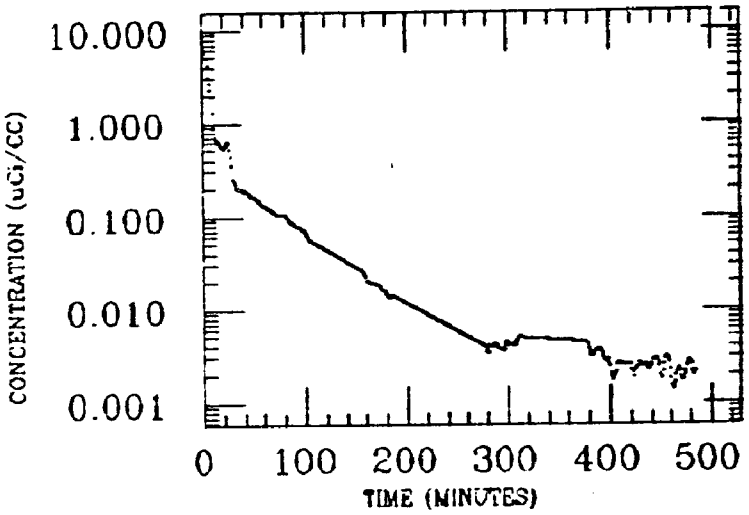

LIVER

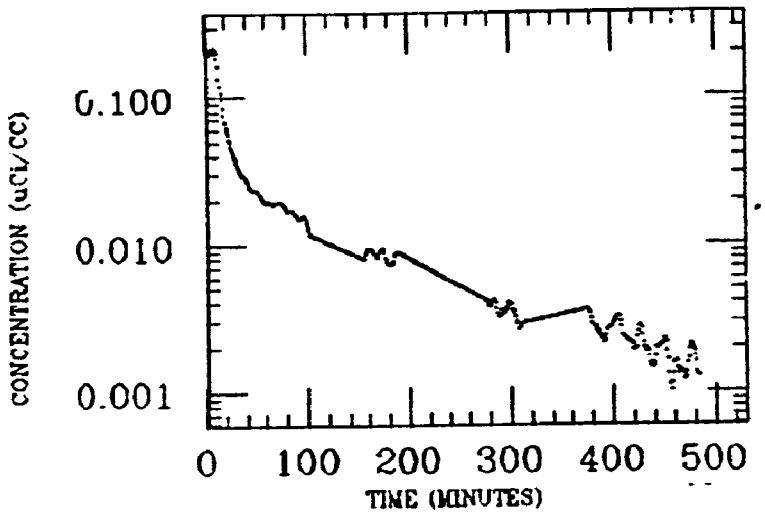

MUSCLE

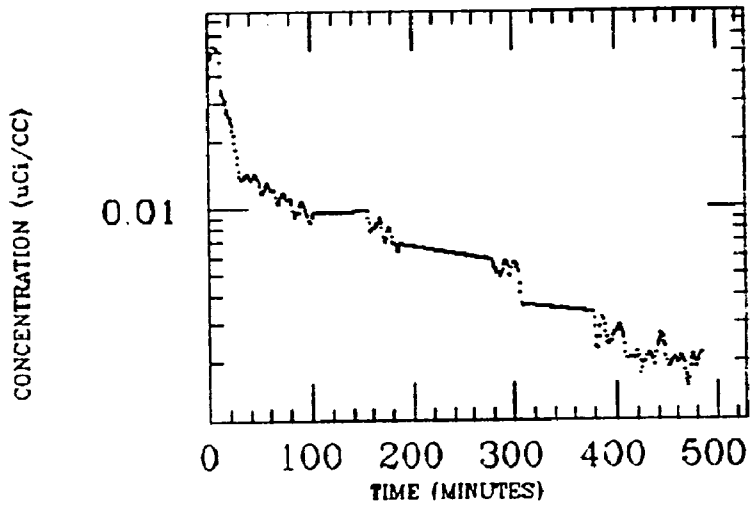

WH FIELD

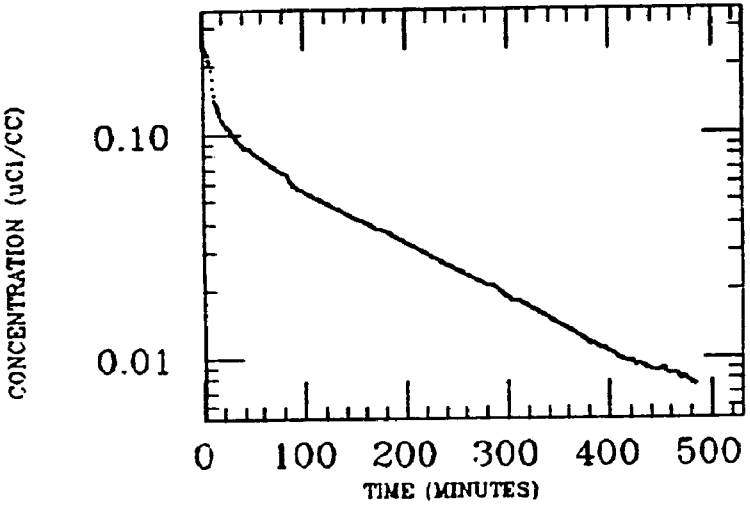

HUTCHINS
XE INGESTION
RADON

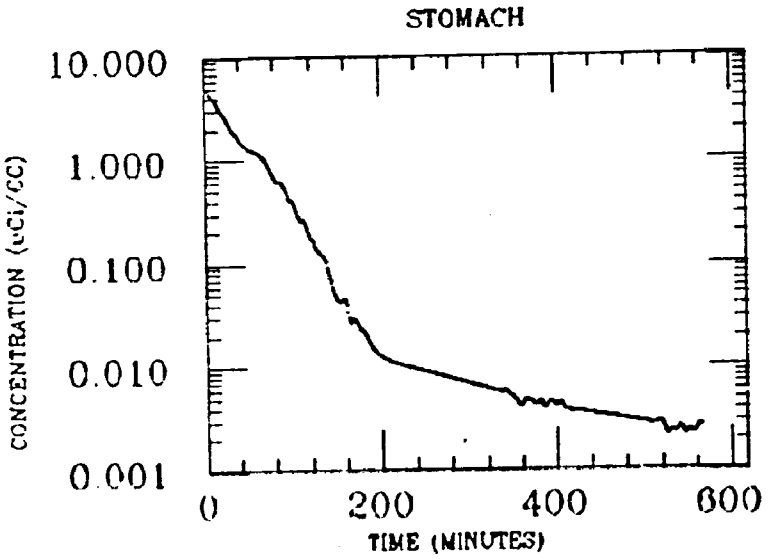

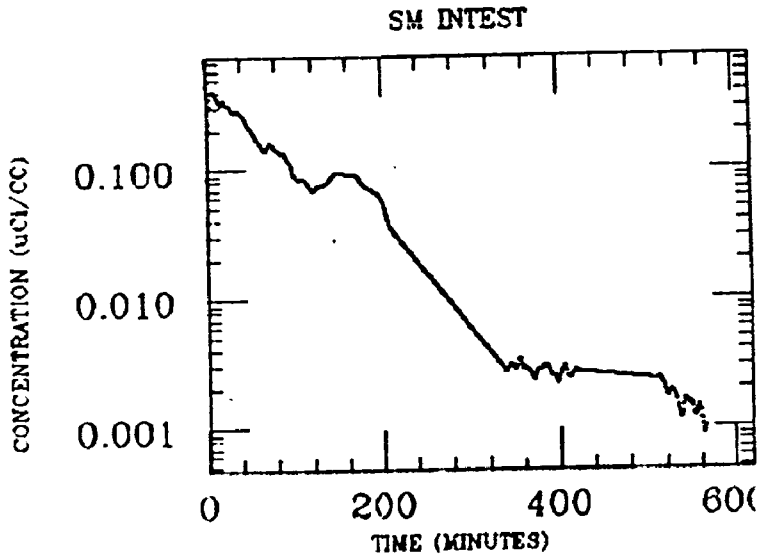

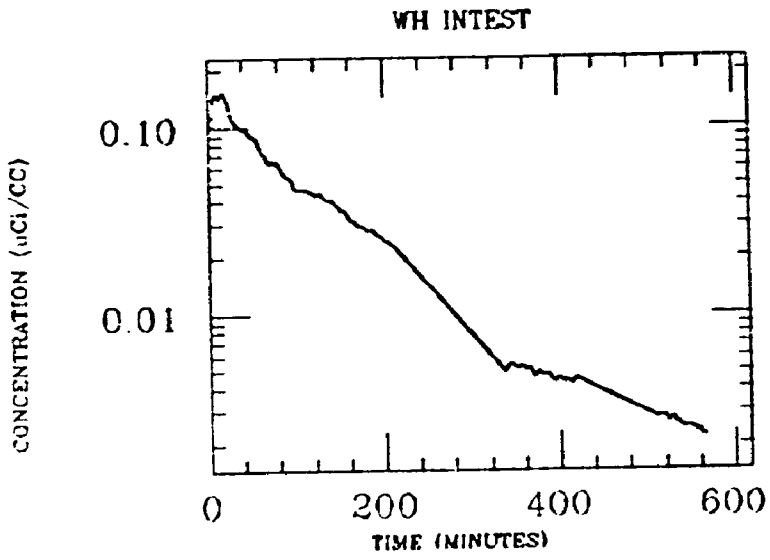

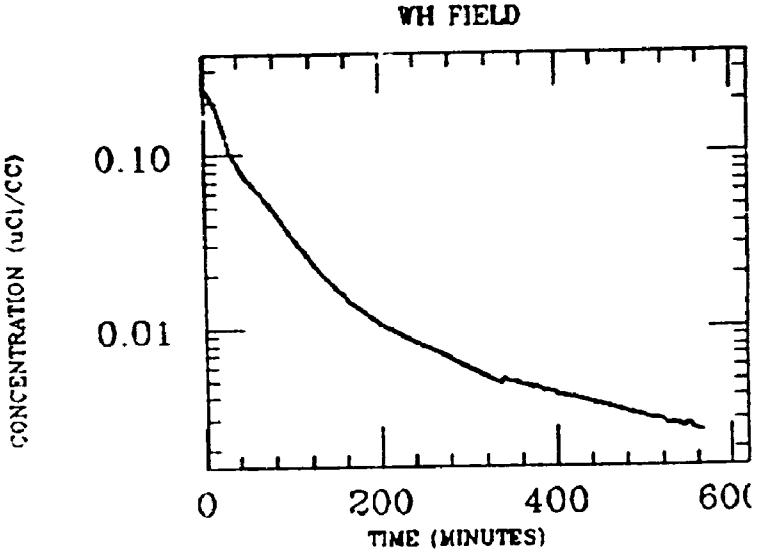

HUTCHINS
XE INGESTION
RADON

DESCENDING

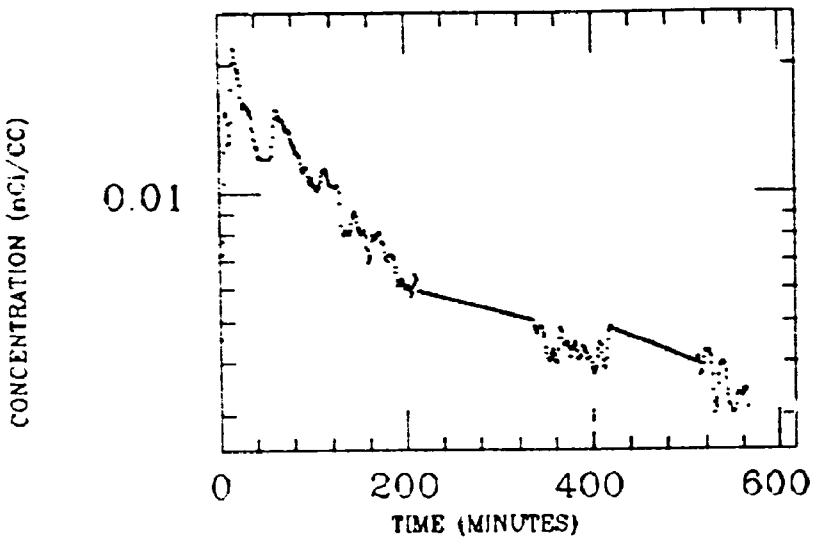

MUSCLE

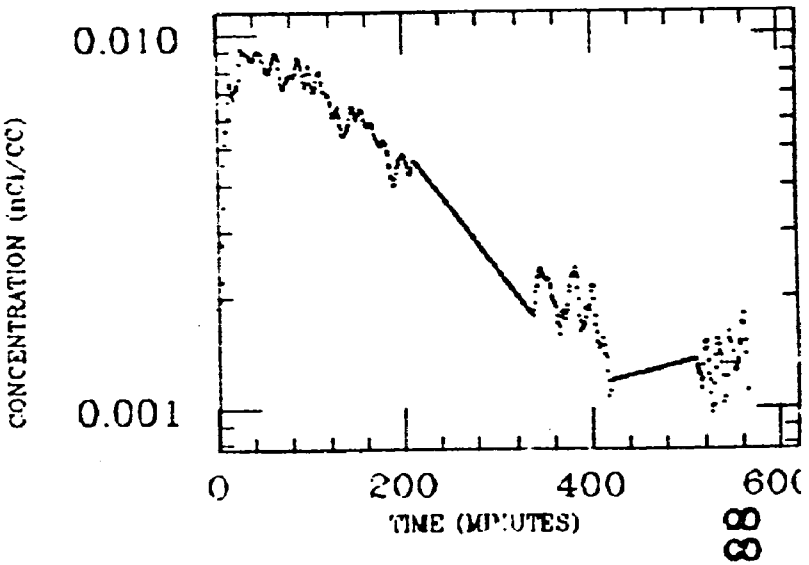

88

HUTCHINS
XE INGESTION
RADON

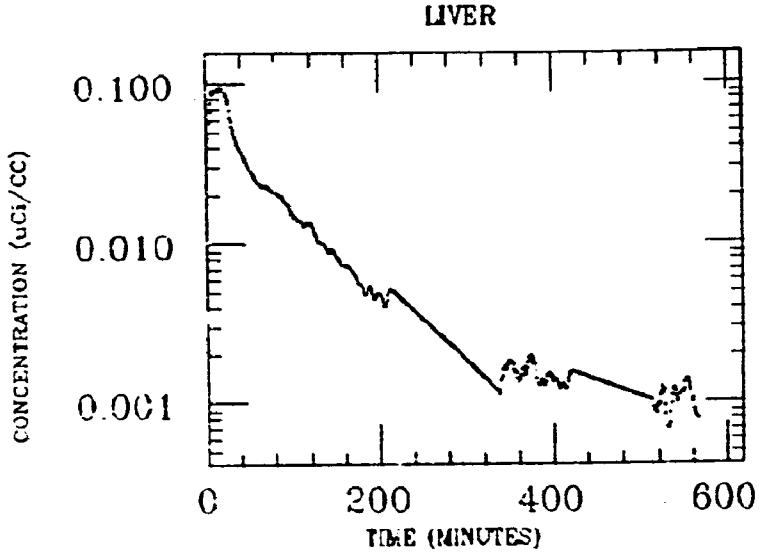

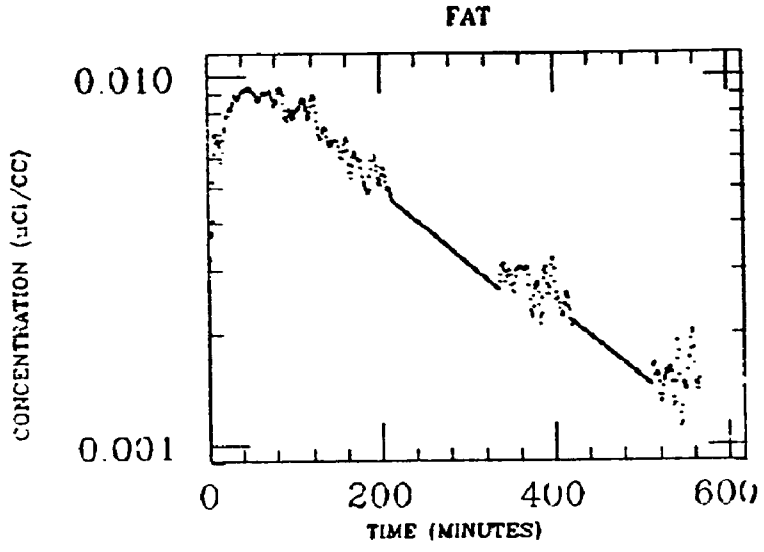

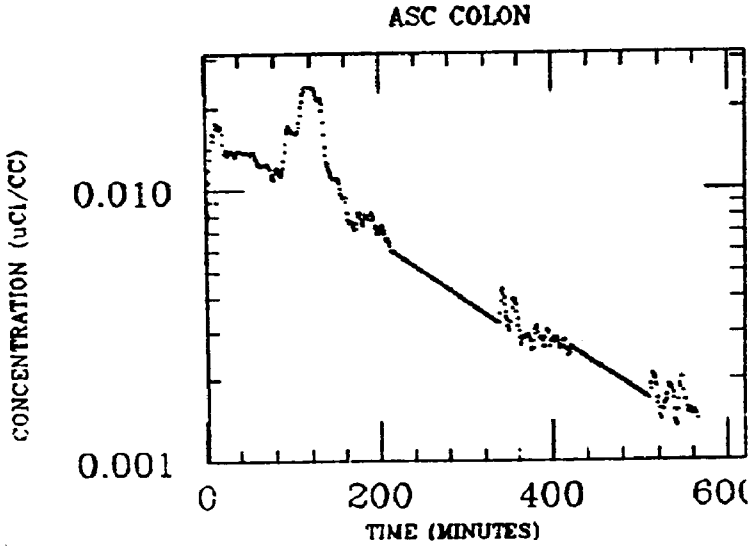

J.MCKINLEY
XE INGESTION
RADON

STOMACH

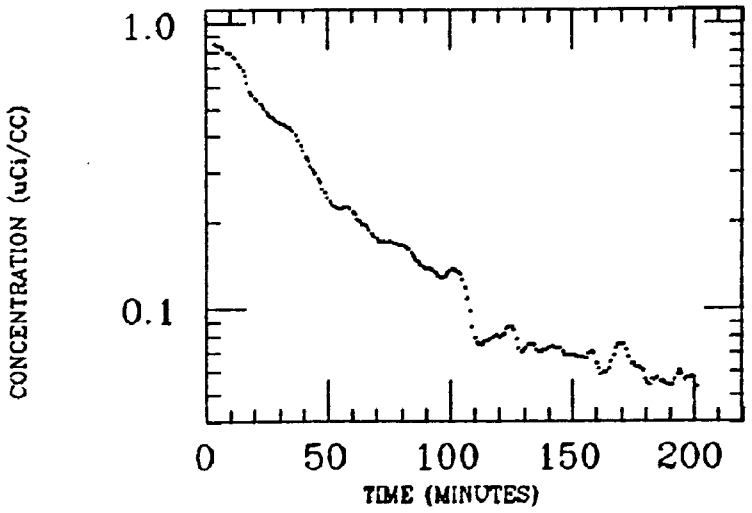

LIVER

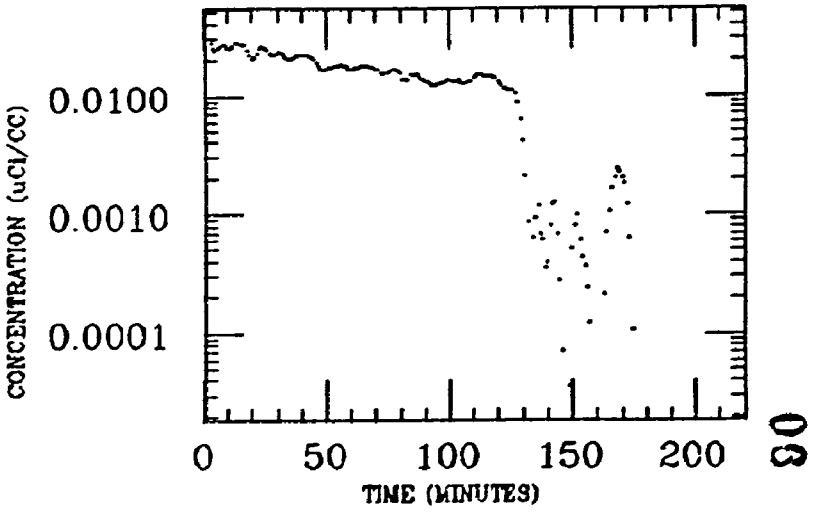

SM INTEST

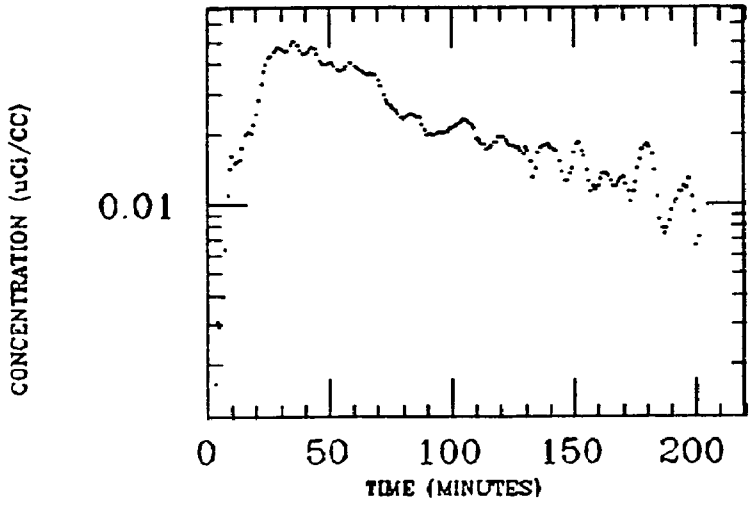

LG INTEST

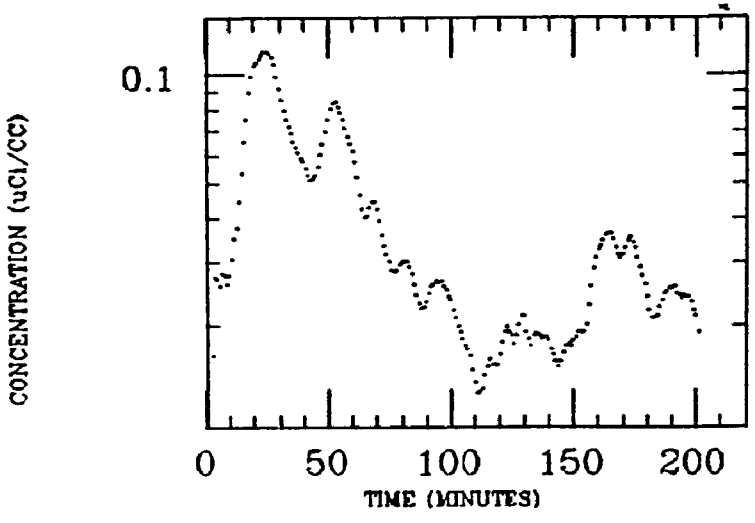

J.MCKINLEY
XE INGESTION
RADON

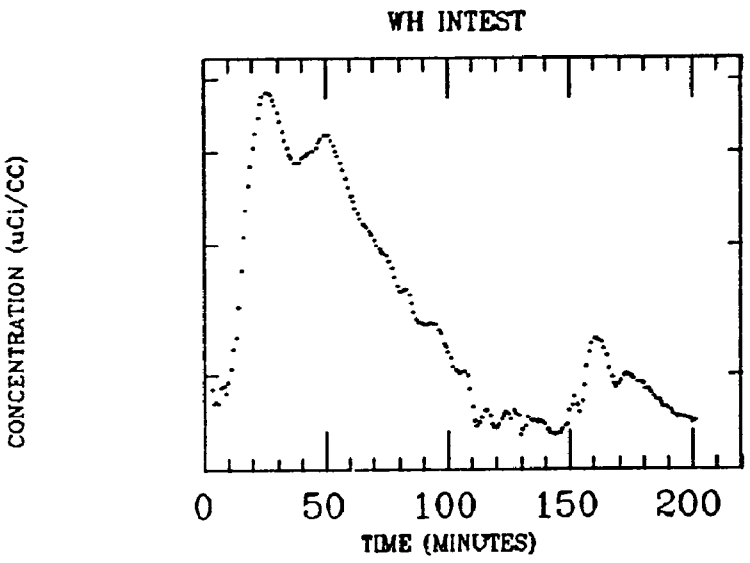

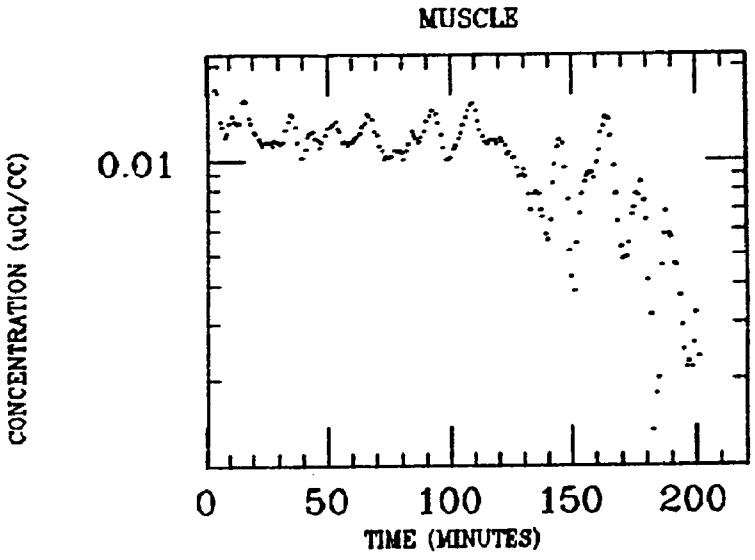

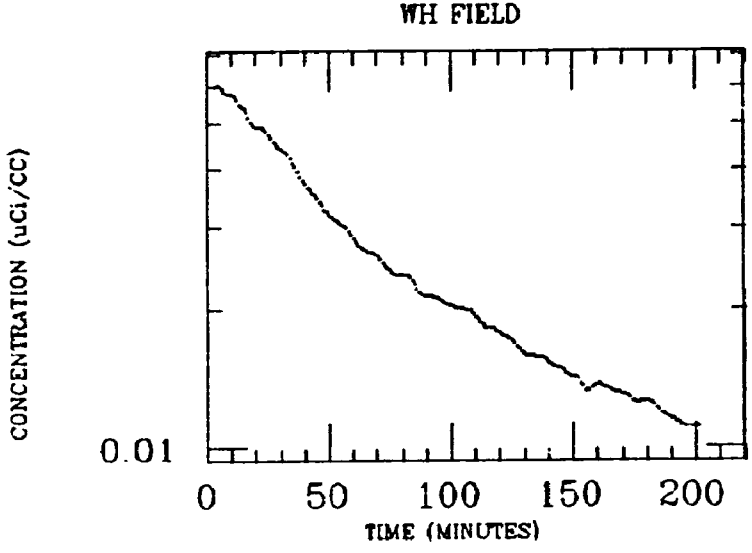

KELLEHER
XE INGESTION
RADON

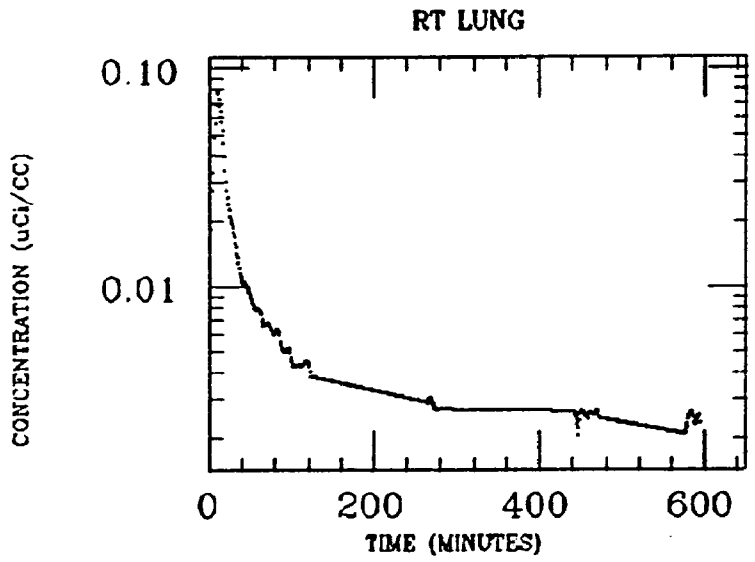

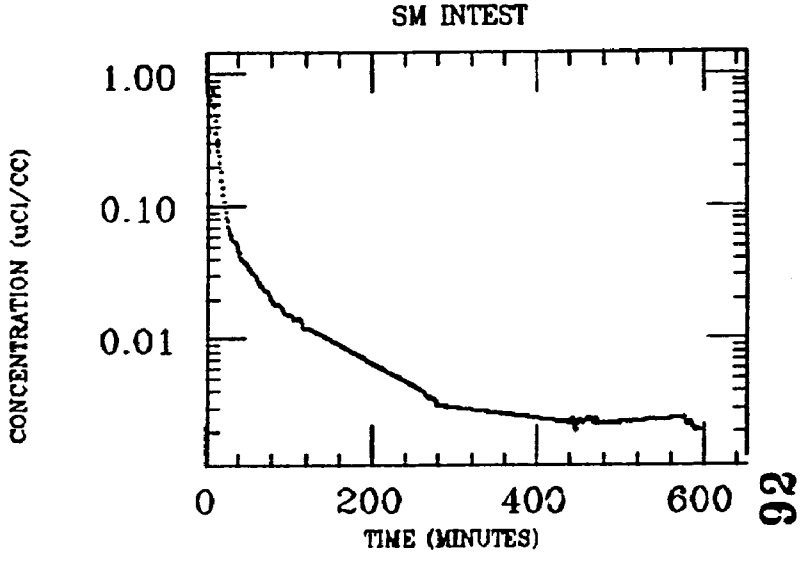

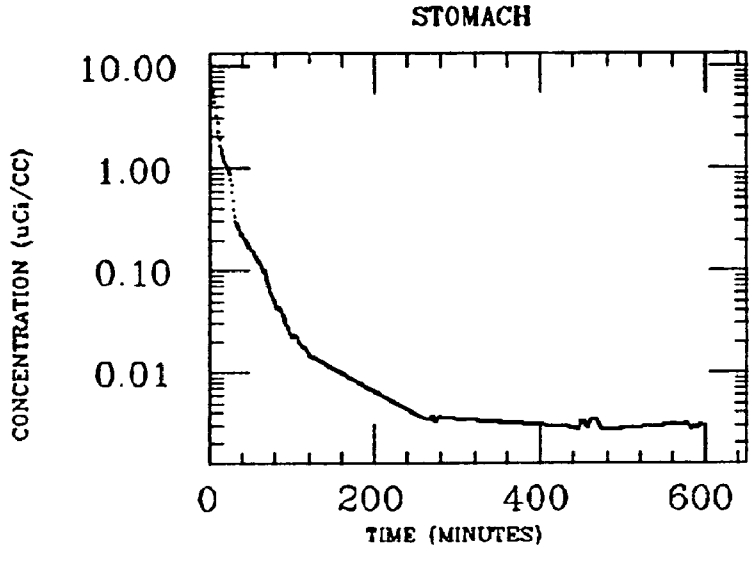

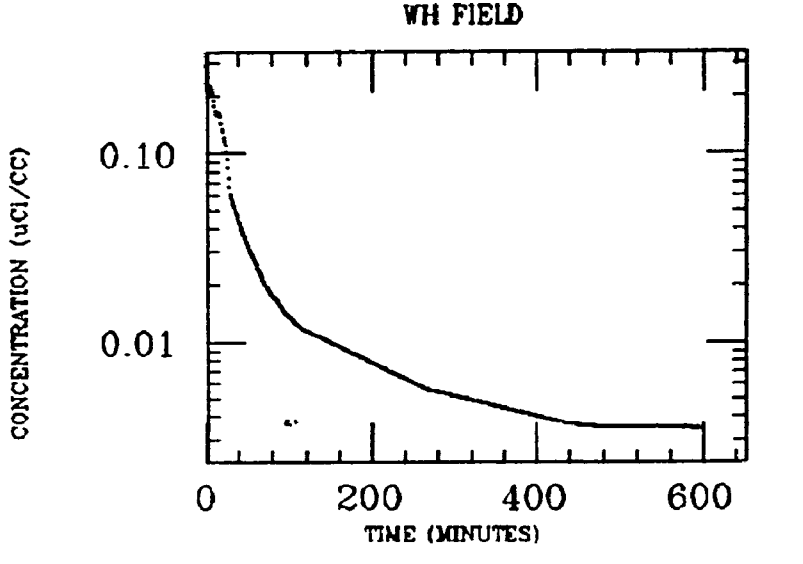

KELLEHER
XE INGESTION
RADON

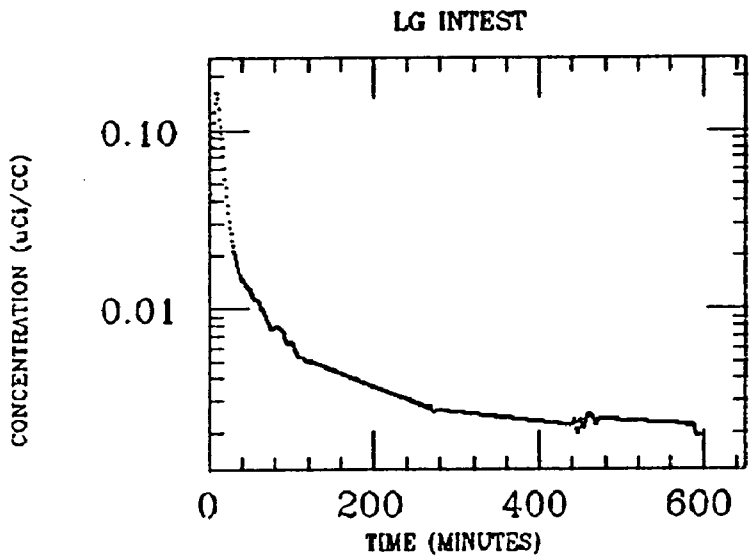

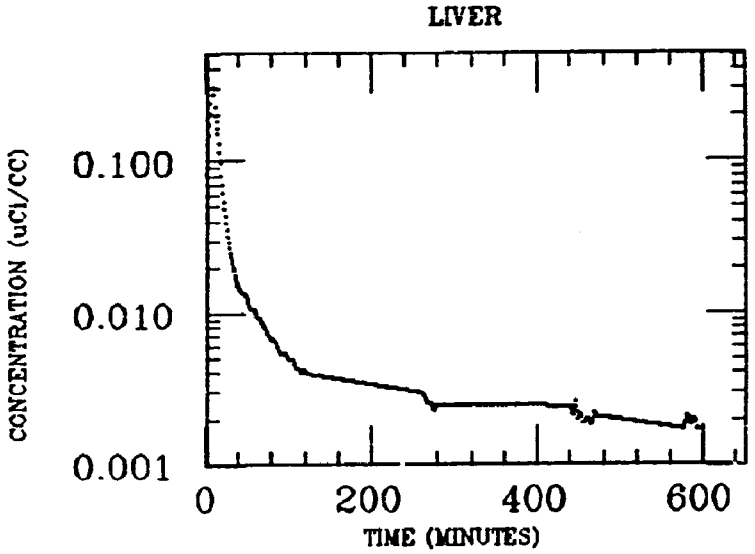

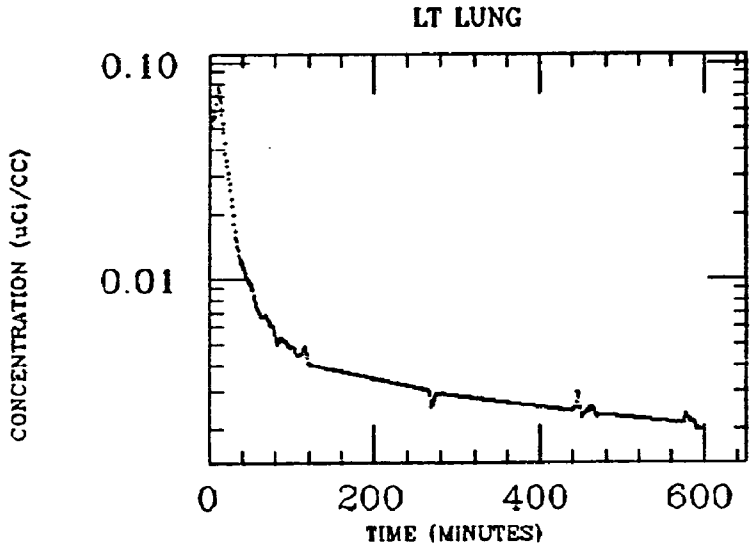

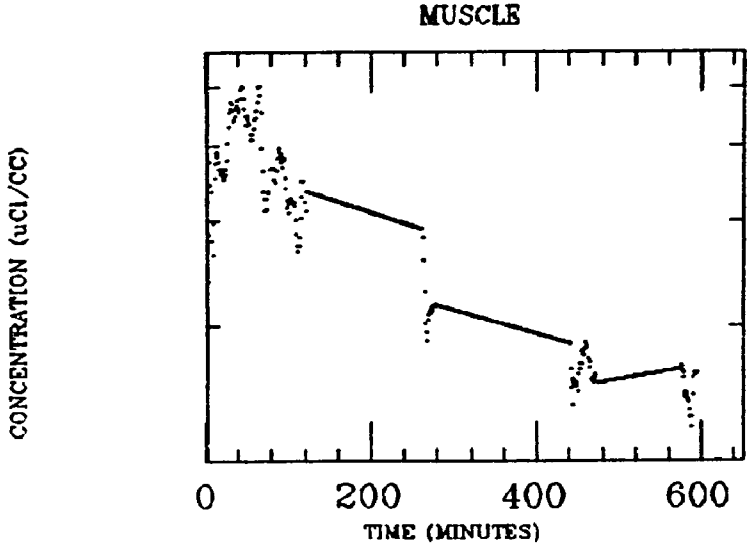

LITTELL
XE INGESTION
RADON

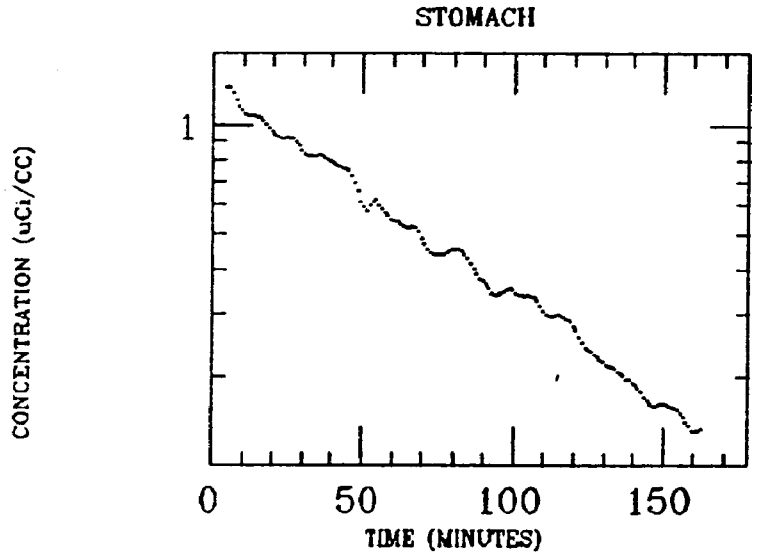

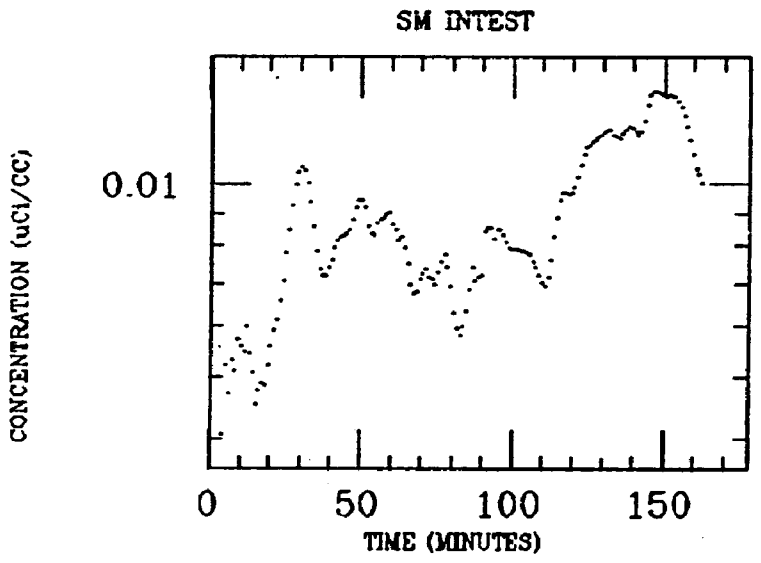

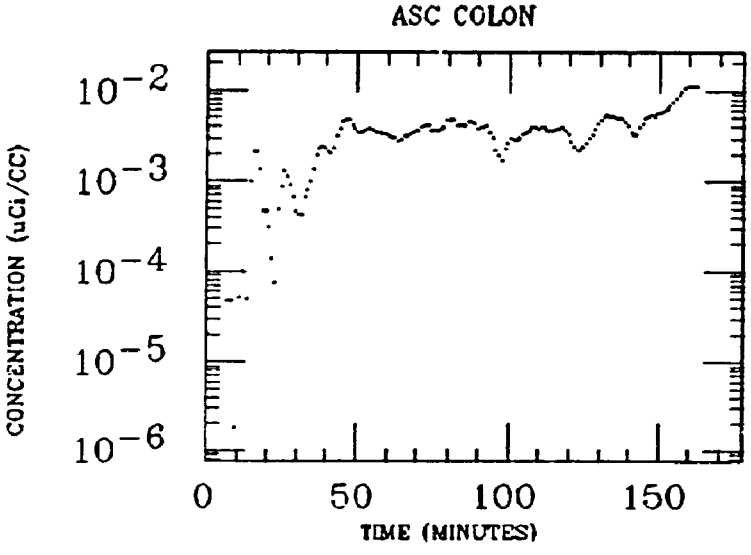

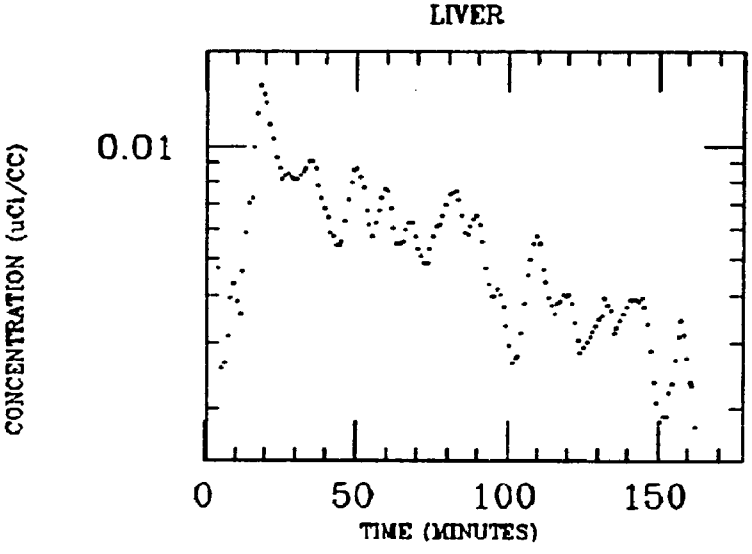

LITTELL
XE INGESTION
RADON

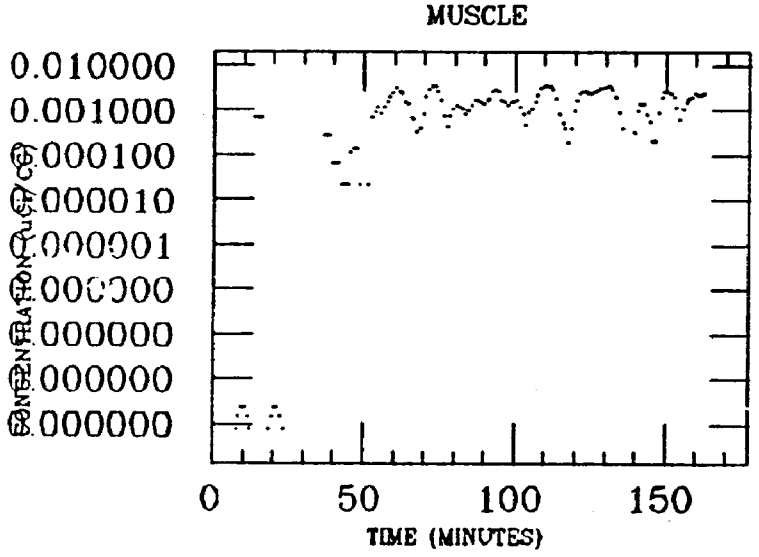

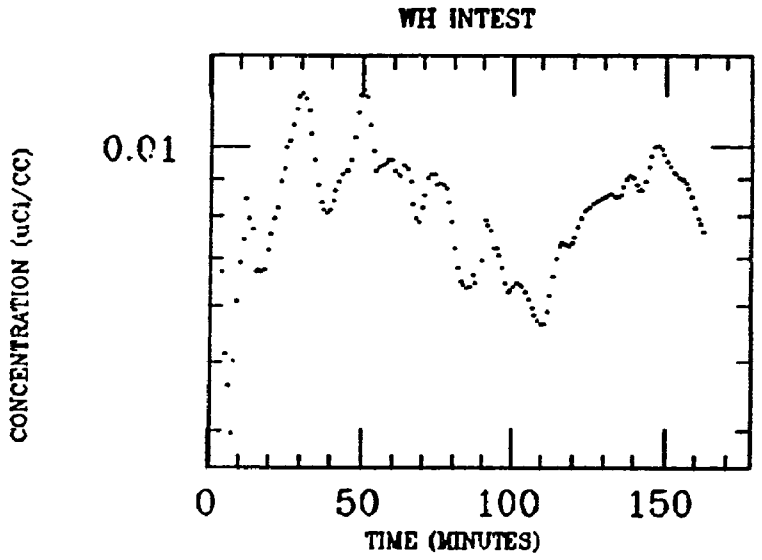

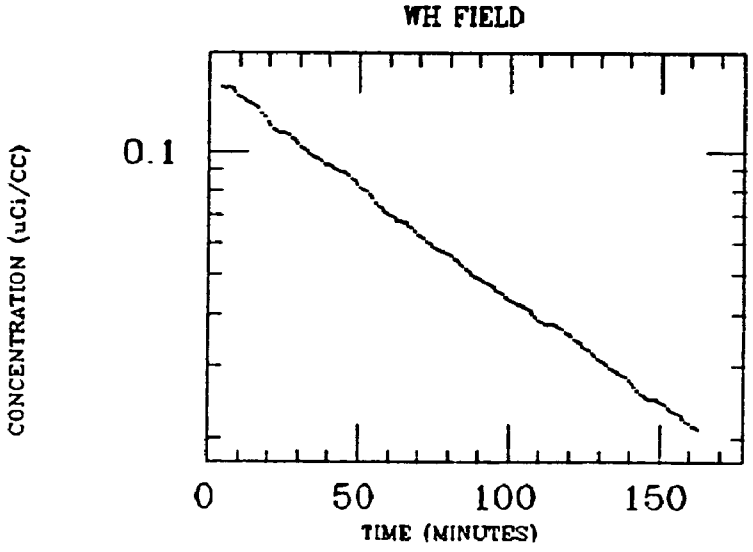

MACMILLAN
XE INGESTION
RADON

ASC COLON

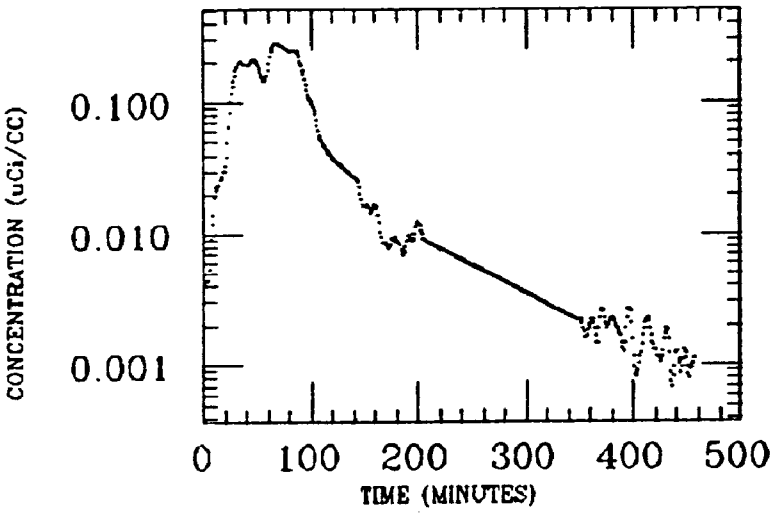

DES COLON

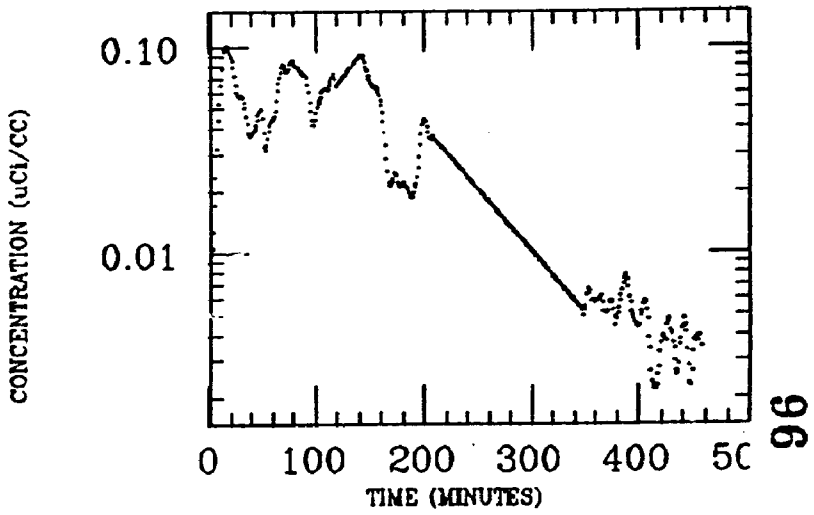

HIP

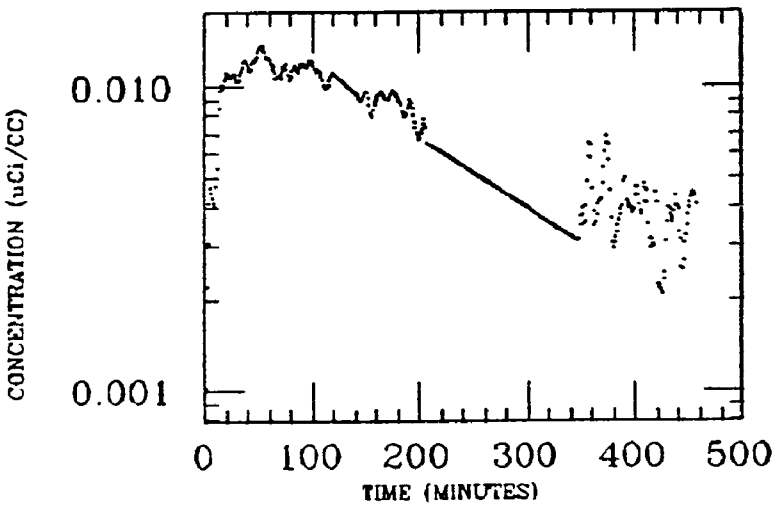

LIVER

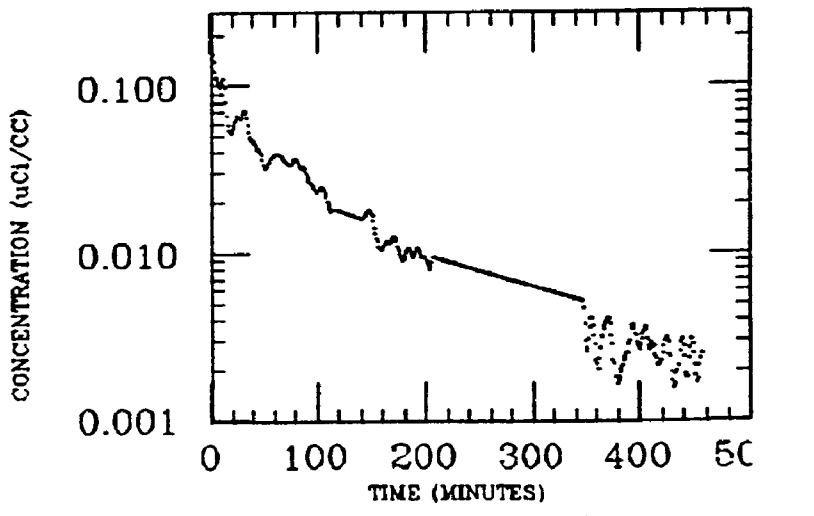

MACMILLAN
XE INGESTION
RADON

SM INTEST

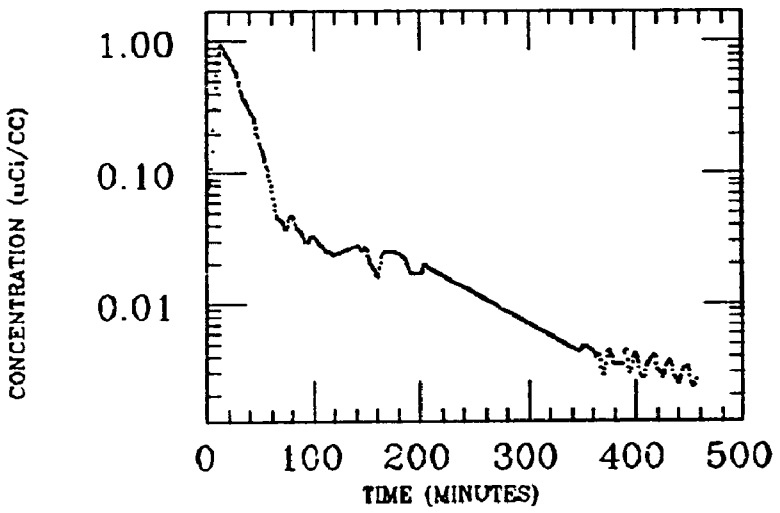

STOMACH

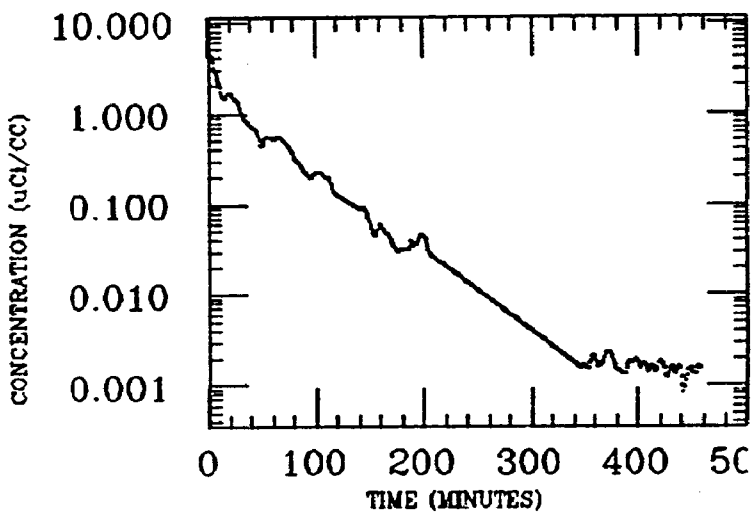

TR COLON

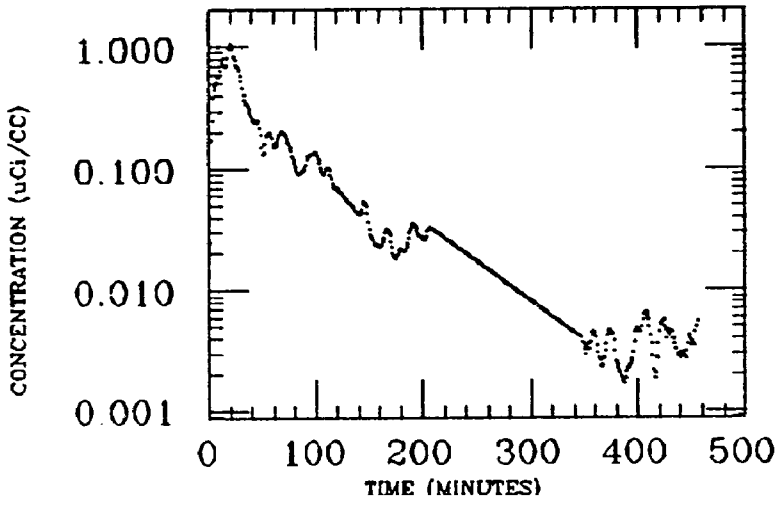

WH INTEST

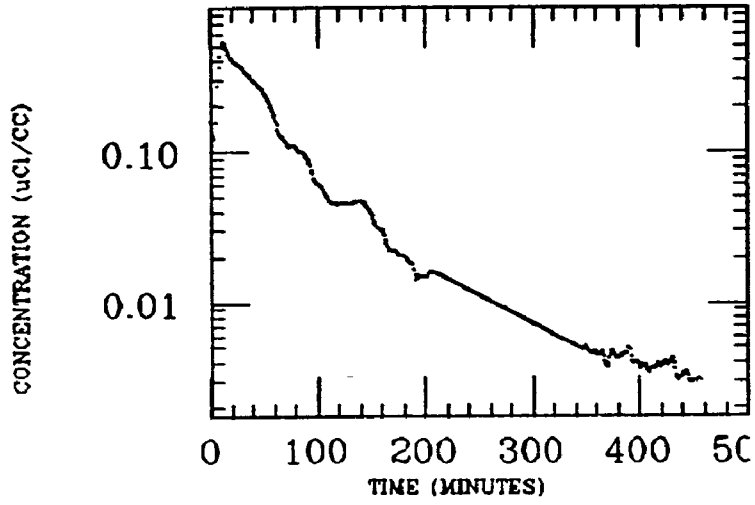

MAIO

XE INGESTION

RADON

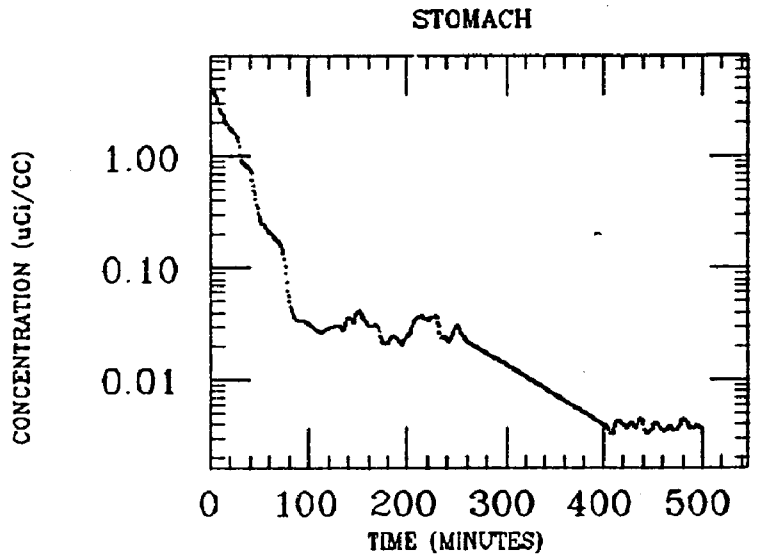

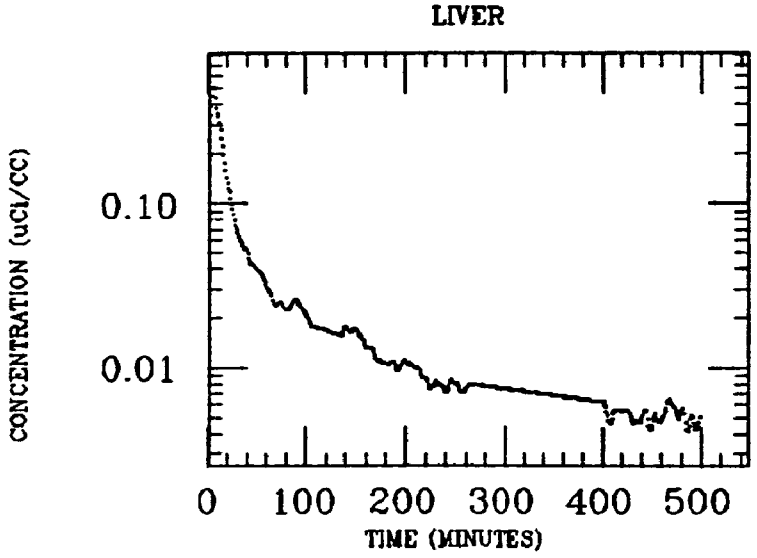

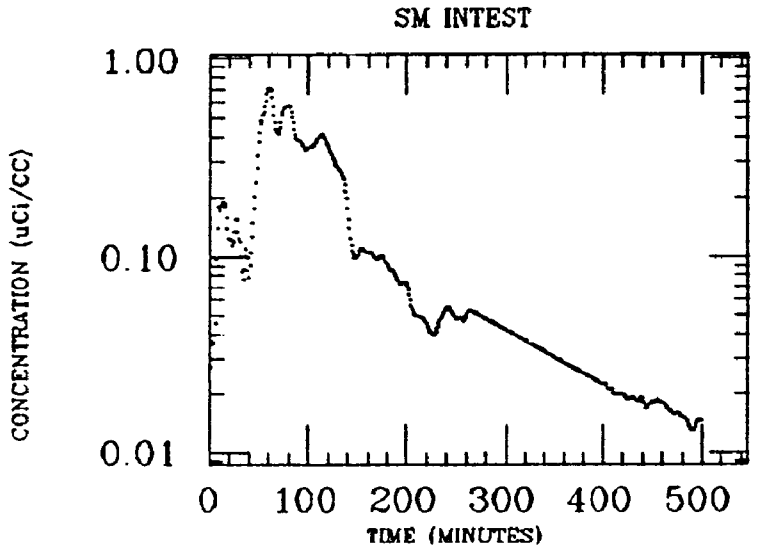

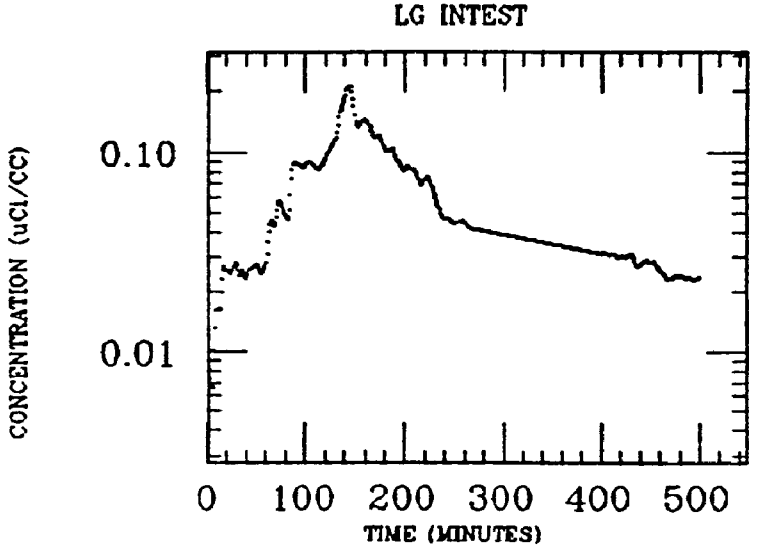

MAIO
XE INGESTION
RADON

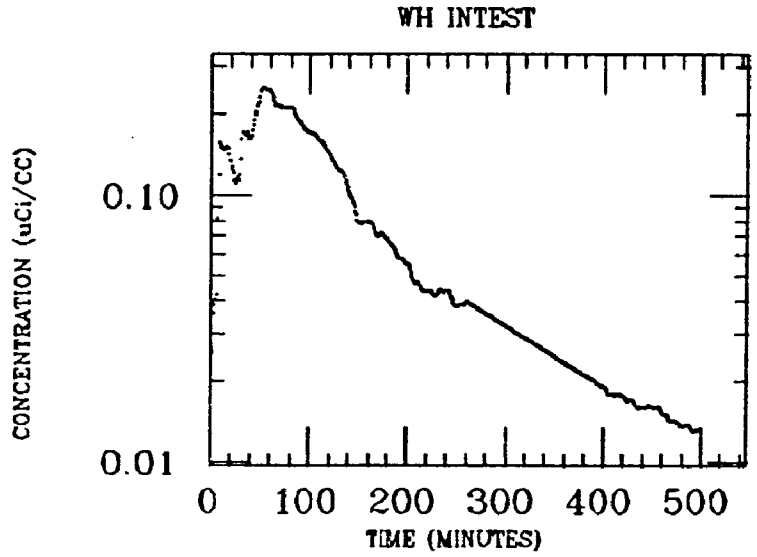

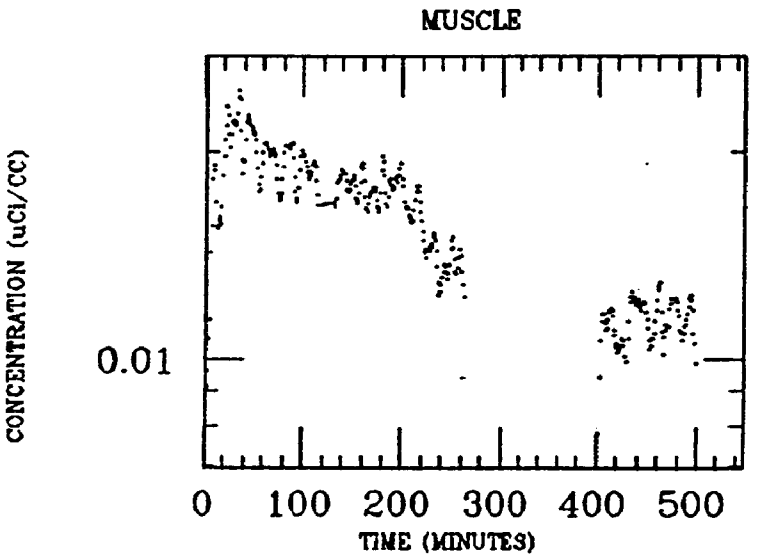

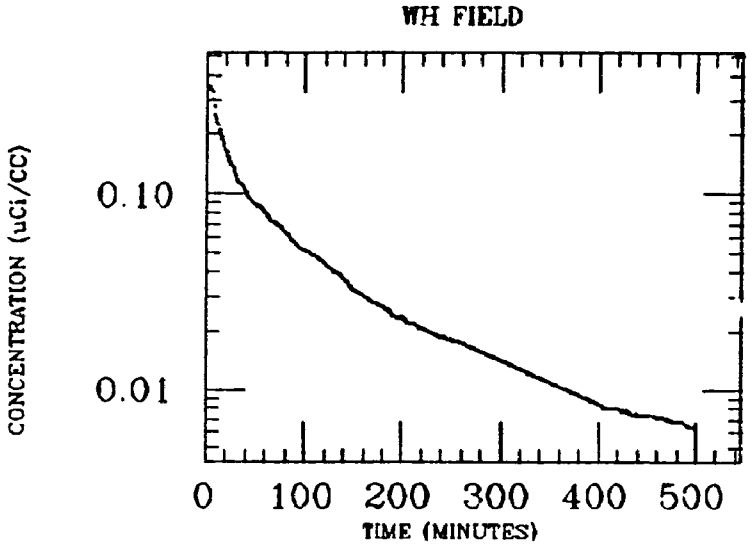

MONROE
XE INGESTION
RADON

STOMACH

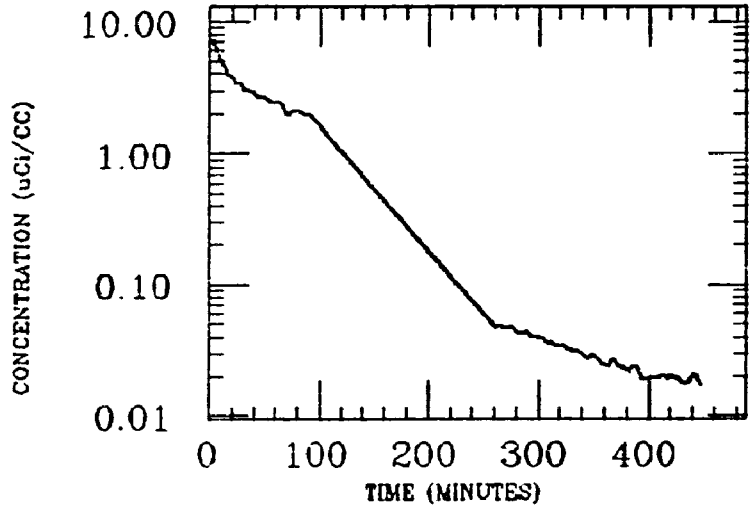

LIVER

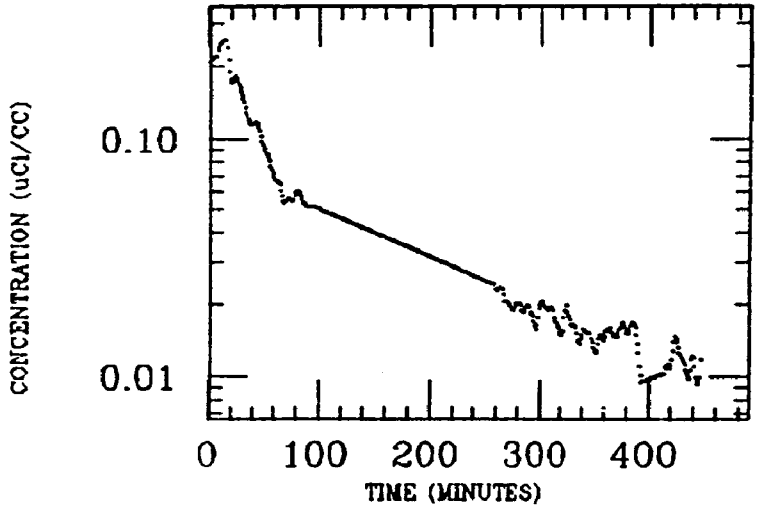

WH INTEST

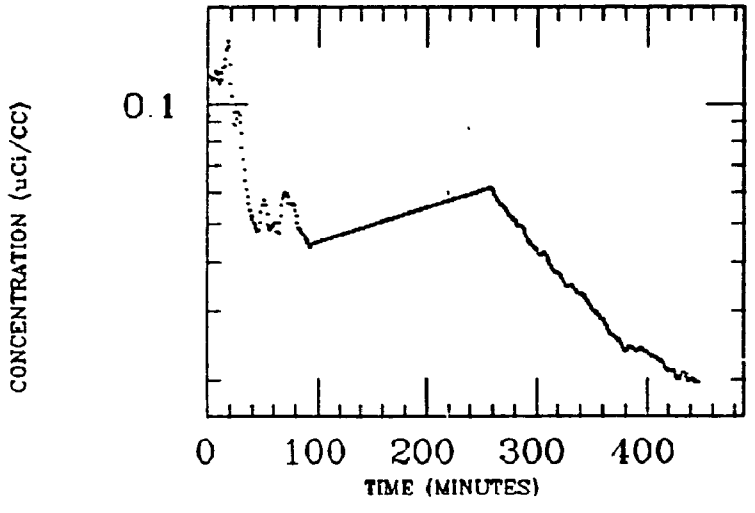

MUSCLE

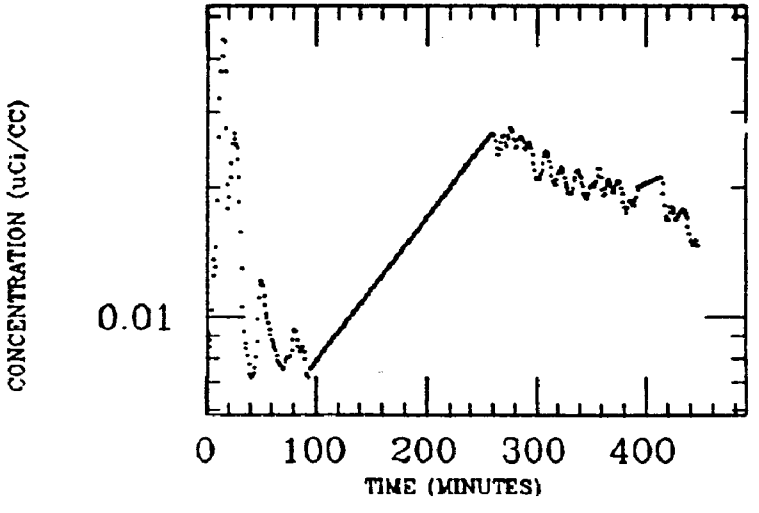

100 1

MONROE
XE INGESTION
RADON

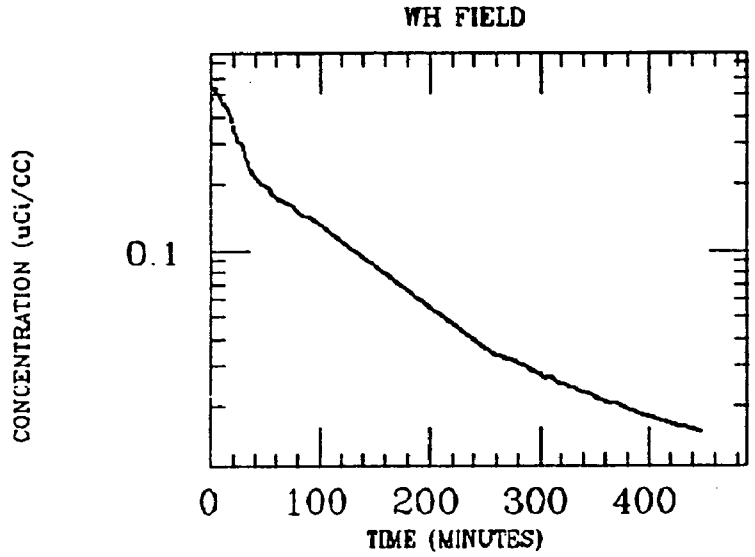

MORGAN
XE INGESTION
RADON

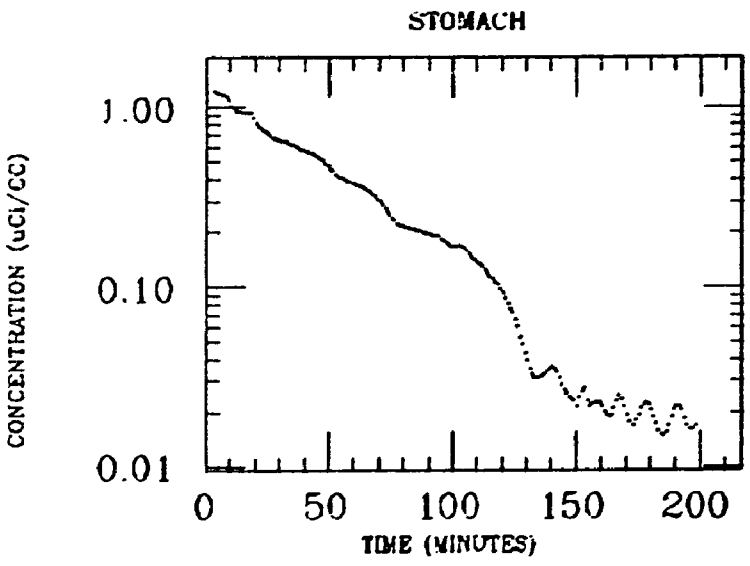

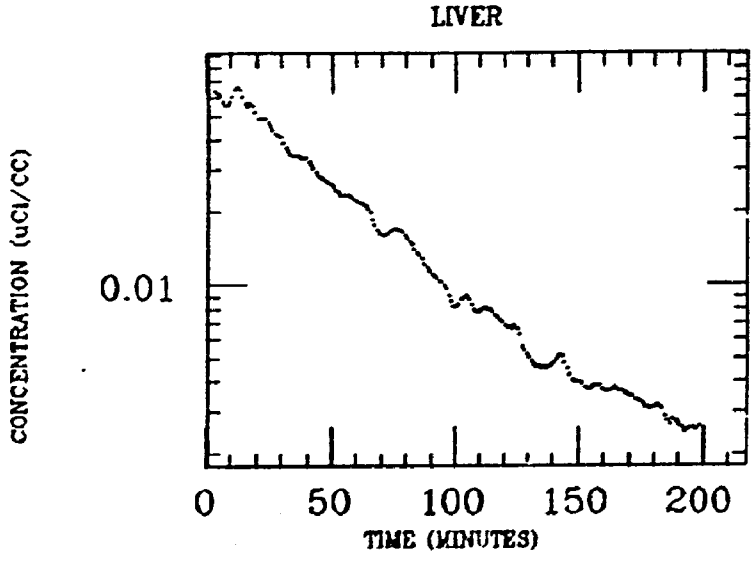

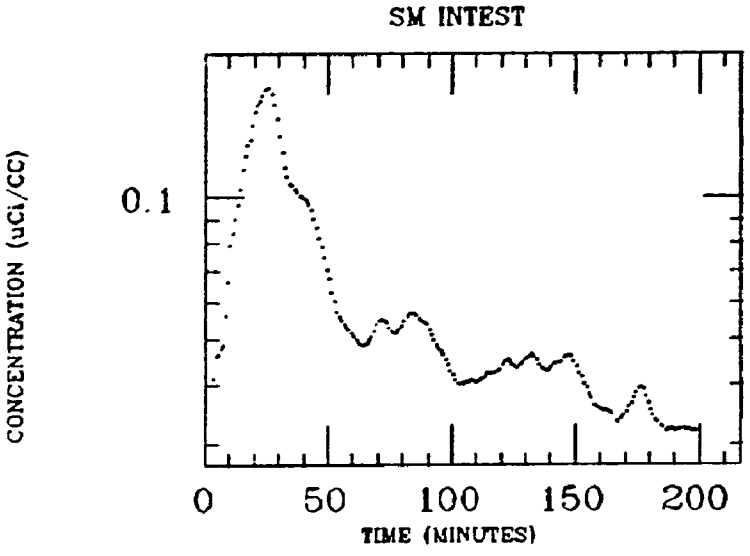

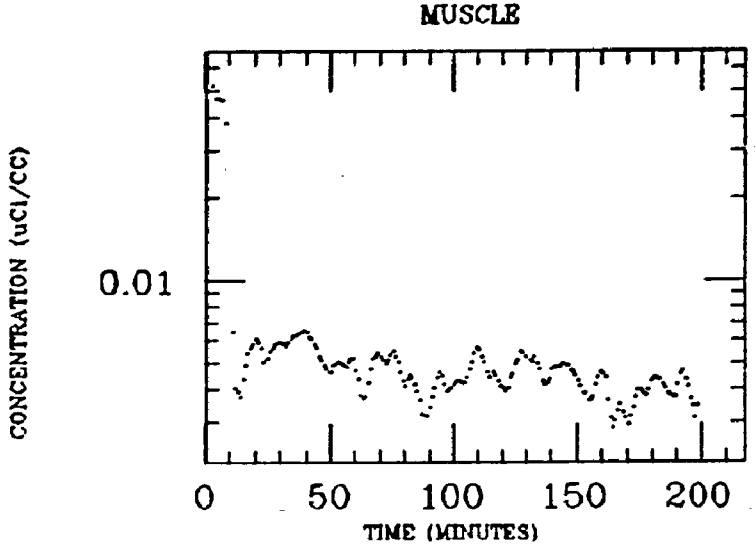

MORGAN
XE INGESTION
RADON

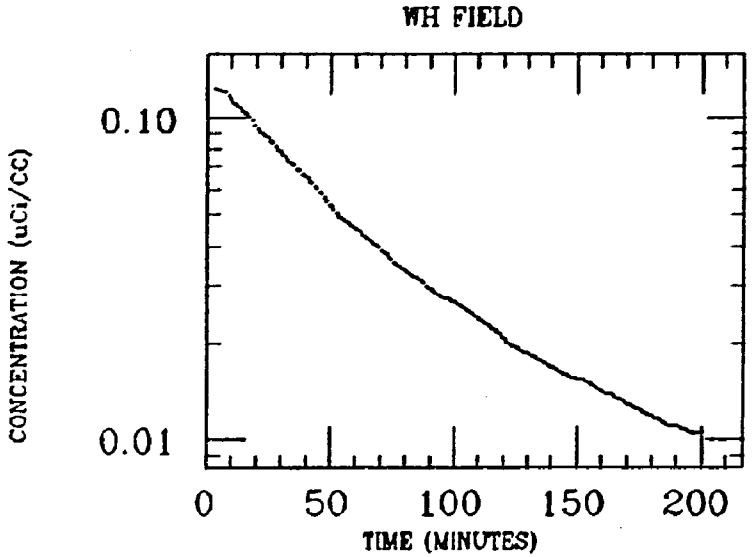

MURCHE
XE INGESTION
RADON

STOMACH

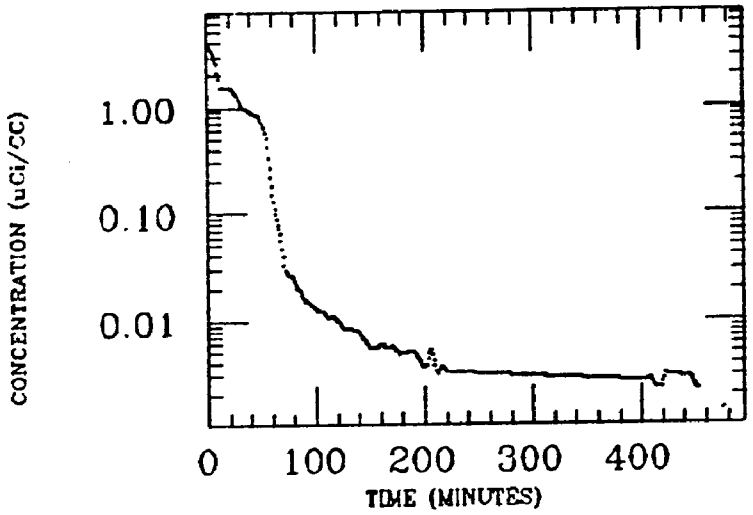

LIVER

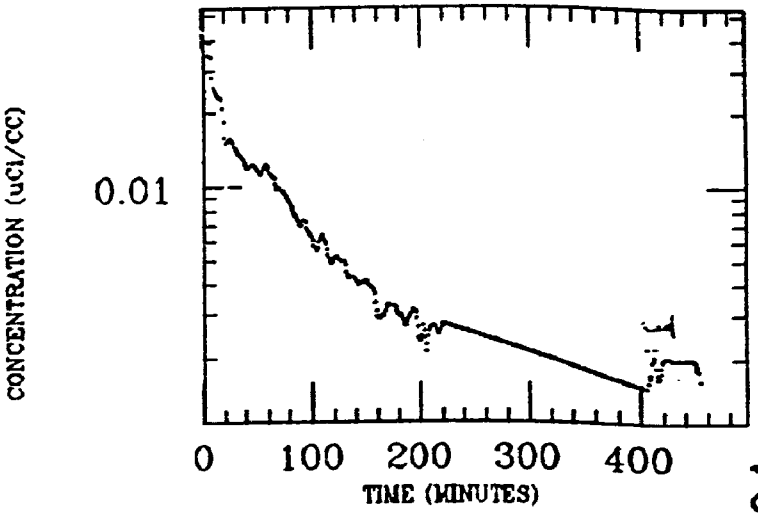

WH FIELD

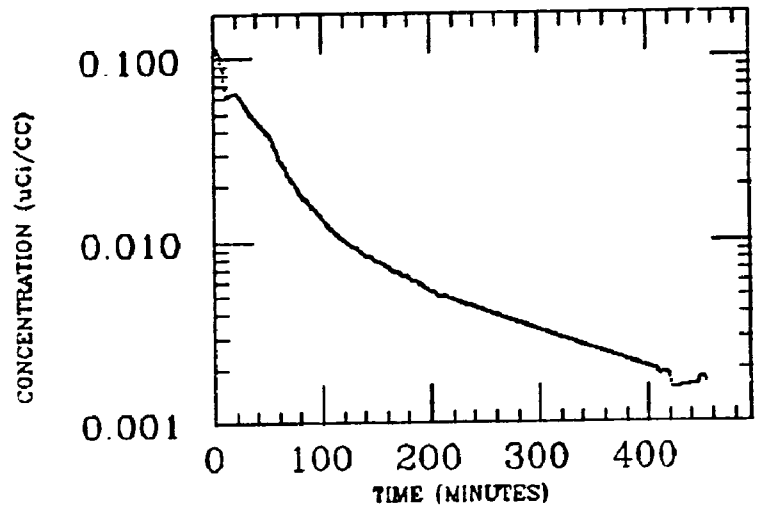

MURCHE
XE INGESTION
RADON

STOMACH

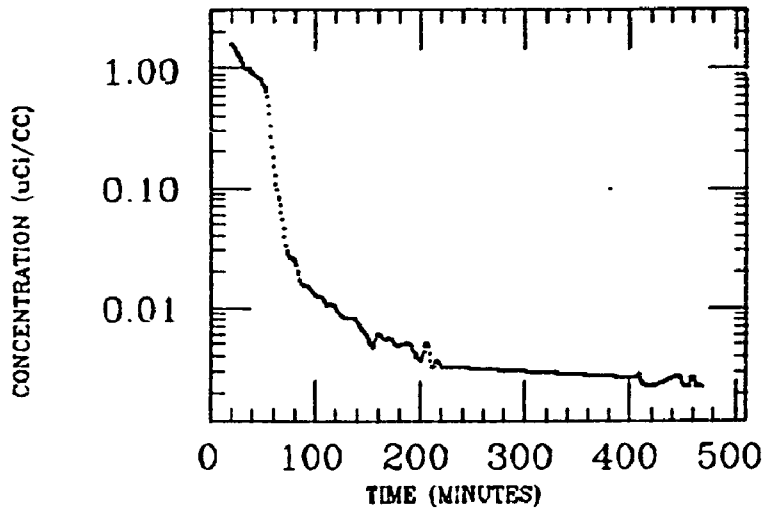

LIVER

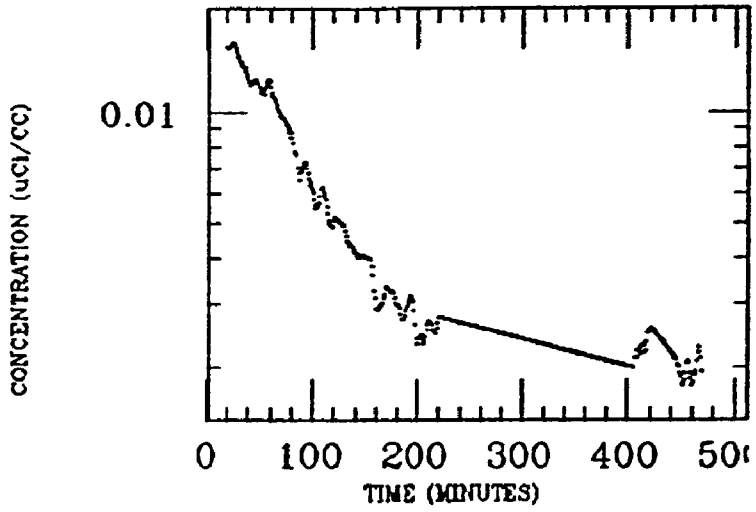

SM INTEST

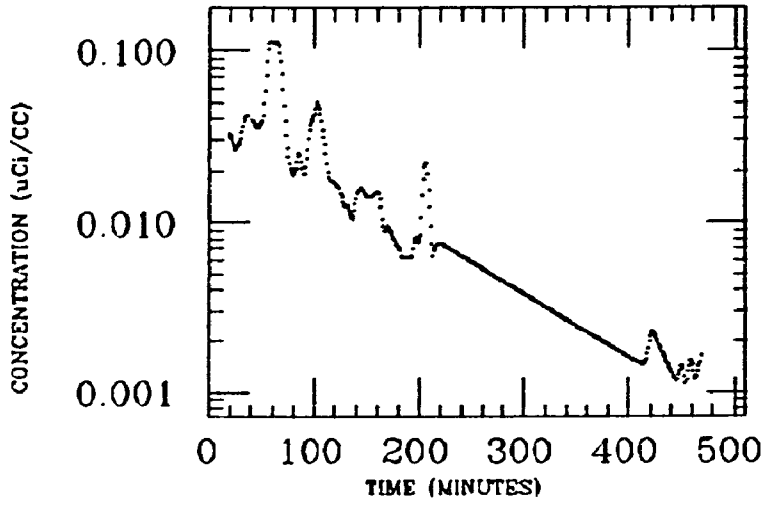

DES COLON

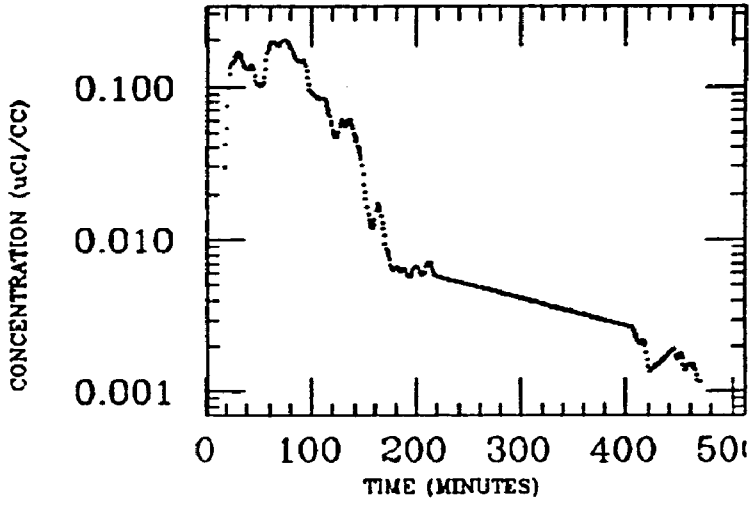

MURCHE
XE INGESTION
RADON

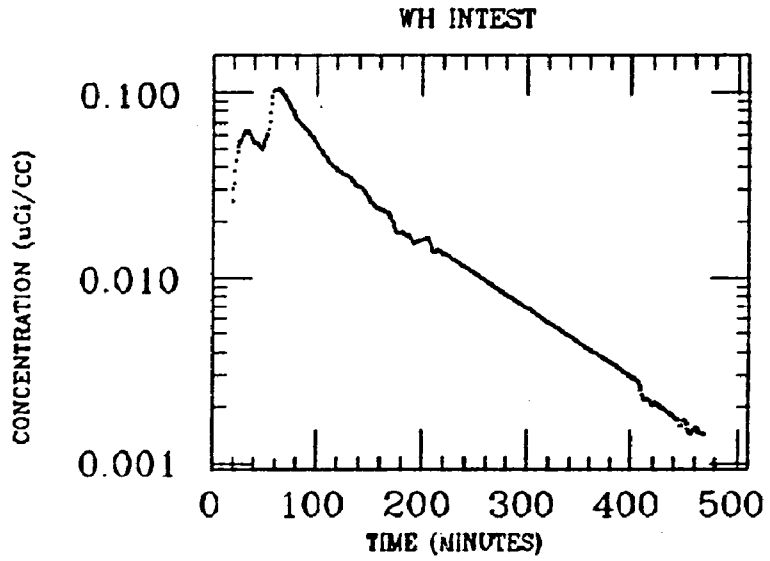

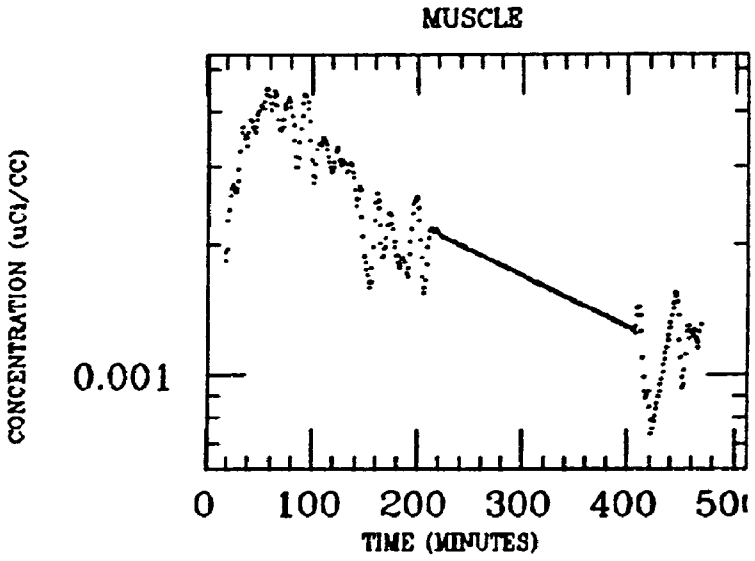

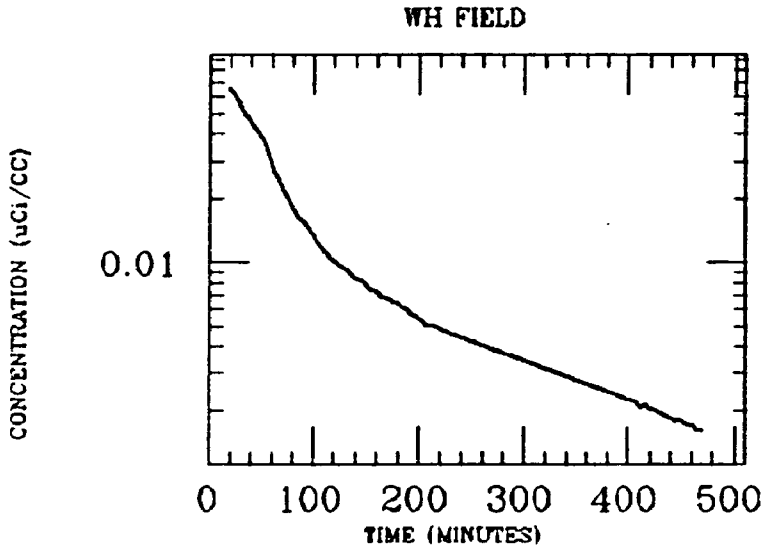

PARK
XE INGESTION
RADON

STOMACH

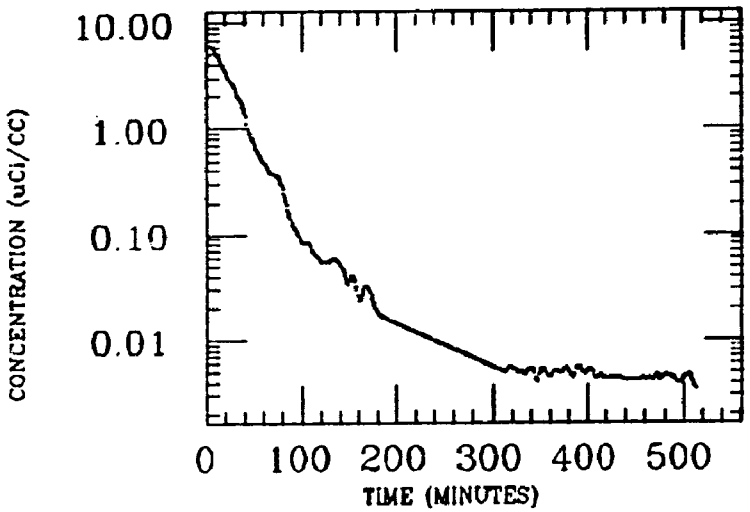

STOMACH 2

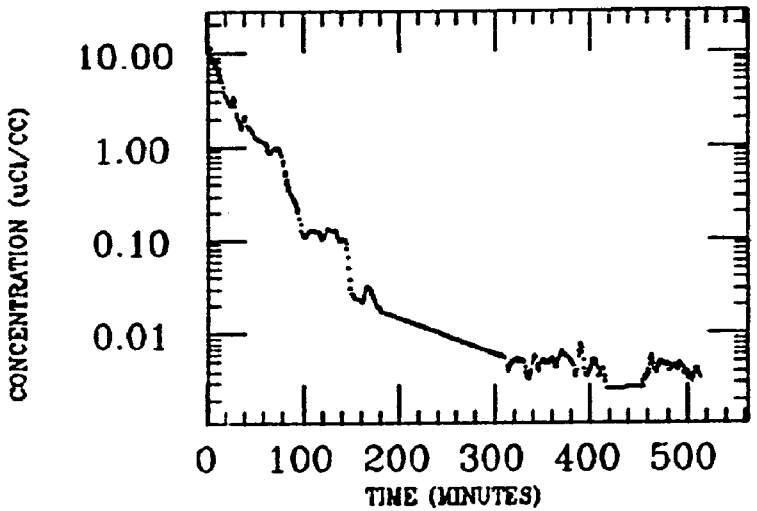

SM INTEST

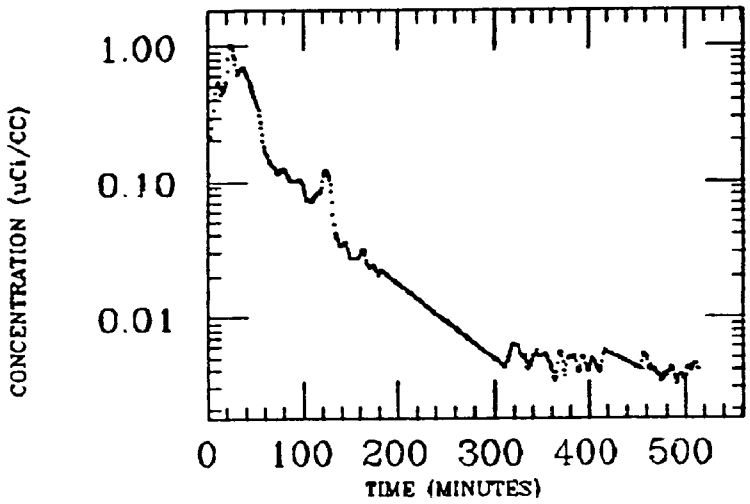

LIVER

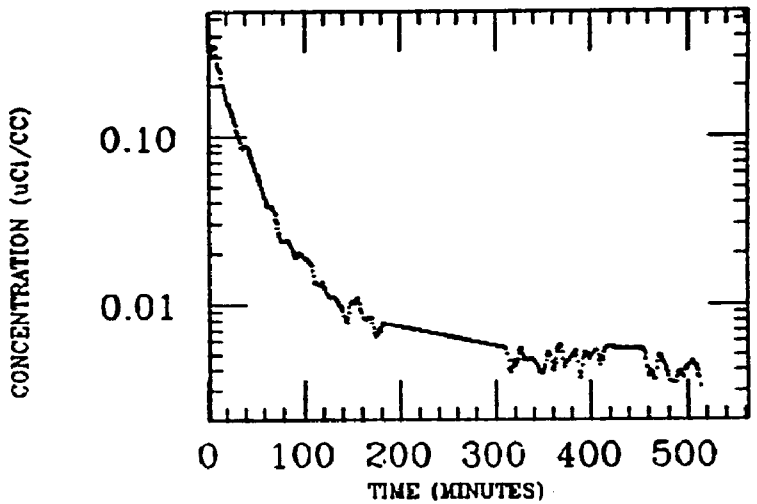

PARK
XE INGESTION
RADON

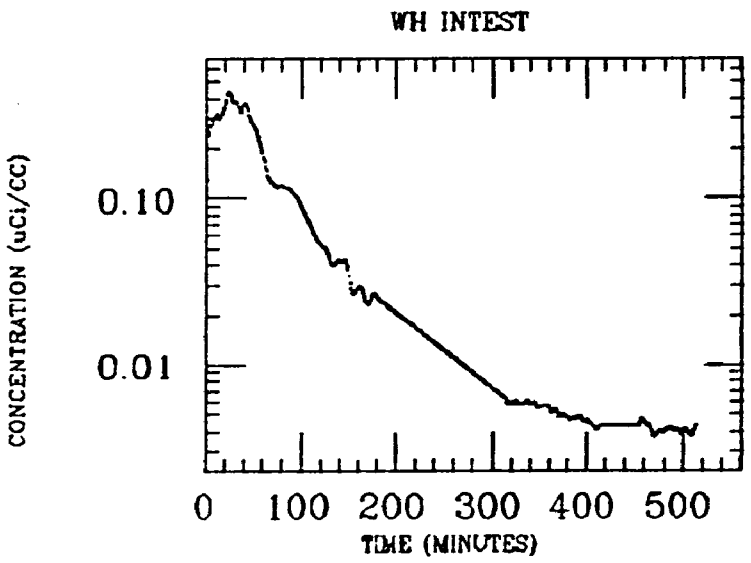

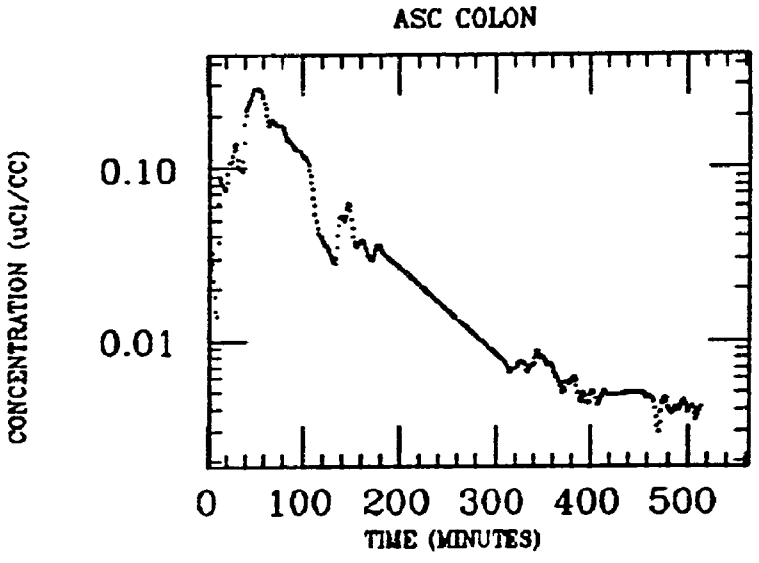

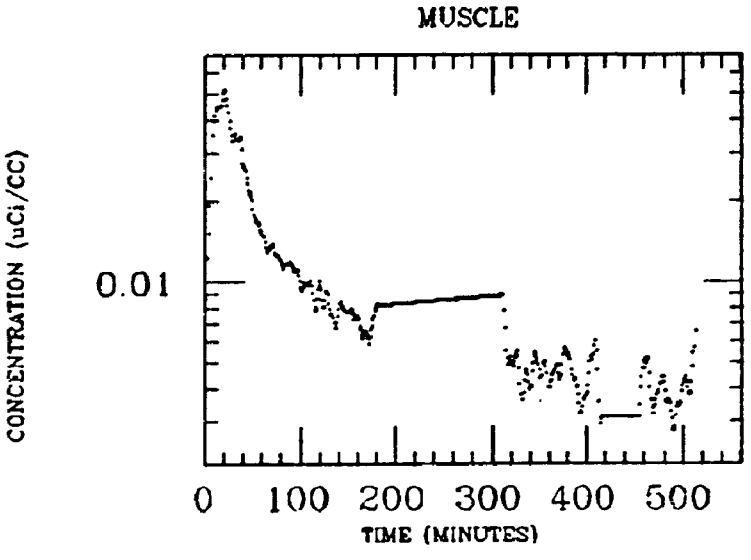

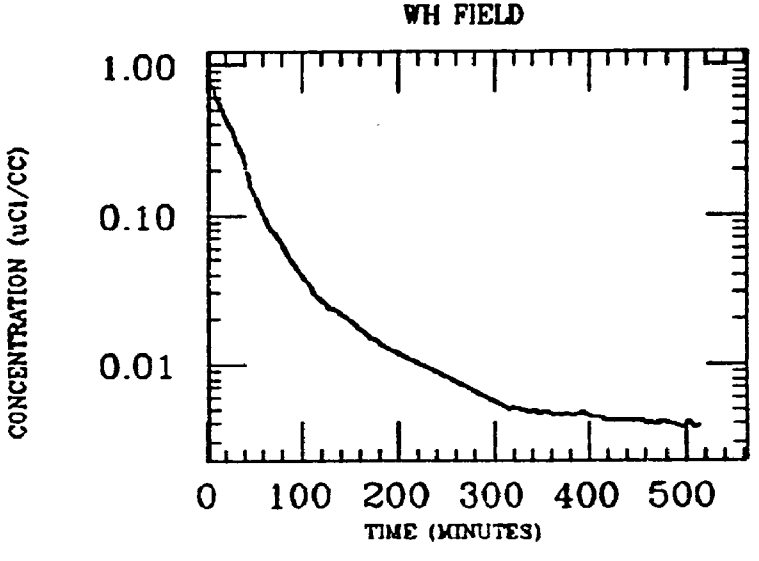

TAATJES
XE INGESTION
RADON

SM INTEST

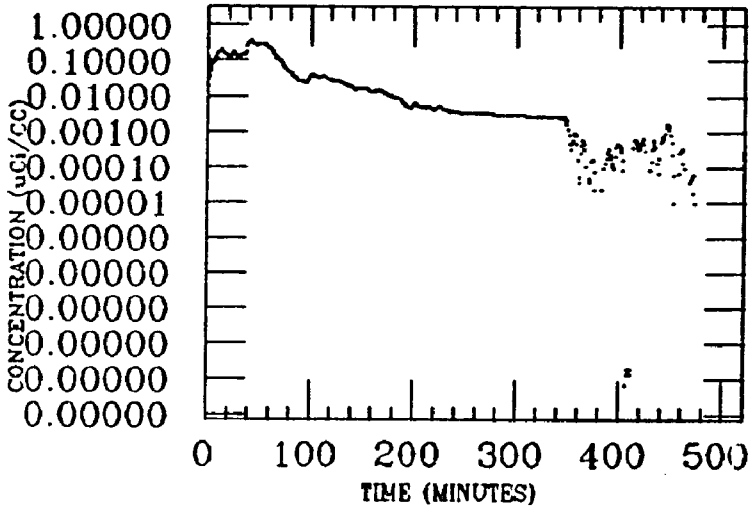

STOMACH

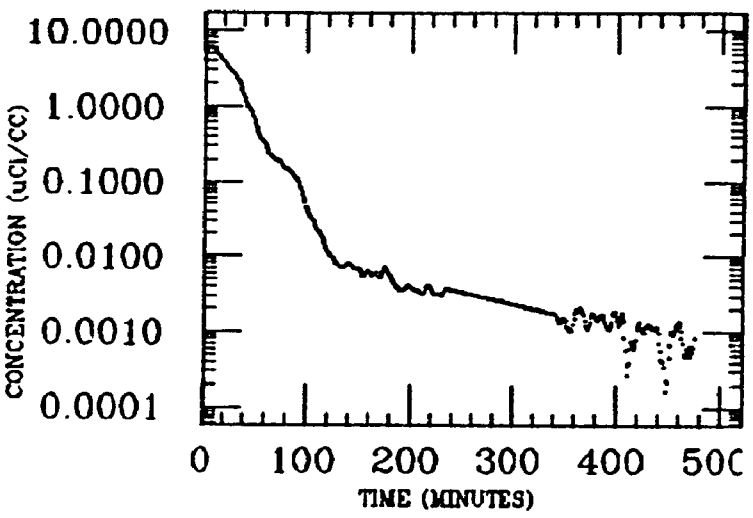

WH FIELD

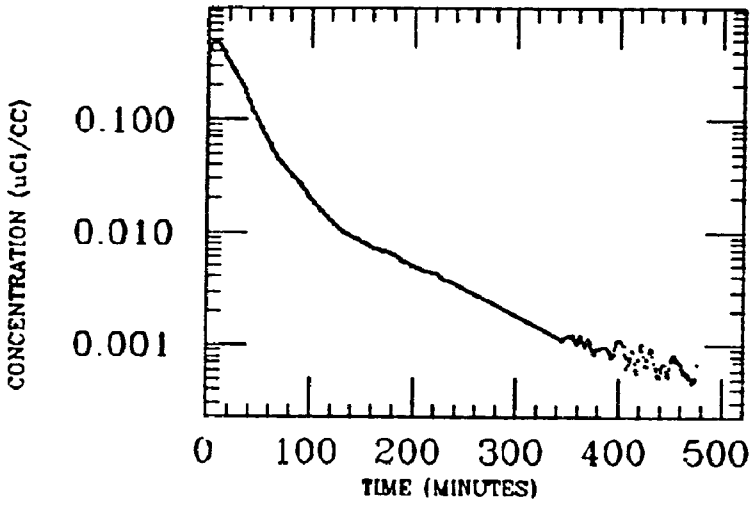

WH INTEST

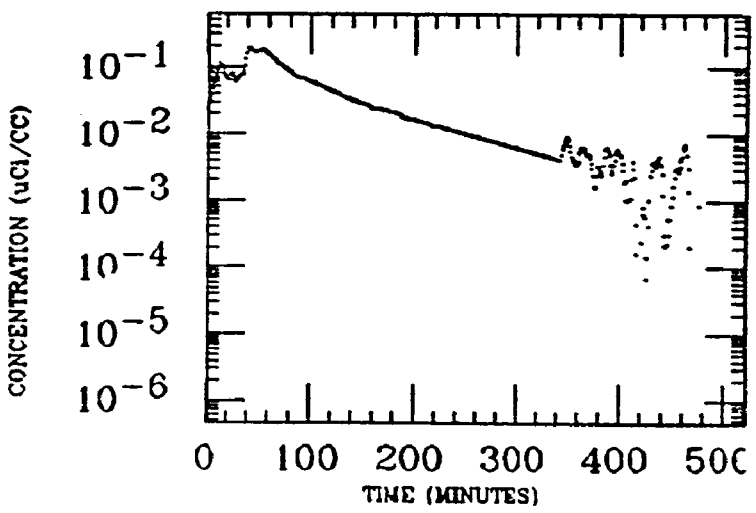

TAATJES
XE INGESTION
RADON

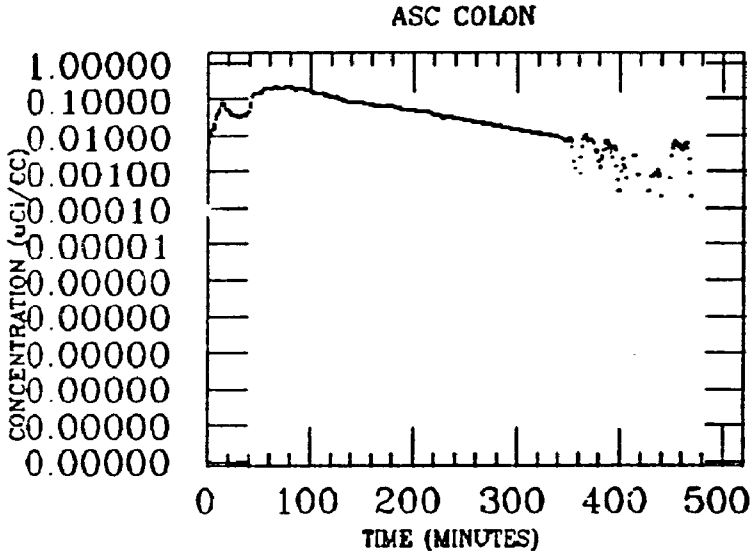

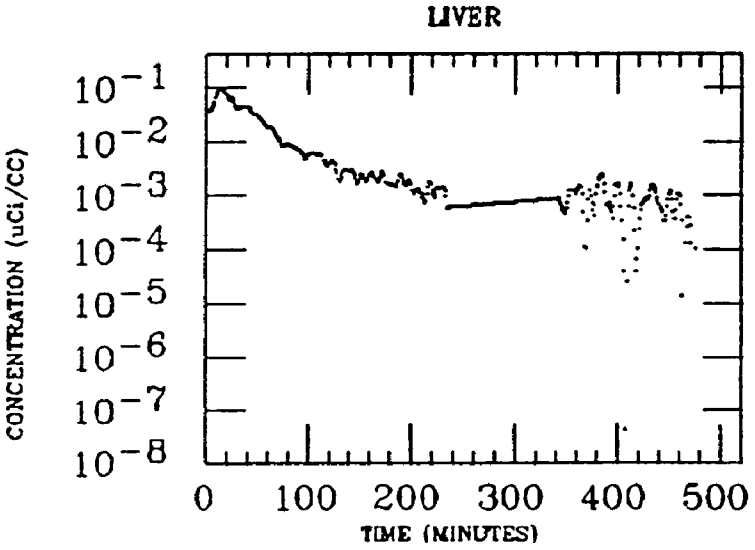

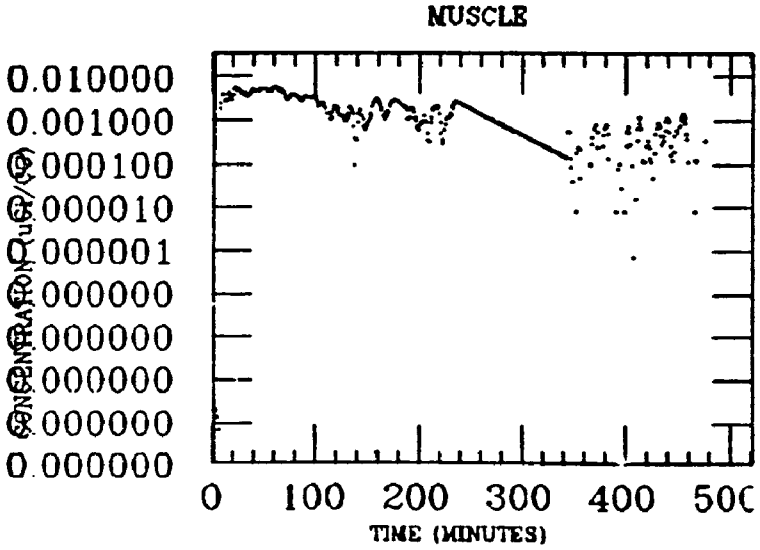

TAYLOR
XE INGESTION
RADON

STOMACH

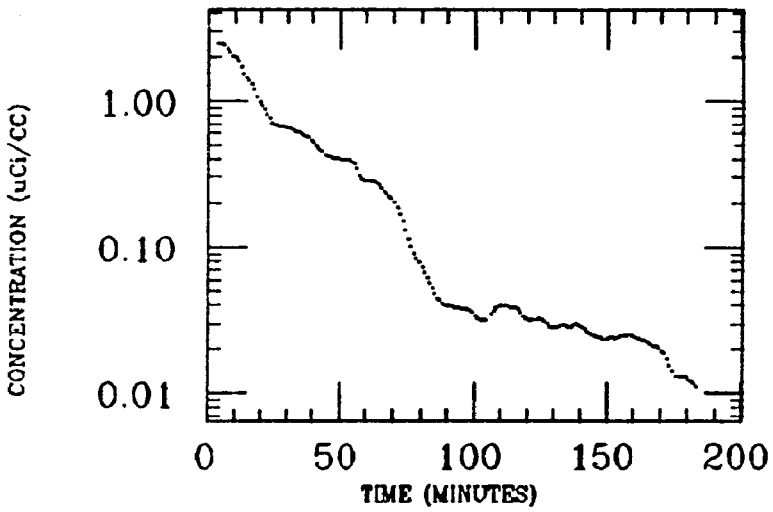

LIVER

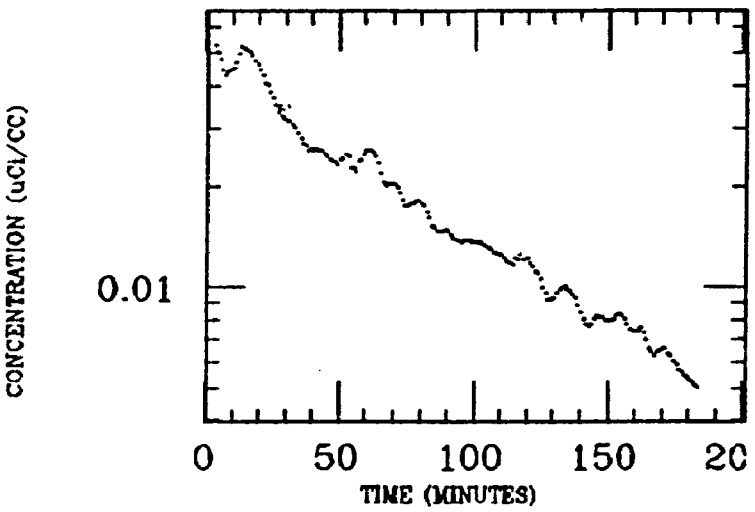

SM INTEST

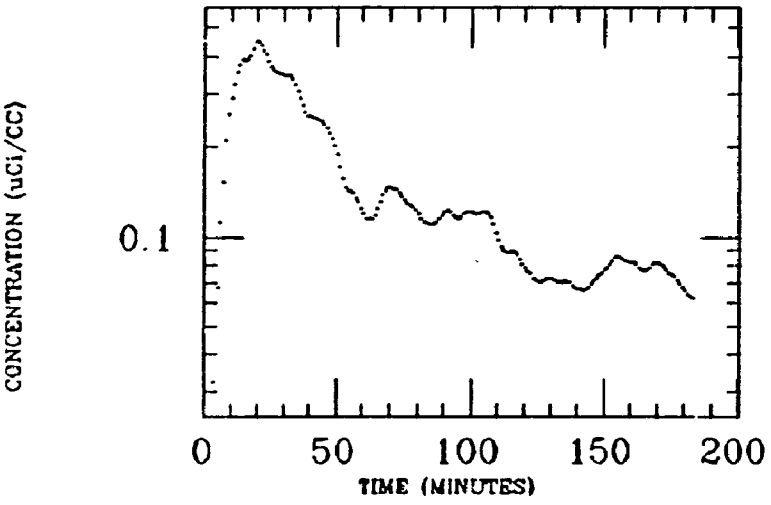

ASC COLON

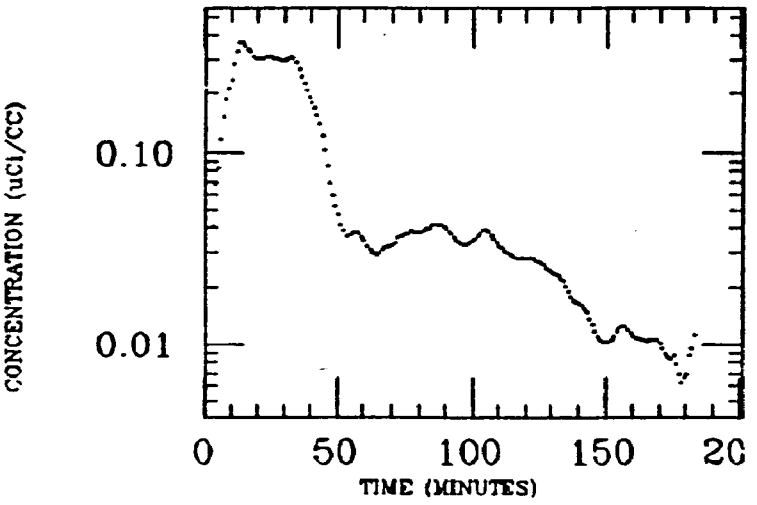

TAYLOR
XE INGESTION
RADON

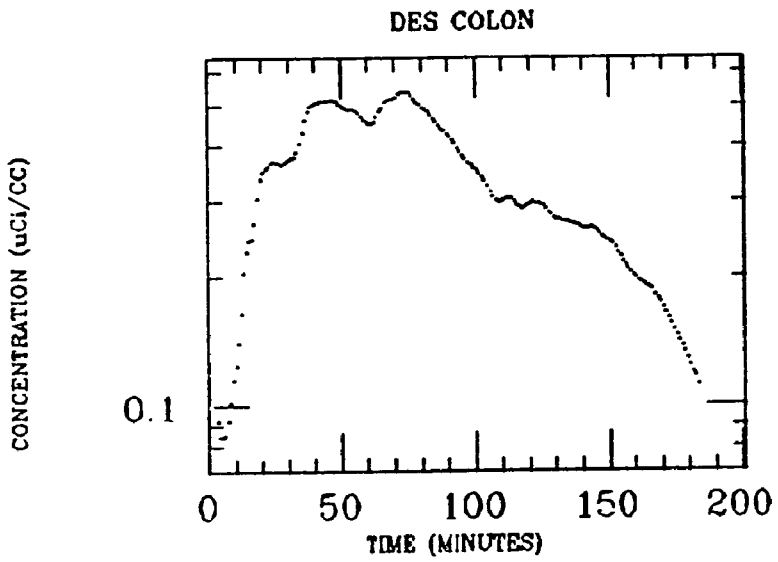

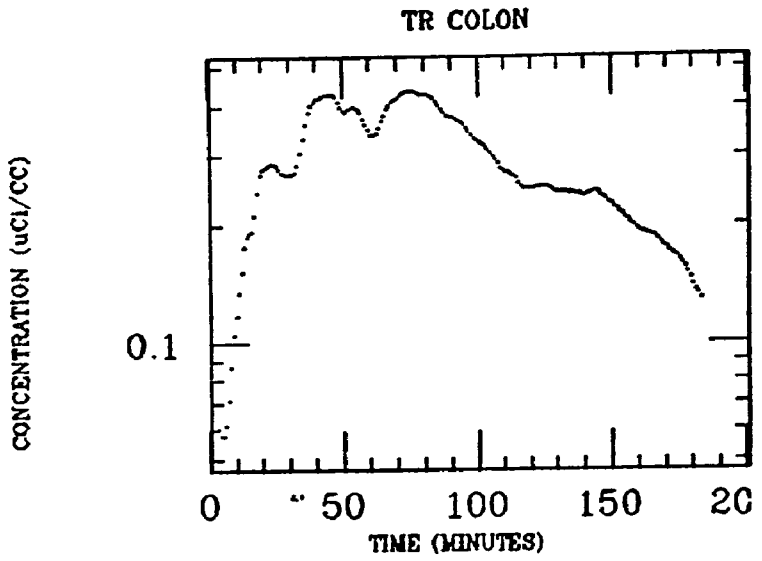

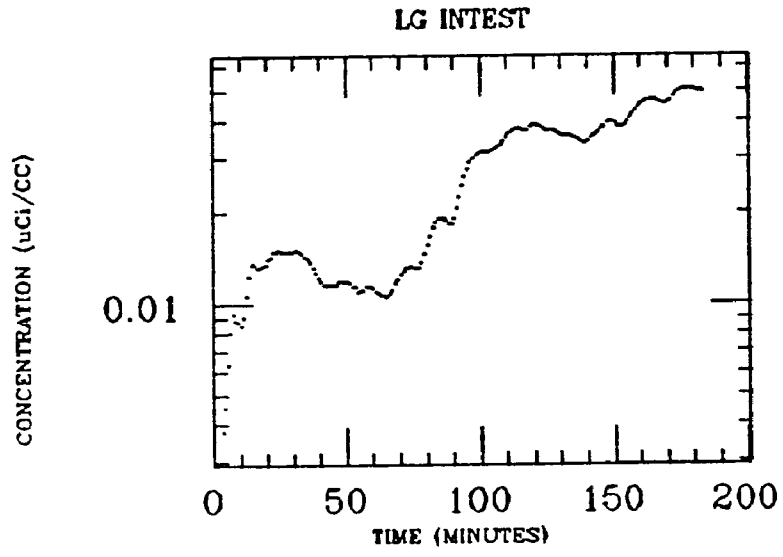

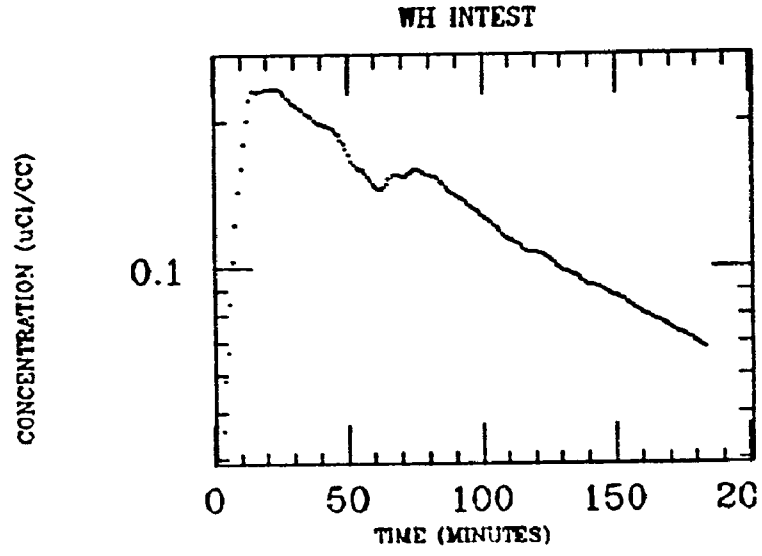

TAYLOR
XE INGESTION
RADON

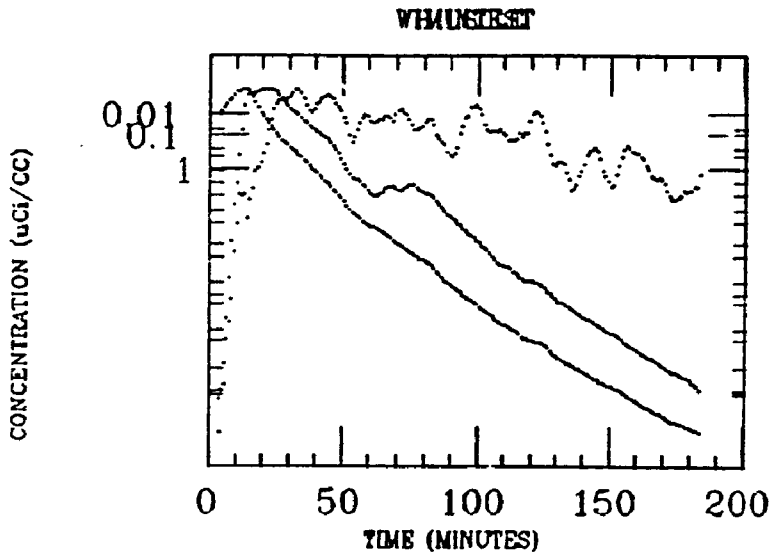

WESOLEK
XE INGESTION
RADON

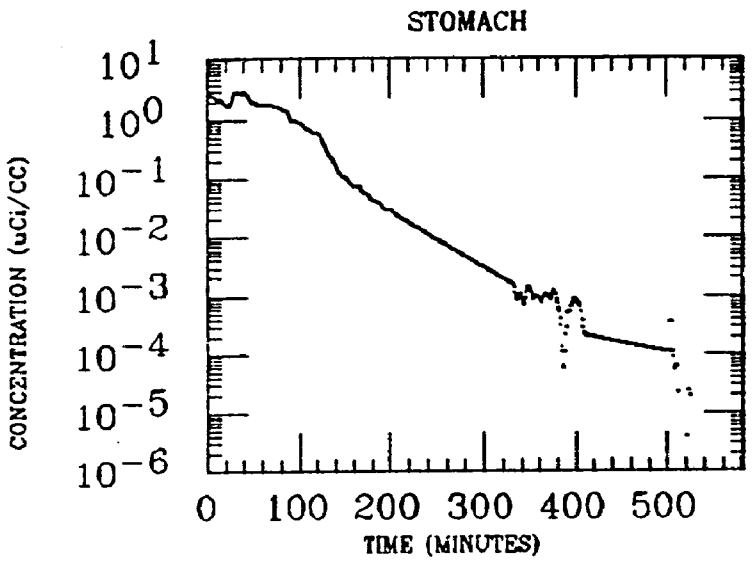

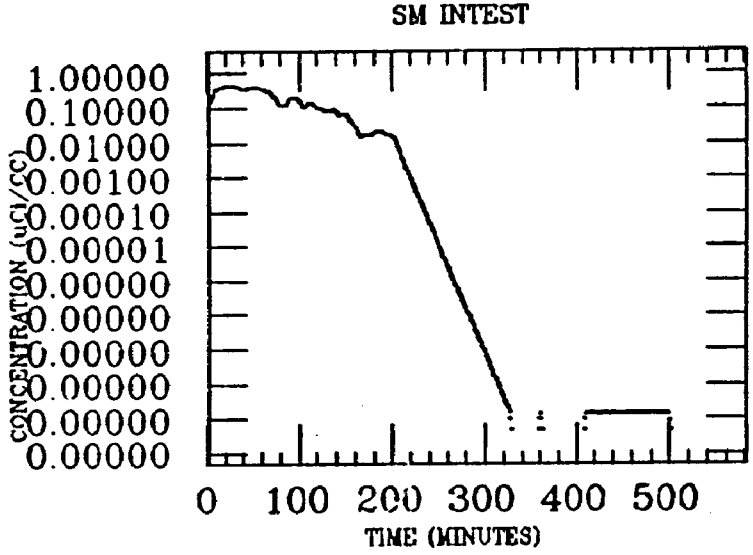

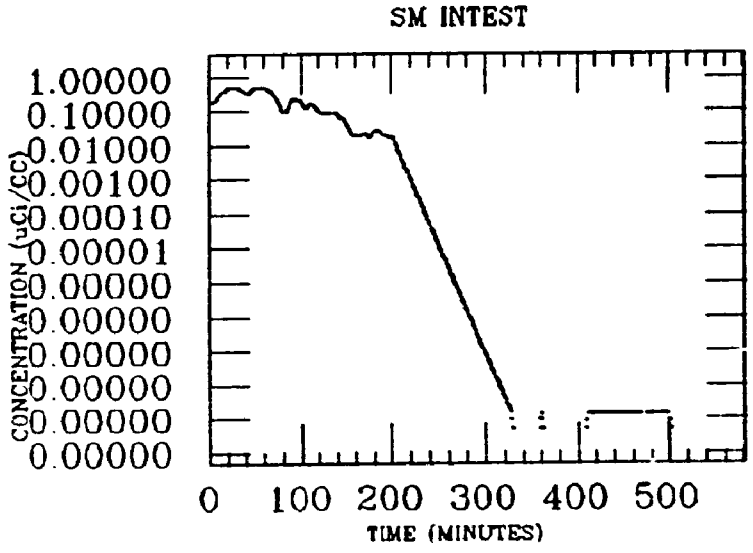

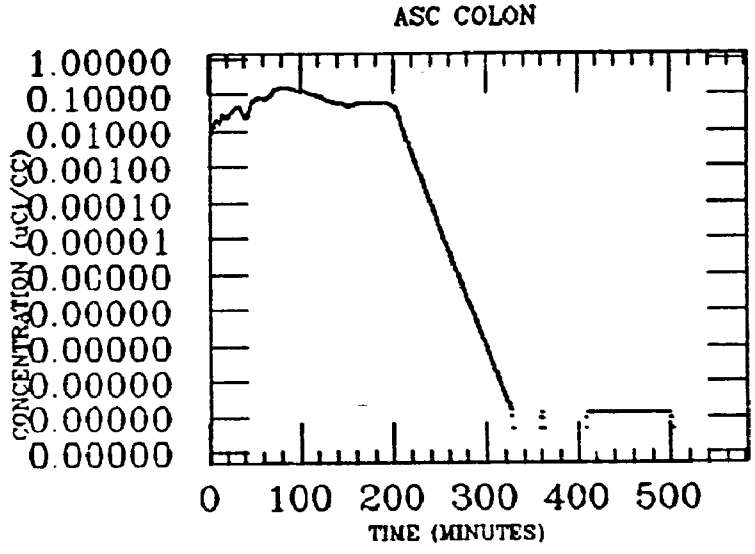

WESOLEK
XE INGESTION
RADON

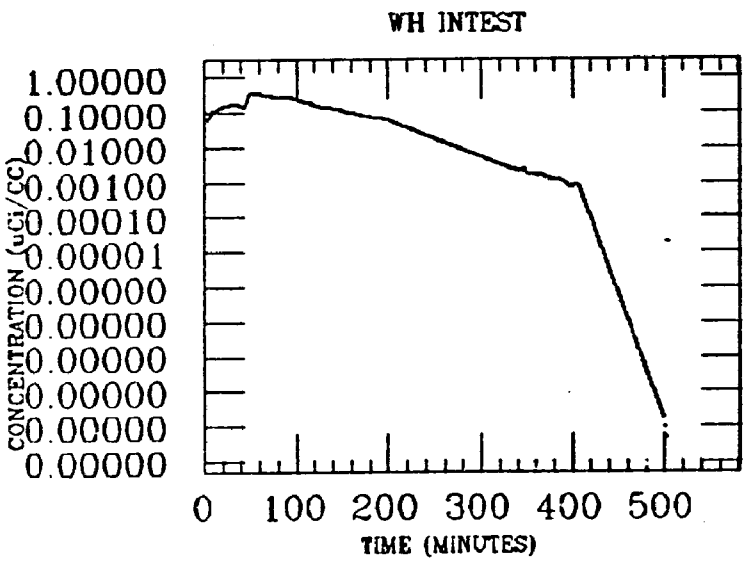

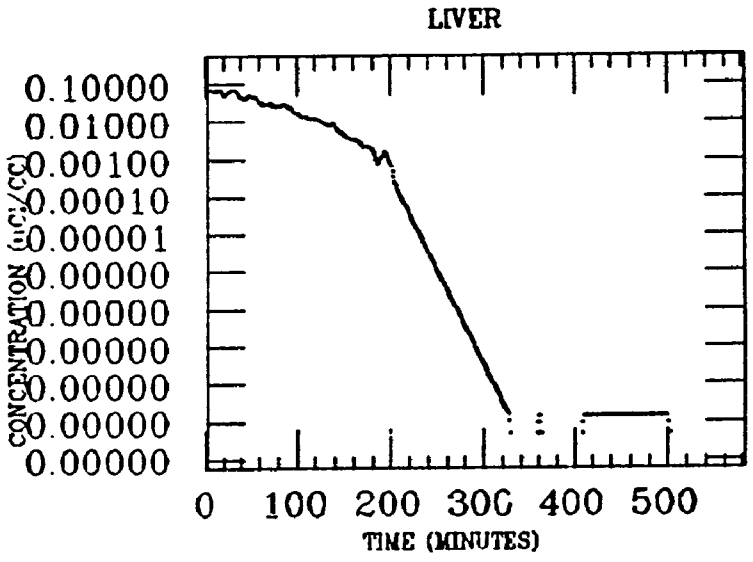

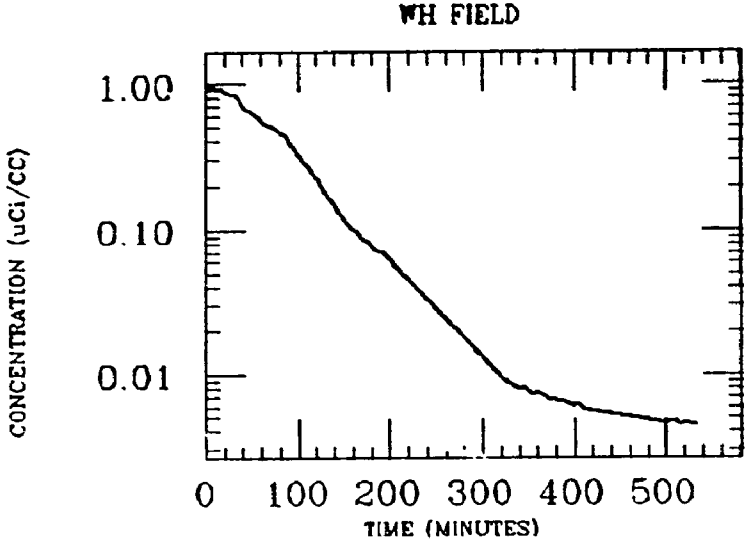

WILTSE
XE INGESTION
RADON

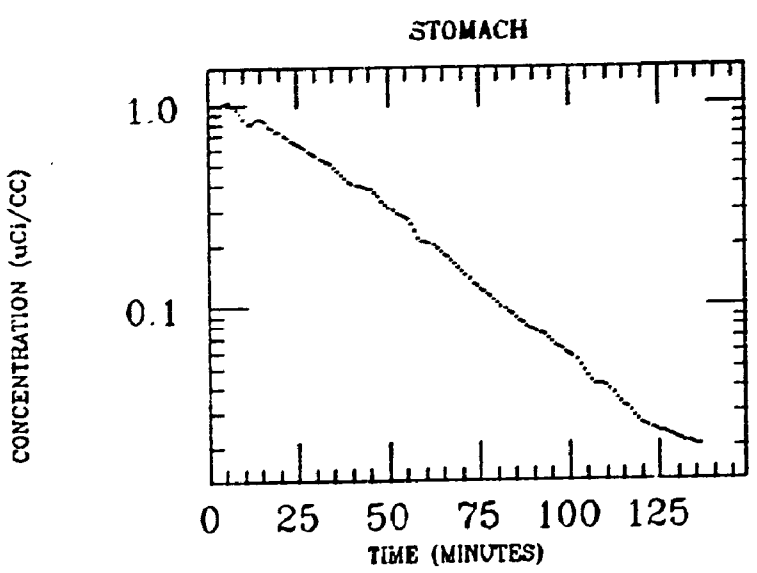

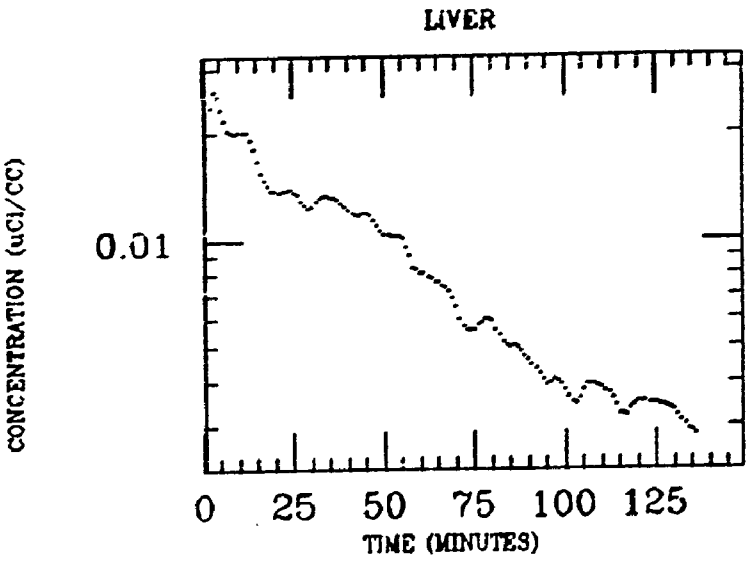

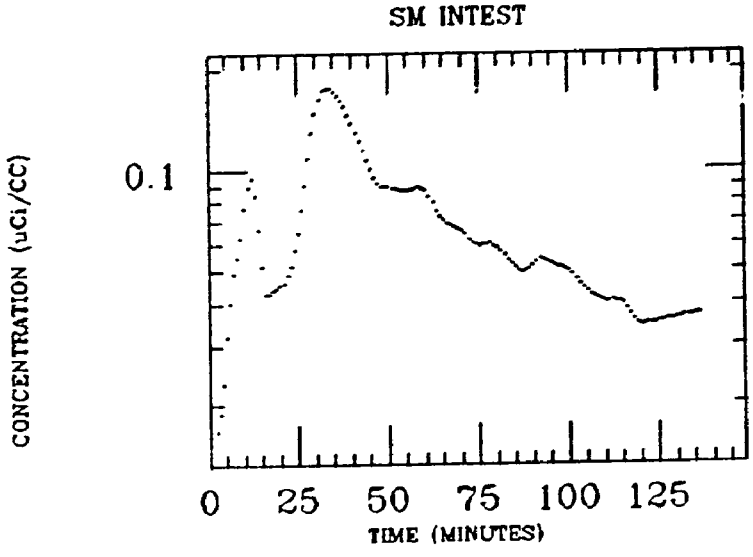

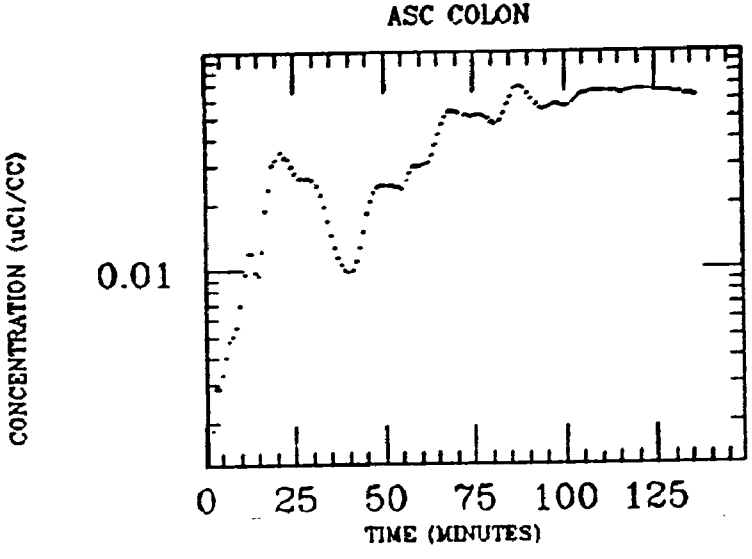

WILTSE
XE INGESTION
RADON

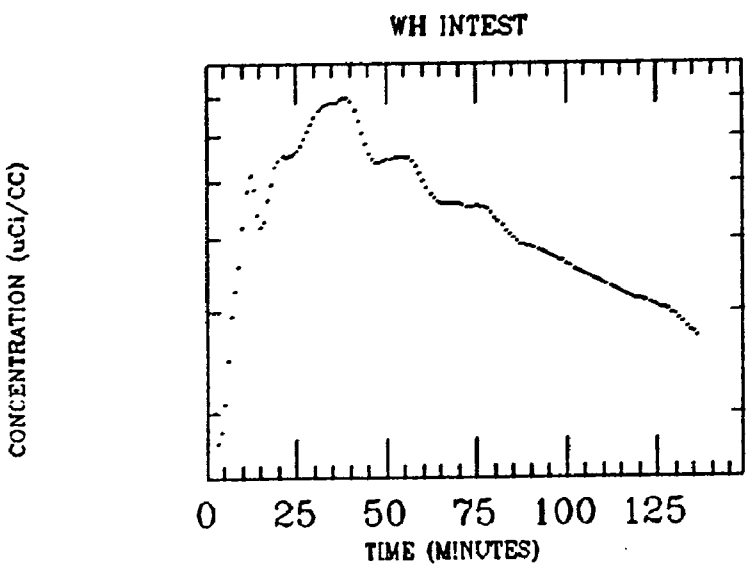

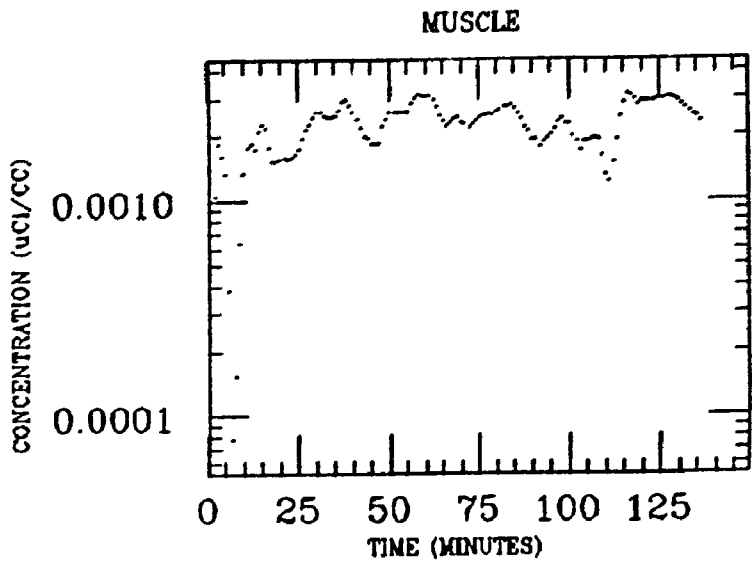

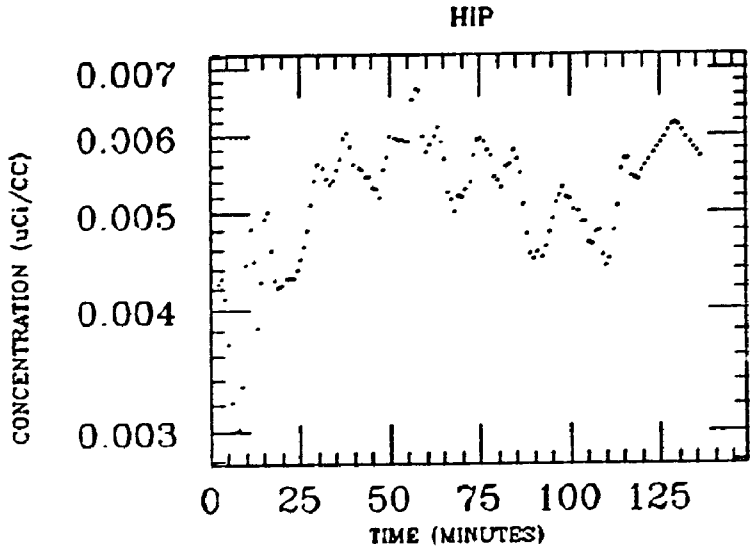

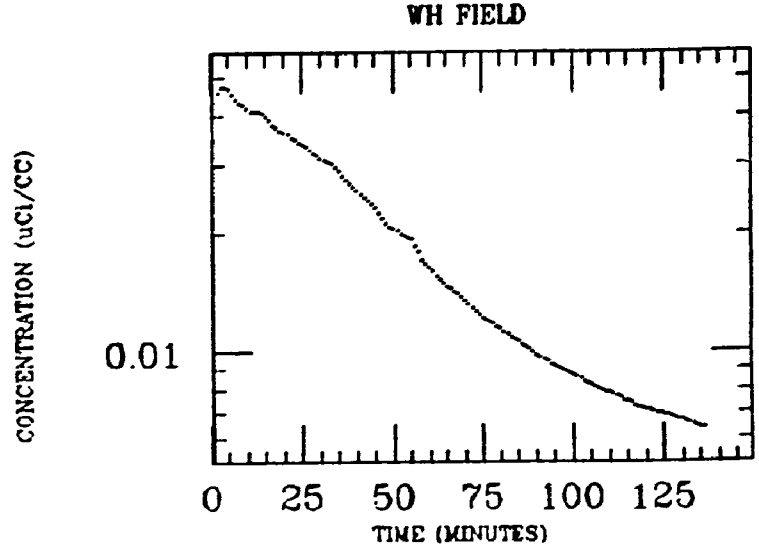

AHERN
XE INGESTION
Po-218

SM INTEST

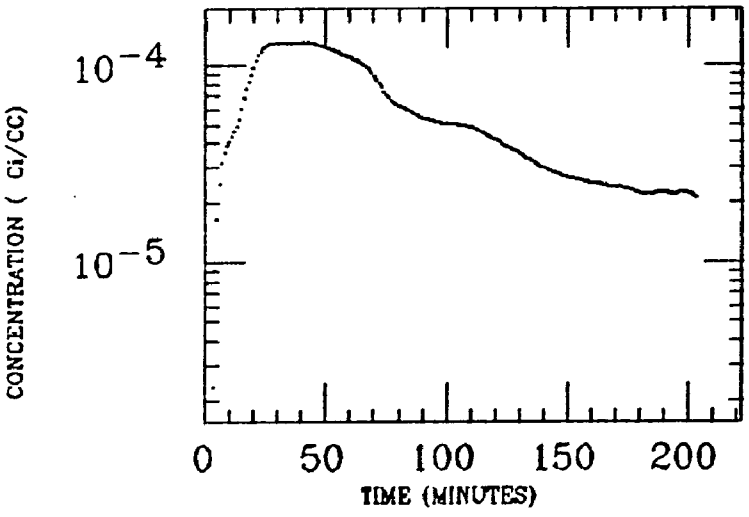

STOMACH

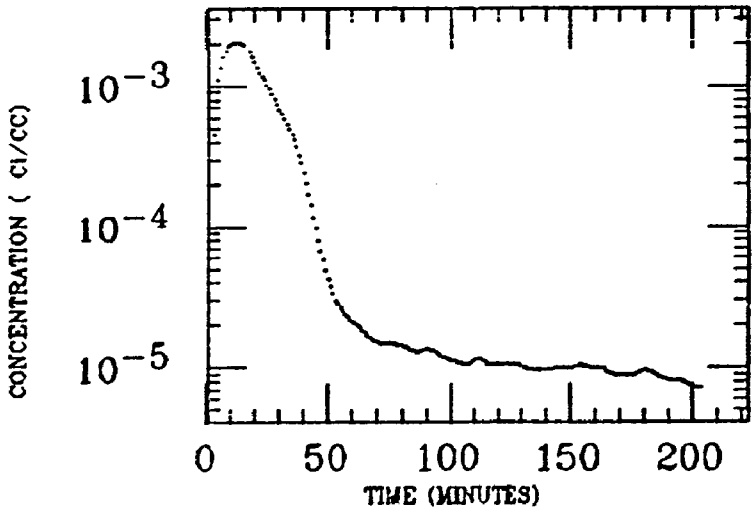

1.18

WH FIELD

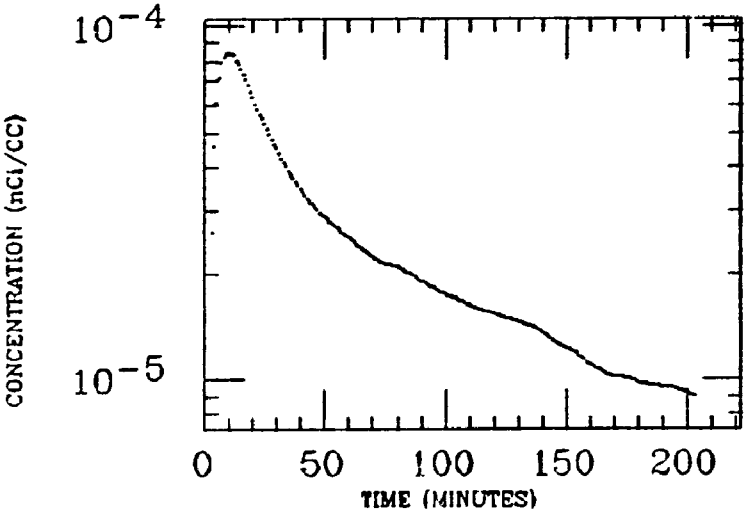

WH INTEST

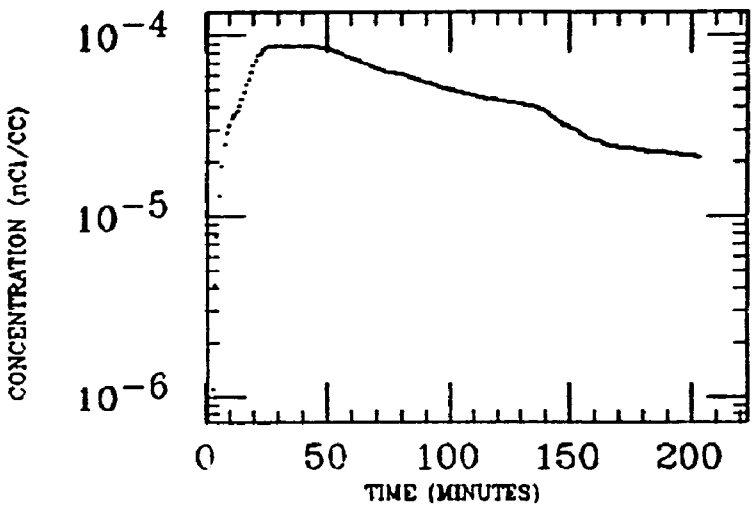

AHERN
XE INGESTION
Po-218

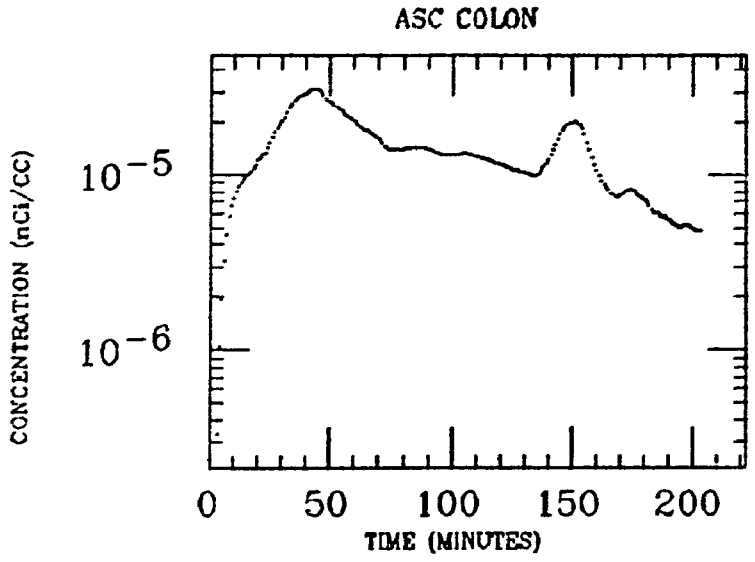

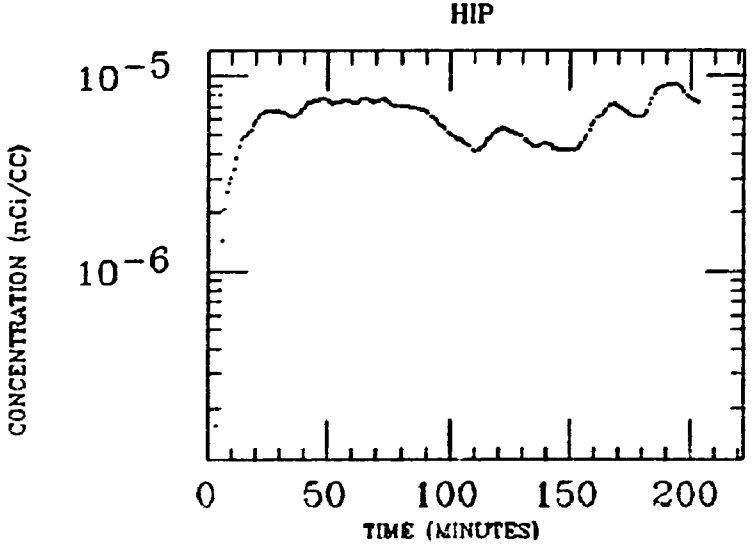

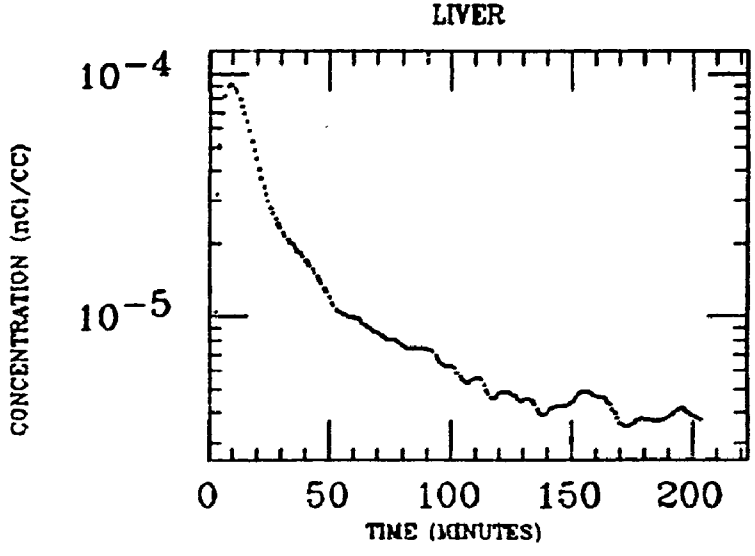

ARROL
XE INGESTION
Po-218

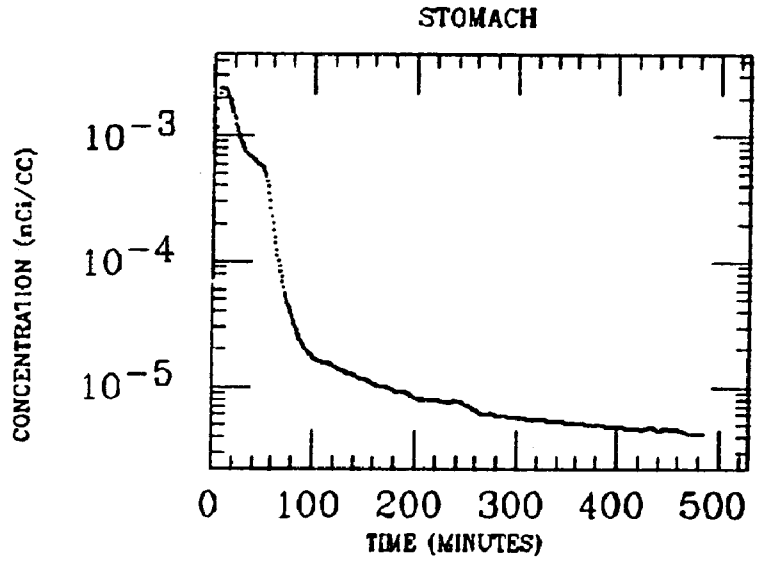

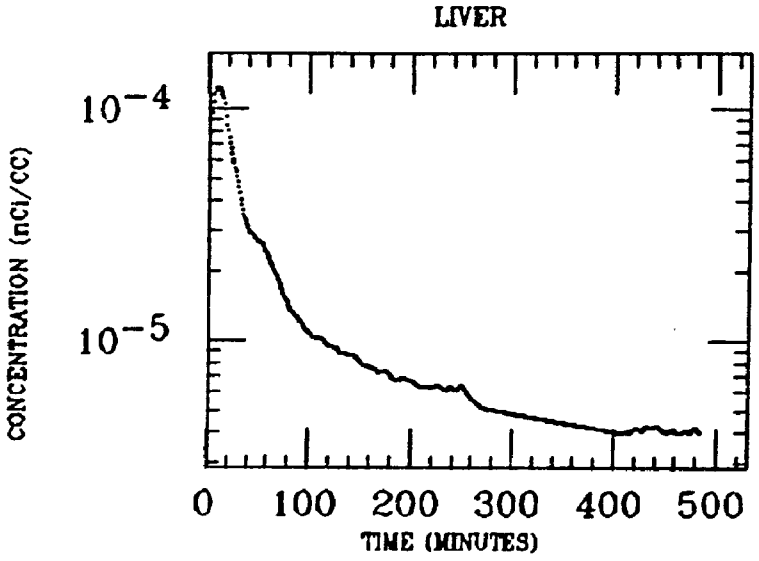

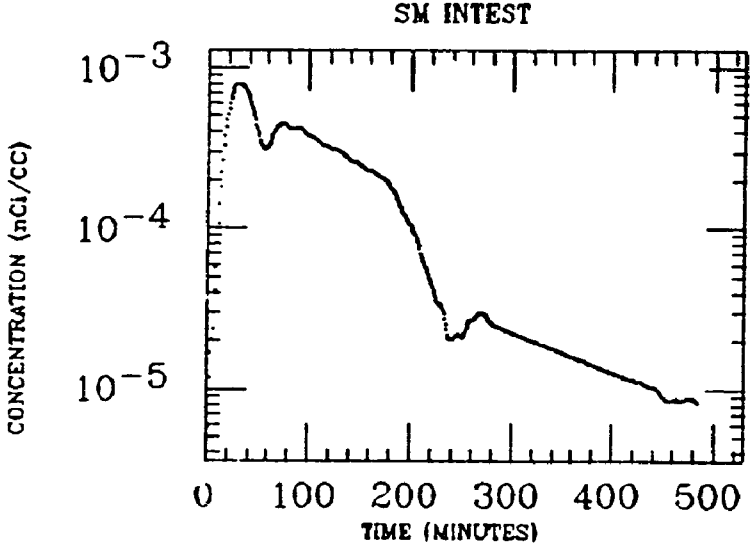

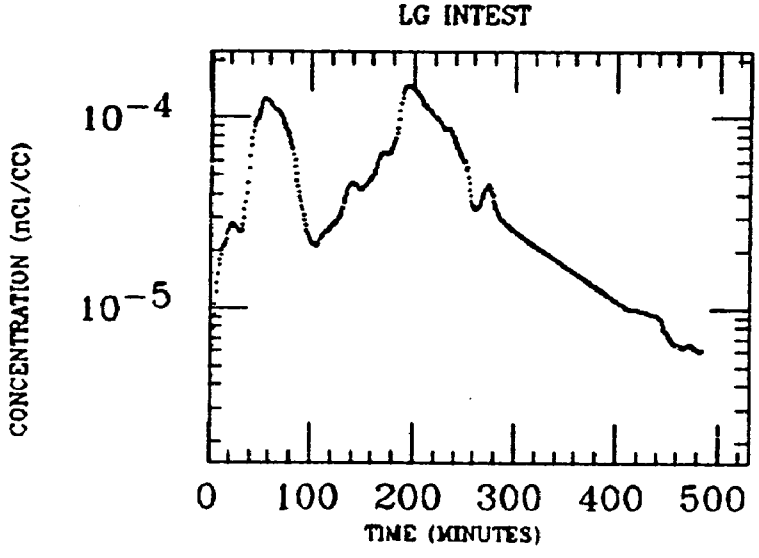

ARROL
XE INGESTION
Po-218

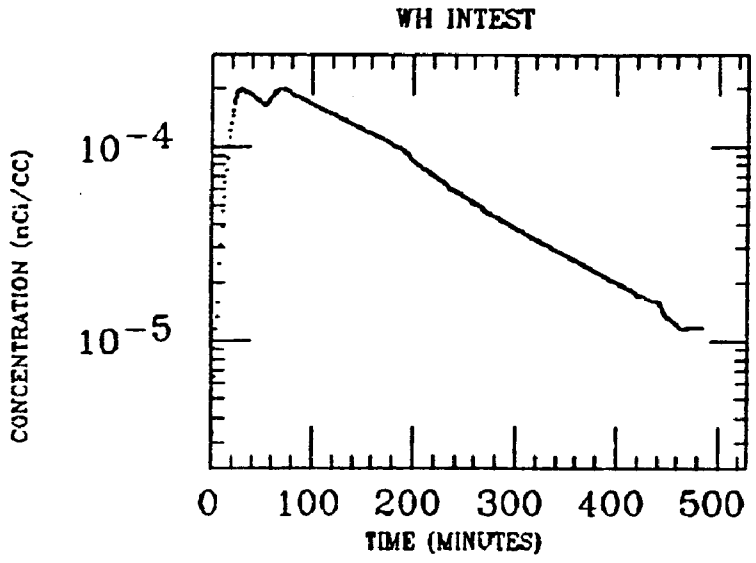

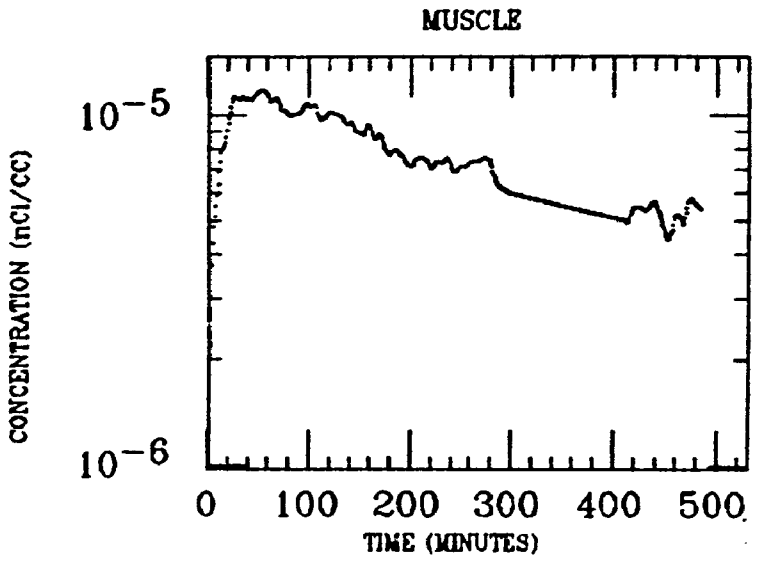

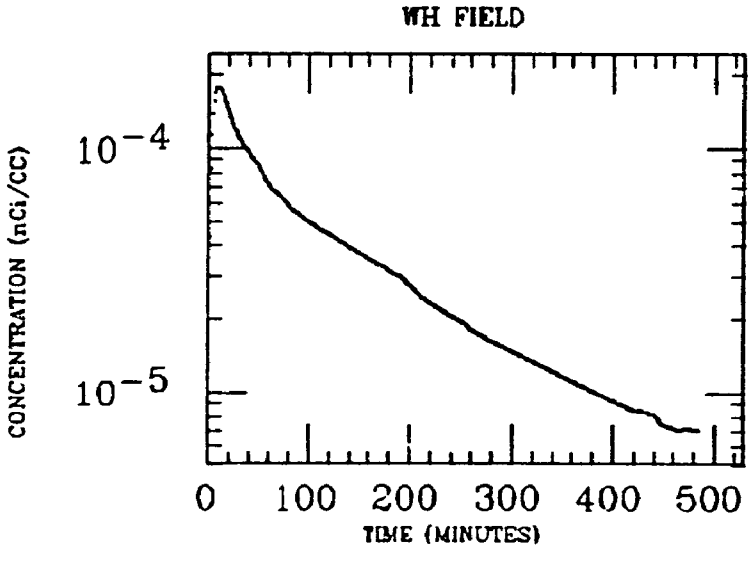

AYER

XE INGESTION

Po-218

STOMACH

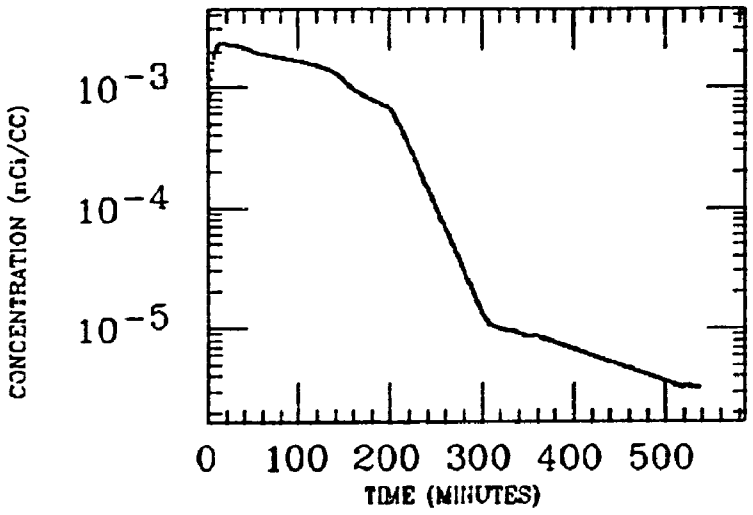

LIVER

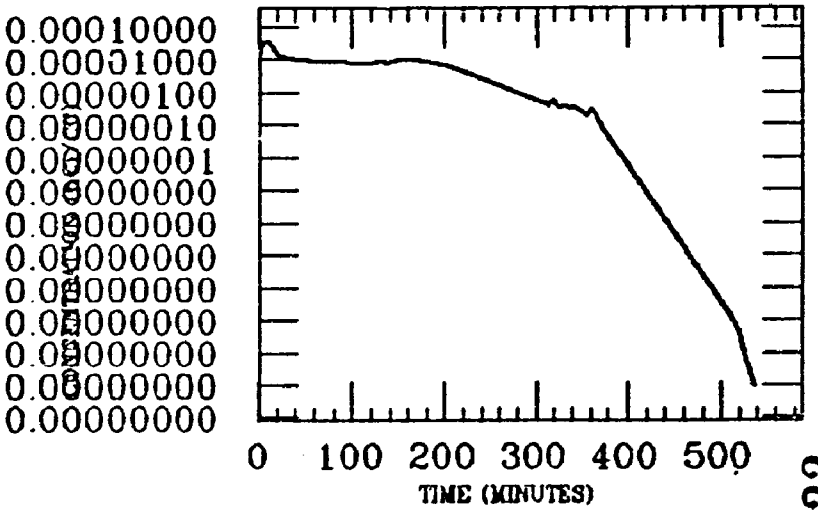

WH FIELD

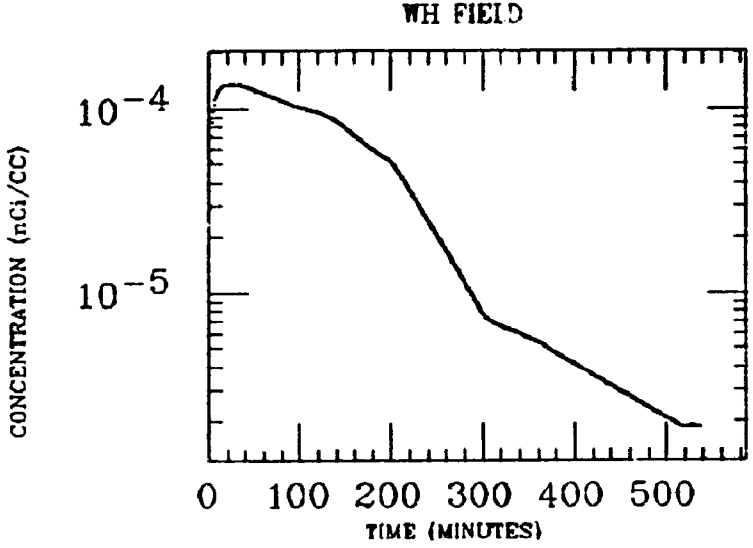

AYER

XE INGESTION

Po-218

ASC COLON

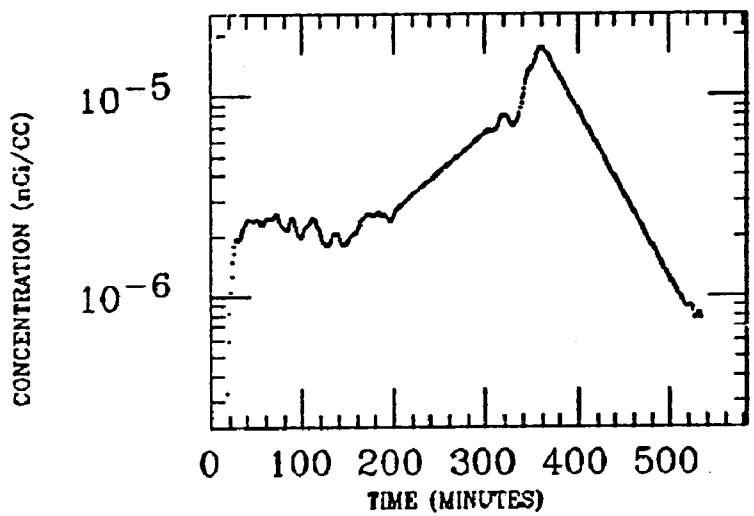

DES COLON

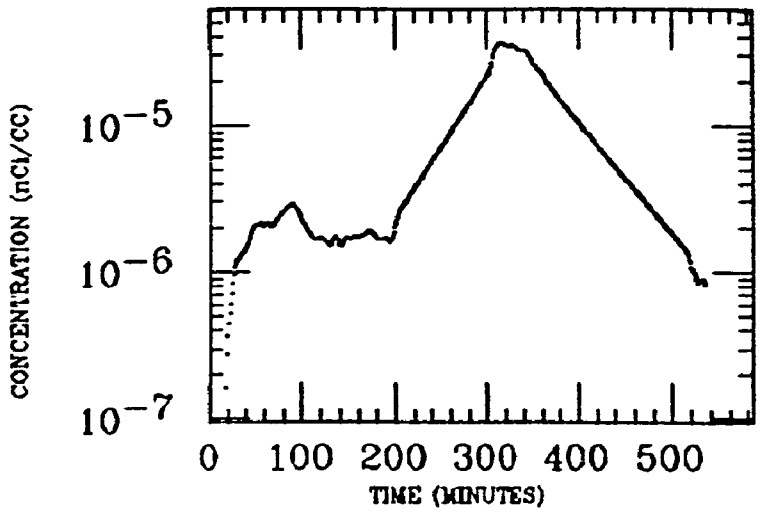

LIVER

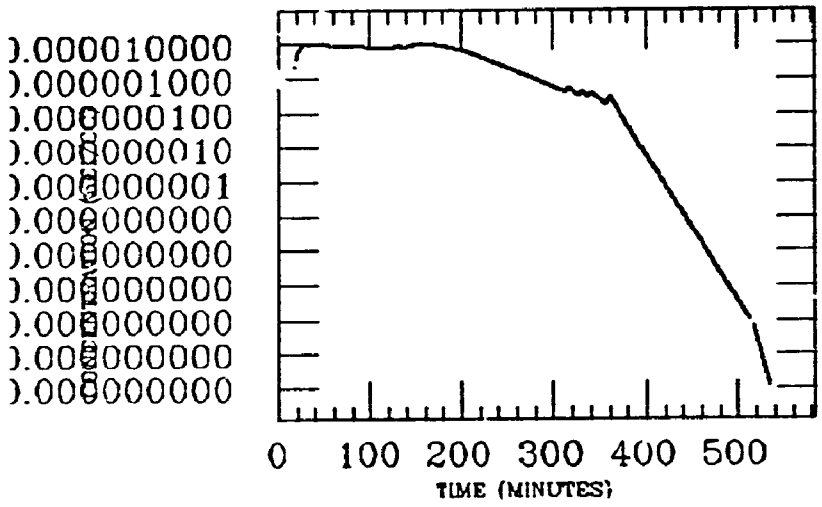

SM INTEST

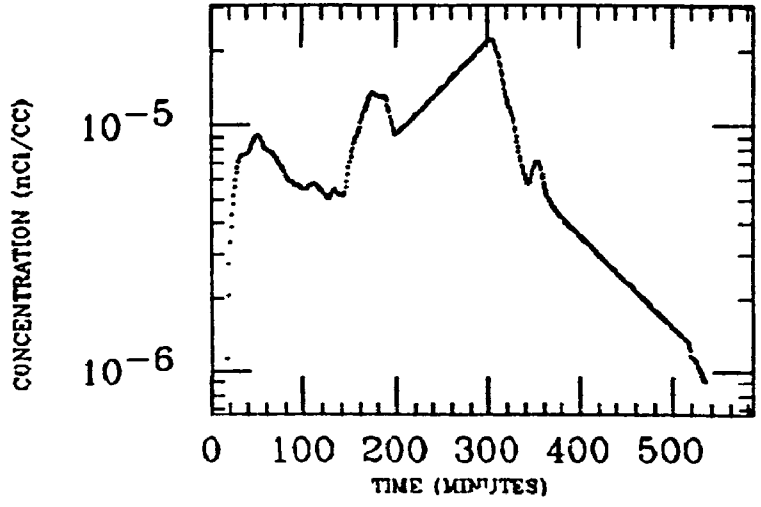

AYER

XE INGESTION

Po-216

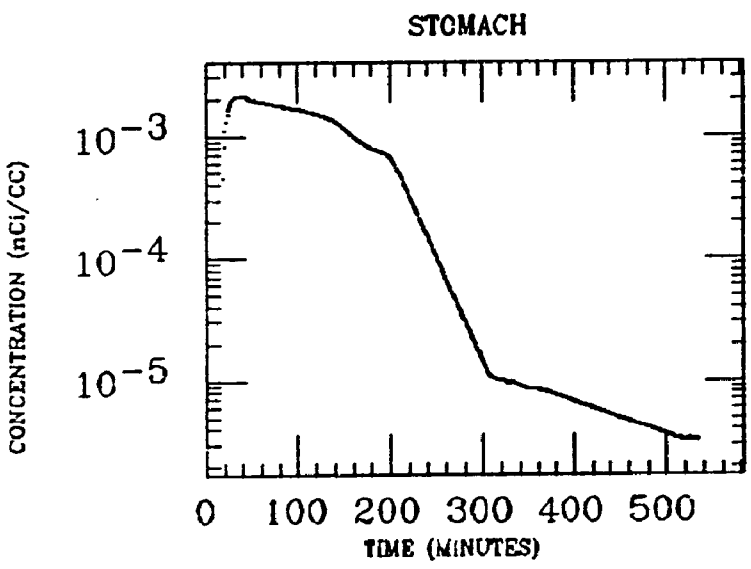

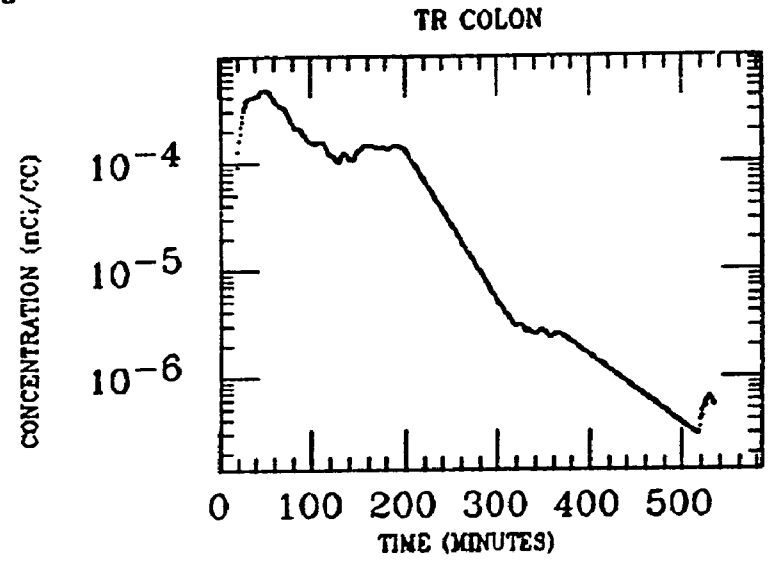

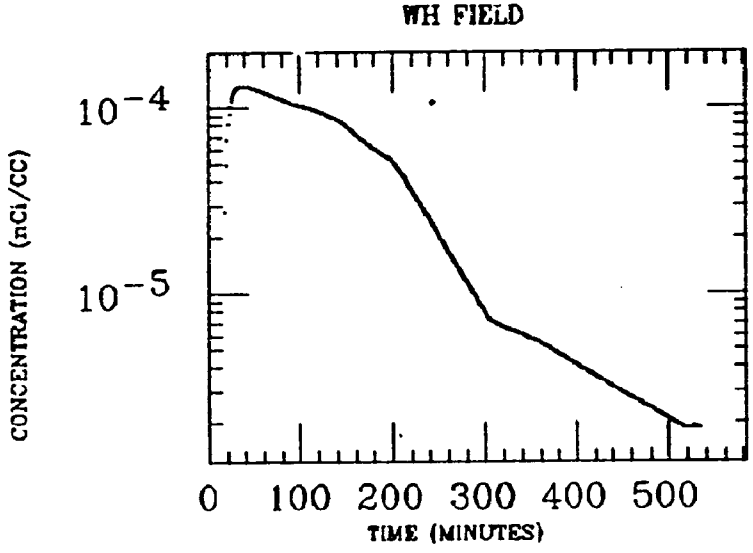

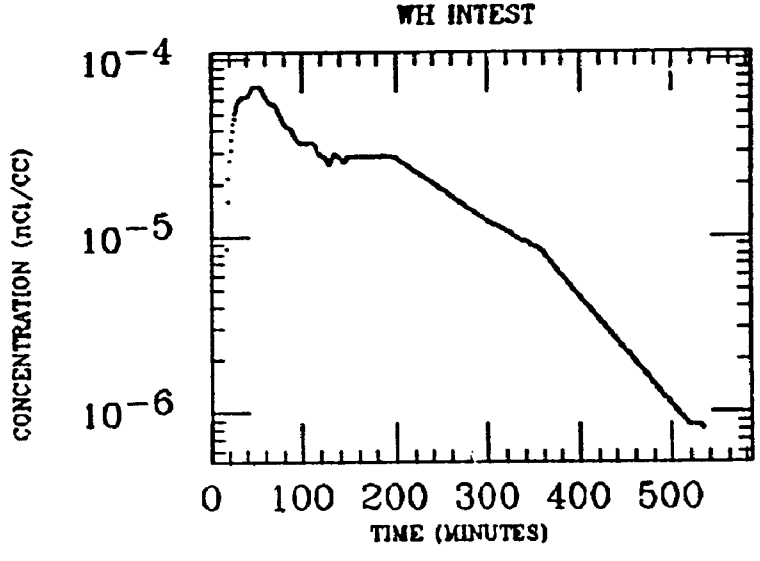

BROCK
XE INGESTION
Po-218

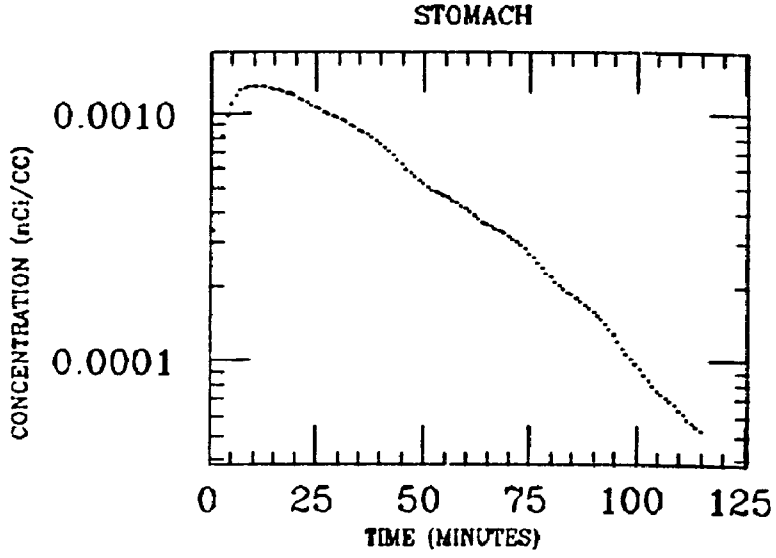

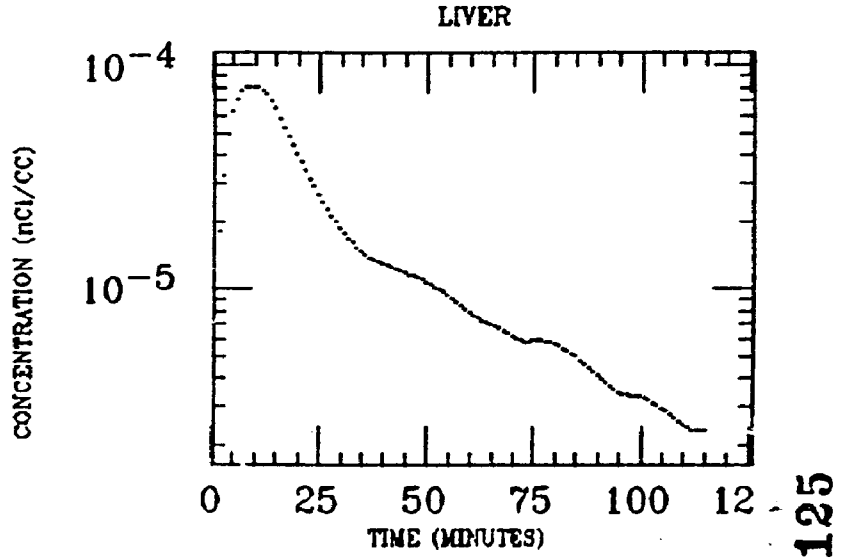

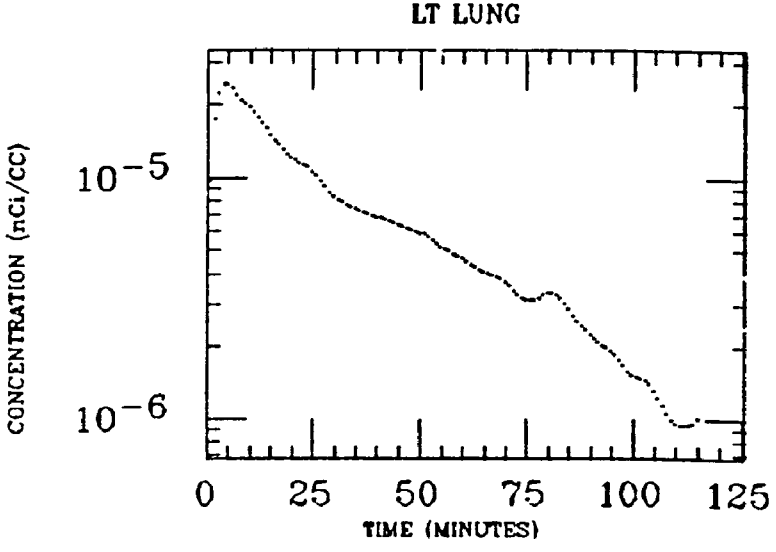

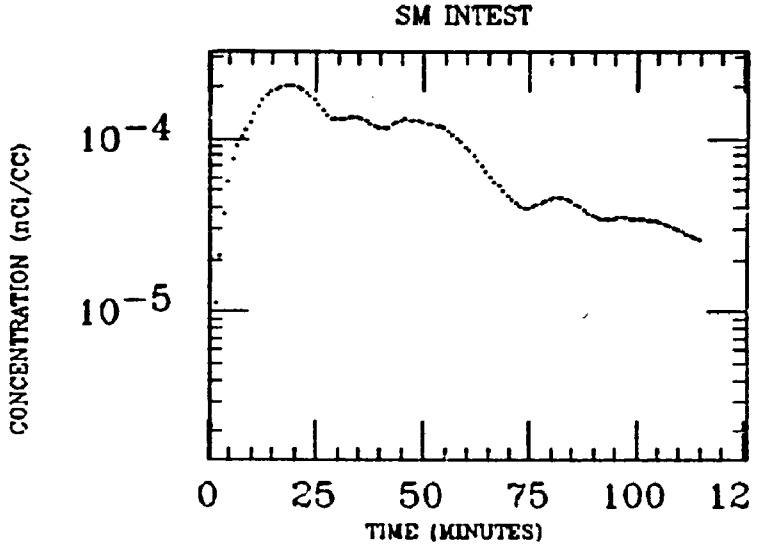

125

BROCK
XE INGESTION
Po-218

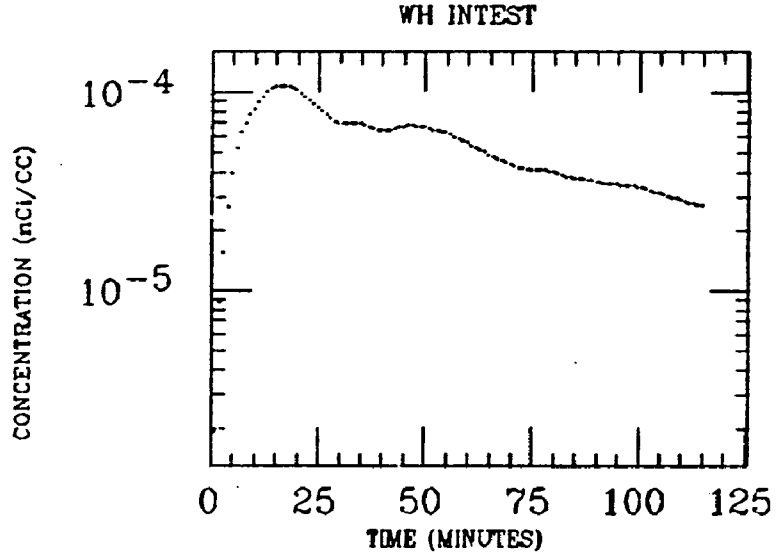

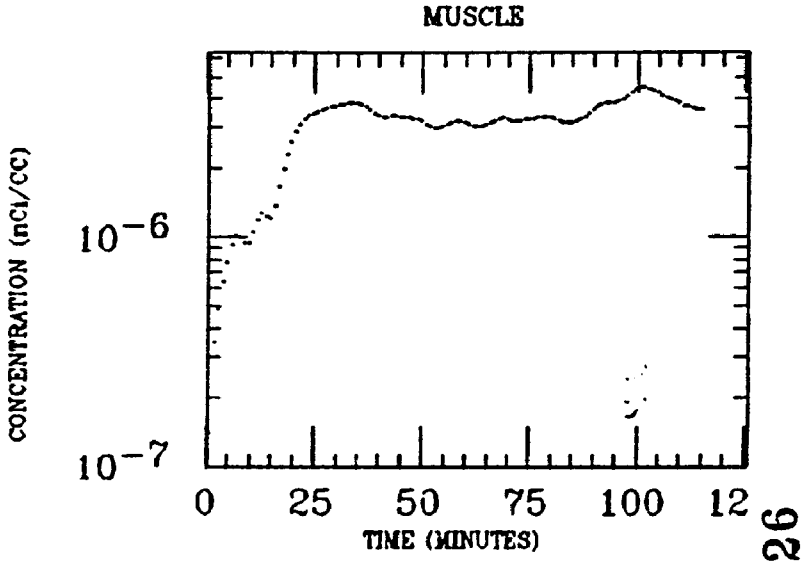

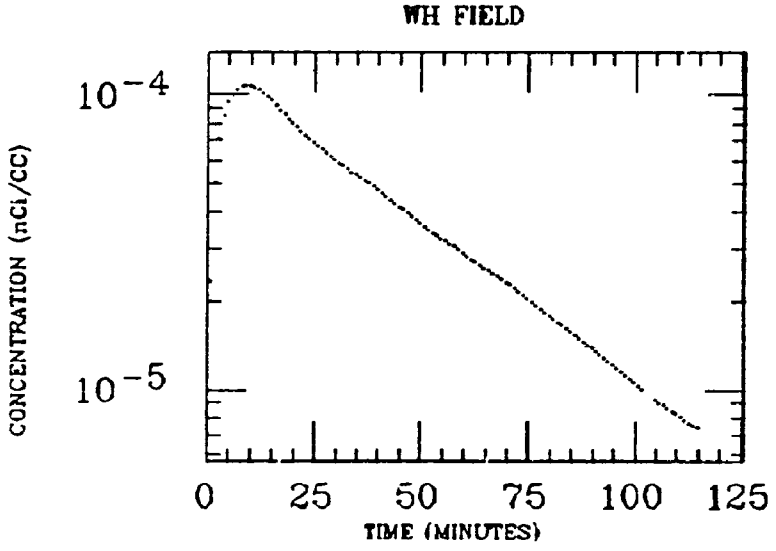

BYRNE
XE INGESTION
Po-218

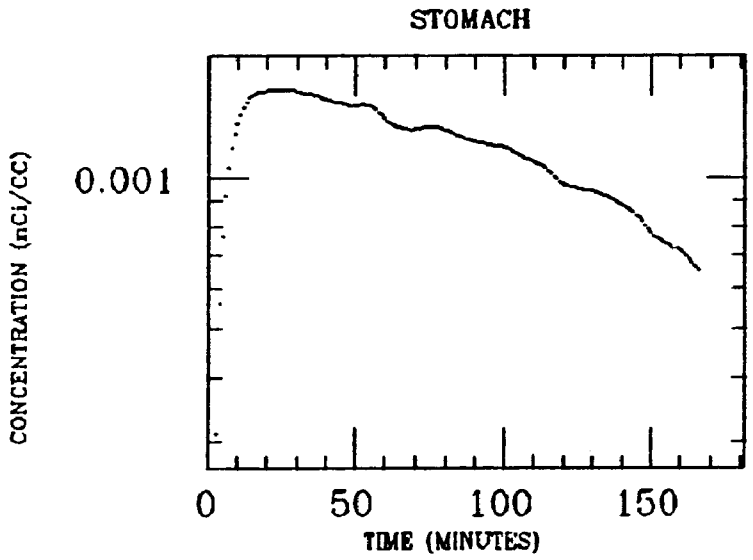

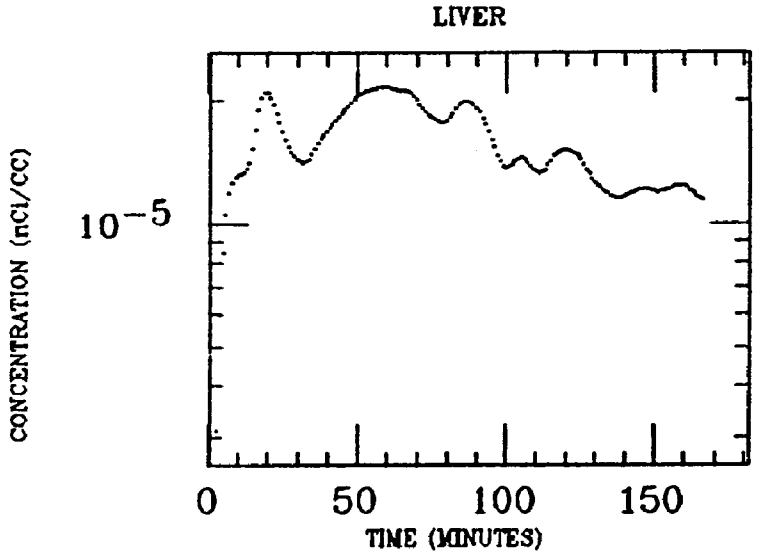

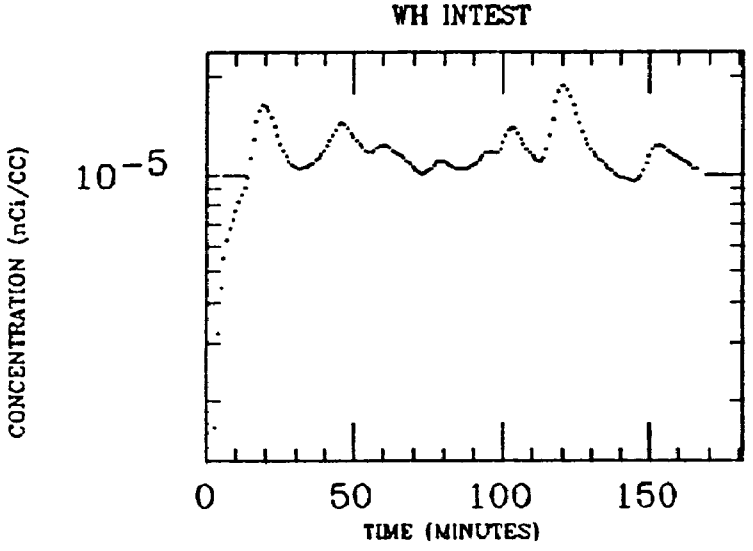

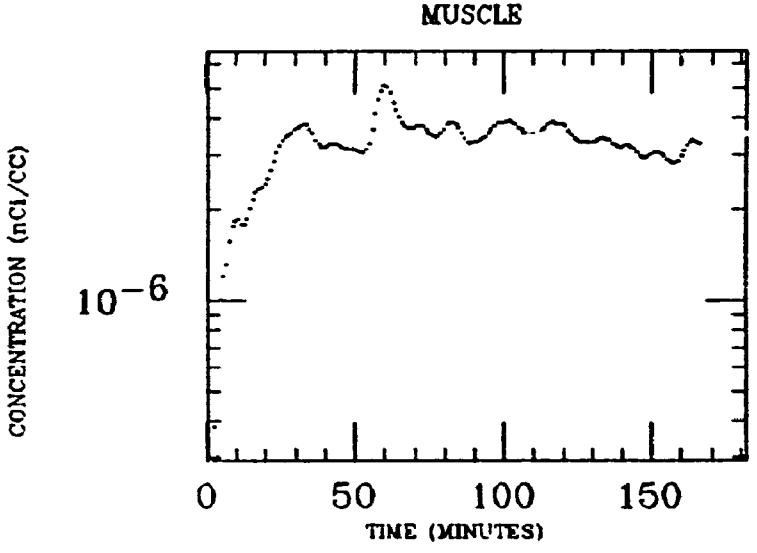

BYRNE
XE INGESTION
Po-218

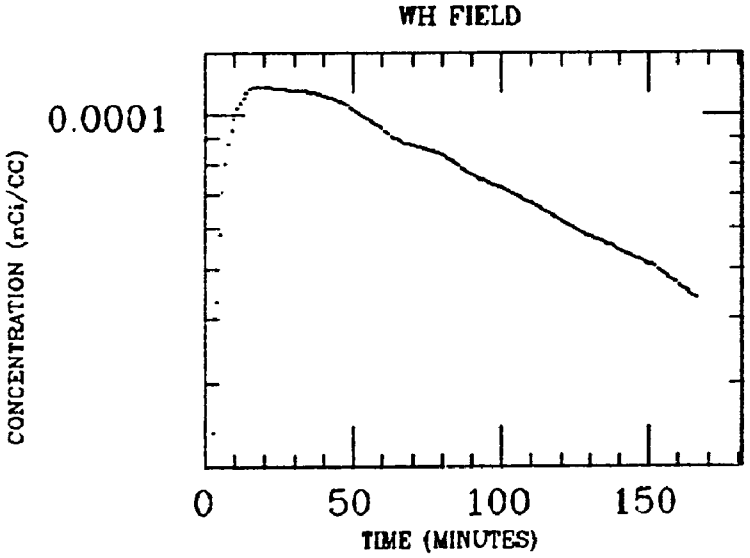

CLINE
XE INGESTION
Po-218

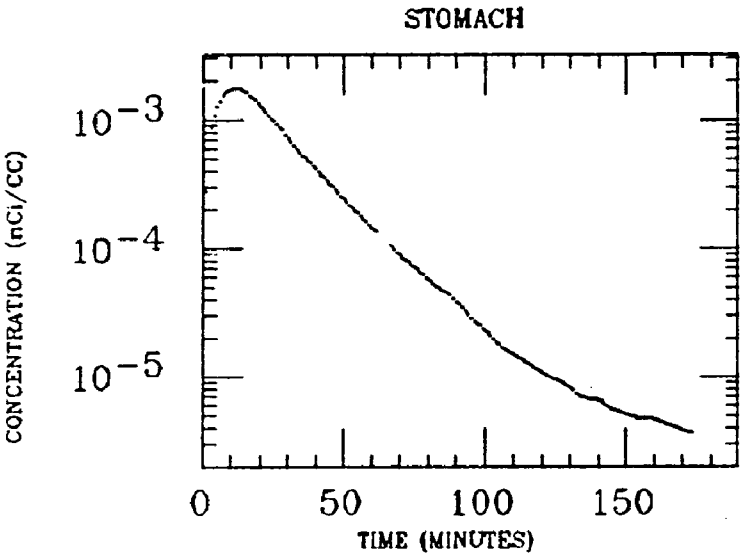

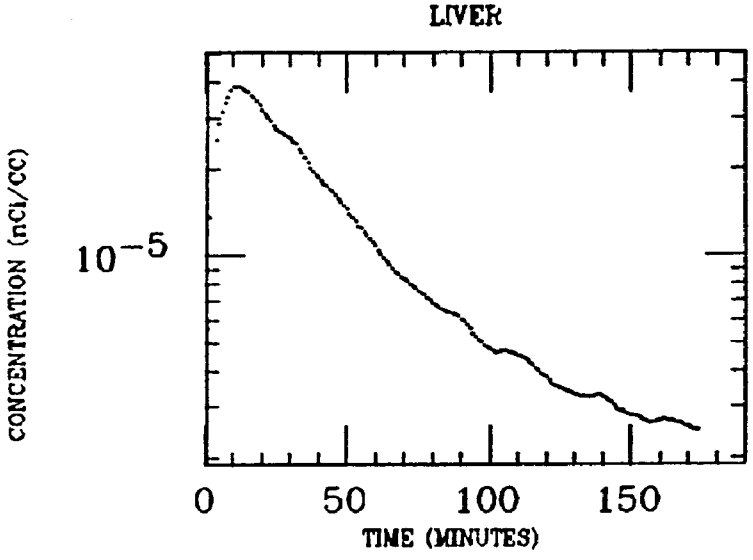

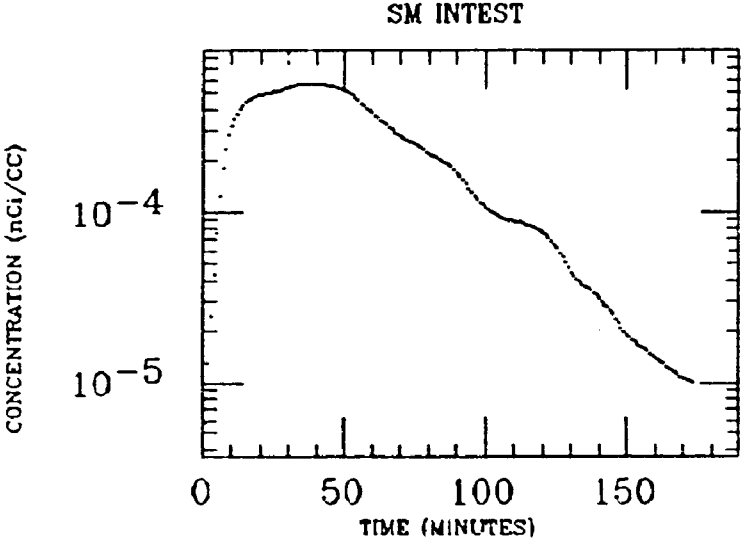

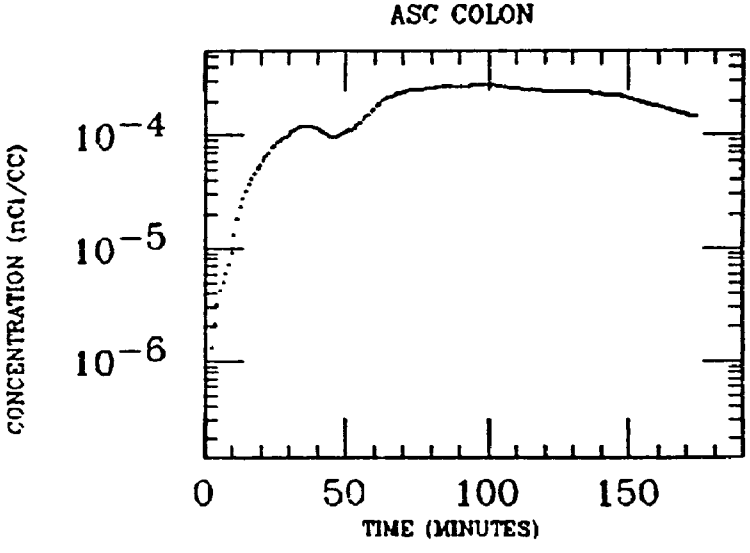

CLINE
XE INGESTION
Po-218

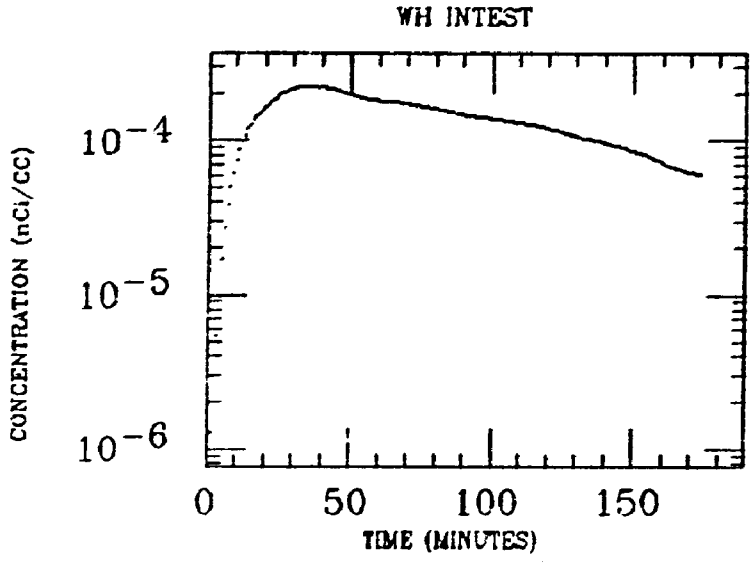

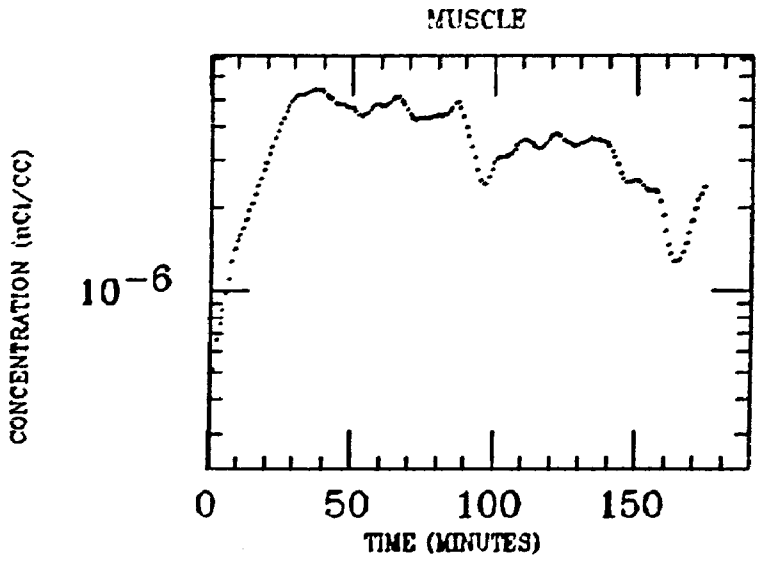

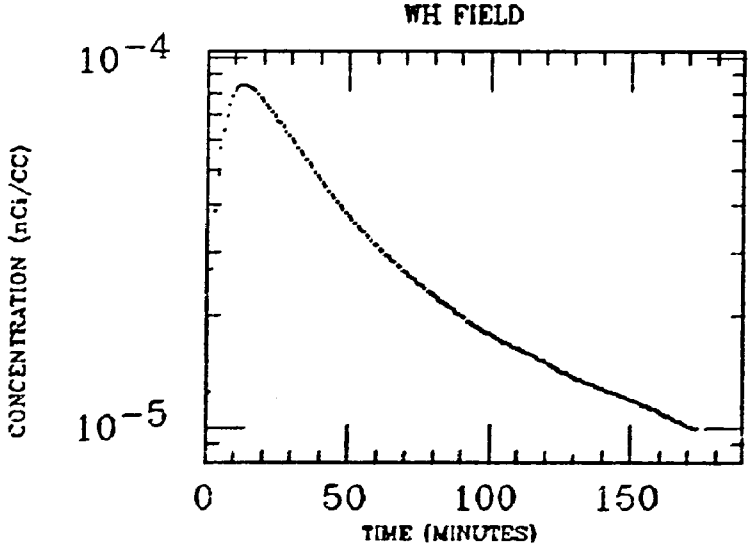

ELMDEN
XE INGESTION
Po-218

STOMACH

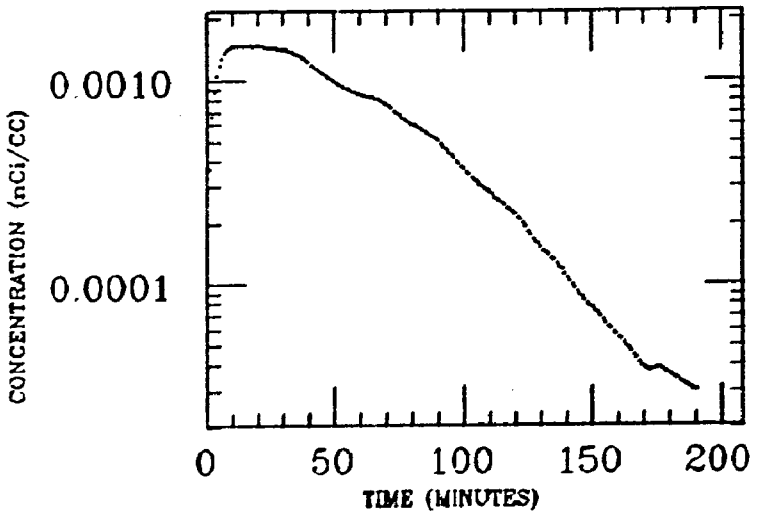

LIVER

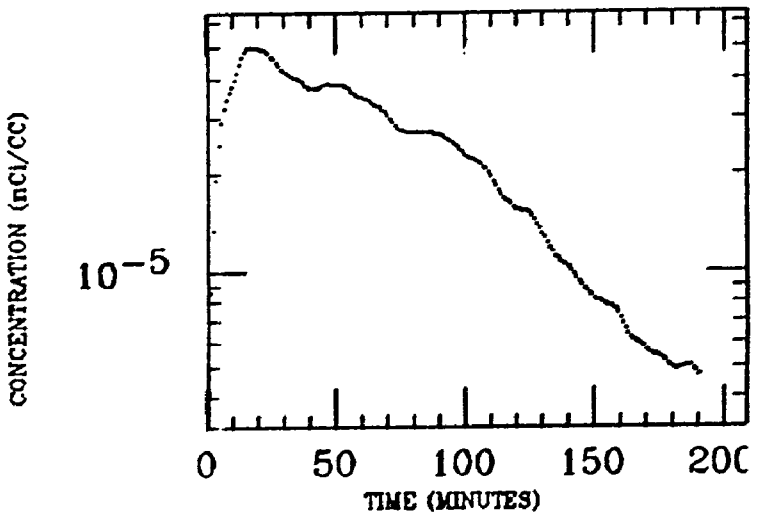

MUSCLE

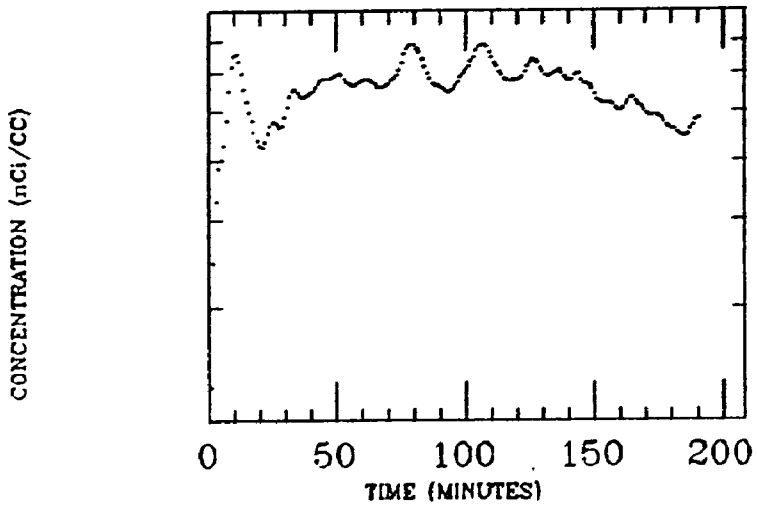

WH FIELD

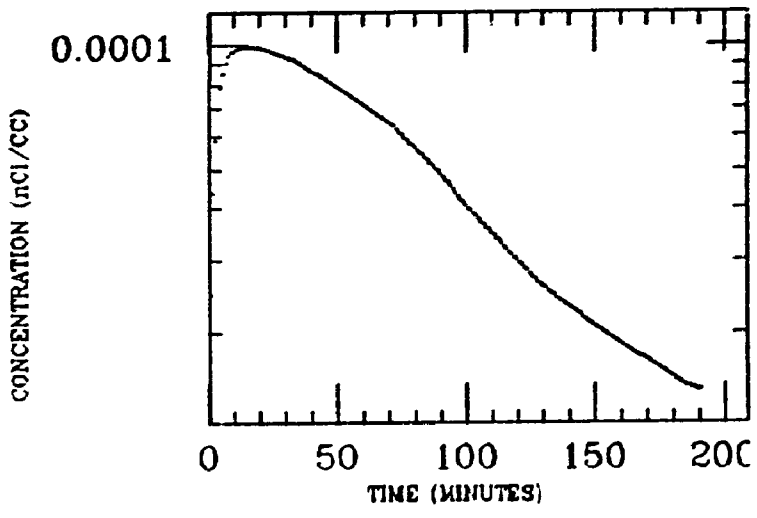

ELMDEN
XE INGESTION
Po-218

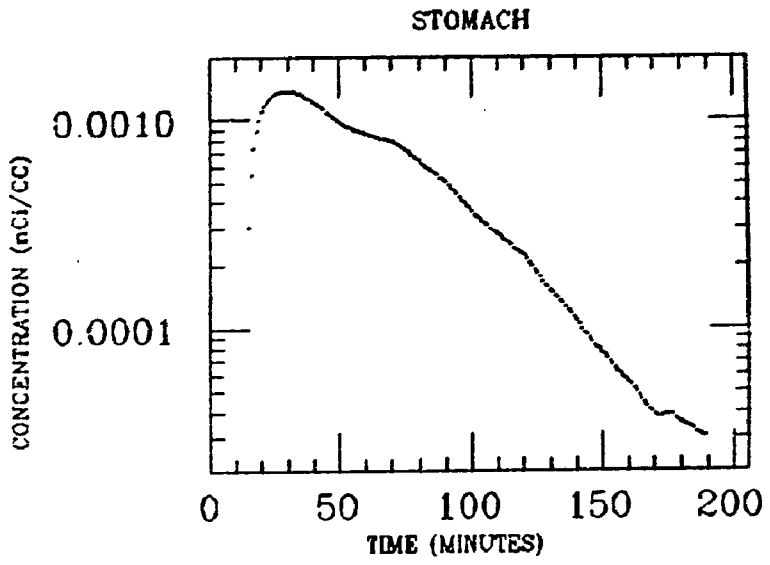

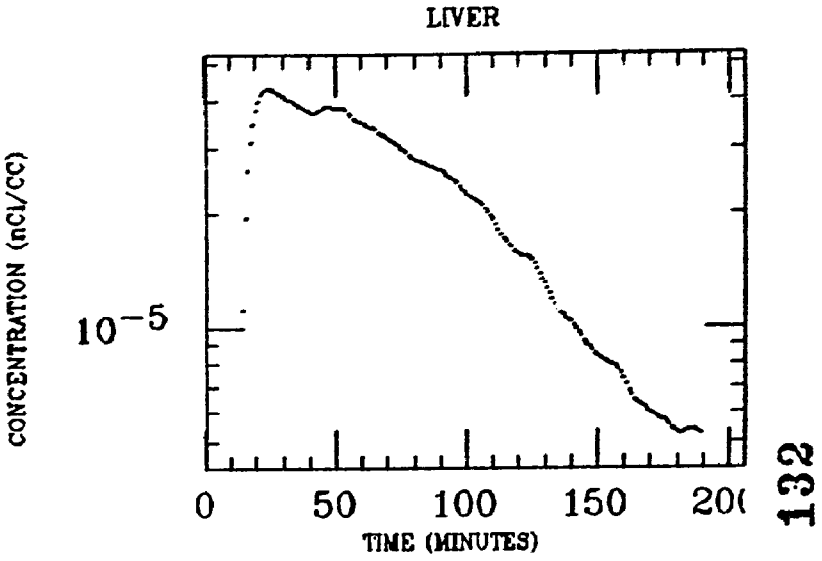

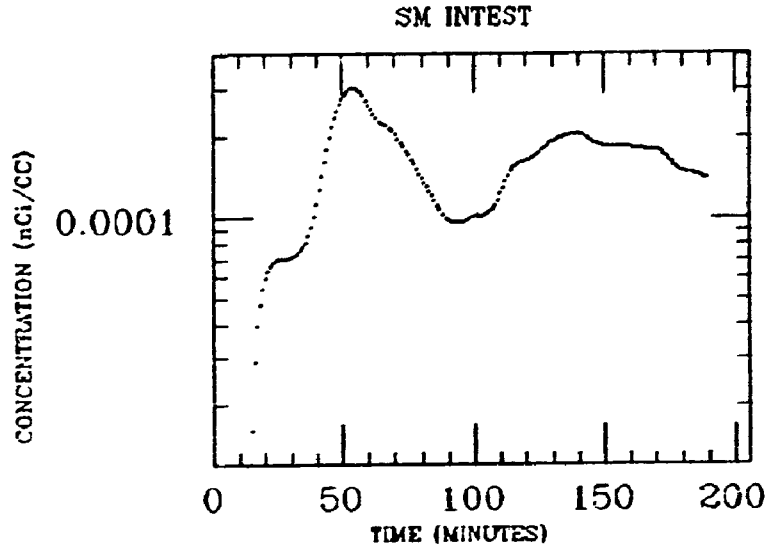

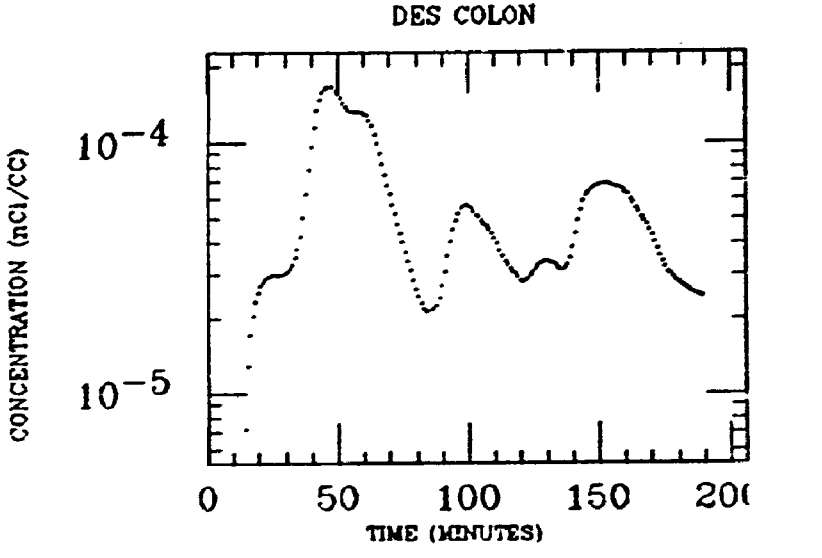

ELMDEN
XE INGESTION
Po-218

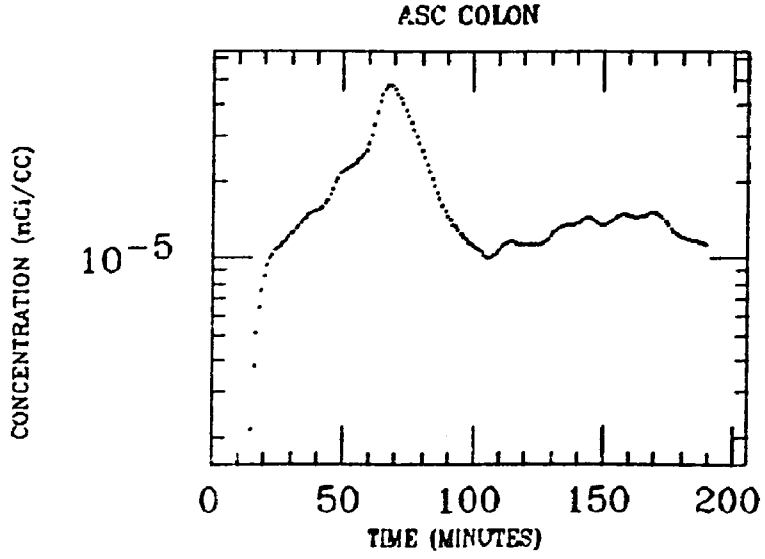

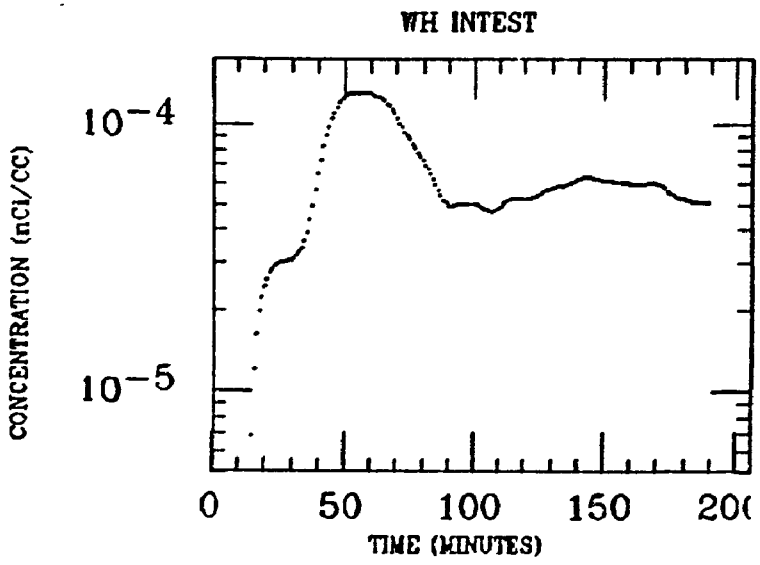

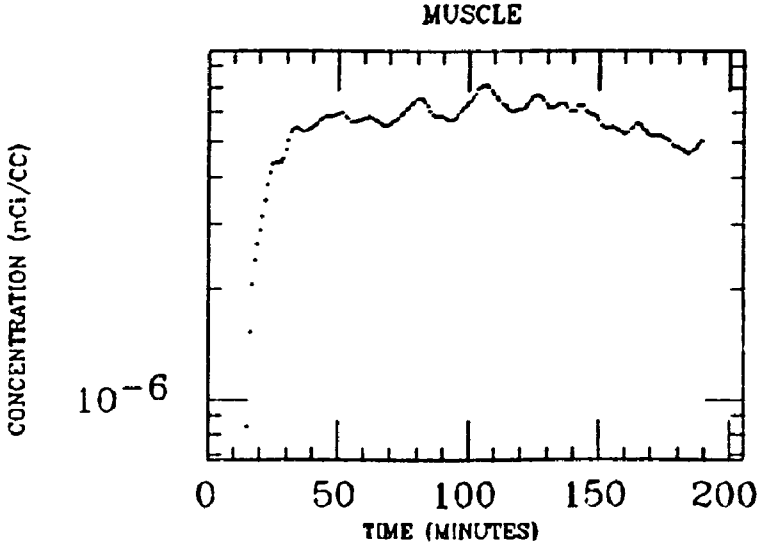

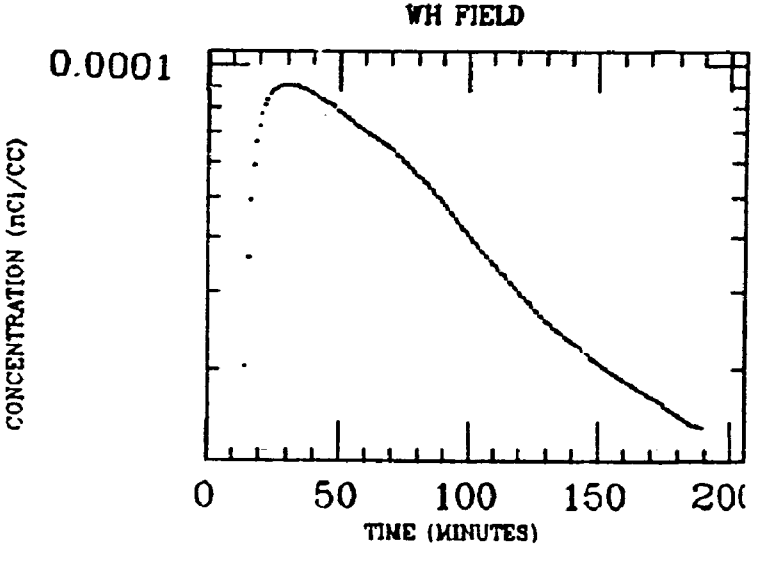

EPLING
XE INGESTION
Po-218

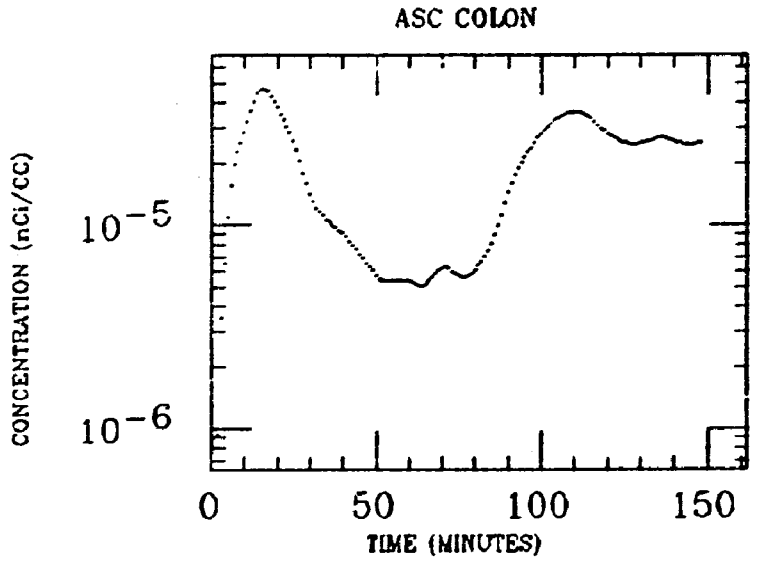

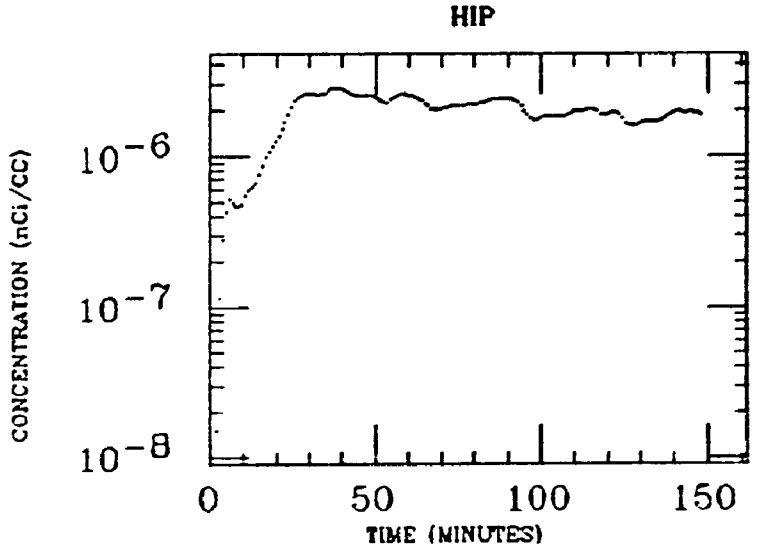

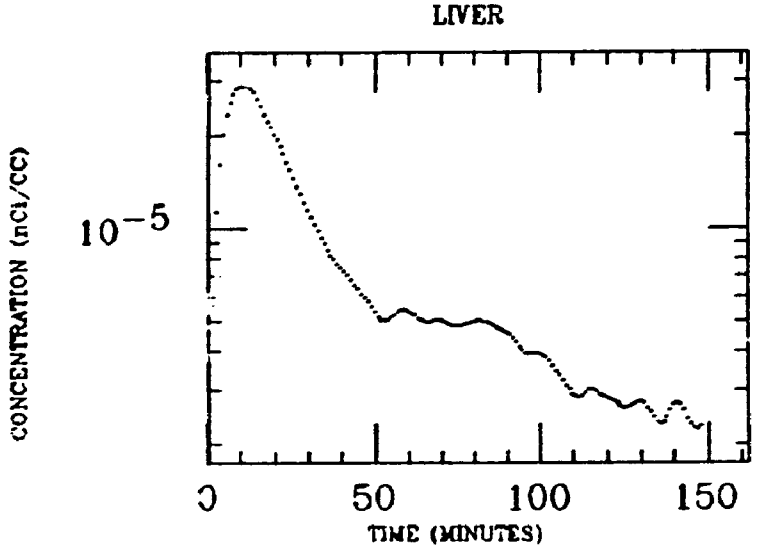

EPLING
XE INGESTION
Po-218

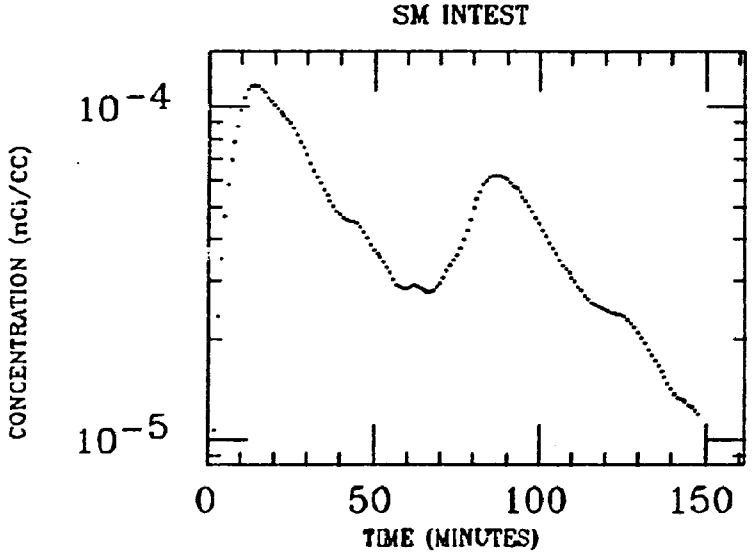

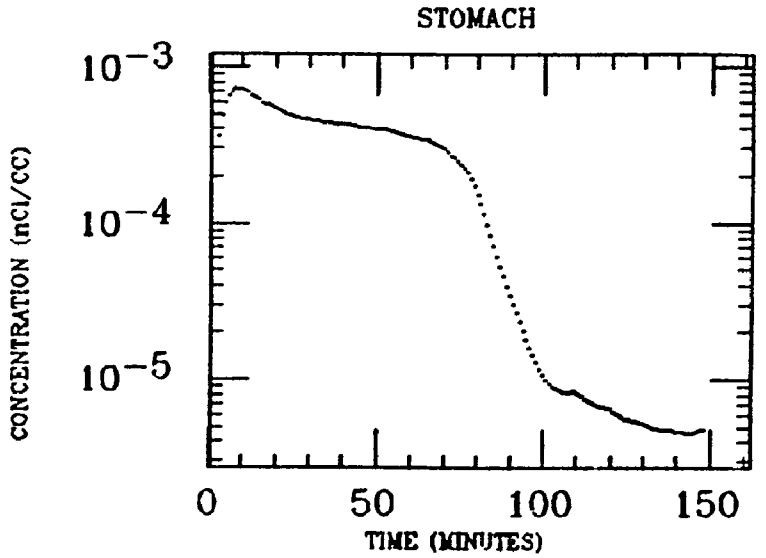

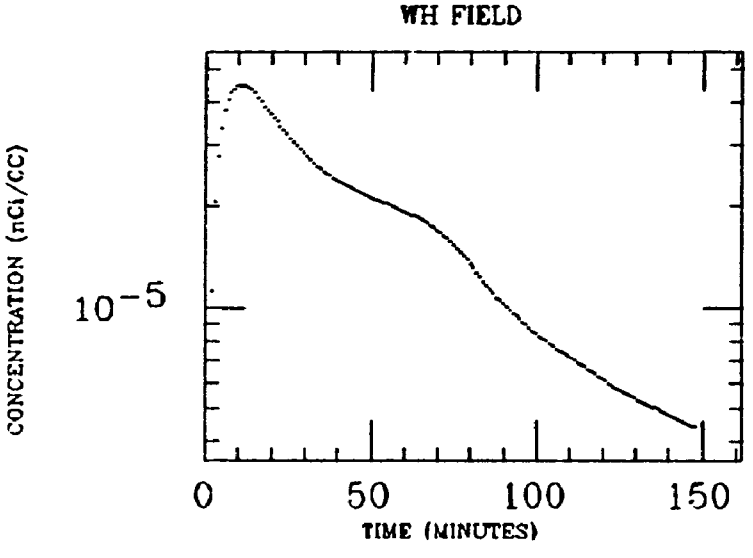

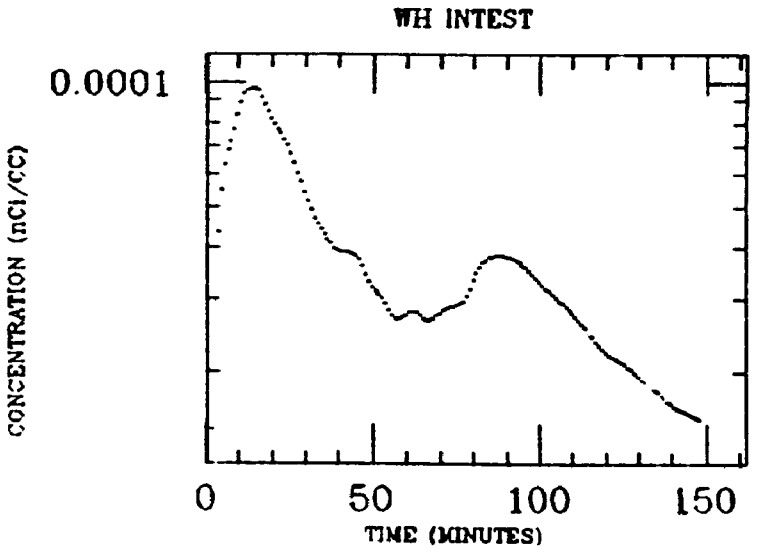

GAILOP
XE INGESTION
Po-218

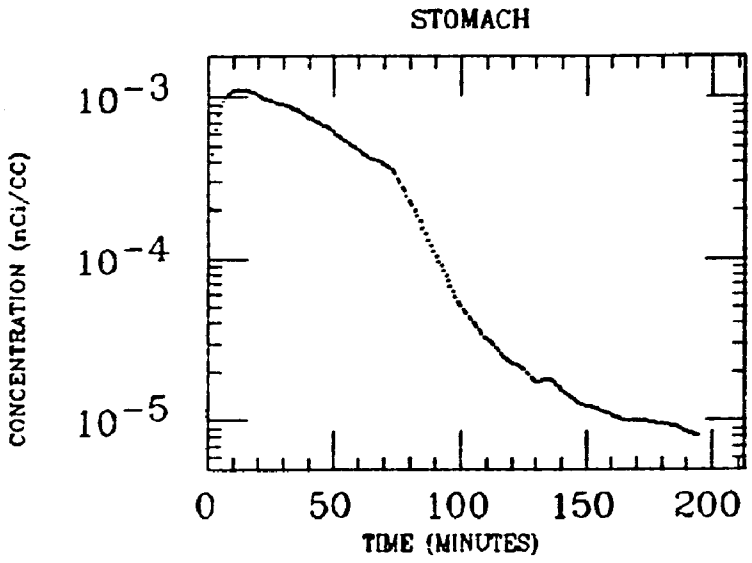

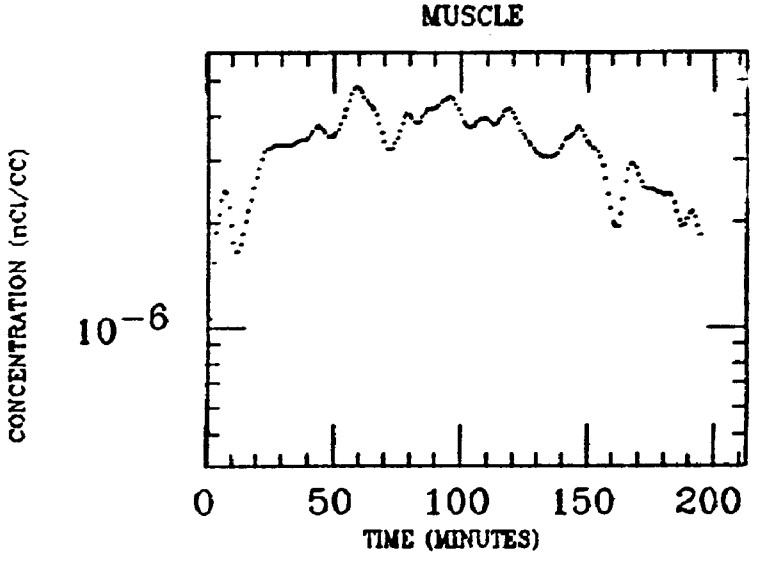

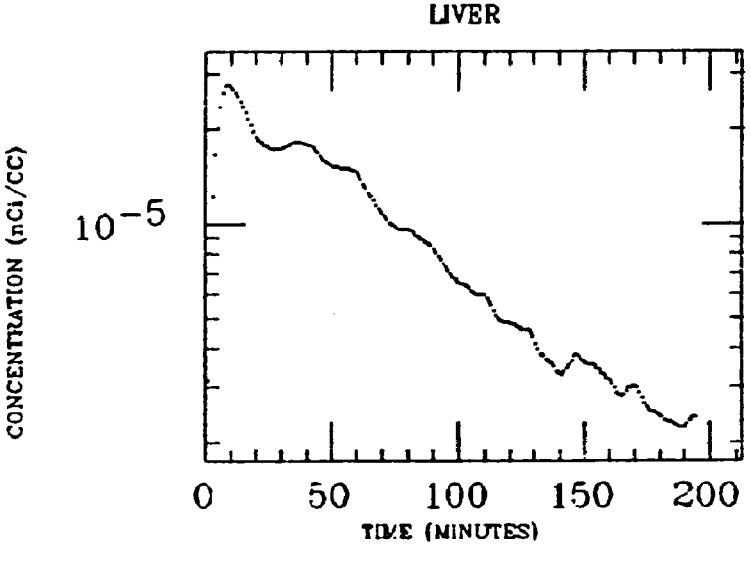

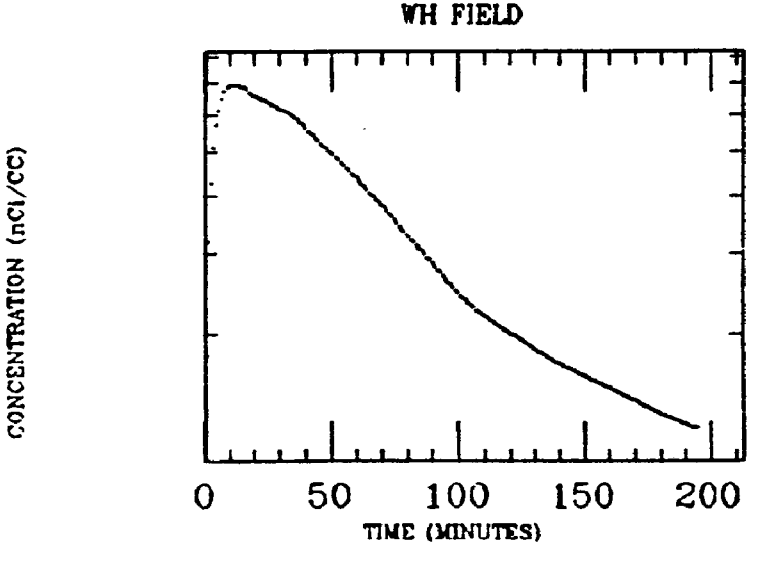

GALLOP
XE INGESTION
Po-218

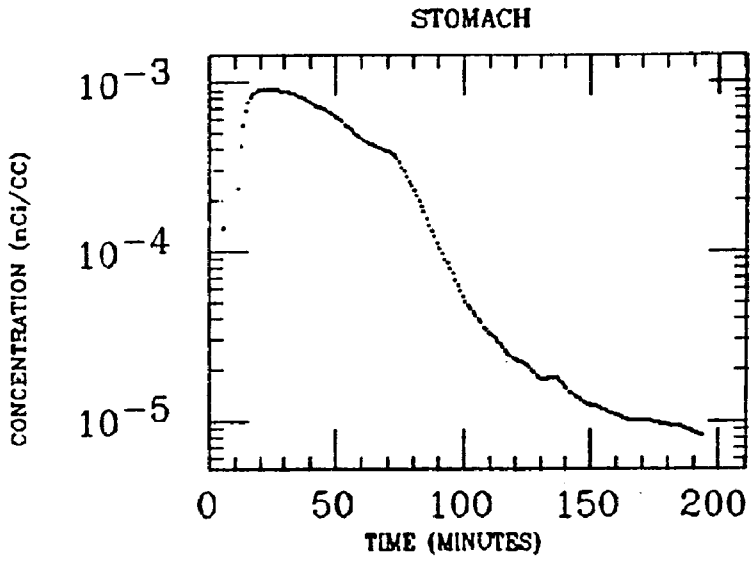

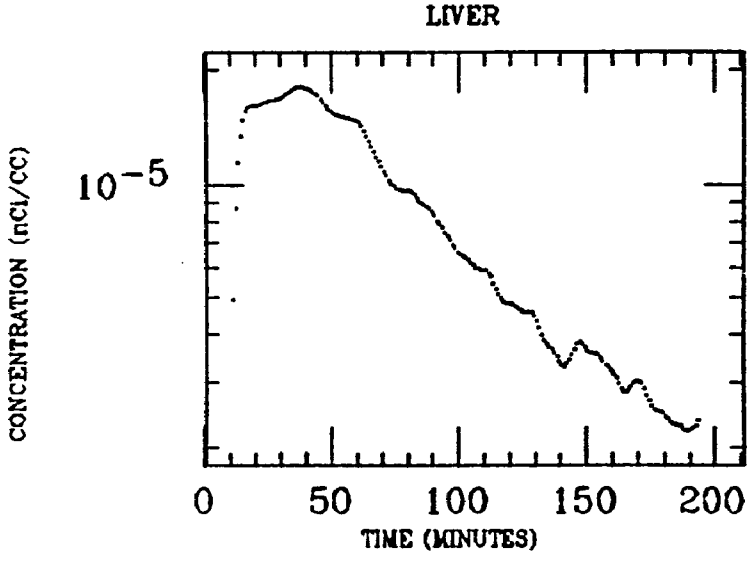

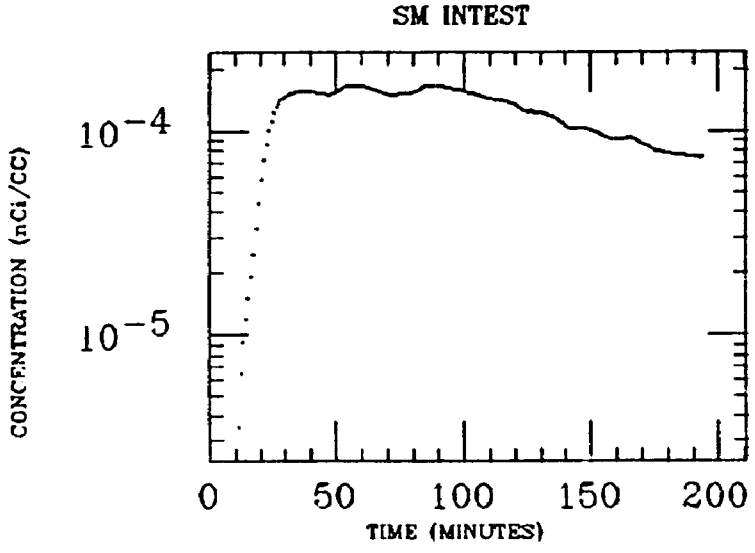

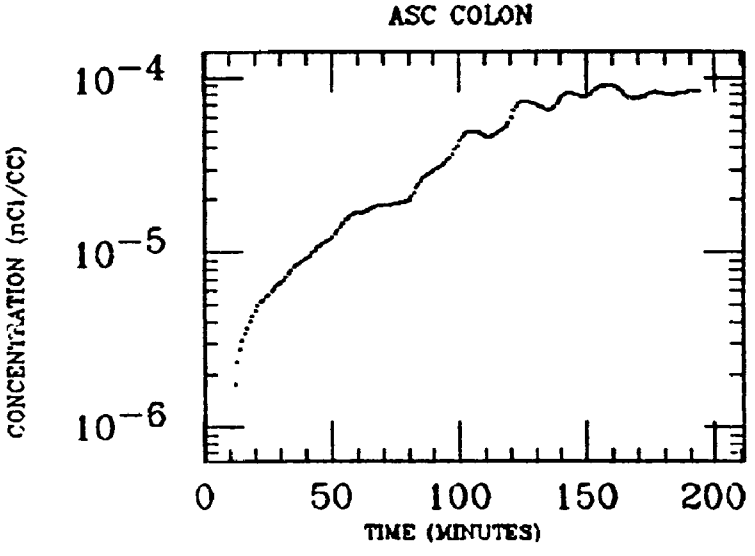

GALLOP
XE INGESTION
Po-218

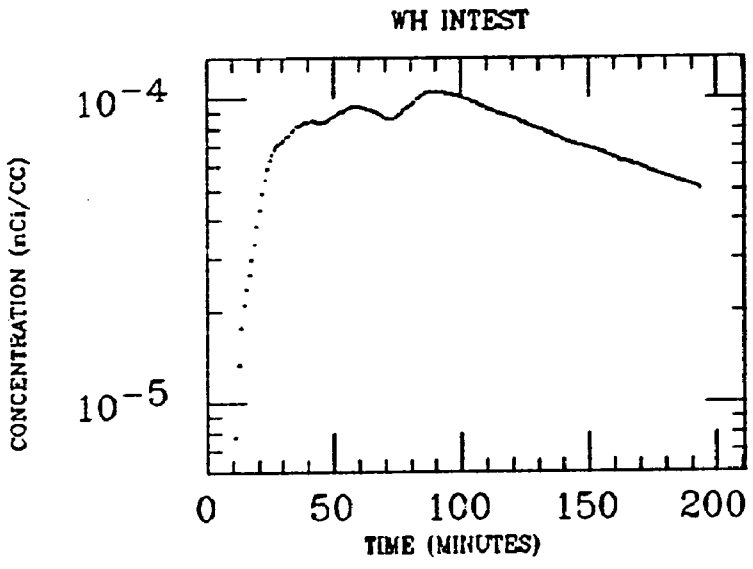

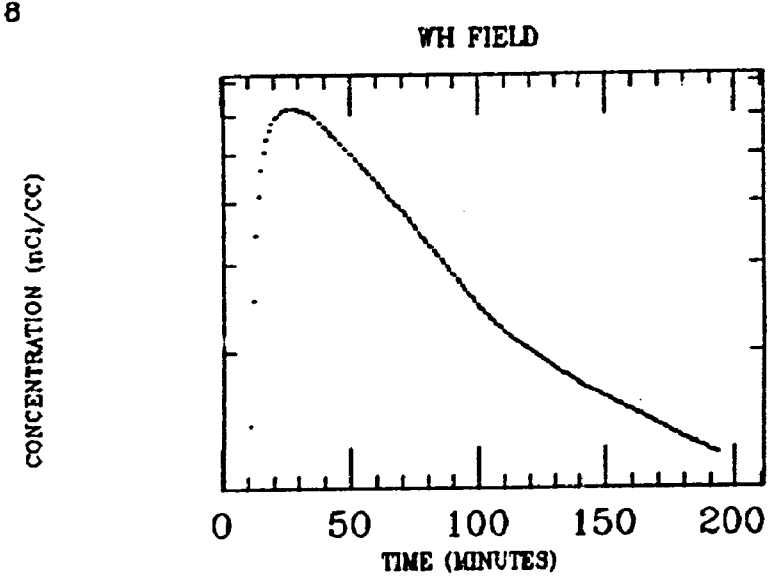

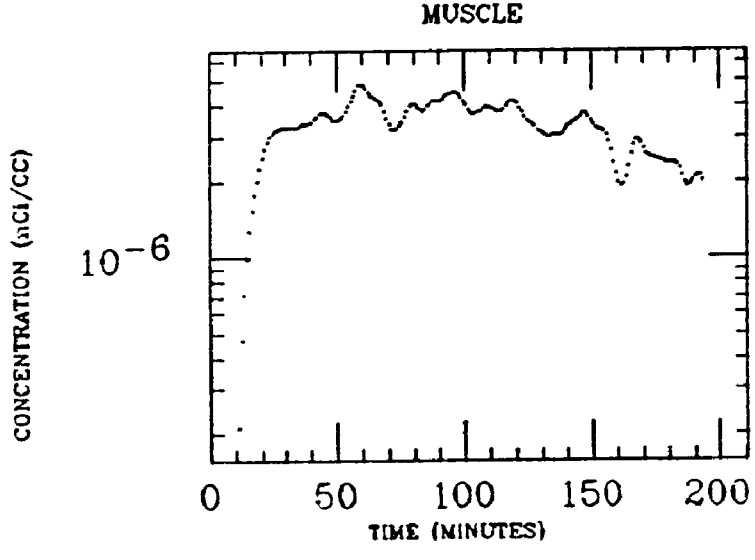

C.MCKINLEY
XE INGESTION
Po-218

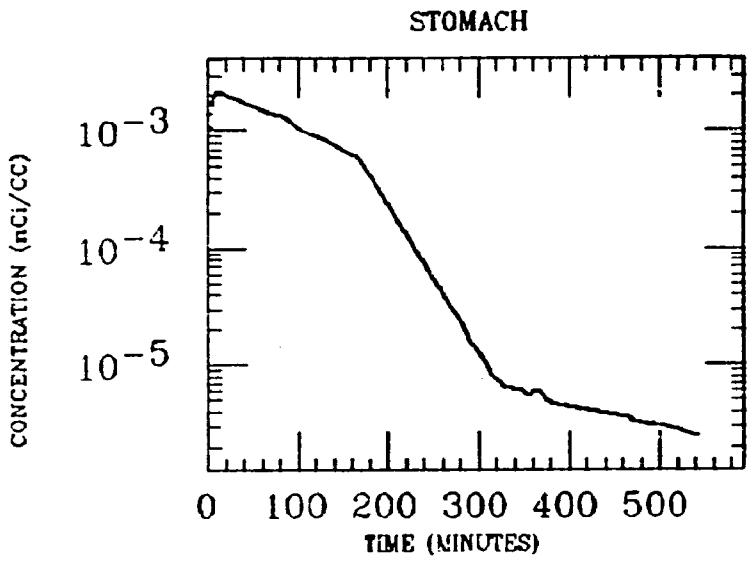

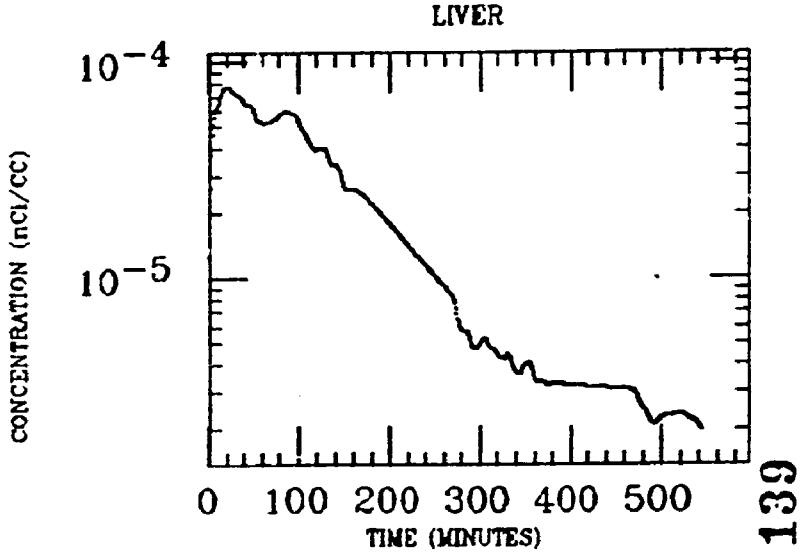

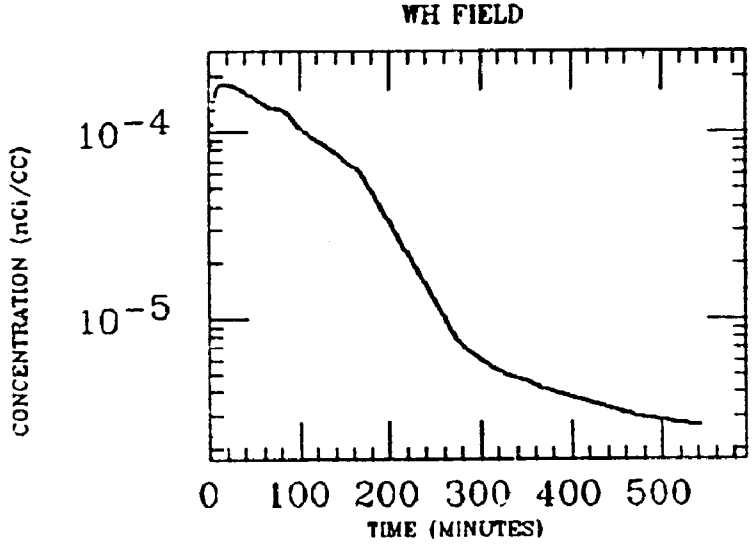

C.MCKINLEY
XE INGESTION
Po-218

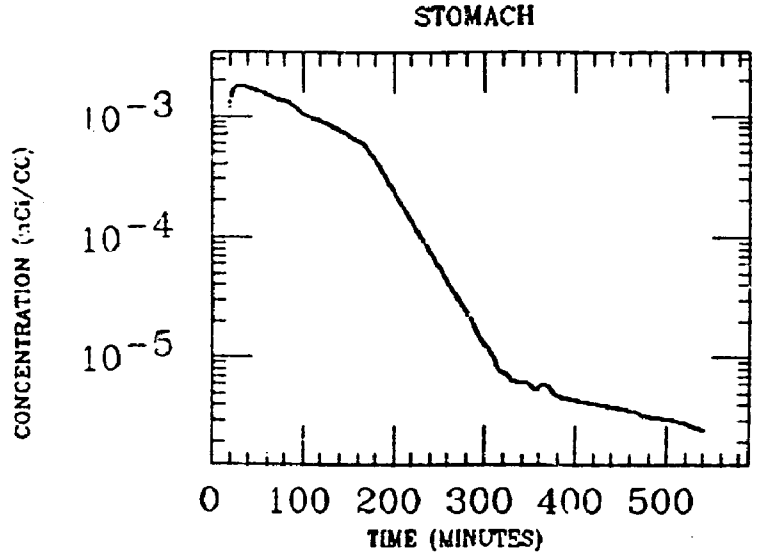

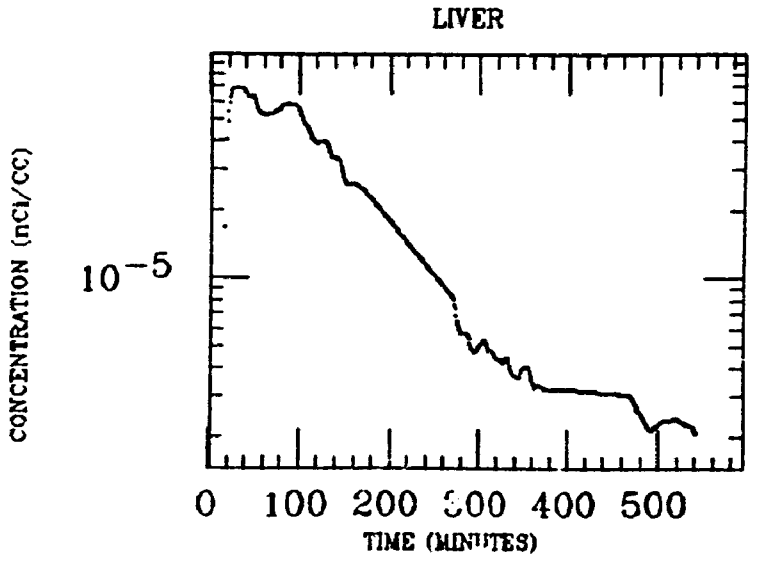

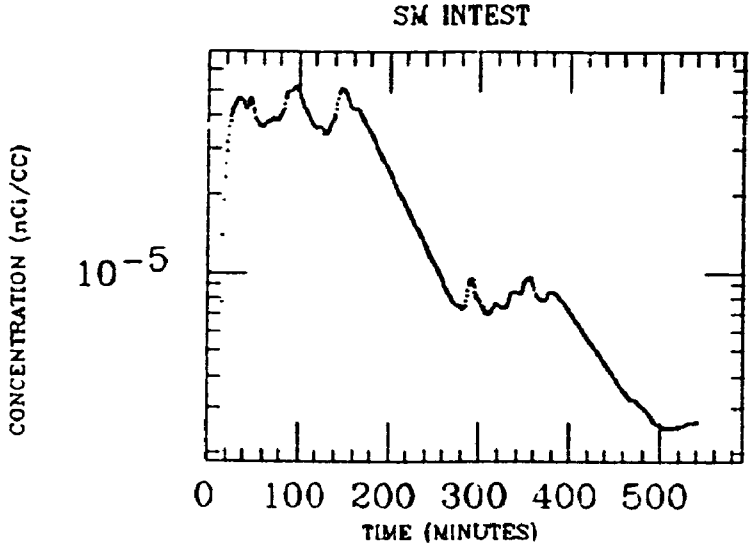

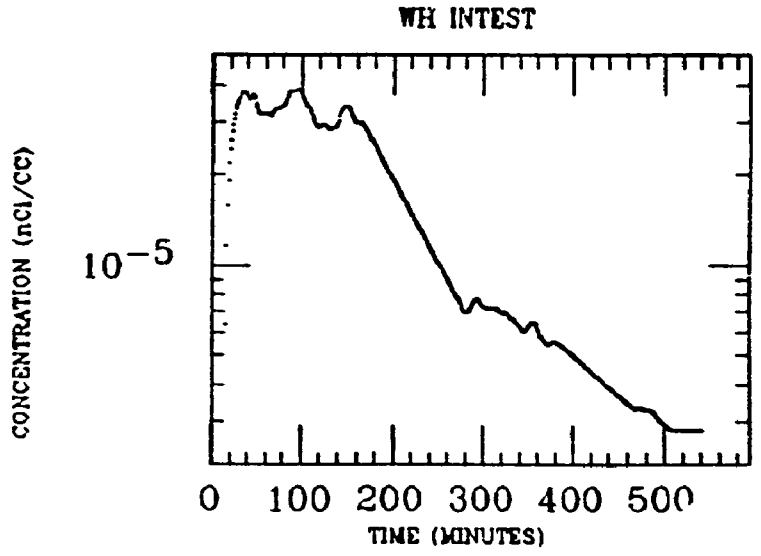

C.MCKINLEY
XE INGESTION
Po-218

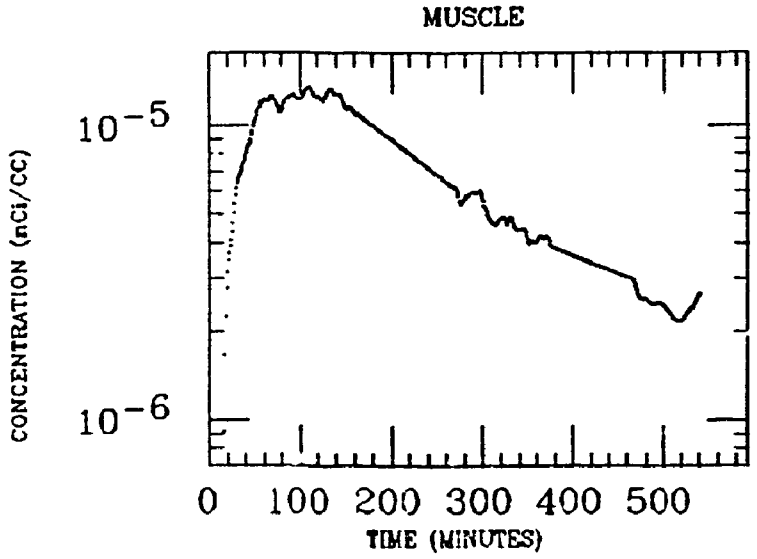

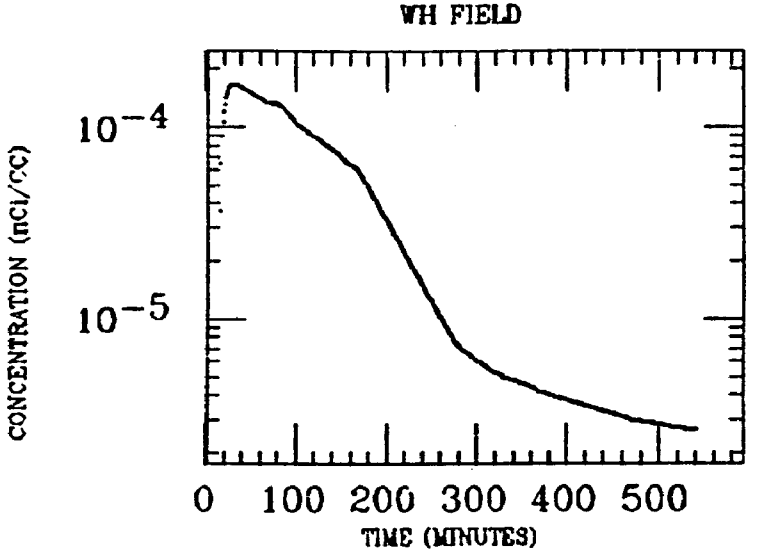

HAND
XE INGESTION
Po-218

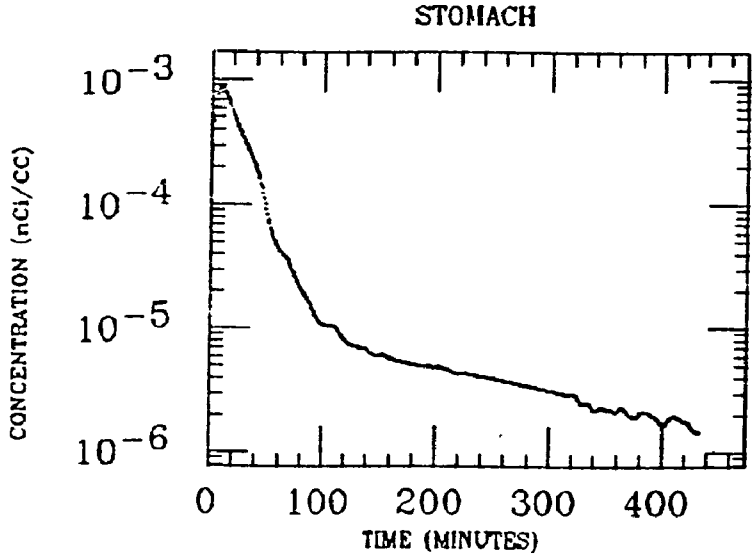

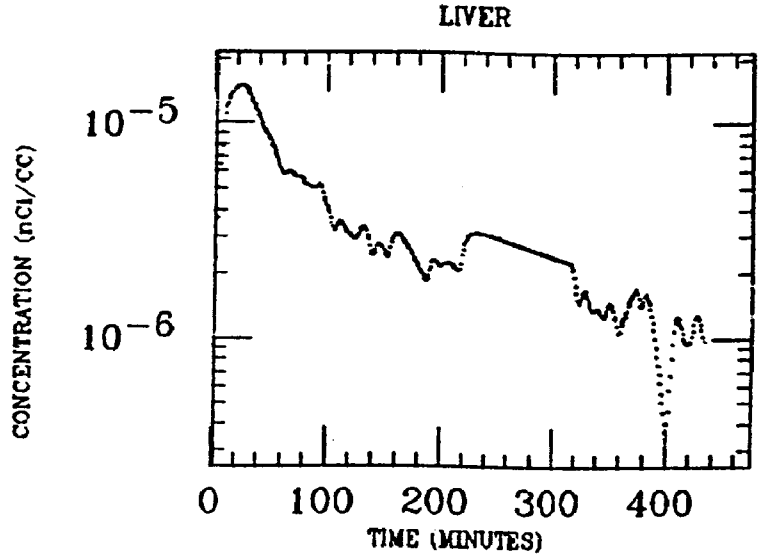

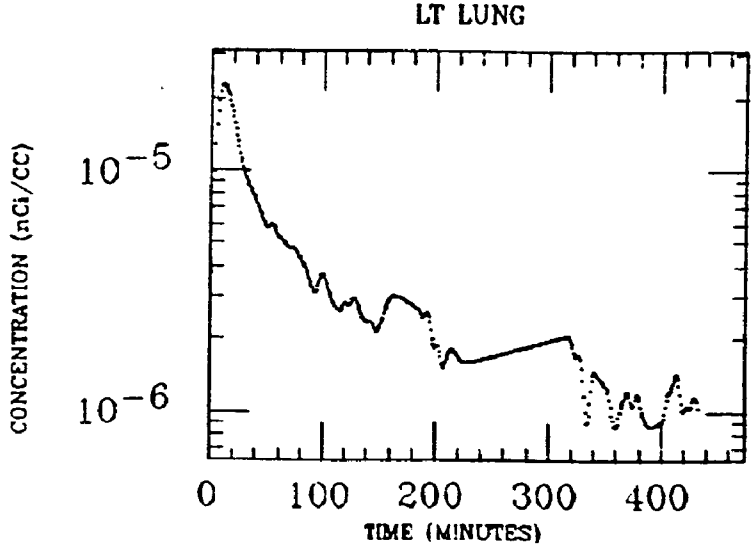

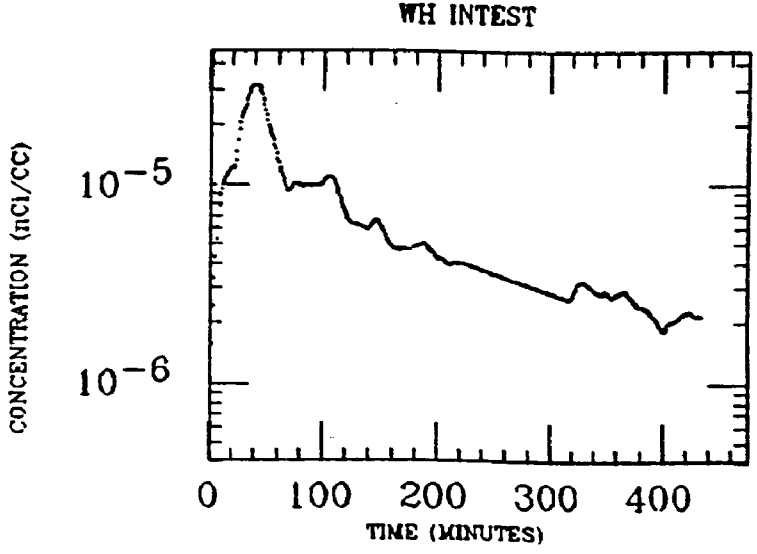

HAND

XE INGESTION

Po-218

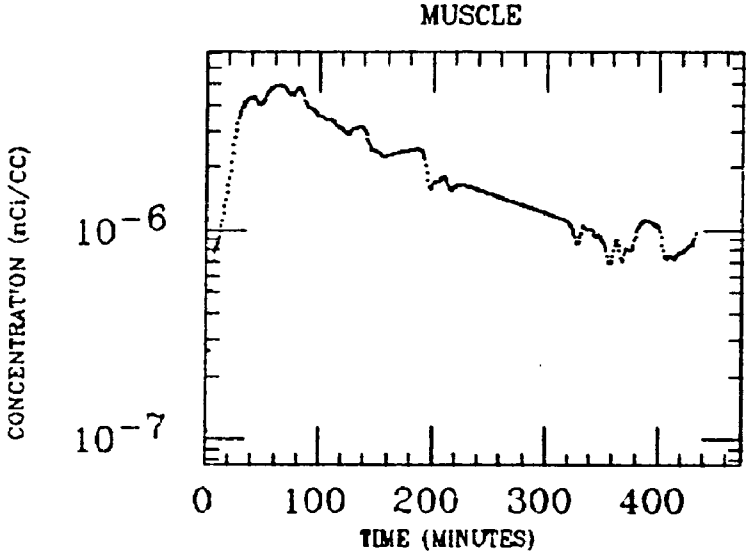

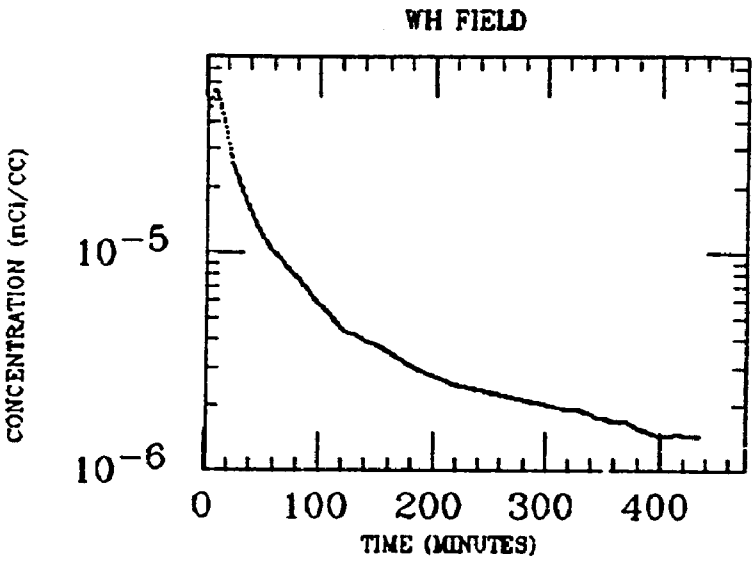

HAND
XE INGESTION
Po-218

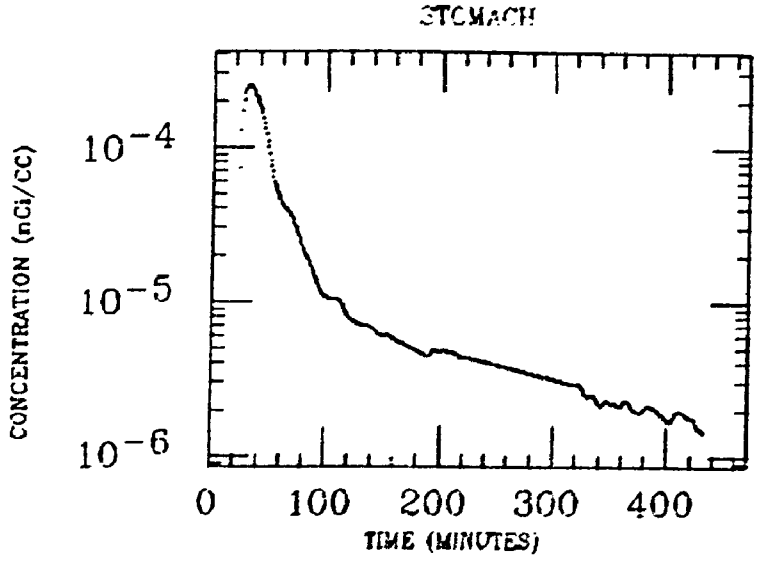

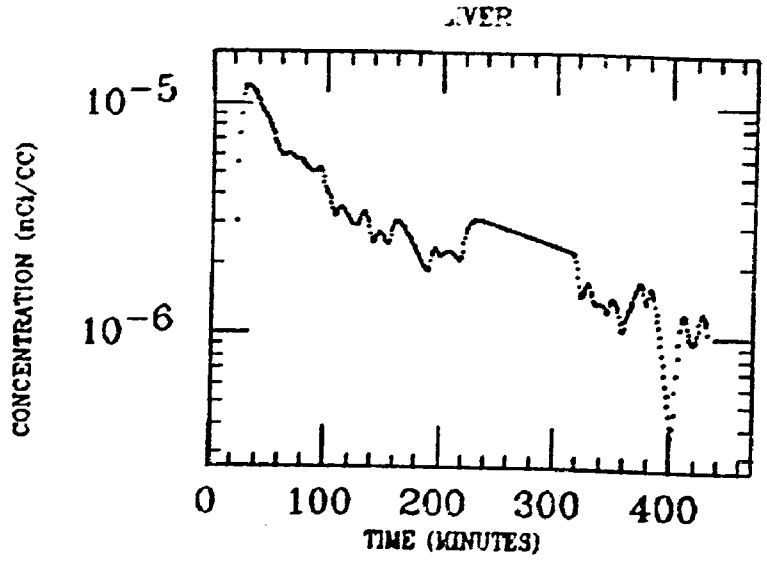

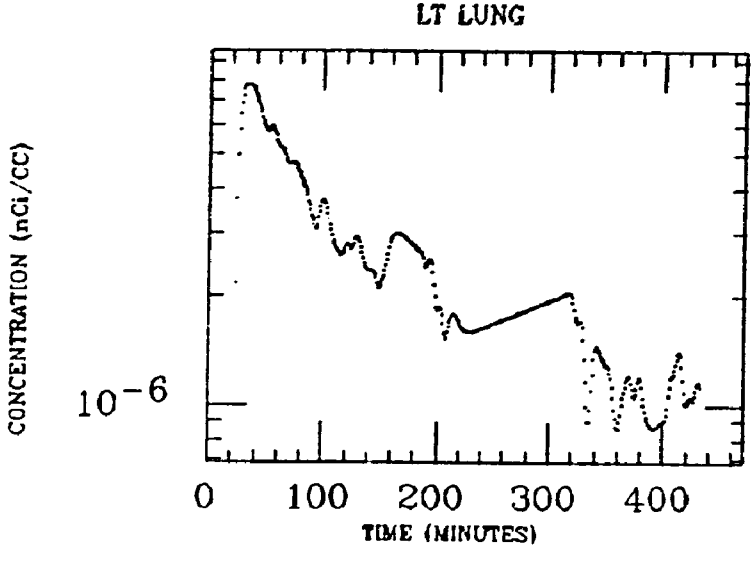

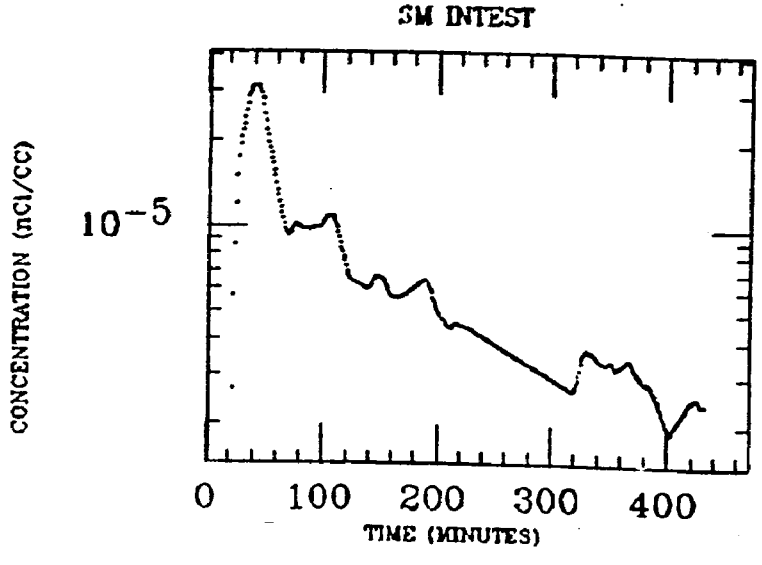

HAND
XE INGESTION
Po-218

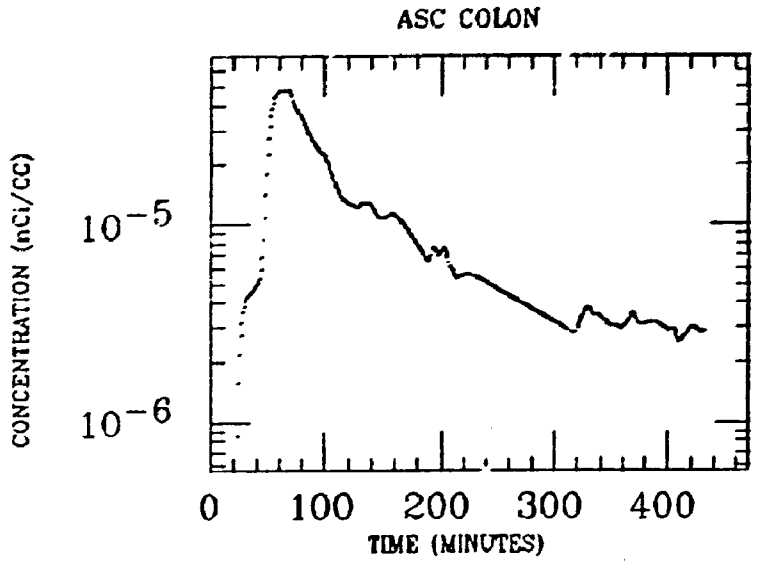

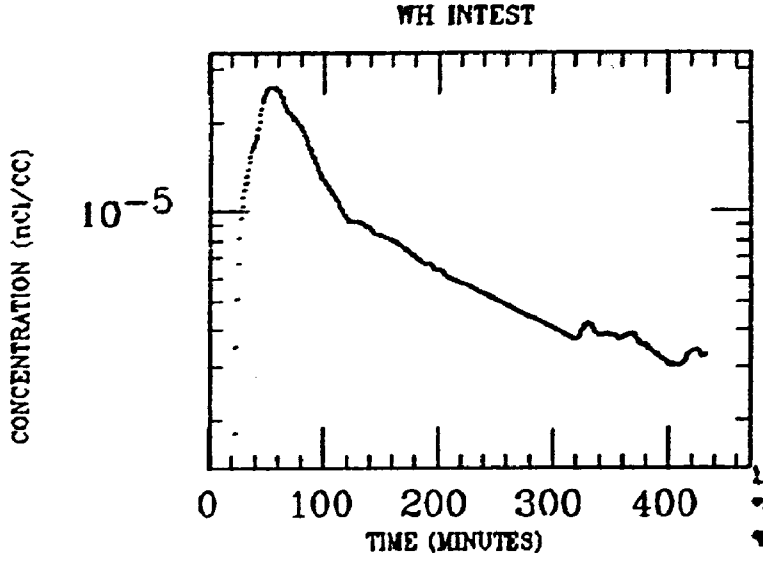

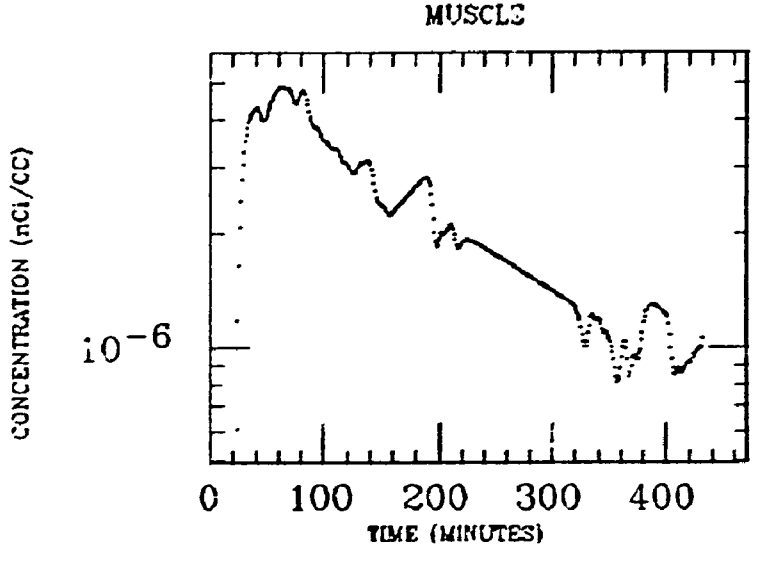

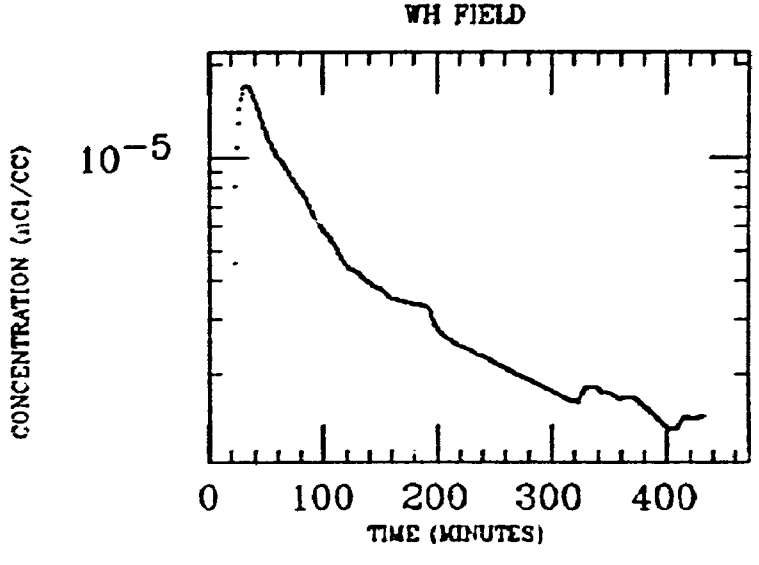

HAWKINS
XE INGESTION
Po-218

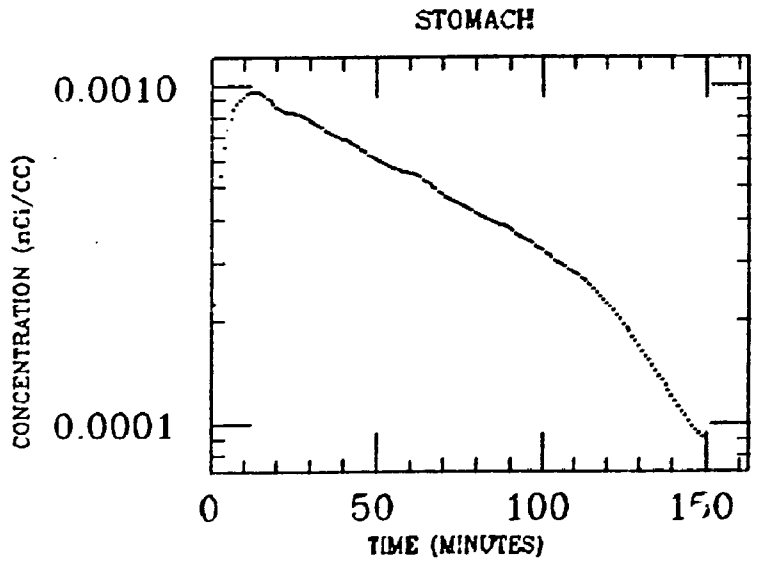

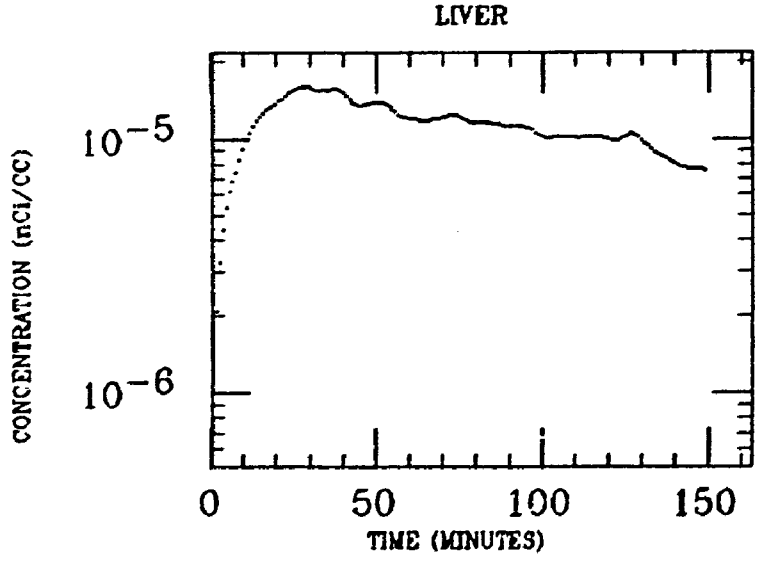

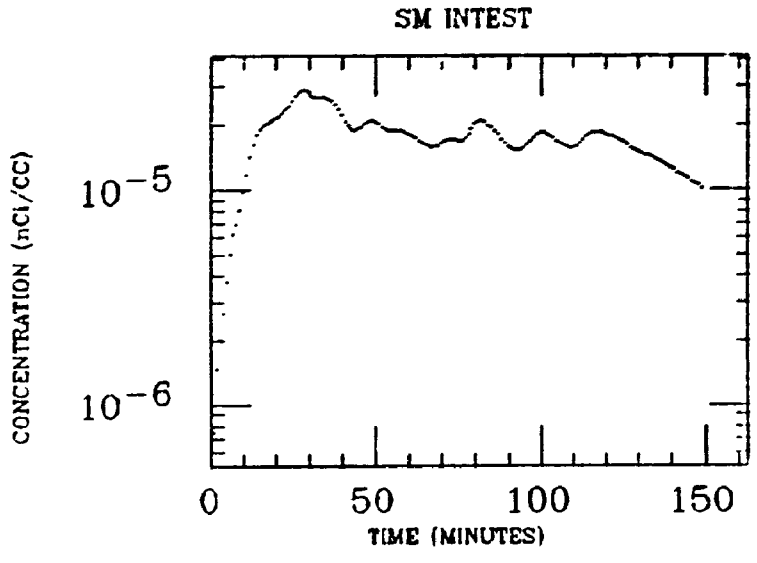

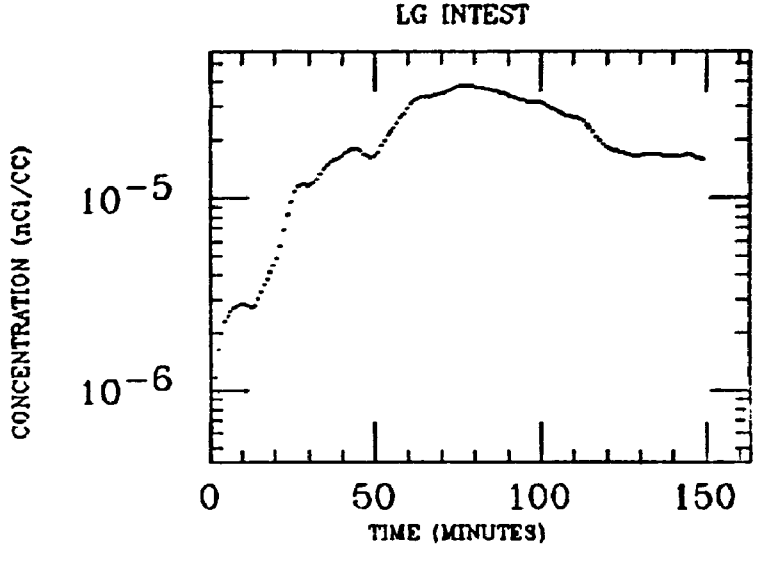

HAWKINS
XE INGESTION
Po-218

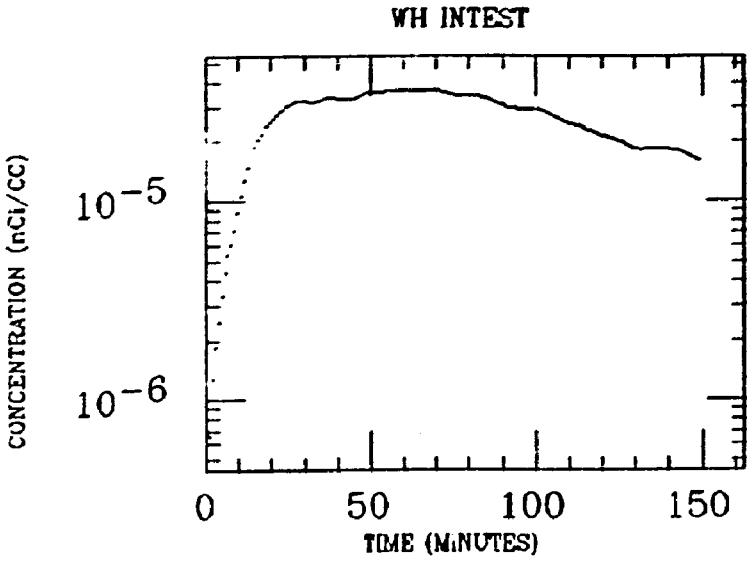

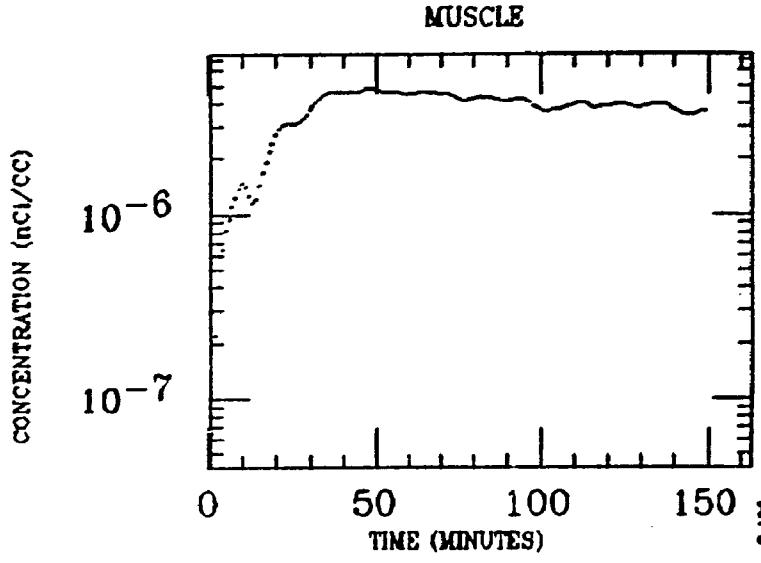

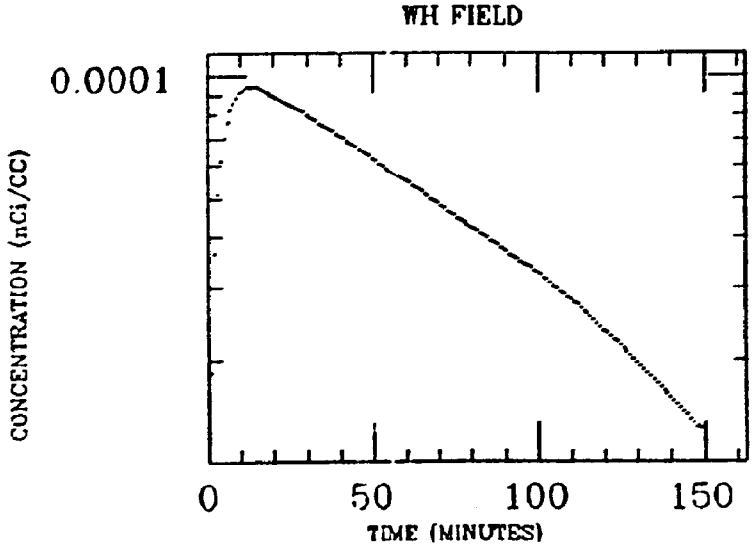

HILL
XE INGESTION
Po-218

SM INTEST

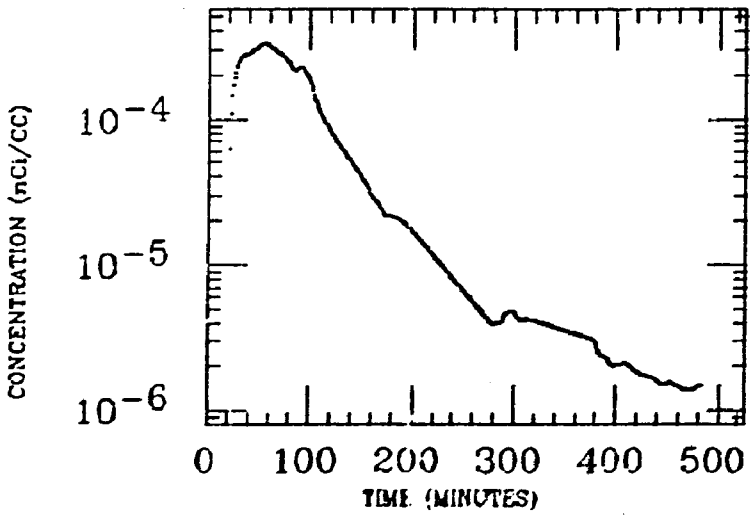

STOMACH

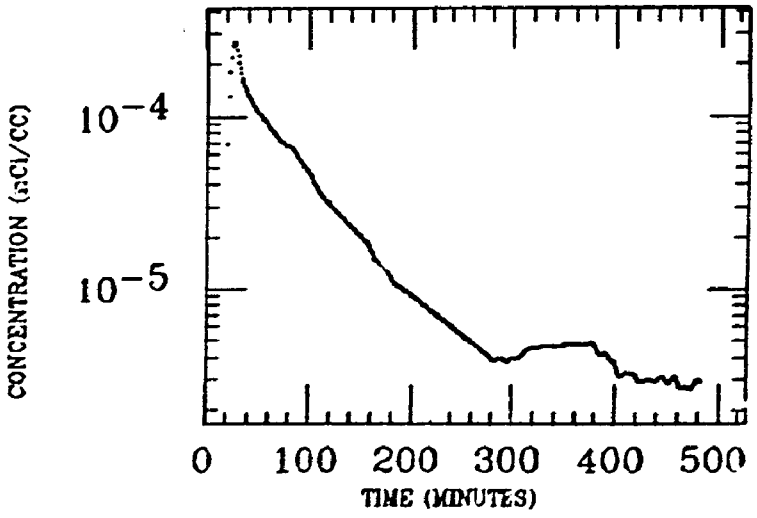

DES COLON

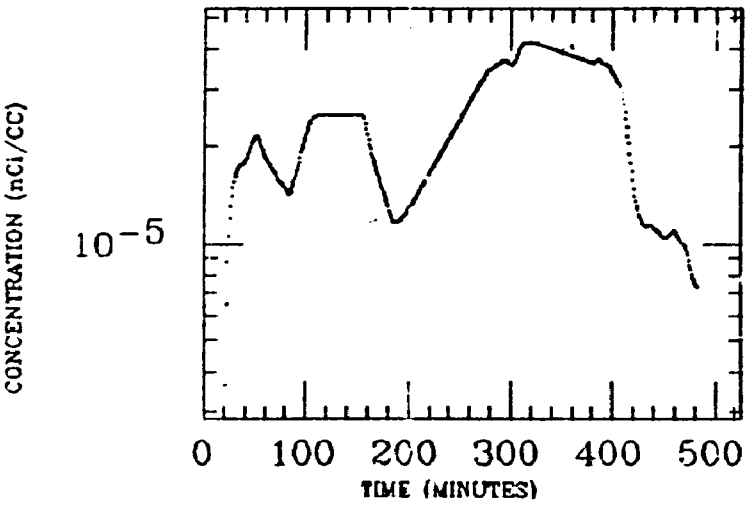

MUSCLE

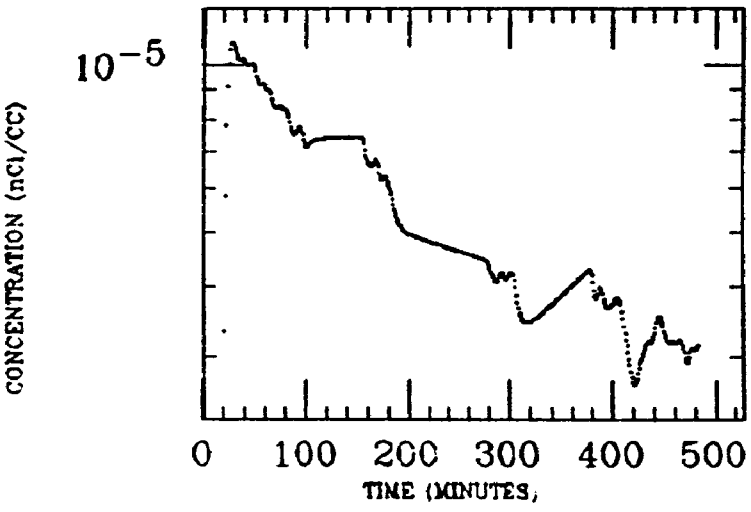

HILL
XE INGESTION
Po-218

LIVER

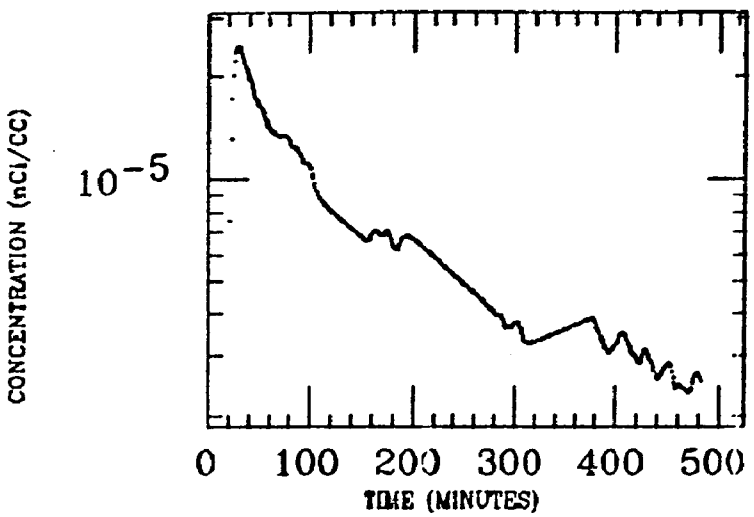

WH FIELD

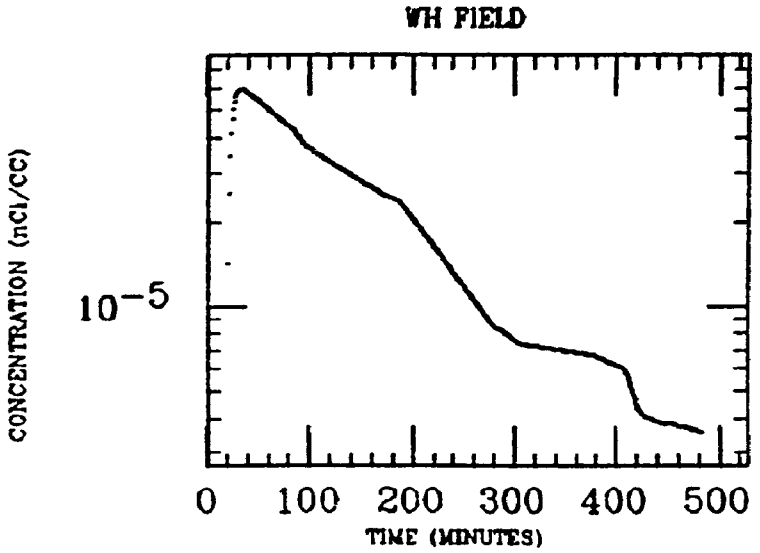

HILL
XE INGESTION
Po-218

STOMACH

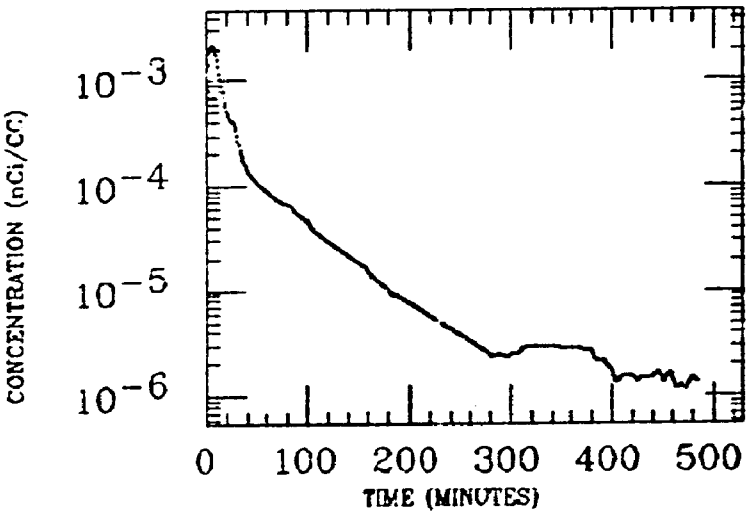

LIVER

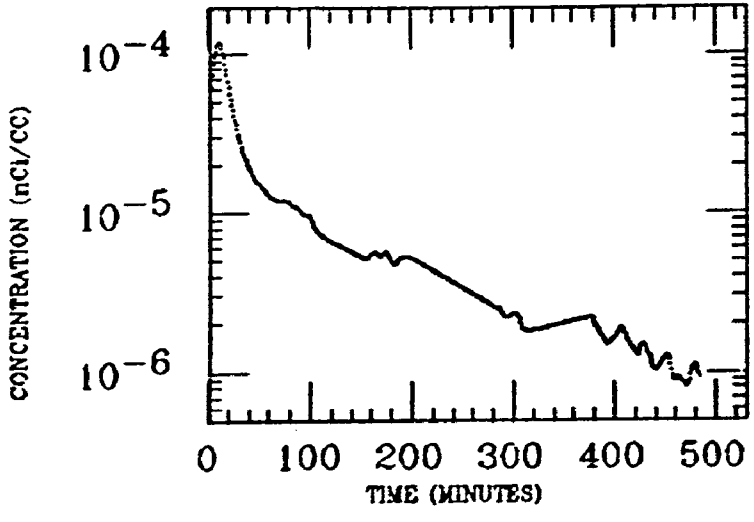

MUSCLE

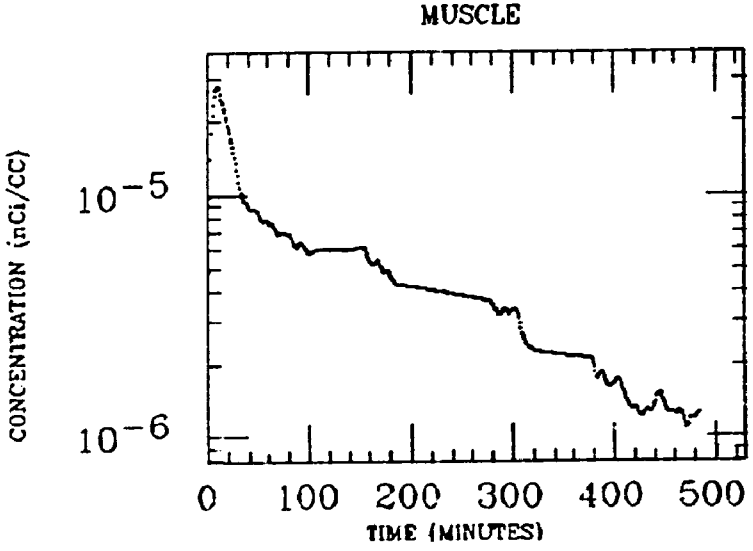

WH FIELD

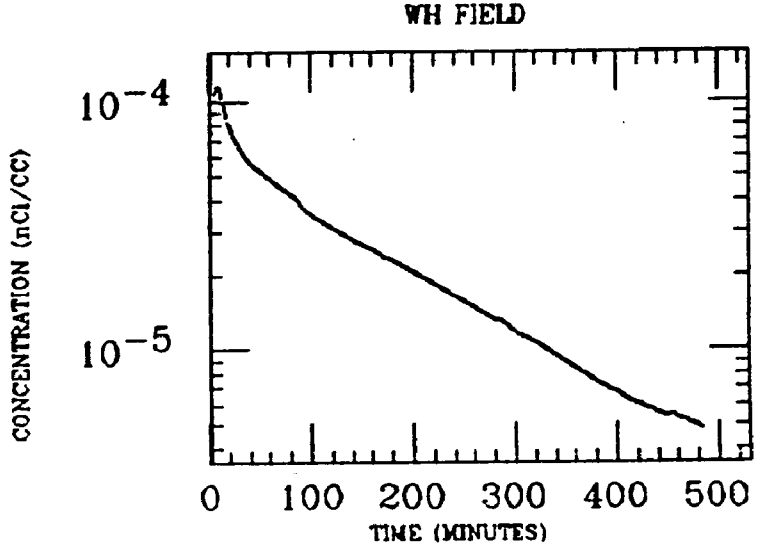

HUTCHINS
XE INGESTION
Po-218

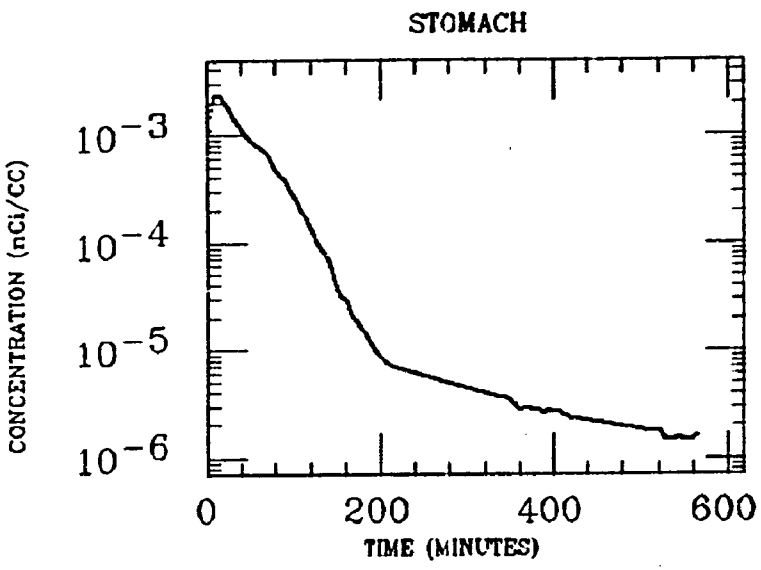

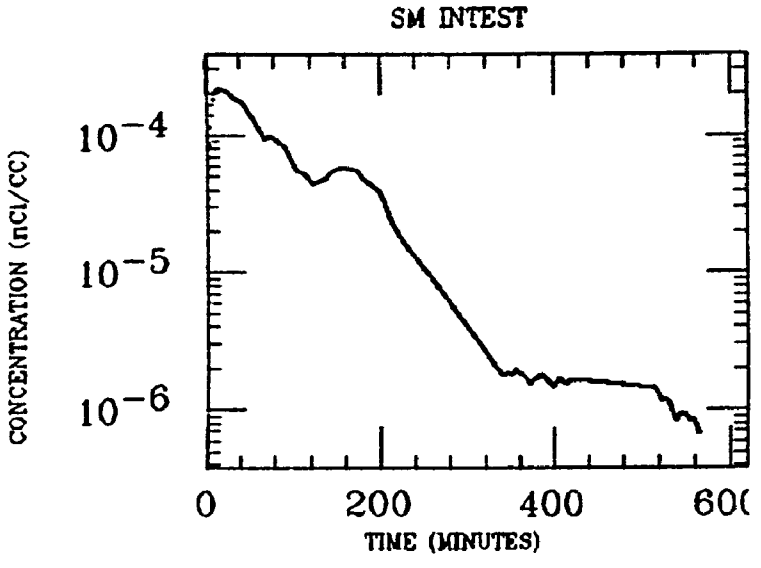

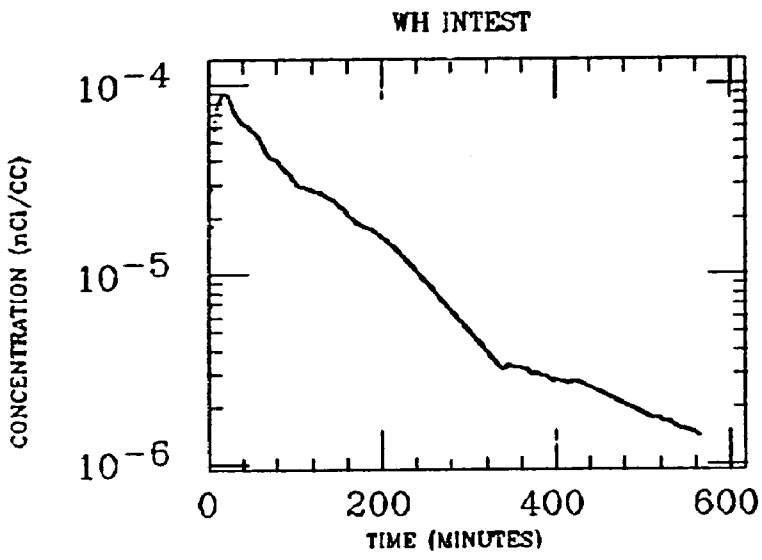

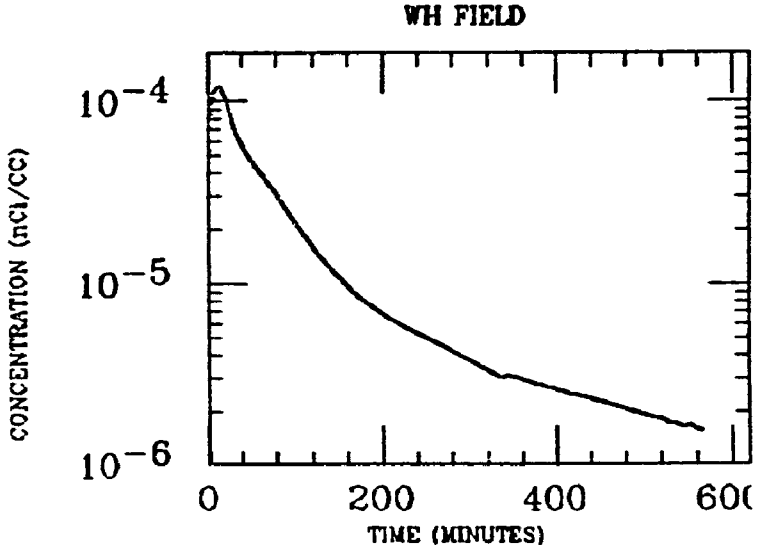

HUTCHINS
XE INGESTION
Po-218

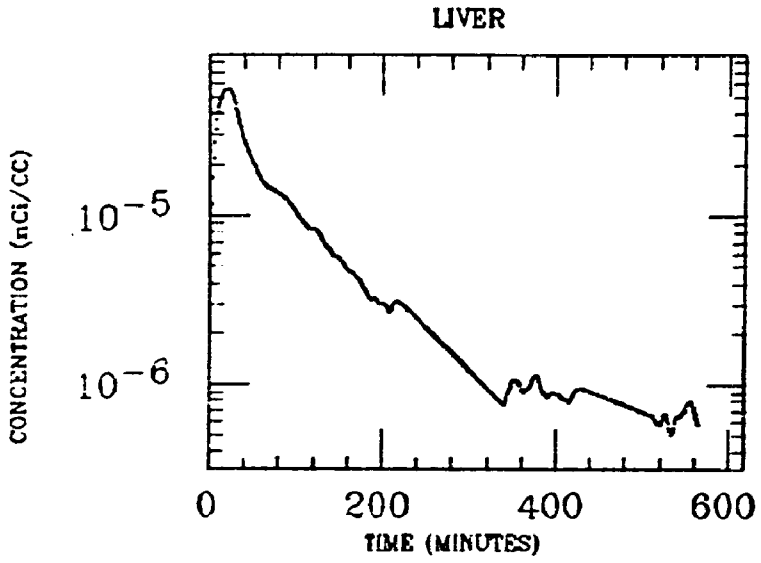

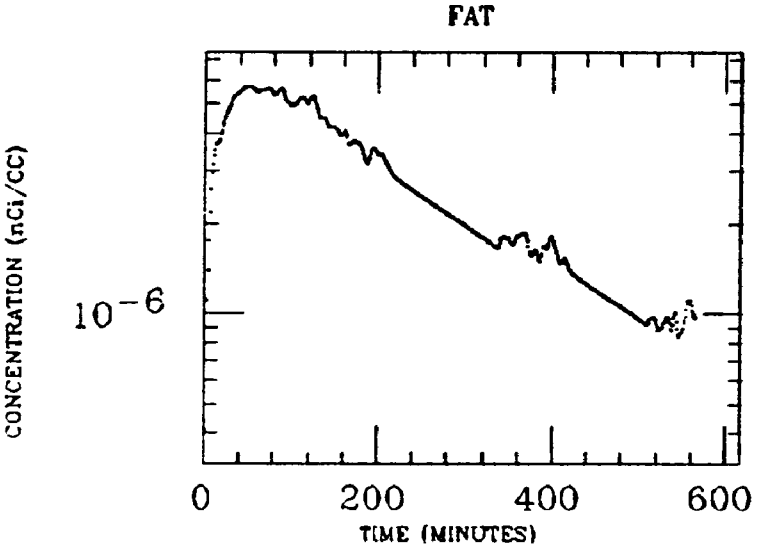

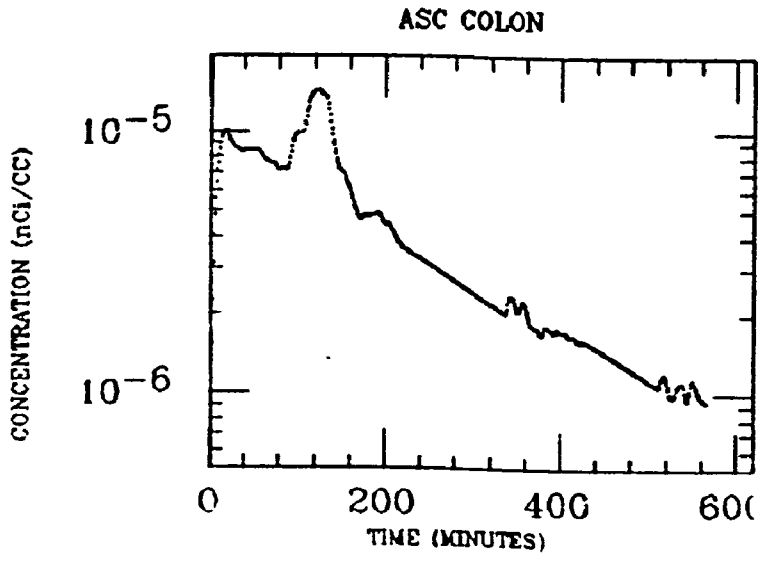

HUTCHINS
XE INGESTION
Po-218

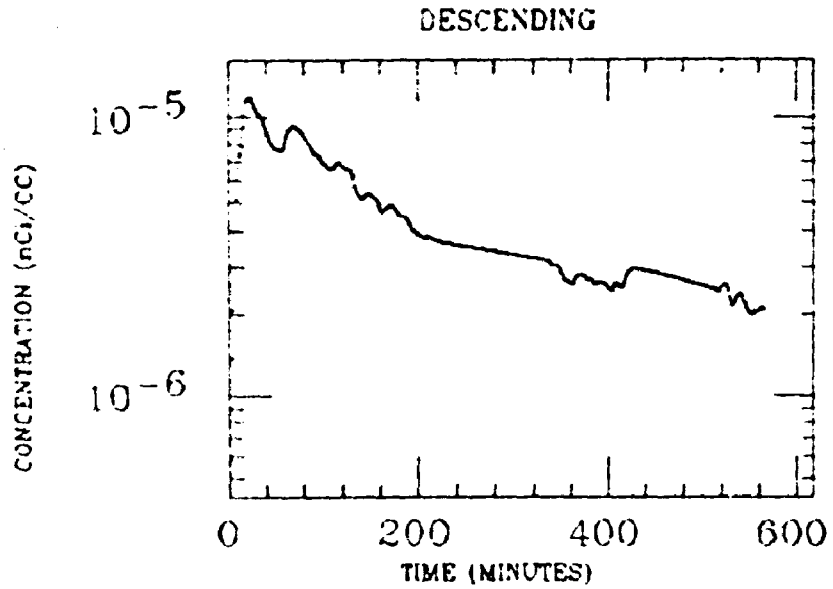

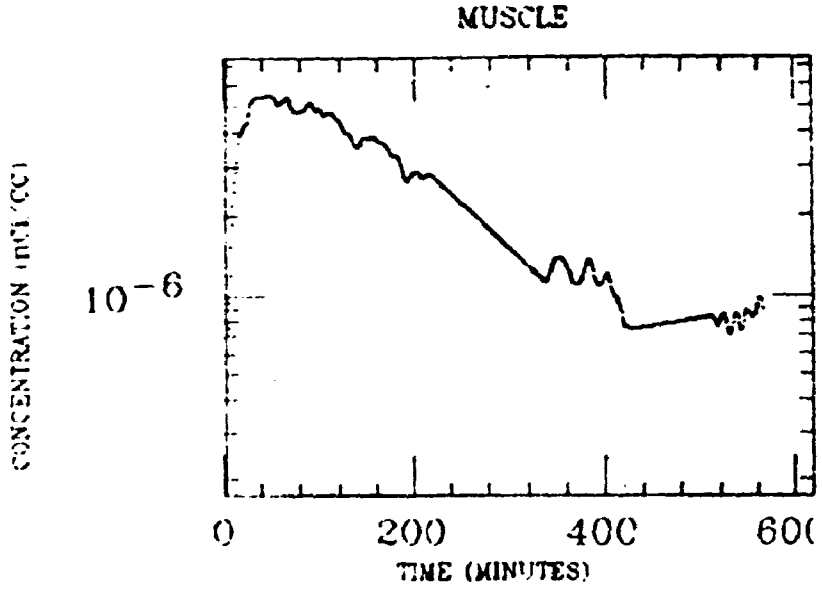

J.MCKINLEY
XE INGESTION
Po-218

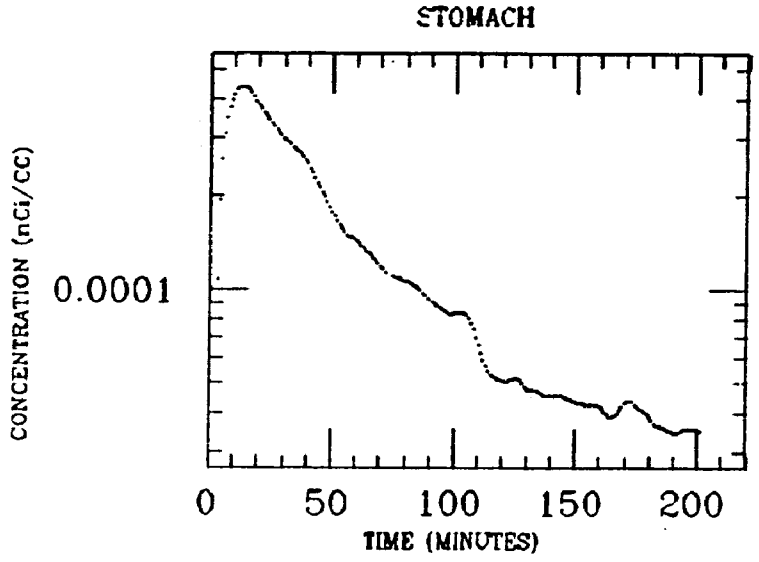

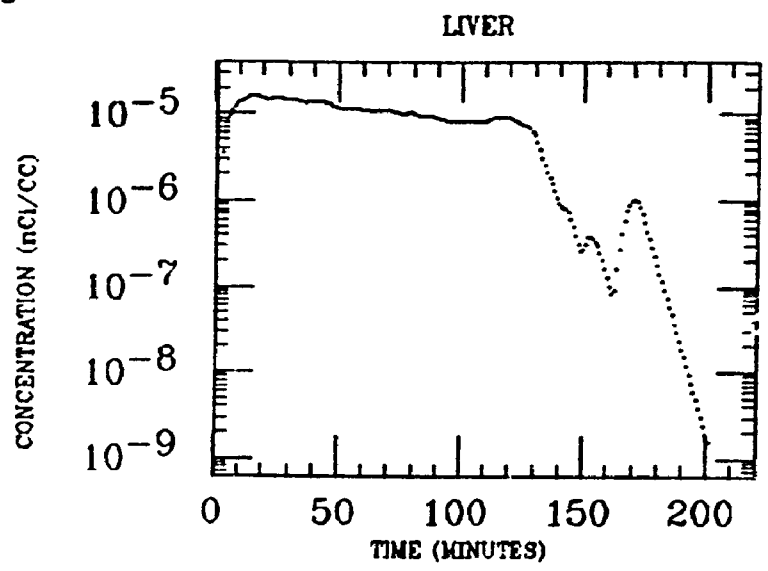

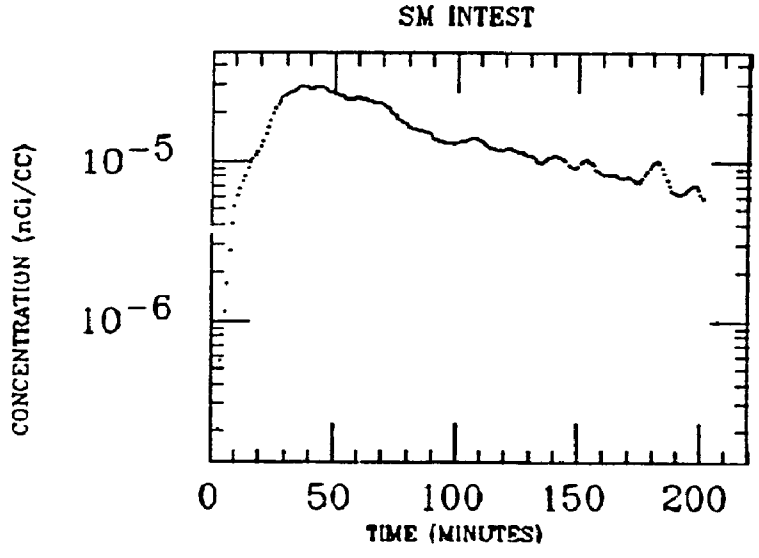

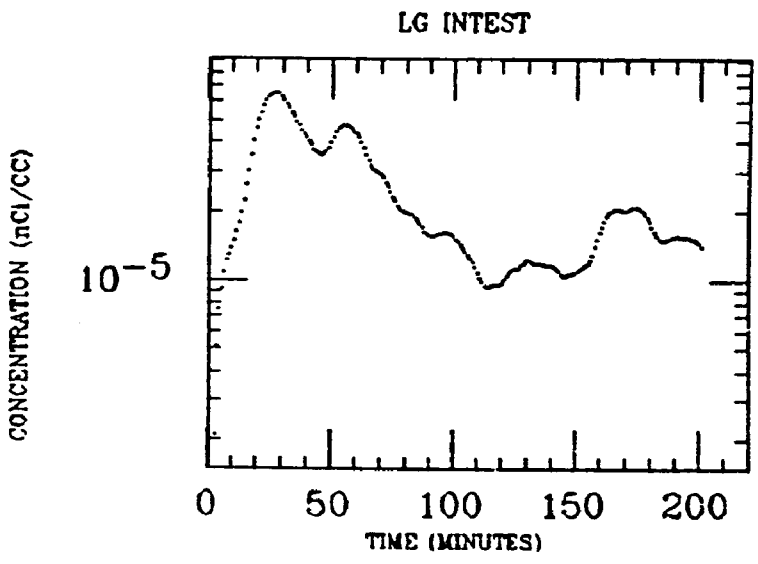

J.MCKINLEY
XE INGESTION
Po-218

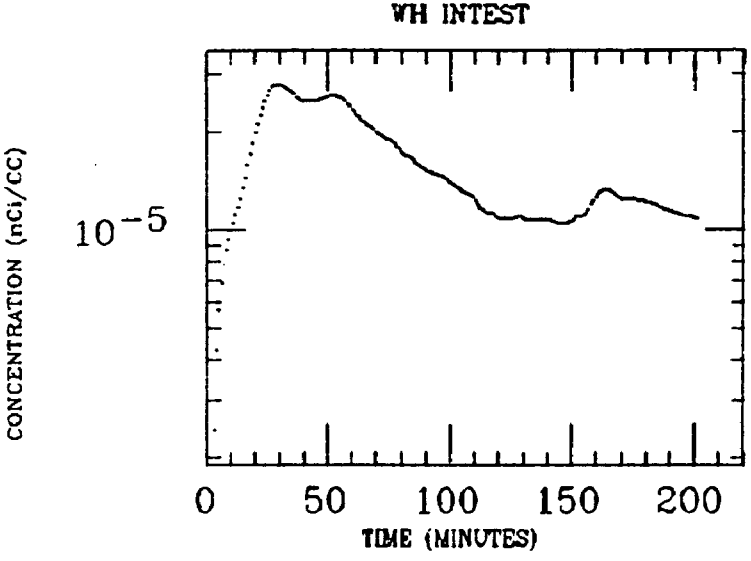

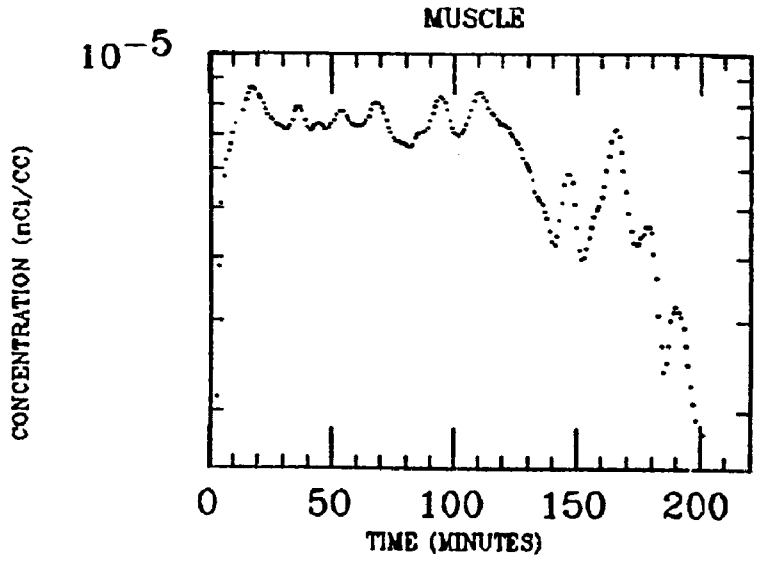

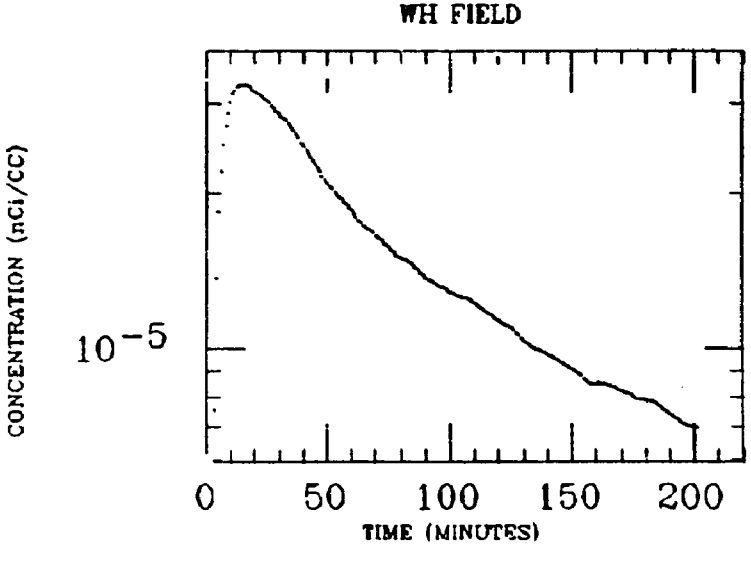

KELLEHER
XE INGESTION
Po-218

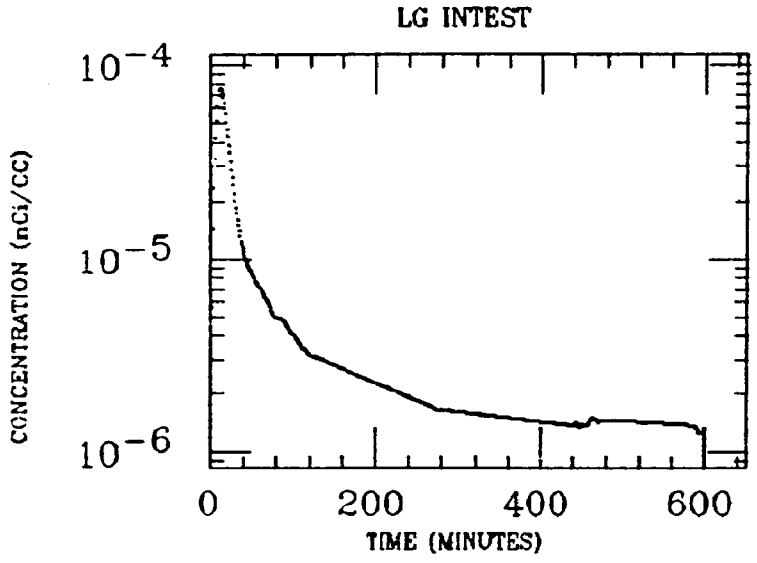

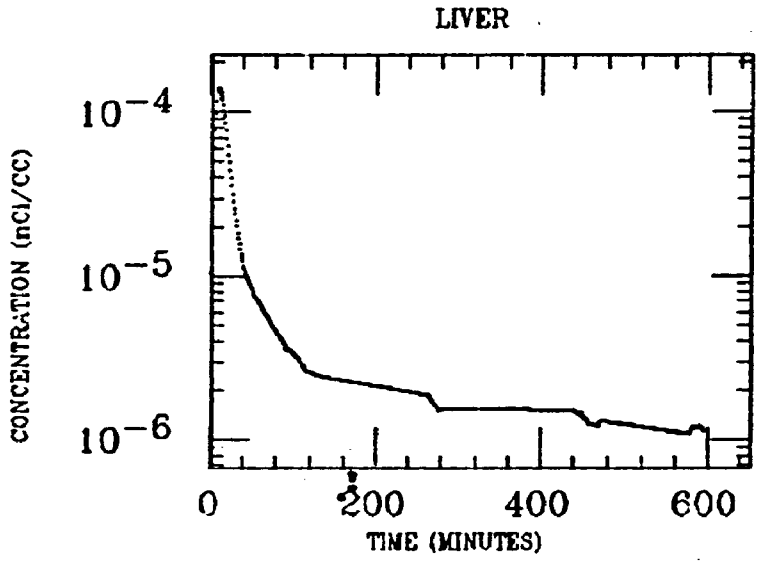

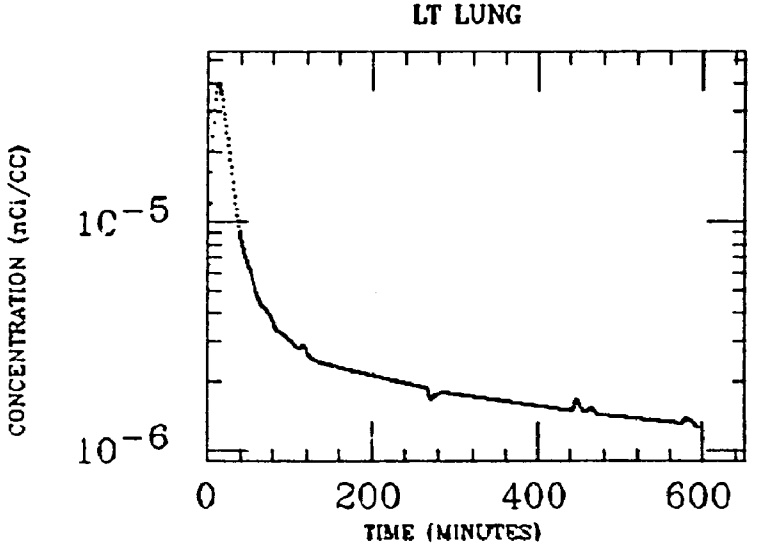

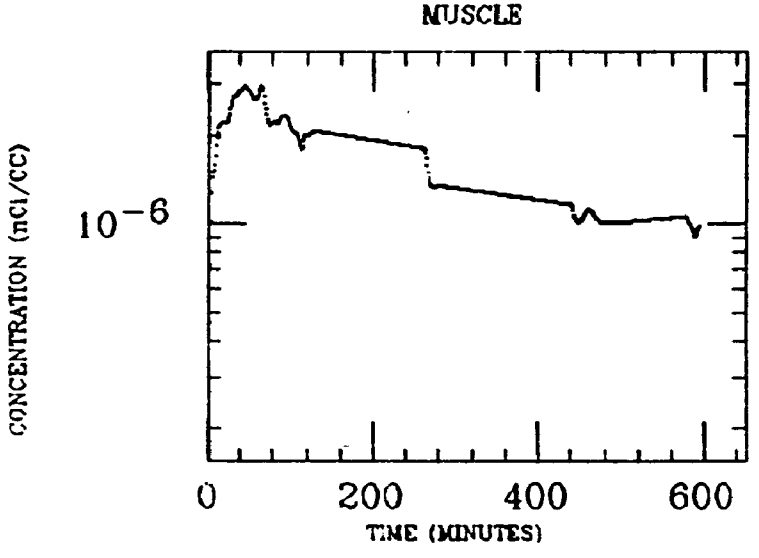

KELLEHER
XE INGESTION
Po-216

RT LUNG

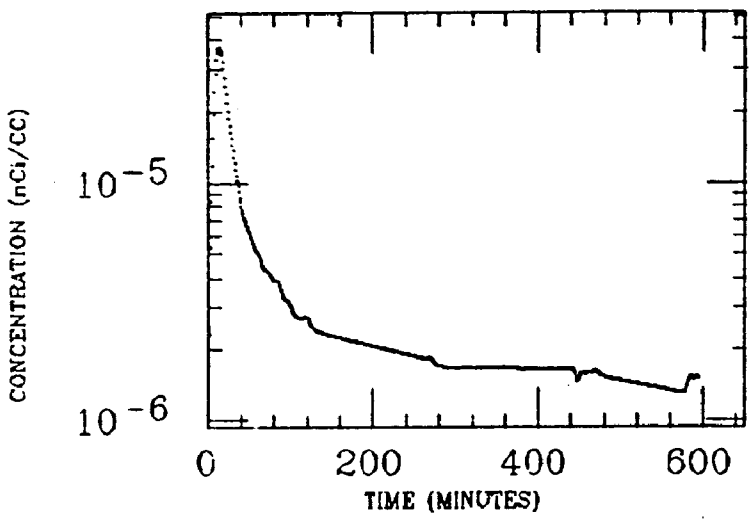

SM INTEST

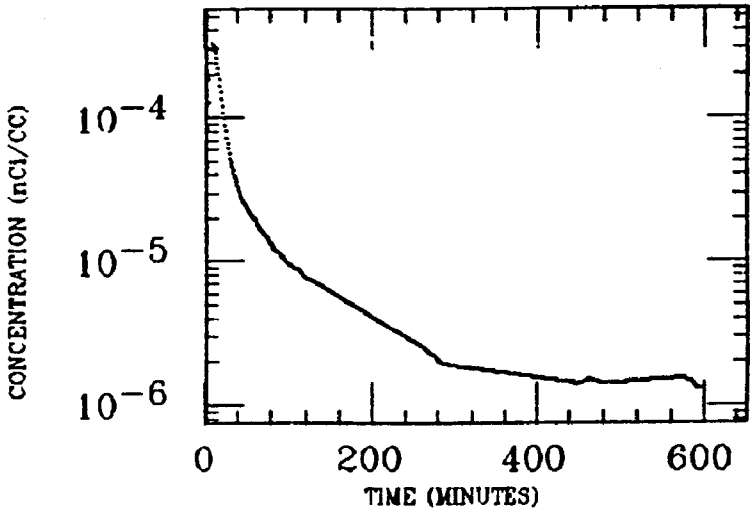

STOMACH

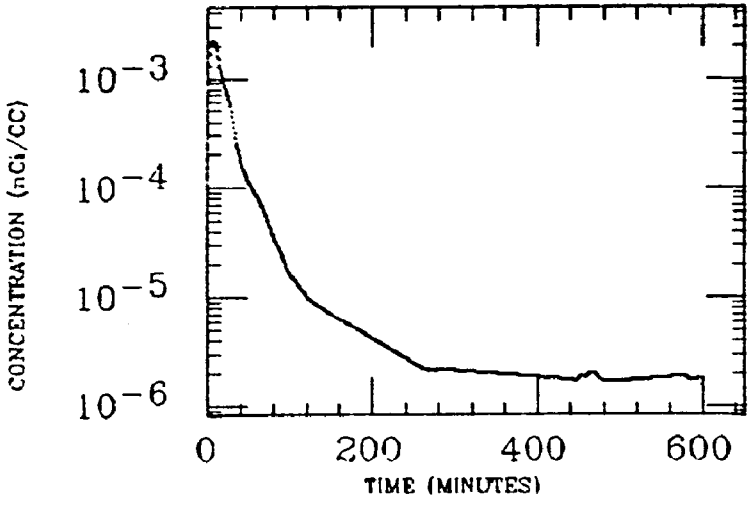

SH FIELD

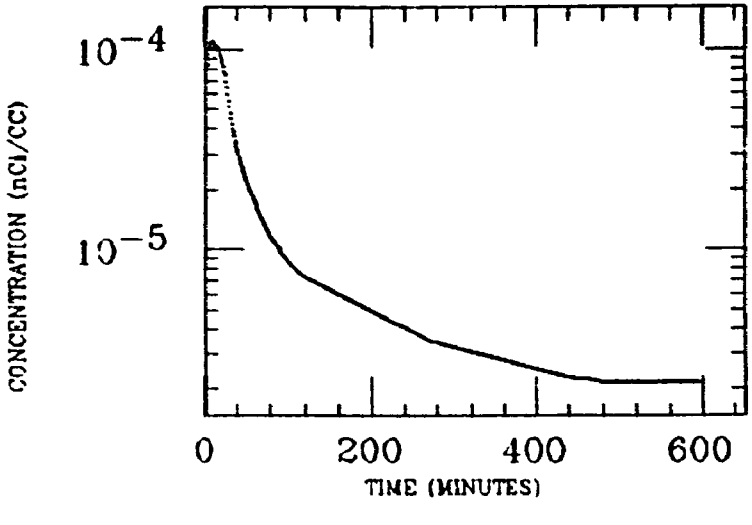

LITTELL
XE INGESTION
Po-218

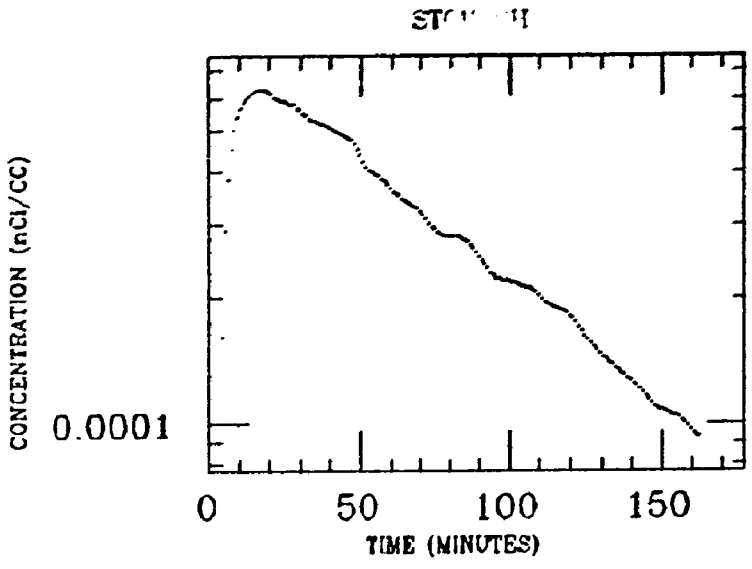

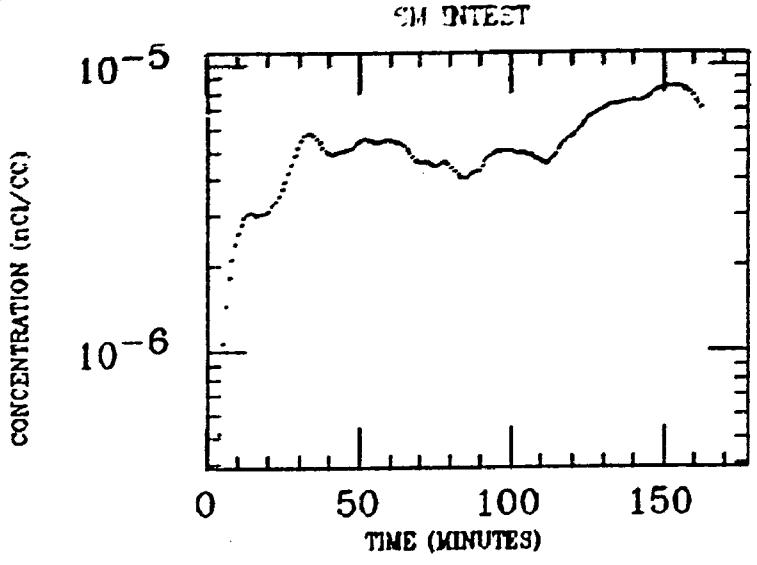

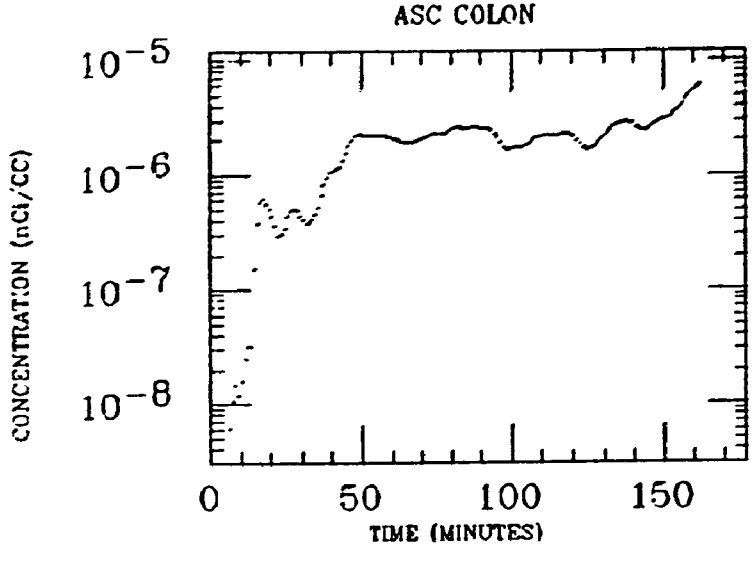

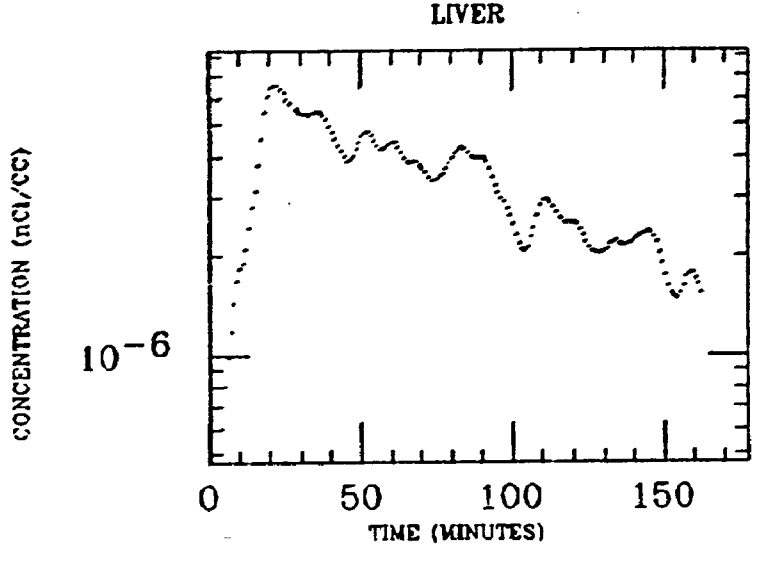

LITTELL
XE INGESTION
Po-218

MUSCLE

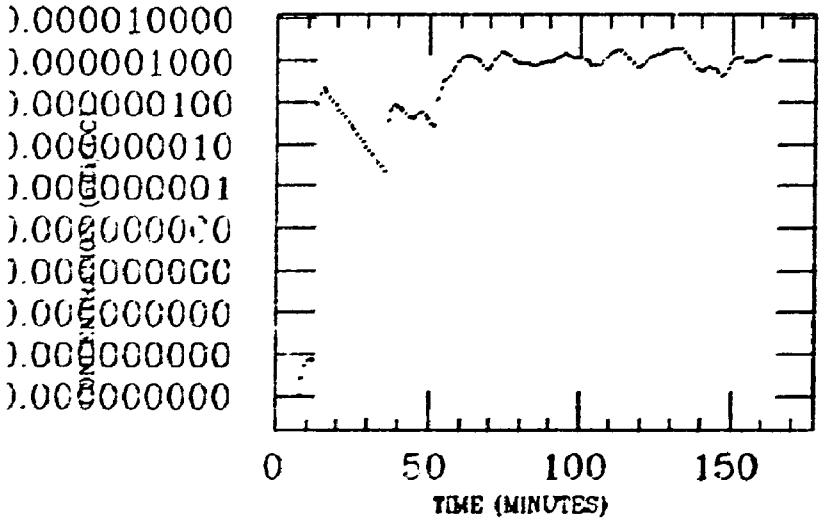

WH INTEST

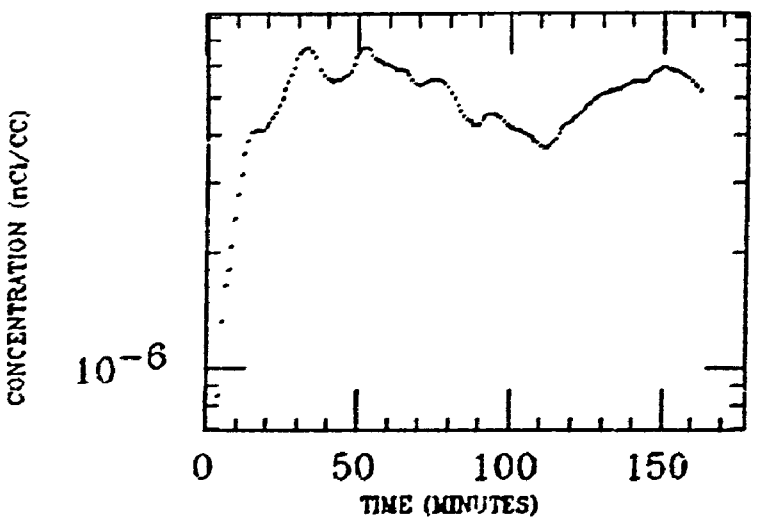

WH FIELD

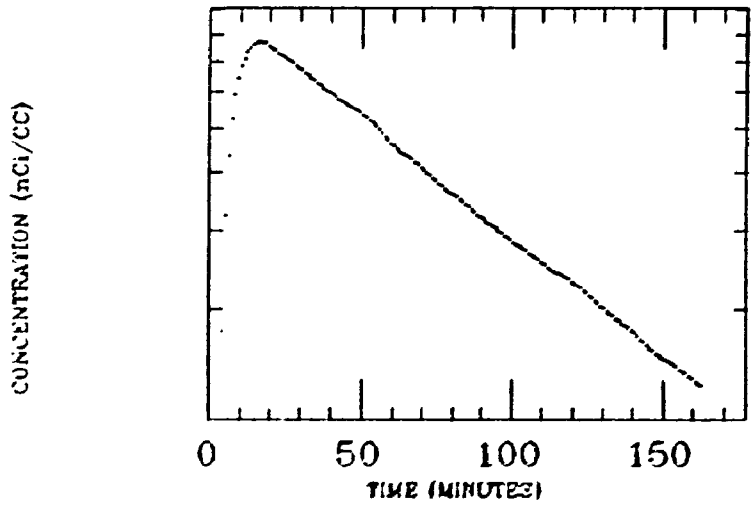

MACMILLAN
XE INGESTION
Po-218

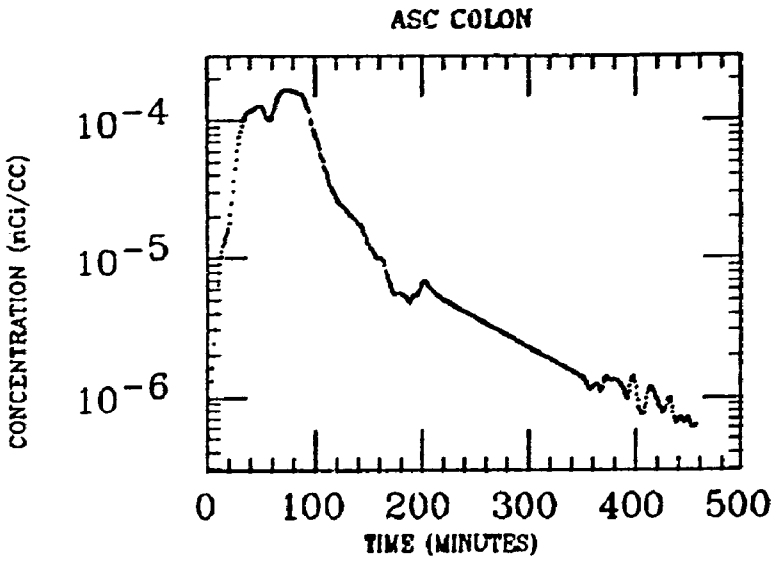

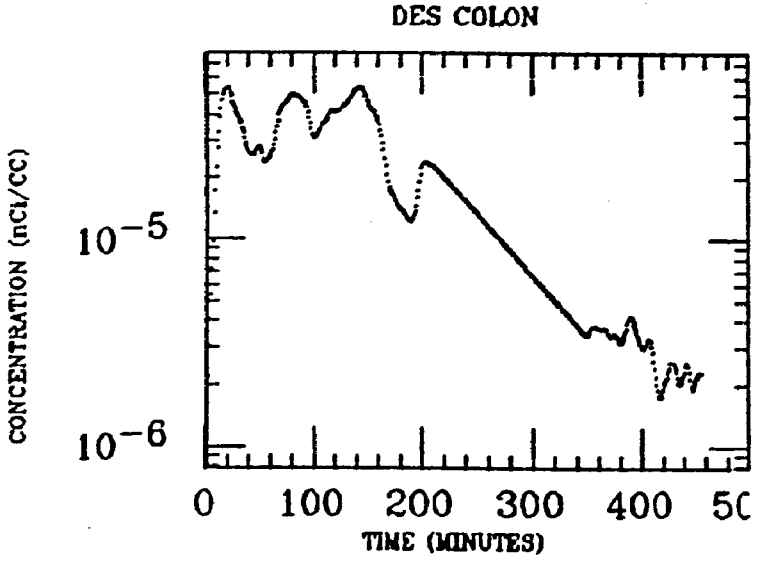

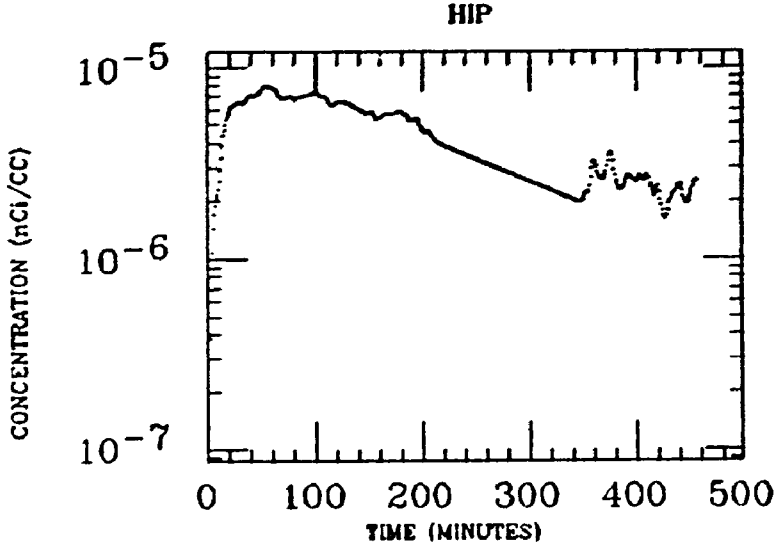

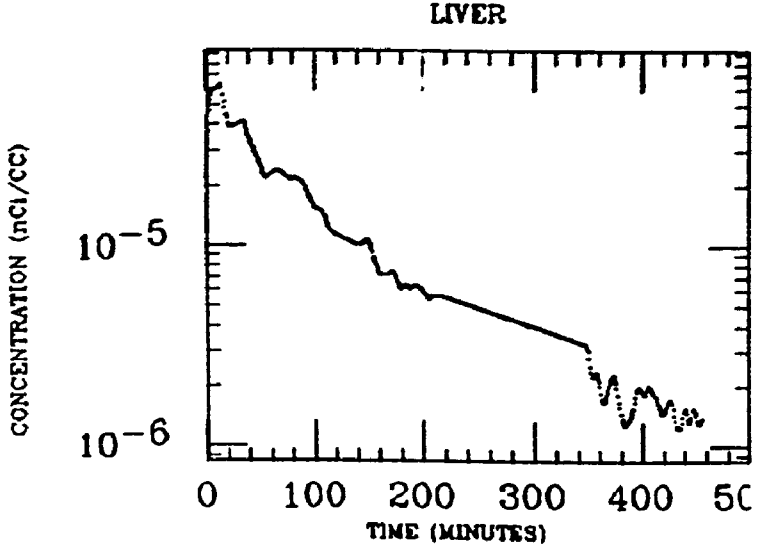

MACMILLAN
XE INGESTION
Po-218

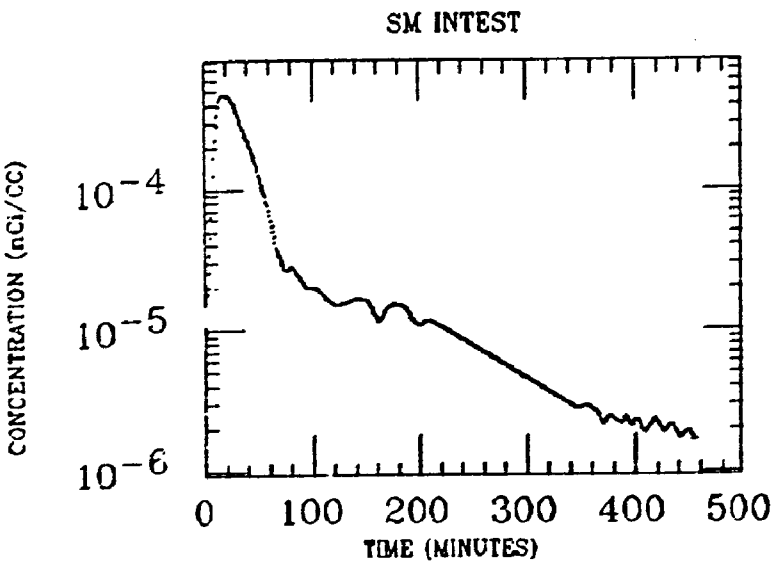

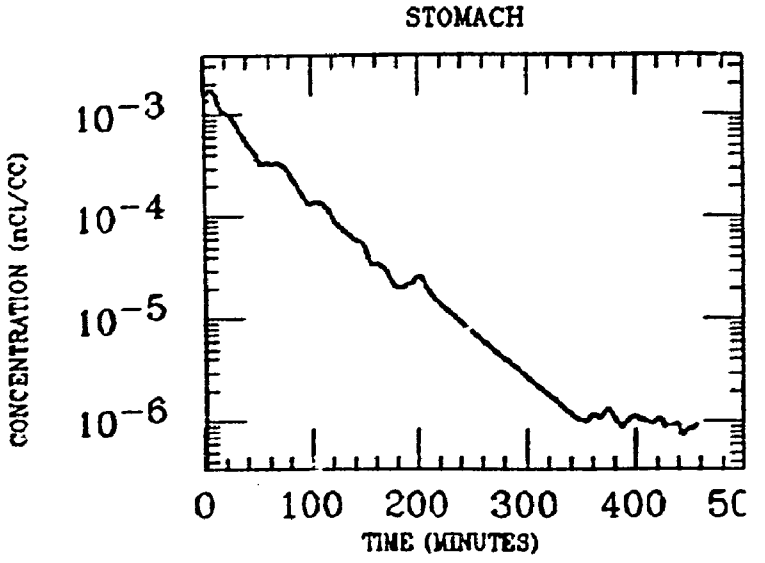

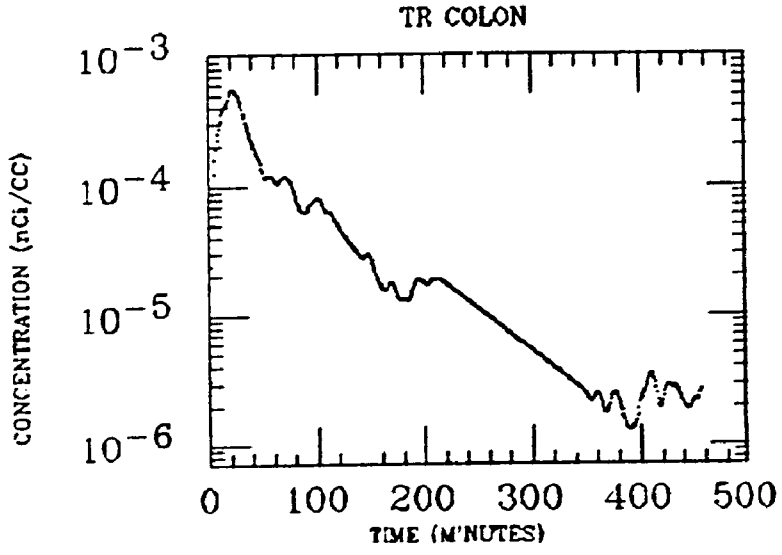

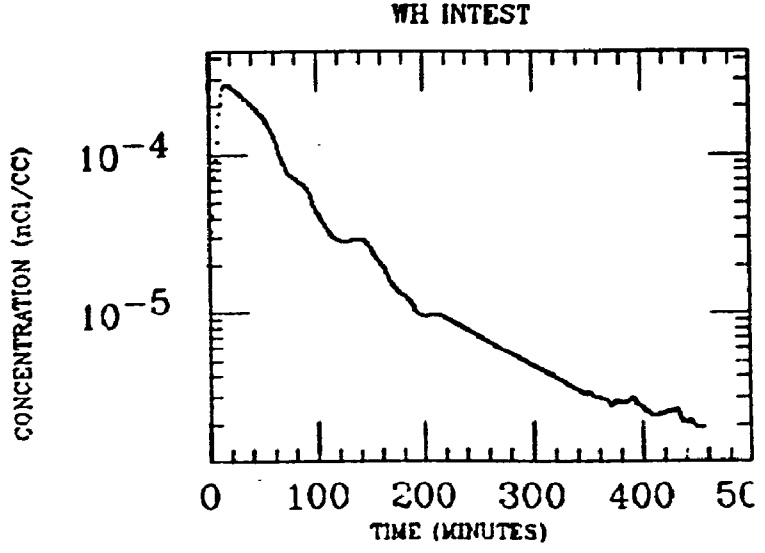

MAIO
XE INGESTION
Po-218

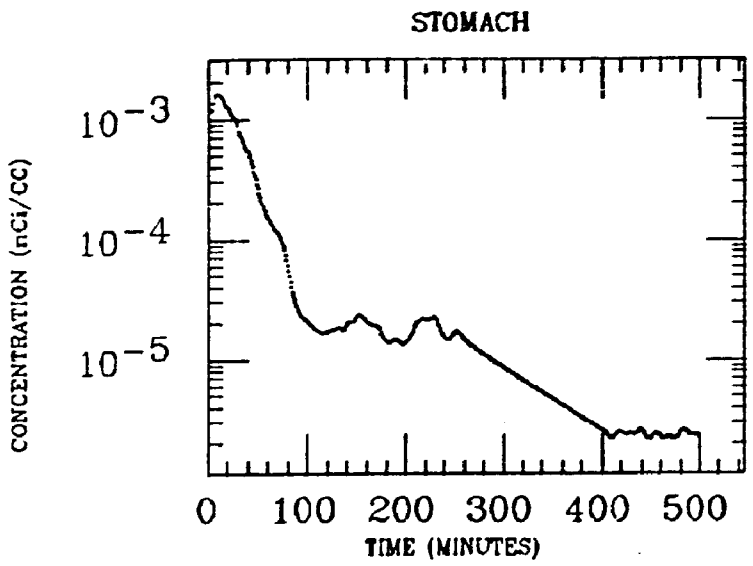

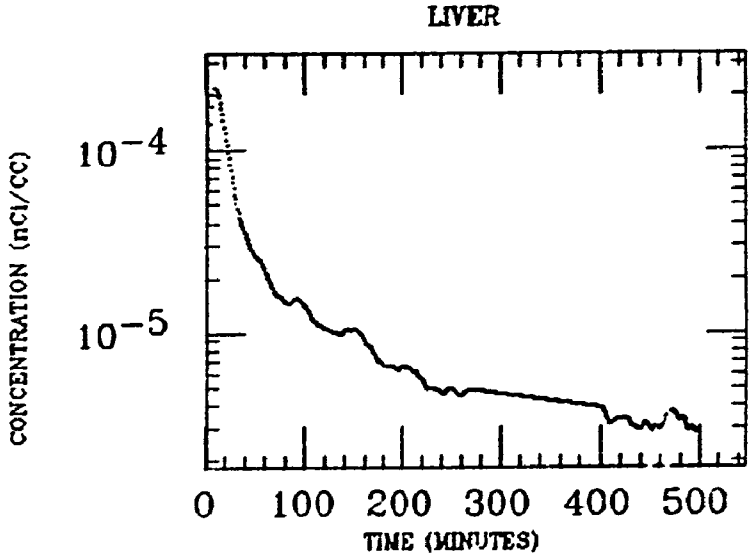

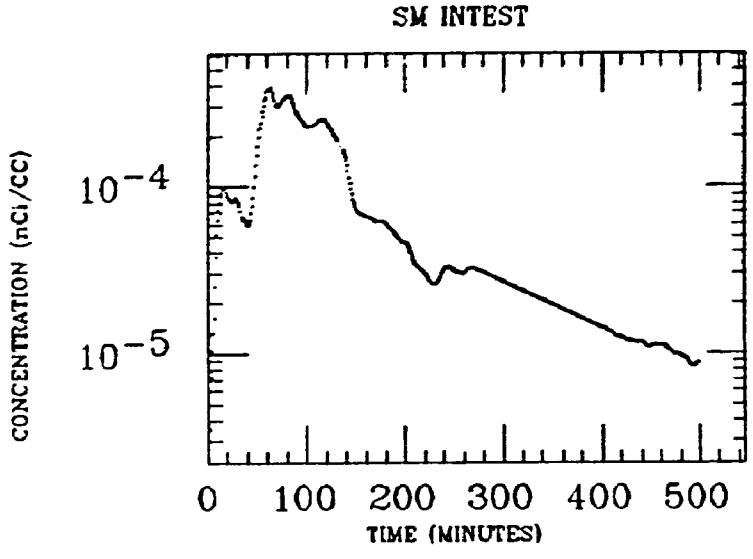

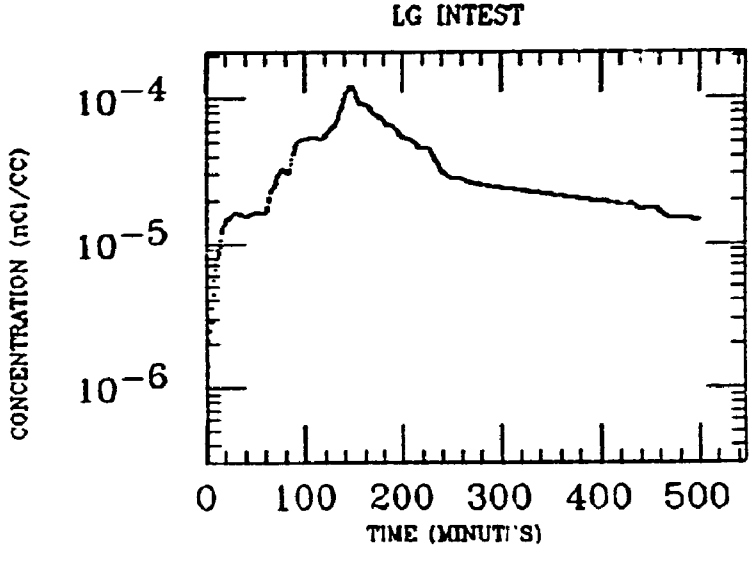

MAIO
XE INGESTION
Po-218

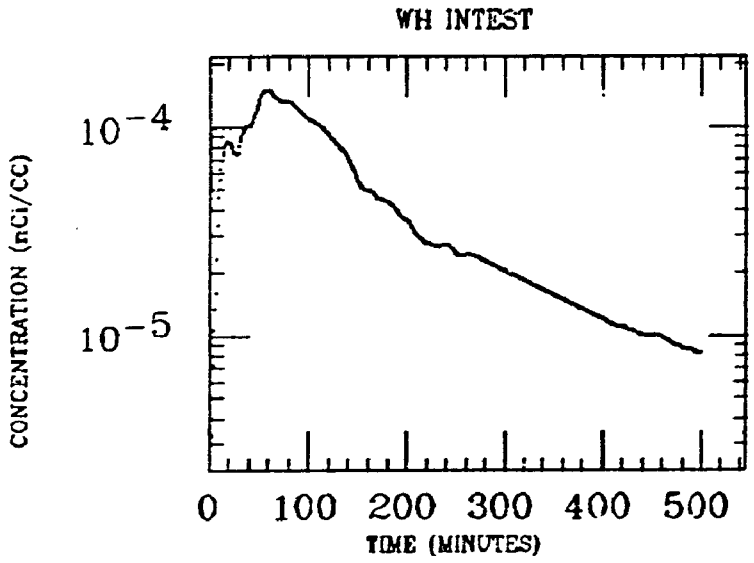

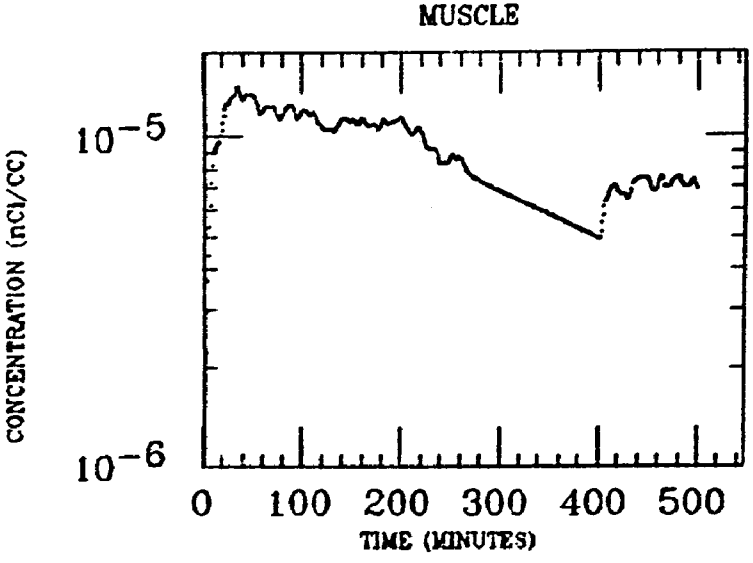

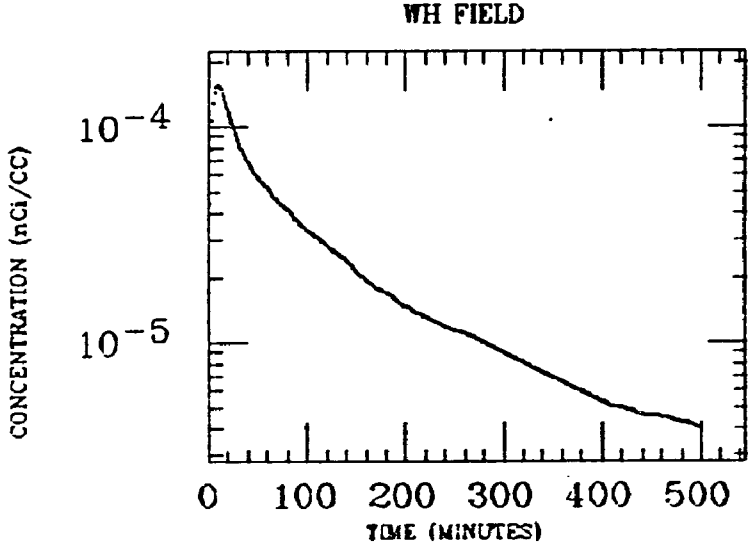

MALCOM
XE INGESTION
Po-218

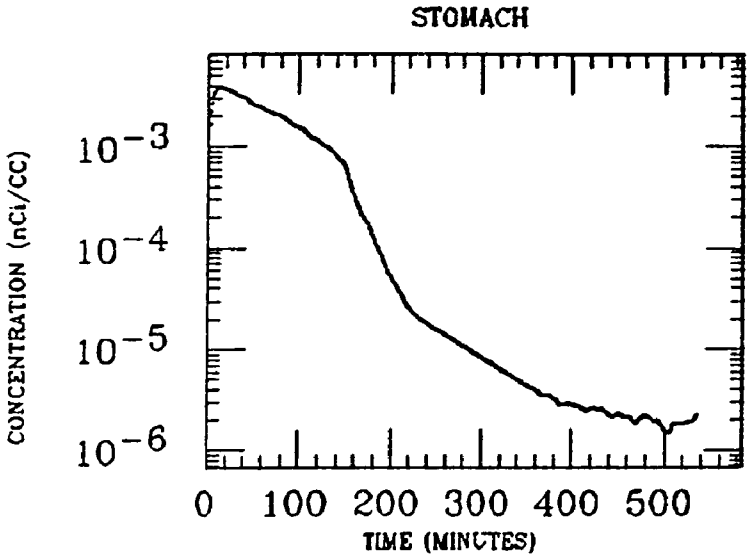

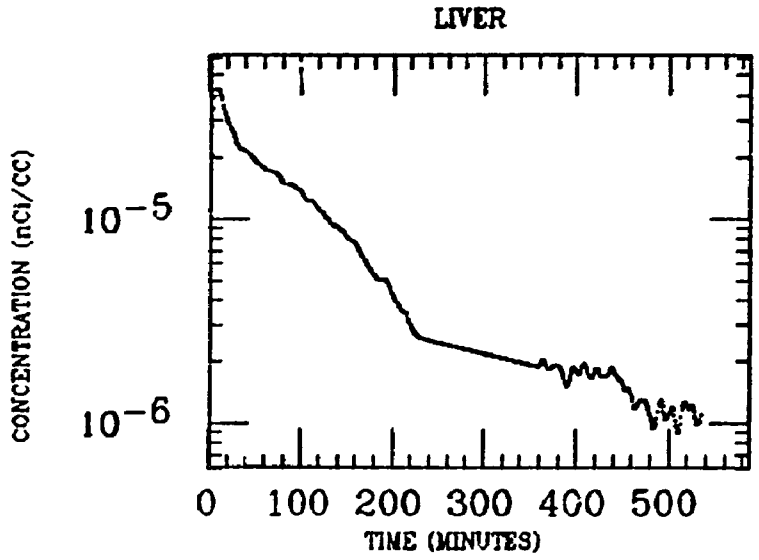

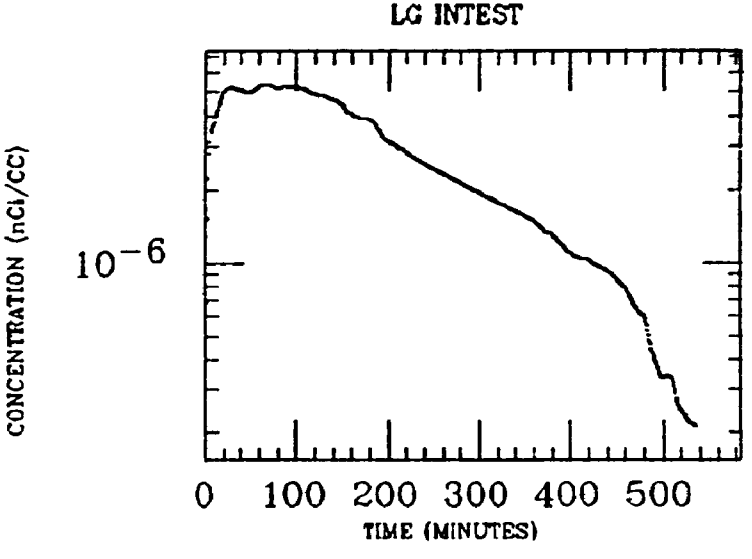

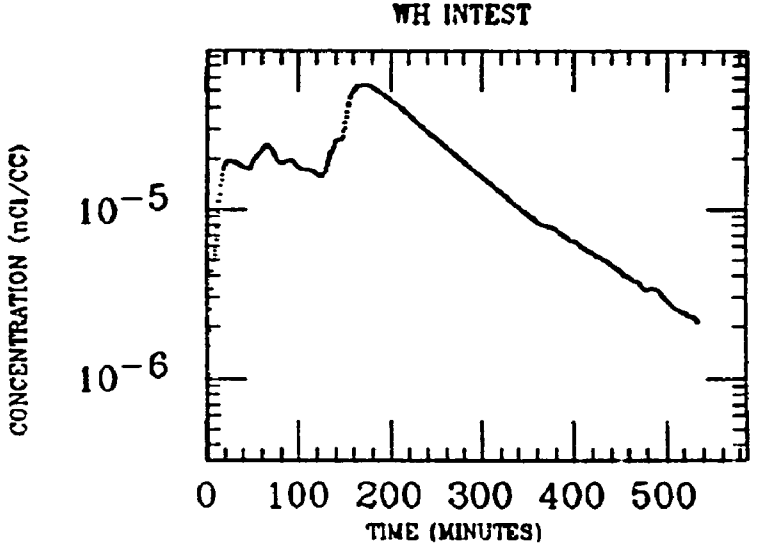

MALCOM
XE INGESTION
Po-218

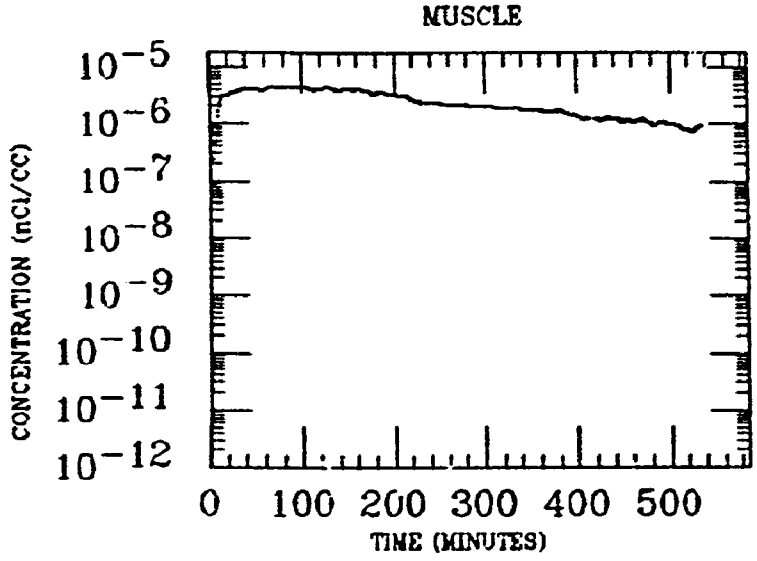

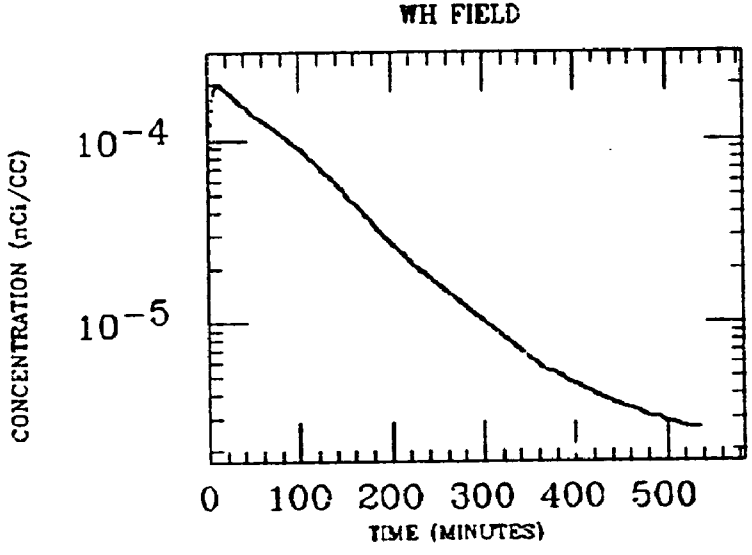

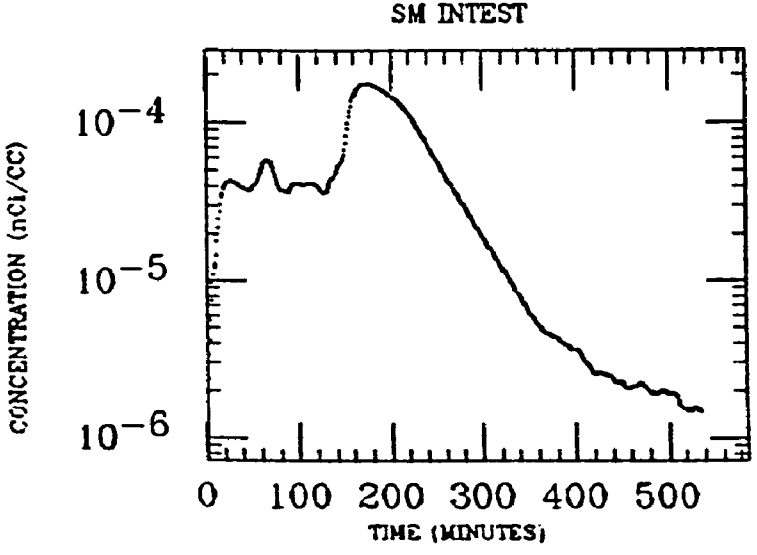

MONROE
XE INGESTION
Po-218

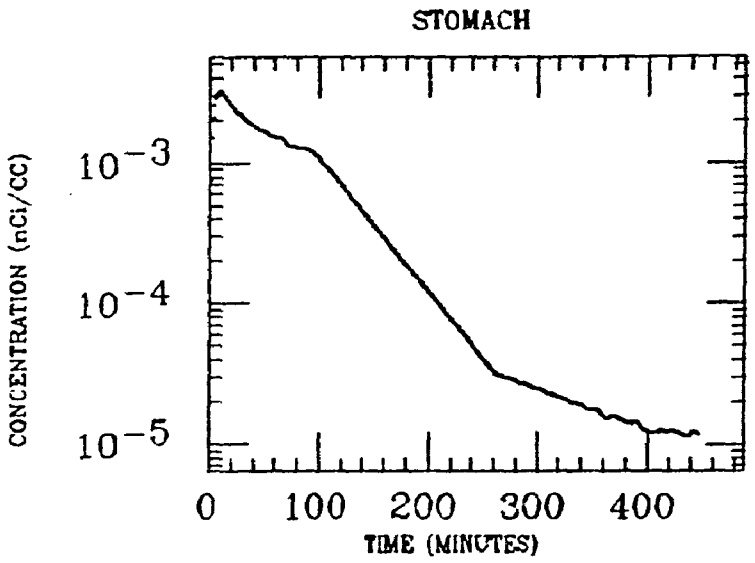

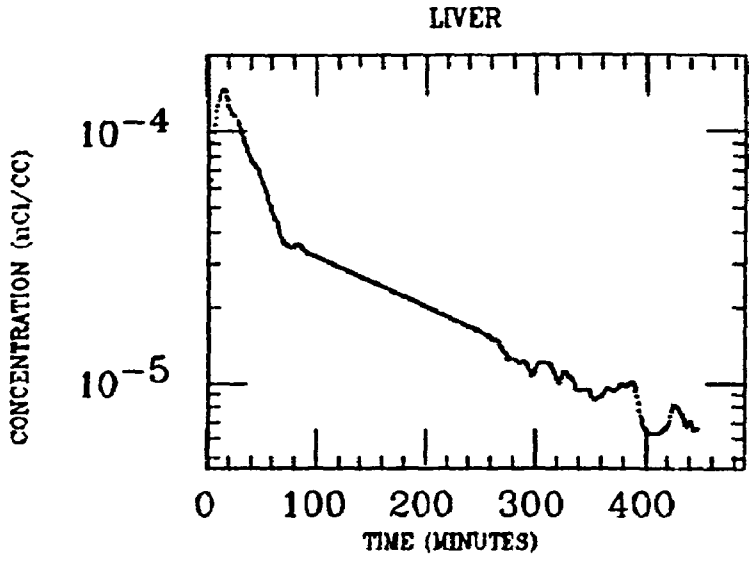

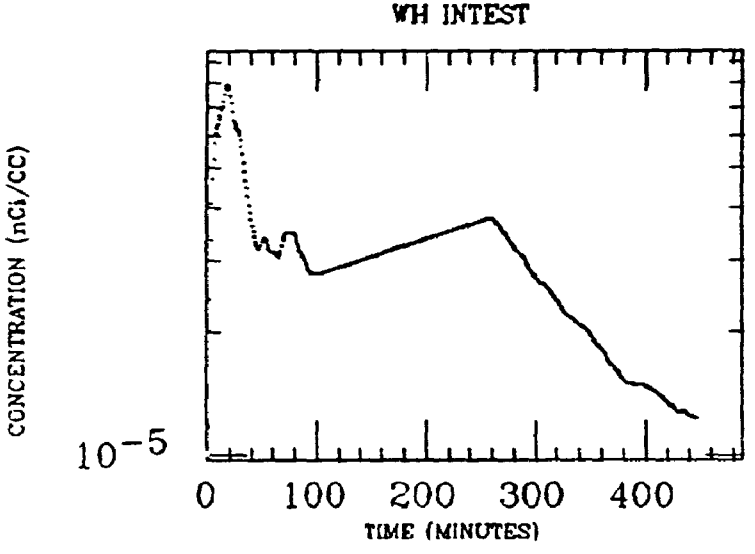

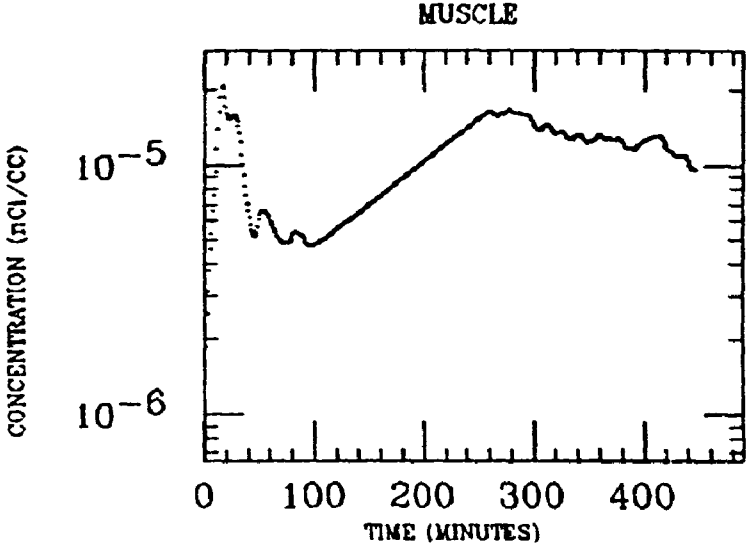

MONROE
XE INGESTION
Po-218

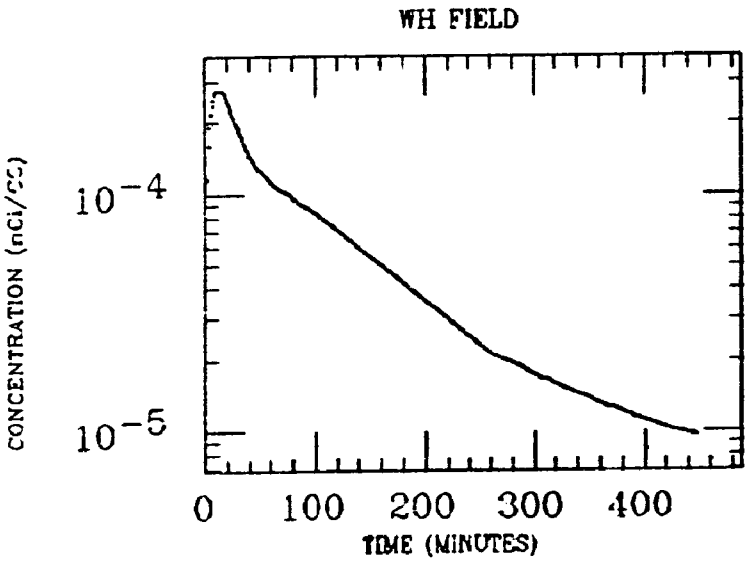

MORGAN
XE INGESTION
Po-218

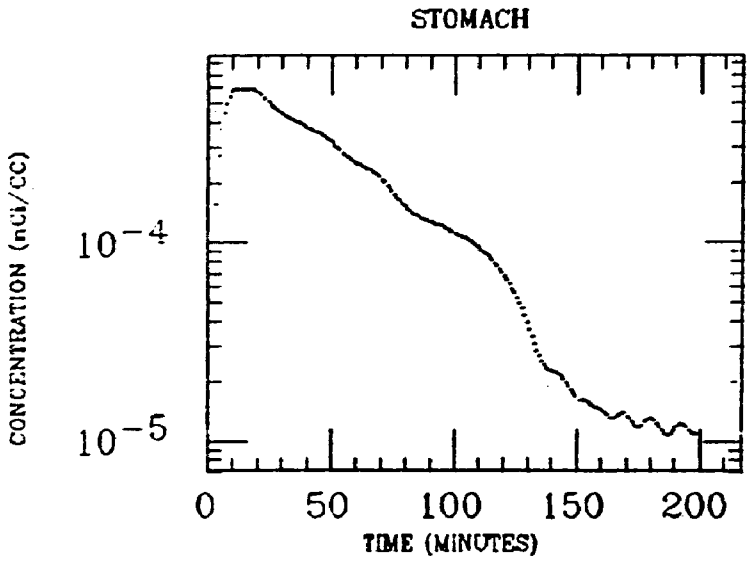

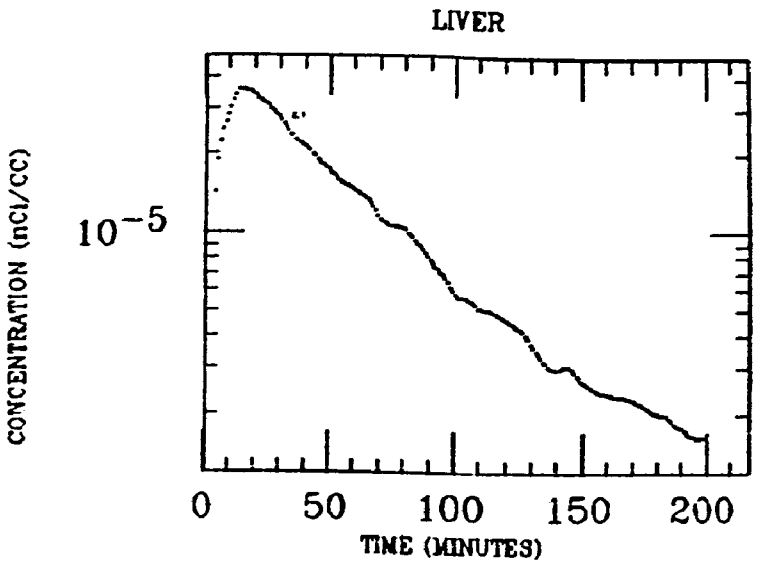

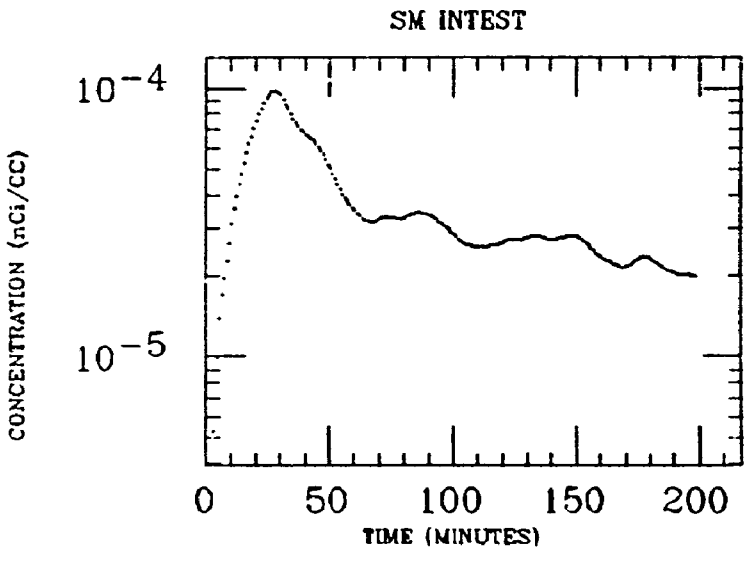

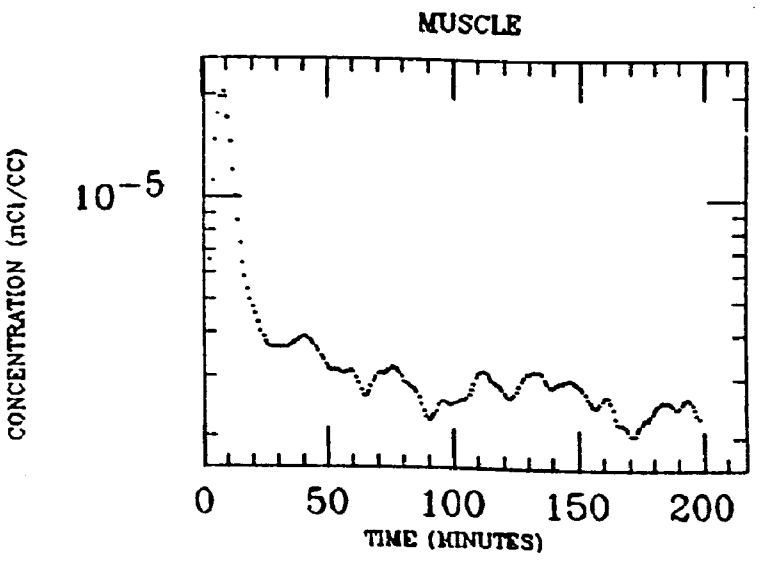

MORGAN
XE INGESTION
Po-218

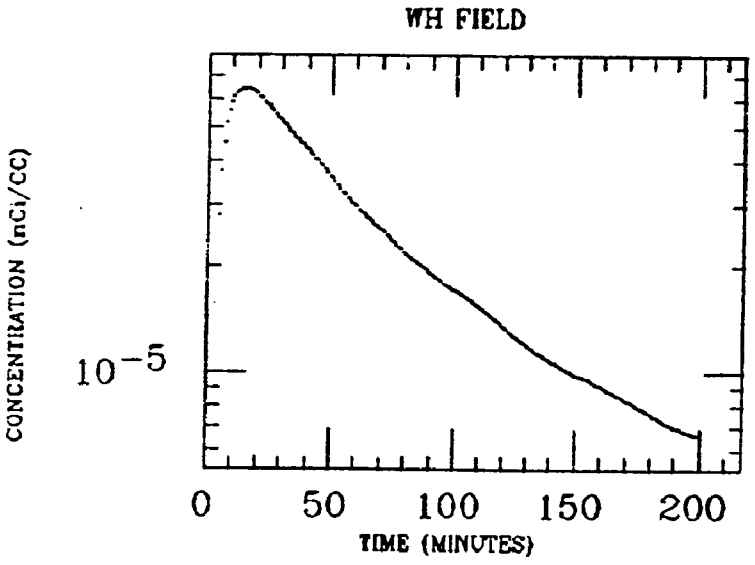

MURCHE
XE INGESTION
Po-218

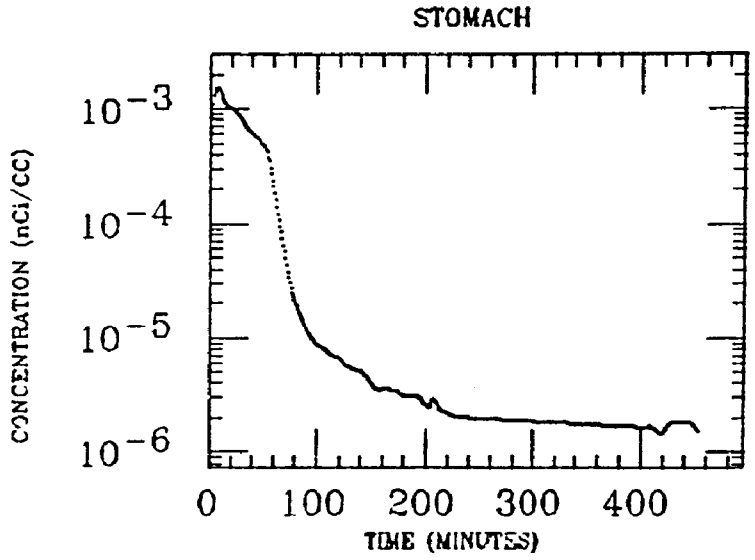

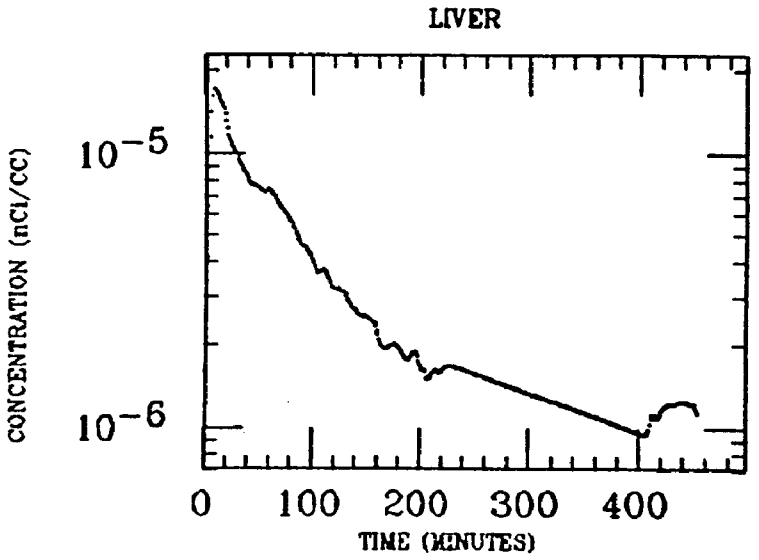

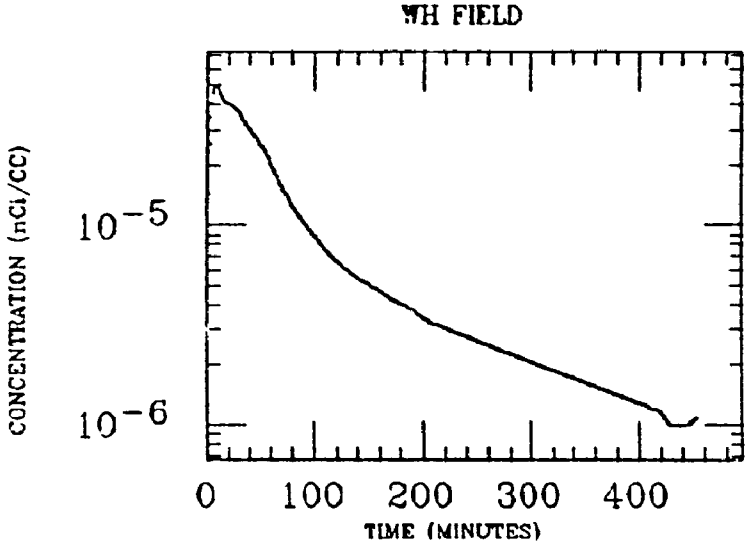

MURCHE
XE INGESTION
Po-218

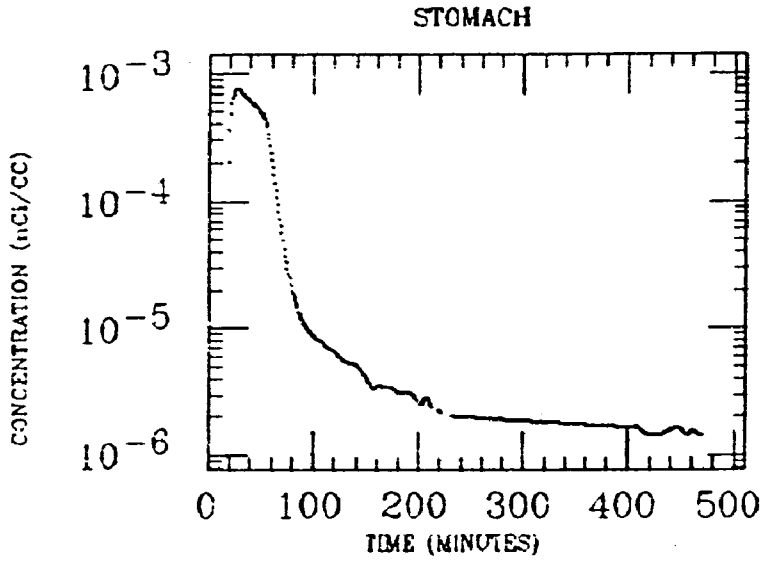

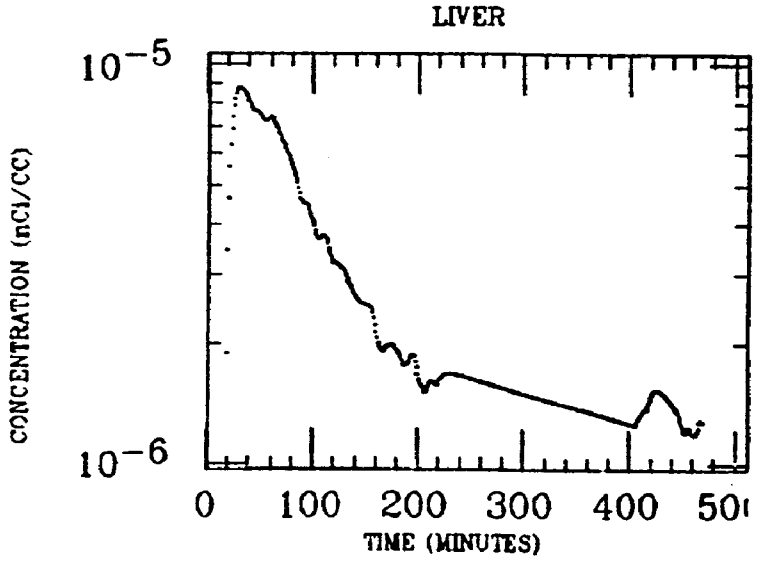

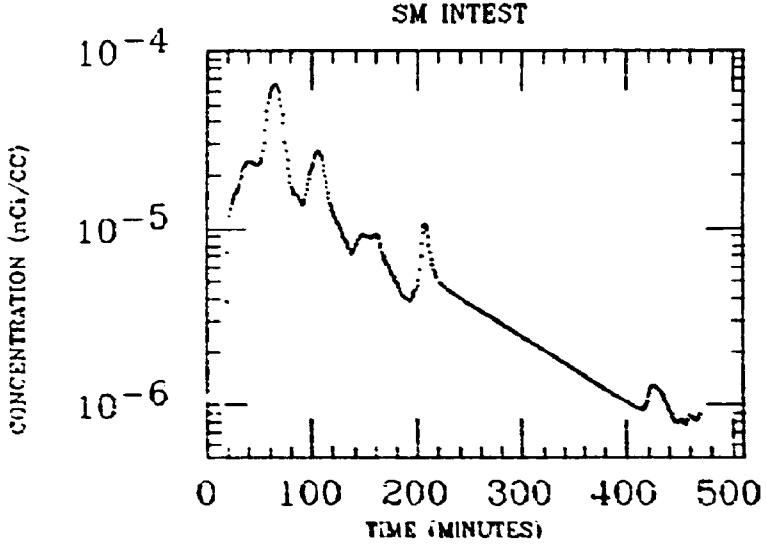

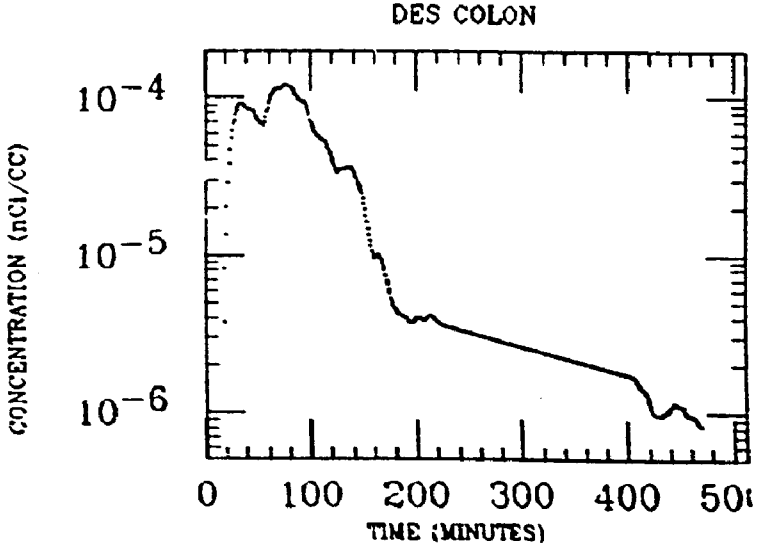

MURCHE
XE INGESTION
Po-218

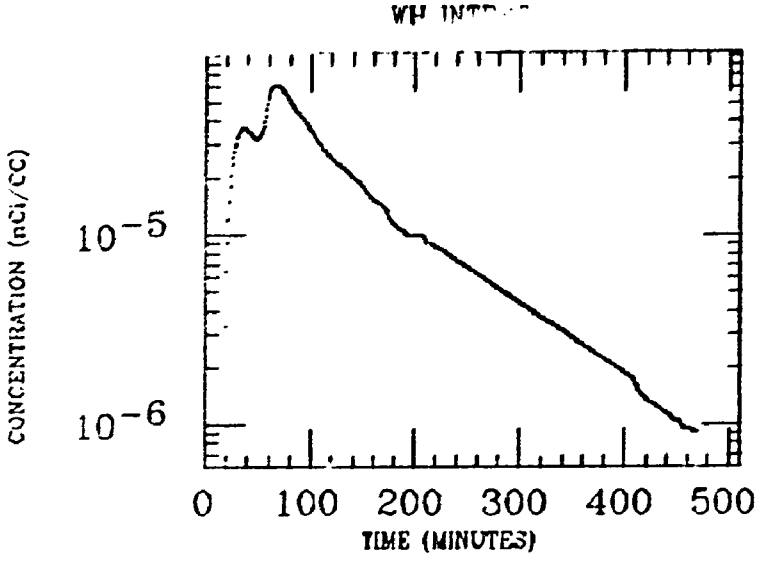

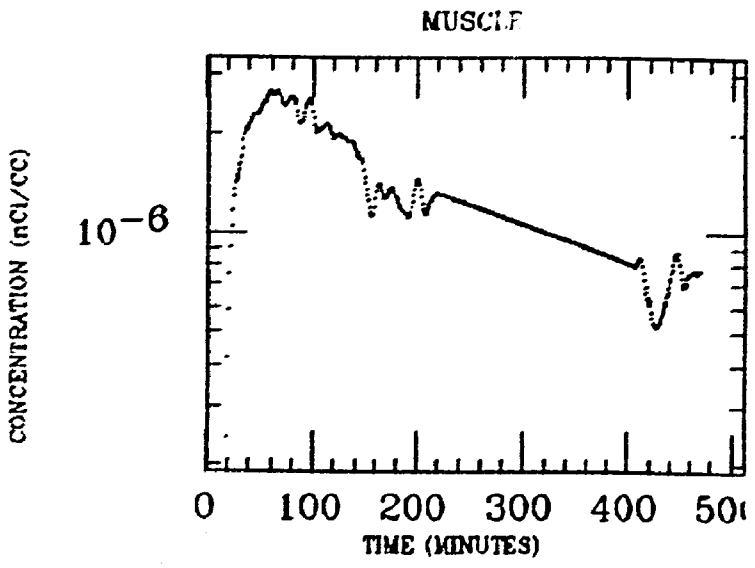

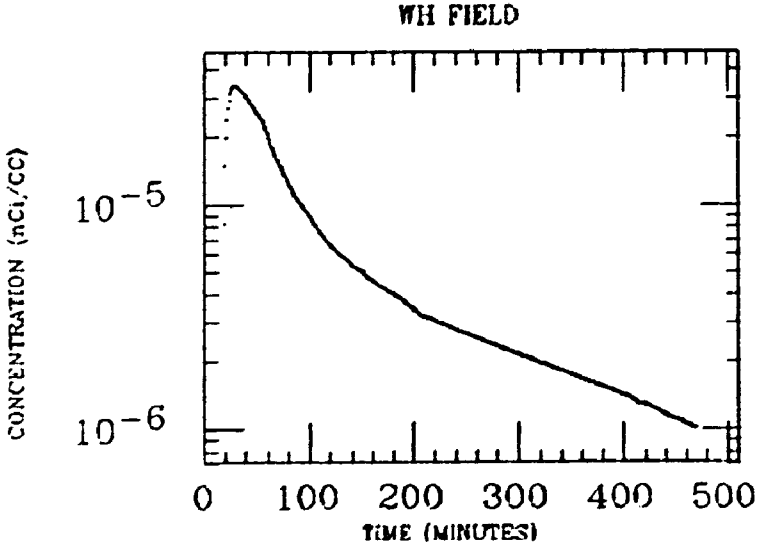

PARK
XE INGESTION
Po-218

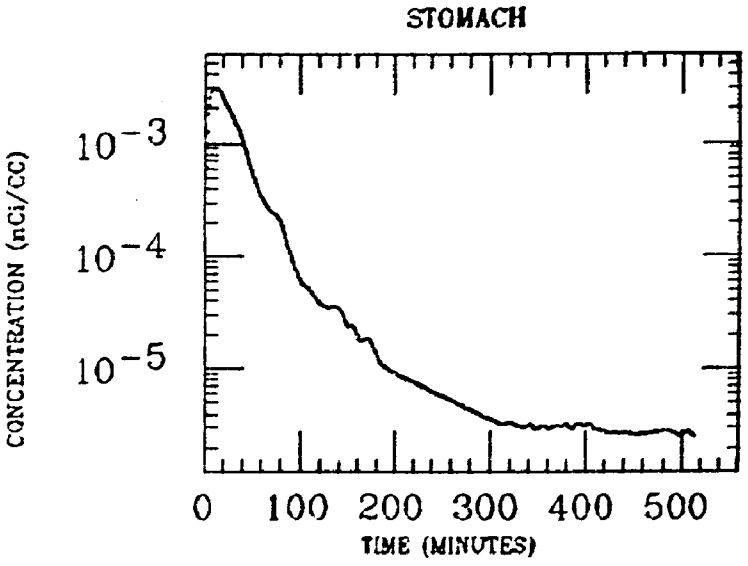

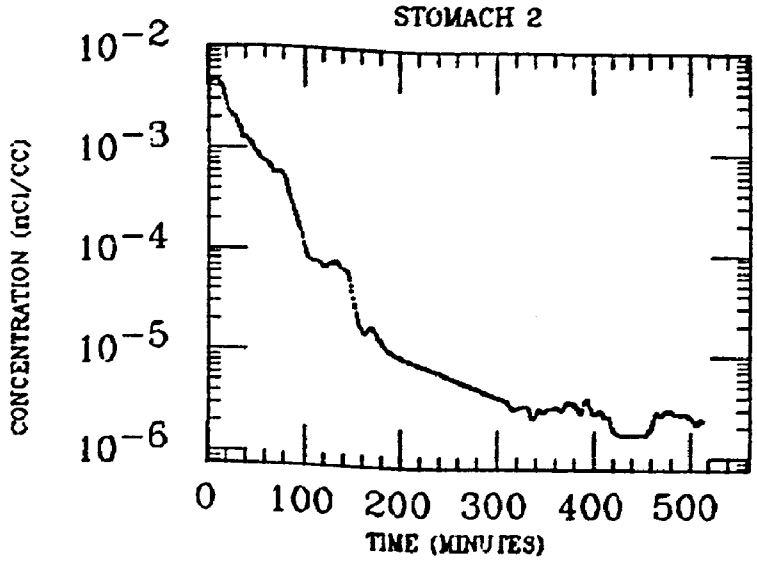

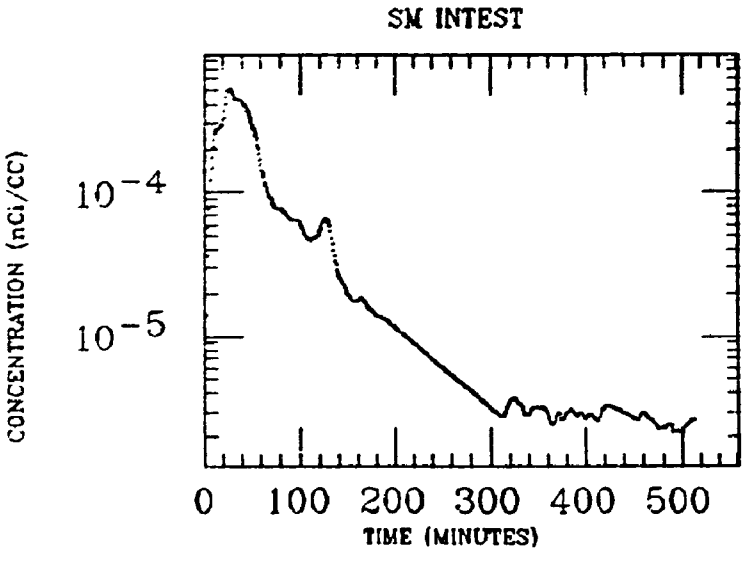

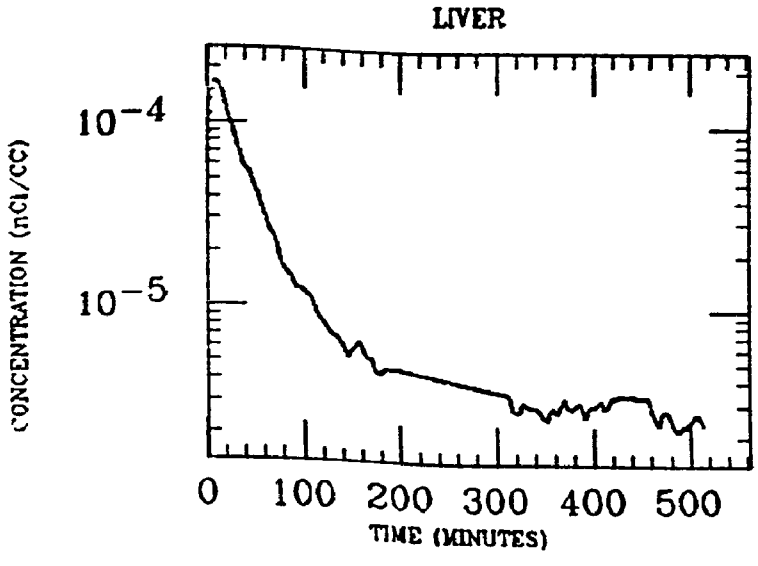

PARK
XE INGESTION
Po-218

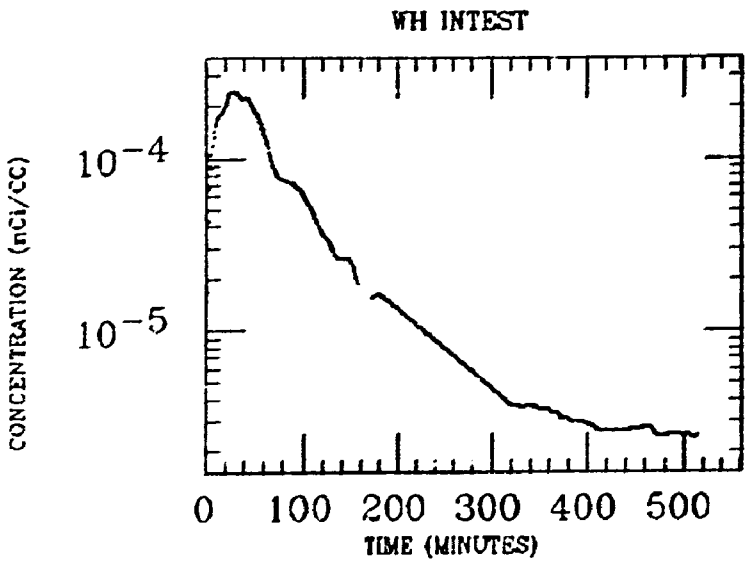

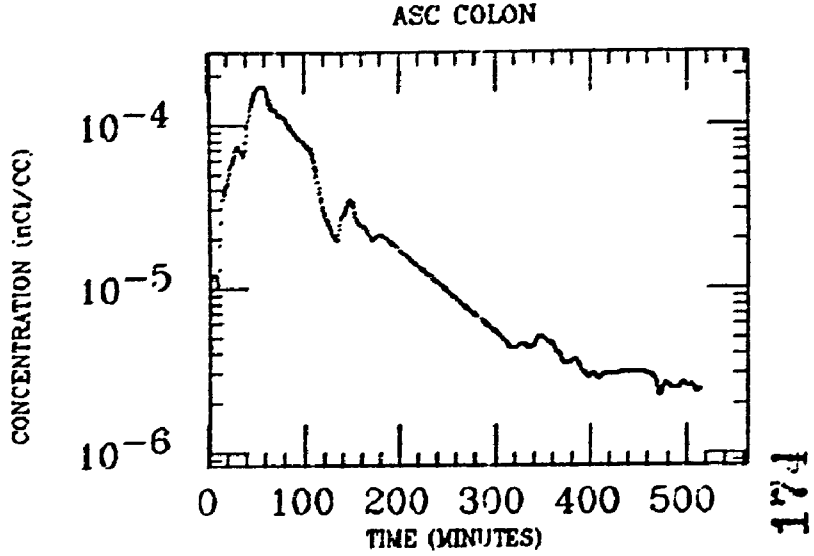

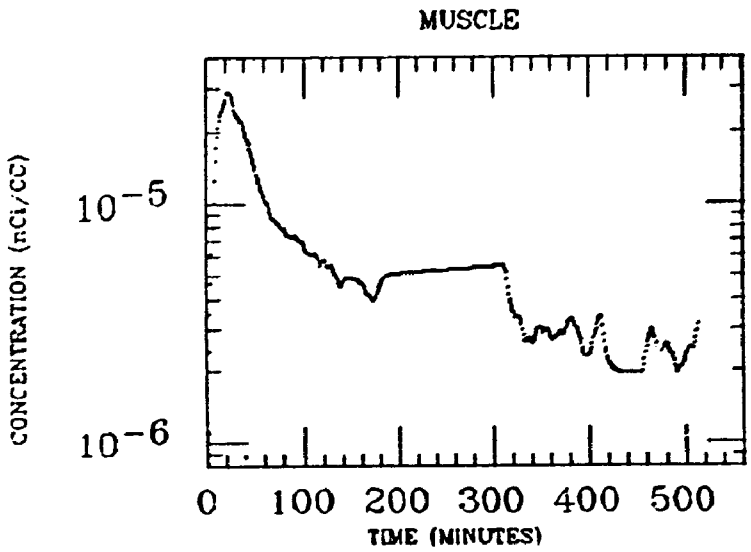

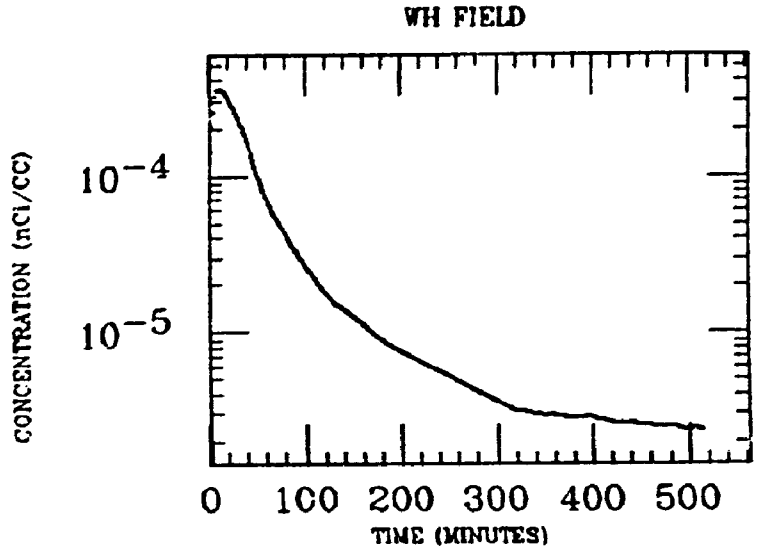

TAATJES
XE INGESTION
Po-218

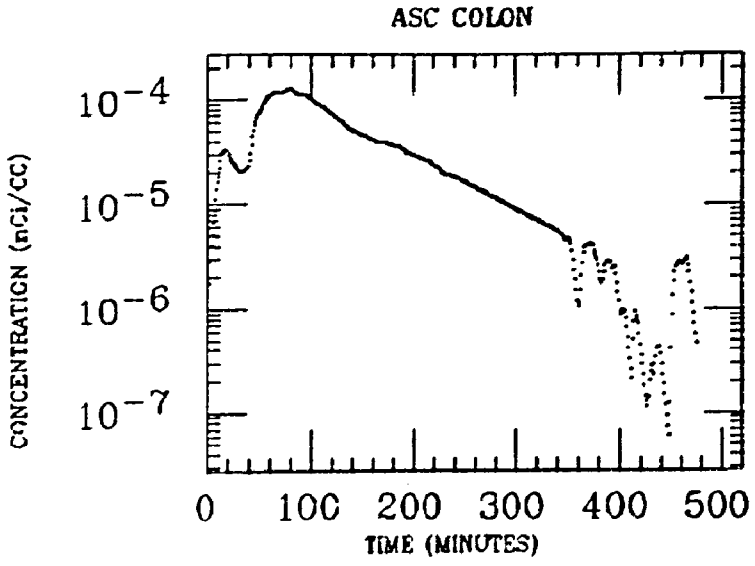

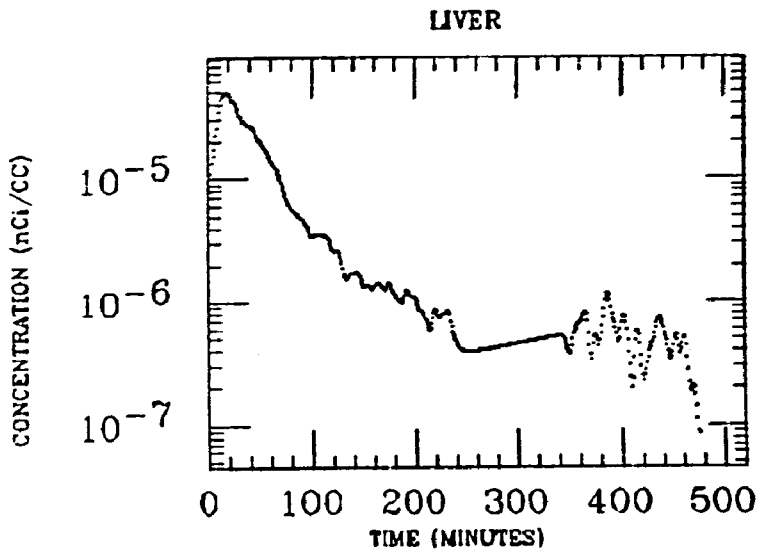

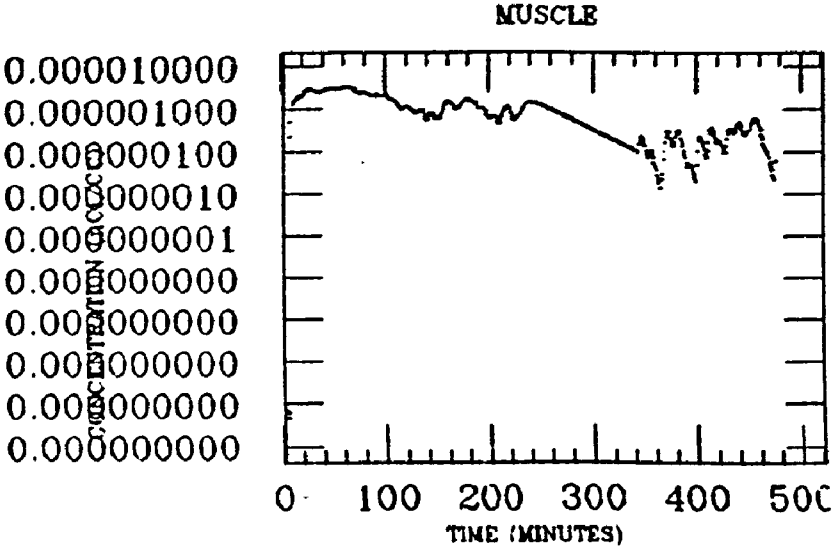

TAATJES
XE INGESTION
Po-218

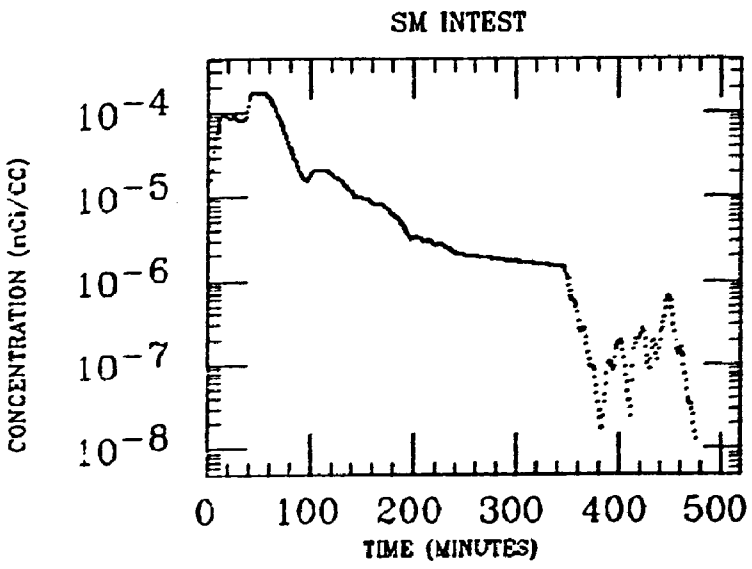

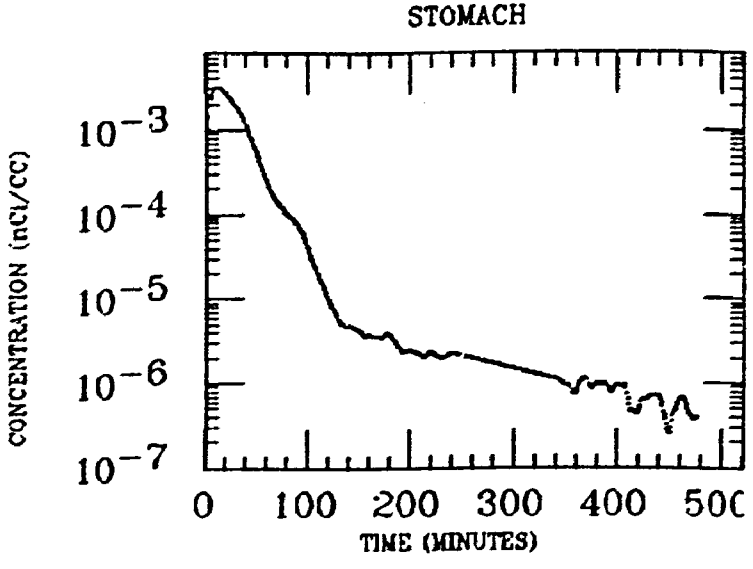

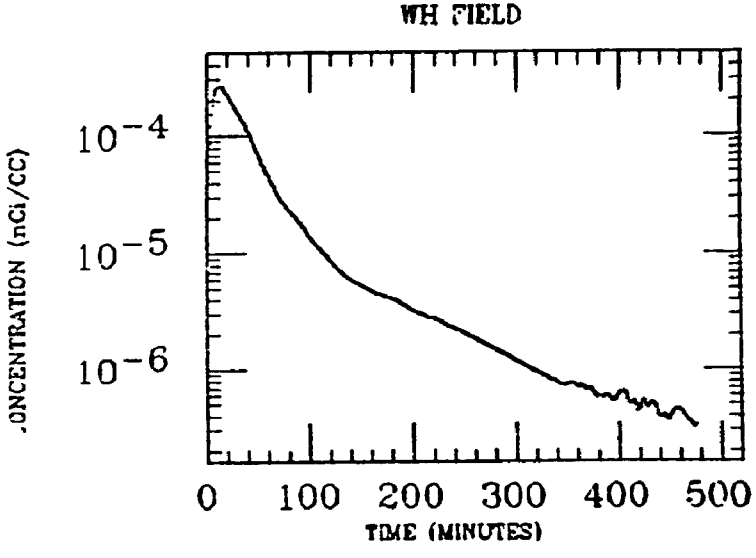

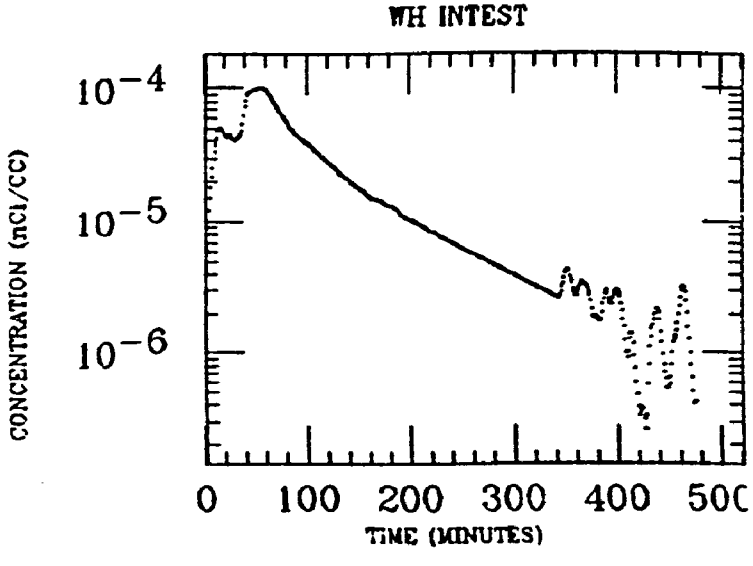

TAYLOR
XE INGESTION
Po-218

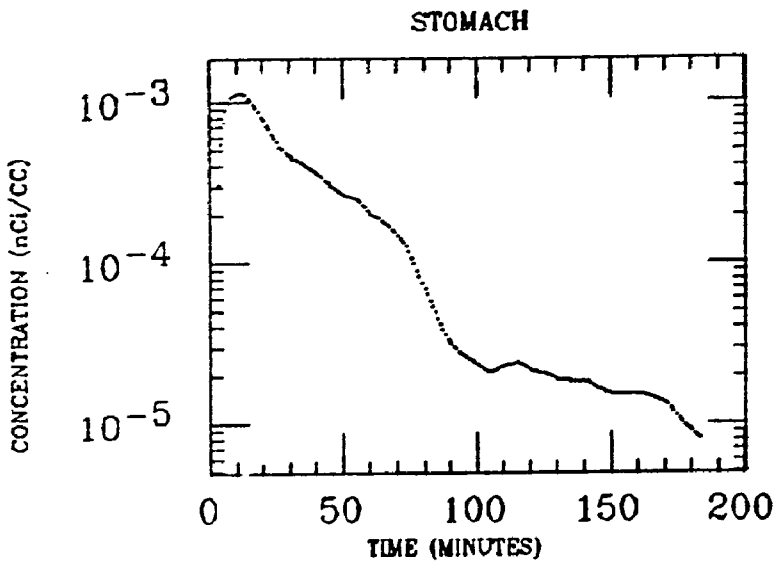

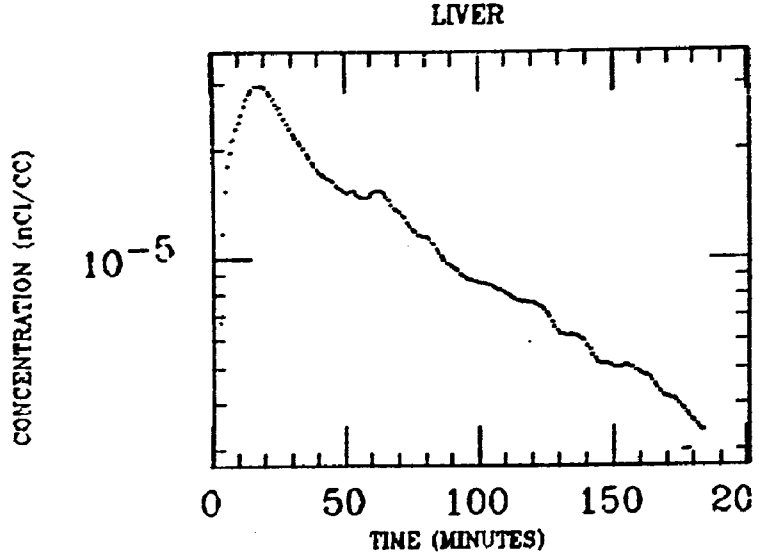

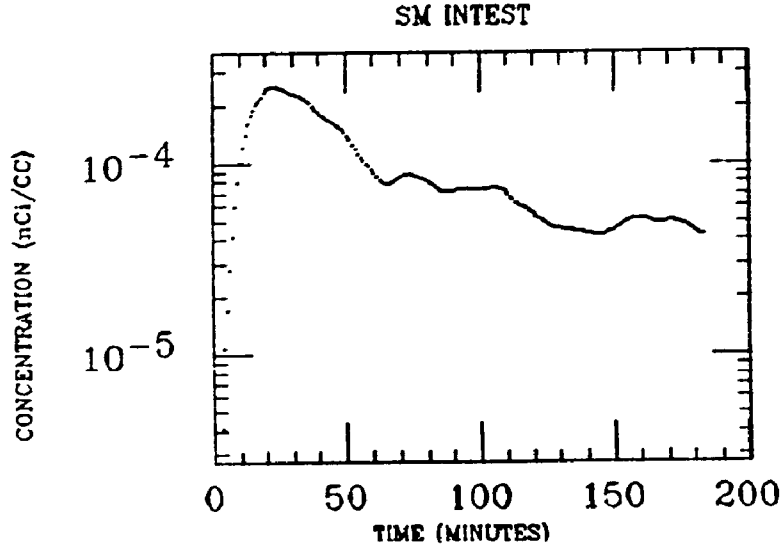

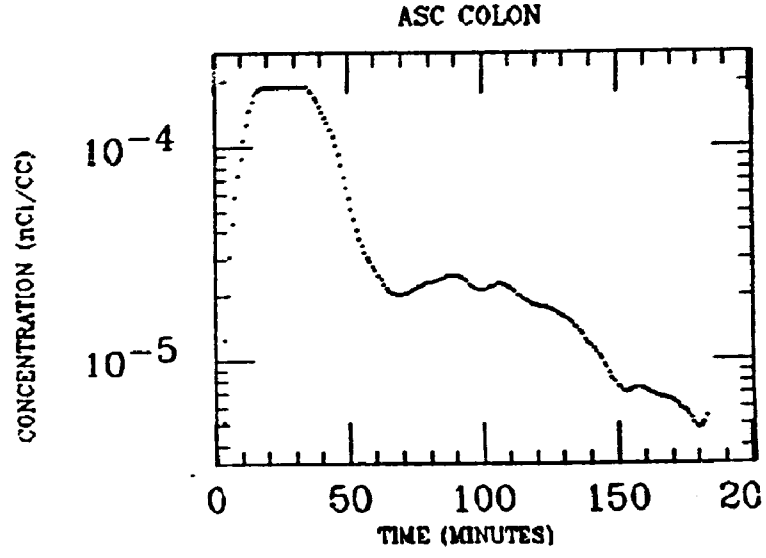

TAYLOR
XE INGESTION
Po-218

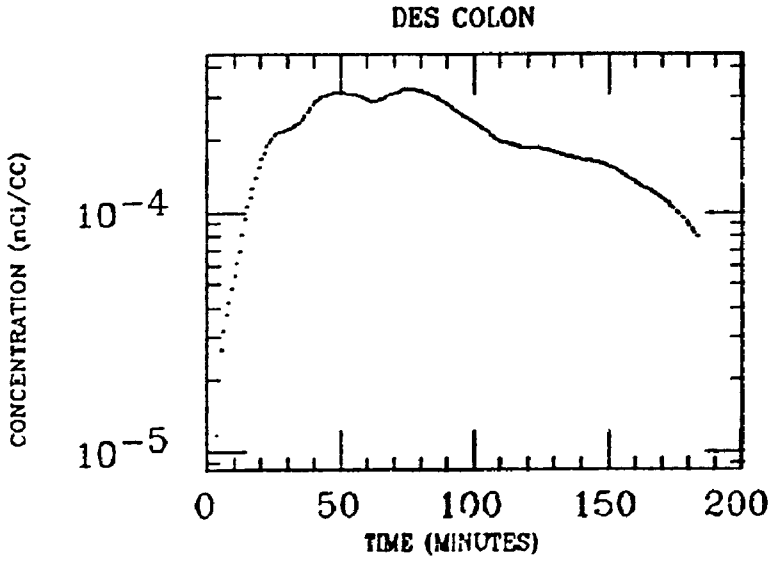

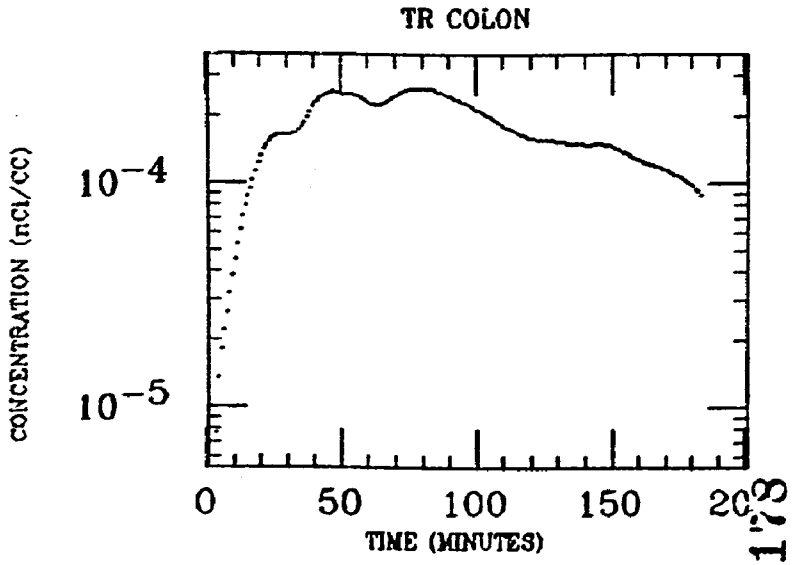

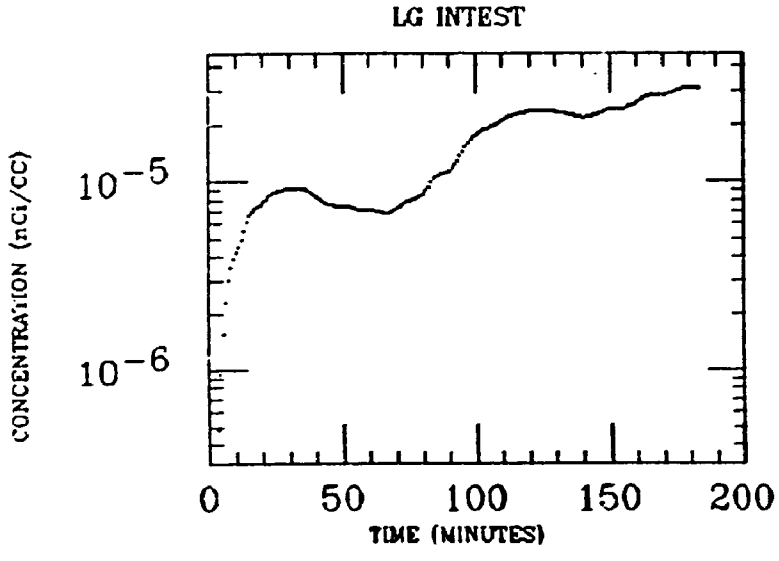

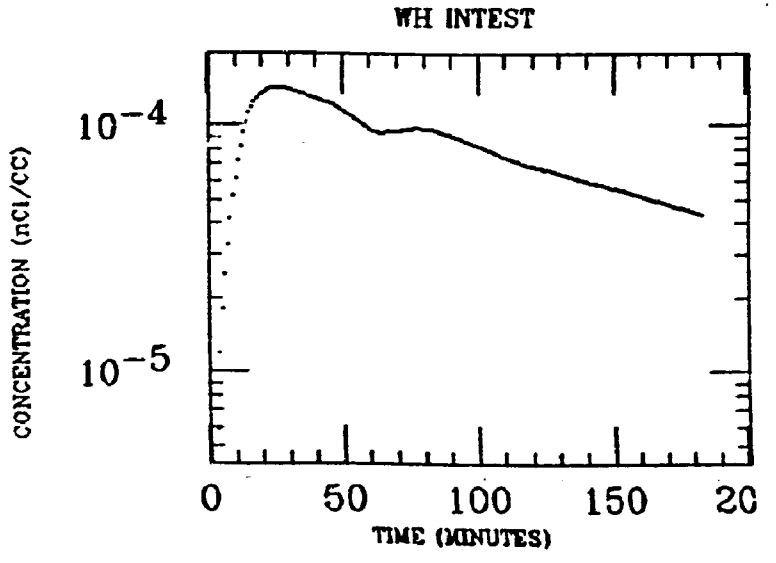

TAYLOR
XE INGESTION
Po-218

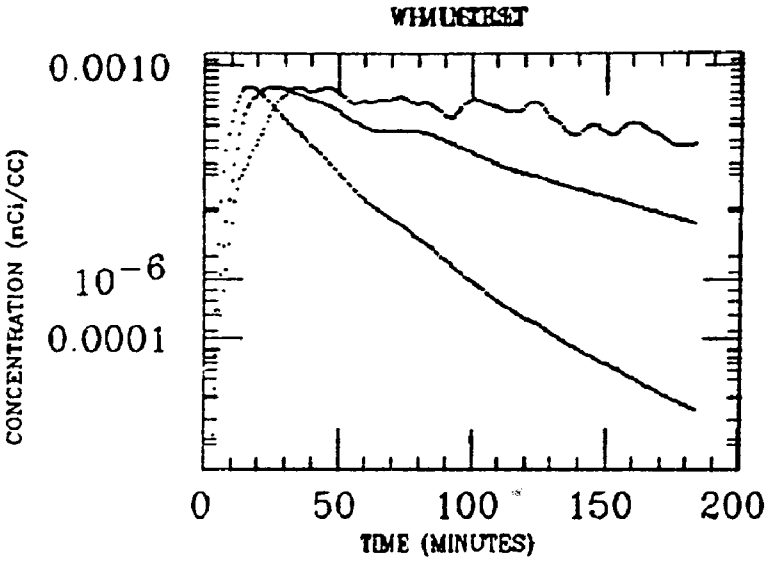

WILTSE
XE INGESTION
Po-218

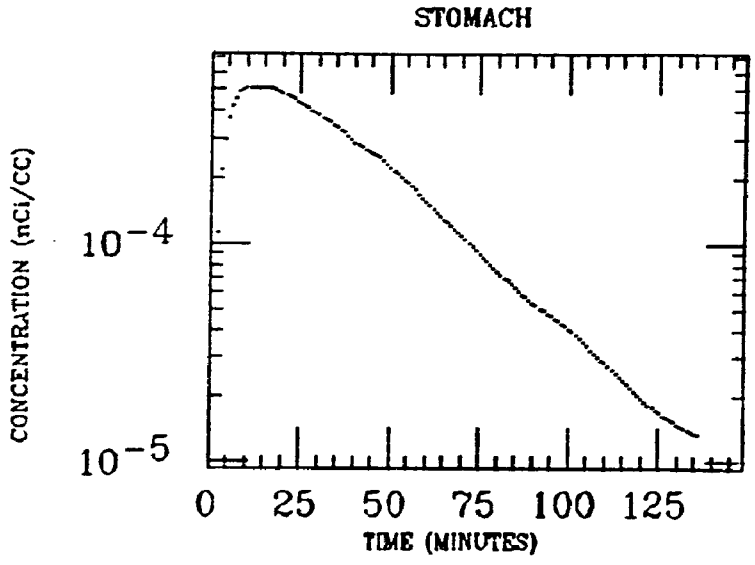

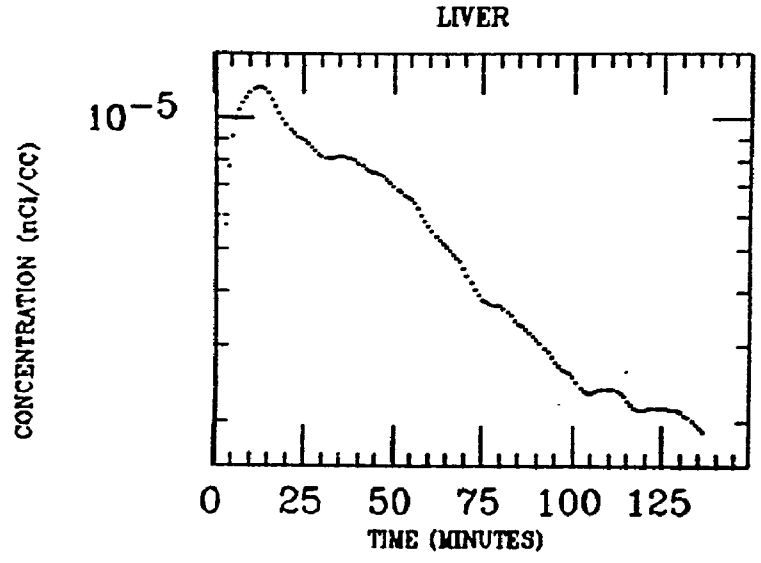

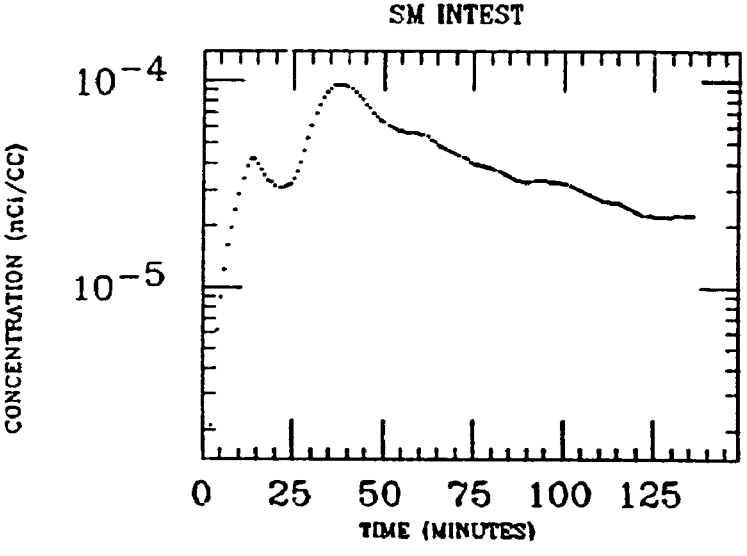

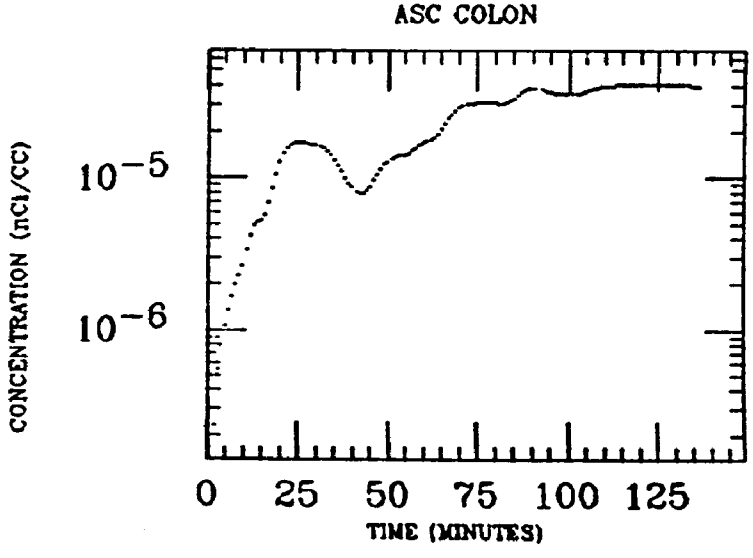

WILTSE
XE INGESTION
Po-218

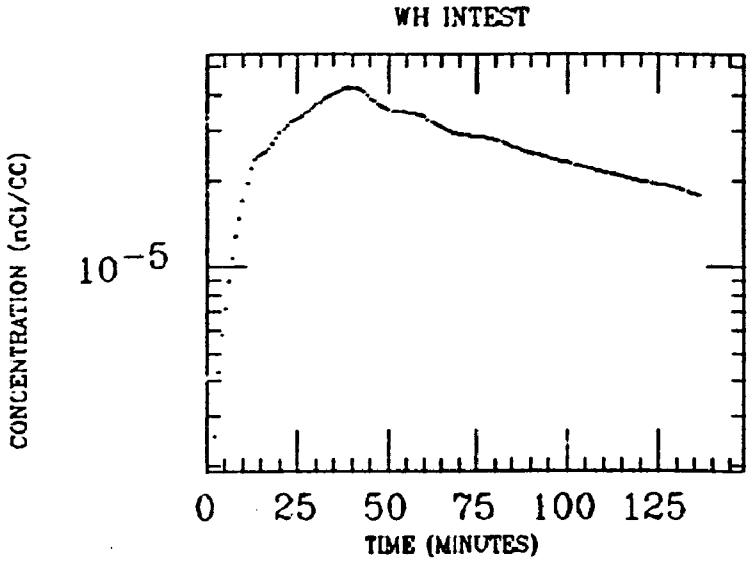

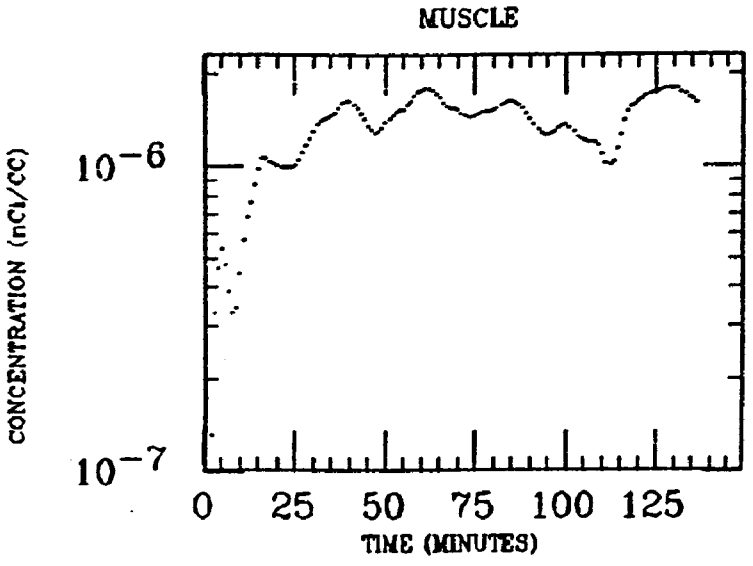

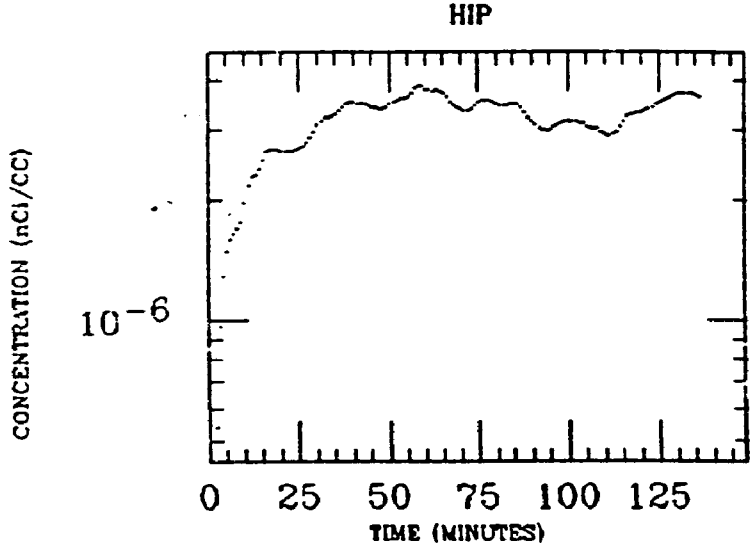

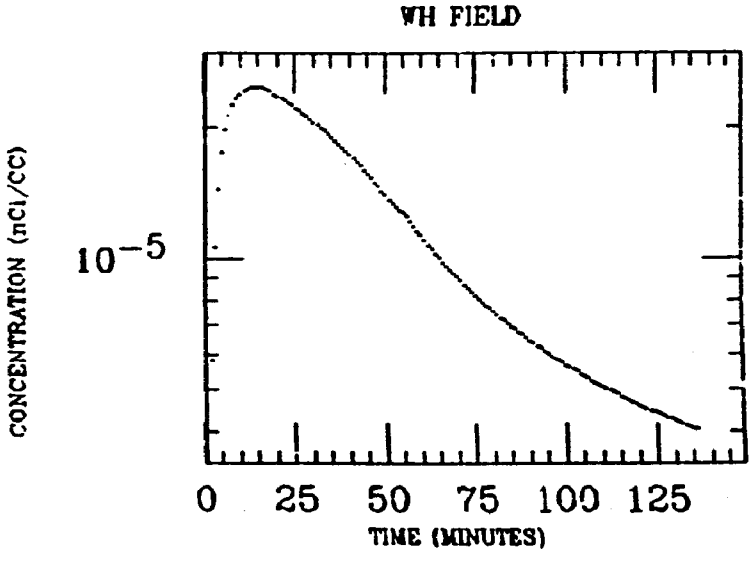

AHERN
XE INGESTION
Pb-214

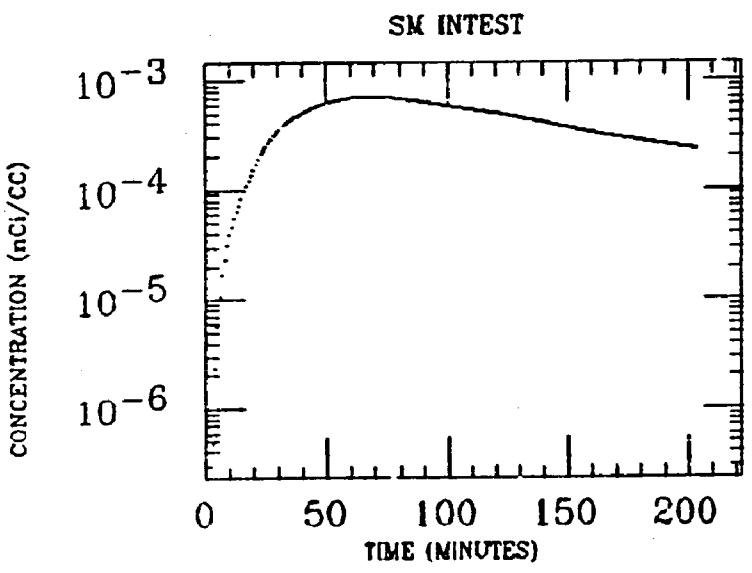

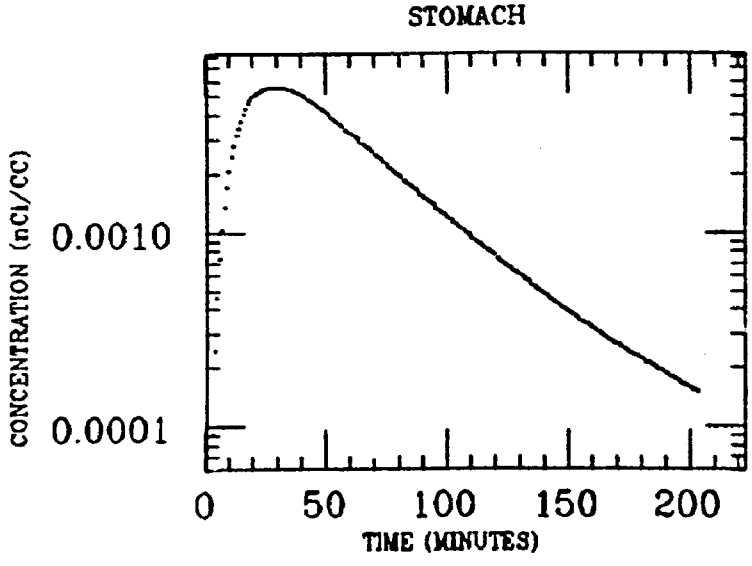

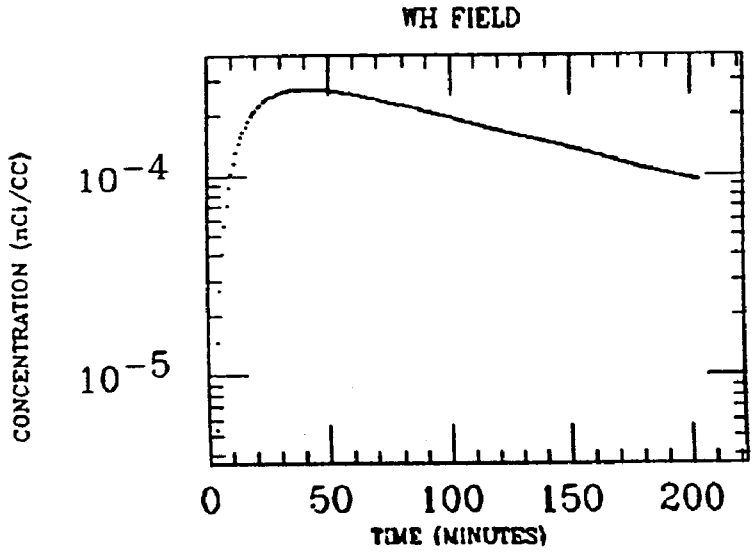

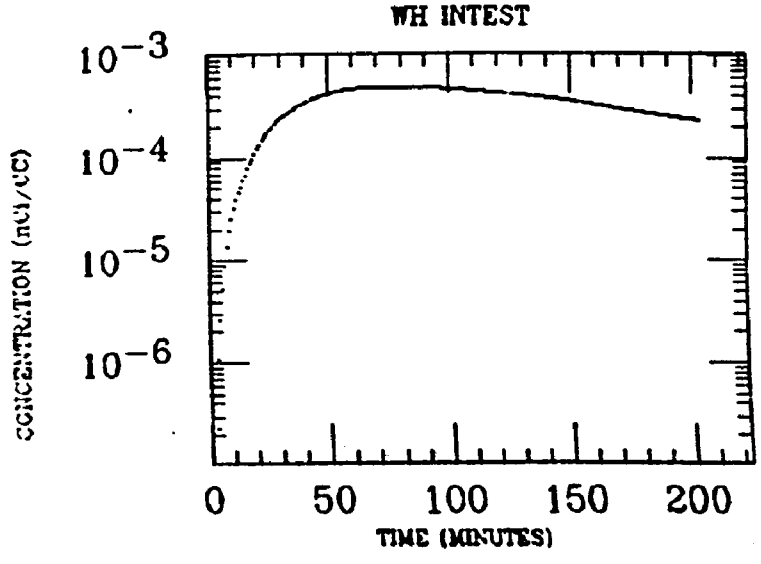

AHERN
XE INGESTION
Pb-214

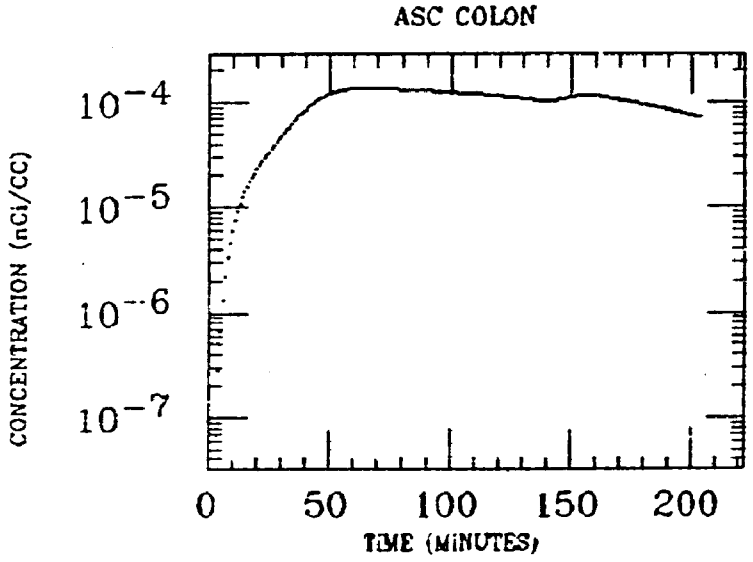

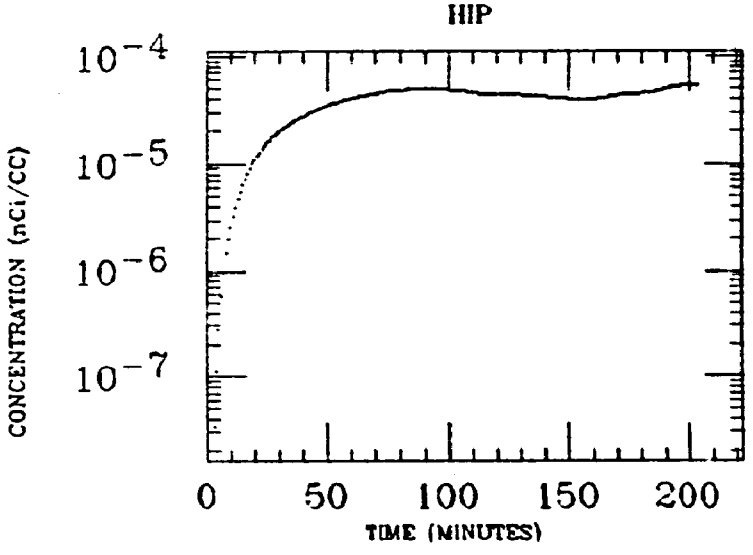

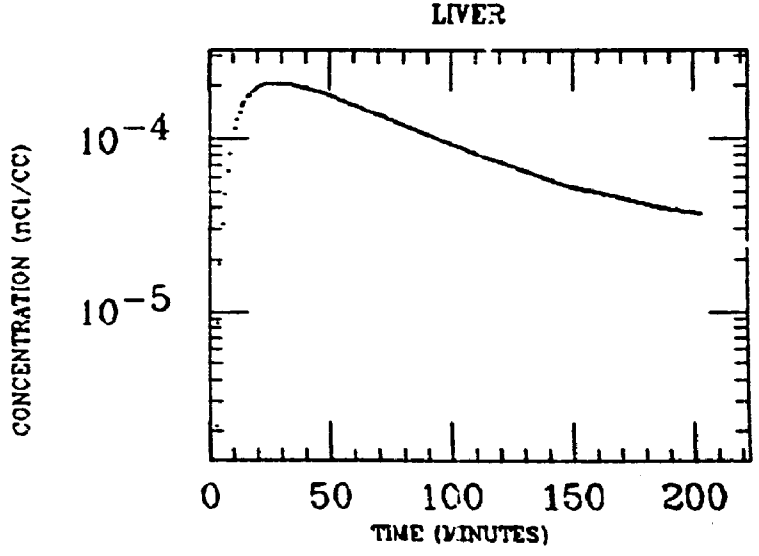

ARROL
XE INGESTION
Pb-214

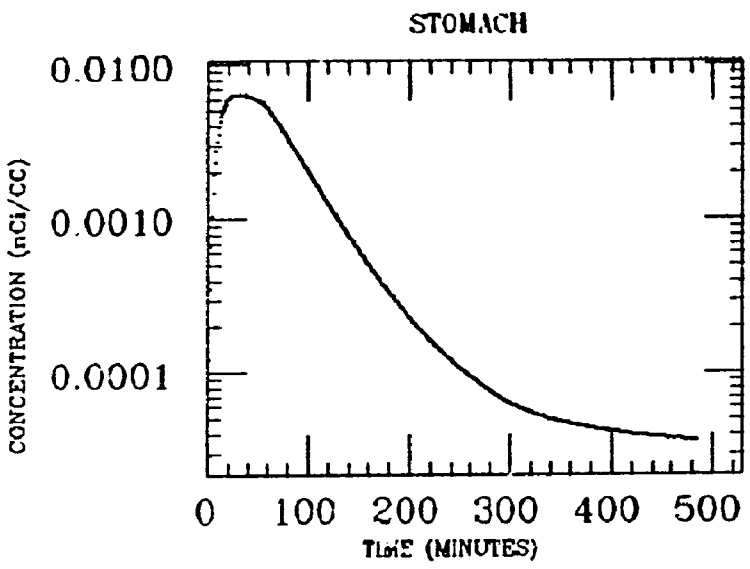

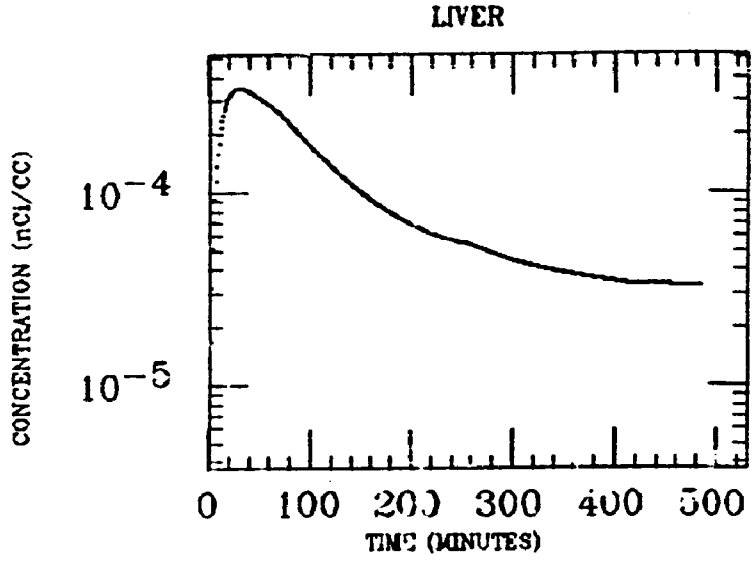

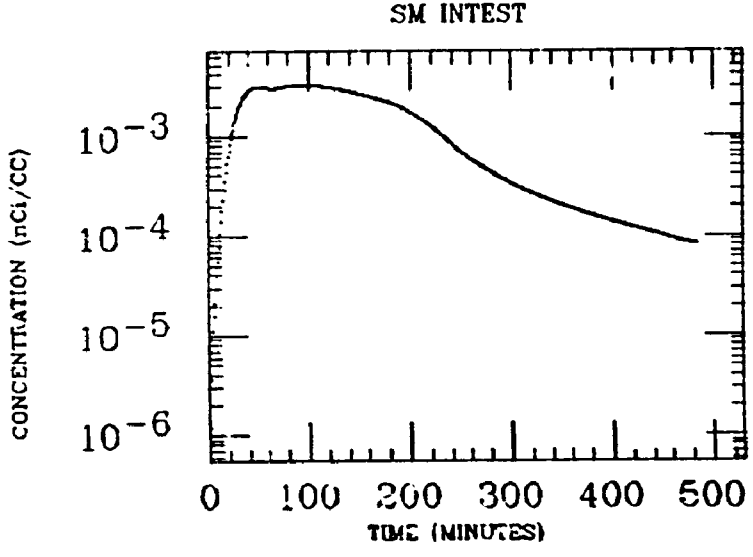

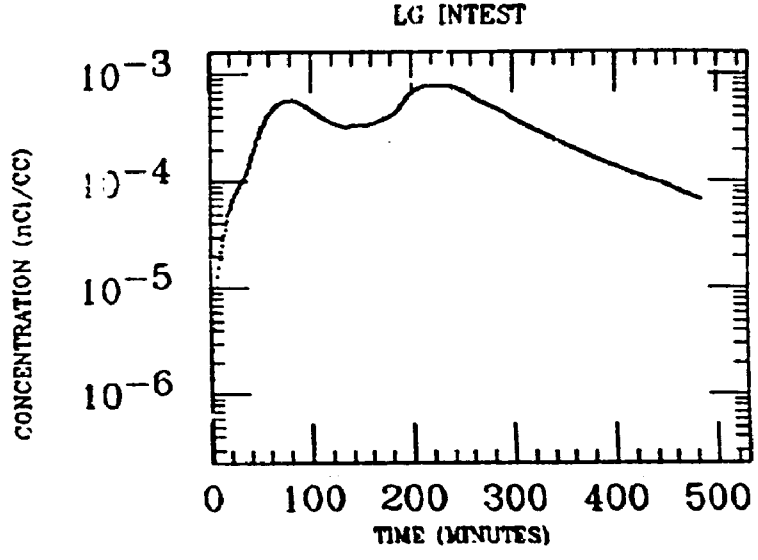

ARROL
XE INGESTION
Pb-214

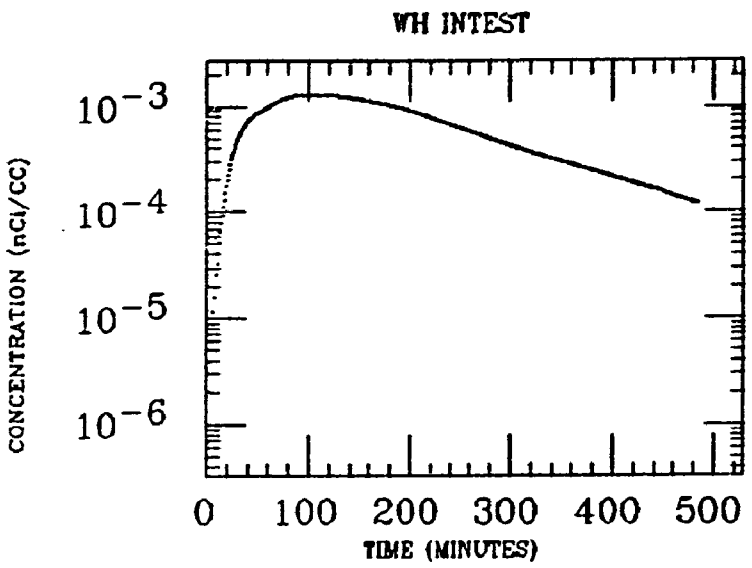

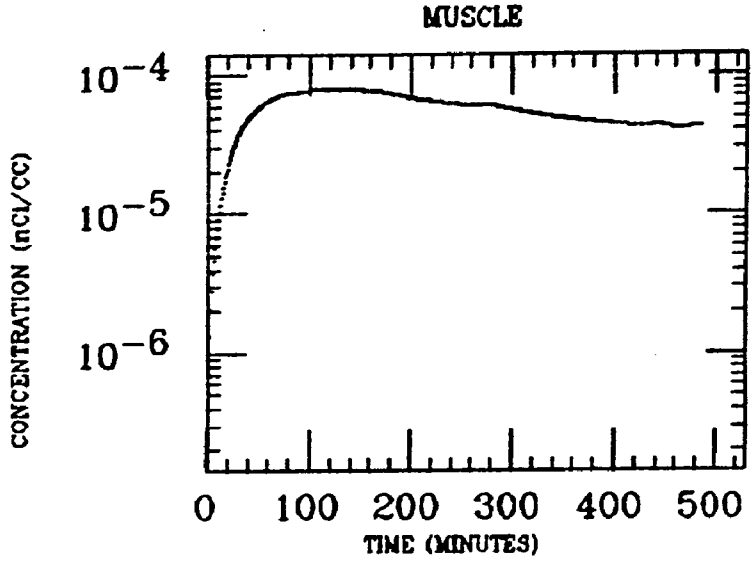

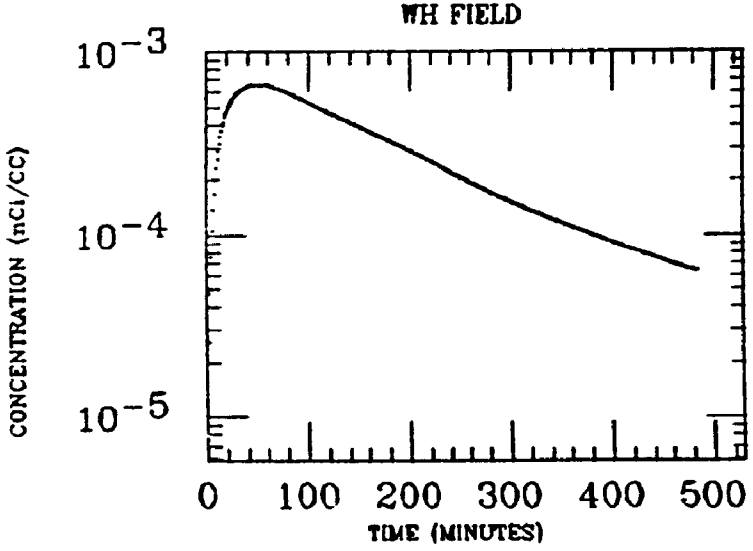

AYER
XE INGESTION
Pb-214

STOMACH

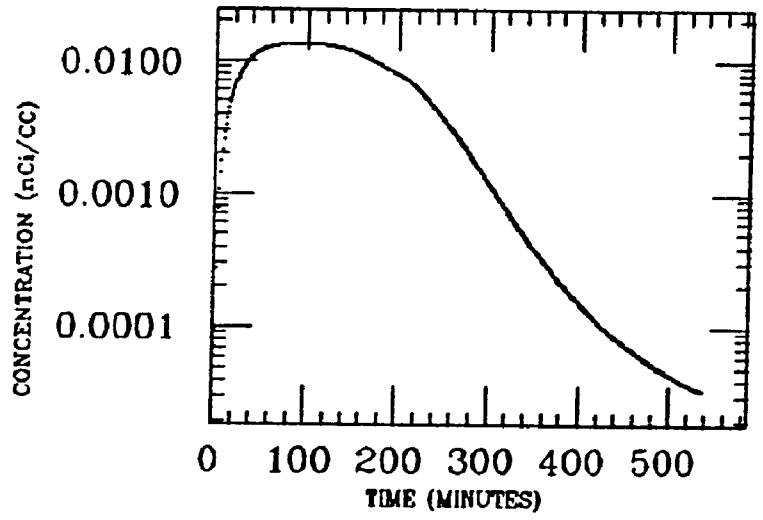

LIVER

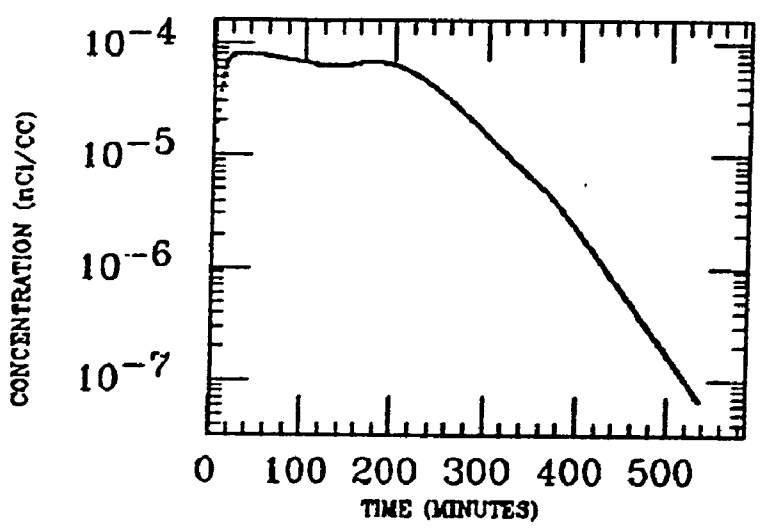

WH FIELD

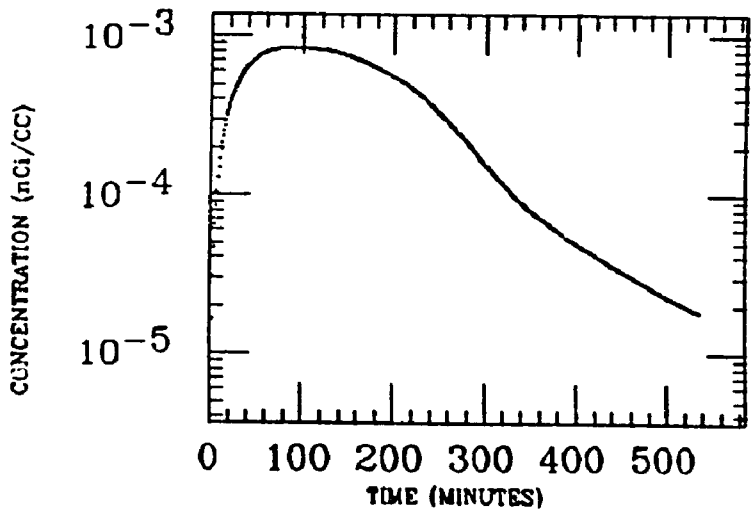

AYER
XE INGESTION
Pb-214

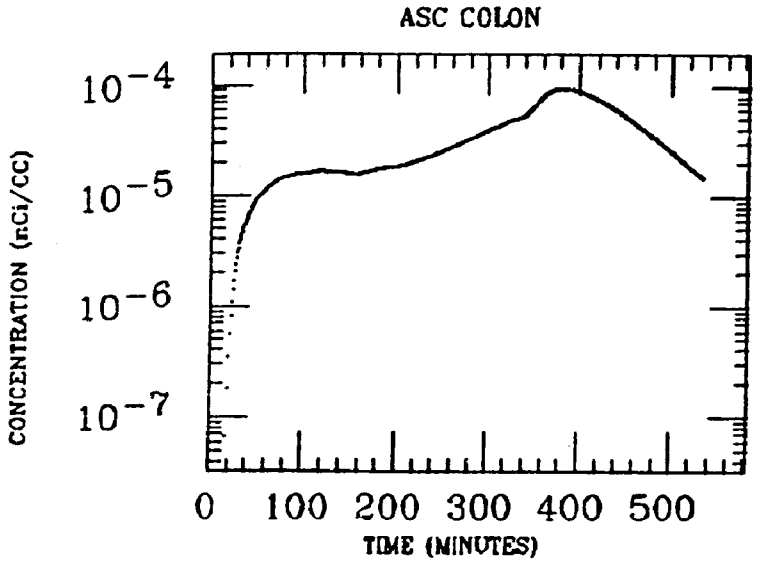

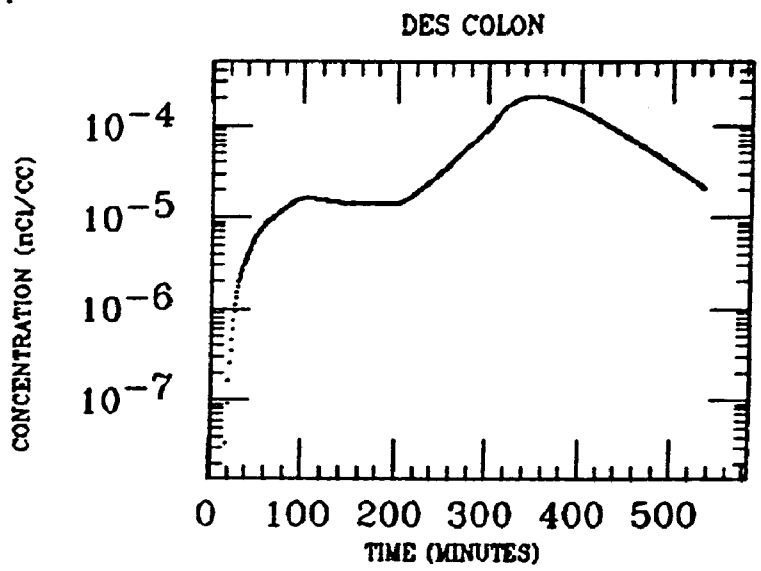

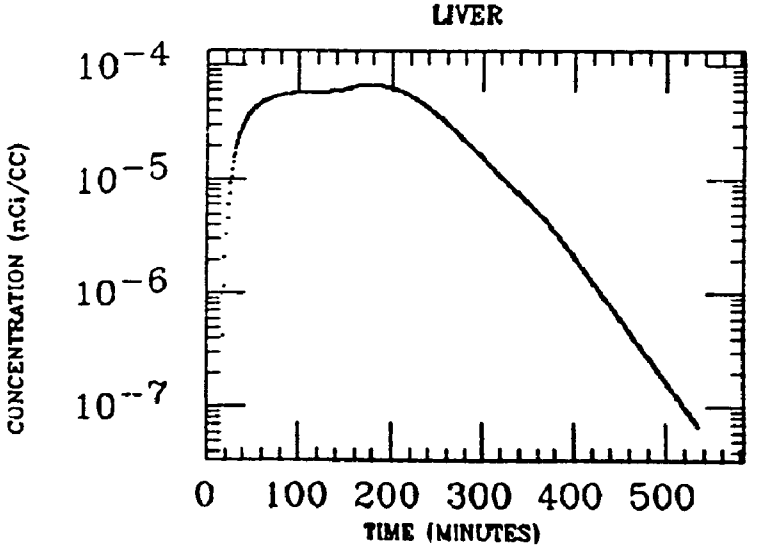

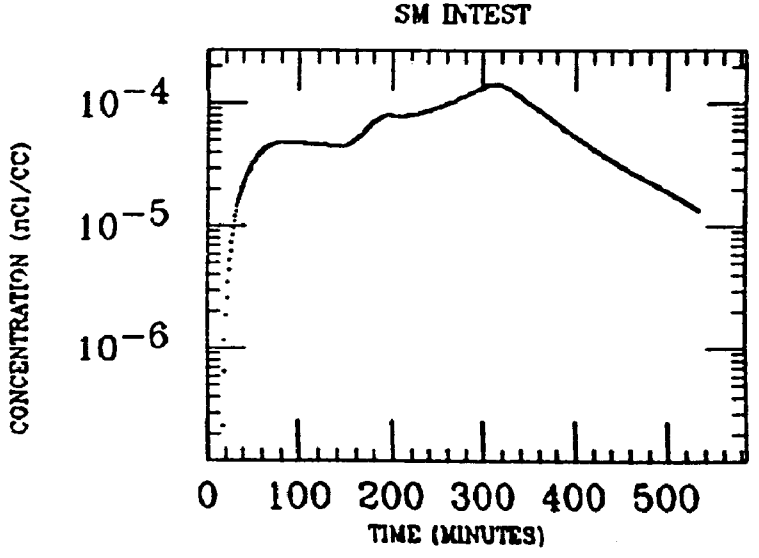

AYER
XE INGESTION
Pb-214

STOMACH

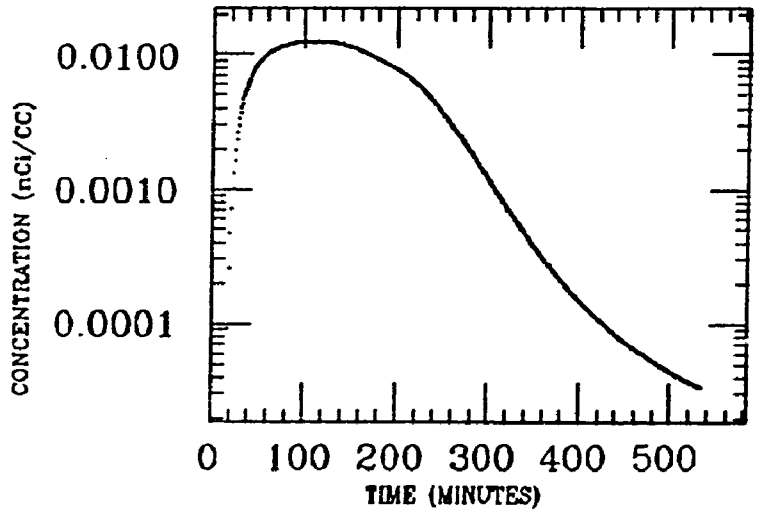

TR COLON

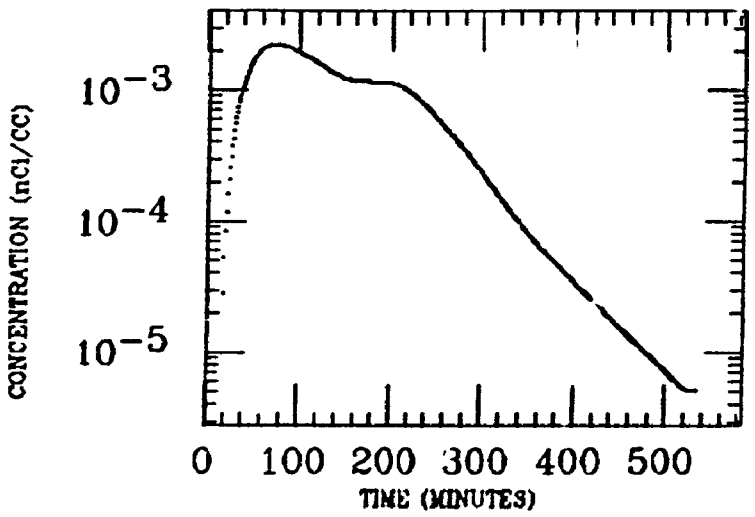

WH FIELD

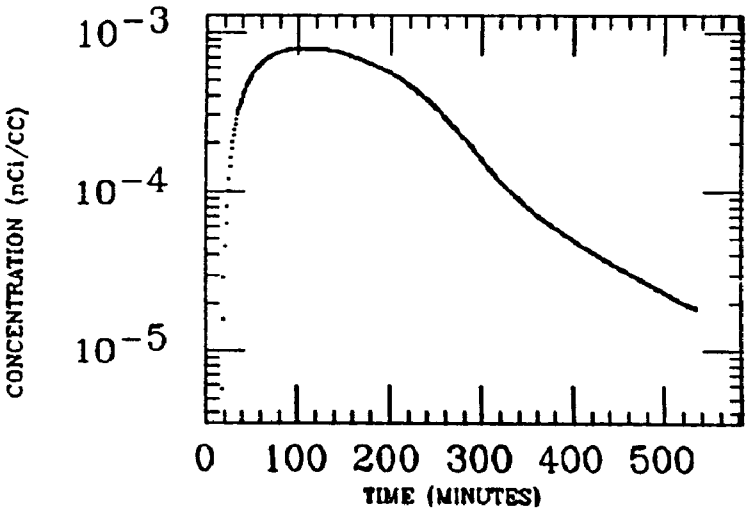

WH INTEST

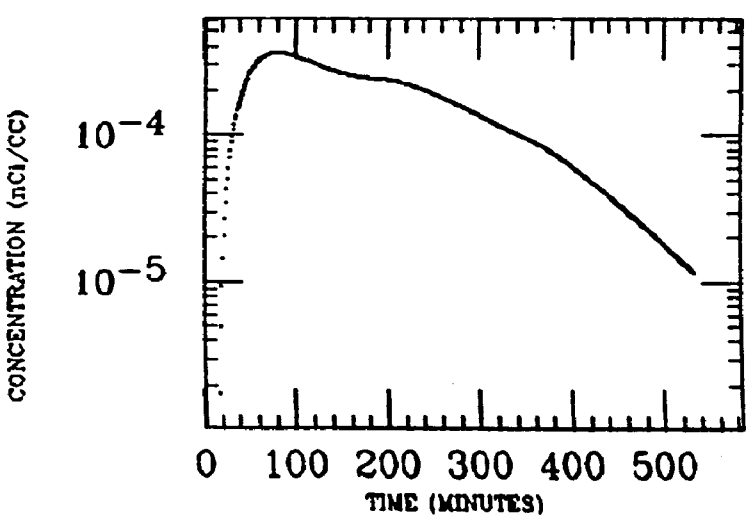

BROCK
XE INGESTION
Pb-214

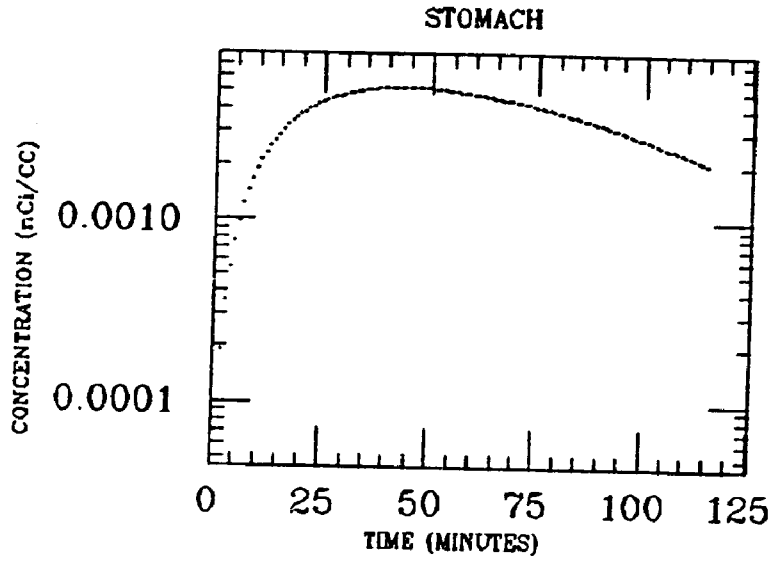

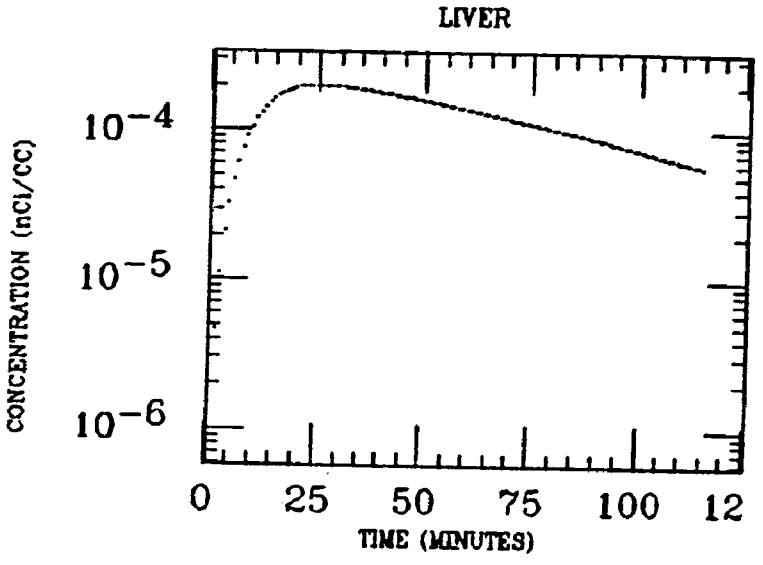

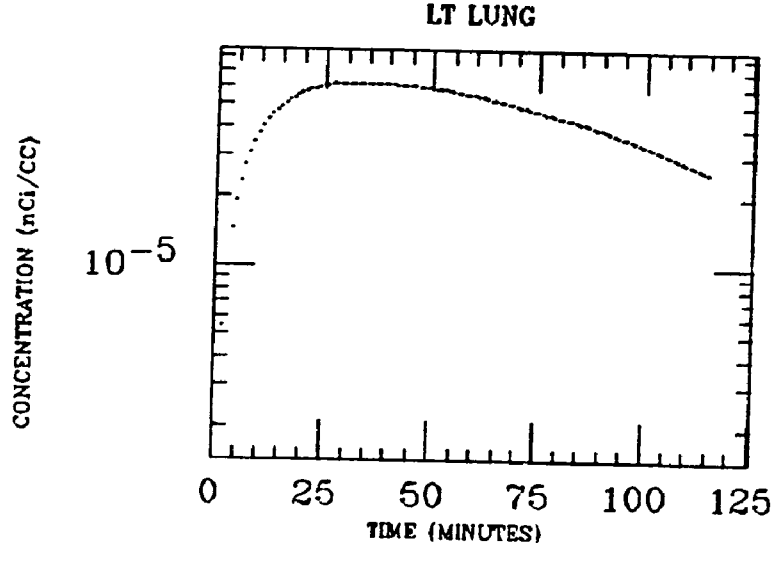

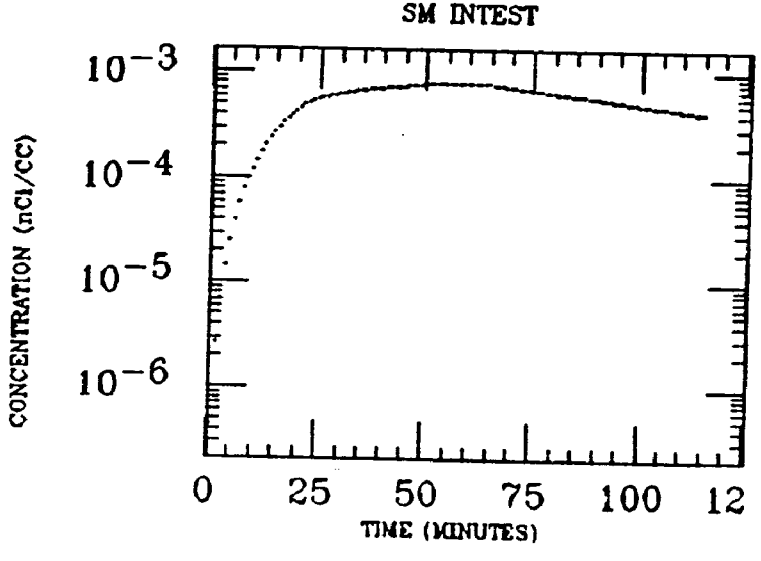

BROCK
XE INGESTION
Pb-214

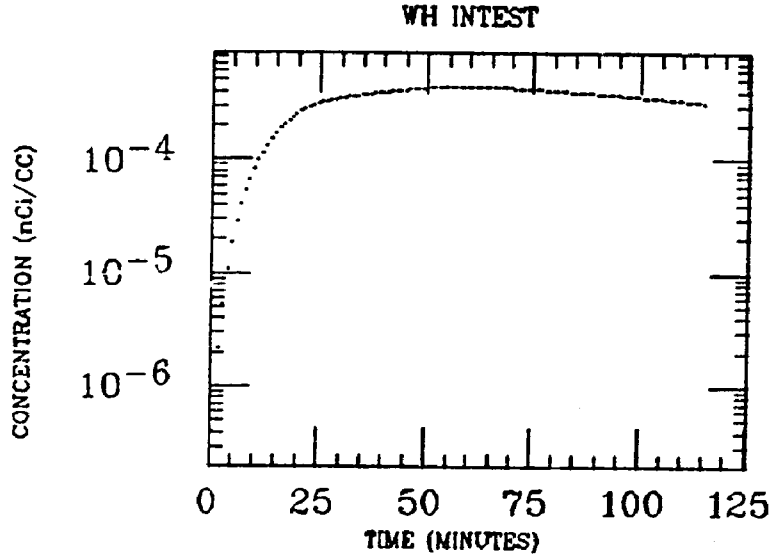

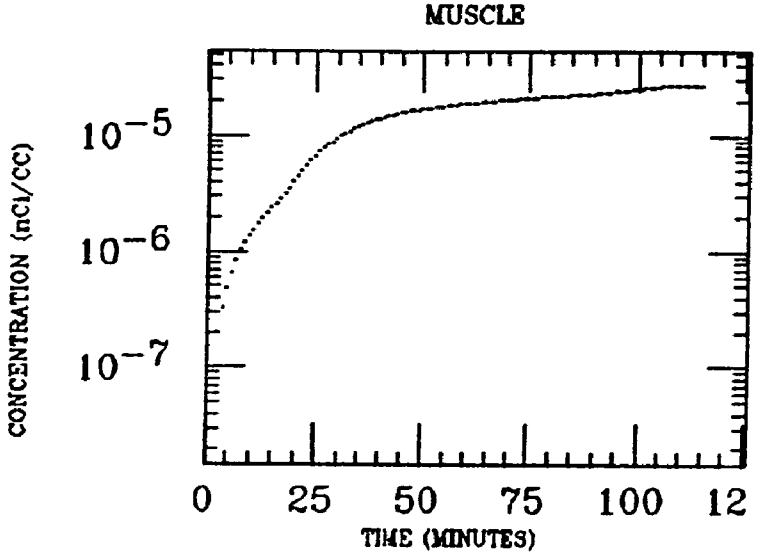

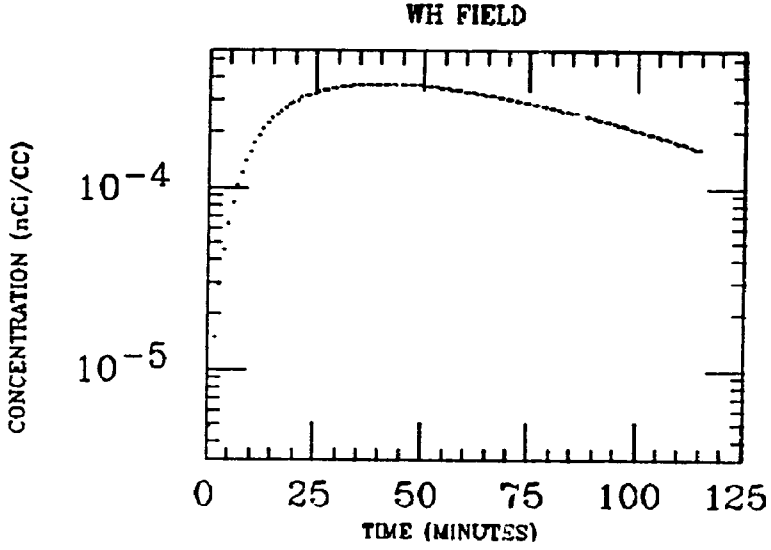

BYRNE
XE INGESTION
Pb-214

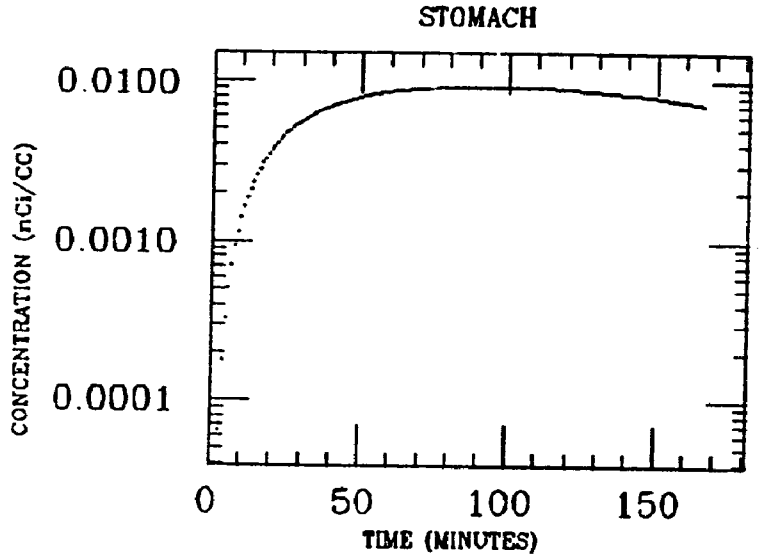

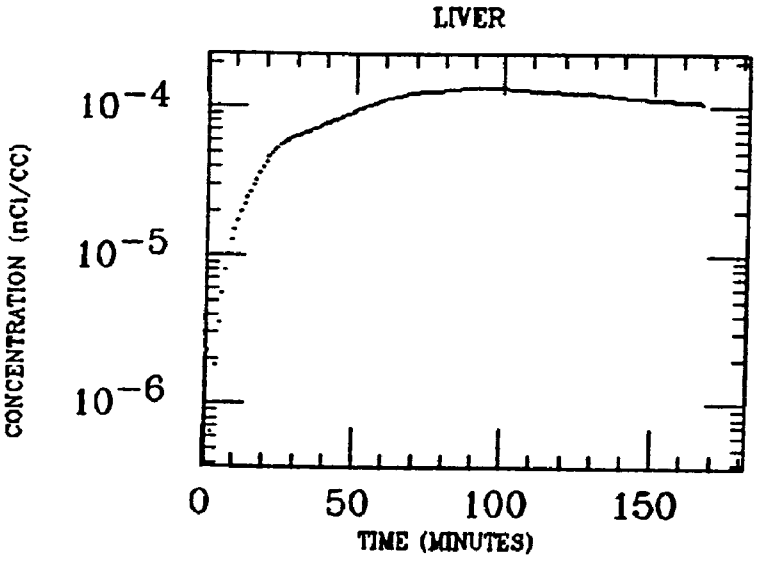

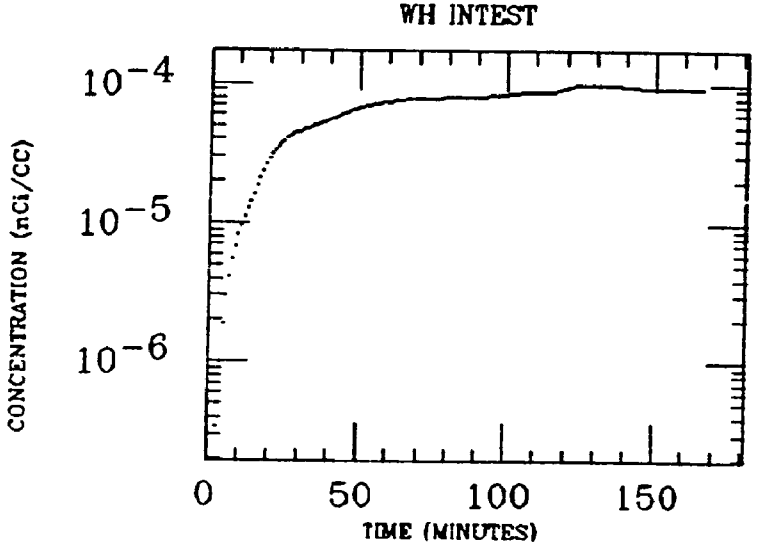

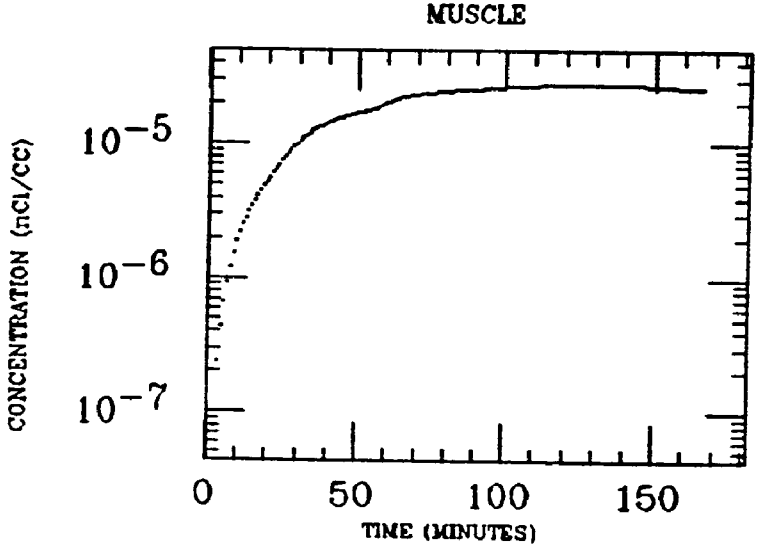

BYRNE
XE INGESTION
Pb-214

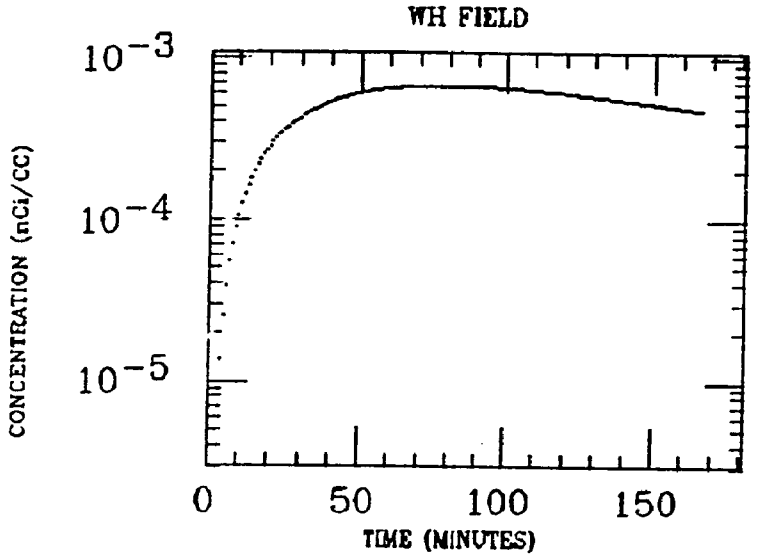

CLINE
XE INGESTION
Pb-214

STOMACH

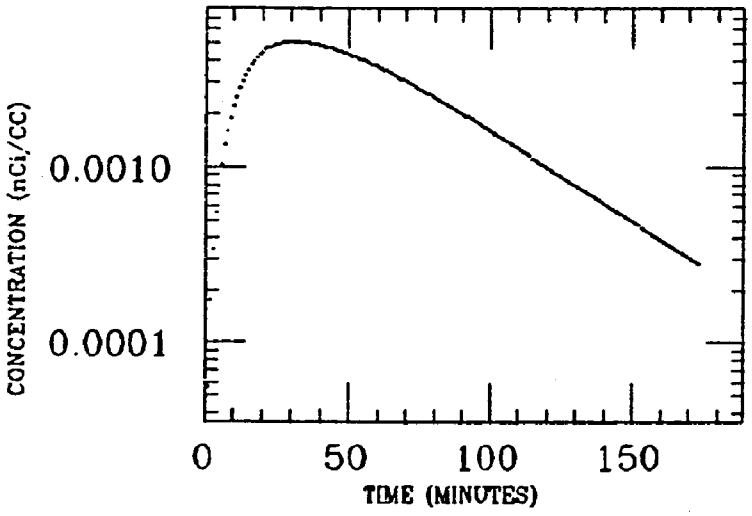

LIVER

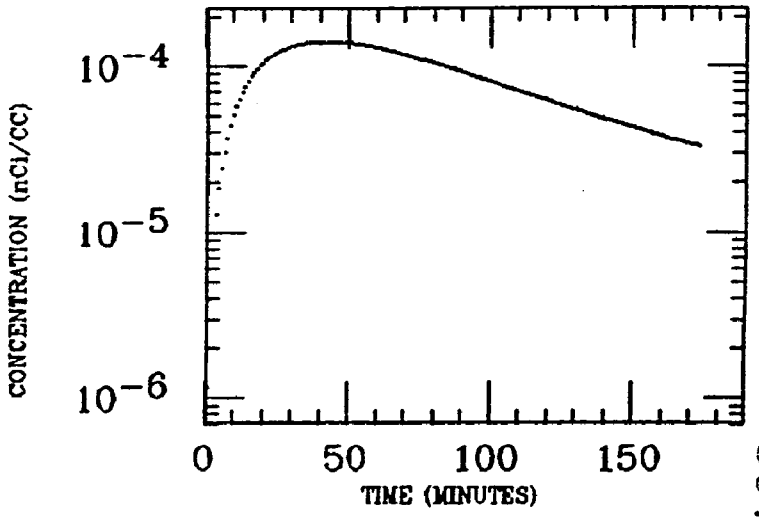

SM INTEST

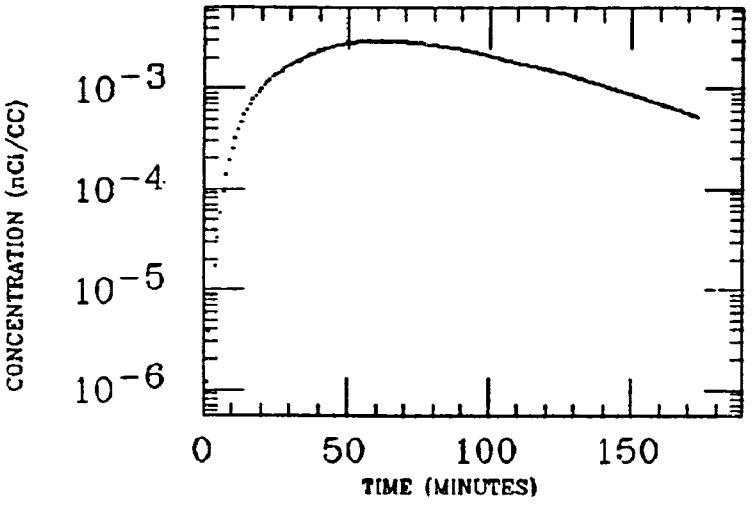

ASC COLON

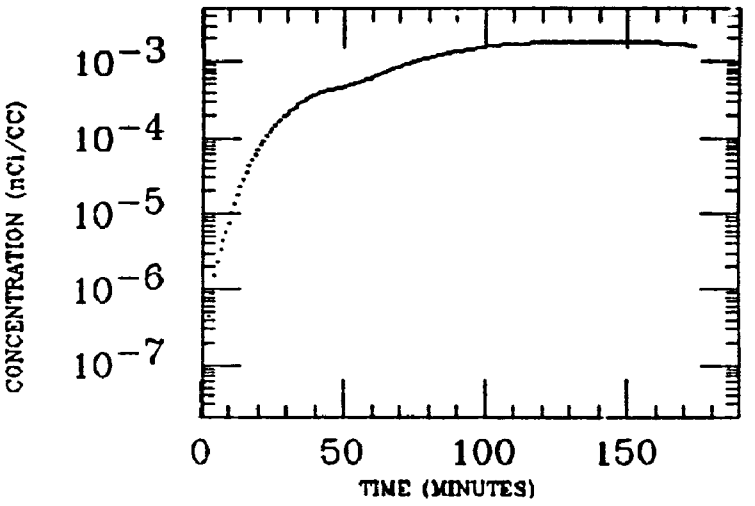

CLINE
XE INGESTION
Pb-214

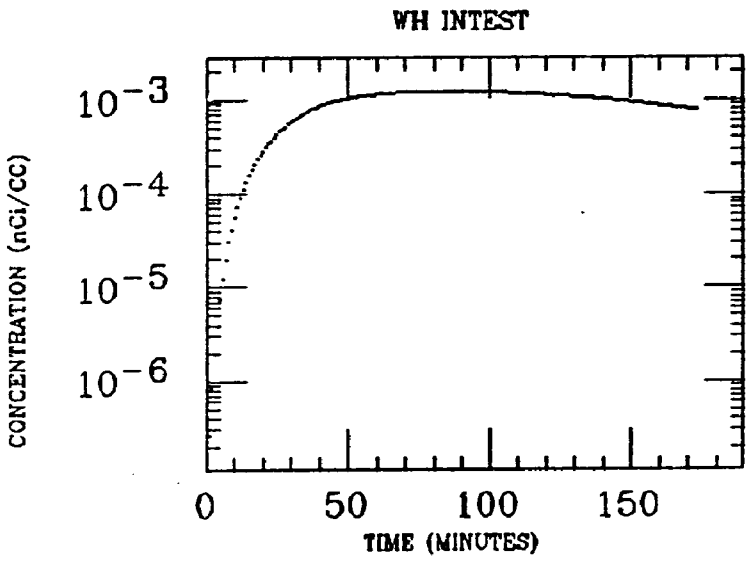

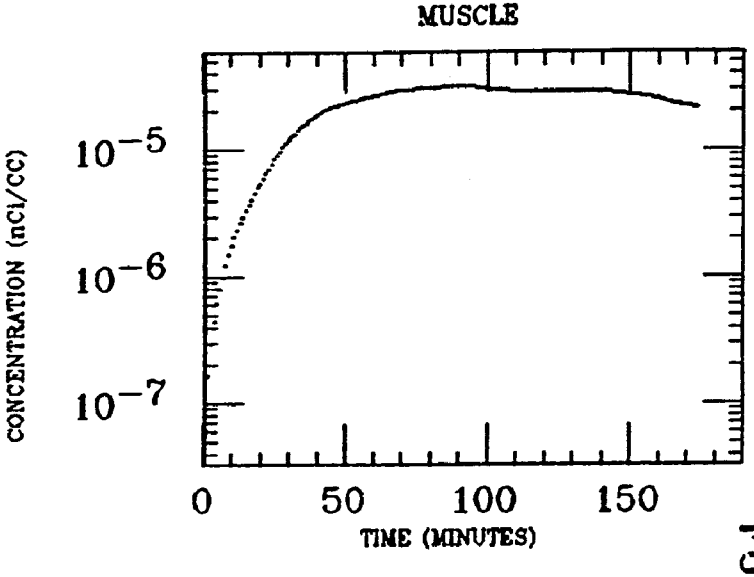

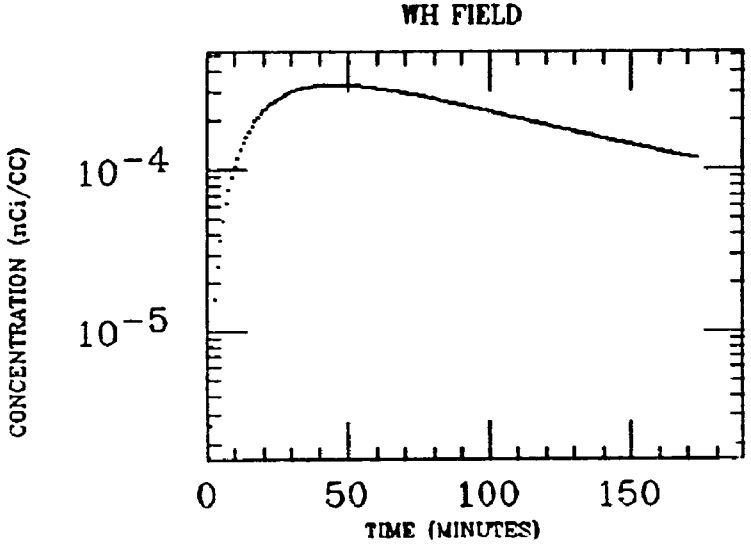

ELMDEN
XE INGESTION
Pb-214

STOMACH

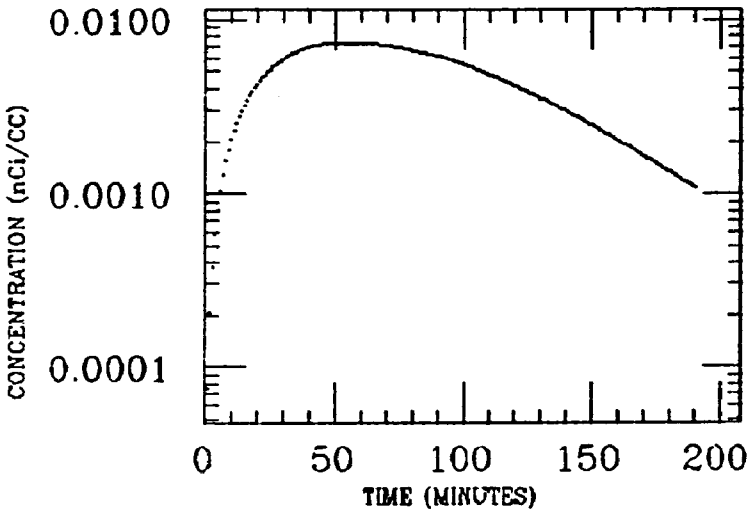

LIVER

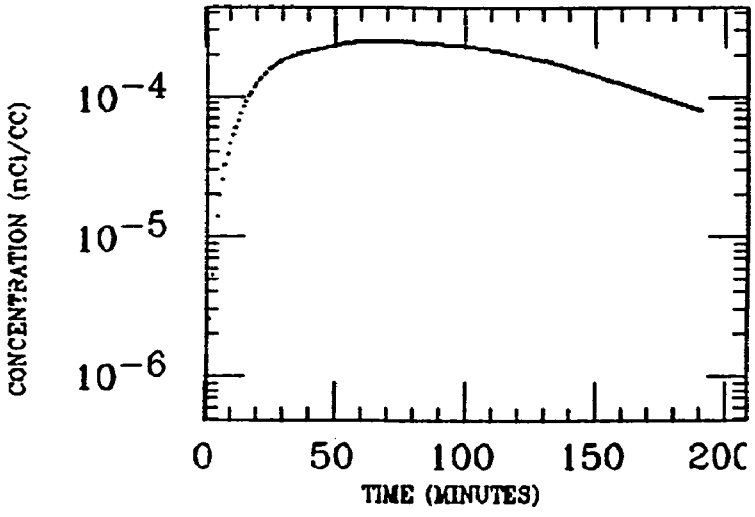

MUSCLE

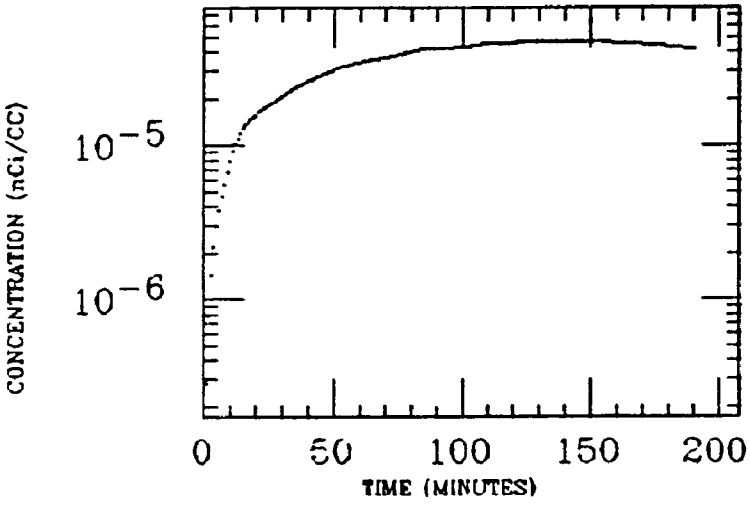

WH FIELD

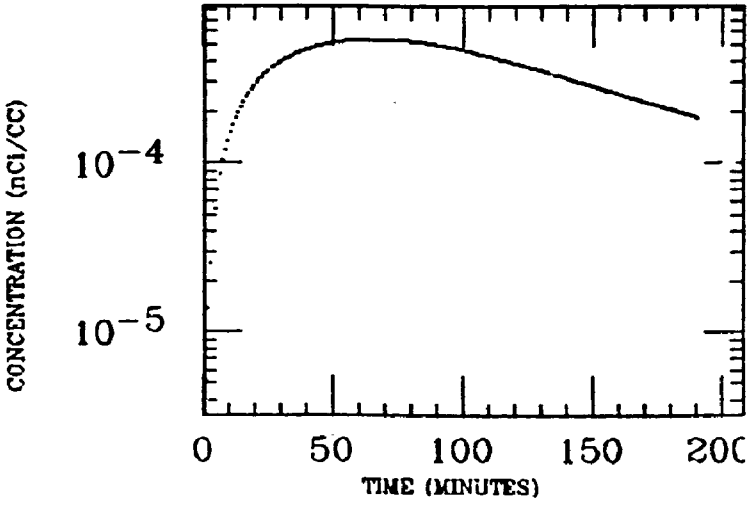

ELMDEN
XE INGESTION
Pb-214

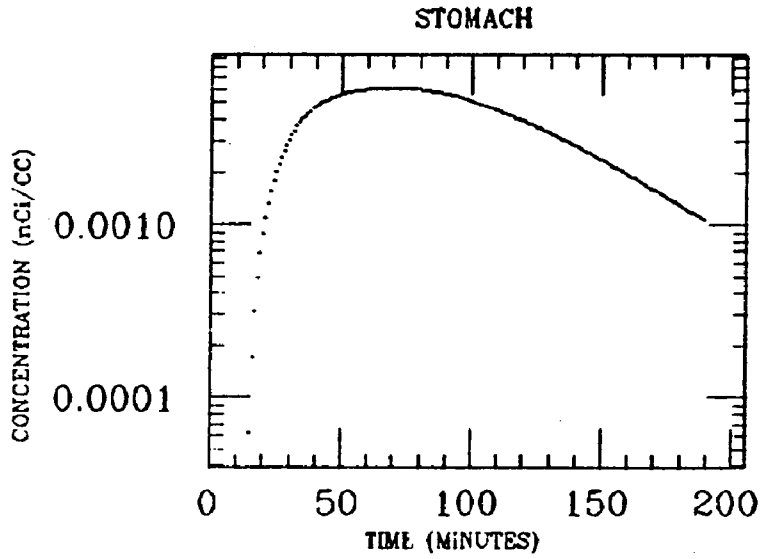

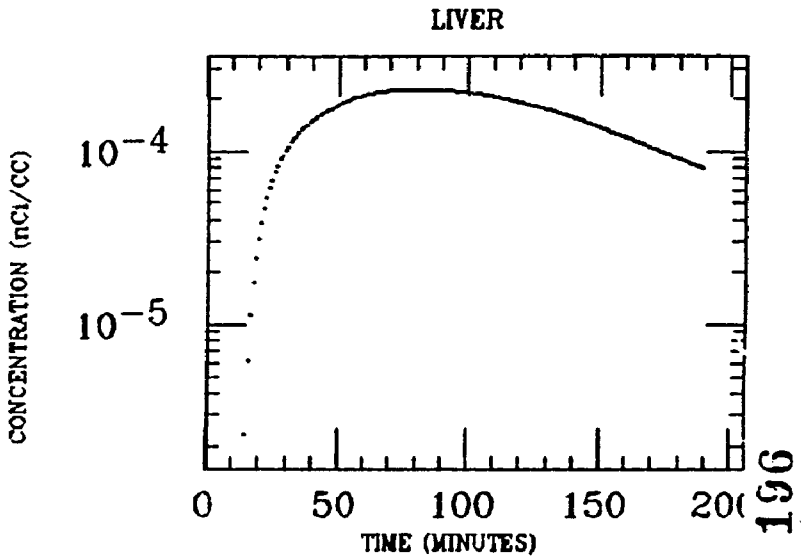

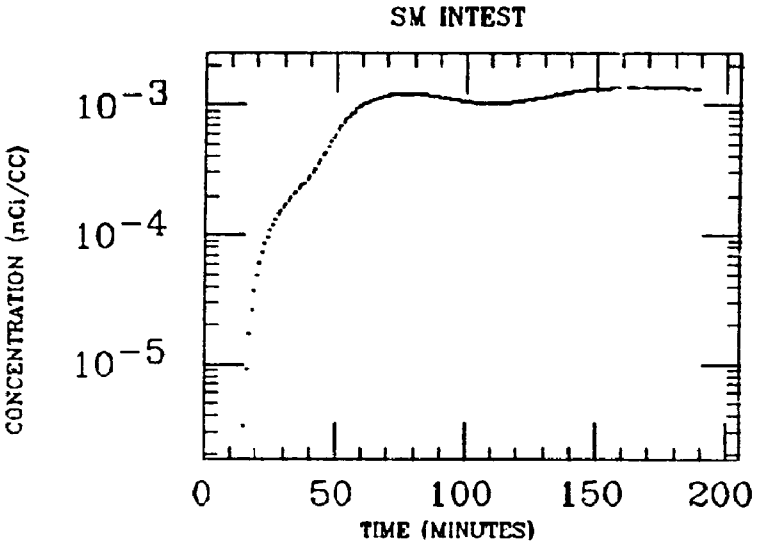

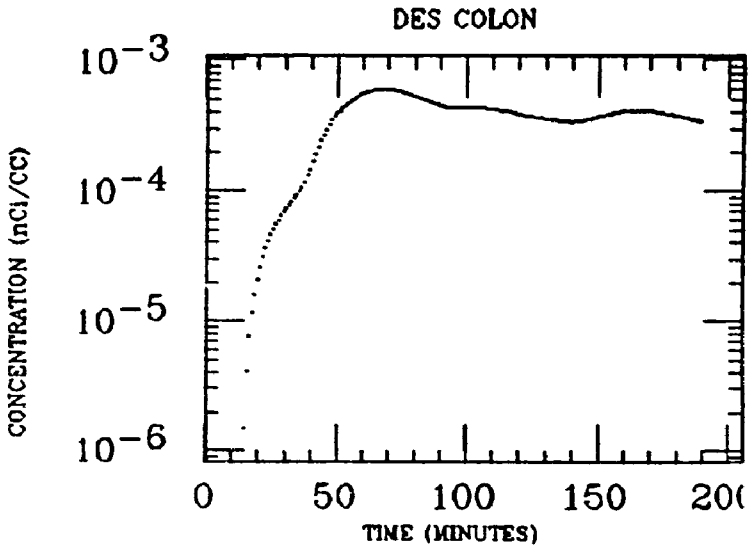

ELMDEN
XE INGESTION
Pb-214

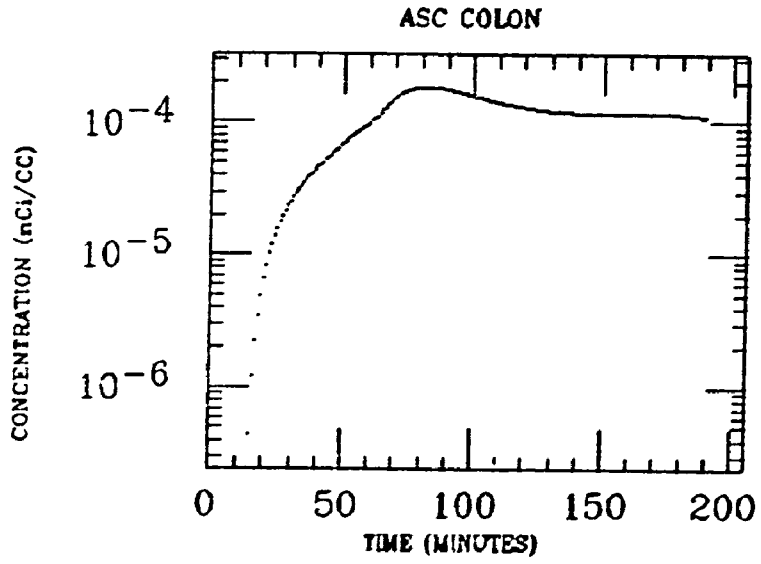

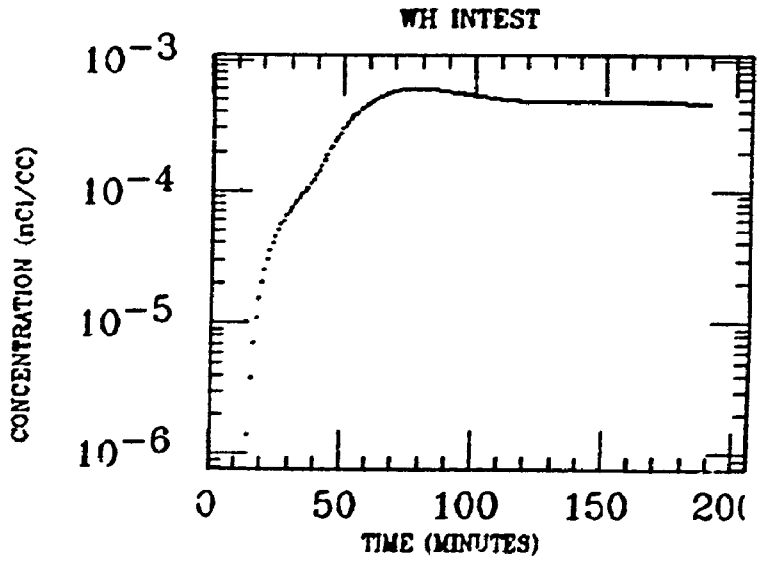

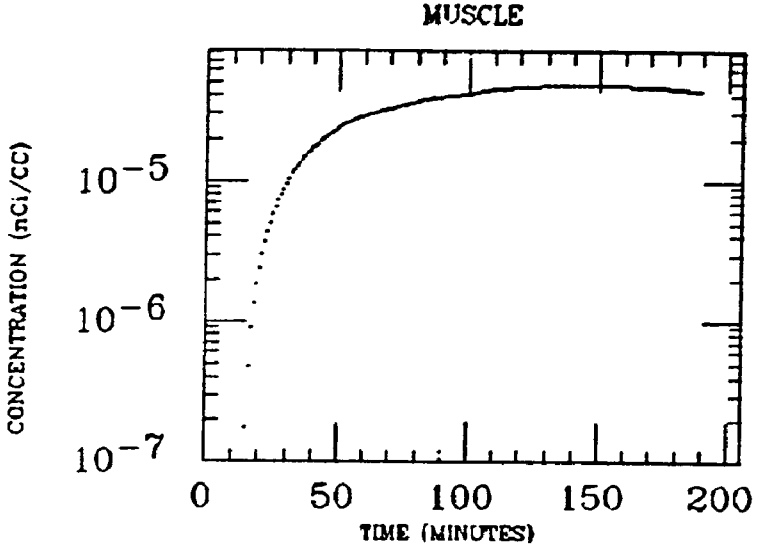

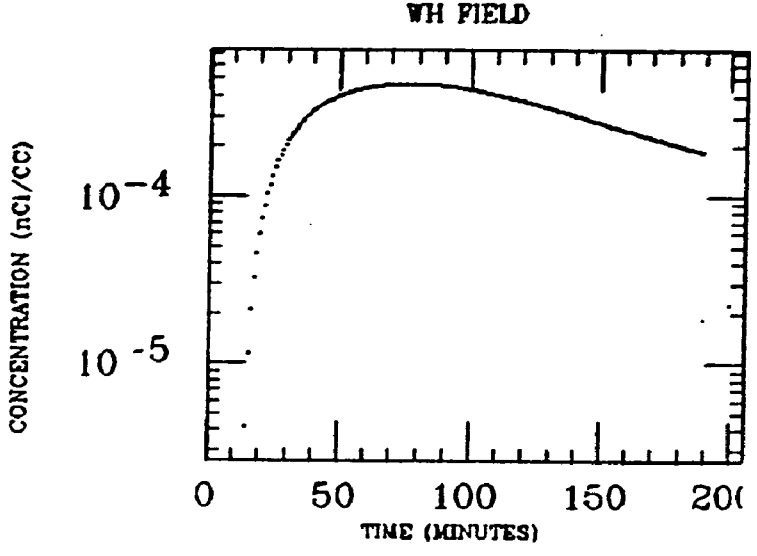

EPLING
XE INGESTION
Pb-214

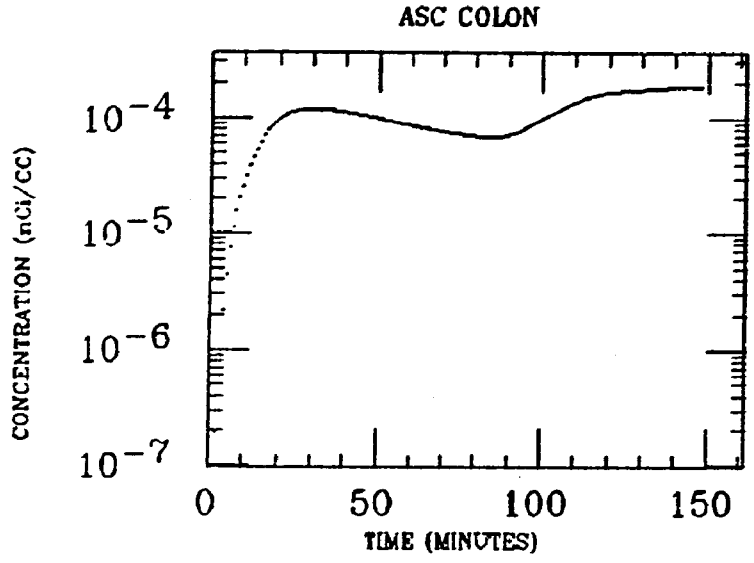

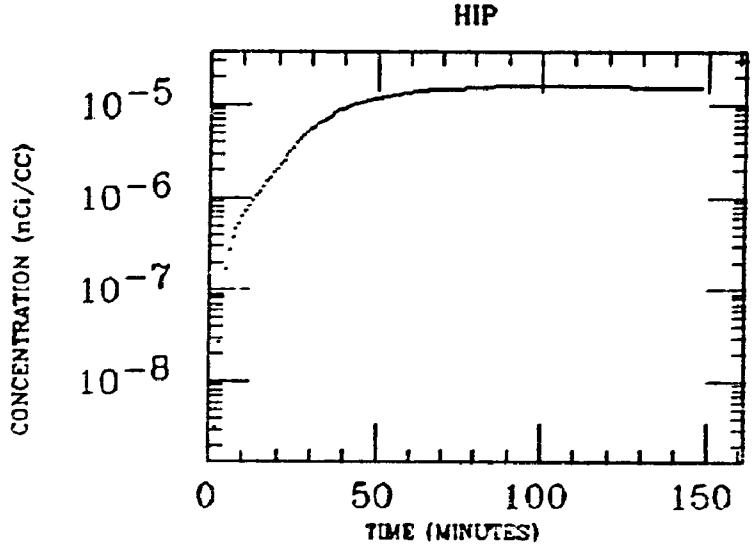

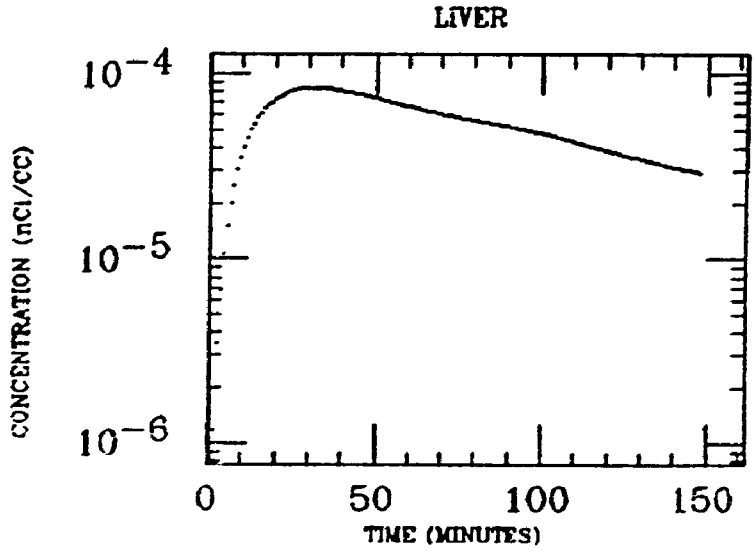

EPLING
XE INGESTION
Pb-214

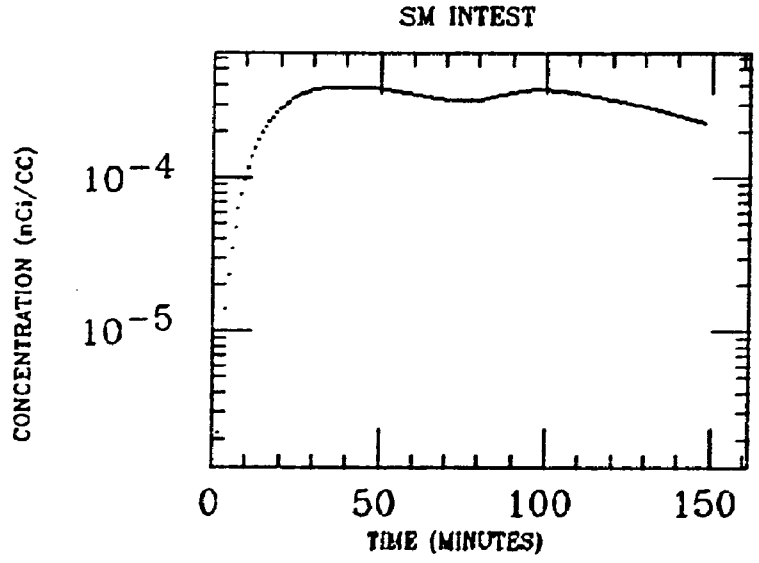

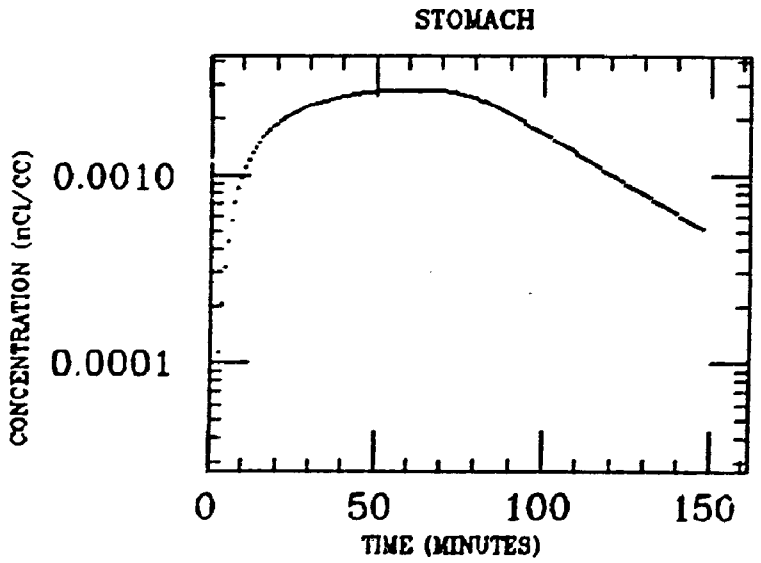

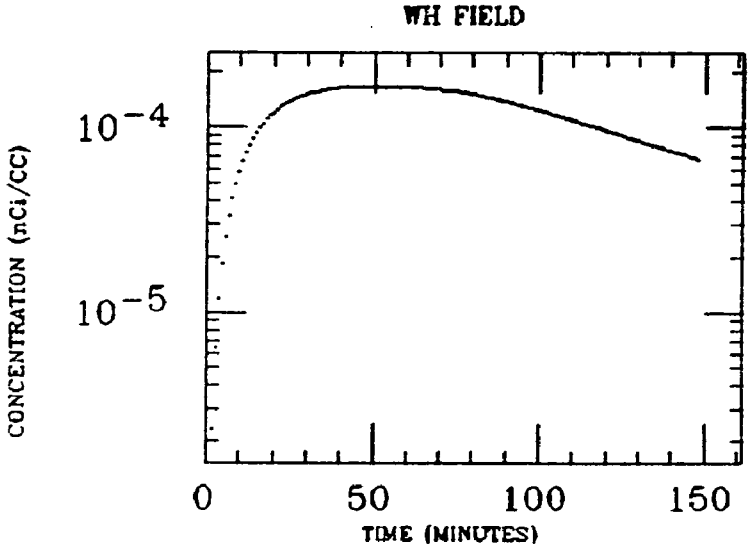

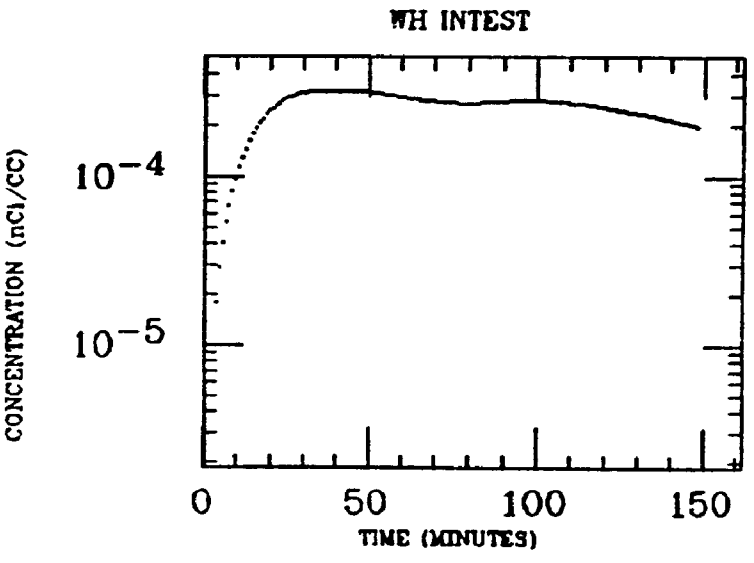

GALLOP
XE INGESTION
Pb-214

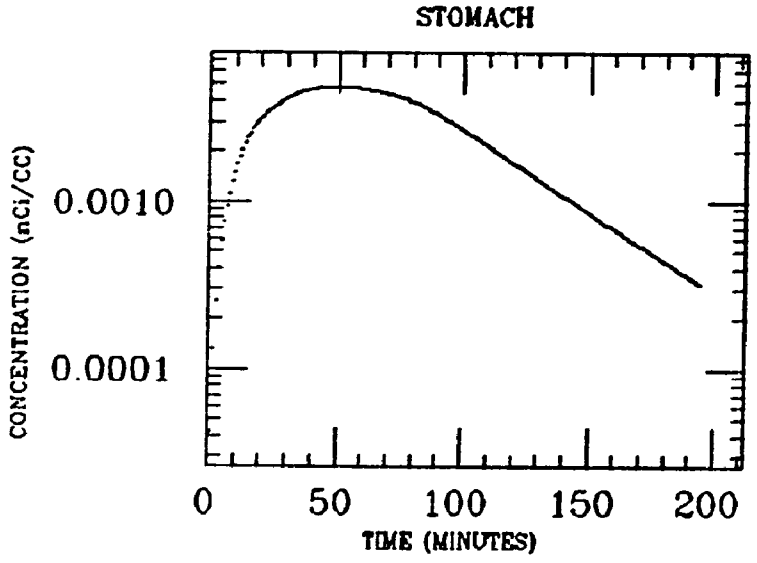

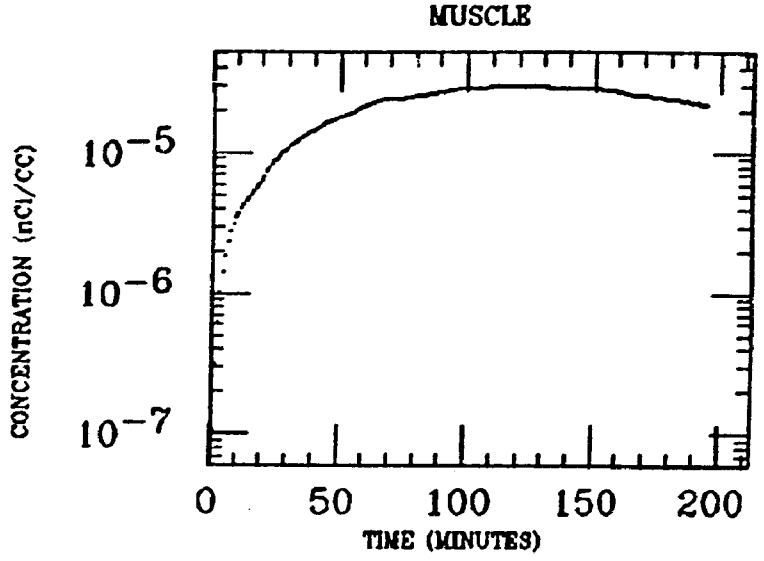

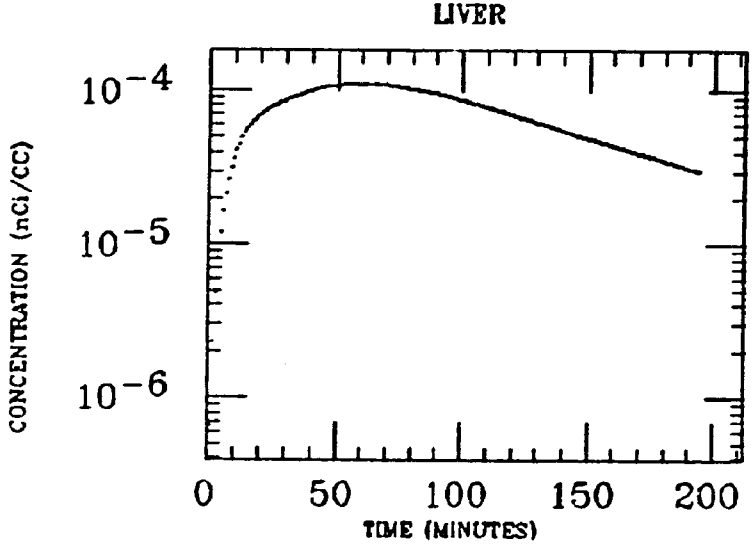

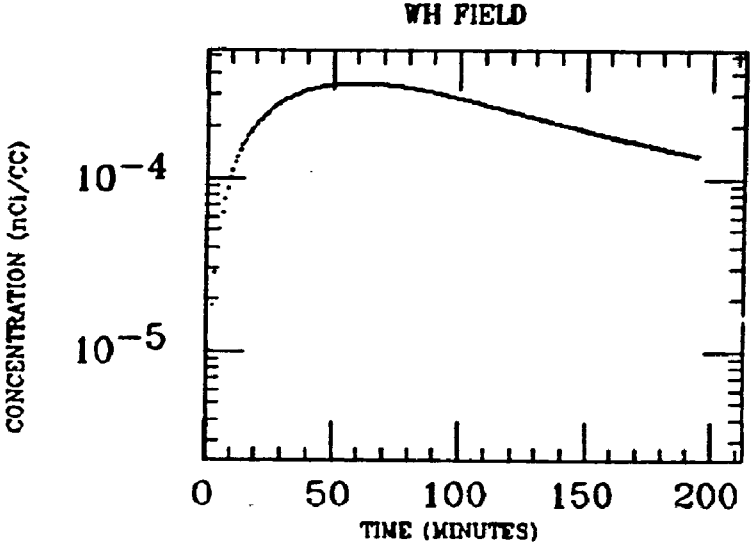

003

GALLOP
XE INGESTION
BI-214

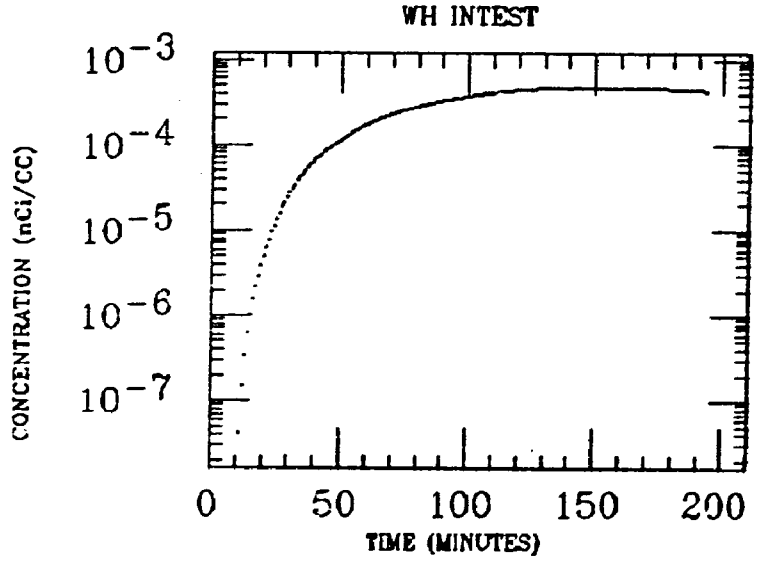

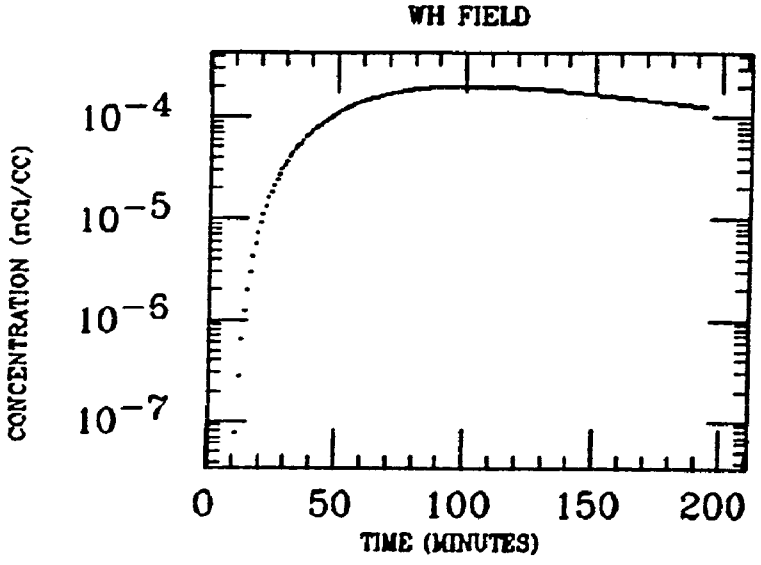

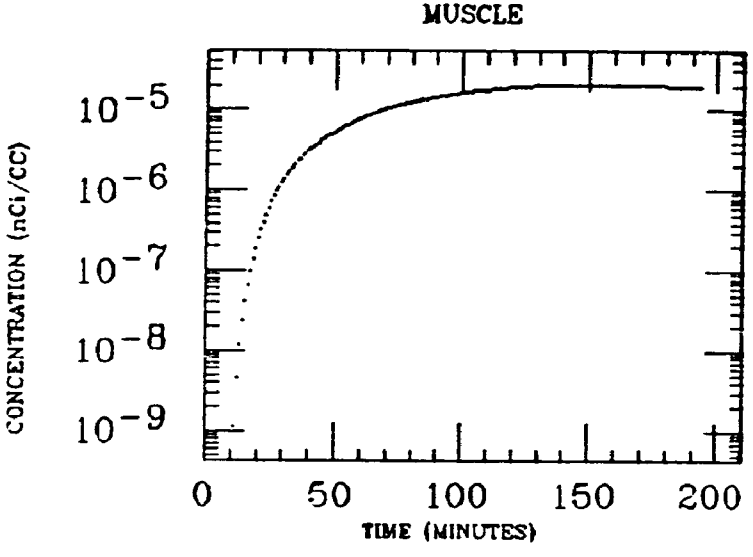

GALLOP
XE INGESTION
Pb-214

STOMACH

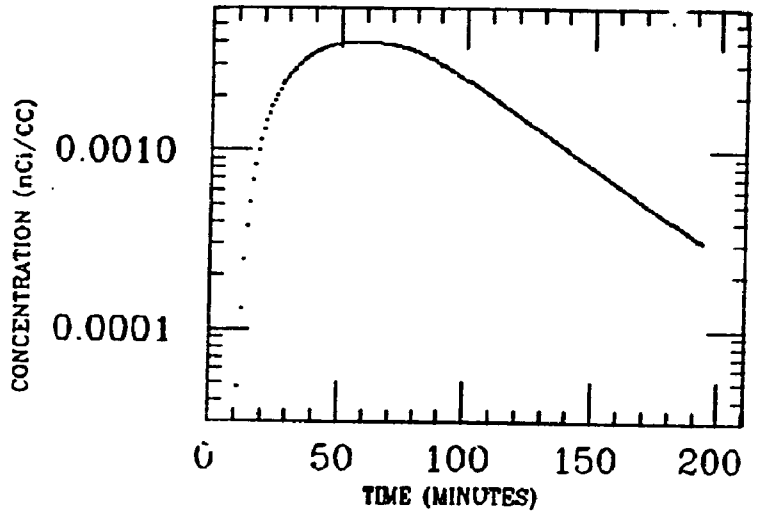

LIVER

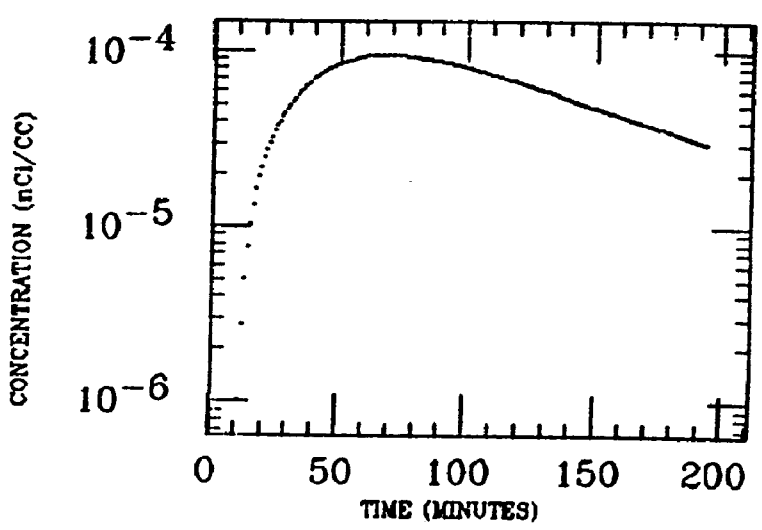

SM INTEST

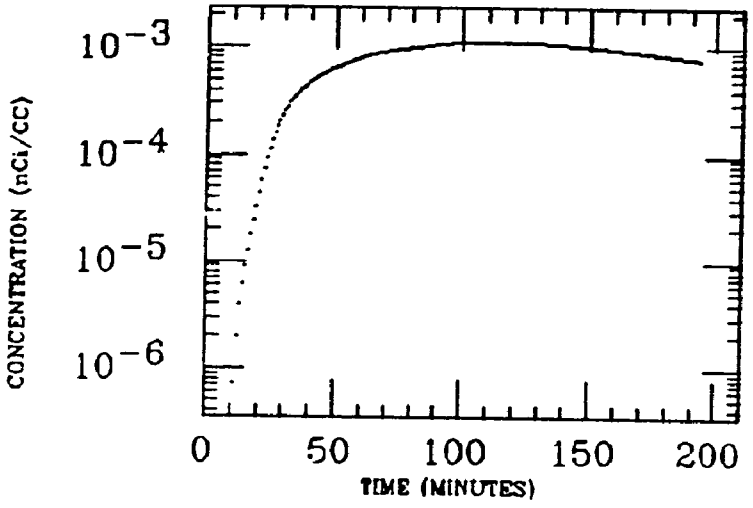

ASC COLON

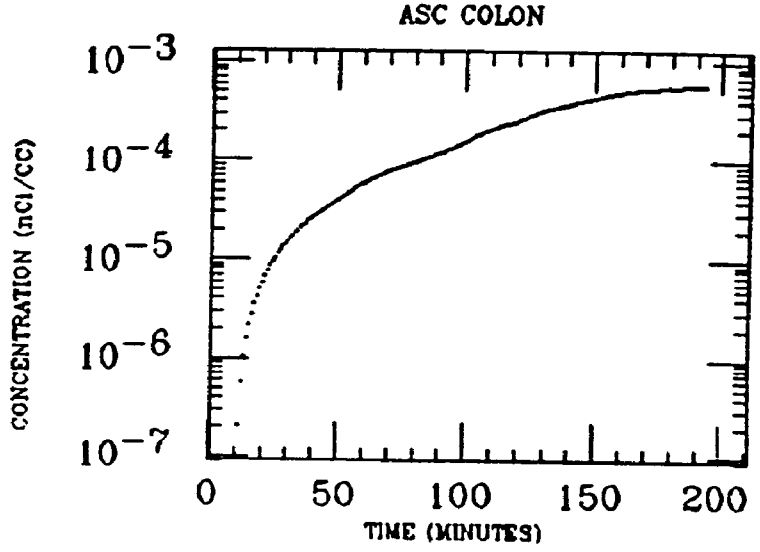

GALLOP
XE INGESTION
Pb-214

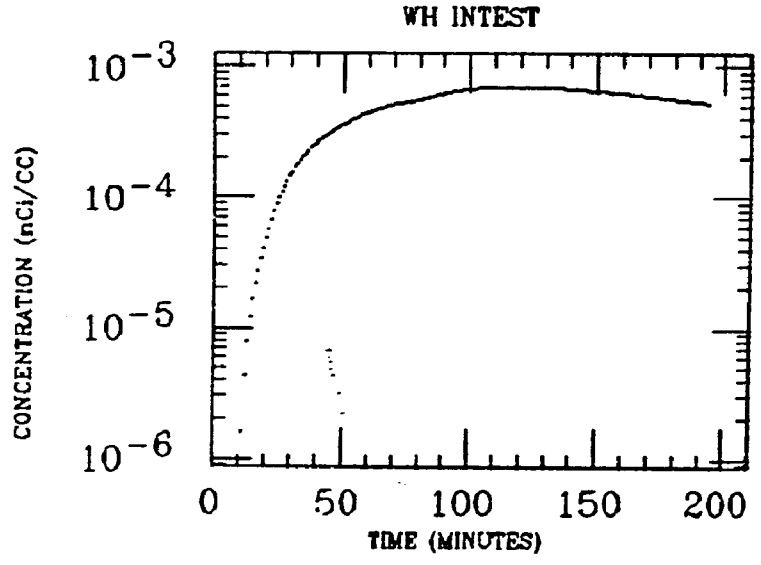

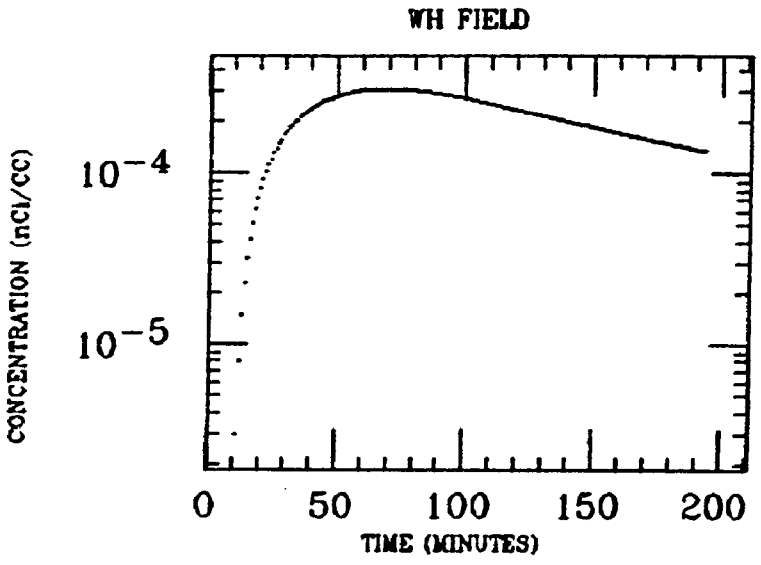

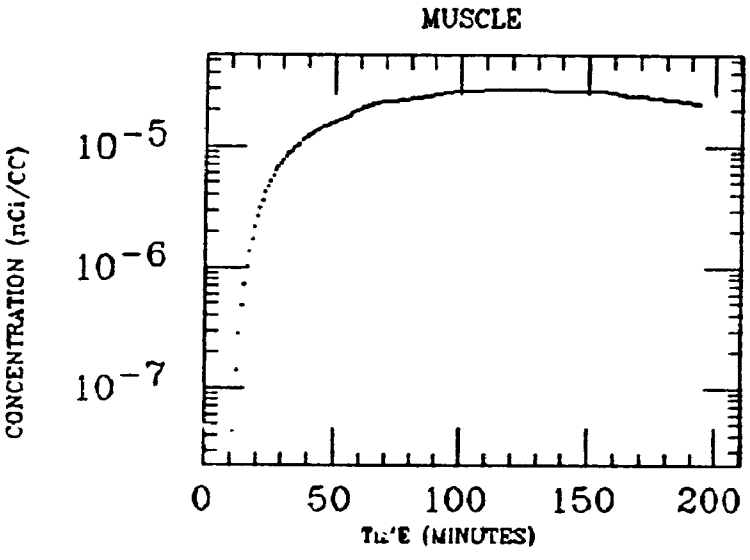

G.MCKINLEY
XE INGESTION
Pb-214

STOMACH

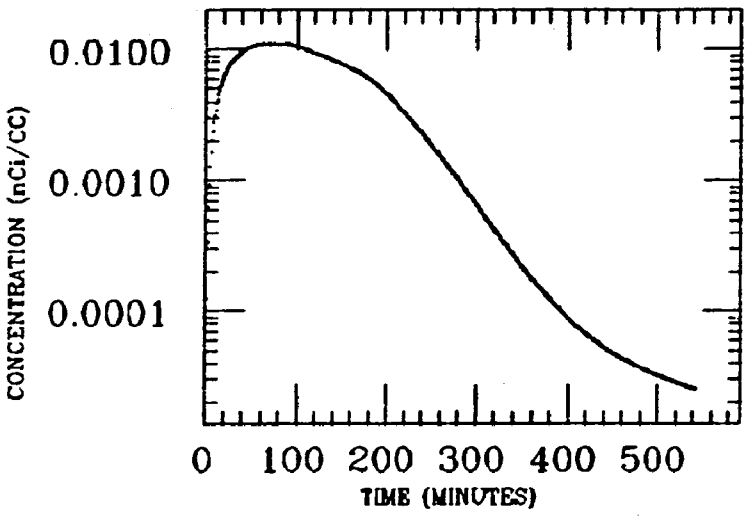

LIVER

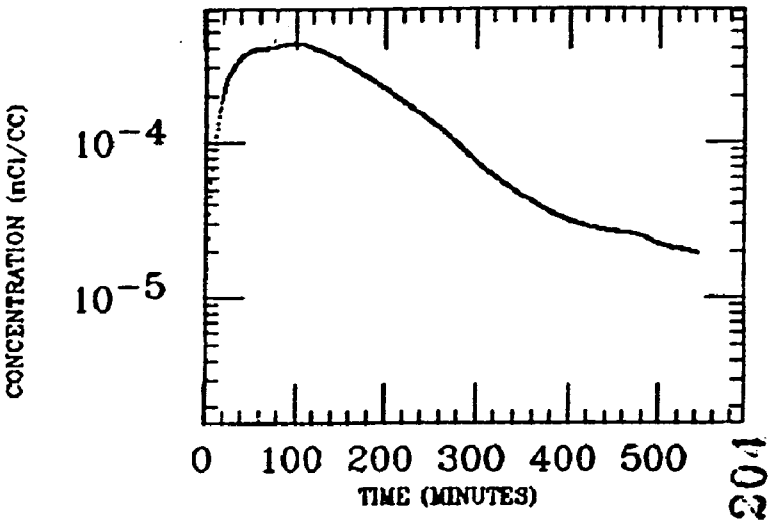

WH FIELD

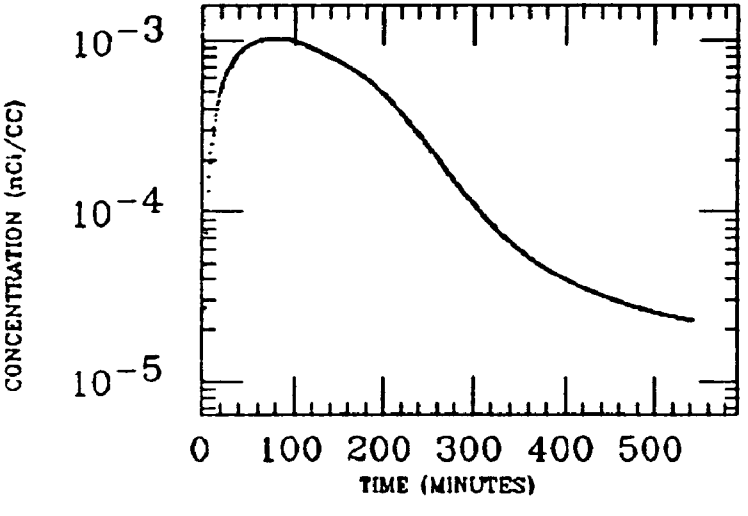

C.MCKINLEY
XE INGESTION
Pb-214

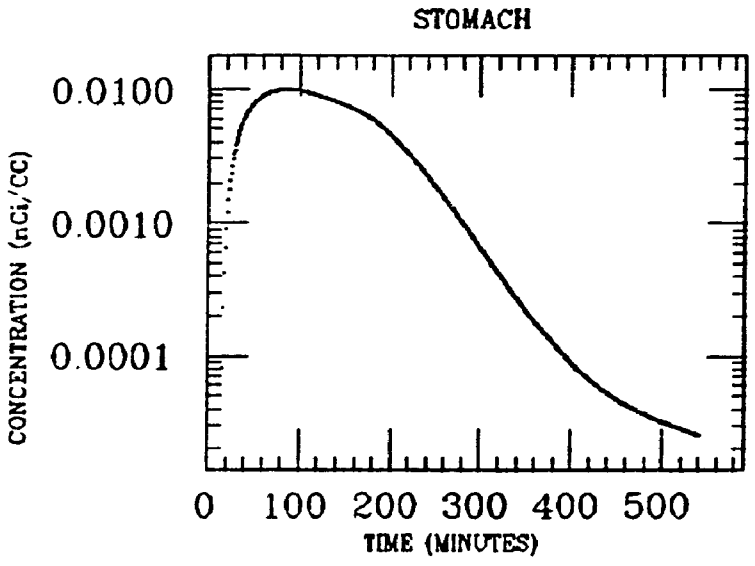

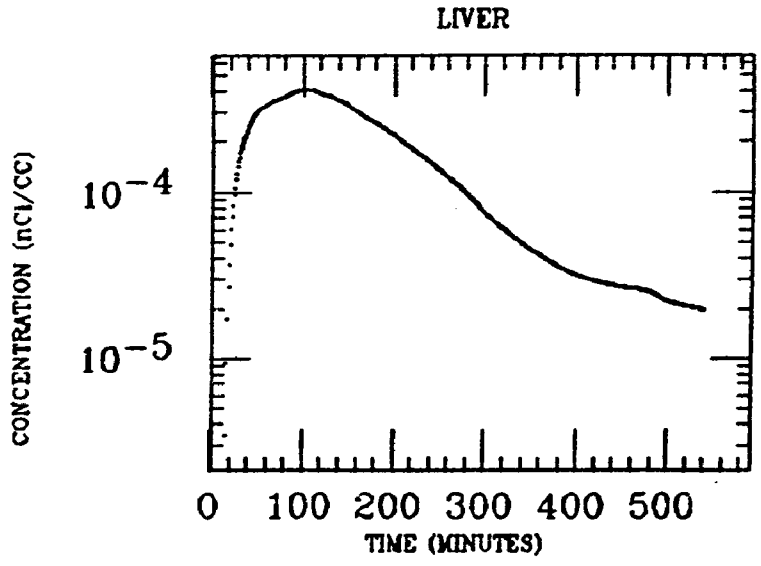

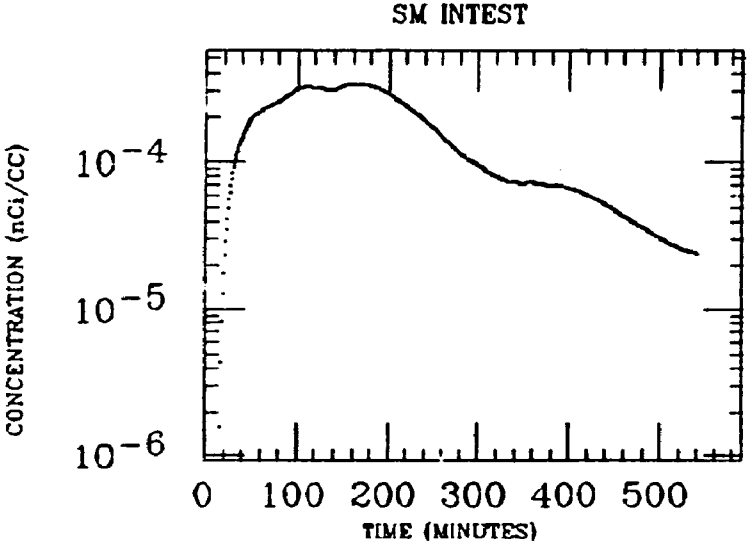

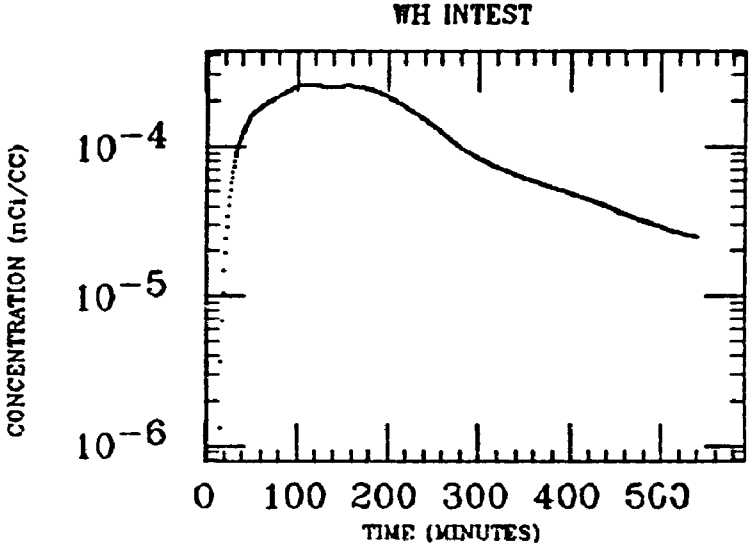

C.MCKINLEY
XE INGESTION
Pb-214

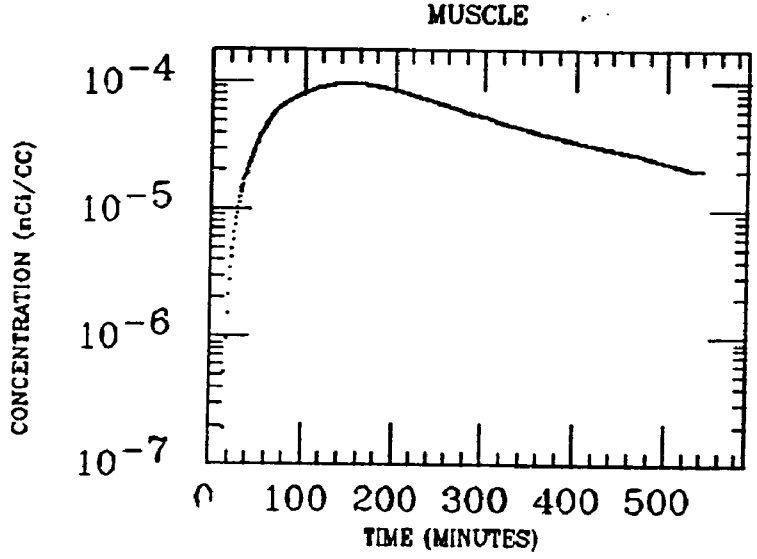

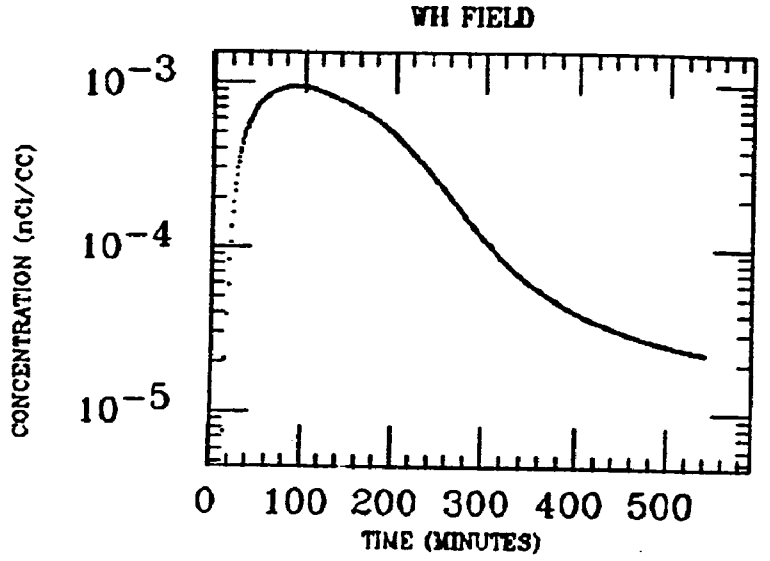

HAND
XE INGESTION
Pb-214

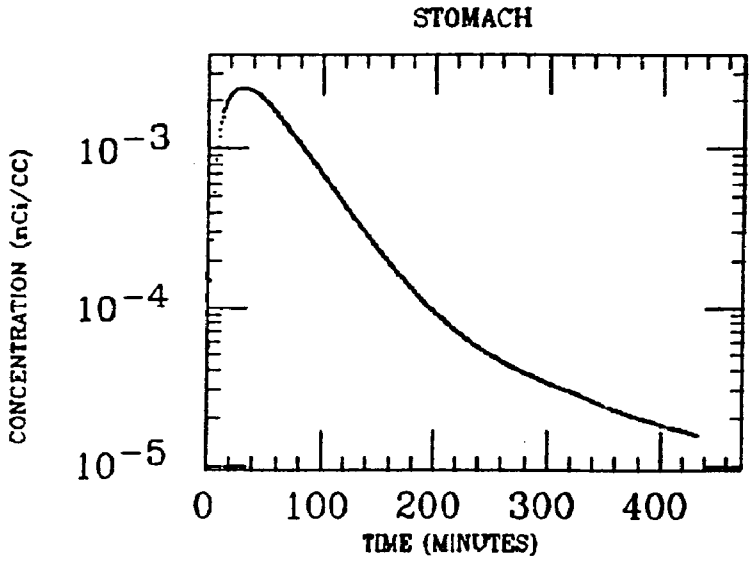

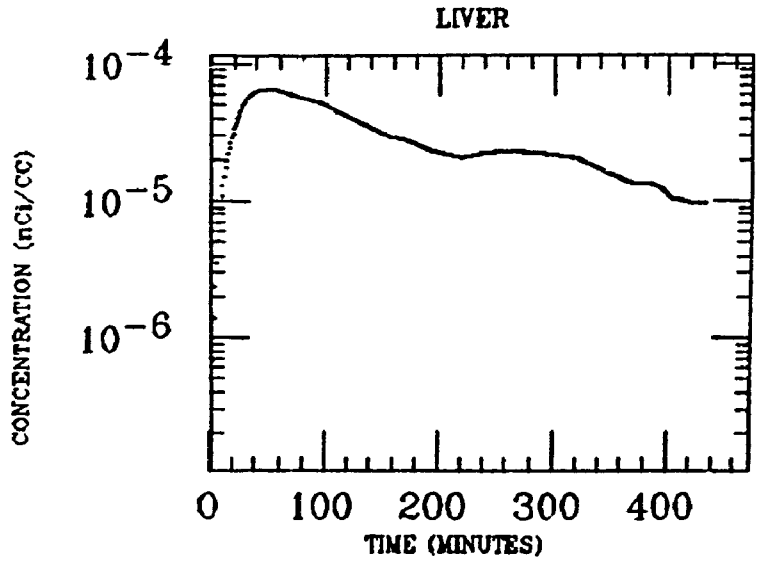

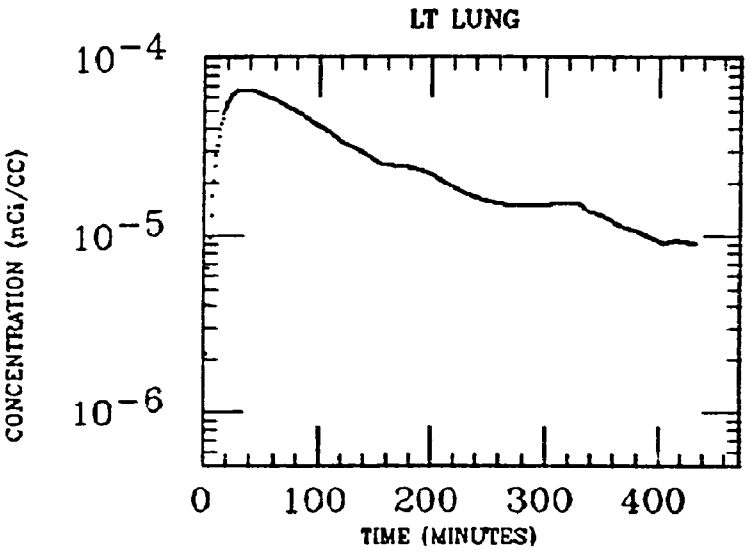

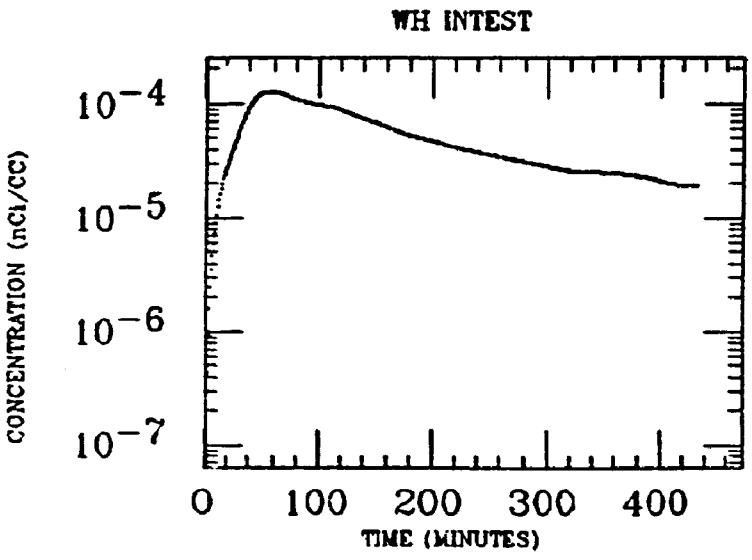

HAND
XE INGESTION
Pb-214

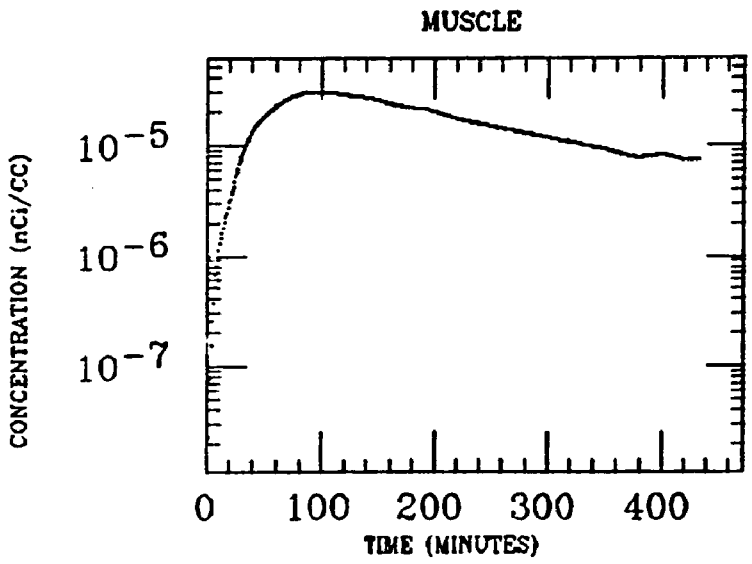

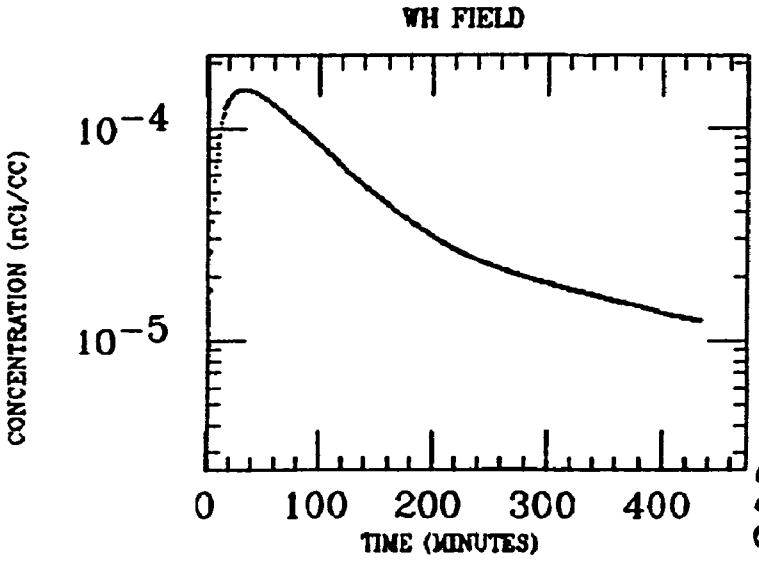

HAND
XE INGESTION
Pb-214

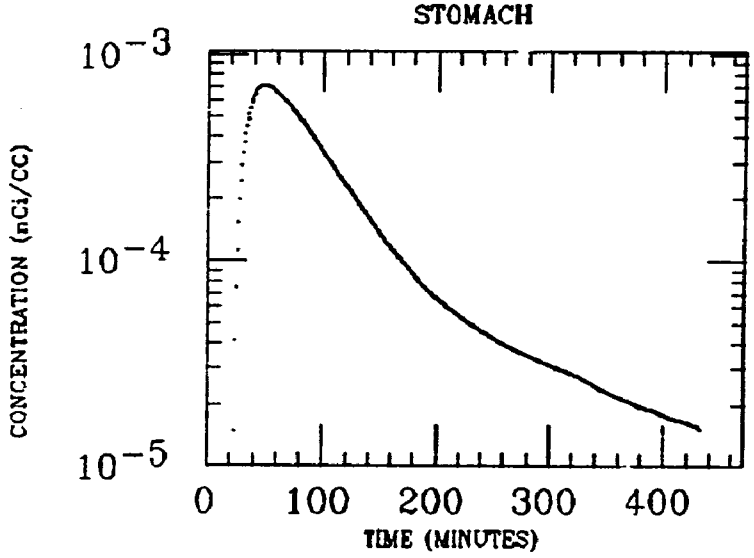

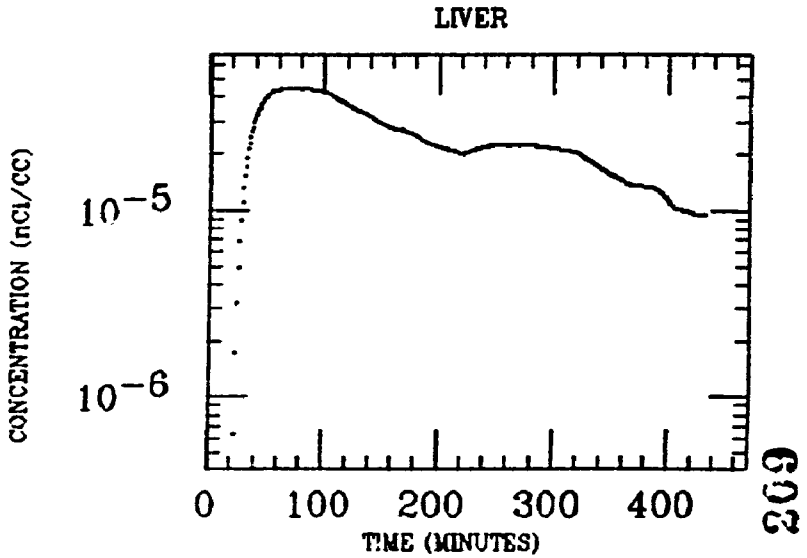

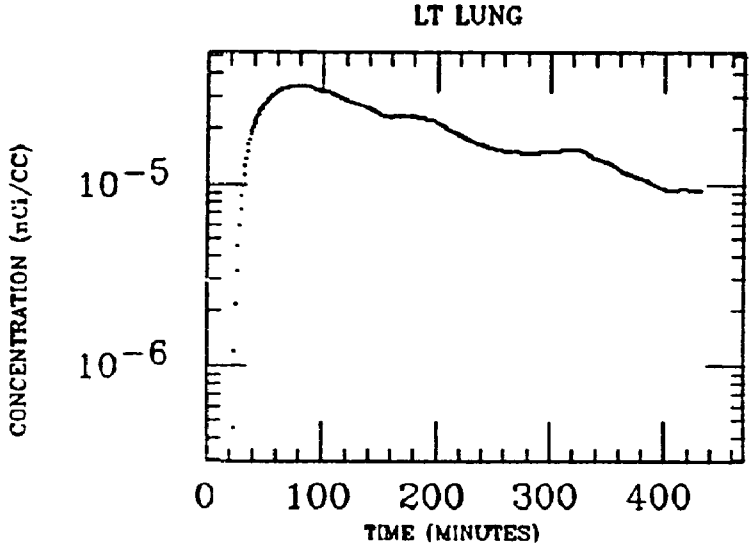

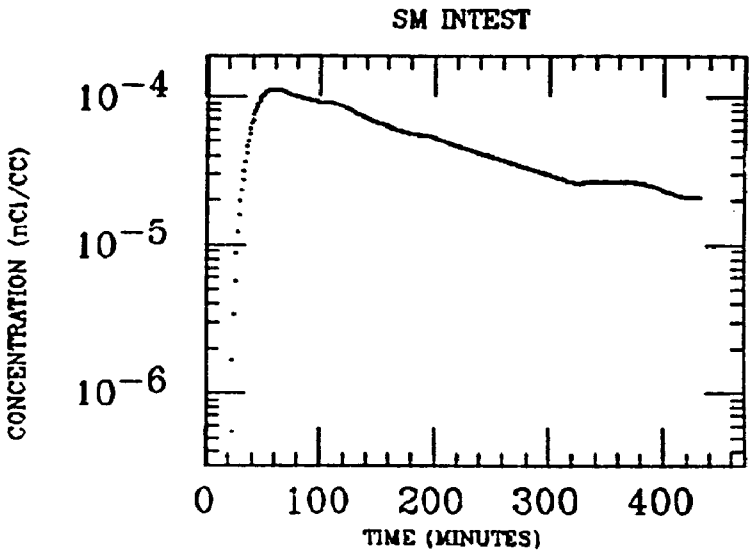

HAND

XE INGESTION

Pb-214

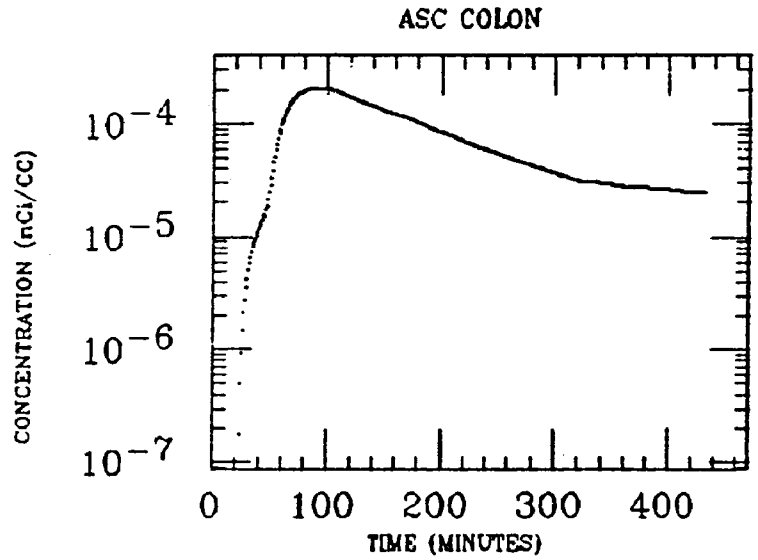

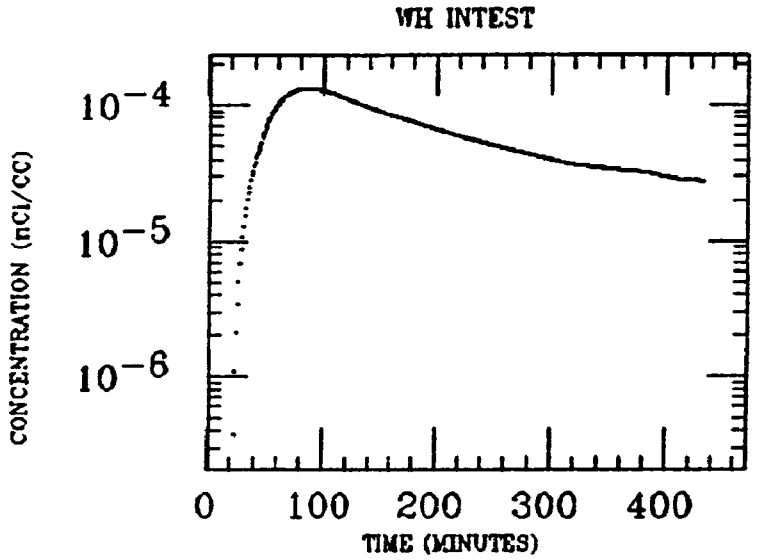

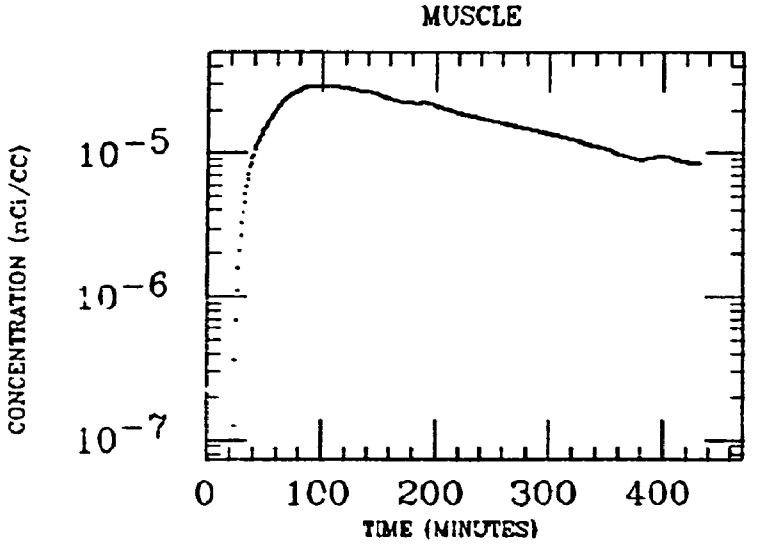

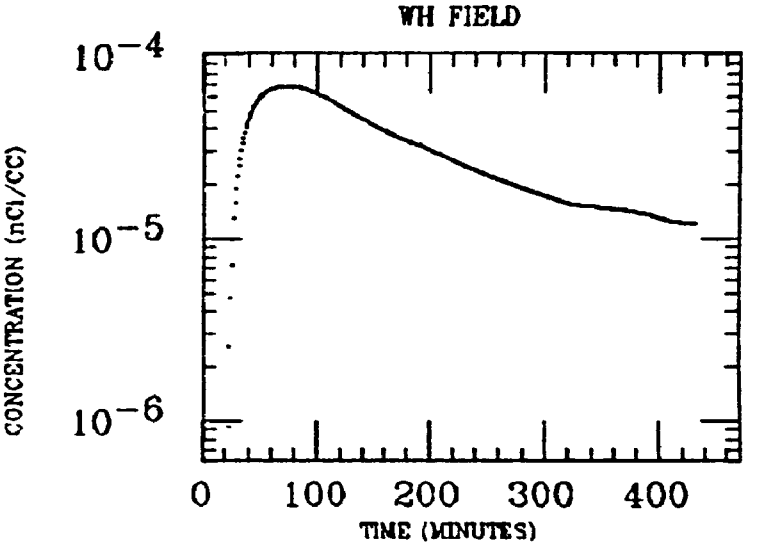

HAWKINS
XE INGESTION
Pb-214

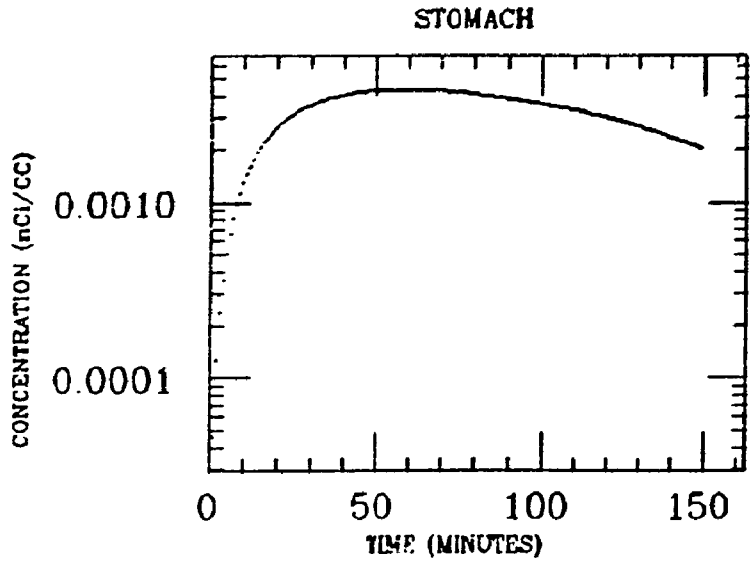

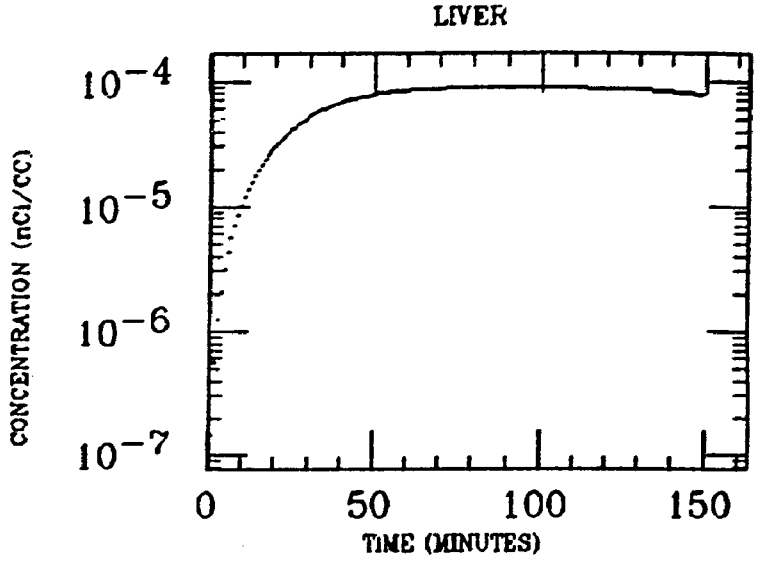

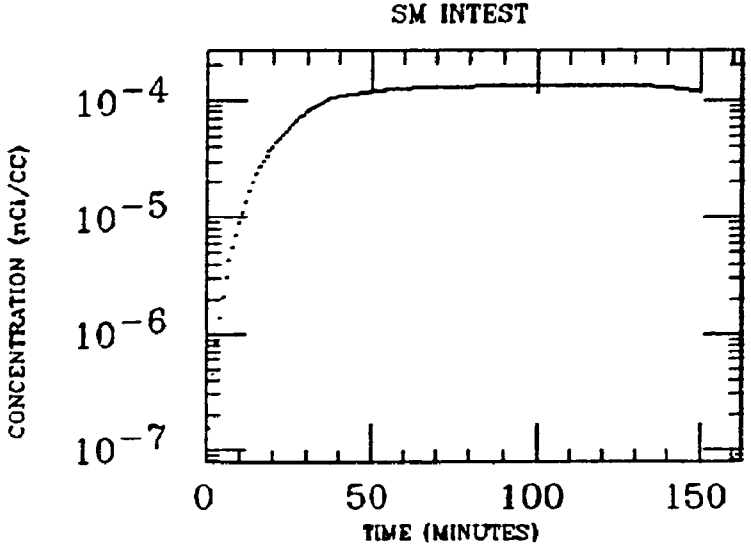

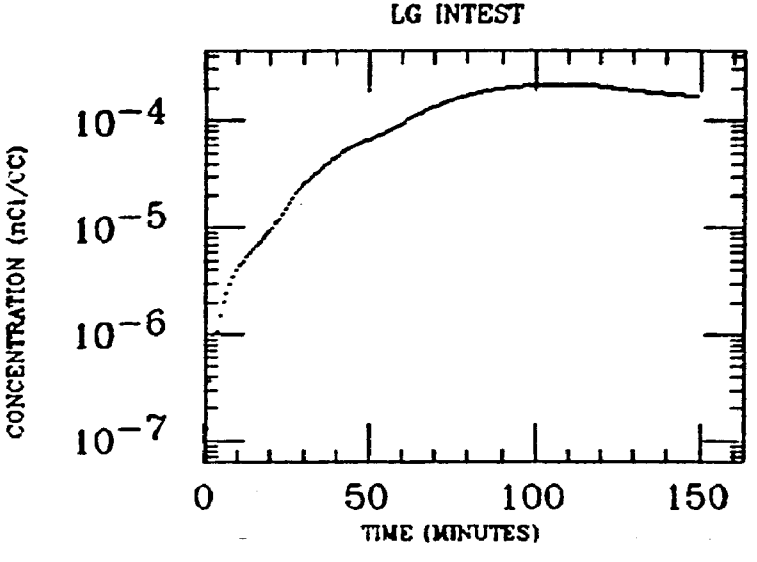

HAWKINS
XE INGESTION
Pb-214

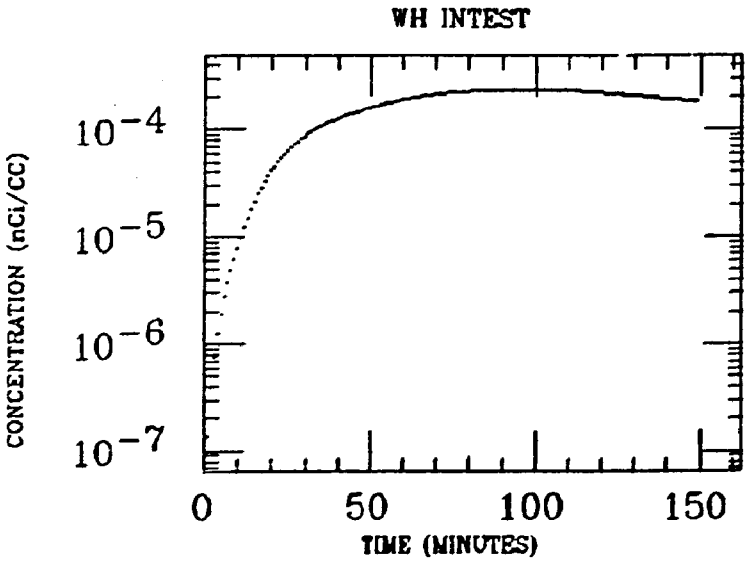

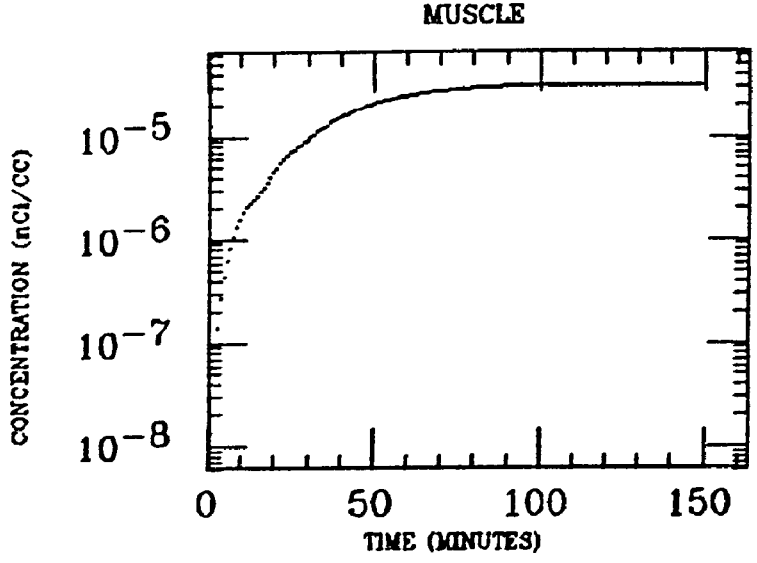

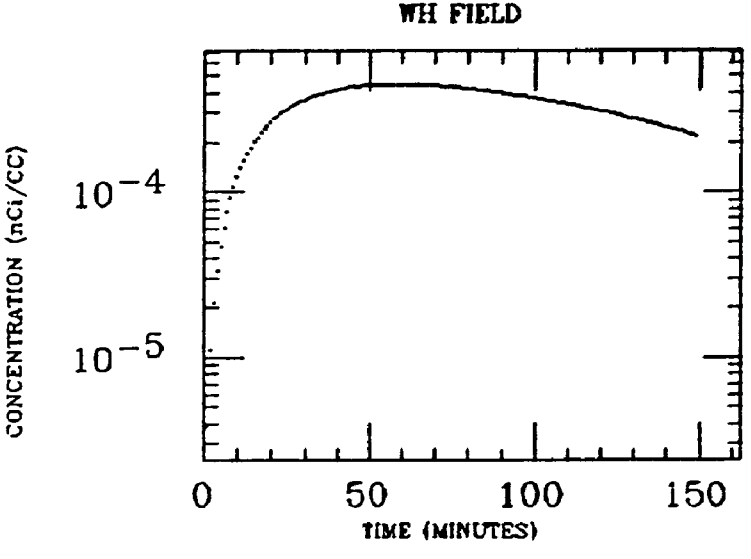

HILL
XE INGESTION
Pb-214

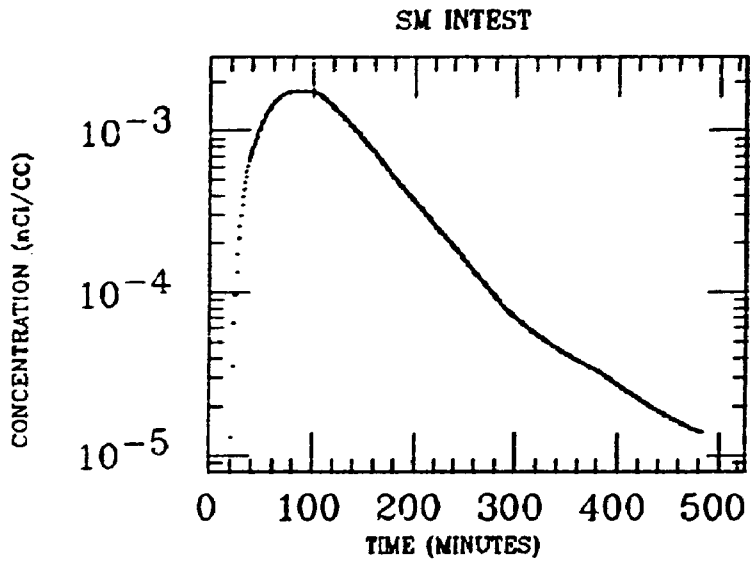

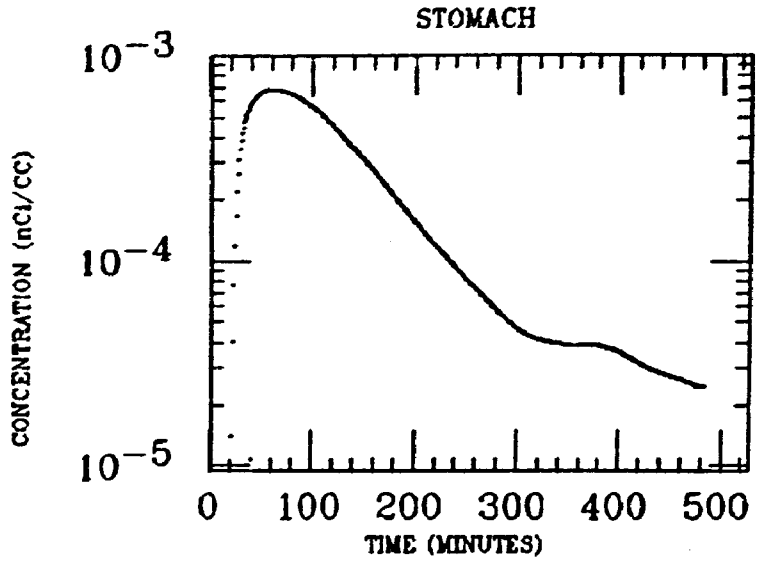

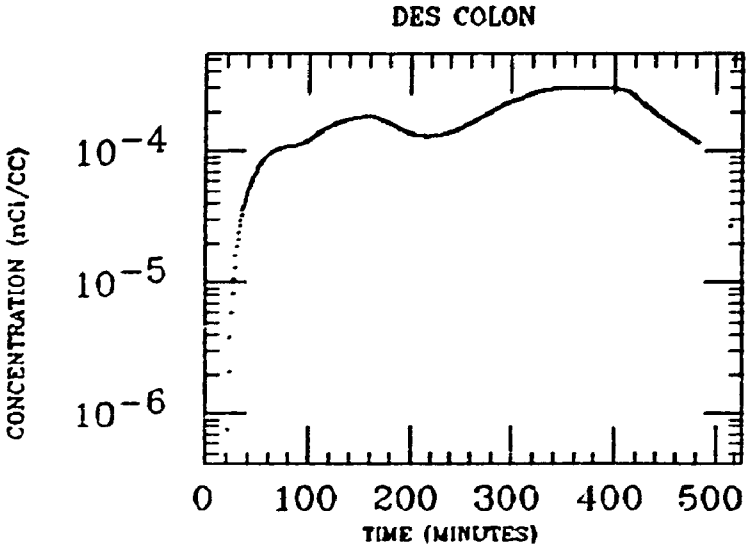

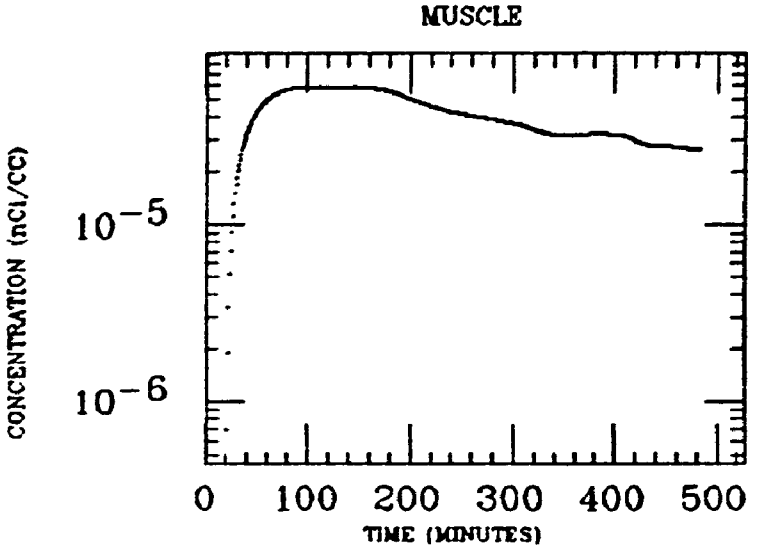

HILL
XE INGESTION
Pb-214

LIVER

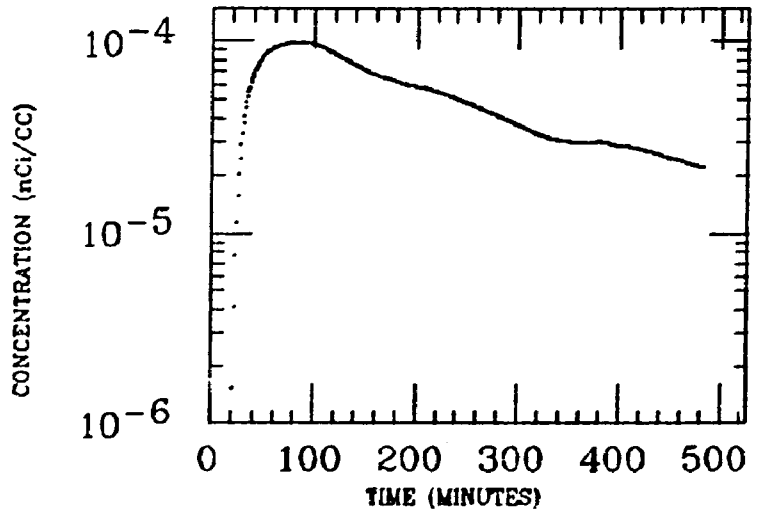

DUODENUM

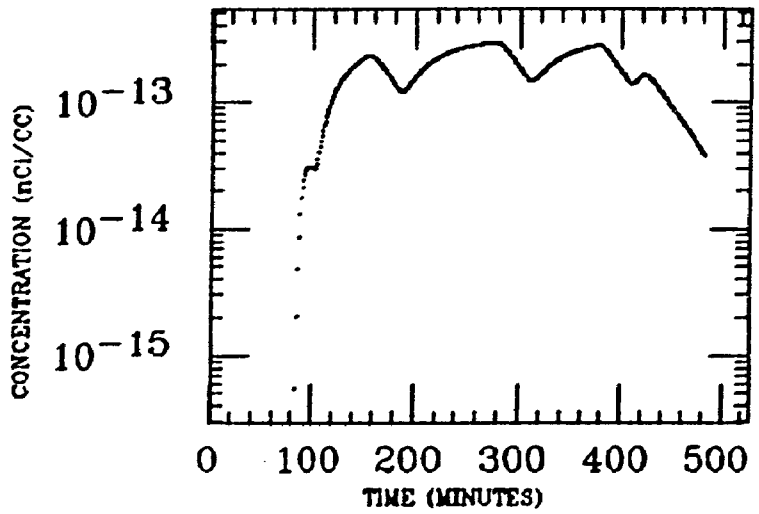

214

LG INTEST

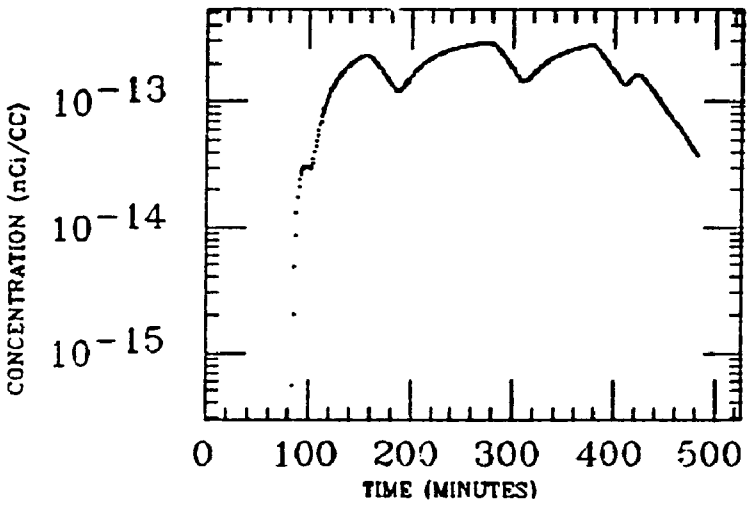

WH FIELD

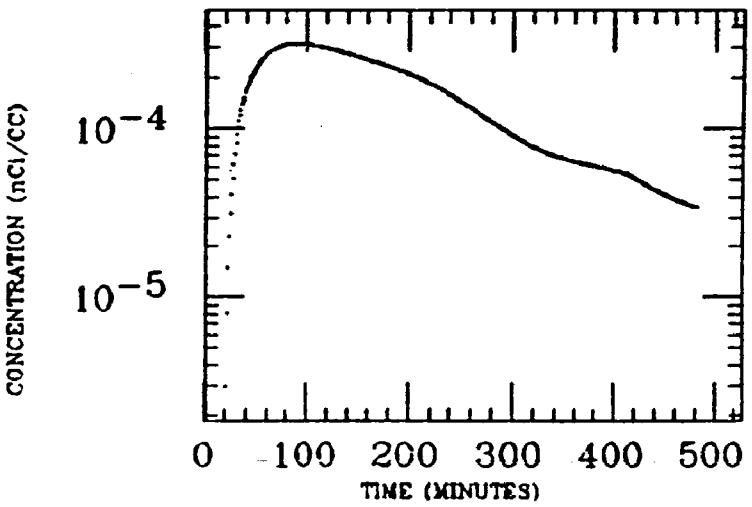

HILL
XE INGESTION
Pb-214

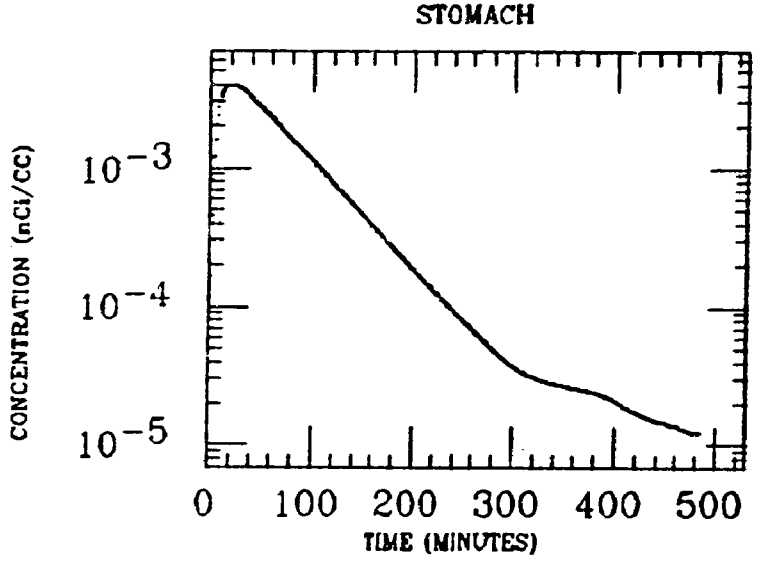

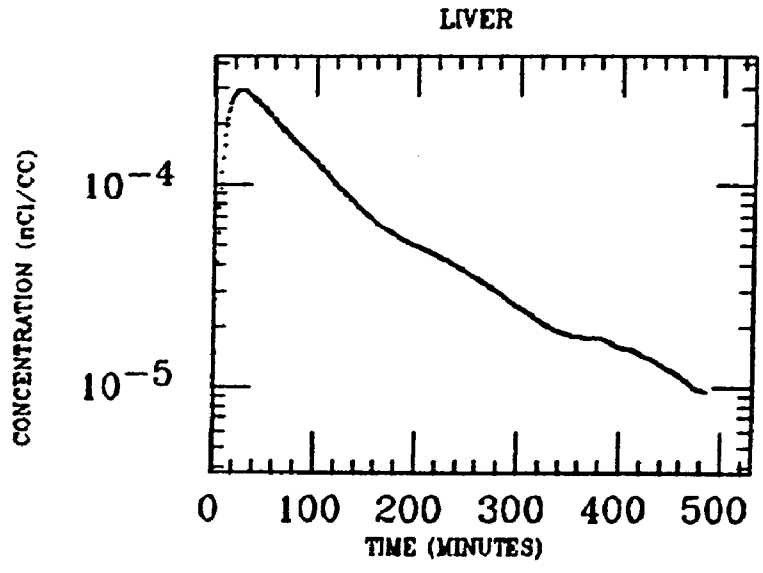

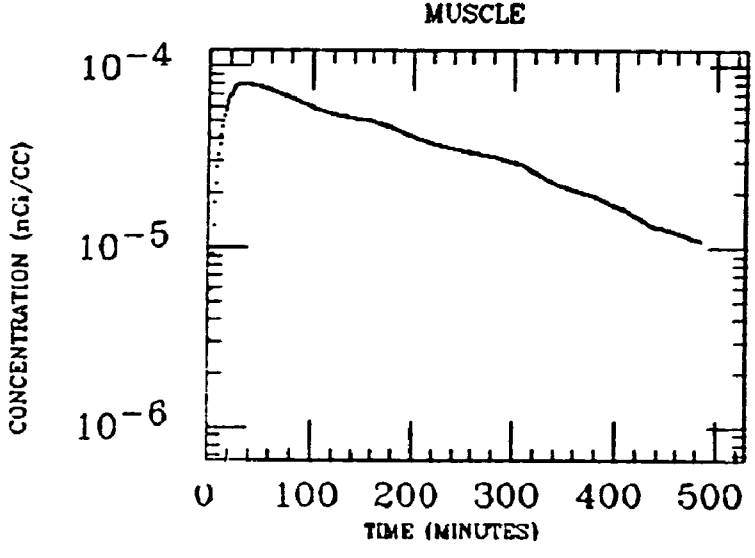

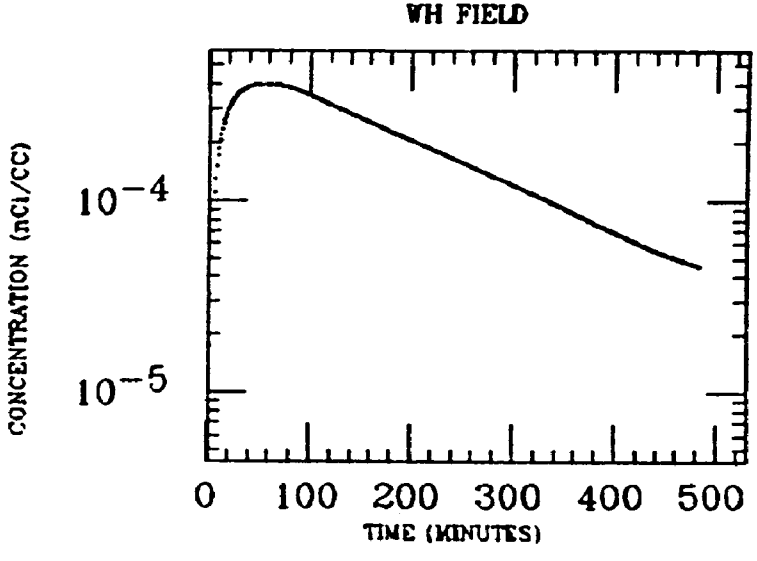

HUTCHINS
XE INGESTION
Pb-214

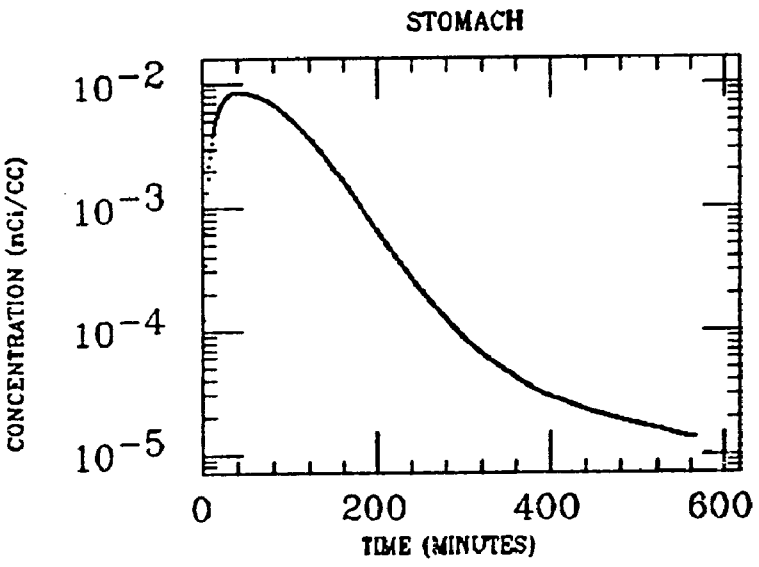

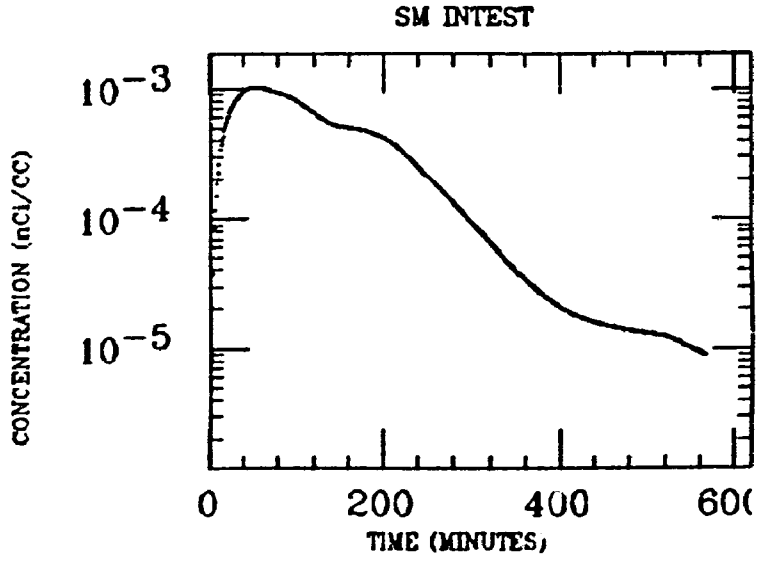

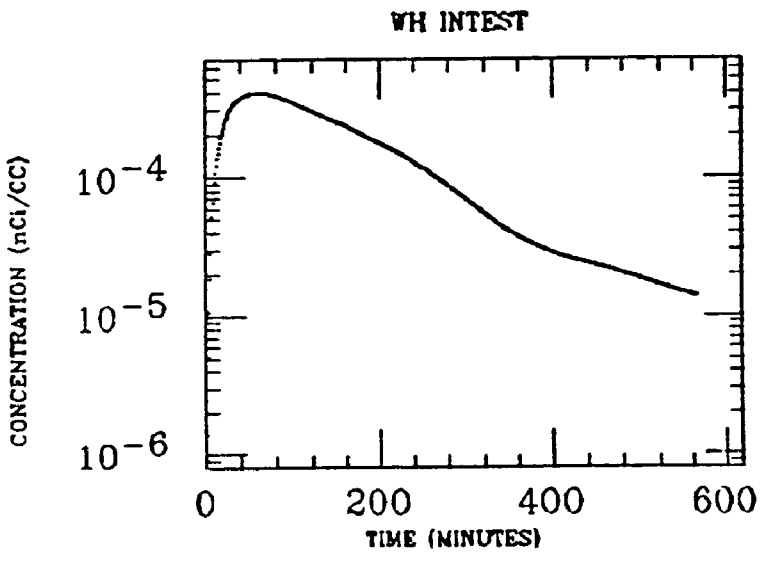

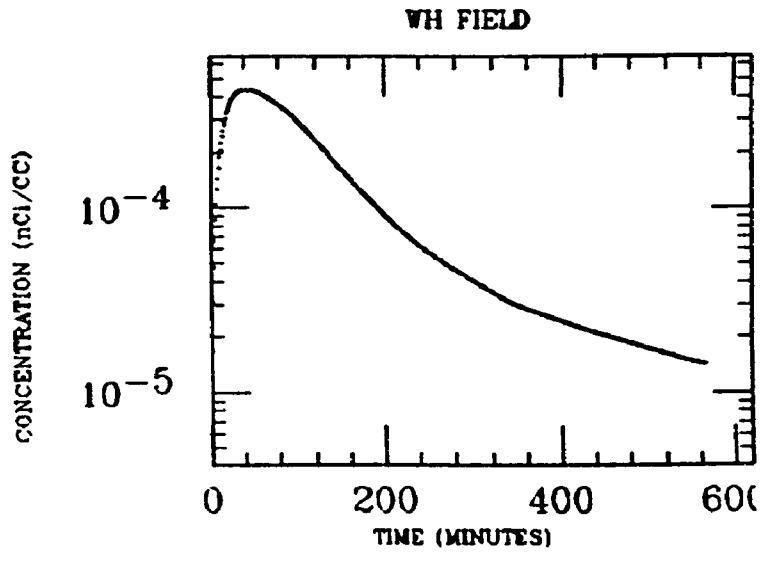

HUTCHINS
XE INGESTION
Pb-214

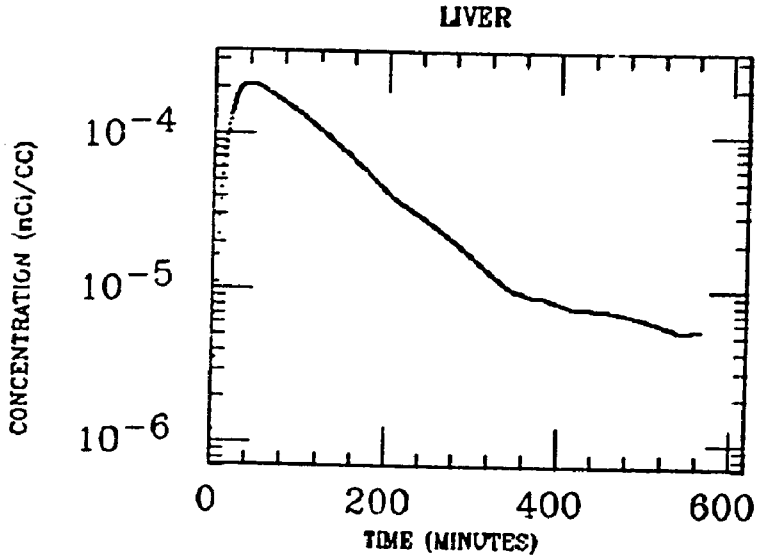

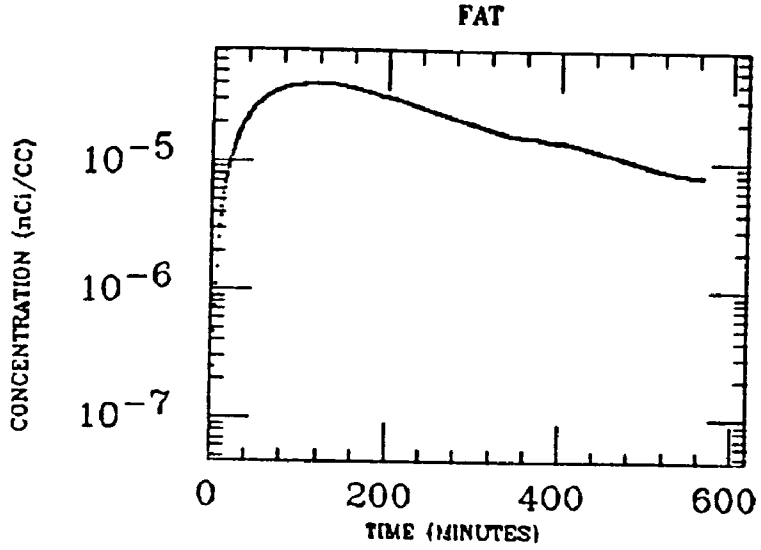

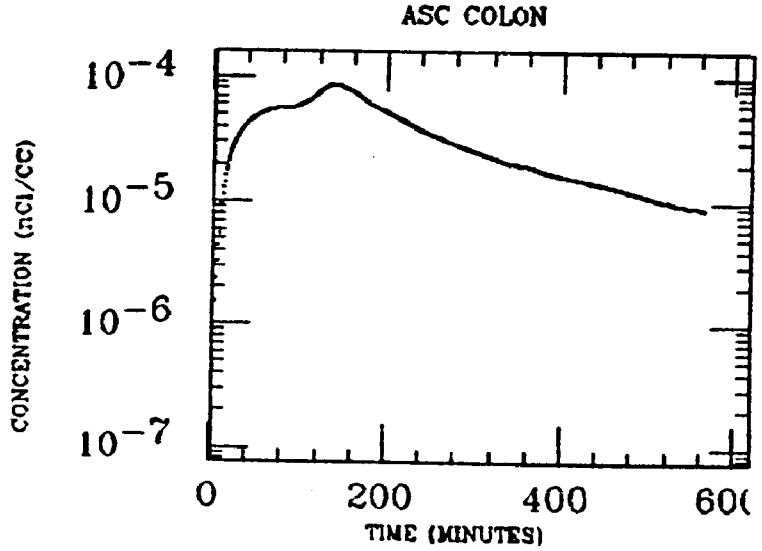

HUTCHINS
XE INGESTION
Pb-214

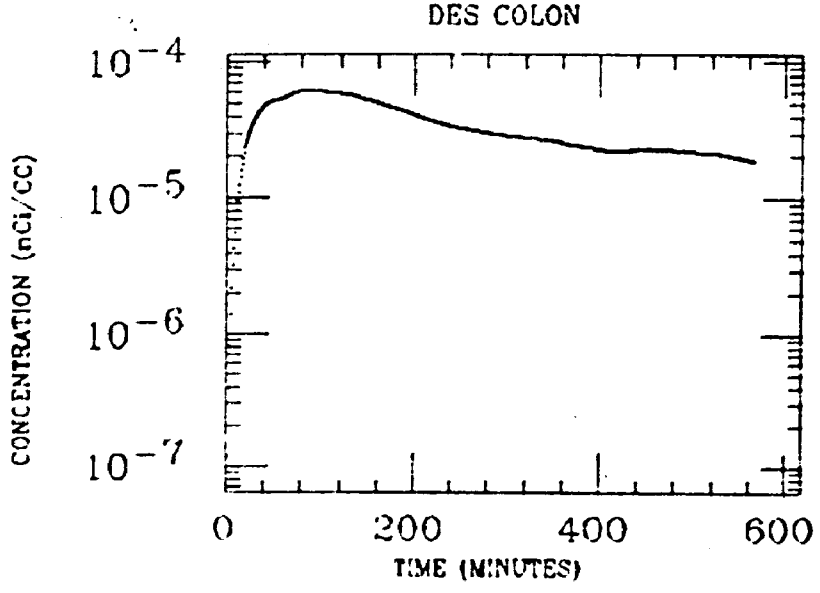

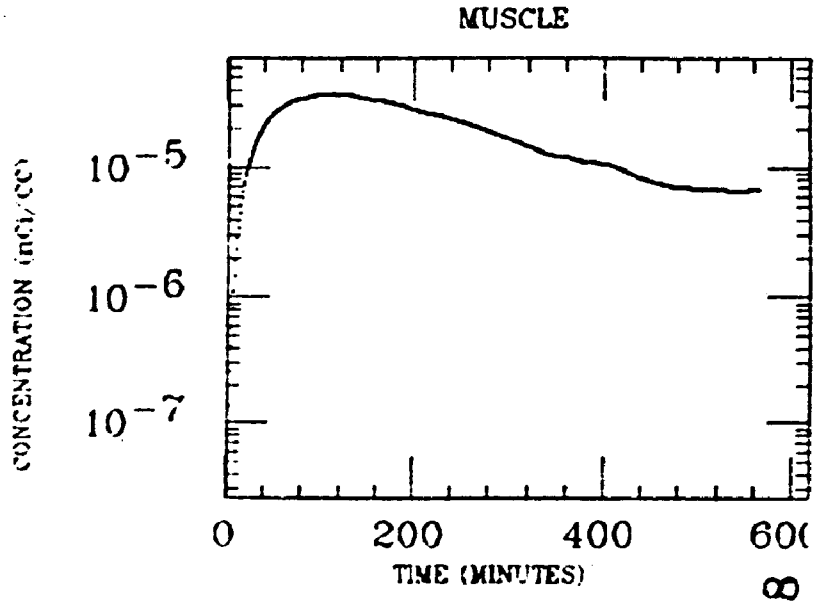

J.MCKINLEY
XE INGESTION
Pb-214

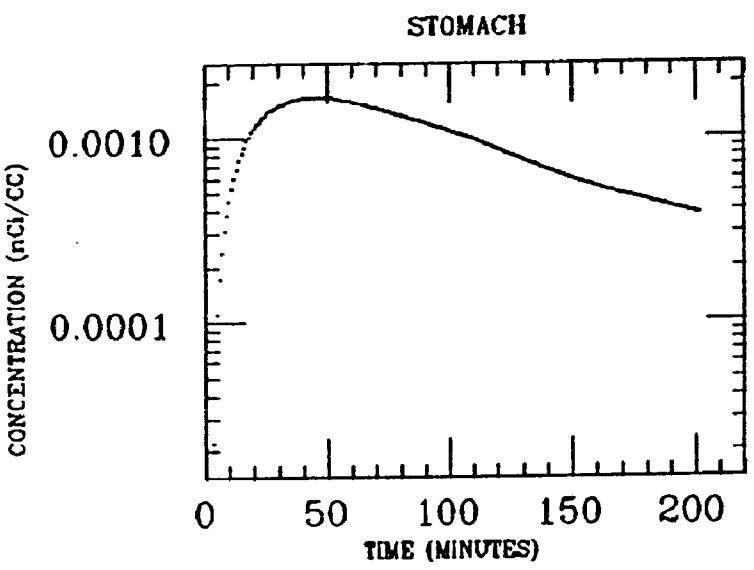

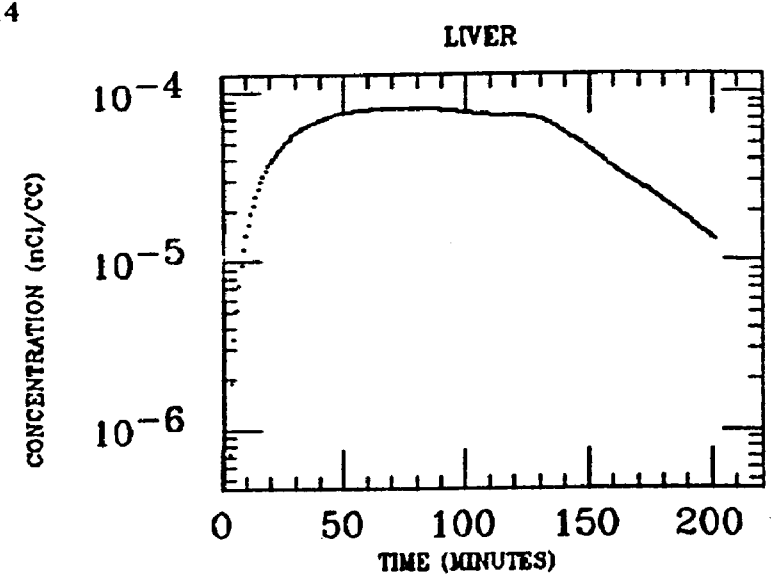

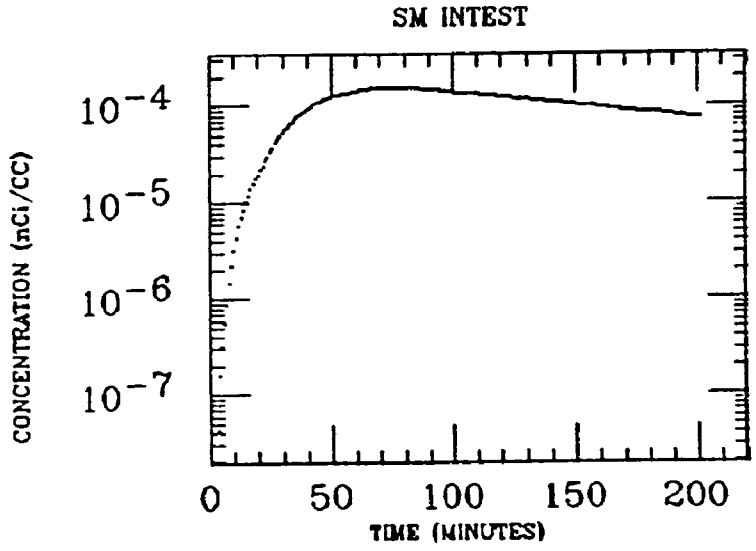

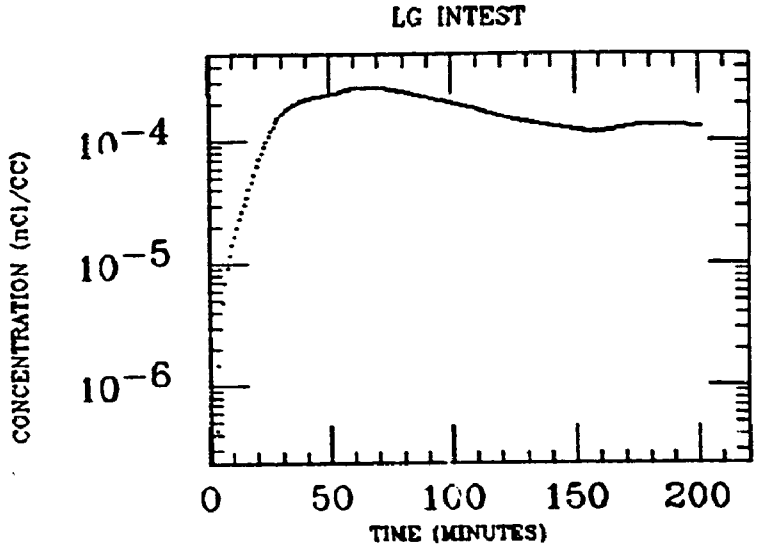

J.MCKINLEY
XE INGESTION
Pb-214

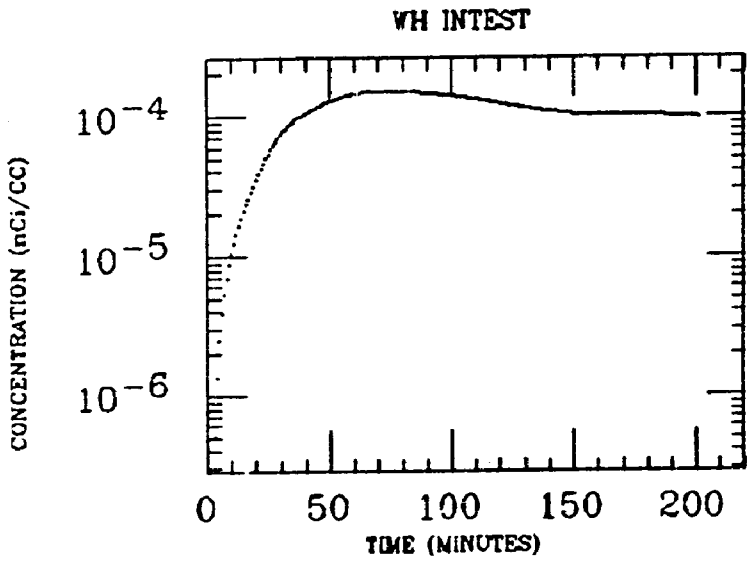

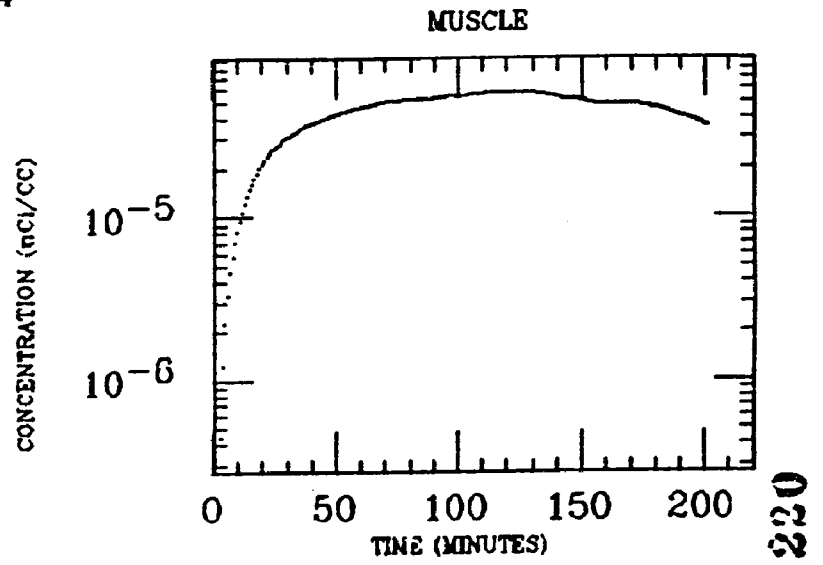

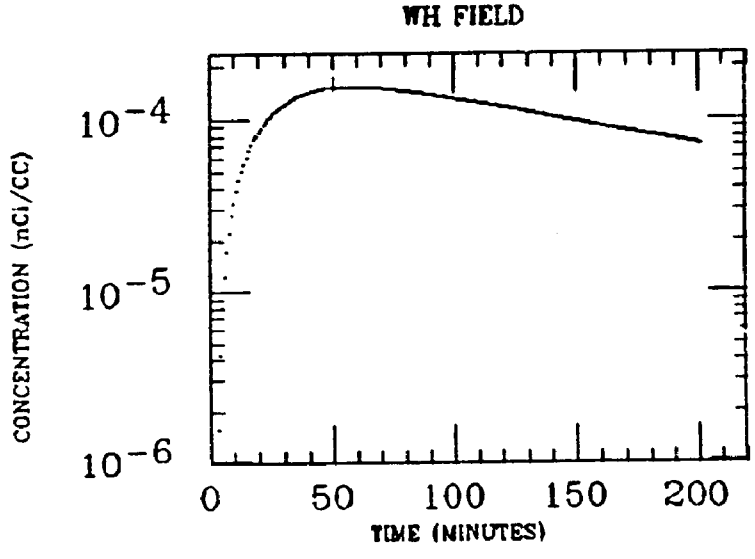

KELLEHER
XE INGESTION
Pb-214

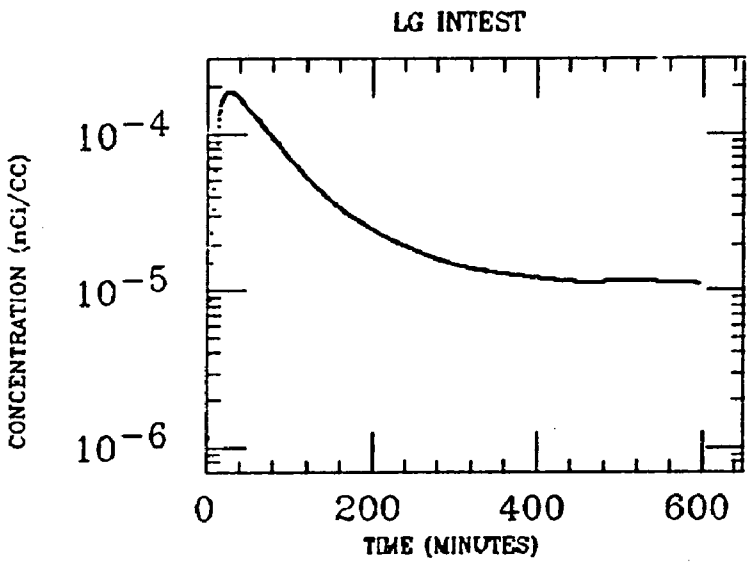

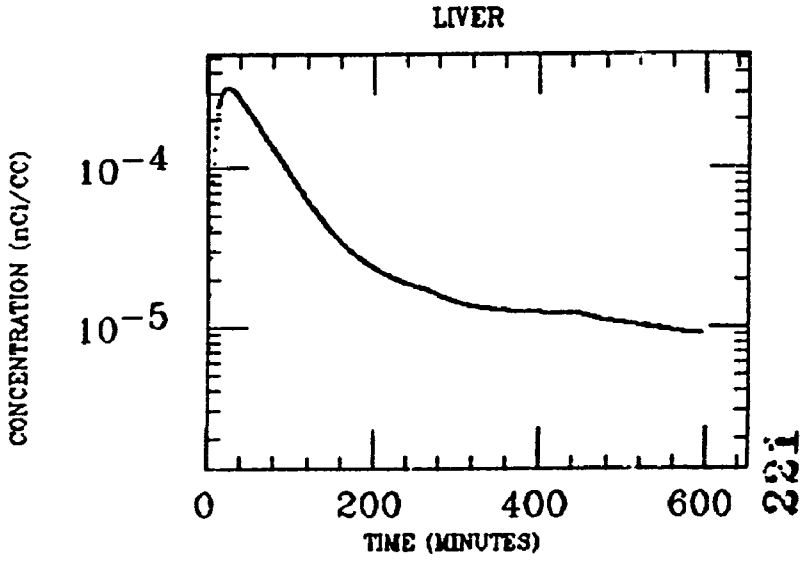

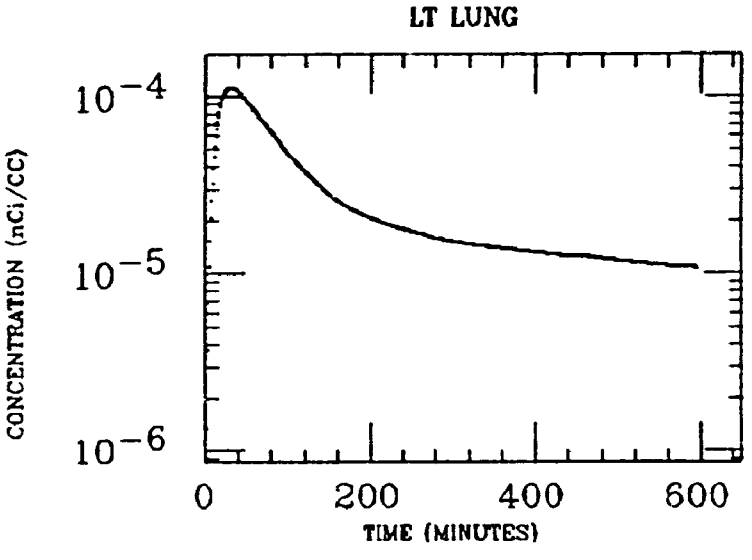

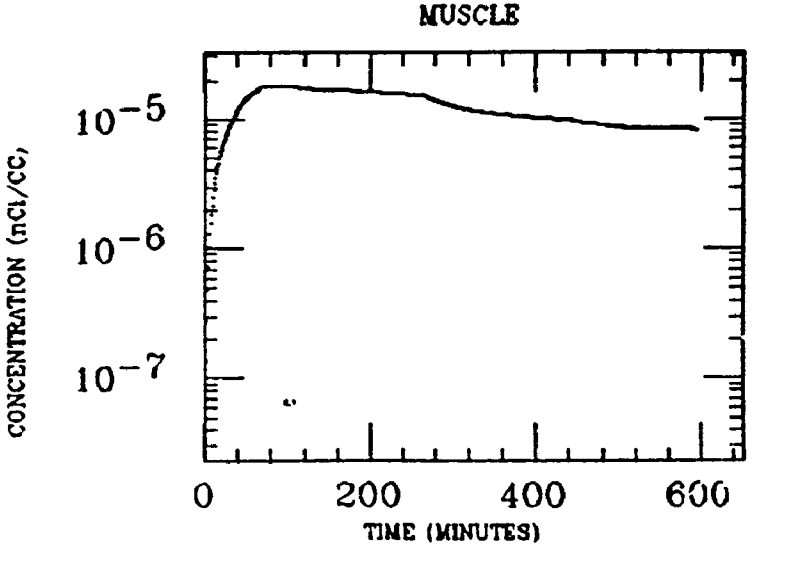

KELLEHER
XE INGESTION
Pb-214

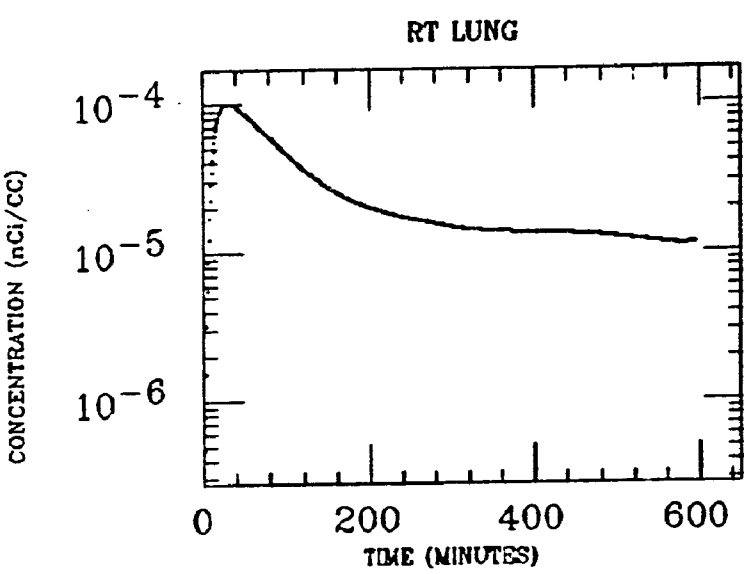

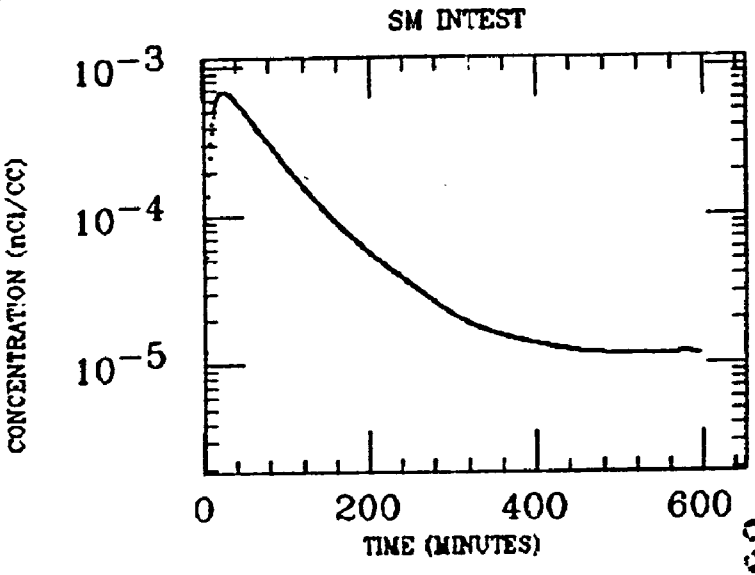

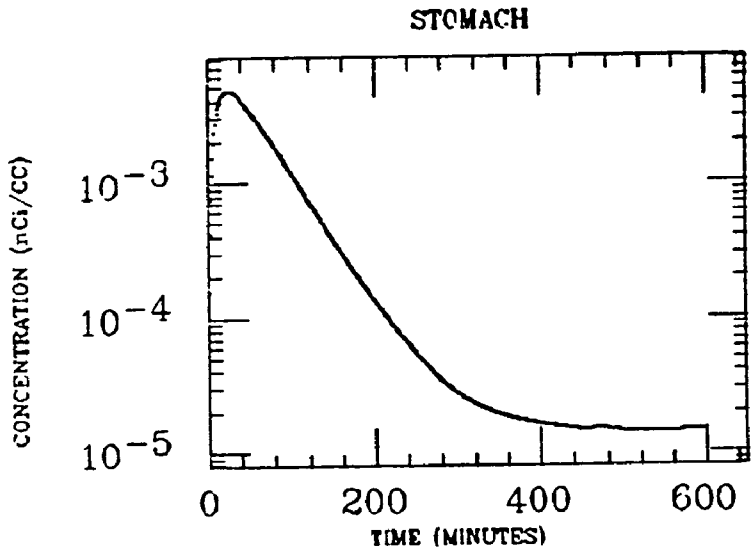

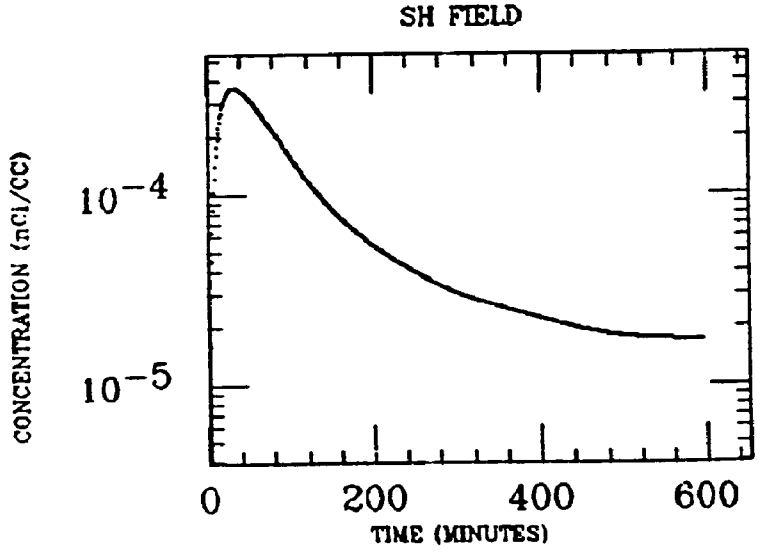

LITTELL
XE INGESTION
Pb-214

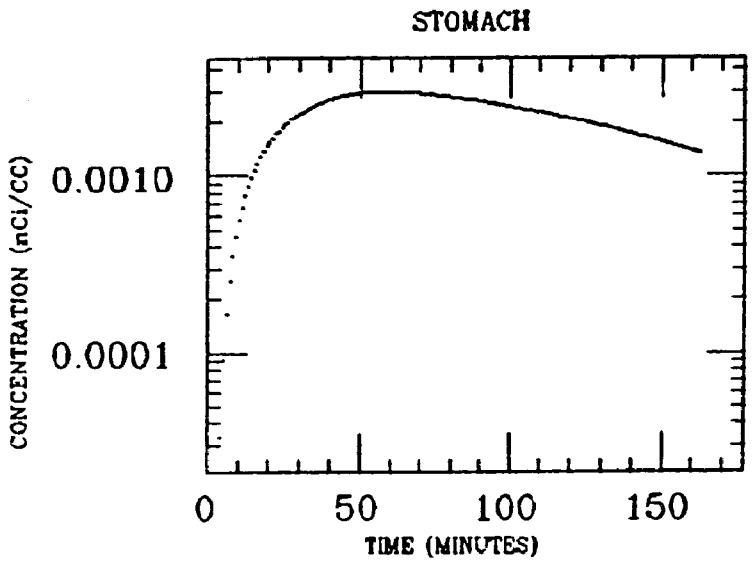

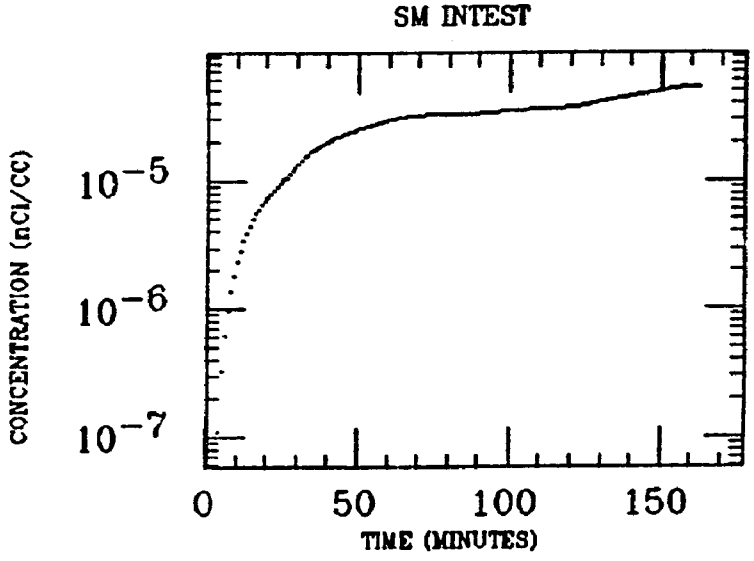

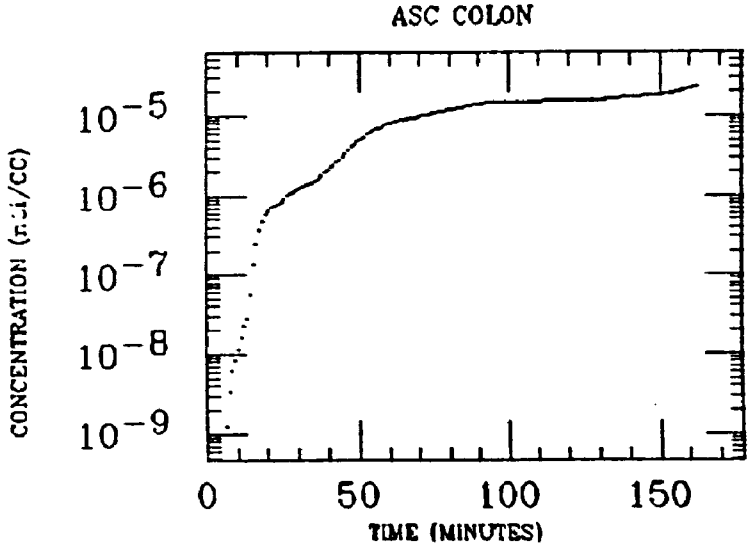

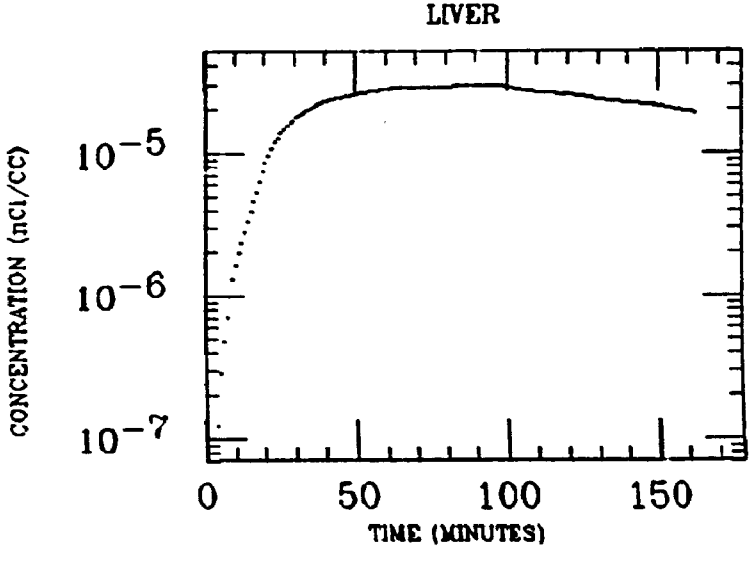

LITTELL
XE INGESTION
Pb-214

MUSCLE

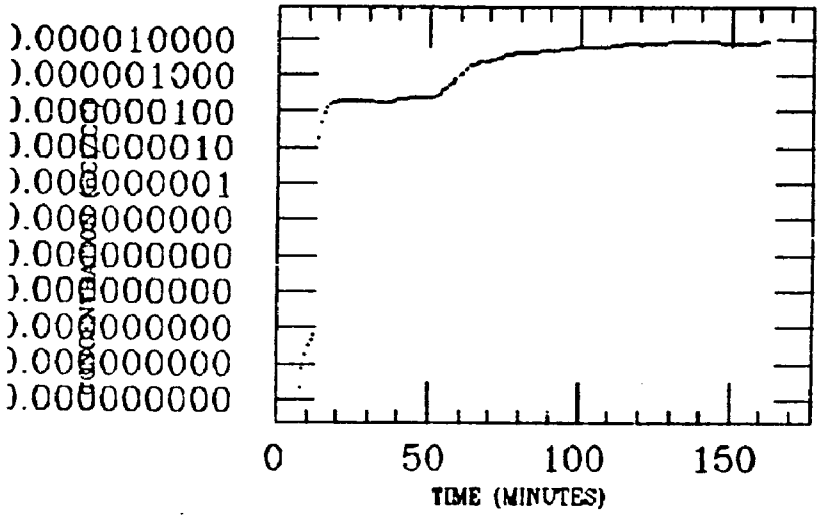

WH INTEST

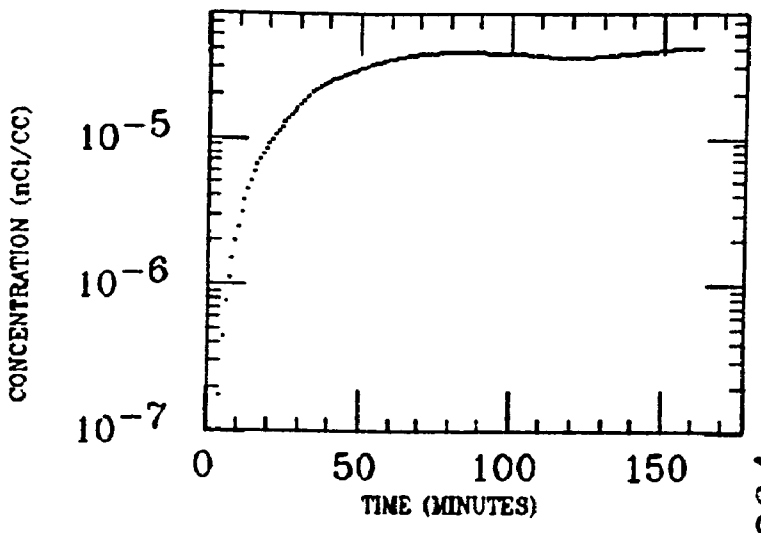

WH FIELD

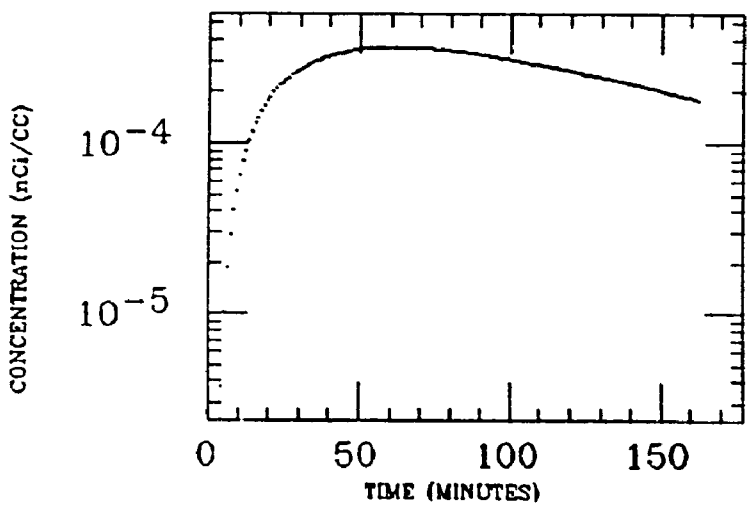

MACMILLAN
XE INGESTION
Pb-214

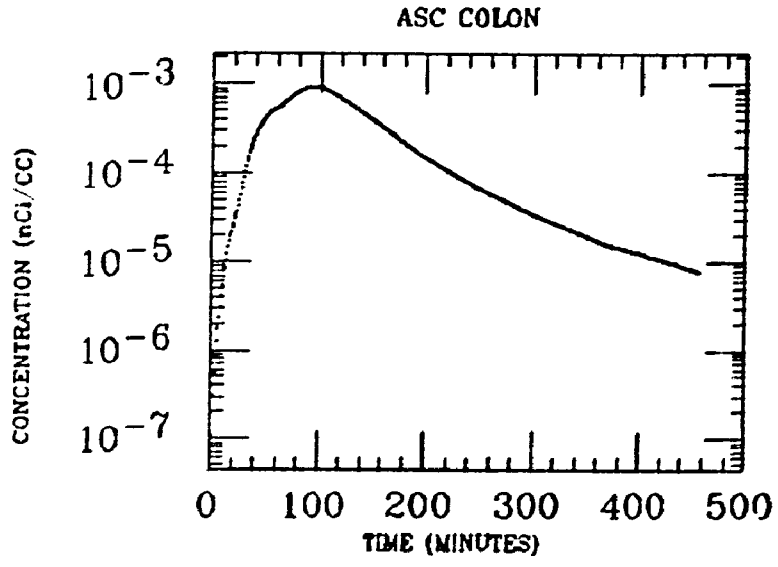

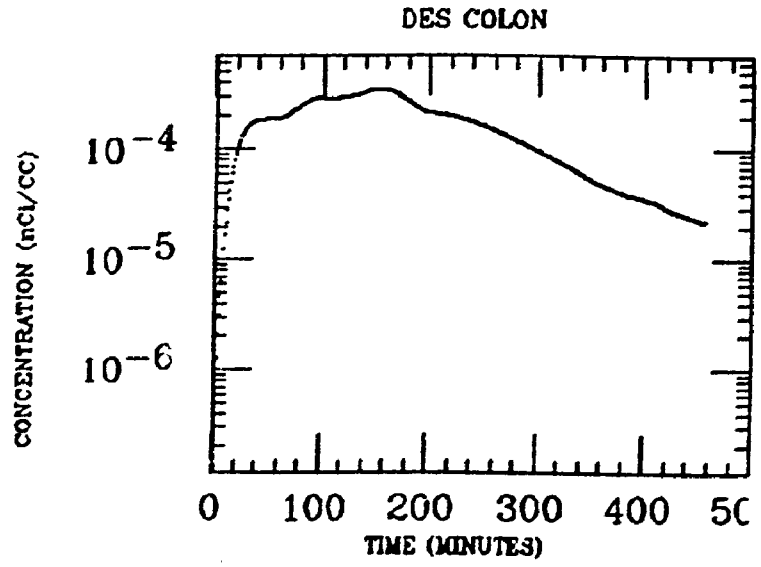

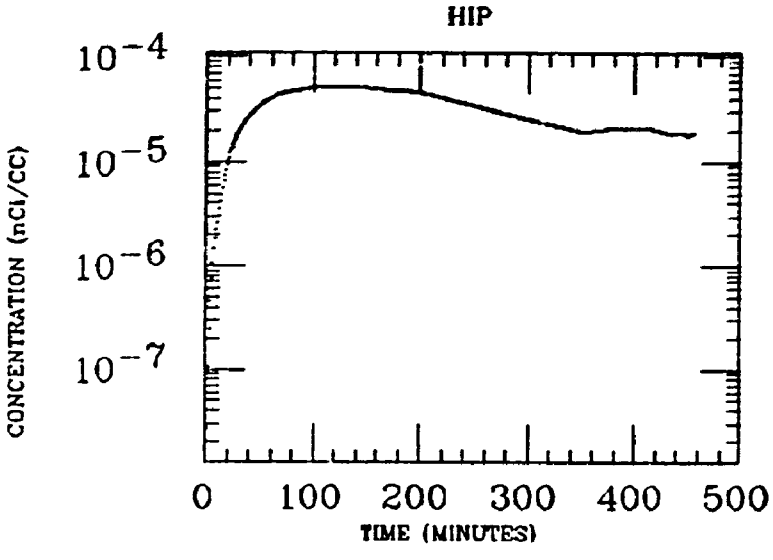

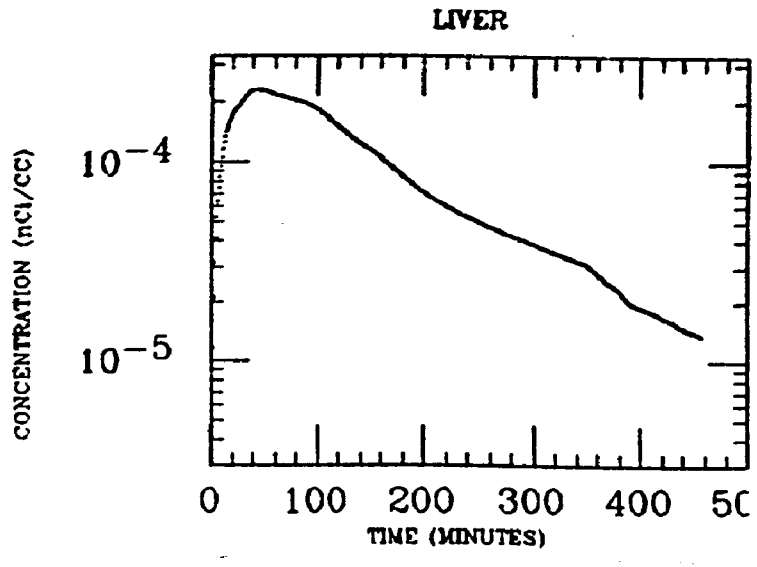

MACMILLAN
XE INGESTION
Pb-214

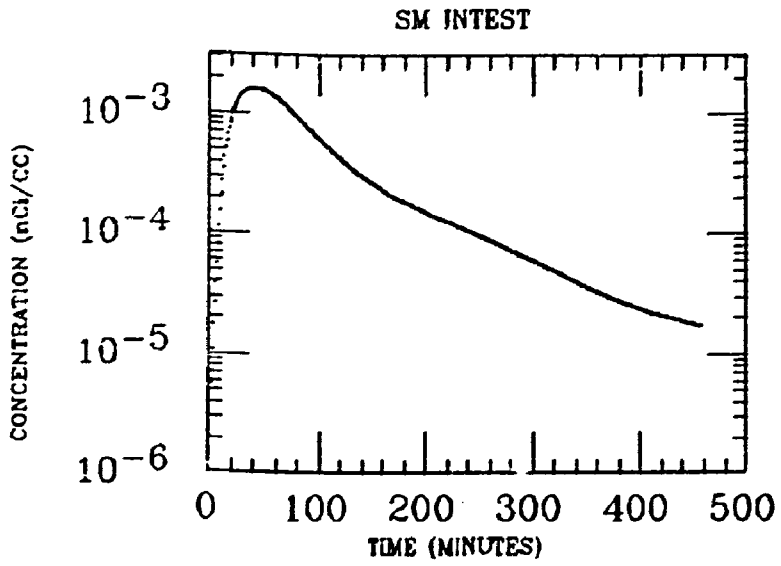

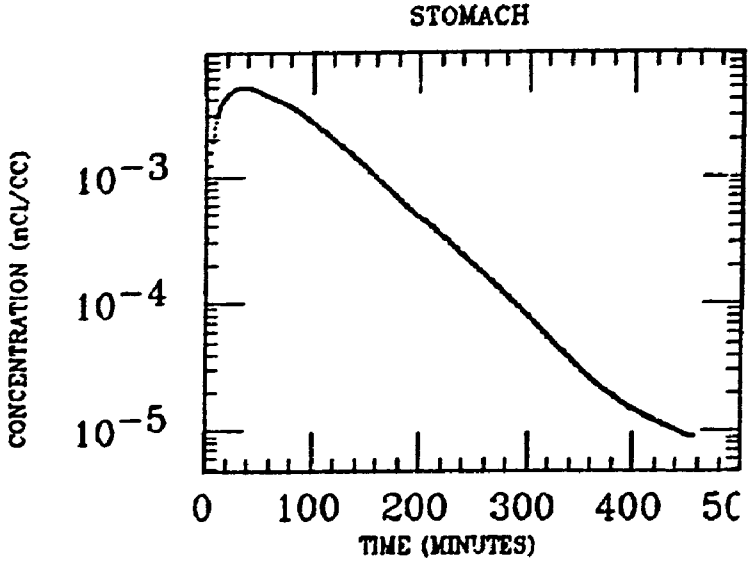

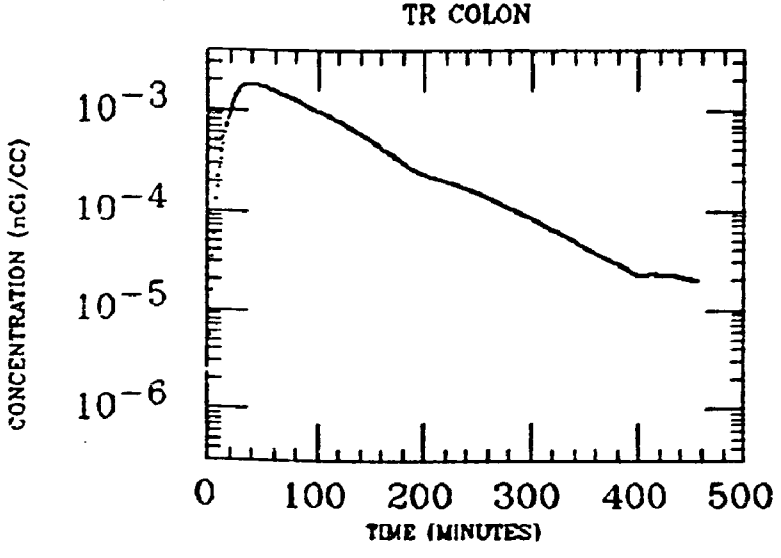

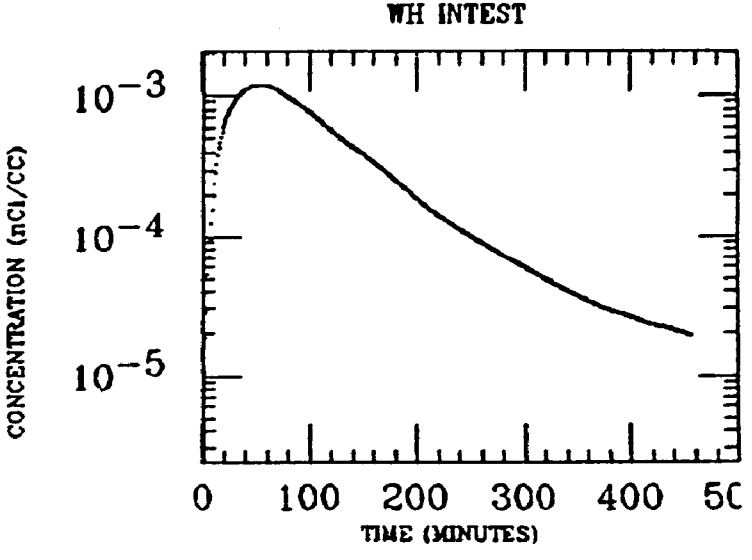

MAIO
XE INGESTION
Pb-214

STOMACH

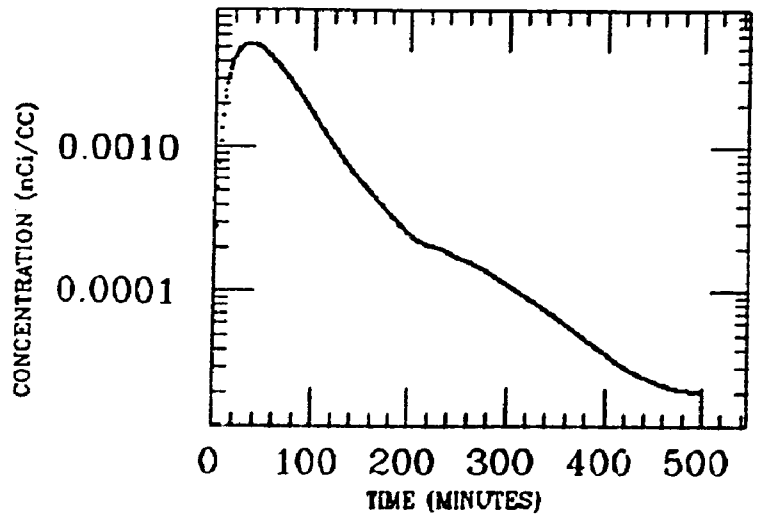

LIVER

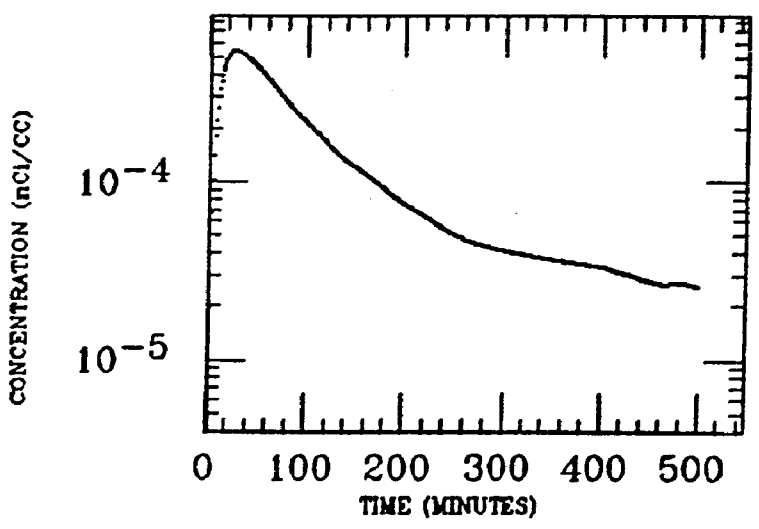

SM INTEST

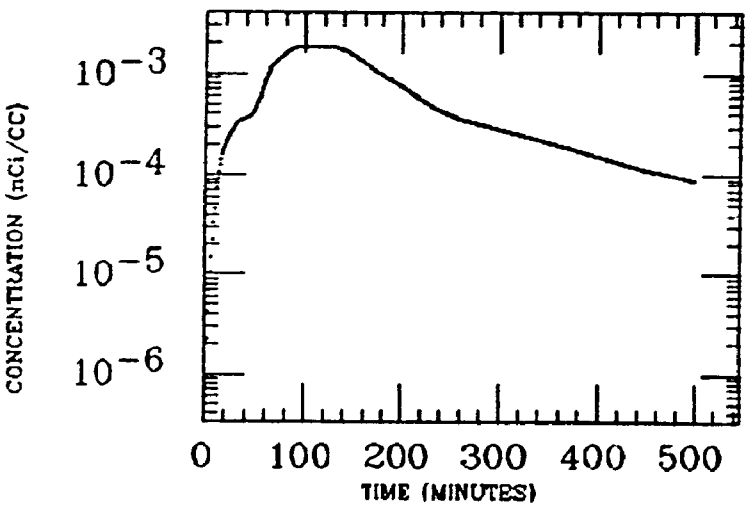

LG INTEST

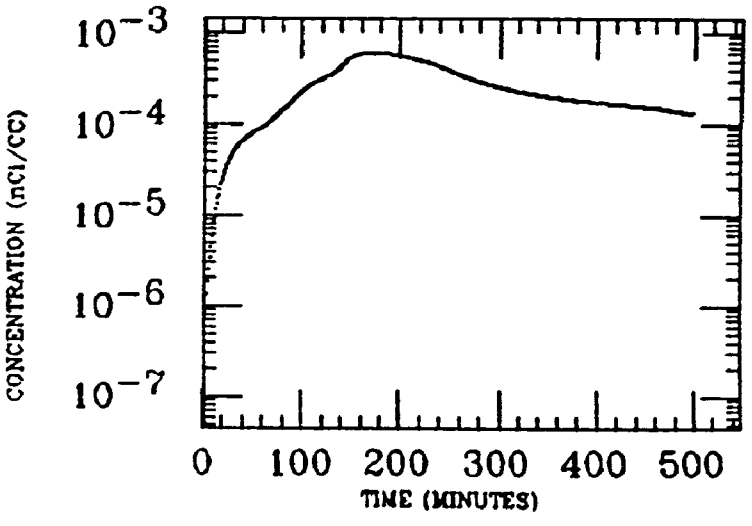

227

MAIO
XE INGESTION
Pb-214

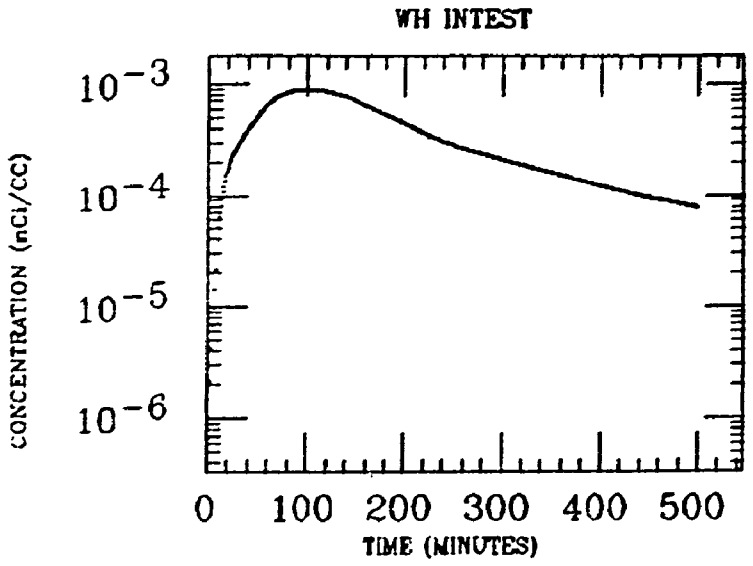

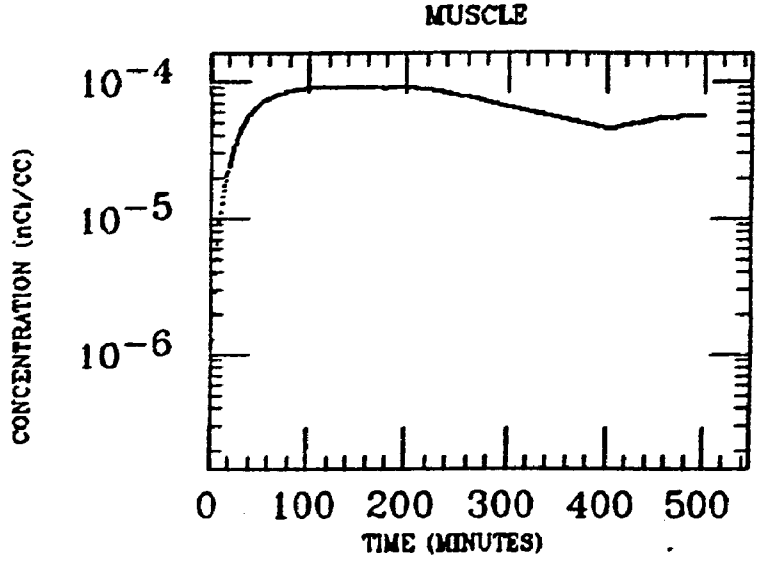

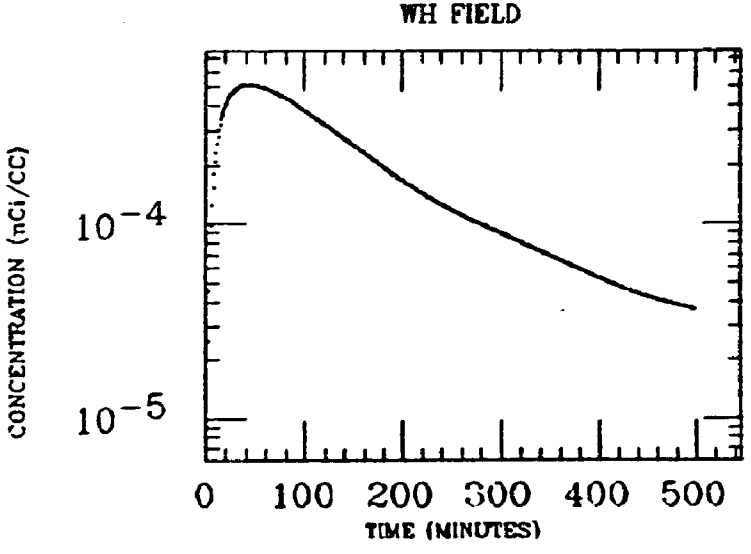

228

MALCOM
XE INGESTION
Pb-214

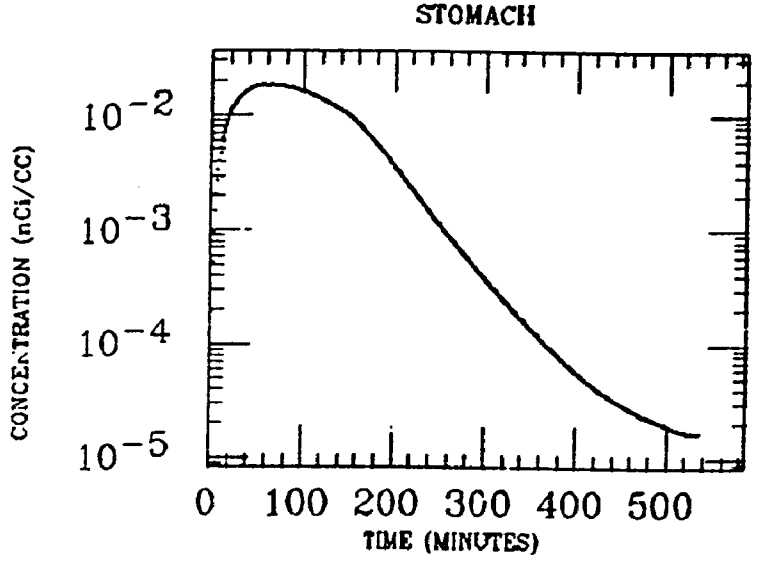

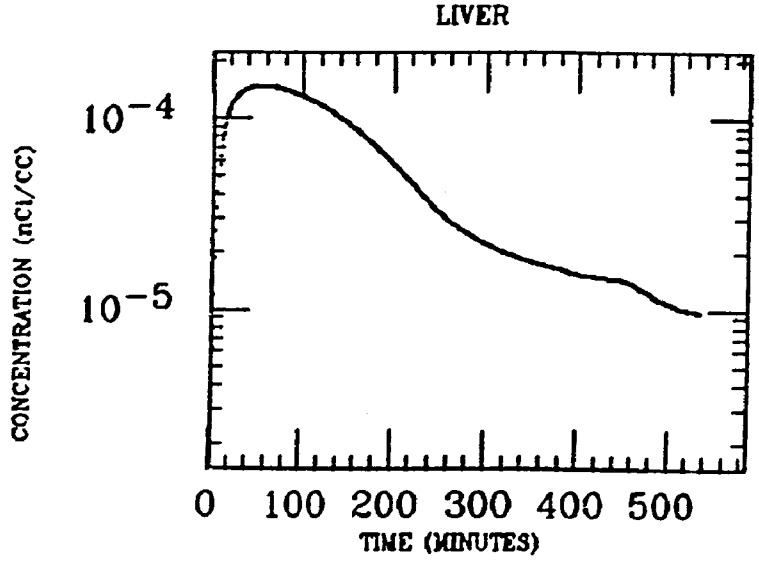

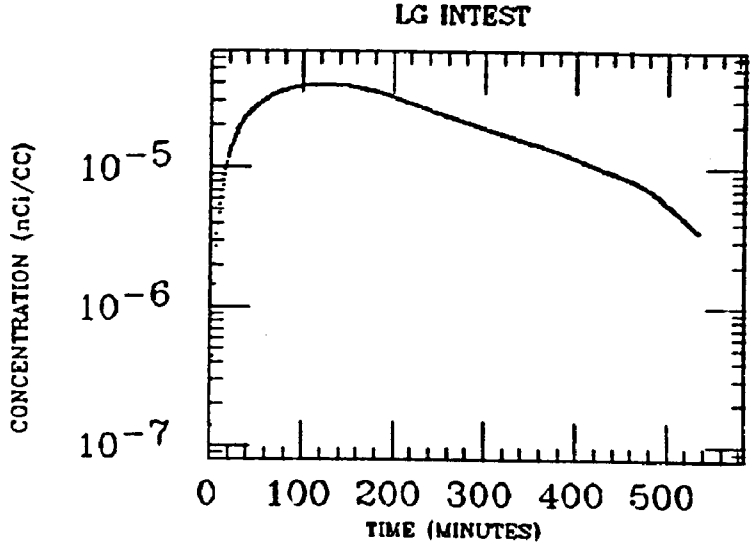

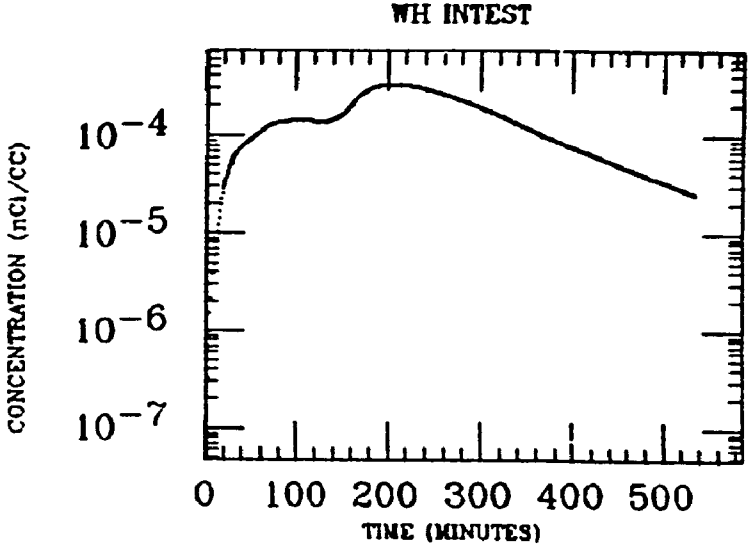

MALCOM
XE INGESTION
Pb-214

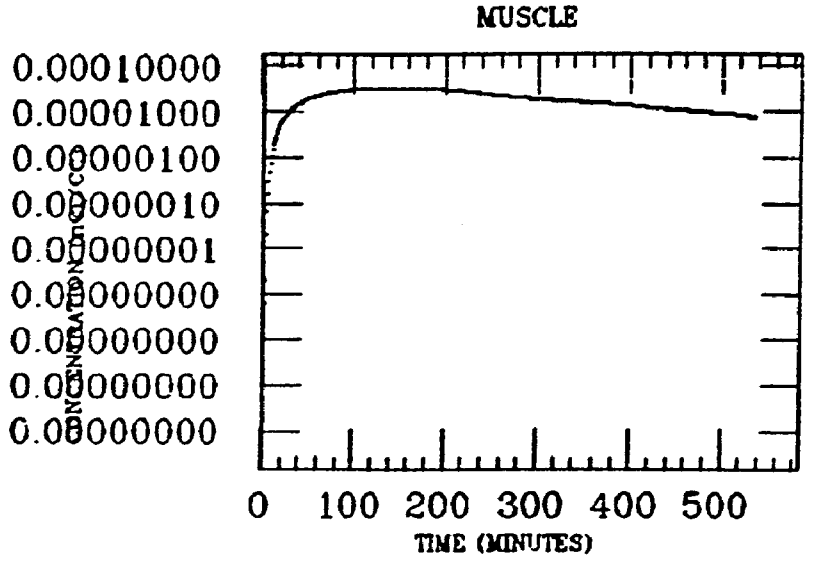

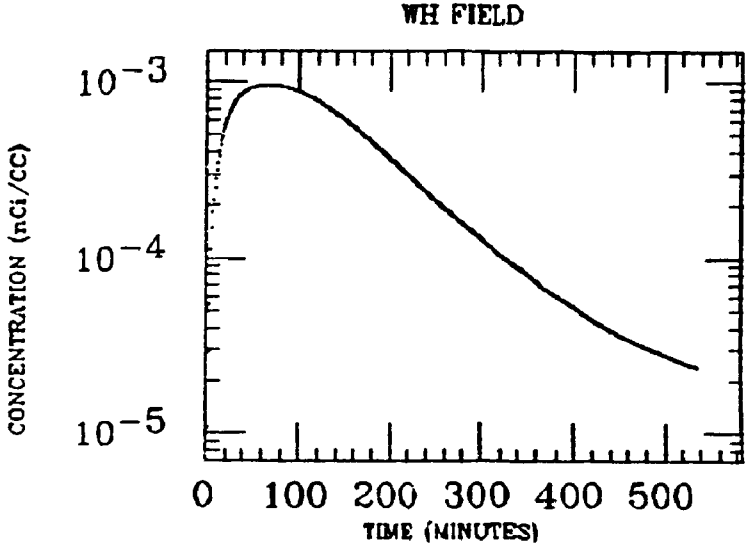

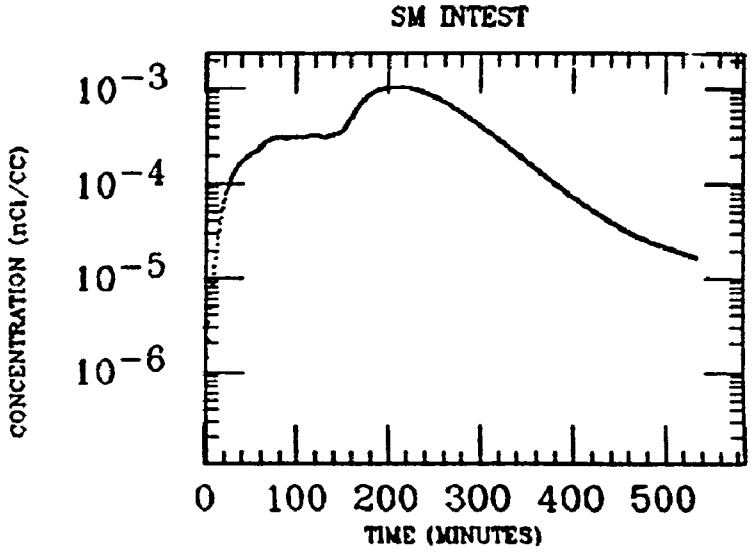

MONROE
XE INGESTION
Pb-214

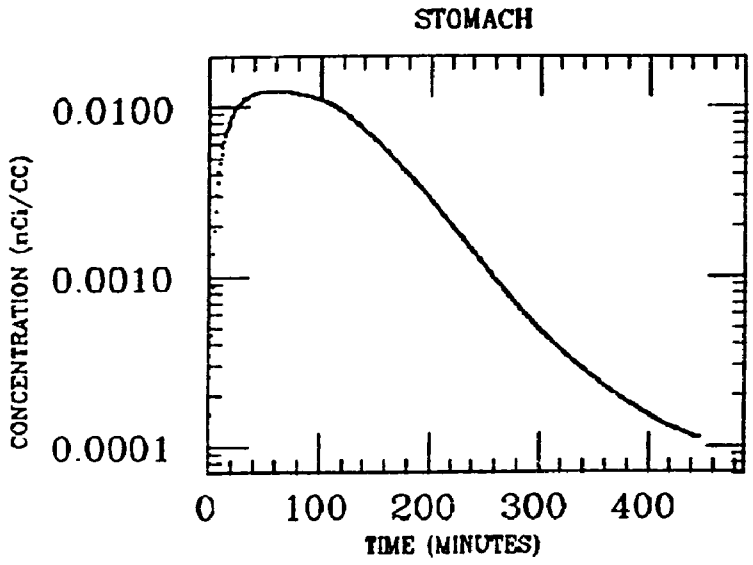

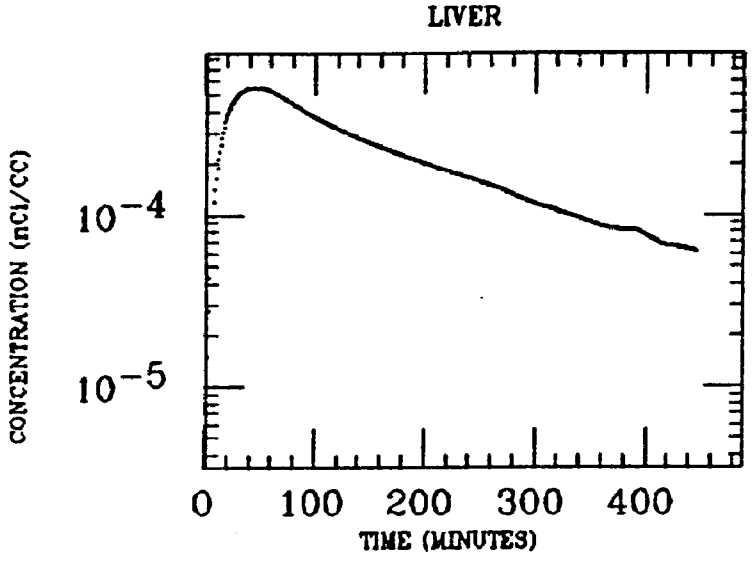

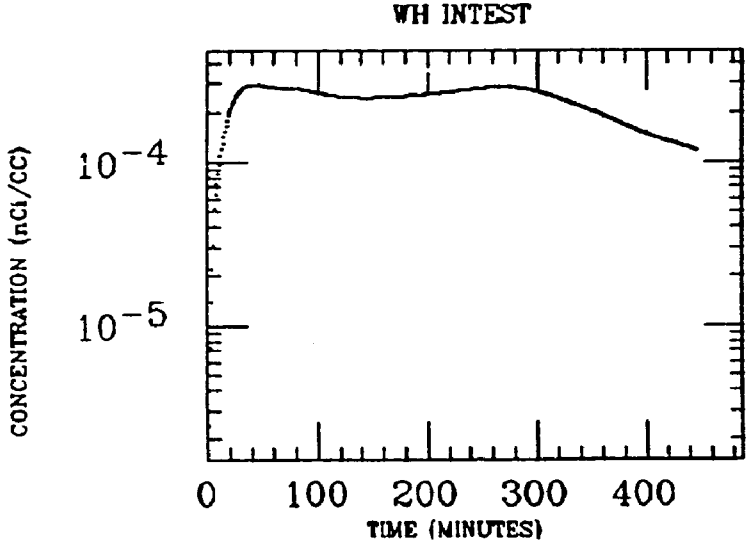

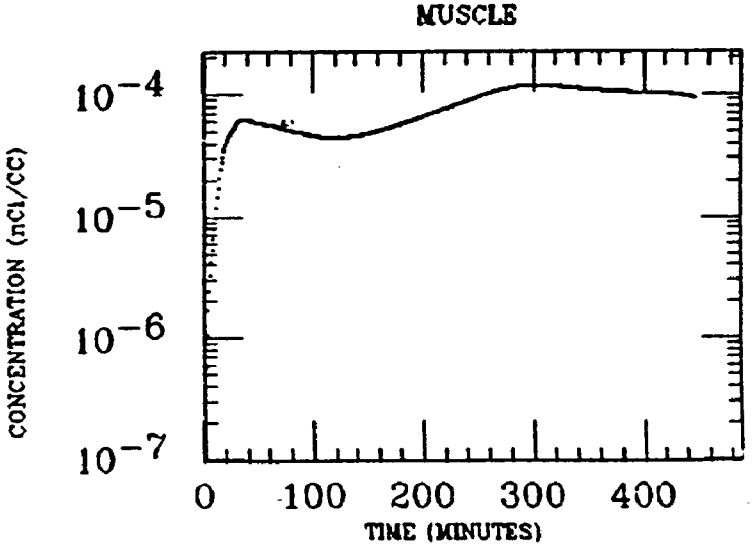

MONROE
XE INGESTION
Pb-214

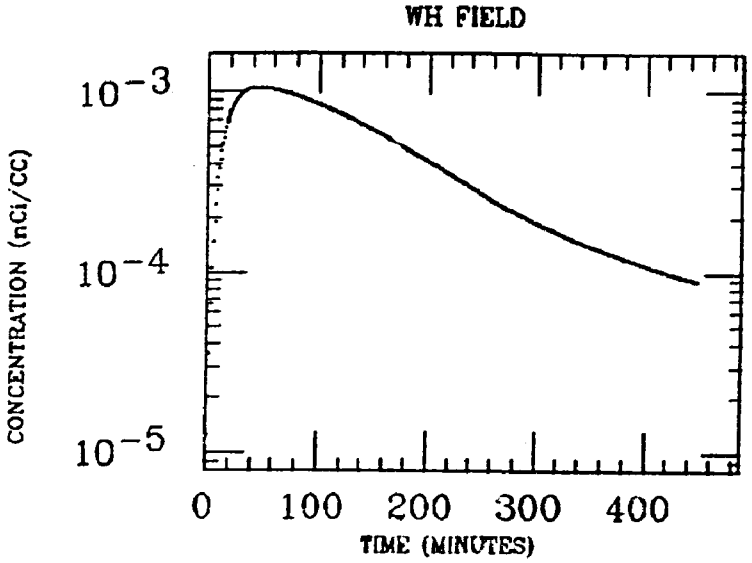

MORGAN
XE INGESTION
Pb-214

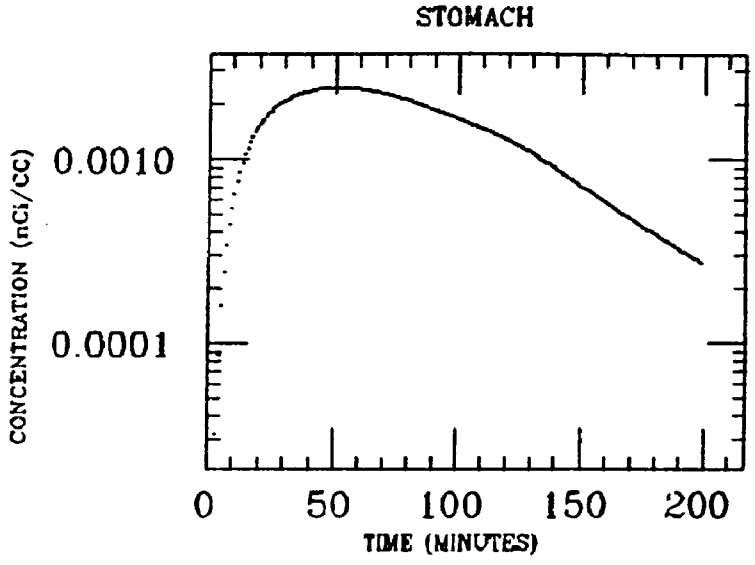

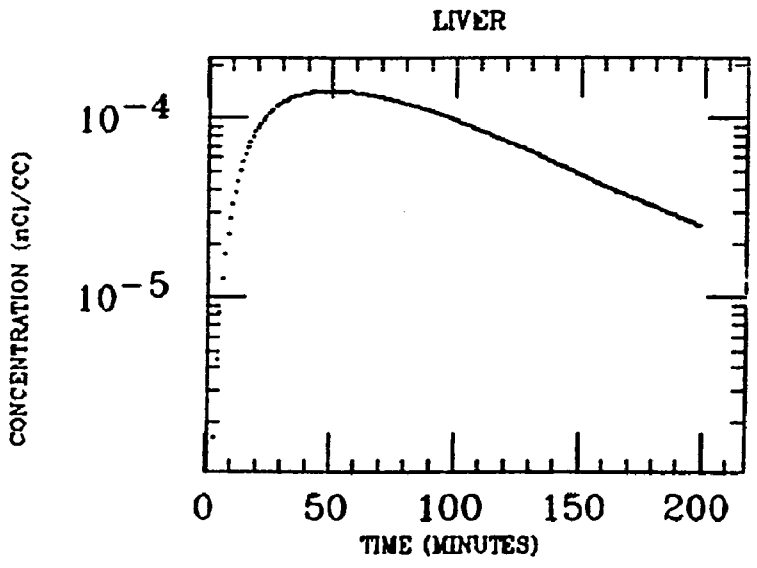

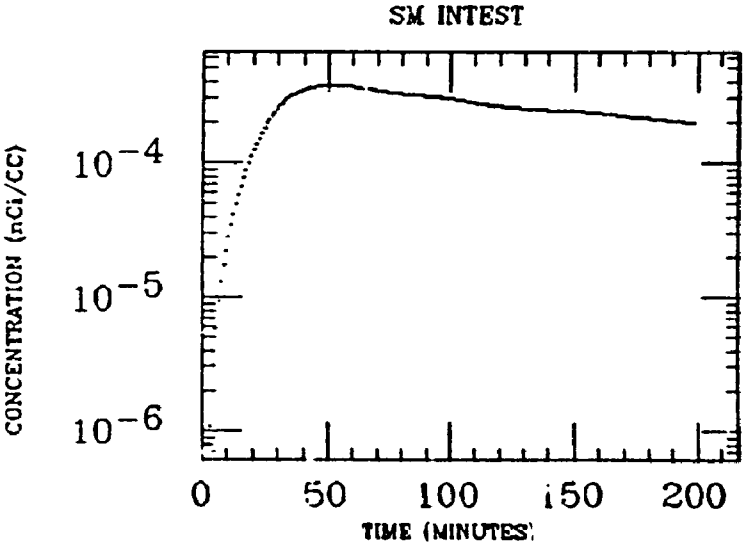

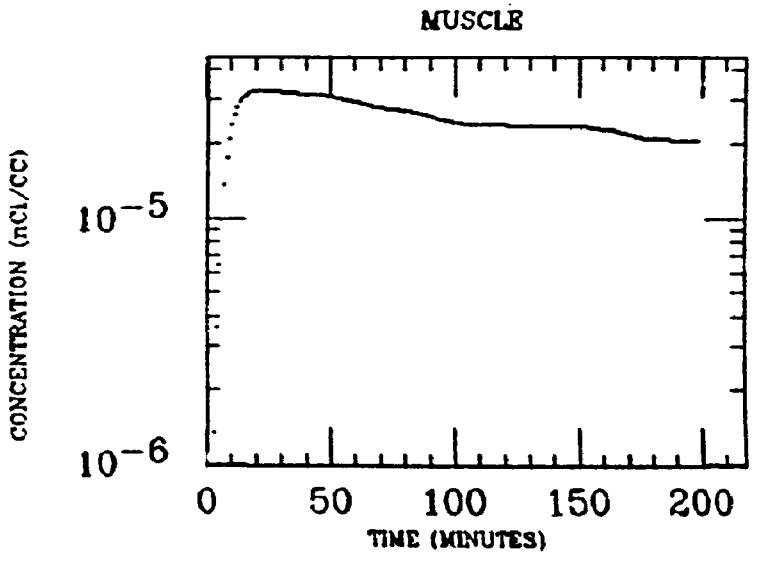

MORGAN
XE INGESTION
Pb-214

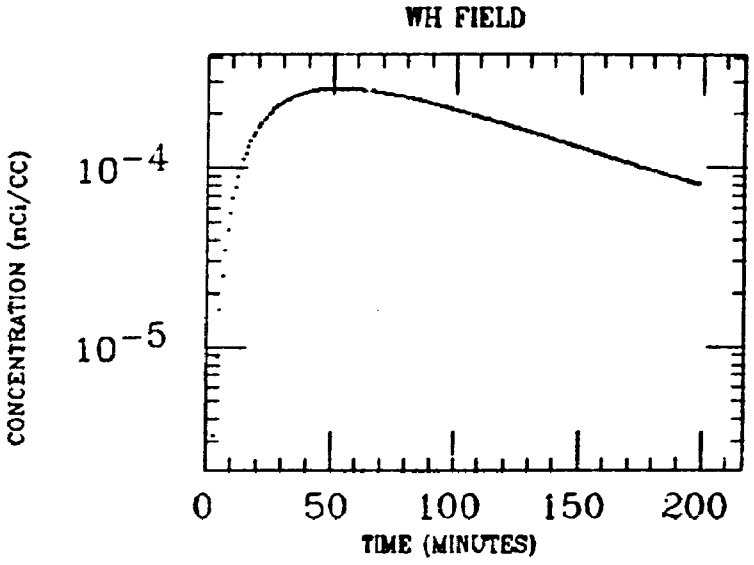

MURCHE
XE INGESTION
Pb-214

STOMACH

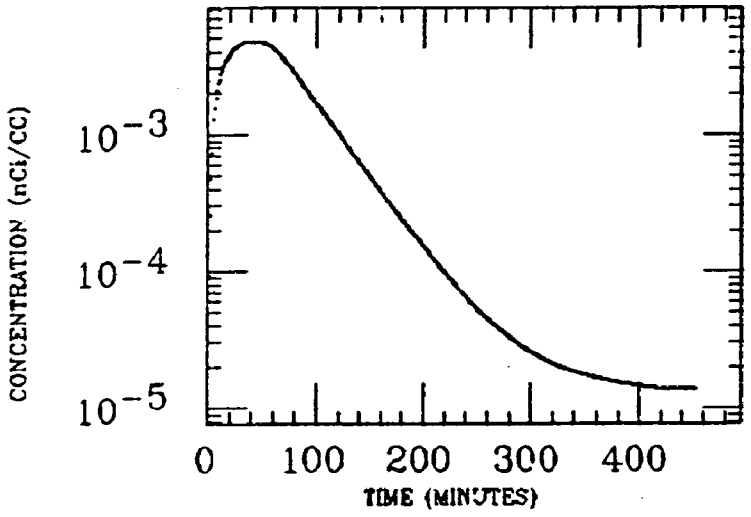

LIVER

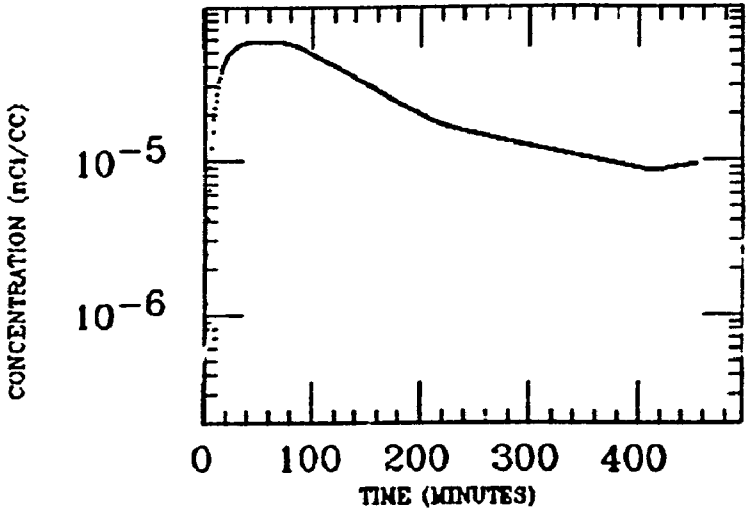

WH FIELD

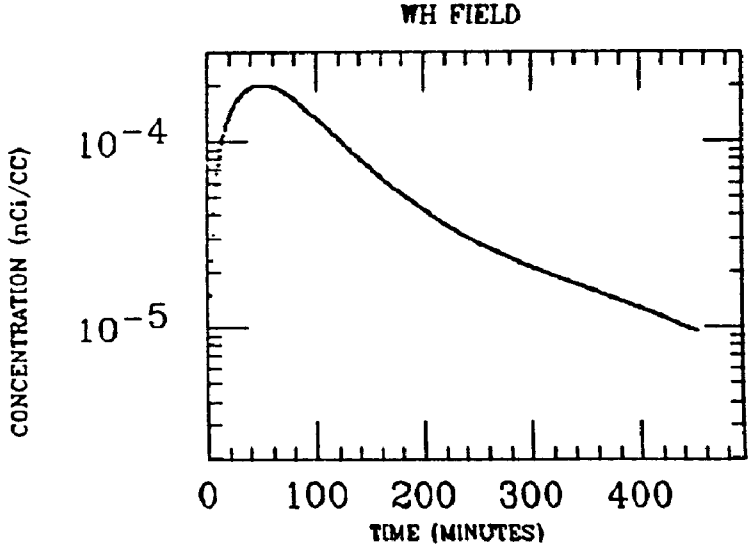

MURCHE
XE INGESTION
Pb-214

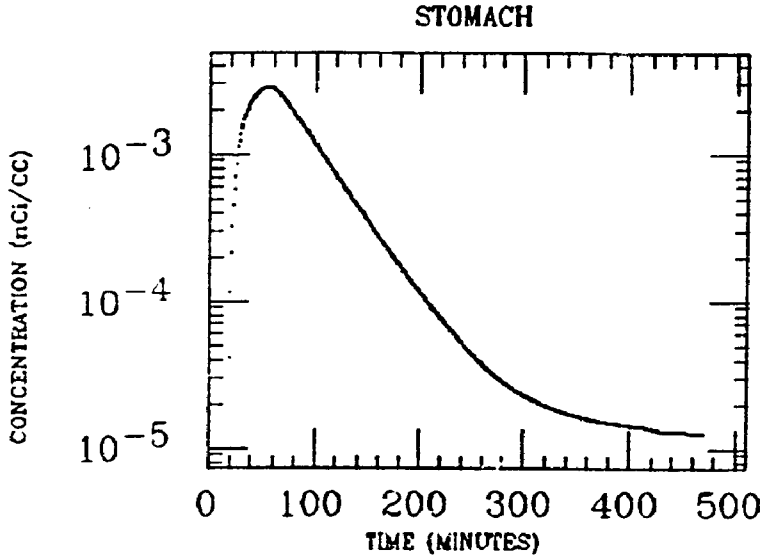

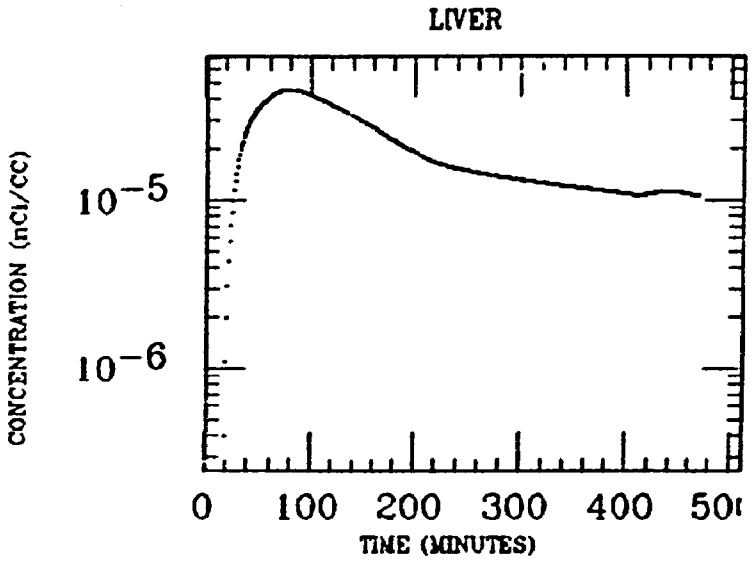

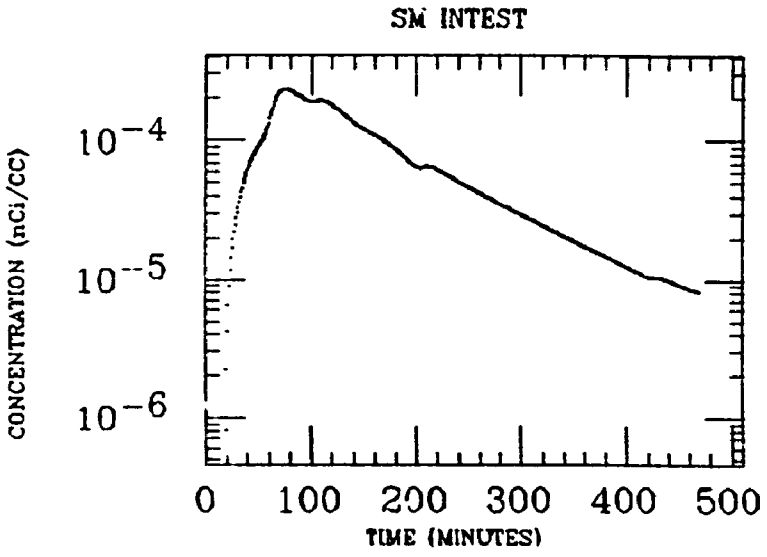

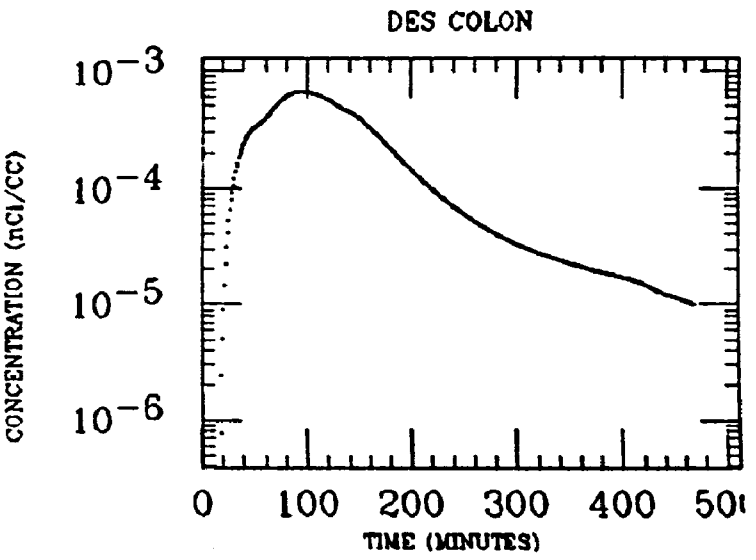

MURCHE
XE INGESTION
Pb-214

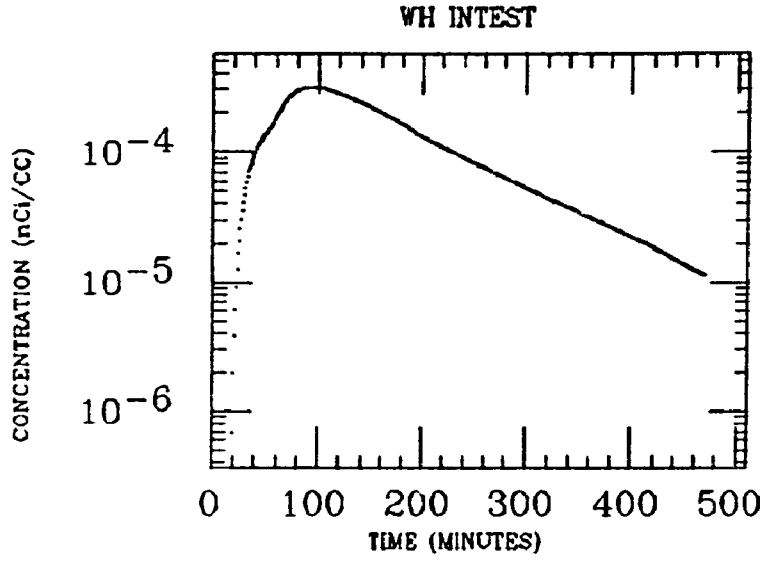

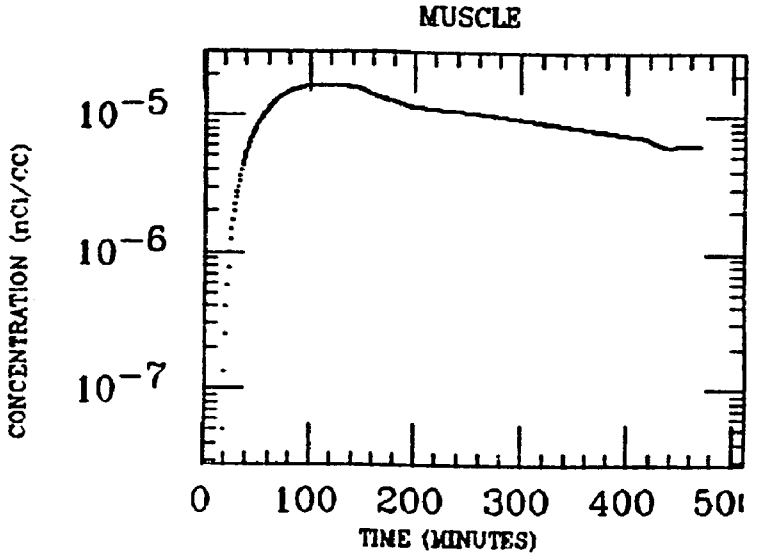

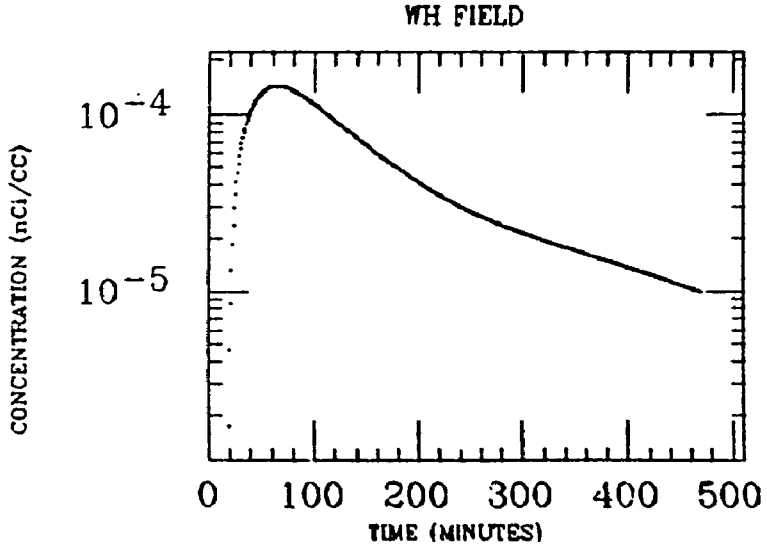

237

PARK
XE INGESTION
PL-214

STOMACH

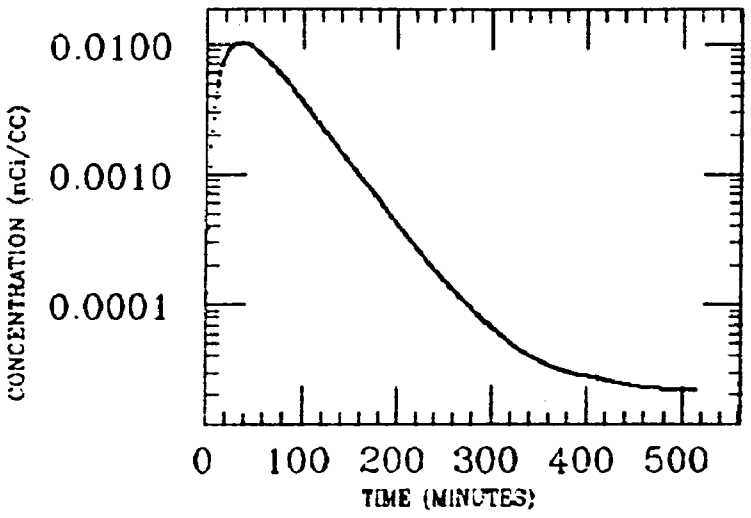

STOMACH 2

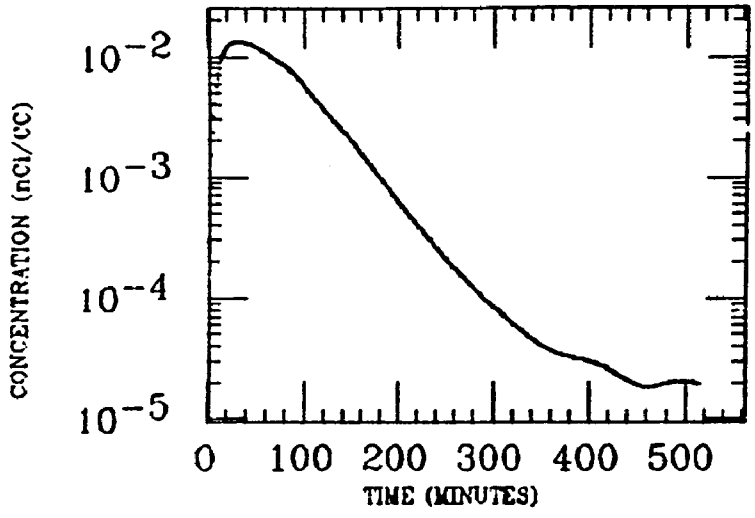

SM INTEST

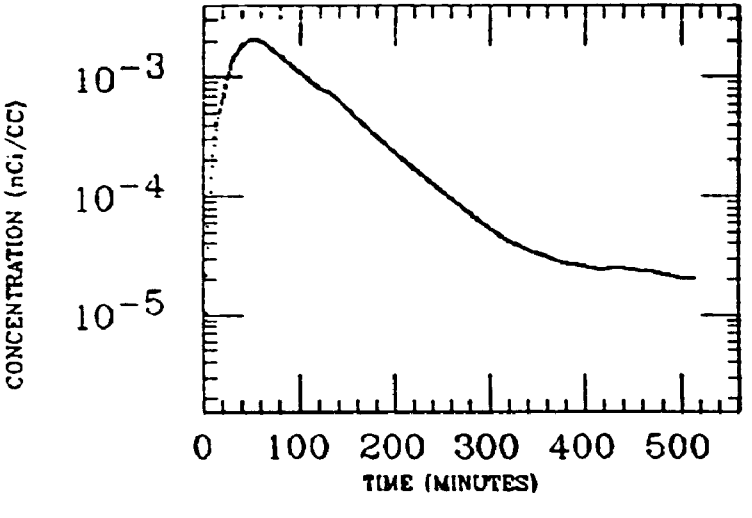

LIVER

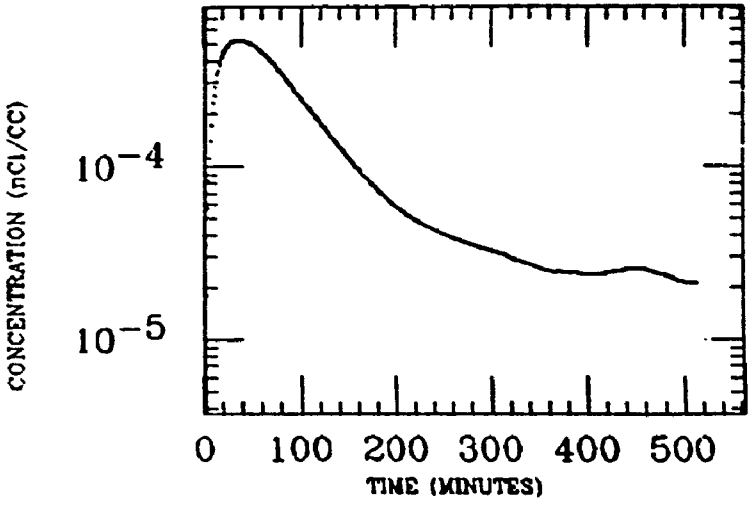

PARK
XE INGESTION
Pb-214

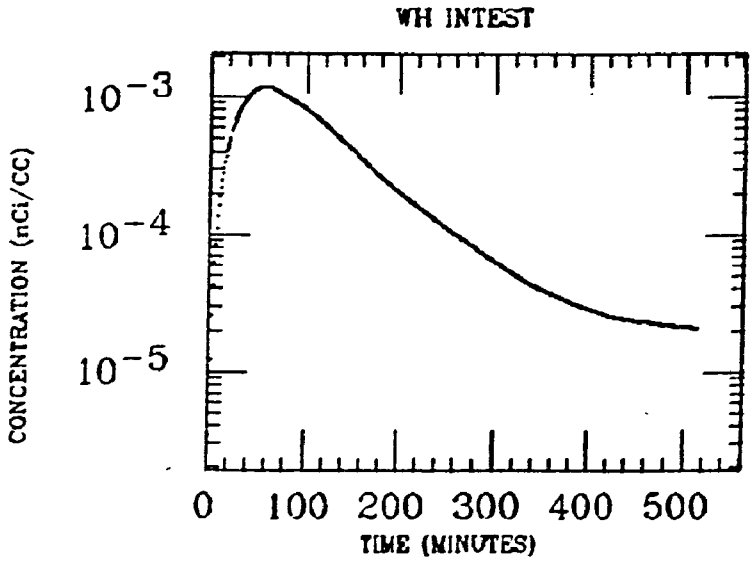

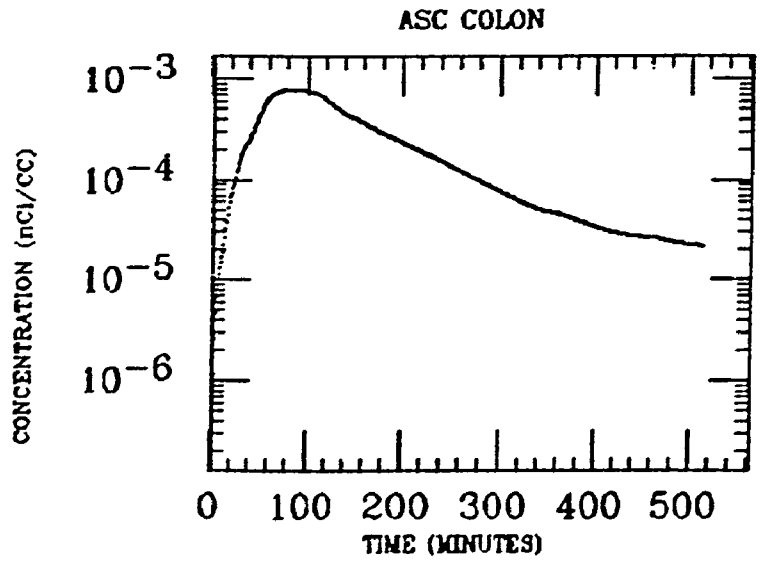

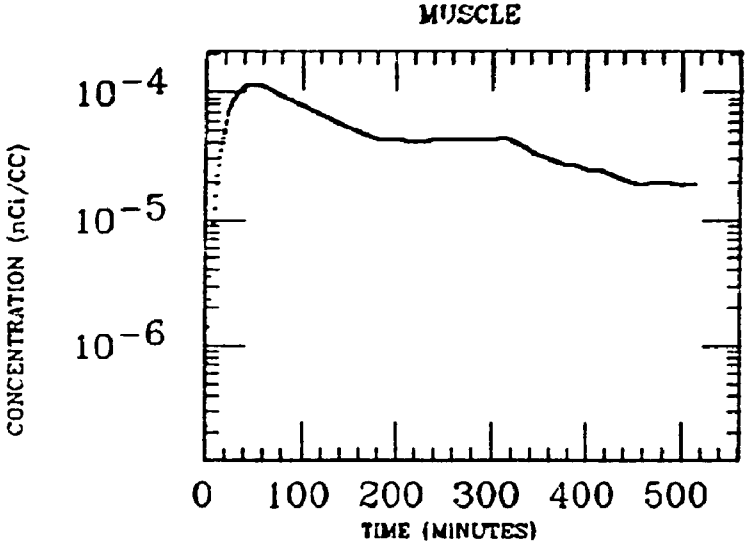

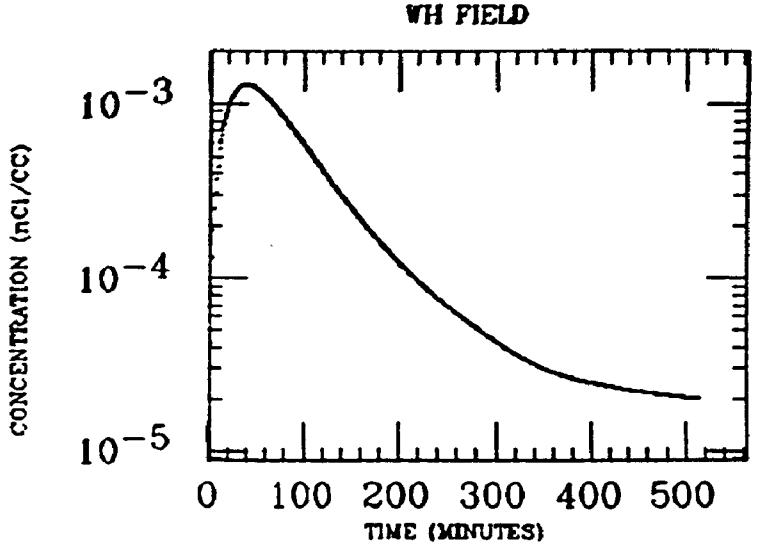

TAATJES
XE INGESTION
Pb-214

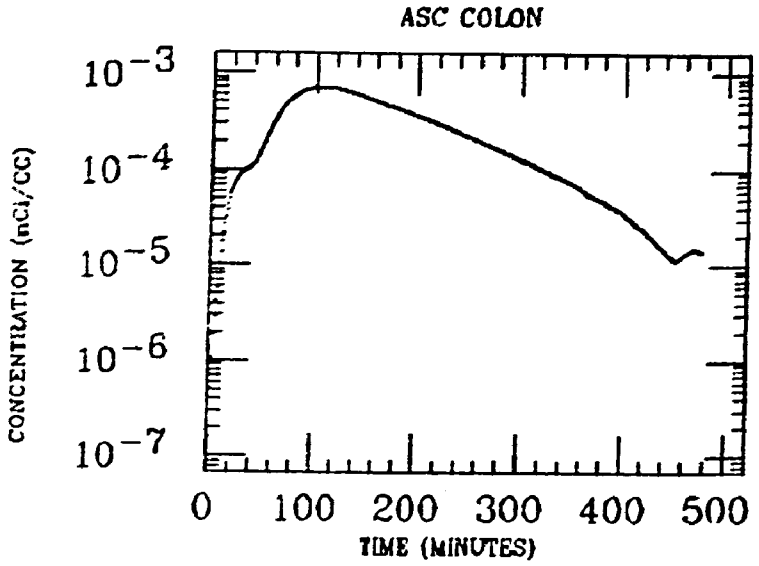

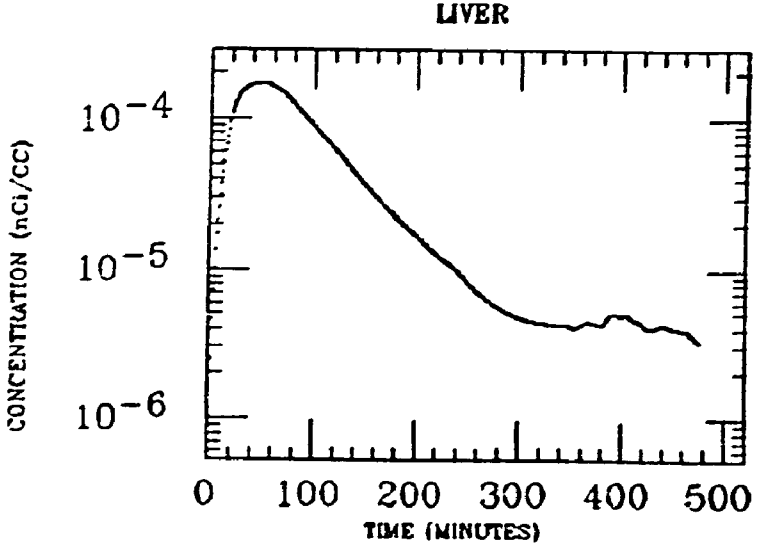

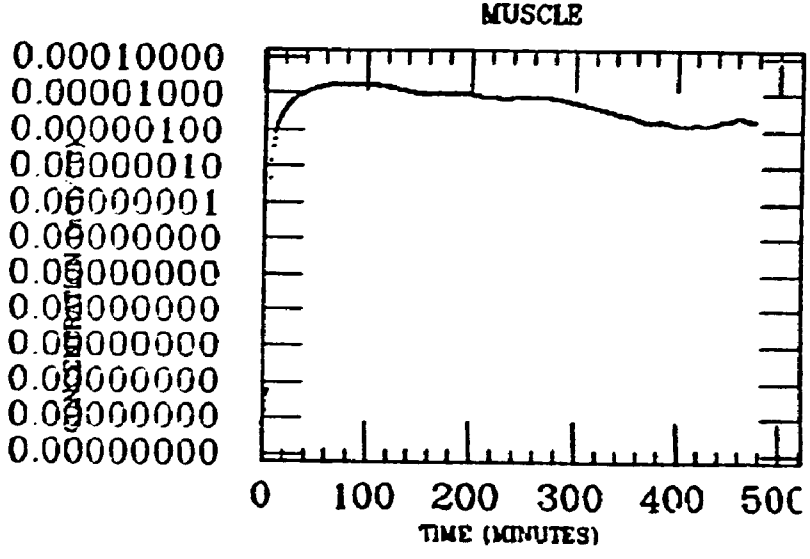

2:10

TAATJES
XE INGESTION
Pb-214

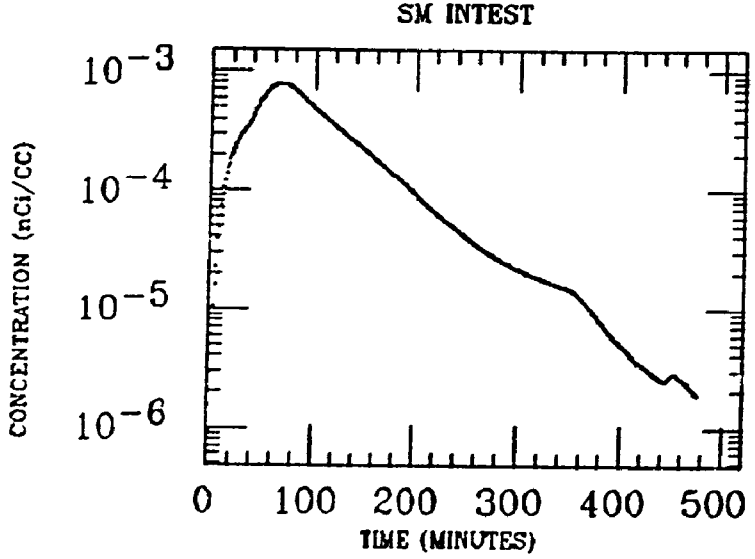

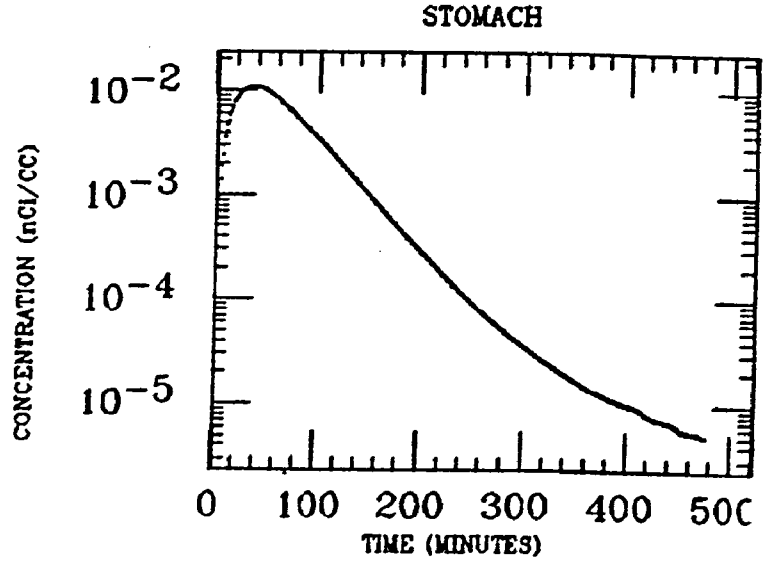

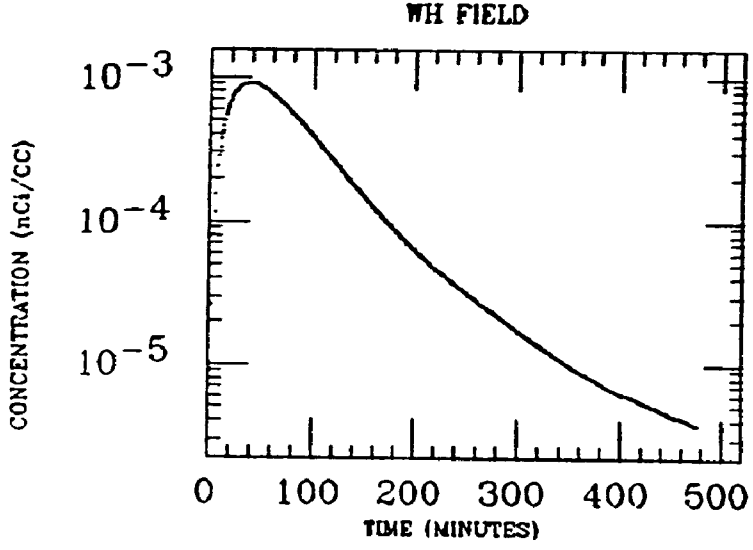

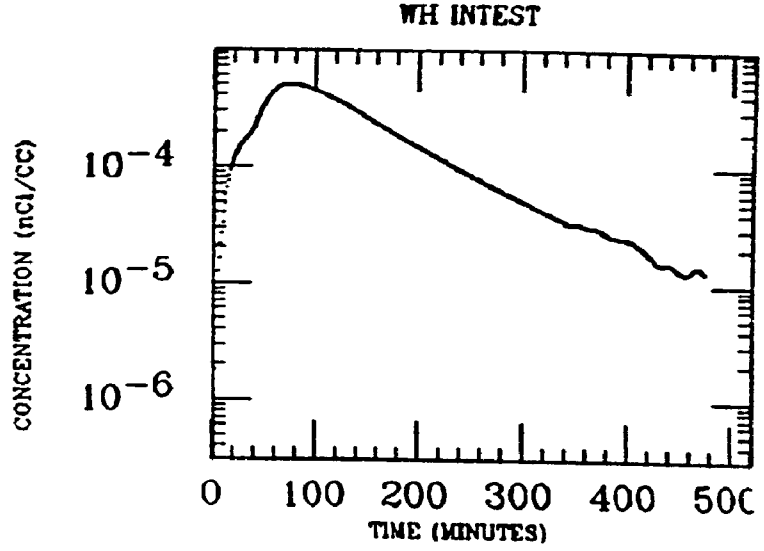

TAYLOR
XE INGESTION
Pb-214

STOMACH

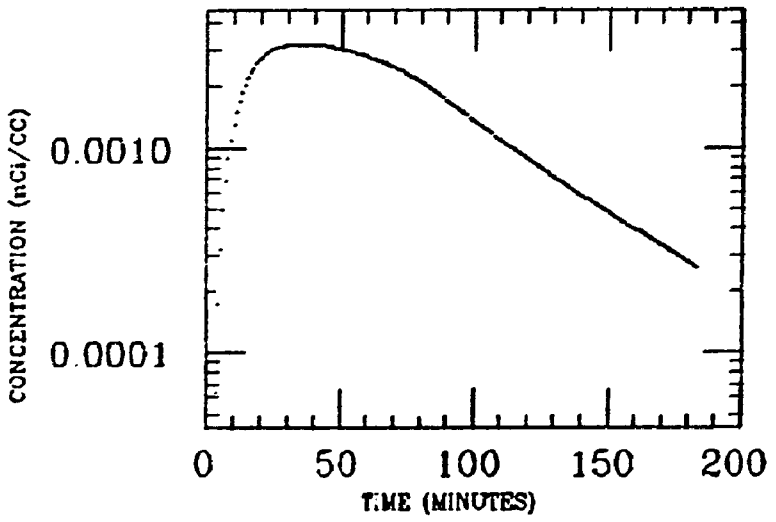

LIVER

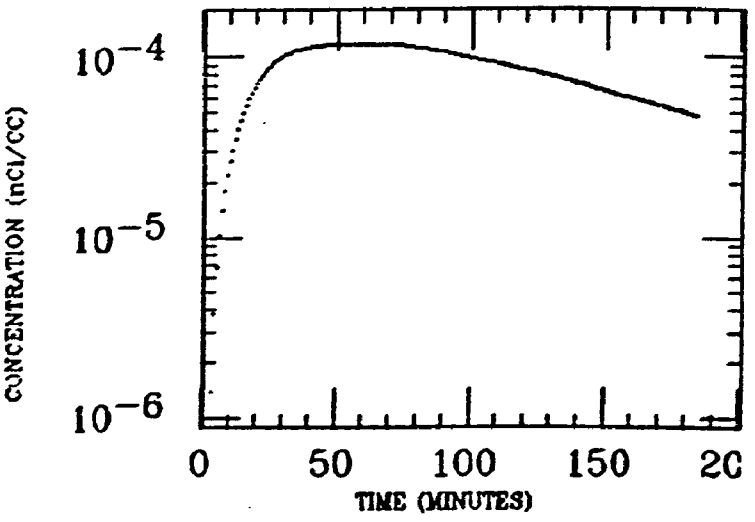

SM INTEST

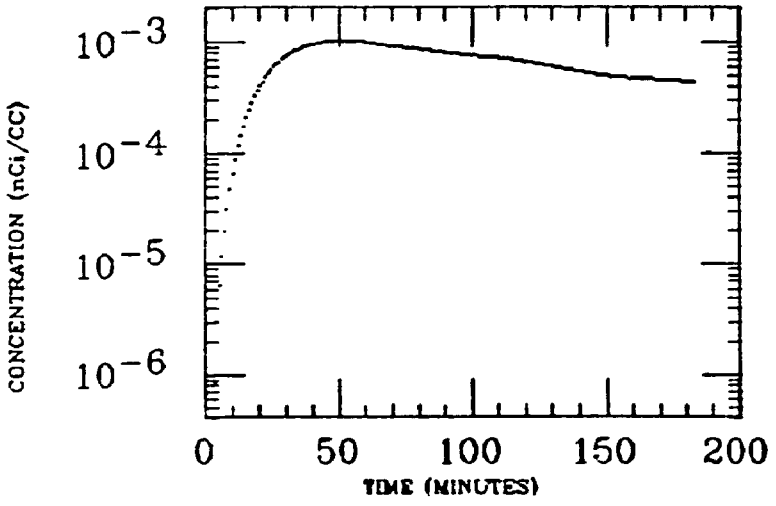

ASC COLON

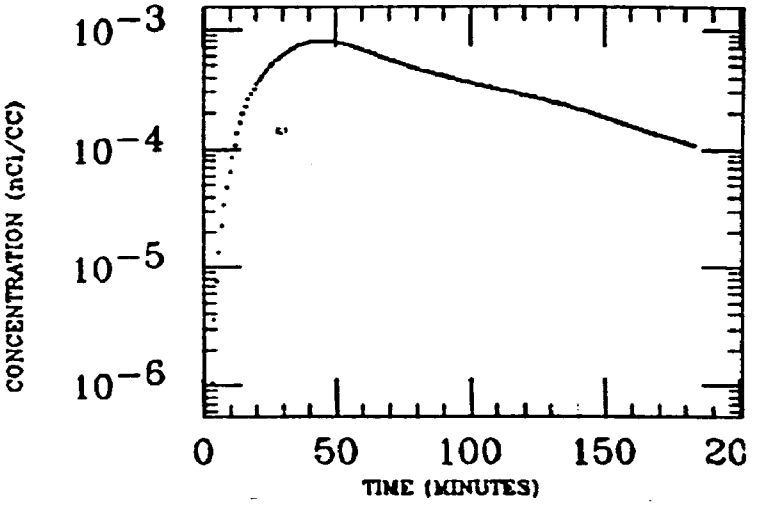

242

TAYLOR
XE INGESTION
Pb-214

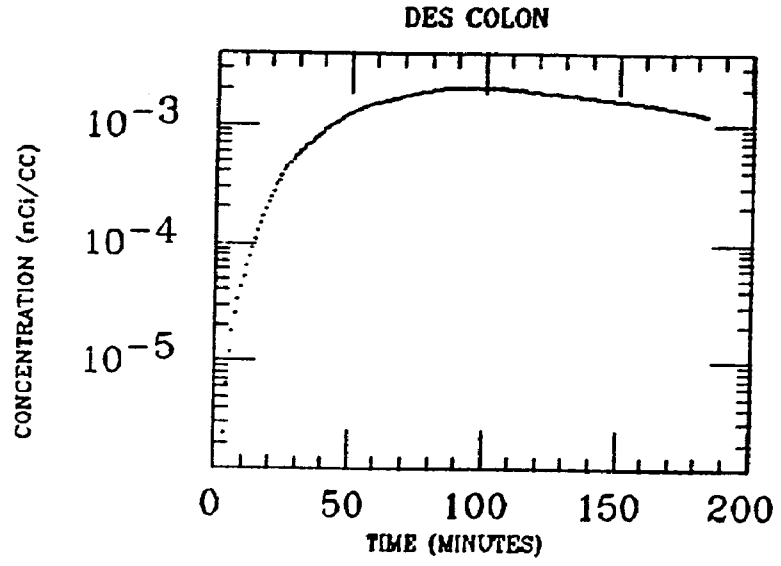

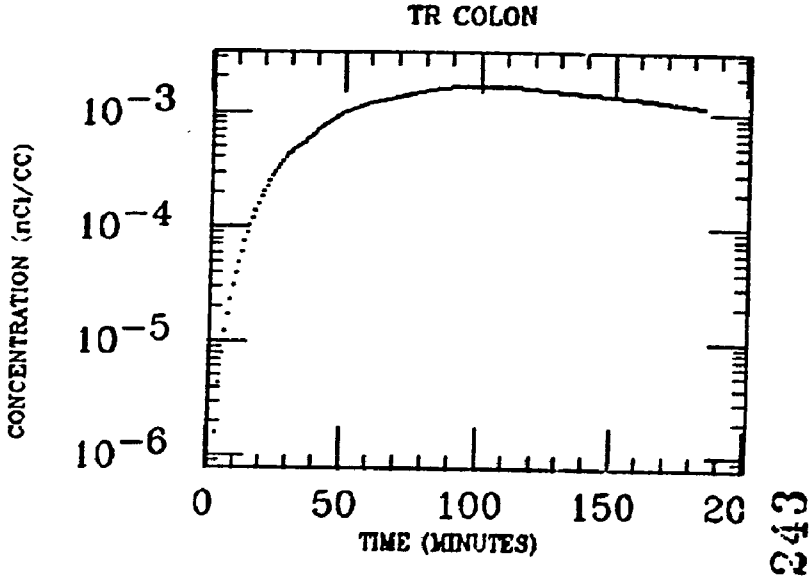

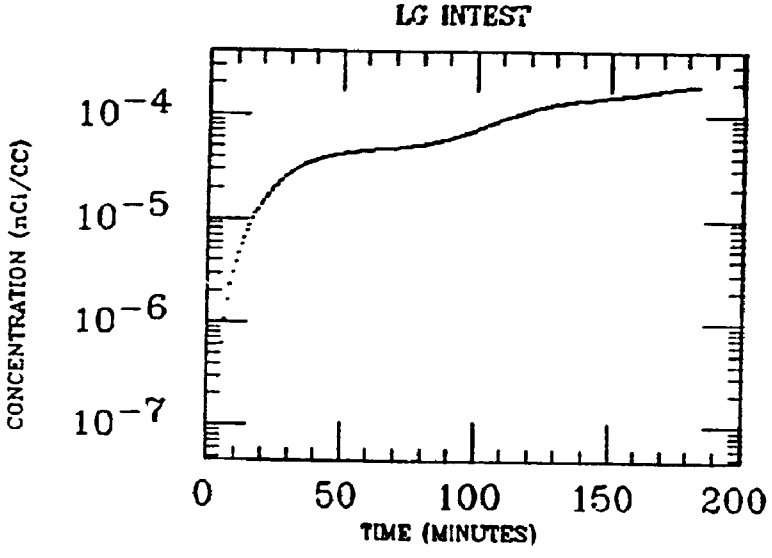

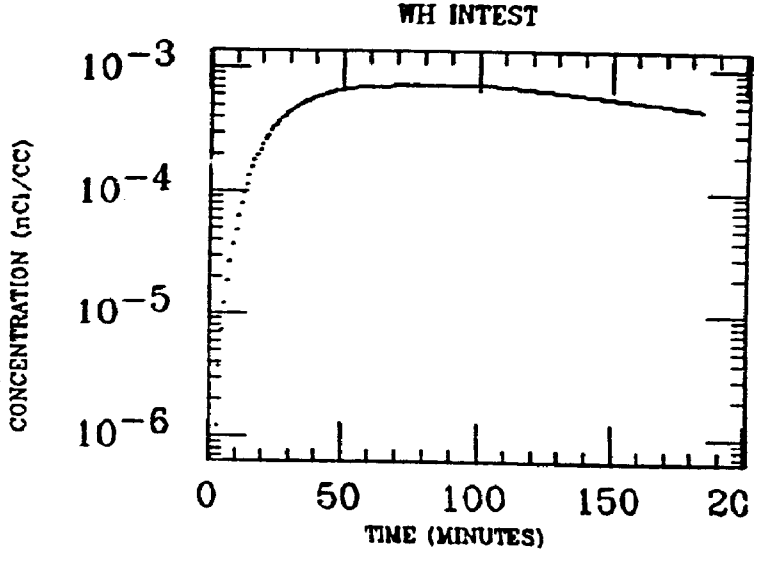

TAYLOR
XE INGESTION
Pb-214

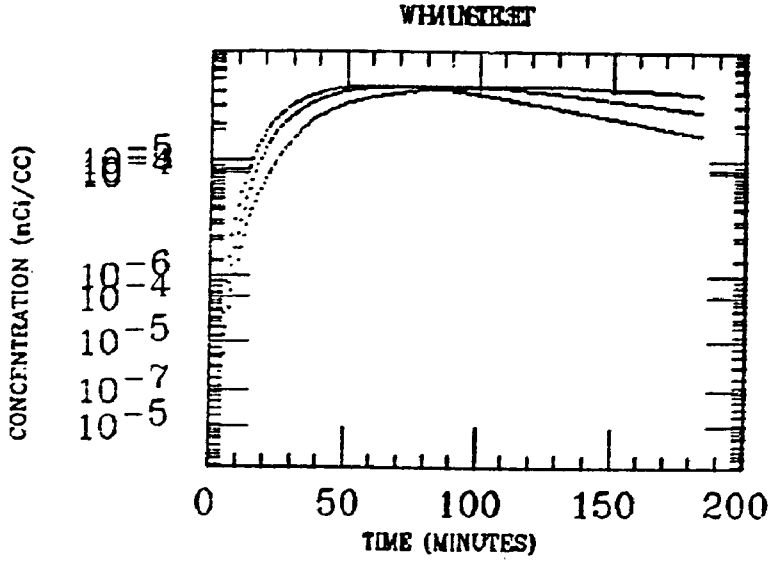

WESOLEK
XE INGESTION
Pb-214

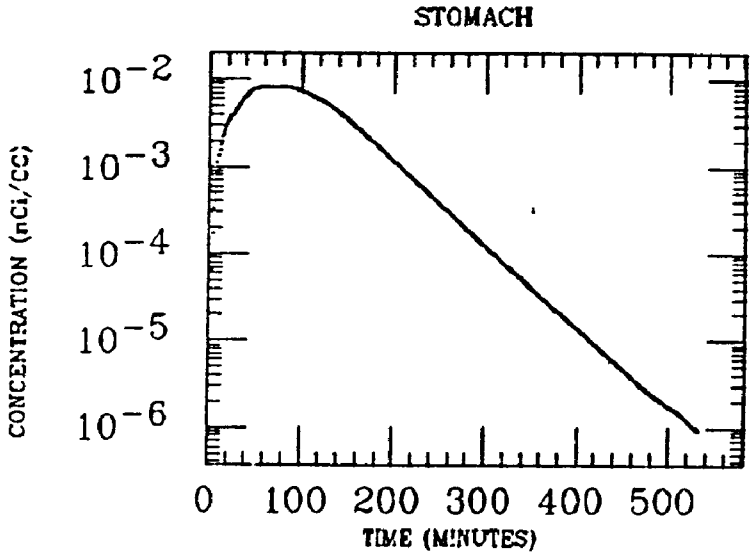

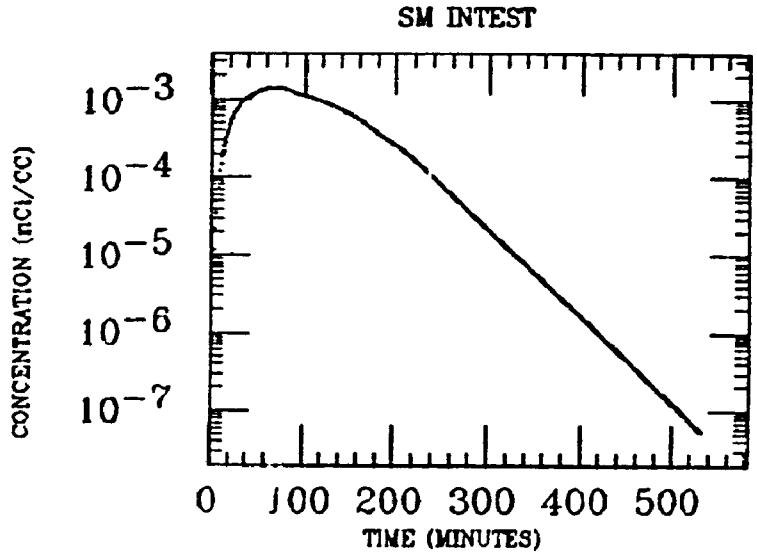

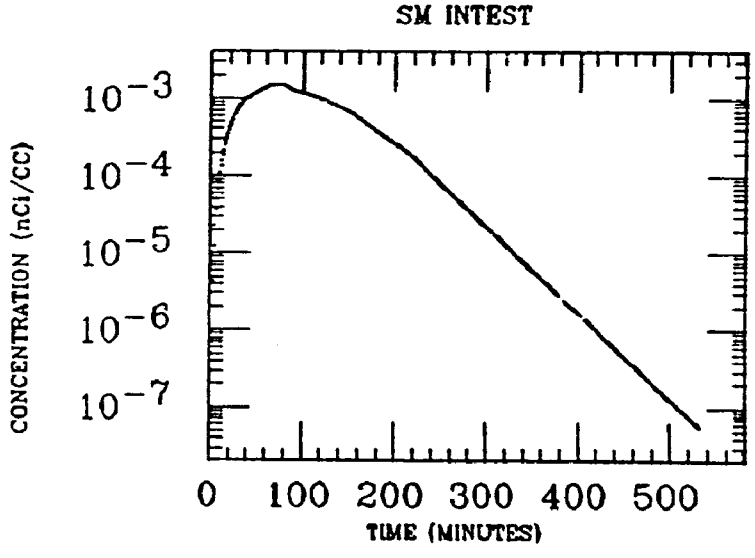

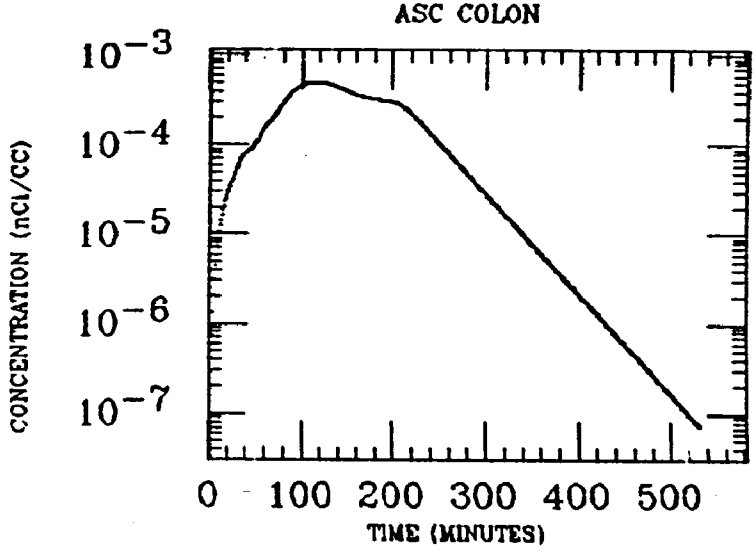

WESOLEK
XE INGESTION
Pb-214

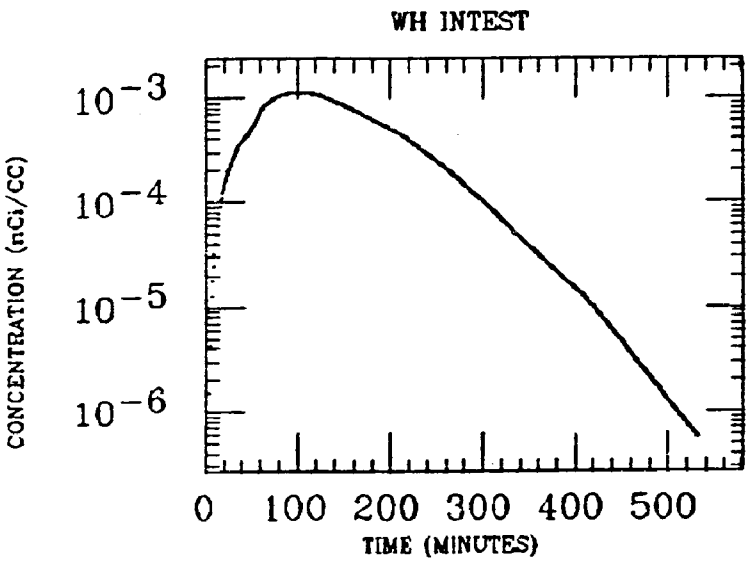

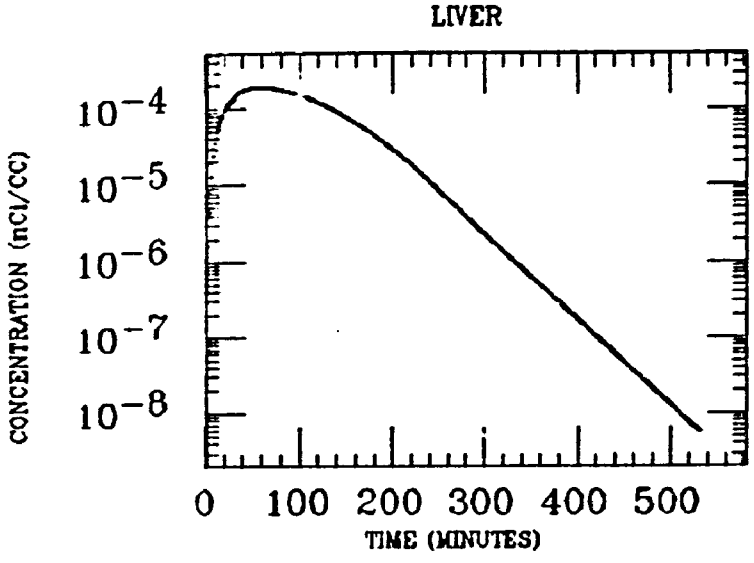

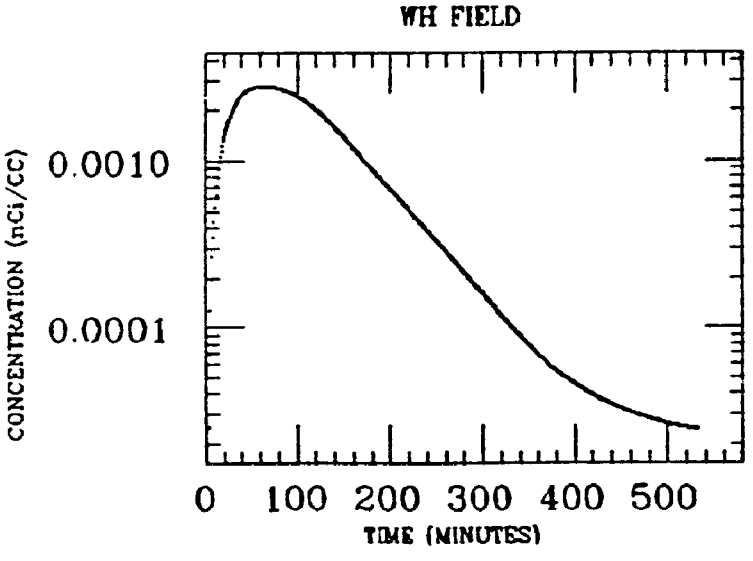

245

WILTSE
XE INGESTION
Pb-214

STOMACH

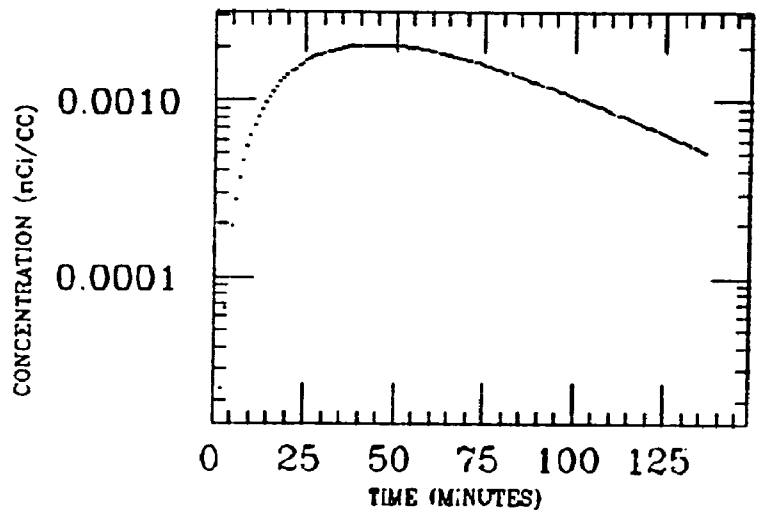

LIVER

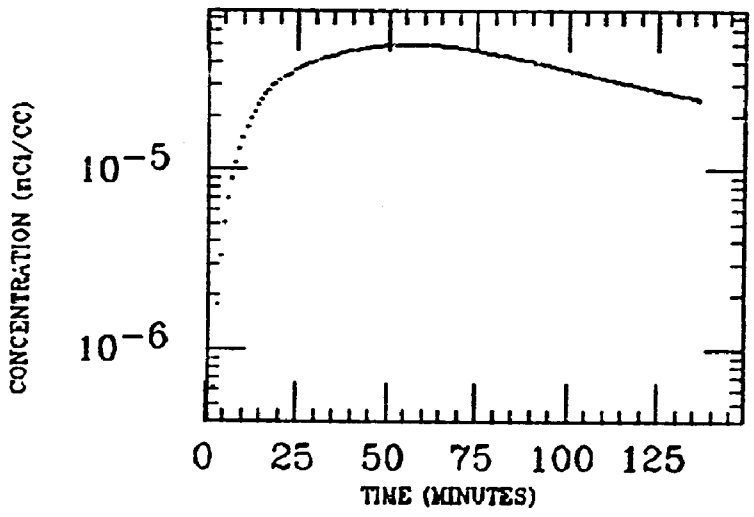

SM INTEST

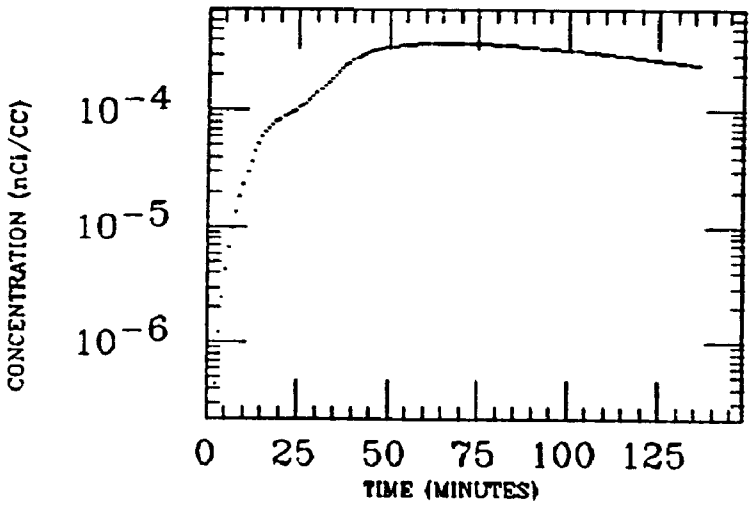

ASC COLON

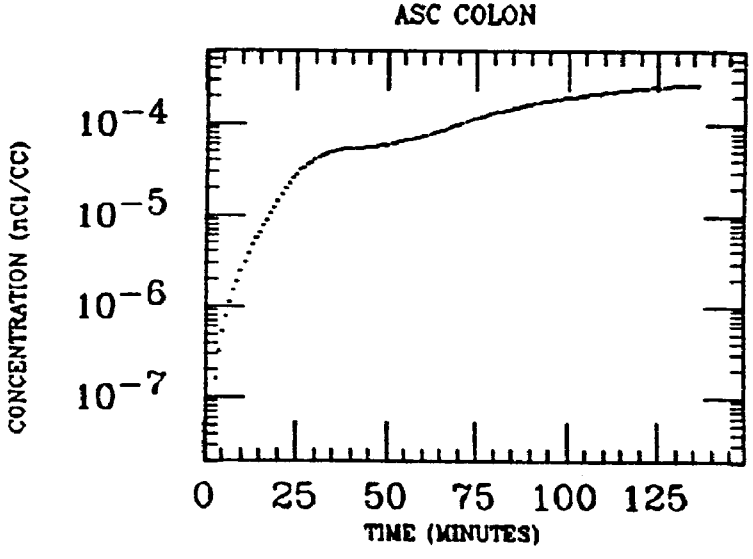

247

WILTSE
XE INGESTION
Pb-214

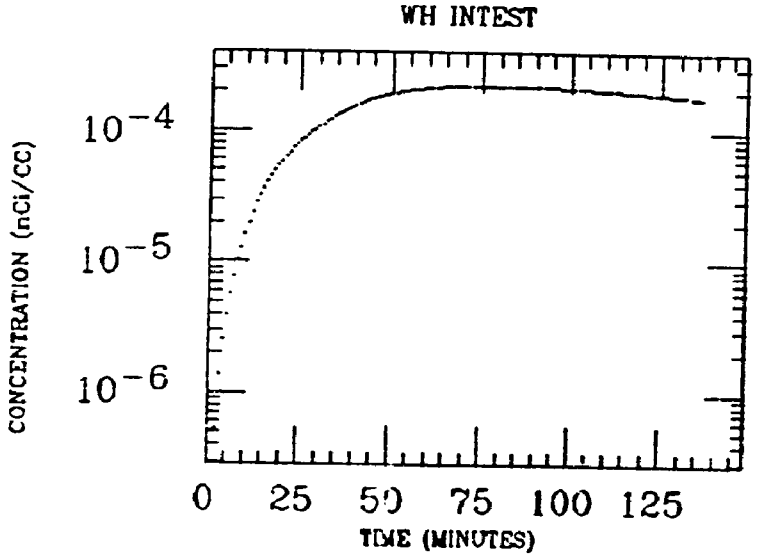

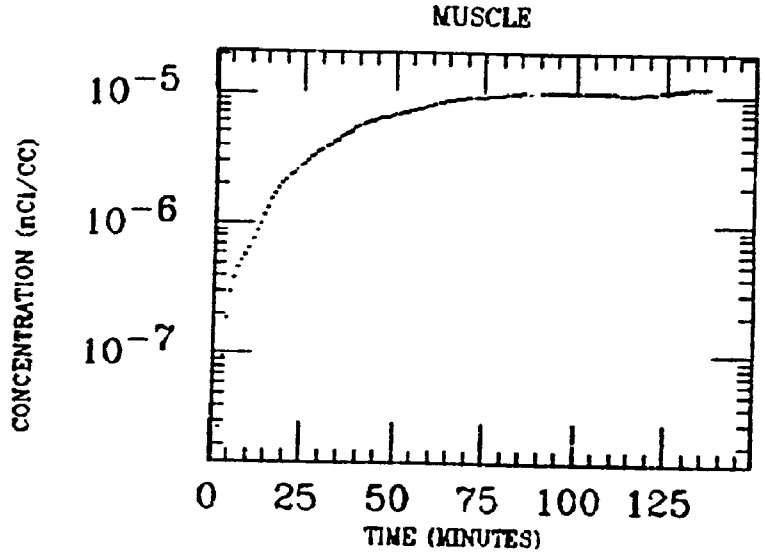

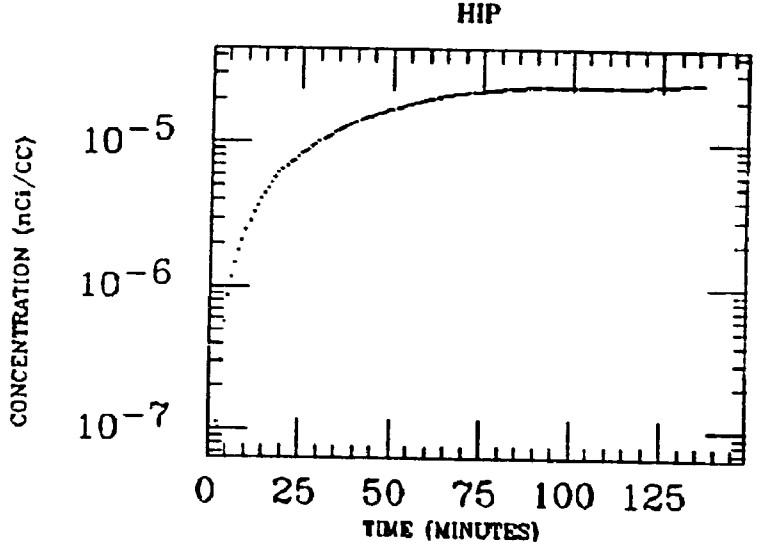

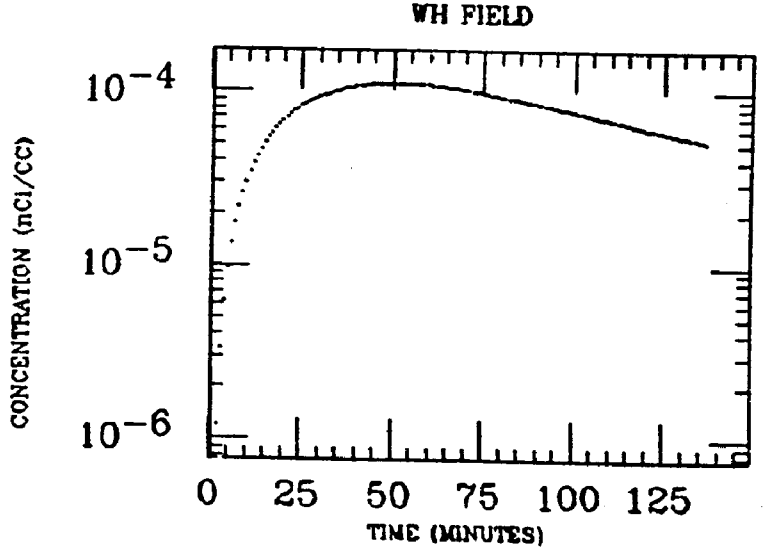

AHERN
XE INGESTION
Bi-214

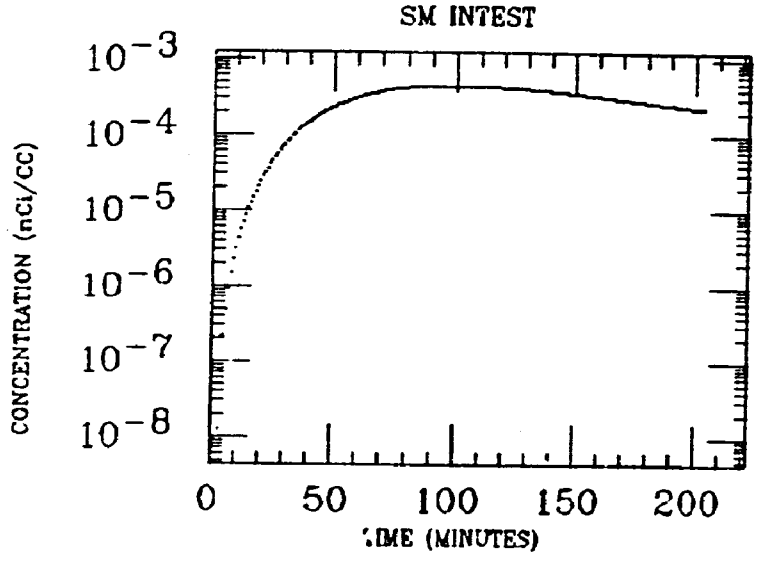

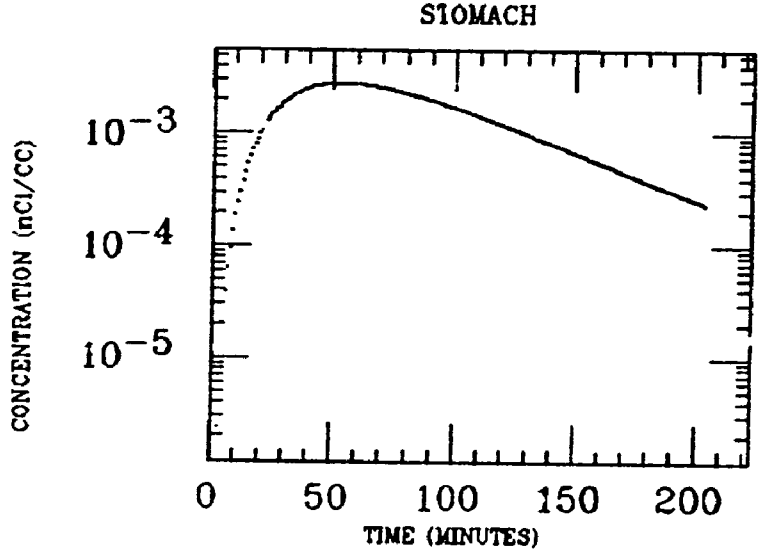

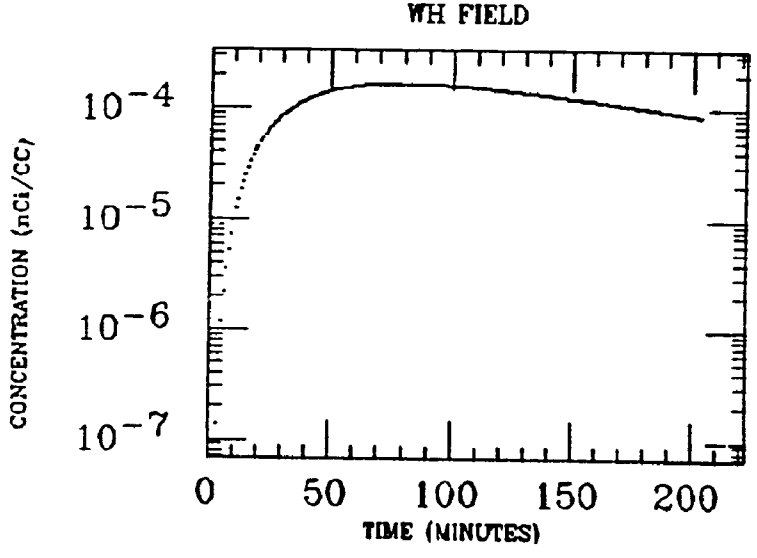

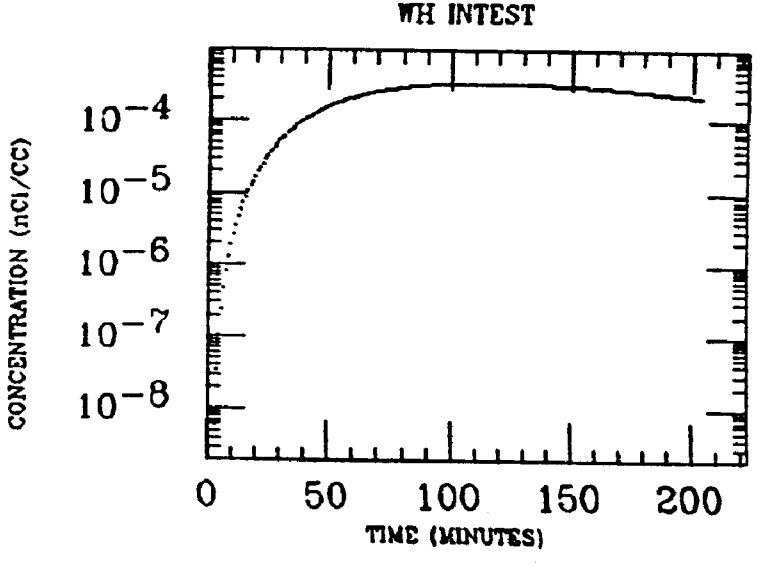

AHERN
XE INGESTION
Bi-214

ASC COLON

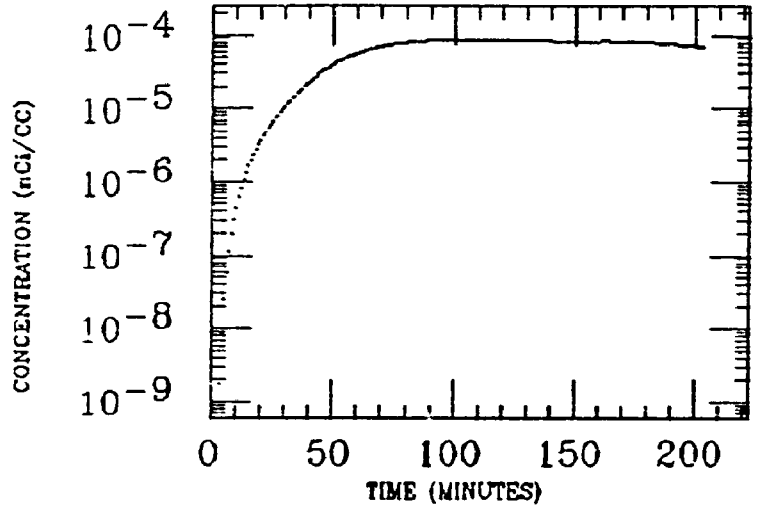

HIP

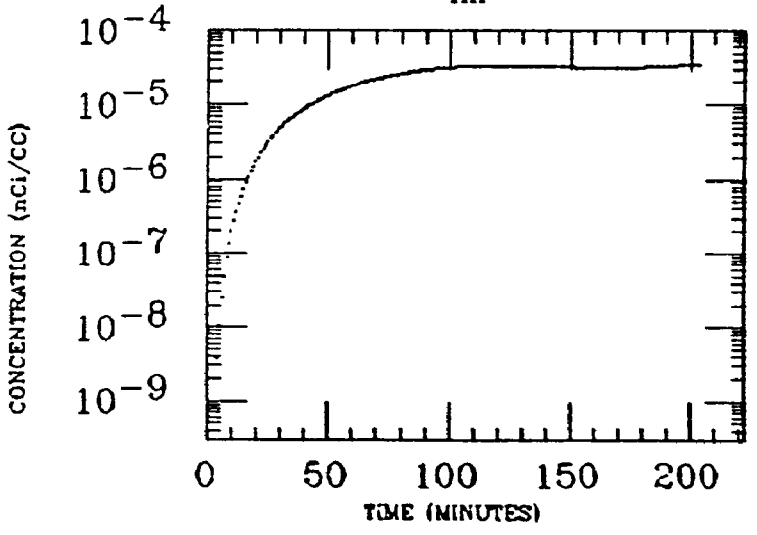

LIVER

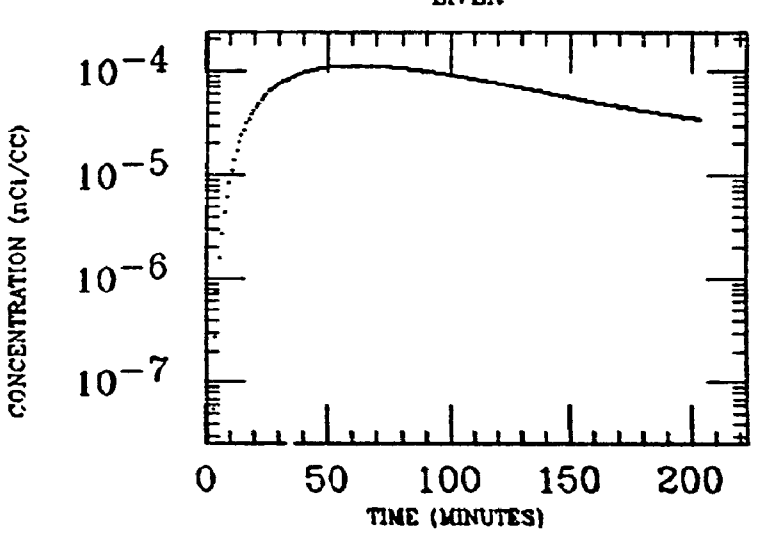

ARROL
XE INGESTION
Bi-214

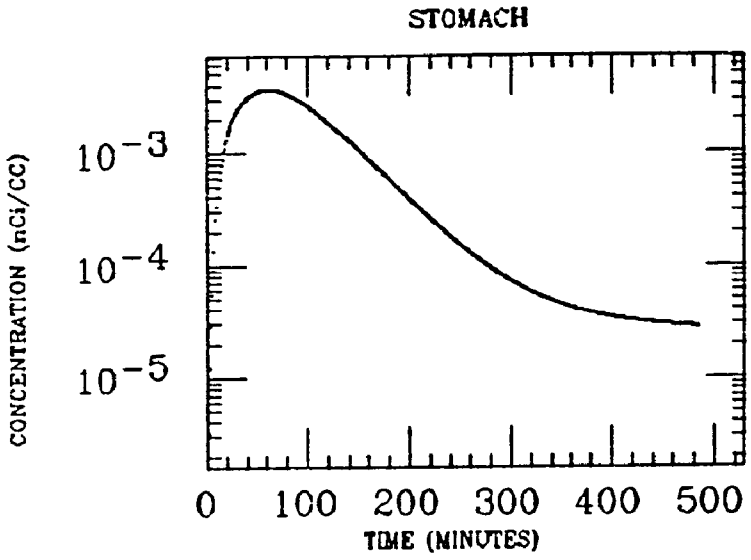

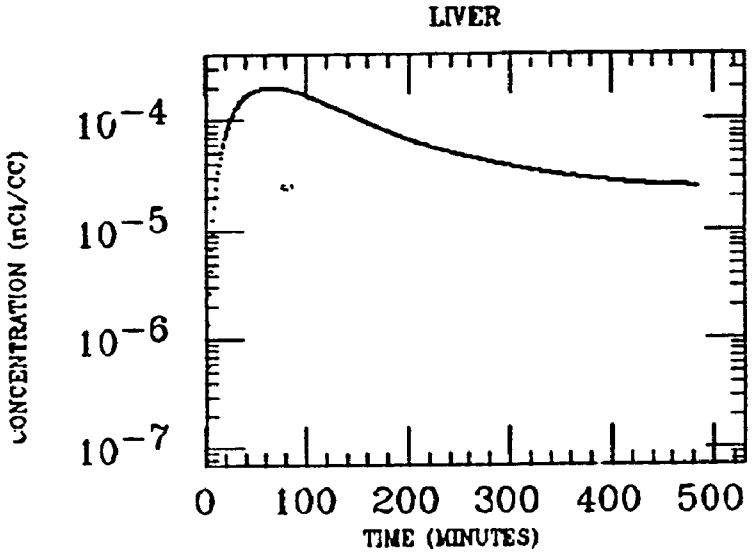

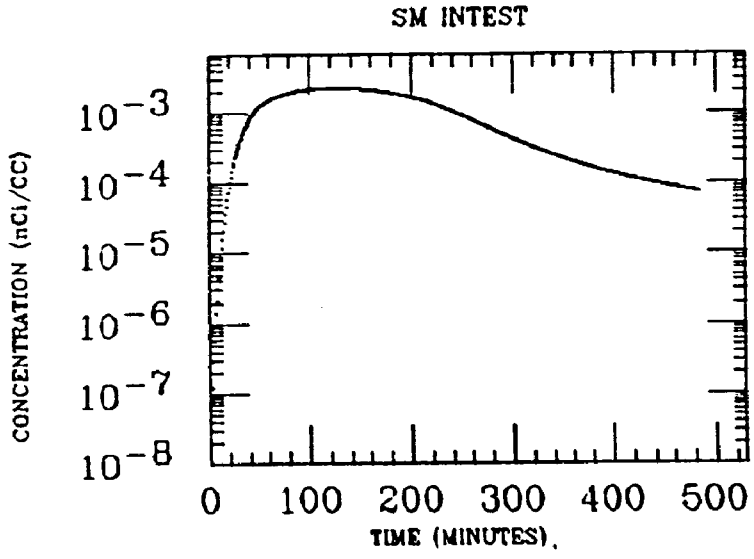

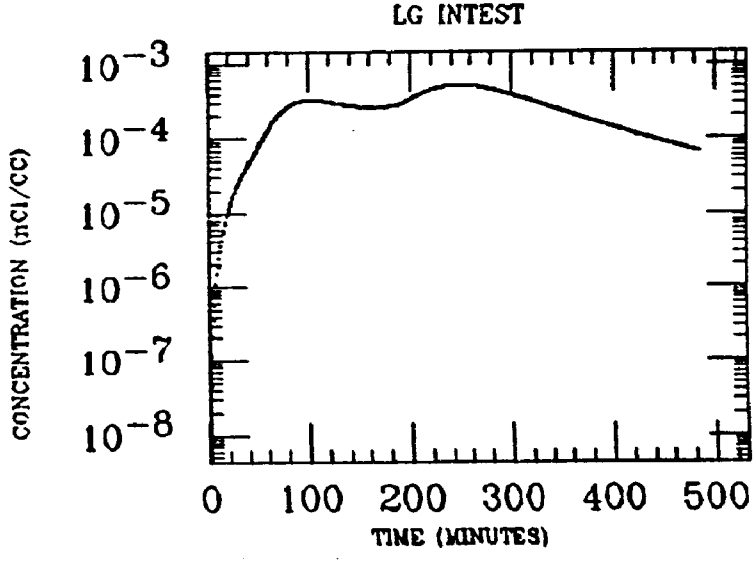

ARROL
XE INGESTION
BI-214

WH INTEST

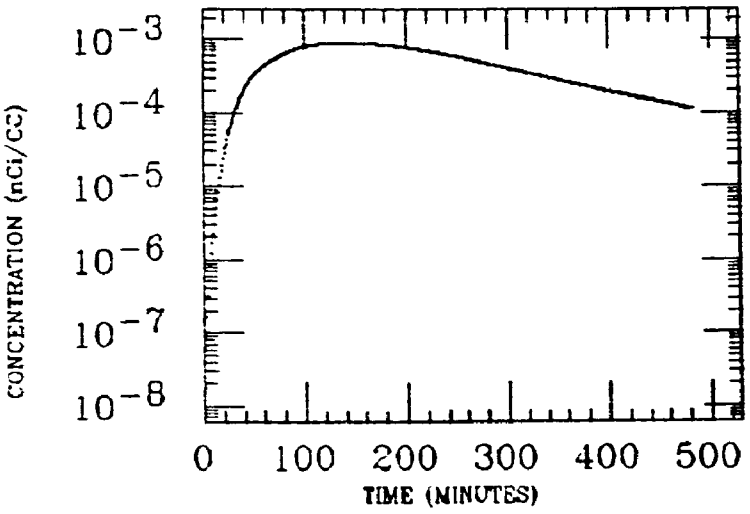

MUSCLE

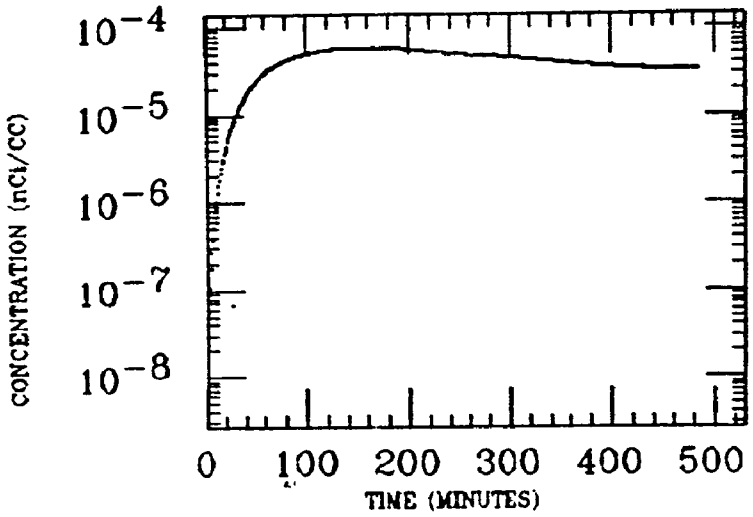

WH FIELD

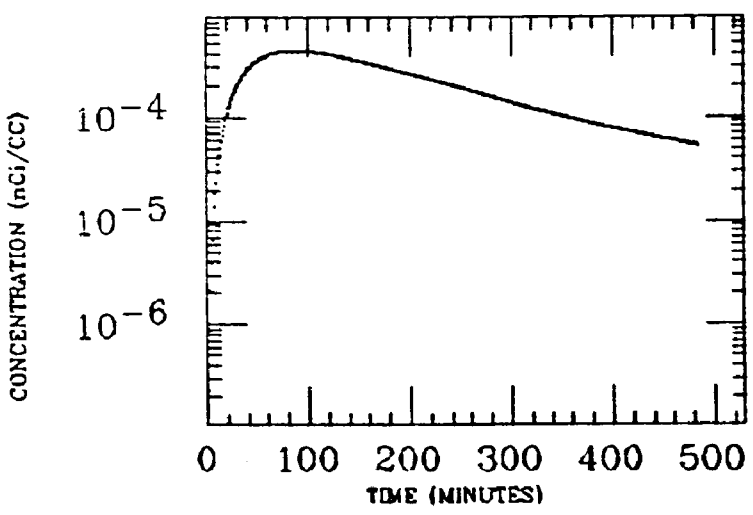

253

AYER

XE INGESTION

BI-214

STOMACH

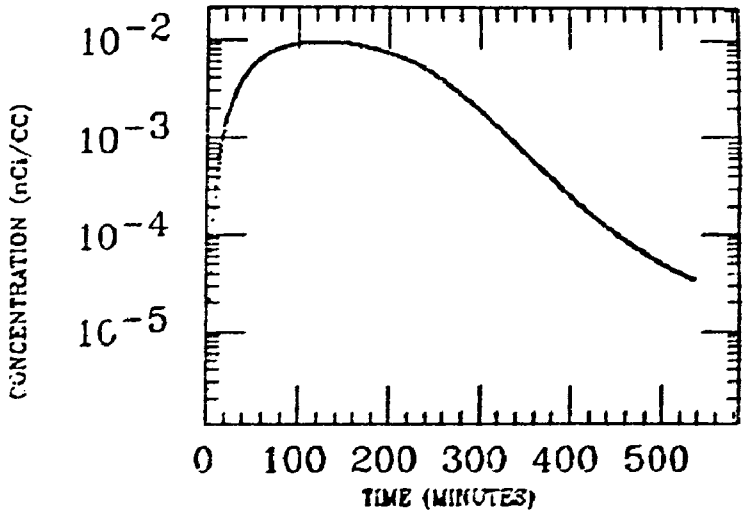

LIVER

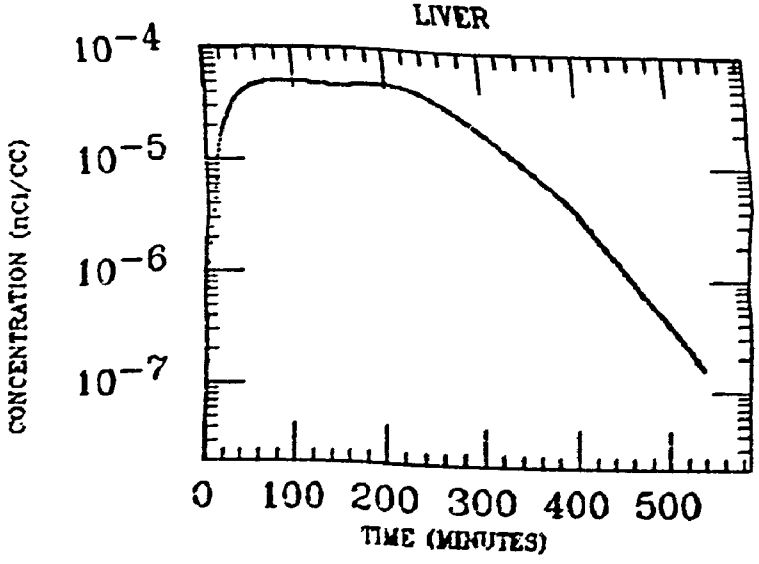

WH FIELD

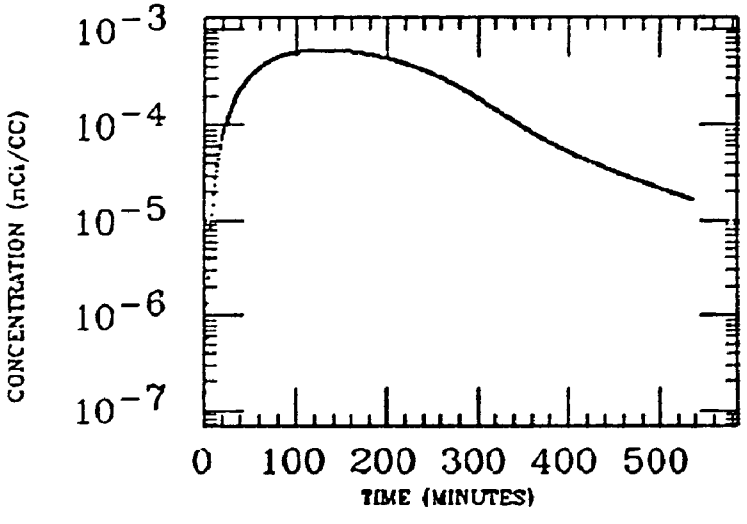

AYER

XE INGESTION

Bi-214

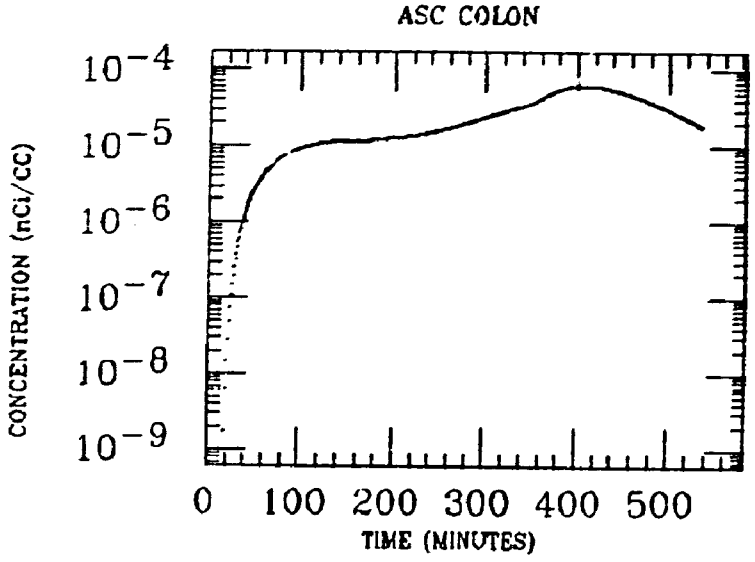

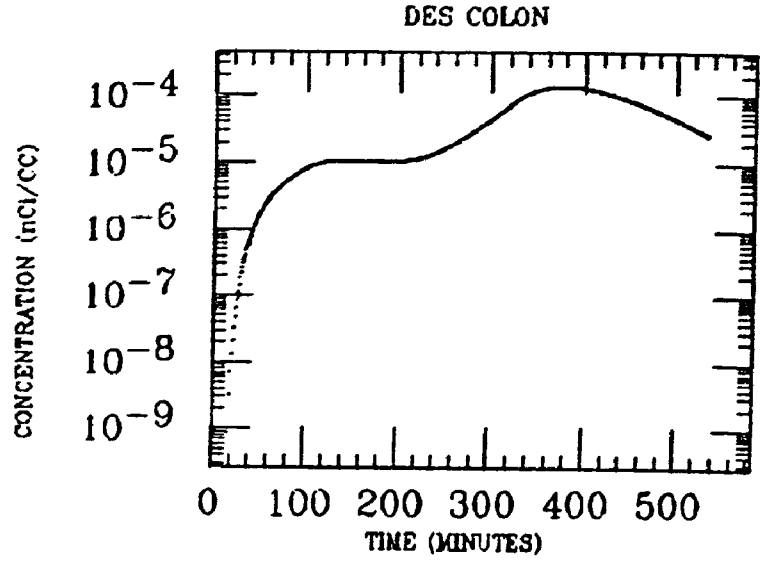

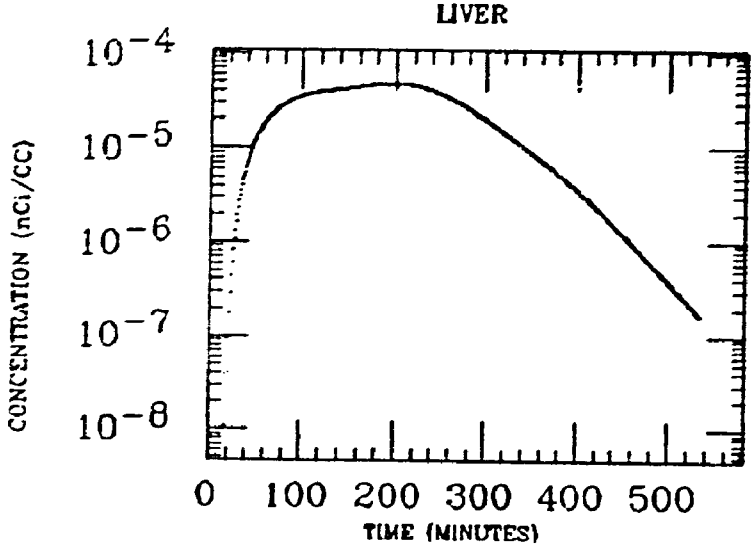

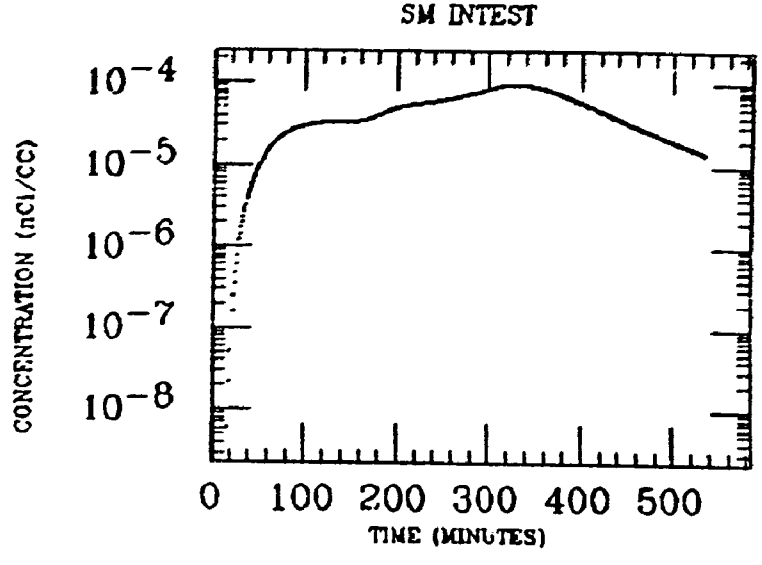

AYER
XE INGESTION
Bi-214

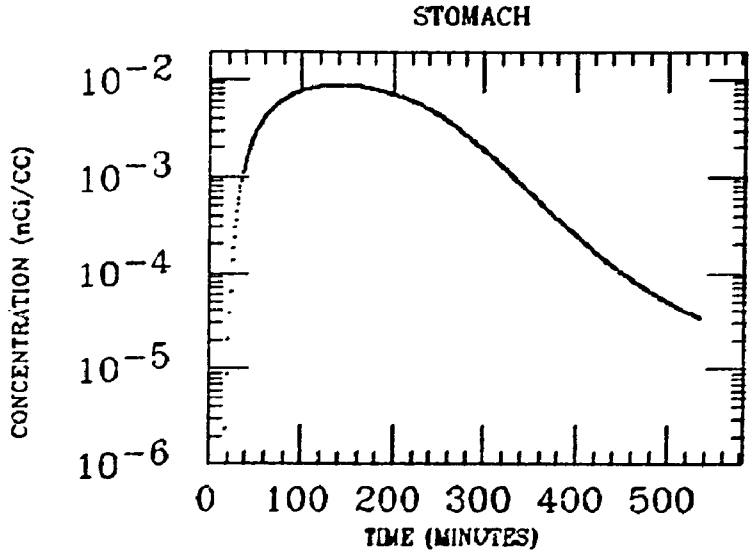

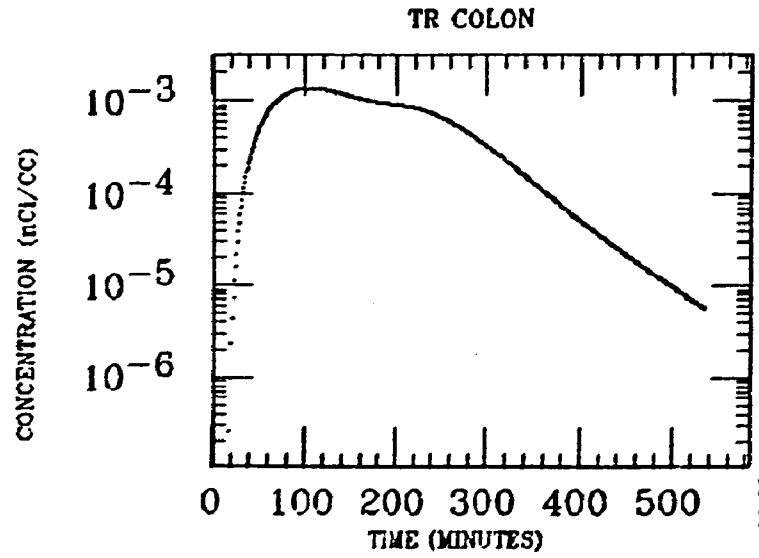

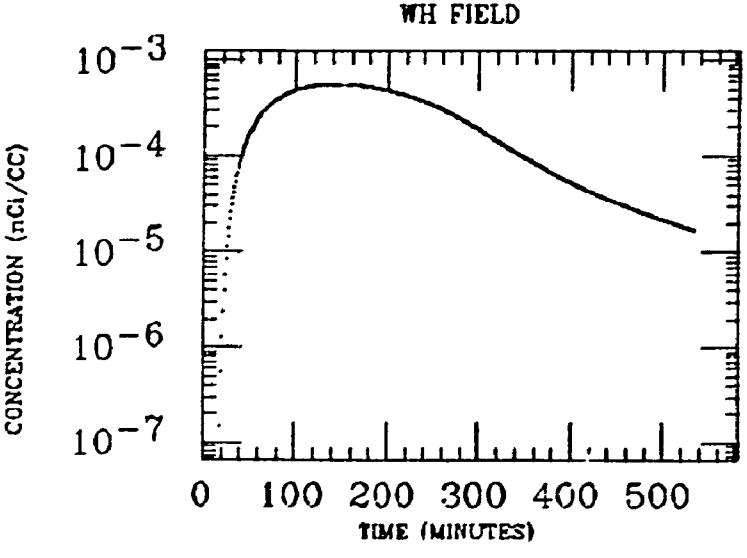

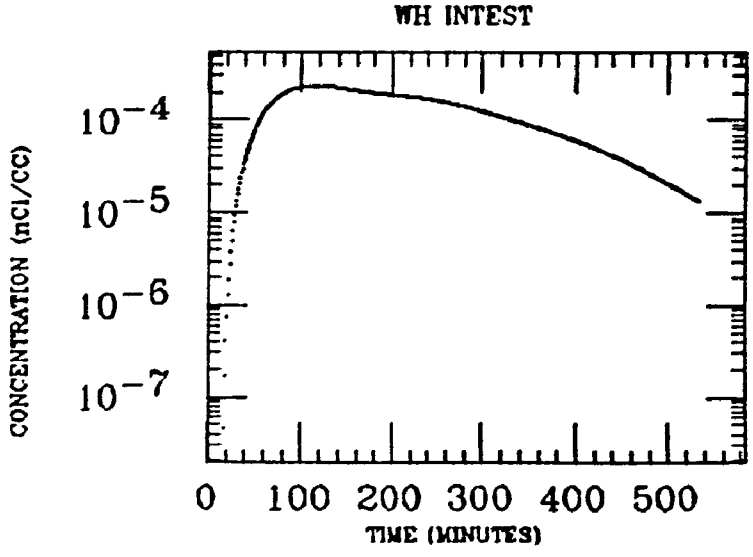

BROCK
XE INGESTION
Bi-214

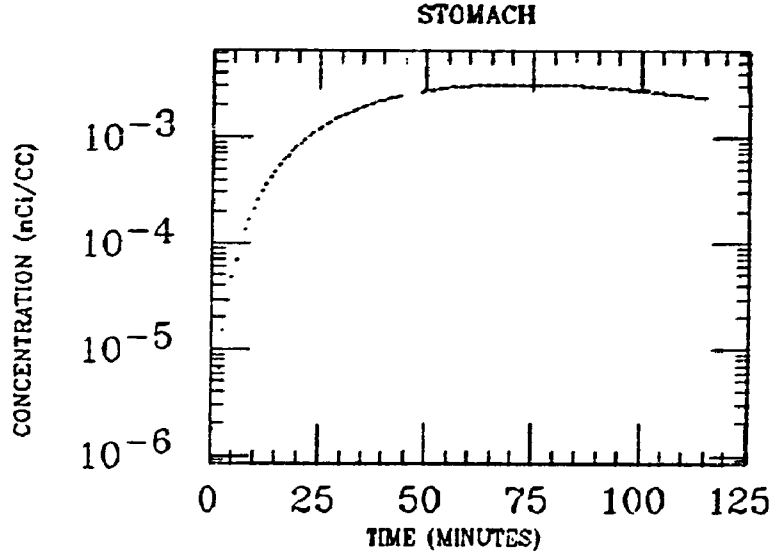

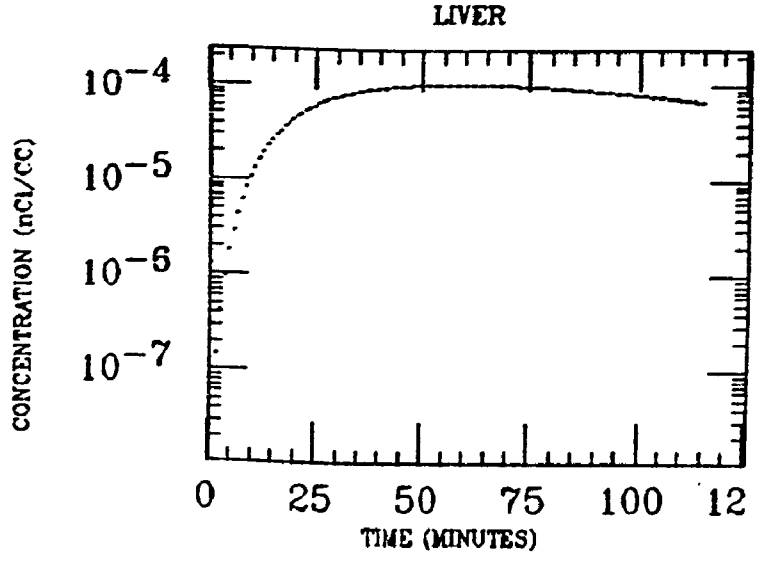

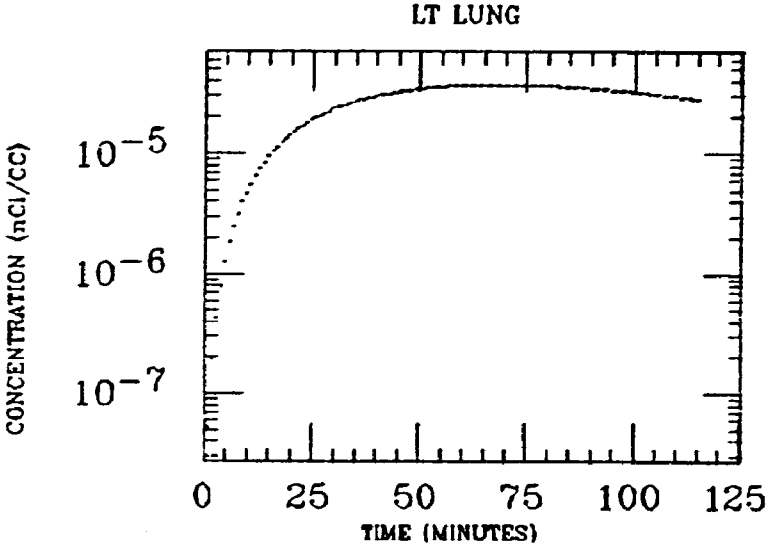

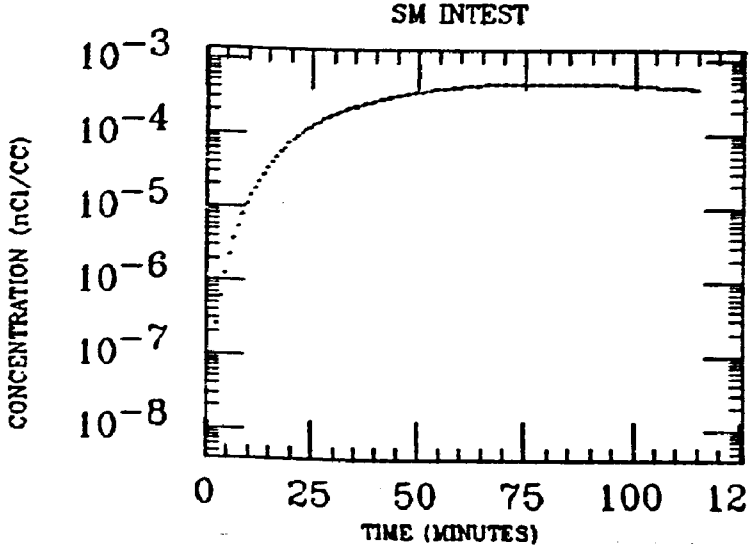

BROCK
XE INGESTION
Bi-214

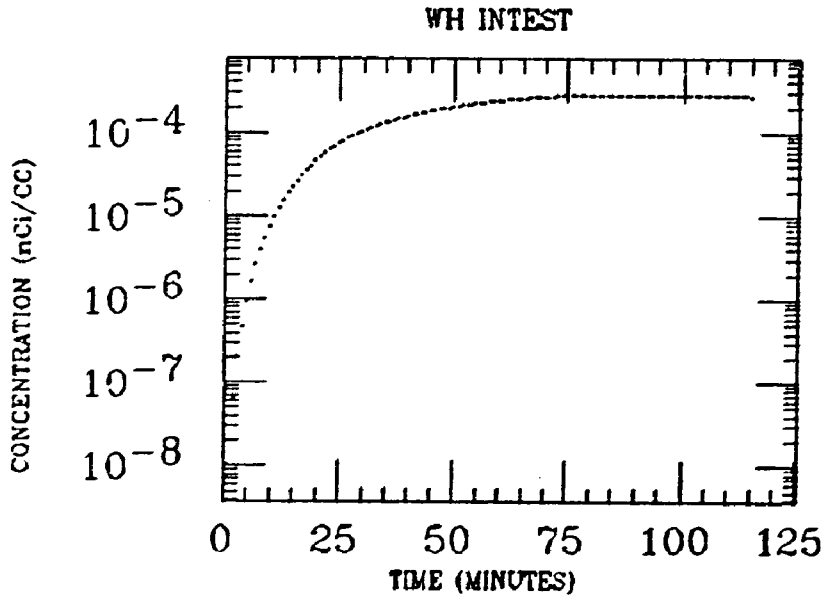

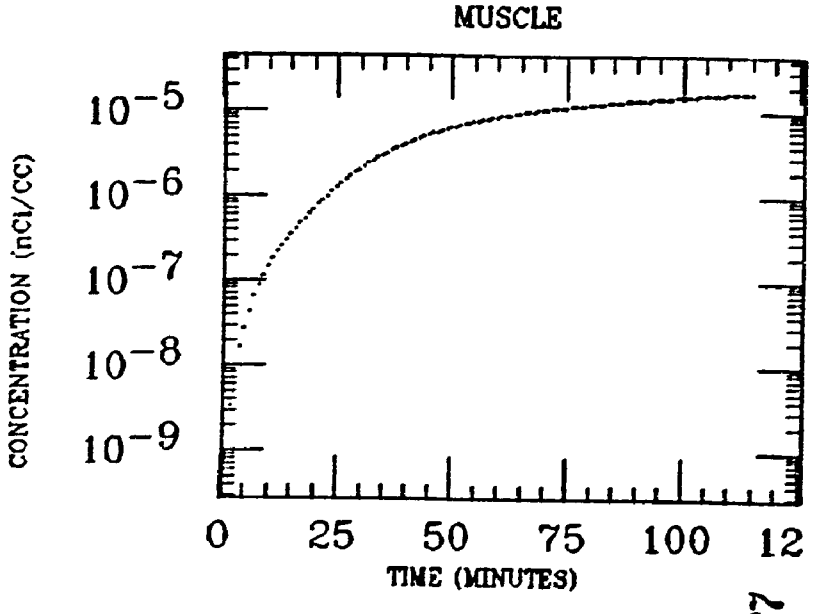

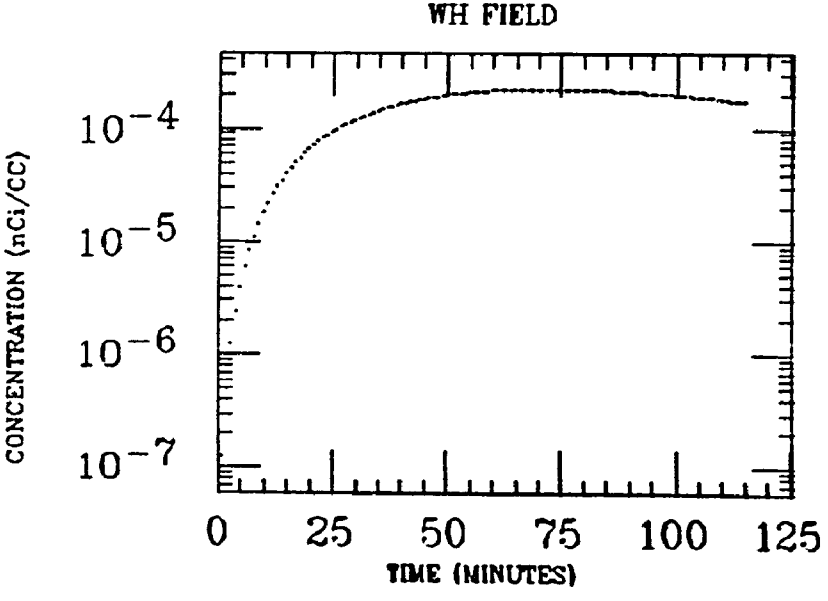

BYRNE
XE INGESTION
Bi-214

STOMACH

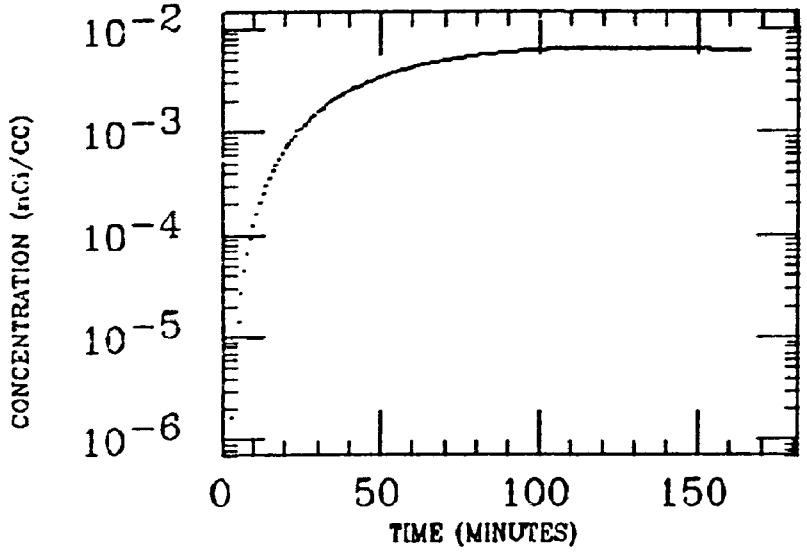

LIVER

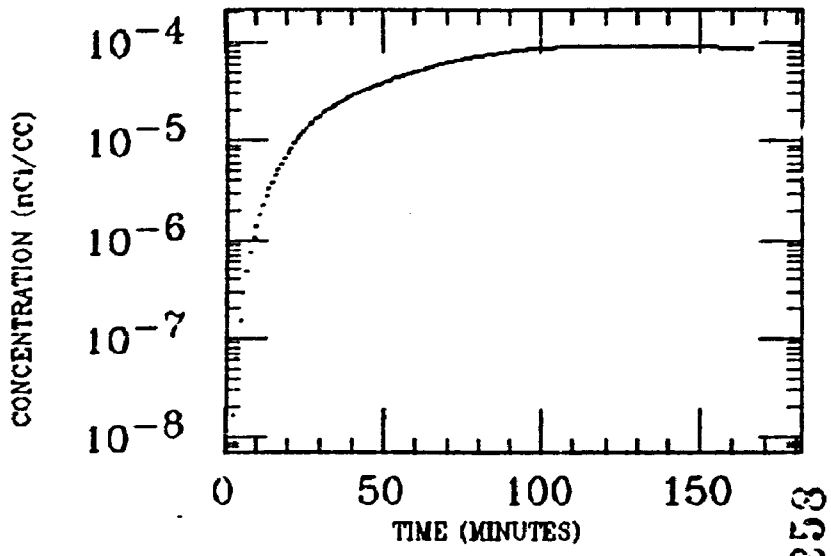

WH INTEST

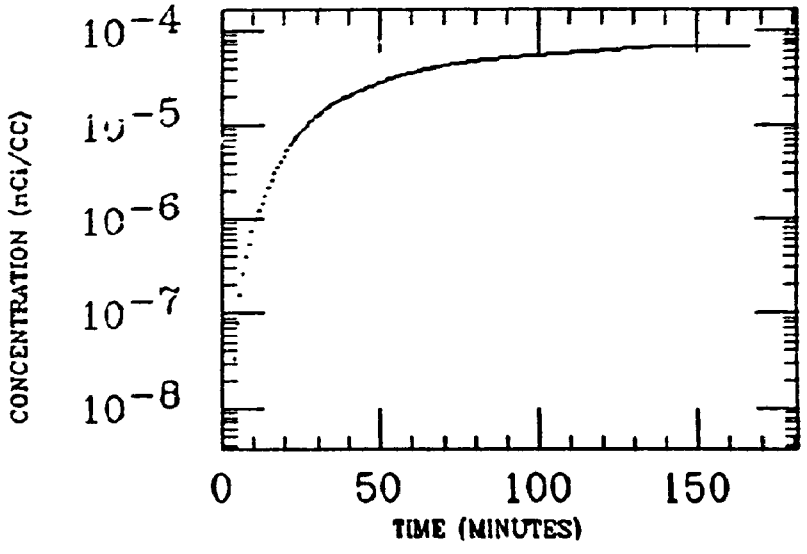

MUSCLE

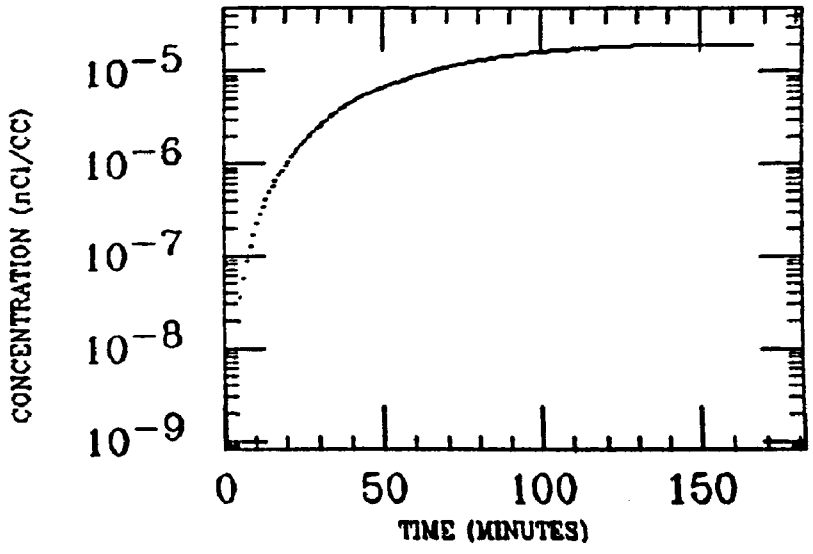

BYRNE
XE INGESTION
Bi-214

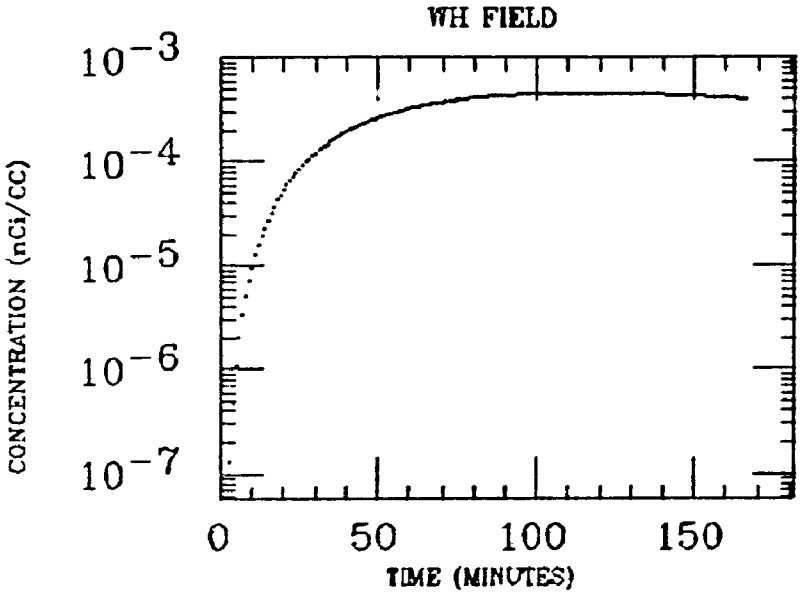

CLINE
XE INGESTION
Bi-214

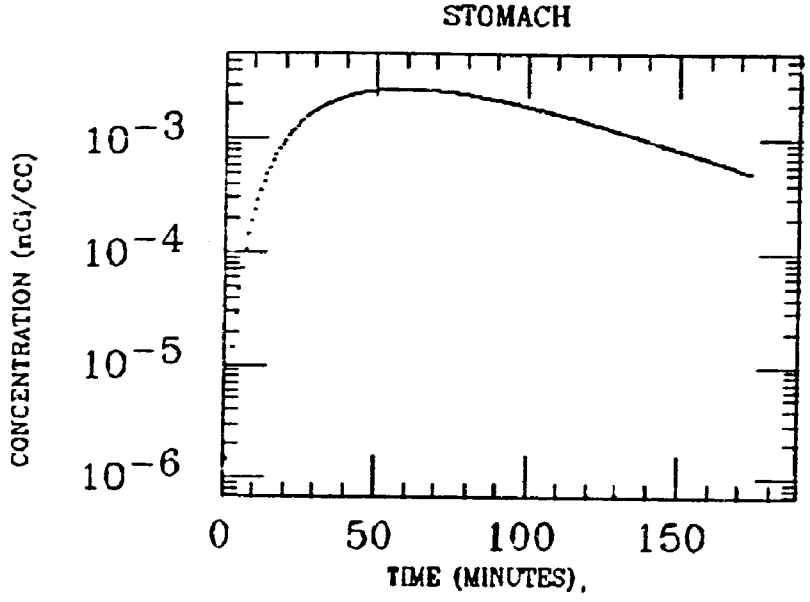

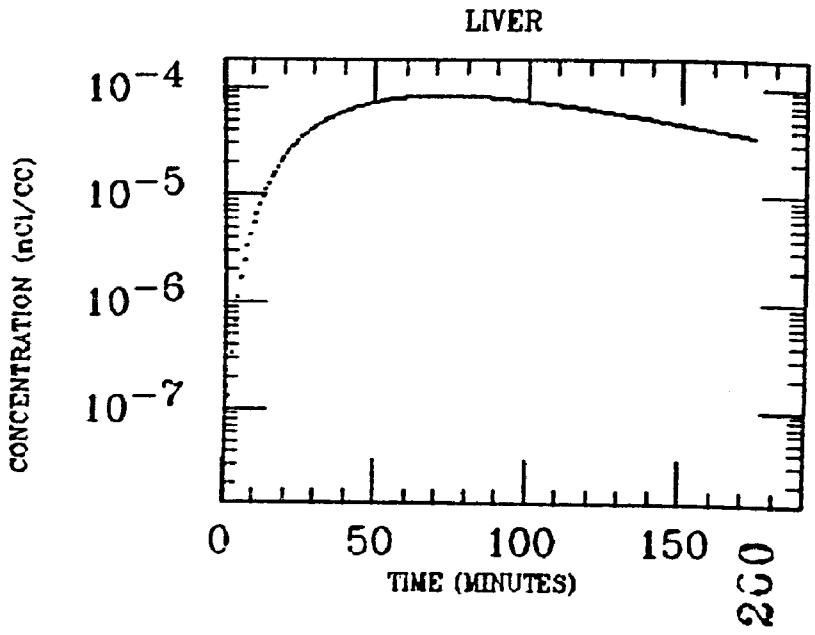

260

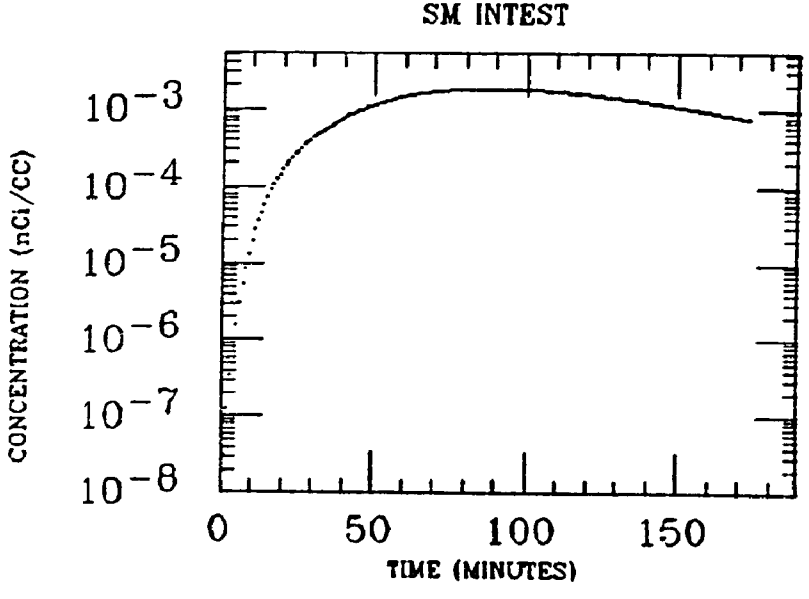

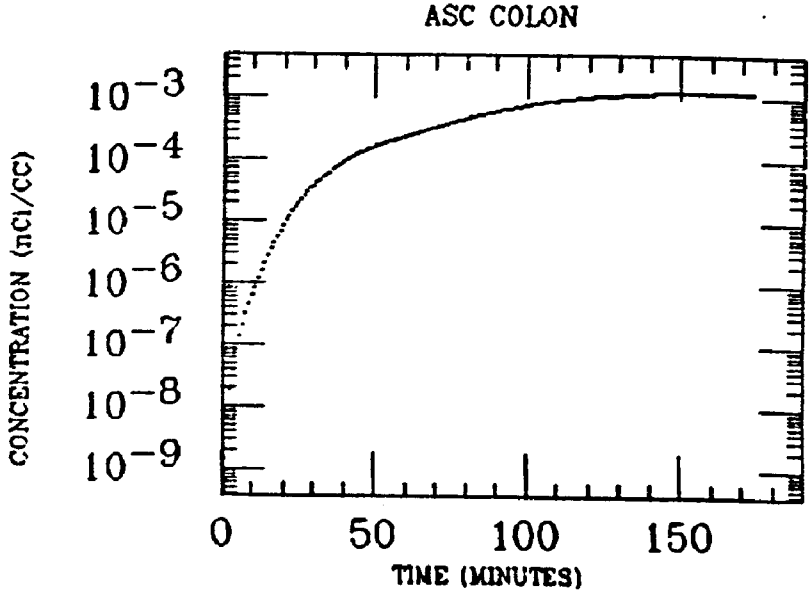

CLINE
XE INGESTION
Bi-214

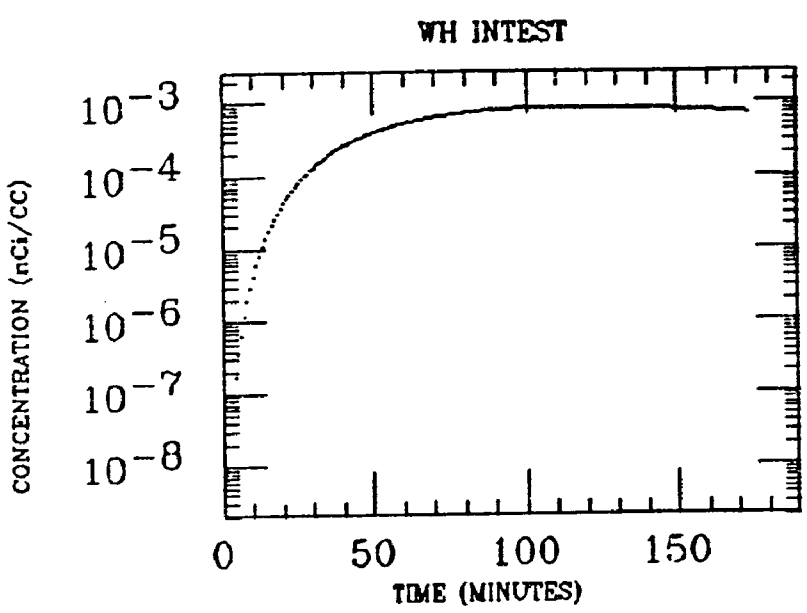

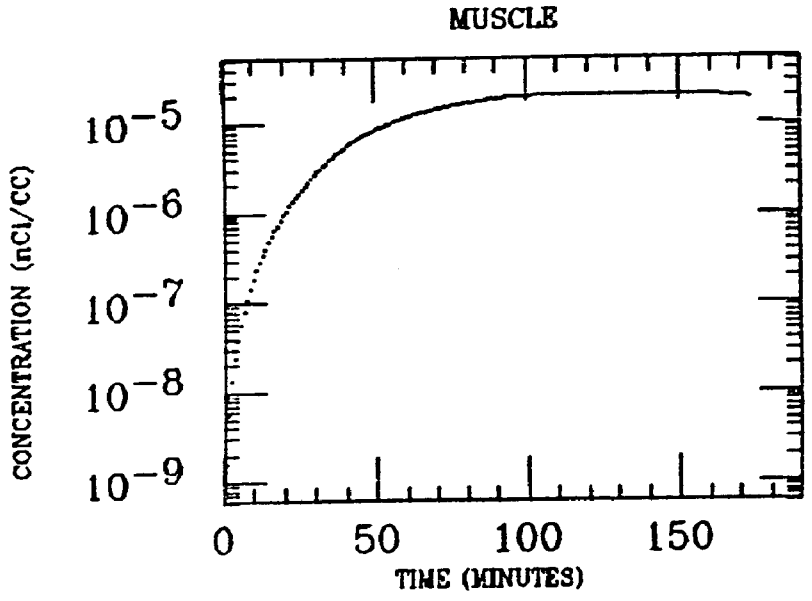

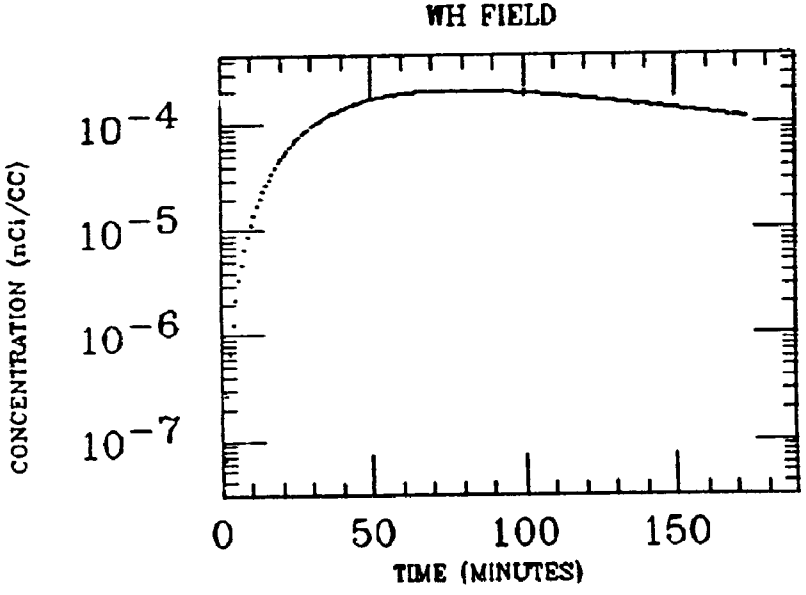

ELMDEN
XE INGESTION
Bi-214

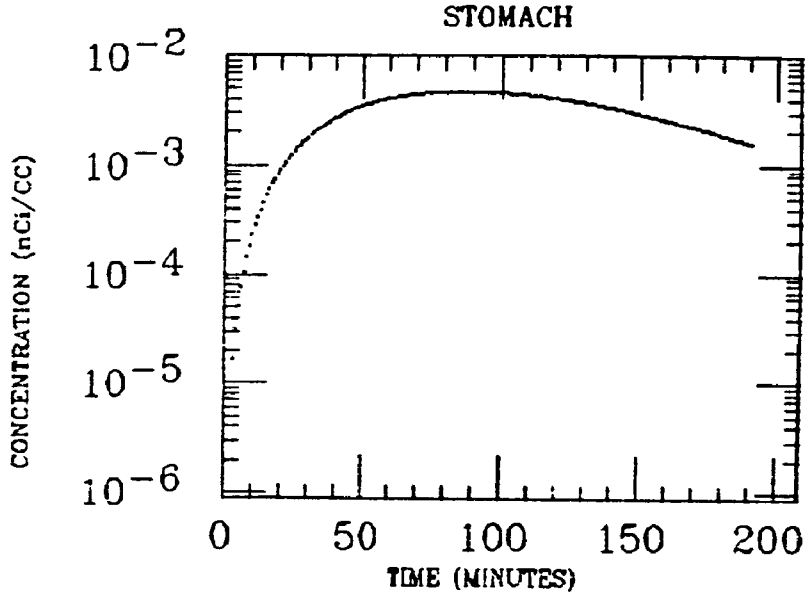

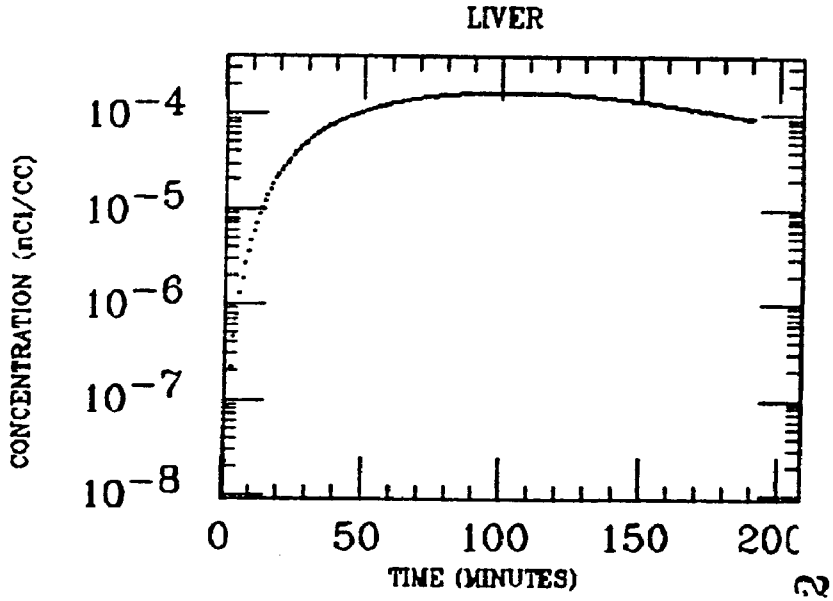

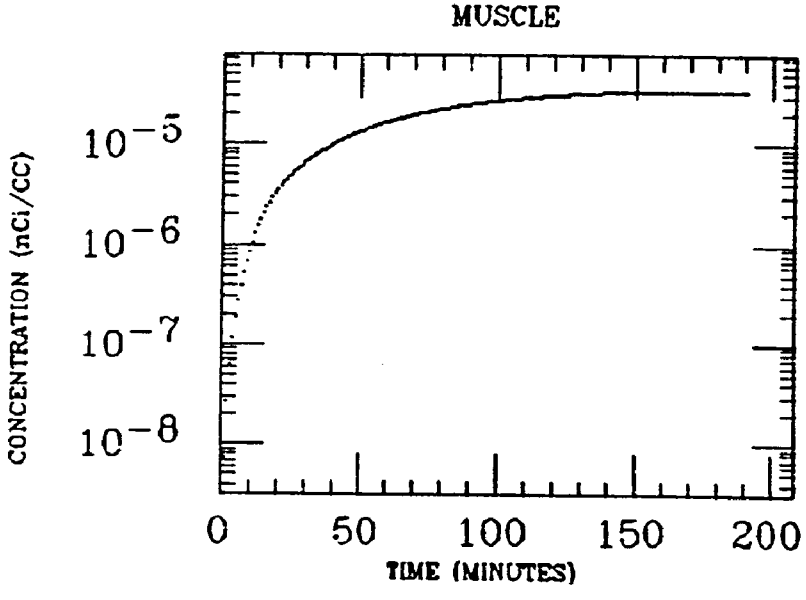

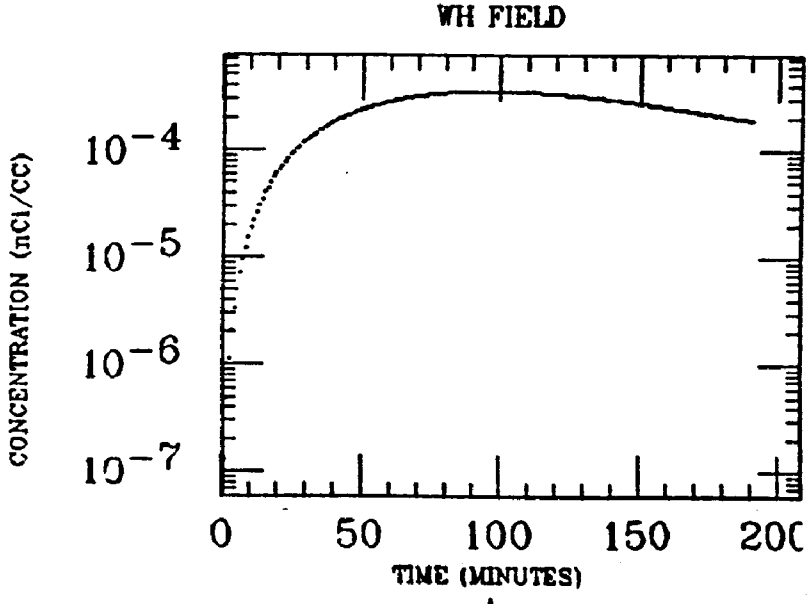

ELMDEN
XE INGESTION
Bi-214

STOMACH

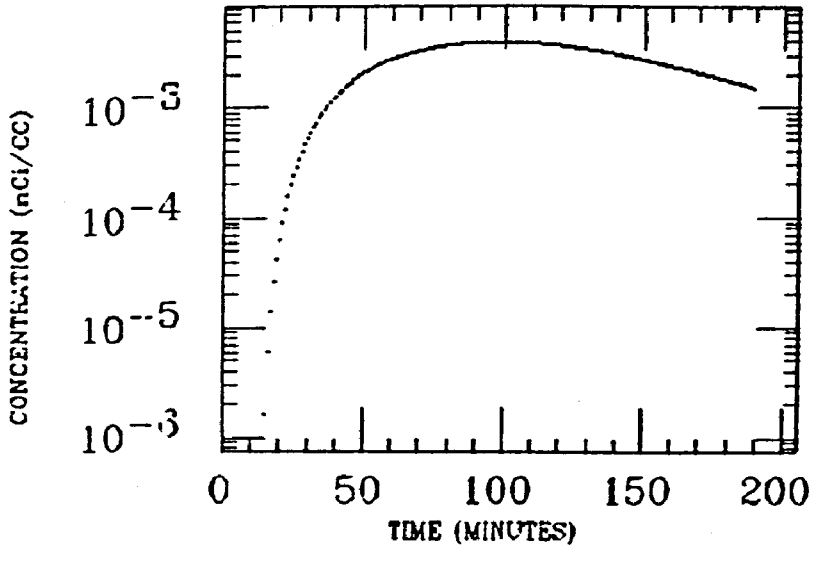

LIVER

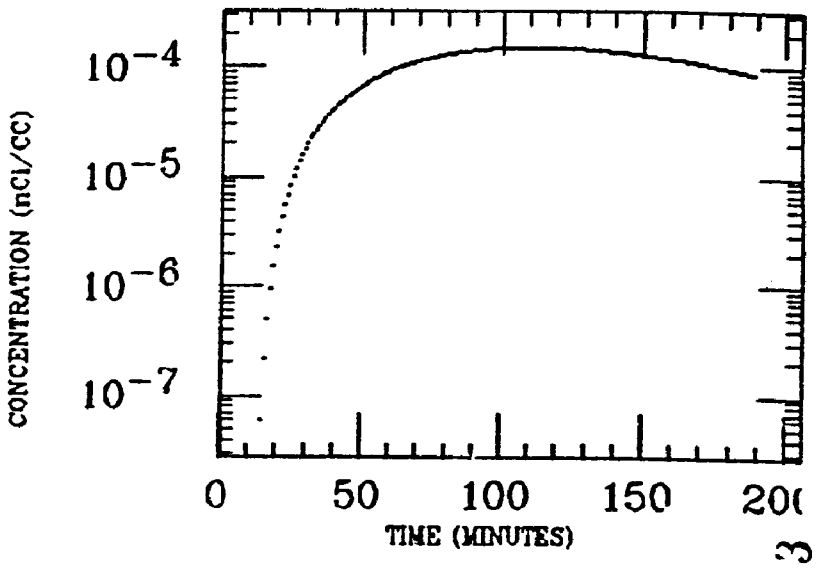

263

SM INTEST

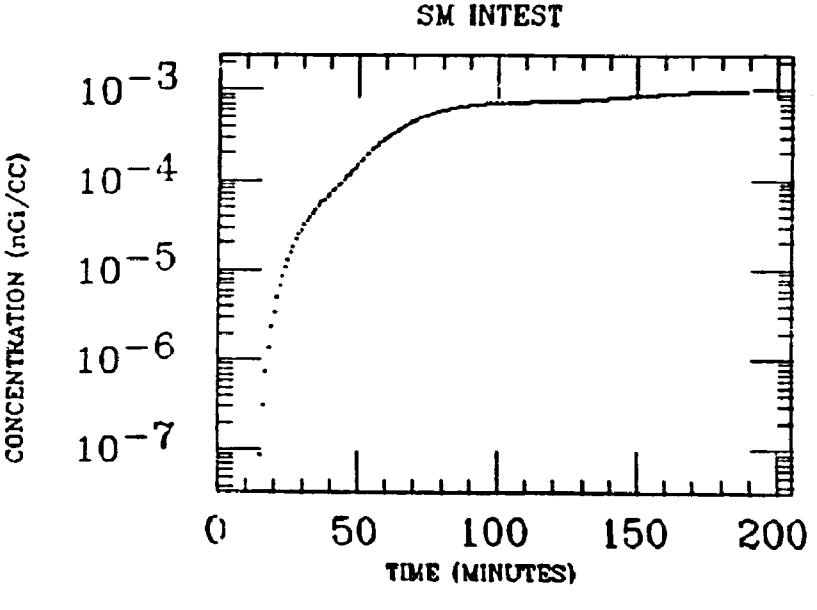

DES COLON

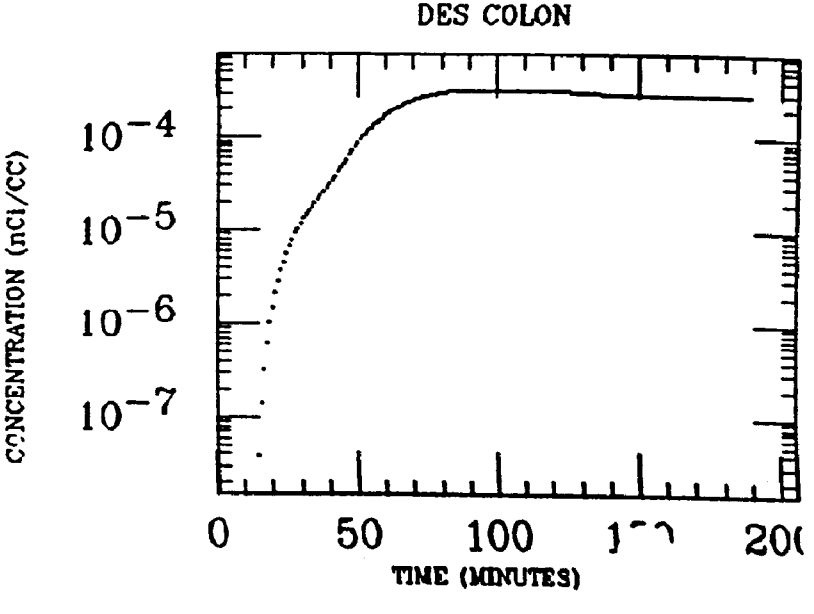

ELMDEN
XE INGESTION
Bi-214

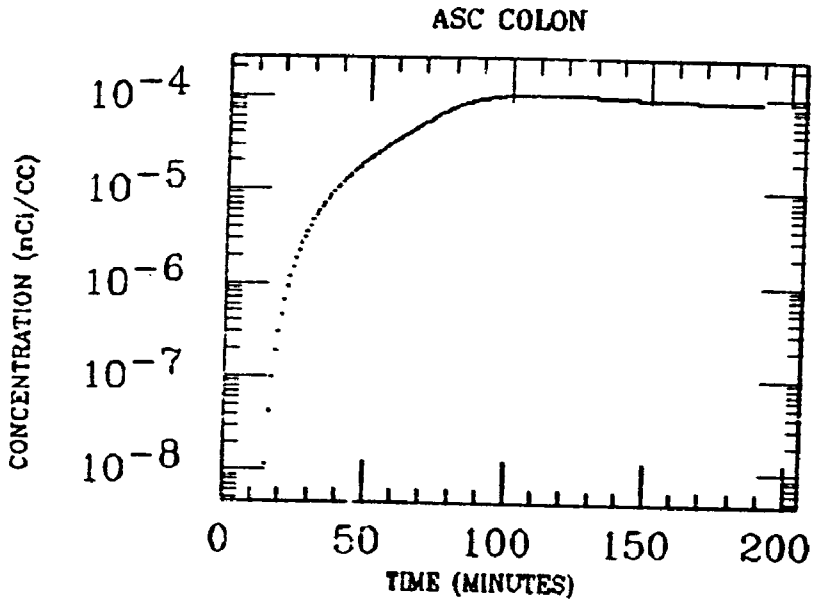

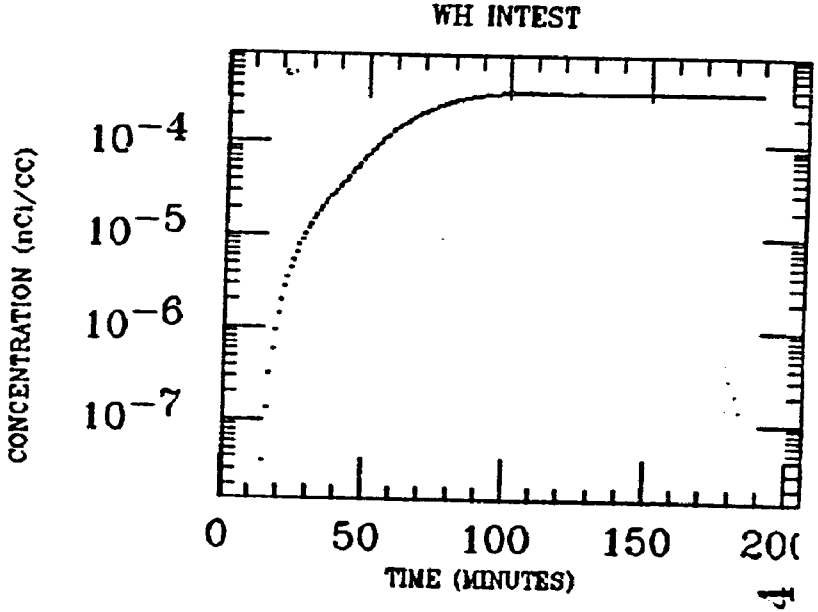

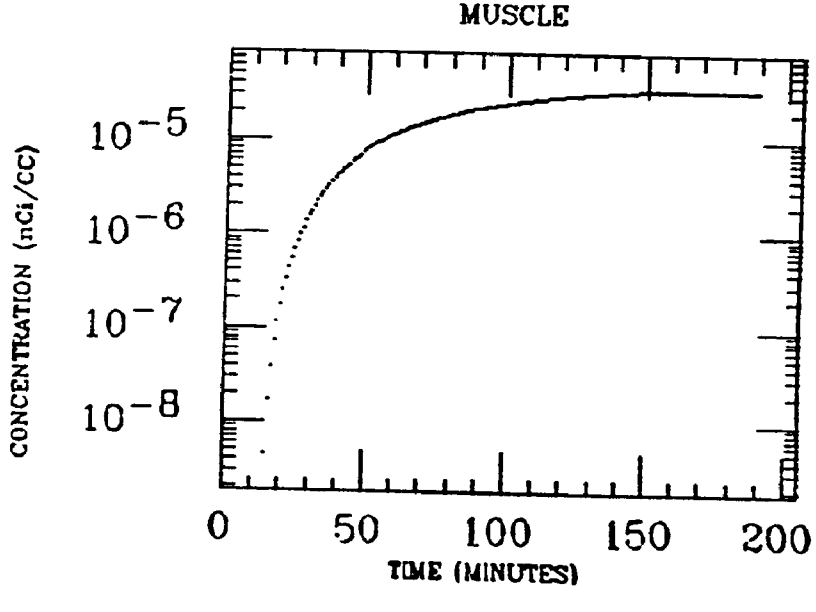

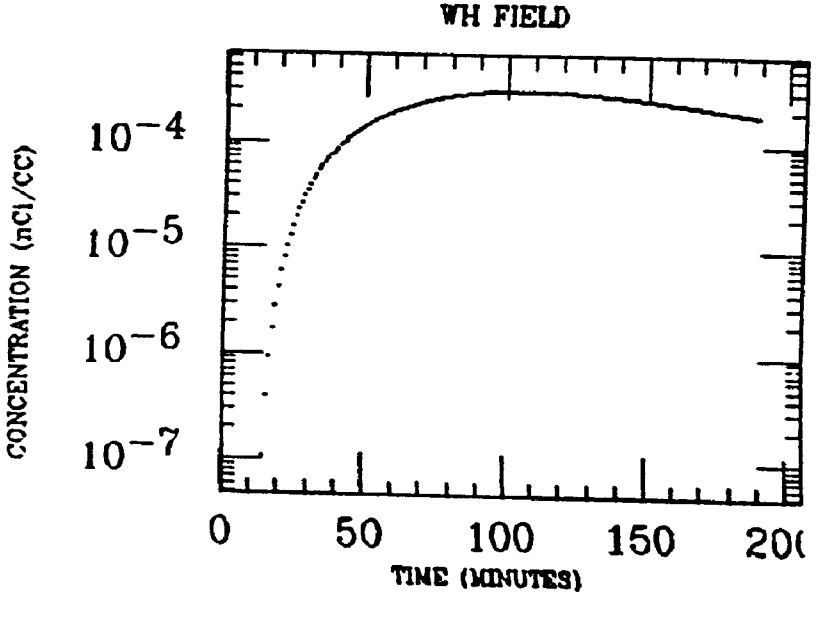

EPLING
XE INGESTION
Bi-214

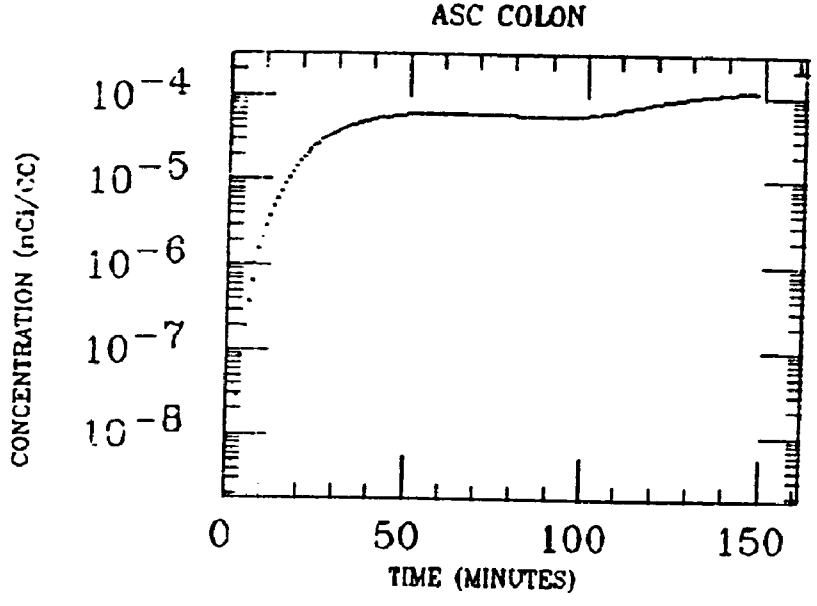

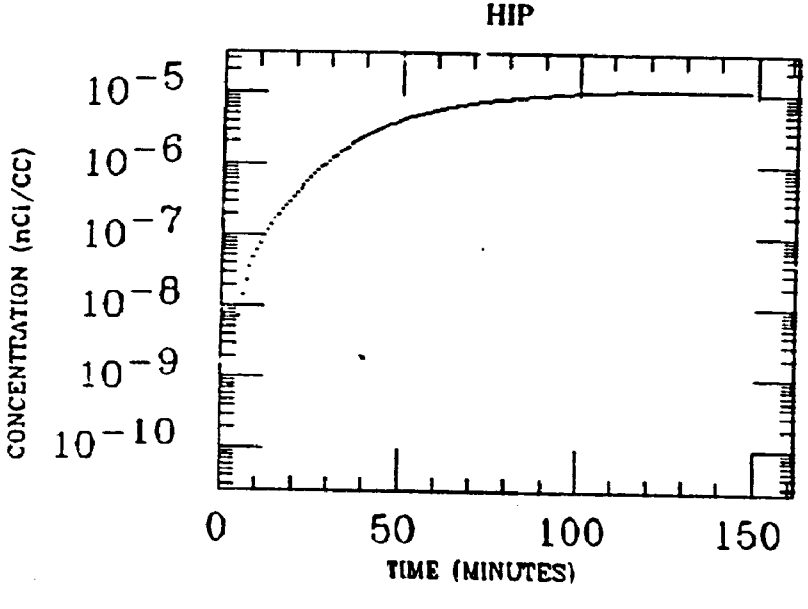

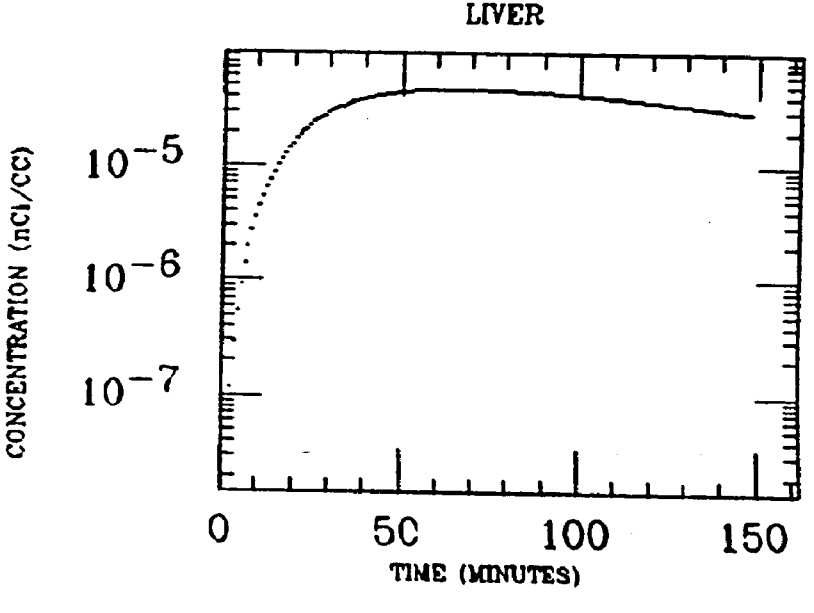

EPLING
XE INGESTION
Bi-214

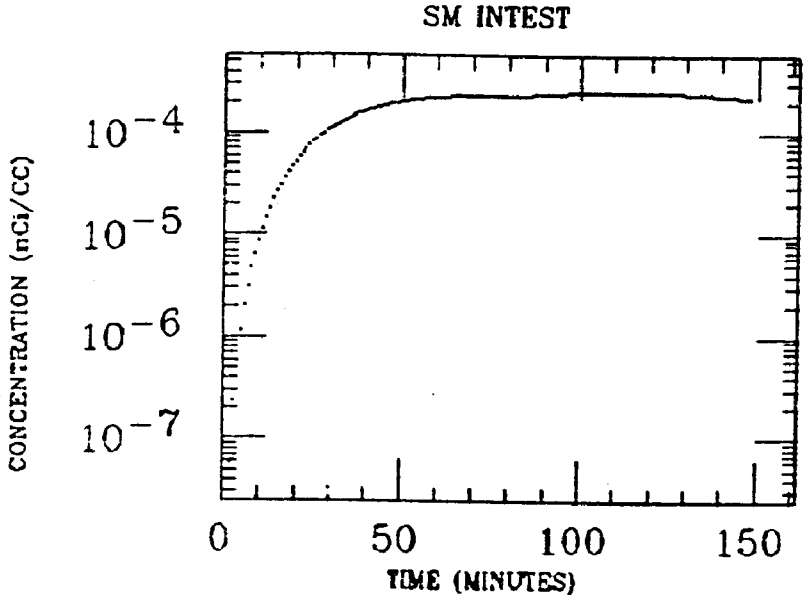

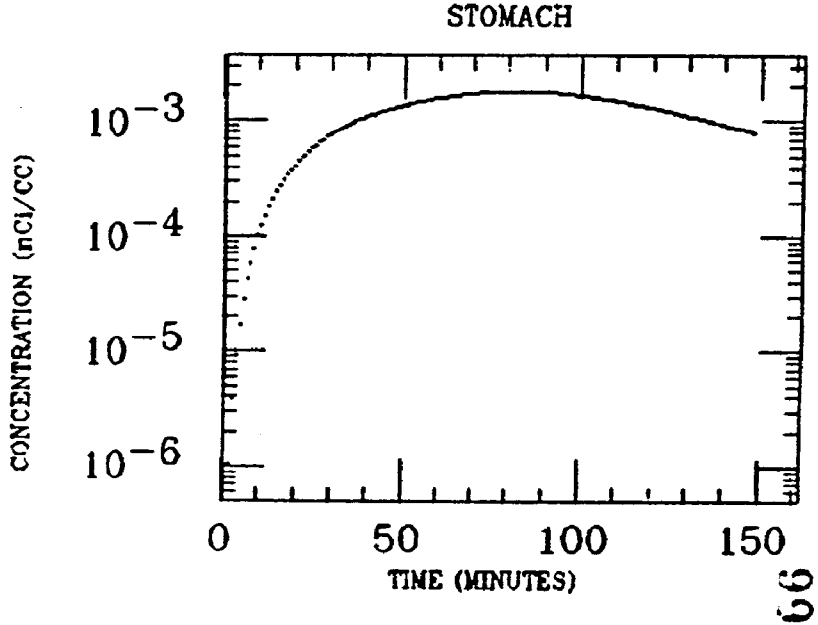

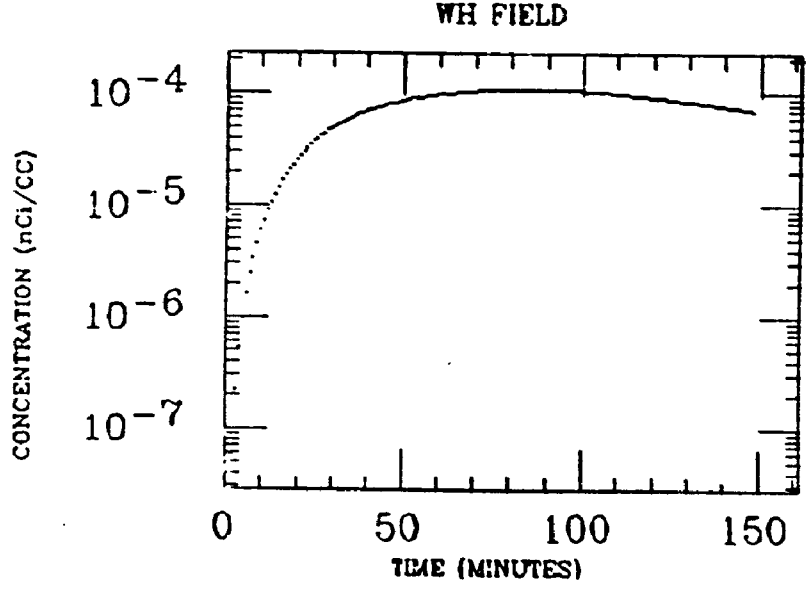

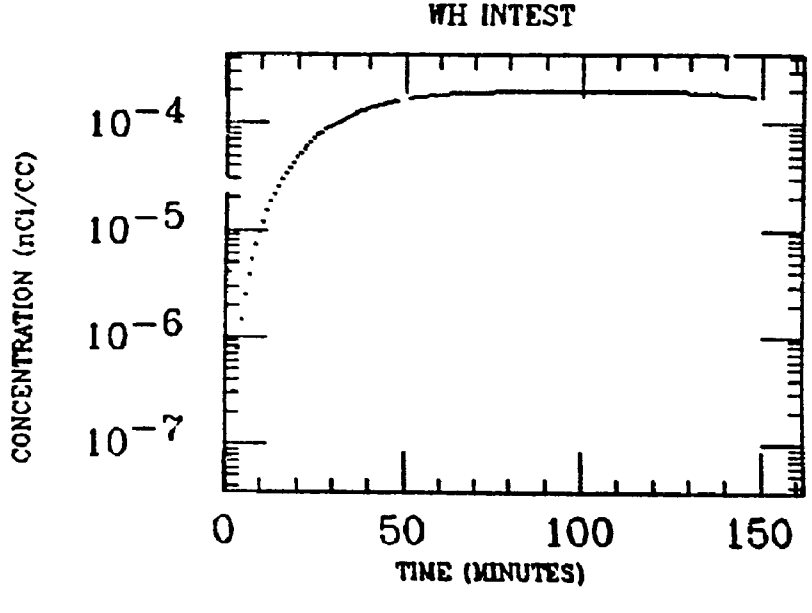

GALLOP
XE INGESTION
Bi-214

STOMACH

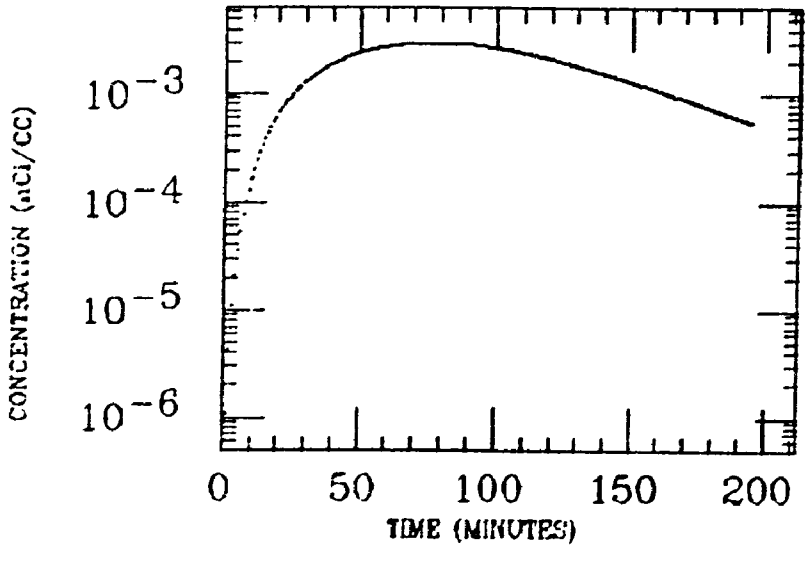

MUSCLE

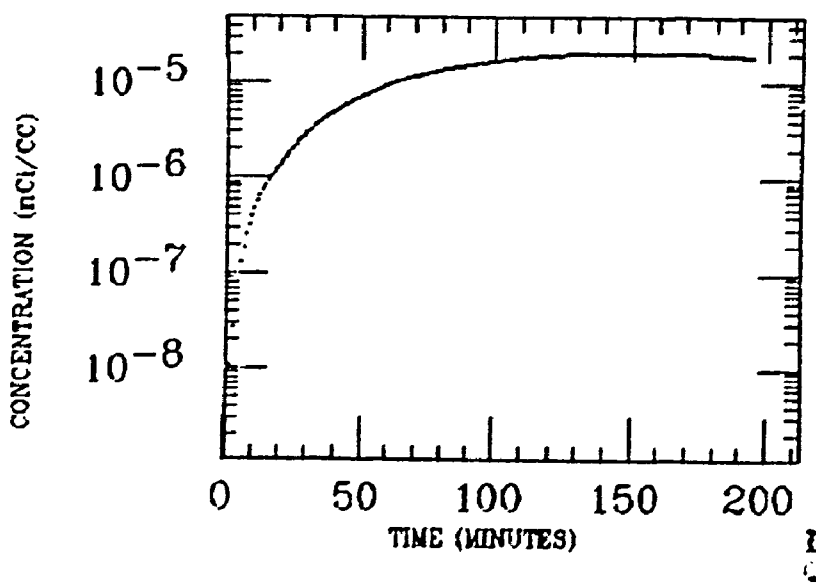

LIVER

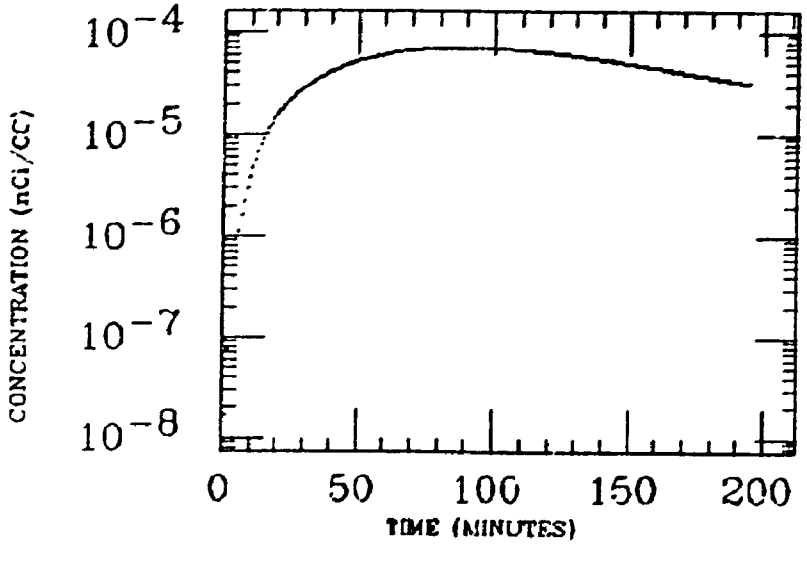

WH FIELD

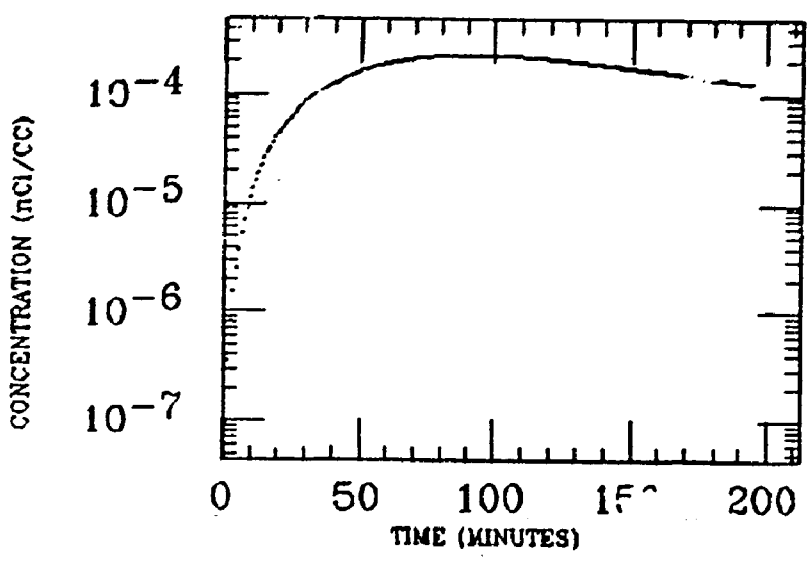

267

GALLOP
XE INGESTION
Bi-214

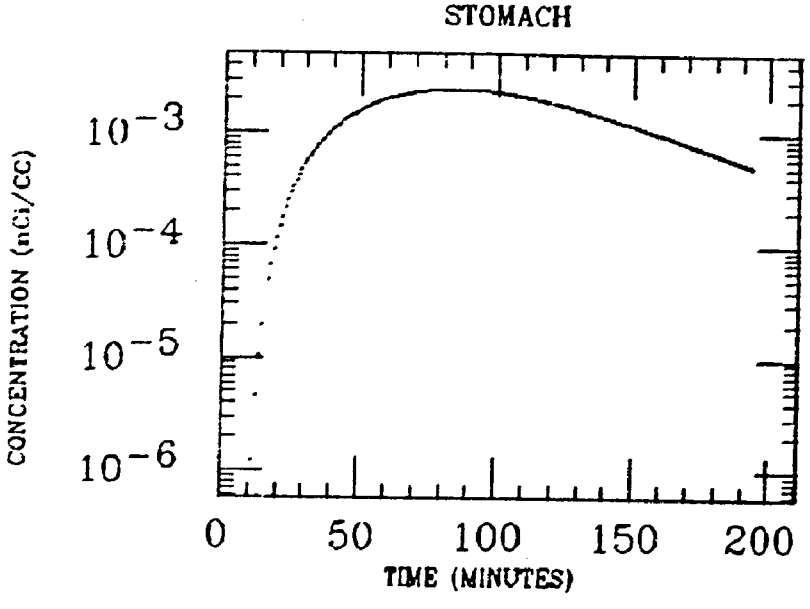

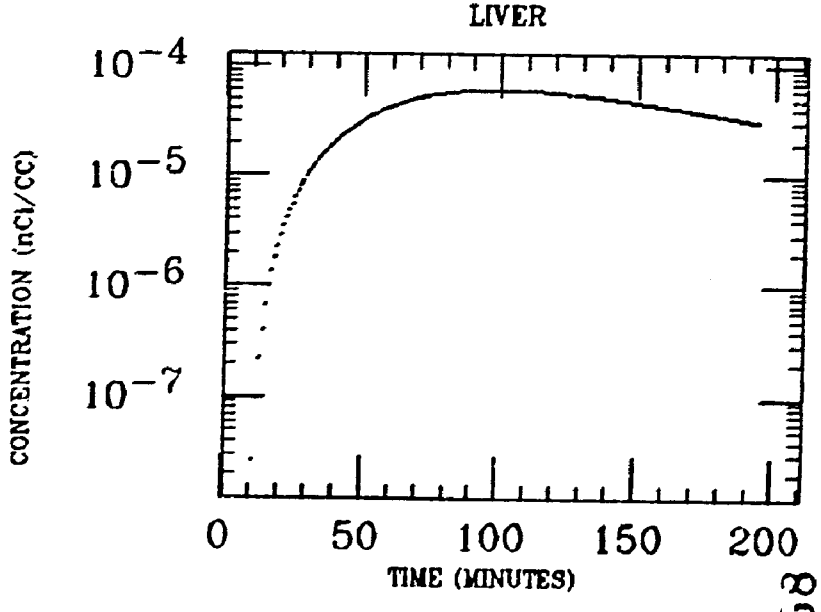

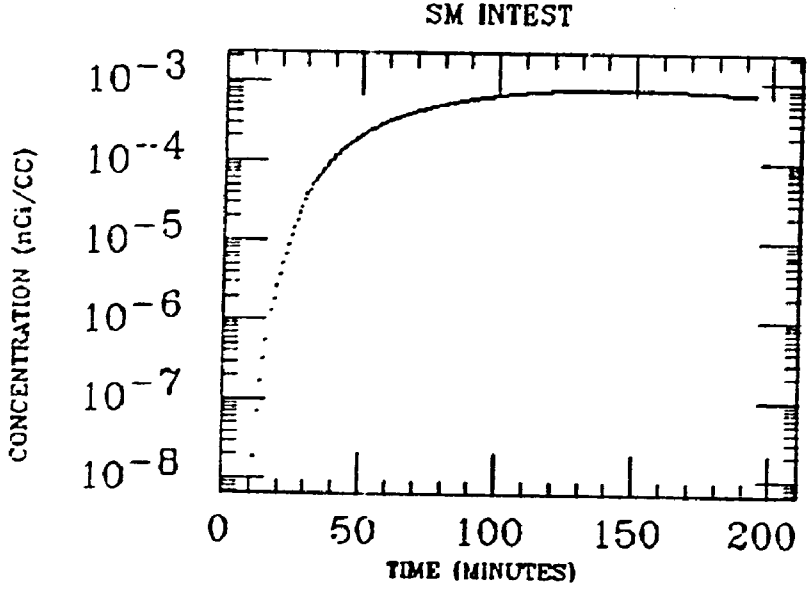

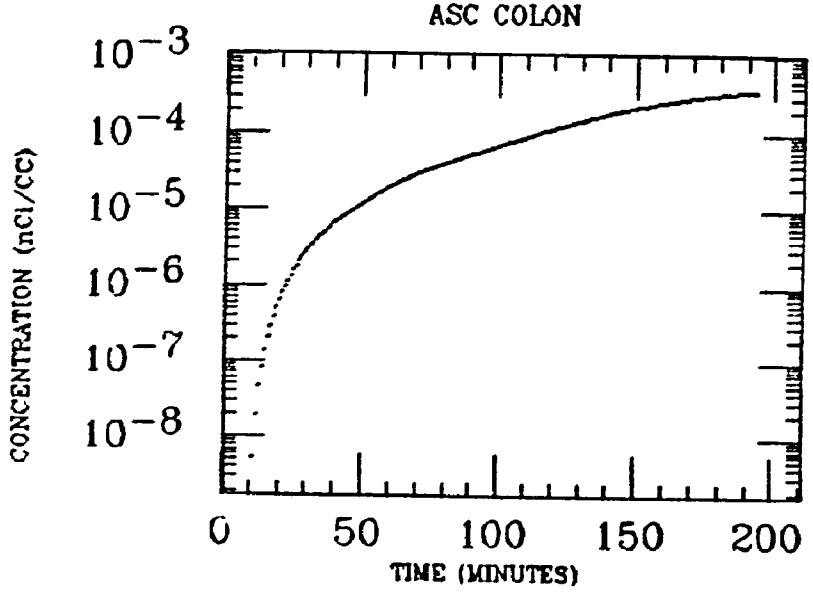

C.MCKINLEY
XE INGESTION
Bi-214

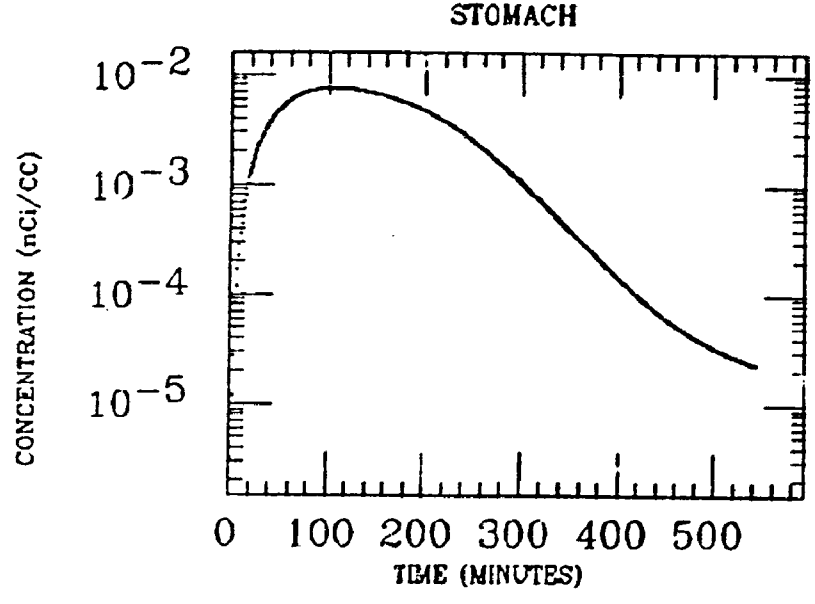

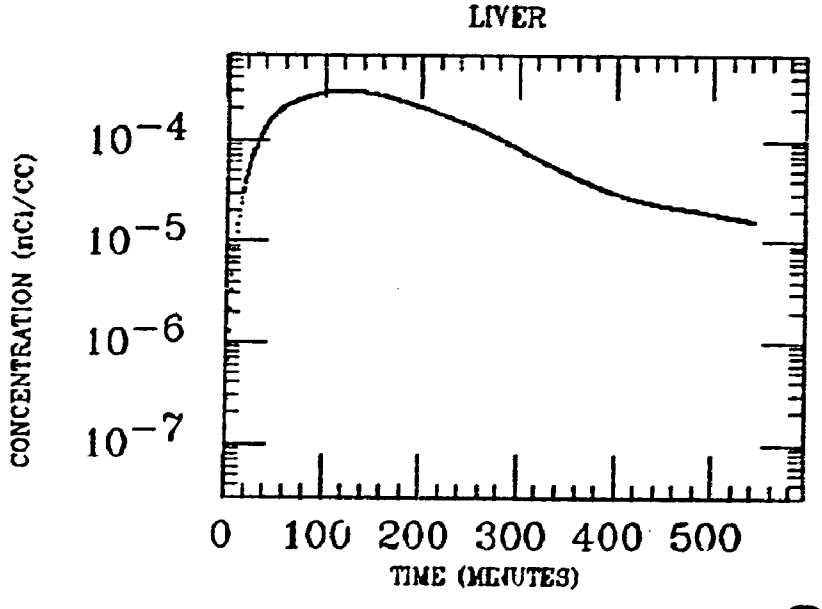

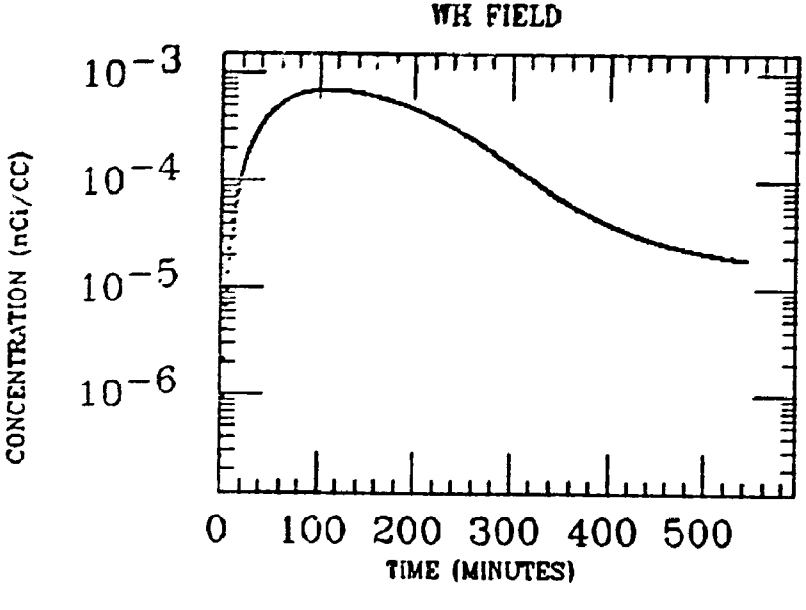

269

G.MCKINLEY
XE INGESTION
Bi-214

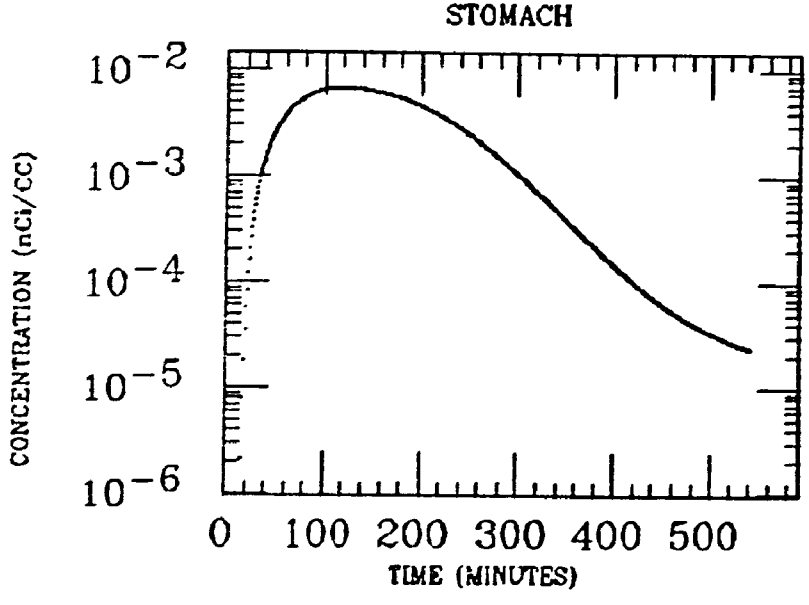

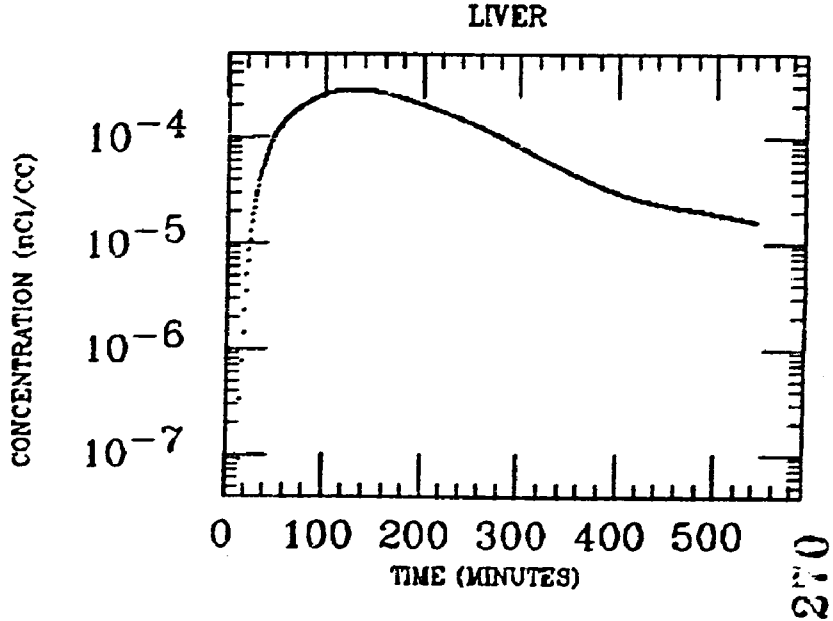

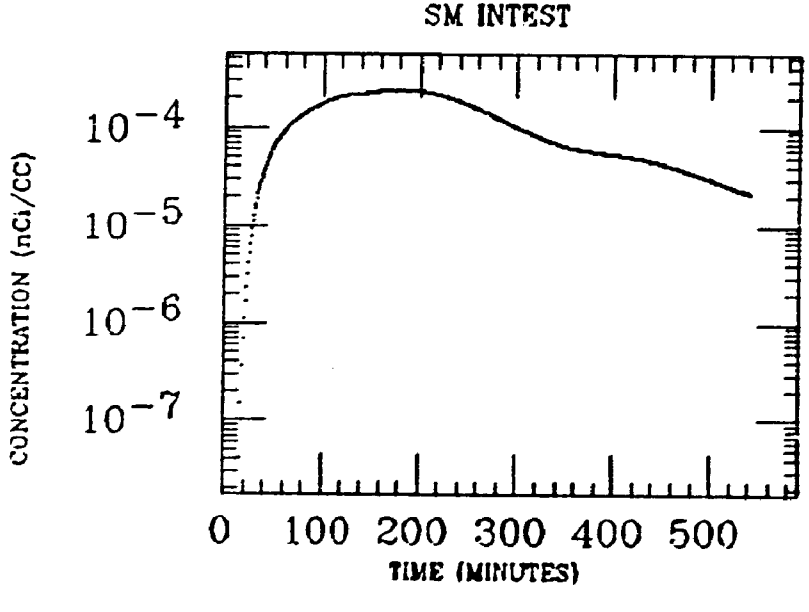

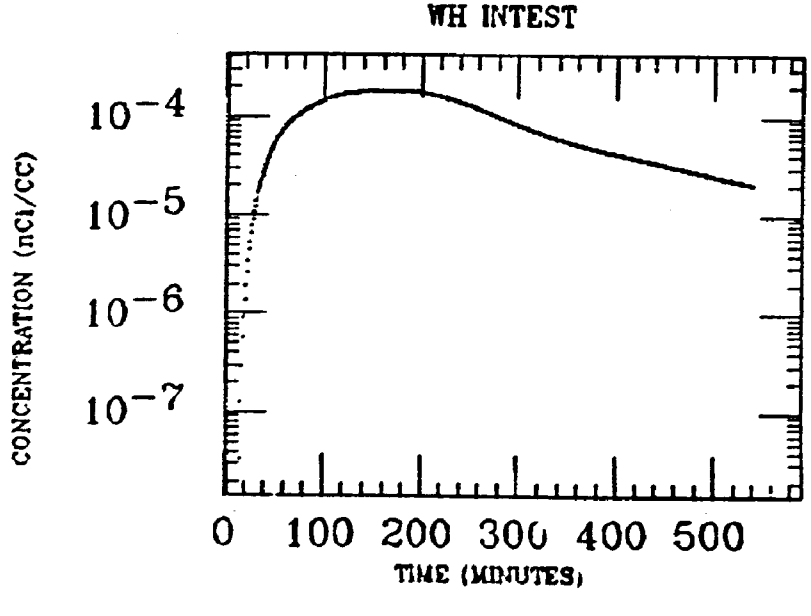

C.MCKINLEY
XE INGESTION
Bi-214

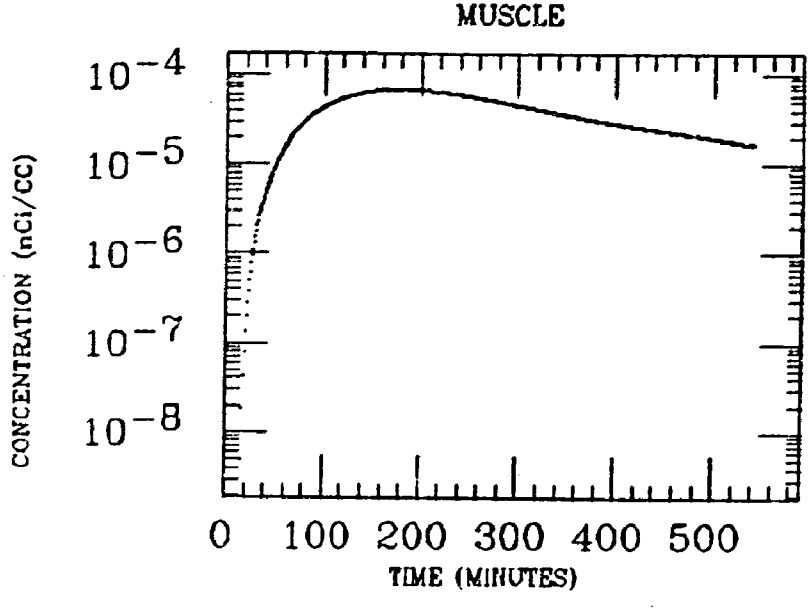

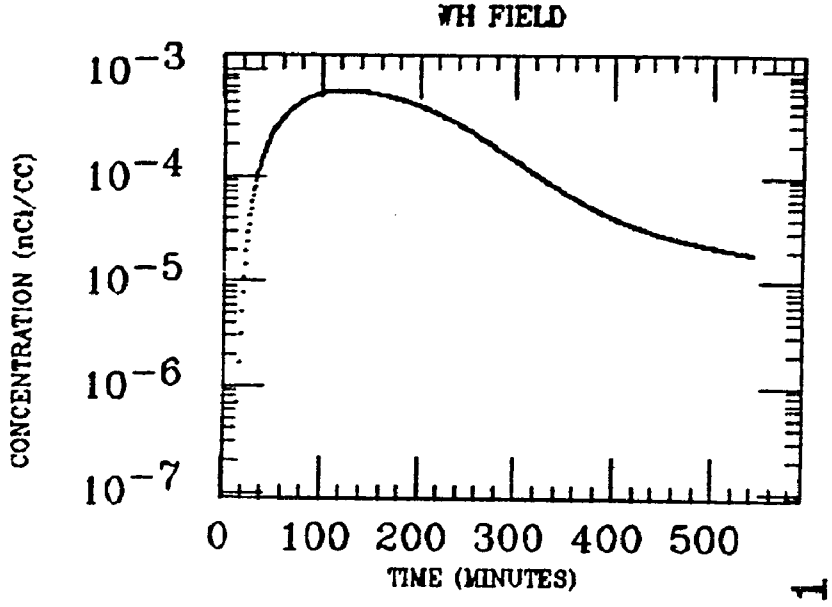

271

HAND
XE INGESTION
Bi-214

STOMACH

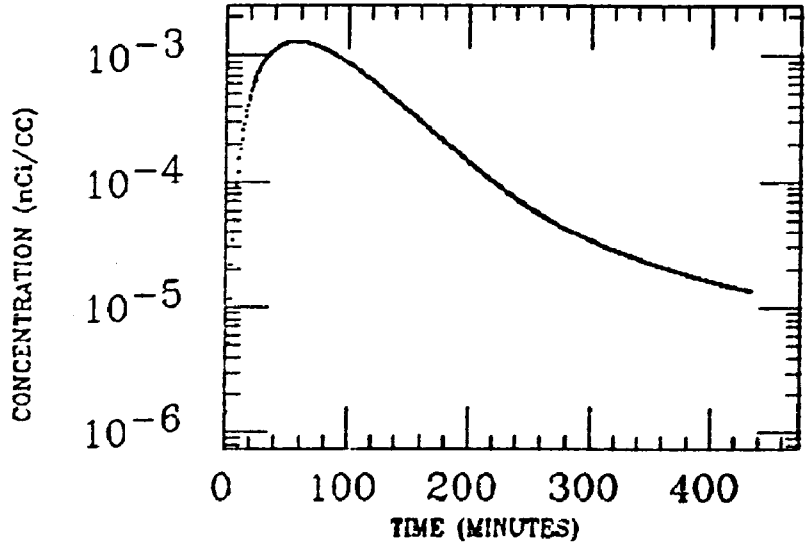

LIVER

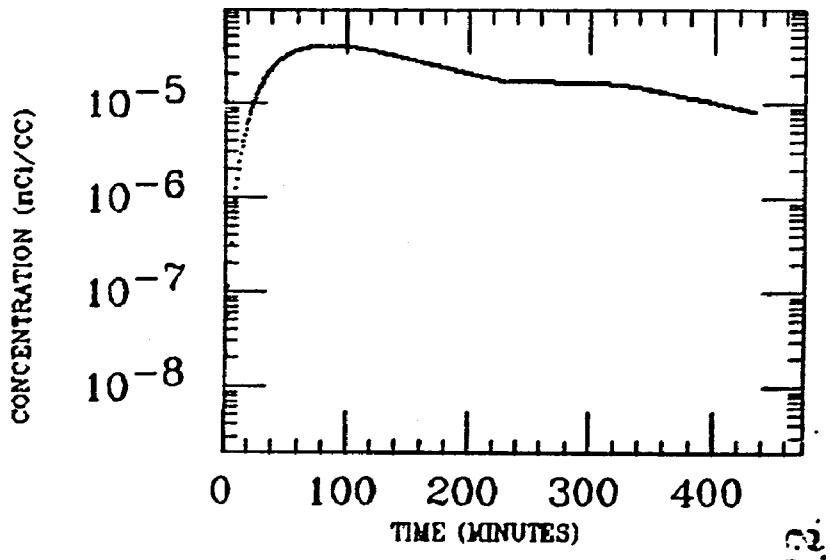

LT LUNG

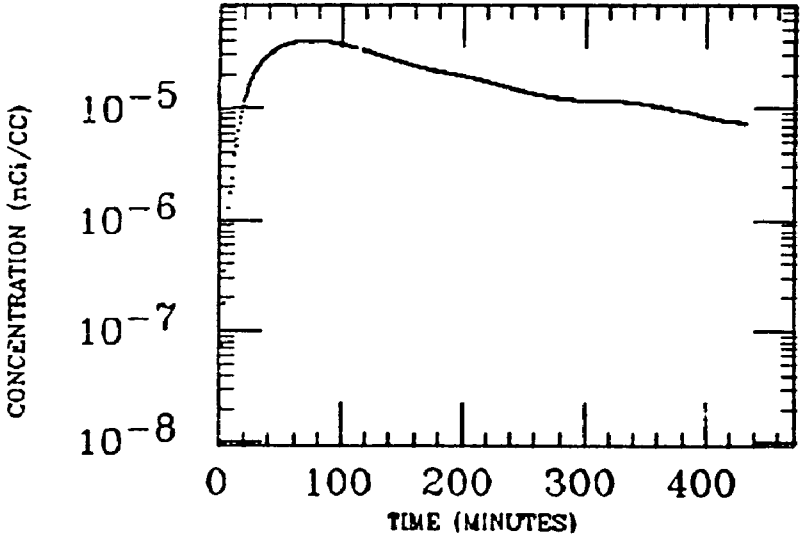

WH INTEST

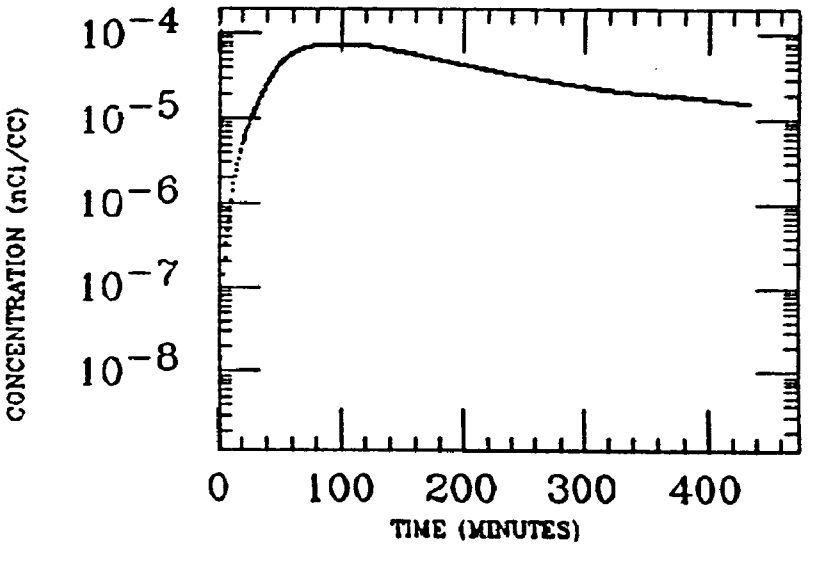

212.

HAND

XE INGESTION

Bi-214

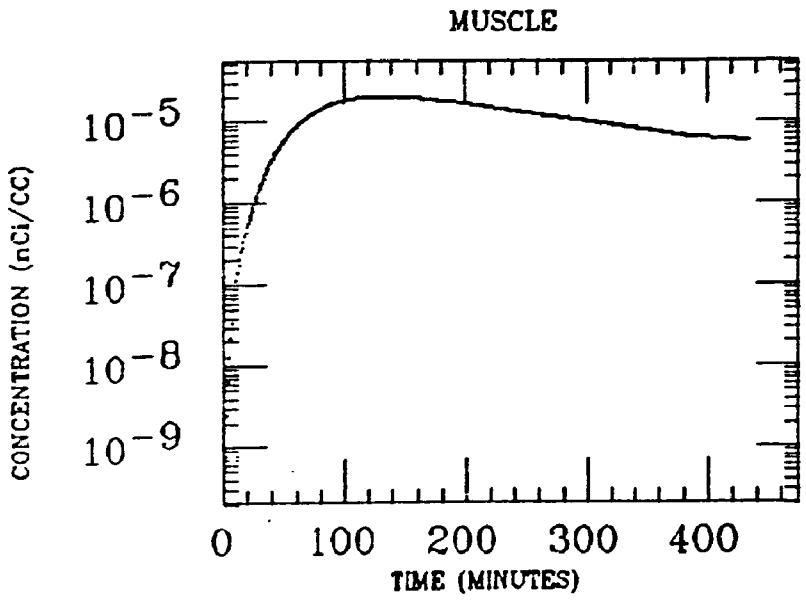

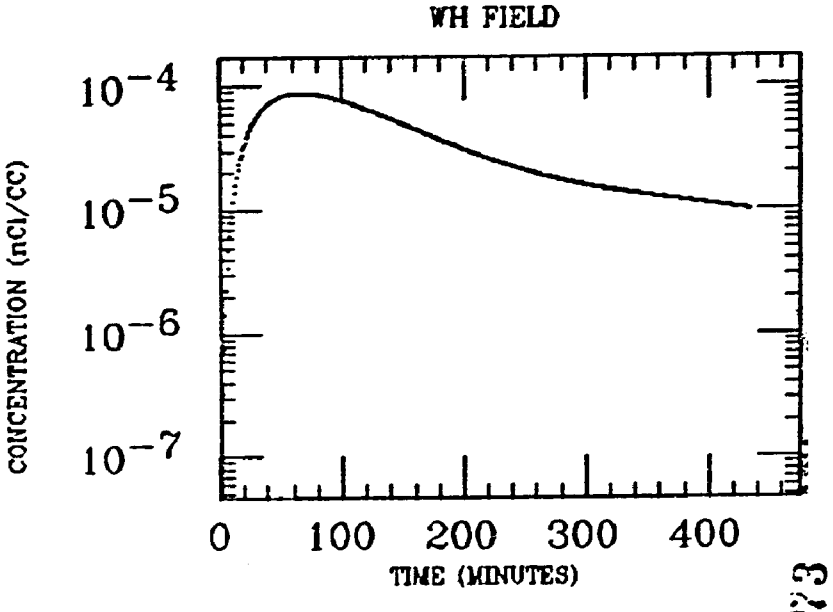

XE INGESTION

Bi-214

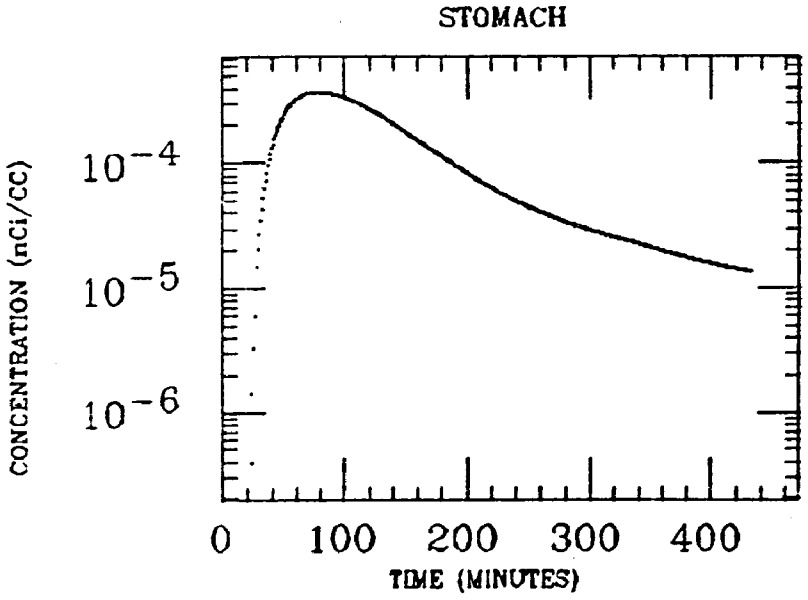

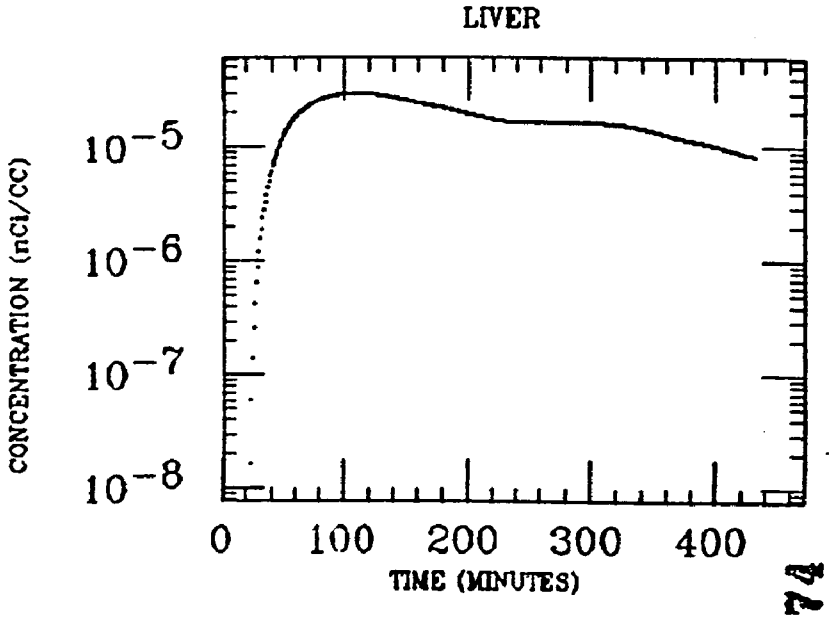

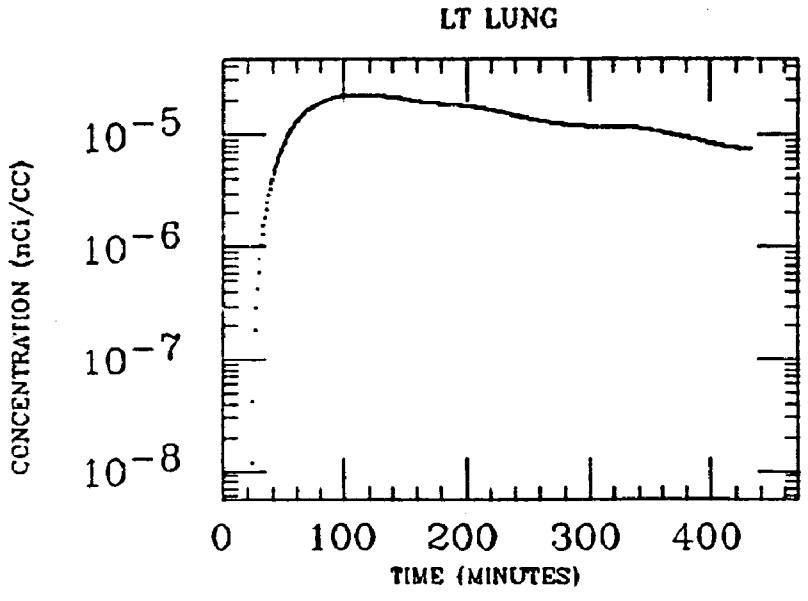

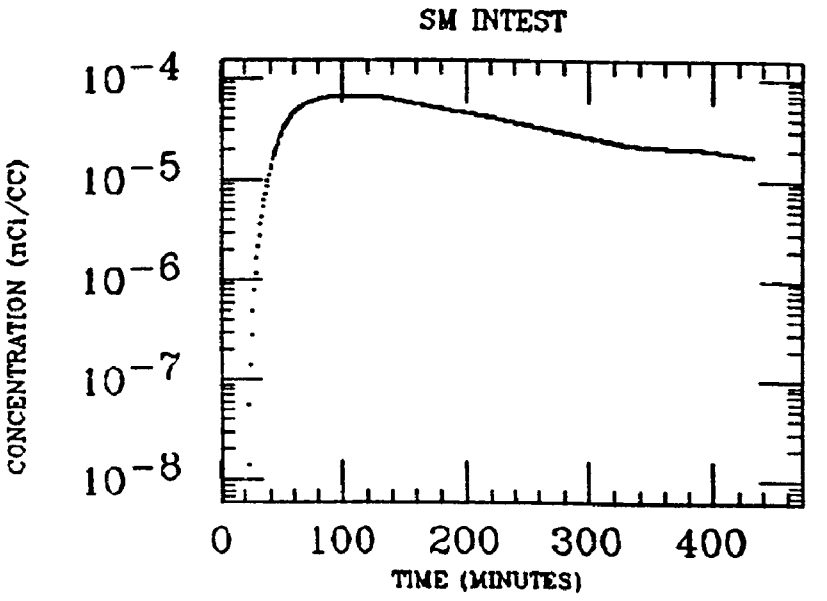

HAND
XE INGESTION
Bi-214

ASC COLON

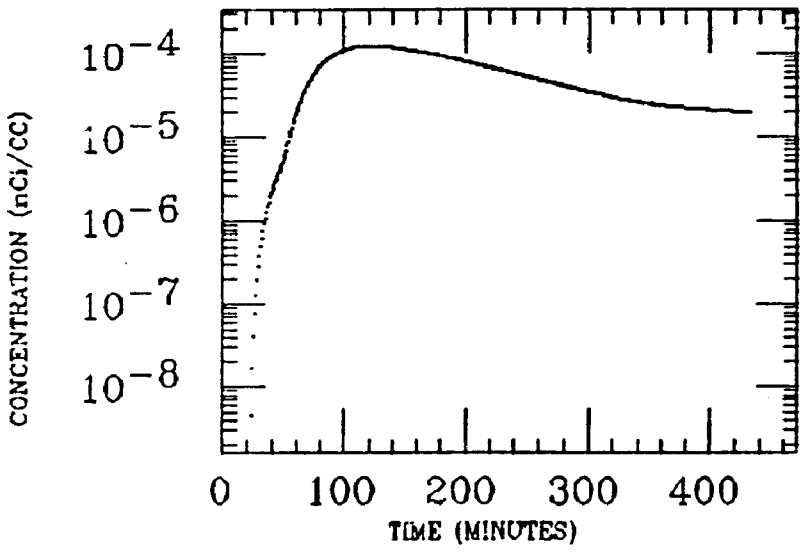

WH INTEST

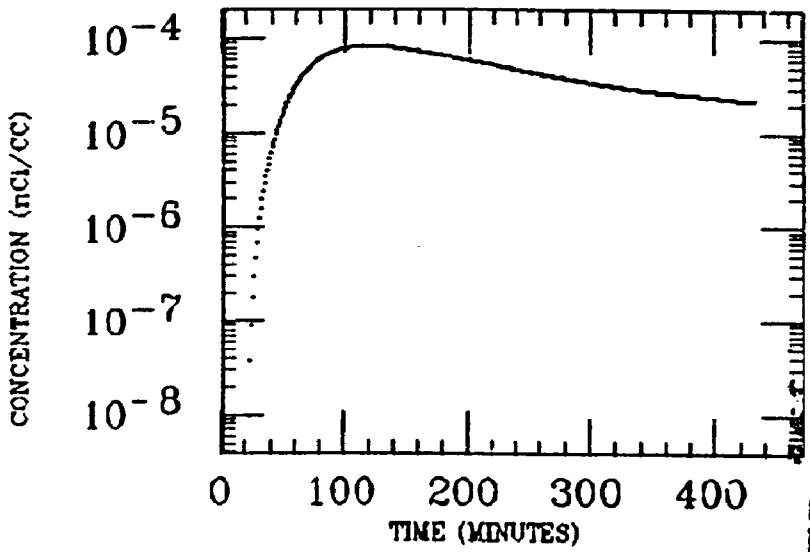

MUSCLE

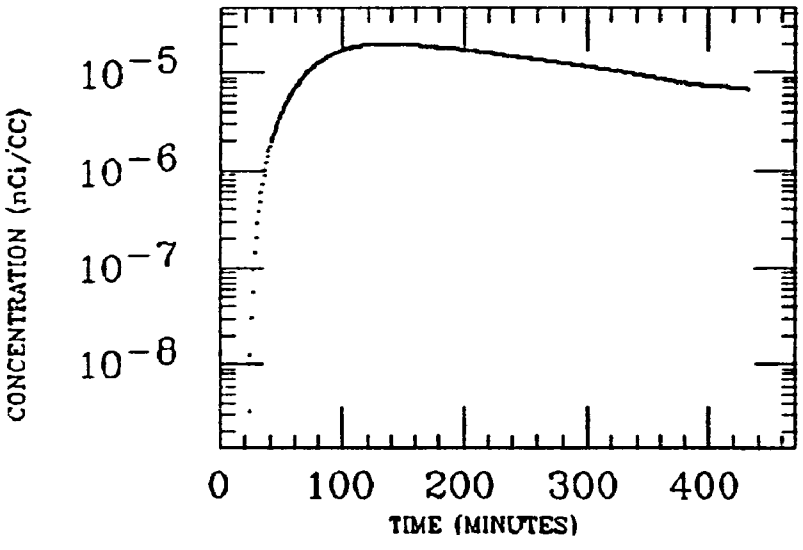

WH FIELD

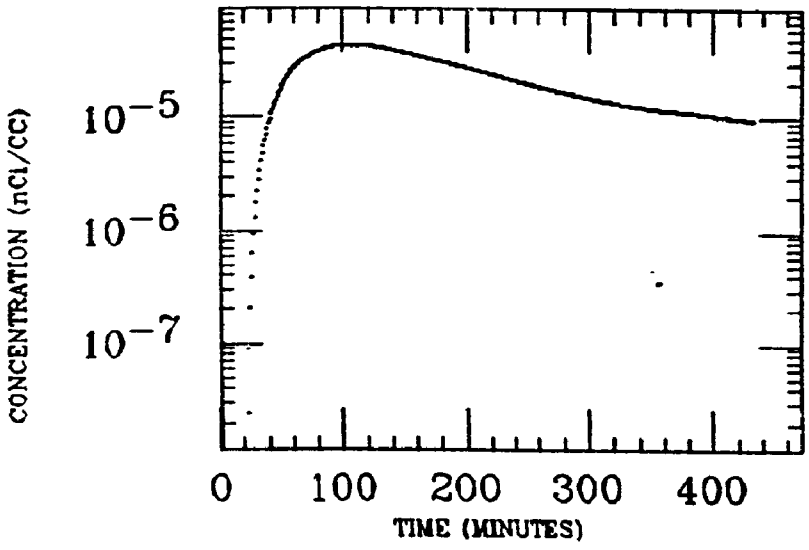

HAWKINS
XE INGESTION
Bi-214

STOMACH

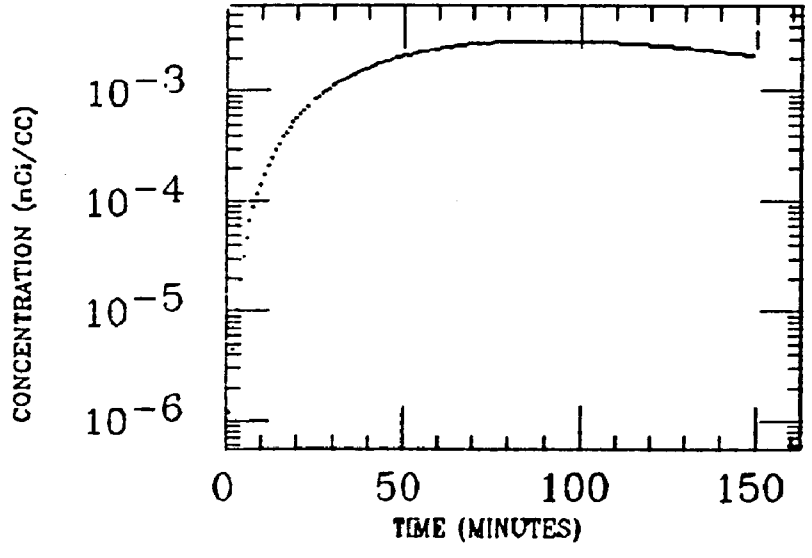

LIVER

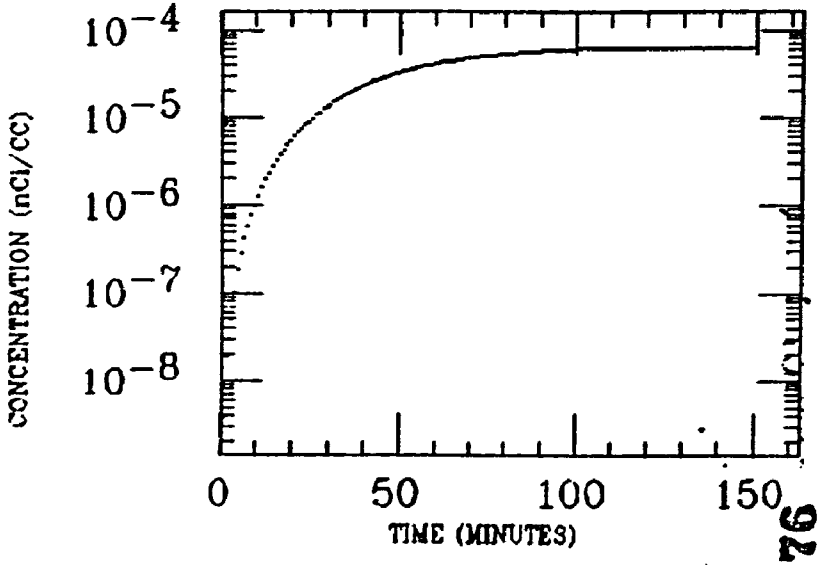

276

SM INTEST

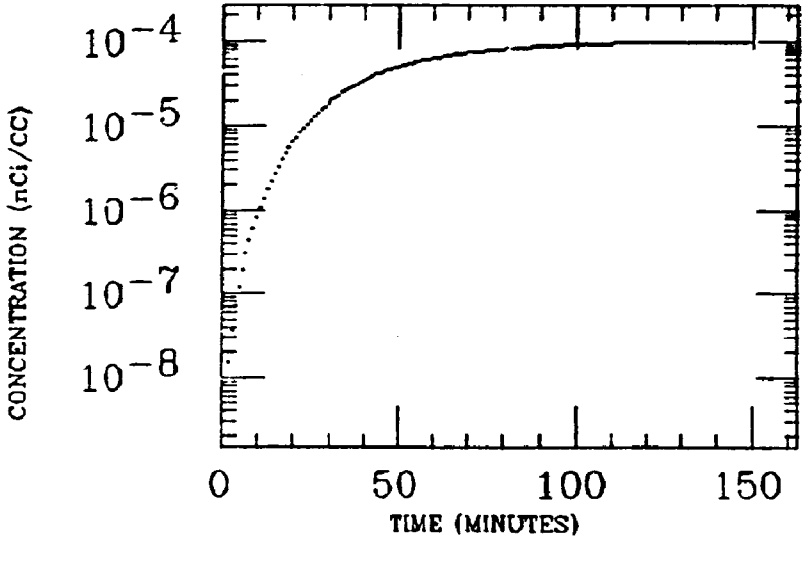

LG INTEST

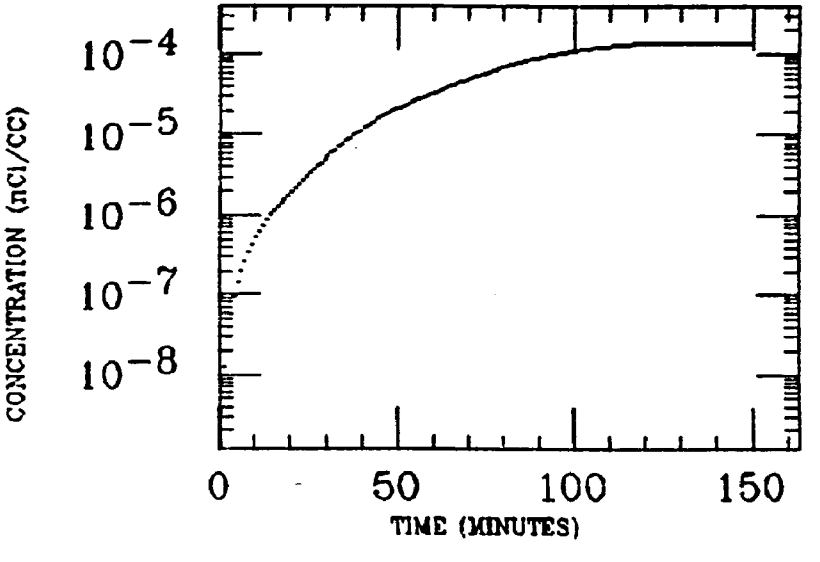

HAWKINS
XE INGESTION
Bi-214

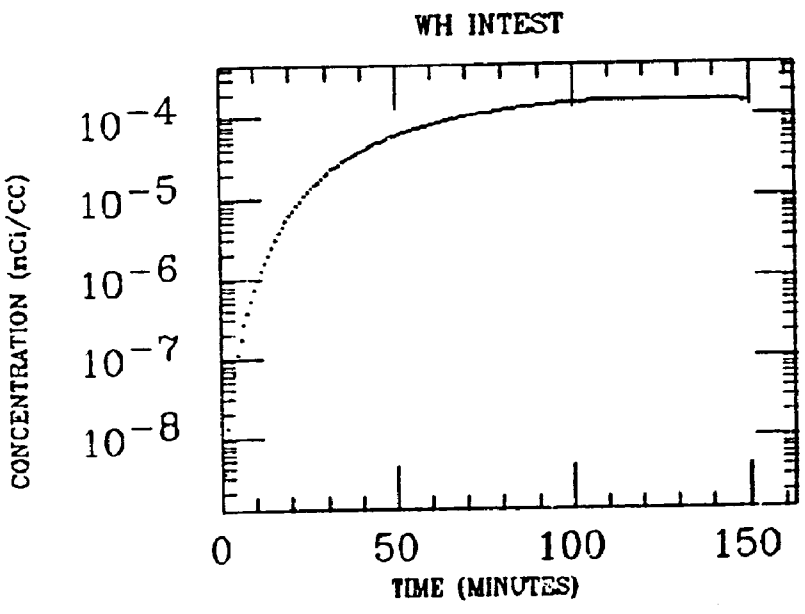

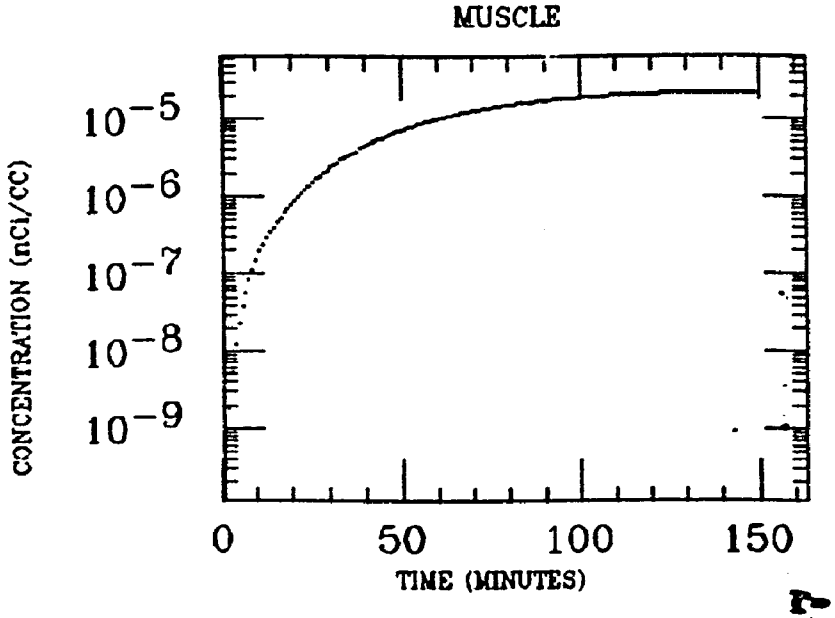

277

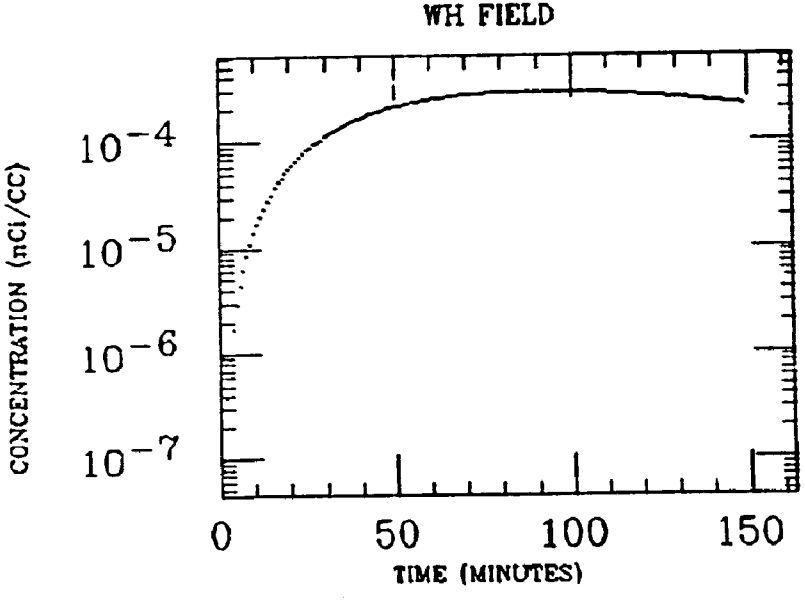

HILL
XE INGESTION
Bi-214

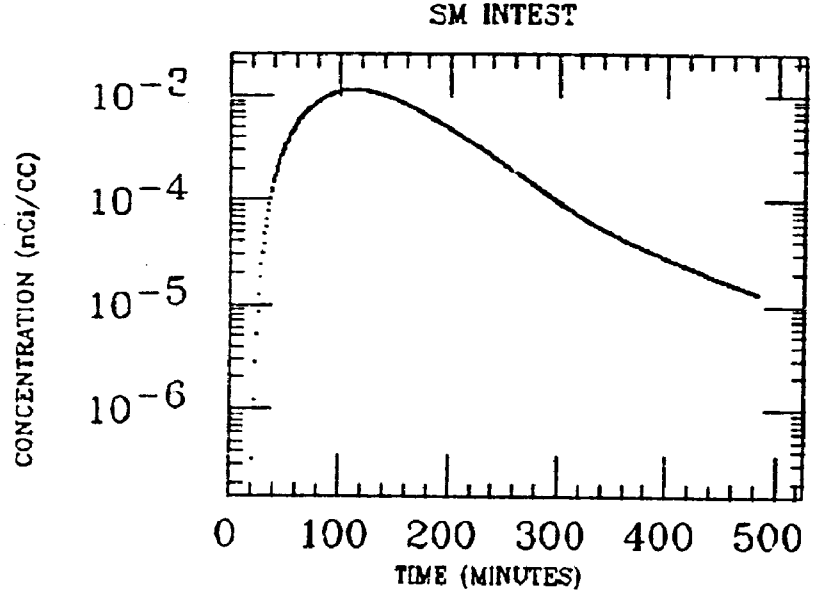

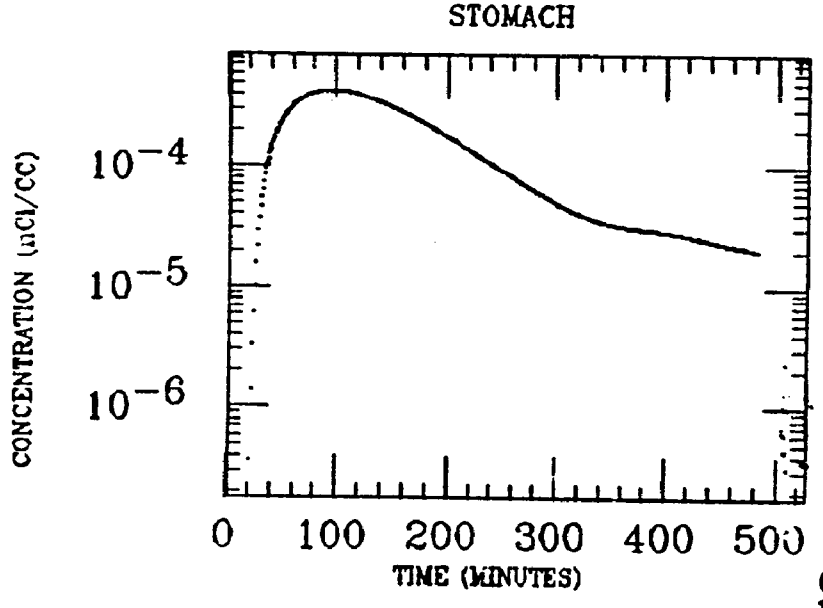

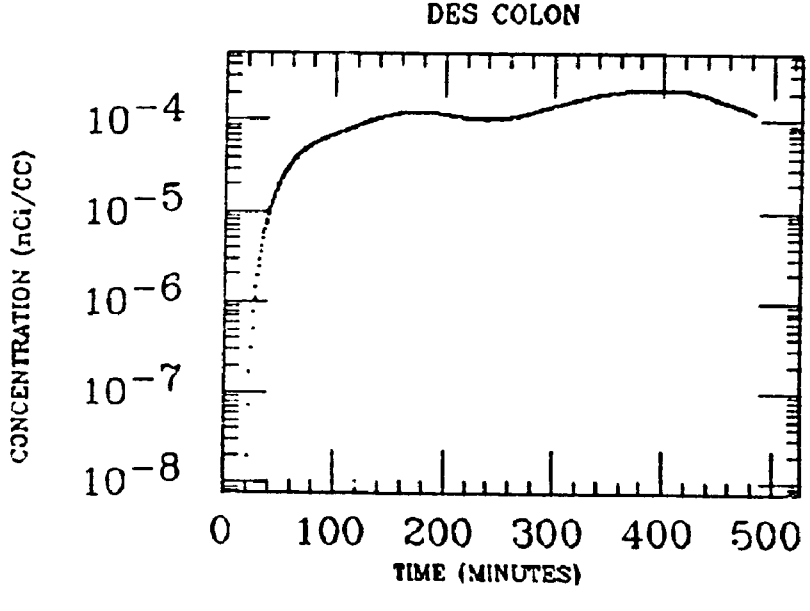

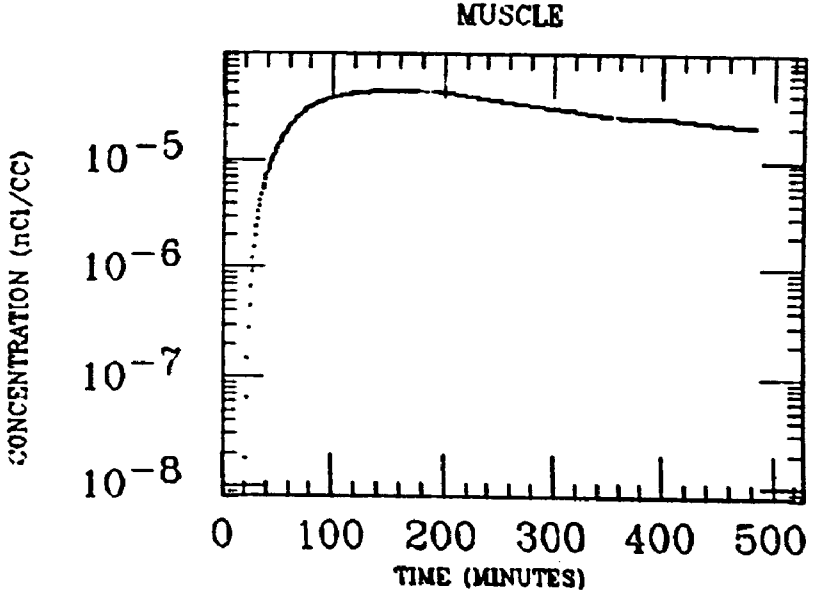

HILL

XE INGESTION

Bi-214

LIVER

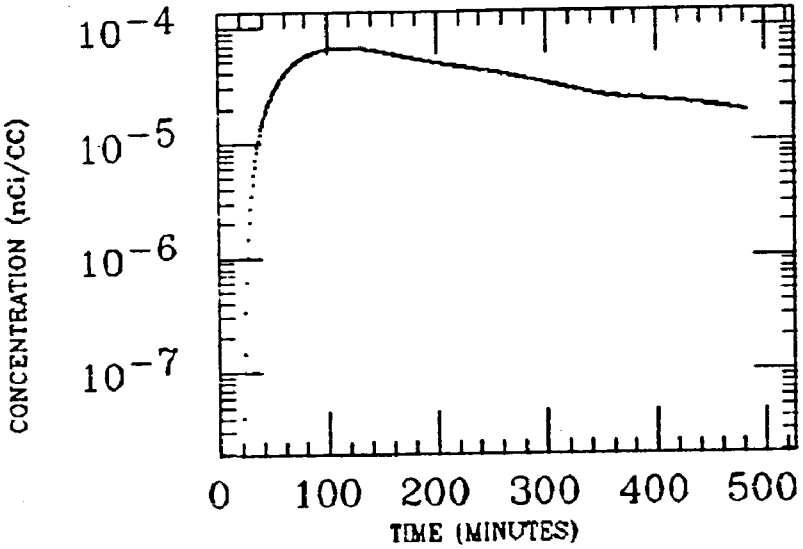

DUODENUM

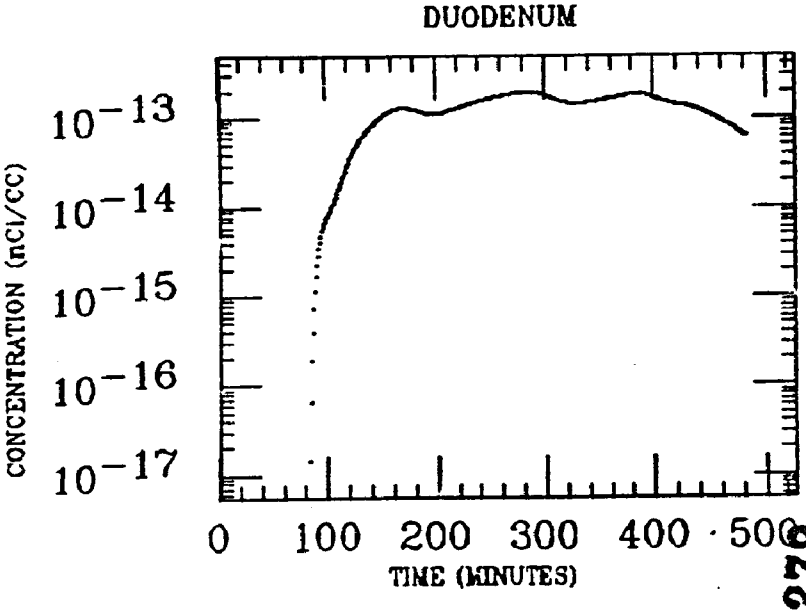

LG INTEST

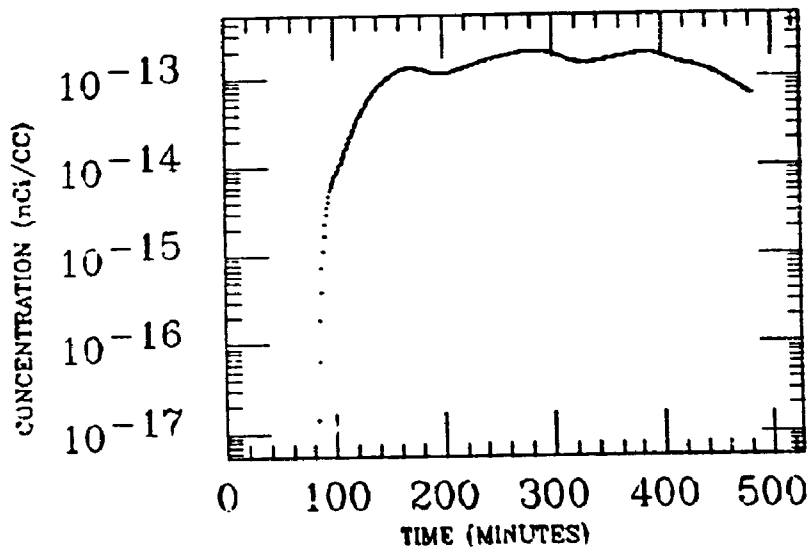

WH FIELD

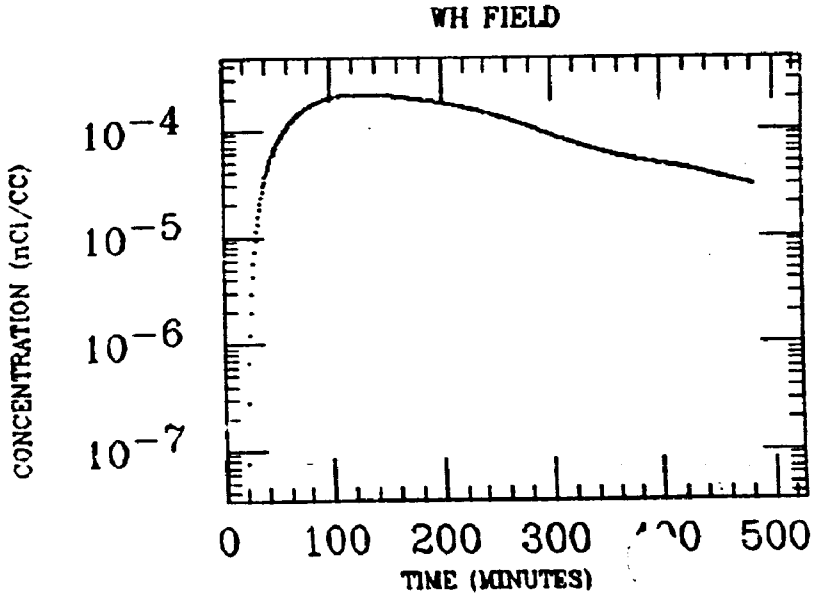

HILL

XE INGESTION

Bi-214

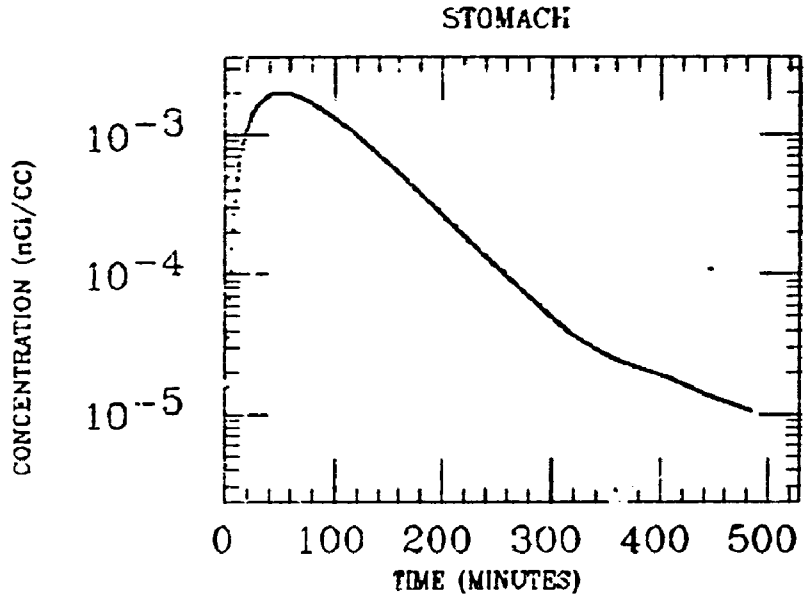

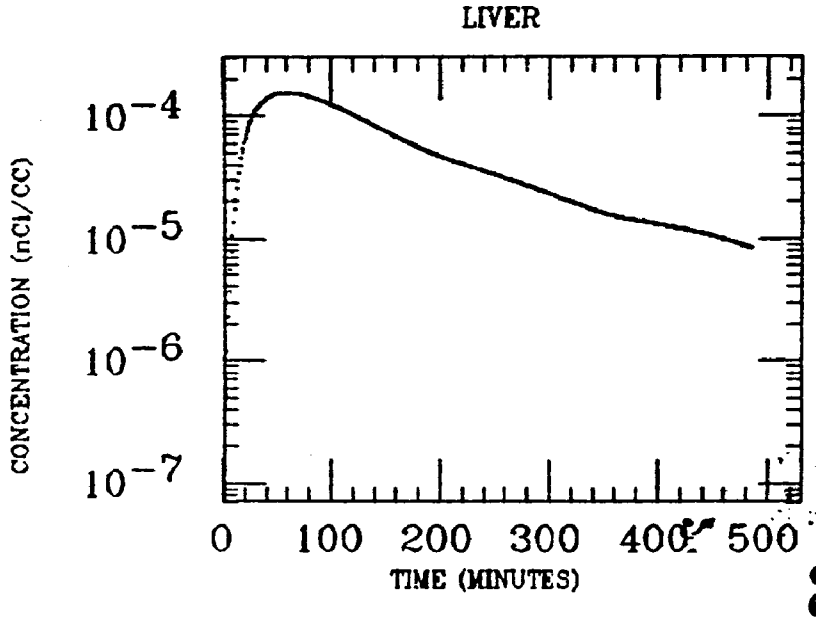

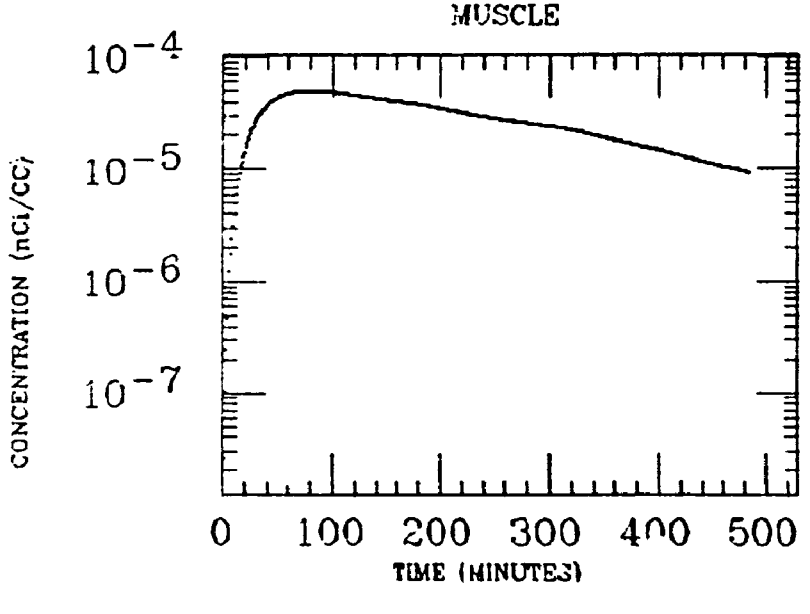

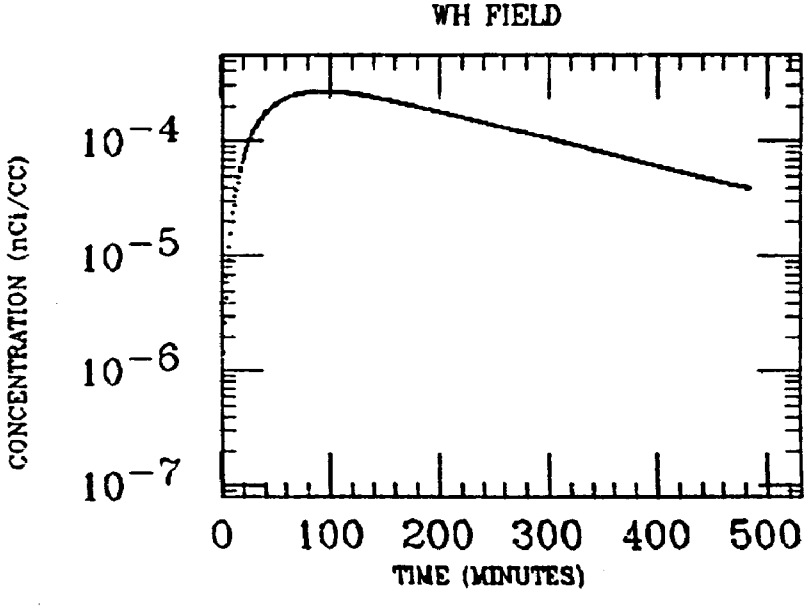

HUTCHINS
XE INGESTION
Bi-214

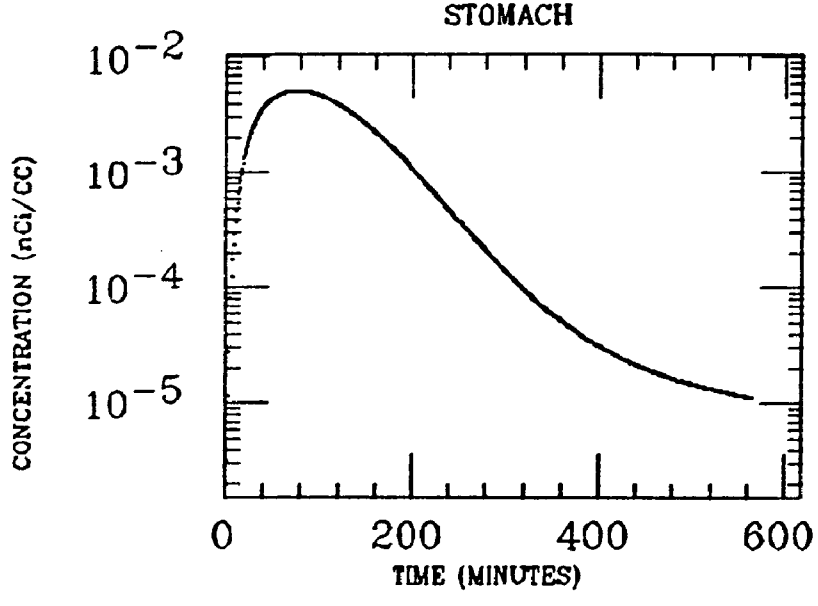

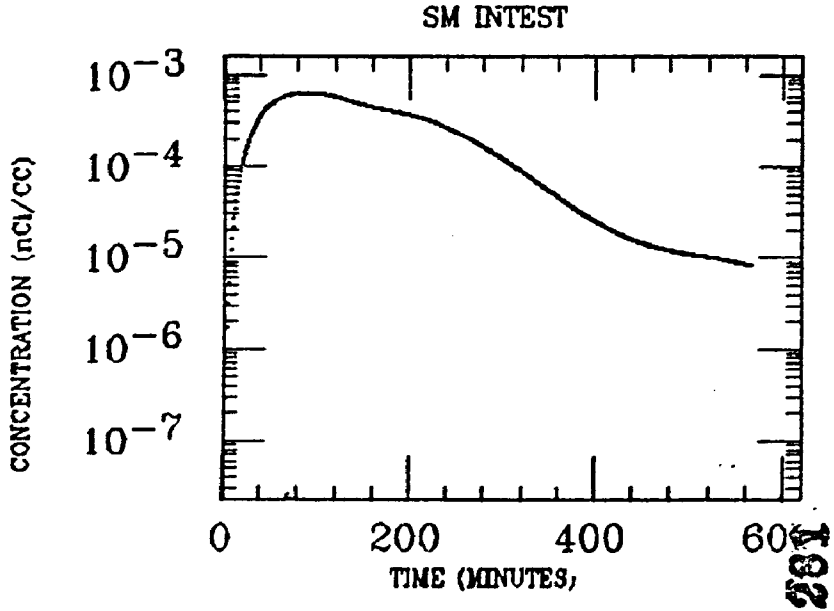

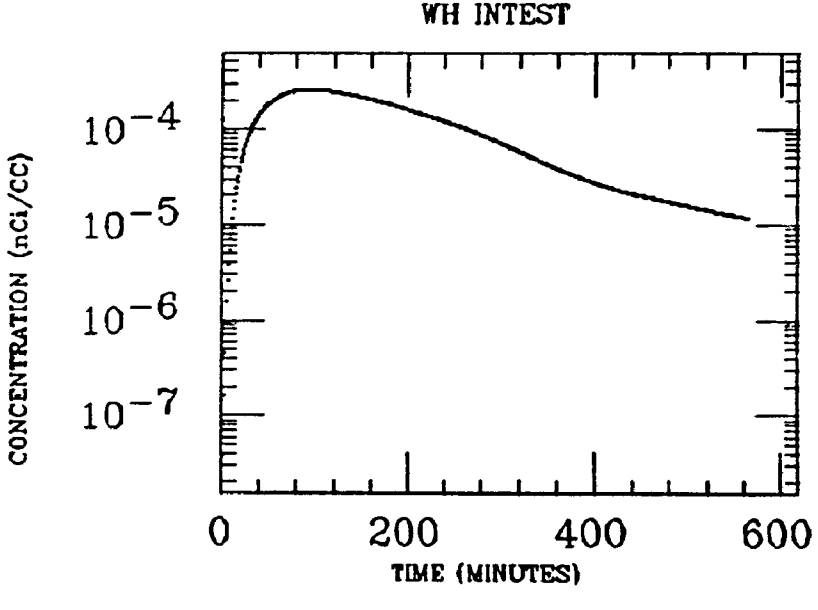

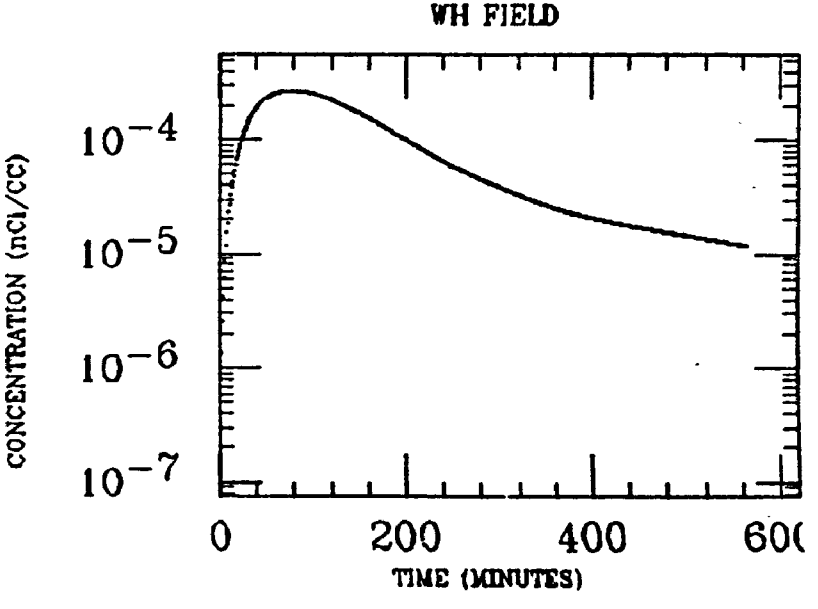

HUTCHINS
XE INGESTION
Bi-214

LIVER

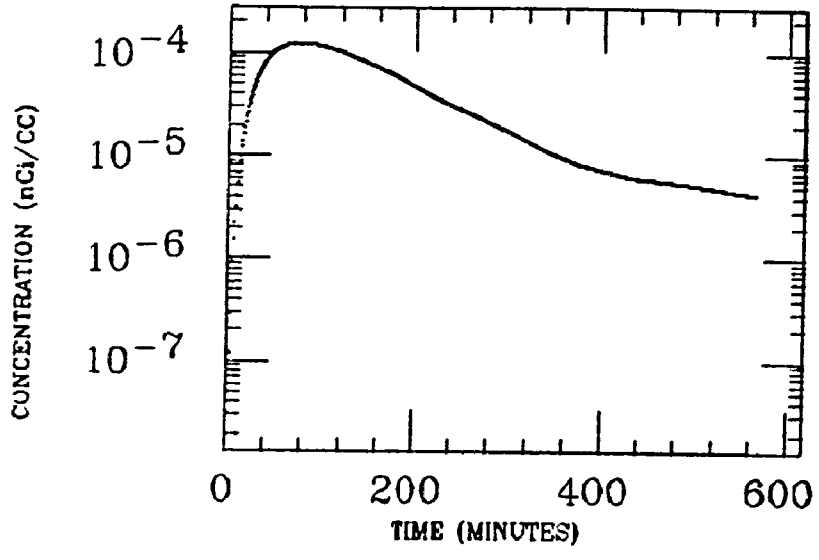

FAT

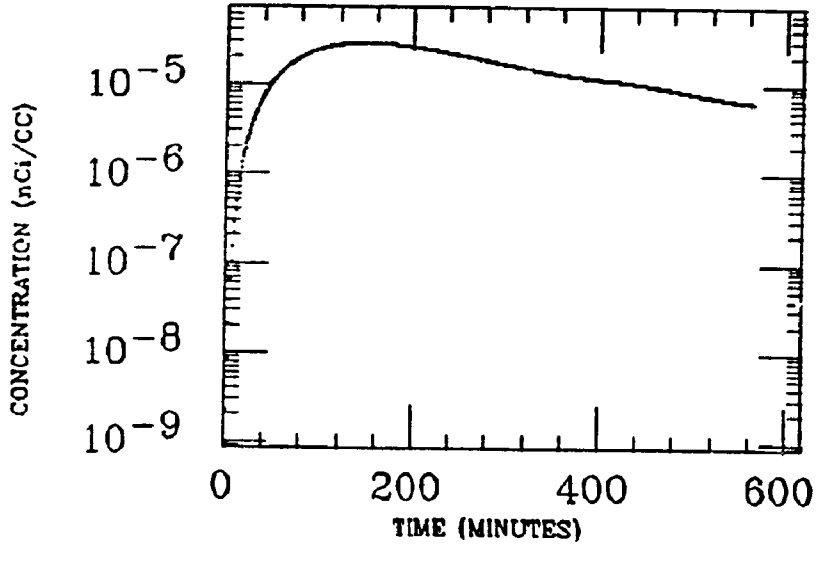

ASC COLON

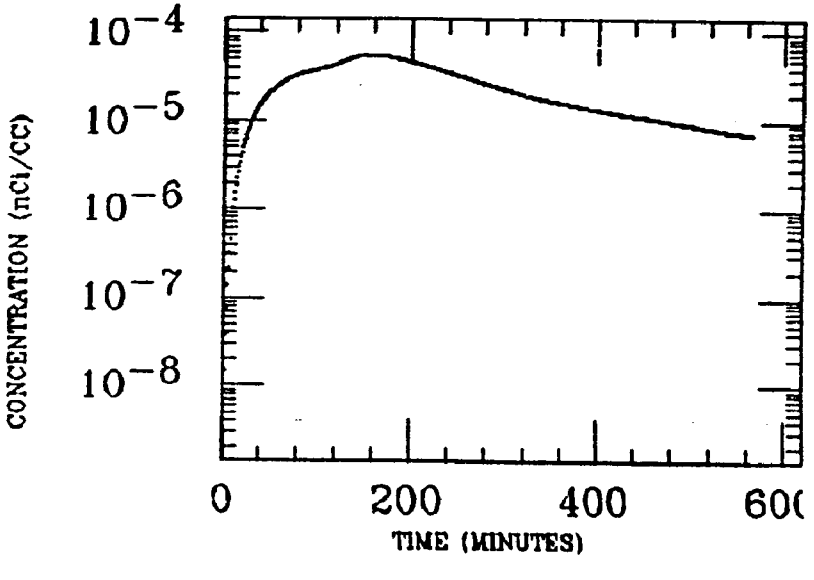

HUTCHINS
XE INGESTION
Bi-214

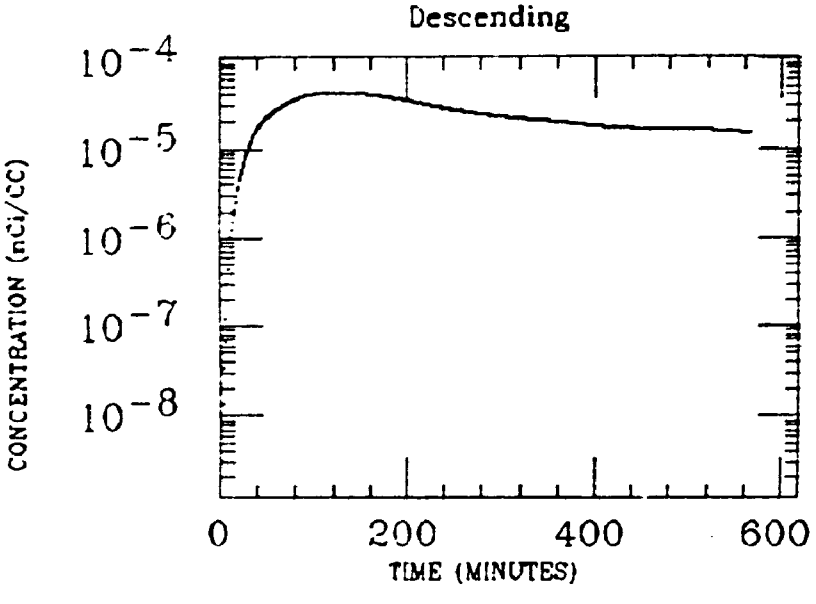

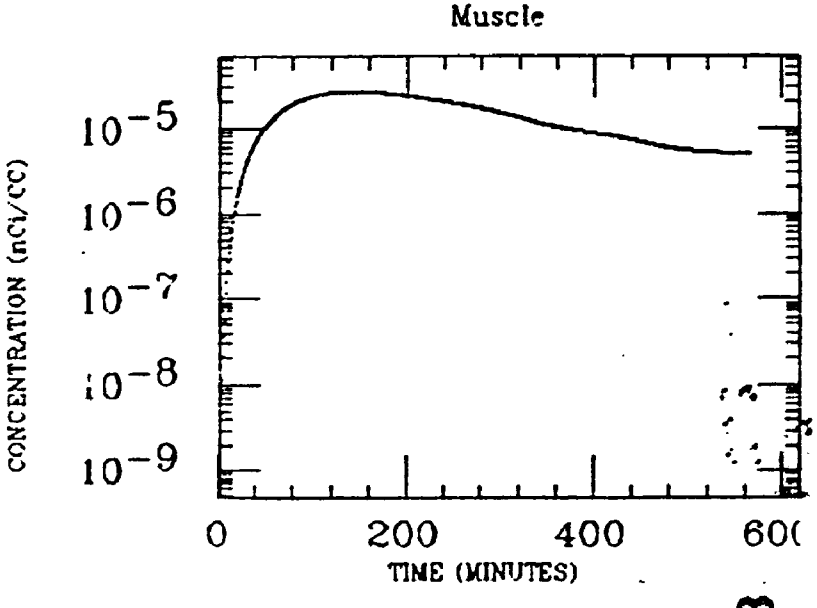

J.MCKINLEY
XE INGESTION
Bi-214

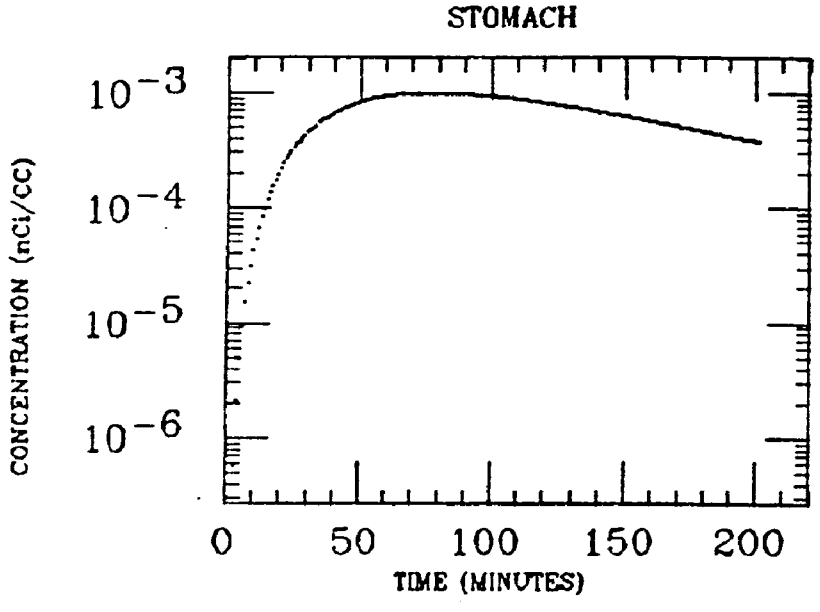

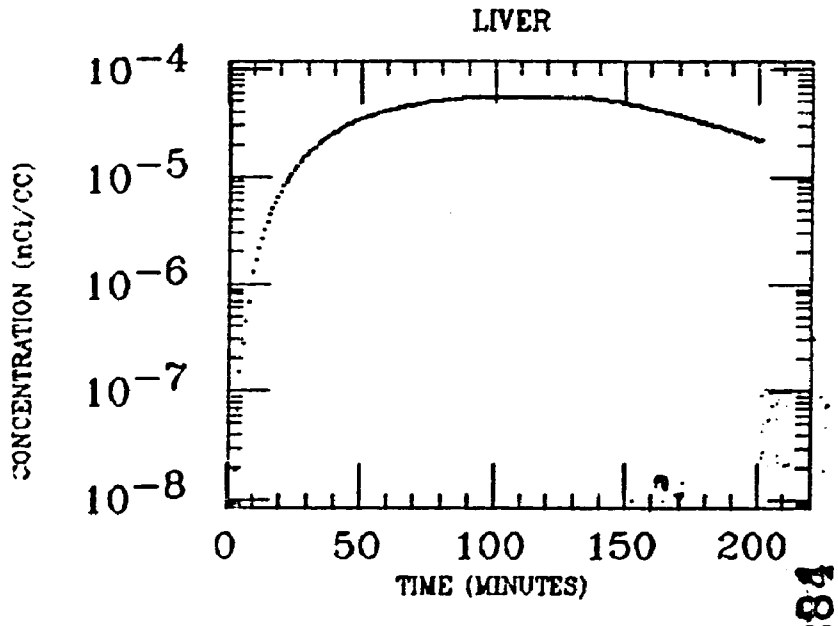

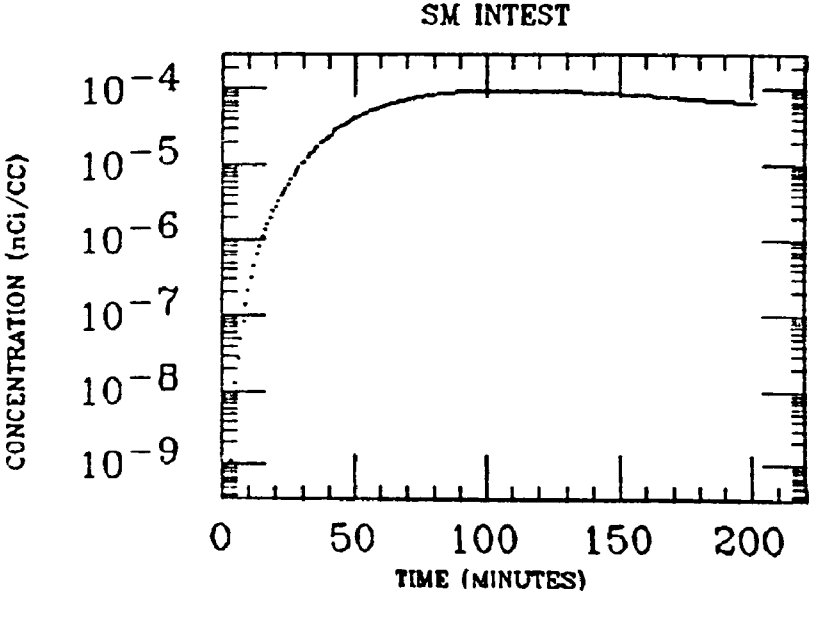

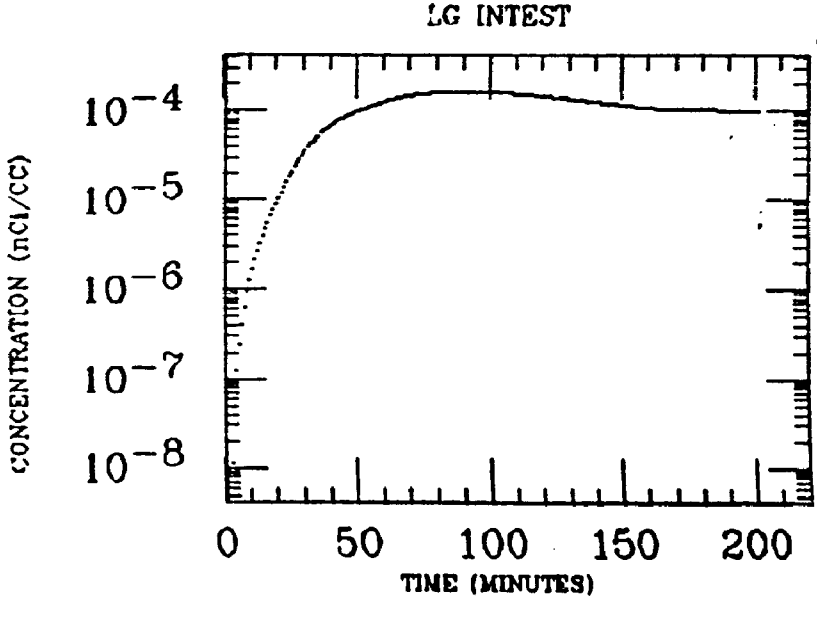

J.MCKINLEY
XE INGESTION
Bi-214

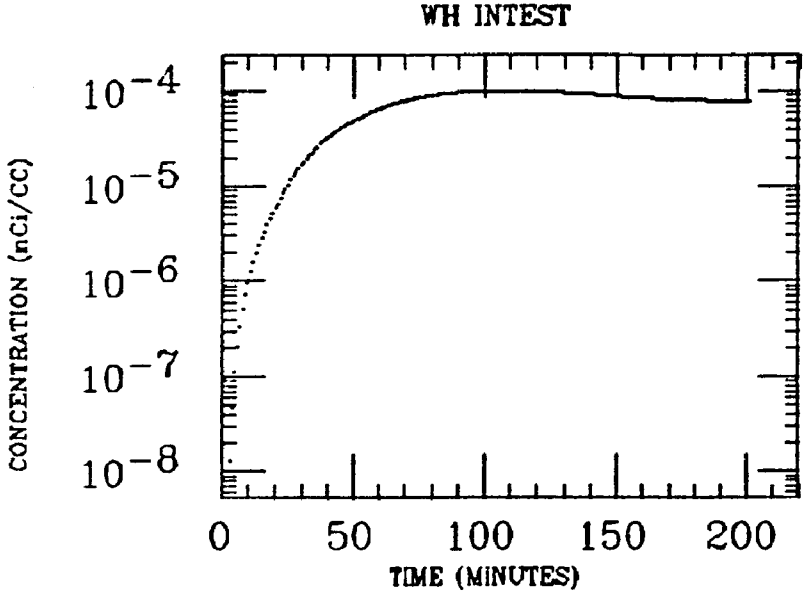

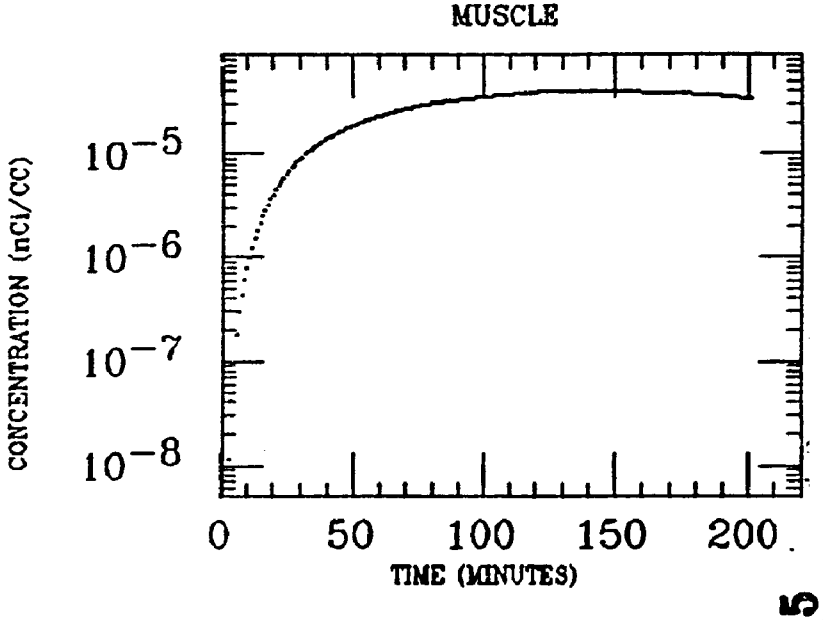

285

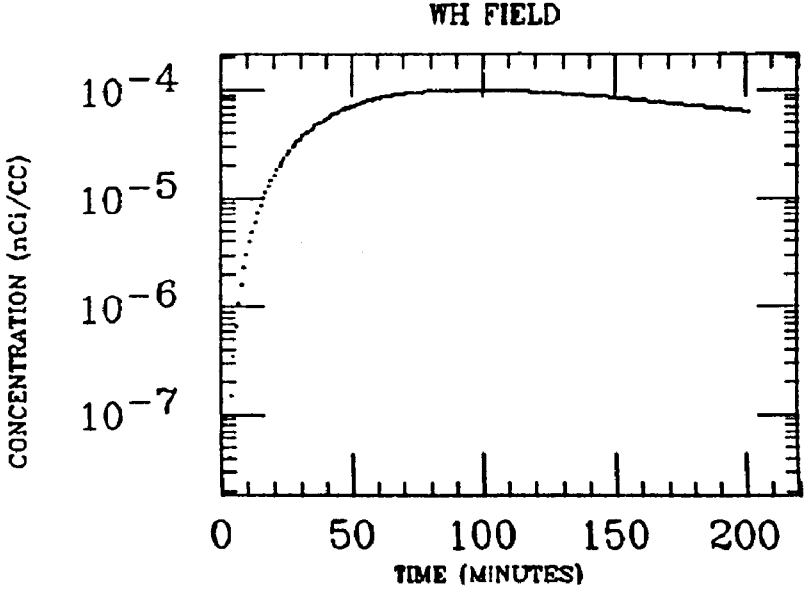

KELLEHER
XE INGESTION
Bi-214

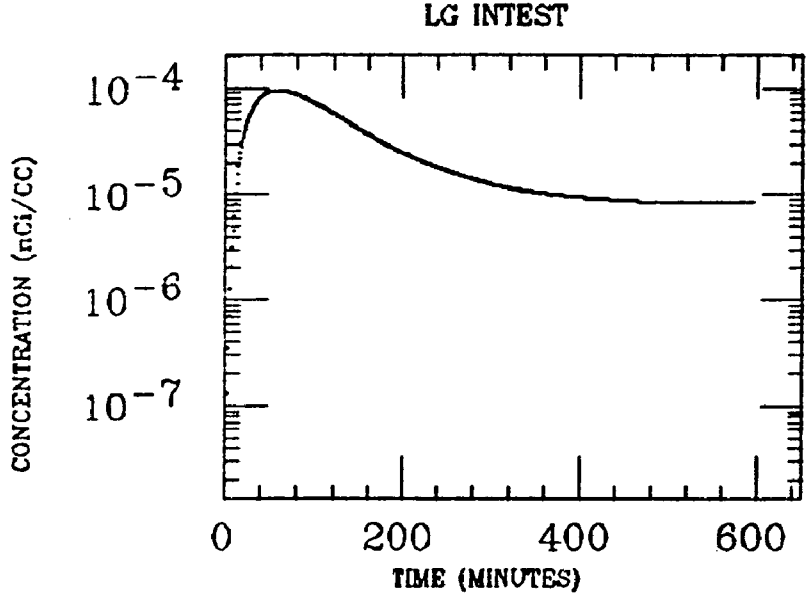

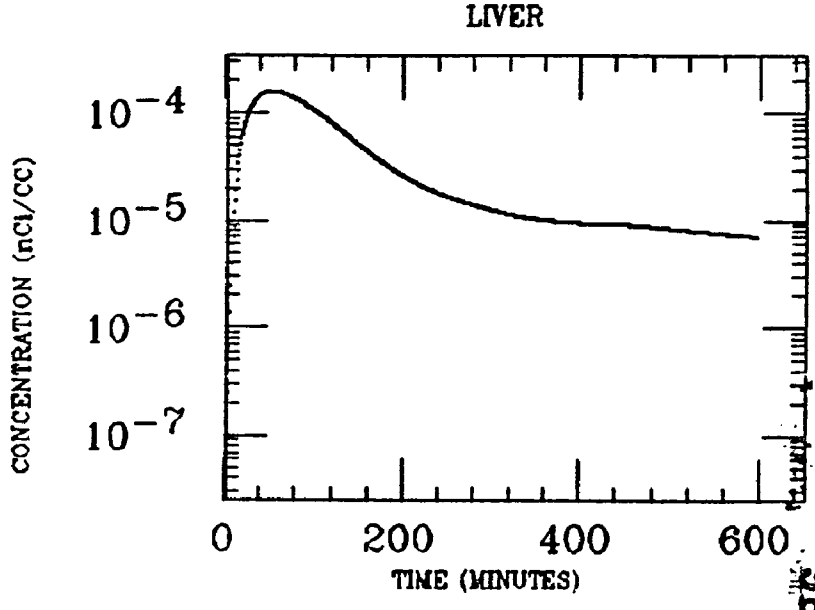

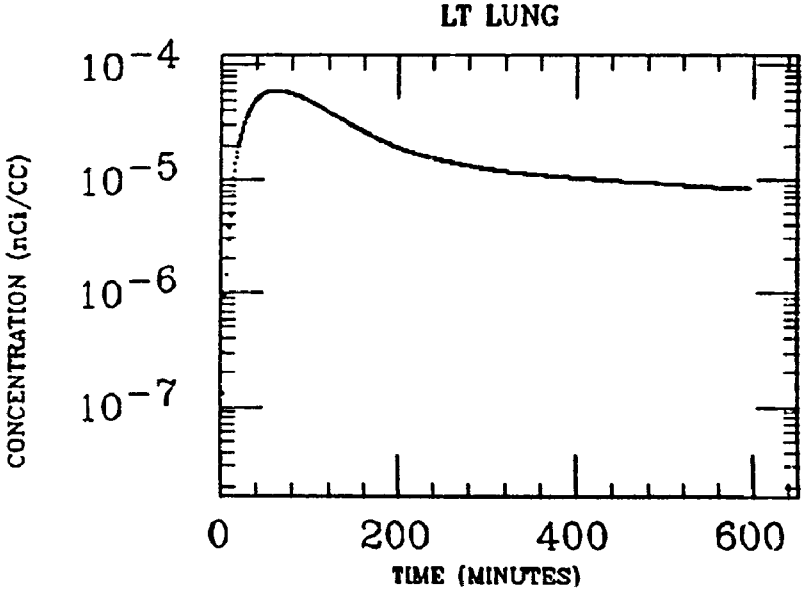

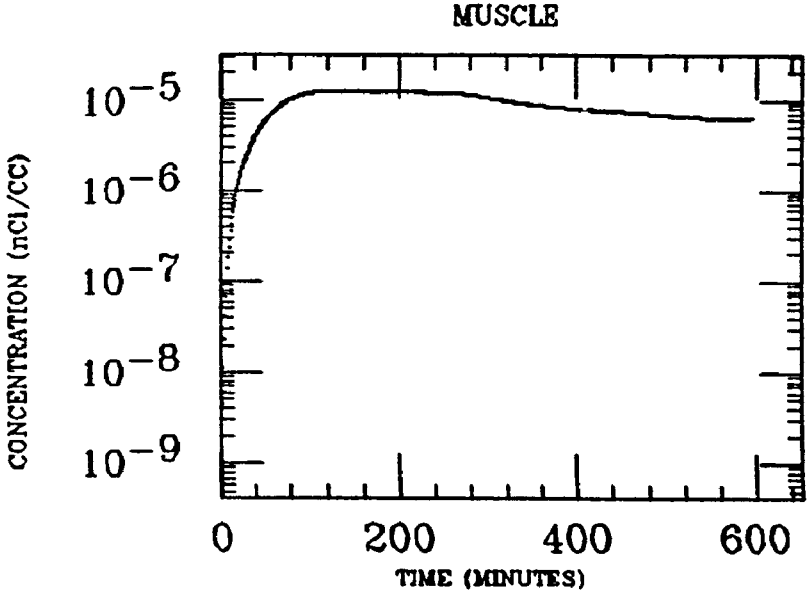

KELLEHER
XE INGESTION
Bi-214

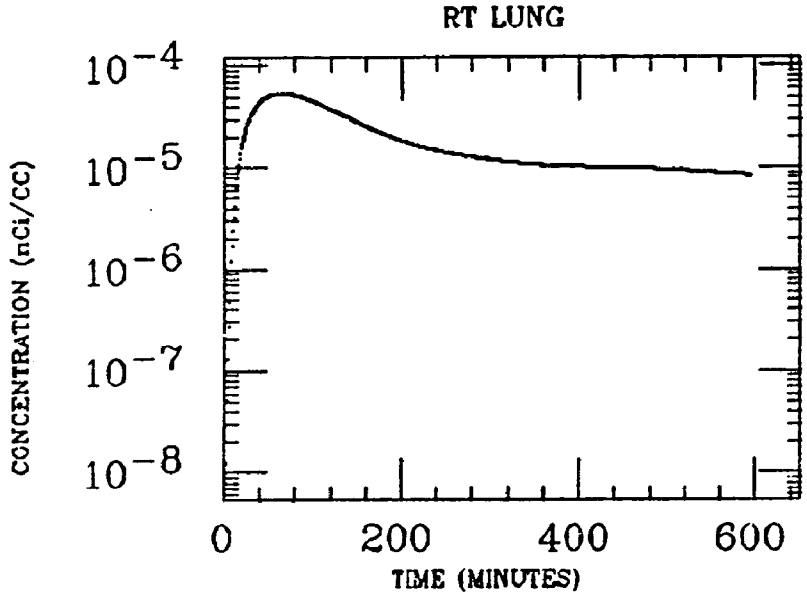

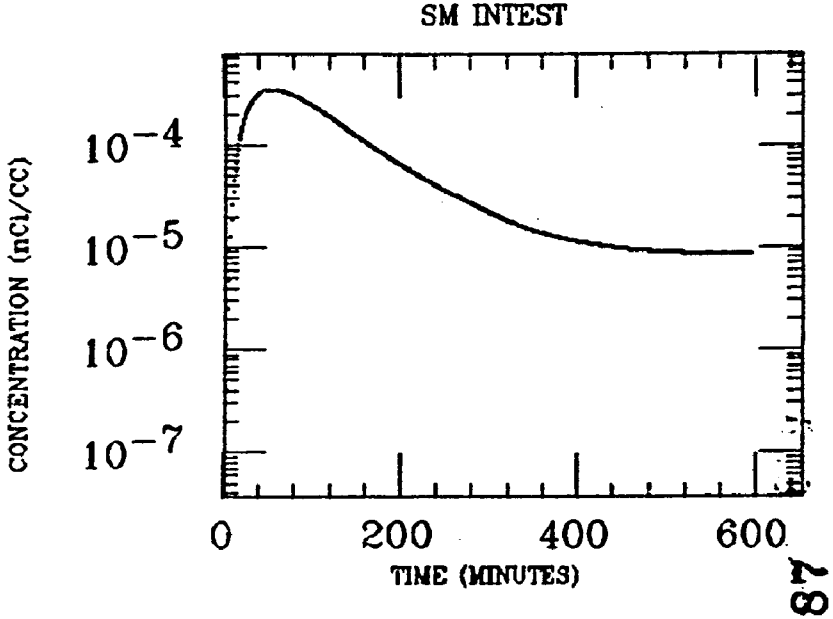

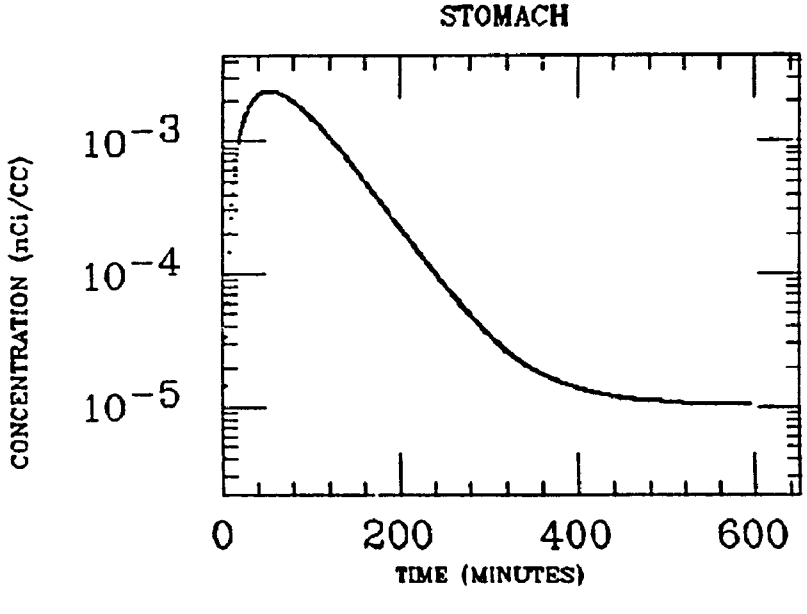

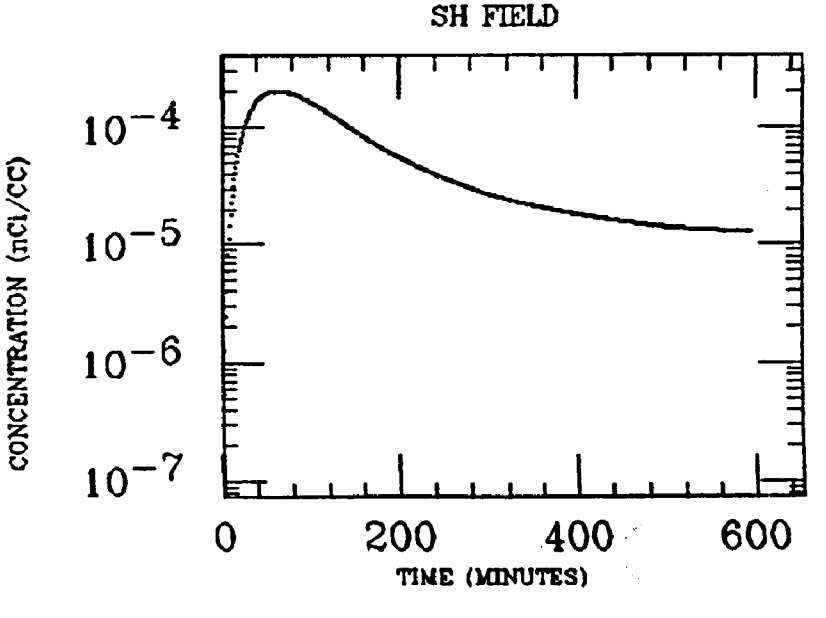

LITTELL
XE INGESTION
Bi-214

STOMACH

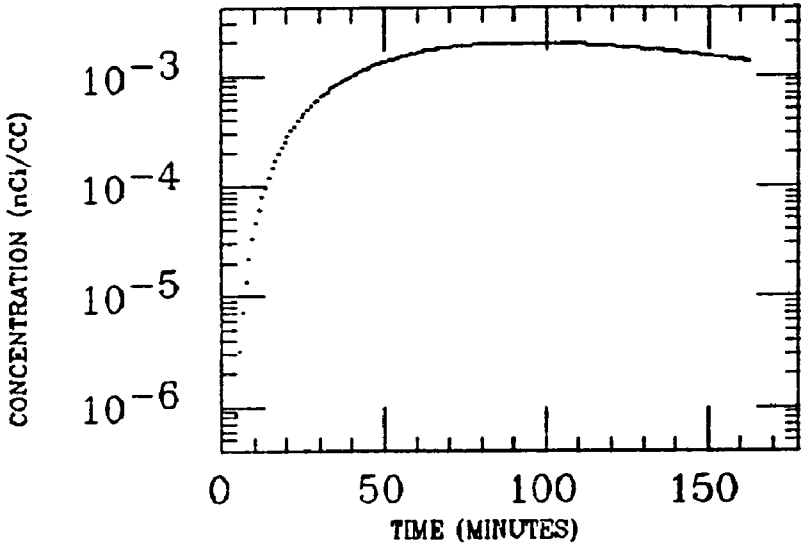

SM INTEST

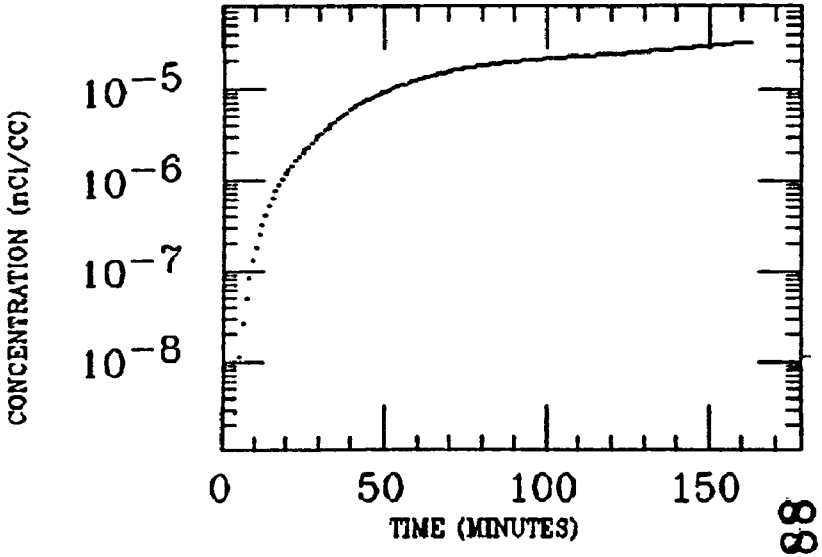

ASC COLON

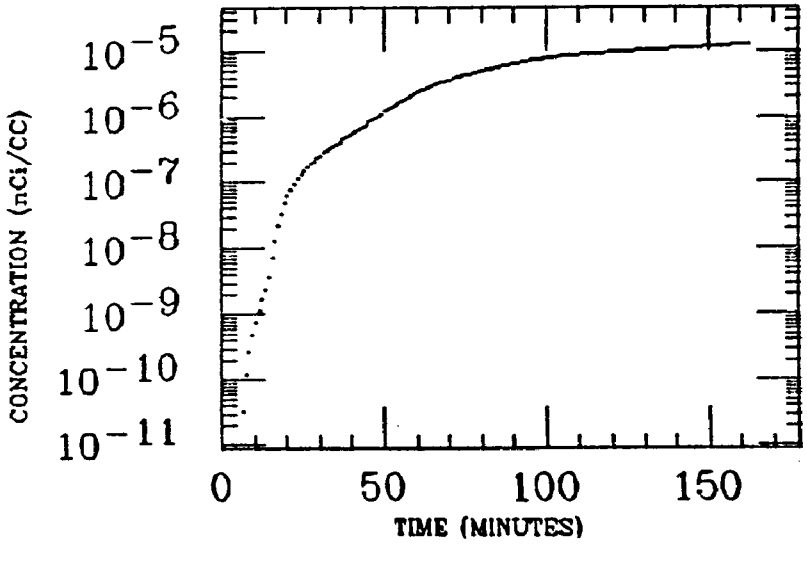

LIVER

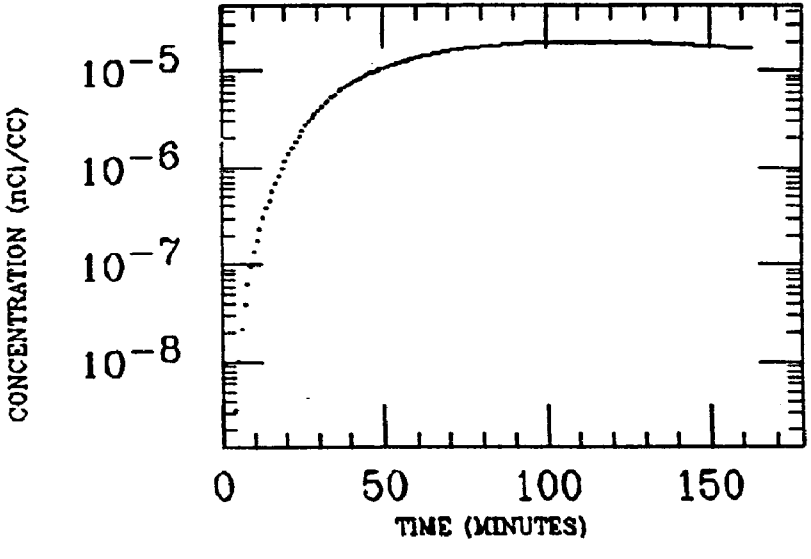

LITTELL
XE INGESTION
Bi-214

MUSCLE

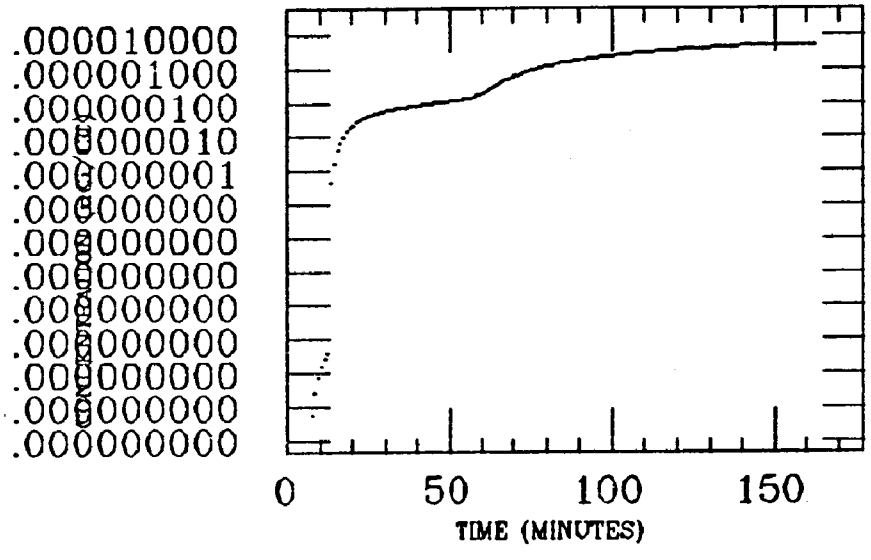

WH INTEST

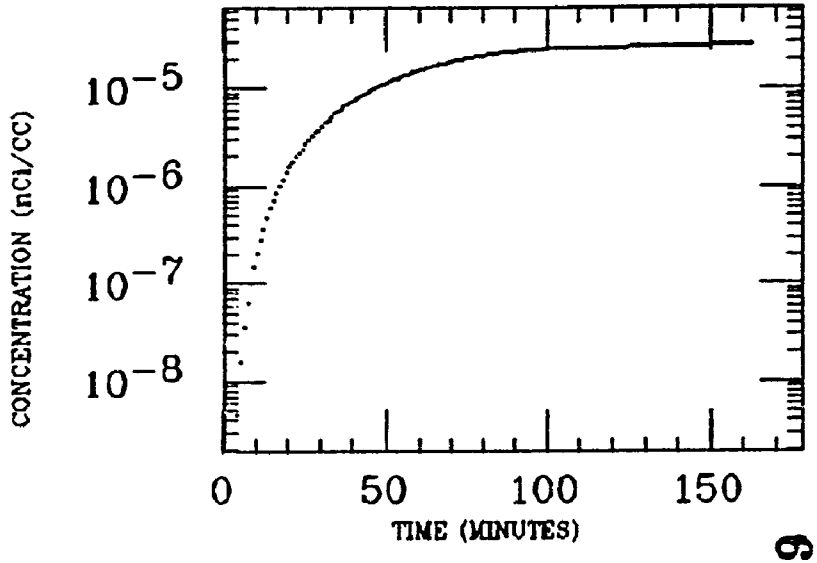

WH FIELD

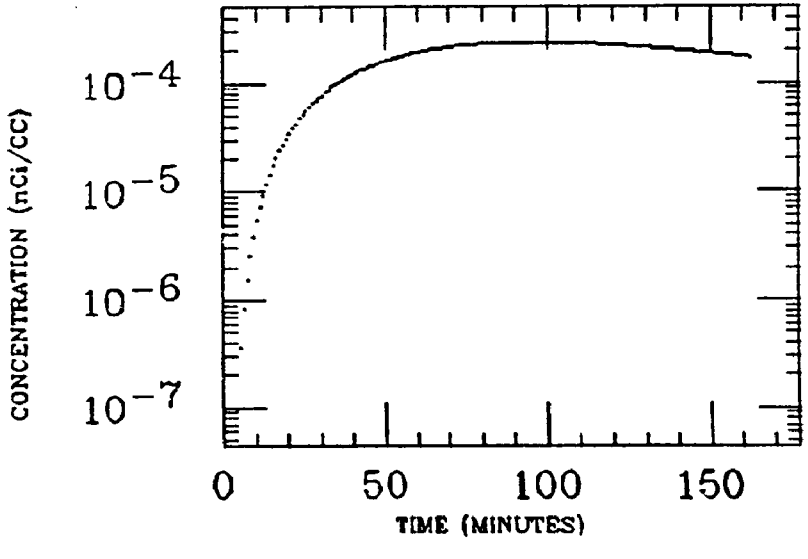

MACMILLAN
XE INGESTION
Bi-214

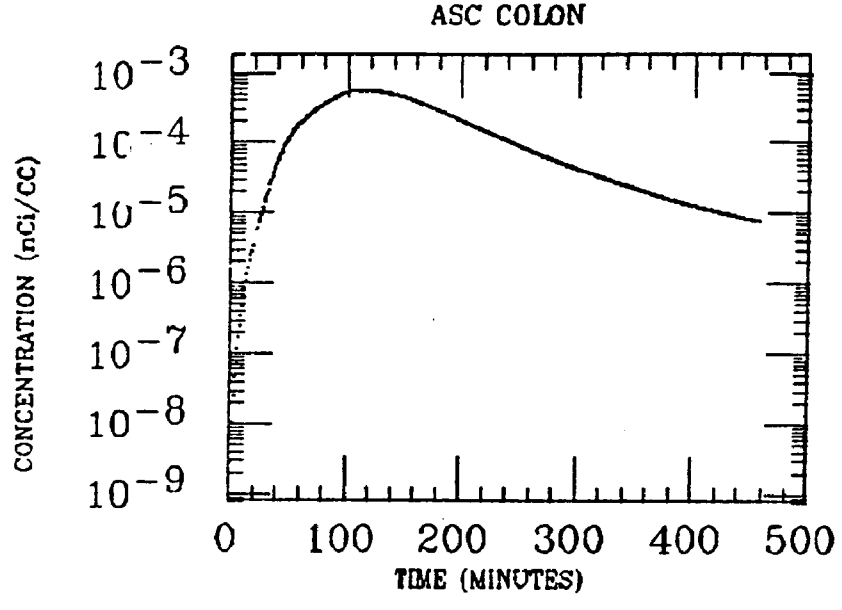

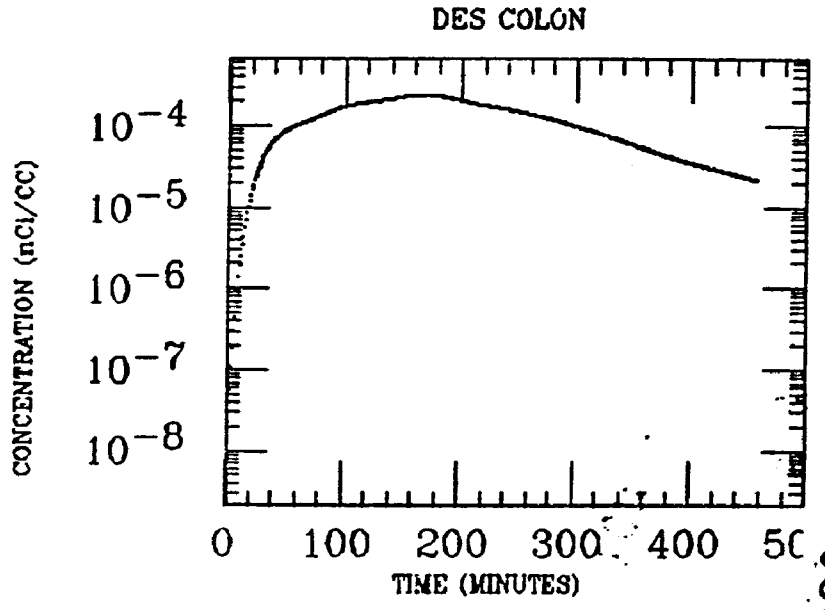

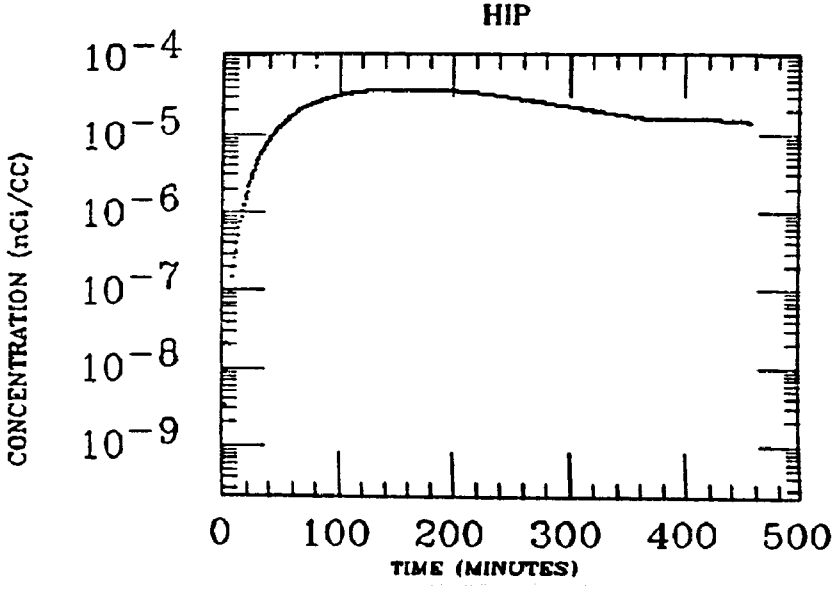

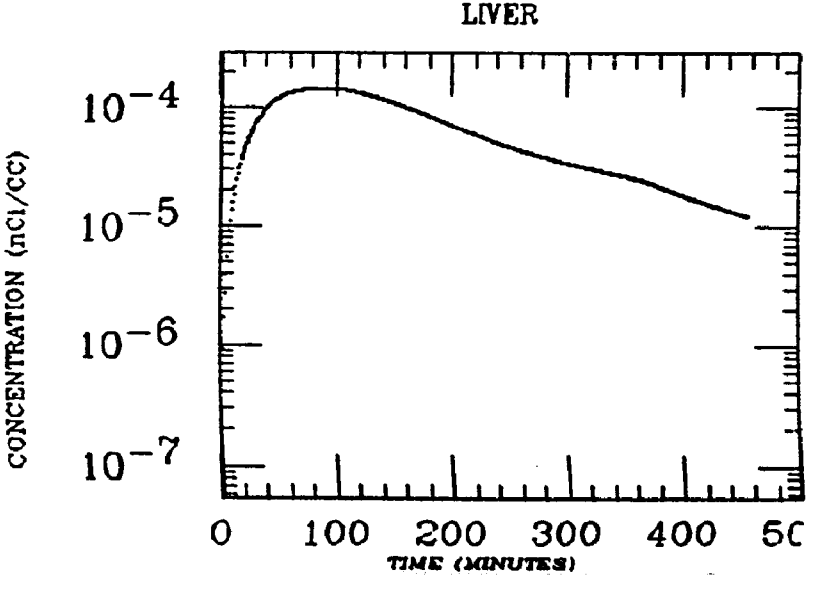

MACMILLAN
XE INGESTION
Bi-214

SM INTEST

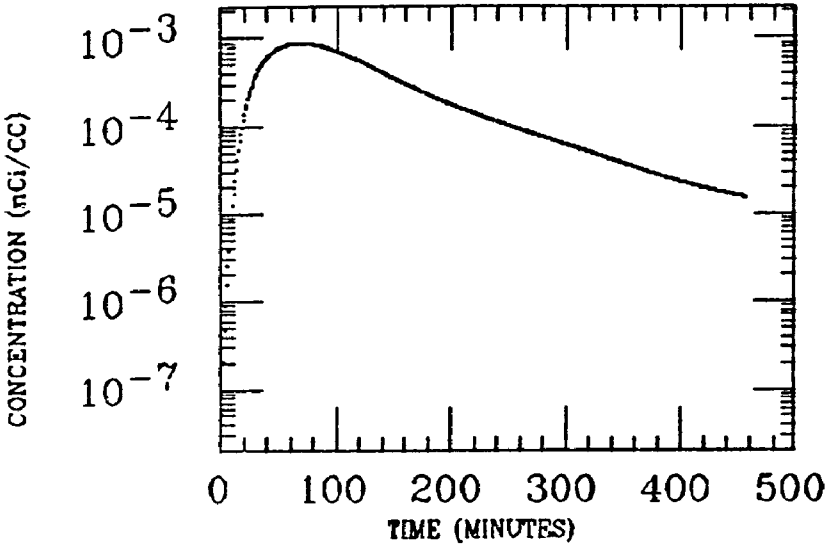

STOMACH

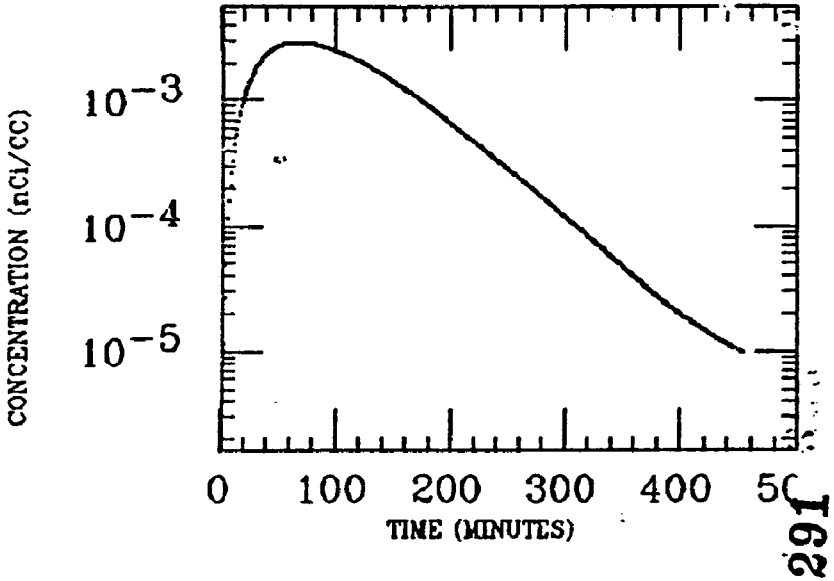

TR COLON

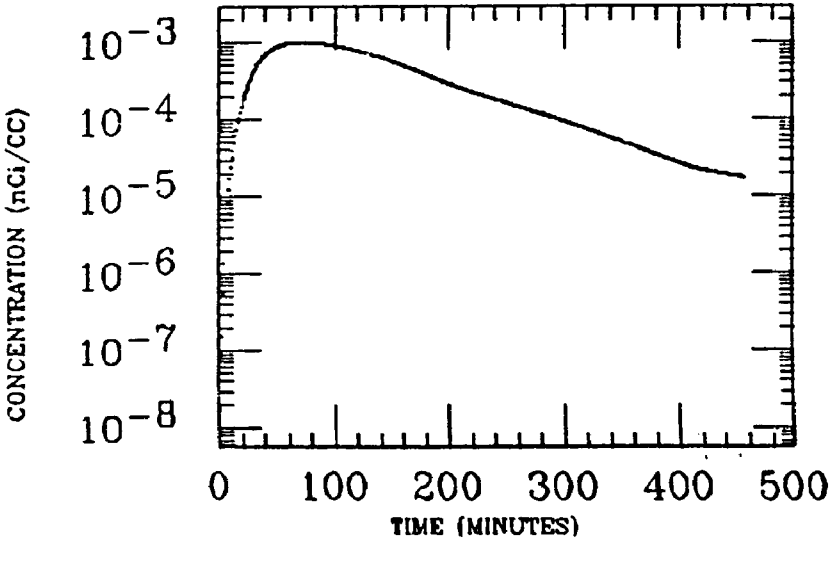

WH INTEST

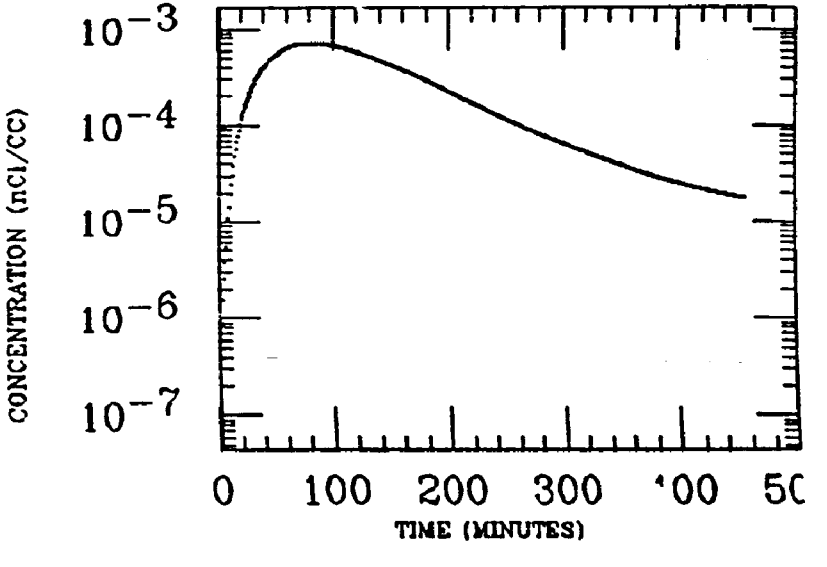

MAIO

XE INGESTION

Bi-214

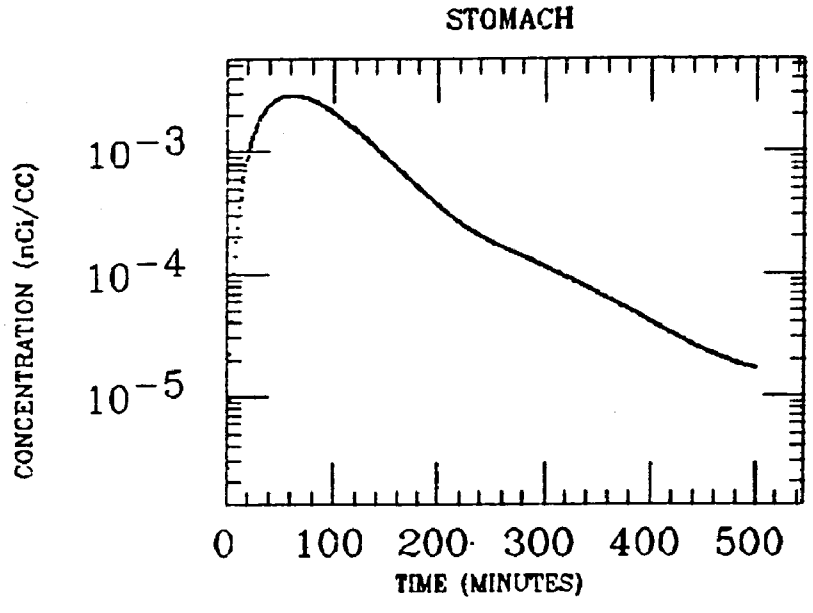

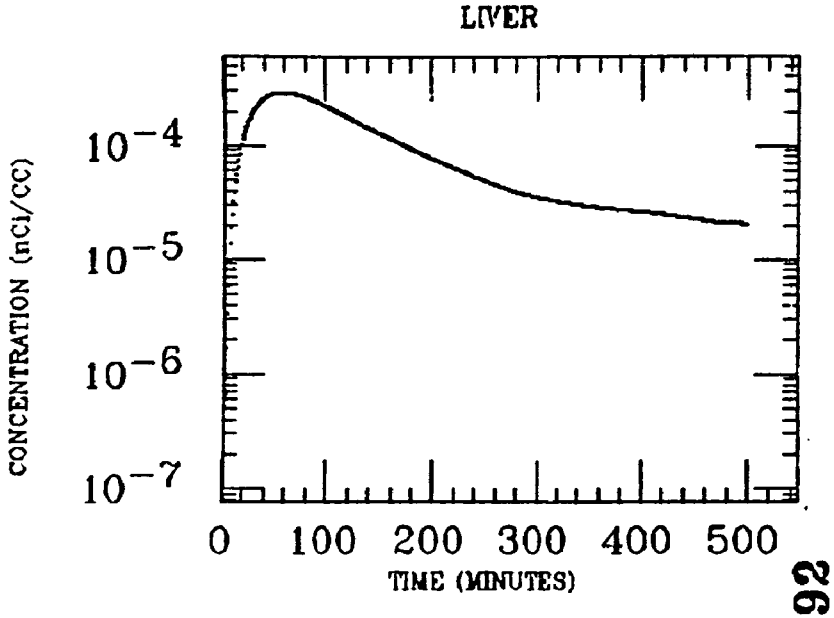

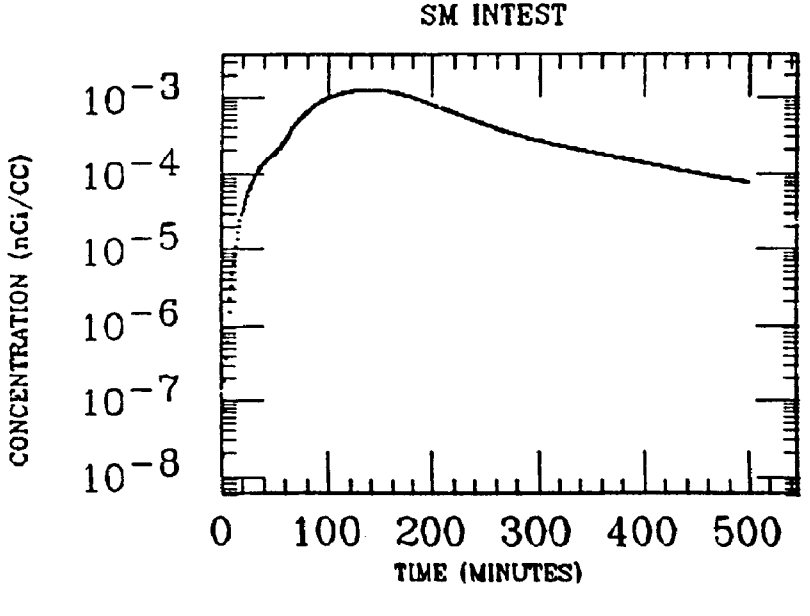

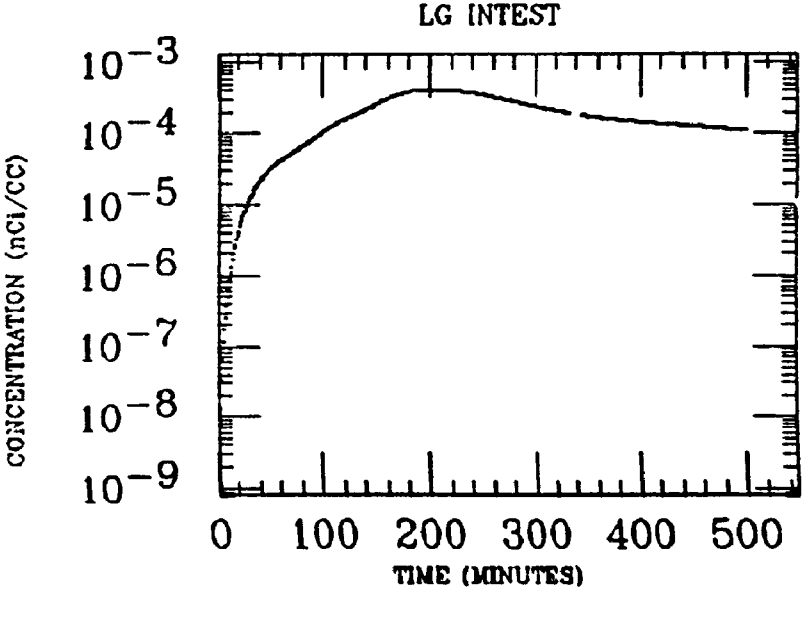

MAIO
XE INGESTION
BI-214

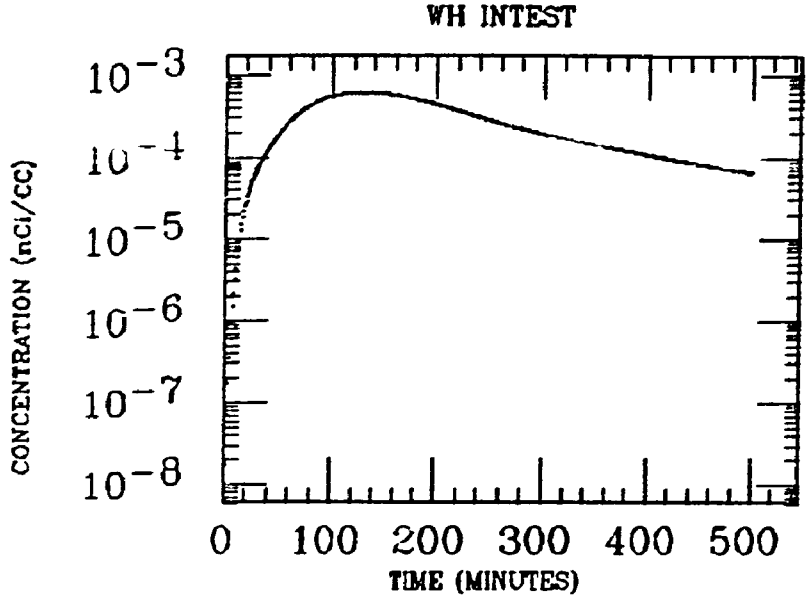

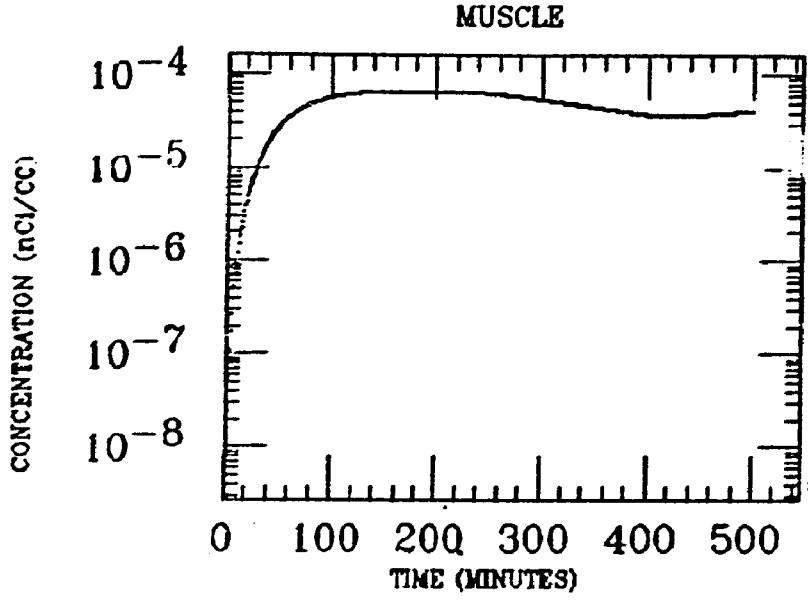

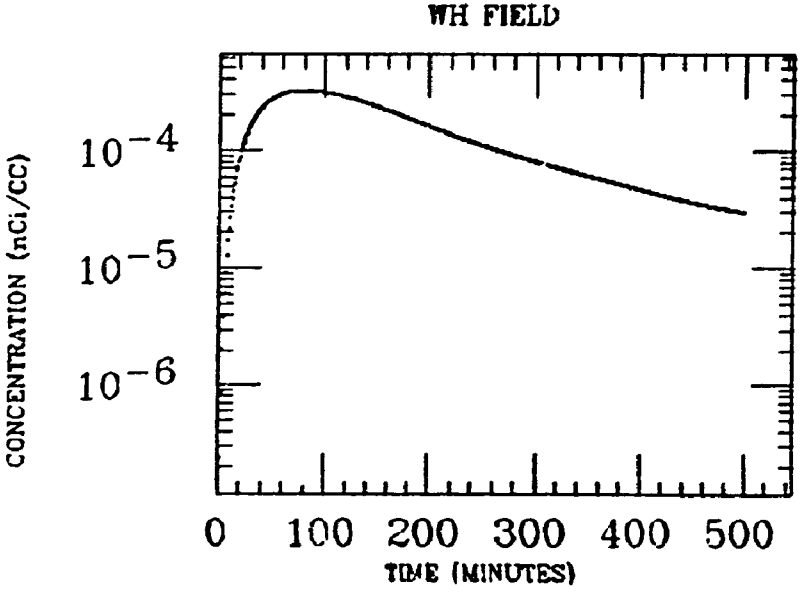

MALCOM
XE INGESTION
Bi-214

STOMACH

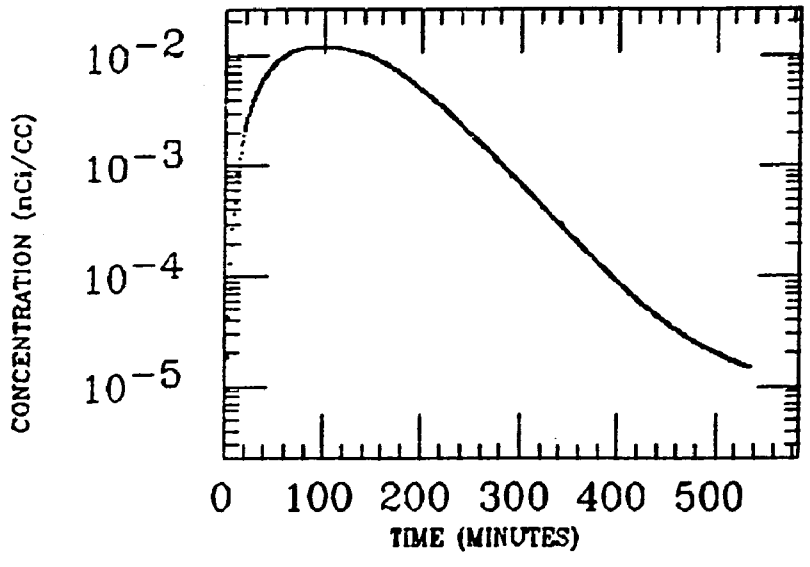

LIVER

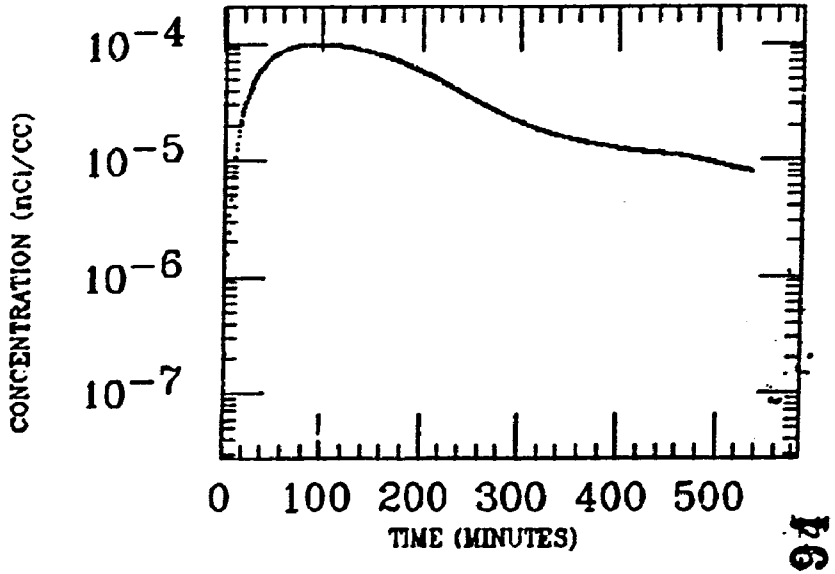

294

LG INTEST

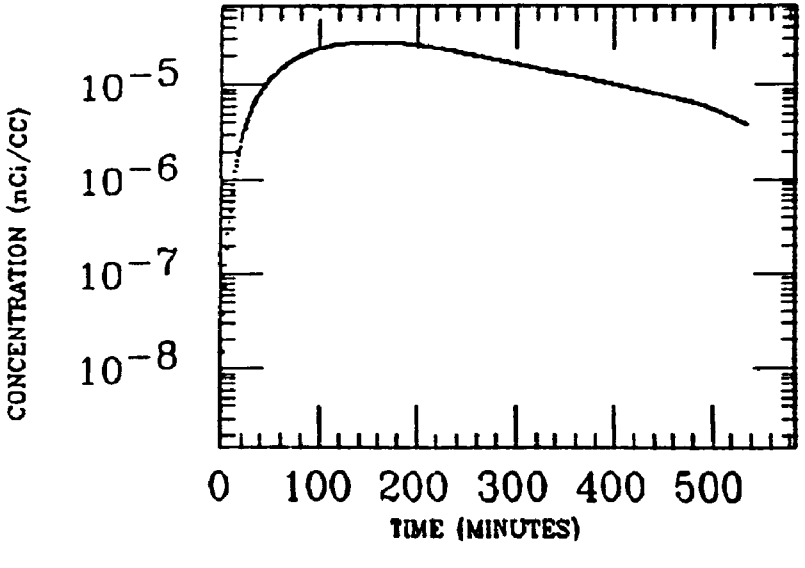

WH INTEST

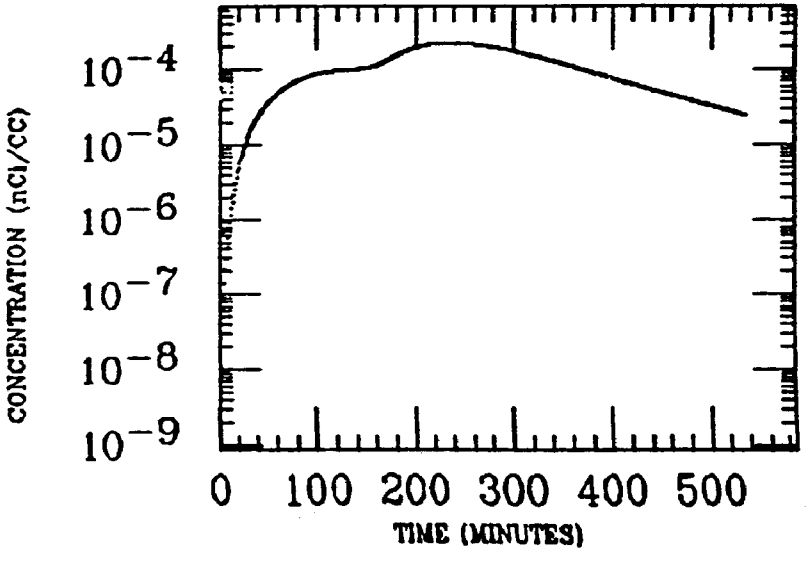

MALCOM
XE INGESTION
Bi-214

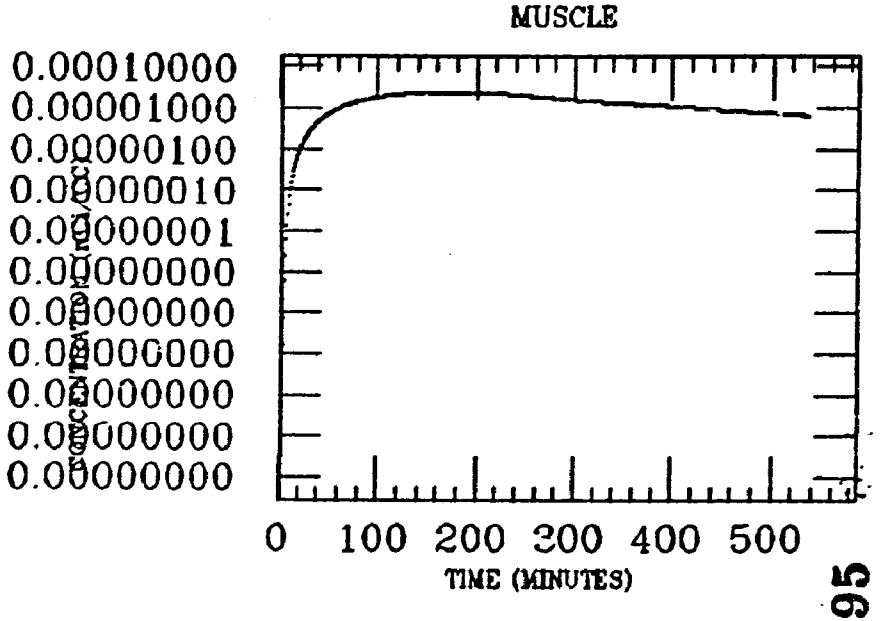

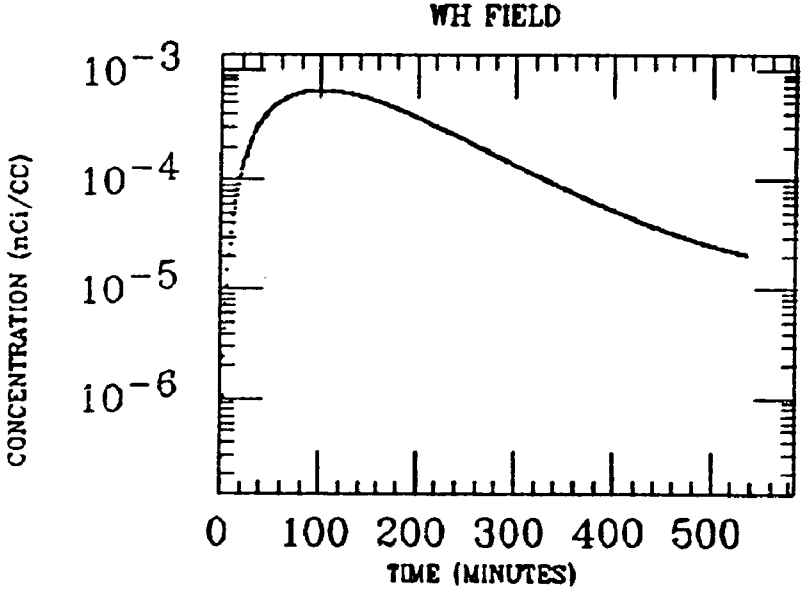

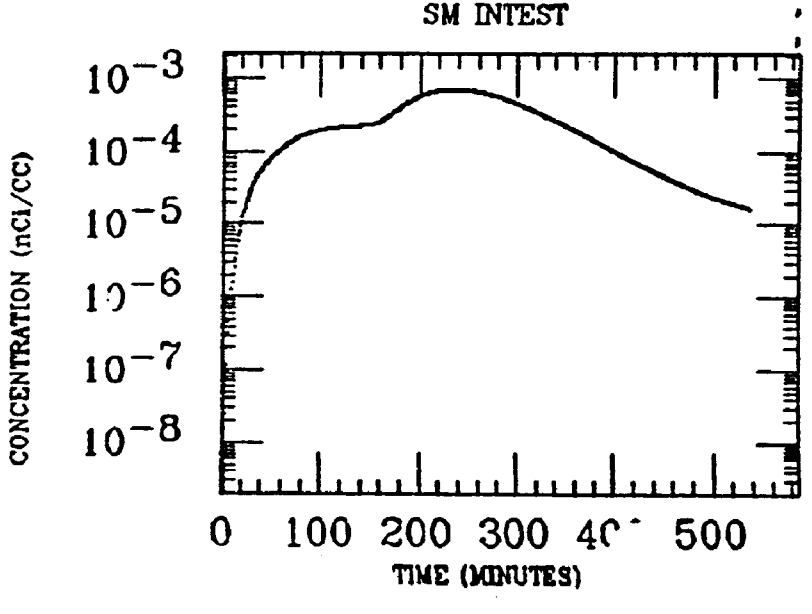

MONROE
XE INGESTION
Bi-214

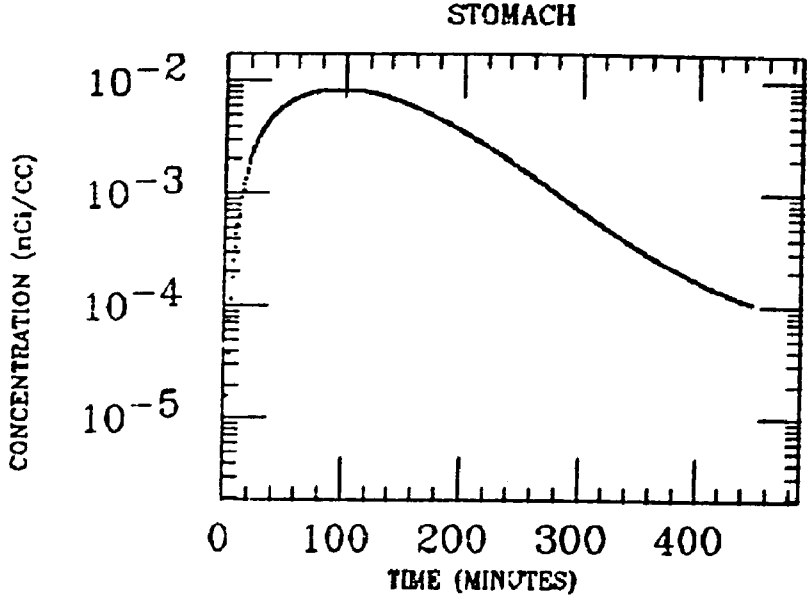

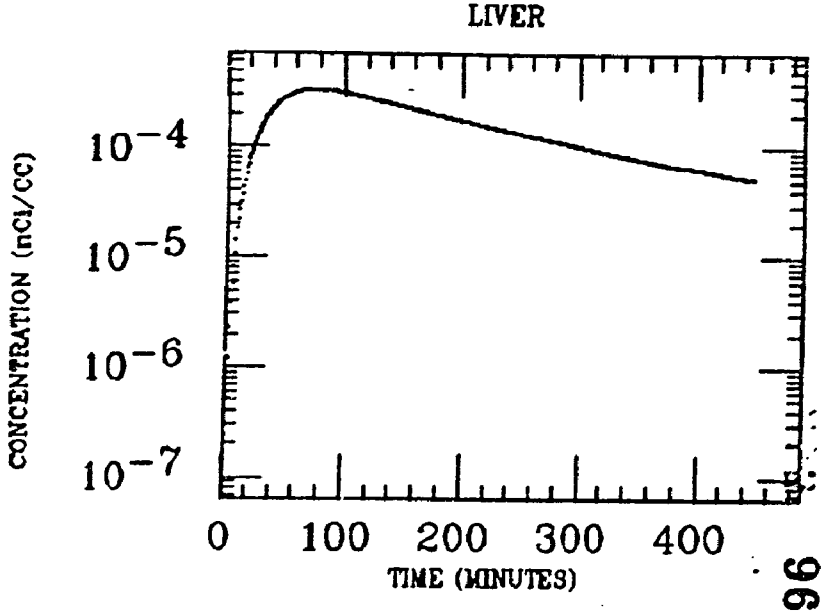

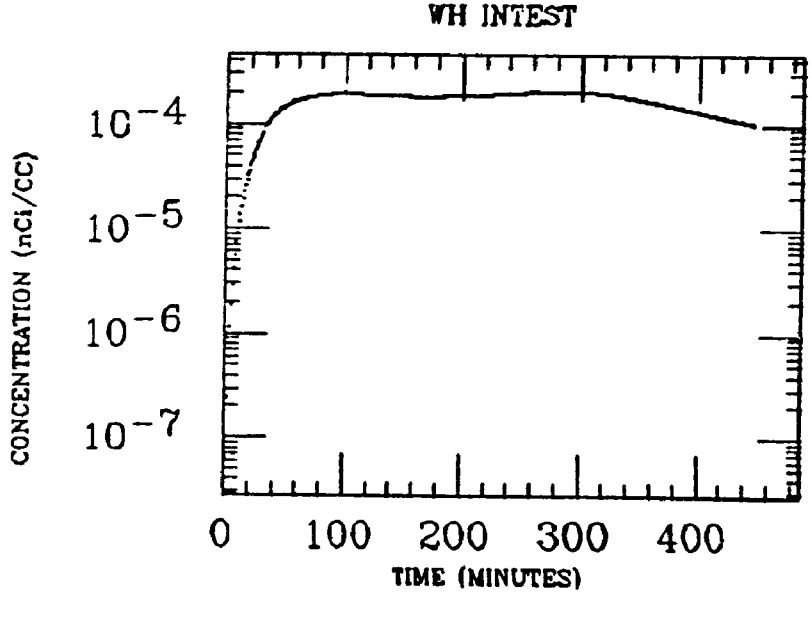

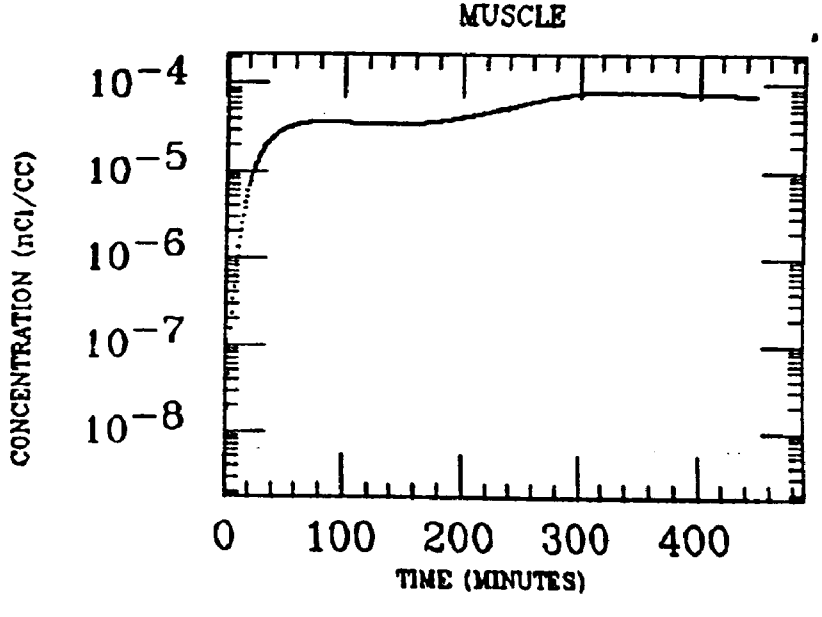

MONROE
XE INGESTION
Bi-214

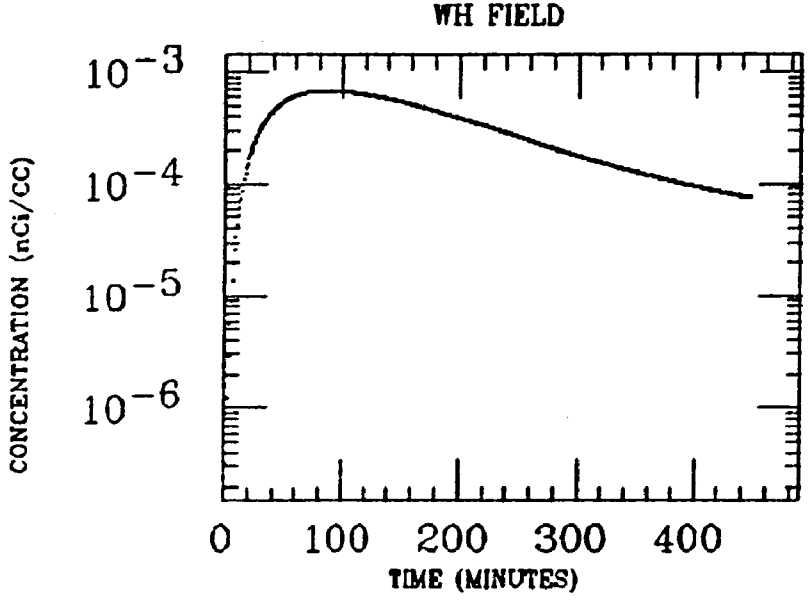

MORGAN
XE INGESTION
Bi-214

STOMACH

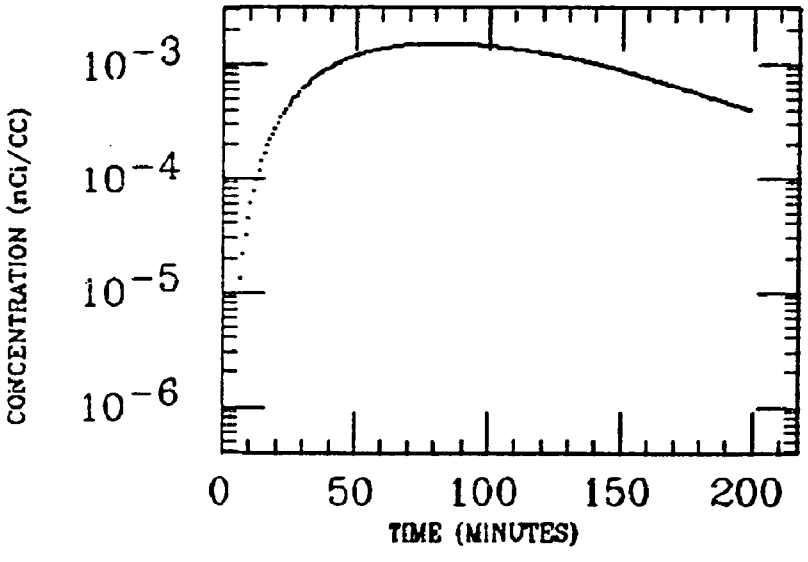

LIVER

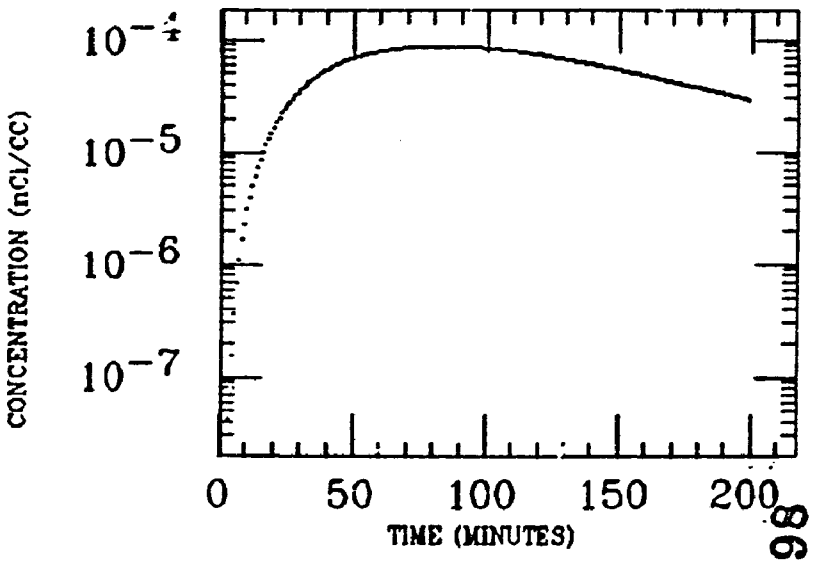

SM INTEST

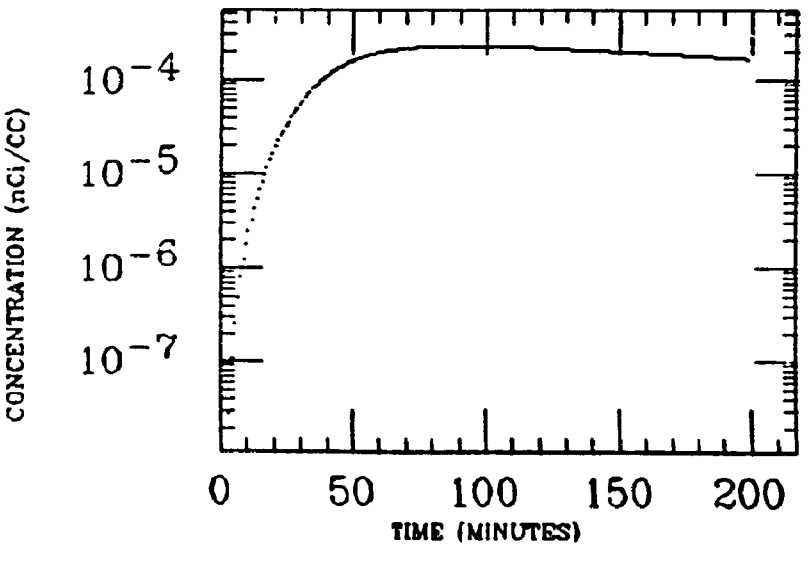

MUSCLE

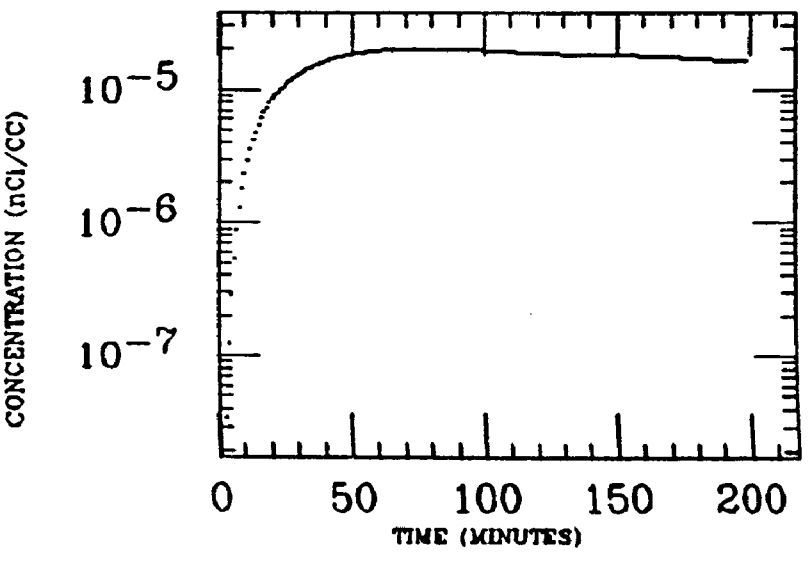

MORGAN
XE INGESTION
Bi-214

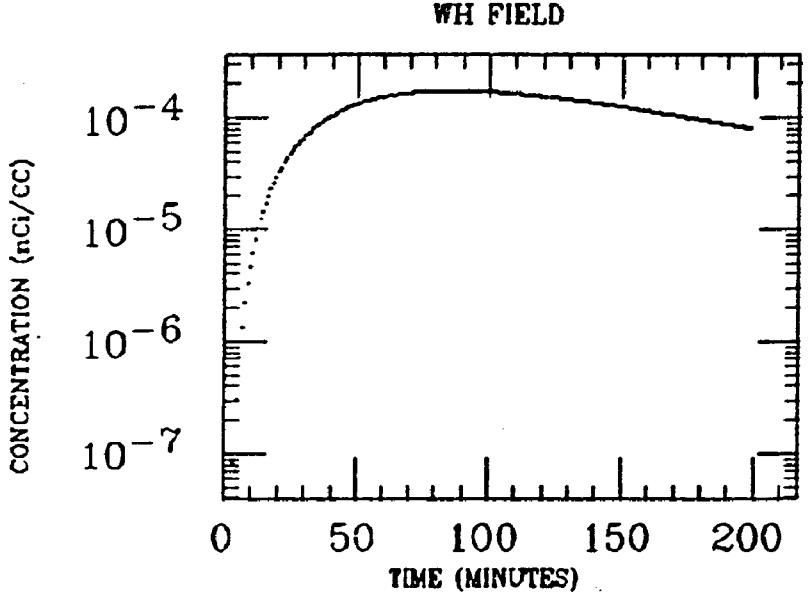

MURCHE

XE INGESTION

Bi-214

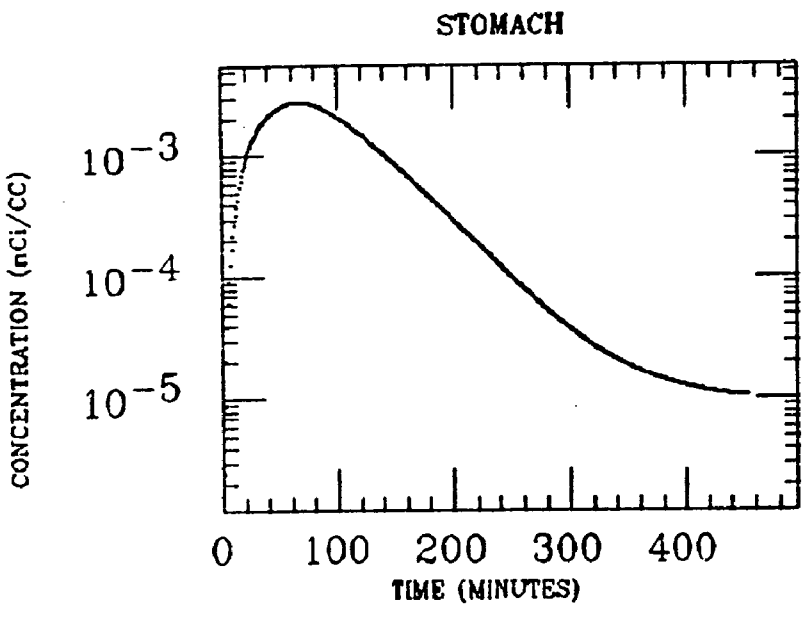

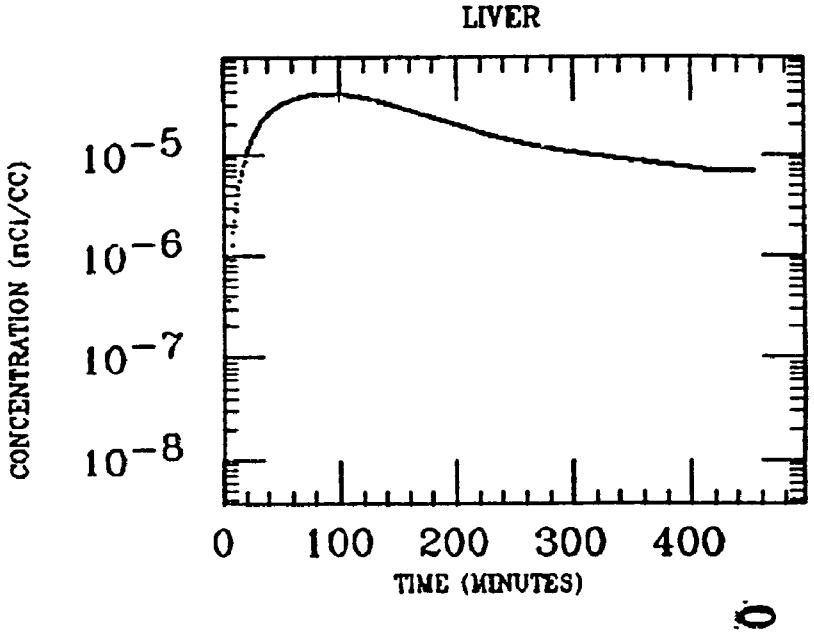

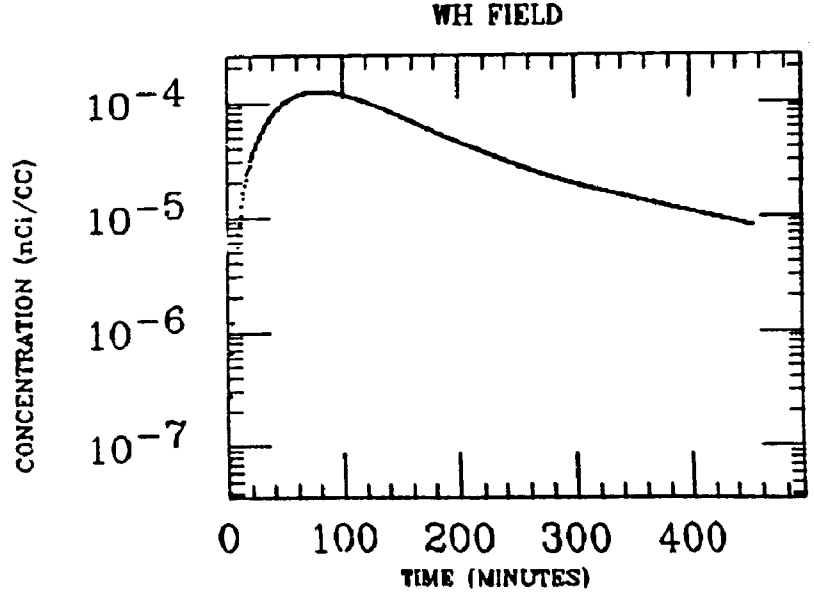

300

MURCHE
Xe INGESTION
Bi-214

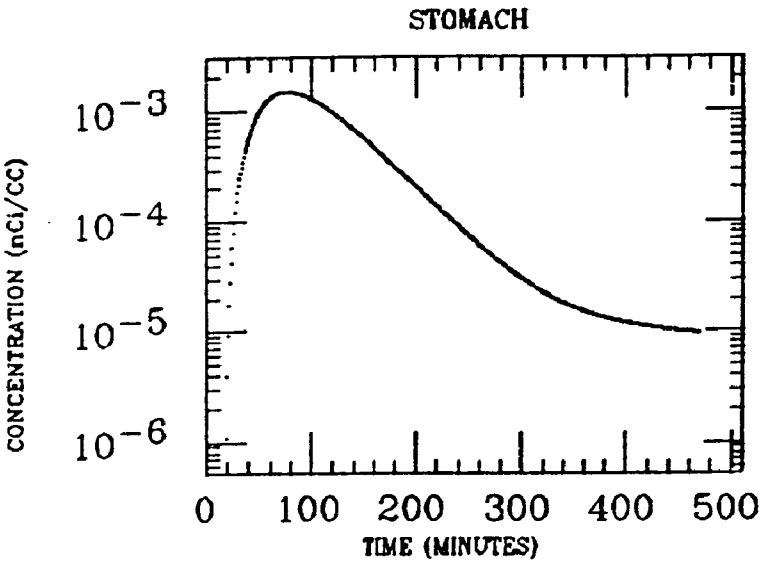

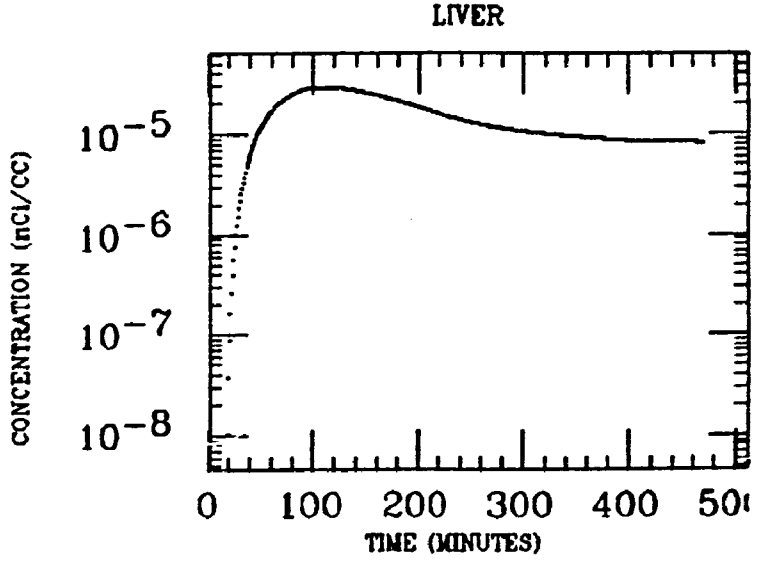

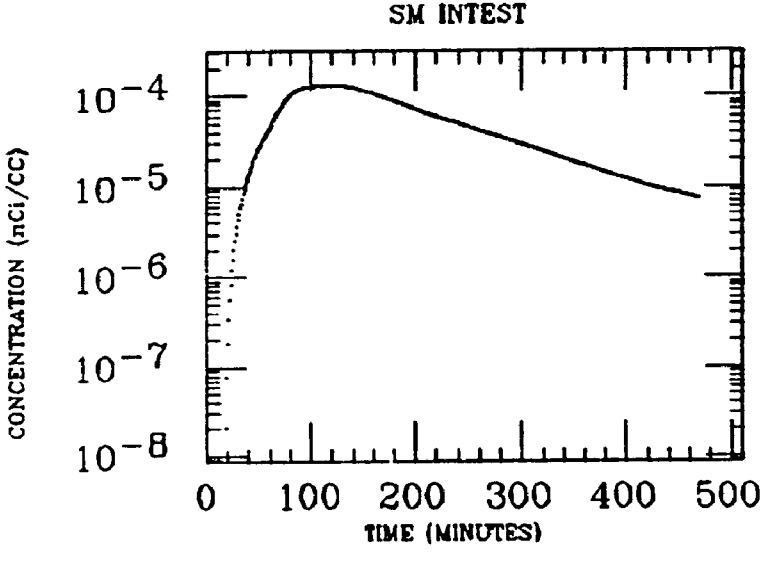

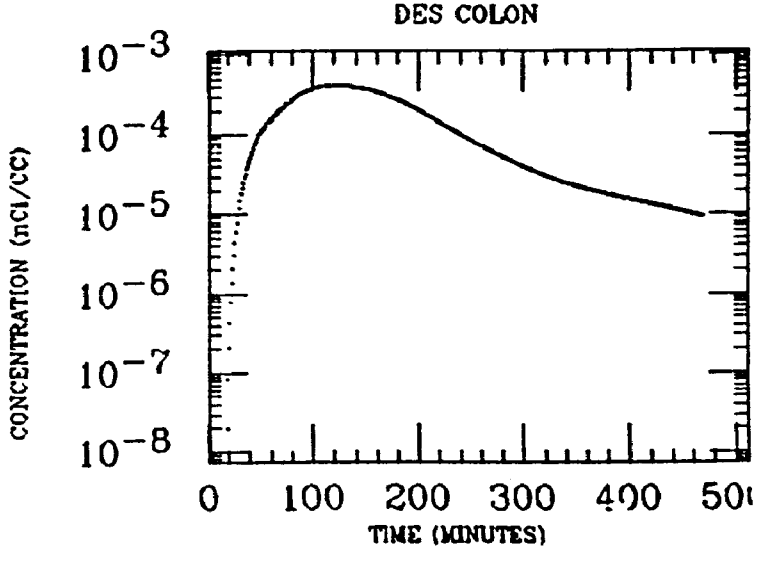

MURCHE
XE INGESTION
Bi-214

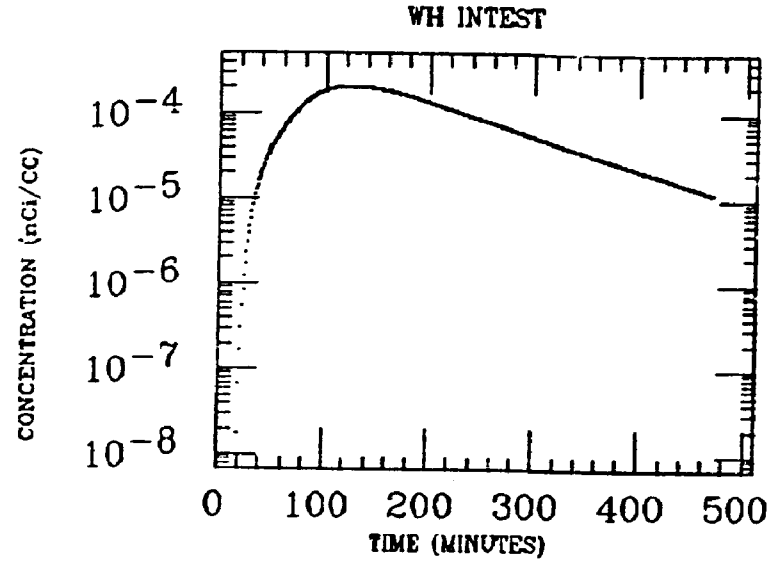

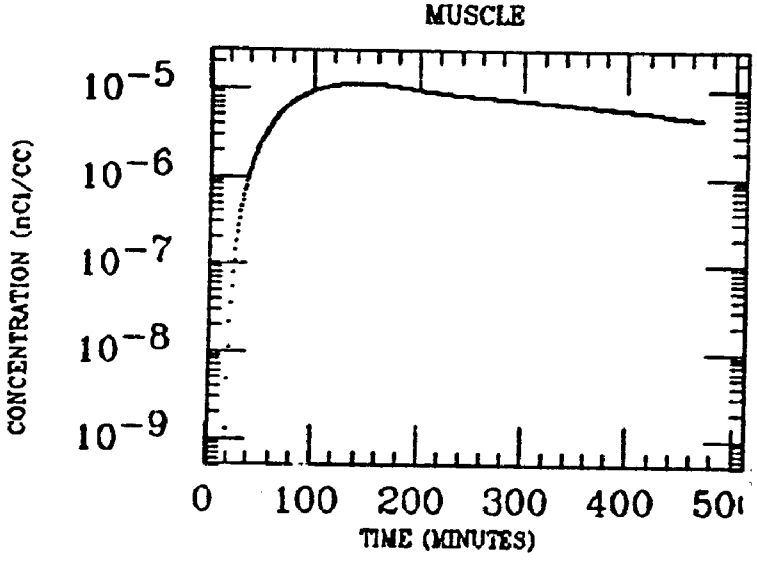

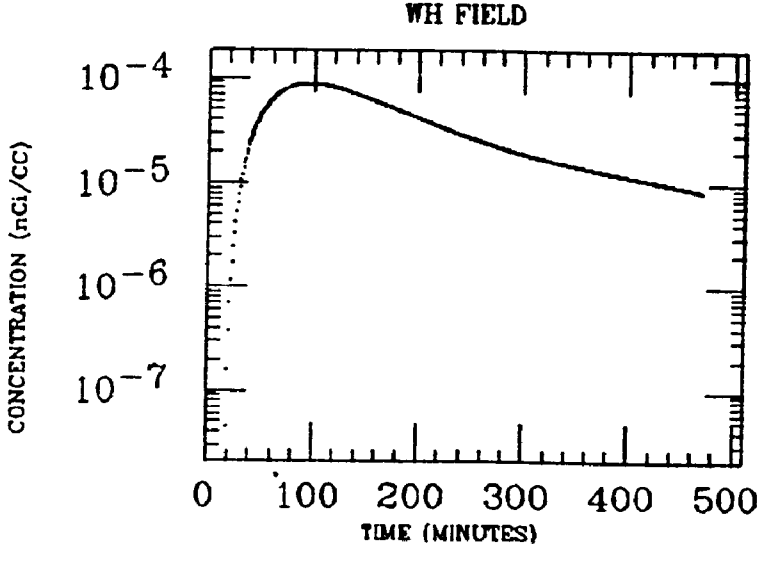

PARK
XE INGESTION
Bi-214

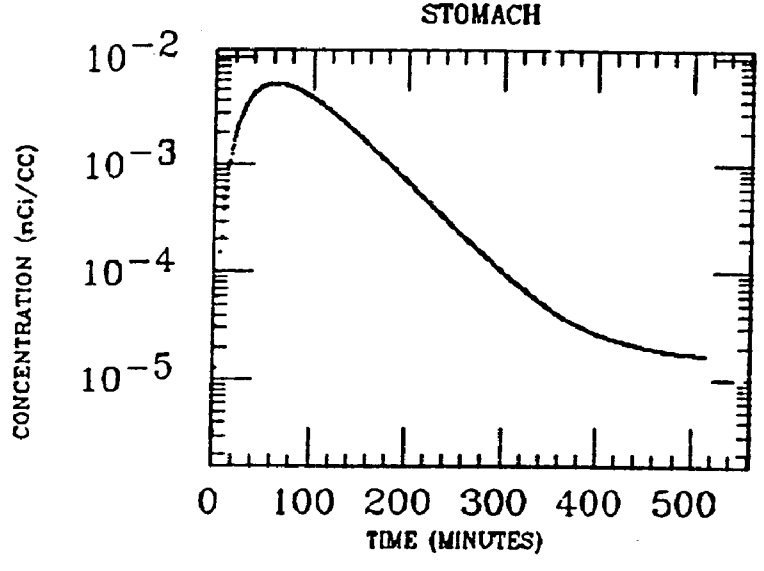

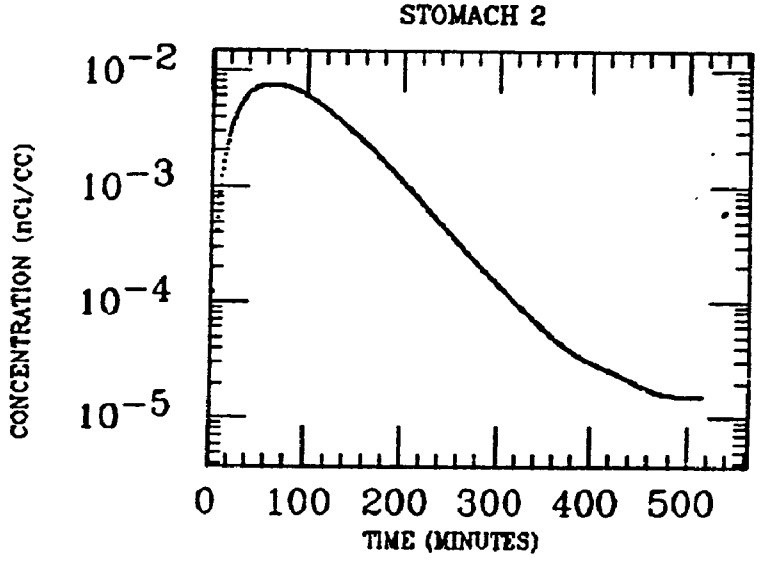

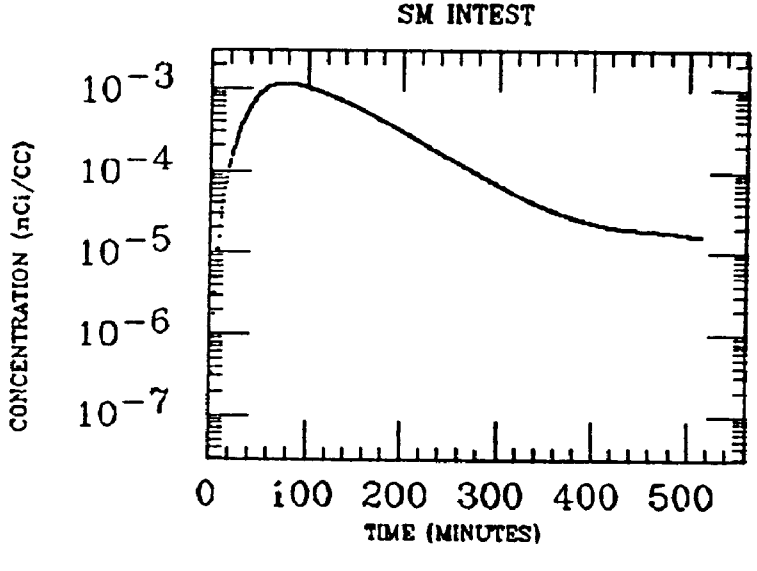

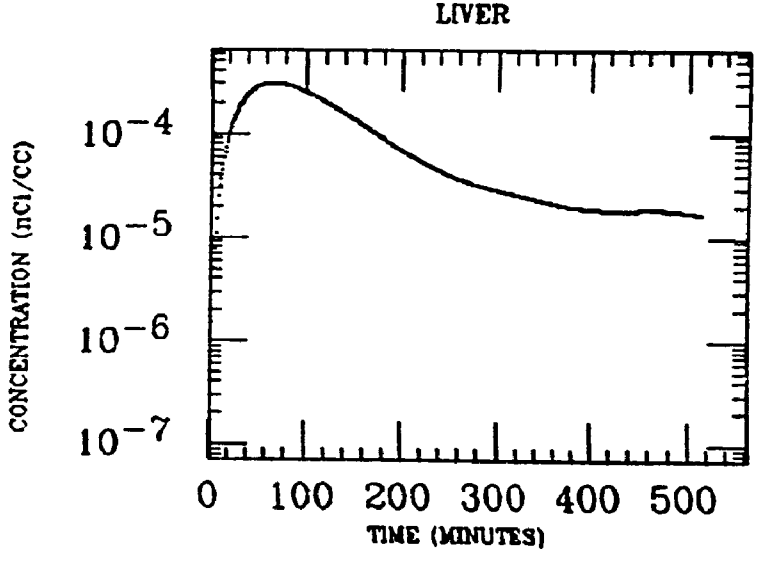

PARK
XE INGESTION
Bi-214

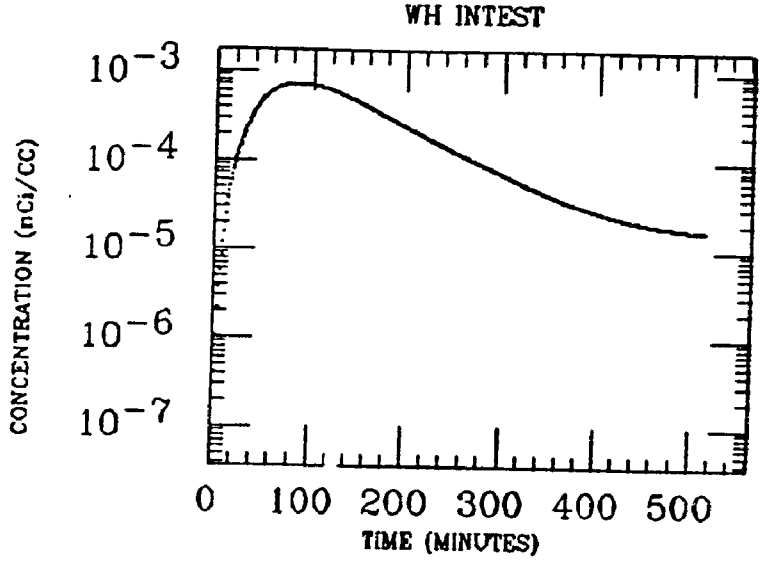

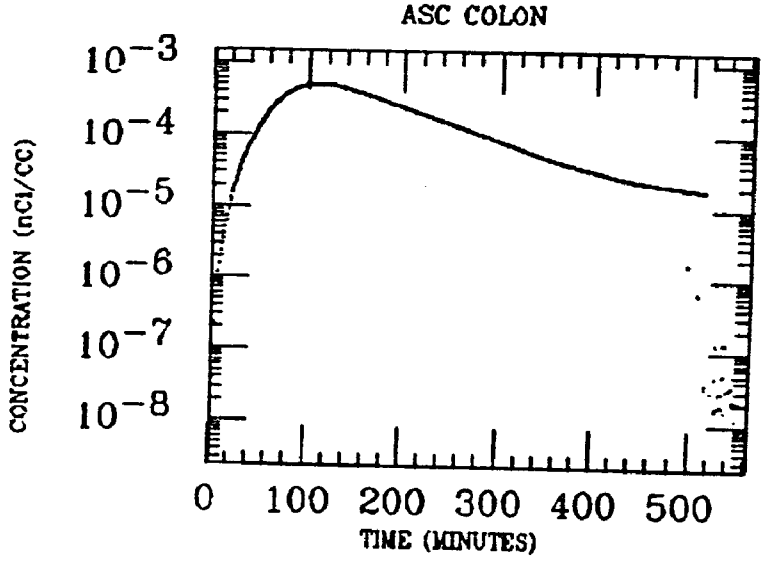

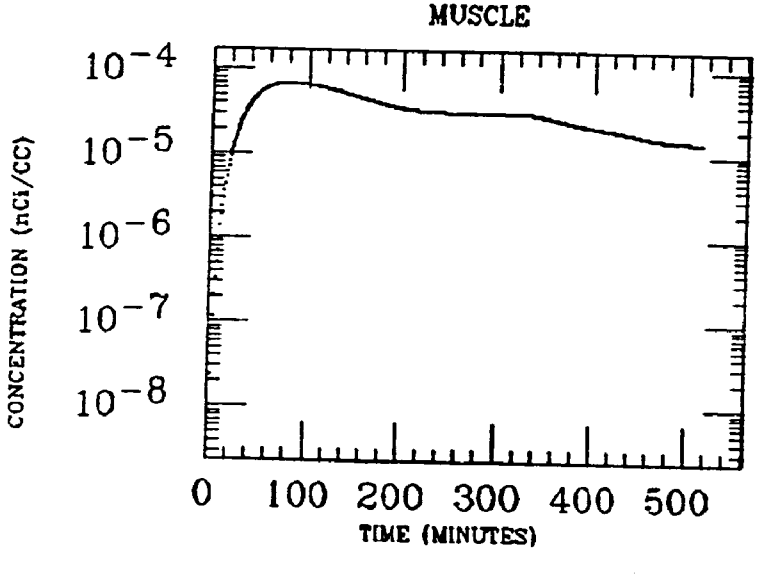

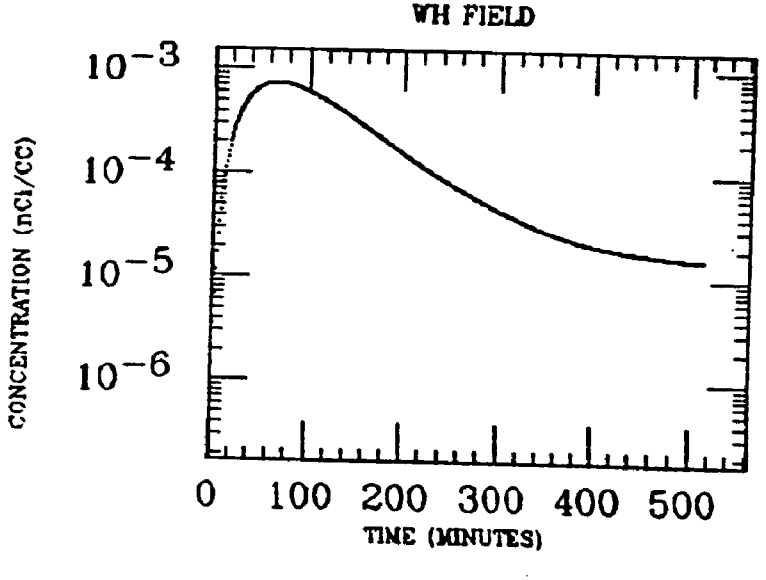

TAATJES
XE INGESTION
Bi-214

TAATJES
XE INGESTION
Bi-214

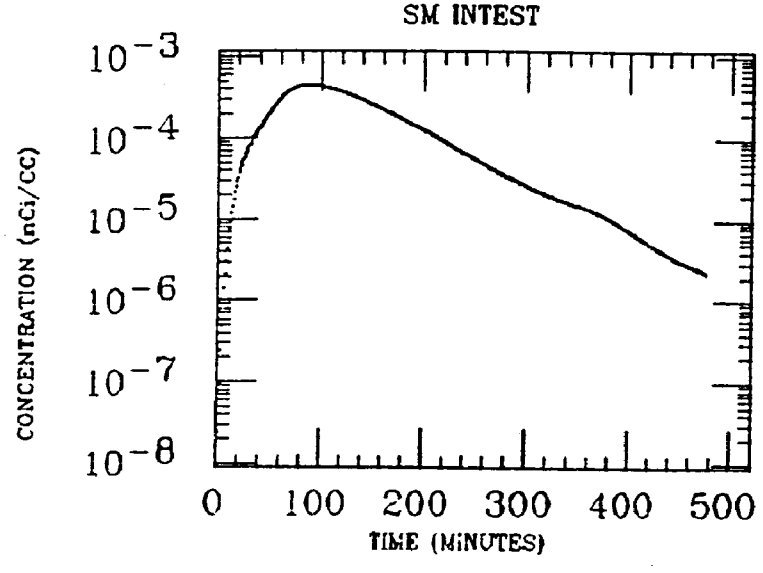

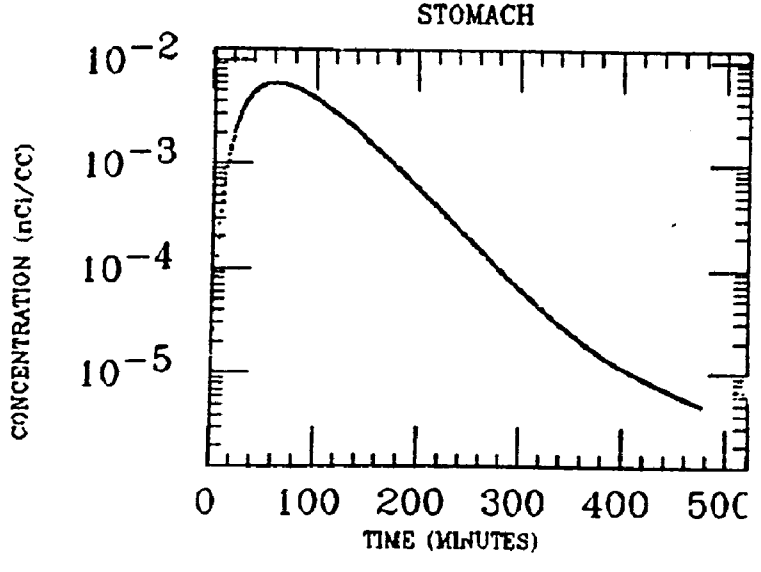

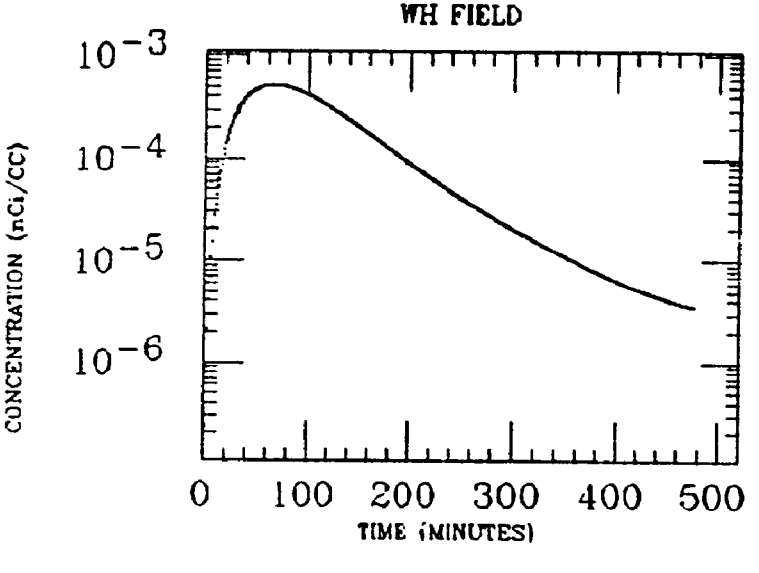

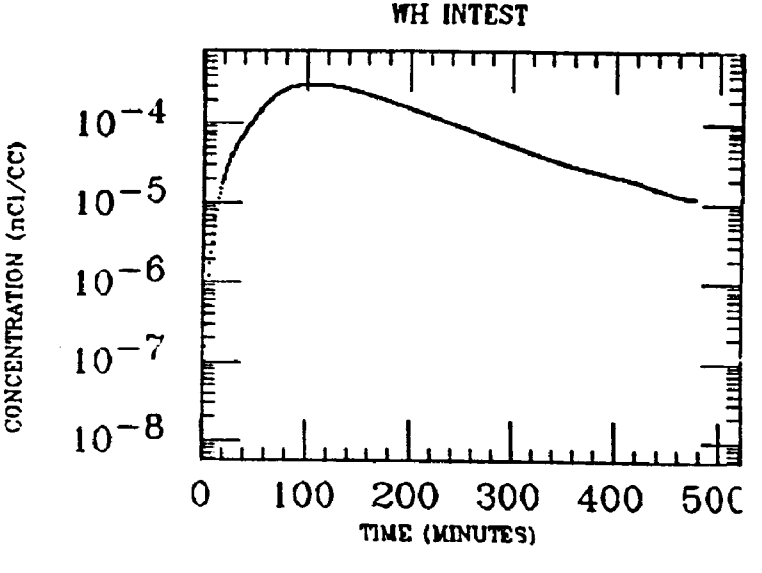

TAYLOR
XE INGESTION
Bi-214

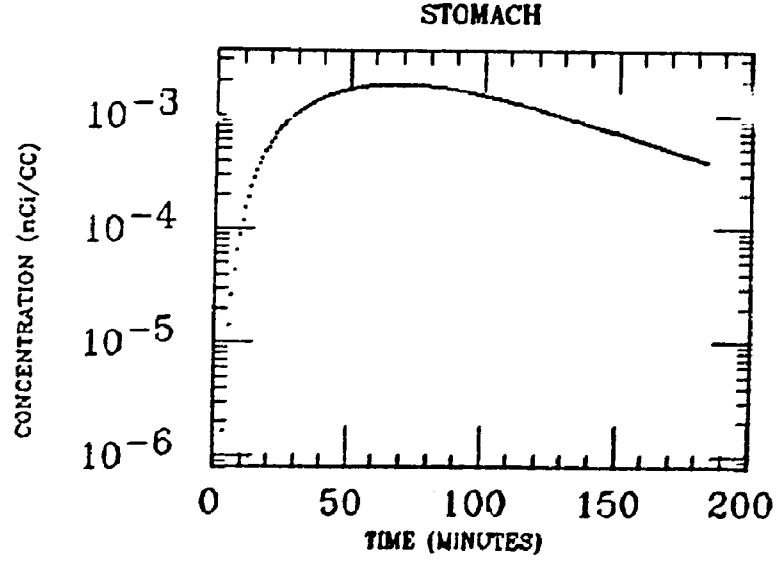

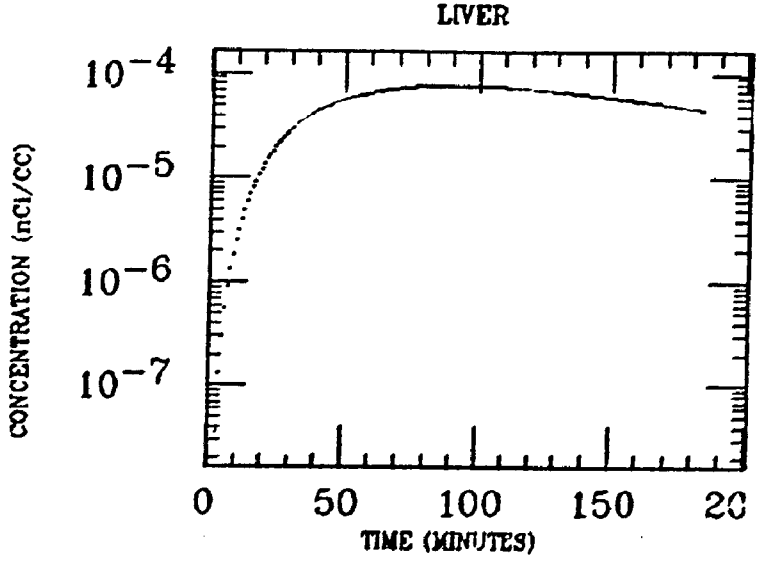

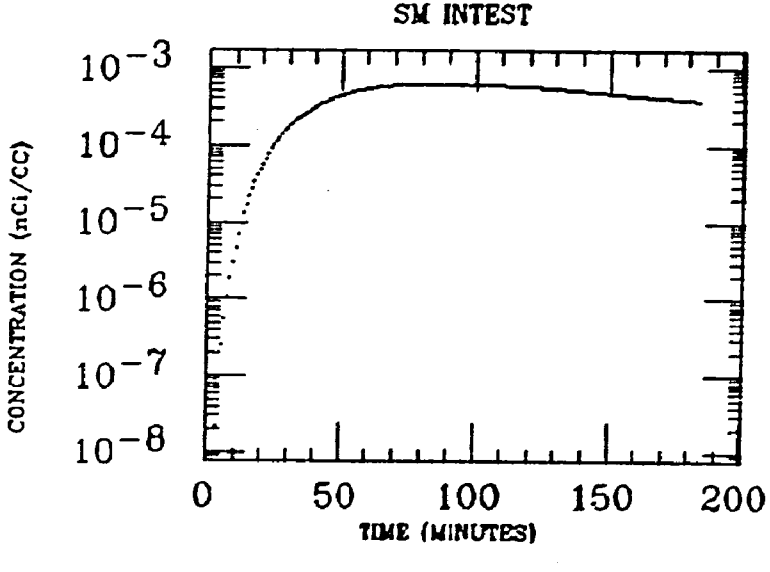

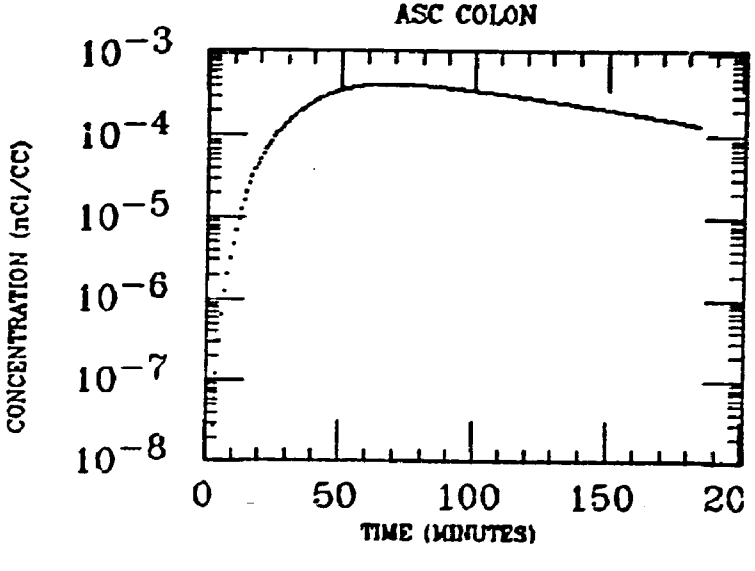

TAYLOR
XE INGESTION
Bi-214

DES COLON

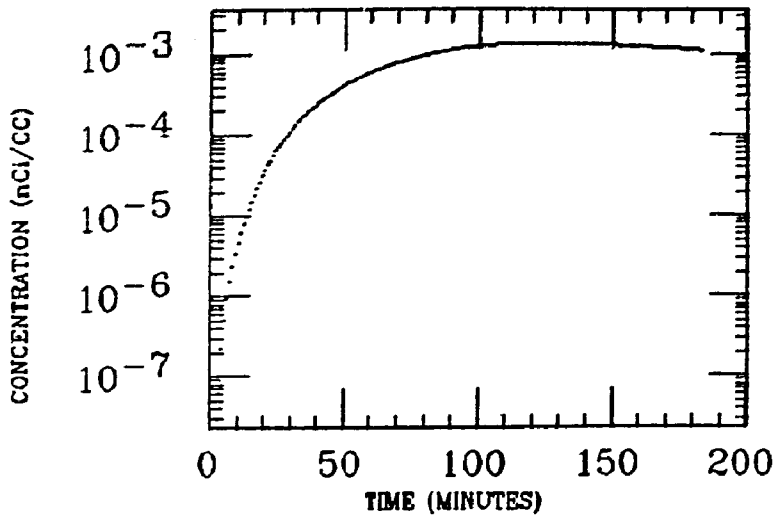

TR COLON

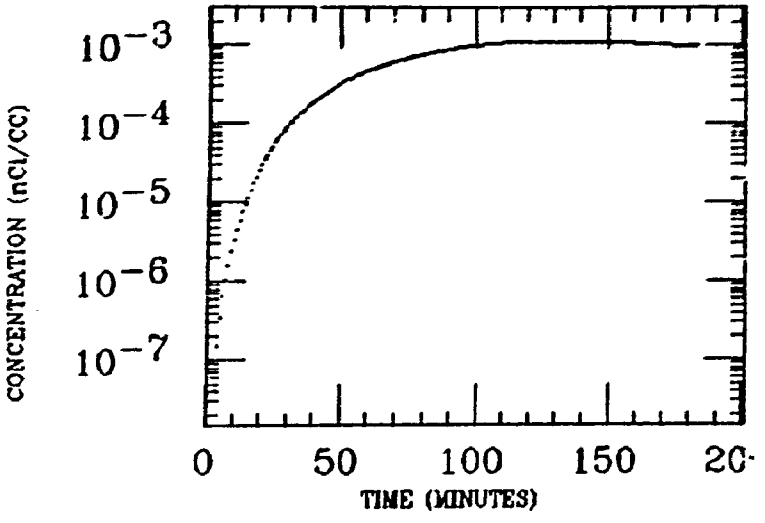

LG INTEST

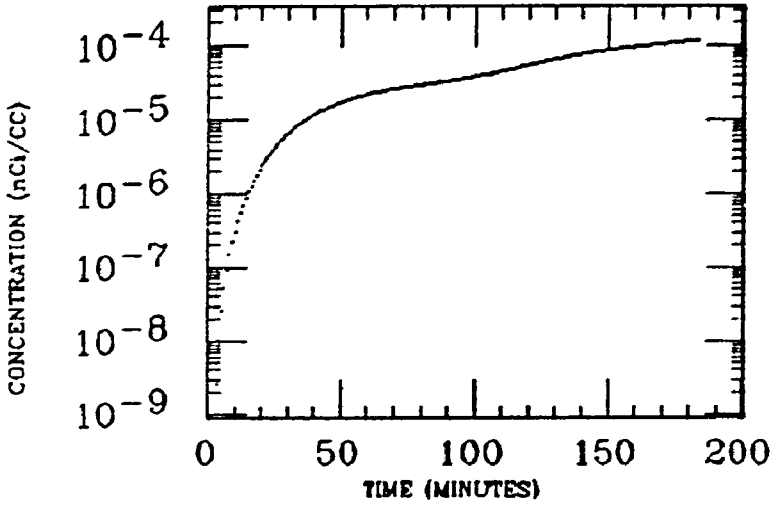

WH INTEST

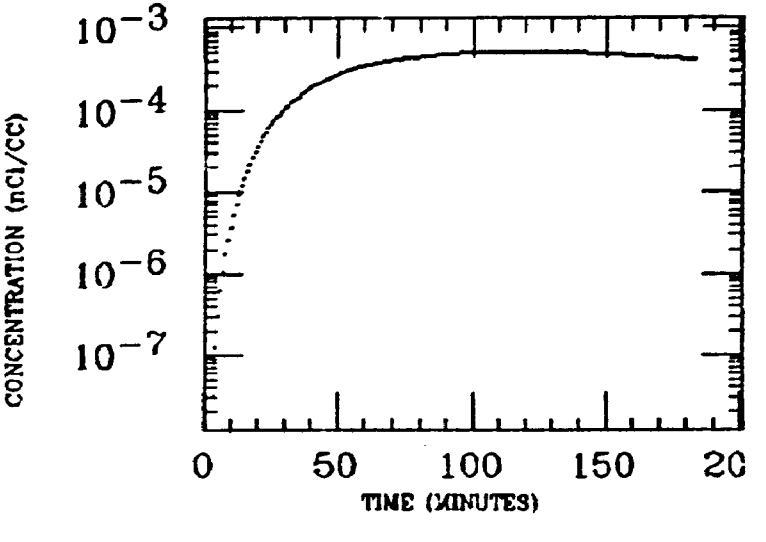

WESOLEK
XE INGESTION
Bi-214

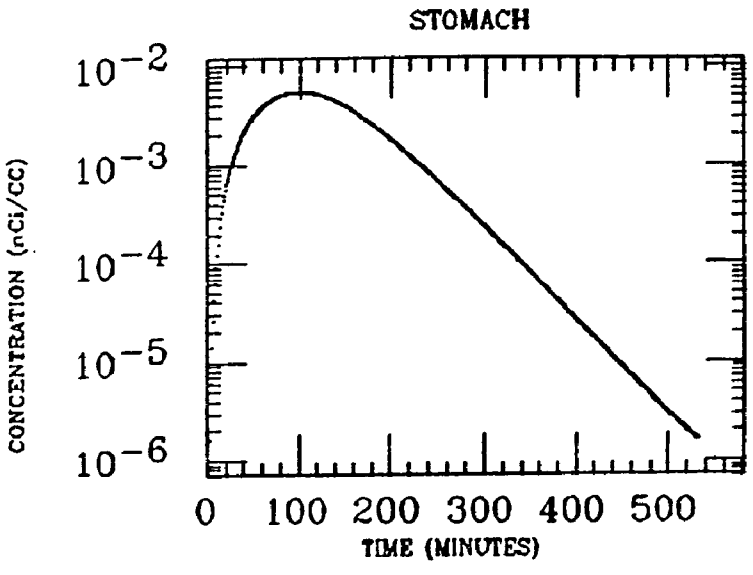

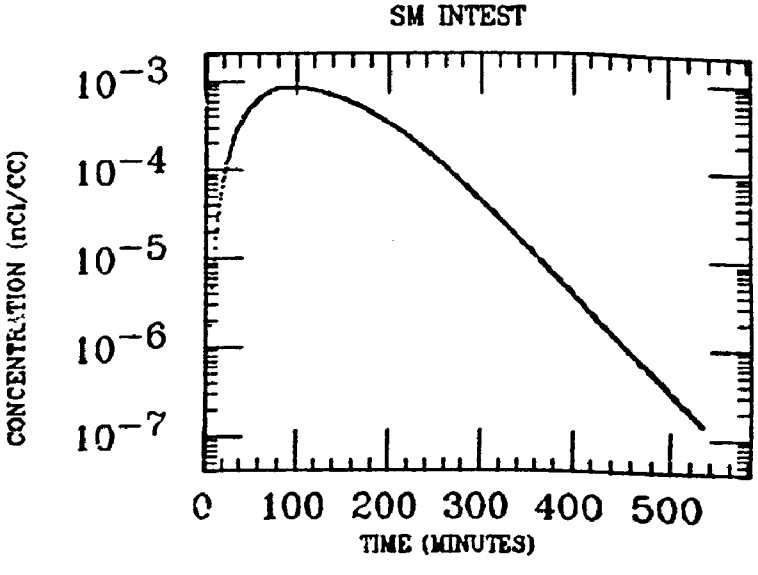

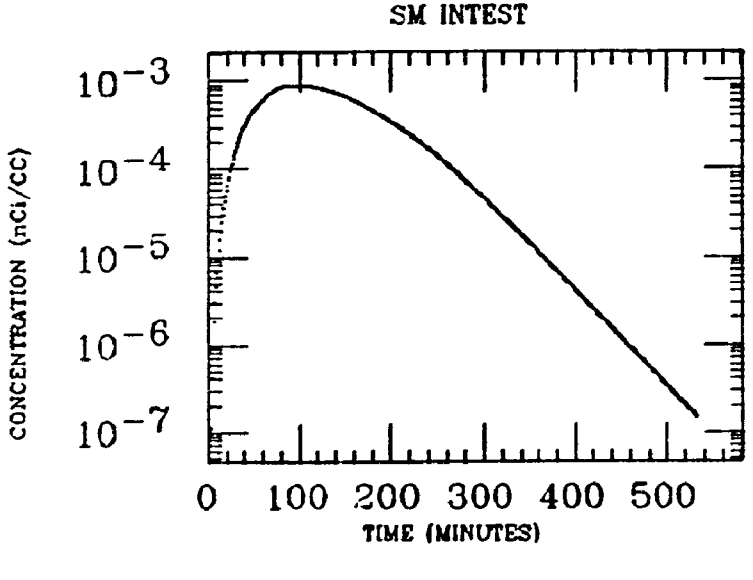

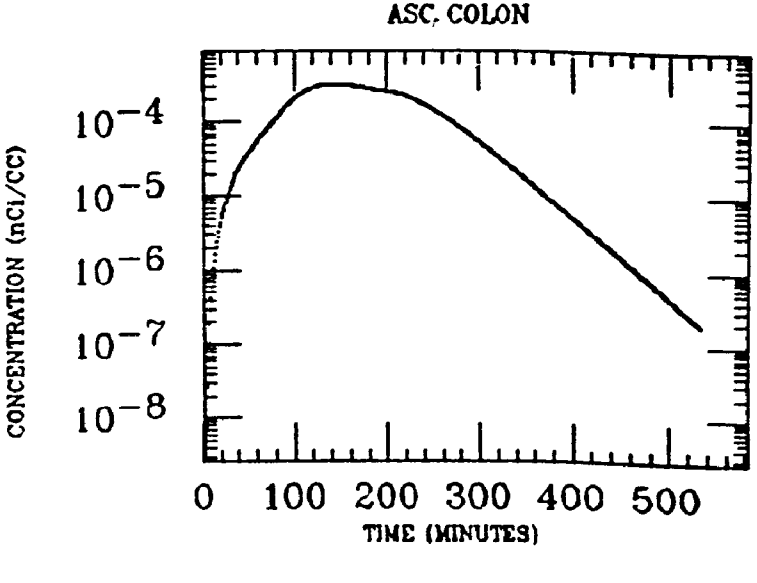

WESOLEK
XE INGESTION
Bi-214

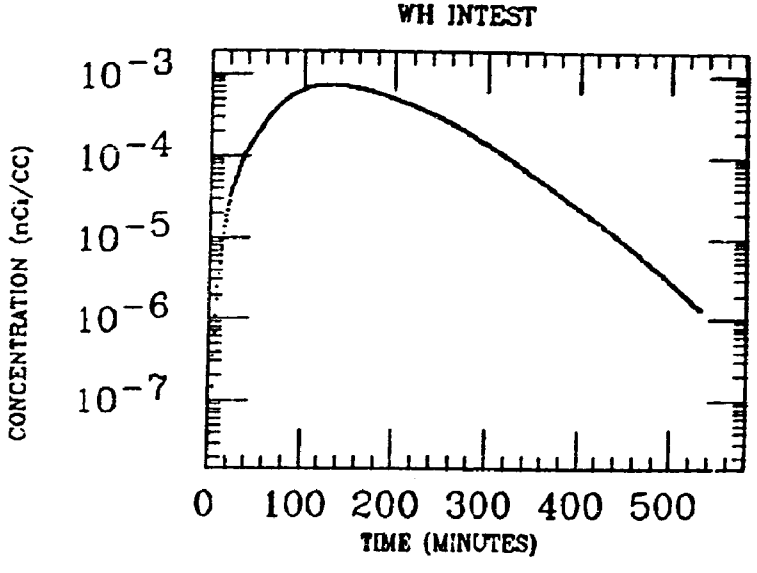

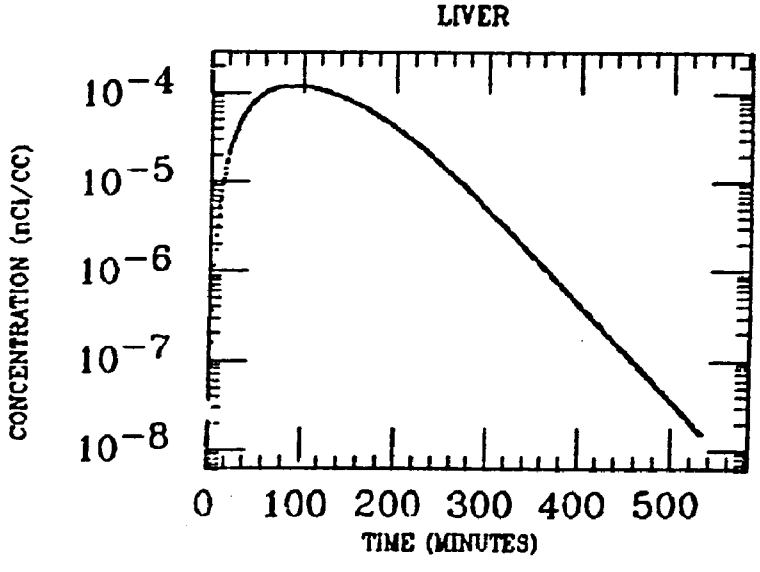

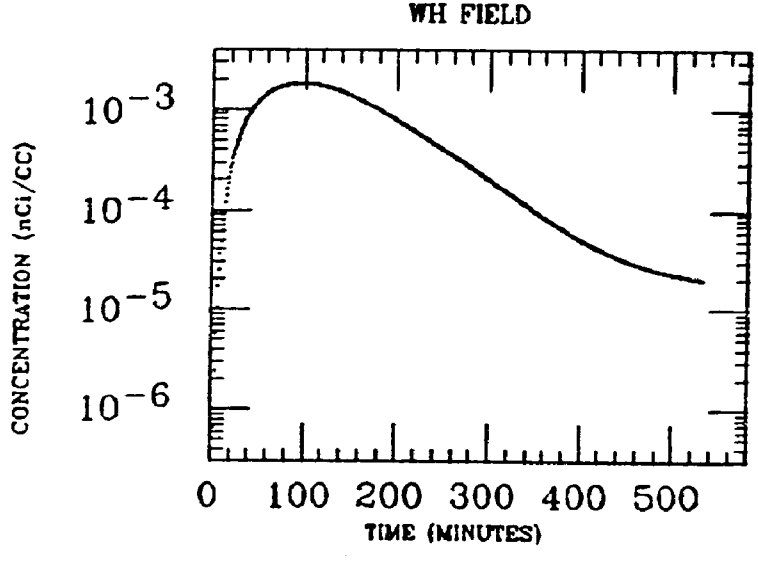

WILTSE
XE INGESTION
Bi-214

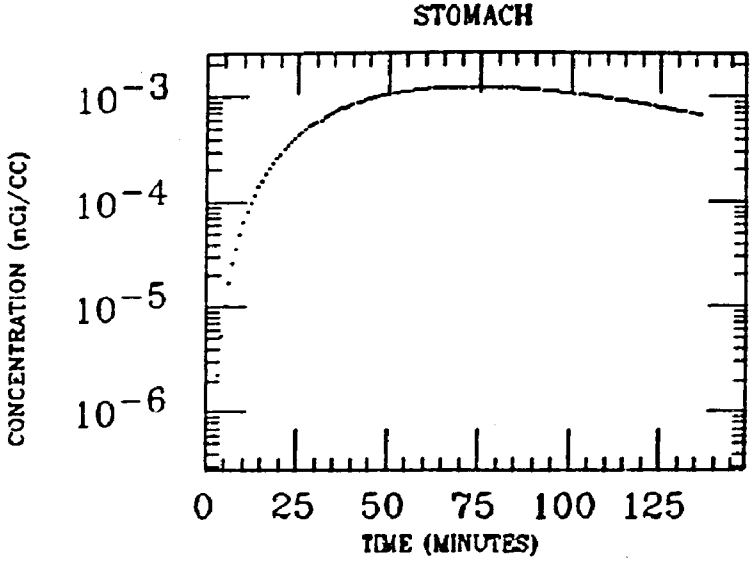

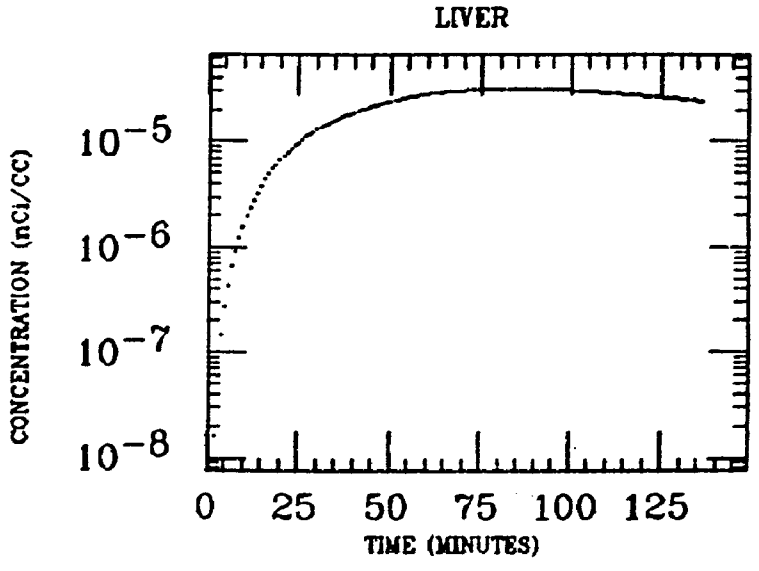

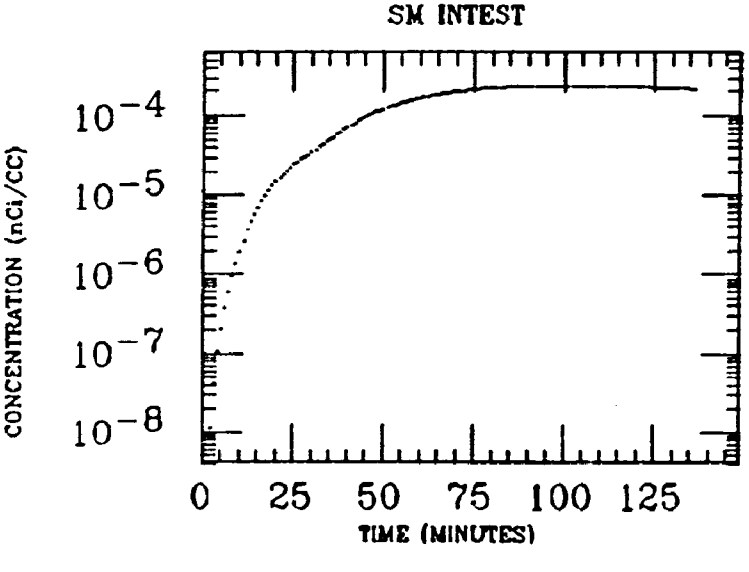

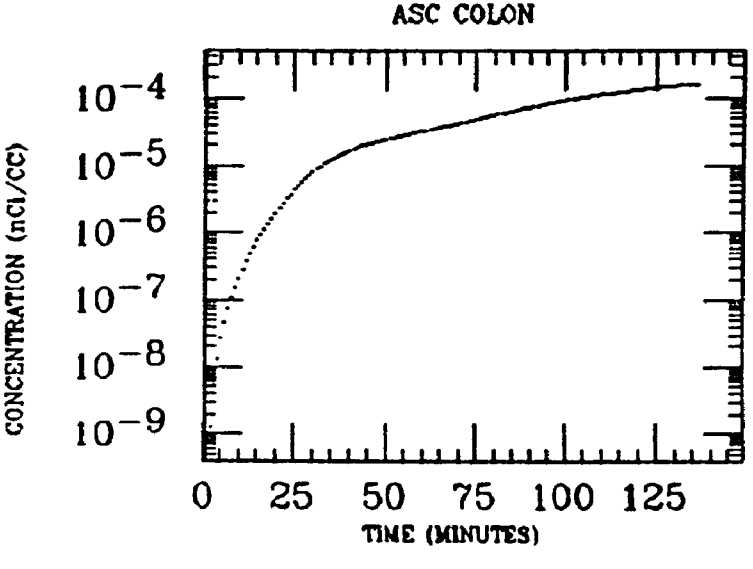

WILTSE
XE INGESTION
BI-214

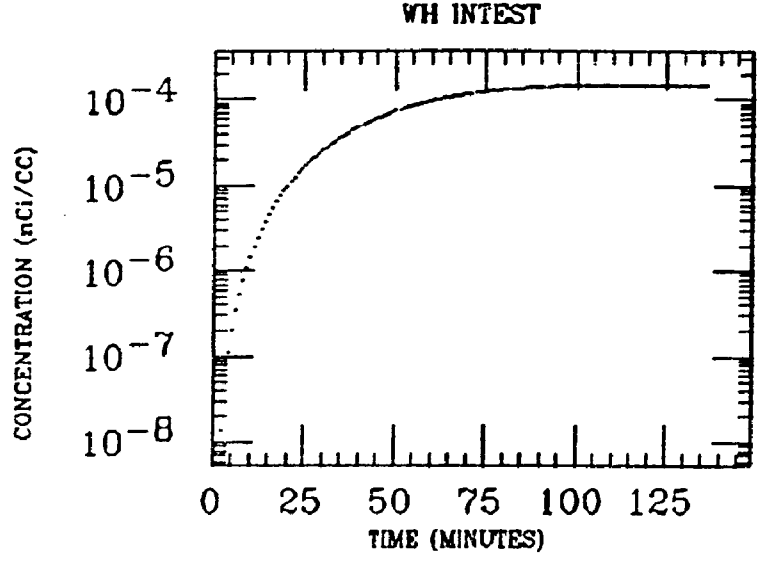

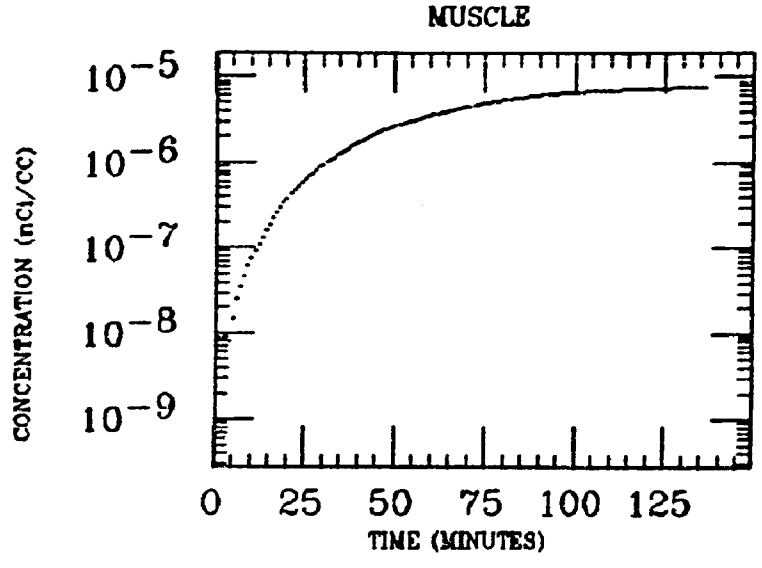

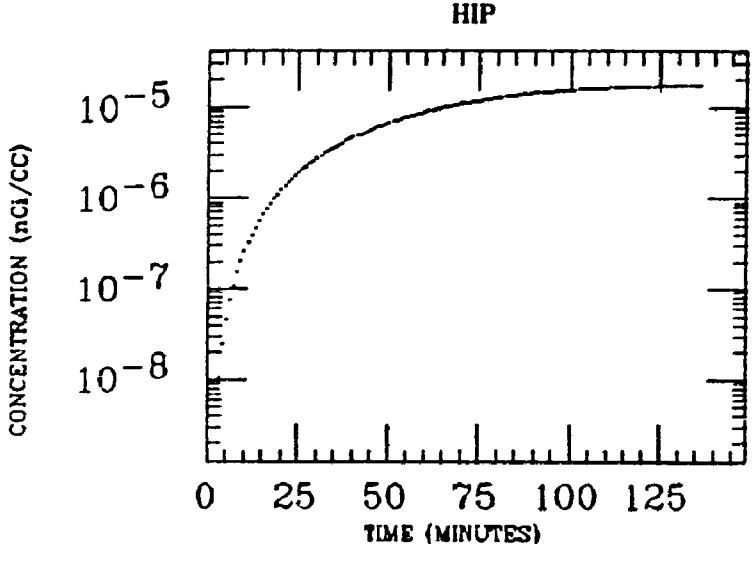

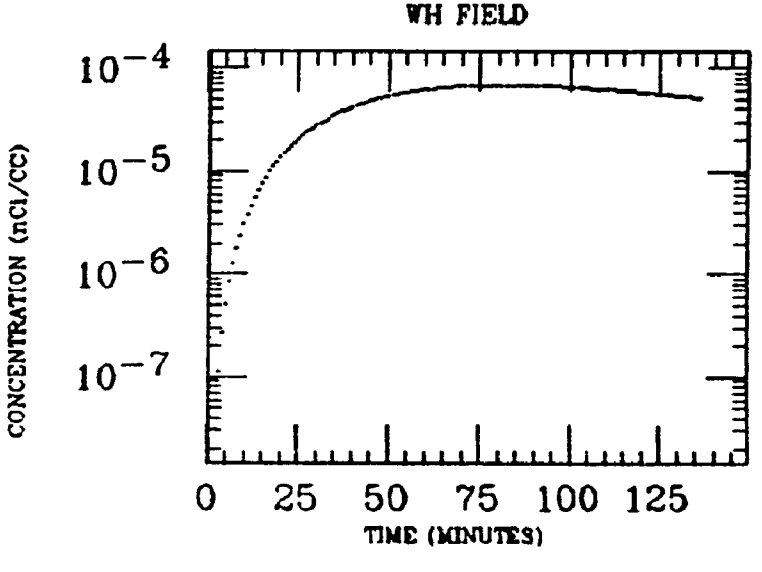

AHERN
XE INGESTION
Po-214

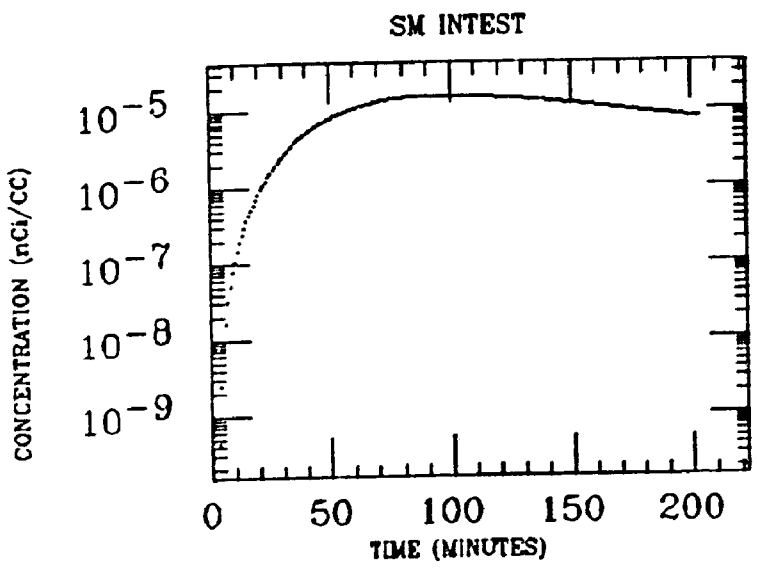

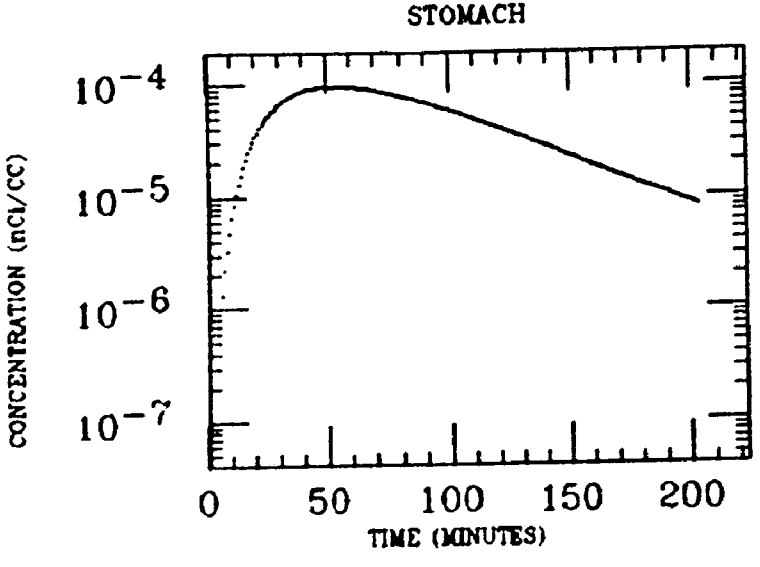

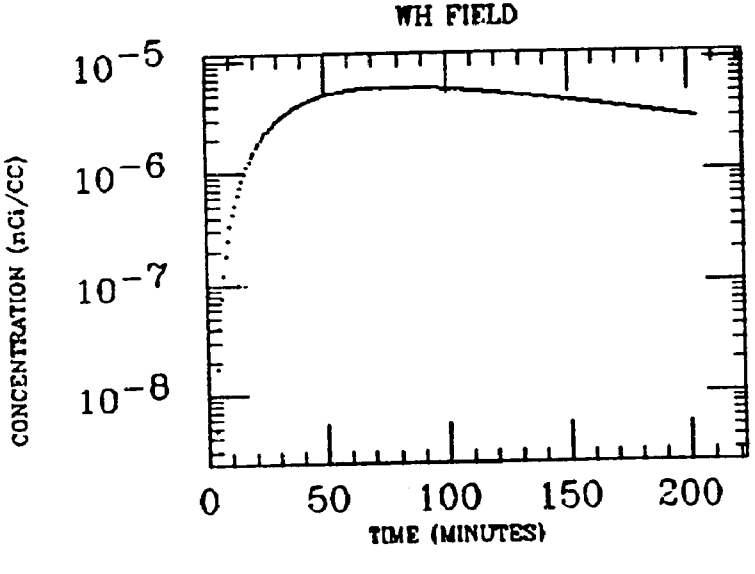

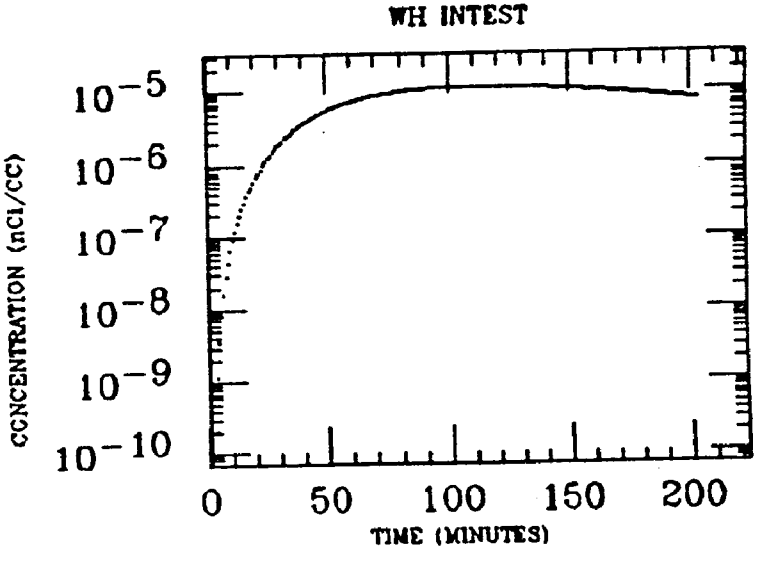

AHERN
XE INGESTION
Po-214

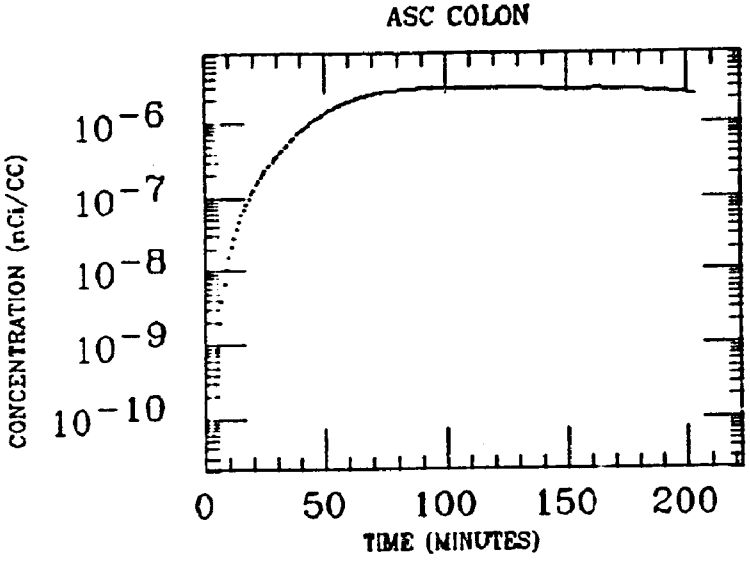

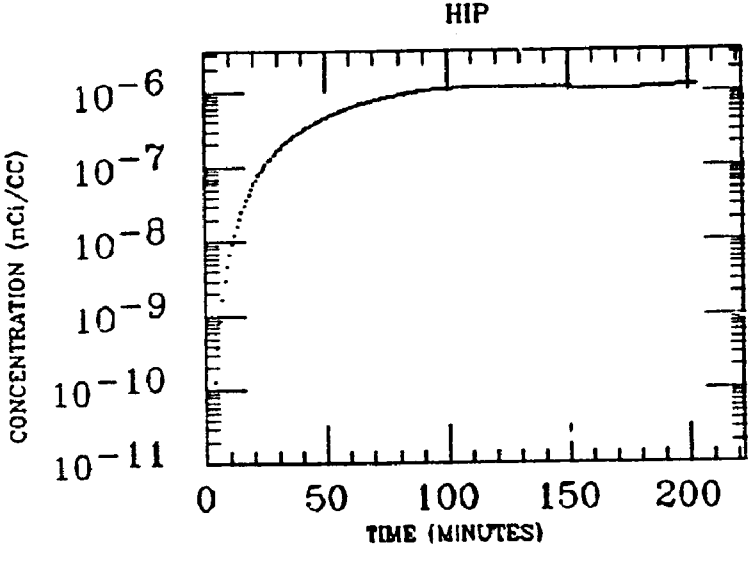

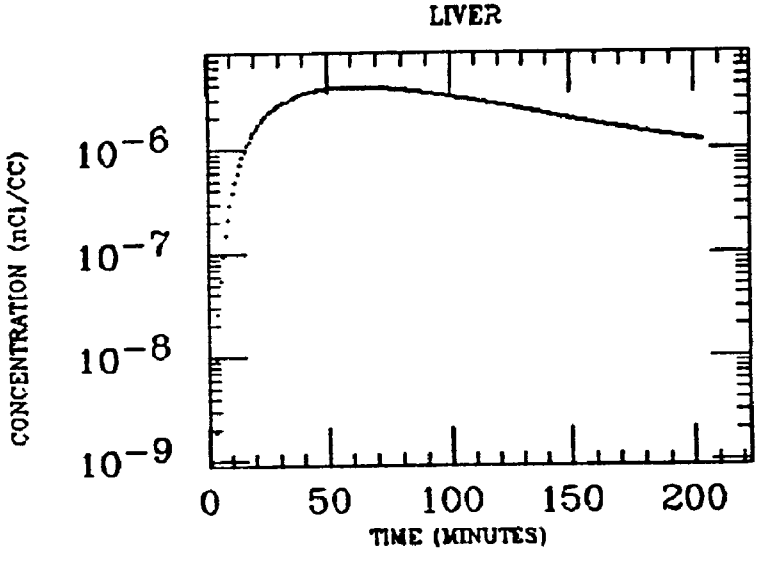

ARROL
XE INGESTION
Po-214

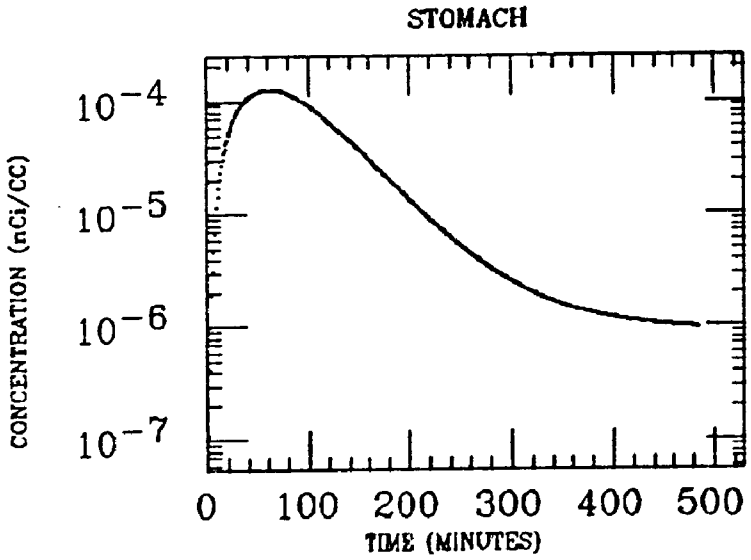

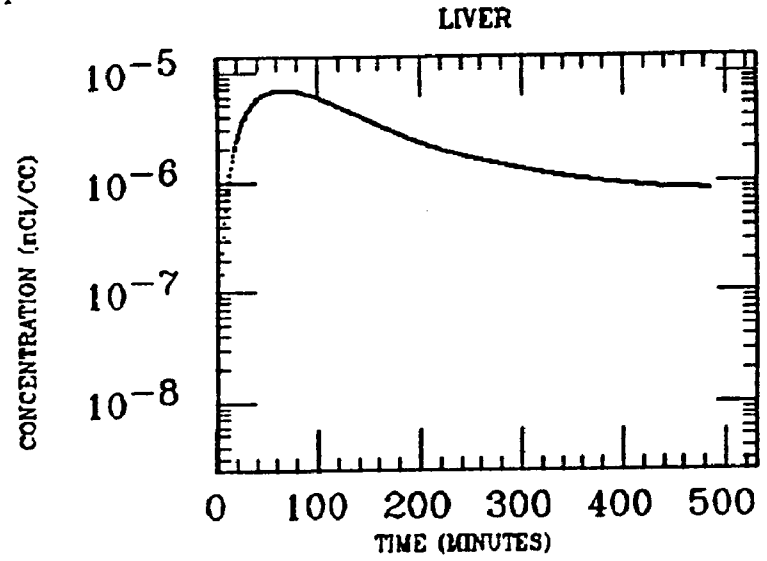

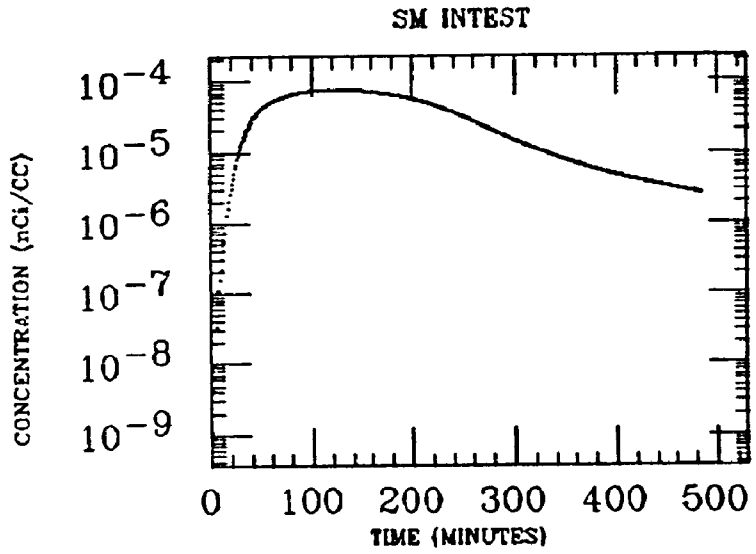

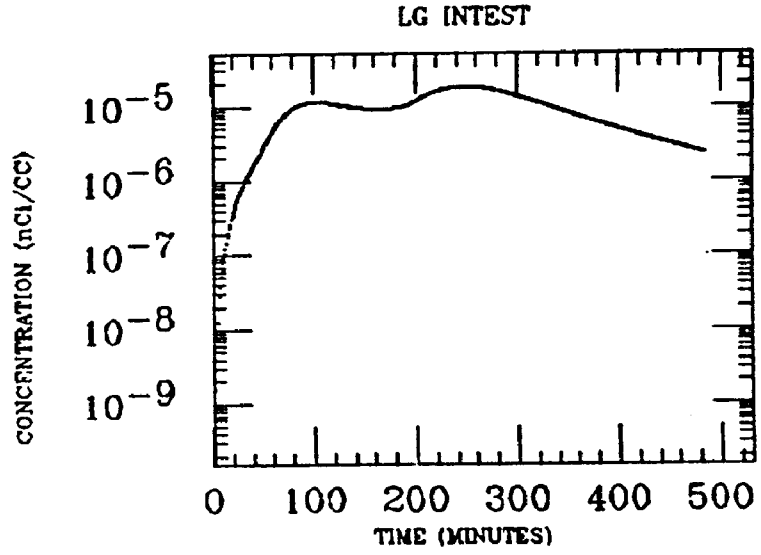

ARROL
XE INGESTION
Po-214

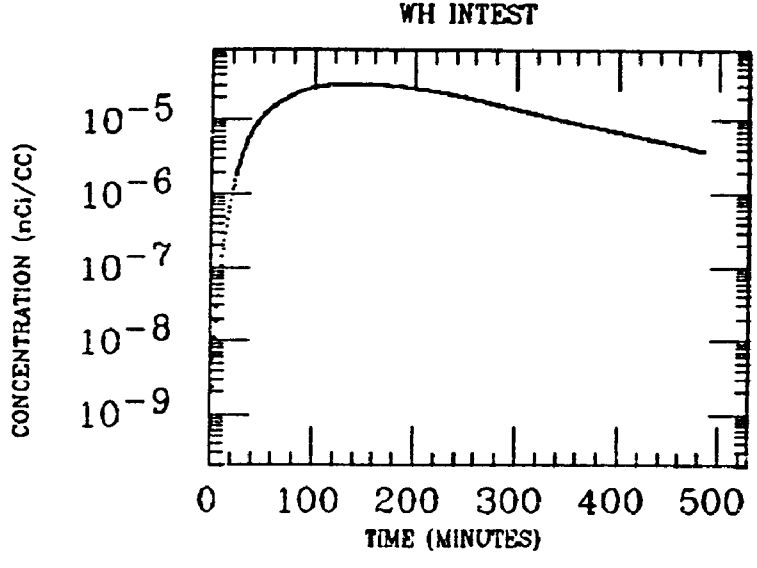

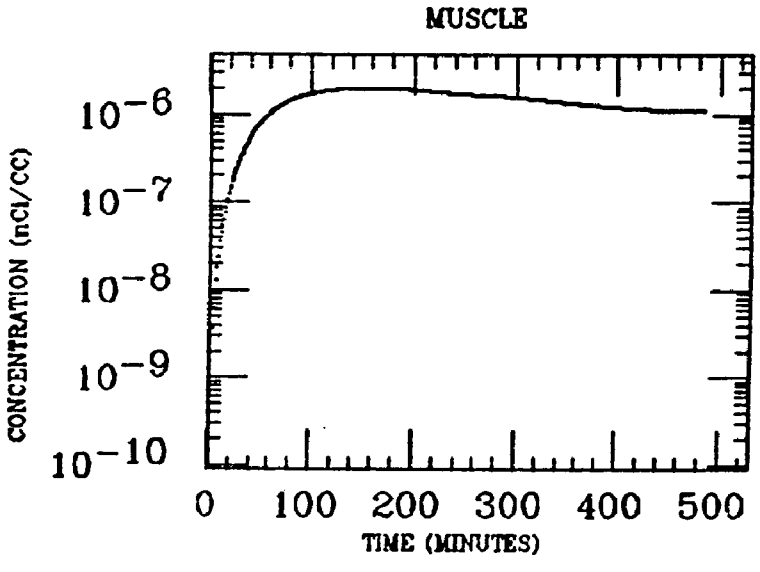

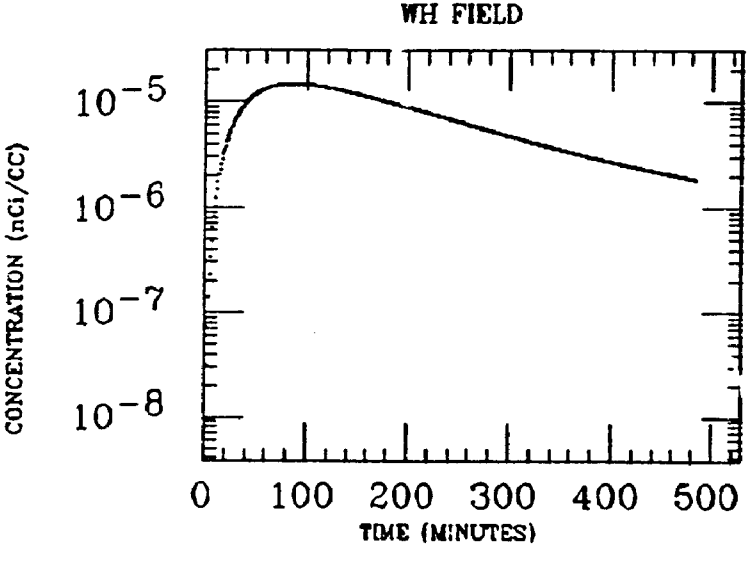

AYER

XE INGESTION

Po-214

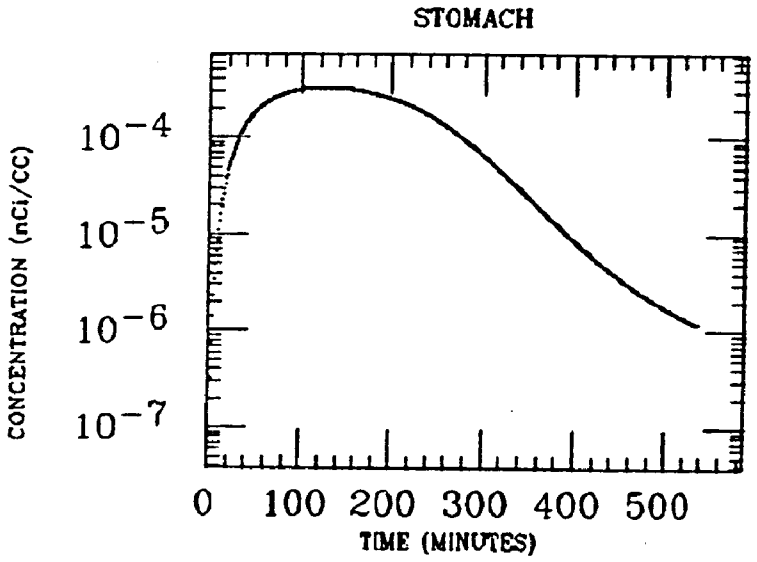

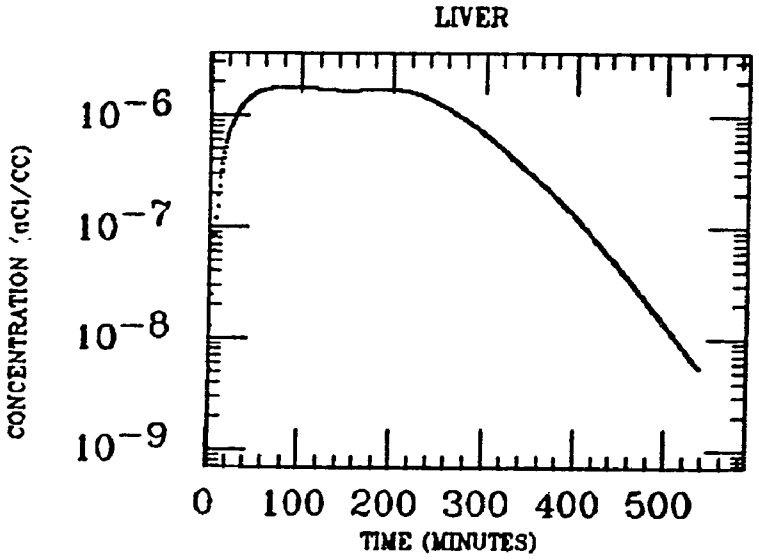

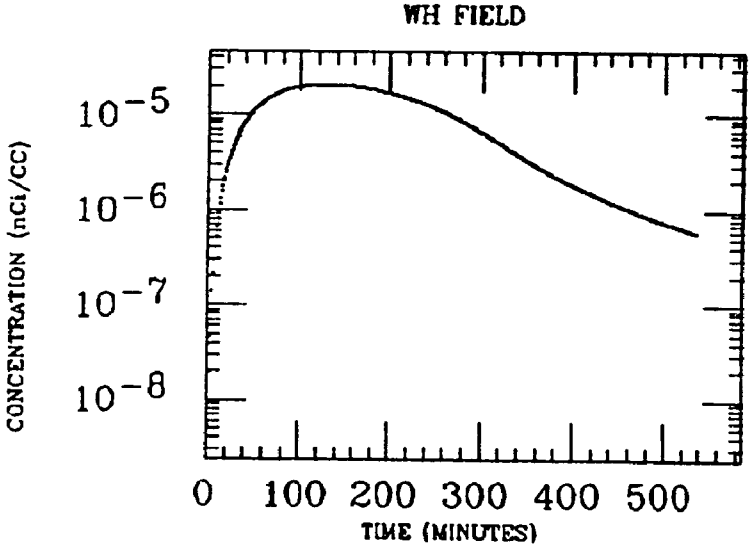

AYER

XE INGESTION

Po-214

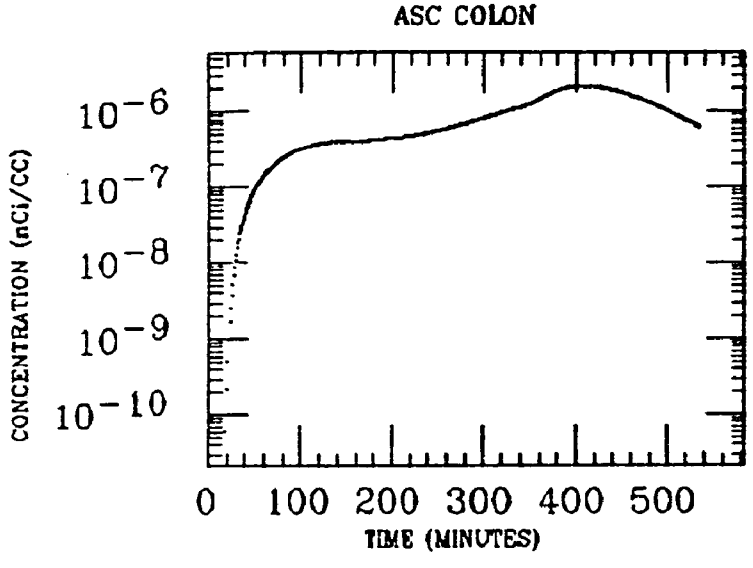

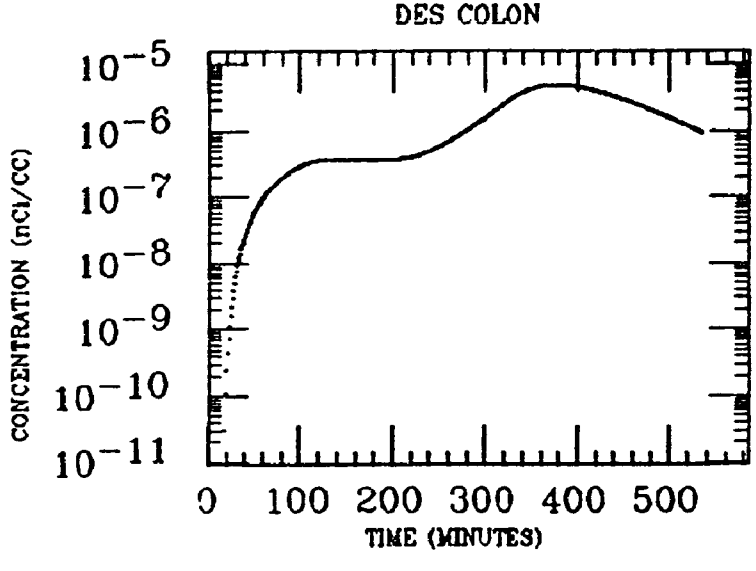

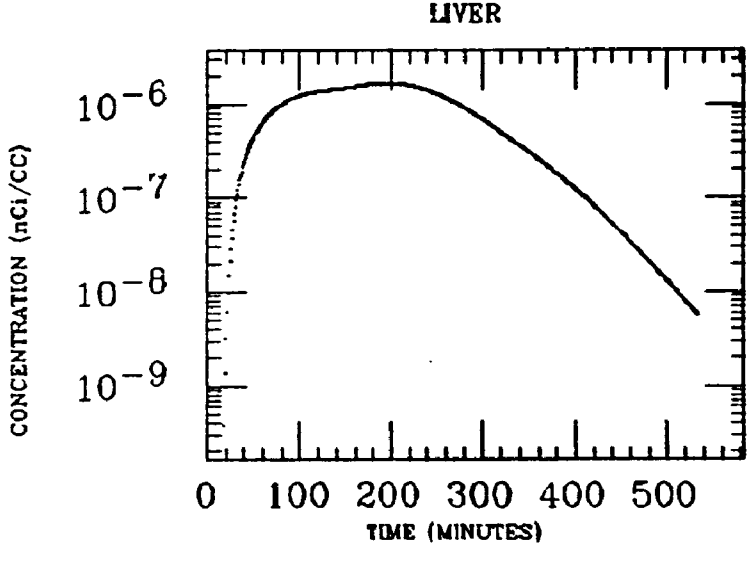

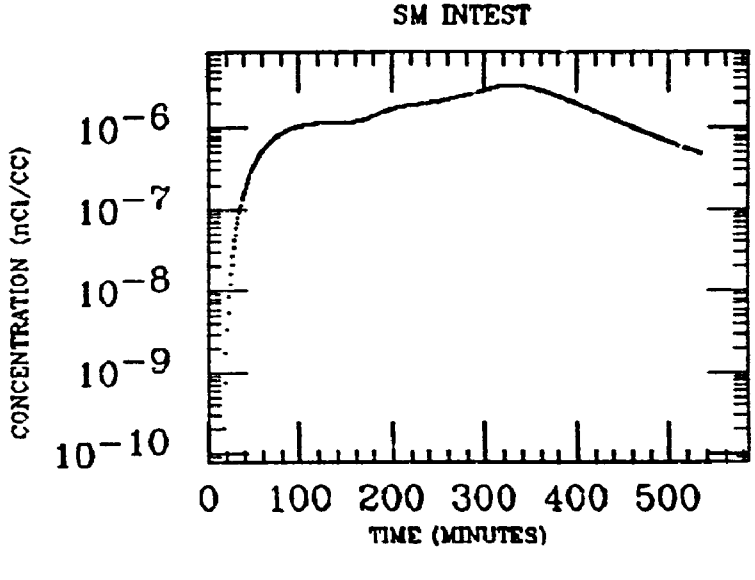

AYER
XE INGESTION
Po-214

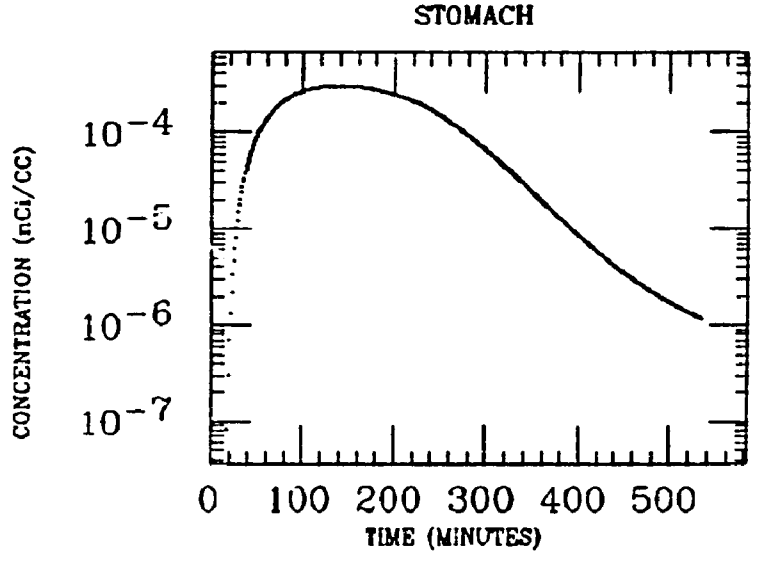

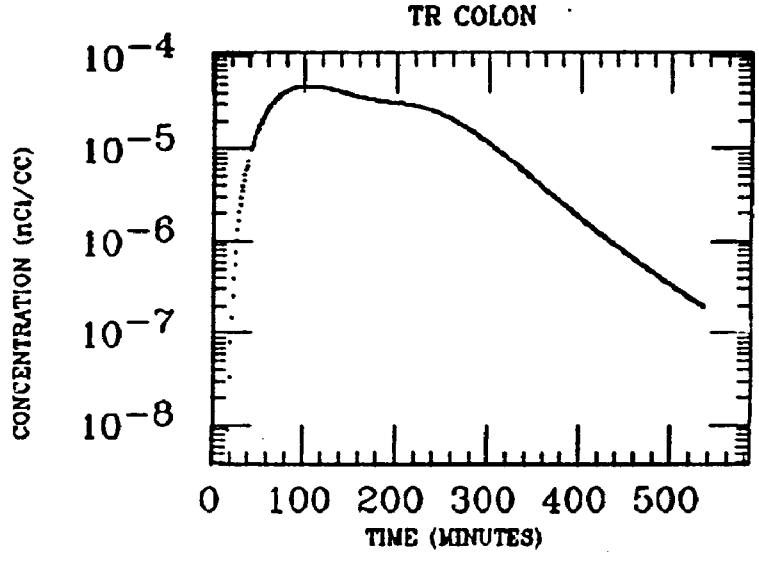

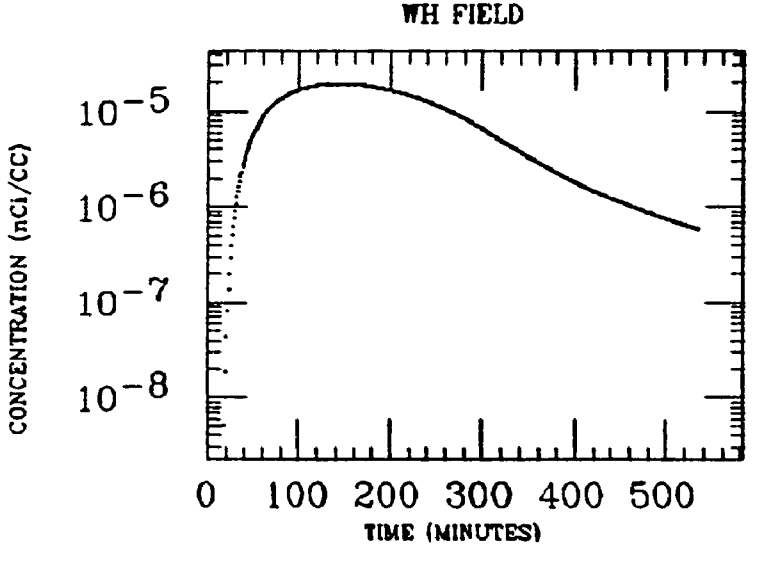

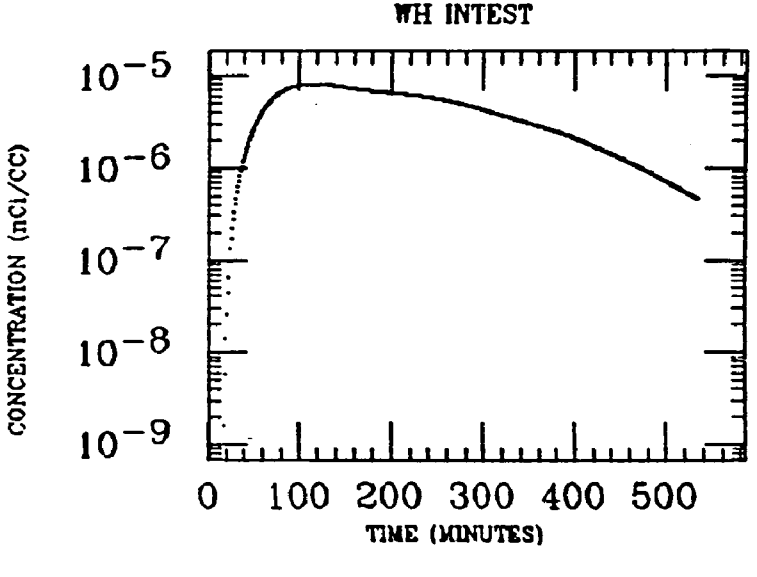

BROCK
XE INGESTION
Po-214

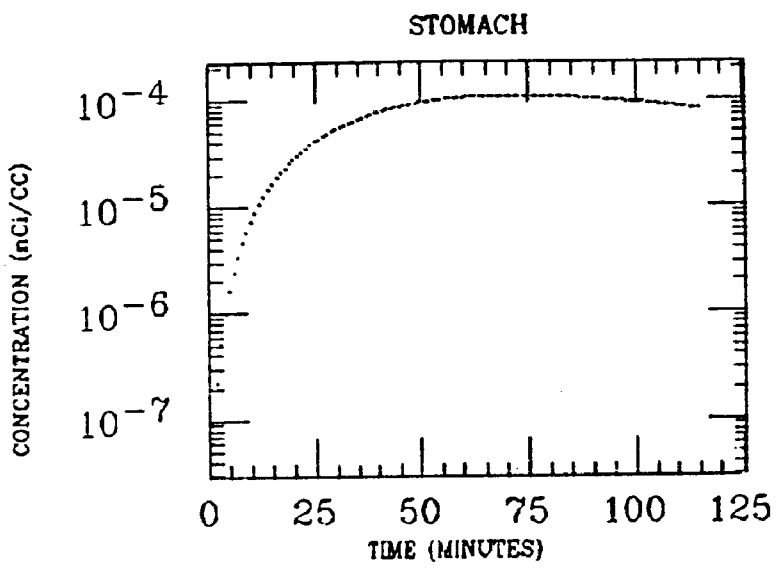

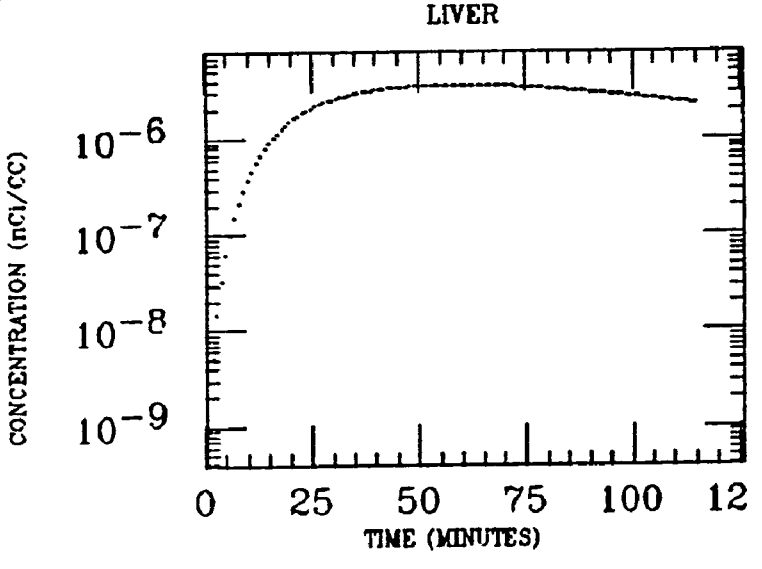

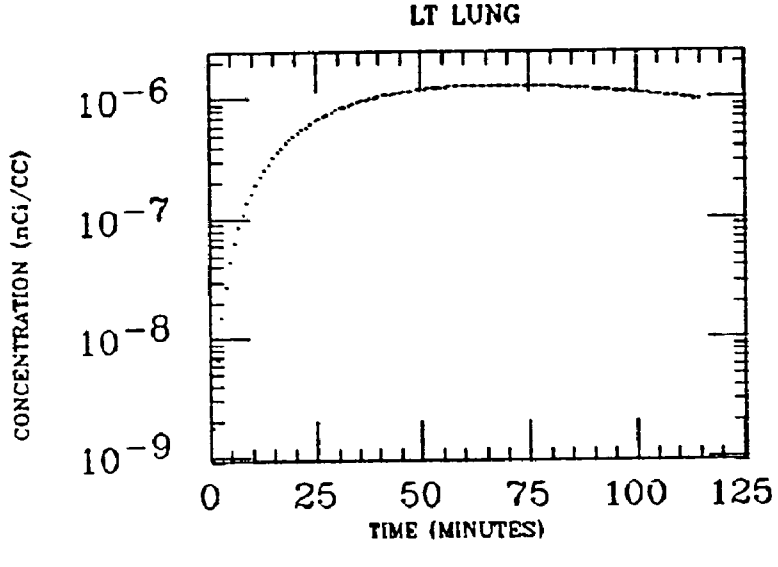

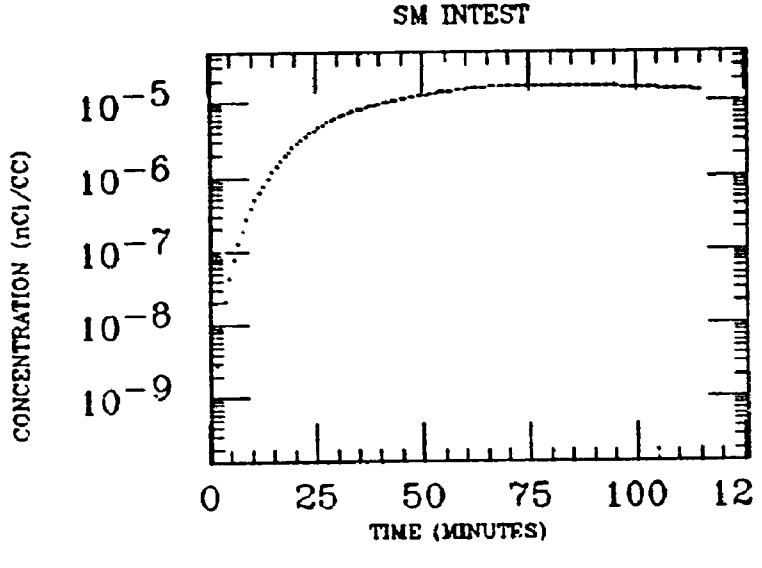

BROCK
XE INGESTION
Po-214

WH INTEST

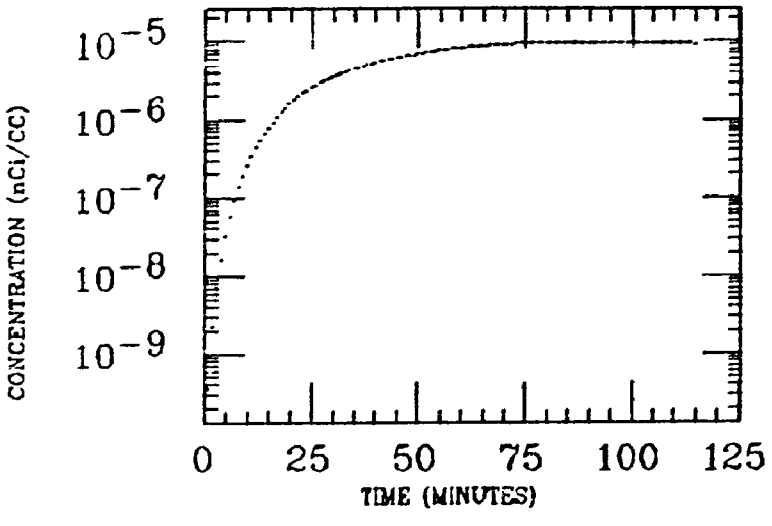

MUSCLE

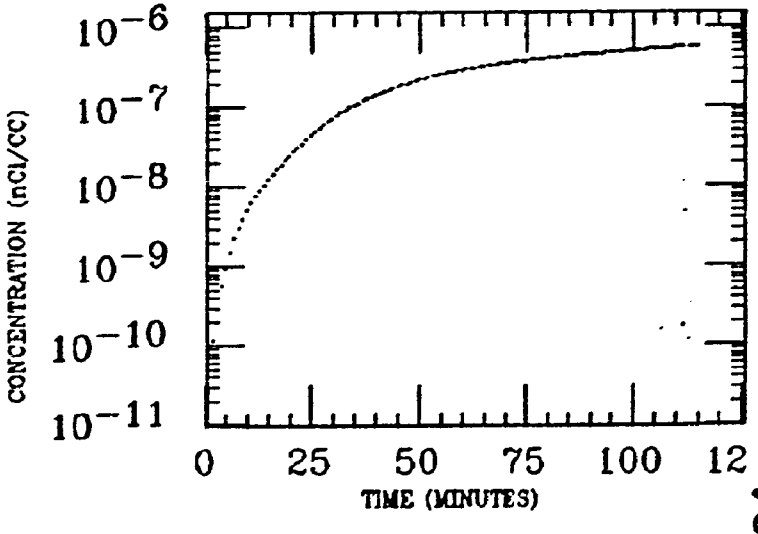

WH FIELD

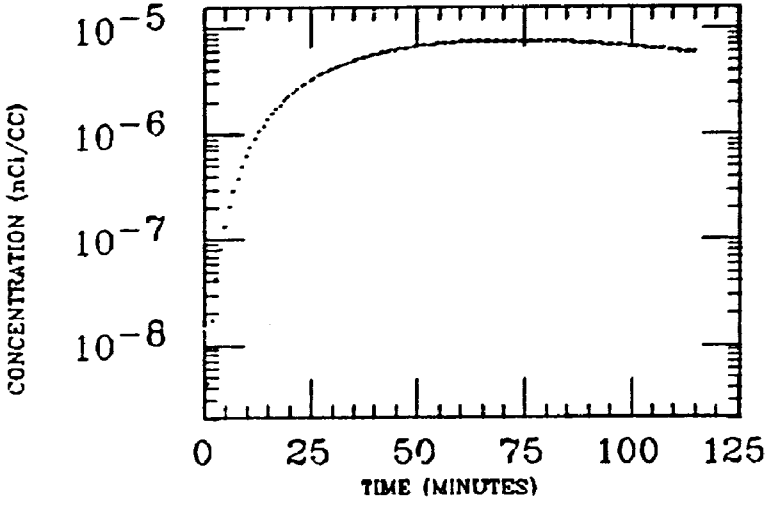

BYRNE
XE INGESTION
Po-214

STOMACH

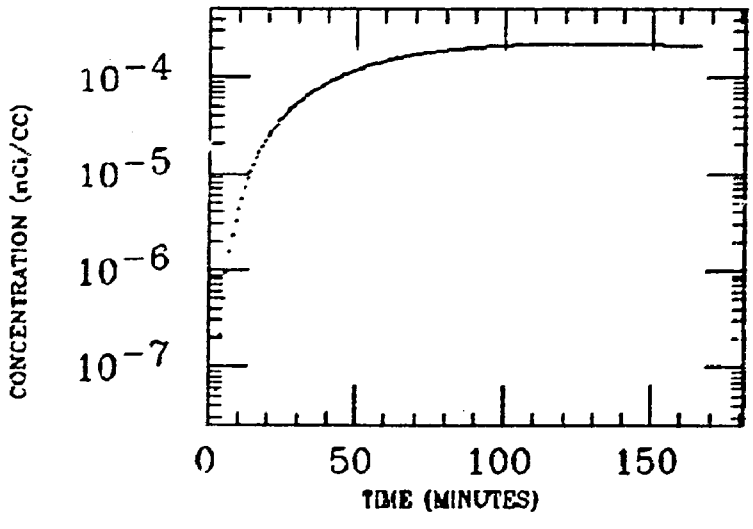

LIVER

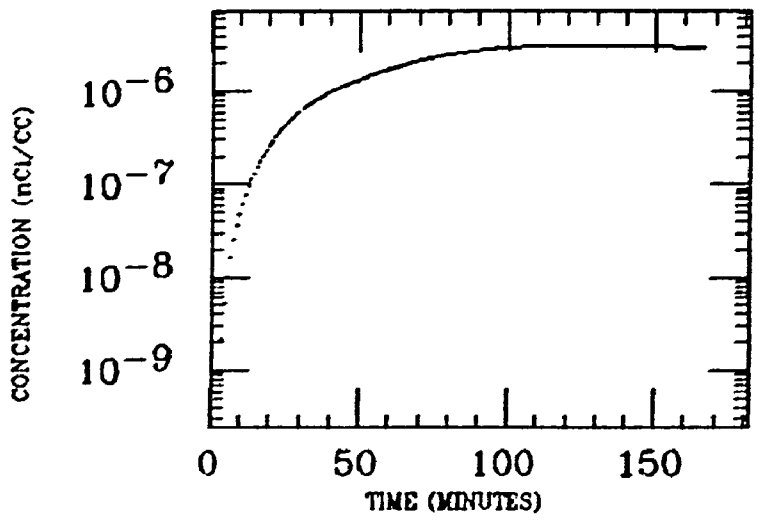

WH INTEST

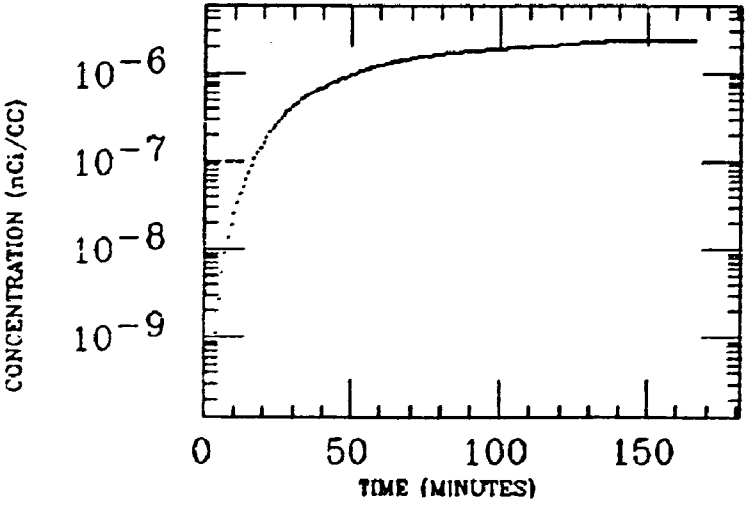

MUSCLE

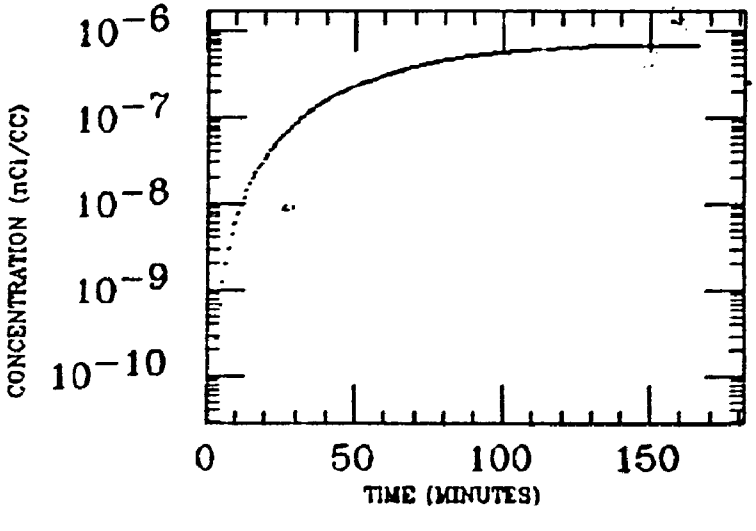

BYRNE
XE INGESTION
Po-214

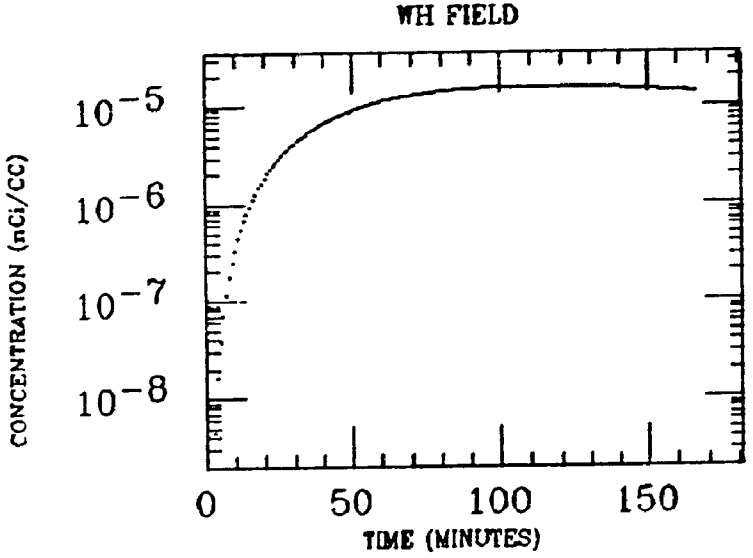

CLINE
XE INGESTION
Po-214

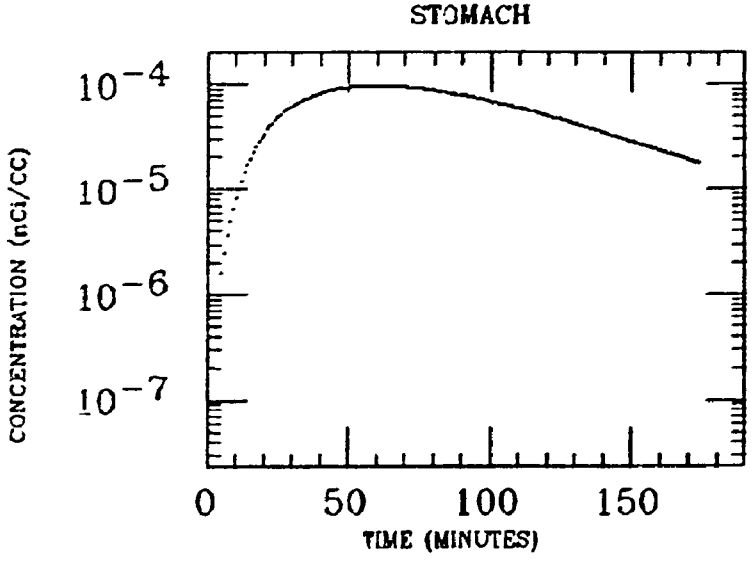

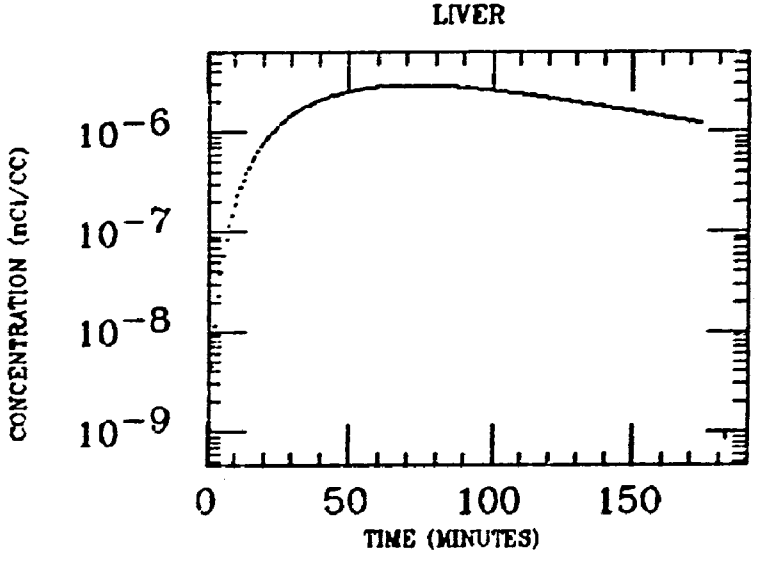

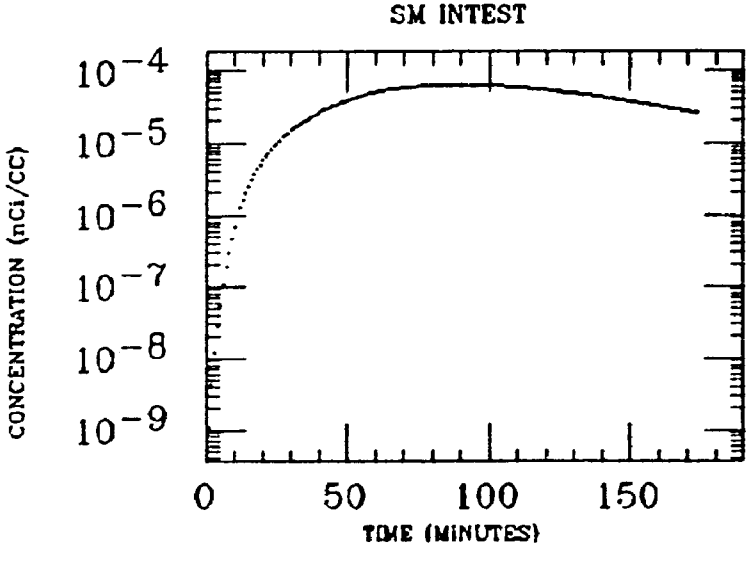

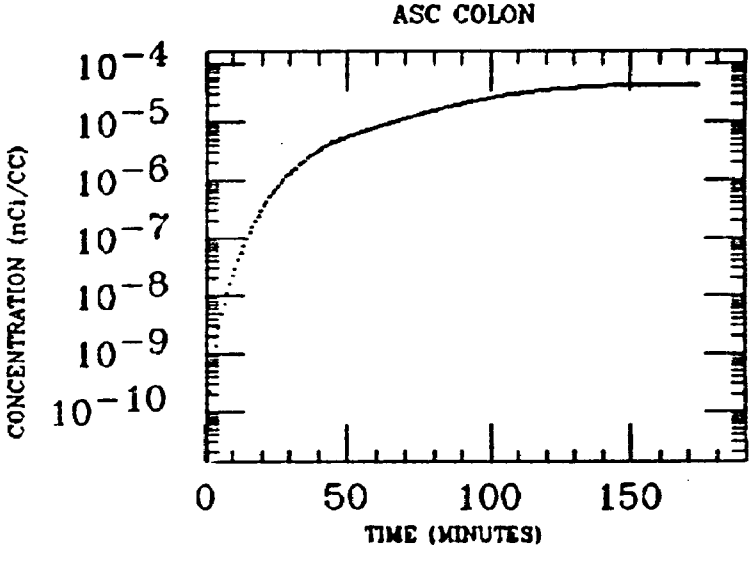

CLINE
XE INGESTION
Po-214

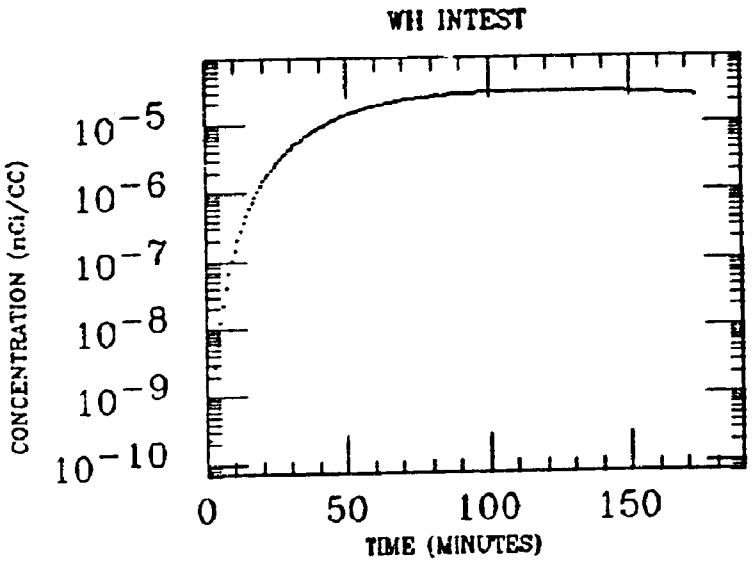

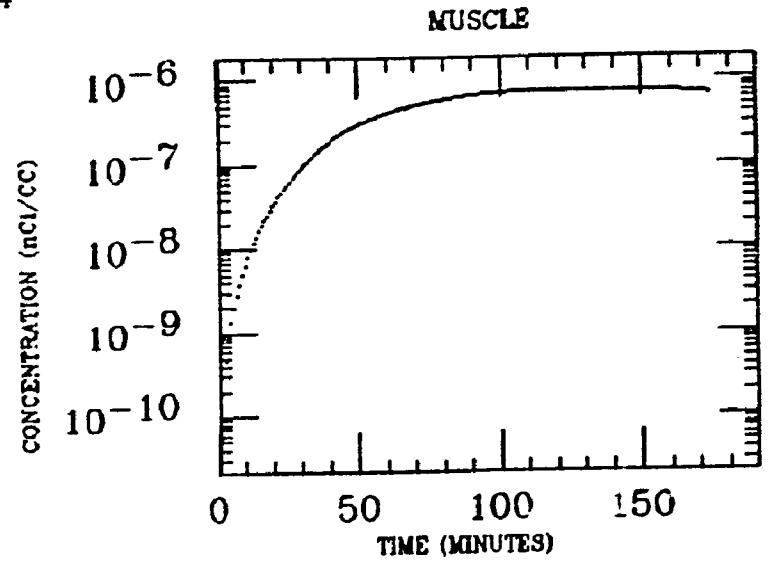

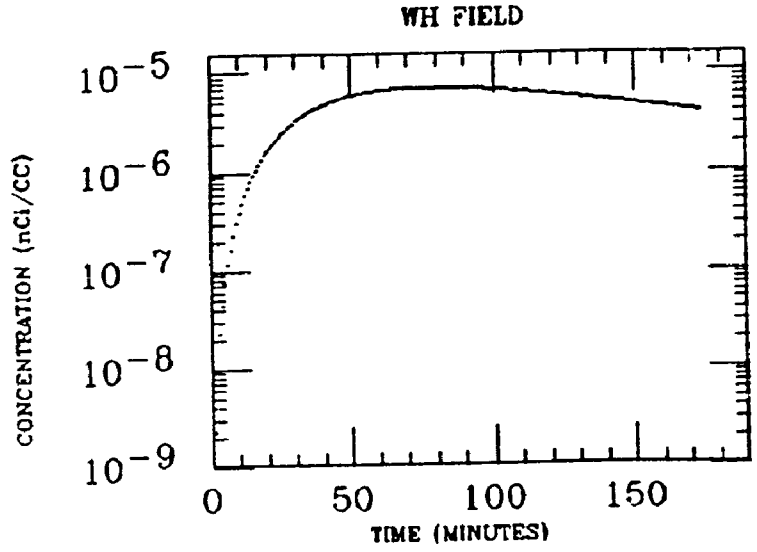

ELMDEN
XE INGESTION
Po-214

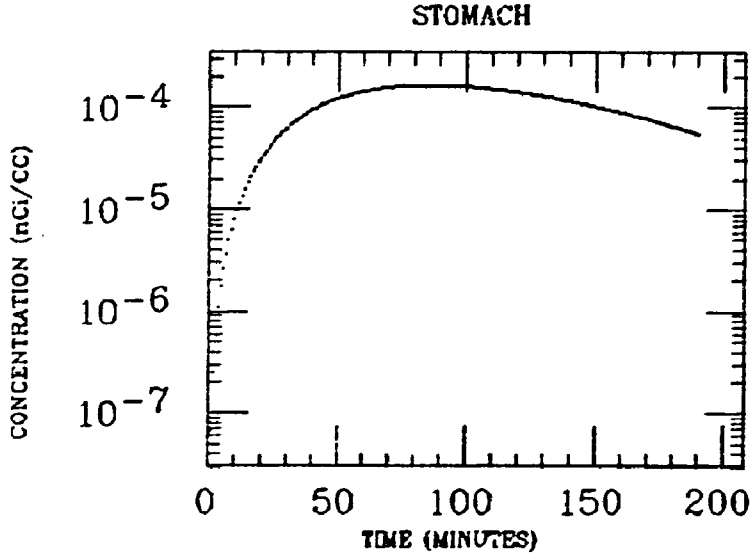

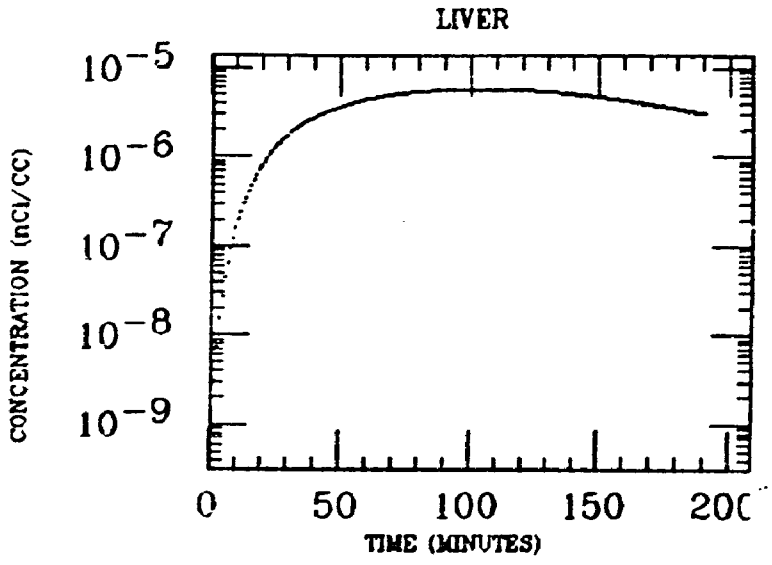

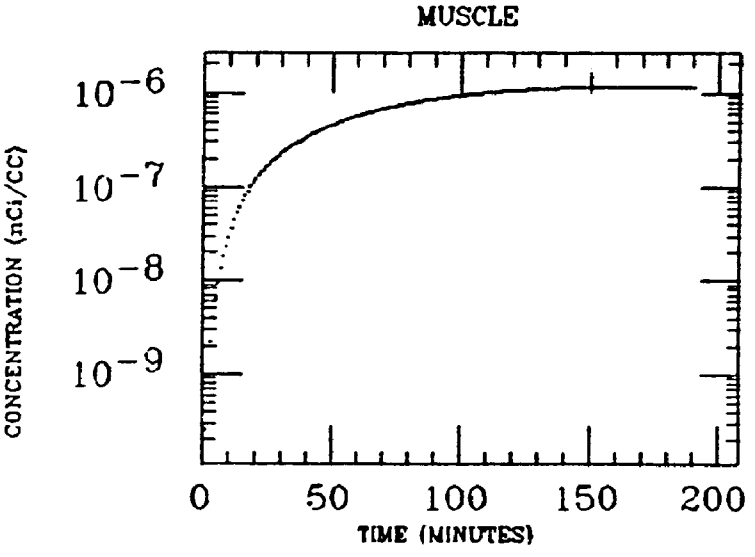

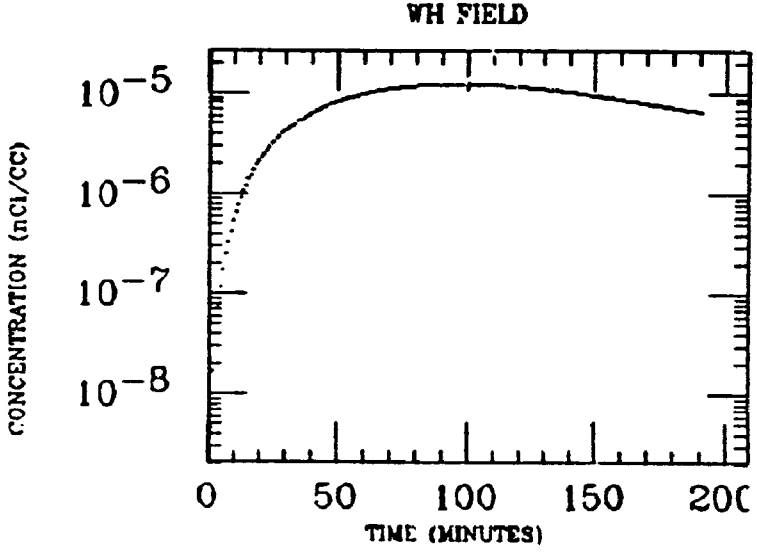

ELMDEN
XE INGESTION
Po-214

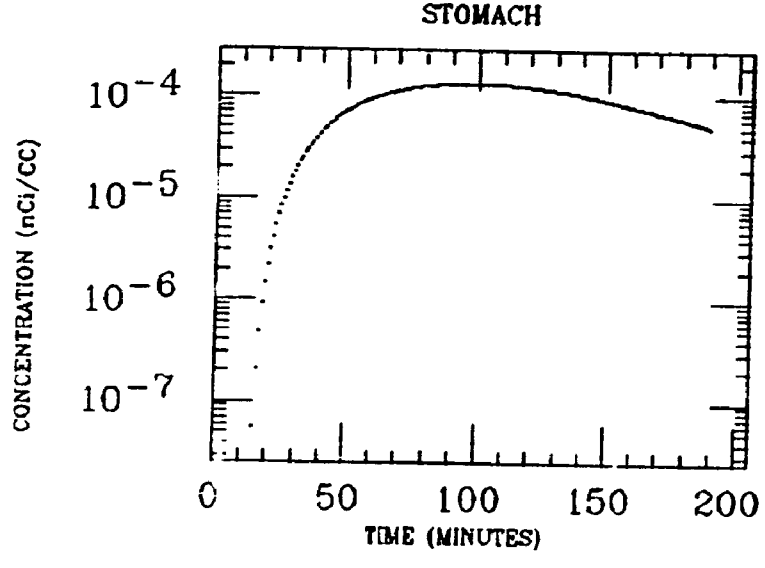

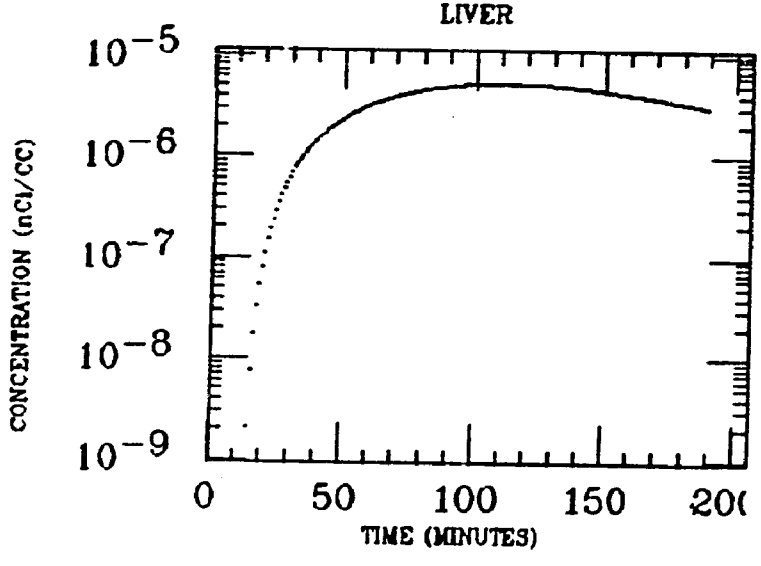

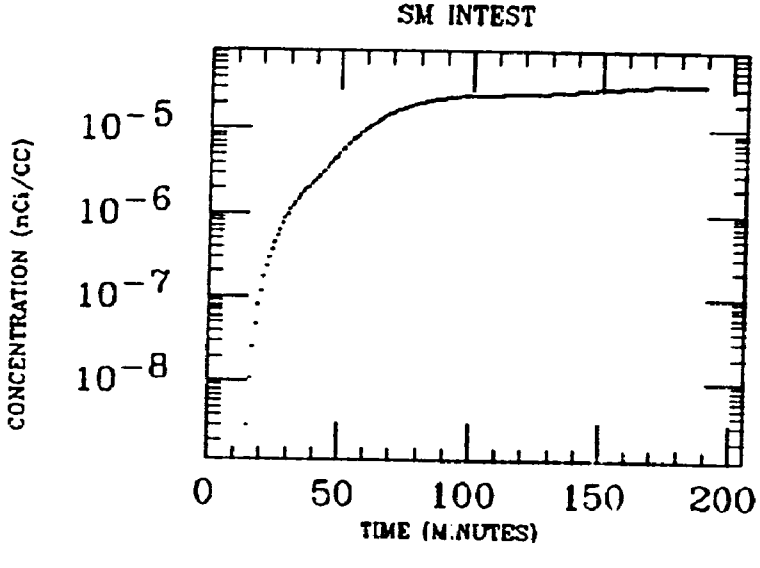

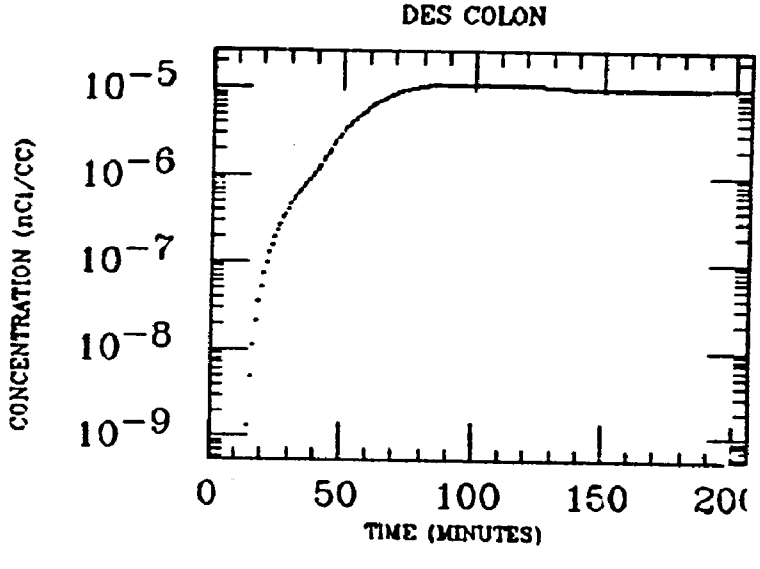

ELMDEN
XE INGESTION
Po-214

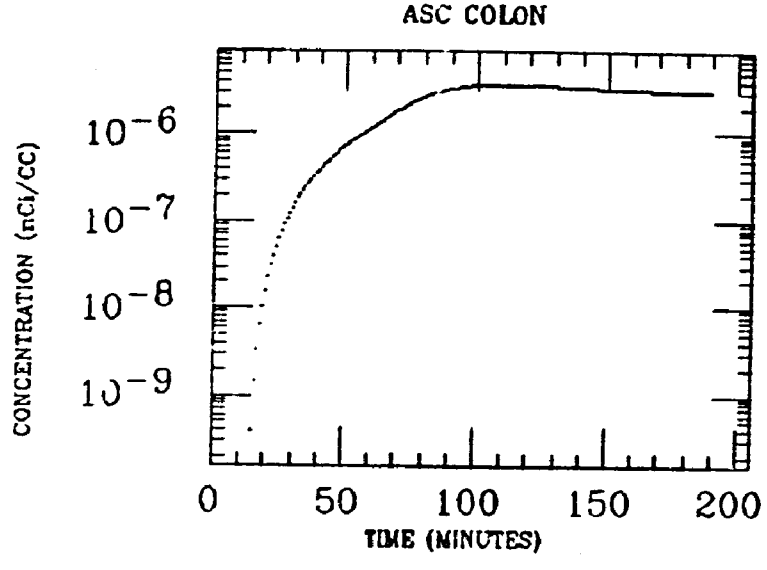

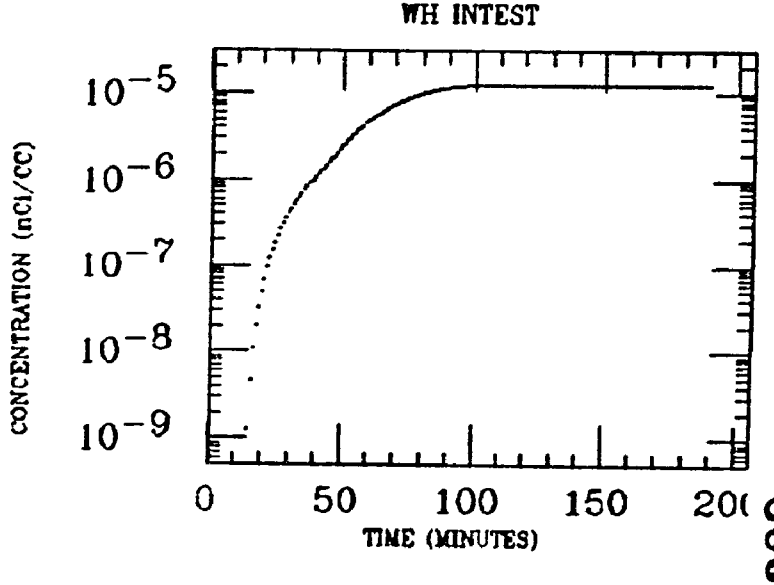

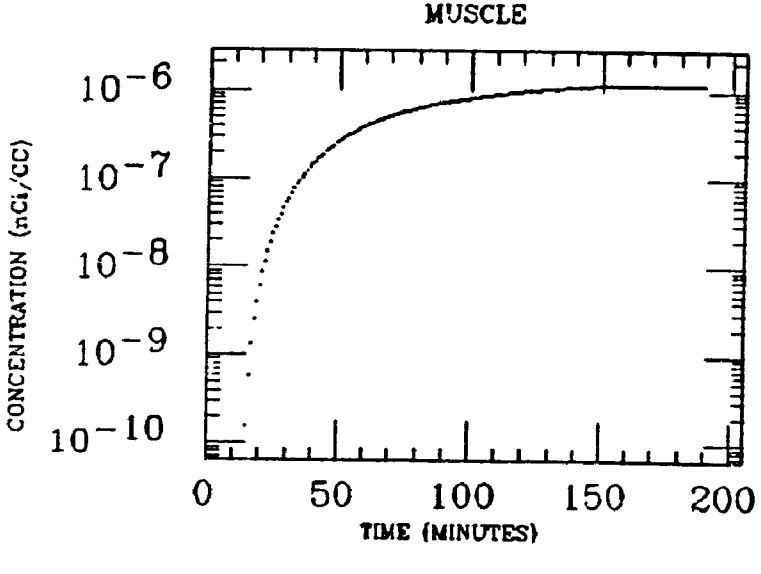

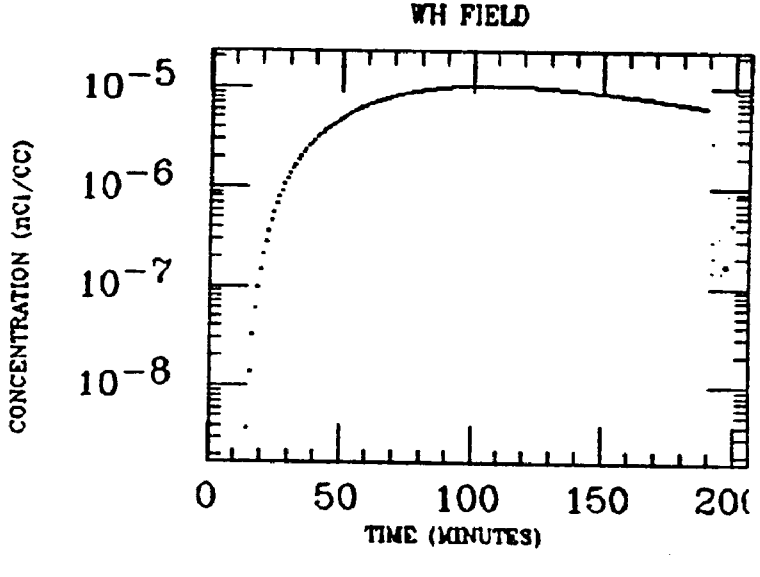

EPLING
XE INGESTION
Po-214

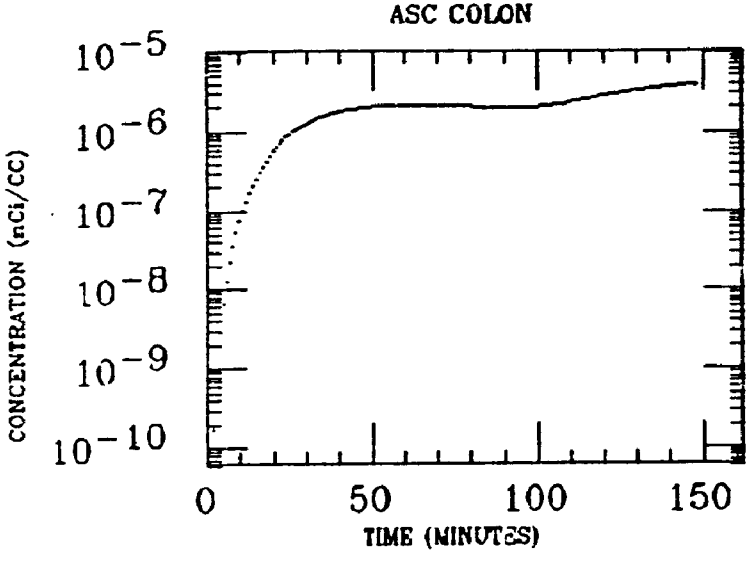

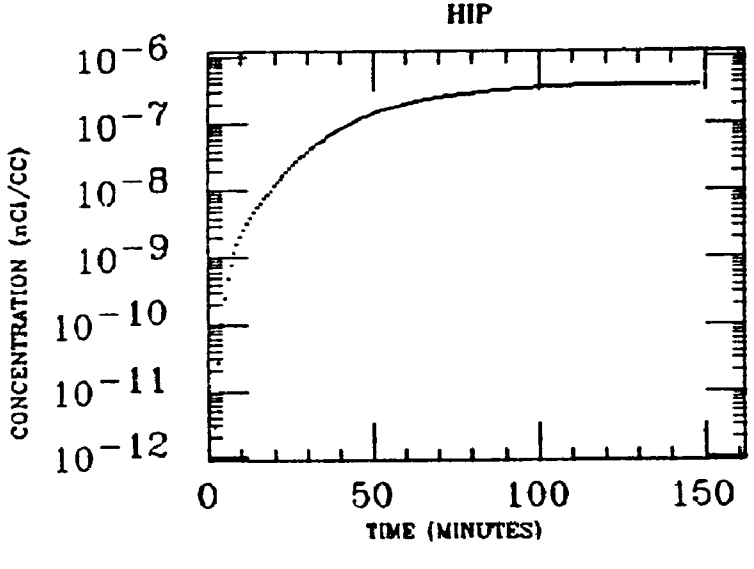

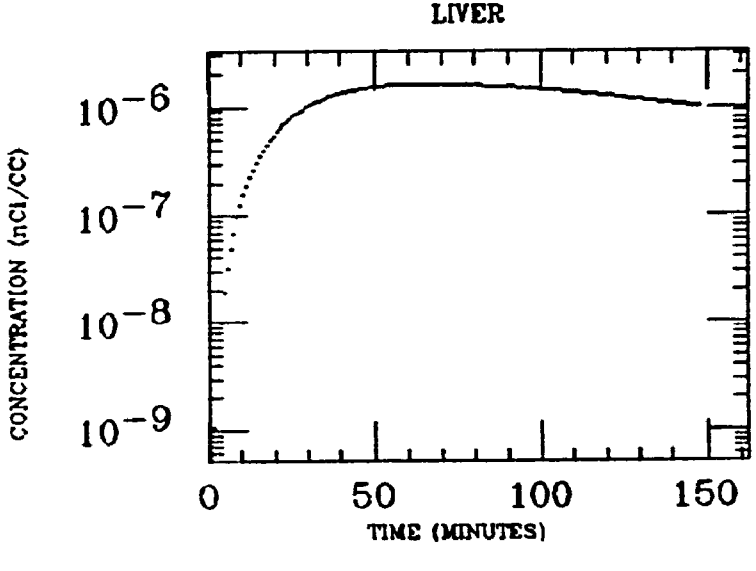

EPLING
XE INGESTION
Po-214

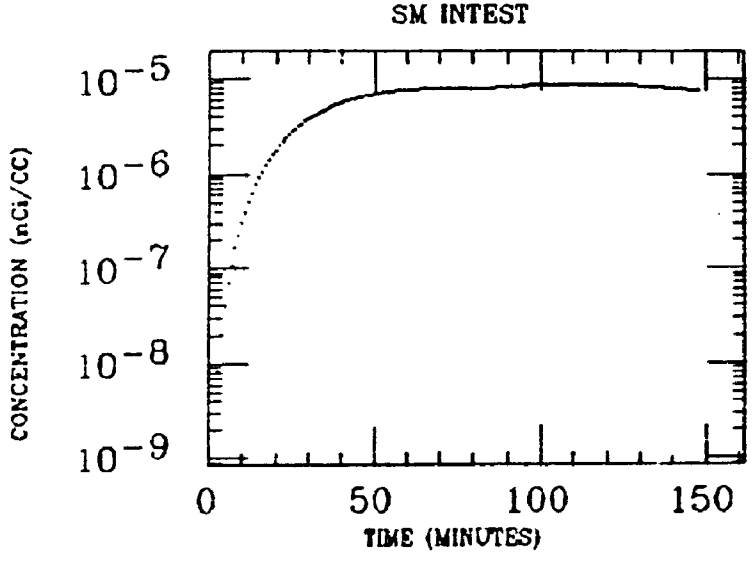

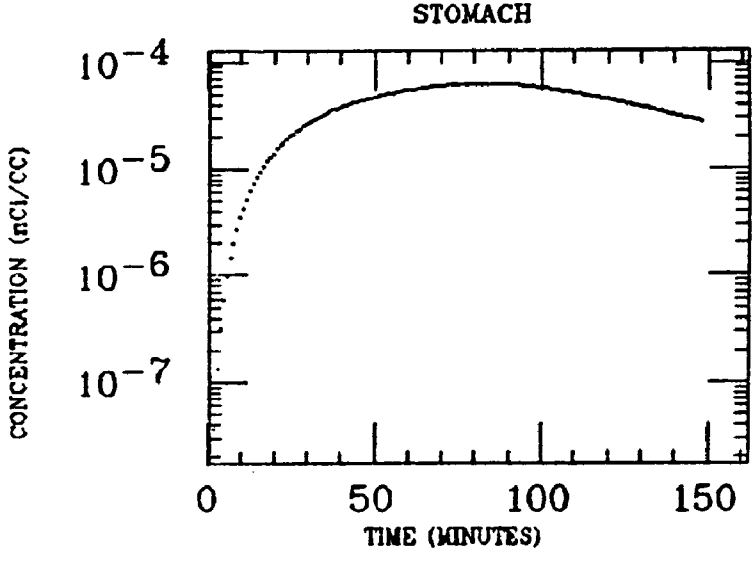

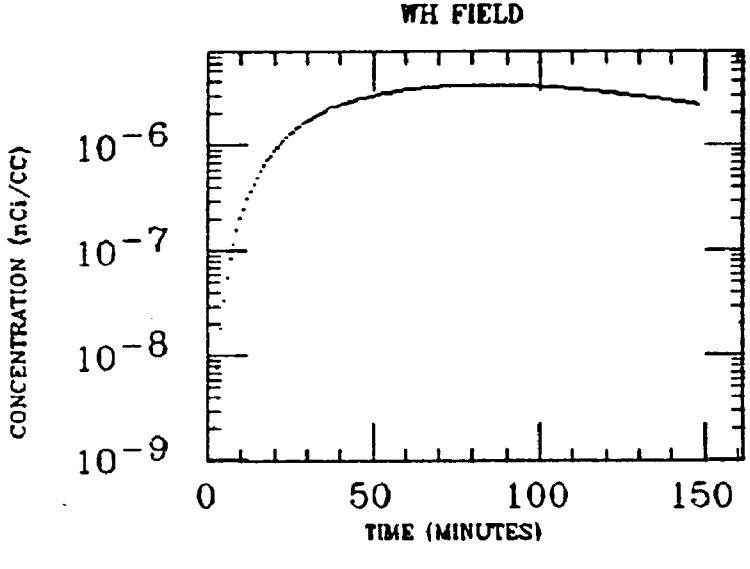

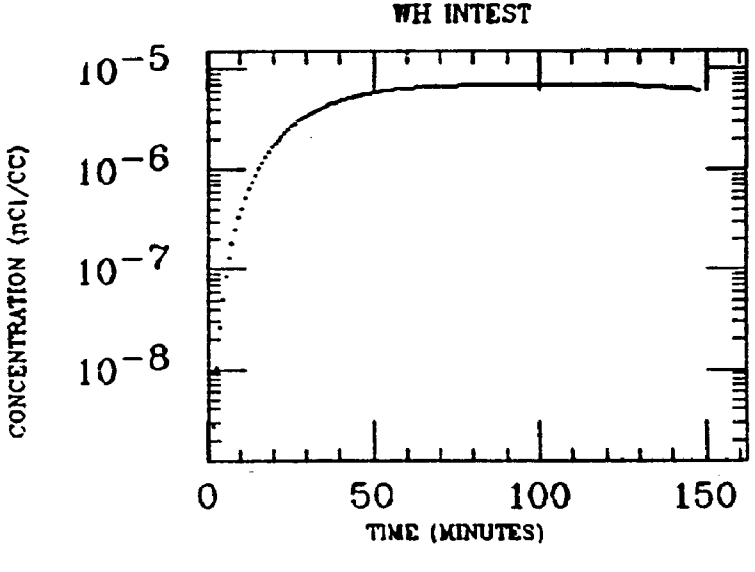

GALLOP
XE INGESTION
Po-214

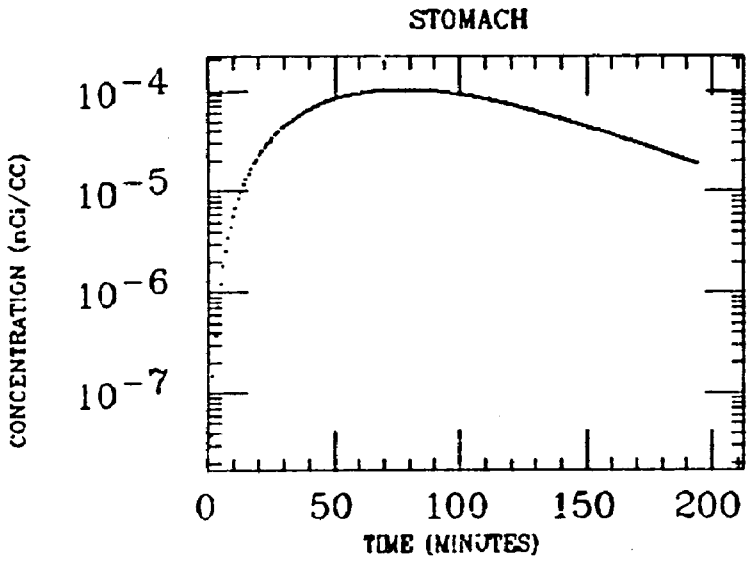

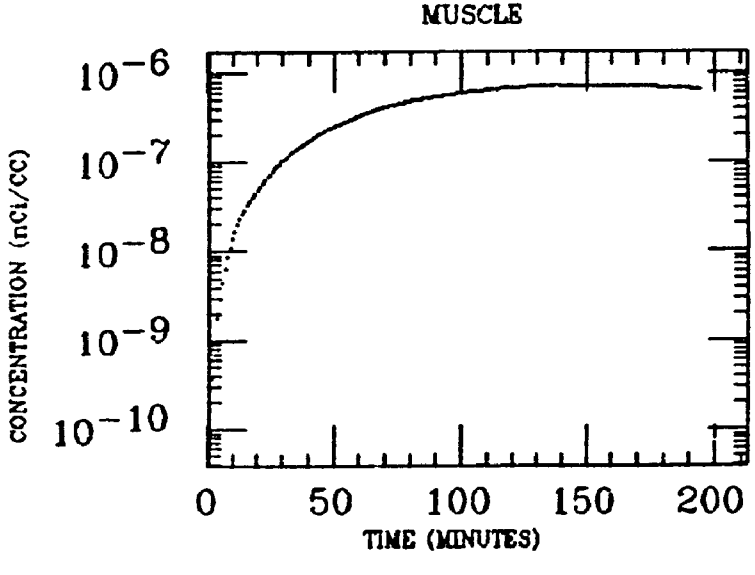

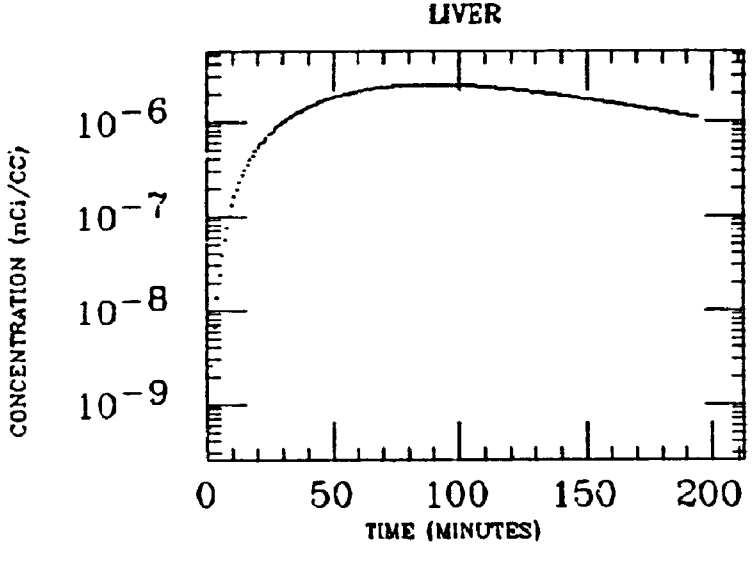

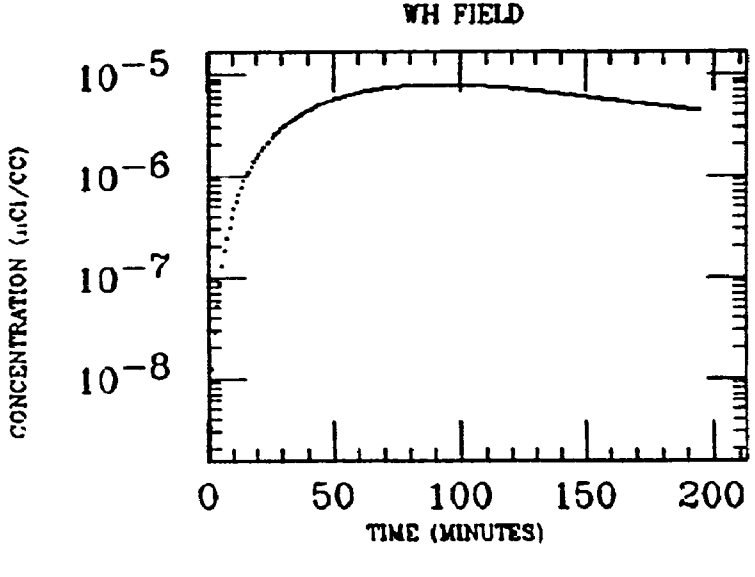

GALLOP
XE INGESTION
Po-214

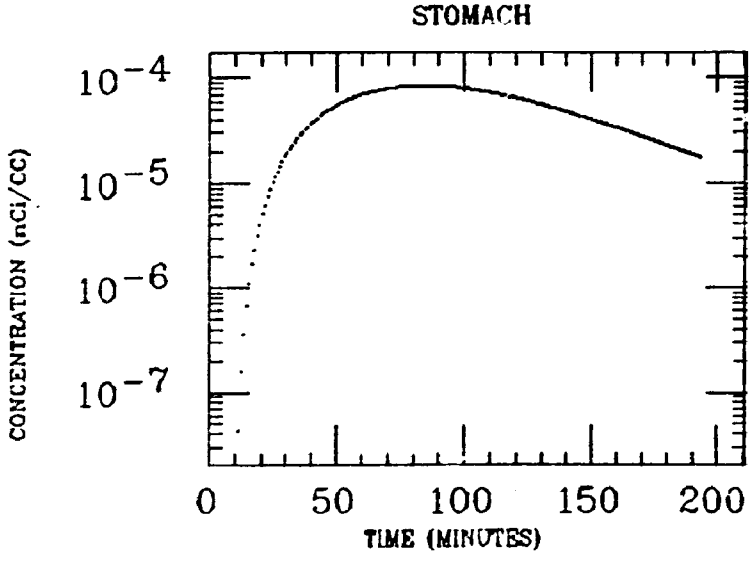

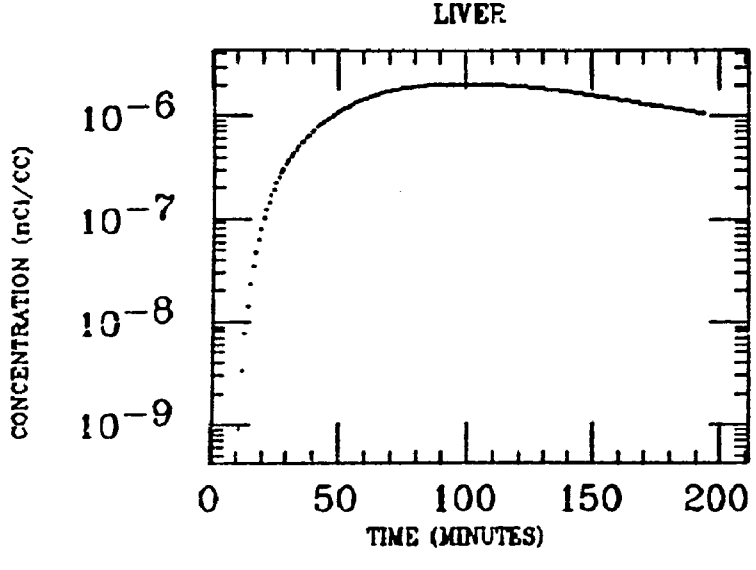

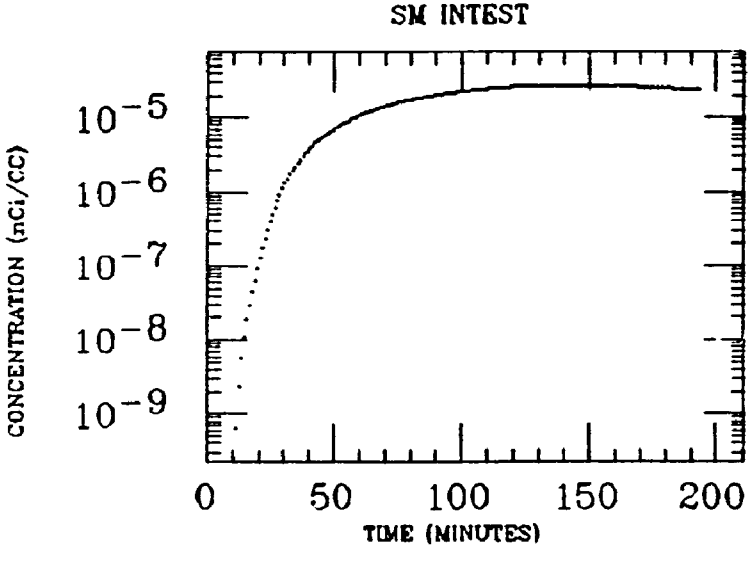

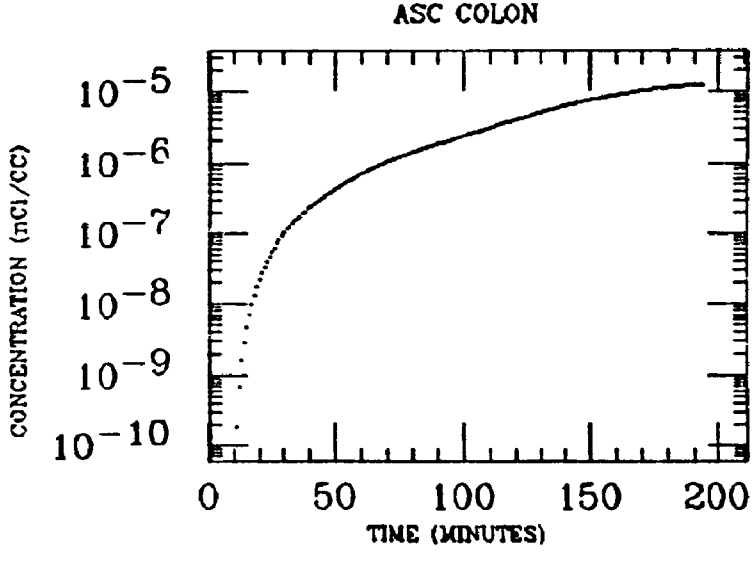

CALLOP
XE INGESTION
Po-214

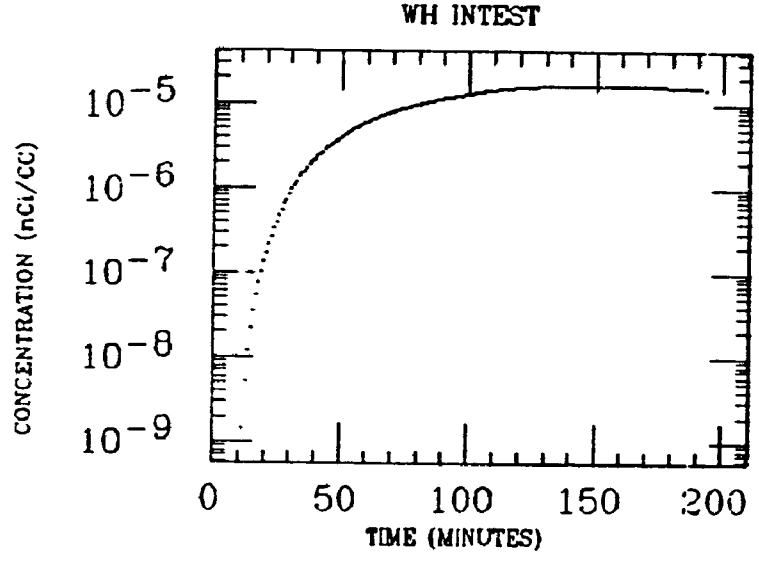

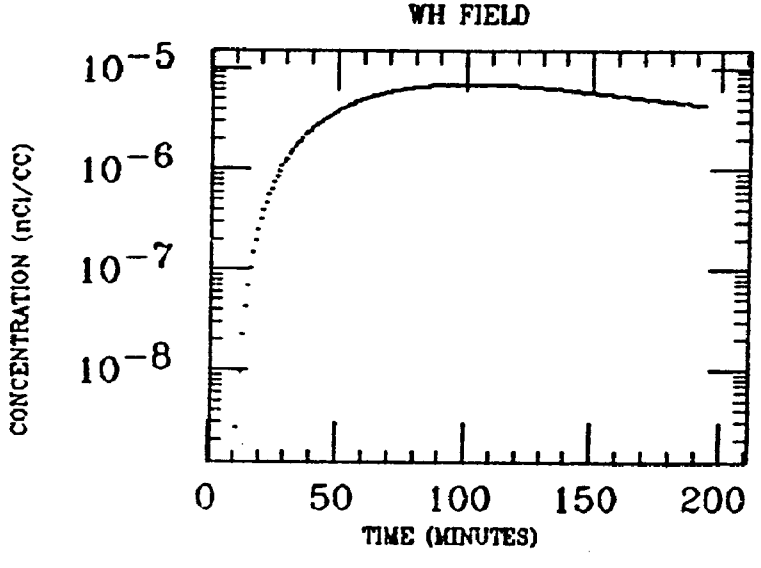

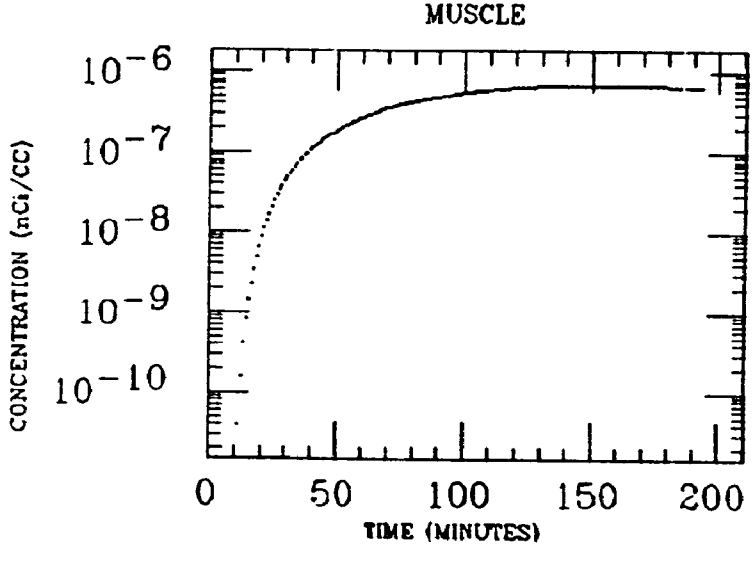

G.MCKINLEY
XE INGESTION
Po-214

STOMACH

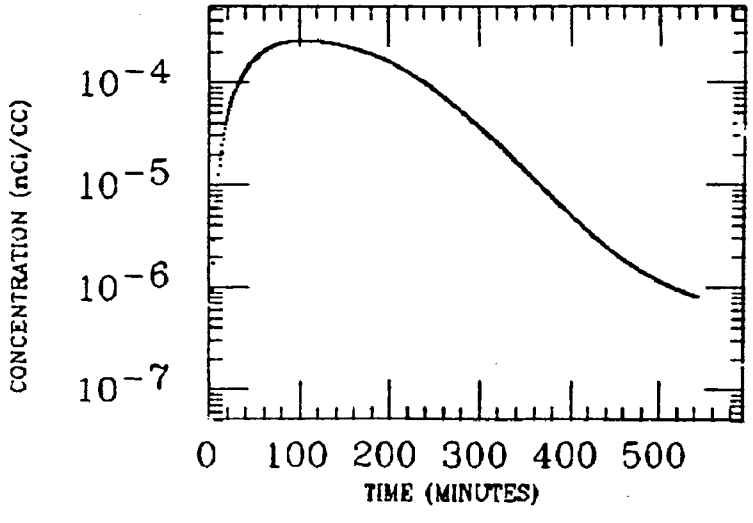

LIVER

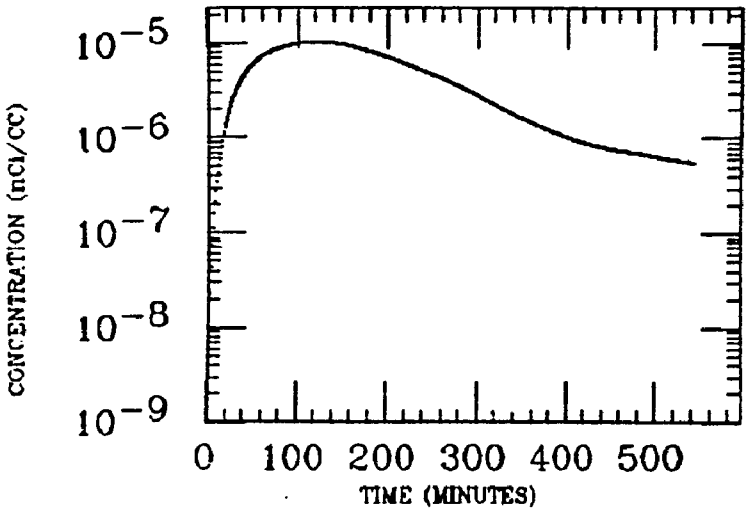

WH FIELD

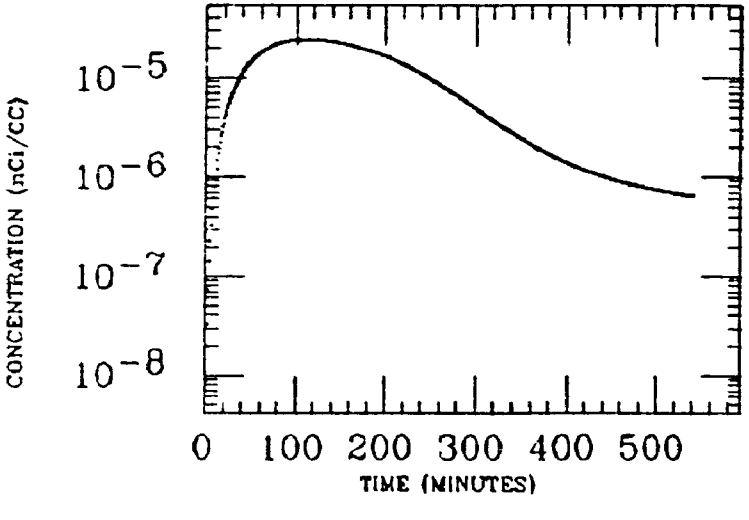

C.MCKINLEY
XE INGESTION
Po-214

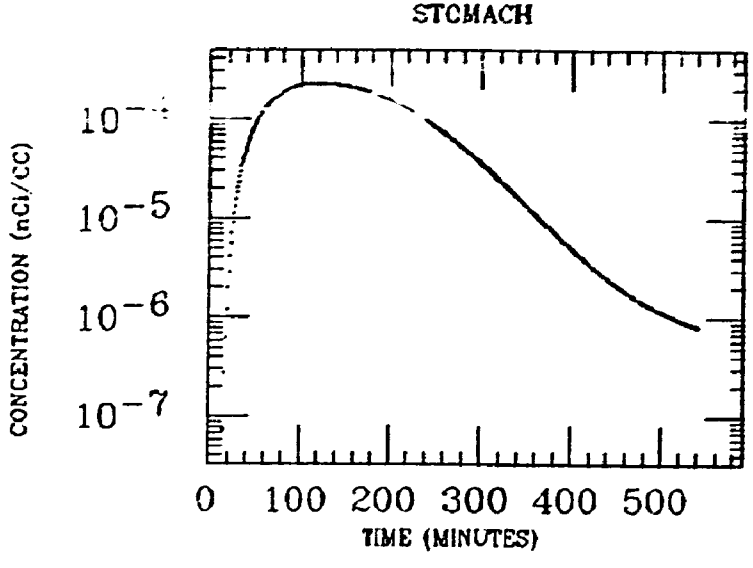

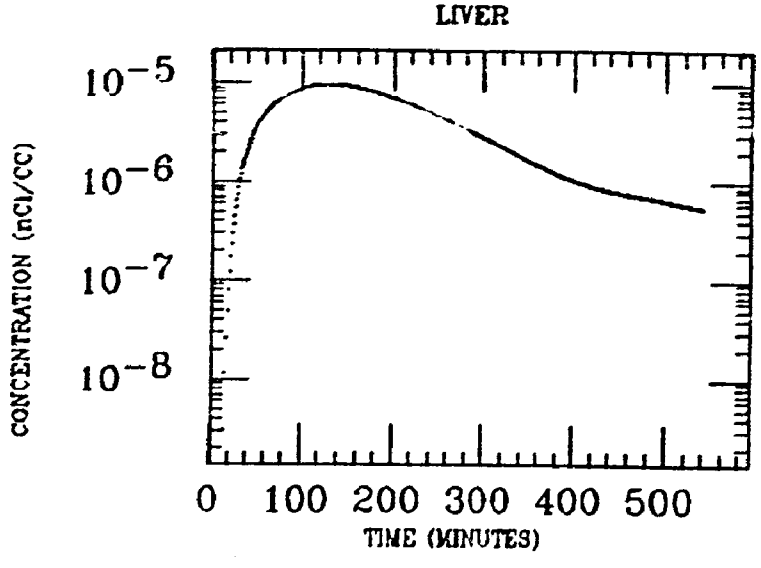

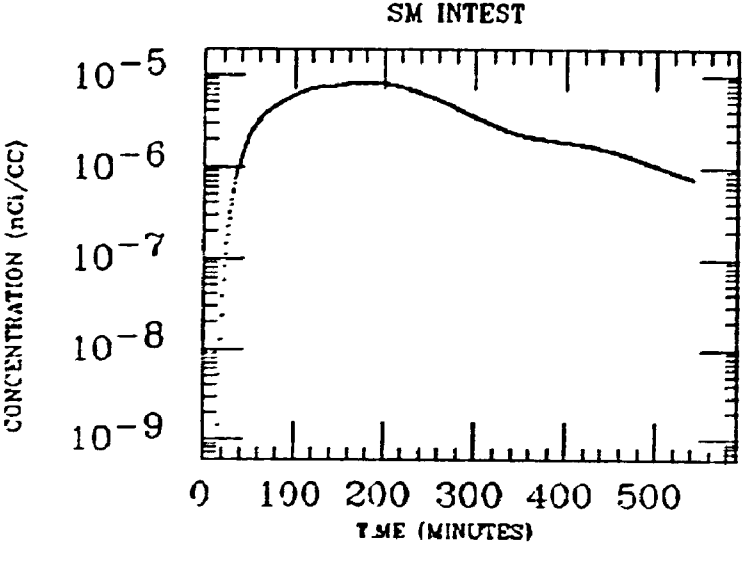

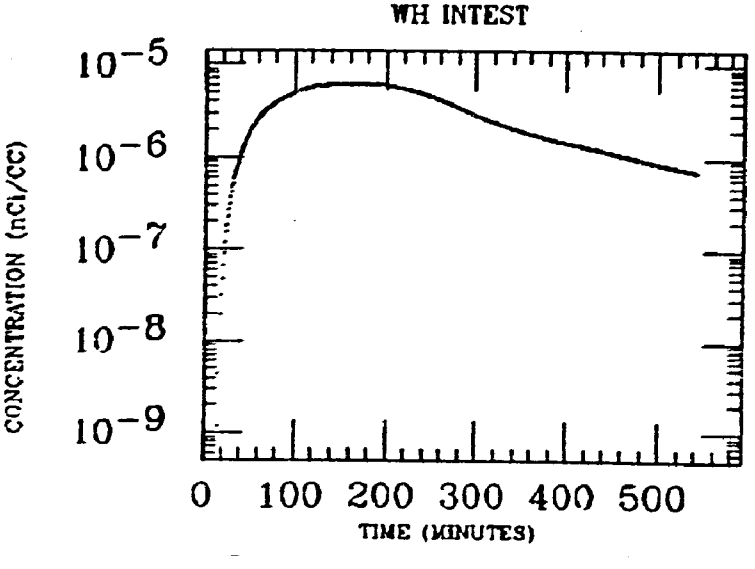

C.MCKINLEY
XE INGESTION
Po-214

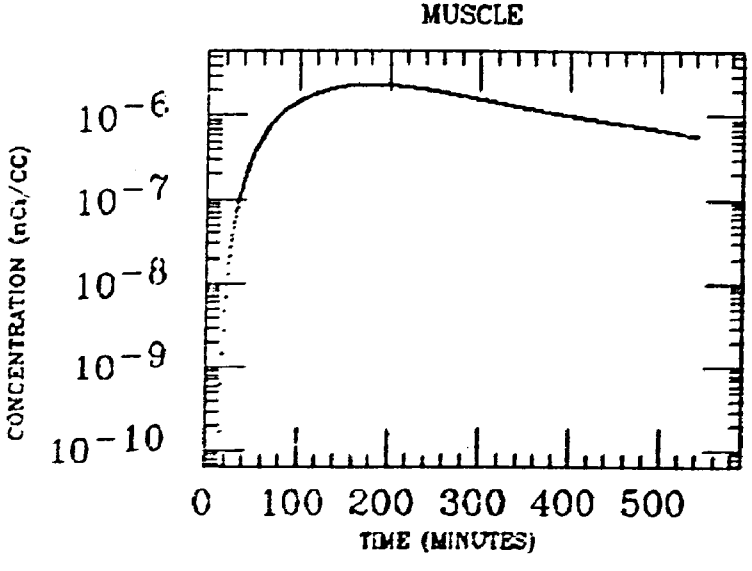

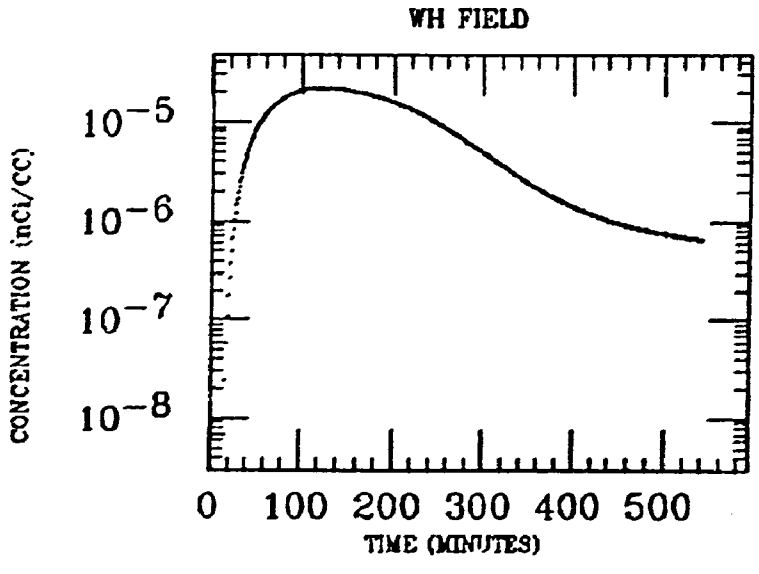

HAND
XE INGESTION
Po-214

STOMACH

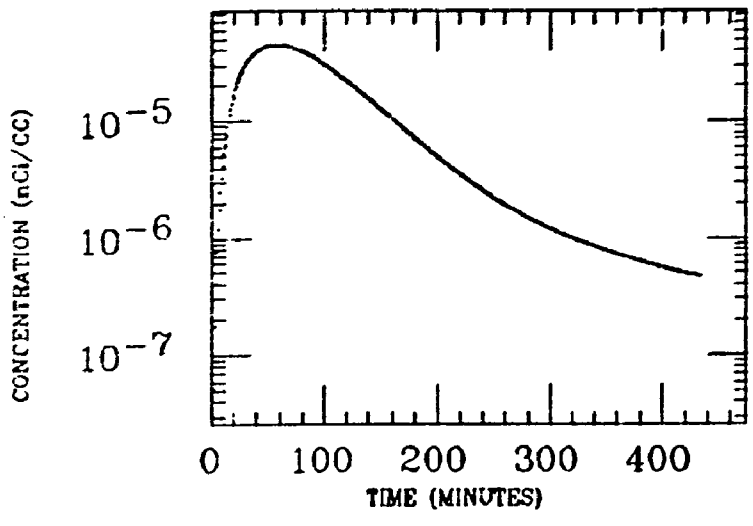

LIVER

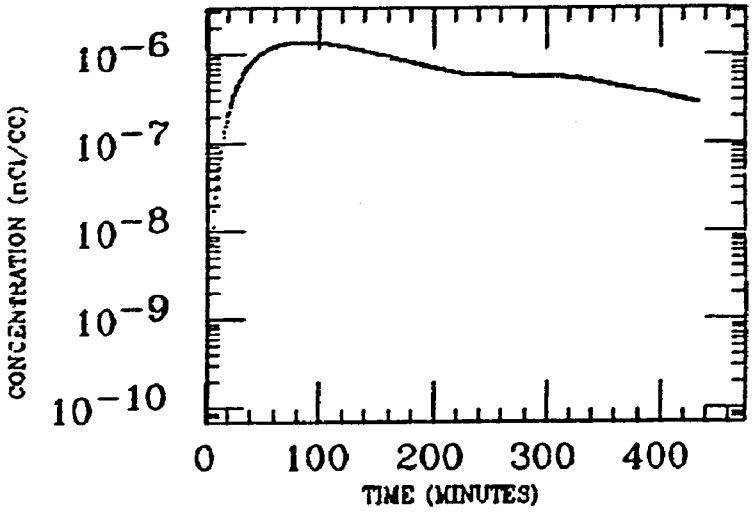

LT LUNG

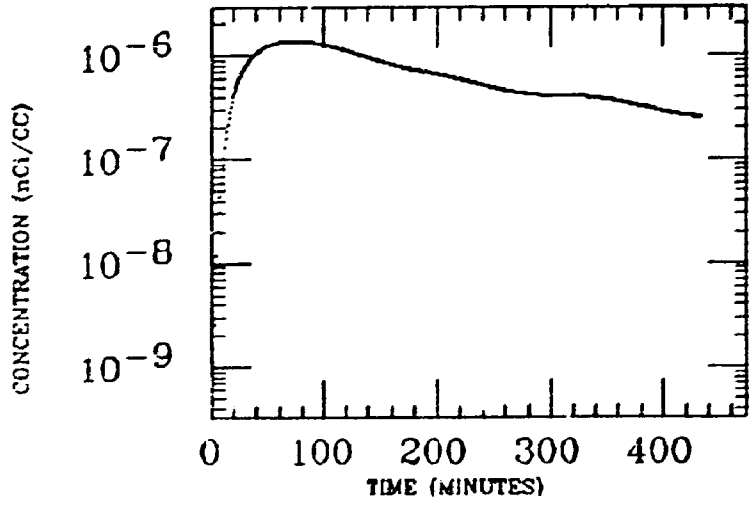

WH INTEST

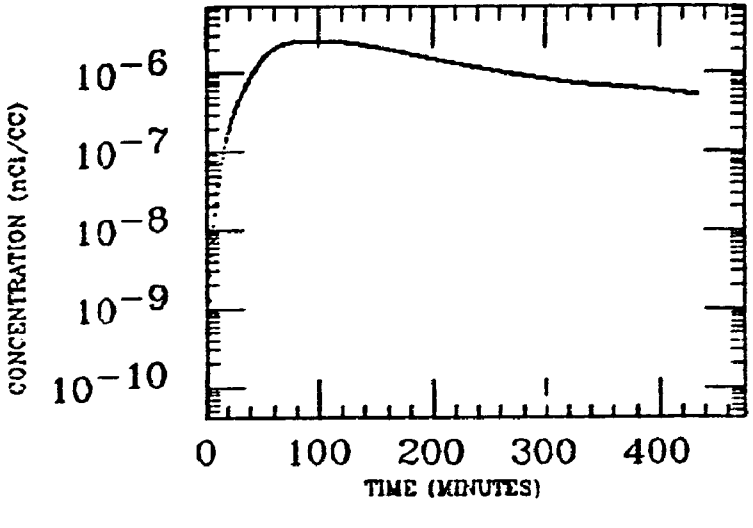

HAND
XE INGESTION
Po-214

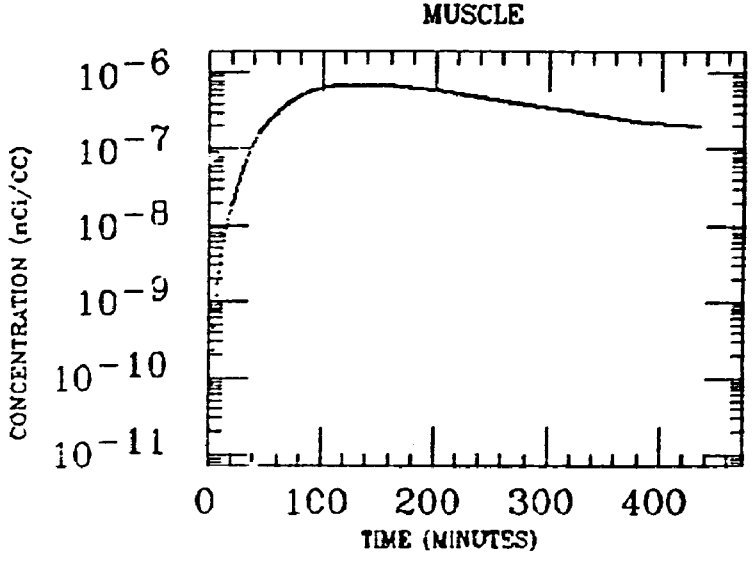

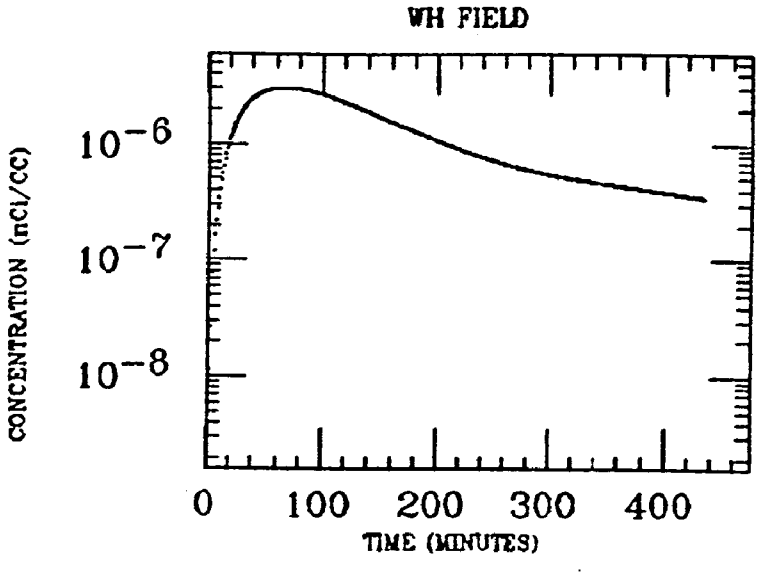

HAND
XE INGESTION
Po-214

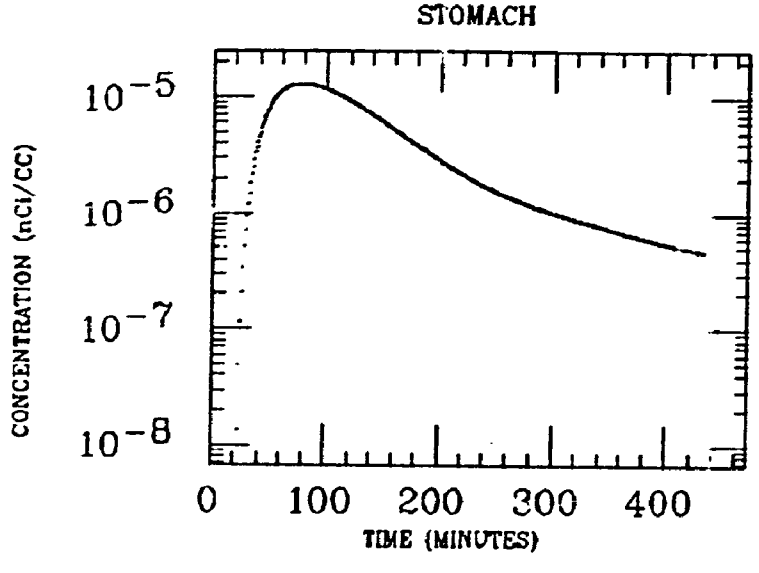

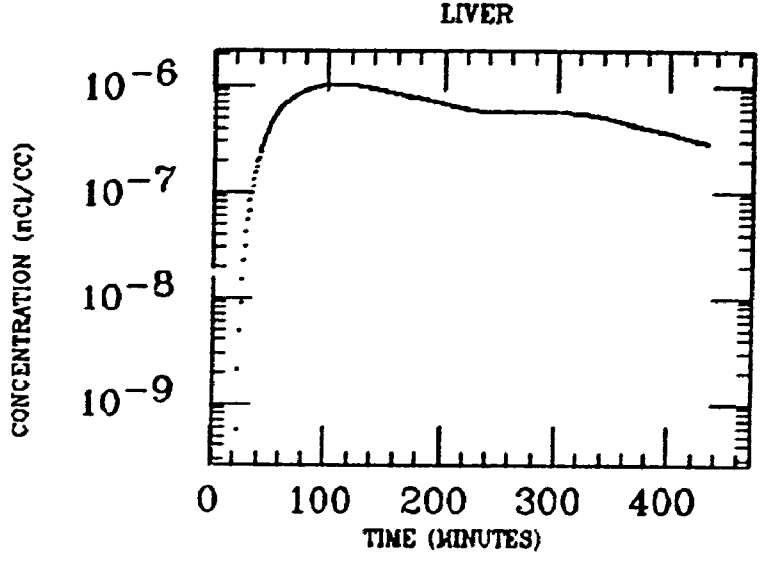

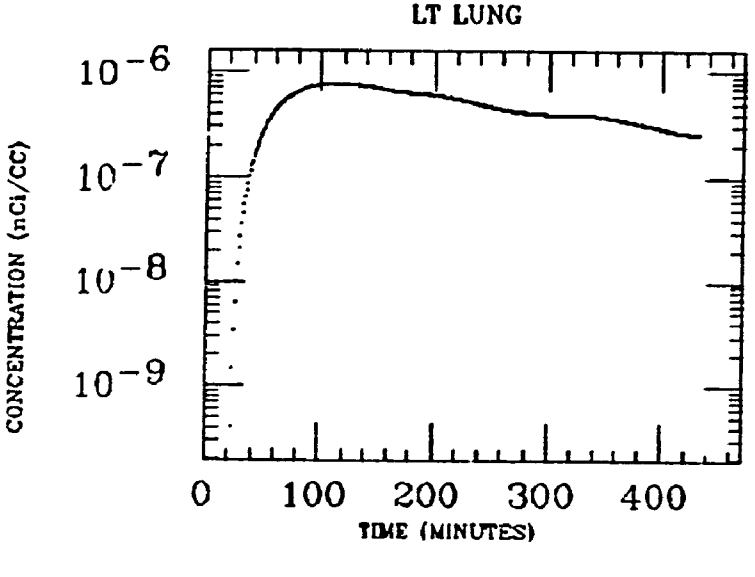

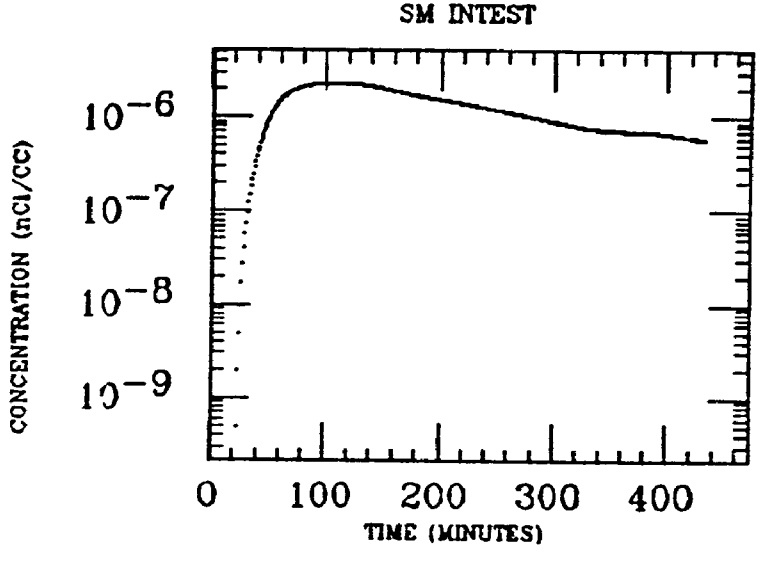

HAND
XE INGESTION
Po-214

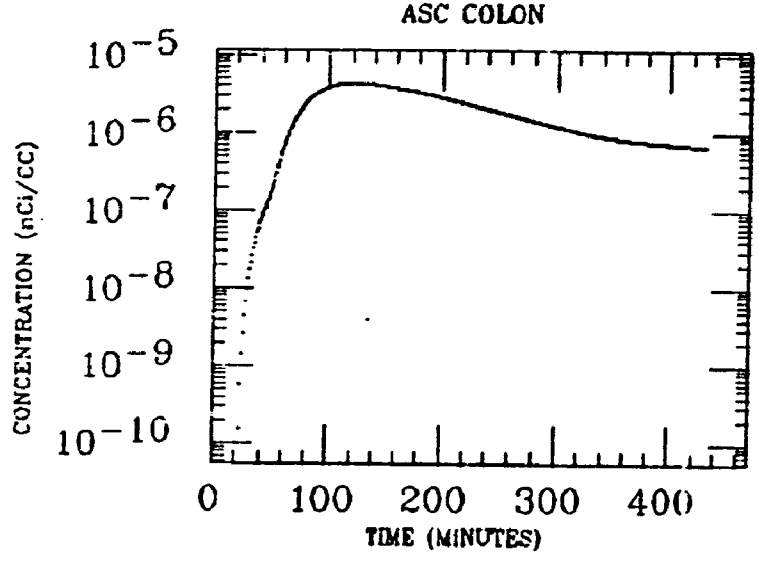

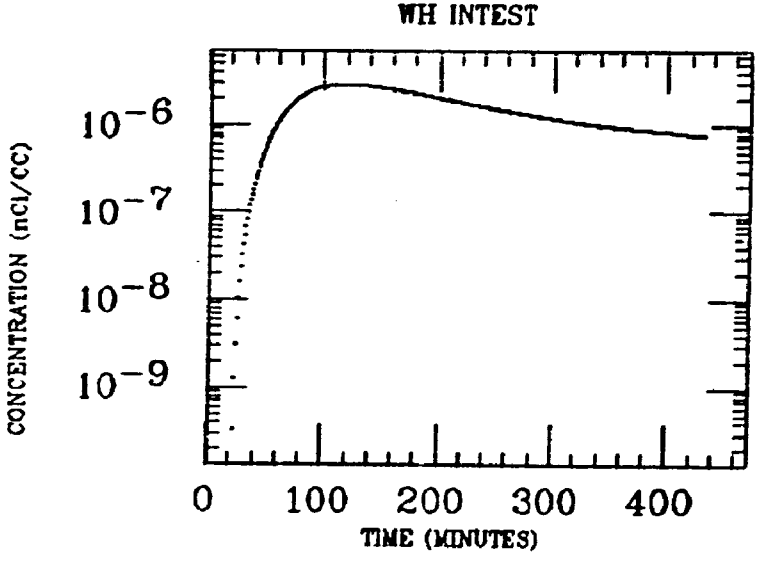

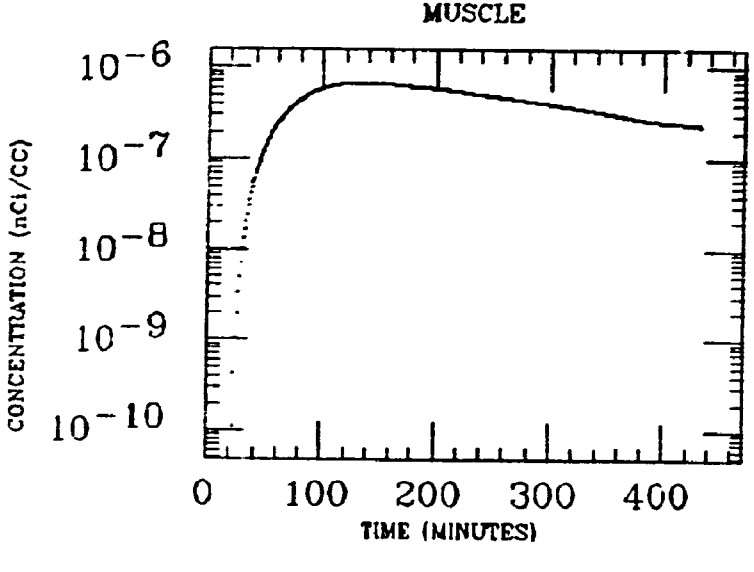

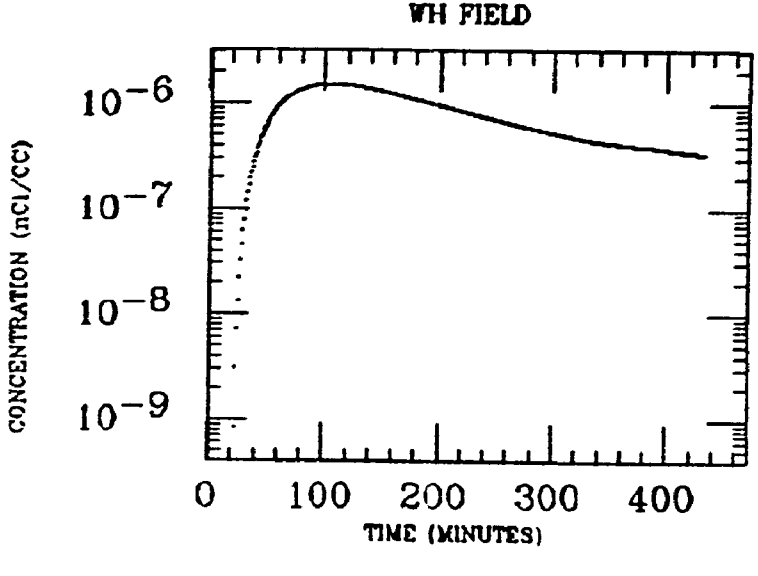

HAWKINS
XE INGESTION
Po-214

STOMACH

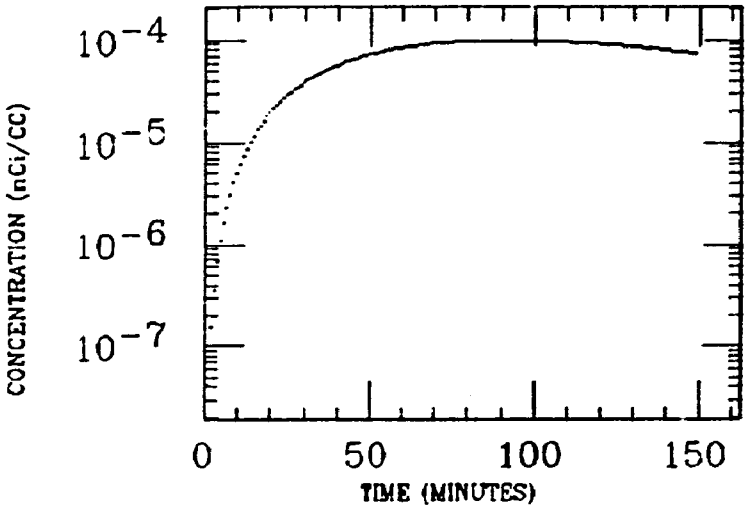

LIVER

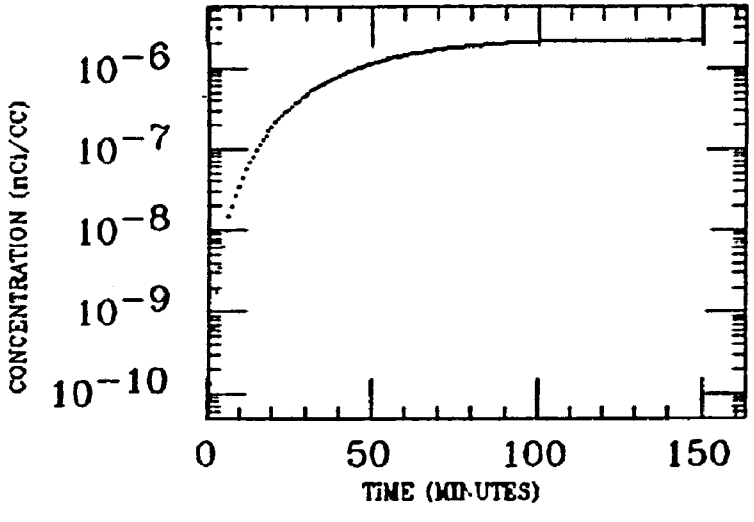

SM INTEST

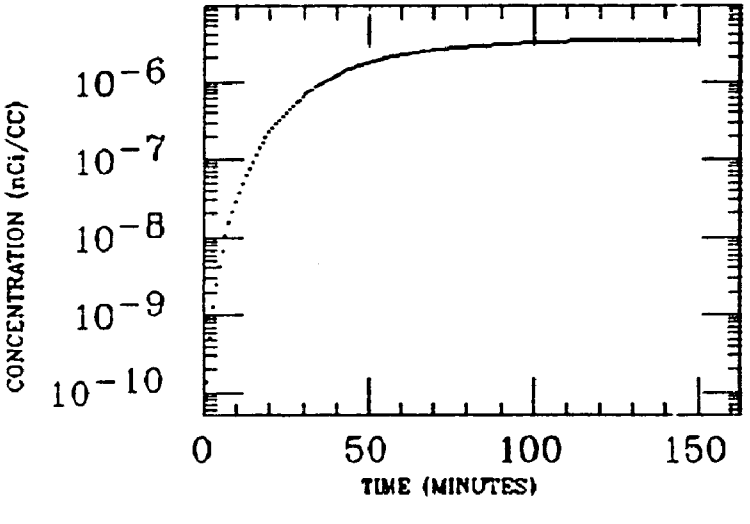

LG INTEST

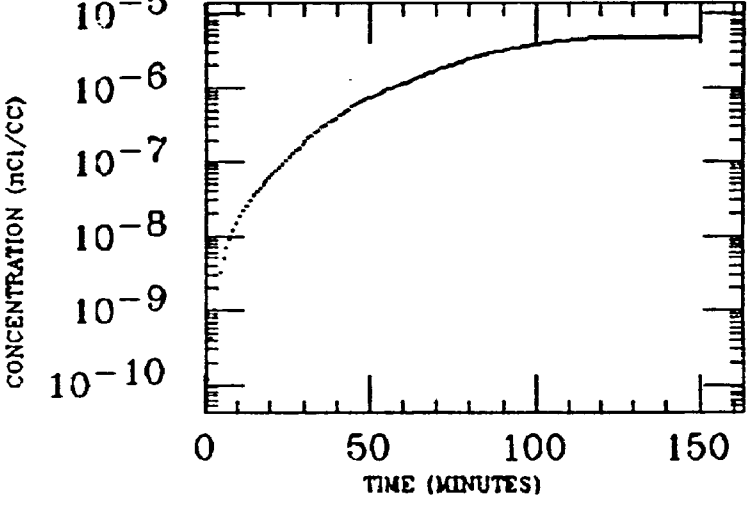

HAWKINS
XE INGESTION
Po-214

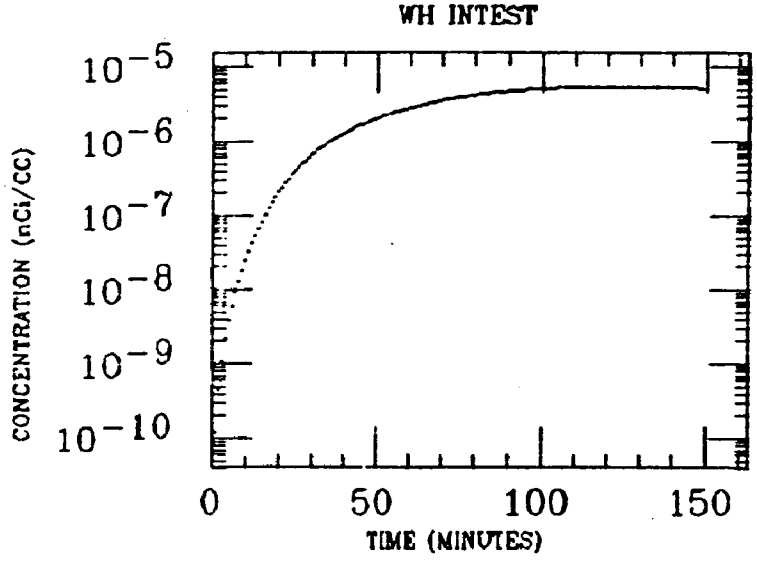

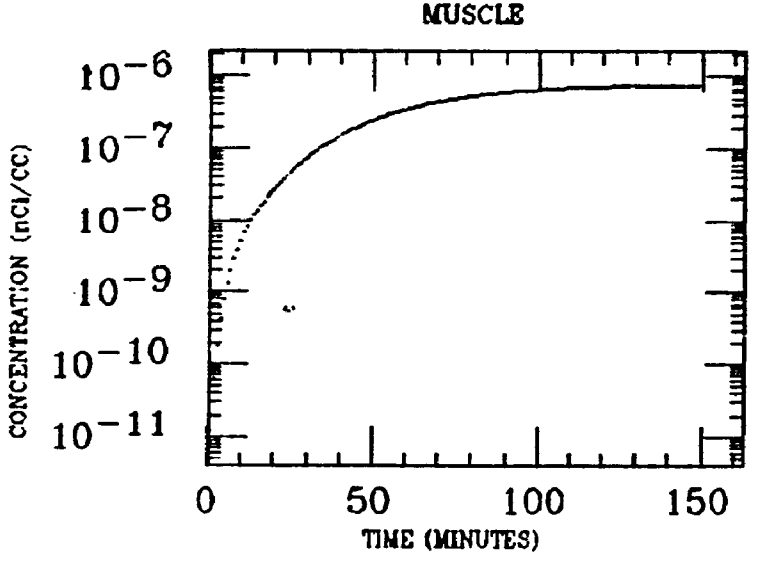

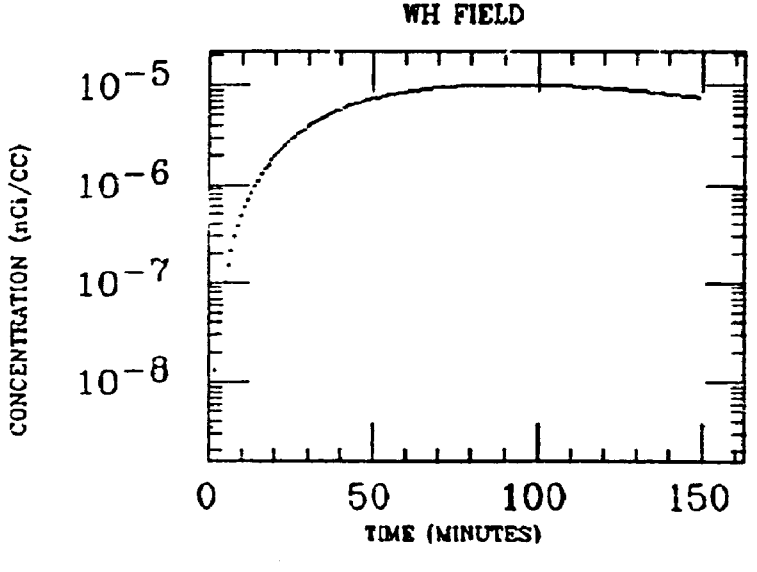

342

HILL
XE INGESTION
Po-214

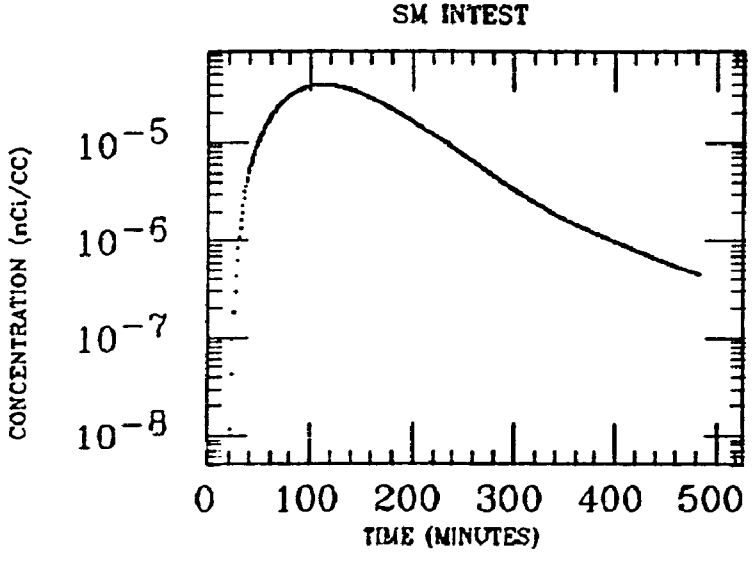

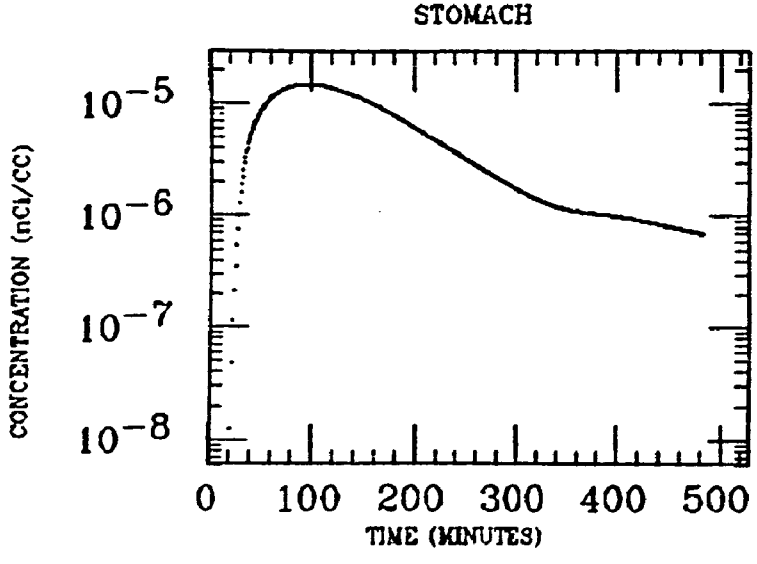

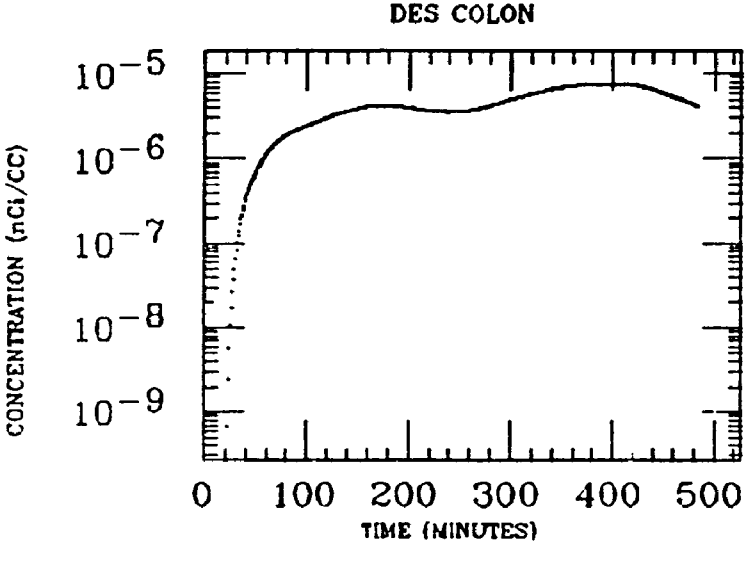

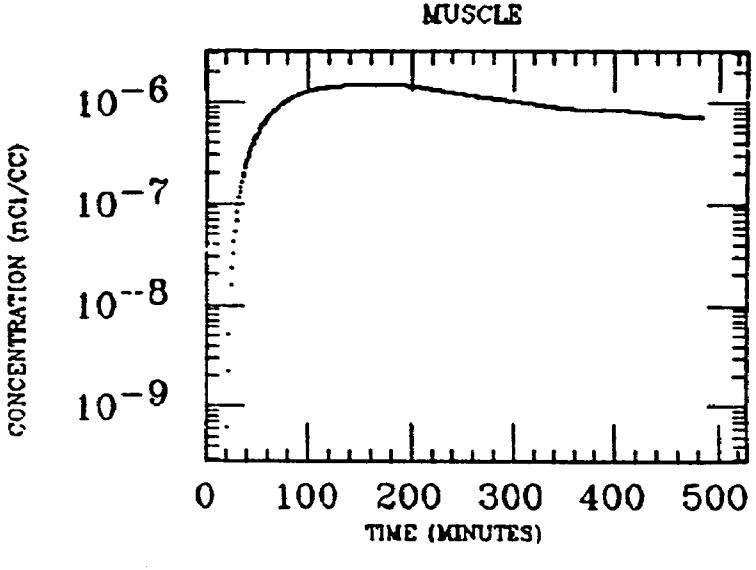

HILL

XE INGESTION

Po-214

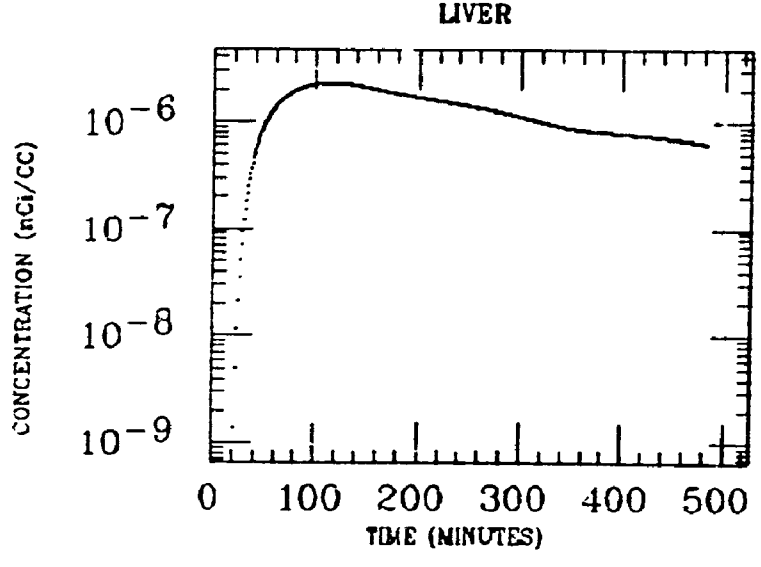

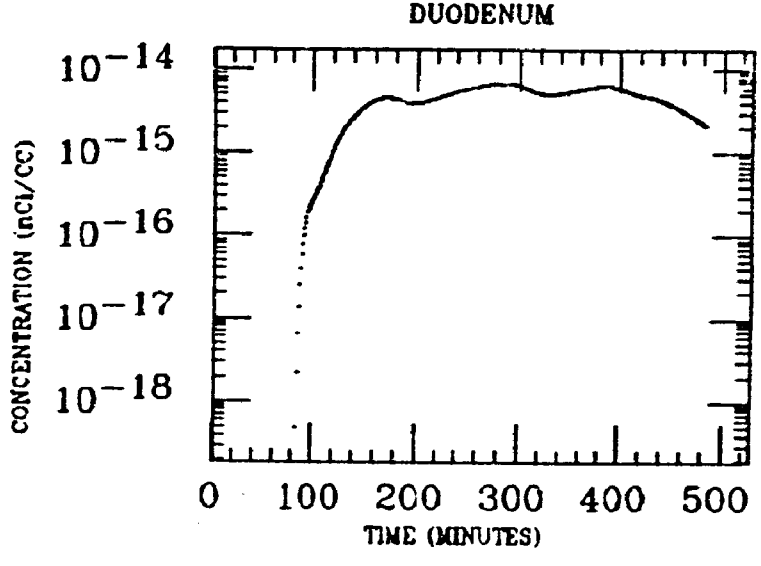

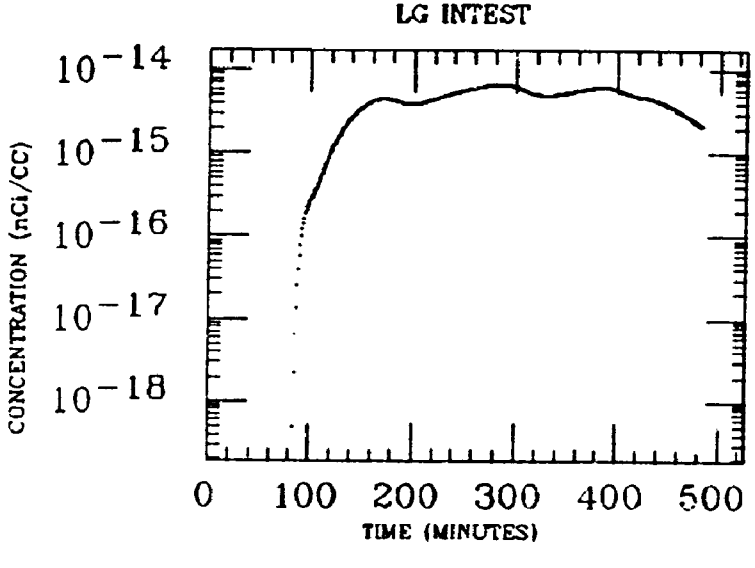

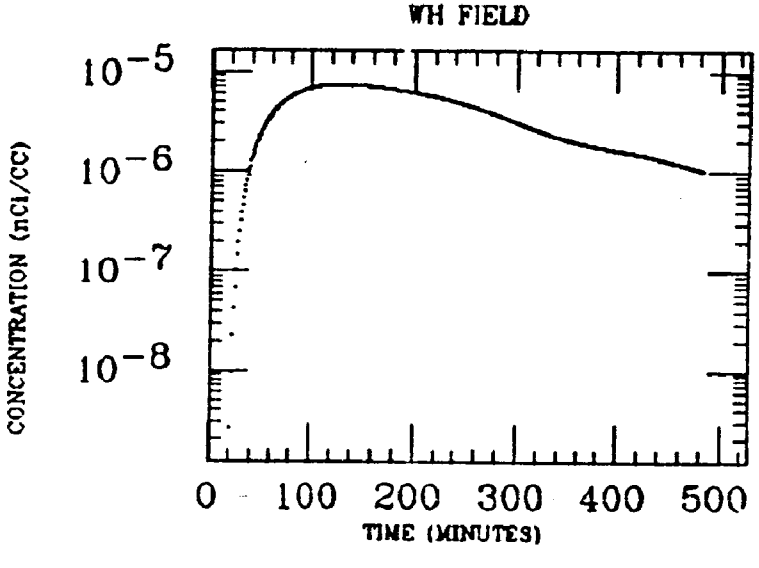

HILL
XE INGESTION
Po-214

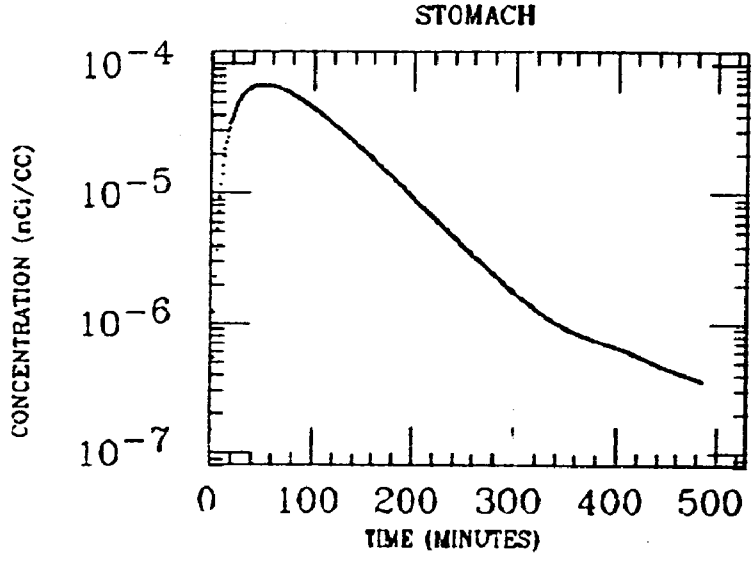

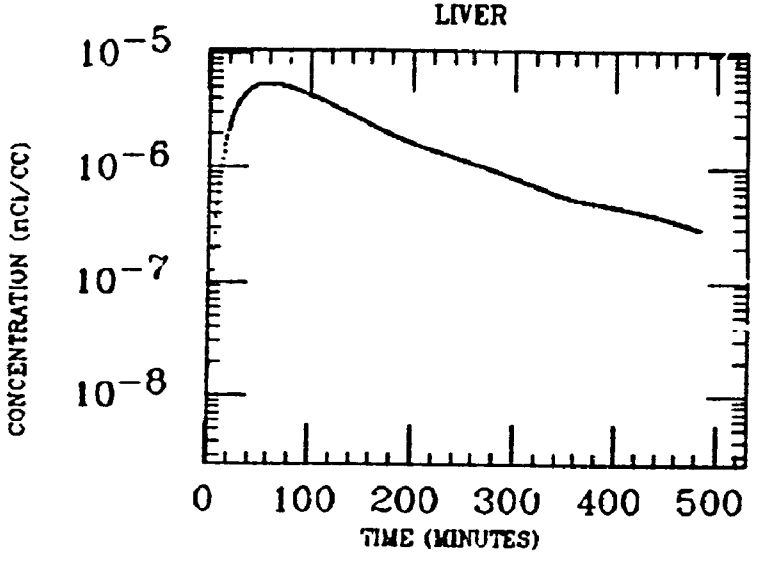

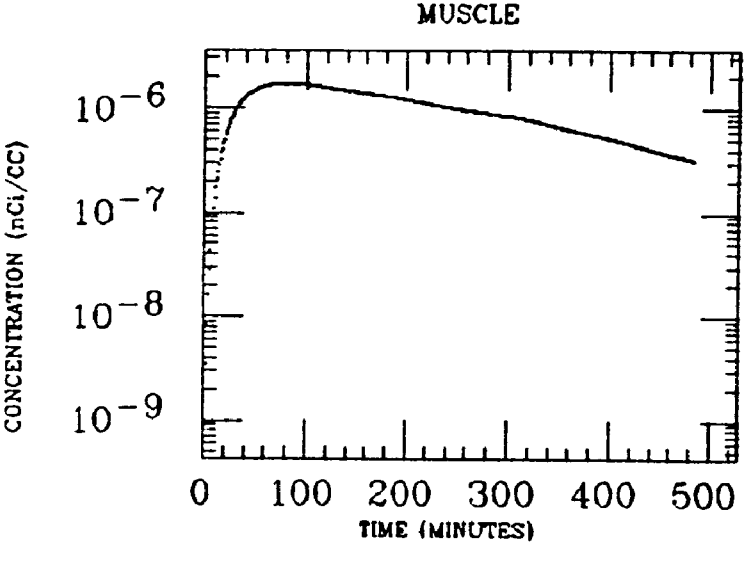

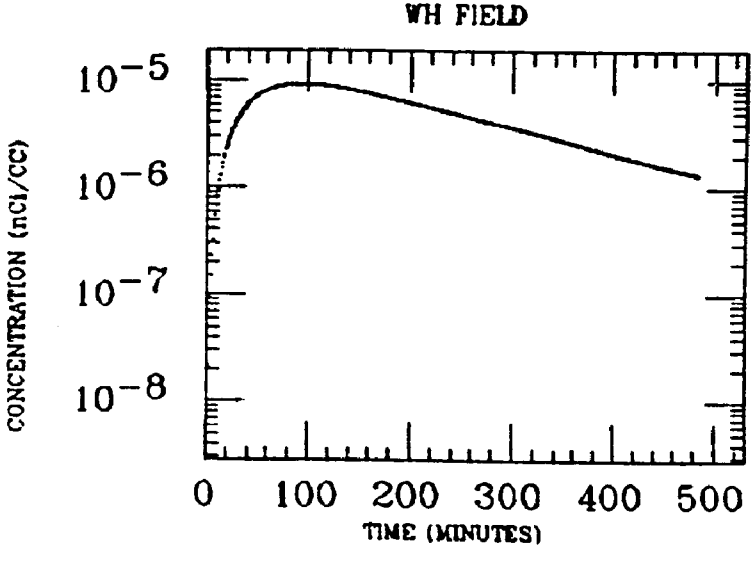

HUTCHINS
XE INGESTION
Po-214

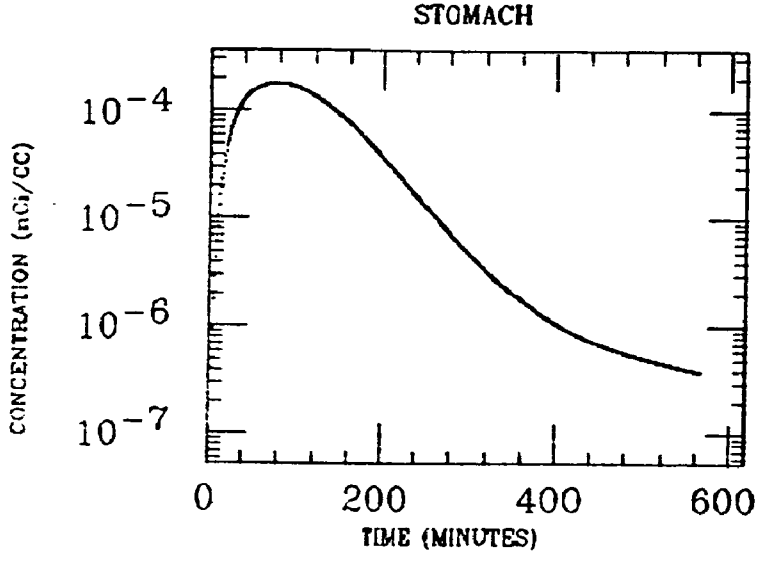

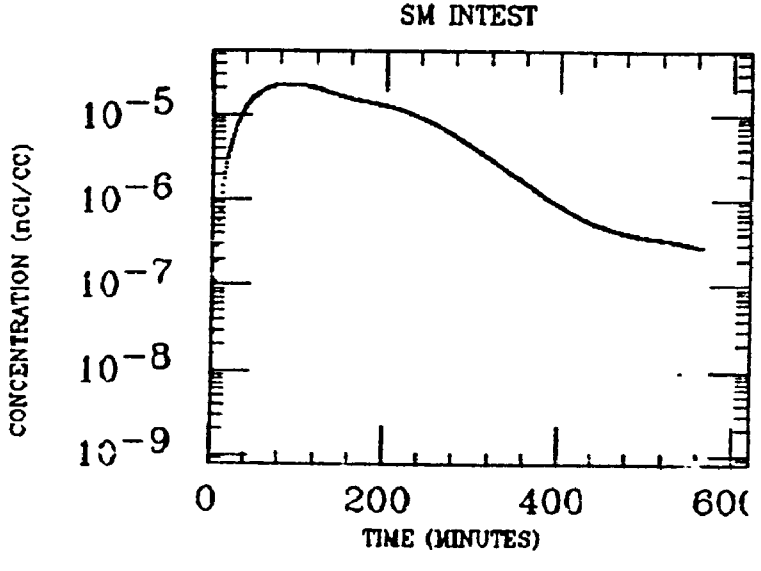

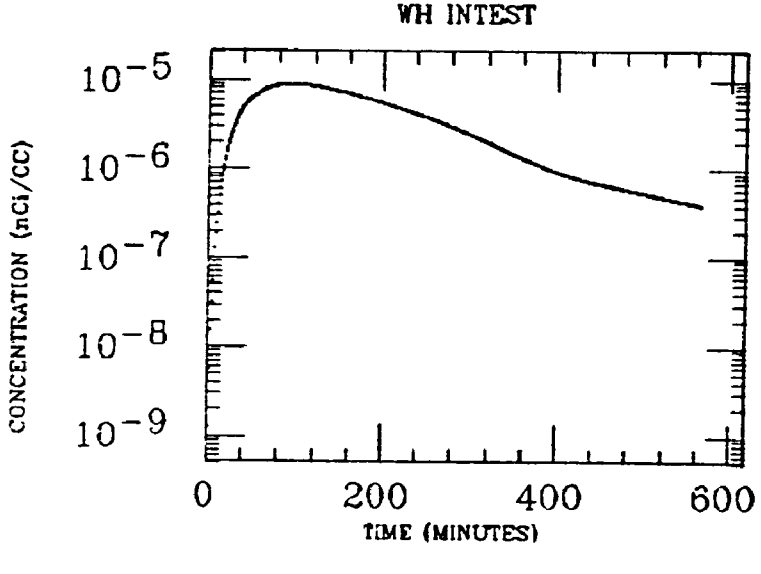

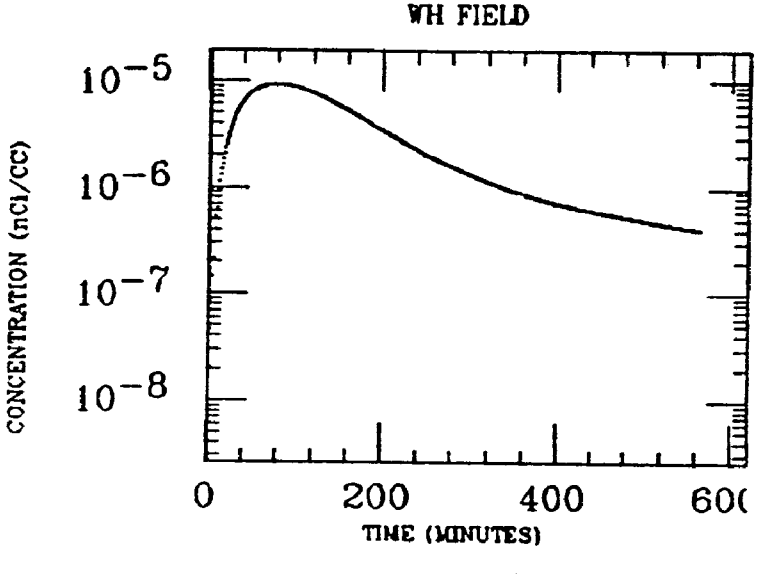

HUTCHINS
XE INGESTION
Po-214

LIVER

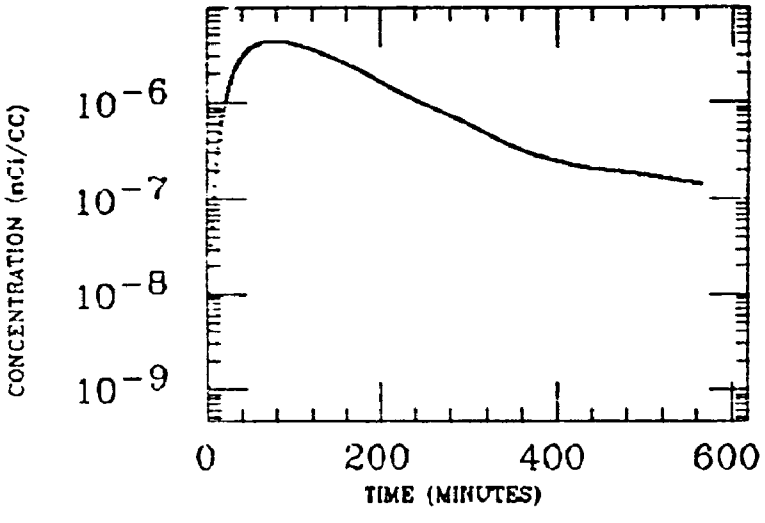

FAT

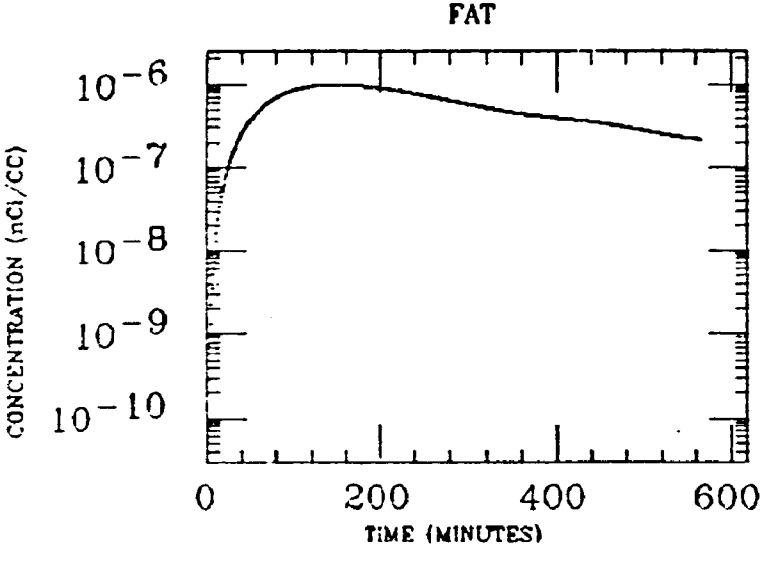

ASC COLON

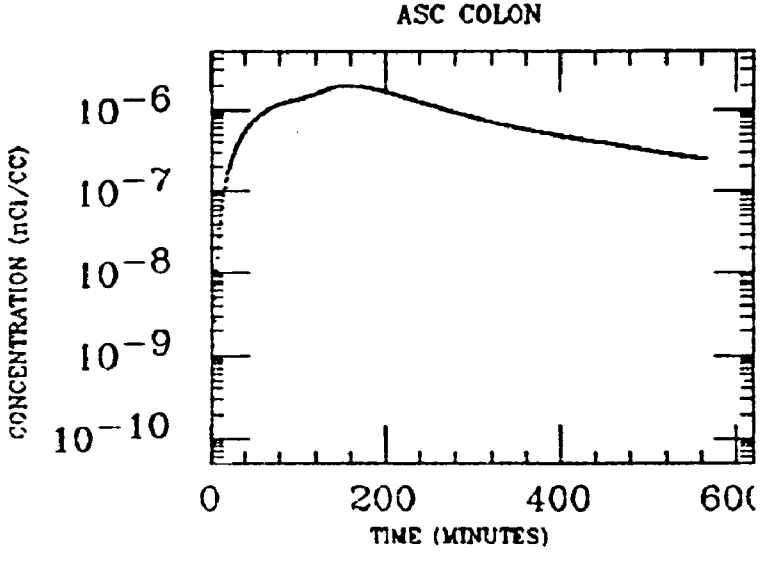

HUTCHINS

XE INGESTION

Po-214

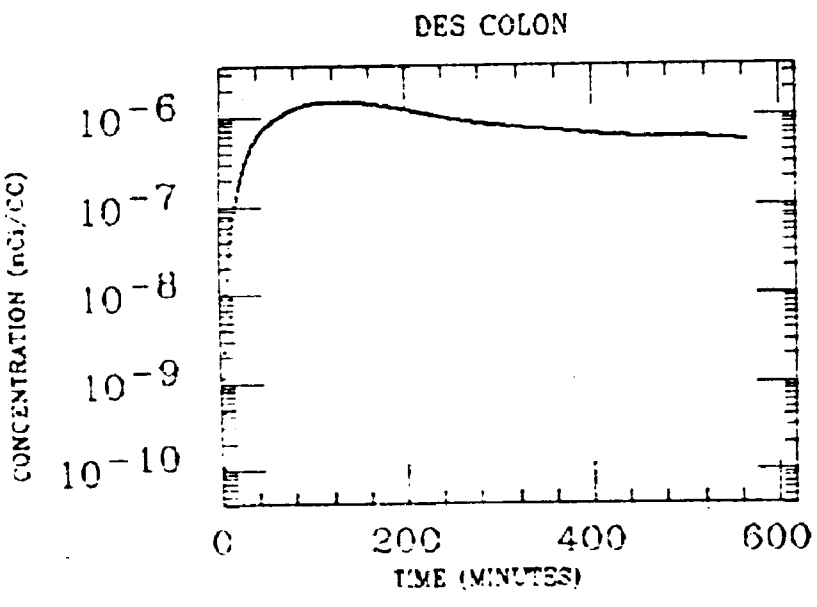

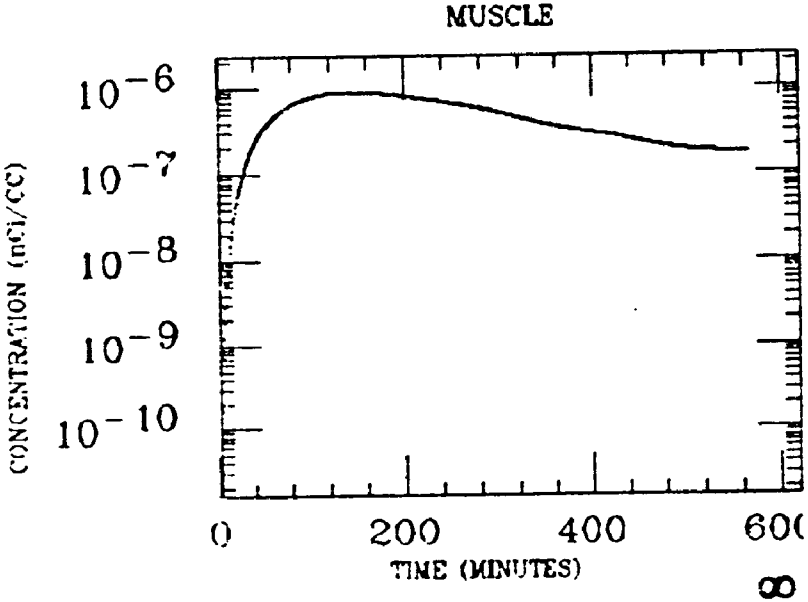

J.MCKINLEY
XE INGESTION
Po-214

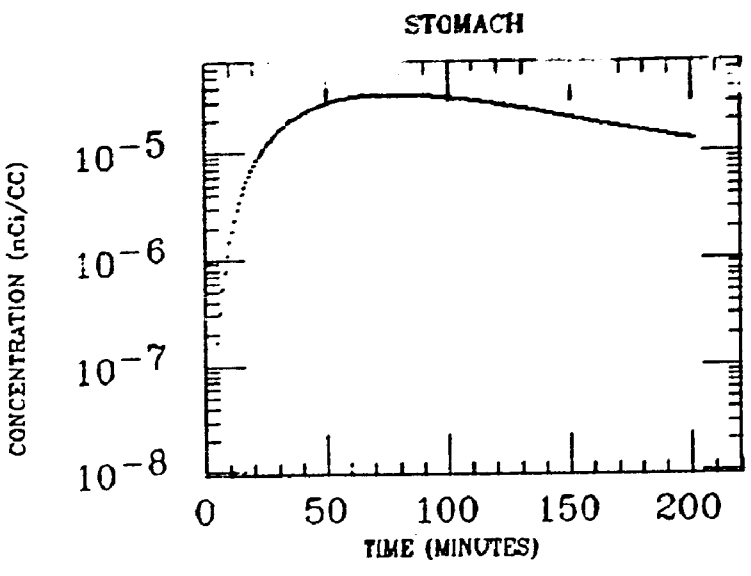

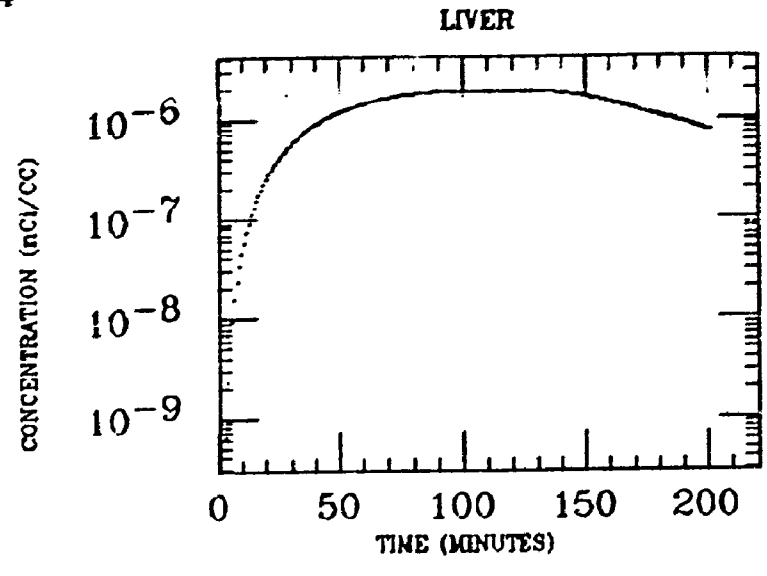

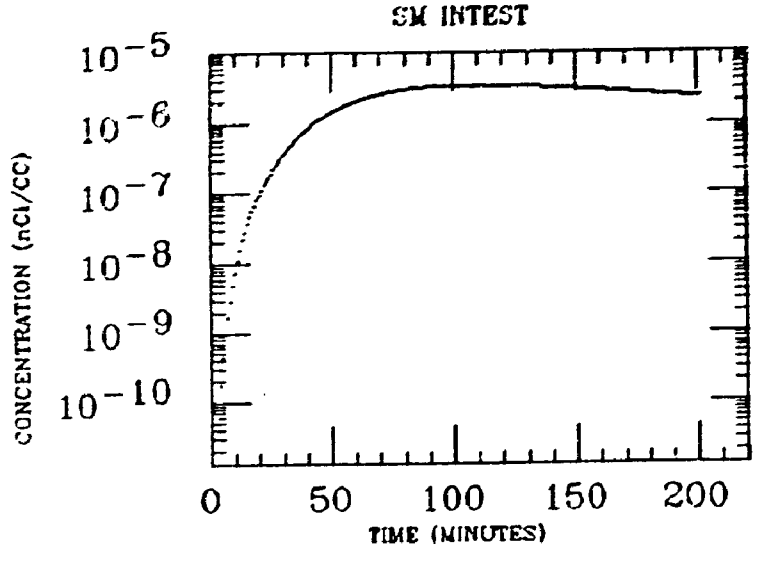

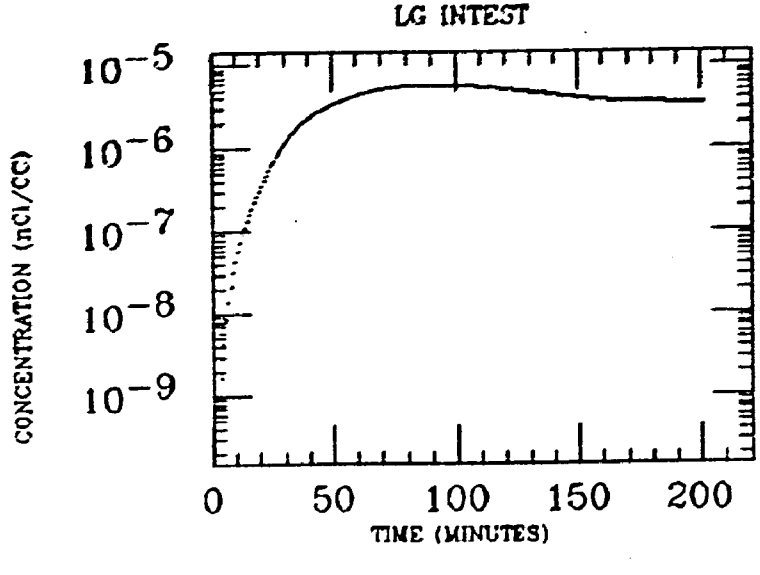

J.MCKINLEY
XE INGESTION
Po-214

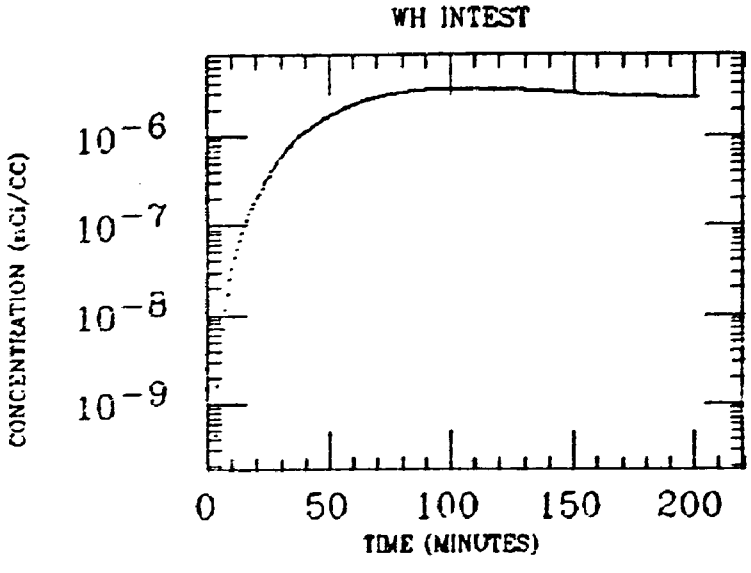

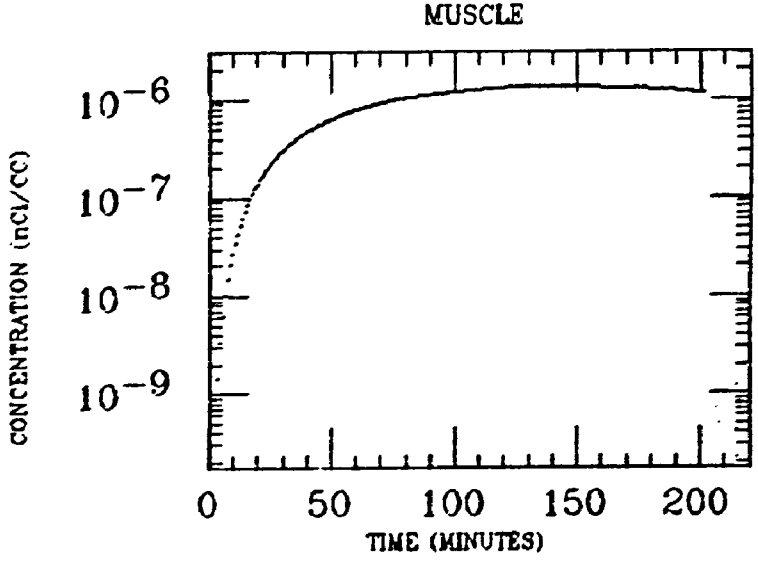

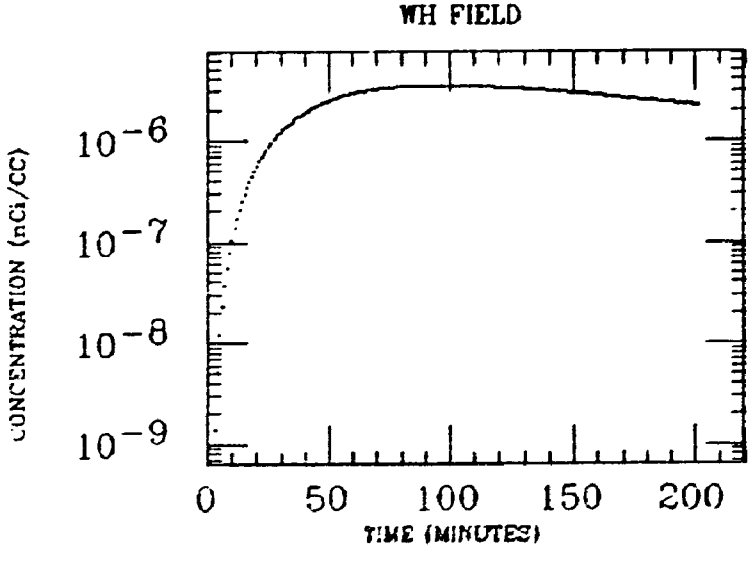

KELLEHER
XE INGESTION
Po-214

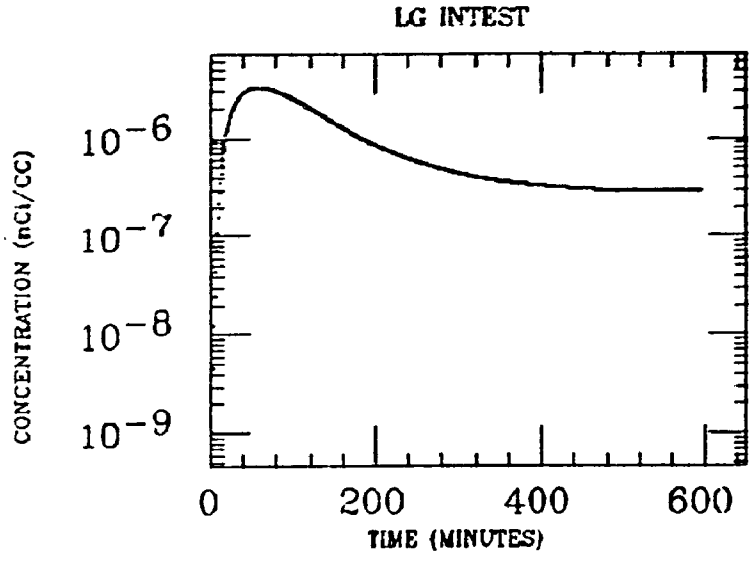

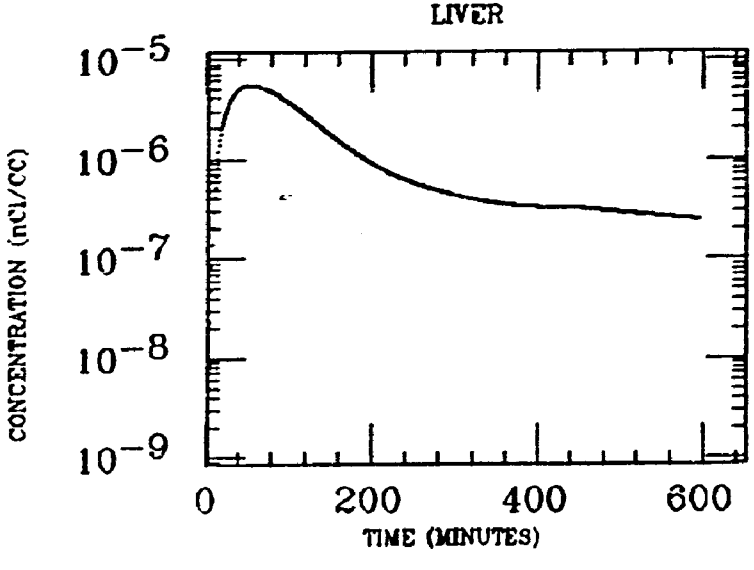

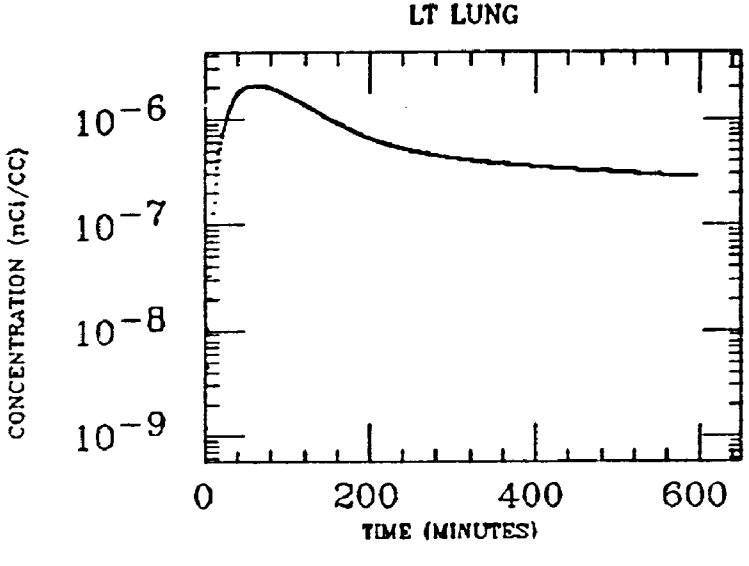

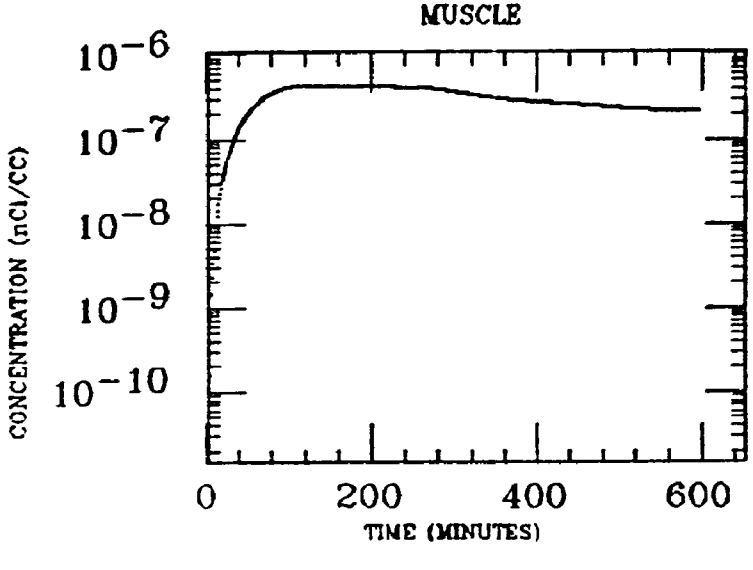

KELLEHER
XE INGESTION
Po-214

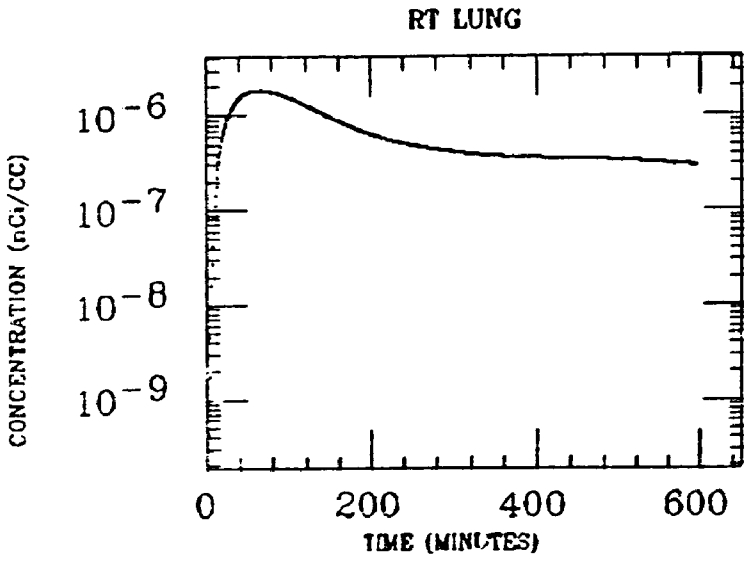

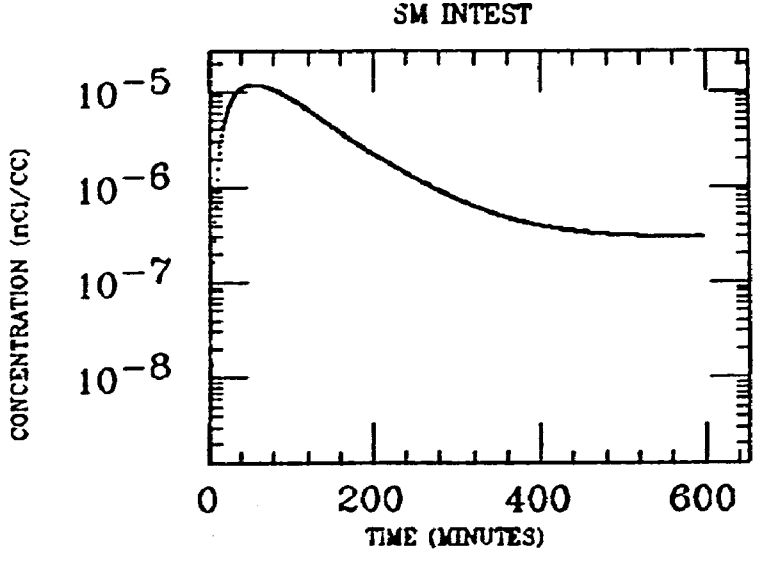

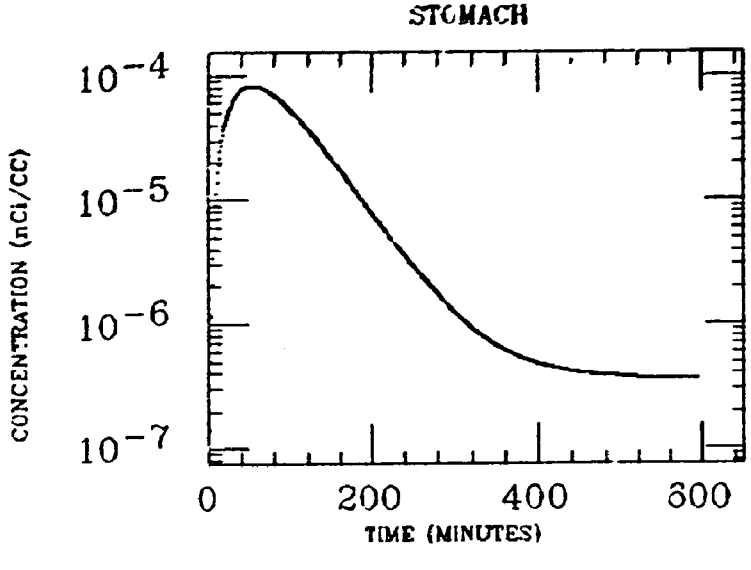

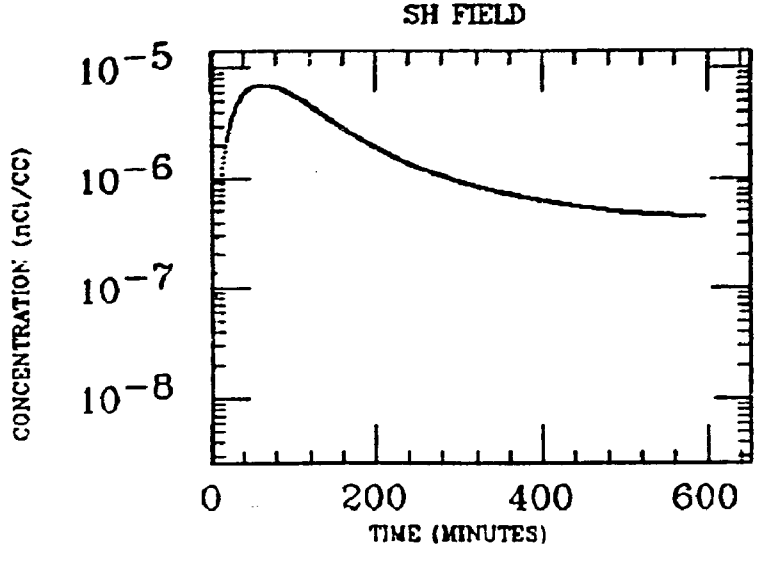

LITTELL
XE INGESTION
Po-214

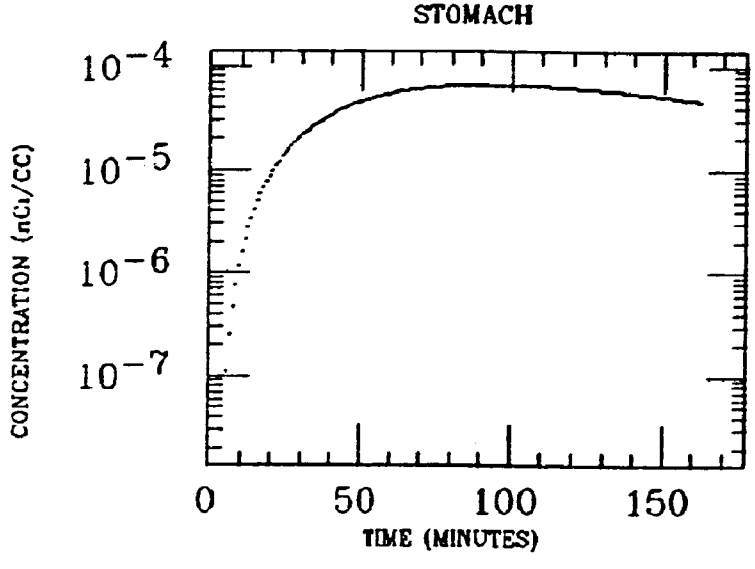

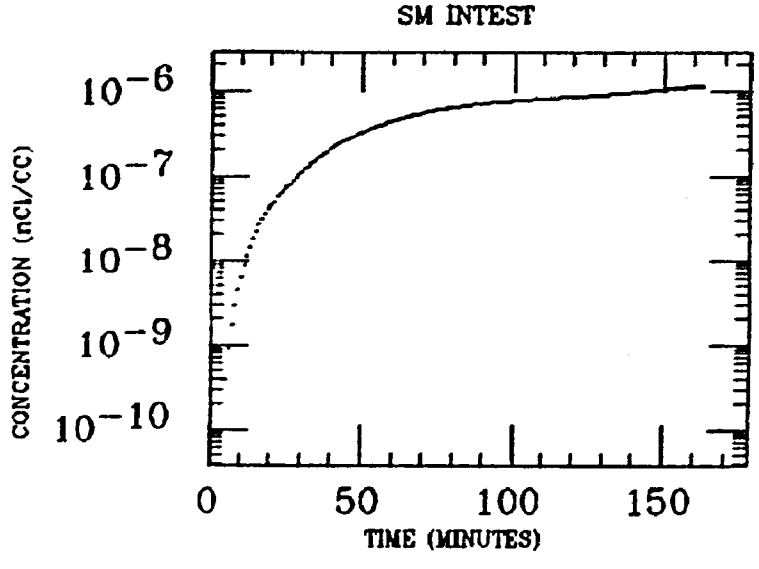

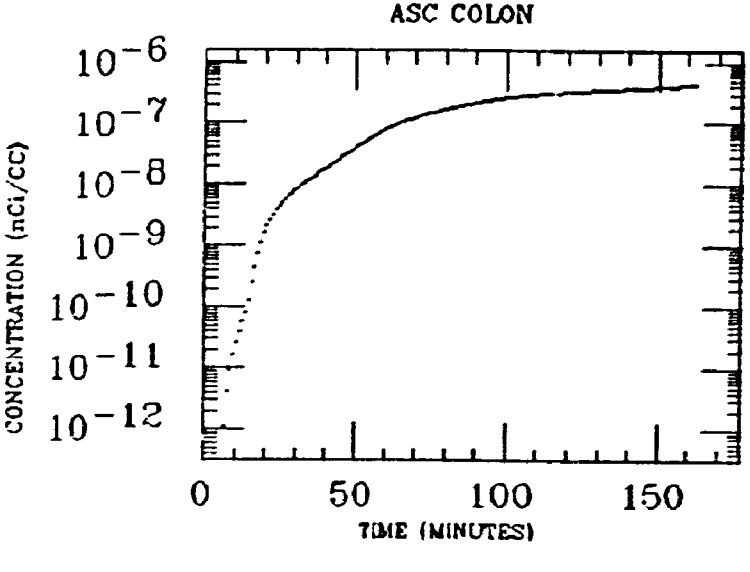

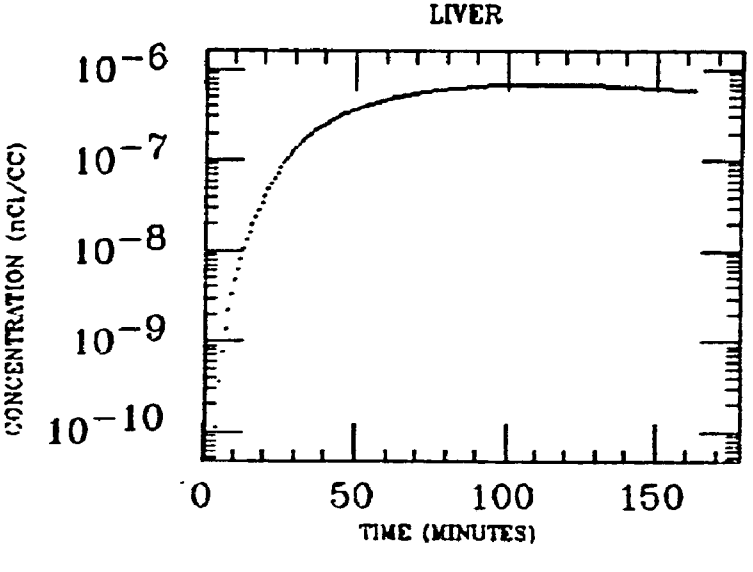

LITTELL
XE INGESTION
Po-214

MUSCLE

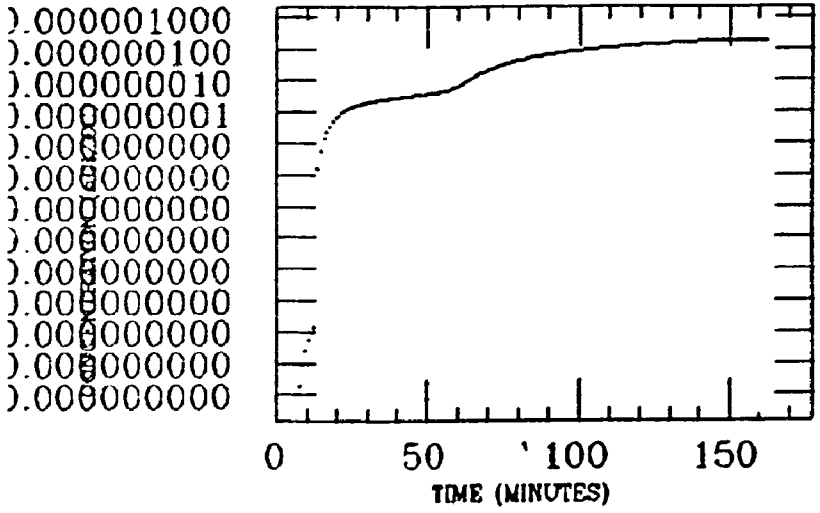

WH INTEST

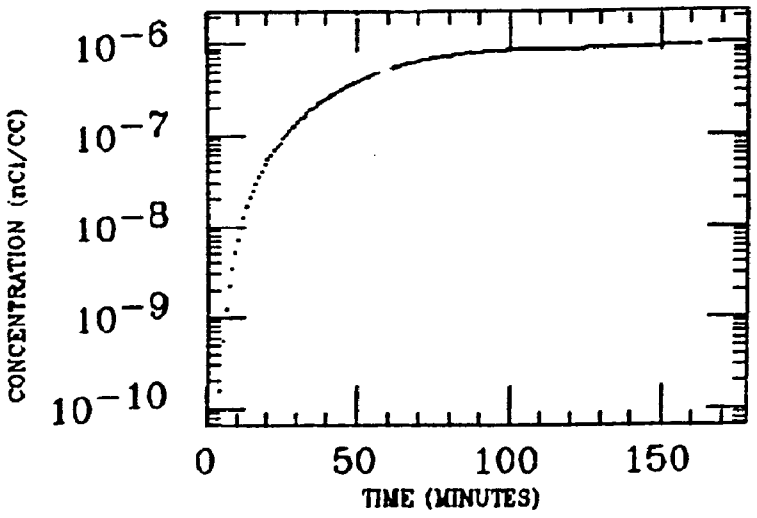

WH FIELD

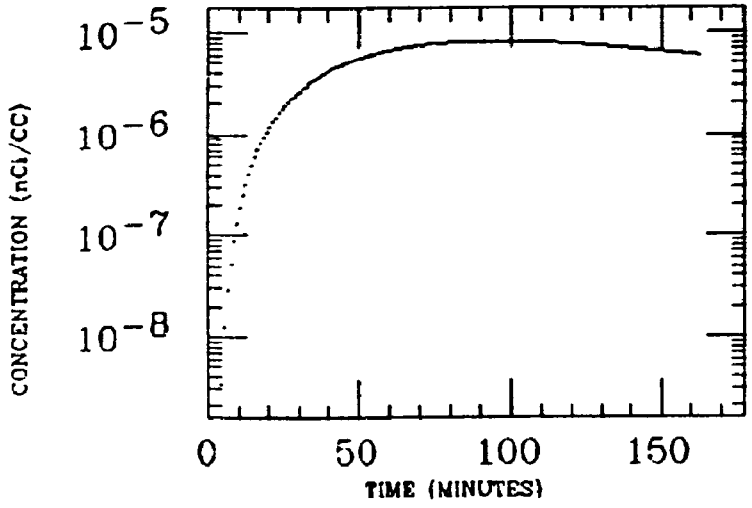

35-1

MACMILLAN
XE INGESTION
Po-214

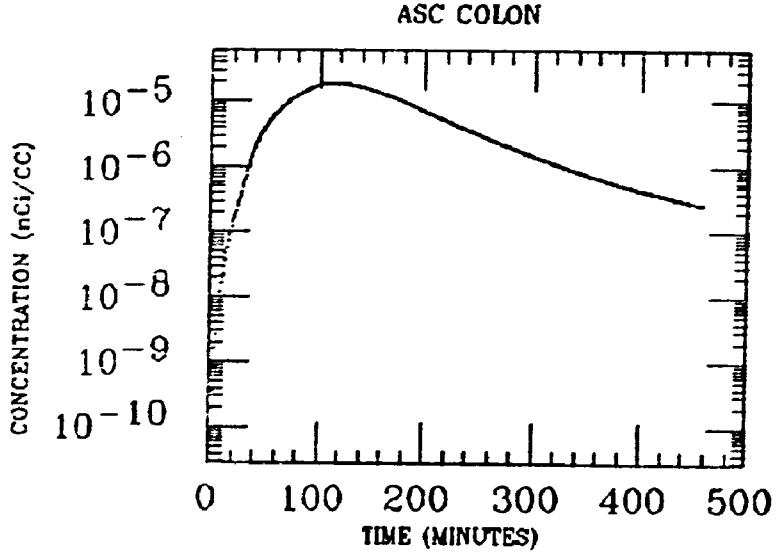

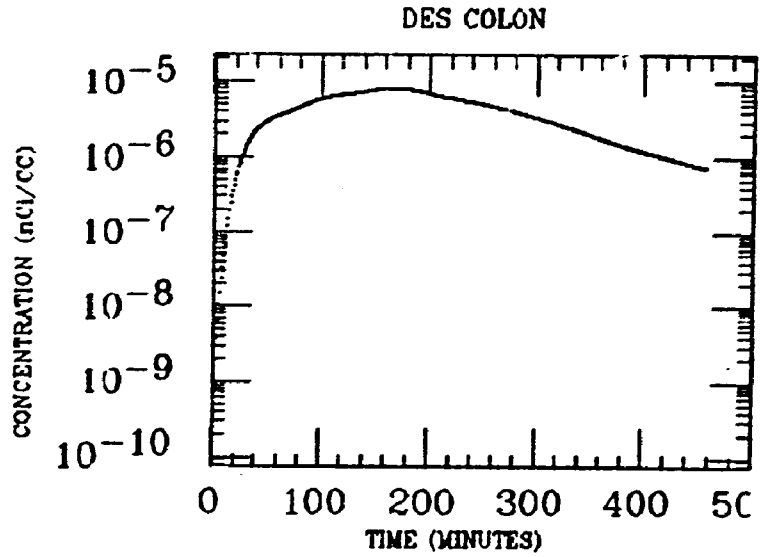

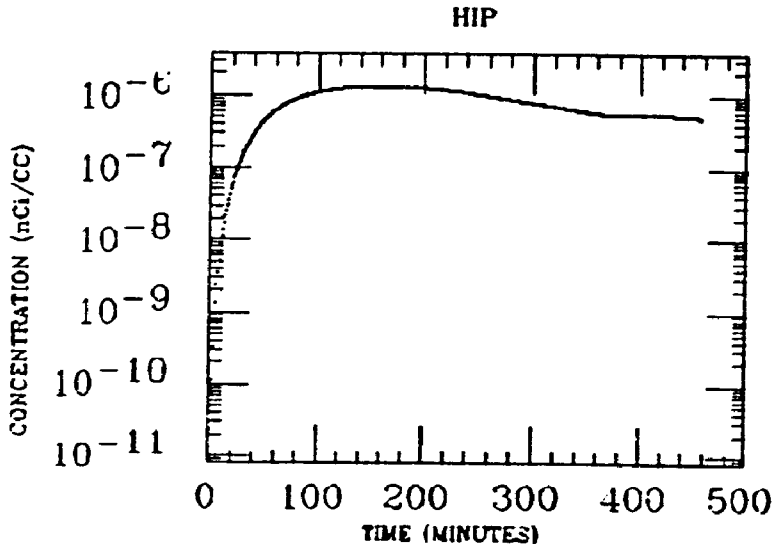

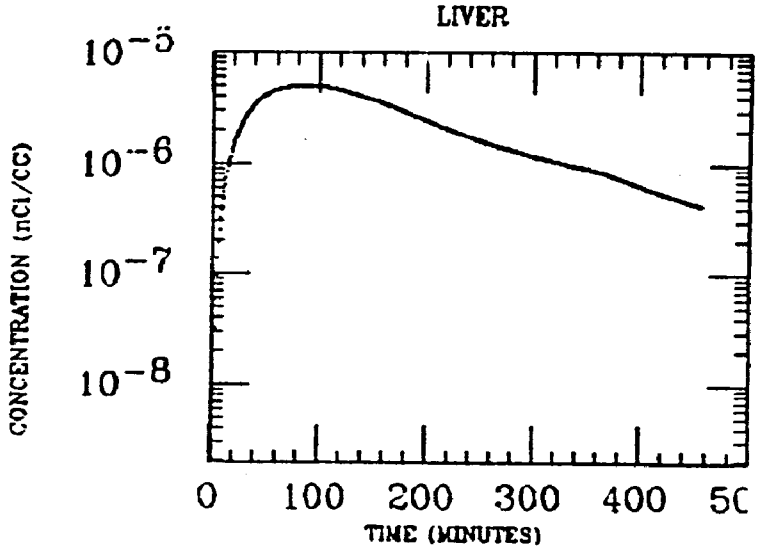

MACMILLAN
XE INGESTION
Po-214

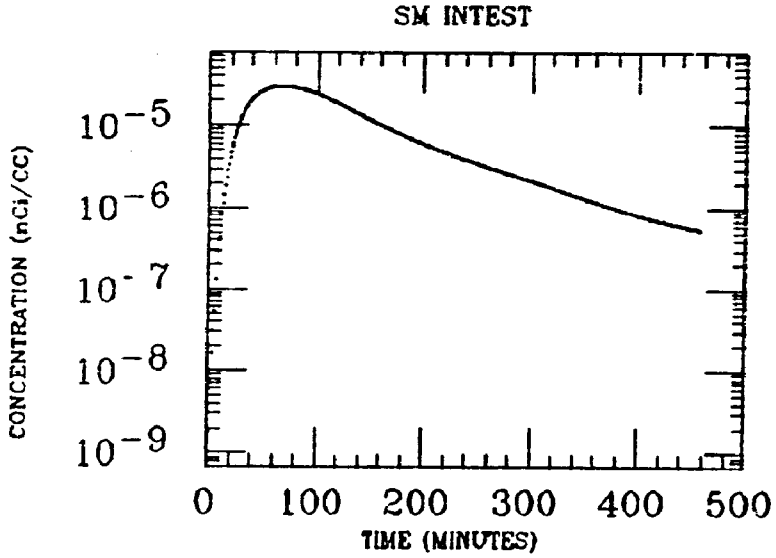

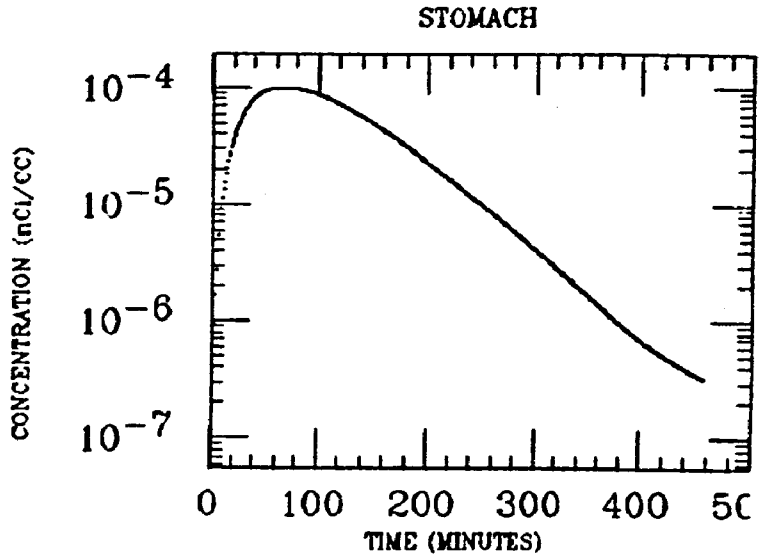

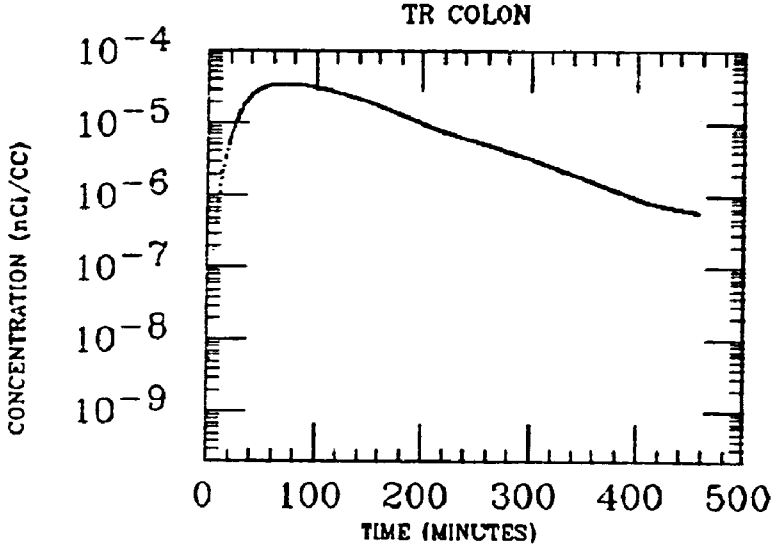

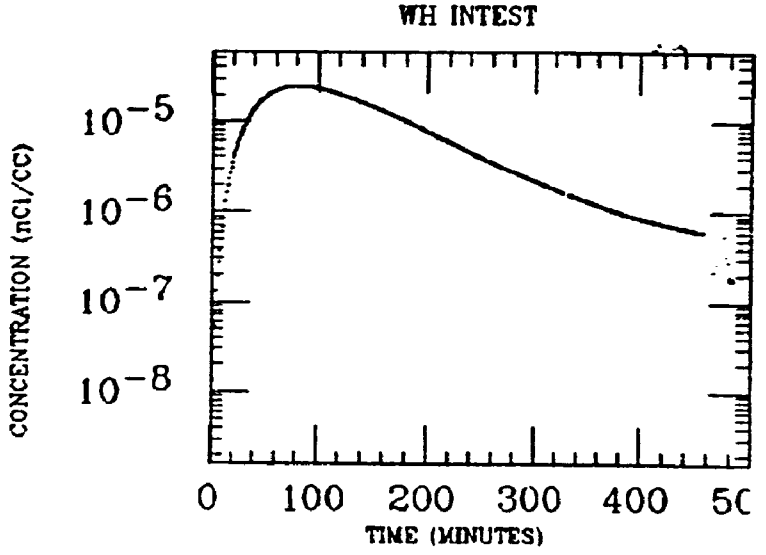

MAIO

XE INGESTION

Po-214

STOMACH

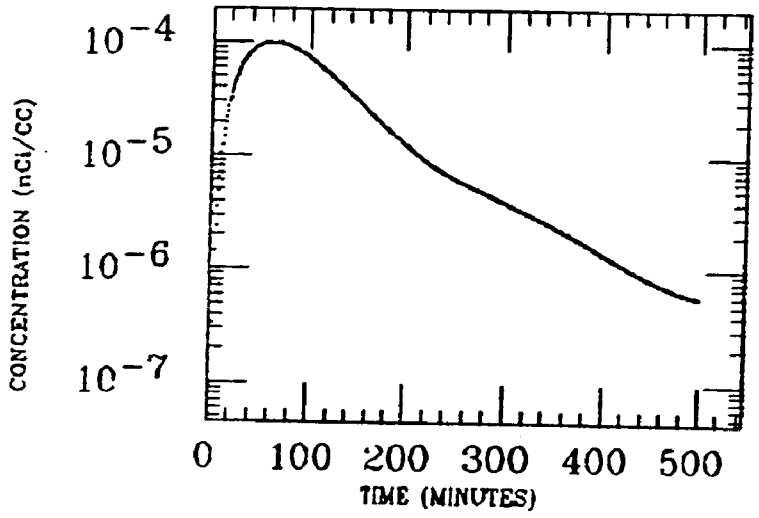

LIVER

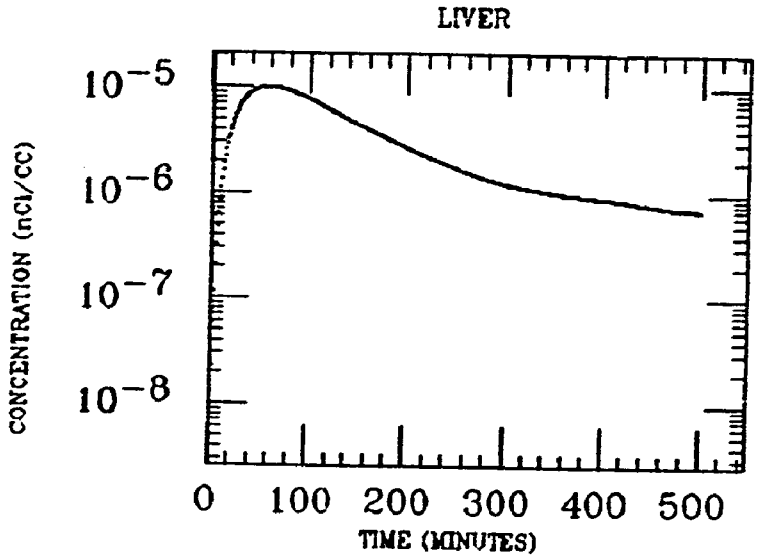

SM INTEST

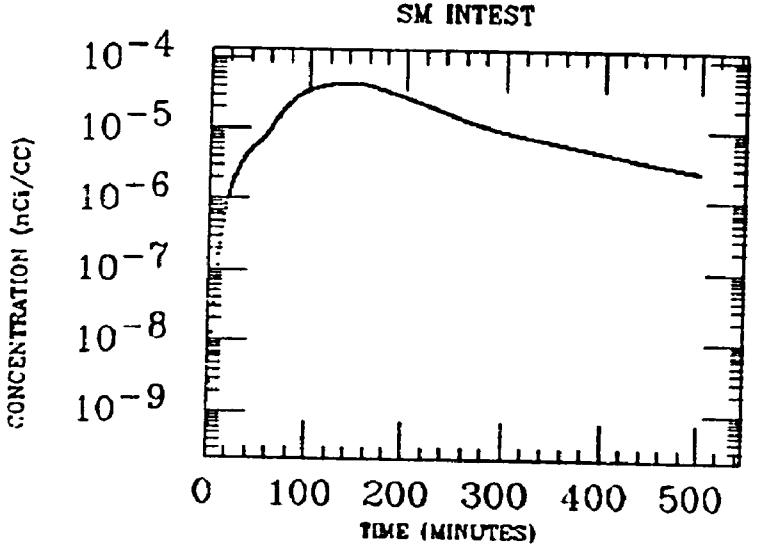

LG INTEST

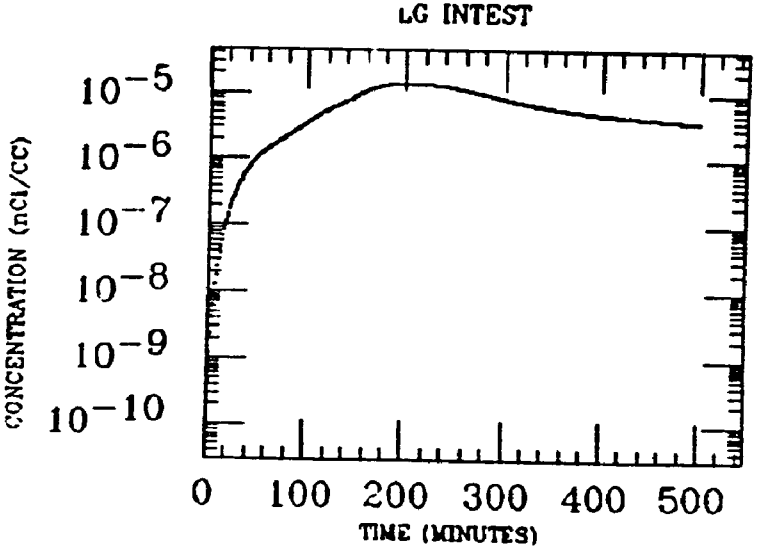

MAIO
XE INGESTION
Po-214

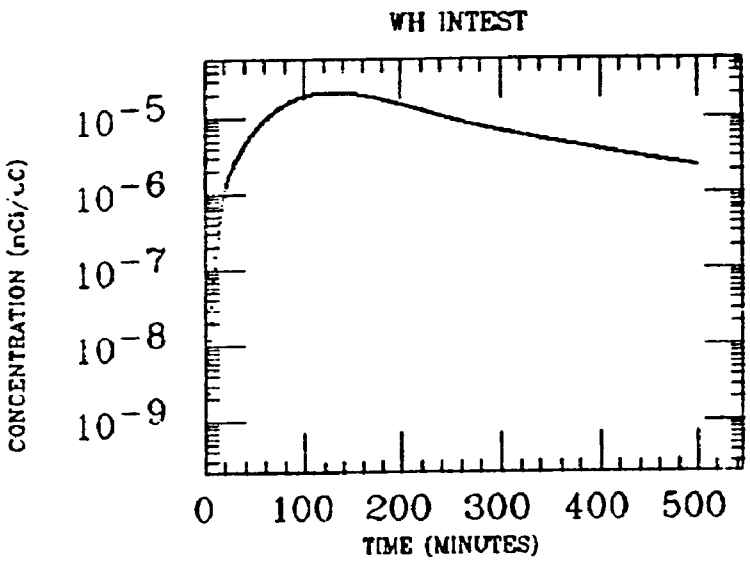

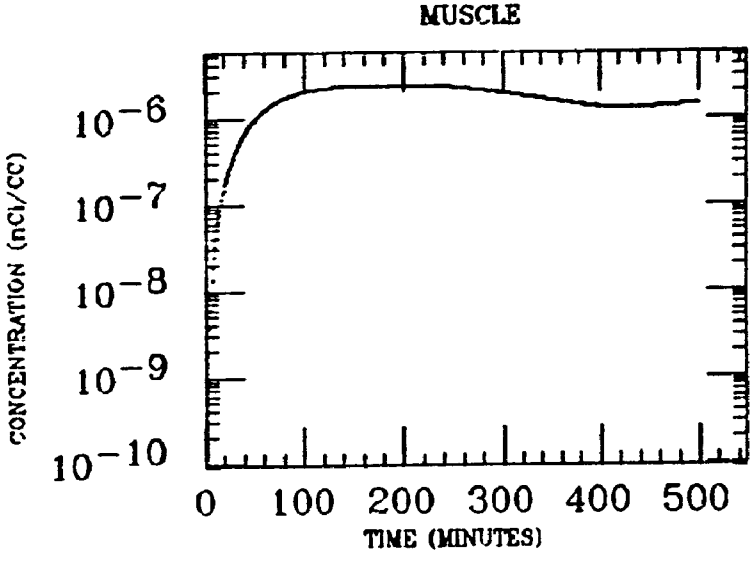

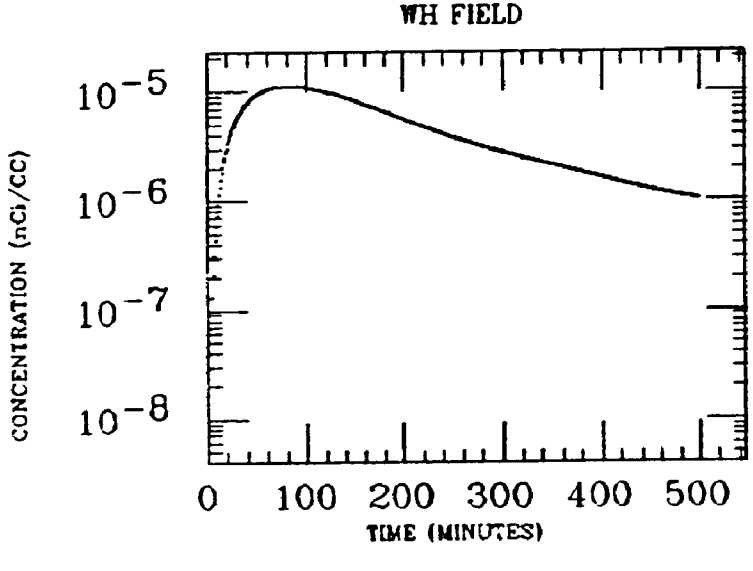

MALCOM
XE INGESTION
Po-214

STOMACH

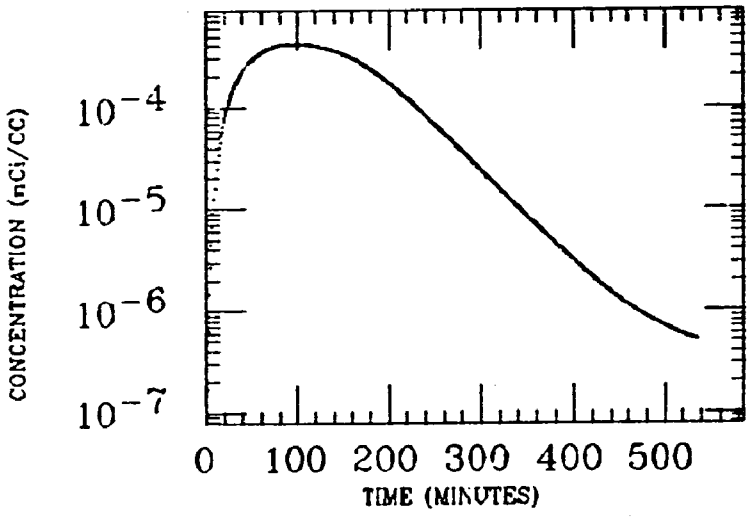

LIVER

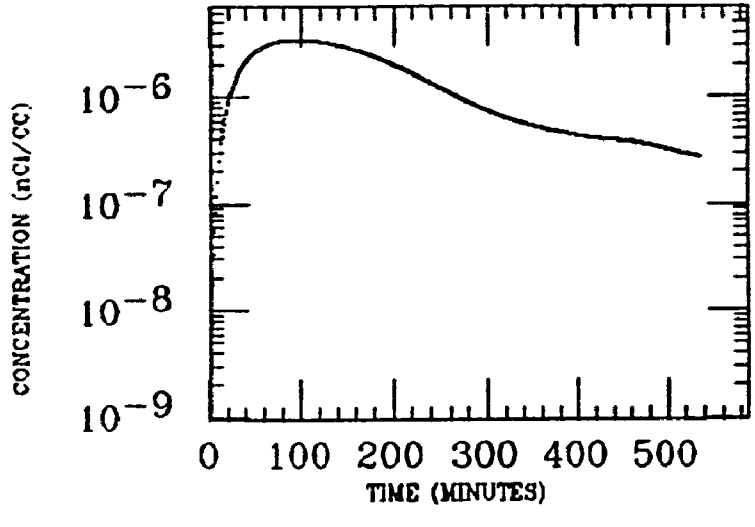

LG INTEST

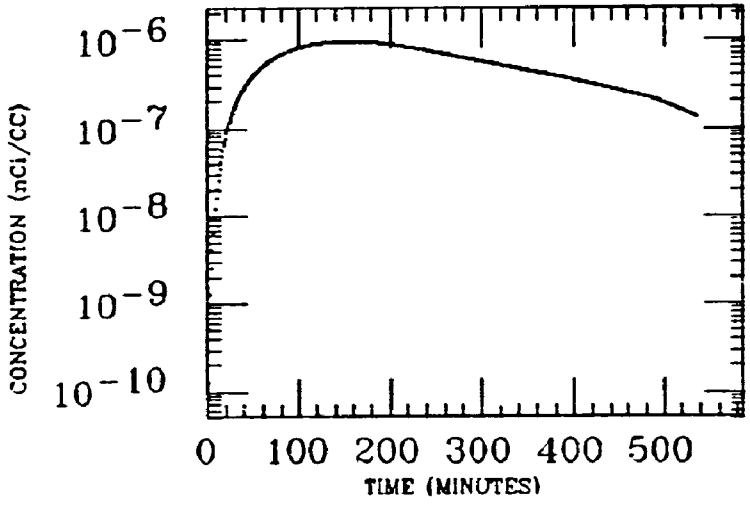

WH INTEST

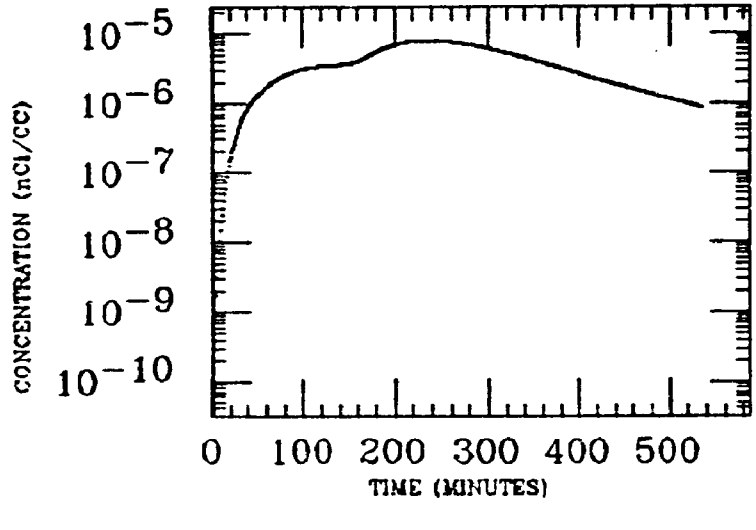

MALCOM
XE INGESTION
Po-214

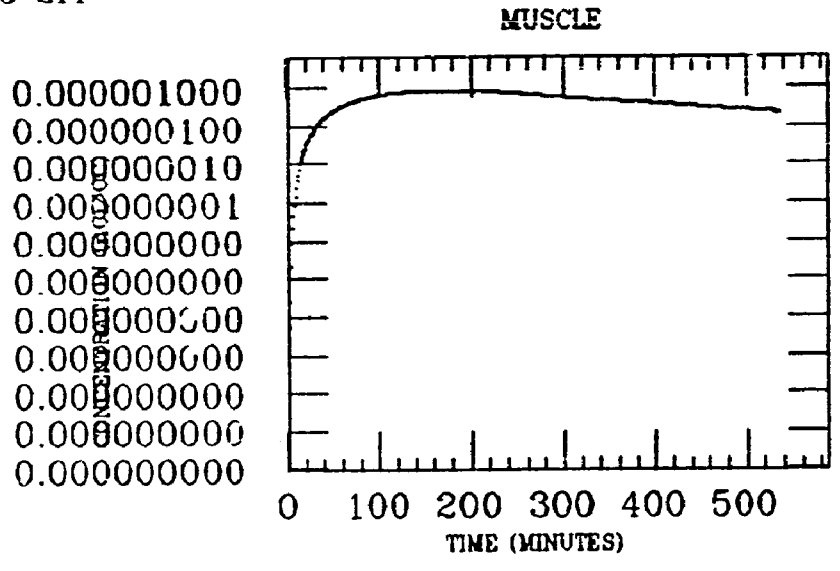

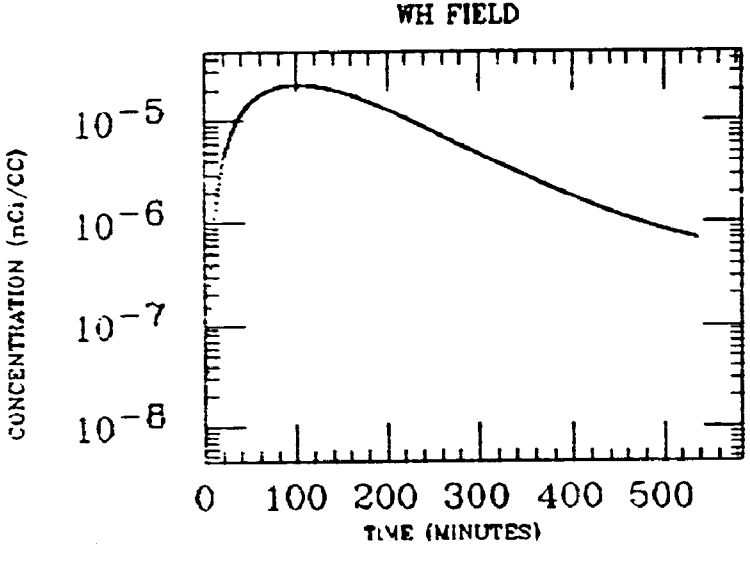

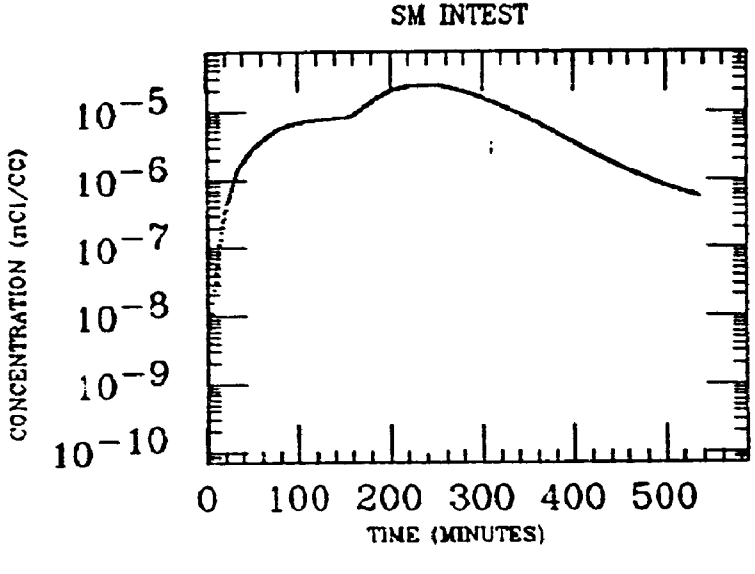

MONROE
XE INGESTION
Po-214

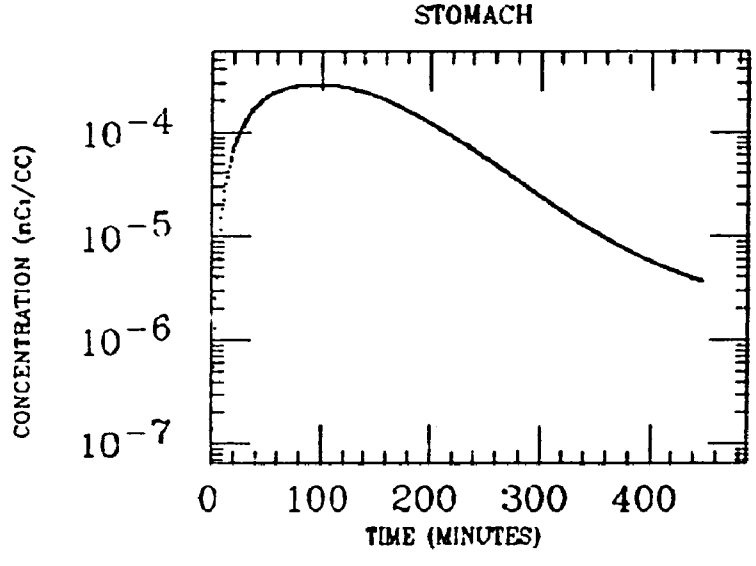

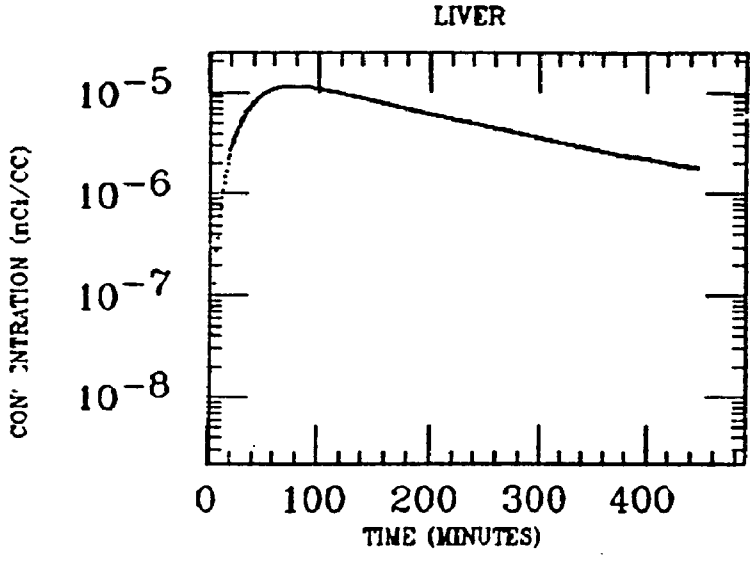

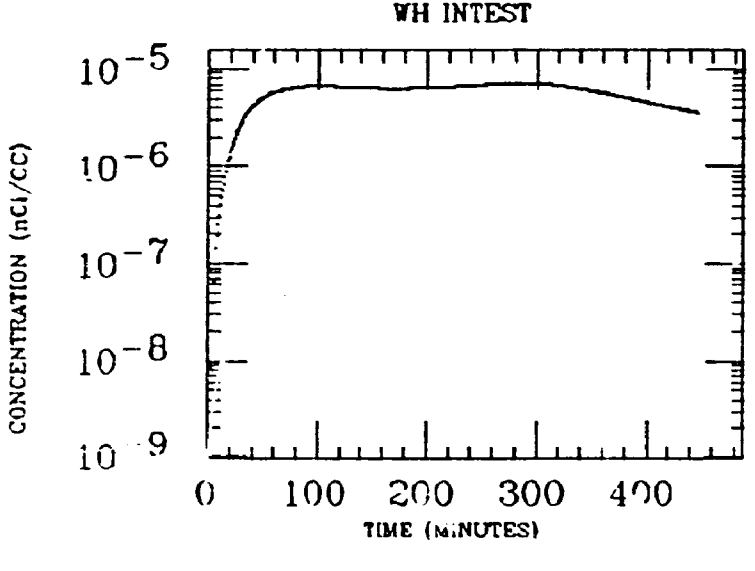

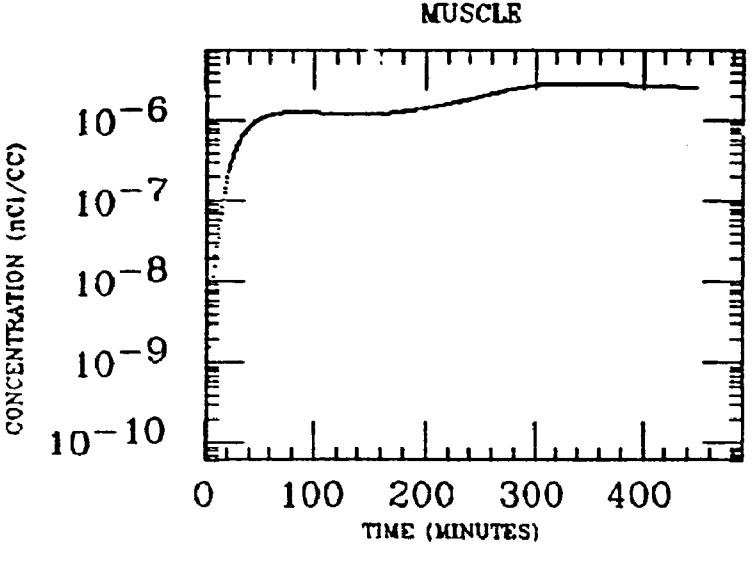

MONROE
XE INGESTION
Po-214

MORGAN
XE INGESTION
Po-214

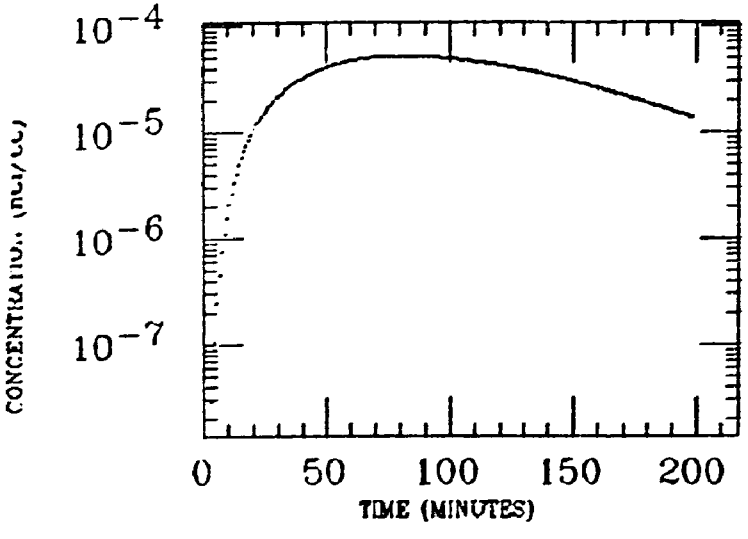

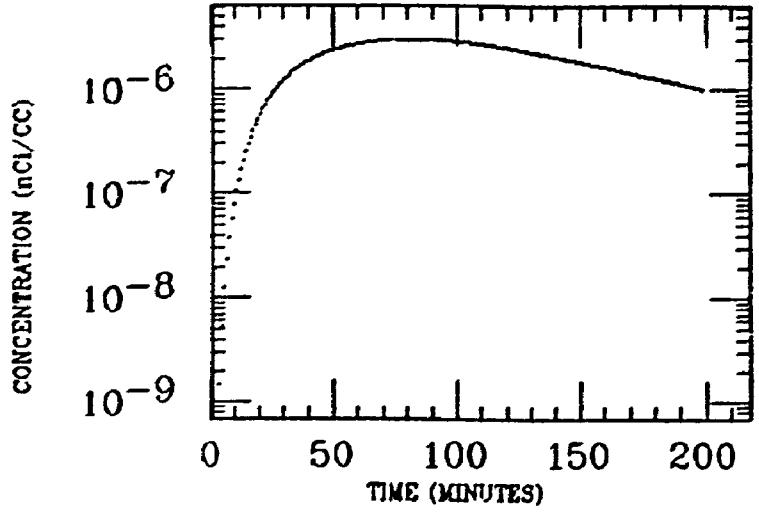

SM INTEST

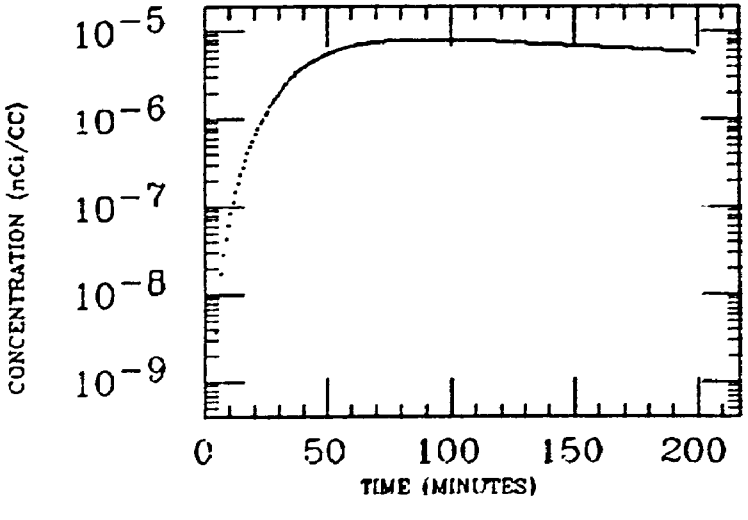

MUSCLE

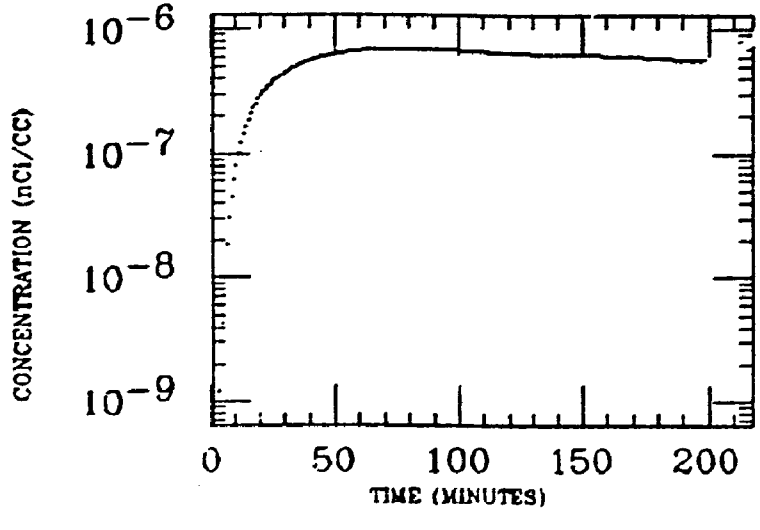

MORGAN
XE INGESTION
Po-214

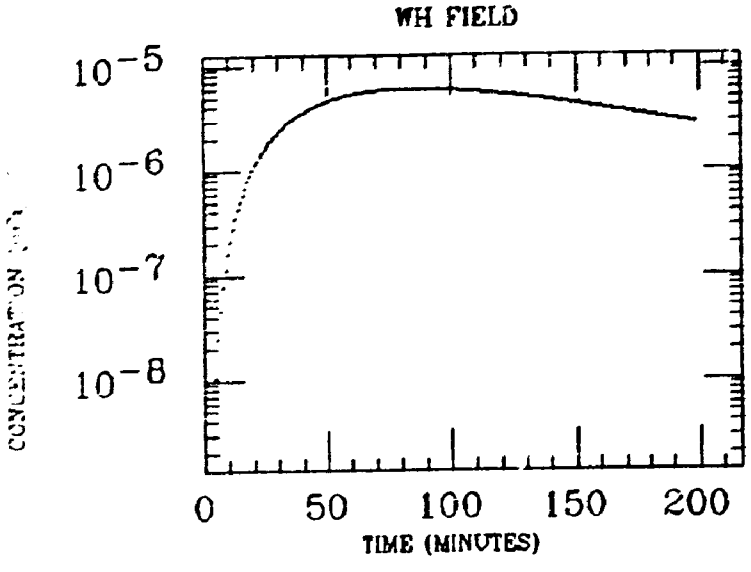

MURCHE
XE INGESTION
Po-214

STOMACH

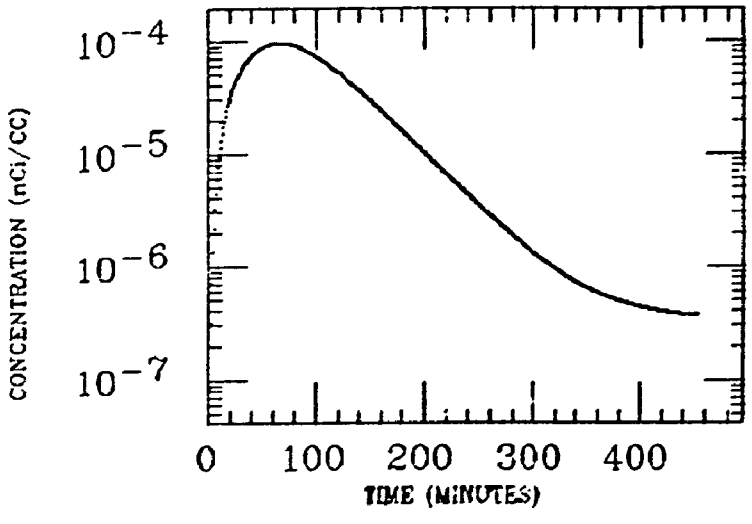

LIVER

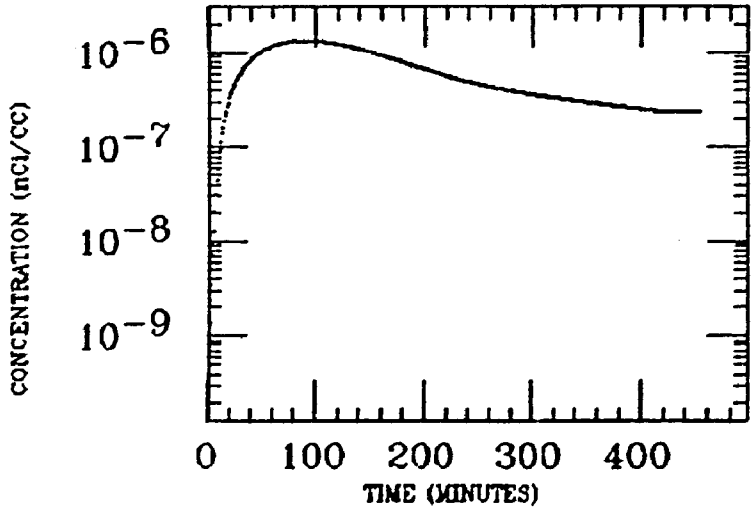

WH FIELD

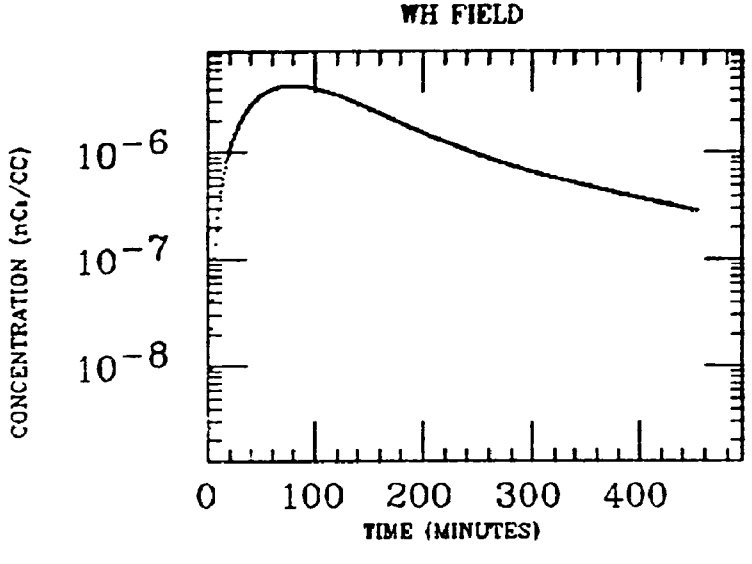

MURCHE
XE INGESTION
Po-214

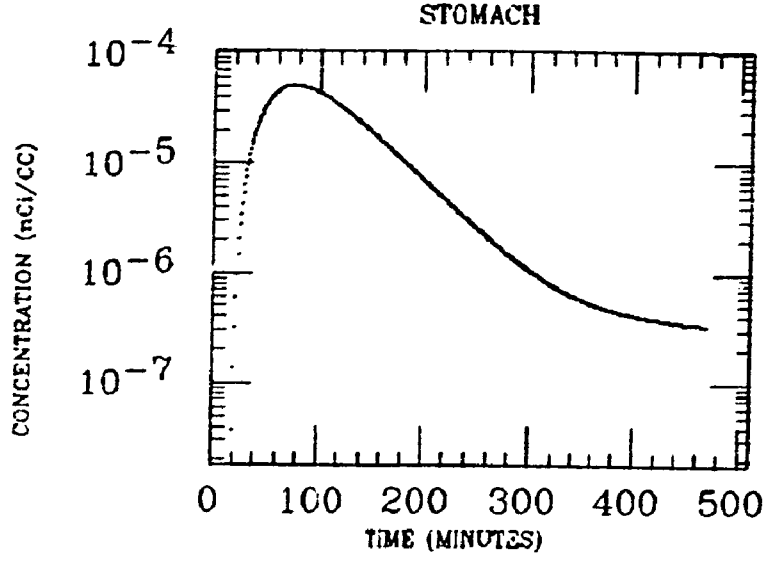

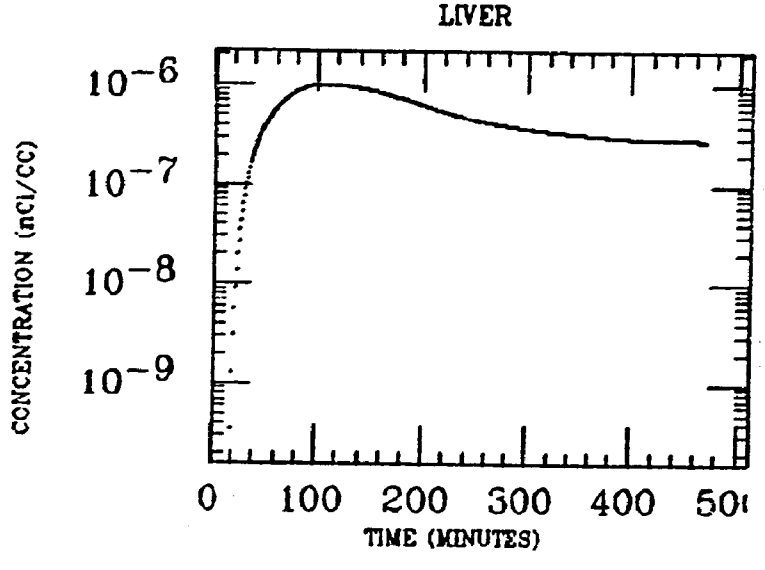

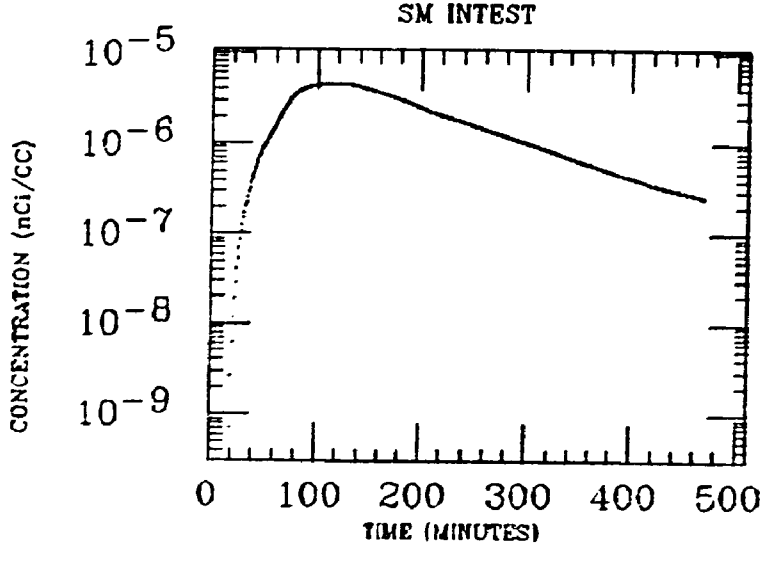

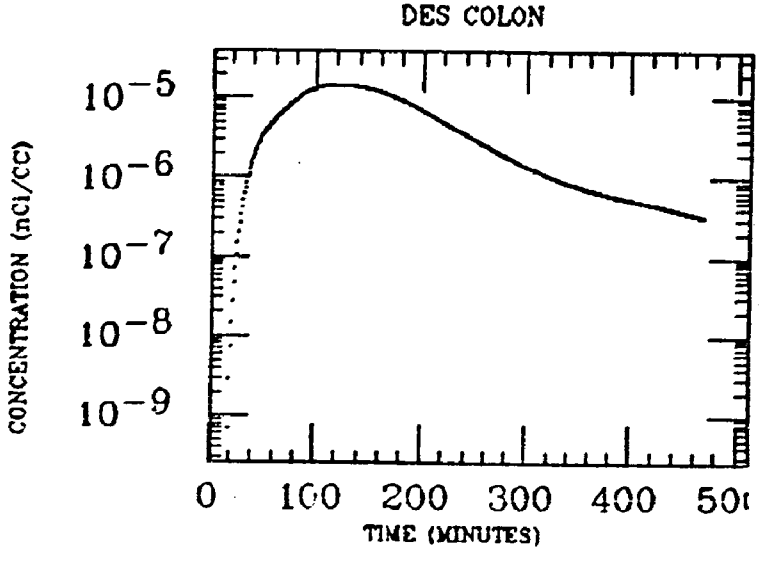

MURCHE
XE INGESTION
Po-214

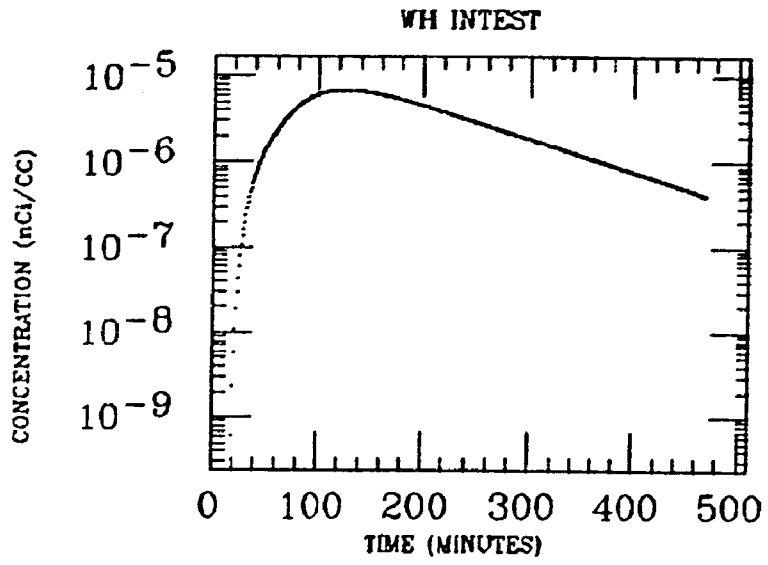

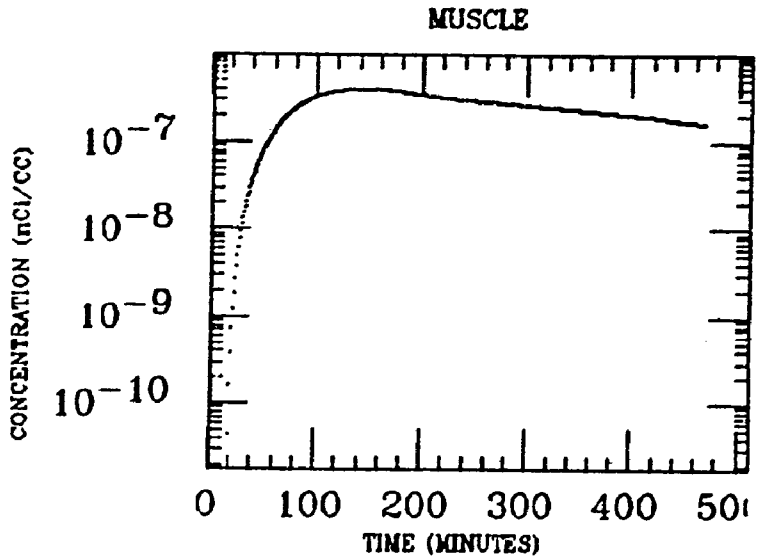

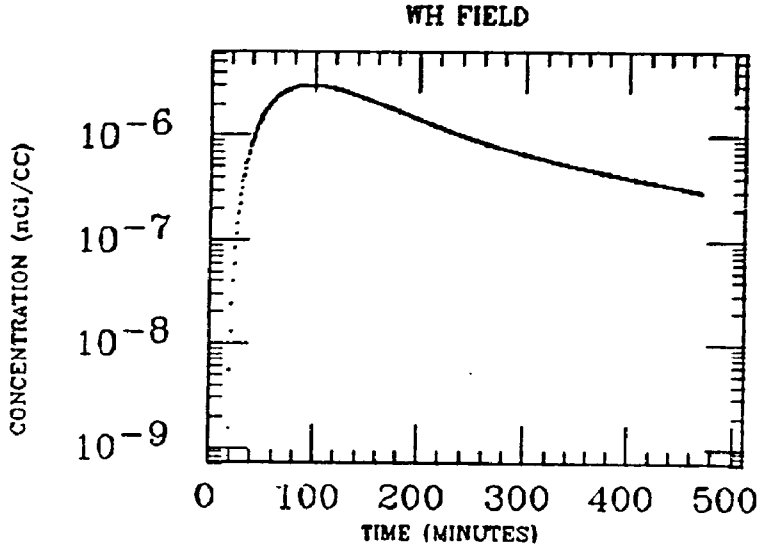

PARK
XE INGESTION
Po-214

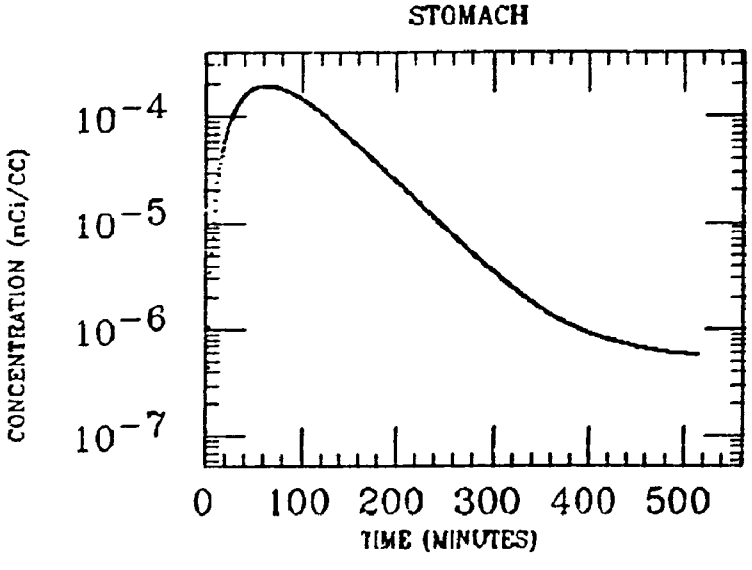

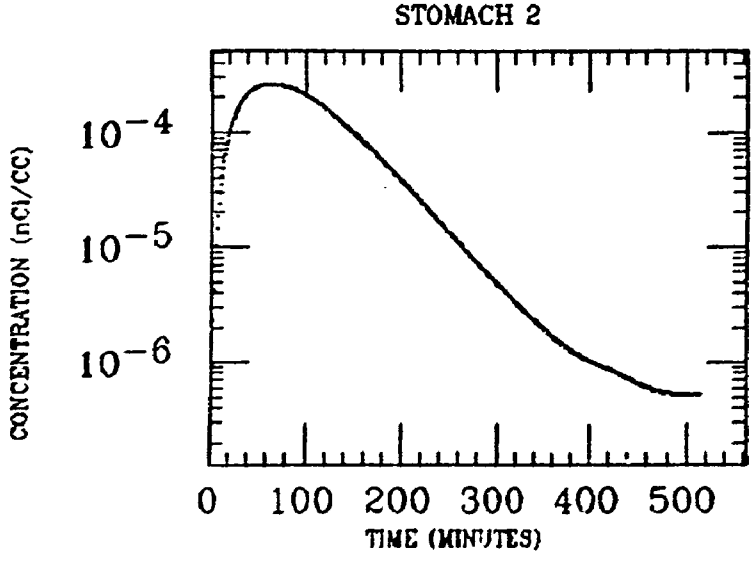

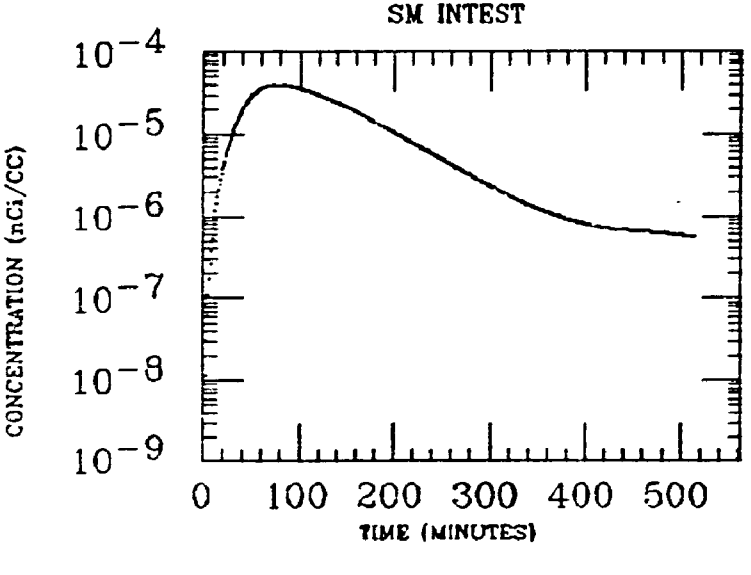

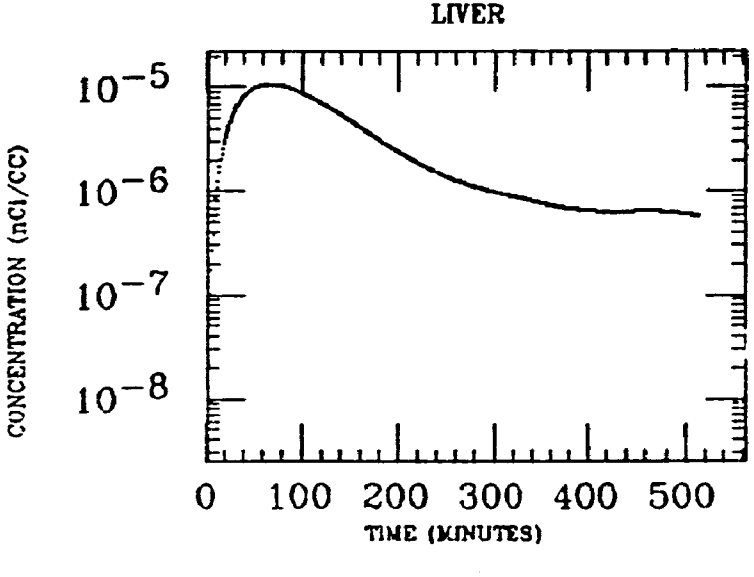

PARK

XE INGESTION

Po-214

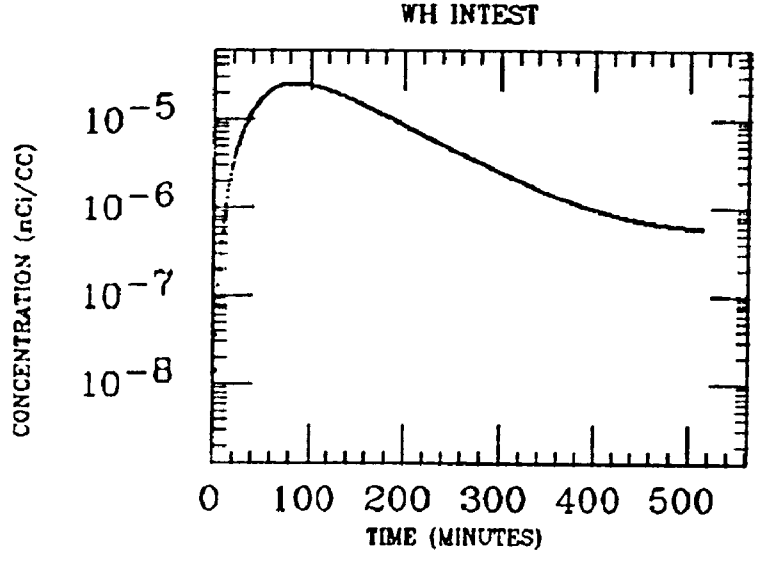

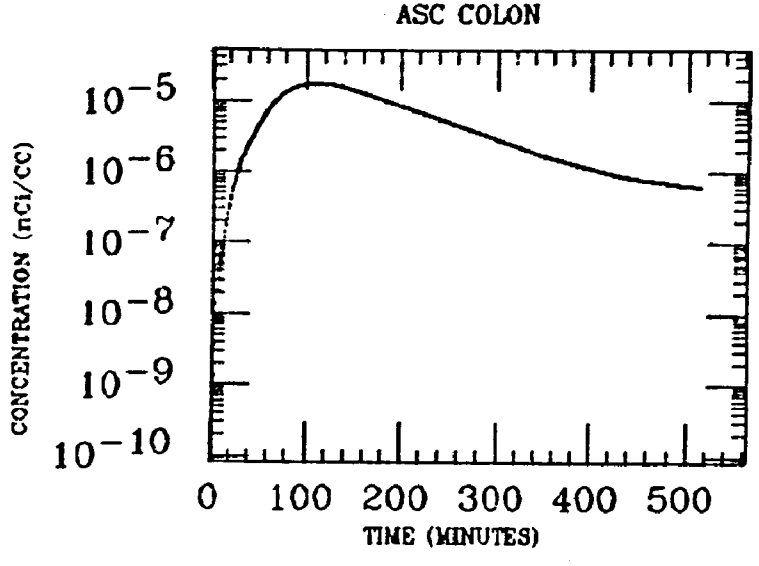

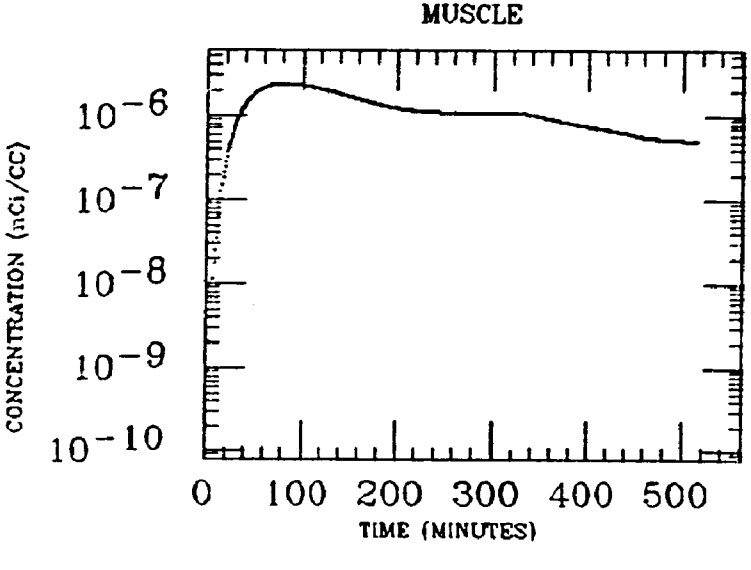

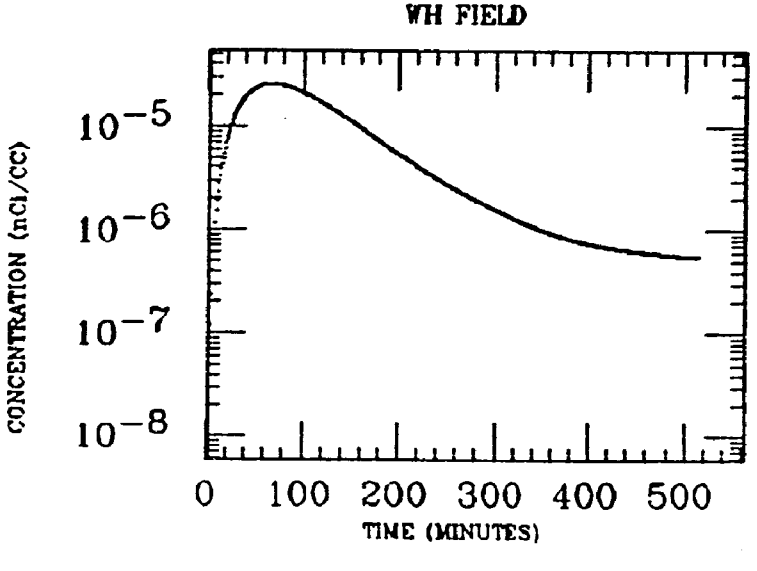

TAATJES
XE INGESTION
Po-214

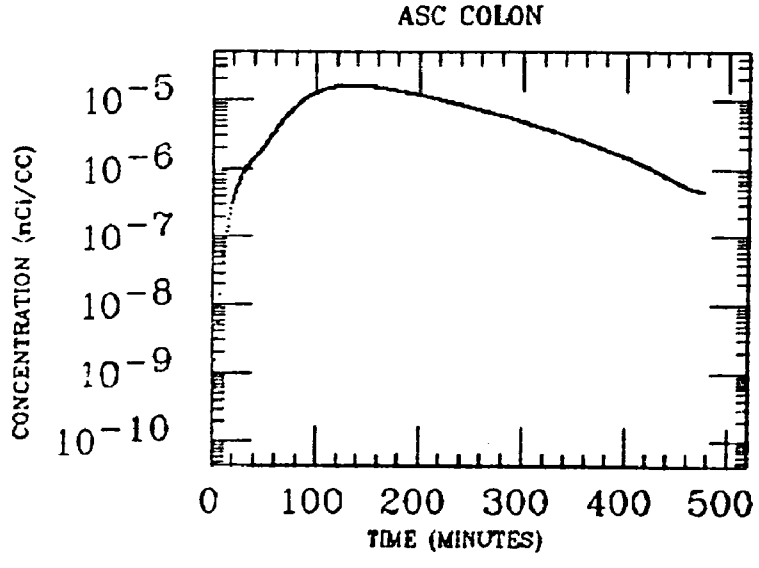

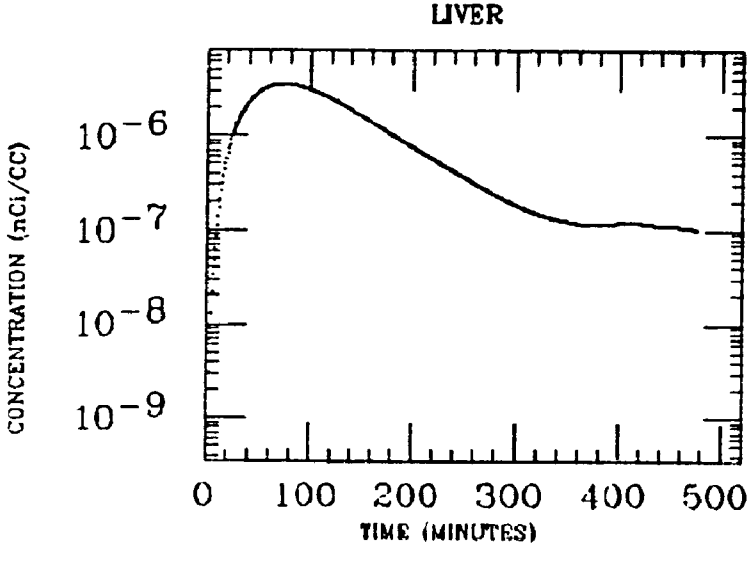

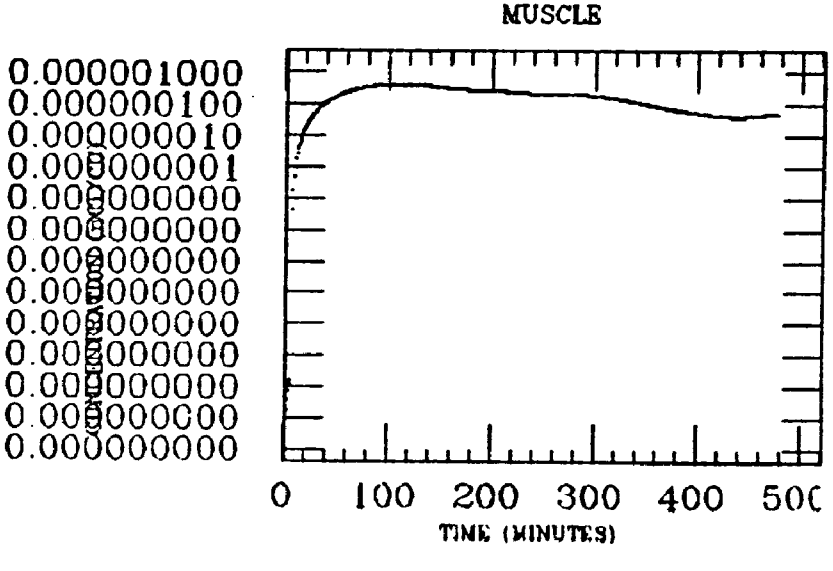

370

TAATJES
XE INGESTION
Po-214

SM INTEST

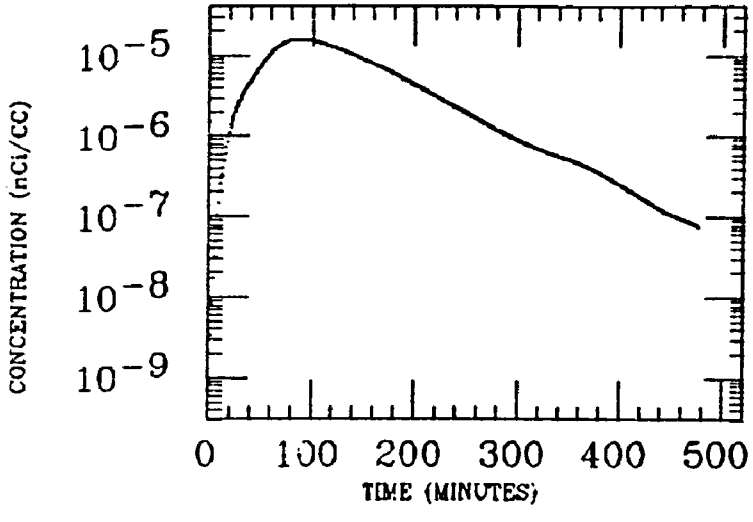

STOMACH

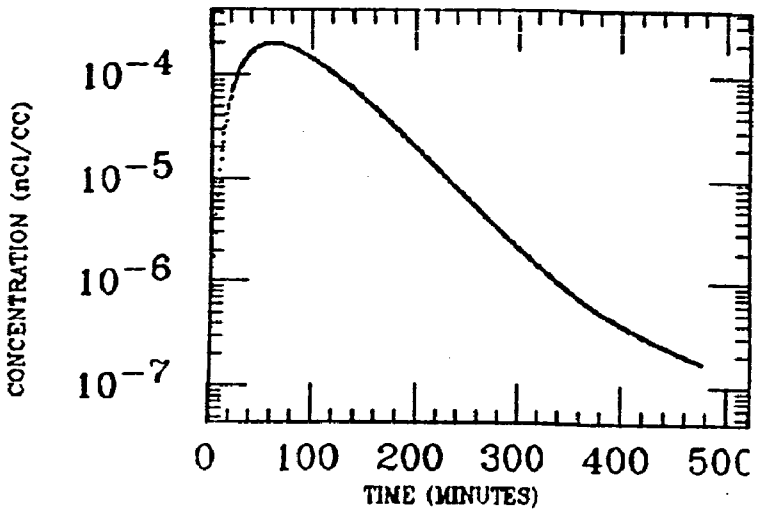

WH FIELD

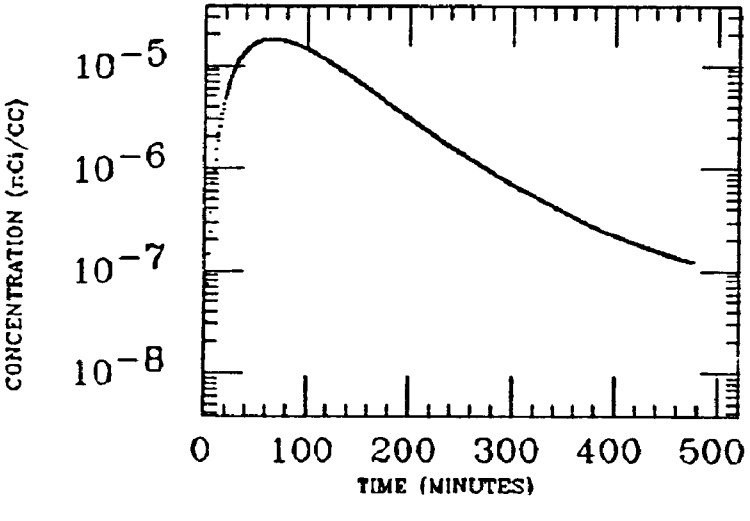

WH INTEST

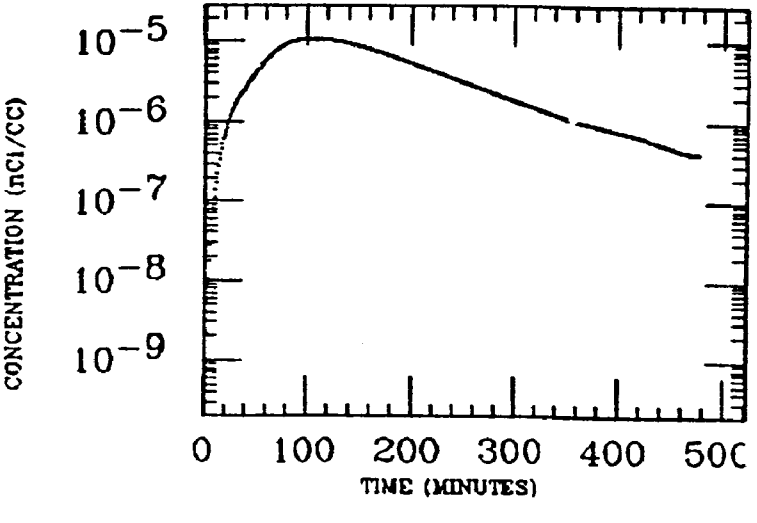

TAYLOR
XE INGESTION
Po-214

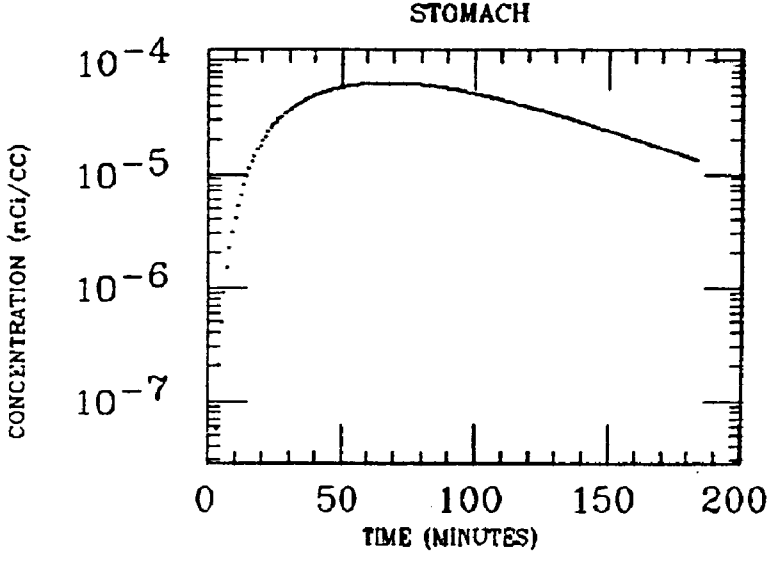

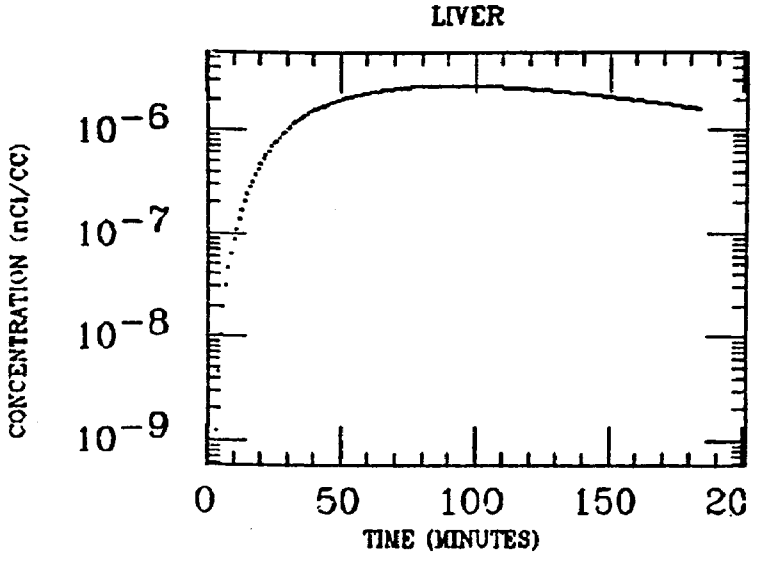

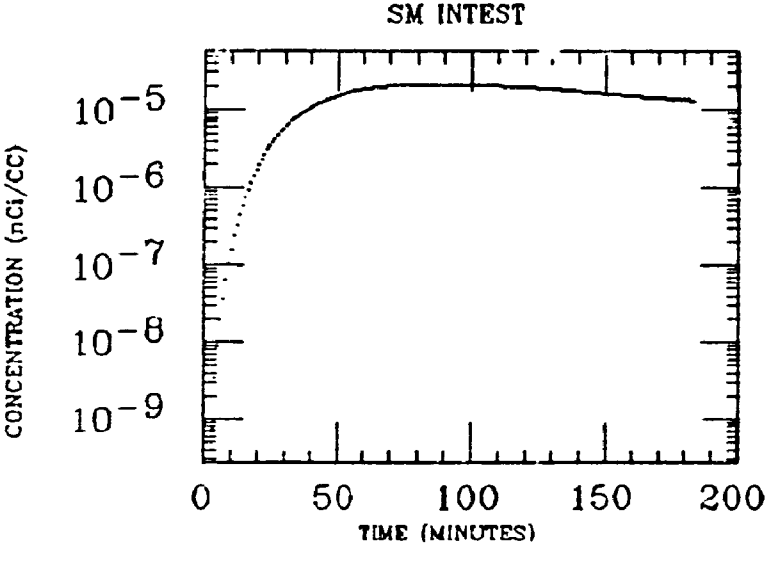

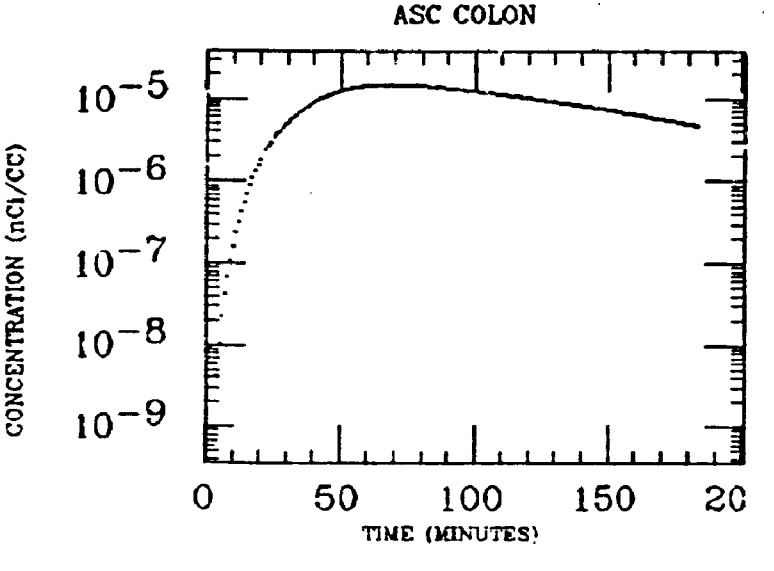

372

TAYLOR
XE INGESTION
Po-214

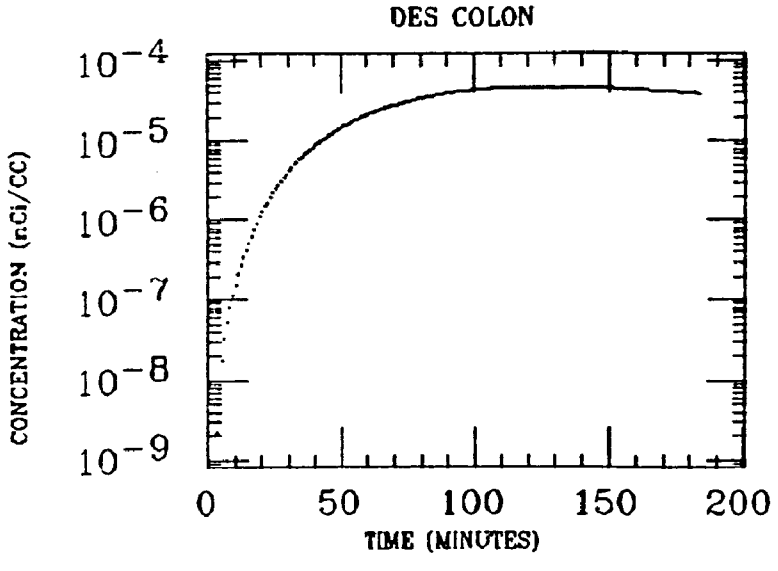

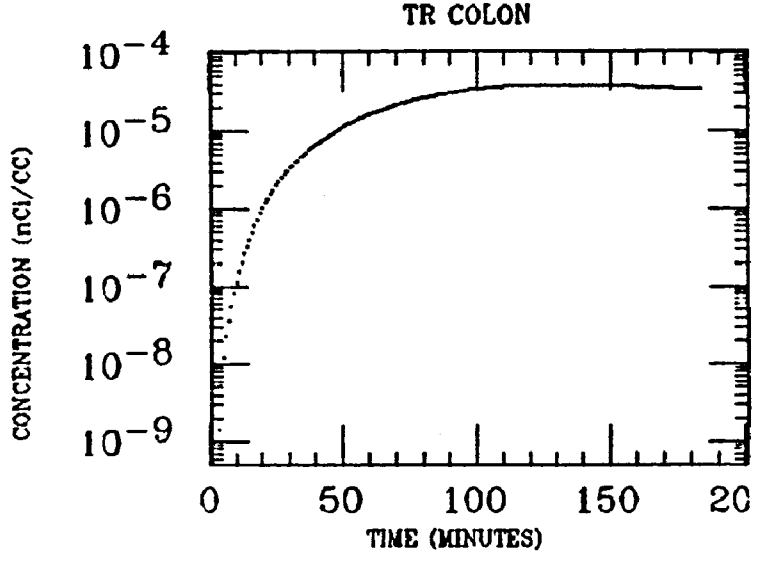

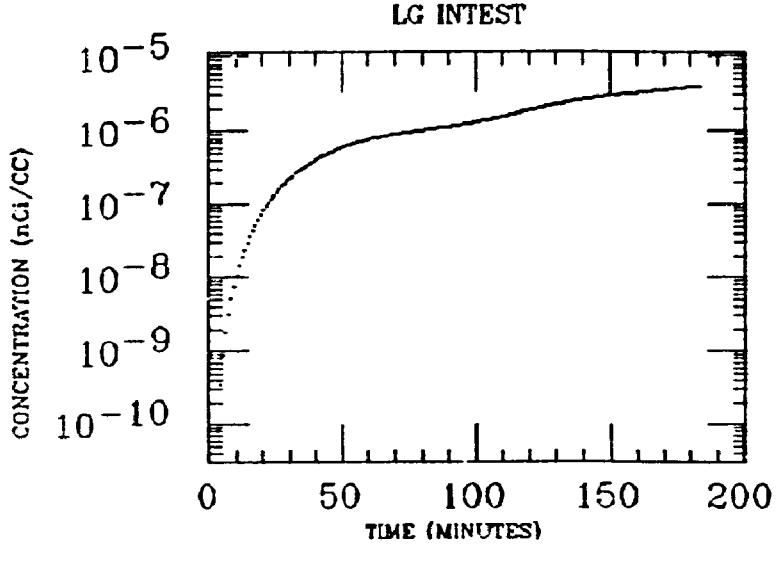

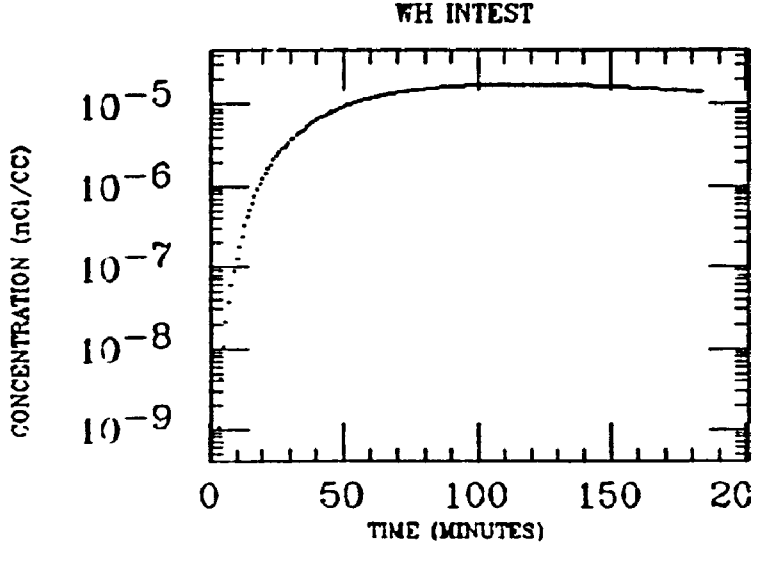

WESOLEK
XE INGESTION
Po-214

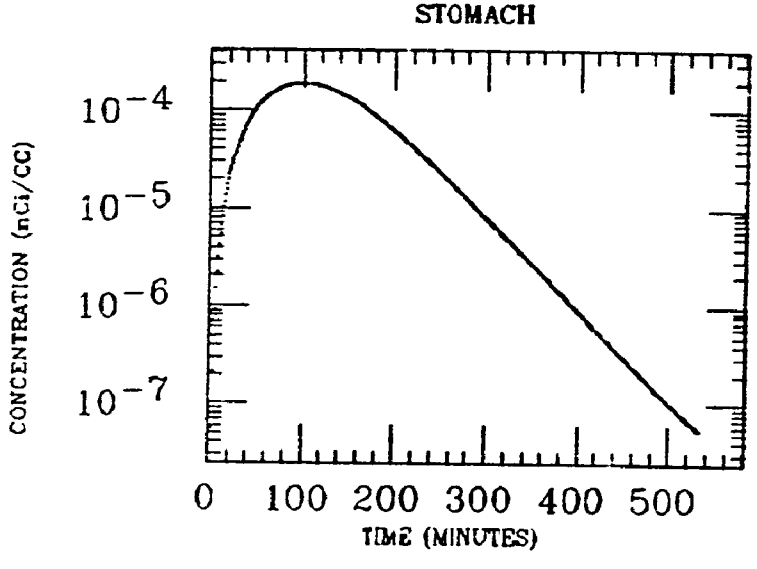

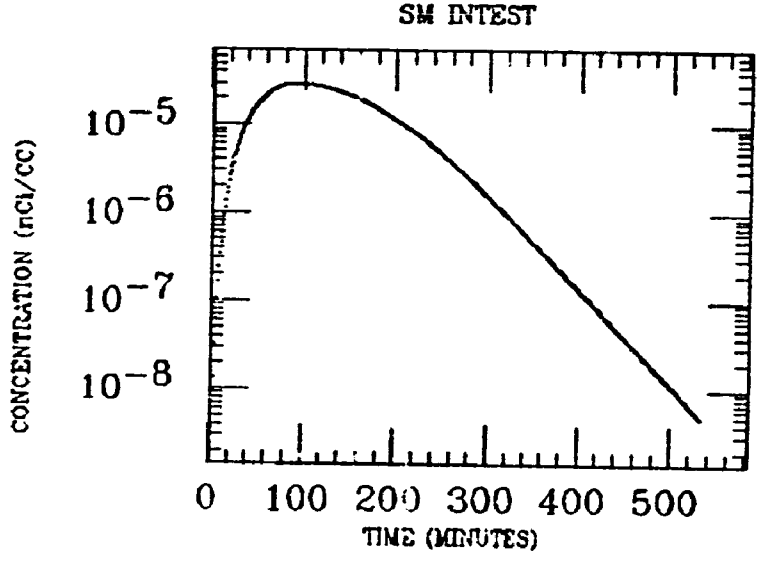

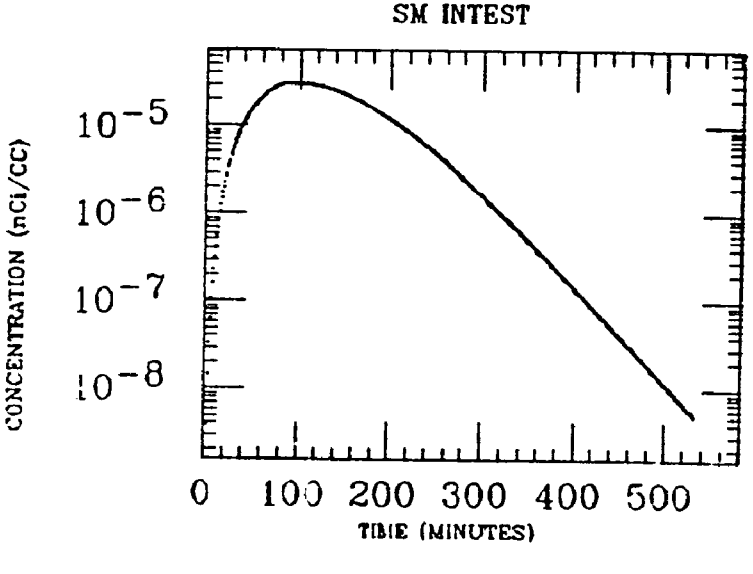

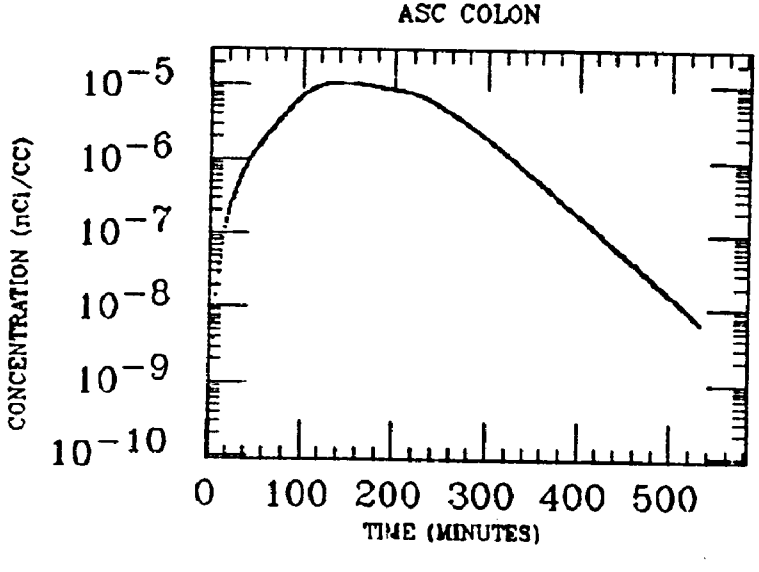

WESOLEK
XE INGESTION
Po-214

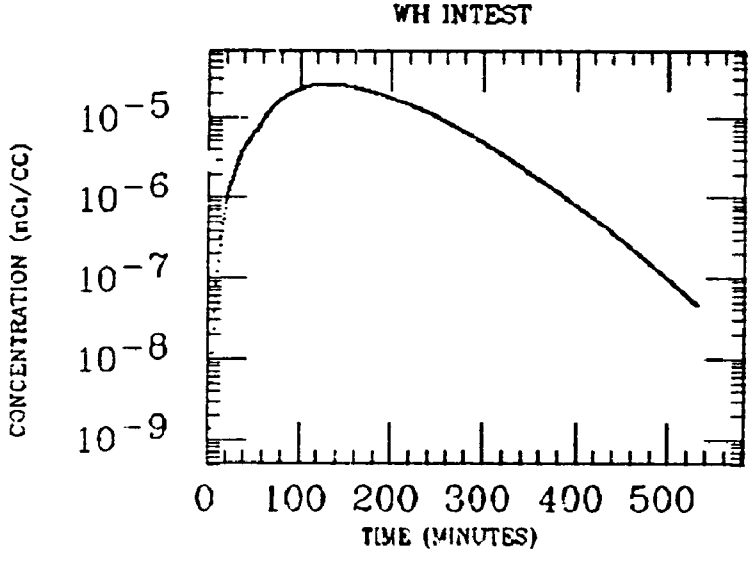

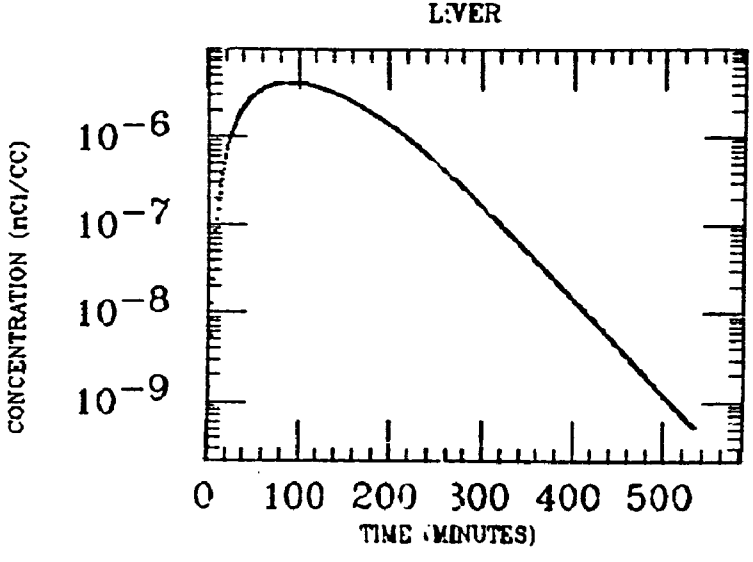

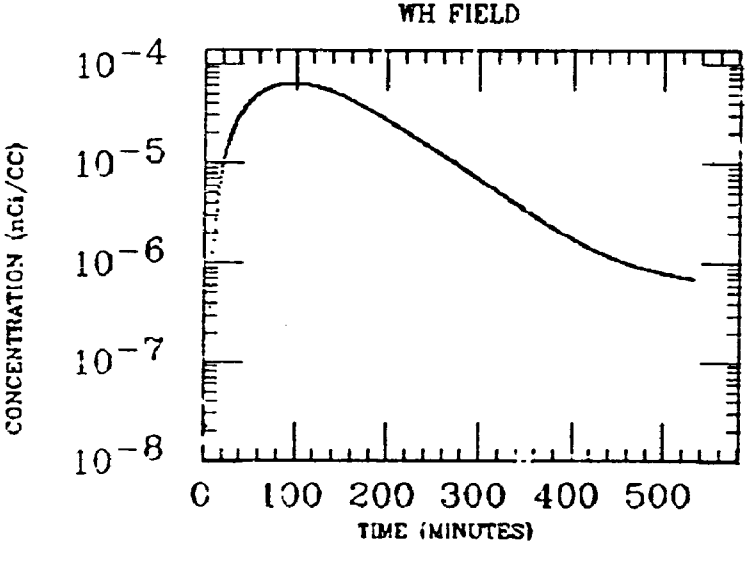

WILTSE
XE INGESTION
Po-214

STOMACH

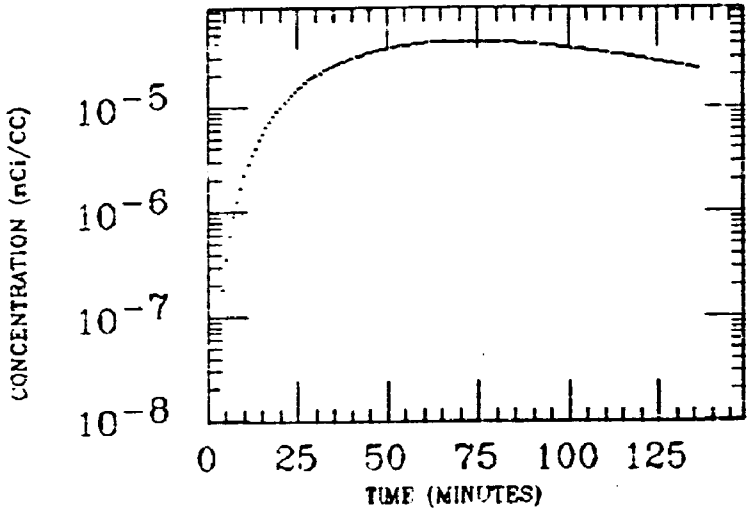

LIVER

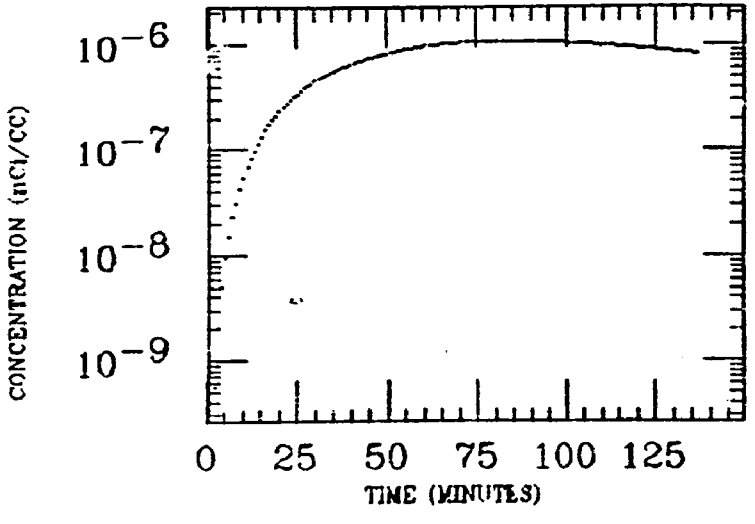

SM INTEST

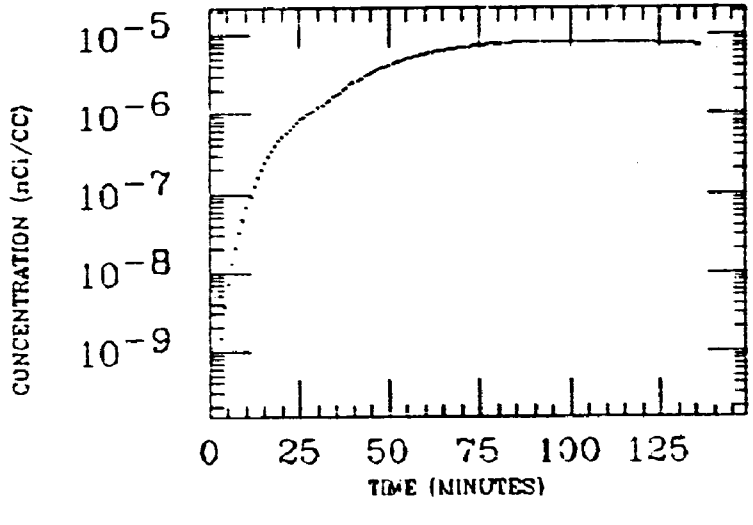

ASC COLON

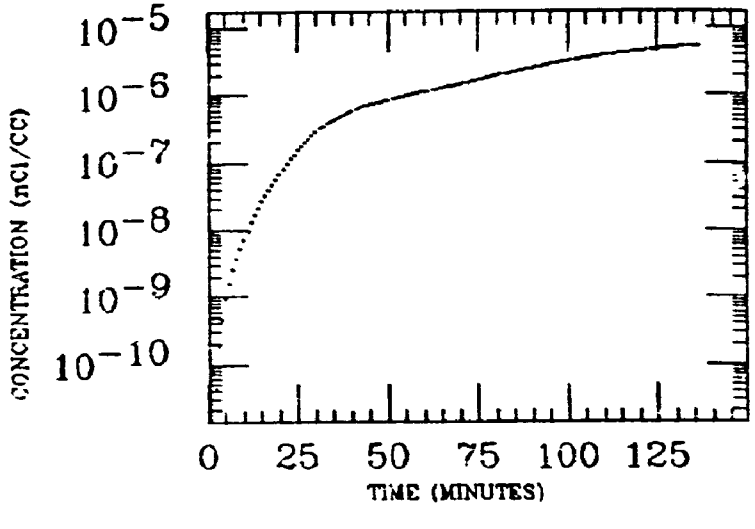

WILTSE
XE INGESTION
Po-214

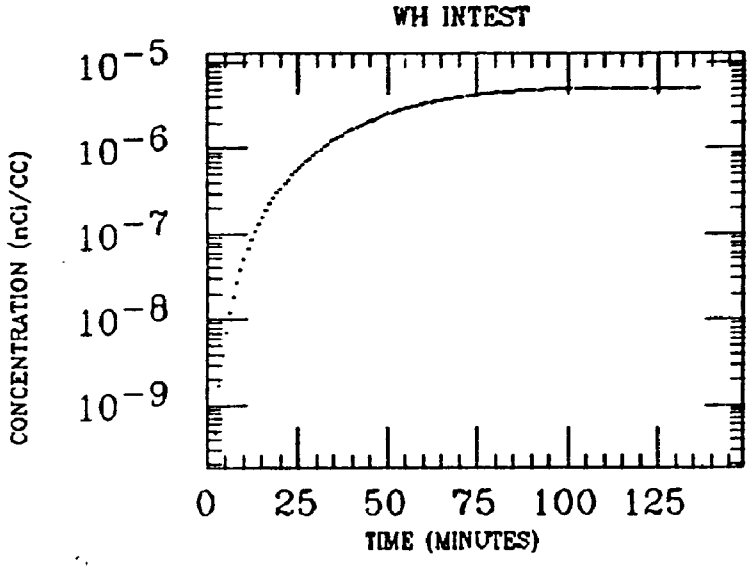

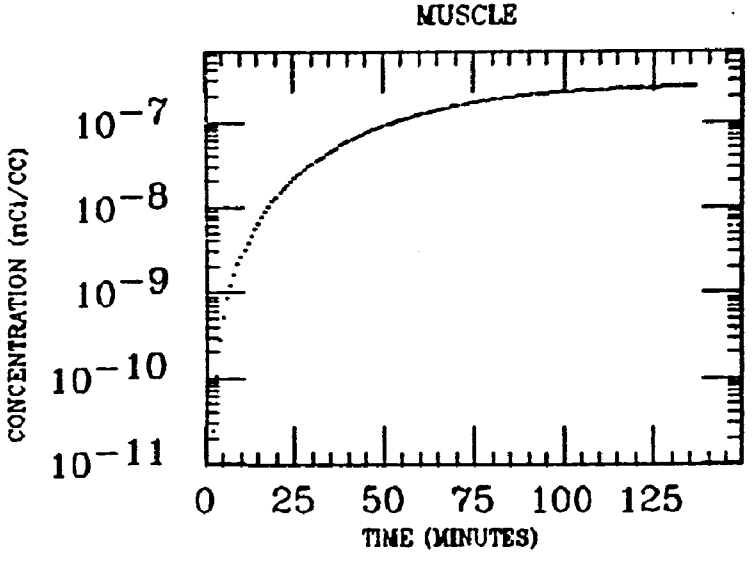

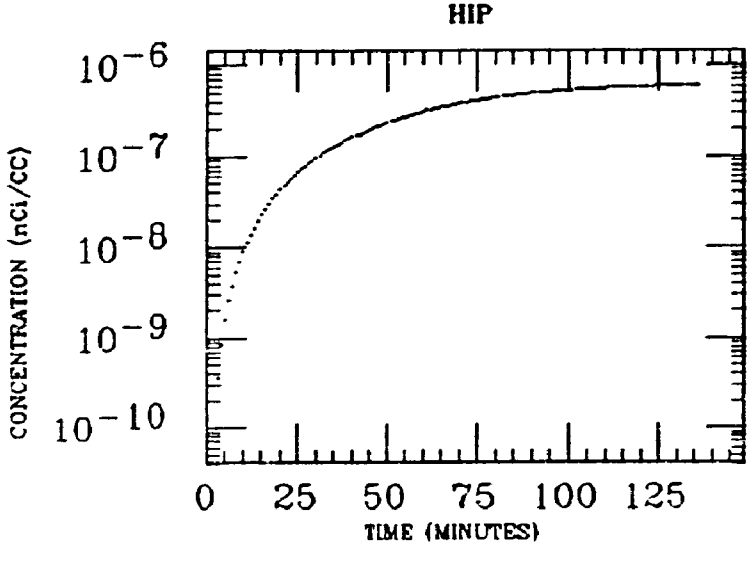

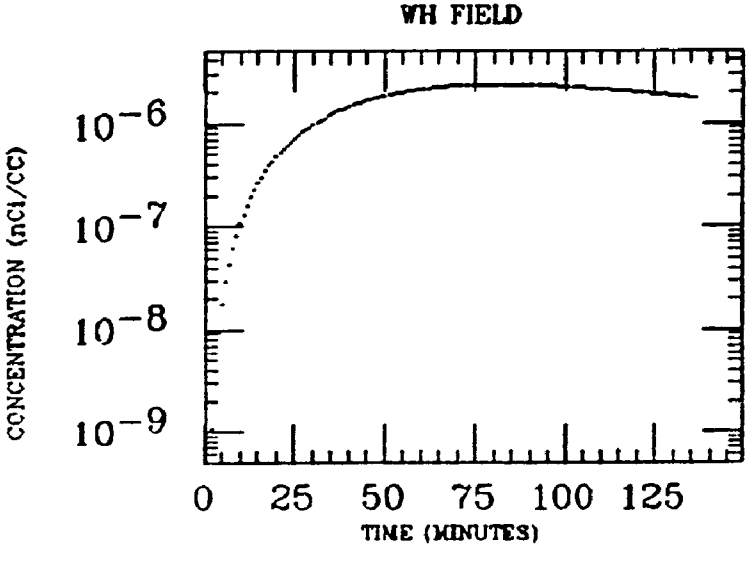

AHERN

XE INGESTION

Pb-210

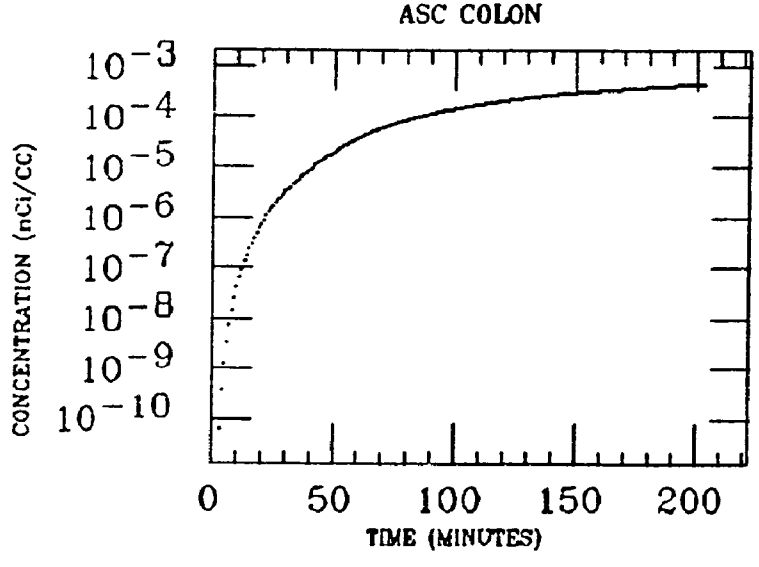

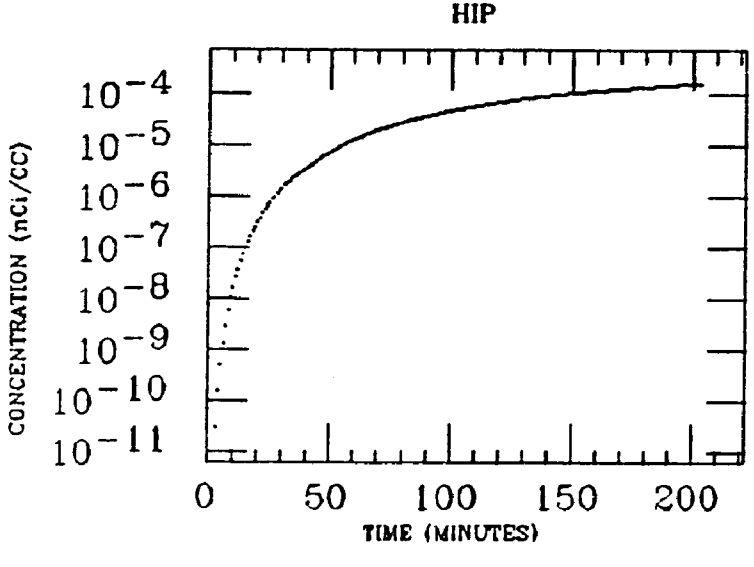

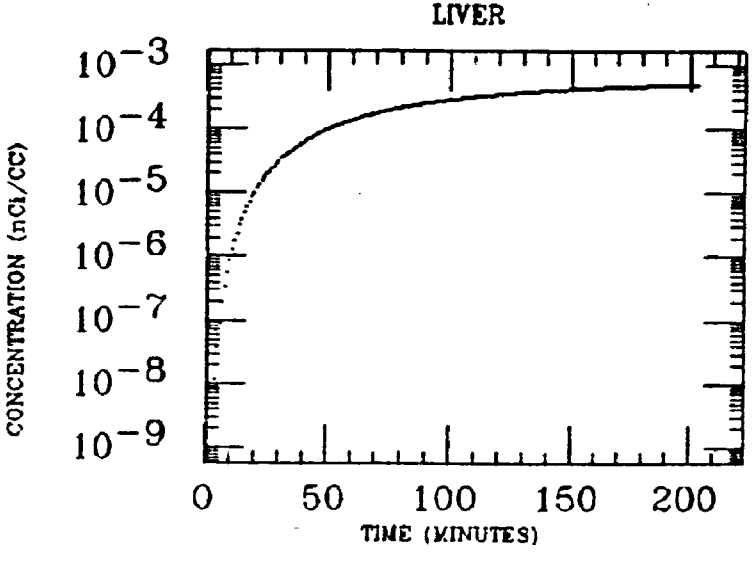

AHERN
XE INGESTION
Pb-210

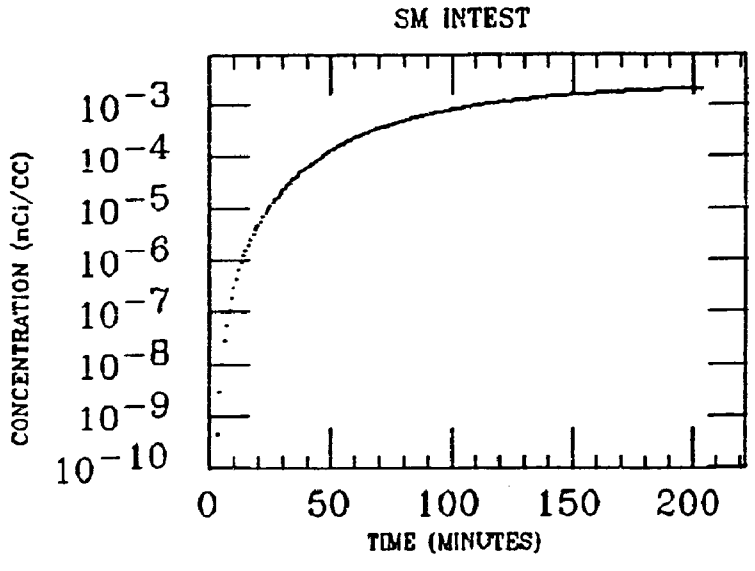

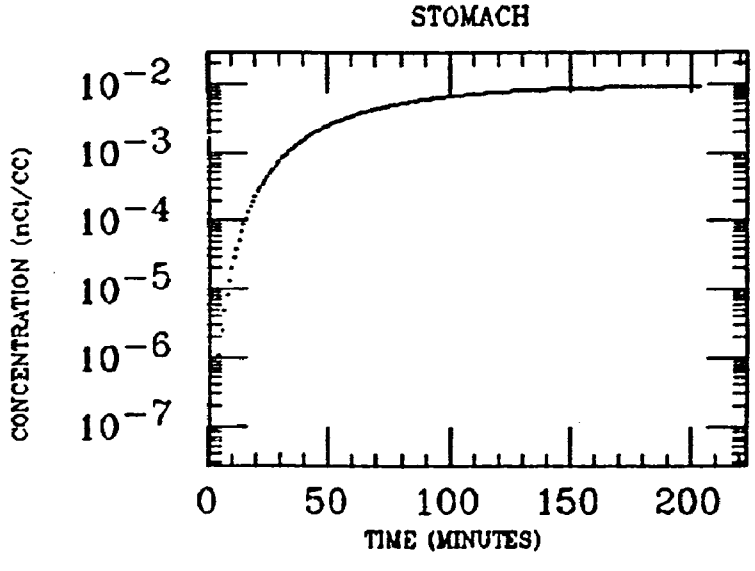

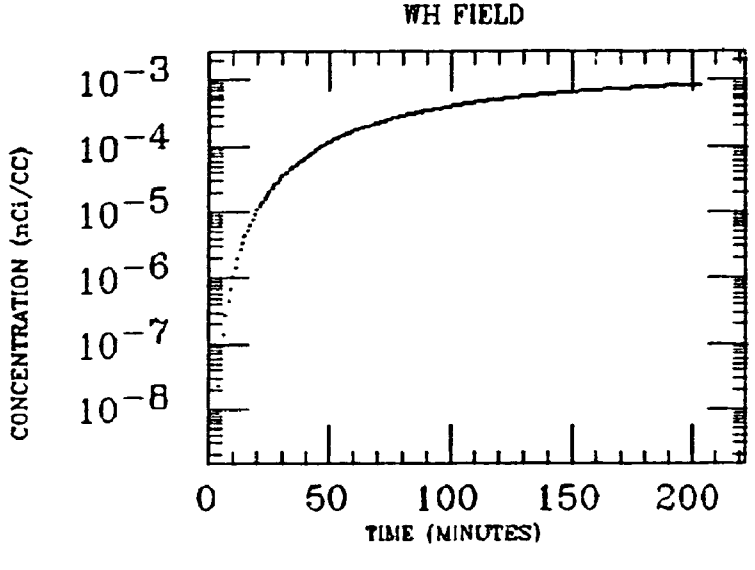

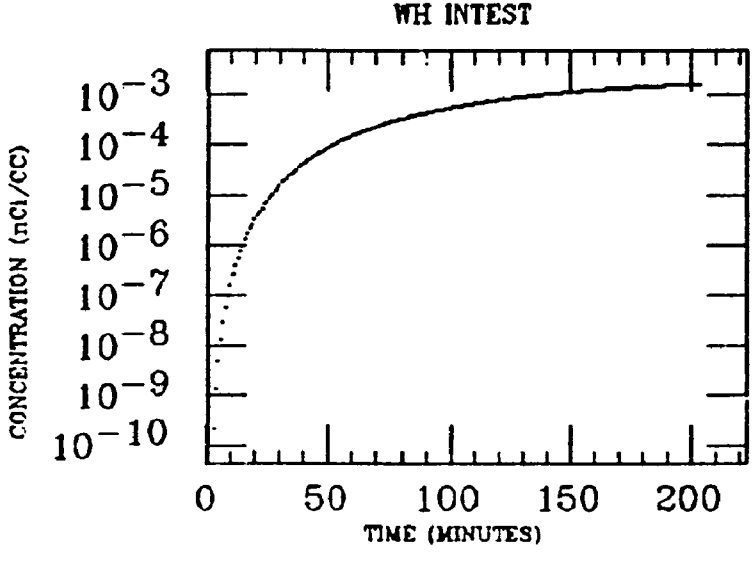

ARROL
XE INGESTION
Pb-210

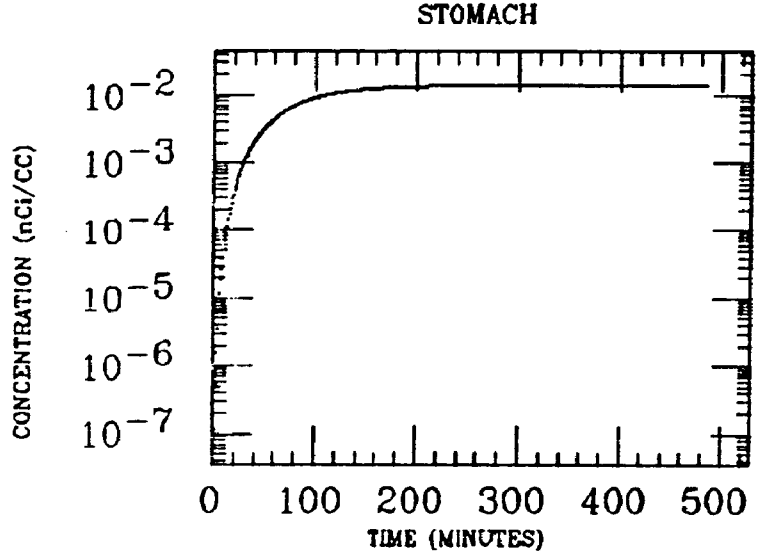

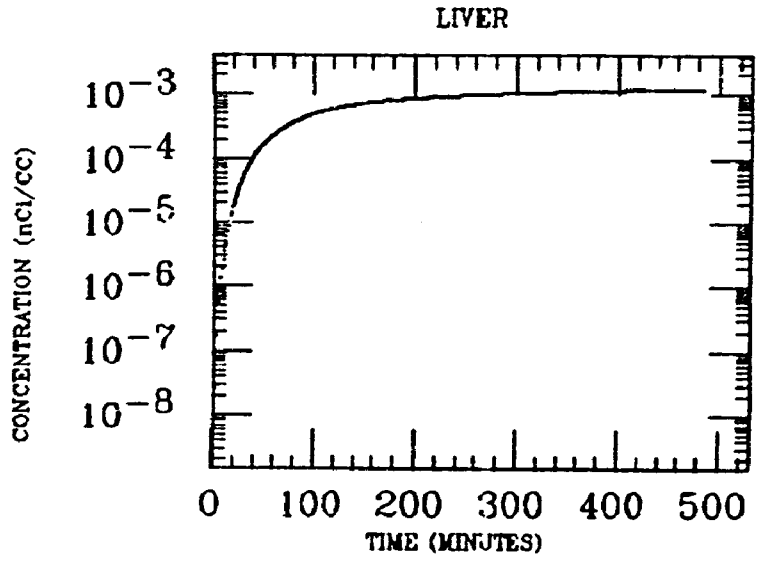

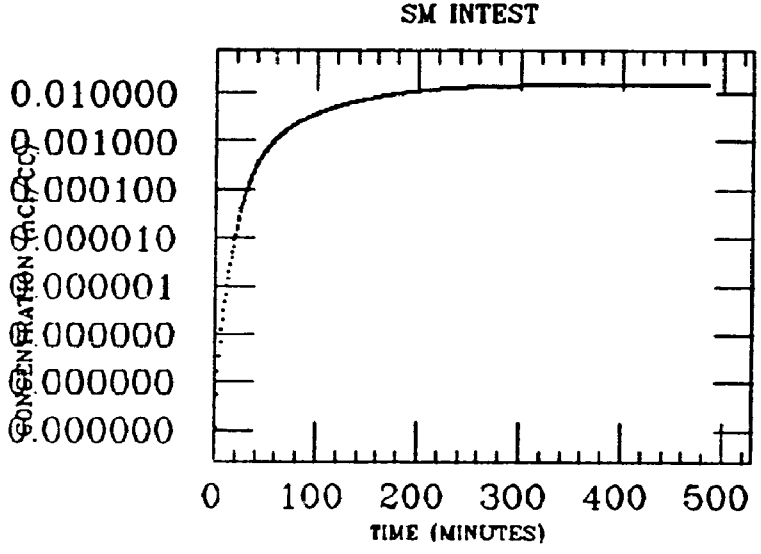

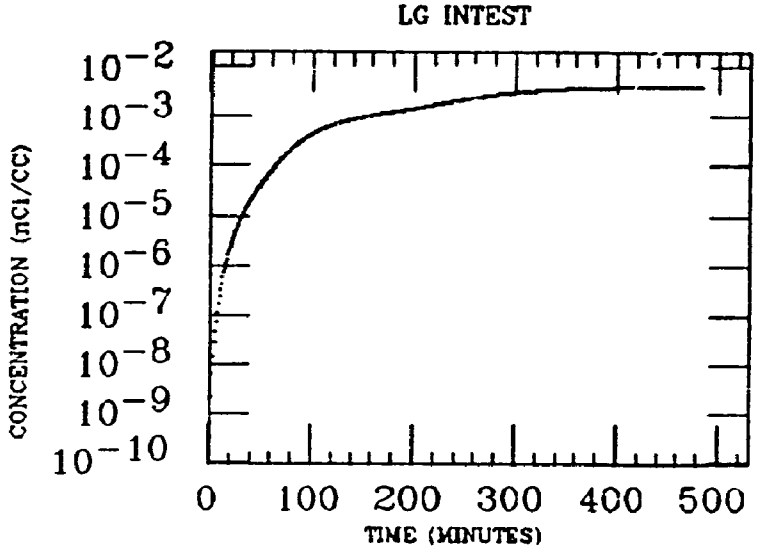

ARROL
XE INGESTION
Pb-210

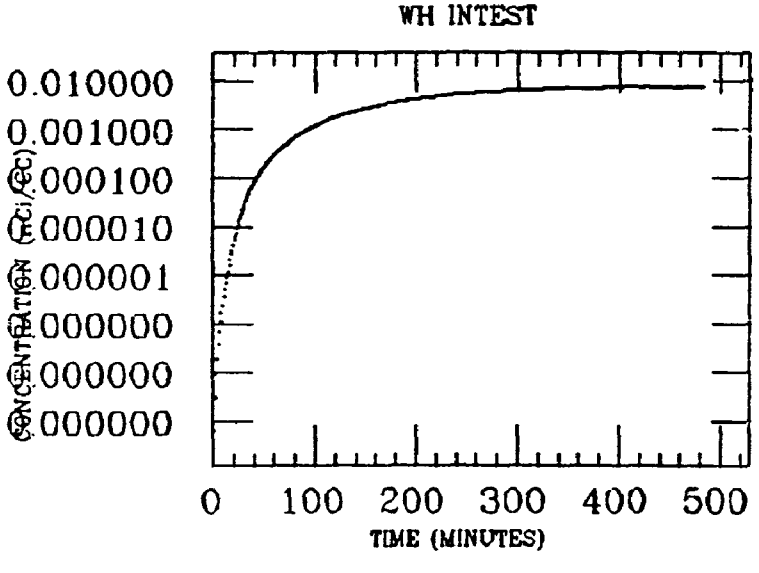

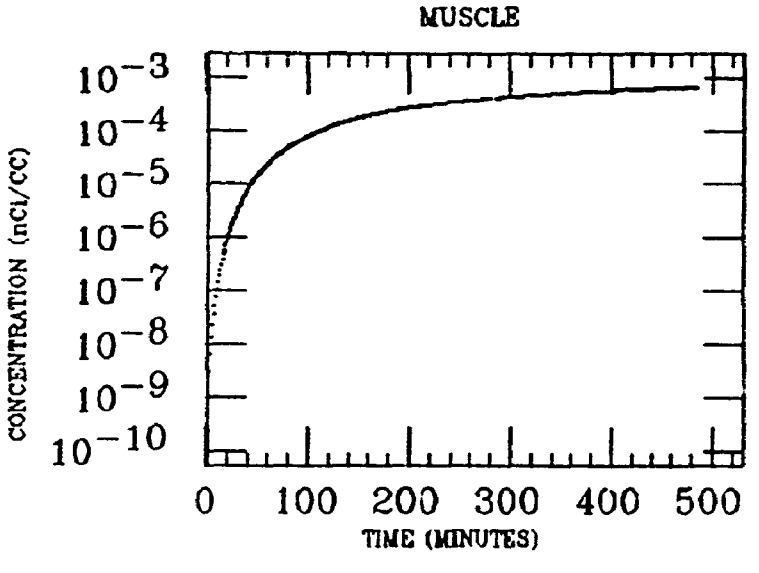

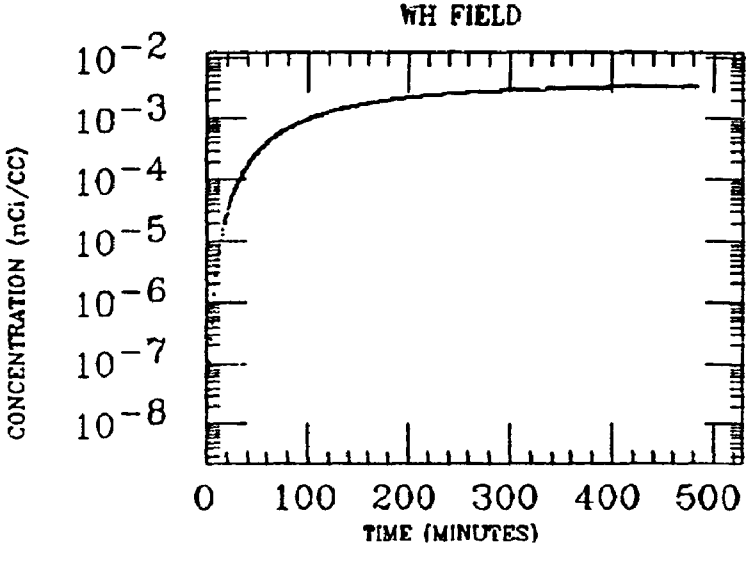

AYER

XE INGESTION

Pb-210

STOMACH

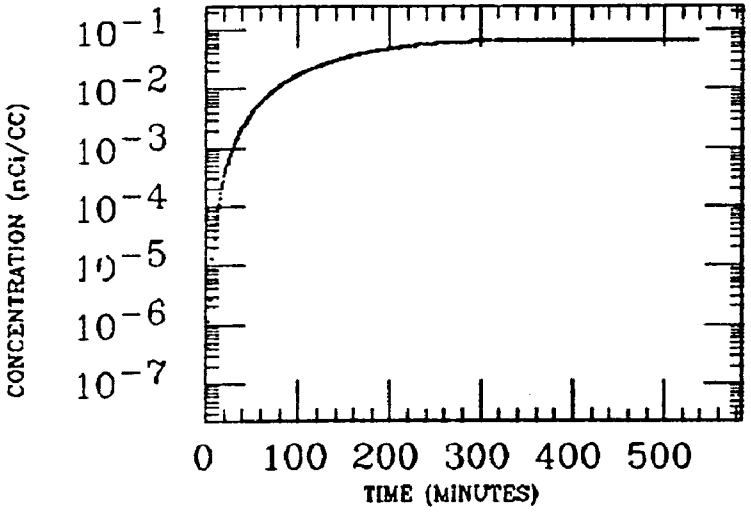

LIVER

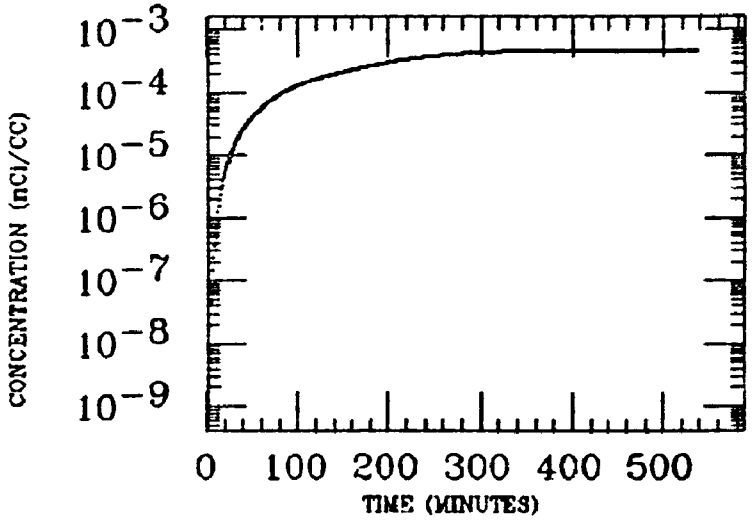

WH FIELD

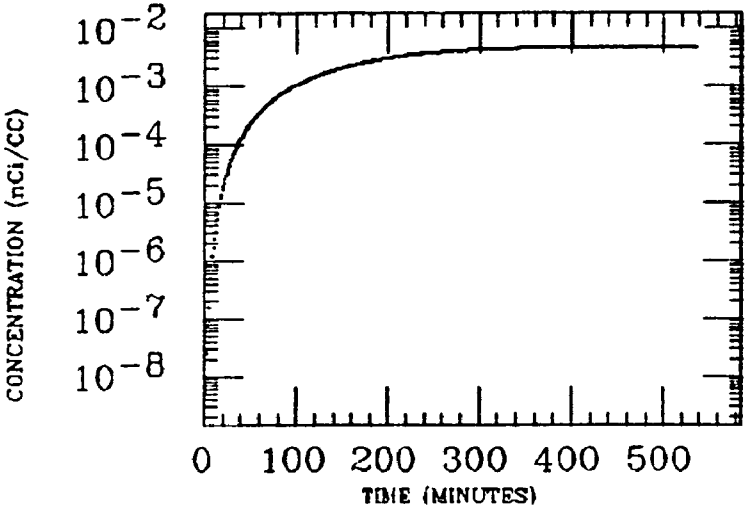

AYER

XE INGESTION

Pb-210

ASC COLON

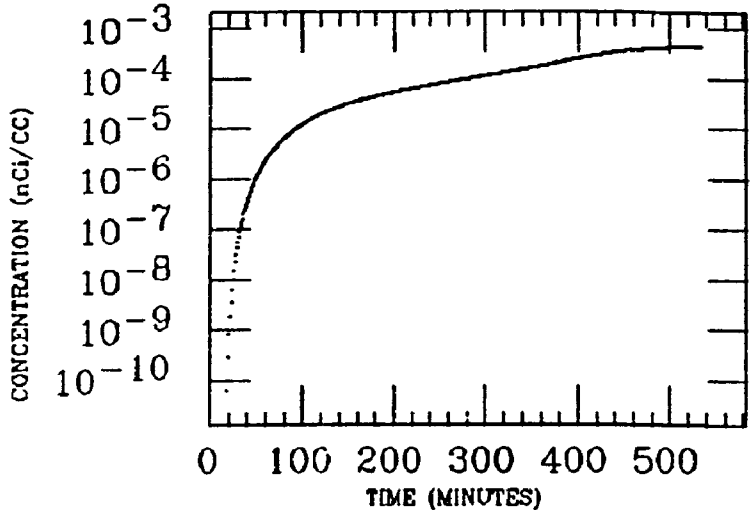

DES COLON

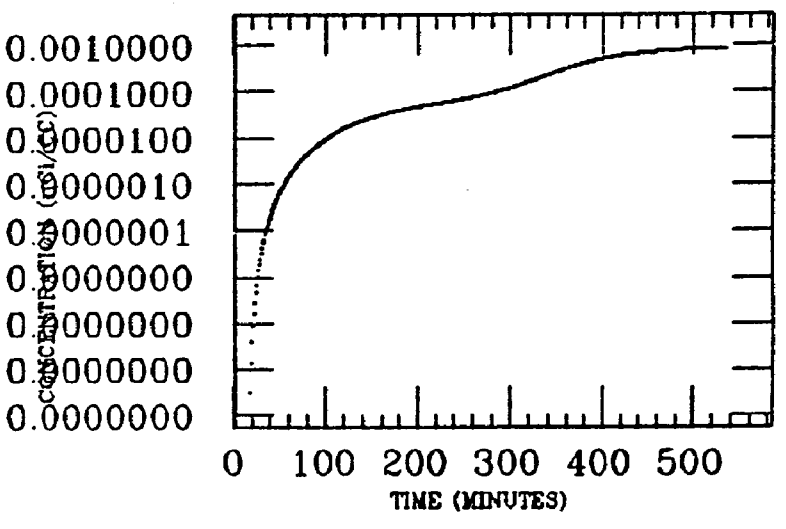

LIVER

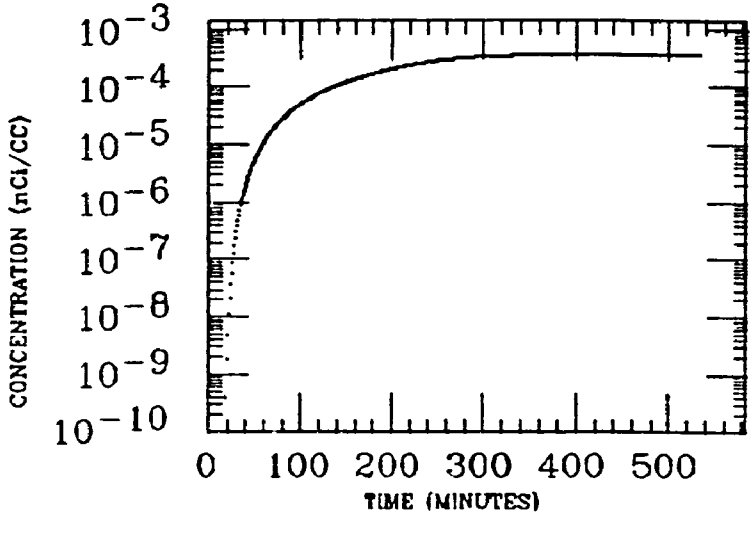

SM INTEST

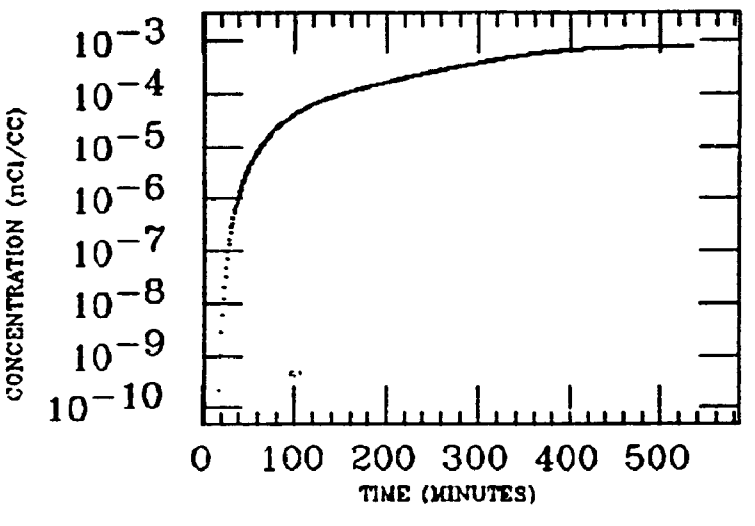

AYER

XE INGESTION

Pb-210

STOMACH

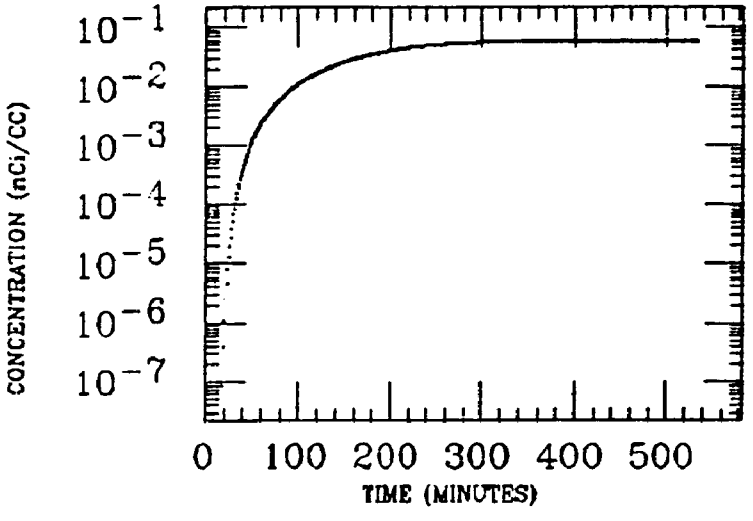

TR COLON

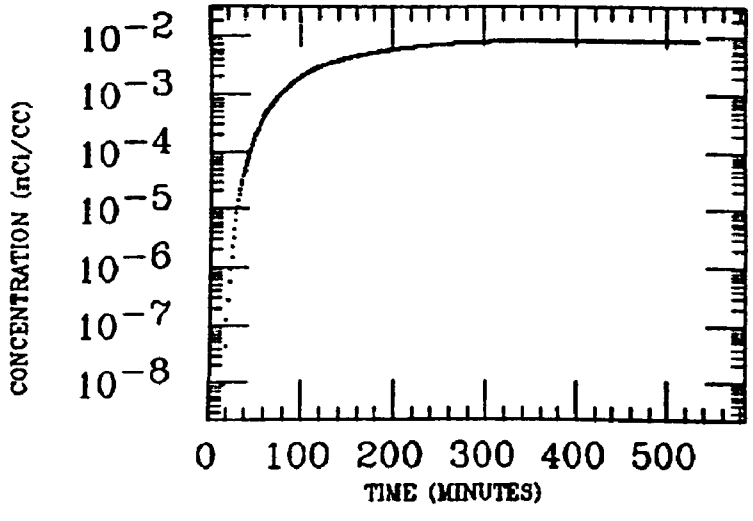

WH FIELD

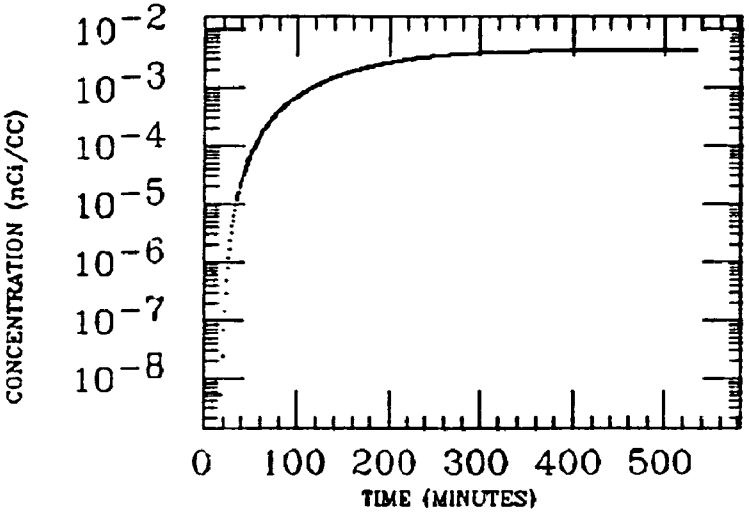

WH INTEST

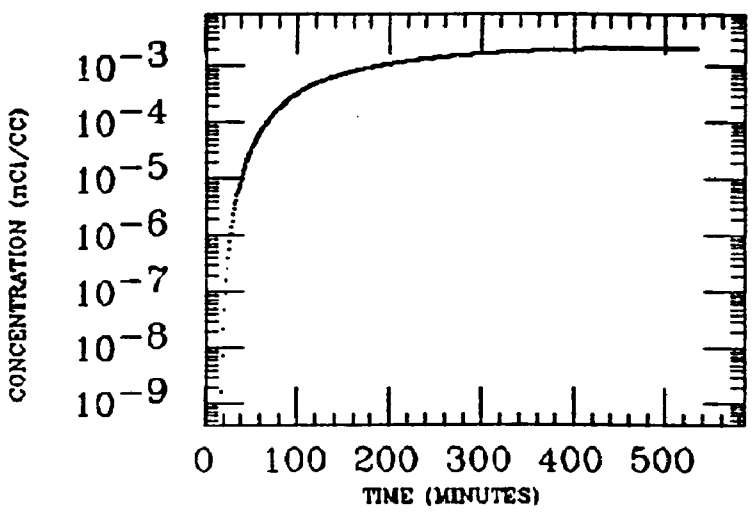

BROCK
XE INGESTION
Pb-210

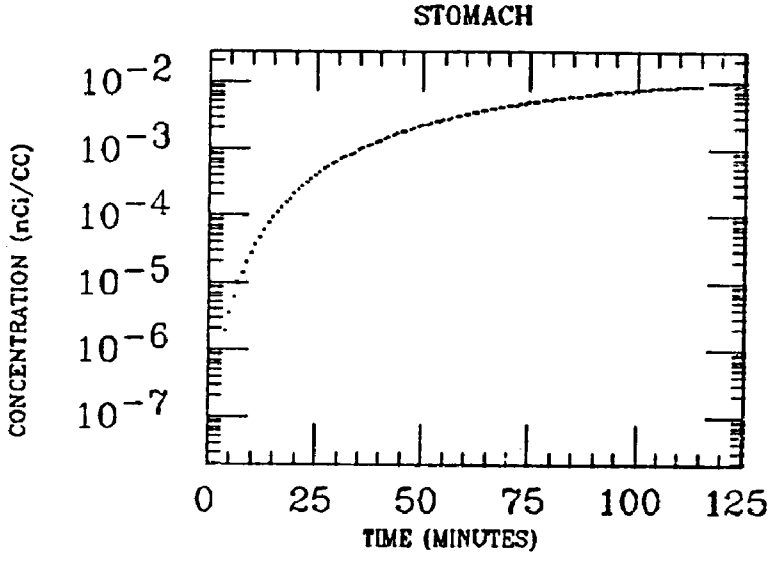

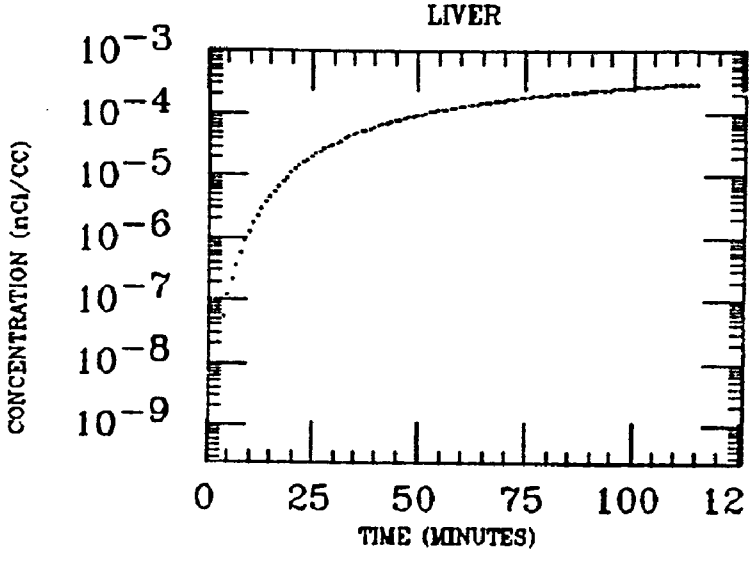

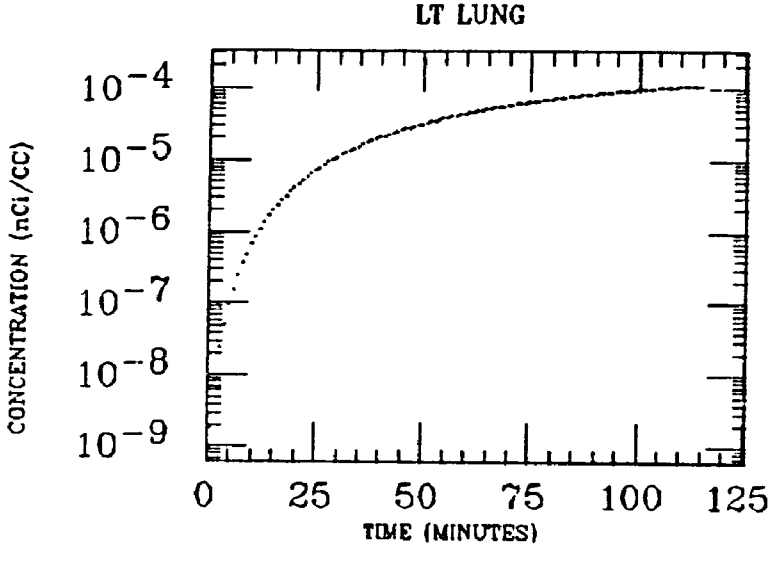

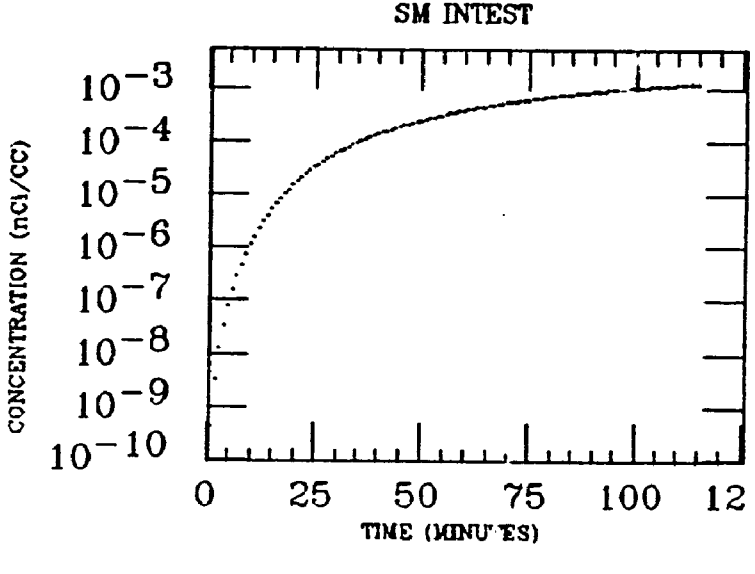

BROCK
XE INGESTION
Pb-210

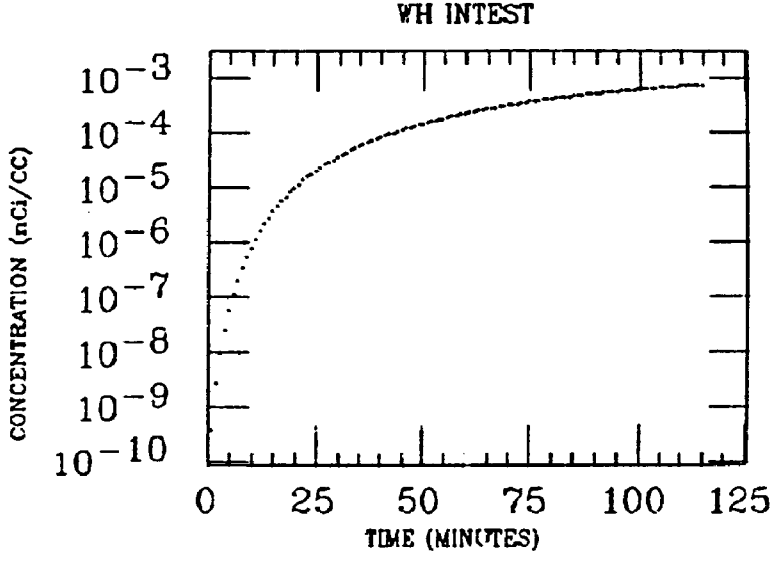

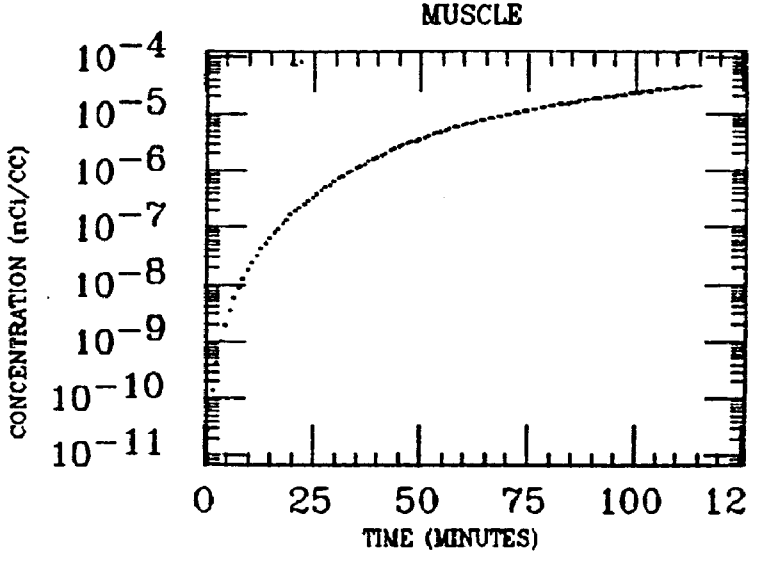

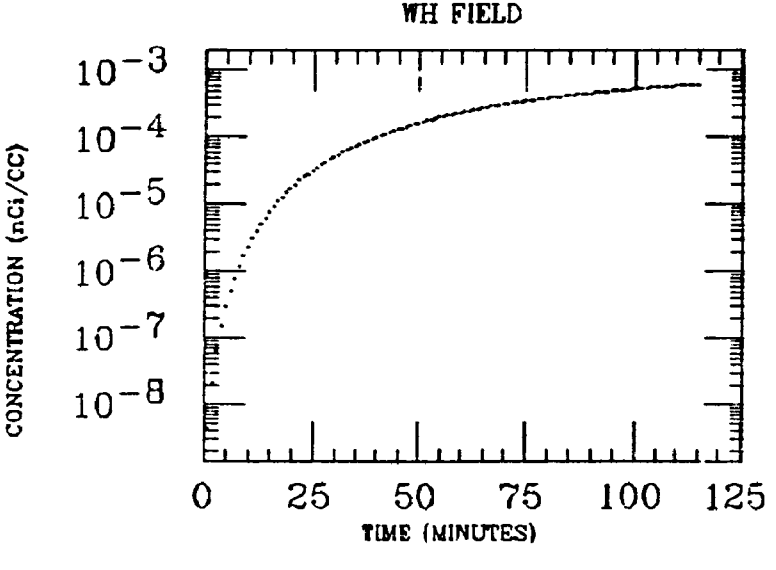

BYRNE
XE INGESTION
Pb-210

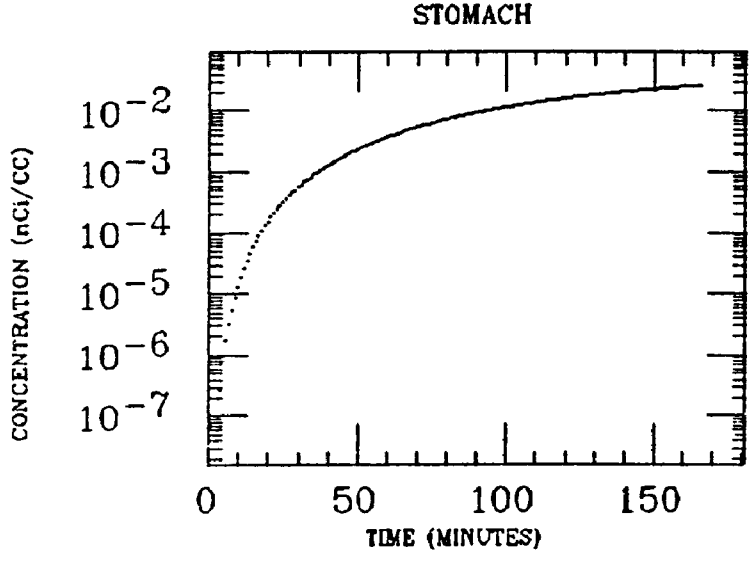

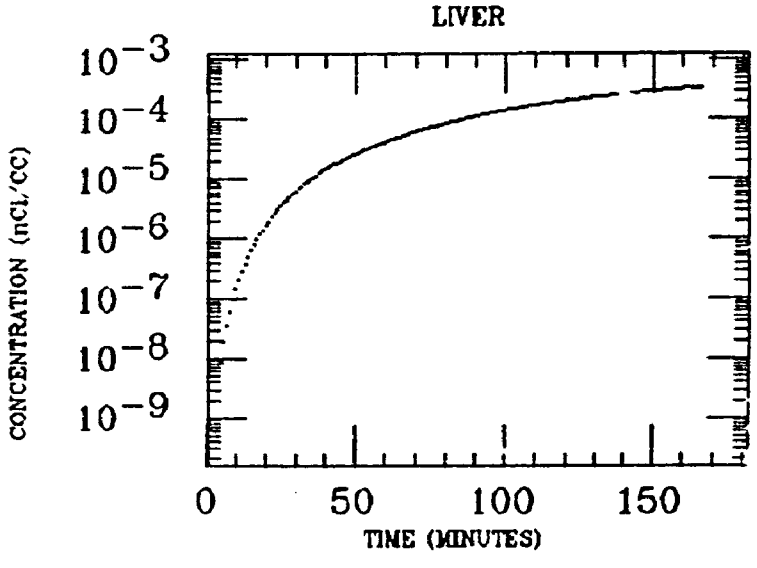

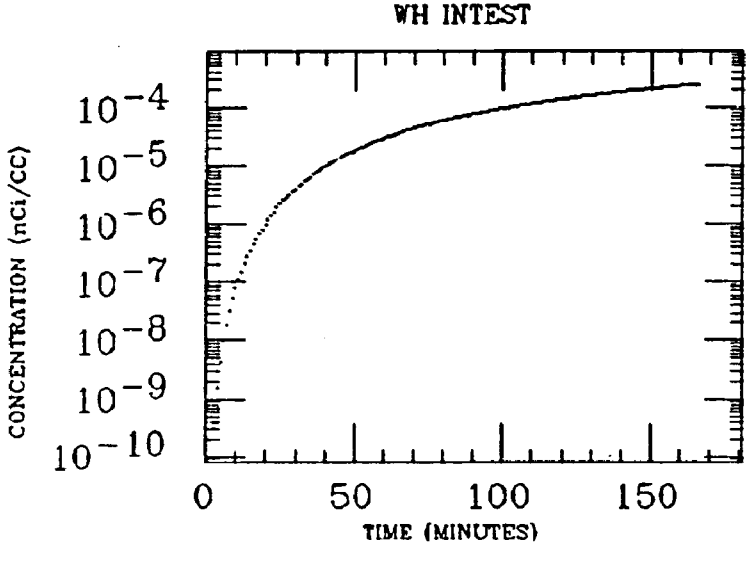

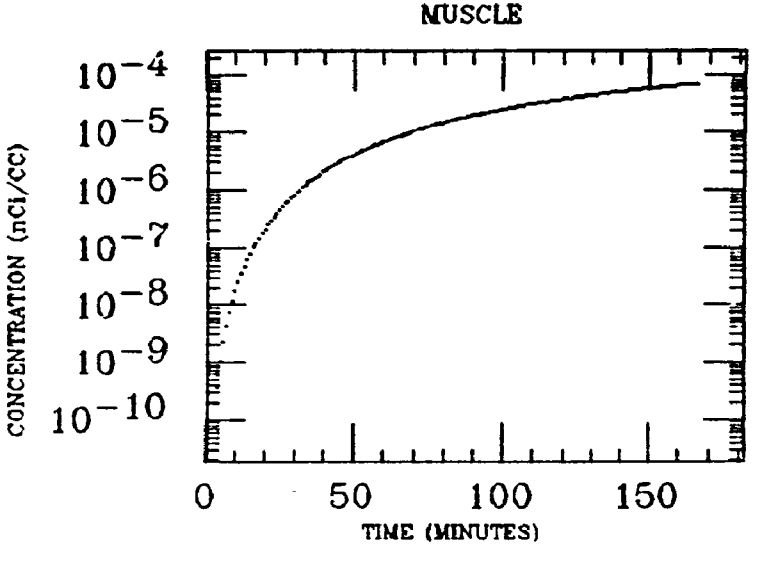

BYRNE
XE INGESTION
Pb-210

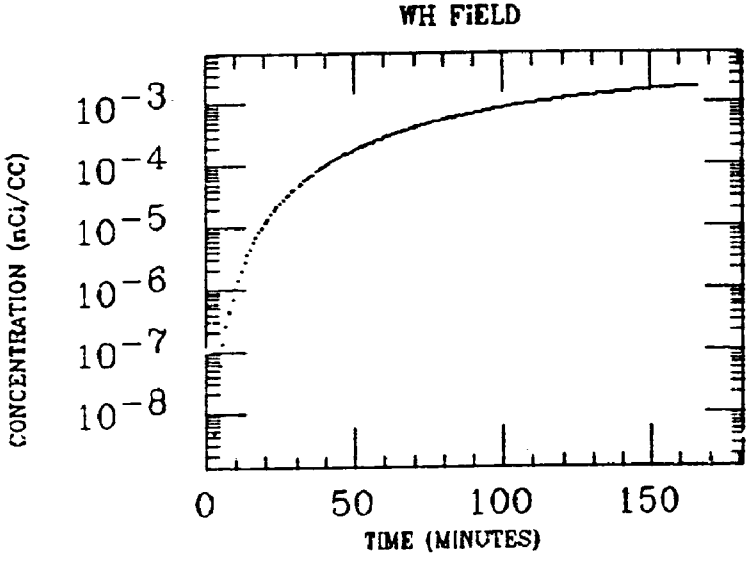

CLINE
XE INGESTION
Pb-210

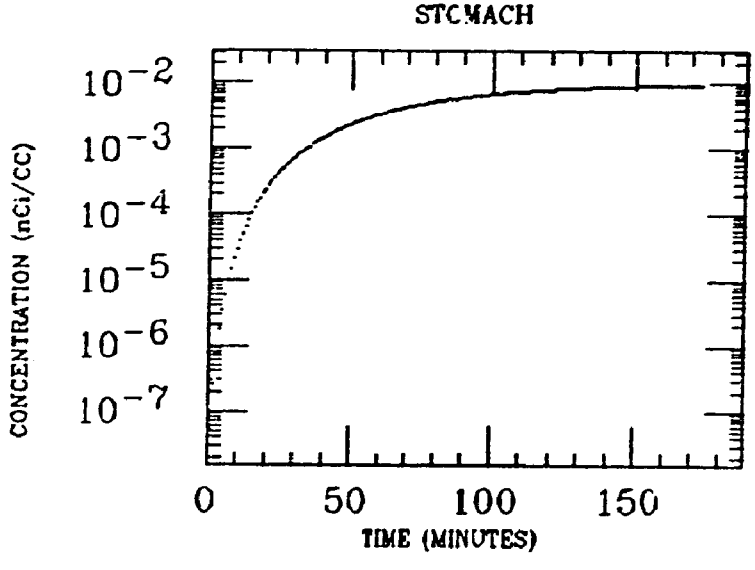

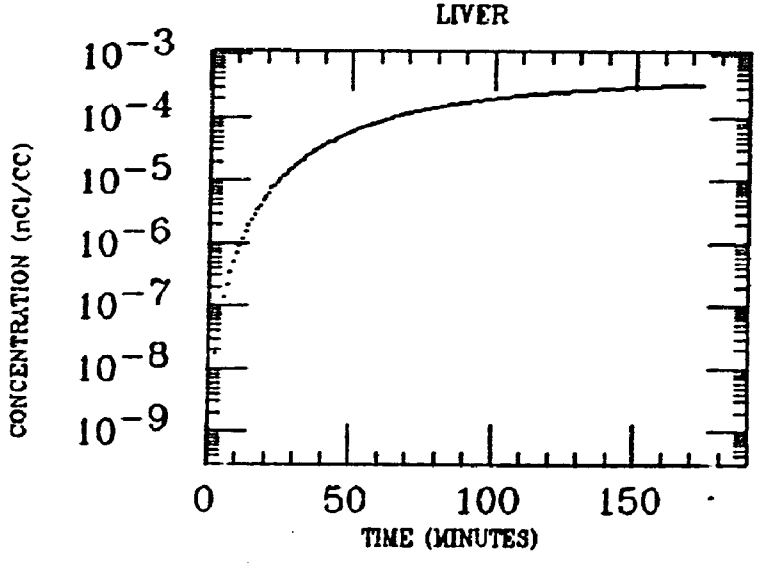

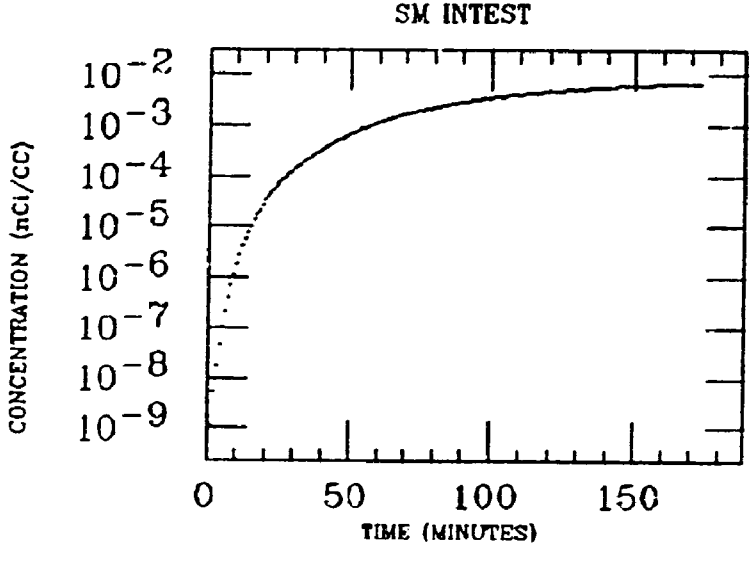

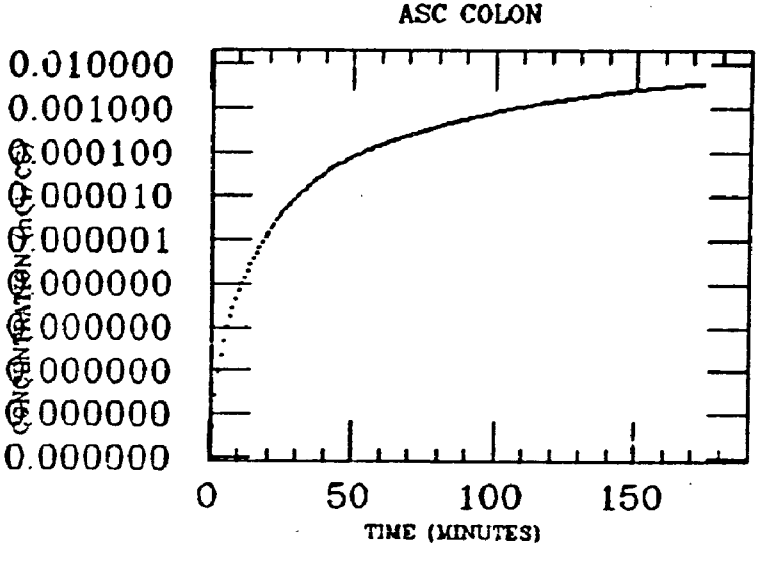

CLINE

XE INGESTION

Pb-210

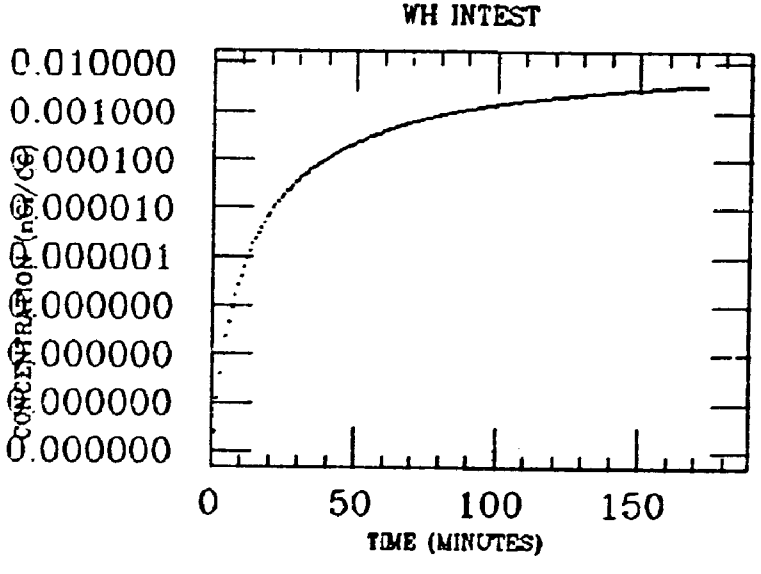

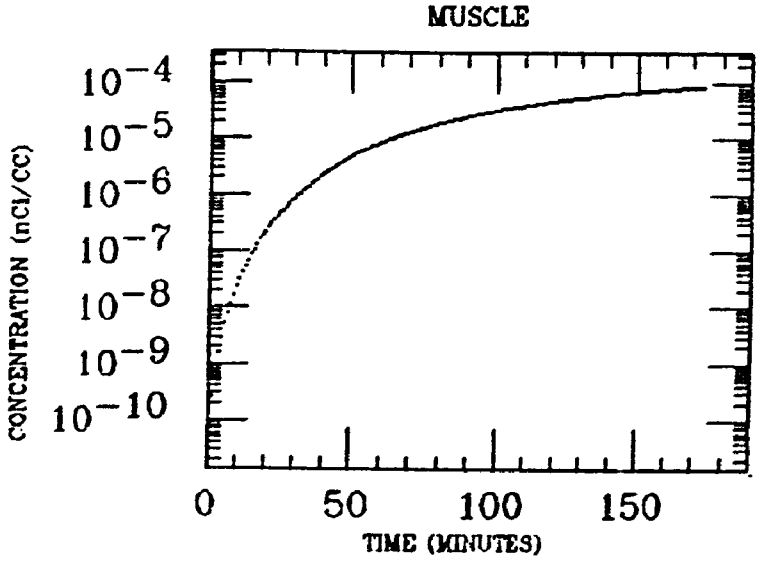

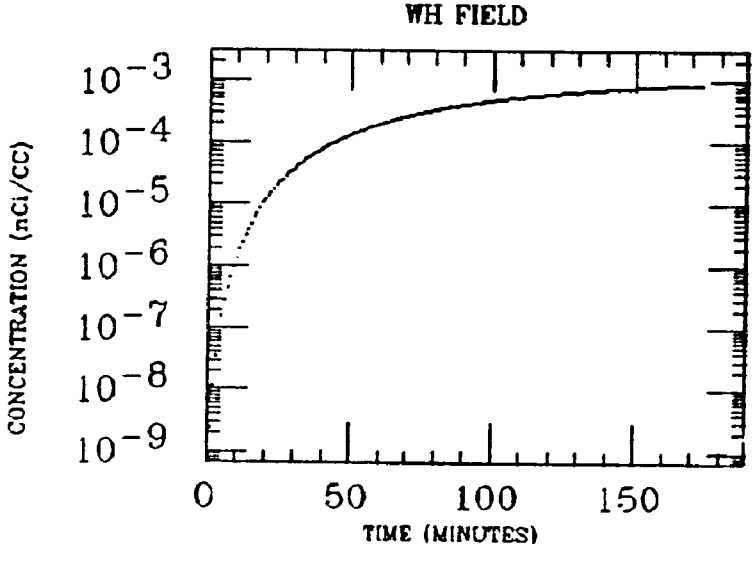

ELMDEN
XE INGESTION
Pb-210

STOMACH

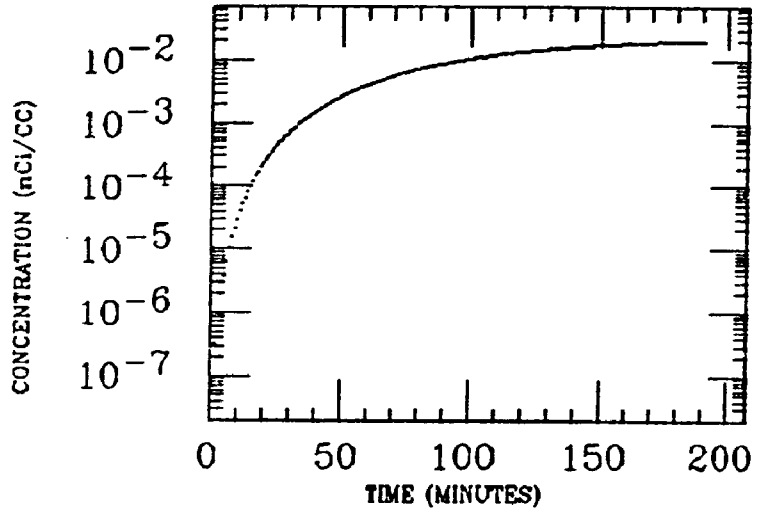

LIVER

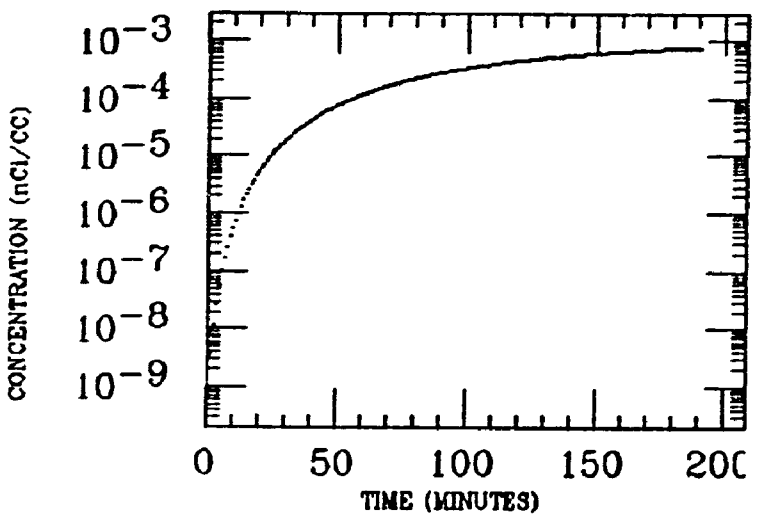

MUSCLE

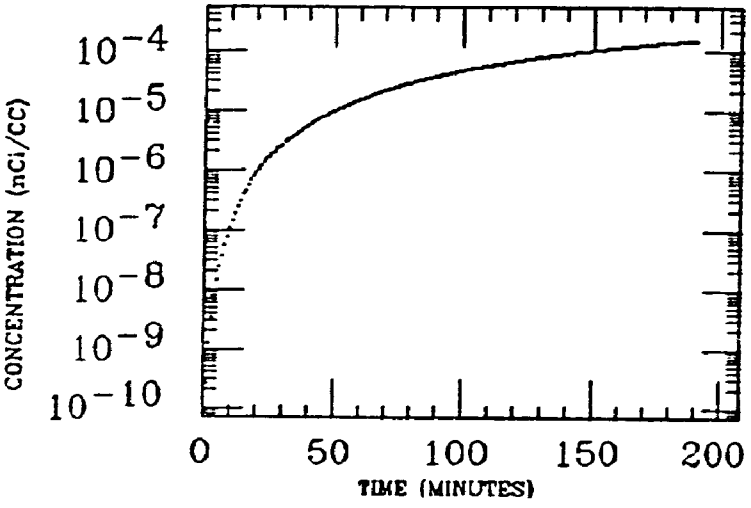

WH FIELD

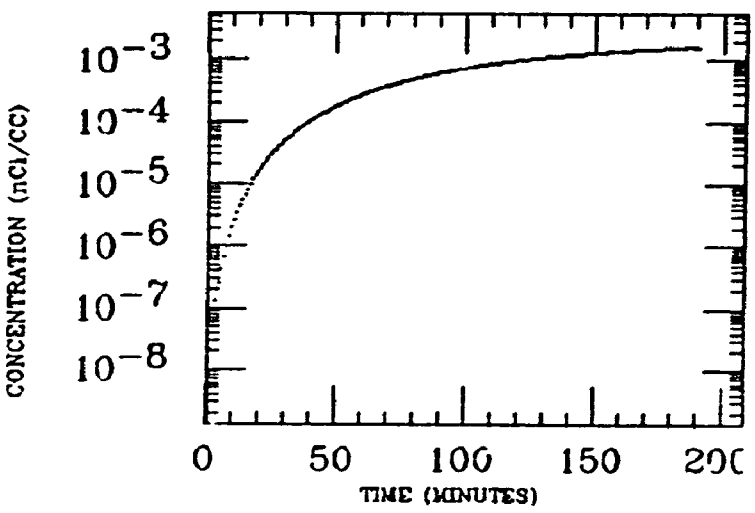

ELMDEN
XE INGESTION
Pb-210

STOMACH

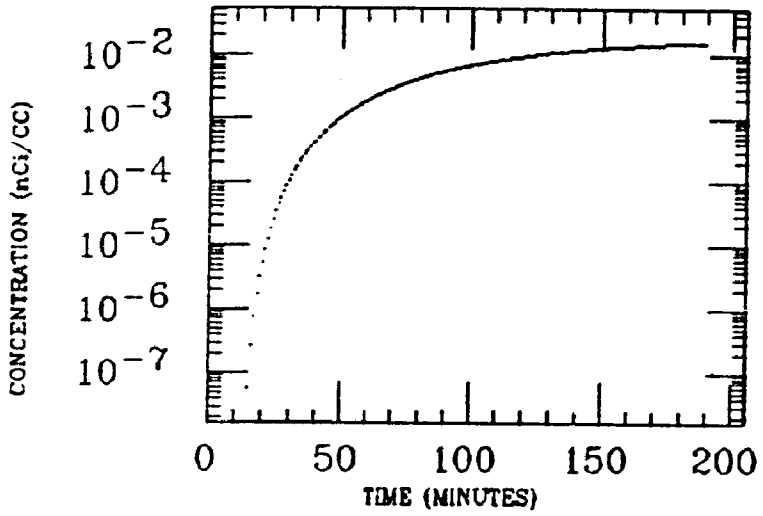

LIVER

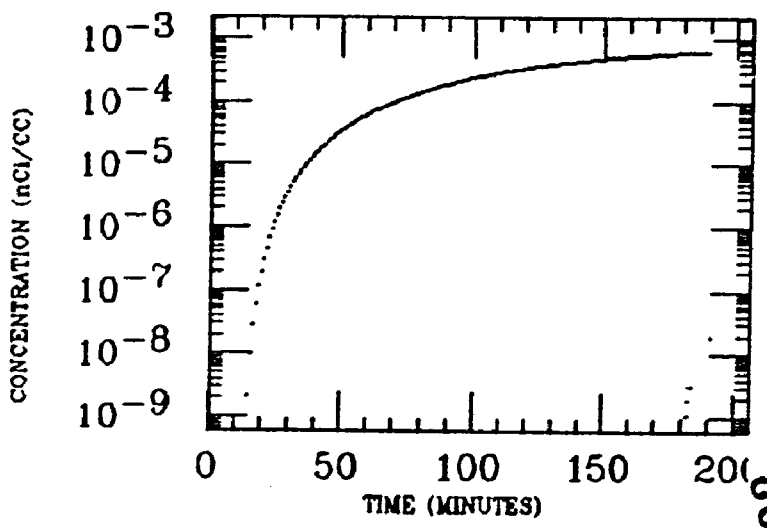

SM INTEST

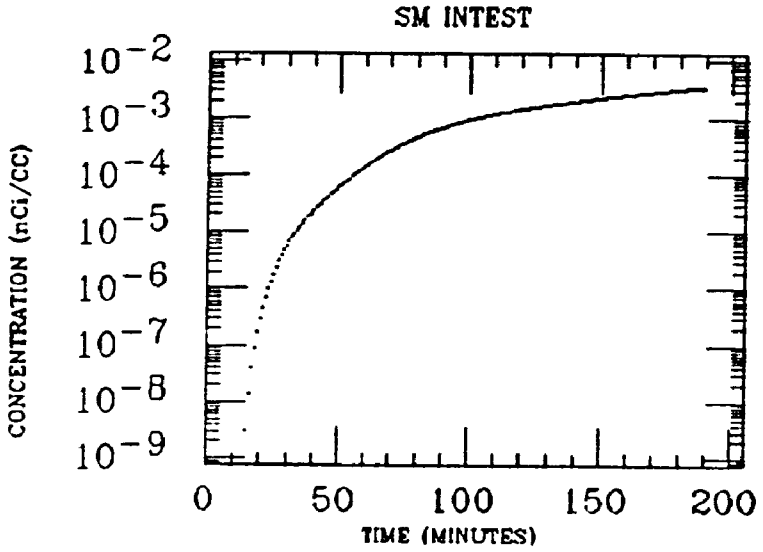

DES COLON

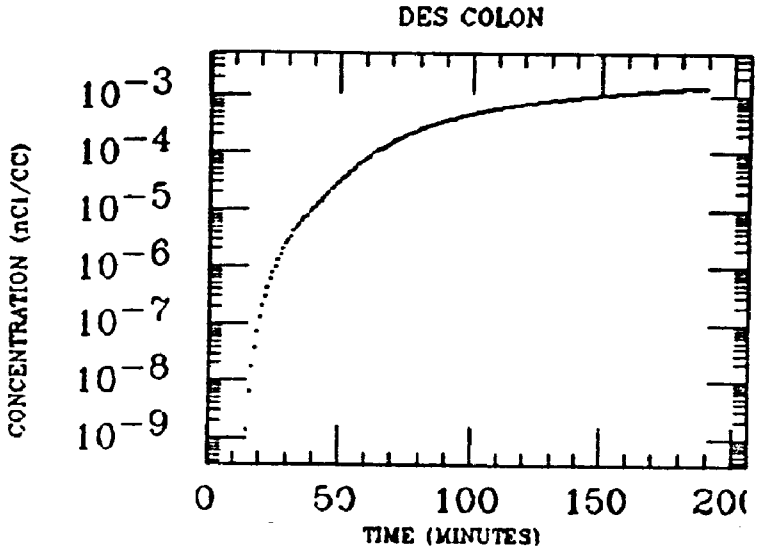

ELMDEN
XE INGESTION
Pb-210

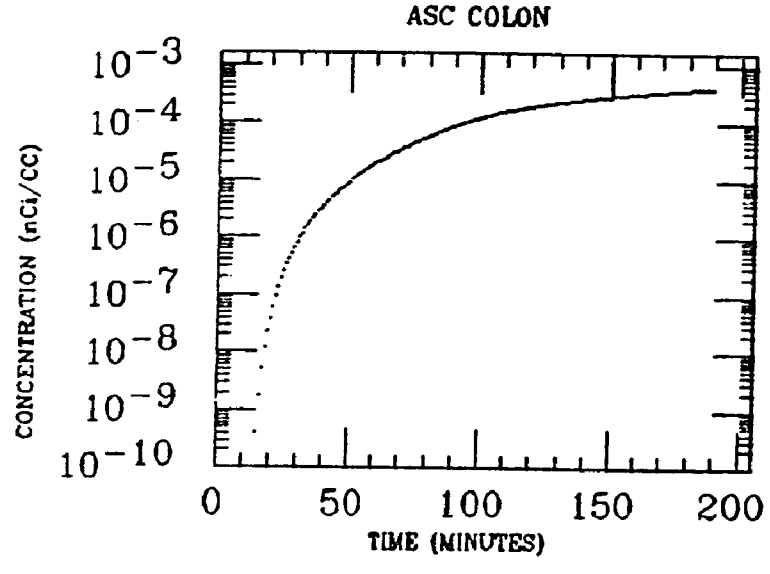

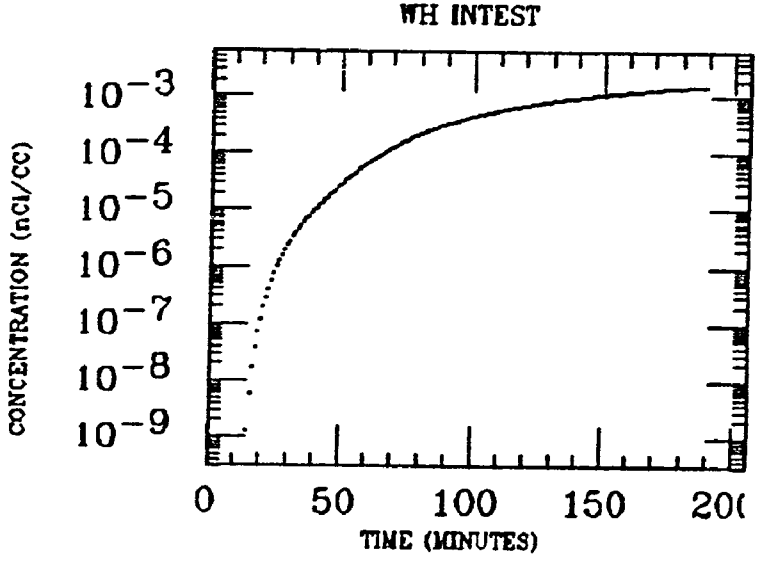

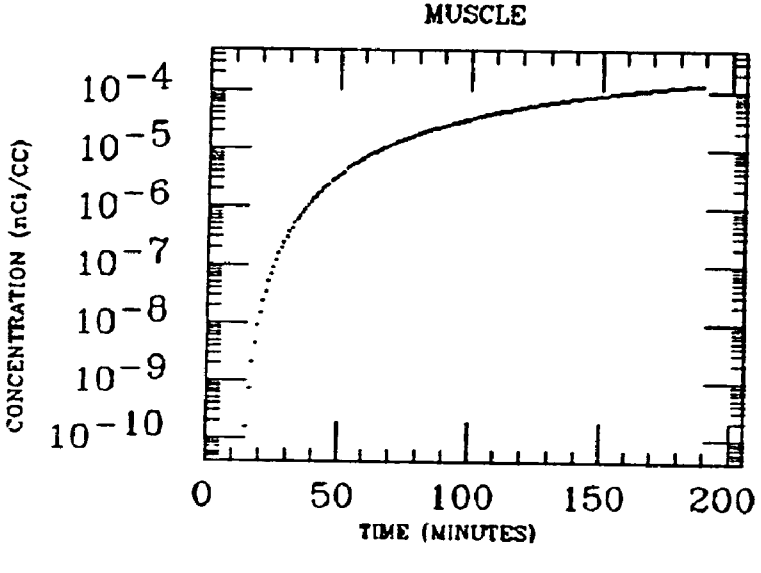

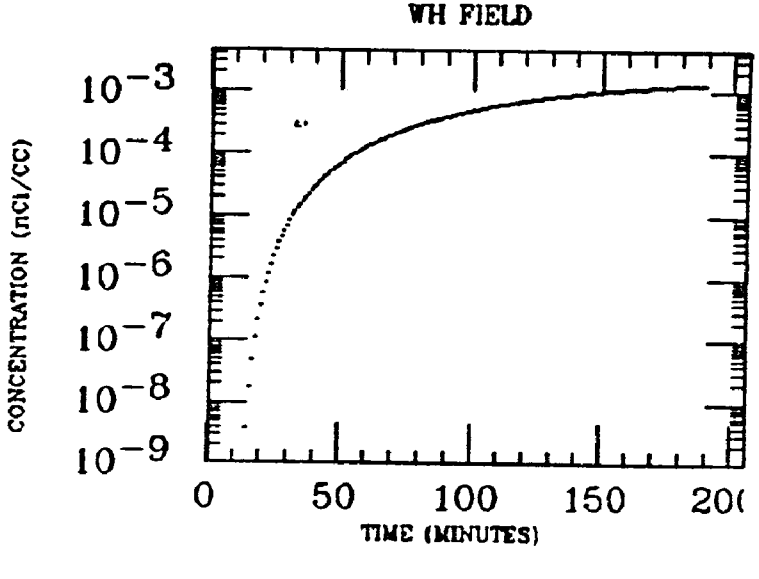

EPLING
XE INGESTION
Pb-210

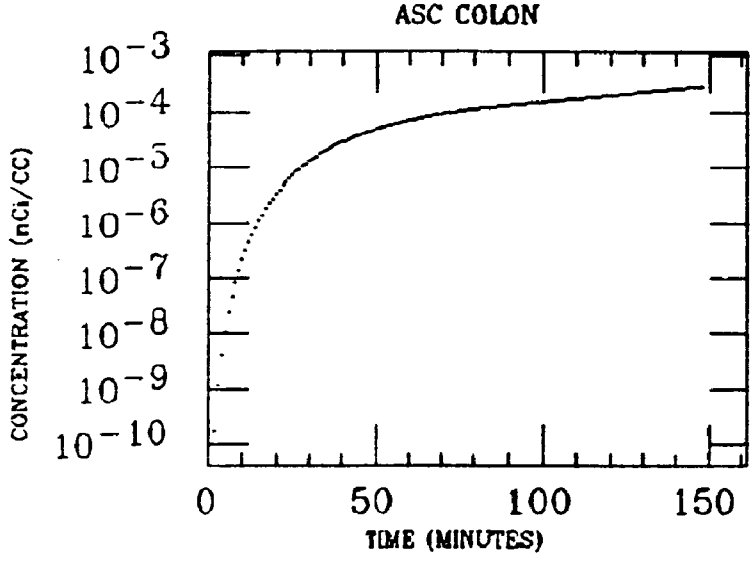

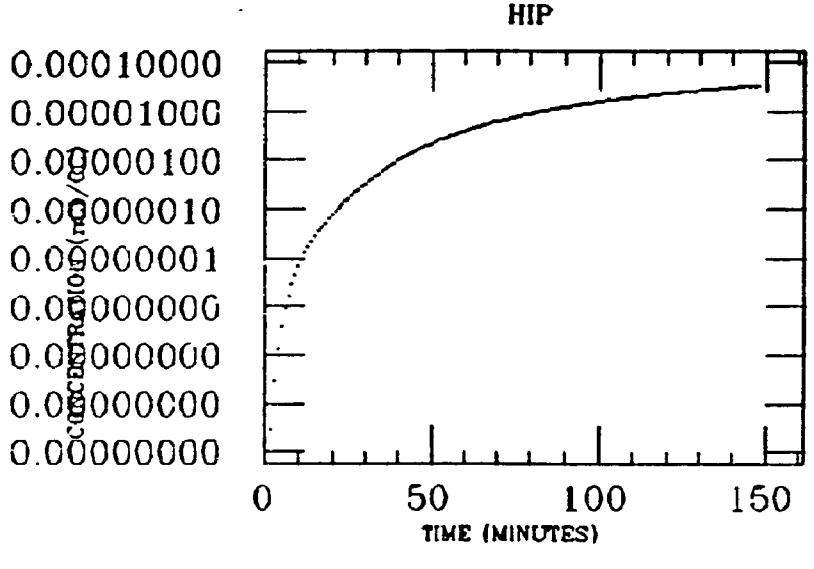

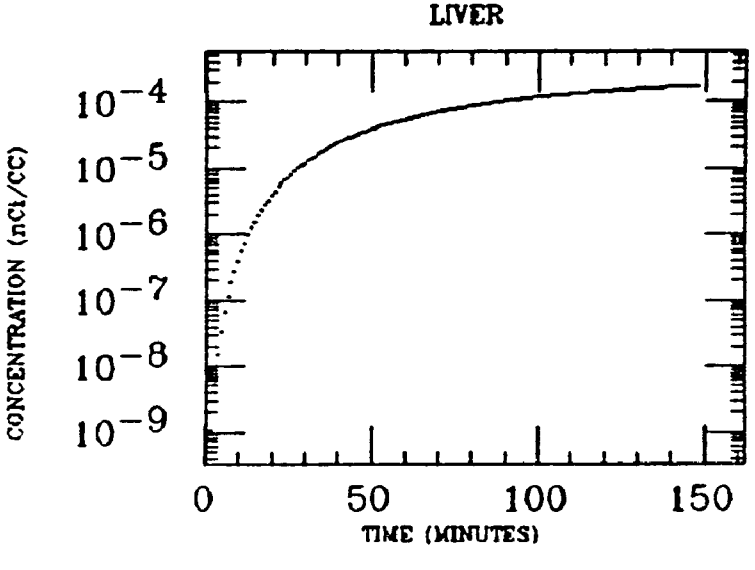

EPLING
XE INGESTION
Pb-210

SM INTEST

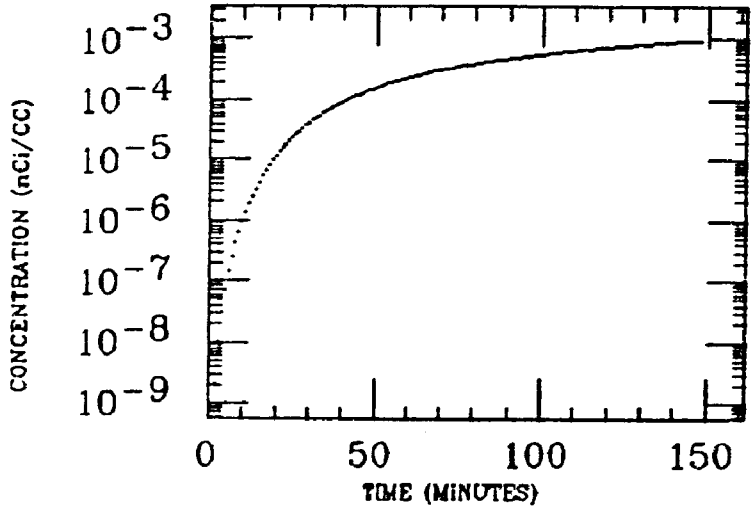

STOMACH

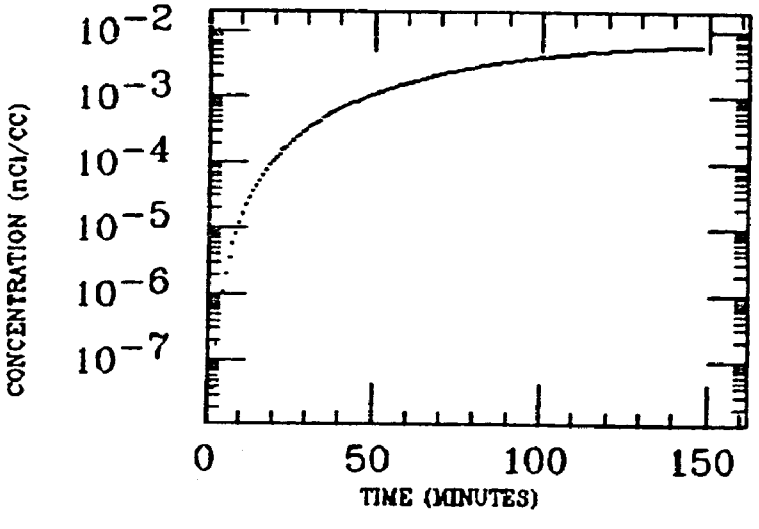

WH FIELD

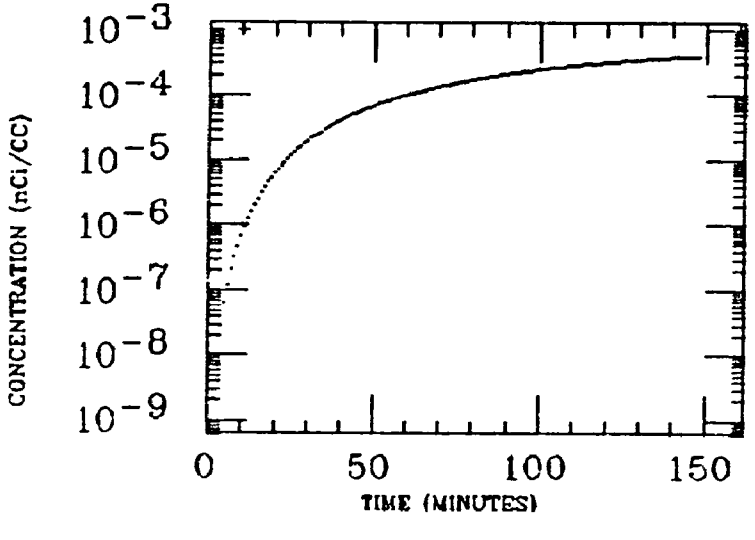

WH INTEST

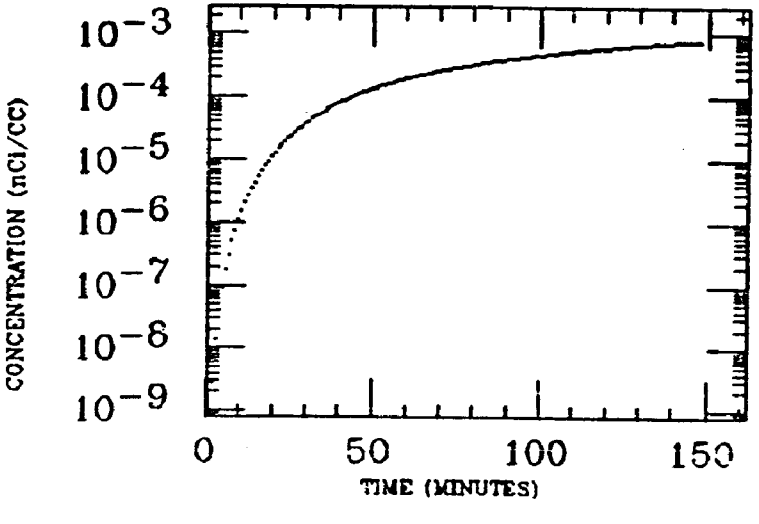

GALLOP
XE INGESTION
Pb-210

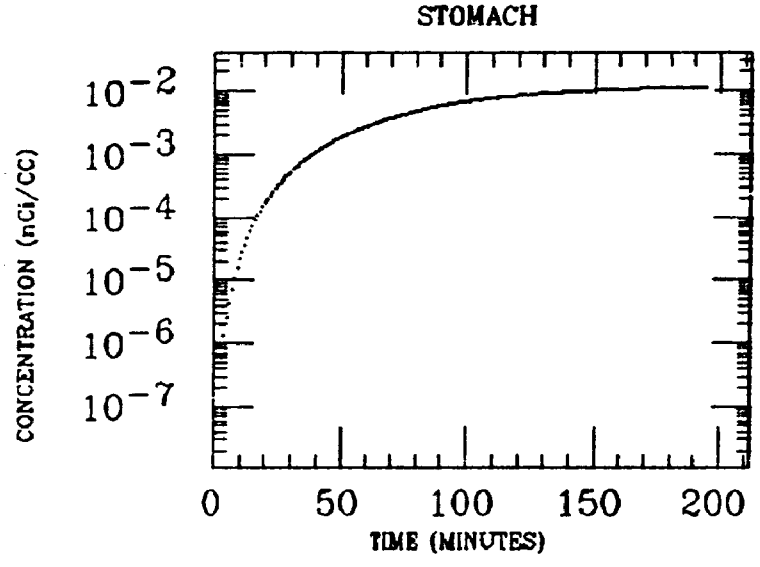

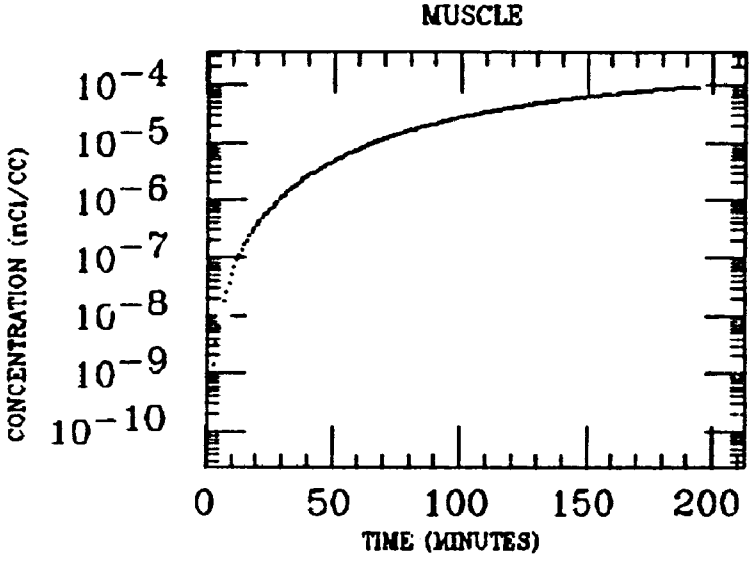

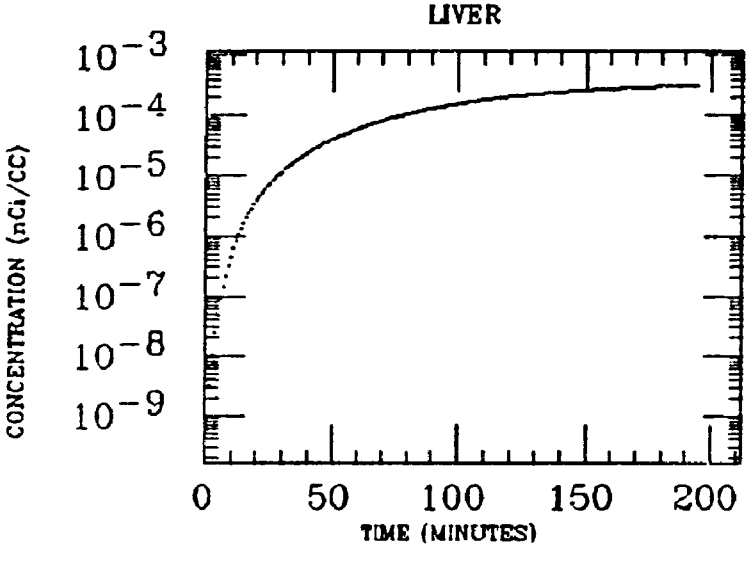

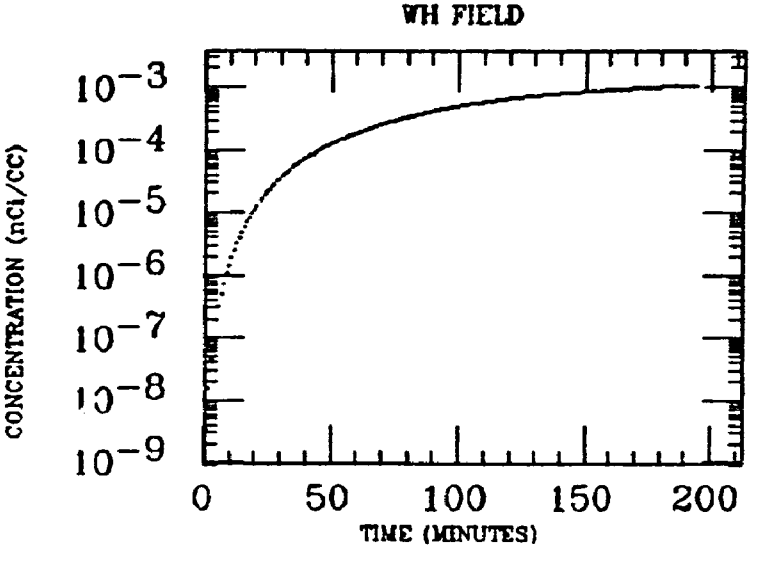

CALLOP
XE INGESTION
Pb-210

STOMACH

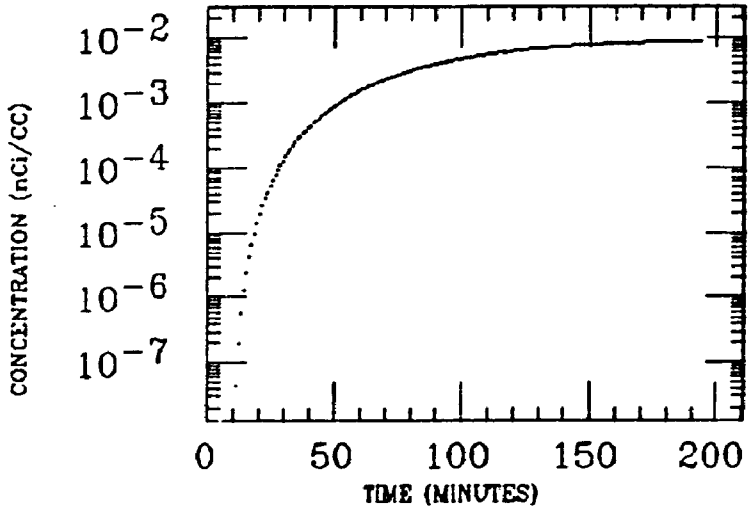

LIVER

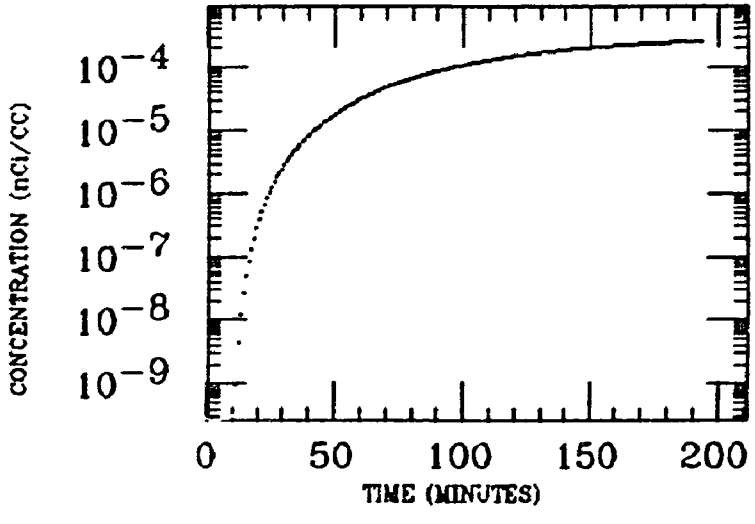

SM INTEST

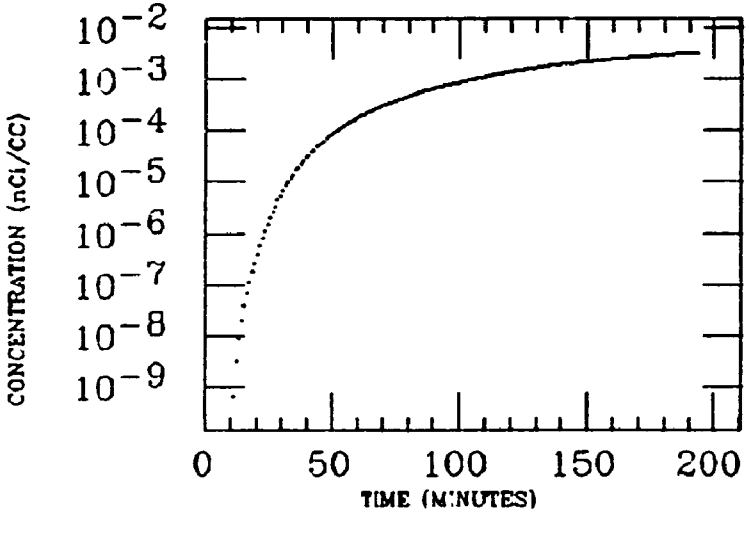

ASC COLON

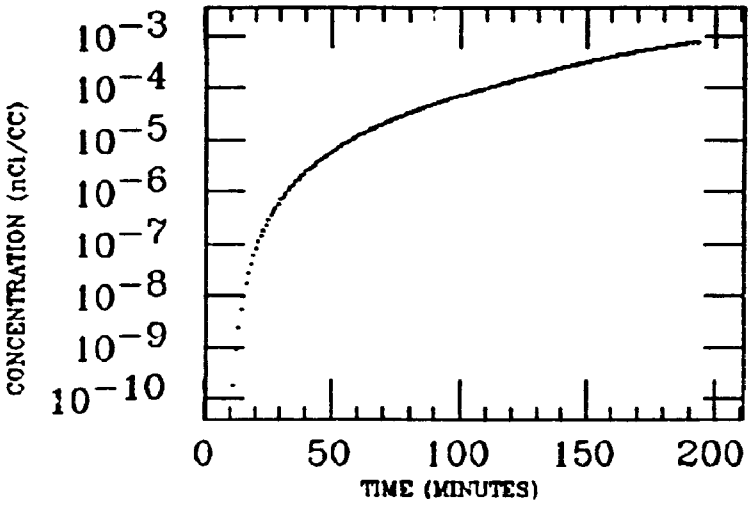

GALLOP
XE INGESTION
Pb-210

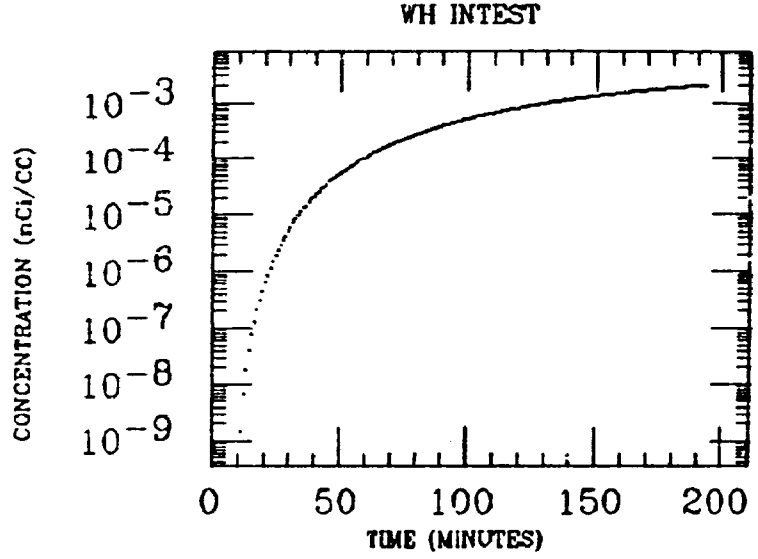

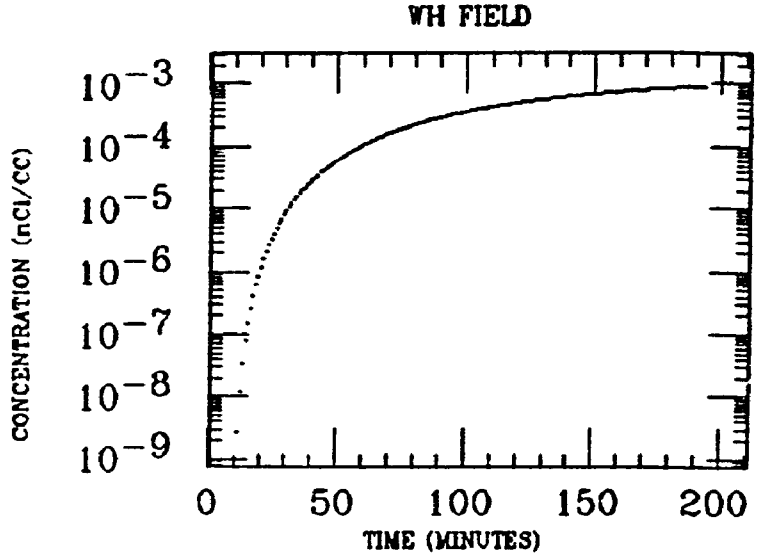

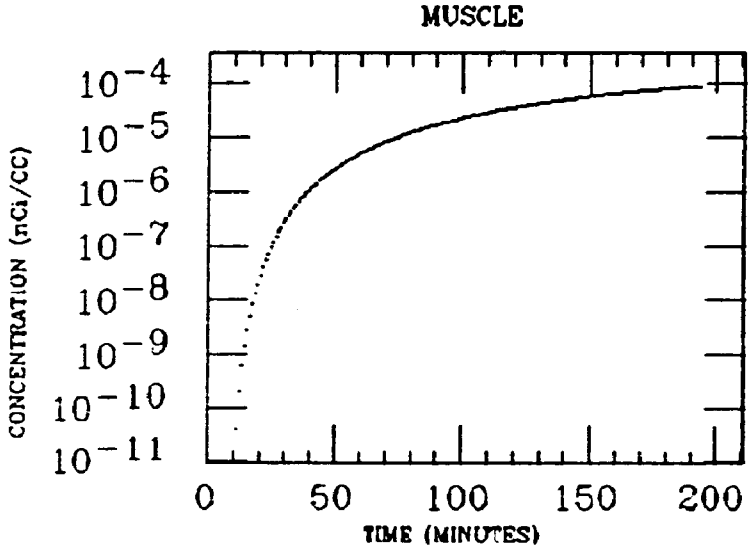

C.MCKINLEY
XE INGESTION
Pb-210

STOMACH

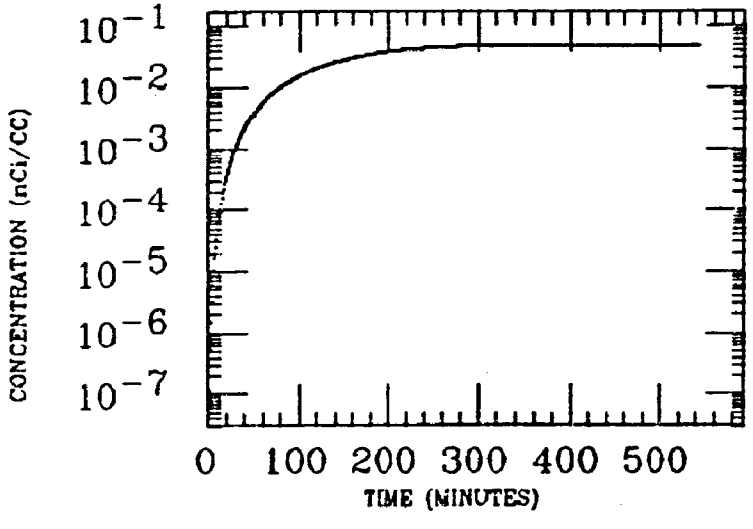

LIVER

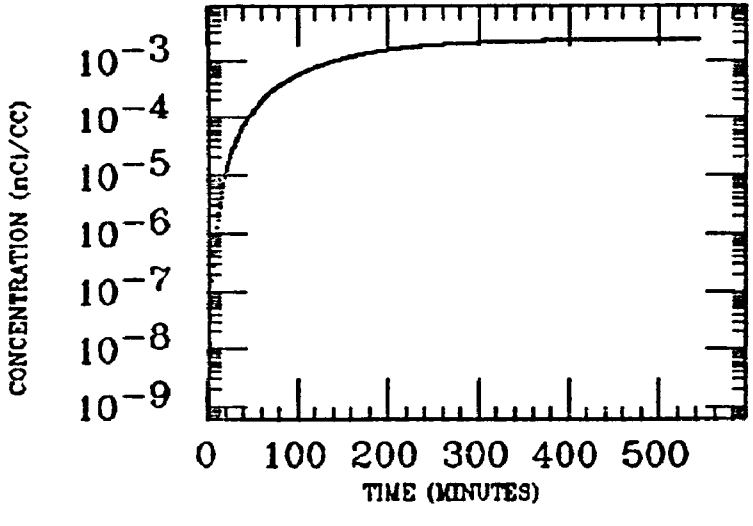

WH FIELD

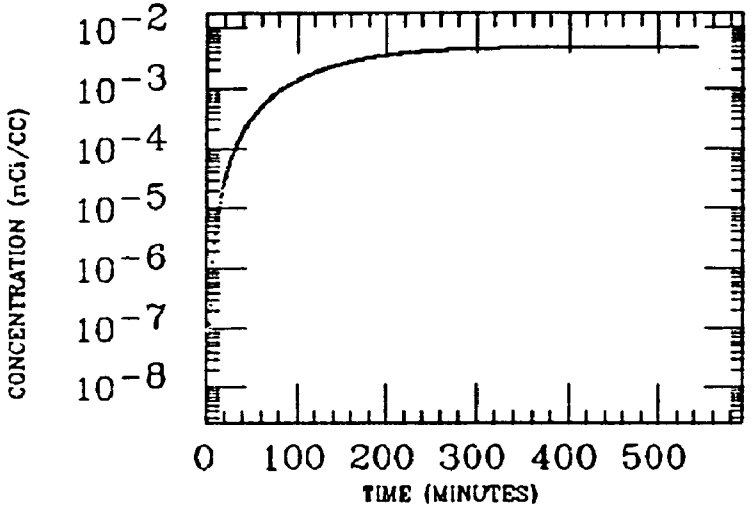

C.MCKINLEY
XE INGESTION
Pb-210

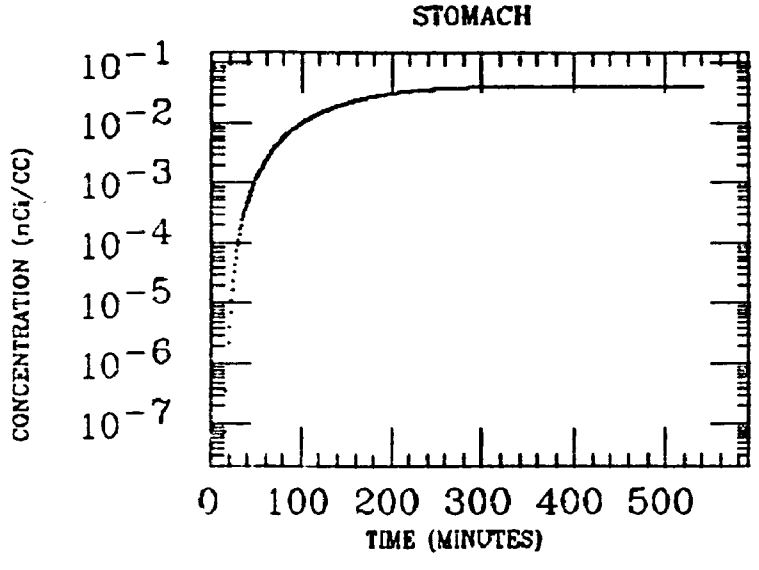

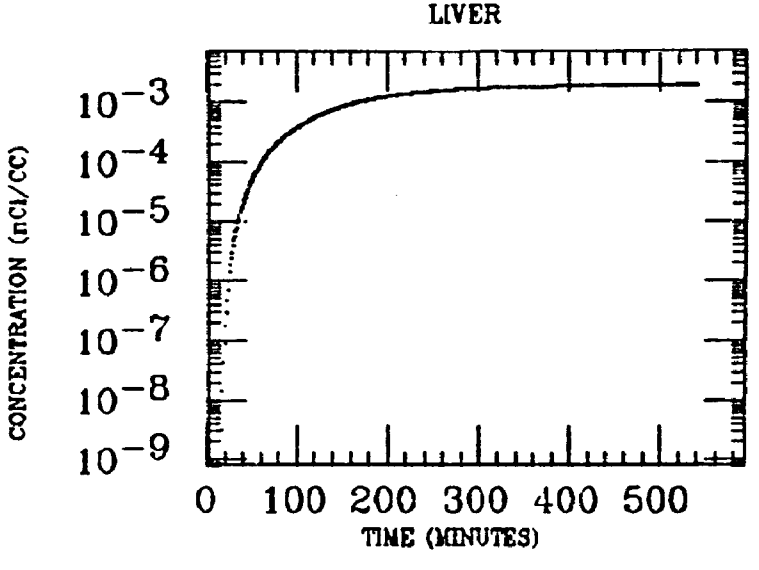

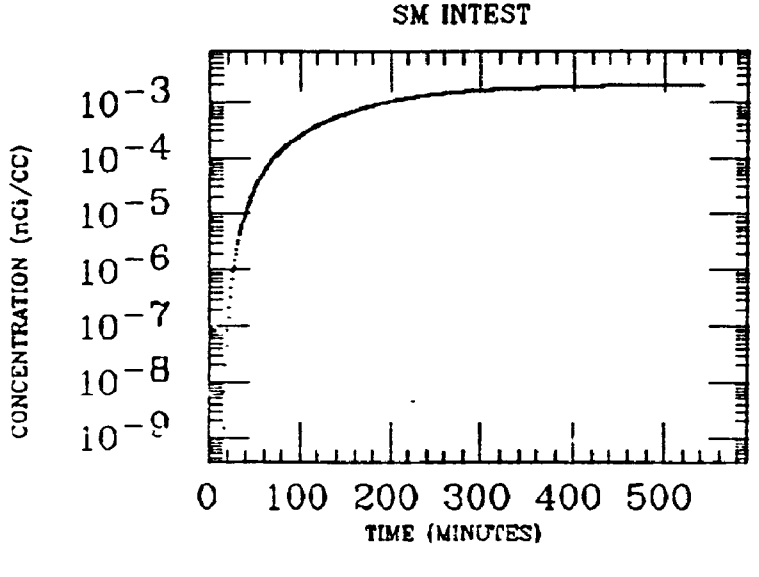

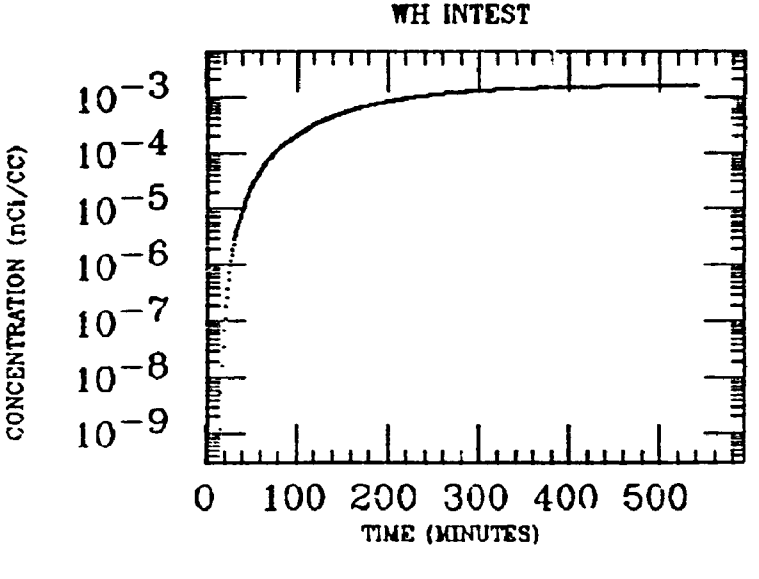

G.MCKINLEY
XE INGESTION
Pb-210

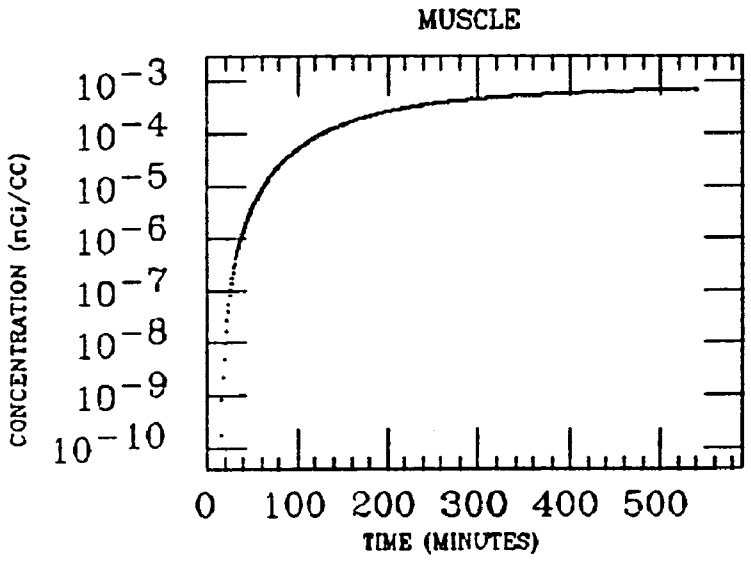

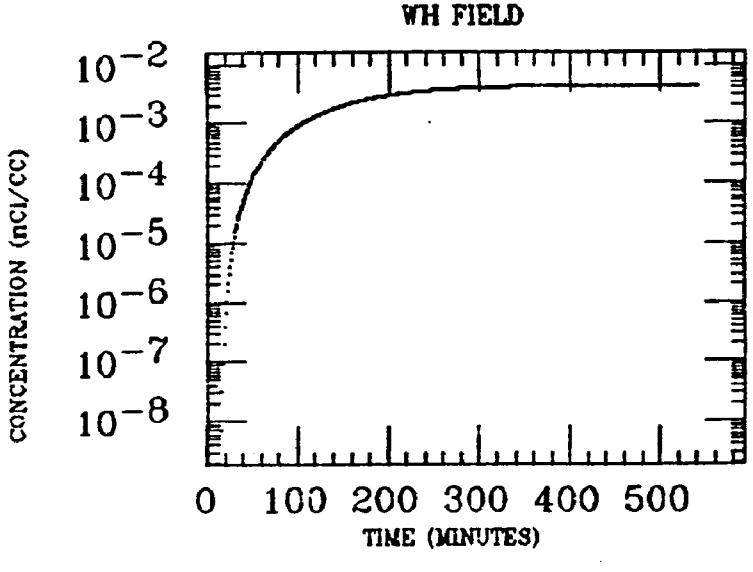

401

HAND
XE INGESTION
Pb-210

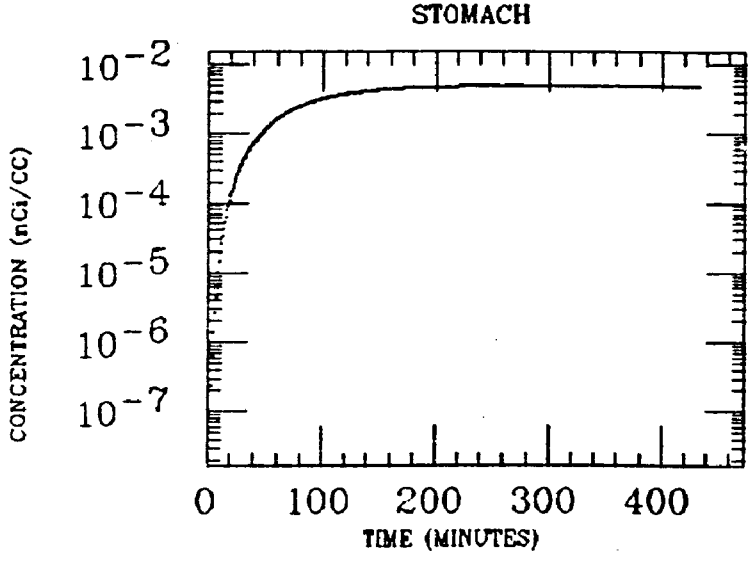

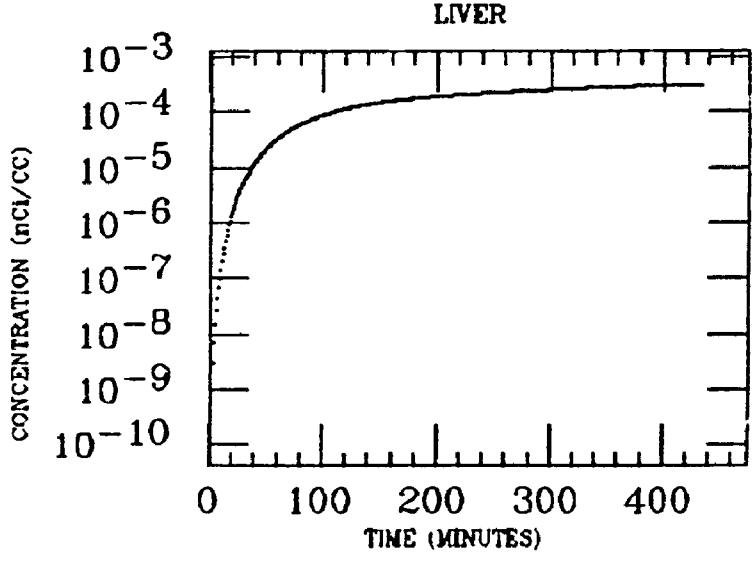

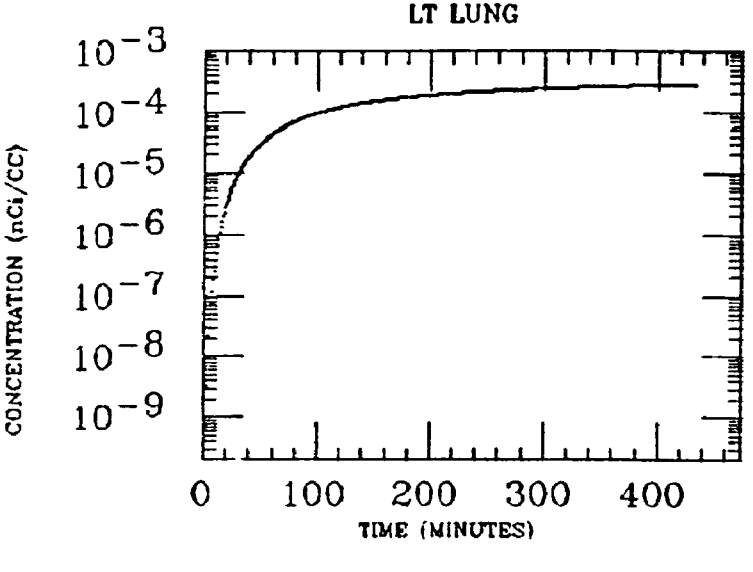

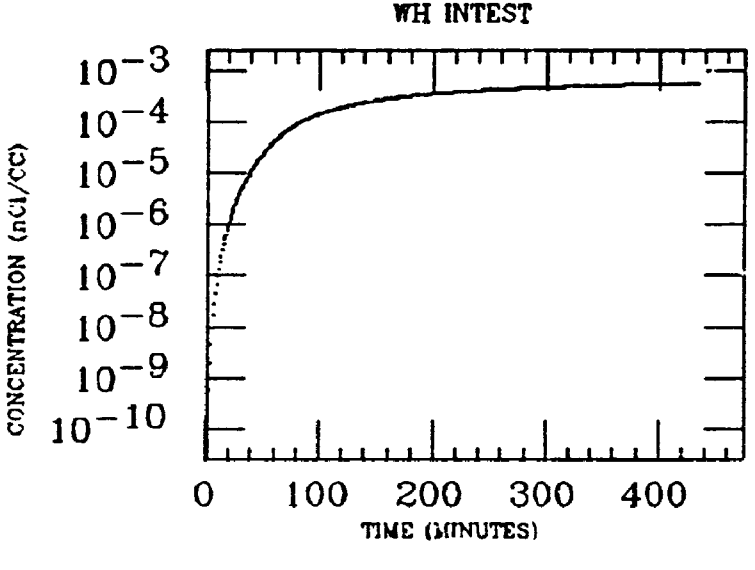

HAND

XE INGESTION

Pb-210

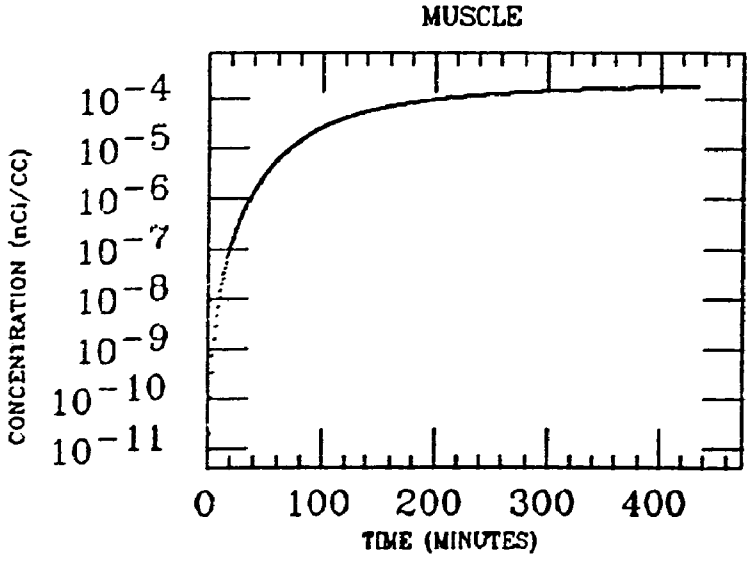

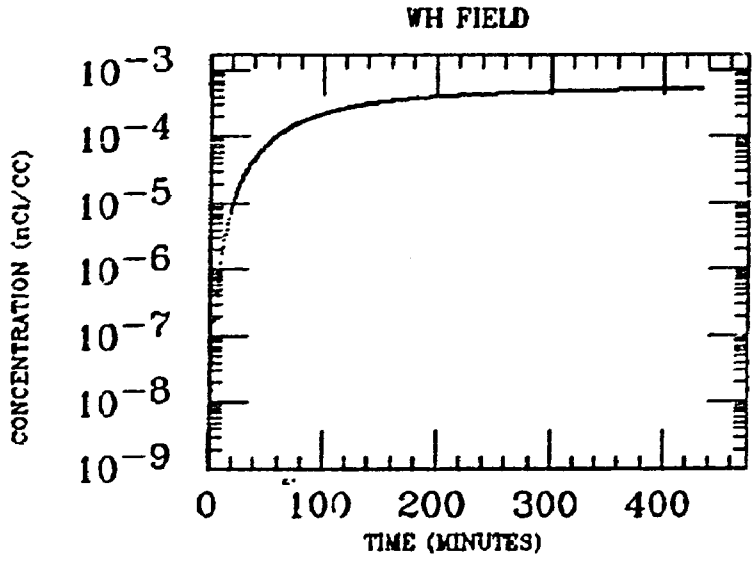

HAND
XE INGESTION
Pb-210

STOMACH

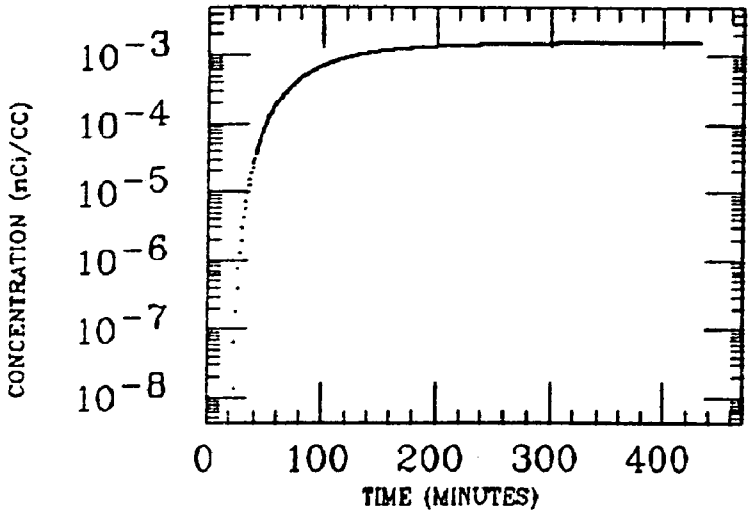

LIVER

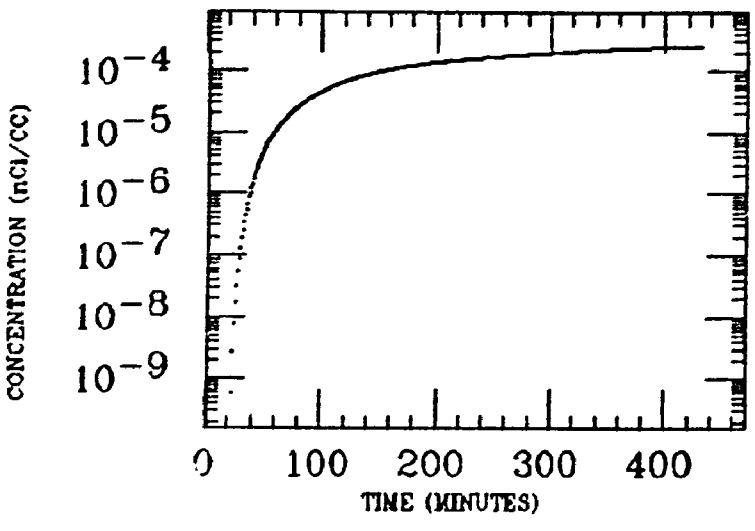

LT LUNG

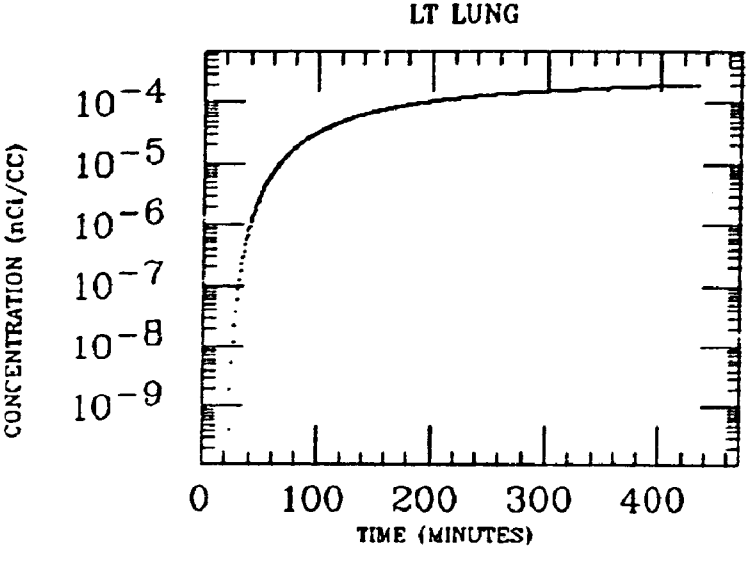

SM INTEST

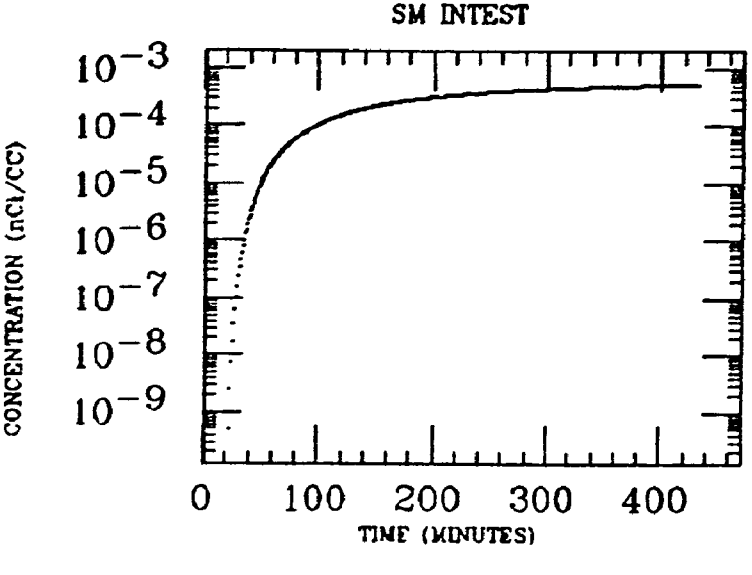

HAND
XE INGESTION
Pb-210

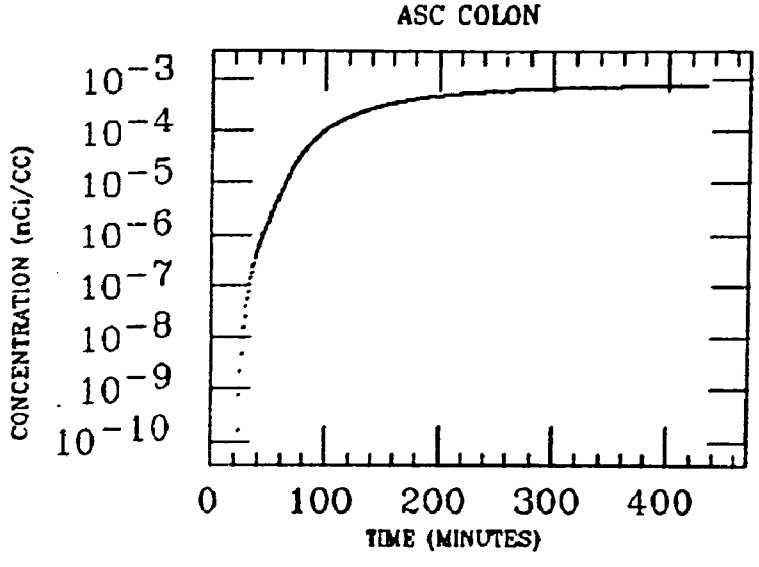

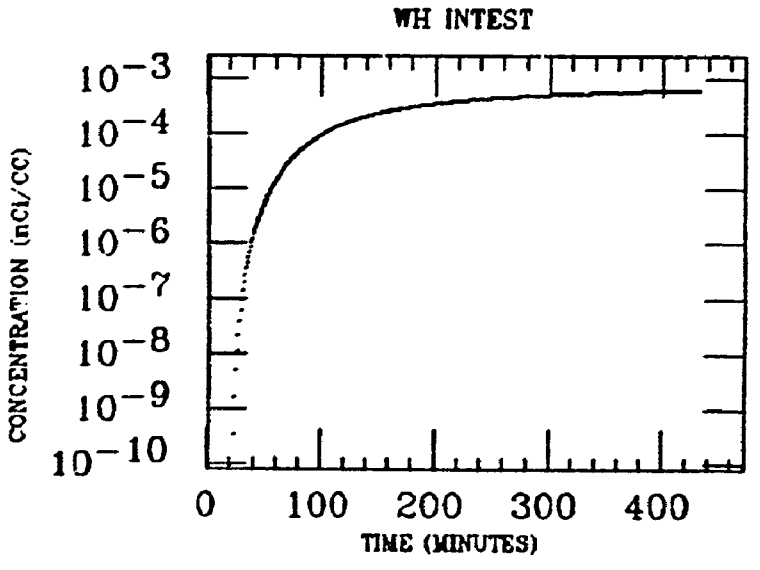

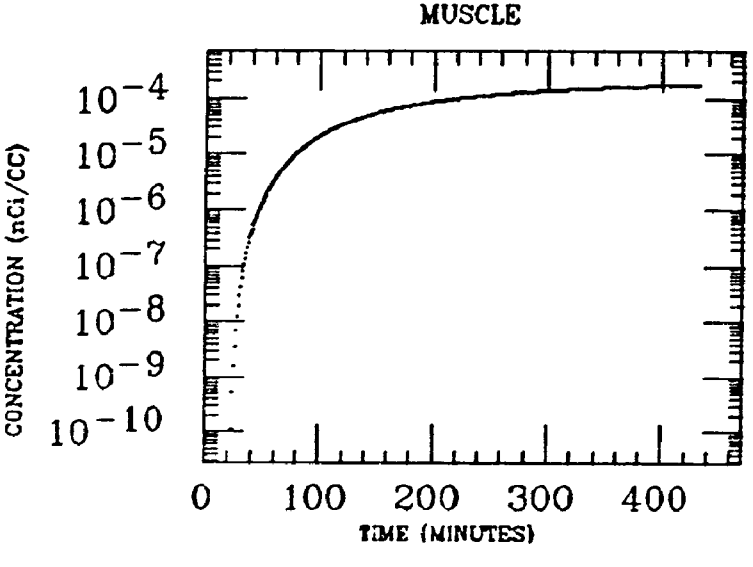

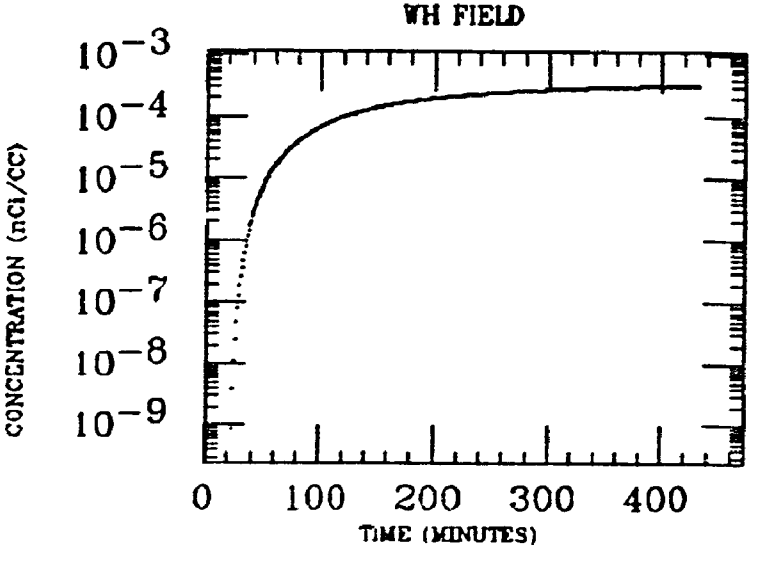

HAWKINS
XE INGESTION
Pb-210

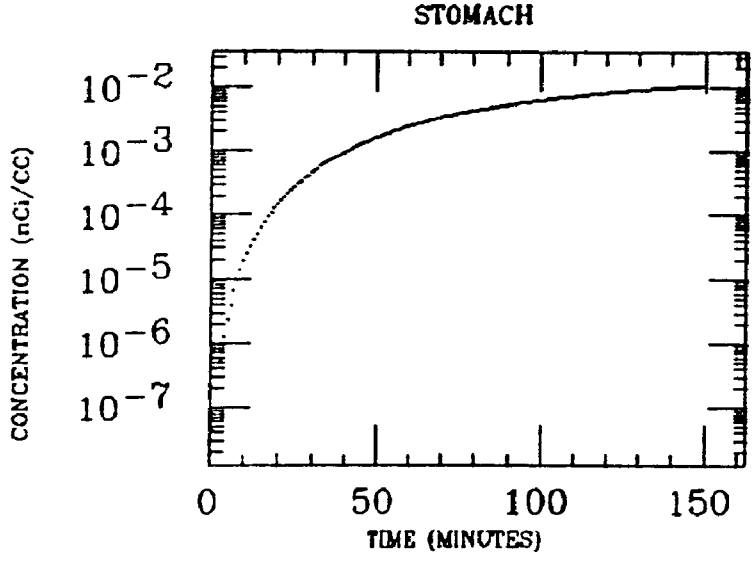

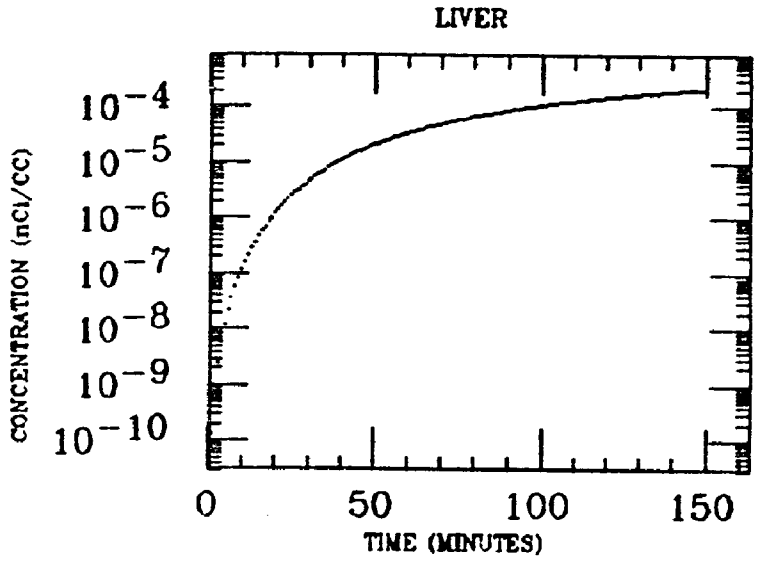

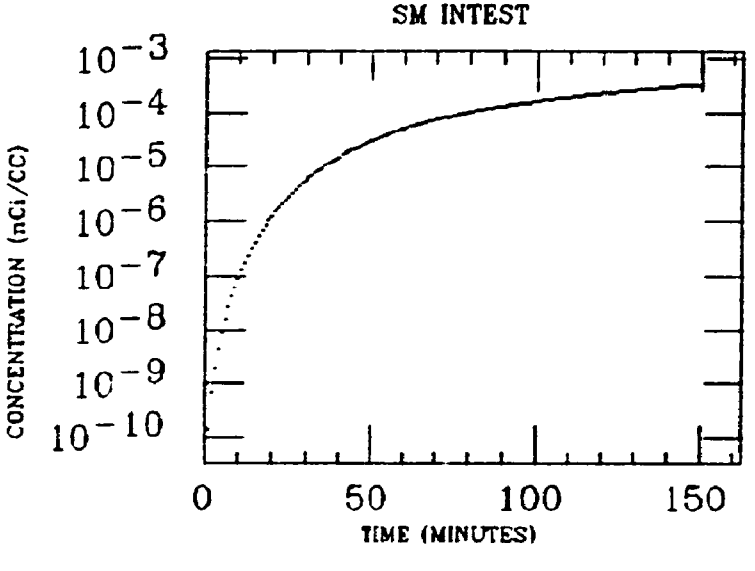

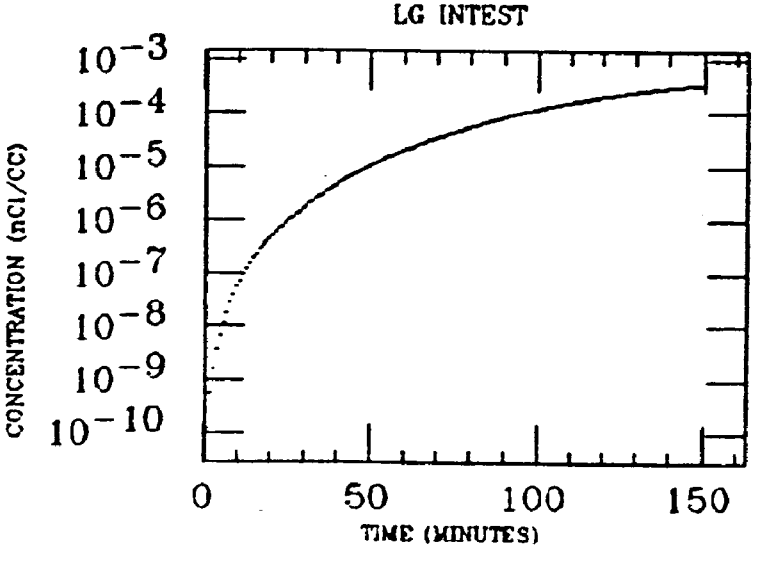

HAWKINS
XE INGESTION
Pb-210

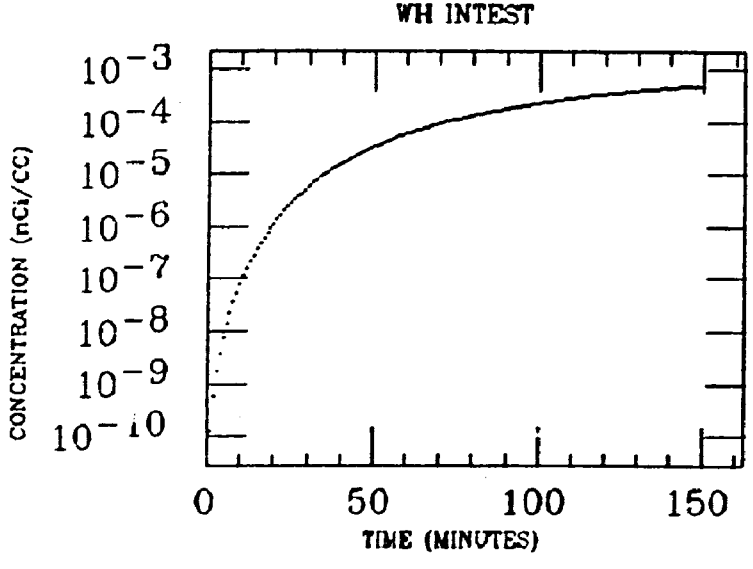

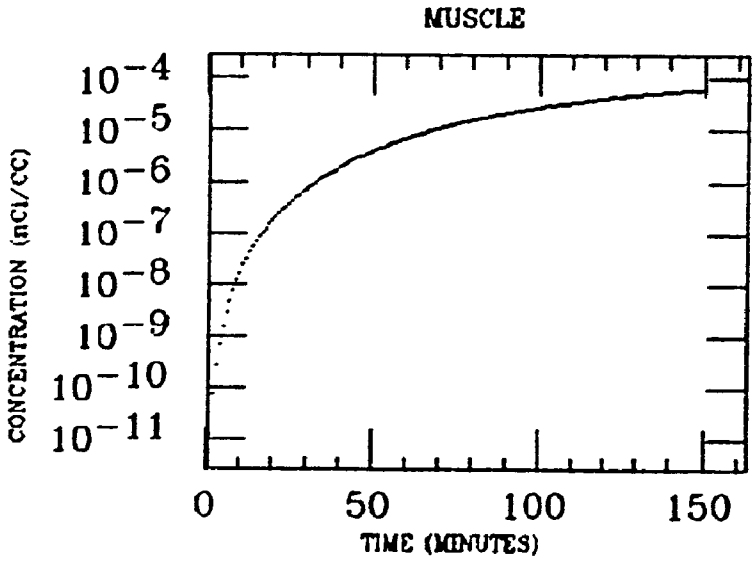

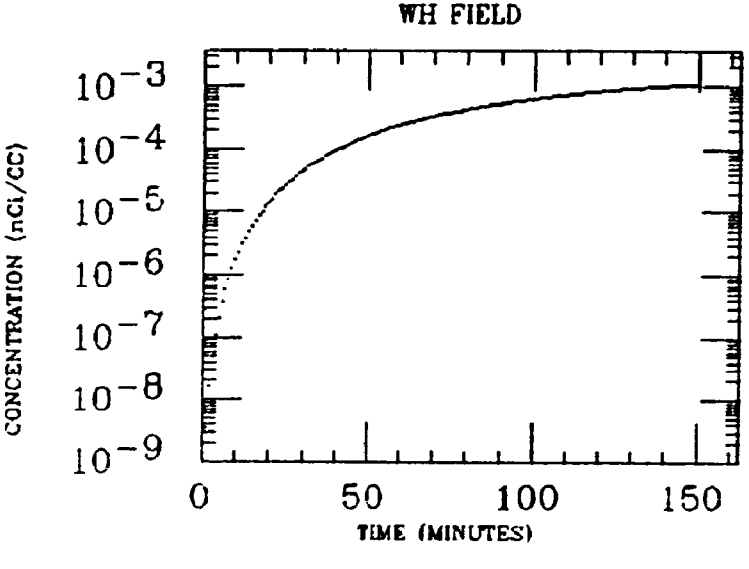

HILL
XE INGESTION
Pb-210

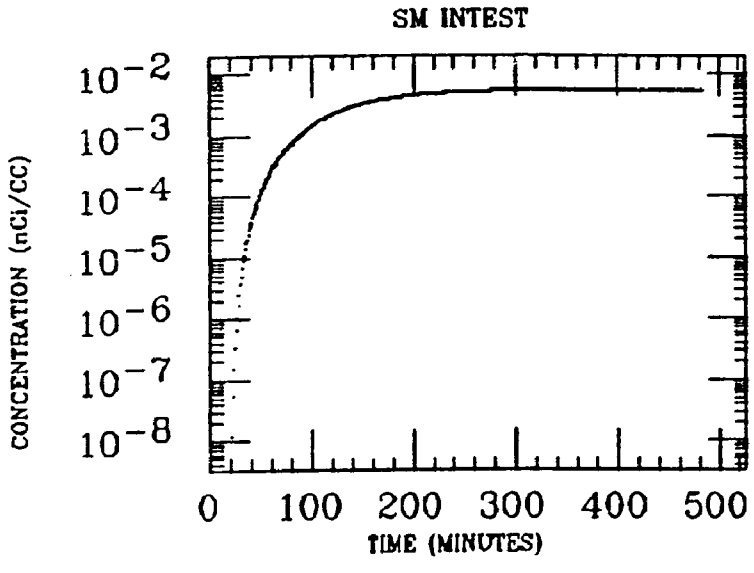

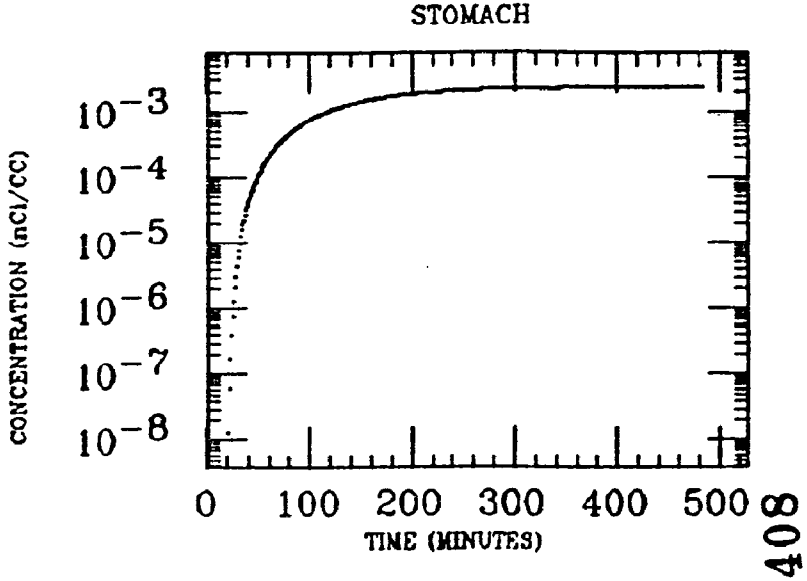

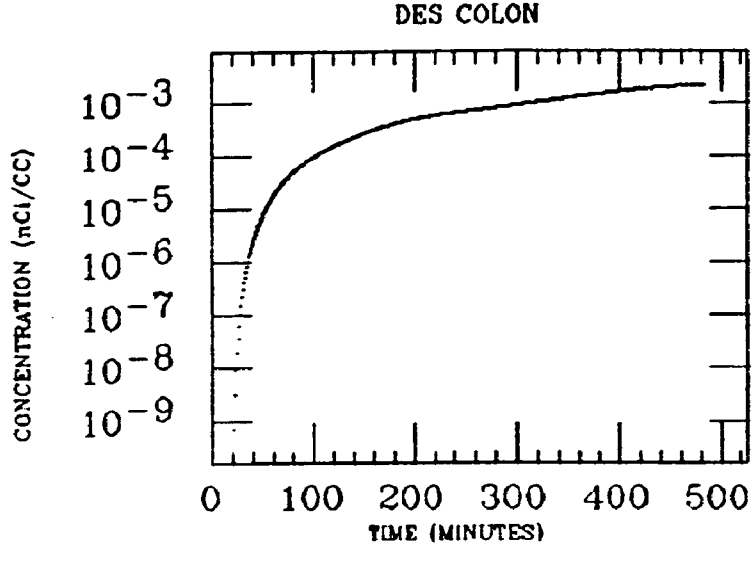

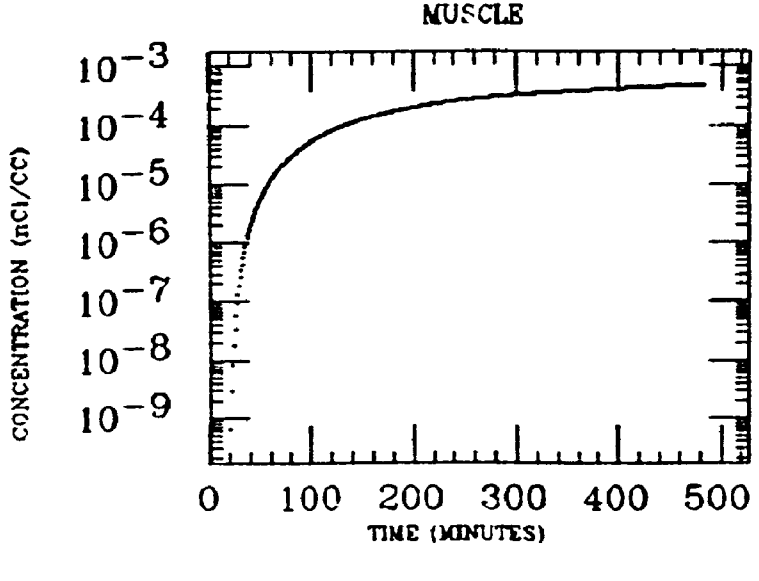

HILL

XE INGESTION

Pb-210

LIVER

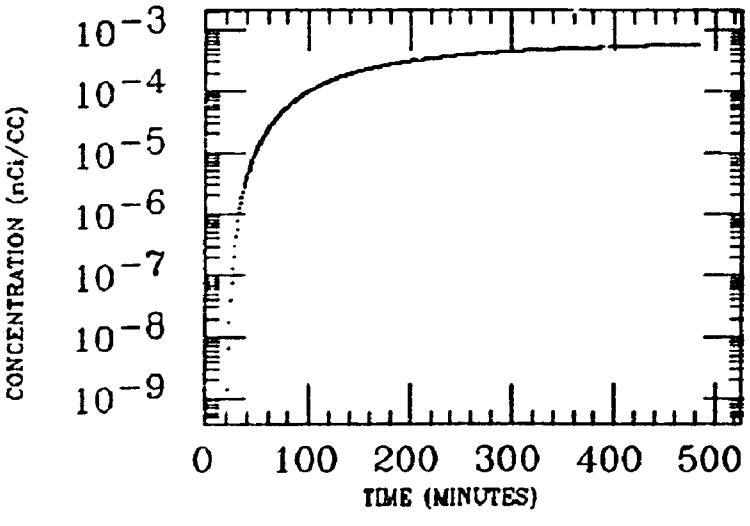

DUODENUM

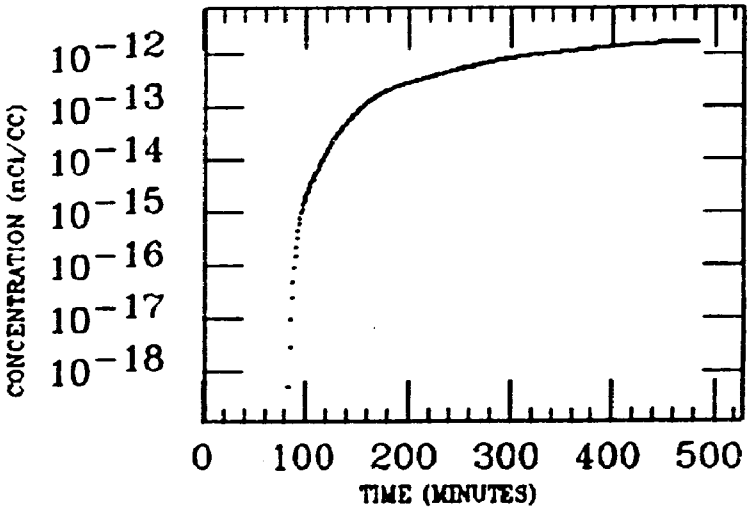

LG INTEST

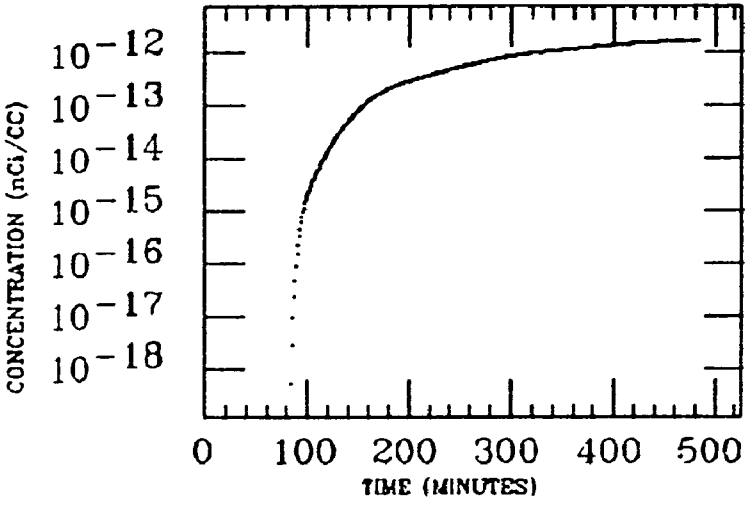

WH FIELD

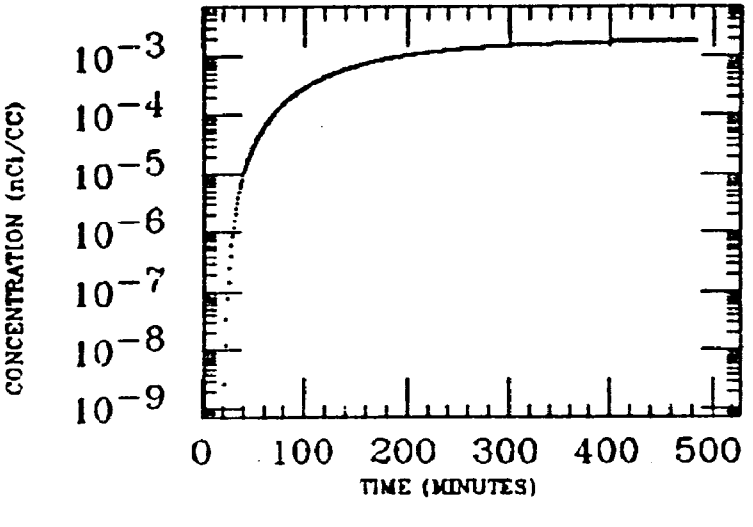

HILL

XE INGESTION

Pb-210

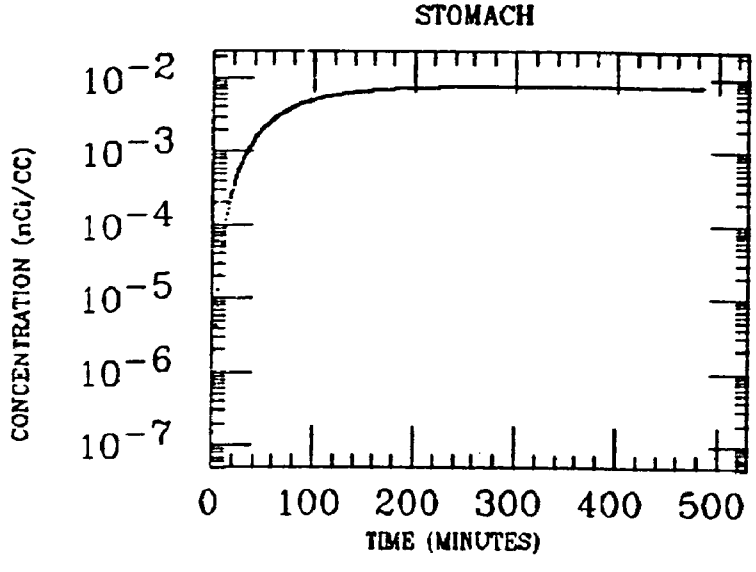

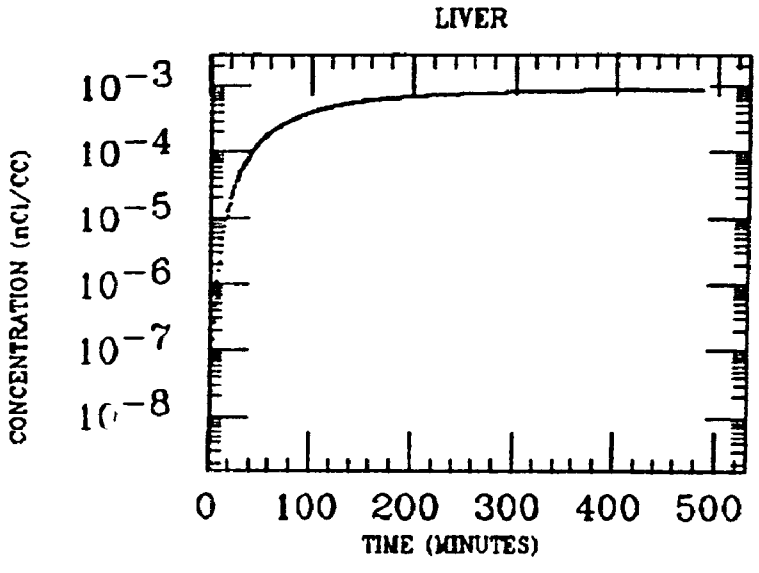

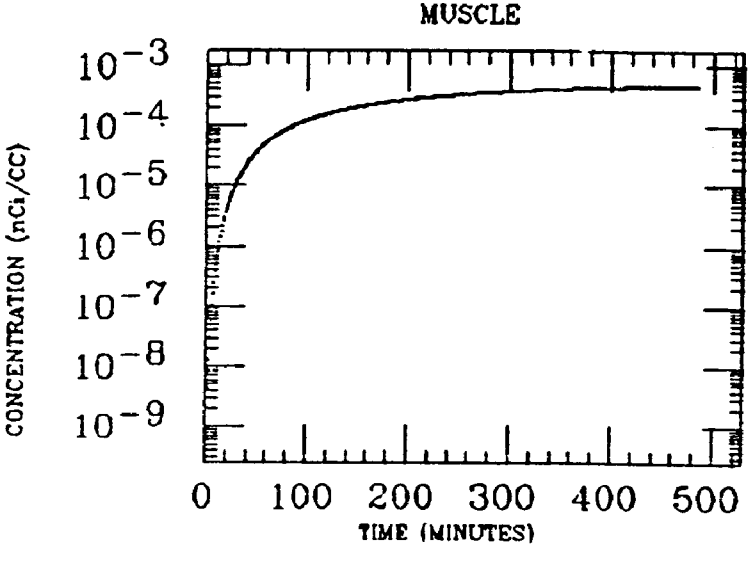

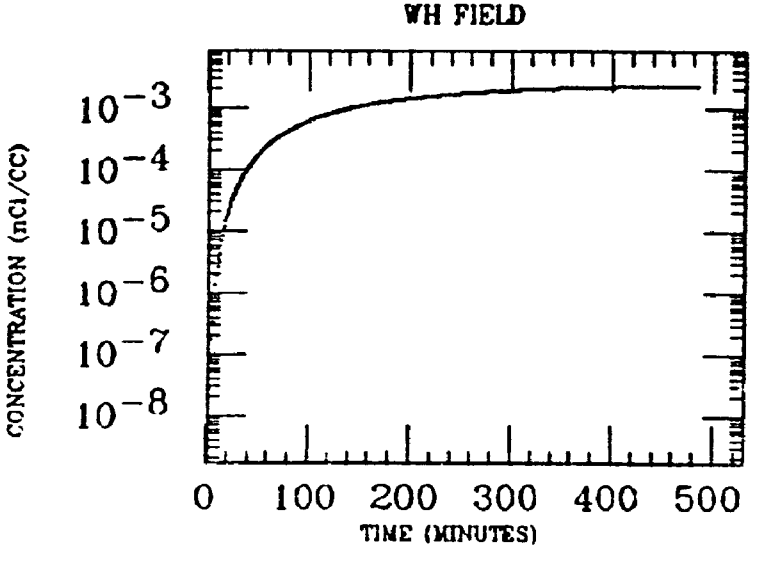

410

HUTCHINS
XE INGESTION
Pb-210

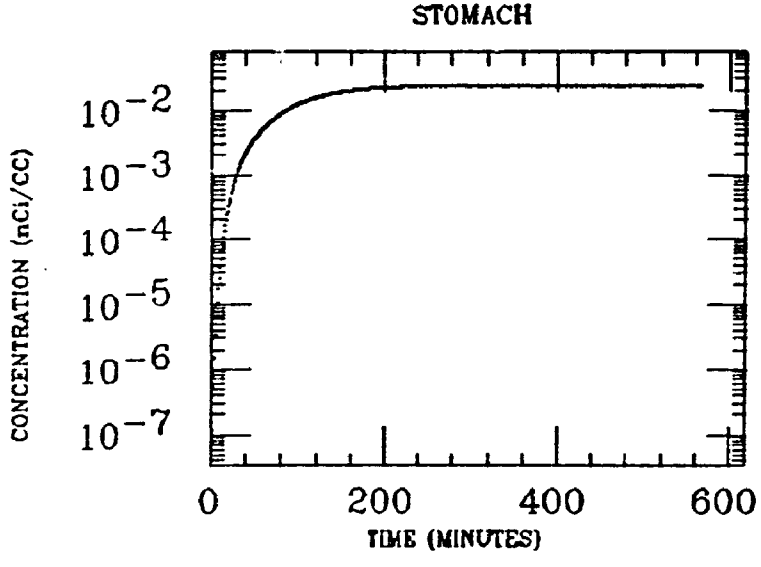

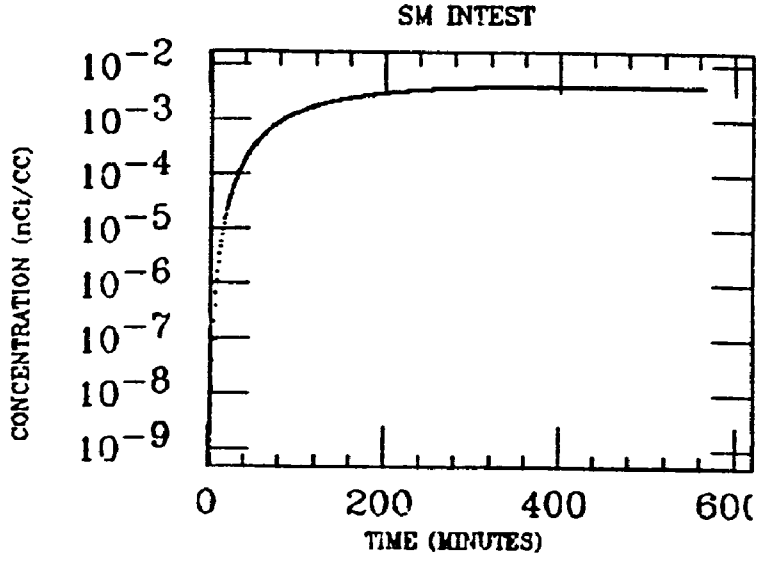

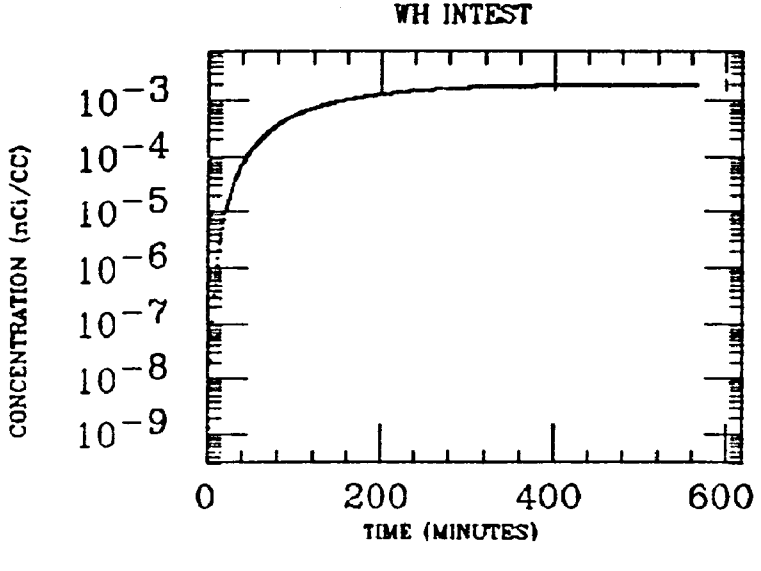

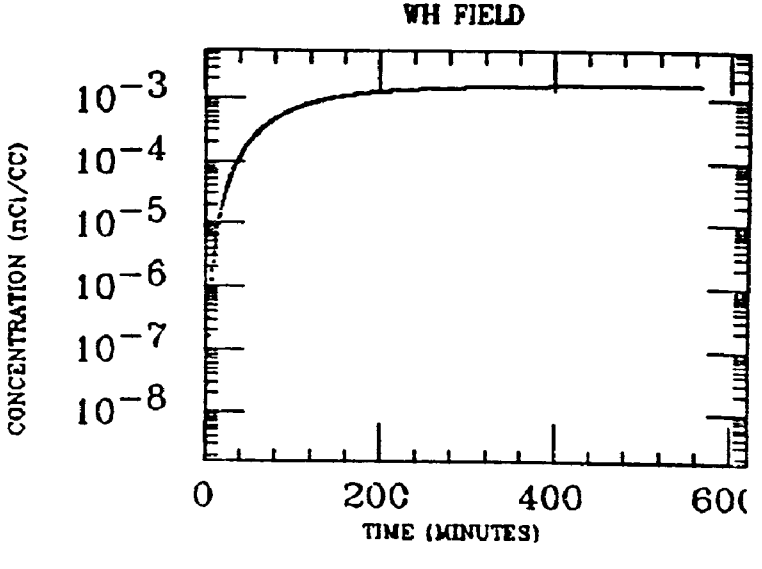

HUTCHINS
XE INGESTION
Pb-210

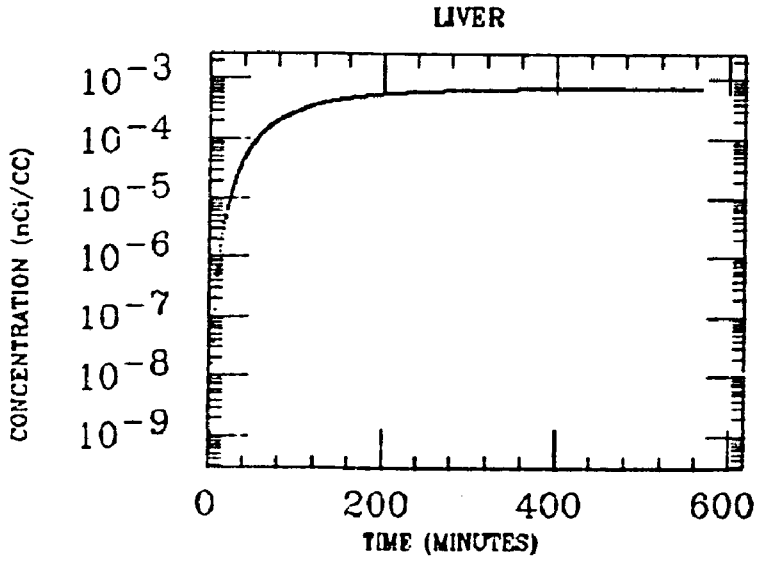

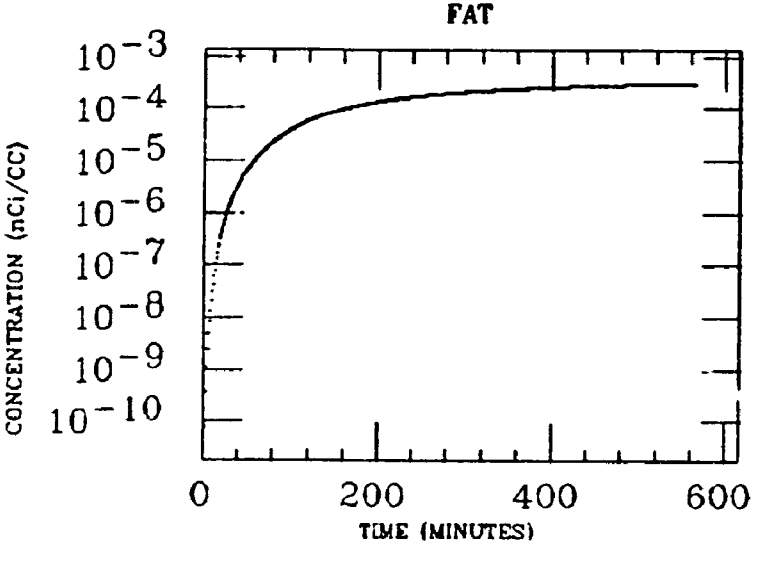

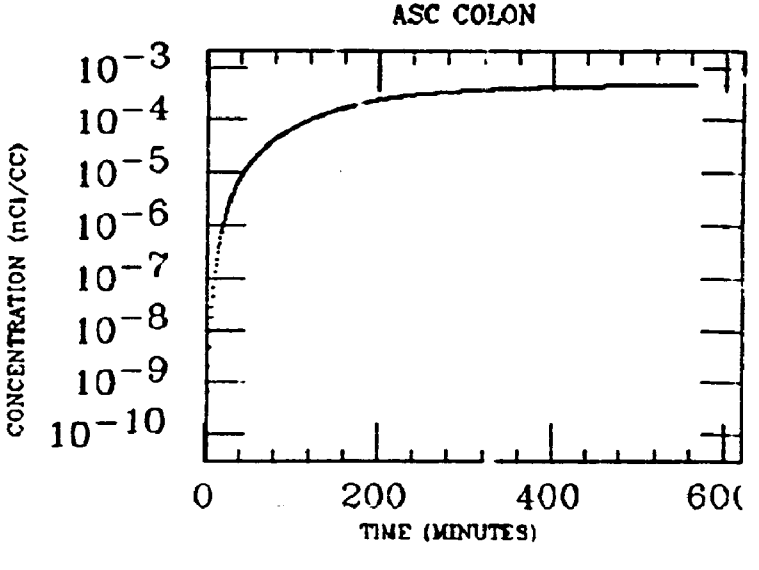

HUTCHINS
XE INGESTION
Pb-210

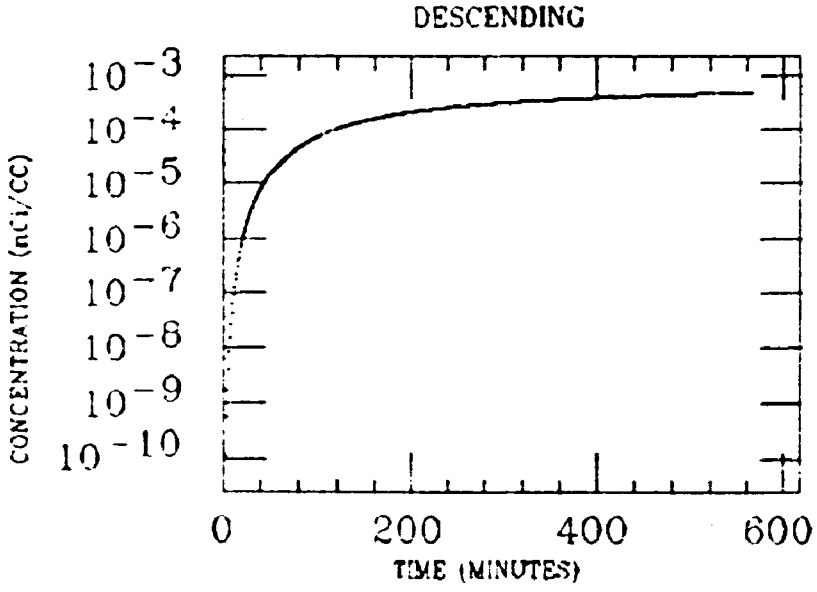

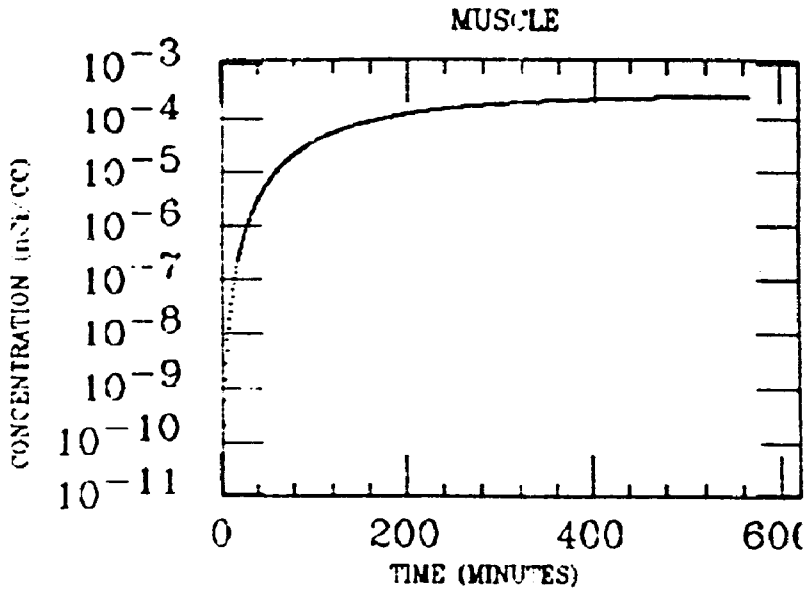

J.MCKINLEY
XE INGESTION
Pb-210

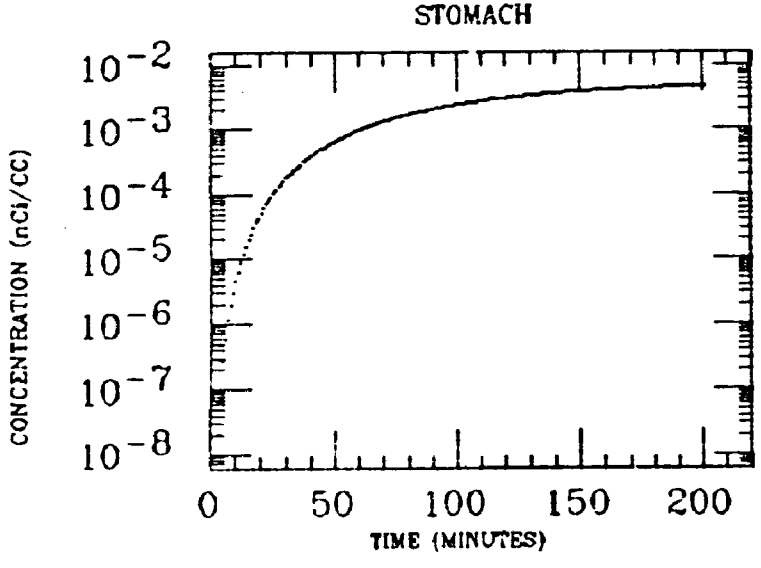

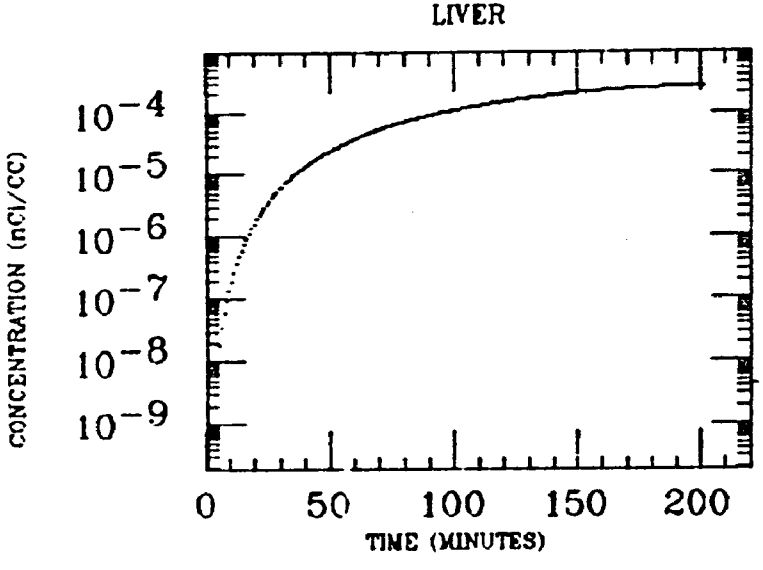

414

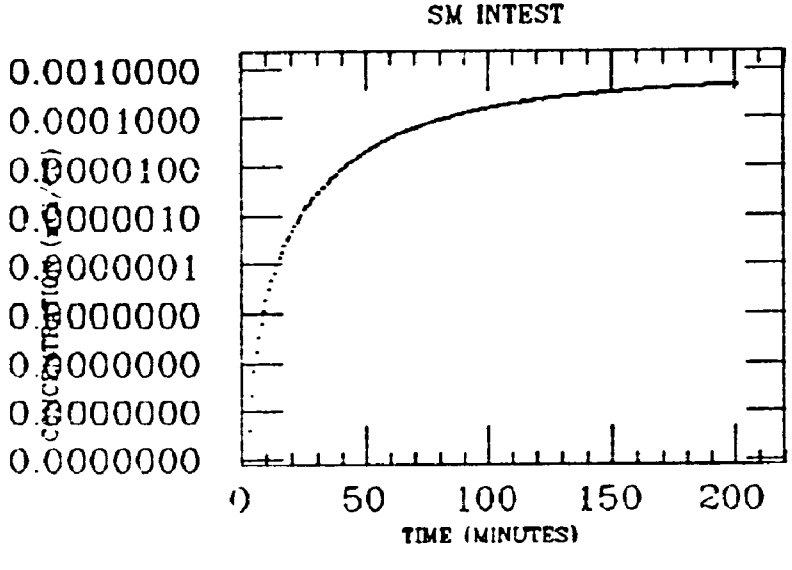

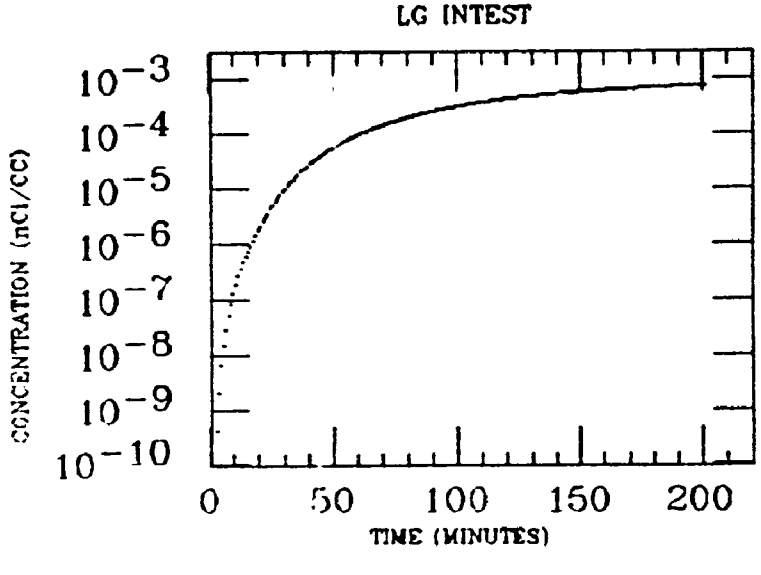

J.MCKINLEY
XE INGESTION
Pb-210

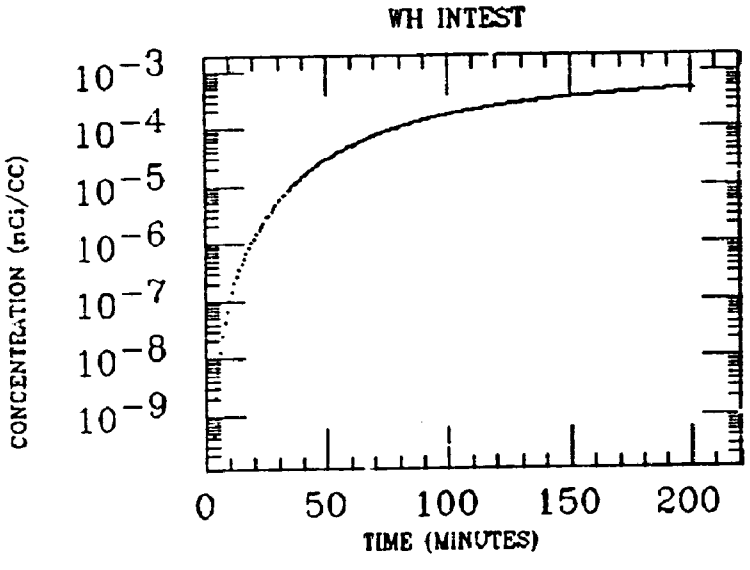

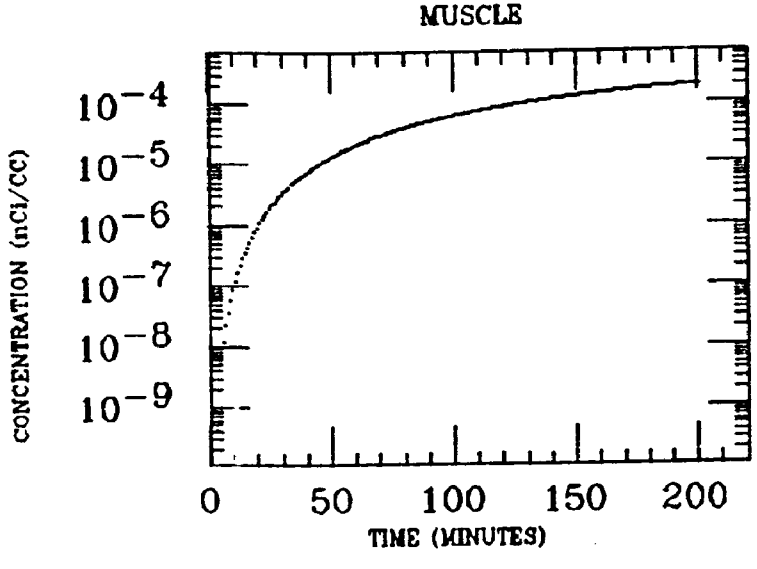

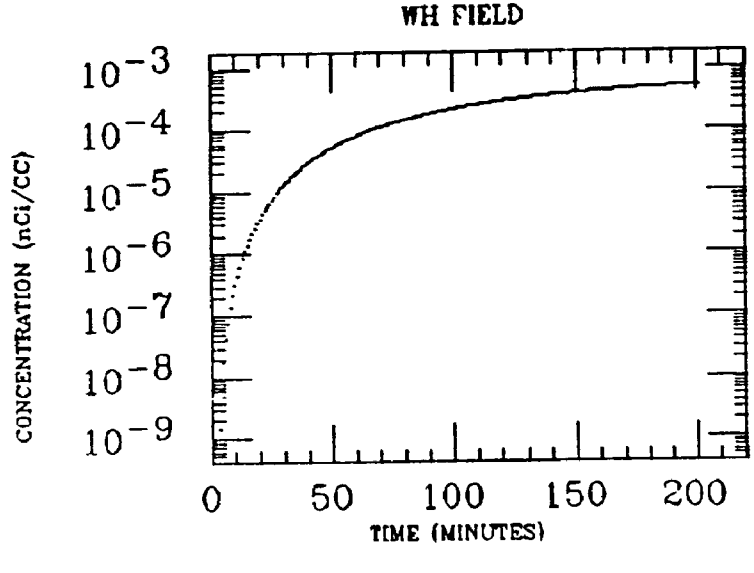

KELLEHER
XE INGESTION
Pb-210

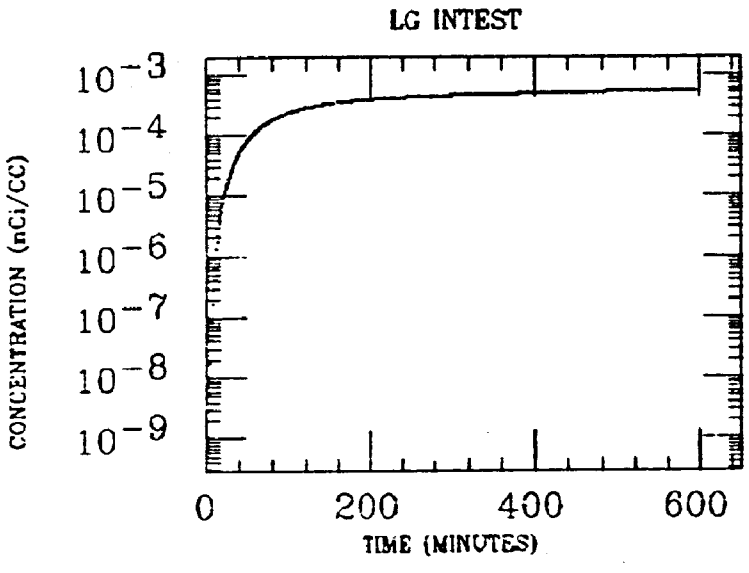

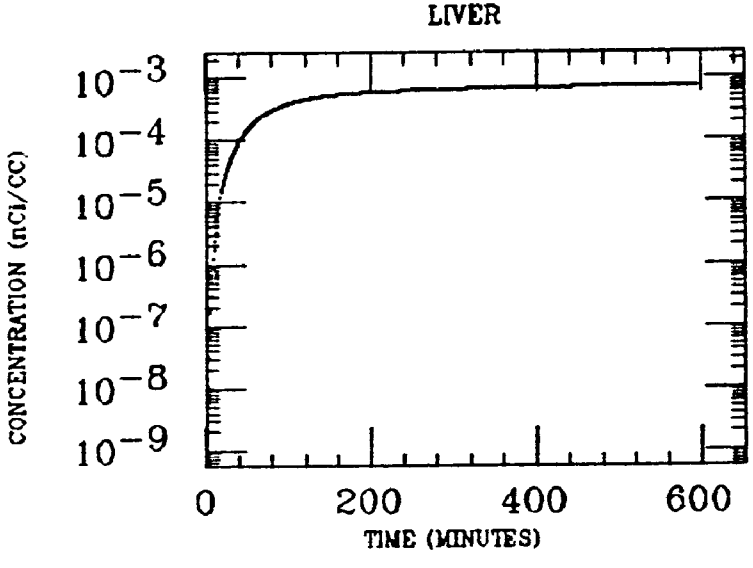

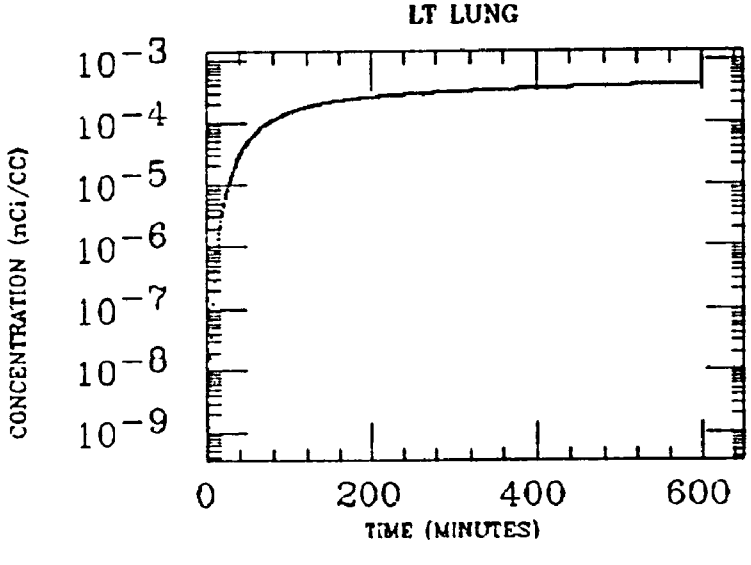

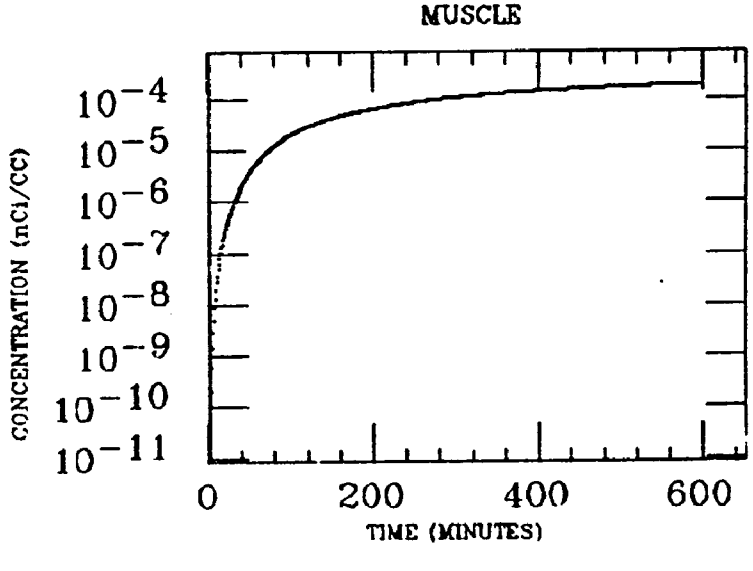

KELLEHER
XE INGESTION
Pb-210

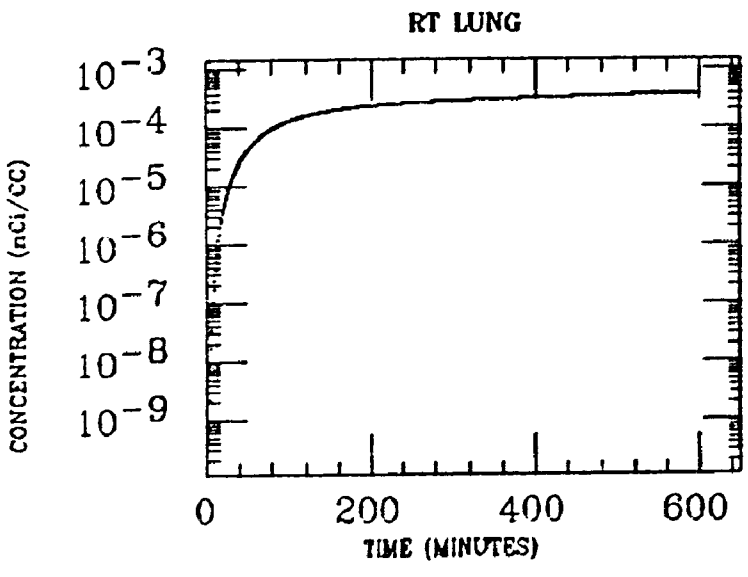

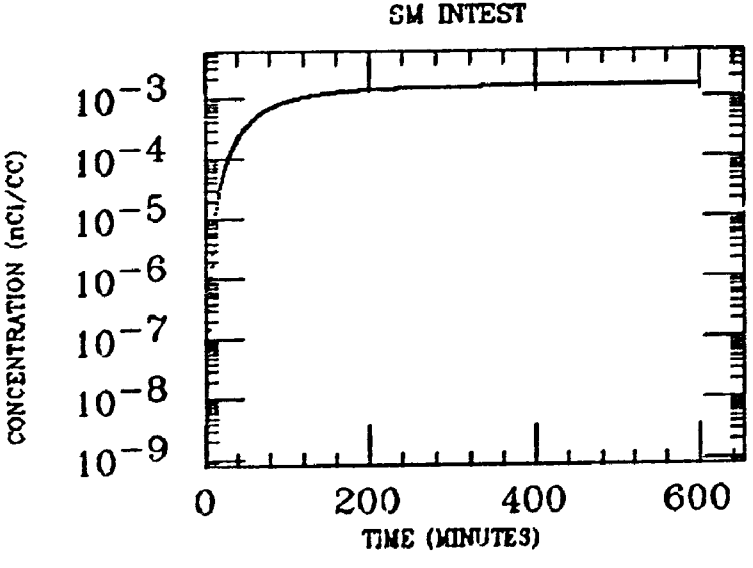

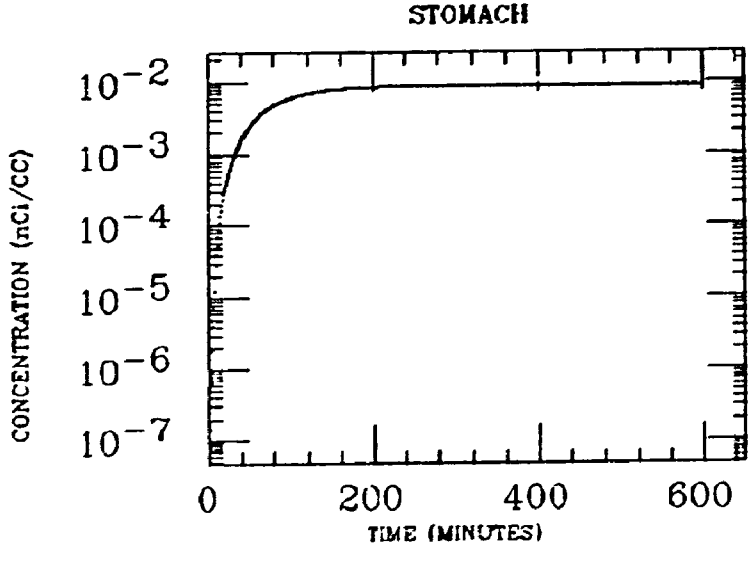

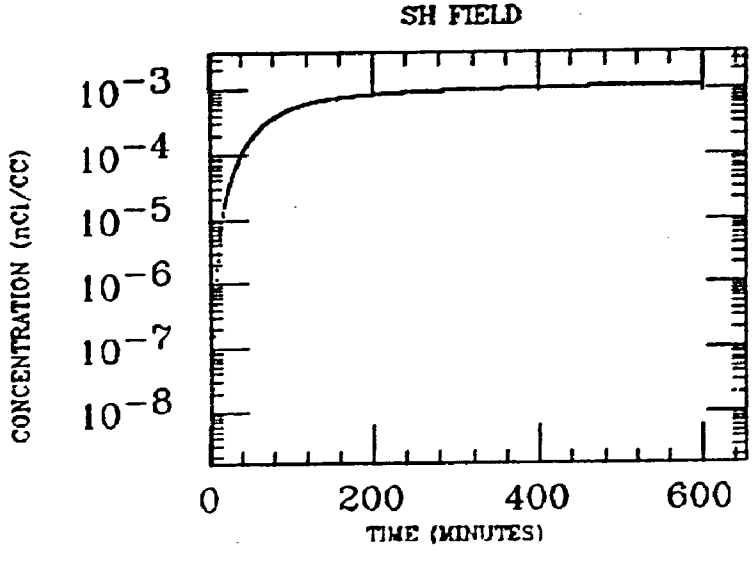

LITTELL
XE INGESTION
Pb-210

STOMACH

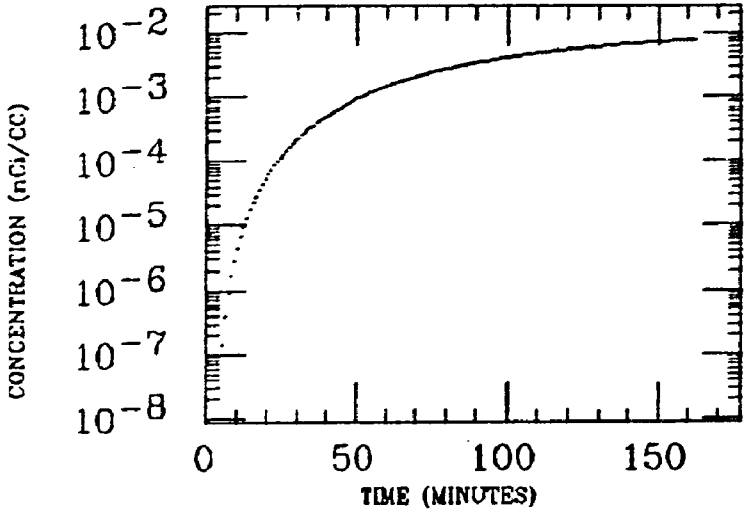

SM INTEST

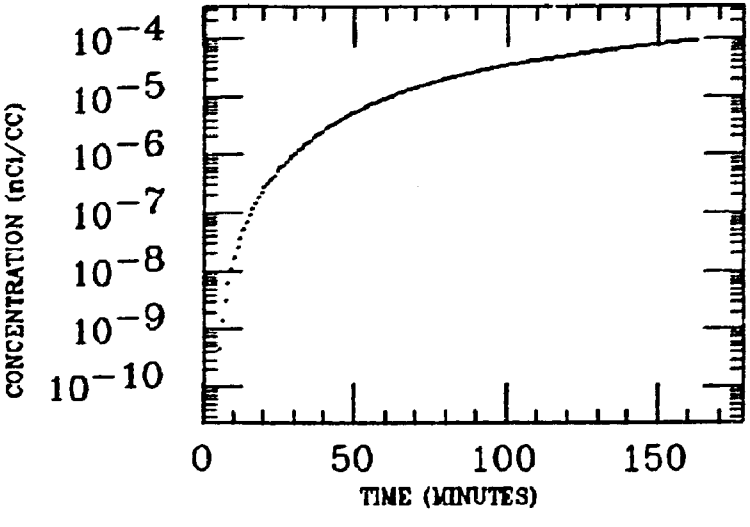

ASC COLON

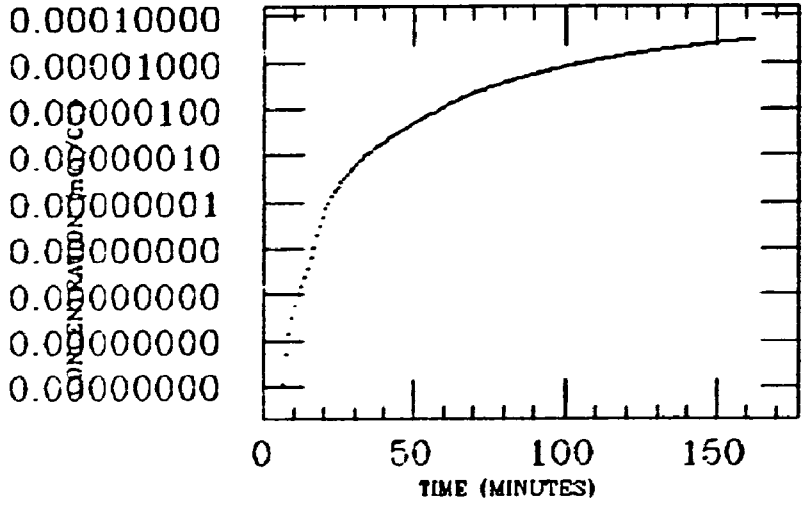

LIVER

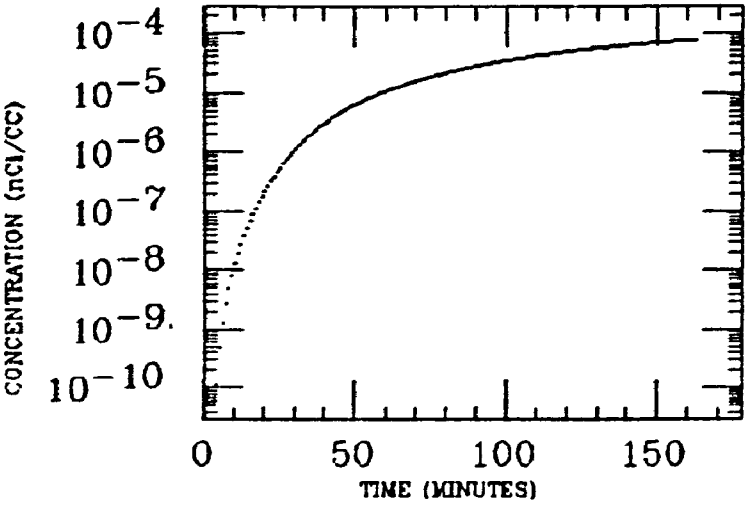

LITTELL
XE INGESTION
Pb-210

MUSCLE

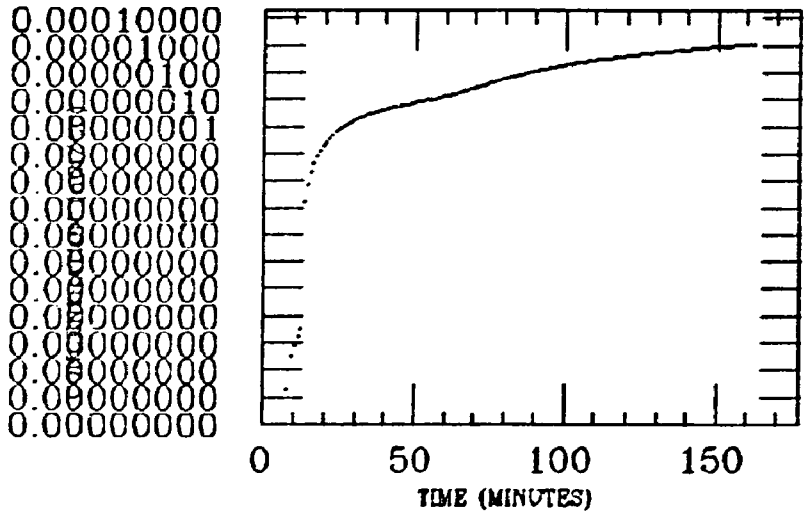

WH INTEST

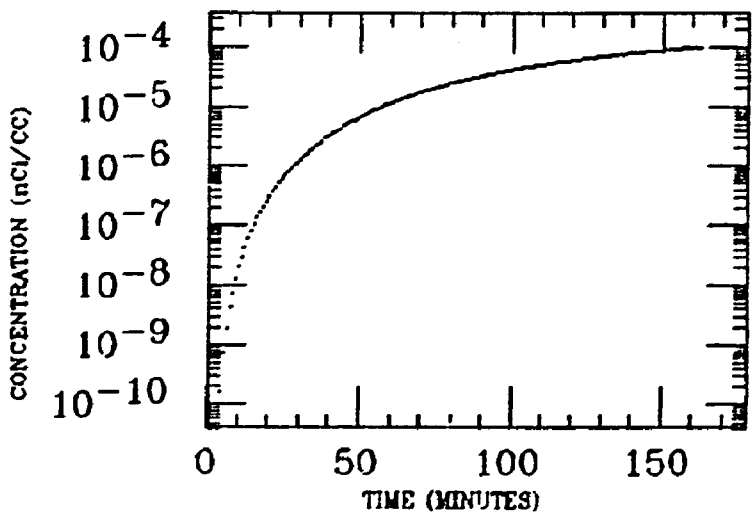

WH FIELD

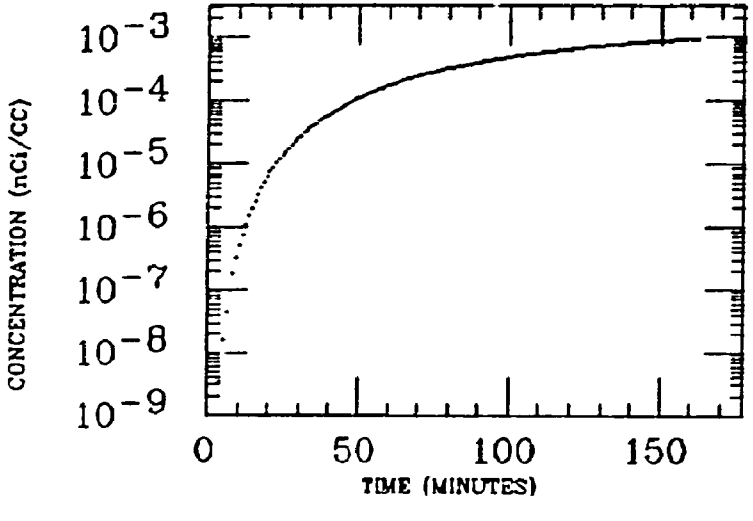

MACMILLAN
XE INGESTION
Pb-210

ASC COLON

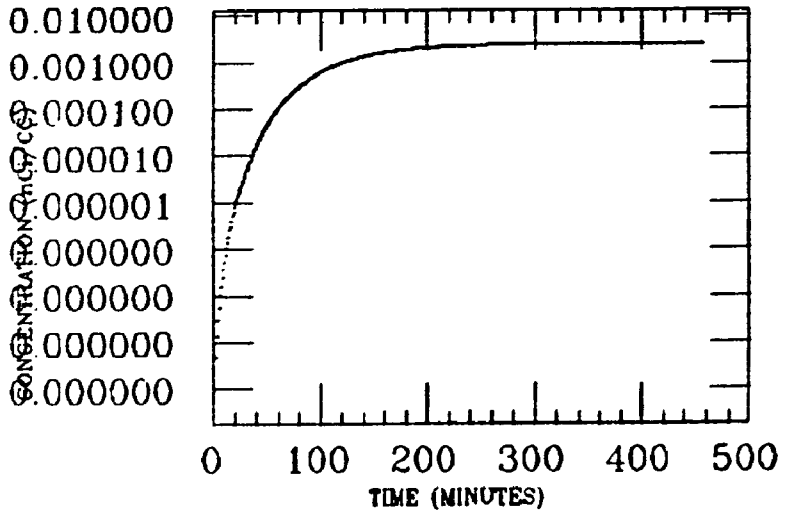

DES COLON

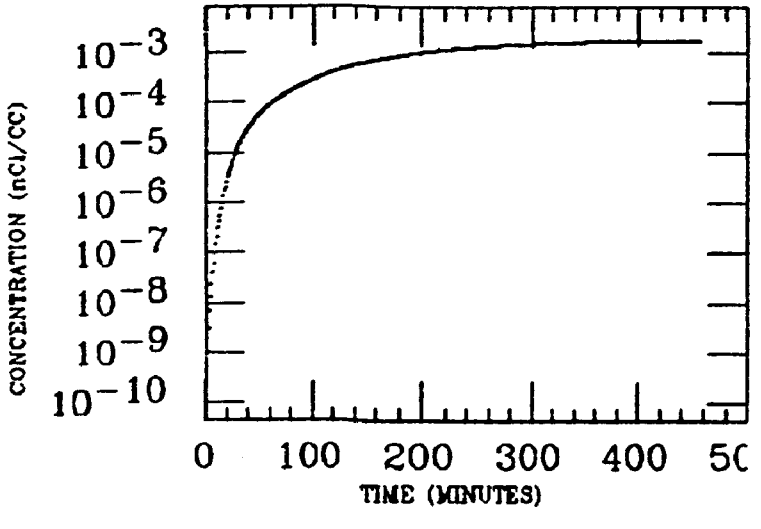

420

HIP

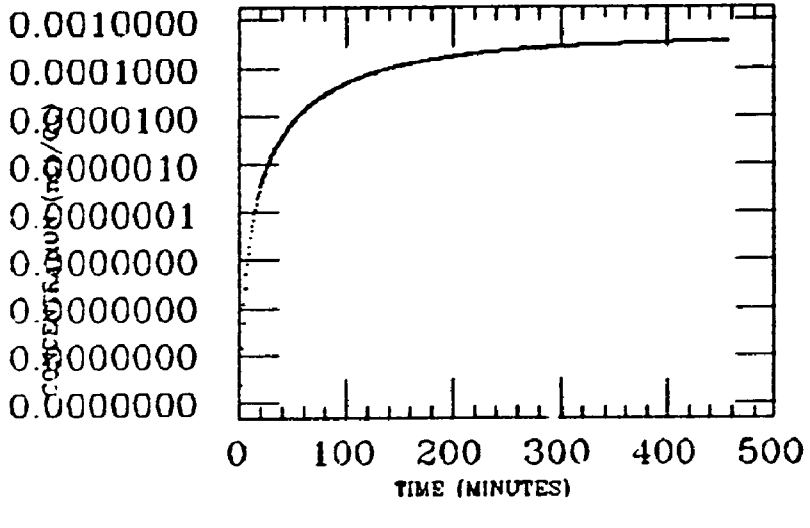

LIVER

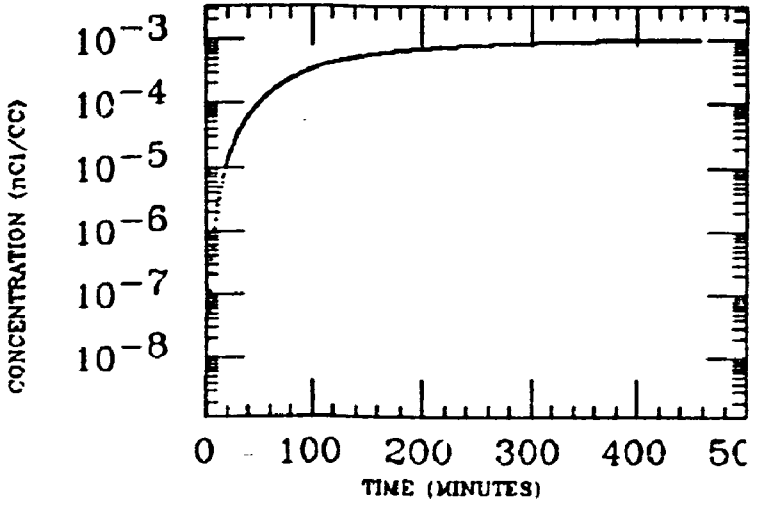

MACMILLAN
XE INGESTION
Pb-210

SM INTEST

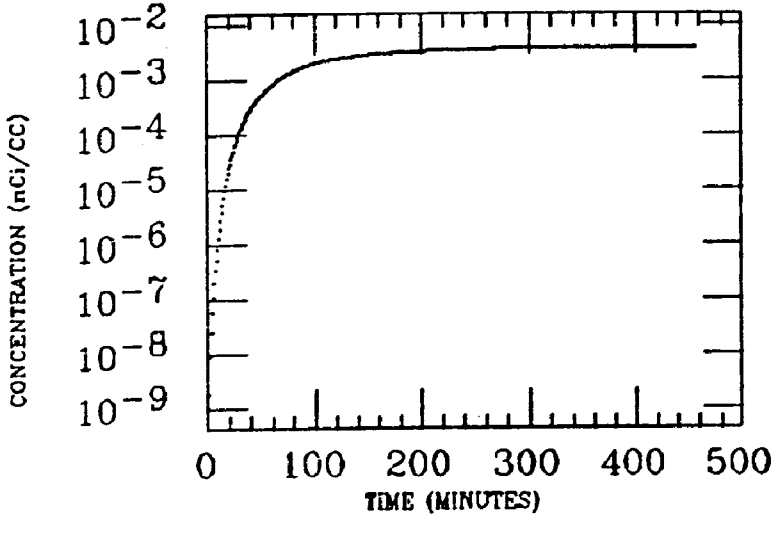

STOMACH

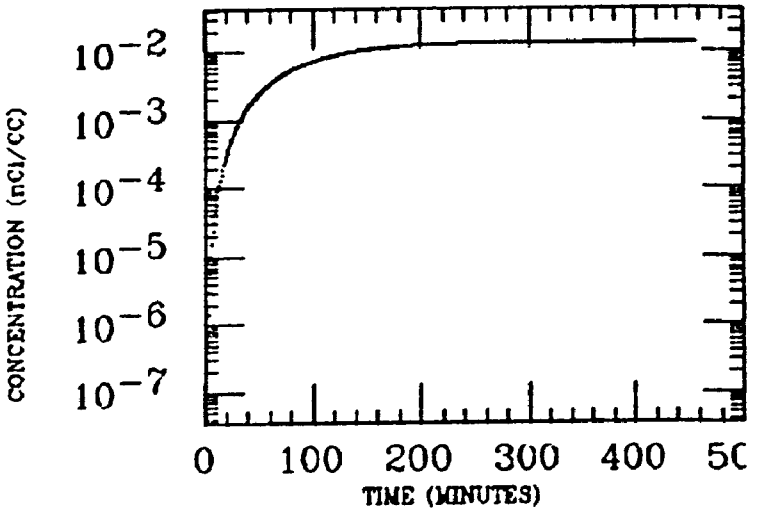

TR COLON

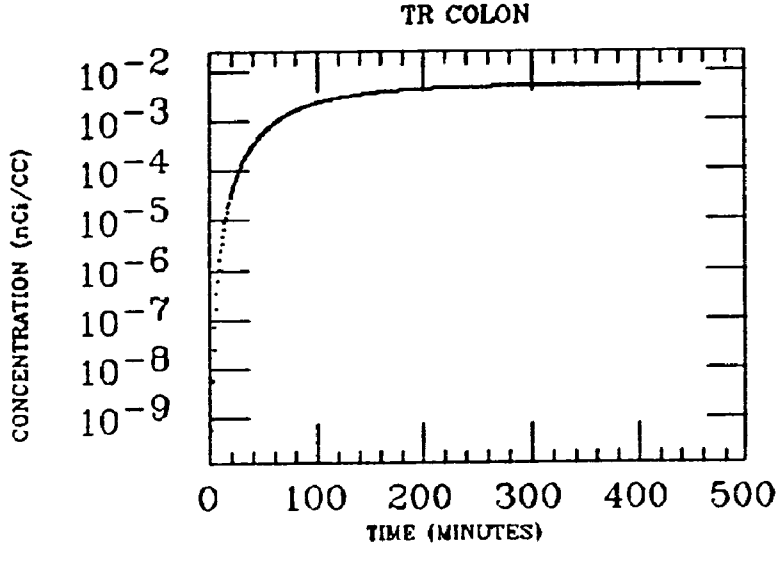

WH INTEST

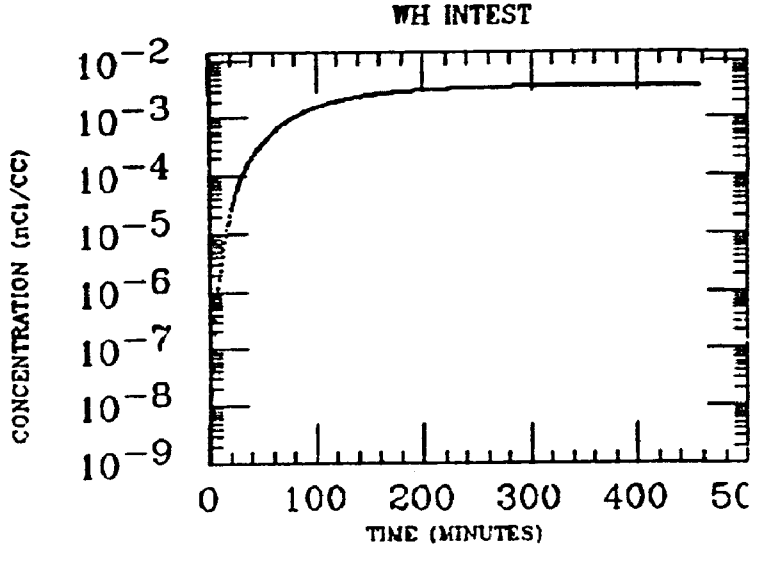

MAIO

XE INGESTION

Pb-210

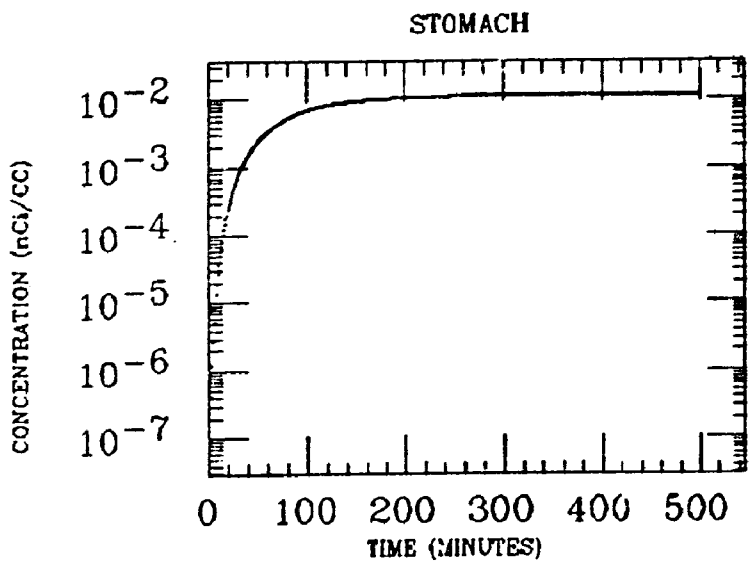

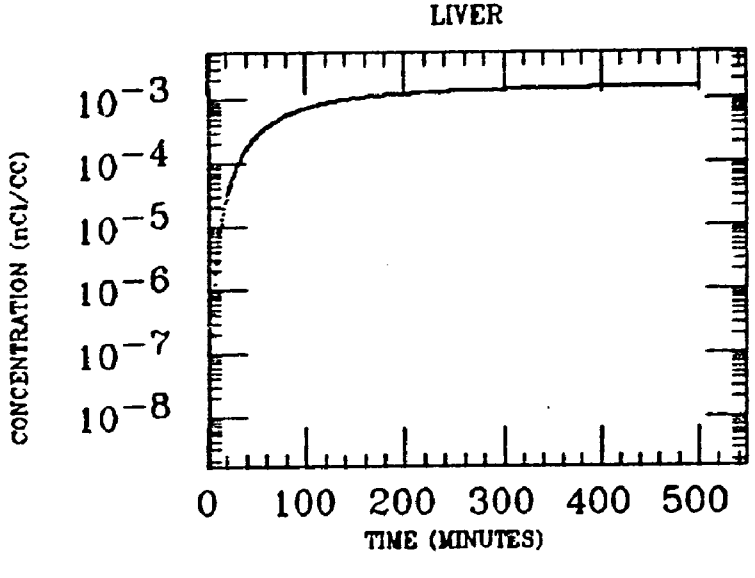

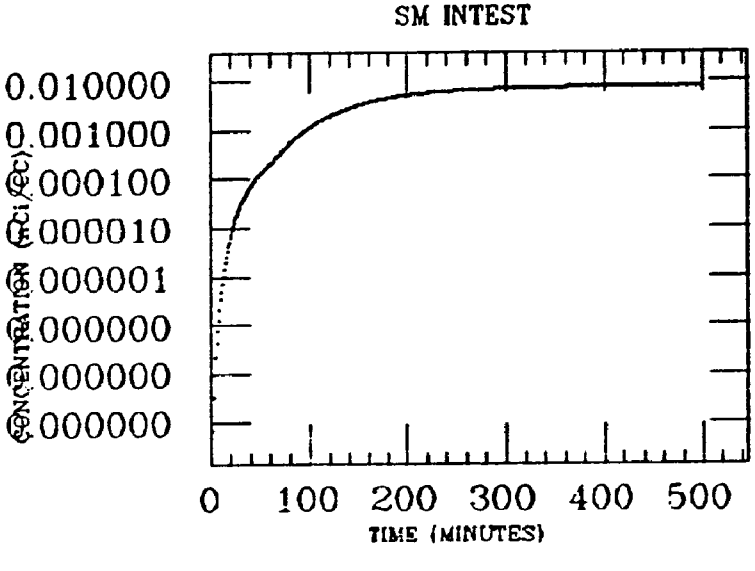

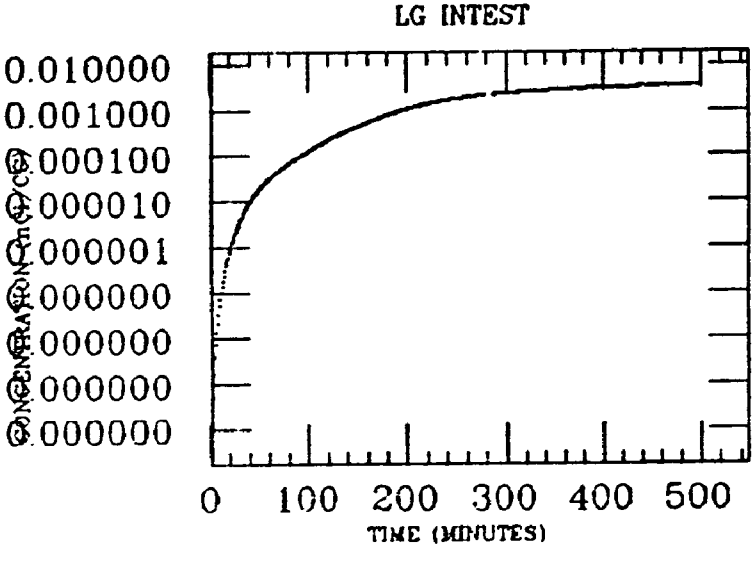

MAIO
XE INGESTION
Pb-210

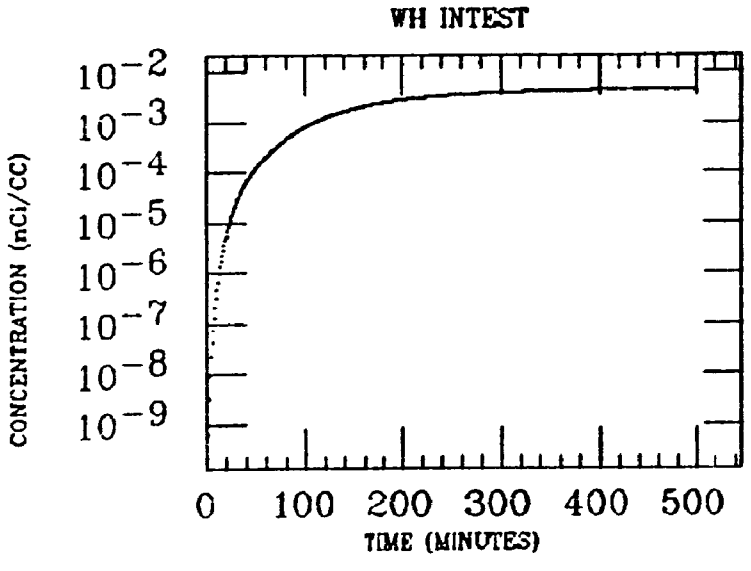

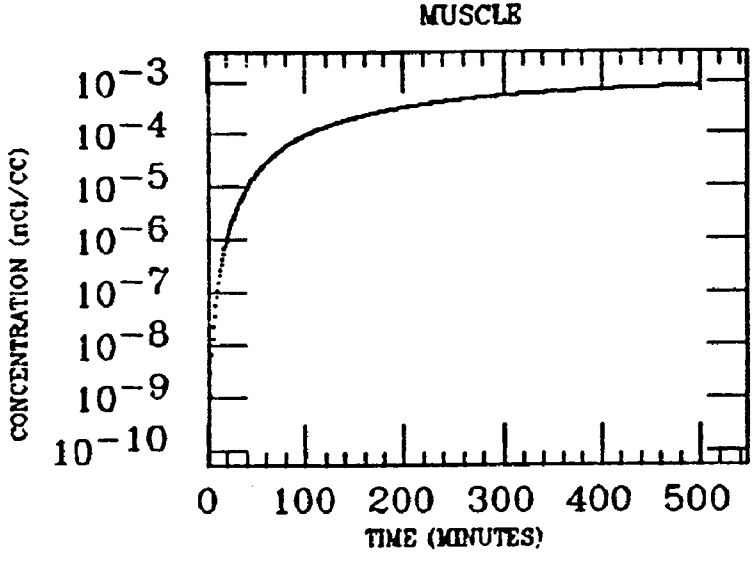

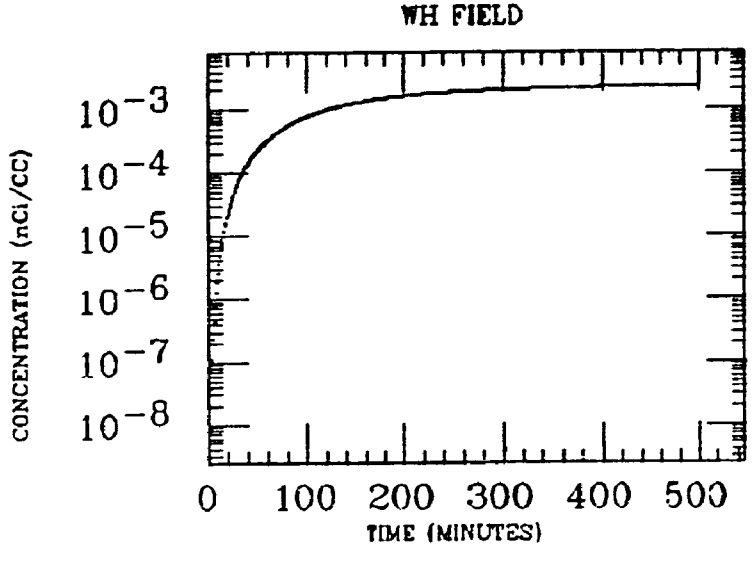

MALCOM
XE INGESTION
Pb-210

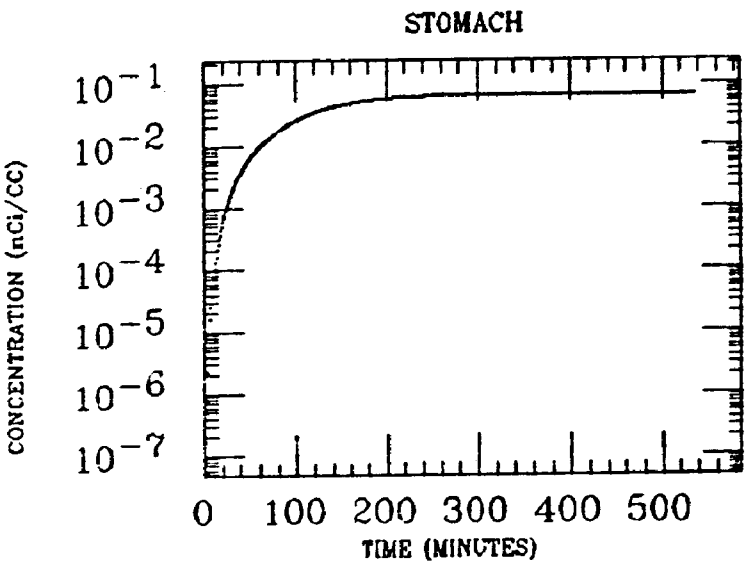

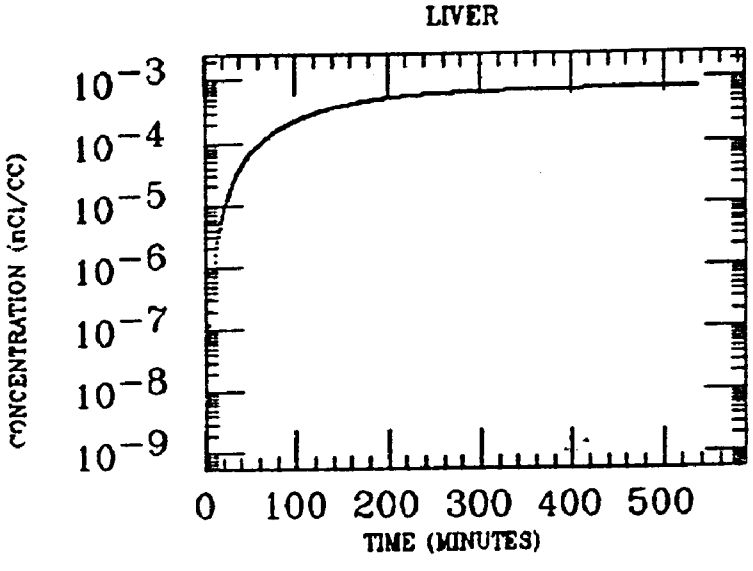

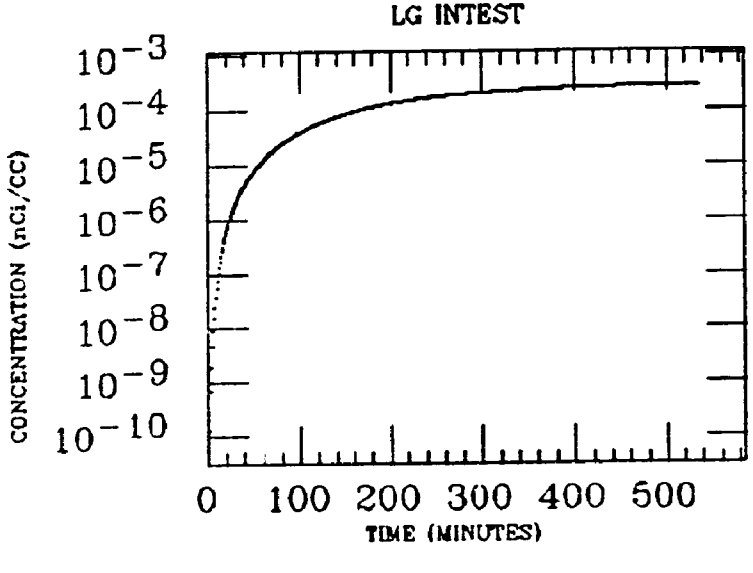

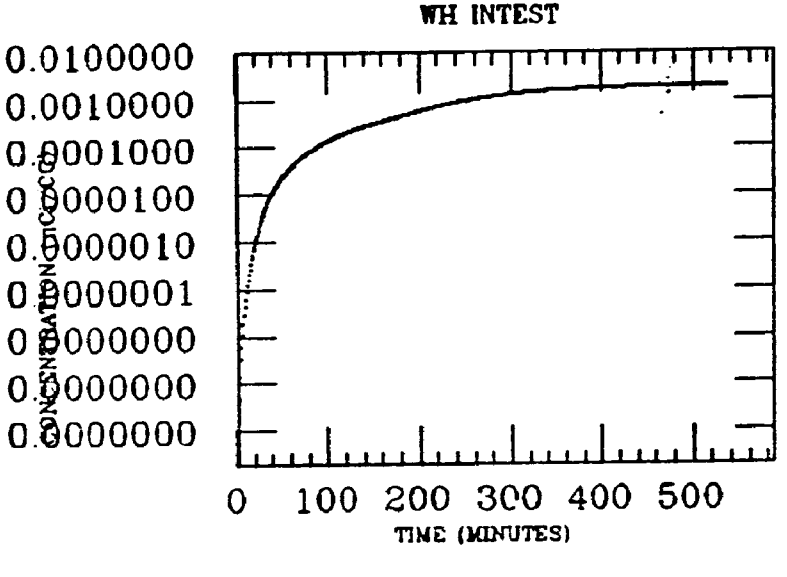

MALCOM
XE INGESTION
Pb-210

MUSCLE

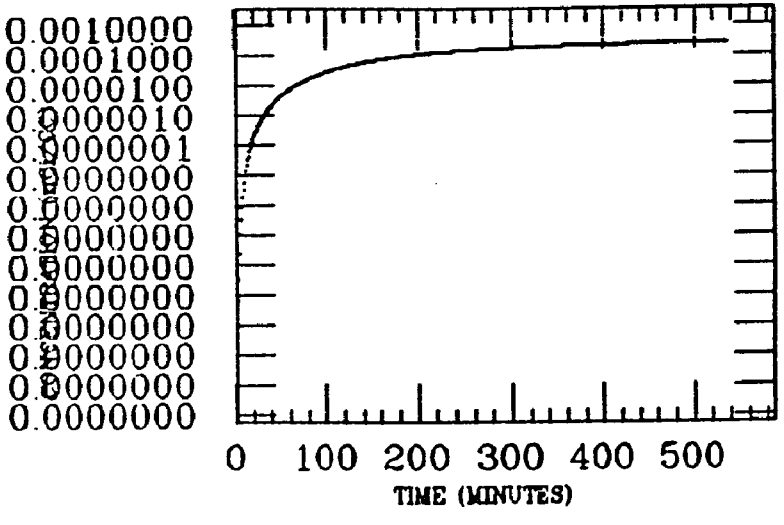

WH FIELD

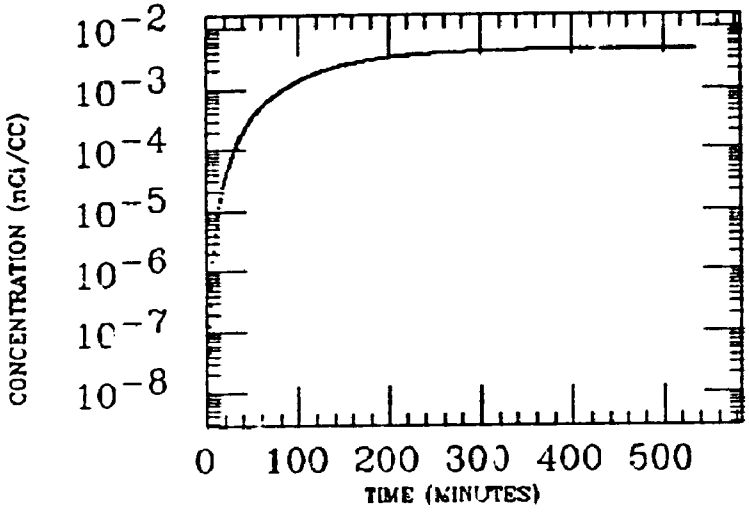

SM INTEST

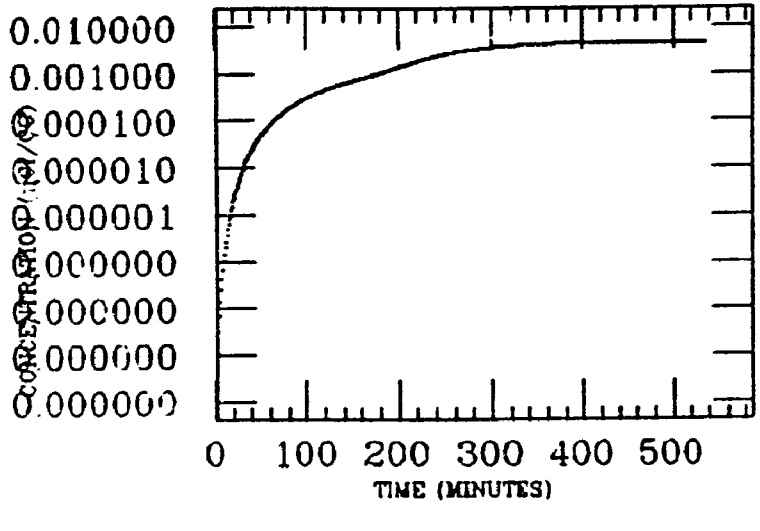

MONROE
XE INGESTION
Pb-210

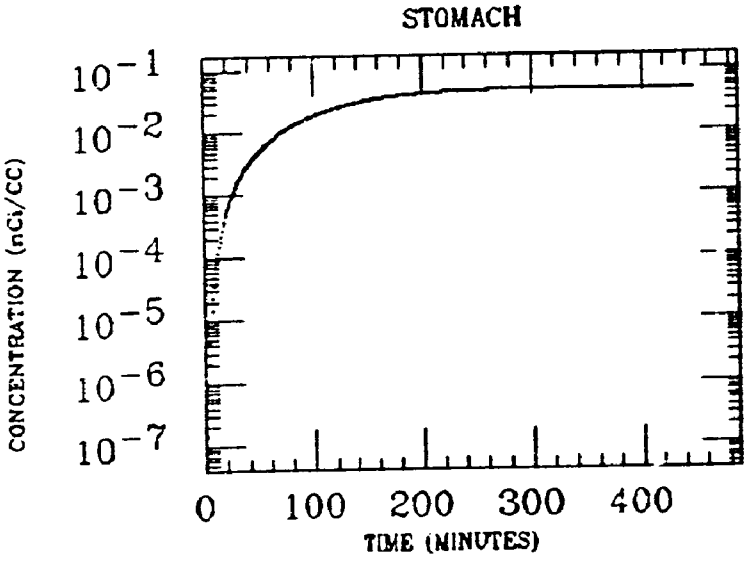

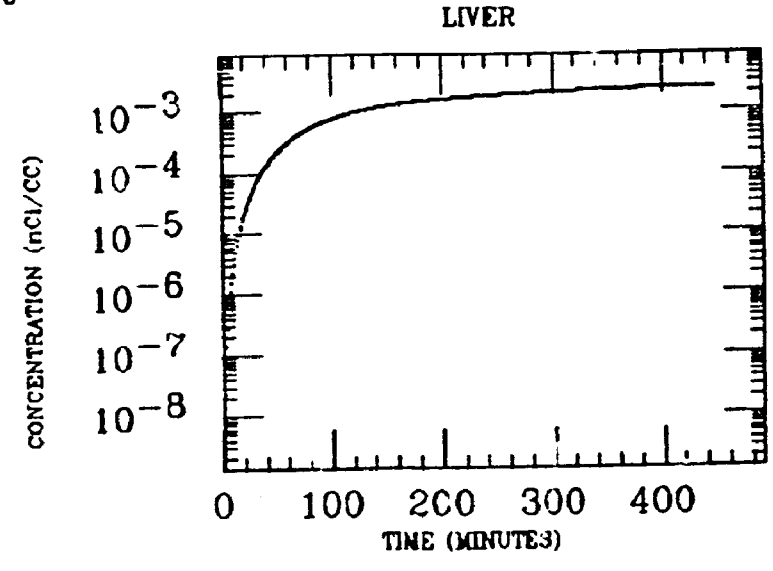

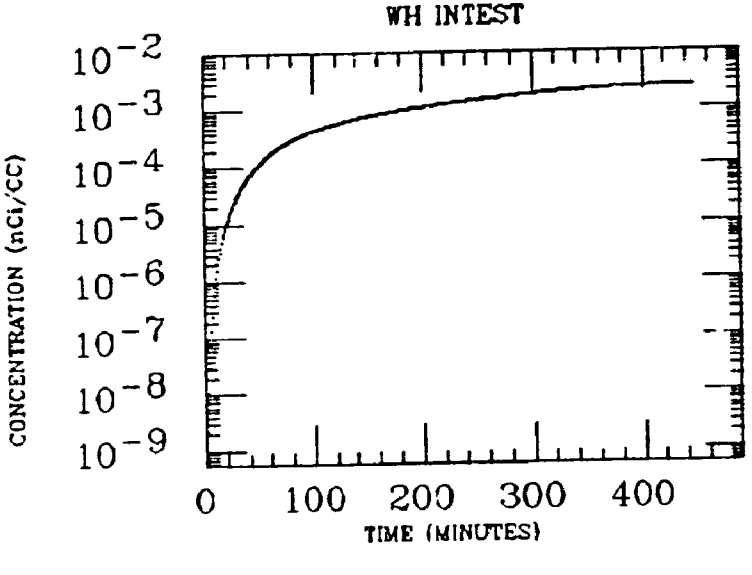

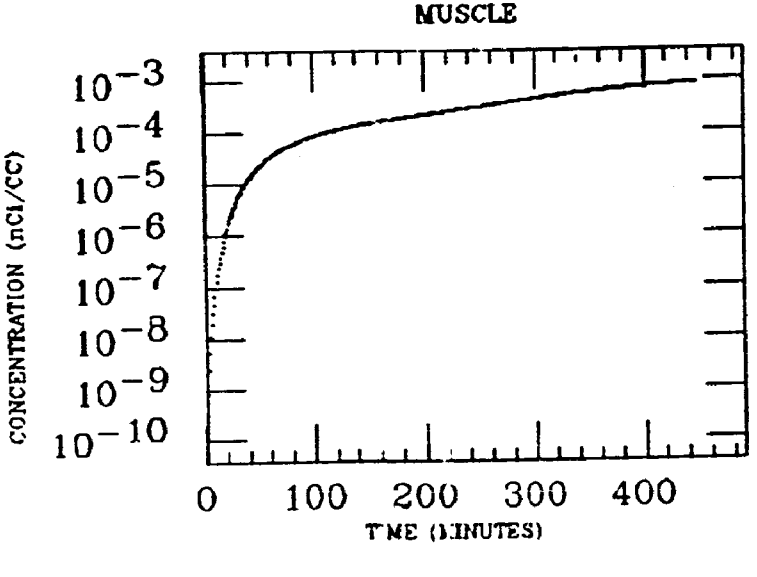

MONROE
XE INGESTION
Pb-210

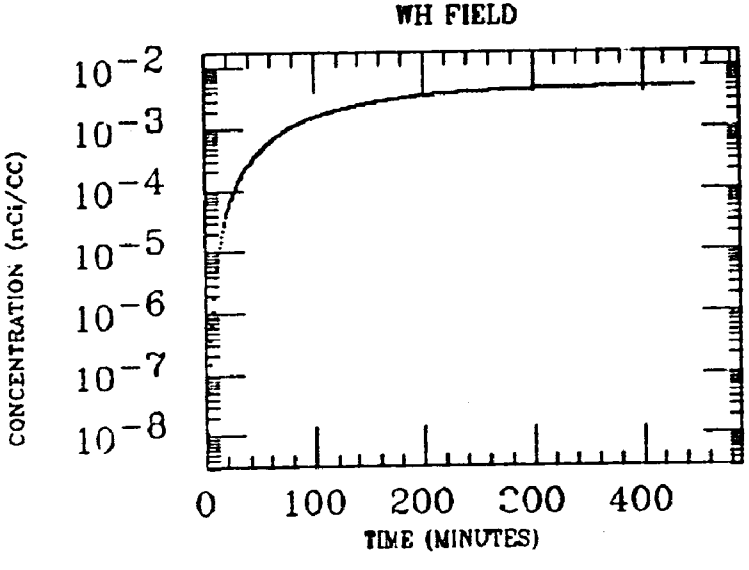

MORGAN
XE INGESTION
Pb-210

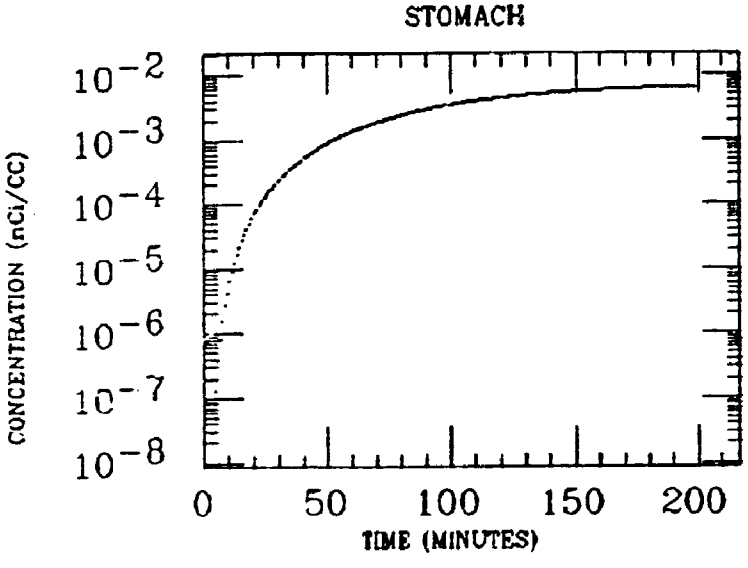

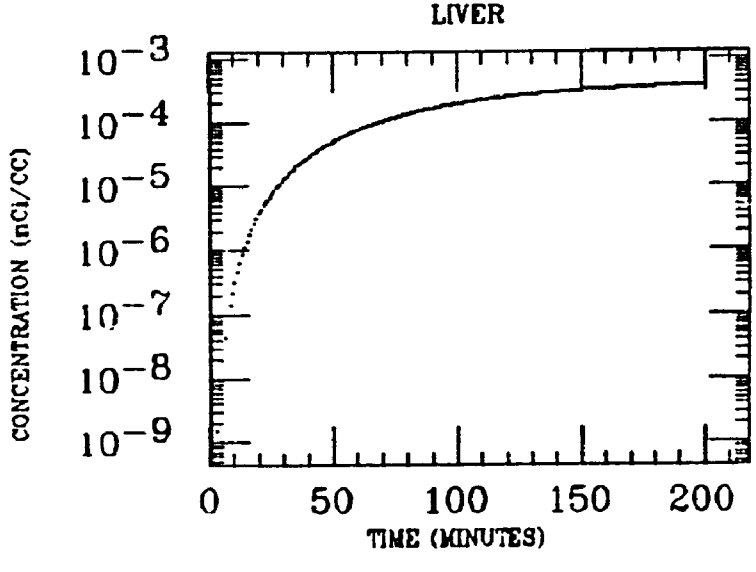

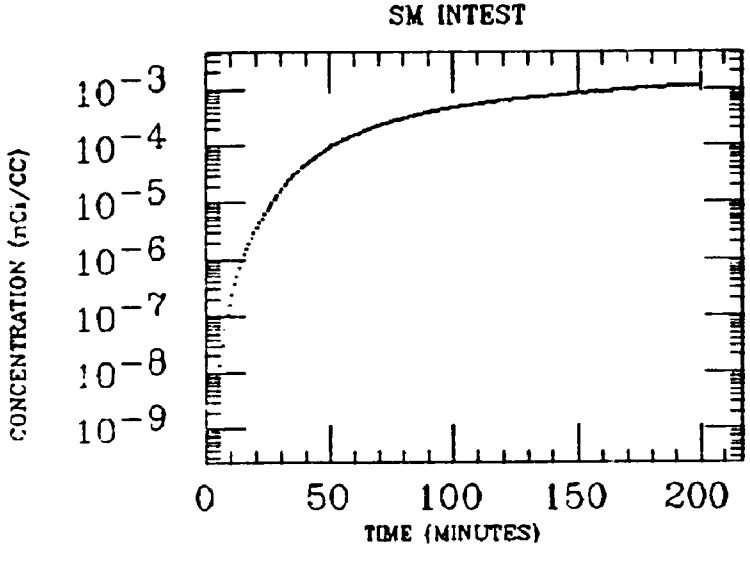

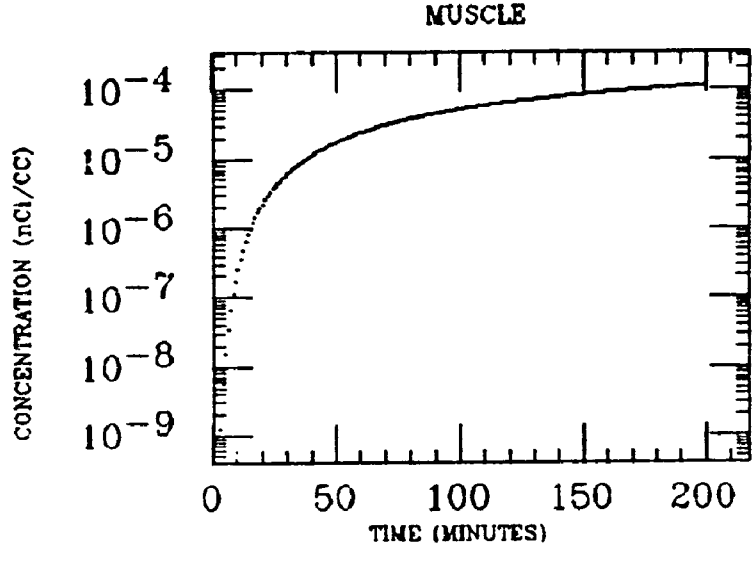

MORGAN
XE INGESTION
Pb-210

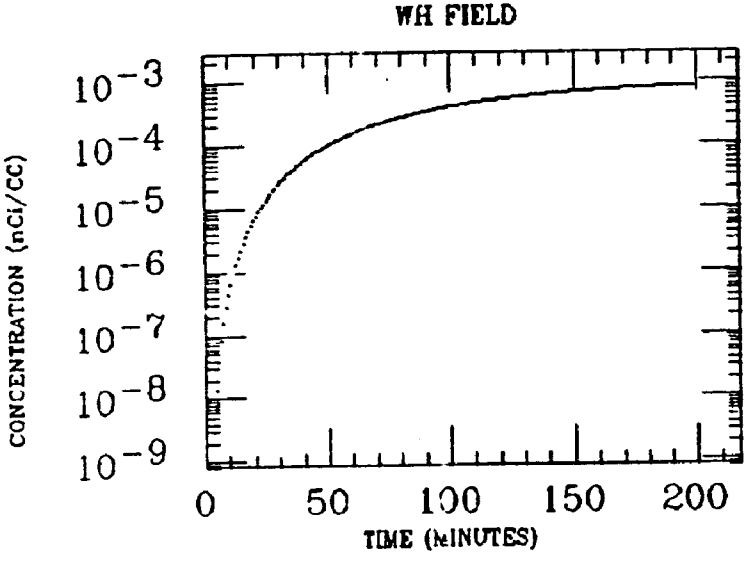

MURCHE
XE INGESTION
Pb-210

STOMACH

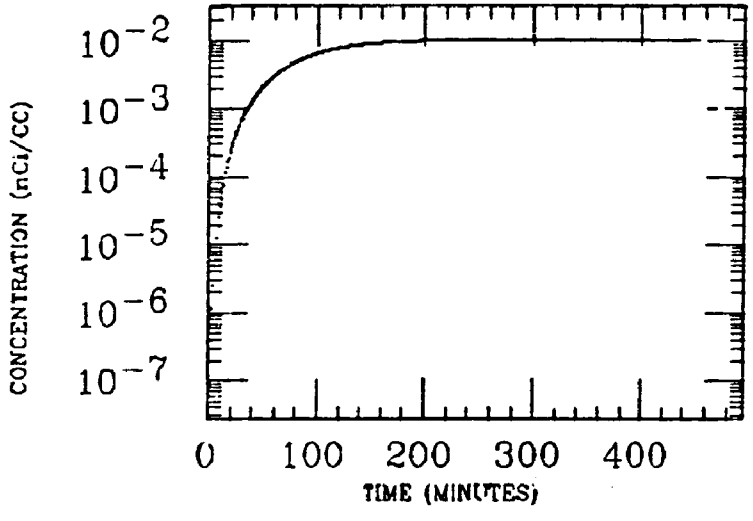

LIVER

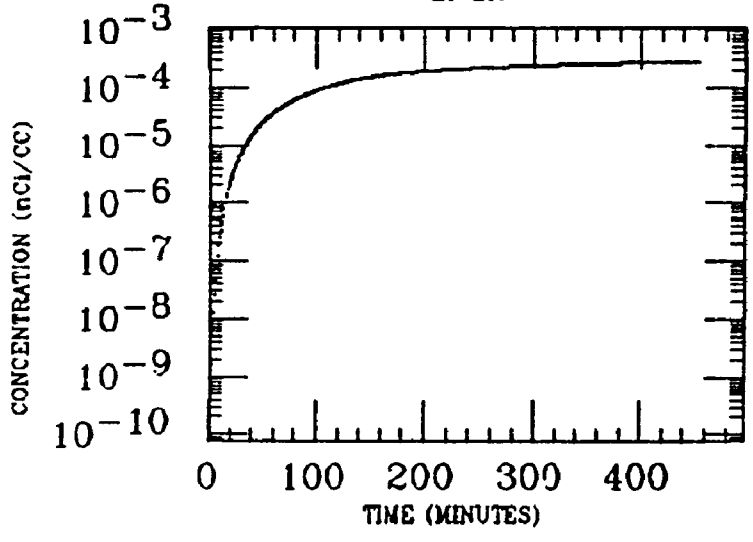

WH FIELD

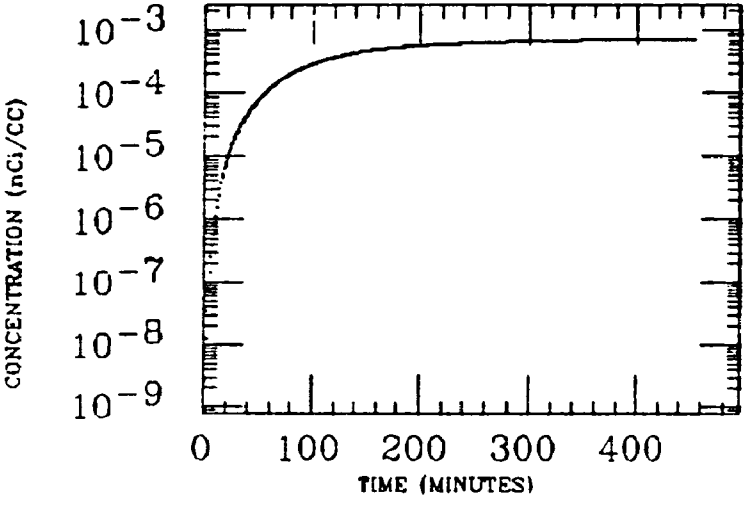

MURCHE
XE INGESTION
Pb-210

STOMACH

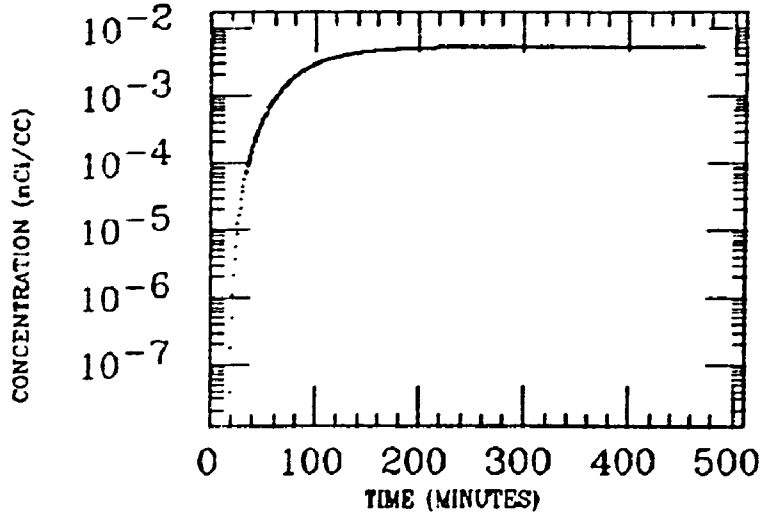

LIVER

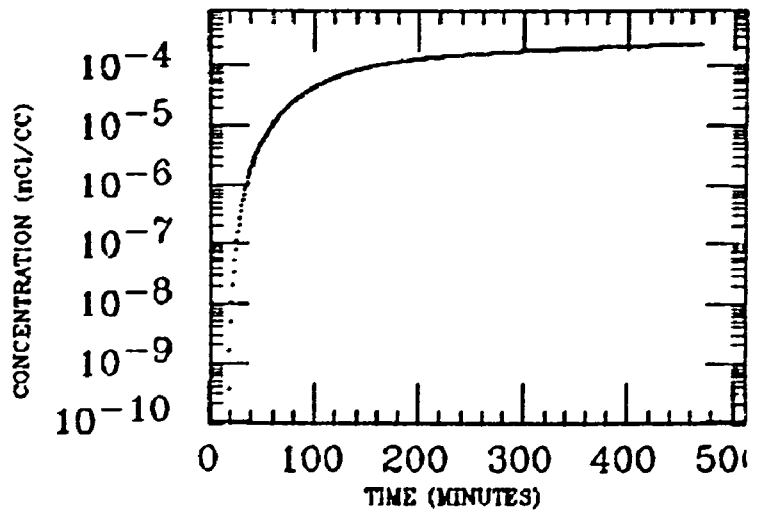

SM INTEST

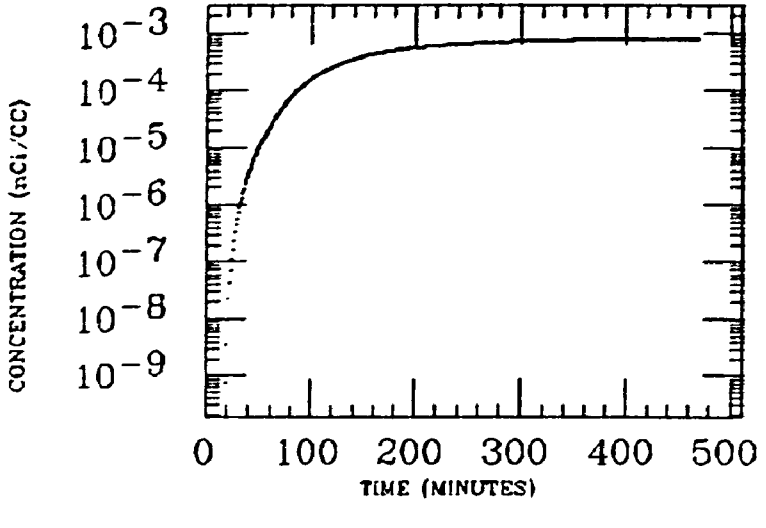

DES COLON

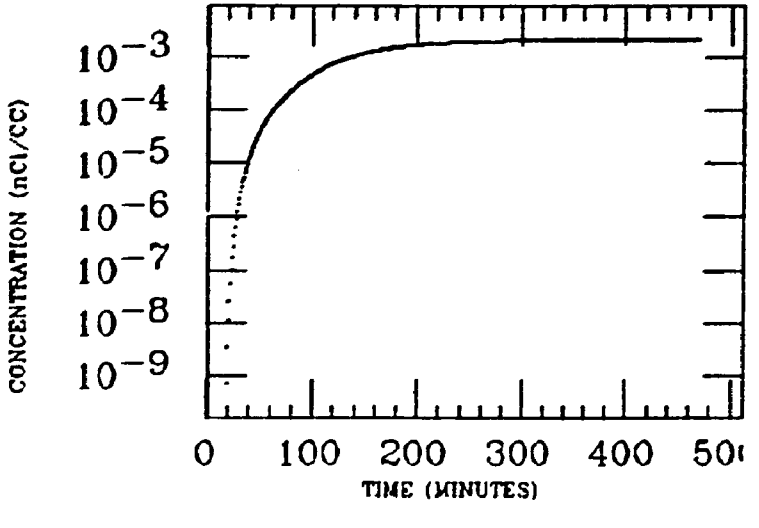

MURCHE
XE INGESTION
Pb-210

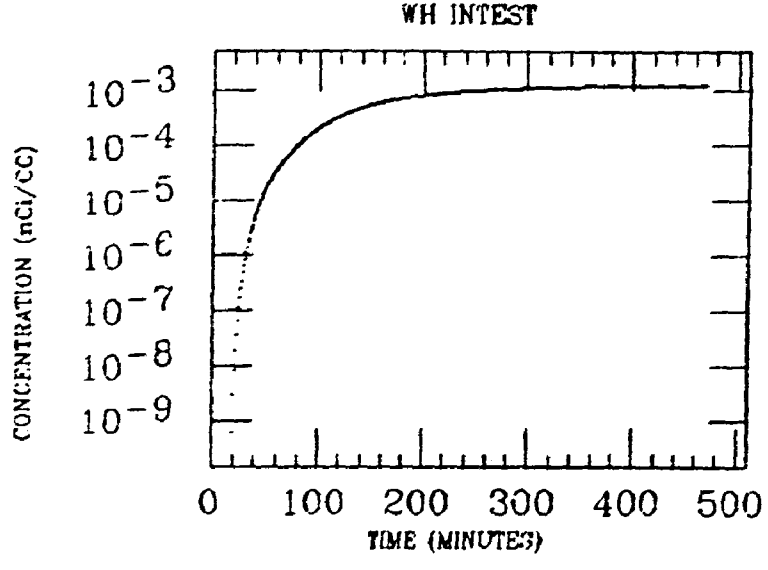

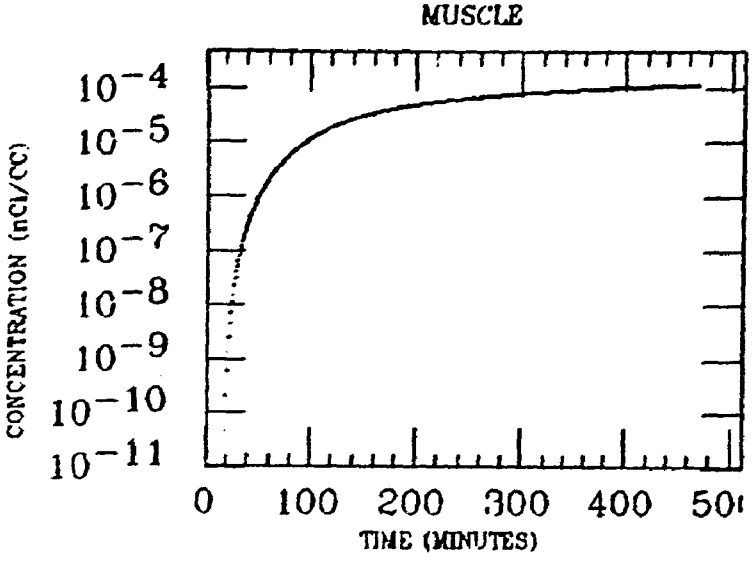

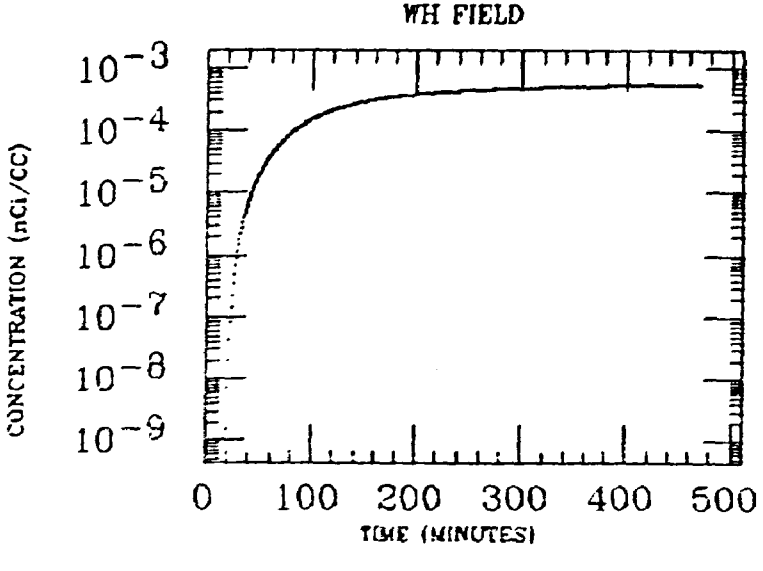

PARK
XE INGESTION
Pb-210

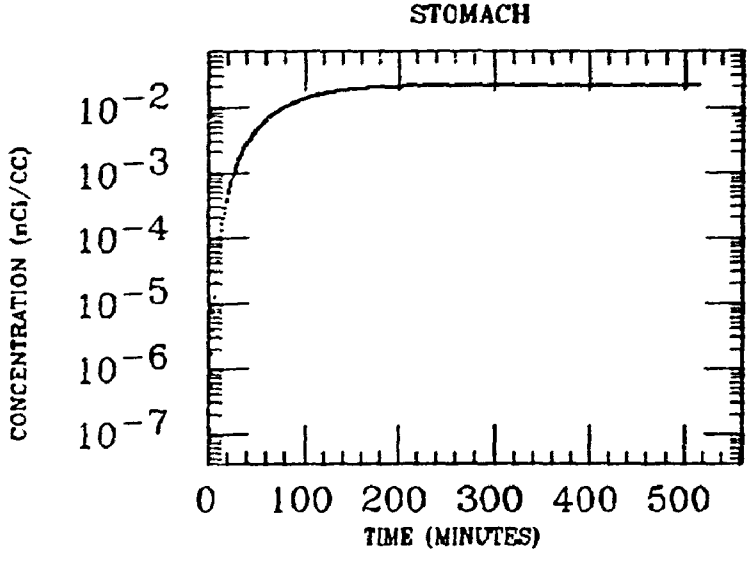

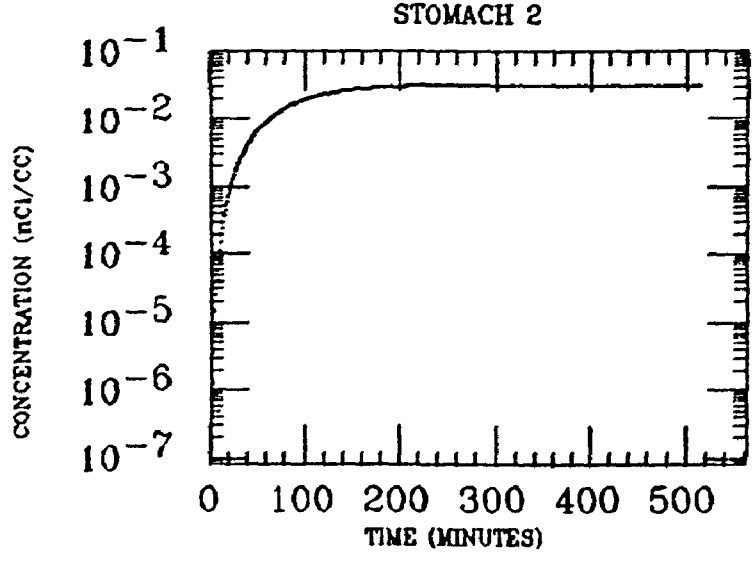

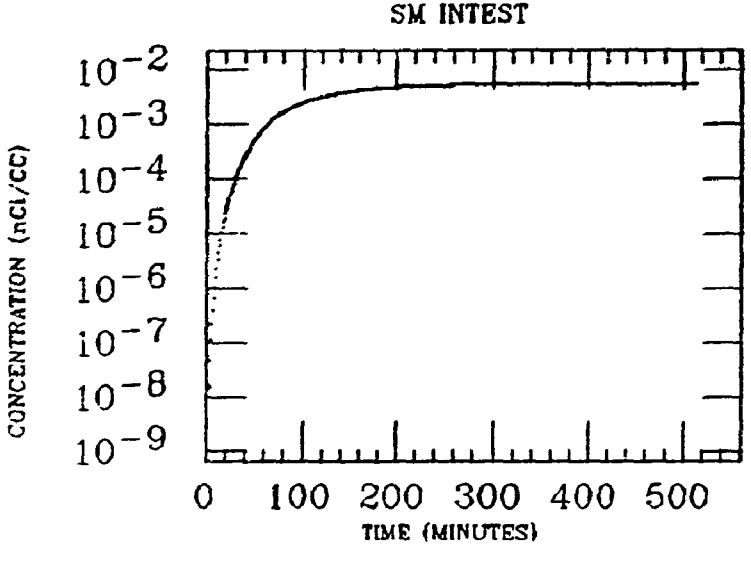

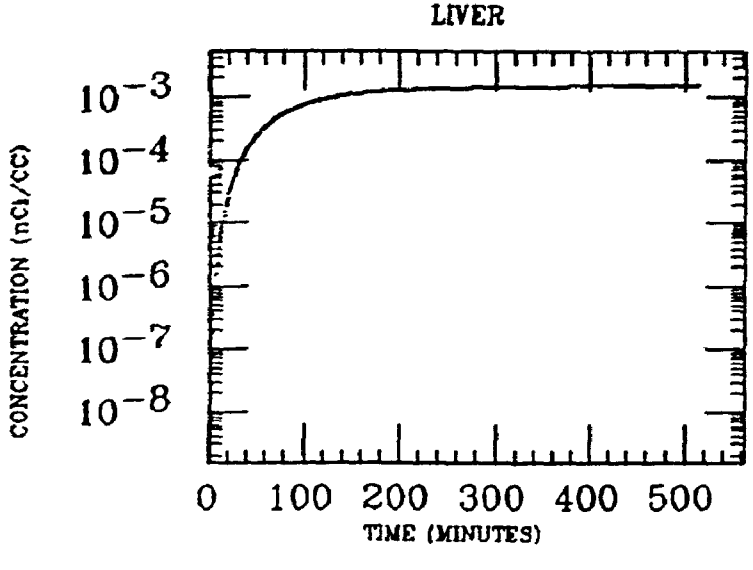

PARK

XE INGESTION

Pb-210

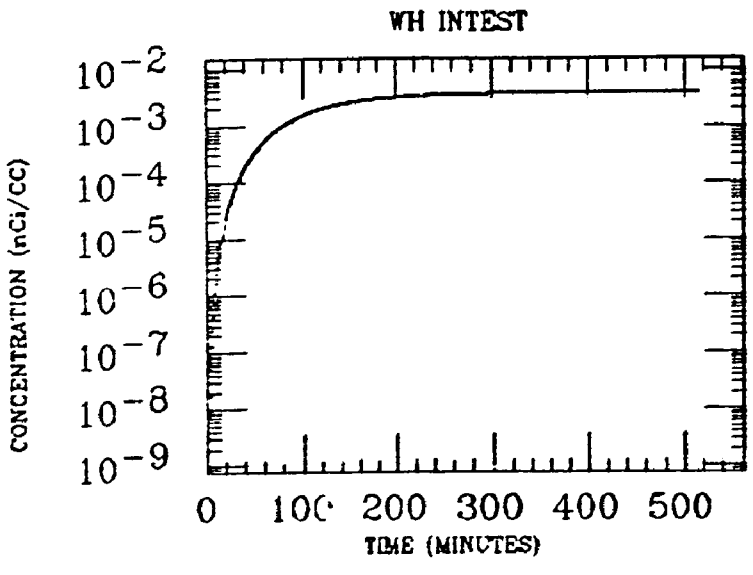

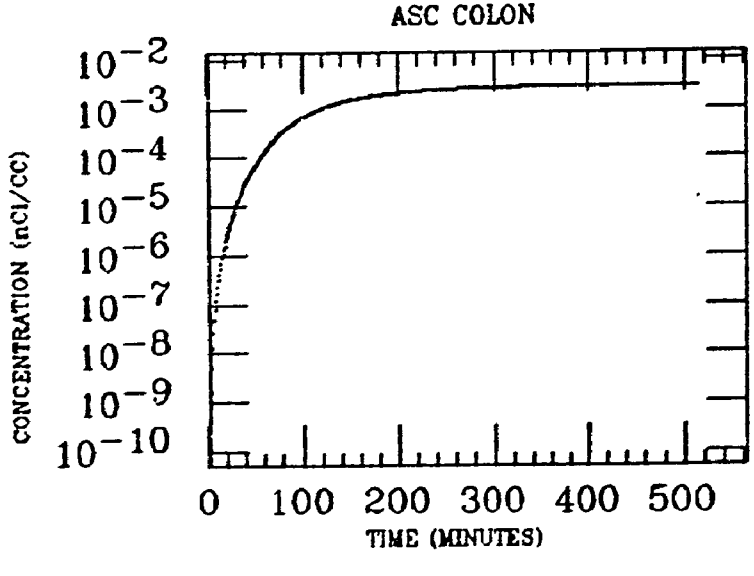

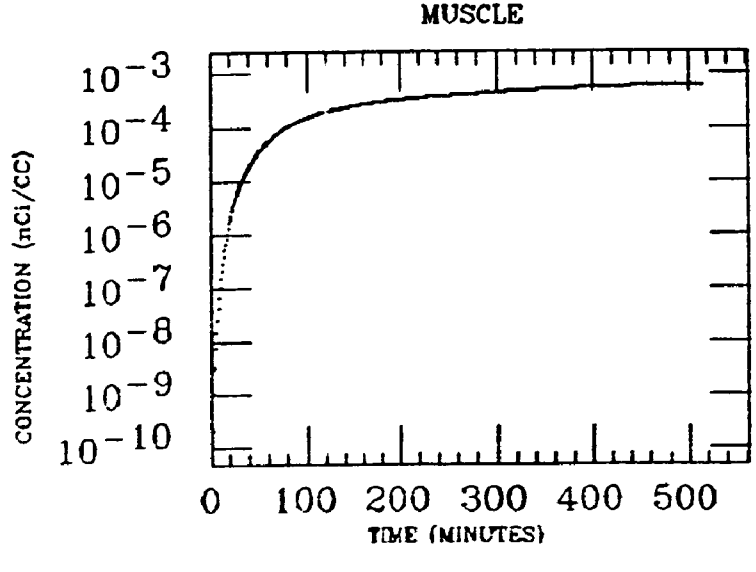

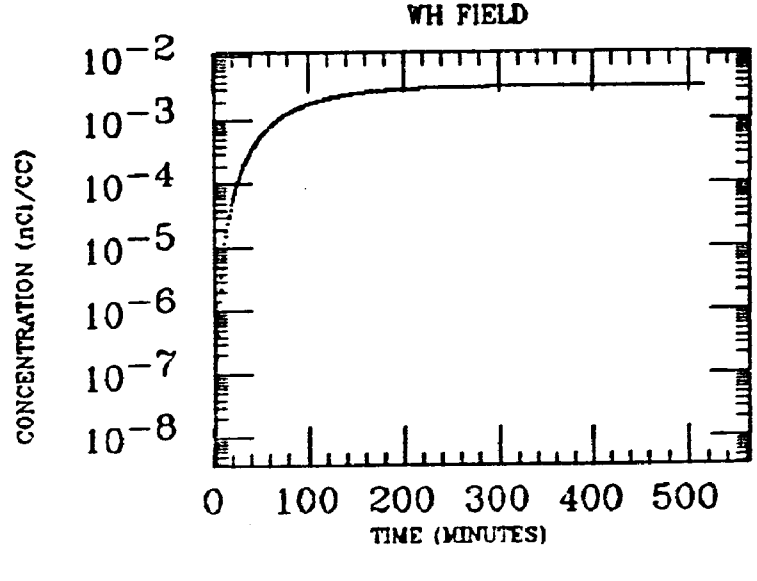

TAATJES
XE INGESTION
Pb-210

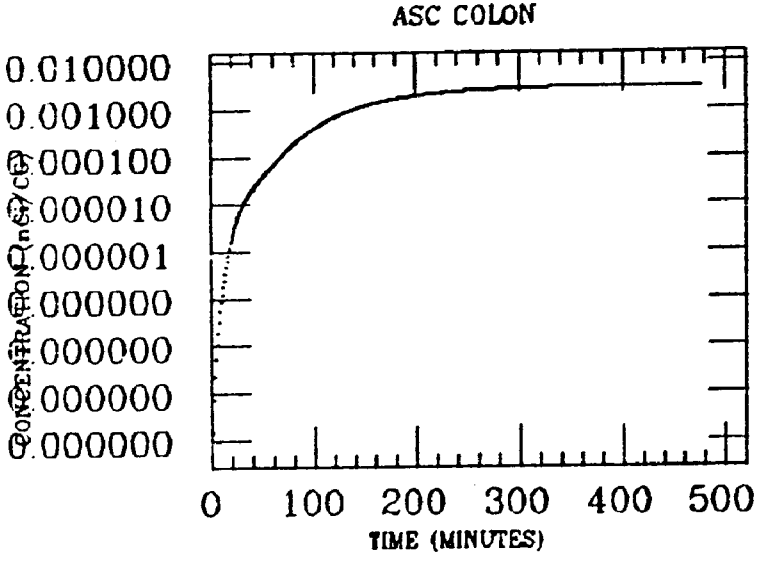

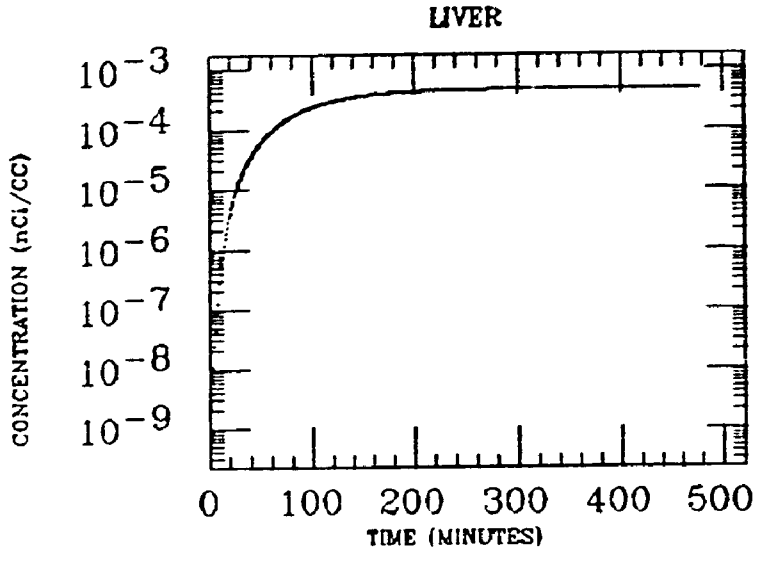

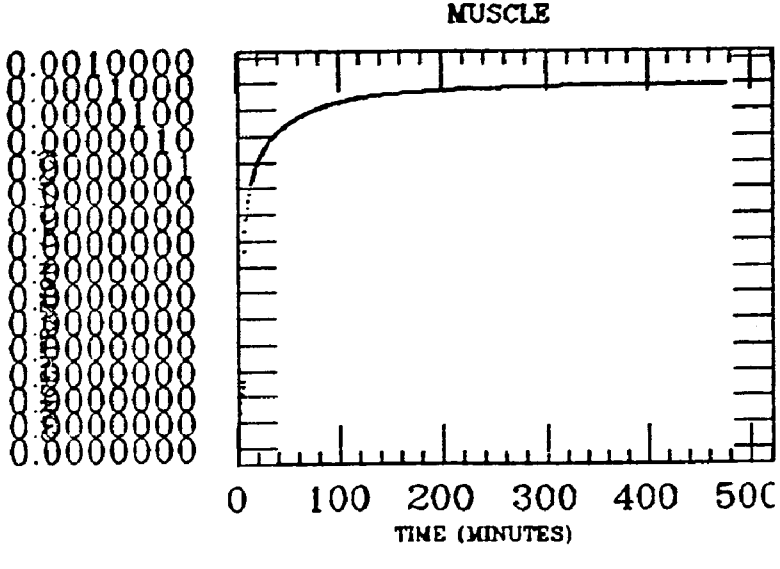

TAATJES
XE INGESTION
Pb-210

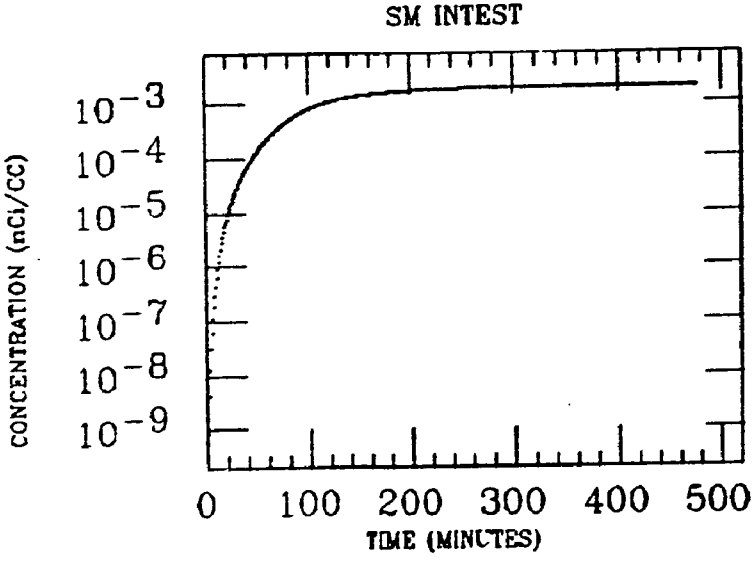

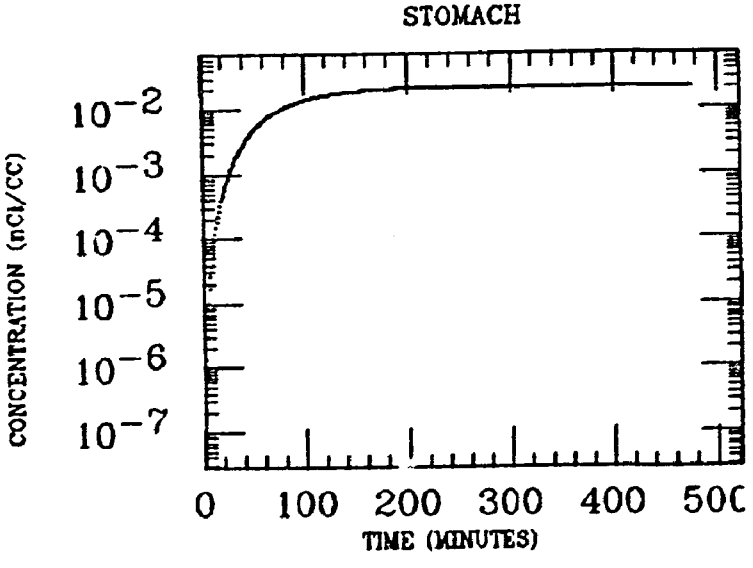

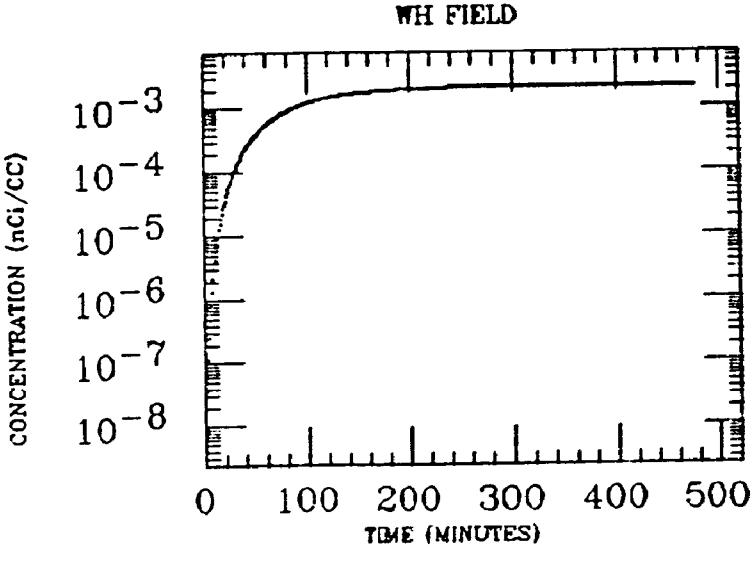

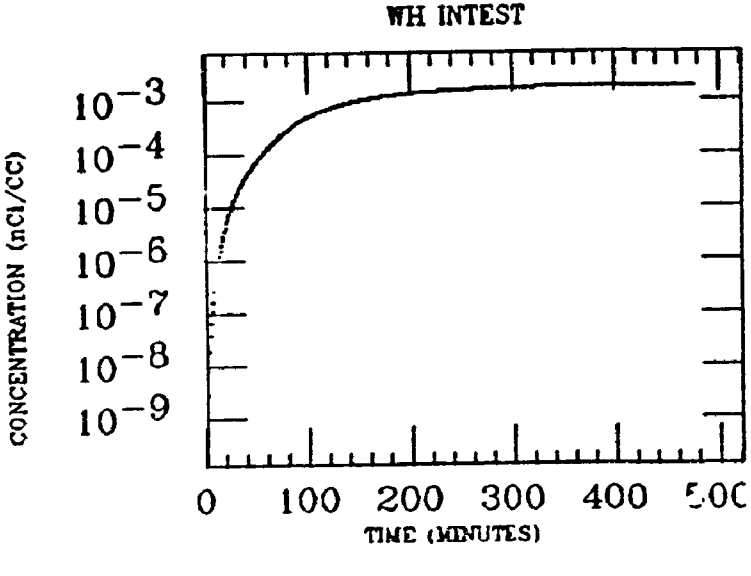

TAYLOR
XE INGESTION
Pb-210

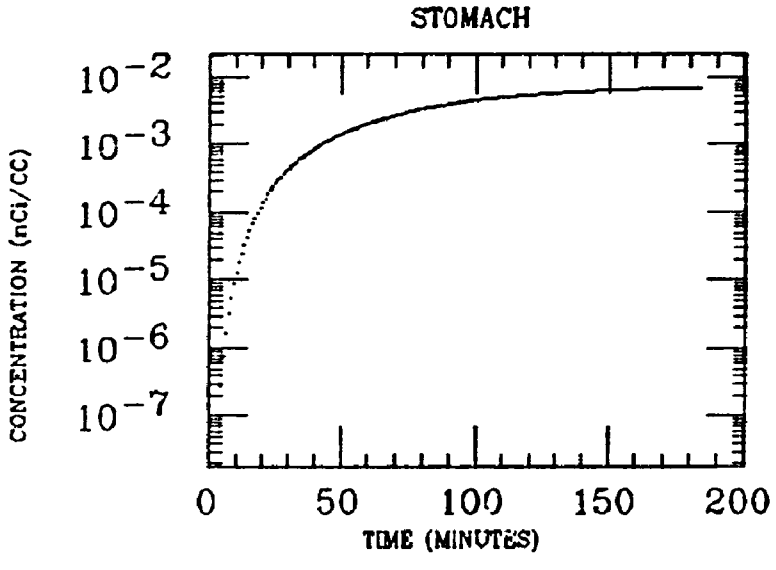

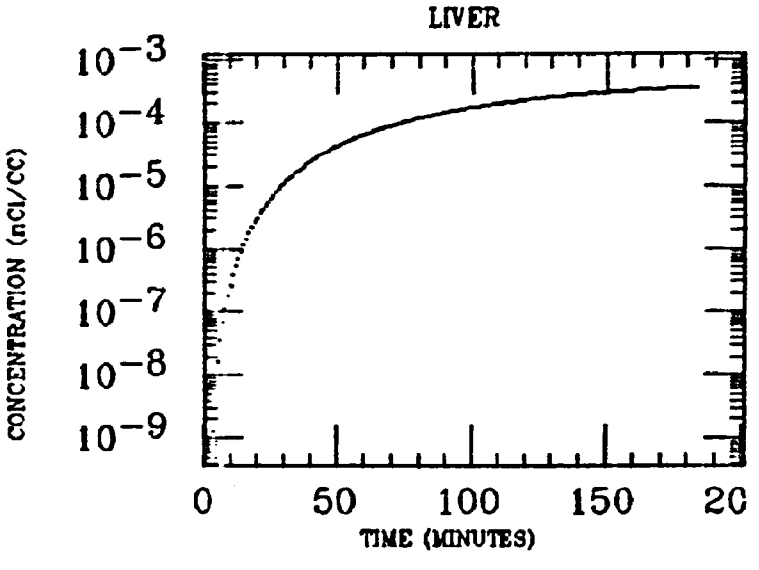

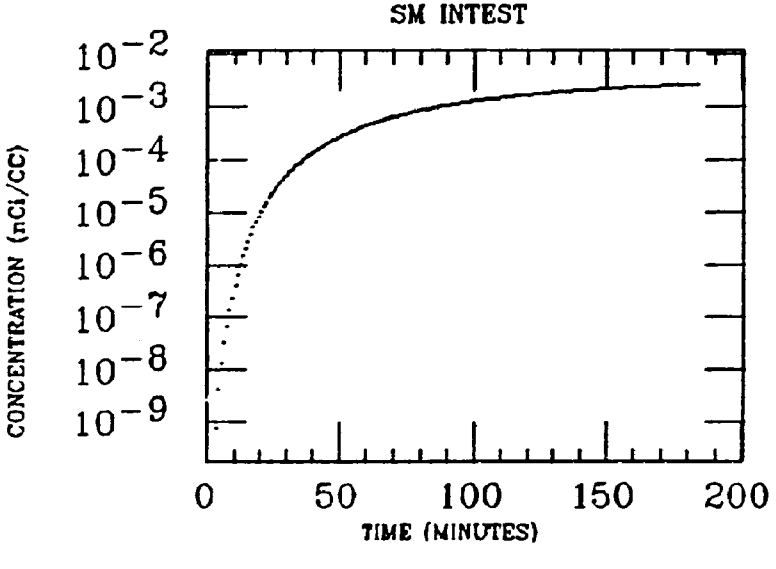

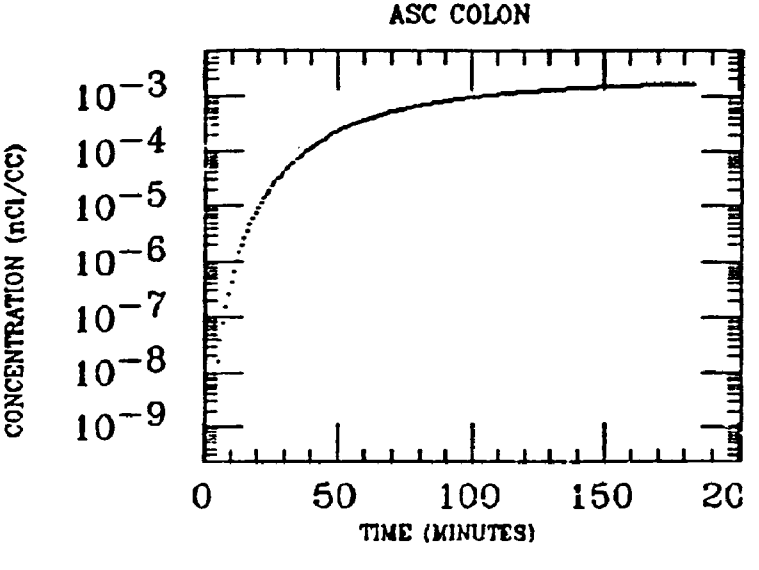

TAYLOR
XE INGESTION
Pb-210

DES COLON

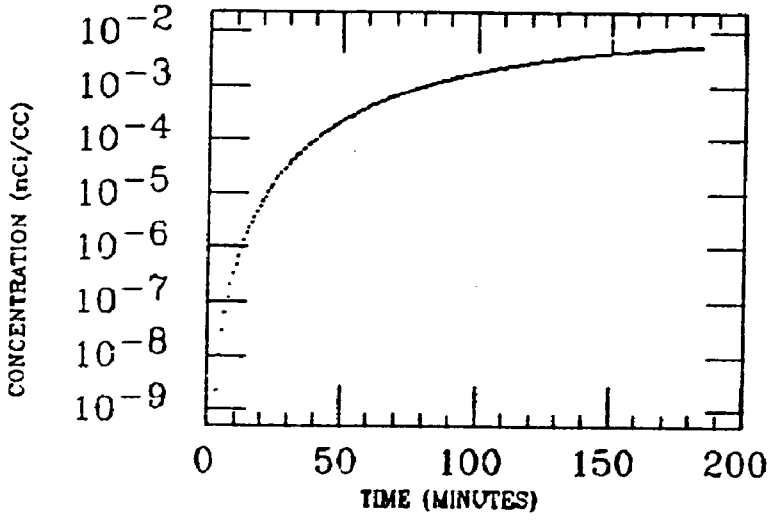

TR COLON

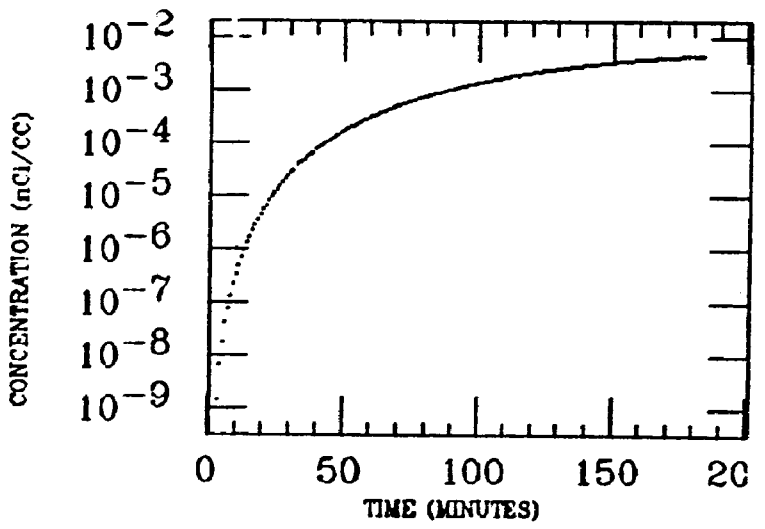

LG INTEST

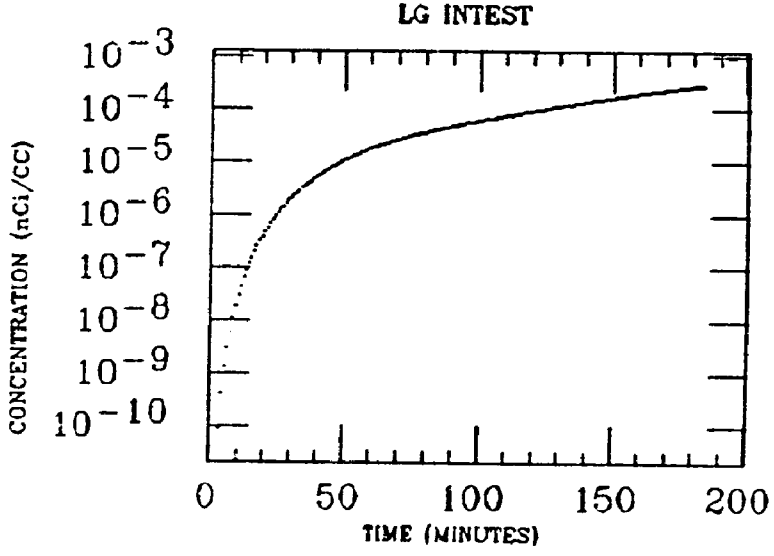

WH INTEST

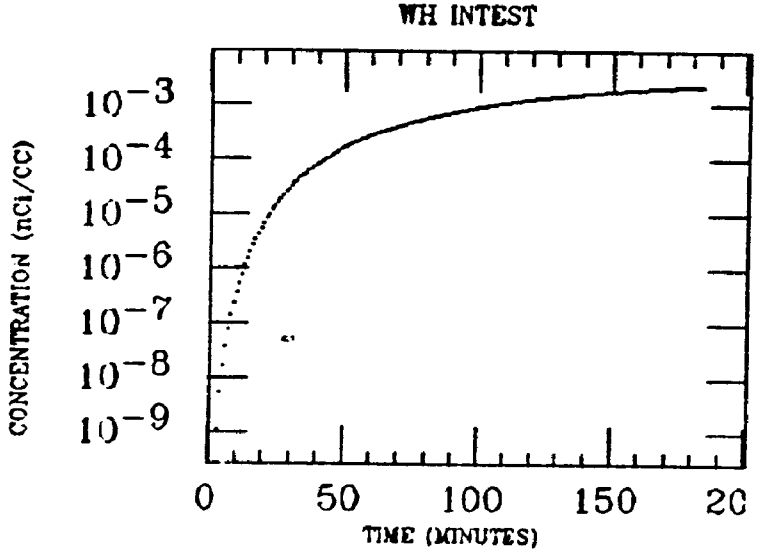

WESOLEK
XE INGESTION
Pb-210

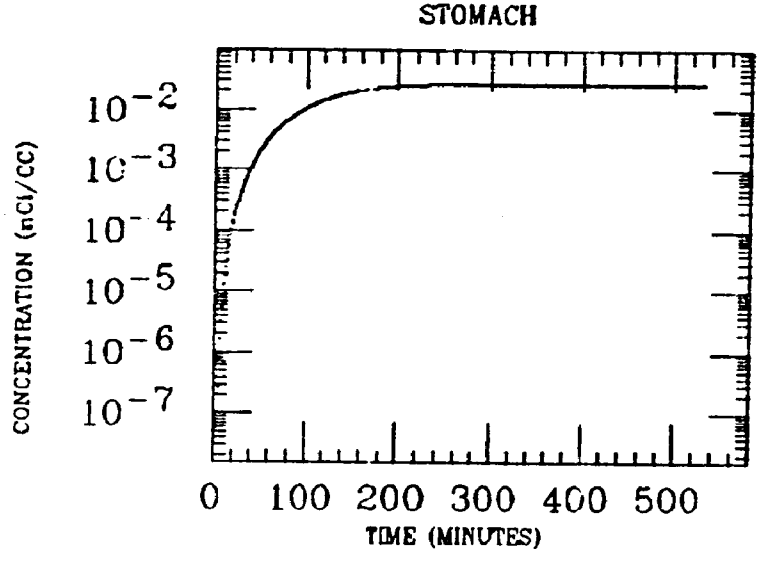

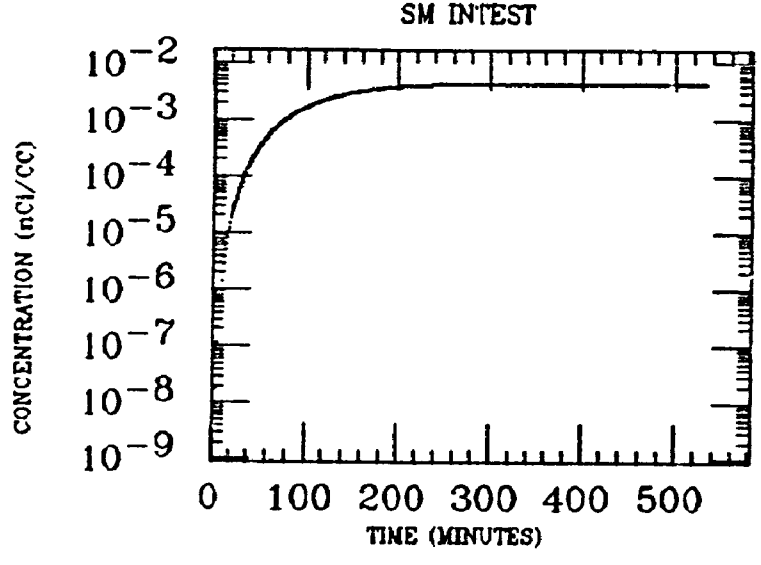

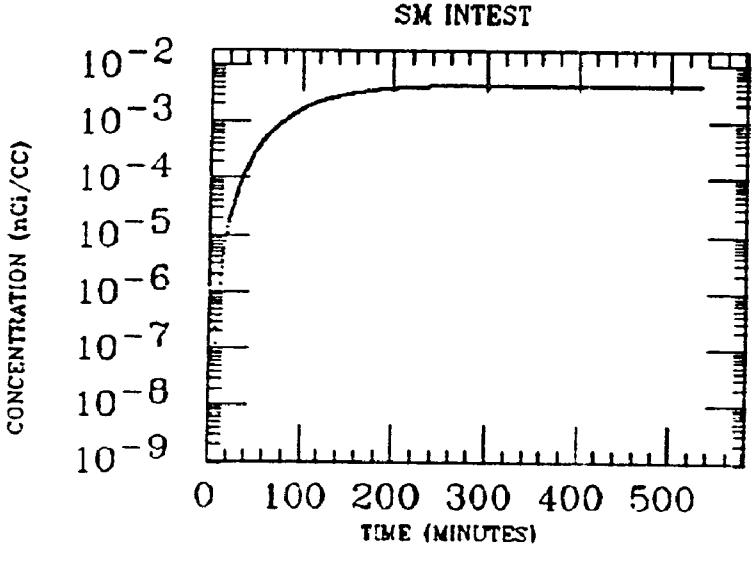

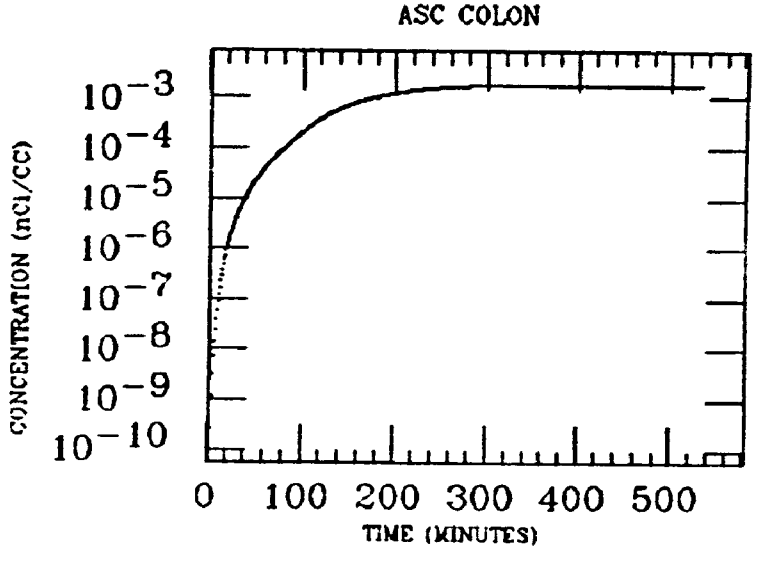

WESOLEK
XE INGESTION
Pb-210

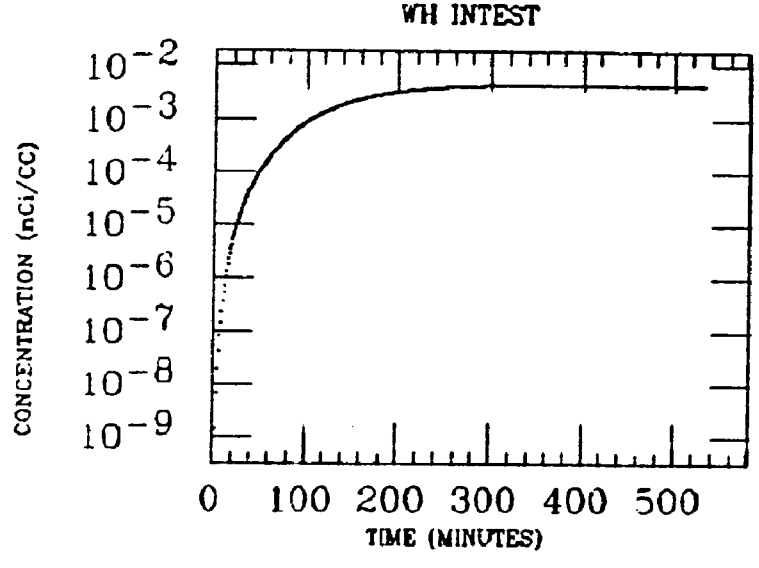

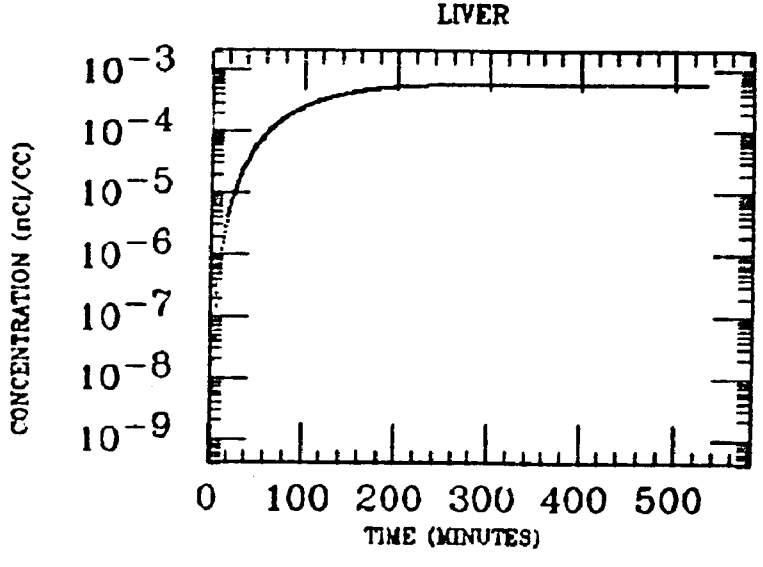

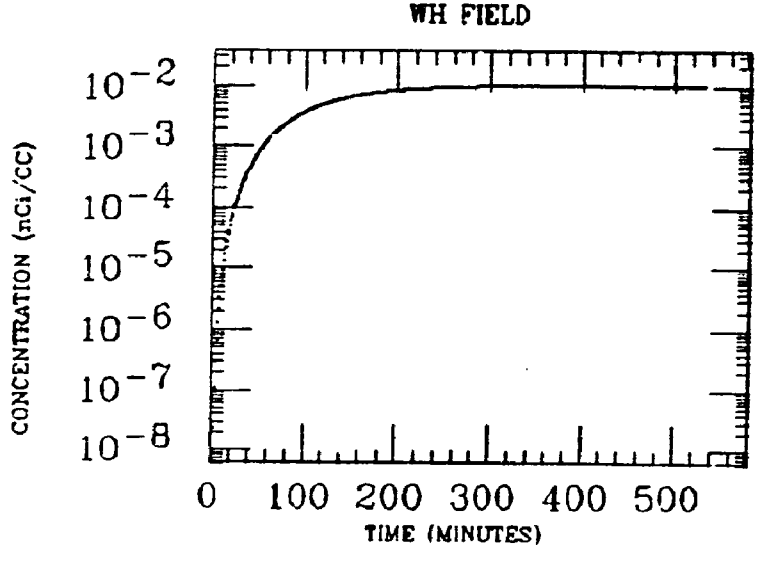

WILTSE
XE INGESTION
Pb-210

STOMACH

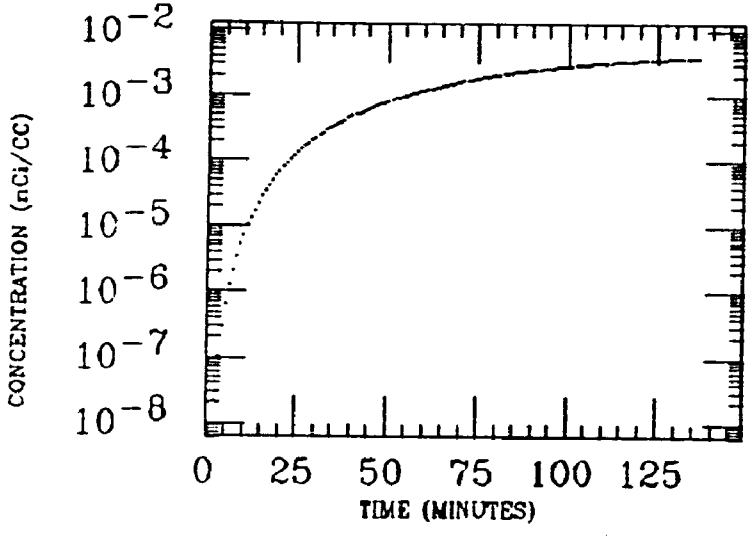

LIVER

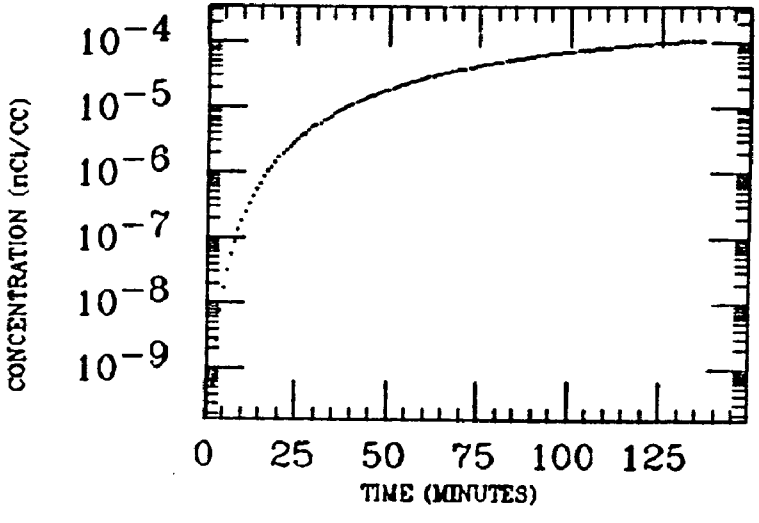

SM INTEST

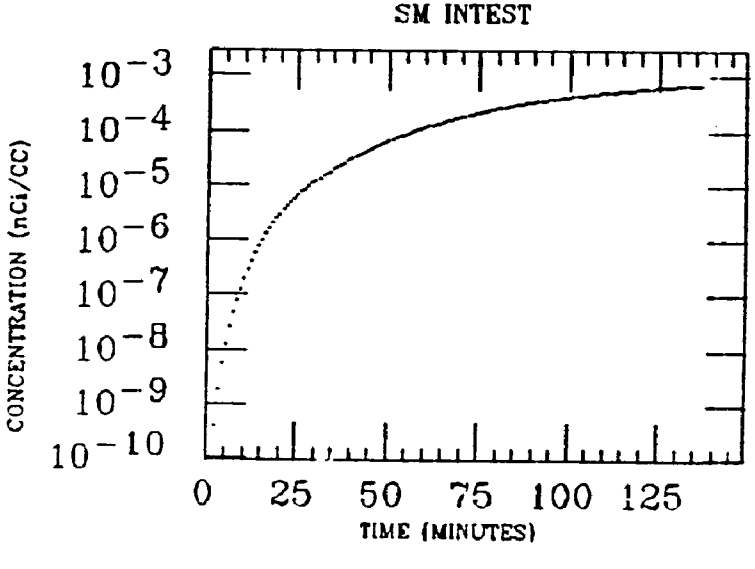

ASC COLON

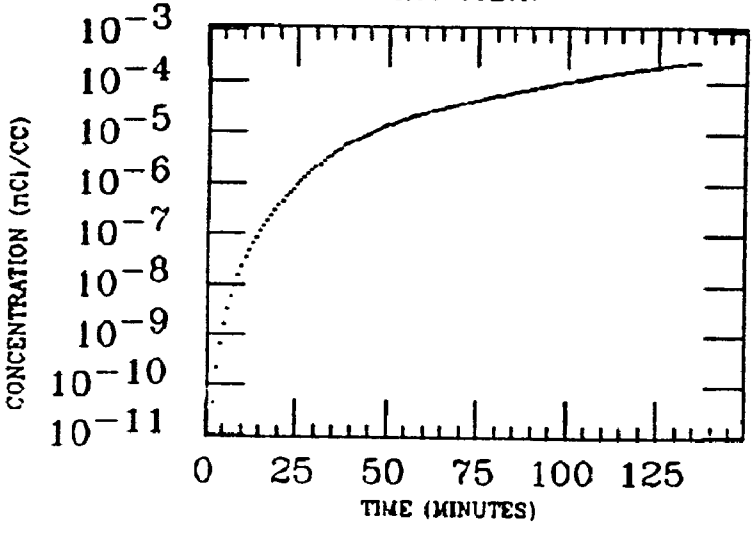

441

WILTSE
XE INGESTION
Pb-210